

AD-769 278

ATMOSPHERIC POLLUTION BY AIRCRAFT
ENGINES

Advisory Group for Aerospace Research and
Development
Paris, France

September 1973

DISTRIBUTED BY:

NTIS

National Technical Information Service
U. S. DEPARTMENT OF COMMERCE
5285 Port Royal Road, Springfield Va. 22151

**Best
Available
Copy**

AD 769 278

NORTH ATLANTIC TREATY ORGANIZATION
ADVISORY GROUP FOR AEROSPACE RESEARCH AND DEVELOPMENT

ORGANISATION DU TRAITE DE L'ATLANTIQUE NORD
GROUPE CONSULTATIF POUR LA RECHERCHE ET LE DEVELOPPEMENT AEROSPATIAL

AD 769278

AGARD Conference Proceedings No.125
ATMOSPHERIC POLLUTION BY AIRCRAFT ENGINES

Reproduced by
NATIONAL TECHNICAL
INFORMATION SERVICE
U S Department of Commerce
Springfield VA 22151

Papers and discussion presented at the 41st Meeting of the AGARD Propulsion and Energetics Panel held at The Meeting Rooms of the Zoological Society of London, Regent's Park, London, United Kingdom, 9-13 April 1973.

THE MISSION OF AGARD

The mission of AGARD is to bring together the leading personalities of the NATO nations in the fields of science and technology relating to aerospace for the following purposes:

- Exchanging of scientific and technical information;
- Continuously stimulating advances in the aerospace sciences relevant to strengthening the common defence posture;
- Improving the co-operation among member nations in aerospace research and development;
- Providing scientific and technical advice and assistance to the North Atlantic Military Committee in the field of aerospace research and development;
- Rendering scientific and technical assistance as requested, to other NATO bodies and to member nations in connection with research and development problems in the aerospace field;
- Providing assistance to member nations for the purpose of increasing their scientific and technical potential;
- Recommending effective ways for the member nations to use their research and development capabilities for the common benefit of the NATO community.

The highest authority within AGARD is the National Delegates Board consisting of officially appointed senior representatives from each member nation. The mission of AGARD is carried out through the Panels which are composed of experts appointed by the National Delegates, the Consultant and Exchange Program and the Aerospace Applications Studies Program. The results of AGARD work are reported to the member nations and the NATO Authorities through the AGARD series of publications of which this is one.

Participation in AGARD activities is by invitation only and is normally limited to citizens of the NATO nations.

The material in this publication has been reproduced directly from copy supplied by AGARD or the author.

Published September 1973

514.71:629.73.03



Printed by Technical Editing and Reproduction Ltd
Harford House, 7-9 Charlotte St, London. W1P 1HD

AGARD PROPULSION AND ENERGETICS PANEL OFFICERS

CHAIRMAN: Professor I.Glassman, Princeton University, New Jersey, USA
DEPUTY CHAIRMAN: Mr F.Jaarsma, National Aerospace Laboratory, Amsterdam, Netherlands

PROGRAM COMMITTEE FOR 41st MEETING

Professor A.Ferri, New York University, USA
Mr M.Barrère, ONERA, Châtillon-sous-Bagneux, France
Professor D.Dini, University of Pisa, Italy
Dr J.Dunham, NGTE, Pyestock, UK
Mr S.E.Høst, NDRE, Kjeller, Norway
Professor P.Monti, University of Naples, Italy
Mr E.C.Simpson, AF Aero Propulsion Laboratory, Wright-Patterson AFB, USA
Dr Ing.W.Alvermann, DFVLR, Germany (co-opted)
Professor R.F.Sawyer, University of California, Berkeley, USA (co-opted)

HOST COORDINATOR FOR 41st MEETING

Mr D.B.Smith, Ministry of Defence, UK

PANEL EXECUTIVE

Major J.B.Catiller, AGARD, France

The Propulsion and Energetics Panel wishes to express its thanks to the hosts – the UK National Delegates to AGARD – for the invitation to hold the meeting at the Meeting Rooms of the Zoological Society in Regent's Park, London, and for the provision of the necessary facilities and personnel to make the meeting possible.

PREFACE

by

Professor A. Ferri
Program Committee Chairman

As part of the growing concern in many developed countries with questions of ecology and environment, aircraft are being heavily criticized as contributing a significant share of pollution. Although the major objection is to noise, objections are also raised concerning smoke, fumes, and smells ascribed to aircraft. As a result, work is in progress to assess the impact of military and civil aviation on pollution levels by determining the nature and quantifying the extent of aircraft produced pollution for comparison with pollution from other sources. The main areas of interest involved in the meeting were:

- (1) effects of pollution at very high altitudes,
- (2) effects of pollution near airports;
- (3) methods for reduction of pollutant production in combustion processes and in engines.

Therefore, the meeting covered both the problem of pollution generation, especially related to nitric oxide, and the problem of diffusion. In addition it discussed some of the effects of the production of pollutants in the atmosphere.

The meeting included a review of physiological effects due to pollutants. This review was presented by the Aerospace Medical Panel. The meeting concluded with Round Table discussions where some of the most important points of the meeting were reviewed and discussed.

Dans le cadre des problèmes d'écologie et d'environnement qui préoccupent de façon croissante de nombreux pays ayant atteint un stade avancé de développement, les avions font l'objet de critiques sévères pour leur importante contribution à la pollution. Bien que, dans ce domaine, les objections essentielles concernent le bruit, elles englobent également la fumée, les vapeurs et les odeurs émises par les avions. Des travaux sont donc actuellement poursuivis en vue d'évaluer l'impact de l'aviation, tant civile que militaire, sur les niveaux de pollution, en déterminant la nature des produits polluants émis par les avions, et en les quantifiant, afin de les comparer aux polluants émis par les avions, et en les quantifiant, afin de les comparer aux polluants provenant d'autres sources. Les principaux domaines d'intérêt traités à l'occasion de cette réunion étaient les suivants:

- (1) les effets de la pollution aux très hautes altitudes;
- (2) les effets de la pollution au voisinage des aéroports;
- (3) les méthodes permettant de réduire la production des polluants provenant des processus de combustion et des moteurs.

La réunion couvrait donc à la fois le problème de la production de polluants, en particulier ceux apparentés à l'oxyde d'azote, et celui de leur diffusion. En outre, y furent étudiés certains des effets de la production de polluants dans l'atmosphère.

La réunion comprenait un bilan des effets physiologiques dont les polluants sont responsables, bilan qui fut présenté par le Groupe de Travail de Médecine Aérospatiale. Elle fut clôturée par une "table ronde" au cours de laquelle furent passés en revue et examinés certains des points les plus importants qui ont été traités.

CONTENTS

	Page
PROPULSION AND ENERGETICS PANEL OFFICERS & PROGRAM COMMITTEE	iii
PREFACE BY THE PROGRAM COMMITTEE CHAIRMAN	iv
 <u>SESSION I - HIGH ALTITUDE POLLUTION</u>	
	Reference
REDUCTION OF NO FORMATIONS BY PREMIXING by A.Ferri	A
UNITED STATES DEPARTMENT OF TRANSPORTATION RESEARCH PROGRAM FOR HIGH ALTITUDE POLLUTION by A.J.Grobecker	1
REACTION OF OZONE WITH NITROGEN OXIDES AT HIGH ALTITUDES by H.S.Johnston and G.Whitten	2
NITROGEN OXIDES, NUCLEAR WEAPON TESTING, CONCORDE AND STRATOSPHERIC OZONE by P.Goldsmith, A.F.Tuck, J.S.Foot, E.L.Simmons and R.L.Newson	3
DETAILED EXHAUST EMISSION MEASUREMENTS OF THREE DIFFERENT TURBOFAN ENGINE DESIGNS by A.W.Nelson	4
PHOTO-OXIDATION OF AIRCRAFT ENGINE EMISSIONS AT LOW AND HIGH ALTITUDES by K.H.Becker and U.Schurath	5
EFFECT OF SUPERSONIC TRANSPORT UPON THE OZONE LAYER, STUDIED IN A TWO-DIMENSIONAL PHOTOCHEMICAL MODEL WITH TRANSPORT by E.Hesstvedt	6
CHEMICAL KINETICS IN THE STRATOSPHERE by G.Brasseur	7
A NEW ANALYTICAL TECHNIQUE FOR CONTINUOUS NO DETECTION IN THE RANGE FROM 0.1 TO 5000 PPM by H.Meinel and Th.Just	8
 <u>SESSION II - LOW ALTITUDE POLLUTION</u>	
PROBLEMS OF CHEMICAL POLLUTION BY AIRCRAFT. THE AIRPORT AND ITS IMMEDIATE ENVIRONMENT by T.V.Lawson	B
RELATIVE AIR POLLUTION EMISSIONS FROM AN AIRPORT IN THE UK AND NEIGHBOURING URBAN AREAS by A.W.C.Keddie, J.Parker and G.H.Roberts	9
GROUND CONTAMINATION BY FUEL JETTISONED FROM AIRCRAFT by N.L.Cross and R.G.Picknett	12
POLLUTION LEVELS AT LONDON (HEATHROW) AIRPORT AND METHODS FOR REDUCING THEM by D.M.Bruton	13
POLLUTION CONTROL OF AIRPORT ENGINE TEST FACILITIES by D.L.Bailey, P.W.Tower and A.E.Fuhs	14

- EXHAUST EMISSION MEASUREMENTS ON THE GE T64-TURBOPROP-ENGINE
by W.Bergt, G.Kappler and G.Meikis

15

SESSION III - BASIC COMBUSTION PROBLEMS

- NO FORMATION IN FUEL RICH FLAMES: A STUDY OF THE INFLUENCE OF THE
HYDROCARBON STRUCTURE
by K.H.Eberius and Th.Just

16

- MESURES DES CONSTITUANTS MINEURS DANS LA STRATOSPHERE PAR
CONCORDE 001
par R.Joatton

17

- SOOT FORMATION IN RICH KEROSENE FLAMES AT HIGH PRESSURE
by F.H.Holderness and J.J.Macfarlane

18

- SOOT OXIDATION KINETICS AT COMBUSTION TEMPERATURES
by J.P.Appleton

20

- PARAMETERS CONTROLLING NITRIC OXIDE EMISSIONS FROM GAS TURBINE
COMBUSTORS
by J.B.Heywood and T.Mikus

21

- FACTORS CONTROLLING POLLUTANT EMISSIONS FROM GAS TURBINE ENGINES
by R.F.Sawyer, N.P.Cernansky and A.K.Oppenheim

22

- A SYSTEMATIC APPROACH TO THE STUDY OF THE CONNECTION BETWEEN
EMISSION AND AMBIENT AIR CONCENTRATIONS
by K.E.Grönskei

23

- ETUDE THEORIQUE DE L'EVOLUTION RESIDUELLE DES PRODUITS POLLUANTS
DANS LES JETS DE TURBOREACTEURS
par R.Borghi

24

- DEVELOPMENT AND VERIFICATION OF AN ANALYTICAL MODEL FOR PREDICTING
EMISSIONS FROM GAS TURBINE ENGINE COMBUSTORS DURING LOW-POWER
OPERATION
by S.A.Mosier, R.Roberts and R.E.Henderson

25

- AN EXPERIMENTAL RESEARCH ON THE BEHAVIOR OF A CONTINUOUS FLOW
COMBUSTION CHAMBER
by C.Casci, A.Coghe, U.Ghezzi and S.Pasini

26

SESSION IV - DESIGN

- OPENING REMARKS
by W.Moe

C

- MODELISATION DES FOYERS DE TURBOREACTEUR EN VUE DE L'ETUDE DE
LA POLLUTION
par M.Barrère

27

- SMOKE SUPPRESSANT ADDITIVE EFFECTS ON PARTICULATE EMISSIONS FROM
GAS TURBINE COMBUSTORS
by P.J.Pagni, L.Hughes and T.Novakov

28

- TECHNOLOGY FOR THE REDUCTION OF AIRCRAFT TURBINE ENGINE EXHAUST
EMISSIONS
by D.W.Bahr

29

- A PRELIMINARY STUDY ON THE INFLUENCE OF FUEL STAGING ON NITRIC OXIDE
EMISSIONS FROM GAS TURBINE COMBUSTORS
by A.H.Lefebvre and R.S.Fletcher

30

	Reference
DESIGN AND EVALUATION OF COMBUSTORS FOR REDUCING AIRCRAFT ENGINE POLLUTION by R.E.Jones and J.Grobman	31
POINT DE VUE DU MOTORISTE SUR LA CONCEPTION DES FOYERS A FAIBLE TAUX DE POLLUTION par A.Quillevéré, R.Briançon et J.Decouflet	32
AIRCRAFT GAS TURBINE POLLUTANT LIMITATIONS ORIENTED TOWARD MINIMUM EFFECT ON ENGINE PERFORMANCE by R.E.Henderson and W.S.Blazowski	33
PHOTOMETRIC MEASUREMENTS OF EXHAUST SMOKE TRAILS BY JET ENGINES by M.Lucchesini and D.Dini	34

SESSION V - PHYSIOLOGICAL EFFECTS OF POLLUTION

ENVIRONMENTAL TOXICOLOGICAL IMPACT OF AIRCRAFT OPERATIONS by K.C.Back	35
ROUND TABLE DISCUSSION	D

APPENDIX A - A selection of AGARD Publications in recent years	App.A
--	-------

APPENDIX B - Participants	App.B
---------------------------	-------

REDUCTION OF NO FORMATIONS BY PREMIXING

Antonio Ferri
 Chairman, Department of Aeronautics and Astronautics
 Astor Professor of Aerospace Sciences
 New York University
 Bronx, New York 10453

1. INTRODUCTION

The possibility that the exhaust gases of a large fleet of future supersonic transports (SST) could substantially alter the equilibrium of the stratosphere must be proved to be extremely improbable, before large scale activities will be approved in the U.S.A. for mass utilization of present SST's and for the development of future SST's. Such possibilities have been formulated on the basis of sound scientific work and therefore should not be minimized. Unfortunately, the probability that such effects will, or will not actually occur will not be ascertained in the near future. At the same time, many decisions on future activities of the SST cannot be delayed for too long a period of time. For this reason, it appears important at this time that the total problem be accurately defined, taking into account all relevant aspects. The purpose of the present paper is to furnish information useful for such a definition.

Many arguments have been raised for and against the SST related to the effects of NO_x on the ozone of the atmosphere. If we move out of the political arena, the present situation can be best summarized by the following statement recently made by Professor H. Johnston of the University of California, Berkeley, "There is strong evidence that nitrogen oxide from SST exhaust could seriously reduce stratospheric ozone. But in every case, the evidence can be matched by a possibility that the SST would have little or no effect." This refers to a large fleet of SST's flying continuously; therefore, it refers to a situation that will exist a few decades in the future and refers to present engine designs. In the present decade, the number of airplanes flying at supersonic speed will probably be substantially smaller than the number considered in the studies related to the effects of NO_x , and the airplanes will have small dimensions. Therefore, initially, the amount of nitric oxide produced will be substantially smaller than the amount considered in such studies. In addition, the possible introduction of new experimental airplanes on the part of the U.S.A. in the immediate future will not change the situation. Therefore, the initiation of new development programs by the U.S.A. will not have any serious consequence, provided that a practical solution to the problem will be available within the period required for such development. On this basis, a sound and responsible technical approach should be as follows:

- a. Continue the scientific investigations related to a better understanding of the chemical processes and diffusion processes in the upper atmosphere. In my opinion, such an effort is of basic importance because it has a much larger scope than the present problem; therefore, independent of the SST, deserves research efforts of the same order of magnitude of the efforts related to deep space investigations. Possibly, these investigations should be organized on a permanent basis.
- b. Develop methods for reducing substantially the amount of pollutants produced by future jet engines. It has been indicated in Reference 1 that the amount of NO_x produced by combustion processes at conditions corresponding to jets for supersonic airplane speed can be reduced by orders of magnitude by generating a flame structure different from the flame structure used in present engines. Such a flame in principle could be created in practical engines provided that different burners are designed. The present paper will enlarge on the points made in Reference 1, and will describe in more detail how the NO_x production can be reduced by orders of magnitude in combustion processes for conditions corresponding to the conditions required by SST engines, provided that the fluid dynamics of the combustion process is modified. The physics for introducing such changes is simple and understood. No reason exists why such flames could not be used for cruise in an SST engine. On this basis, it appears logical to assume that if an effort in this direction parallels the effort mentioned before in upper atmospheric physics, a good possibility exists that the problem of NO_x can be resolved.

While the design of an actual engine using the combustion process described below will require a substantial effort and expensive development cycle, it appears logical to assume that the development of a new combustion design can be achieved within the period of several years, available between now and the period when production of 500 large SST's will be initiated. Therefore, the possibility of unacceptable effects due to the NO_x formation due to present design as predicted today, should not be a main reason for delaying decisions on the initiation of SST prototypes, provided that substantial efforts are initiated in parallel toward the development of new burner designs that apply the principle described below.

The problem related to such a development is extremely complex; therefore, it is conceivable at the first stage of the effort that a burner design be considered that uses the new combustion flame described below only during supersonic cruise to be generated in a separate combustion zone created for this purpose, while the existing burner concept is used at low speed for the transient operations. A burner having two sets of injector systems and two sets of flame generators, is more complex than present designs; however, such an approach would reduce substantially the time required for development because the burner to be developed using the flames that produce low NO_x during cruise will be designed for single operational characteristics.

2. DESCRIPTION OF THE ENGINE REQUIREMENTS

Present engines to be used for near future SST's are turbojet engines. The cycle requirements for such engines are that the temperature of the gases downstream of the burner be as uniform as possible, and be at temperatures that are dictated by the turbine structure requirements.

Present engine technology, because of the life requirements for the engine, limits the gas temperatures of the flow entering the turbine at cruise conditions to values that are as low as 1280°K (2300°R). It can therefore be concluded that combustor designs capable of producing gases in the 1200° to 1800°K range (3200°R) are practical for future SST engines at cruise. At these temperatures, the amount of NO_x that can be generated in a few milliseconds is very small, and on the order of 10⁻³ to 10⁻² g/Kg of fuel. This value is several orders of magnitude lower than the value measured in present engines. Typical values in present engines are 1-3x10¹ g/Kg fuel. The reason for this difference is due to the fact that in present combustor designs, the chemical reaction between fuel and oxidizer occurs approximately at stoichiometric conditions, then the maximum temperatures reached by the gas correspond to a stoichiometric mixture and are much higher than the final required temperature. The NO_x formed at the maximum temperature remains frozen during subsequent cooling due to the mixing and therefore remain in the gas.

3. DESCRIPTION OF PRESENT COMBUSTOR DESIGN

Present combustor designs are based on combustion controlled by mixing. The fuel is injected in the air that moves in the combustor at low speed. Because of the rapid reaction rates corresponding to the flame temperature, the heat release occurs rapidly and is close to equilibrium conditions; then the flame sheet model approximation applies. In this model, the flame region can be divided in two regions; one fuel rich close to the fuel injector, the other oxygen rich outside of this region. The temperature of the gas is maximum at the line that divides the two regions where the mixture is stoichiometric. Here the temperature is close to equilibrium conditions for stoichiometric mixtures. Such temperatures depend on the initial temperature of the air before combustion and is given in Fig. 1 as a function of the air temperature before combustion. The time involved in the combustion process is very short; however, it is sufficiently long to permit formation of a substantial amount of NO_x, once NO_x is formed it then remains frozen during cooling. An example of such a flame is shown in Fig. 2. Here the fuel is injected at the axis and air is flowing outside. Combustion is initiated near the wall of the jet by a heat source. The fuel is a gas and diffuses in the air, combustion propagates downstream, and the maximum temperature reached locally is of the order of 2300°K independent of the amount of air involved in the process and therefore of the final temperature. The combustion products are diluted by the excess air and therefore are cooled off. A schematic representation of the combustion process taking place in present type combustors is shown in Fig. 3. Here the initial temperature of the air is assumed to be 450°K, the fuel is burned first at stoichiometric mixture and then additional air is added to decrease the gas temperature. Again, the fuel air combustion is initiated by a high temperature source. The time involved in cooling the gas from 2400°K is extremely short. It must be noted that all fuel crosses the high temperature region. These data have been calculated taking into account mixing and chemical reactions.

The NO_x formed in this process is equal to 10 g/Kg of fuel. This value can be reduced by increasing the speed of the process or by decreasing the fuel air ratio in the outside region; then lower maximum temperatures are obtained. For these conditions, values on the order of 5 to 10 g/Kg fuel have been calculated. These values are in approximate agreement with the values measured in existing engines.

Because the maximum temperature in the flame is a function of initial temperature, which depends on the flight Mach number and compression ratio across the compressor, the NO_x formed in this process when measured in grams of NO per Kg of fuel is independent of the conditions of the combustion gases at the entrance of the turbine and therefore is not a function of the final temperature, but depends only on the initial temperature, and therefore on the flight Mach number and pressure ratio of the compressor.

4. PREMIXED FLAMES

The only requirement for the combustor at cruise is to produce chemical reaction in air fuel mixtures with average value of the composition on the order of 0.3 to 0.5 of stoichiometric. Therefore, the high temperatures corresponding to stoichiometric mixtures can be avoided, provided that the combustion can be generated and sustained in the stream. Assume, as described in Reference 1, that we premix the fuel and the air before combustion, and that the stoichiometric fuel to air ratio in the mixture is uniform and below stoichiometric; however, sufficient amount of fuel is present so that the flame can be sustained. Then if we ignite the mixture at one point, the heat release due to reaction is sufficiently high to generate a stable flame that propagates to all the mixture. Because the flame is a heat conduction flame, in a uniformly premixed mixture the maximum local temperature is determined by initial temperatures and by the local fuel to air ratio. Because the mixture is below stoichiometric, the maximum temperature reached locally is lower than in a diffusion type flame.

Recent analyses and laboratory experiments indicate that such a flame can be maintained in a wide range of pressure, and in mixtures where the fuel concentration is much lower than the stoichiometric value provided that the flame is initiated at a point. Results of analyses of such flames are shown as examples in Figs. 4 and 5. Figure 4a gives the isotherms of one of the flames. The flame is a heat conduction flame in a uniform mixture of hydrocarbon fuel and air (JP4 and air) at a fuel to air ratio capable of producing a final temperature of 1820°K. The initial temperature of the mixture is 720°K and the static pressure is 5760 lb/ft², the fuel to air ratio is 0.45 of stoichiometric. Such conditions are typical for supersonic flights at M on the order of 2, and at 65,000 ft. altitude. The velocity of the mixture is 450 ft/sec. The flame is initiated locally by a hot region of the flow (a pilot) having 1722°K, and moving at lower velocity 250 ft/sec. The flow is axially symmetric.

The mass fraction of NO (% of total mass) along selected streamlines is given in Fig. 4b, as a function of the distance. The curves are defined by the values of the initial radius y at $x = 0$.

The NO formation occurs first near the center, then in the outside region. The flame is about 2 ft long. There is substantial delay between the station where maximum temperature is reached and the point where high concentration of NO is present. The mass fraction of NO is on the order of 2 to 3×10^{-6} which corresponds to an emission index of 6.6×10^{-2} g/Kg fuel.

One of the most important problems to be solved in this type of flame is related to maintaining a stable flame across the mixture. Combustion of hydrocarbons and air at values of fuel to air ratio somewhat lower than the values used in Fig. 4 and the same initial temperature cannot be maintained. While if the fuel air ratio is increased and therefore the final temperature is increased, then the NO concentration increases. For example, if the fuel to air ratio is on the order of .024 combustion cannot be maintained for the given initial temperature selected while if the value becomes .040 then the final temperature reaches a value of 2130° and the NO index becomes 2 g/Kg fuel. The amount of NO produced does not change if we increase the Mach number of flight, or the compression ratio of the compressor provided that we keep constant the final temperature. In this type of flame, the concentration of NO is independent of initial temperature and only depends on the final temperature and static pressure. This characteristic is different from the characteristic of diffusion flames presently used in engines where the NO concentration depends only on the initial temperature, and is independent of the final temperature. However, the increase of initial temperature facilitates the propagation of the flame.

Figure 5a gives the isotherms for a premixed flame having initial temperature of 1111°K and $10,500 \text{ lb/ft}^2$ pressure, and reaching a final temperature of 1850°K . These conditions are typical for an engine operating at $M = 3.5$ at 65,000 ft altitude. In this case, the flame propagates faster and the combustor length for the conditions selected is approximately 1/2 of the combustion length required for 720°K temperature. The fuel to air ratio for this case corresponds to 0.3 of stoichiometric. The mass formation of NO is 1×10^{-6} , that corresponds to approximately 6×10^{-2} g/Kg fuel.

Many other cases have been calculated. The results have been summarized in Fig. 6 which gives the grams of NO per Kg fuel as a function of the final temperature.

This chart indicates that for cruise conditions corresponding to the engines required for the SST, the NO concentration could be reduced by two orders of magnitude with respect to present engines using the present knowledge of rate of combustion processes.

Unfortunately, this direction which has been proposed by the author as early as 1970 has not yet been actively pursued. Experiments of a proprietary nature performed by the Advanced Technology Laboratories, Inc., have confirmed the analytical results.

5. CONCLUDING REMARKS

The type of flame described here has been obtained in many laboratory experiments and can be generated safely and with stable conditions on a laboratory scale.

If the concept of a more complex burner design, where two sets of injectors are used is acceptable, one of the type used in present engines to be used at low speed and during transients, and a second that incorporates the present concept to be used only for cruise, then the many objections raised by combustor designers related to operational properties of such a flame at conditions different from cruise are eliminated. The two types of injectors increase the complexity of the engines; however, they can probably be introduced in actual engine burners without too large a penalty in volume and weight, and therefore will not be noticeable in the airplane's performance. On this basis, it appears logical to conclude that no sound reason presently exists in delaying the development of the SST because of the NO effects on the ozone even if the present estimates are proved valid. A sound scientific program should enlarge the research of the effect of upper atmospheric pollution and in parallel should develop burner concepts that use the concepts described above in the development of new engines for SST's should include the possibility of a different burner design.

6. REFERENCES

1. Ferri, A., "Better Marks on Pollution for the SST." *Astronautics and Aeronautics*, July 1972.

7. ACKNOWLEDGEMENT

This work has been performed with the help of Dr. A. Agnone and Mrs. F. Kung. The numerical program used has been supplied by the Advanced Technology Laboratories, Inc., and has been generated by Dr. P. Baronti and Dr. A. Rubel.

The work reported herein was supported partially by the National Aeronautics and Space Administration under Grant No. NGR-35-016-131.

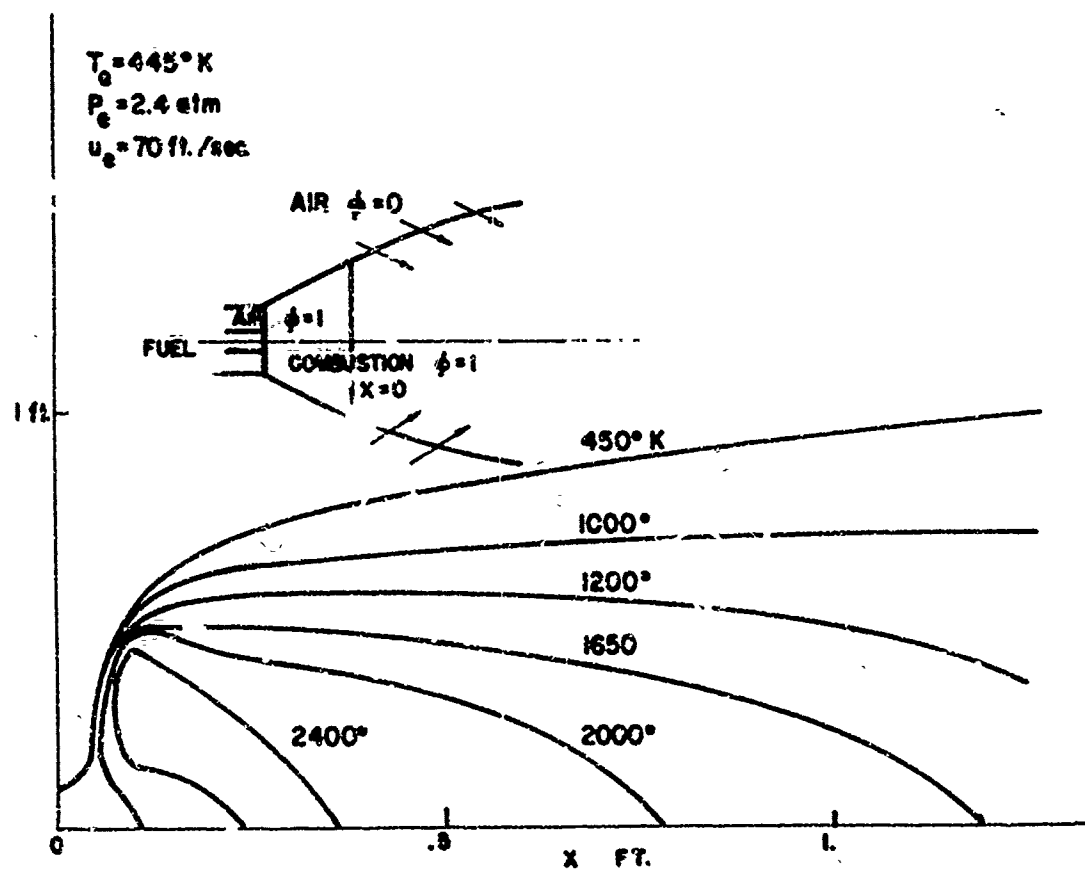


Fig. 3 Isotherms in a Pilot Ignited Mixture of JP-4 and Air.

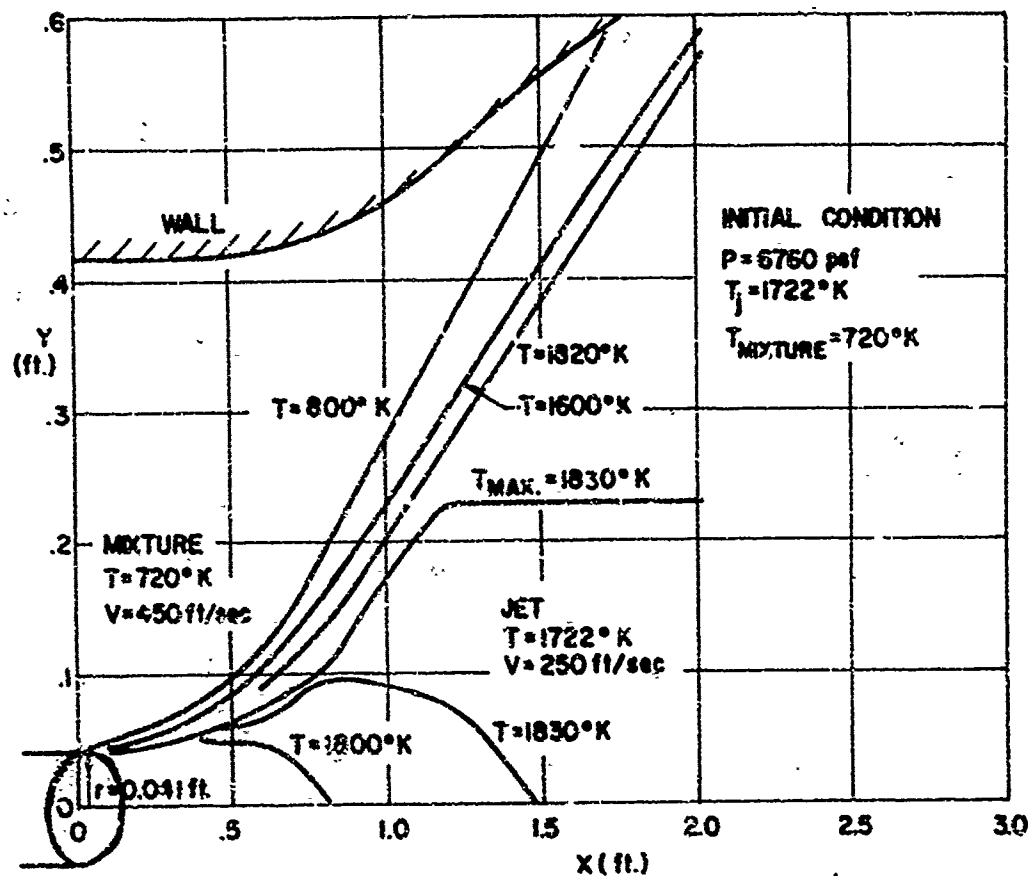


Fig. 4a Isotherms of Plane of Premixed Gases.

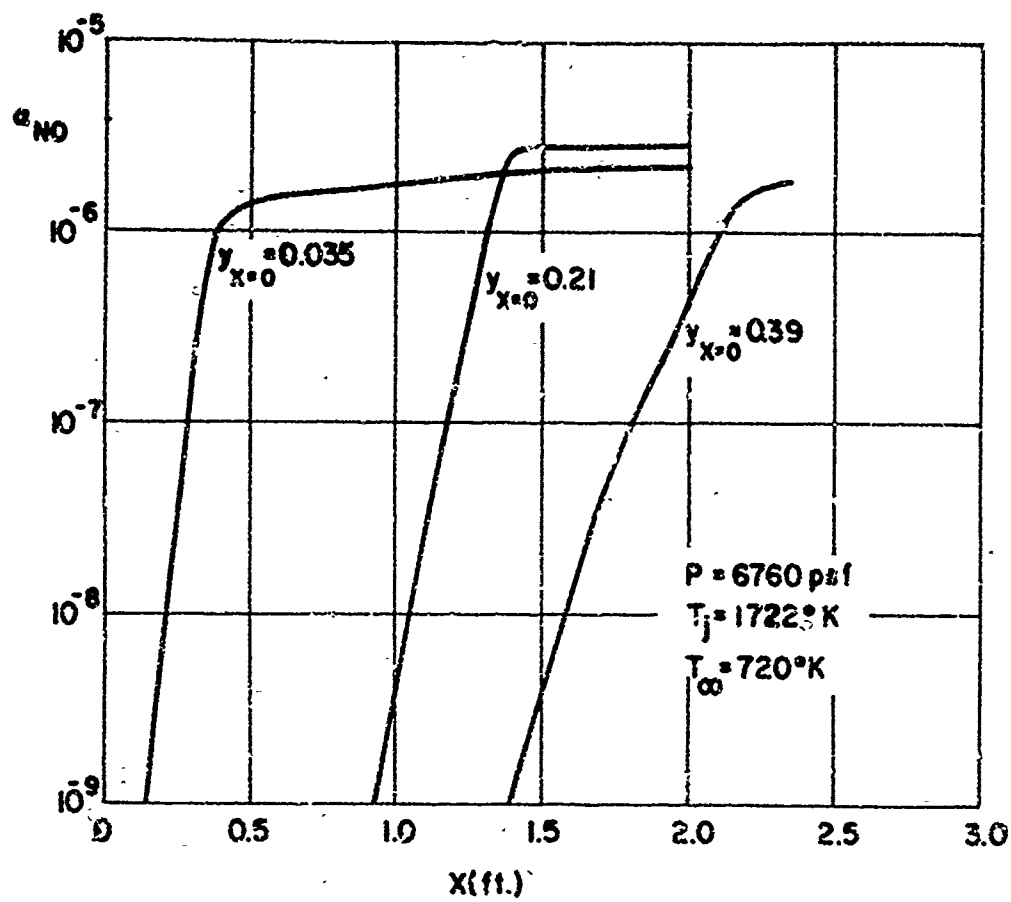


Fig. 4b Mass Fraction of NO Along Selected Streamlines

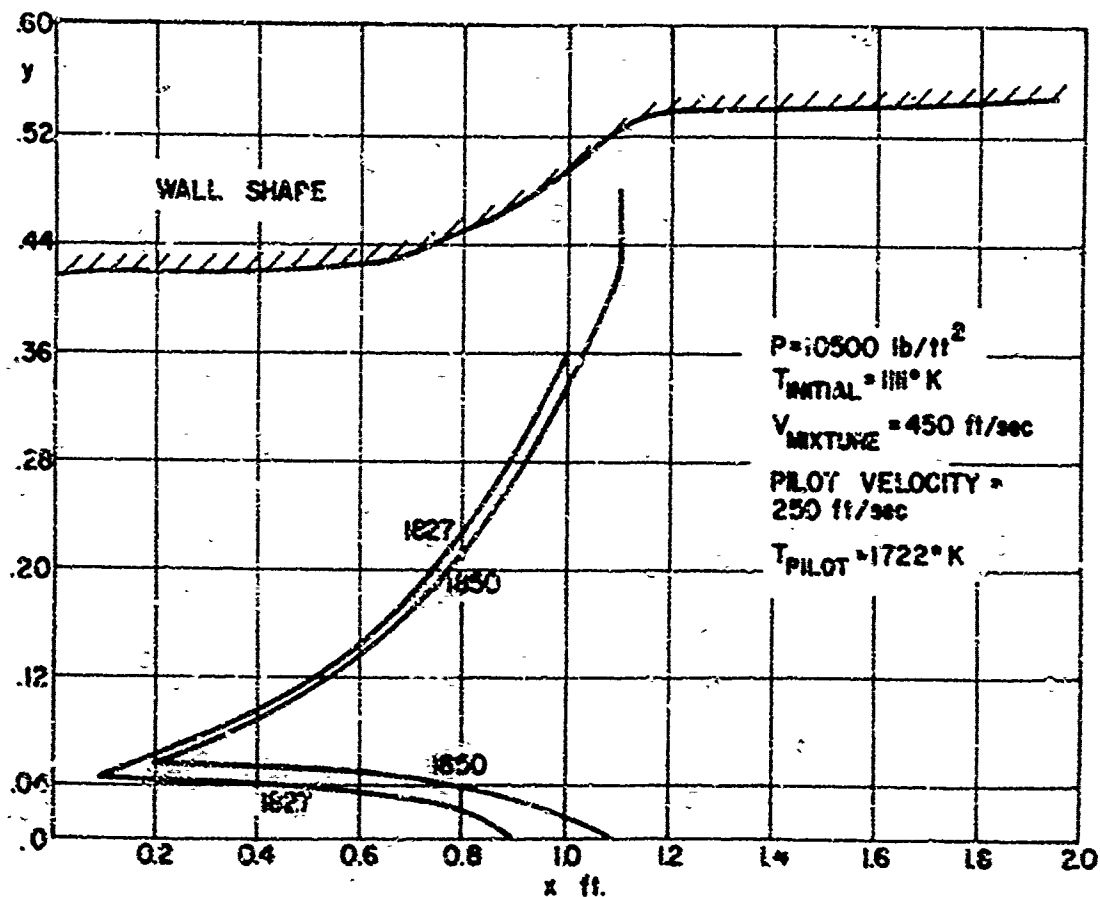


Fig. 5a Isotherms of Flame of Premixed Gases.

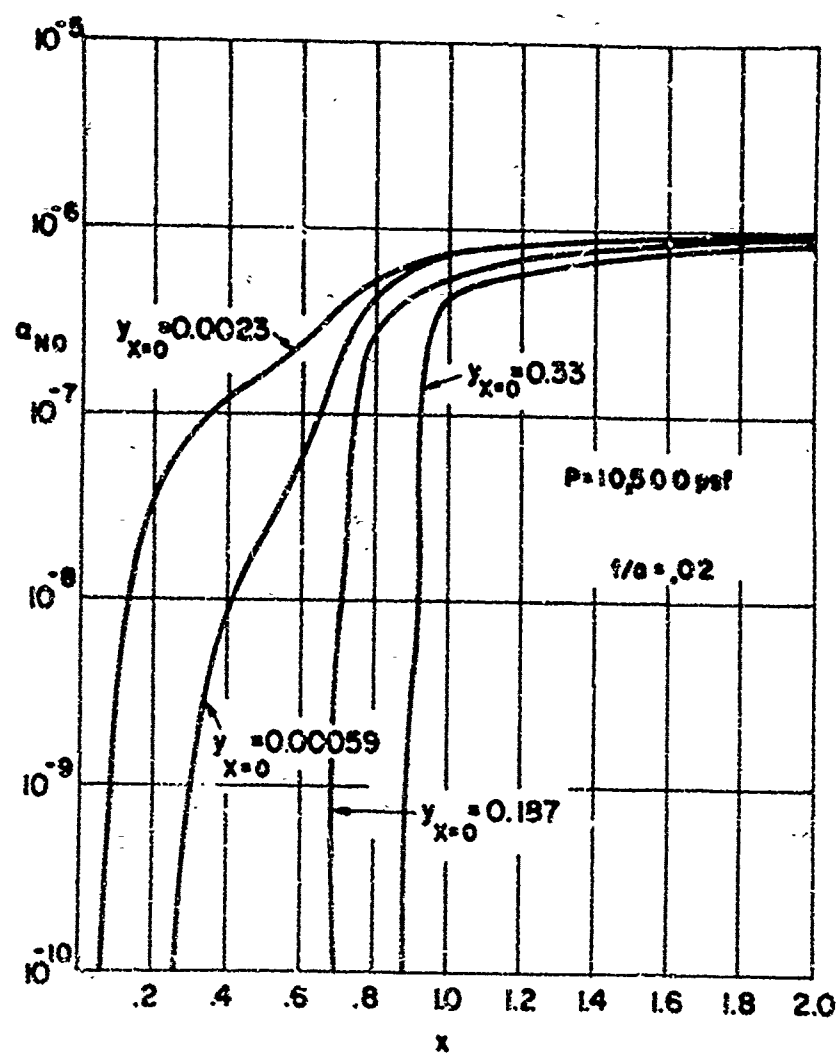


Fig. 5b Mass Fraction of NO Along Selected Streamlines.

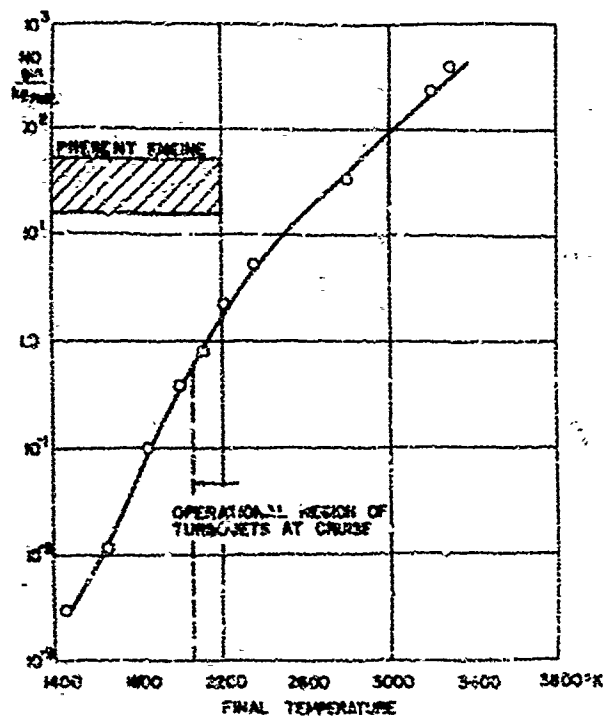


Fig. 5 Final Temperature

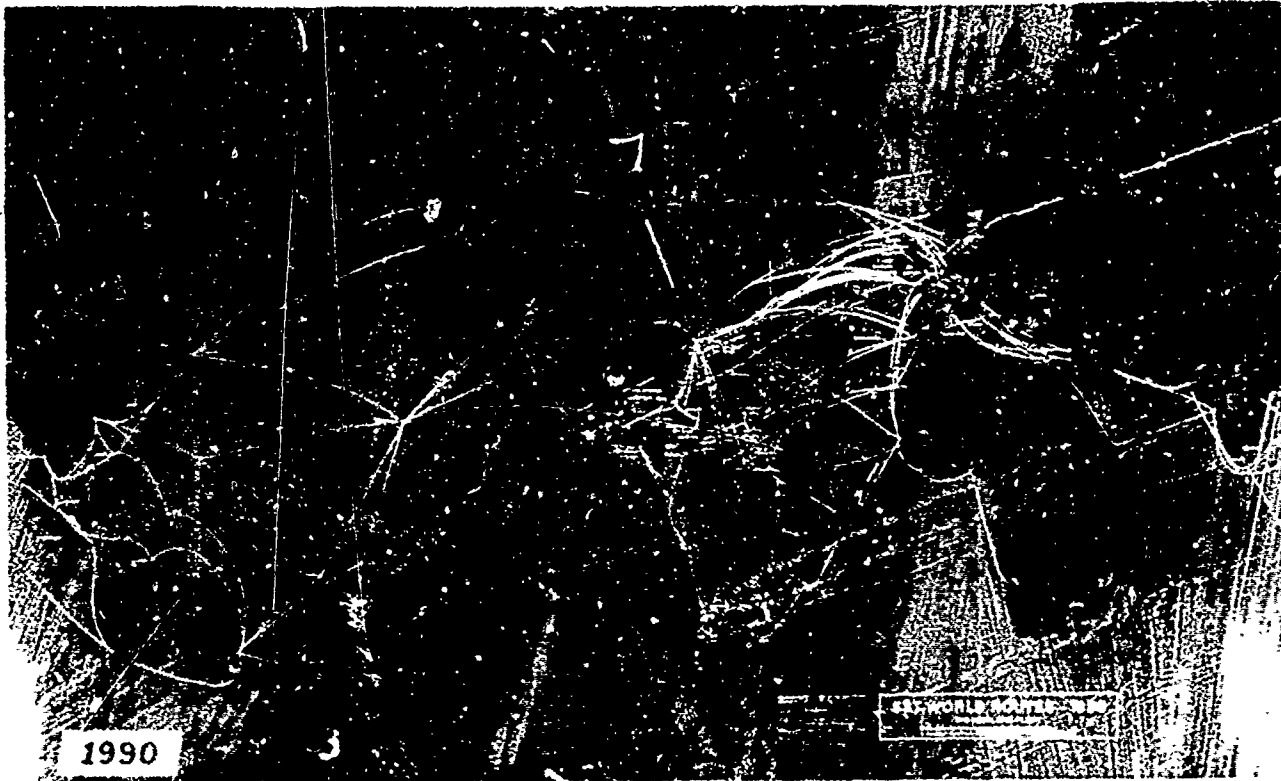
Discussion on Paper A
"Reduction of NO Formations by Premixing"
presented by A. Ferri

A.E. Fuhs: In your paper you have outlined an excellent approach to reduce NO. However, does the proposed combustor design offer good combustion efficiency, blow out limits, relight capability, favorable volumetric heat release, etc.?

A. Ferri: The loss in efficiency at high temperatures (high M and high compression ratio) is due mainly to incomplete mixing. Then the use of a premixed vaporized mixture should improve combustion efficiency.

In connection with the second part of the question published experiments performed under my direction at U.A.S.L. indicate that it is possible to burn at moderate pressure and at low temperature for ϕ as low as 0.2 - 0.3. In any case the premixed fuel air could be used only at supersonic cruise, as a first step, while the standard mixer system is used for all other conditions.

1974



UNITED STATES DEPARTMENT OF TRANSPORTATION
RESEARCH PROGRAM FOR HIGH ALTITUDE POLLUTION

UNITED STATES DEPARTMENT OF TRANSPORTATION RESEARCH PROGRAM FOR HIGH ALTITUDE POLLUTION

by

Alan J. Grobecker
Office of the Secretary (TST-91)
Department of Transportation
400 Seventh Street, S.W.
Washington, D.C. (U.S.A.) 20591

SUMMARY

This is a review of a United States program to provide an assessment by 1974 of the impact on man, plants and animals of climatic changes due to perturbations of the upper atmosphere by the propulsion effluents of a world high-altitude aircraft fleet as projected to 1990.

Some physical considerations which must be taken into account in this program are described, including representations of the stratosphere in its unperturbed state, of the effluents of vehicles expected in 1990, of the perturbed stratosphere of 1990, of the perturbed troposphere of 1990 and 2020, of the effects of climatic changes on the biosphere and of social and economic measures of these biological effects.

* * * *

This is a review of a United States Department of Transportation program to provide an assessment, by 1974, of the impact on people, plants and animals of climatic changes resulting from perturbing the upper atmosphere by the propulsion effluents of a world high-altitude aircraft fleet as projected to 1990. The report of the assessment has as its principal purpose, the provision of answers to environmental questions concerning the operation of supersonic transports, for which Federal decisions will be needed on or before 1974. While primarily ecological in its consideration, the report will take into account the possibilities, via developing technology, of remedies for the suggested problems.

The program of which I speak, called the Department of Transportation's Climatic Impact Assessment Program, with acronym "CIAP," has involved to date the participation of 56 contractors for which funding is about equally divided between government activities, universities, profit-making organizations, and nonprofit-making organizations. There are more than 50 government organizations, other than DOT, which are actively contributing pieces required for solution to the problem. Many of these are funded independently of DOT to achieve objectives of their several agencies. There is as well an extensive international participation, with principal investigators in France, England, Belgium, Japan, Sweden, Germany, Switzerland, Canada, Australia and, hopefully, the USSR and India.

The schedule for the accomplishment of this work is indicated by the data flow shown in Figure 1. It covers a period of three years ending in 1974. The work consists of measurements aloft, laboratory chemistry experiments and engine exhaust tests, extensive modeling including modeling of the aircraft wakes, of the dispersion and transport in the mesoscale stratosphere and of the circulation and chemistry of the global-scale stratosphere. In addition, the work includes estimation of changes in the tropospheric climate, and of impact on the biosphere and the economies of the world. The reported work will be recapitulated in a Report of Findings, due by the end of 1974 and based on appendices comprising a series of six monographs. The six monographs are entitled: "The Natural Stratosphere of 1974," "The Engine Emissions in the Stratosphere of 1990 A.D.," "The Perturbed Stratosphere of 1990 A.D.," "The Perturbed Troposphere of 1990 and 2020 A.D.," "The Biological Effects of the Tropospheric Changes," and "The Social and Cost Measurements of the Biological Changes."

I will now describe in reverse order the monograph treatment in terms of some considerations which led to the problem outline.

The final outcome of the CIAP Study is concerned with the social and economic costs, to be treated in Monograph VI, as listed in Table 1. Included will be analyses of economic impacts on agricultural markets, forestry resources and fisheries, expressed in terms of direct costs to the United States, of direct costs to the other nations, and of secondary costs of employment changes, national income changes, balance of payment changes and trade flow changes. Another type of economic impact is that on urban resources, to be measured in direct costs. The impact on human health is to be measured by direct costs as represented by three approaches: defensive expenses, hospitalization expenses, and willingness-to-pay expenses. The economic impact on aesthetic resources is also measured as a direct cost, in terms of willingness-to-pay expenses and representation by pictorial examples of change. Also to be included in Monograph VI are the factors which affect decision analysis: the uncertainties of the physical, biological and socio-economic considerations. The analysis-of-variance technique will be applied and there will be consideration of feedback relations as well as remedial alternatives.

Monograph V, "The Biological Effects of Tropospheric Changes," describes biological impacts on fauna and flora. The National Cancer Institute will conduct epidemiological studies of the incidence of skin cancer in six U.S. cities to augment similar and earlier studies in Australia and Ireland. National Cancer Institute also expects to study further the effects of ultraviolet radiation inducing carcinogenesis in mice. Temple University, with the assistance of Donald Robertson of the University of Queensland, will prepare instruments for measuring erythema dosage. Studies of the effects of ultraviolet radiation on insects and fish are contemplated but have not yet been defined. A rough indication of biological effects is shown by preliminary findings of the Third National Cancer Survey of skin cancer which finds a strong correlation of skin cancer incidence with latitude. These results confirm findings of surveys in Australia and elsewhere.

The effects on flora of climatic changes in temperature, winds, precipitation and ultraviolet radiation are being studied by the University of Florida and Utah State University and the U.S. Department of Agriculture. These field and laboratory studies will determine the sensitivity of representative food crops such as corn and tomatoes, and of trees and of other vegetation to changes of climate. As a beginning for parametric studies, the following changes in the troposphere are being examined for effect:

$$-2^{\circ}\text{C} < \Delta \bar{T} < 0.2^{\circ}\text{C}$$

$$-0.16 < \Delta \bar{P}/\bar{P} < +0.06$$

$$-0.16 < \Delta |\bar{V}|/|\bar{V}| < +0.06$$

$$0.1 < \Delta \bar{\Phi}_{3070\text{Å}}/\bar{\Phi}_{3070\text{Å}} < 2.0$$

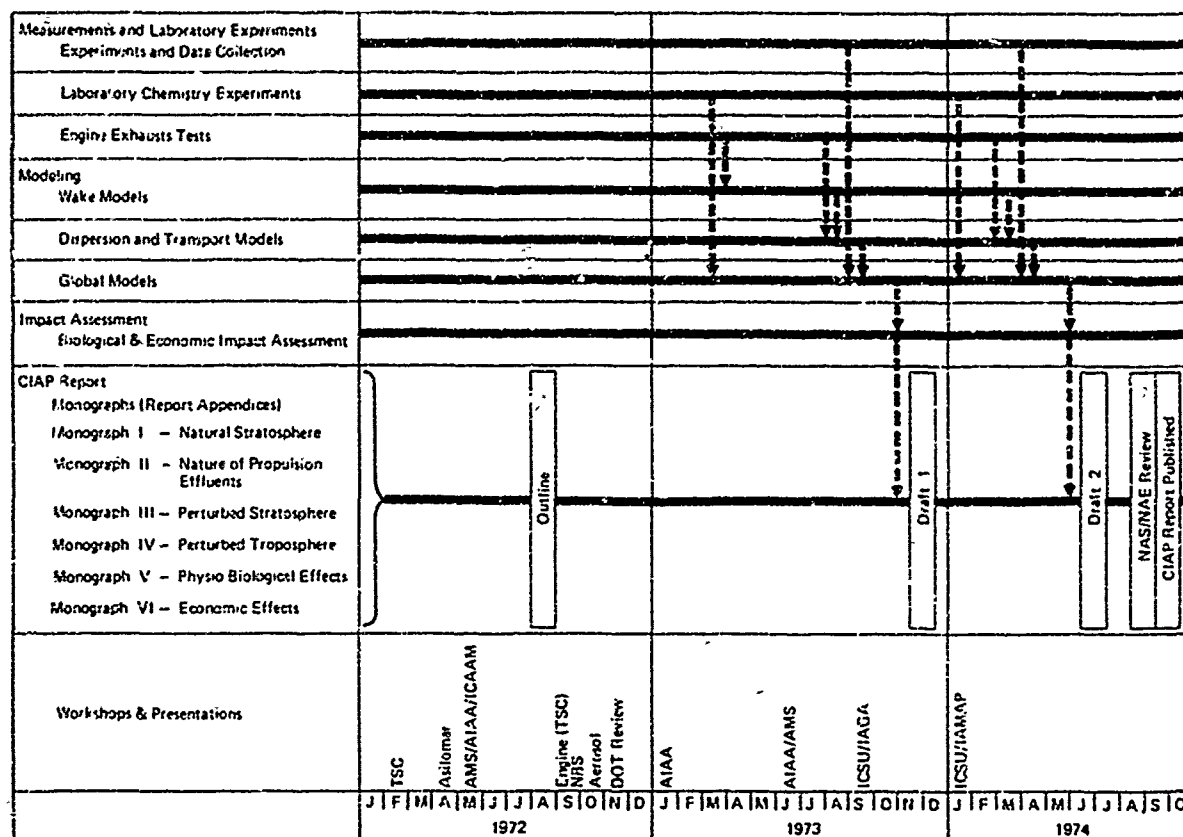


Figure 1. CIAP Data Flow

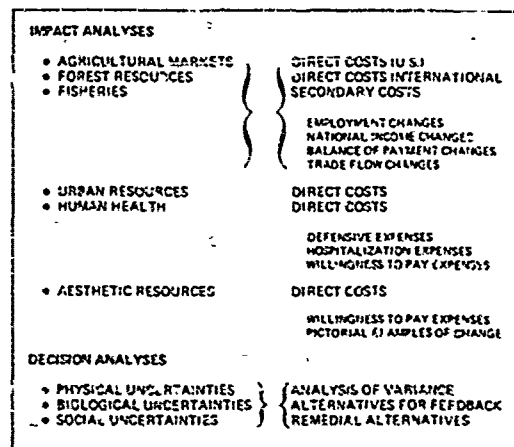


Table 1. Monograph VI - Social and Economic Costs

wherein \bar{T} is mean temperature, \bar{P} is mean precipitation, \bar{V} is mean mid-latitude wind speed, and $\bar{\Phi}$ is mean ultraviolet flux at 3070 Å. Not yet formulated but necessary are additional studies of effects of ultraviolet on plankton.

The treatment of climatic change is the topic of Monograph IV, "The Perturbed Troposphere of 1990 and 2020 A.D." The studies consider the effects felt immediately in the lower atmosphere as a result of the perturbed stratosphere of 1990 as well as the long-term effects felt after 30 years of a 1990 stratosphere. The long-term effects are felt more gradually because of the large heat capacity of the sea which will slow the cooling of the troposphere in response to changes in radiative heating.

The studies of the troposphere may be approached in several ways. One of these ways is by the use of numerical climatic models; another is by the use of closed expressions which are analytical in form. Both of these are to be used in the CIAP approach. As shown in Figure 2, one of these, attributed to Mintz, 1961 [Ref. 1] found that the mean square velocity of mid-latitude winds varied by a factor of two between winter and summer and that the planetary wave number (that is the number of nodes of the north, south excursions of the horizontal waves of the mid-latitude air stream) varies from seven to

eight in the summer to five and six in the winter. These computations, approximating observations, suggest ways in which the climate may be affected, illustrated in the sketch. "W" suggests the schematic trajectory of winds in the northern hemisphere troposphere near, but south of, the polar front in the winter time under the assumption that the shape is dominantly positioned by the persistent high-pressure region of continental Siberia. "S" indicates the summer wind trajectory having a small shift of phase within the continental United States in the summer time. Both the summer and winter winds, from the standpoint of the United States, seem to originate in Alberta, bringing dry air down from the northwest until the mean wind trajectory reaches about Oklahoma. The trajectory there turns toward the northeast, carrying with it masses of moist tropical air dragged from the Gulf of Mexico area alternating with masses of dry polar air. A consequence of this process is that the United States west of the Mississippi is generally dry in contrast with the United States east of the Mississippi, which is humid.

Possible effects of a markedly less insolation of the troposphere resulting from increased aerosols in the stratosphere may be speculated. As inferred from the Mintz study [Ref. 1], the winds may be weaker, resulting from a weakened poleward temperature gradient. An extreme effect would be a marked phase shift of the polar front. This may bring, as the sketch suggests, warm humid air to the shores of the Pacific northwest, with polar dry air coming down into the eastern part of the United States. If realized, such an effect may strongly affect the U.S. climate and similarly, the middle latitude regions of the world. Such speculations may be tested by climatological simulation.

Monograph III treats "The Perturbed Stratosphere of 1990." This work will be the climatological starting point for estimation by computational projection of changes in chemistry and transport in the vehicle wake, dispersion of effluents from the flight trajectory and transport by global circulation. The output of this monograph, required for subsequent stages of the study, to be described in Monograph IV, includes new values of the insolation at the tropopause and of the distribution of densities of species and light-diffusing particles.

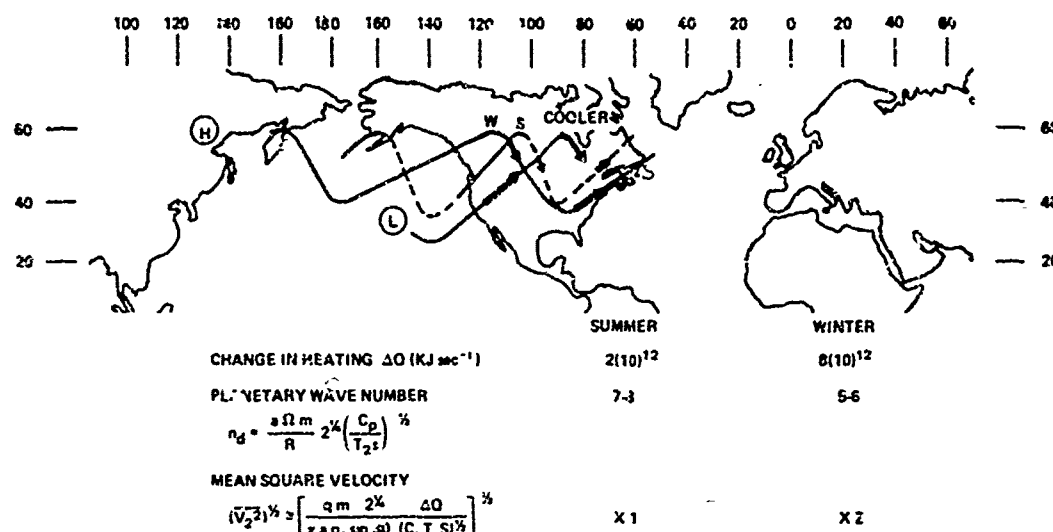


Figure 2. Implications of Climatic Change (after Mintz, 1961 [Ref 1])

As shown in Table 2, atmospheric modeling for CIAP considers each of four regimes in which the treatment must be different. At the top of Table 2 is a representative differential equation of number continuity, which includes dynamic terms involving diffusivity, mean winds and gradient of species in one bracketed frame, the chemical production and loss terms involving radiative effects as well as nonradiative kinetic reactions in the second bracketed frame, and in the third group are the terms of higher order involving densities, reaction coefficients, velocities, fluctuations of velocities and diffusivities.

Of the regimes considered, Regime I is one in which the dominant factors are the velocity of the jet and the rapidly cooling temperatures of the jet after it passes the nozzle. This regime continues for about 10 seconds, during which time the wake enlarges to a cross-sectional dimension of about 1 meter. In Regime II the wake gases are at the ambient temperatures of the stratosphere but are strongly moved by the vortices due to the passage of the vehicle. Regime II lasts until about one thousand seconds after the gases have left the nozzle exit. The dimensions of the wake at that time are of the order of 100 meters both horizontally and vertically. Regime III is influenced by the mesoscale motions of the stratosphere. In this regime, wakes of successive aircraft passages have cumulative effects, and enlarge to horizontal dimensions of about 1,000 kilometers and vertical dimensions of about 1 kilometer. The additive wake effects in this scale become features of a size usefully introduced into the global models described in Regime IV and which are used to define the equilibrium condition of the earth's atmosphere. The important terms of the number continuity equation, listed at the top of Table 2, may be established by the criteria indicated. The chemical reactions, important for Regime I are those involving densities smaller than 10 times the chemical production and loss terms. Those important in Regime II are those involving densities smaller than 10³ times the chemical production and loss terms. Those important in Regime III are those involving densities smaller than 10⁶ times the chemical production and loss terms. By these criteria, all possible chemical reactions are important in Regime IV.

$\frac{\partial n_i}{\partial t} = \left[(\nabla \cdot \mathbf{K} + \bar{\mathbf{U}}_i) \cdot \nabla n_i \right] + \left[\frac{J_k n_k + k_{ki} n_k n_i - J_i n_i - k_{ij} n_i n_j}{(P-L)} \right] + H(n_i, n_j, n_k, n_l, k_{kl}, k_{ij}, K, \bar{\mathbf{U}}, \bar{\mathbf{U}}')$				
	DYNAMICS		CHEMISTRY	HIGHER ORDER
	REGIME I	REGIME II	REGIME III	REGIME IV
SCALES:				
TIME FROM NOZZLE, sec	0	10	10 ³	10 ⁶
HORIZONTAL SCALE, m			10 ²	10 ⁶
VERTICAL SCALE, m			10 ³	10 ⁶
IMPORTANT TERMS:				
a. CHEMISTRY IMPORTANT IF:	$n_i < 10 [P-L]$	$n_i < 10^3 [P-L]$	$n_i < 10^6 [P-L]$	all n_i
b. DYNAMICS IMPORTANT IF:	$n_i < 10 \bar{\mathbf{U}}_j \cdot \nabla n_i$	$n_i < 10^3 \bar{\mathbf{U}}_j \cdot \nabla n_i$	$n_i < 10^6 (\nabla \cdot \mathbf{K}_i + \bar{\mathbf{U}}_i) \cdot \nabla n_i$	all n_i (primarily $\bar{\mathbf{U}}_i \cdot \nabla n_i$)
c. HIGHER ORDER IMPORTANT IF:	$n_i < 10 H_i$	$n_i < 10^3 H_i$	$n_i < 10^6 H_i$	None
CIAP/NOT INVESTIGATORS	LMSC a, b	LMSC a, b	LLL a, b AEROSPACE a, b ARAP a, b, c	3D - UCLA GCM MIT 2D - LLL ZAM NOAA Special Chemistry U.C.B. U.WASH U.COLO SANDIA
OTHER INVESTIGATORS				GFDL, GISS, NCAR NASA AMES

The dynamics terms are important in Regime I if the density is less than 10 times the dot product of the jet velocity and the density gradient; in Regime II if the density is smaller than 10^3 times the dot product of the vortex velocity and the density gradient, and in Regime III if the density is smaller than 10^6 times a dot product which takes into account the diffusivity as well as the mean velocity. Higher-order terms are determined to be important by comparable criteria.

Indicated by acronyms in the lower box of Table 2 are a number of experimenters addressing problems in each of the four Regimes. The participants also include some engaged in the data collection. The models of the several regimes work in logical sequence to provide estimates of the equilibrium distribution of species and particles in a stratosphere perturbed by engine effluents introduced along the routes of world travel in the stratosphere. Since many of the problems have never been modeled before, parallel efforts by several investigators in each of the areas are encouraged. Each of several models addressing the same regime problems may illuminate different facets of the problem. A composite picture, from all of the modeling studies, may be the best picture available in the time for this study.

In Figure 3, H. Hoshizaki, et al. 1972 [Ref. 2], is shown the scaling model for the jet and vortex regimes by which the rate of dilution and expansion of the gases leaving the engine nozzle may be estimated. This model is given in terms of a characteristic length based on the wing-span dimension and a characteristic time which is a function of density, velocity, wing span and weight of the vehicle. The wakes in the jet (Regime I) grow uniformly in height and width dimension. In Regime II, where the effect of the vortex motion dominates, the expansion of the height is much more rapid than the width which remains nearly constant. This model of near-wake behavior has been validated by comparison with a time history of B-52 exhaust trails at 41,000 feet, probably just above the tropopause.

That the chemistry in Regimes I and II does not materially change from the distribution that it had when it left the nozzle exit is indicated in Figure 4, after Hoshizaki, et al. 1972 [Ref. 2], which shows the centerline concentration profiles of the GE-4 secondary nozzle and exhaust under the condition that there is zero CH_4 as the gases leave the engine exit nozzle. This is the condition of a most efficiently burning engine. The case for the afterburning engine shows that hydrocarbon radicals are scavenged by water vapor radicals, but in other respects the principal long-term stable constituents of the exhaust including the nitrogen oxides are unchanged for distances out to 24 meters. The inference from these studies by Hoshizaki, et al. is that in Regimes I and II the chemical species are not materially changed except by purely mechanical dilution as a consequence of the expansion of the wake.

In Regime III the characteristics of the stratosphere, the region in which the gases are introduced, are important and dominate the dispersion. In Figure 5, after Newell, 1969 [Ref. 3], is shown a temperature distribution; on the left, the temperature is shown by contours as a function of altitude, and on the right, the temperature profile is shown for tropical and polar latitudes. The figures on the right illustrate typical flight altitudes of vehicles like the B-747 (about 13 kilometers), of SST types like the Concorde (18 to 20 kilometers), and of the hypersonic transports (about 35 kilometers). The significant characteristic of the stratosphere is the large positive-upward temperature gradient between the tropopause at about 20 kilometers and the stratopause at about 50 kilometers. This large temperature gradient, is indeed the major factor which makes the stratosphere a collector of materials. The stratospheric lifetime of materials may vary from a month to years compared to the tropospheric lifetime of species which may be as short as days as a consequence of rainout. A further characteristic of the stratosphere is that the temperature gradient is positive poleward; the temperature varies from a low in the tropics to a high at the poles. Since the mean motion in the stratosphere moves from the equator to the poles, the stratosphere behaves as a refrigerator by comparison with the engine-like behavior of the troposphere below it, where the motion from the equator to the poles moves energy from the high-temperature equator to the low-temperature poles.

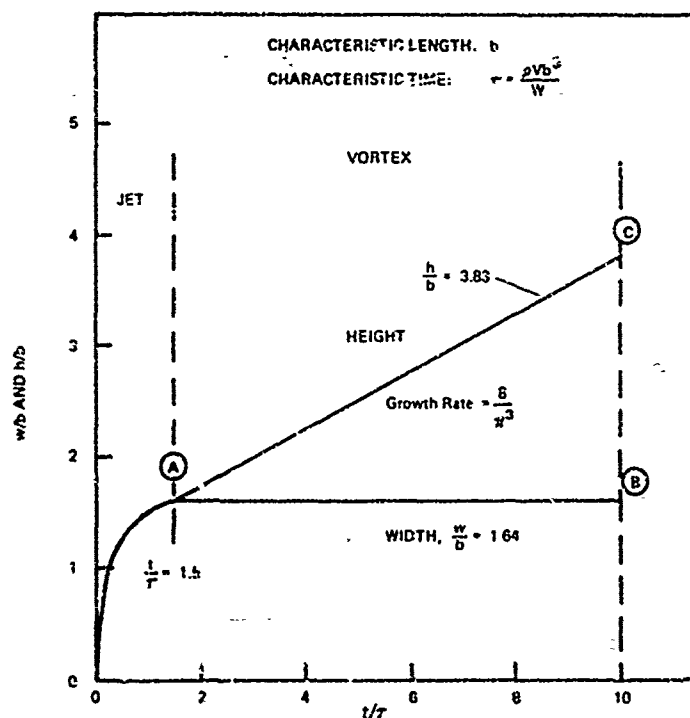


Figure 3. Scaling Model for Jet and Vortex Regimes (H. Hoshizaki et al. 1972 [Ref. 2])

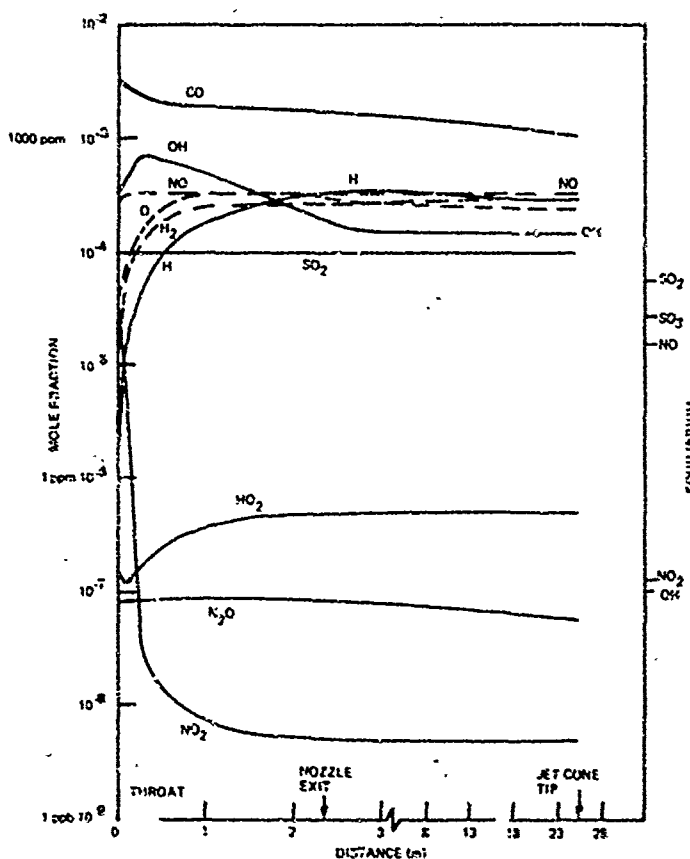


Figure 4. Centerline Concentration Profiles, GE-4 Secondary Nozzle and Exhaust (Zero CH_4) (after H. Hoshizaki et al., 1972 [Ref. 2])

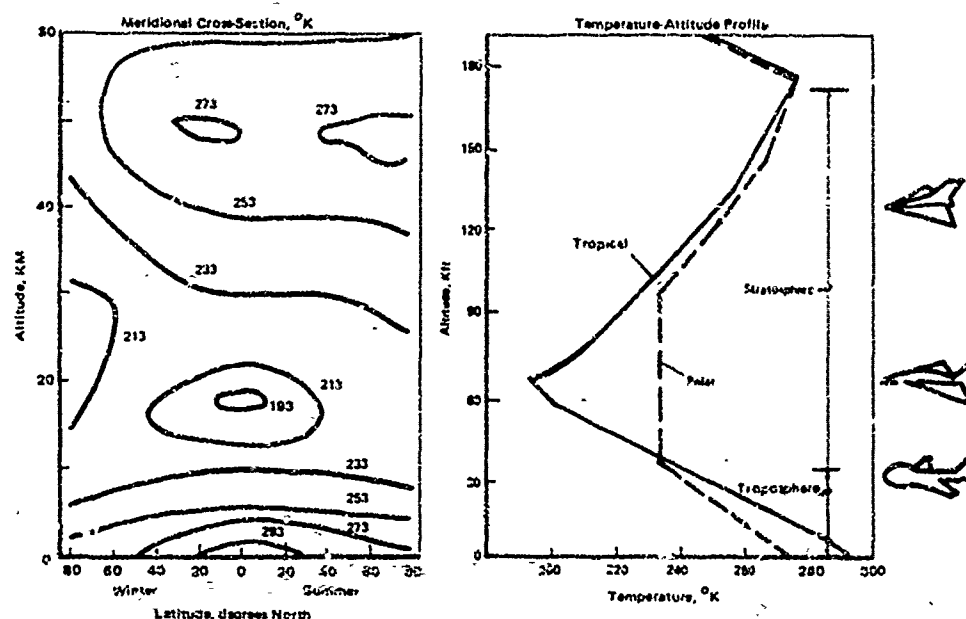


Figure 5. Temperature (Stratospheric Temperature Gradient Inhibits Vertical Mixing) (after R. E. Newell, 1969 [Ref. 3]).

In Figure 6, after R. E. Newell, 1969 [Ref. 3], is shown the mean zonal wind expressed in meters per second. Between 20 and 50 kilometers, the winds have a direction from west to east in the winter hemisphere, which is the same direction as the winds in the troposphere below it; but in the summer hemisphere the winds are from east to west oppositely directed to those in the troposphere below it. This difference in wind directions has an effect on the rates of mixing of materials down from the stratosphere into the troposphere.

In Figure 7, after R. E. Newell, 1969 [Ref. 3], is shown the standard deviation of meridional wind components. Since the meridional motion in the stratosphere is a stochastic effect of wind fluctuations, the mean meridional dispersion is proportional to the wind variability. This measure, attributed to Newell 1969, indicates that in the stratosphere the meridional wind fluctuations are smaller by factors of 5 to 10 than those which exist in the troposphere.

In Figure 8, after R. E. Newell, 1969 [Ref. 3], is shown the ratio of the standard deviation of meridional winds to standard deviation of the vertical winds, indicating that in the stratosphere the variability of vertical winds is about three orders of magnitude smaller than the variability of meridional winds. The vertical transport of species in the stratosphere is much smaller than that of the troposphere.

The horizontal eddy diffusivity, which is the eddy counterpart of molecular diffusivity, accounts for the diffusion of sources of species, and is a function of the dimension of the phenomena. This scaling relationship, as described by E. Bauer 1972, Figure 9 [Ref. 4], is shown as a function of mean cloud width. The features of dimension 10^3 kilometers, which characterize Regime IV, are

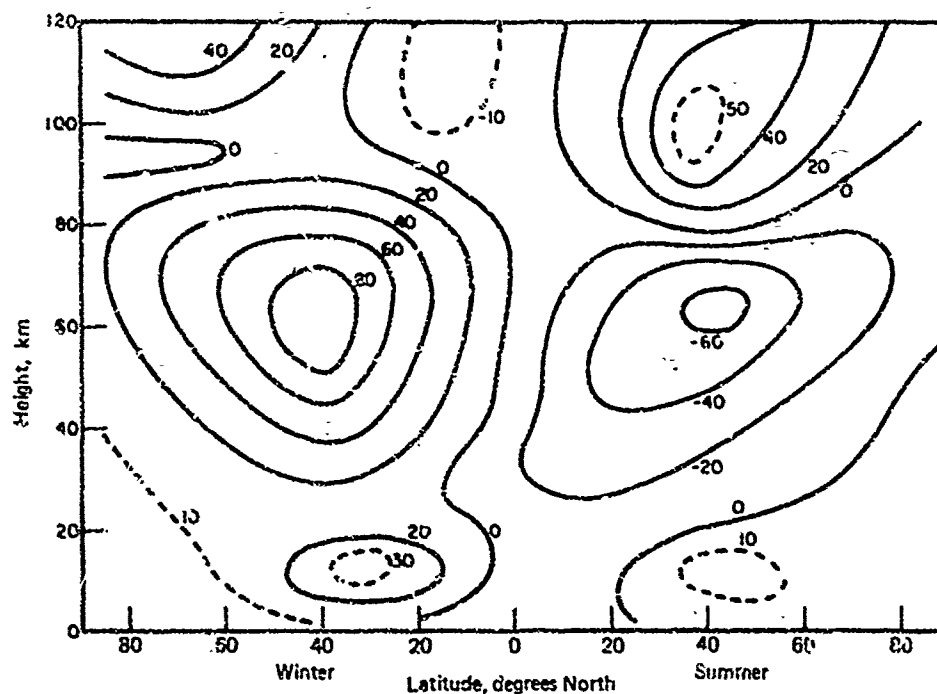


Figure 6. Mean Zonal Wind (m/sec) (after R. E. Newell, 1969 [Ref. 3])

characterized by an eddy diffusivity value of about $10^9 \text{ cm}^2 \text{ sec}^{-1}$; but features such as the output of Regime II and input of Regime III of dimension 100 meters, are characterized by a horizontal eddy diffusivity of about $10^3 \text{ cm}^2 \text{ sec}^{-1}$. These differences in eddy diffusivity must be taken into account. To a large extent, the further characterizing of small-scale eddy diffusion will be developed from data derived by Air Force Project HICAT.

The important chemistry which characterizes Regime III, as we now understand it, involves about 21 reactions, as shown in Table 3, due to F. Hudson, 1972 [Ref. 5]. Seven of these are reactions due to photoytic effects and the remaining 14 are associative and rearrangement reactions.

The chief computational problems of Regime III take into account mesoscale motions of the stratosphere which are little understood and measured, and compute the superposition of material laid along the trajectory routes by the successive flights of engines expected to be flying in 1990.

Monograph II appraises "The Engine Effluents in the Stratosphere of 1990." It considers the product of the effluents from all the individual engines, taking into account the numbers of flights on various routes and altitudes that such engines will be flying. Results of emission tests of the YJ-93-GE-3 engine under stratospheric conditions are shown in Table 4, after A. K. Forney, 1972 [Ref. 6], as functions of altitude and whether the engines are being operated under a so-called military power setting or afterburning. In general, several independent methods of measuring were used and these in general give comparable results.

In Figure 10, after Rummel, 1972 [Ref. 7], is shown one estimate of SST relative flight density by 1990. Flights are projected for both the Anglo-French Concorde and the Boeing SST. It is clear that there is a great variability in estimates of engine outputs and

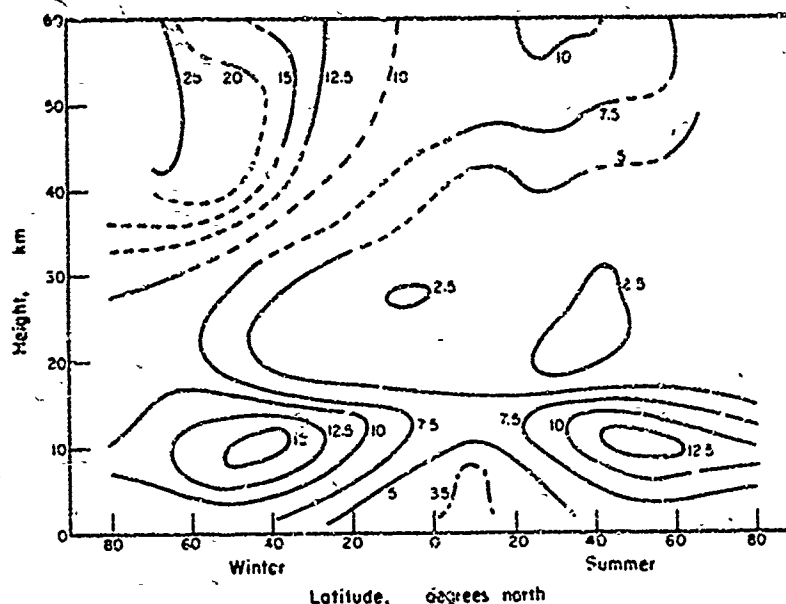


Figure 7. Standard Deviation of Meridional Wind σ_v (m/sec) (after R.E. Newell, 1969 [Ref. 3])

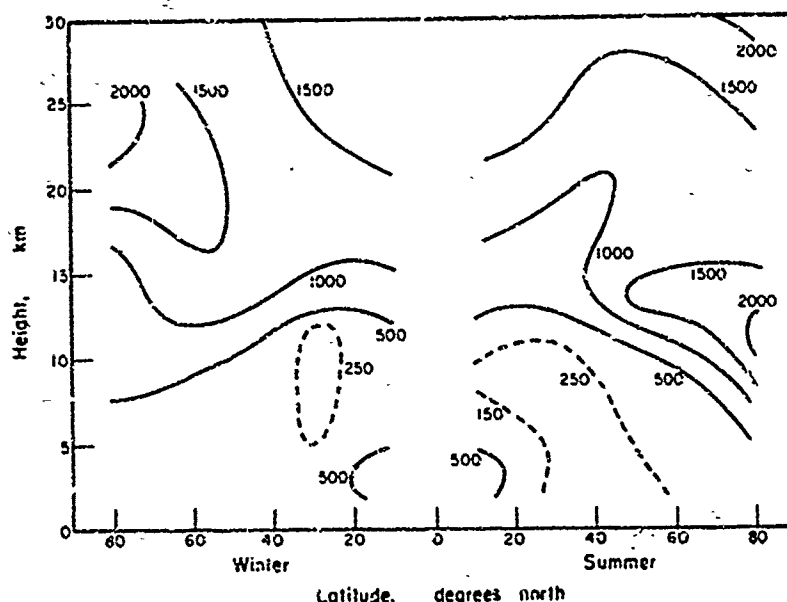


Figure 8. Ratio of Standard Deviations of Meridional and Vertical Winds σ_v/σ_w (after R.E. Newell, 1969 [Ref. 3])

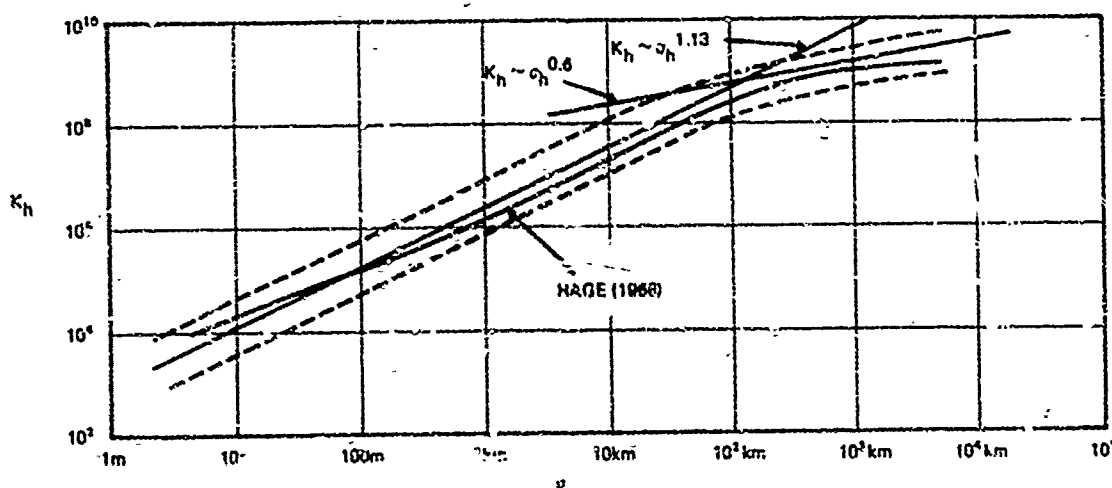


Figure 9. Horizontal "Eddy Diffusivity" K_h (cm^2/sec) as a Function of Mean Cloud Width σ_c (after E. Bauer, 1972 [Ref. 4])

1. $O_2 + hv \rightarrow O + O$	8. $O + O_2 + M \rightarrow O_3 + M$	15. $O_3 + OH \rightarrow O_2 + H_2O$
2. $O_3 + hv \rightarrow O + O_2$	9. $O + NO_2 \rightarrow O_2 + NO$	16. $NO + HO_2 \rightarrow OH + NO_2$
3. $NO_2 + hv \rightarrow O + NO$	10. $O + NO_2 \rightarrow NO_3 + hv$	17. $NO_2 + NO_3 + M \rightarrow N_2O_5 + M$
4. $NO_3 + hv \rightarrow O + NO_2$	11. $O_3 + NO \rightarrow O_2 + NO_2$	18. $H_2O_5 + M \rightarrow NO_2 + NO_3 + M$
5. $NO_3 + hv \rightarrow O_2 + NO$	12. $O_3 + NO \rightarrow O_2 + NO_2 + hv$	19. $N_2O_5 + H_2O \rightarrow HNO_3 + HNO_3$
6. $N_2O_5 + hv \rightarrow O + NO_2 + NO_2$	13. $O_3 + NO_2 \rightarrow O_2 + O_2 + NO$	20. $OH + HO_2 \rightarrow O_2 + H_2O$
7. $HNO_3 + hv \rightarrow OH + NO_2$	14. $O_3 + NO_2 \rightarrow O_2 + NO_3$	21. $OH + NO_2 + M \rightarrow HNO_3 + M$

Table 3. Regime III Chemistry (after F. Hudson, 1972 [Ref. 5])

ALT PS	CO NDIR-S	CO NDIR-L	NO CID	NO NDIR	NO ₂ NDUV	NO _x CID+	THC FID
0 MIL	7.2	—	3.2	3.1	—	5.6	0.67
0 A/B	37.9	—	1.1	1.6	—	4.1	7.92
30K MIL	7.0	—	3.1	3.4	—	5.1	0.18
30K A/B	3.3	—	2.3	2.3	—	3.5	0.05
36K MIL	15.4	—	—	2.4	0.5	4.0	0.15
36K MIL	8.7	10.8	2.7	2.4	—	4.6	0.17
36K A/B	37.6	—	1.1	1.6	—	2.9	1.78
55K MIL	4.6	5.5	3.9	4.1	—	6.6	0.10
55K A/B	18.4	—	1.8	2.4	—	4.0	4.49
65K MIL	10.3	8.6	3.1	—	—	5.5	0.31
65K A/B	33.4	—	1.7	—	—	3.2	7.71
65K MIL	3.2	—	7.2	6.8	1.8	12.2	0.26
65K A/B	39.7	—	2.8	2.4	—	6.0	13.3
75K MIL	13.7	13.0	2.5	2.4	—	3.6	0.28
75K A/B	73.0	—	1.0	1.2	—	1.9	18.33

SYMBOLS: ALT = ALTITUDE IN FEET
 PS POWER SETTING: MIL = MAX NON-AFTERBURNING; A/B = AFTERBURNING
 NDIR = NON-DISPERSIVE INFRARED; -S = SHORT PATH; -L = LONG PATH
 CID = CHEMILUMINESCENCE + CHEMILUMINESCENCE WITH THE TMAI CONVERTER
 FID = FLAME IONIZATION DETECTOR
 NOTE: ALL NUMBERS ARE EMISSION INDEXES IN POUNDS PER 1000 POUNDS OF FUEL BURNED

Table 4. YJ93-GE-3 Engine Emissions Test—Summary of Results: On-Line Instrumentation (after A.K. Forney, 1972 [Ref. 6])

the routes and frequency of travel over these routes if one takes into account uncertainties in predicting the possibilities of future development. As far as route travel predictions are concerned, the study will establish a number of route projections and consider the effects of the least and the greatest of these. As far as reductions of engine effluents are concerned, performance of present-day engines is considered, as well as that of engines with desirable characteristics of low nitrogen-oxide output being developed by NASA's Lewis Laboratory.

Since the CIAP study is projecting the effects of a 1990 fleet of vehicles, it is important that this projection take into account the developments of the next 20 years. With this concern the projection of route frequencies is being based primarily on the demographic projections of the population growth of the world and on the projections of the gross domestic products of the countries of the world. With these taken into account, together with the possibilities for technical development, the transportation which would be required using vehicles traveling in the stratosphere, attain the benefits of the high velocity of travel or the short travel time, may be estimated. Although no travel distance smaller than one thousand kilometers is considered in this study, in all likelihood stratospheric travel will involve transit distances of many thousands of kilometers, coupling the two hemispheres as well as the continents within the northern hemisphere.

Also to be taken into account is the development of new engines and new aircraft types. There are developments currently under way to decrease by several orders of magnitude the nitrogen oxide output of the engines currently in use and being tested. There are also new vehicle types to augment the subsonic vehicles, which will fly at altitudes of 13 to 15 kilometers. There are jet type aircraft like the Concorde and the TU-144 which fly at about 20 kilometers altitude. In addition, there will be hypersonic transports which may use ramjet propulsion and fly at between 25 and 35 kilometers as well as the beginnings of boost-glide vehicles, such as are being demonstrated by the U.S. Space Shuttle, for long-haul transport of premium cargo such as passengers.

It will be a particularly satisfying part of the CIAP program to show that where present conventional designs pose large ecological problems that there is indeed a direction in which these problems can be attacked and notably minimized. In the design of most stratospheric vehicles, minimizing untoward ecological effects may be fully as important as other engineering objectives such as development of high thrust for engines or high lift/drag characteristics or anti-flutter qualities, or whatever.

Of course, the basis for all the studies must be the present knowledge of the stratosphere. This is the subject of Monograph I, "The Natural Stratosphere of 1974." The natural stratosphere of 1974 is a complicated chemical mix of reactive species as partially illustrated in Figure 11. This figure portrays the results of computational analyses accomplished by Bortner and Kummier in 1969 [Ref. 8]. Upward of about 40 species were taken into account but only the most important ones are shown in Figure 11. We see that, in general, the total species number density is about 10^{18} cm^{-3} , that water vapor, methane, and ozone comprise about one part in a million or 10^{12} cm^{-3} , and that nitric oxide and OH and other radical species are of the orders of one part per billion or even less.

In considering the distribution of species in the natural stratosphere, it is important not only to consider the mean values based on a computational balance as in Figure 11, but also the variations. Figure 12 shows the total ozone content as a column thickness expressed in units of 10^{-3} cm STP at STP, attributed to measurements made in a Nimbus satellite and reported by

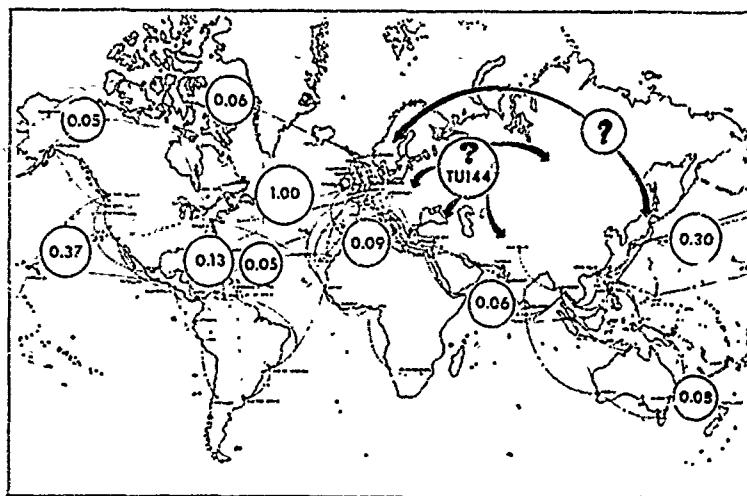


Figure 10. SST Estimated Relative Flight Density by 1990 (Concorde Plus U.S. SST) (after Rummel, 1972 [Ref. 7])

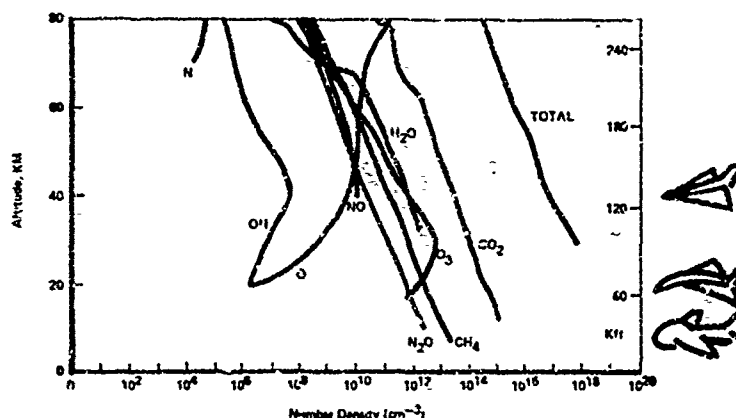


Figure 11. Daylight Atmosphere Chemistry (Bortner & Kummier, 1969 [Ref. 8])

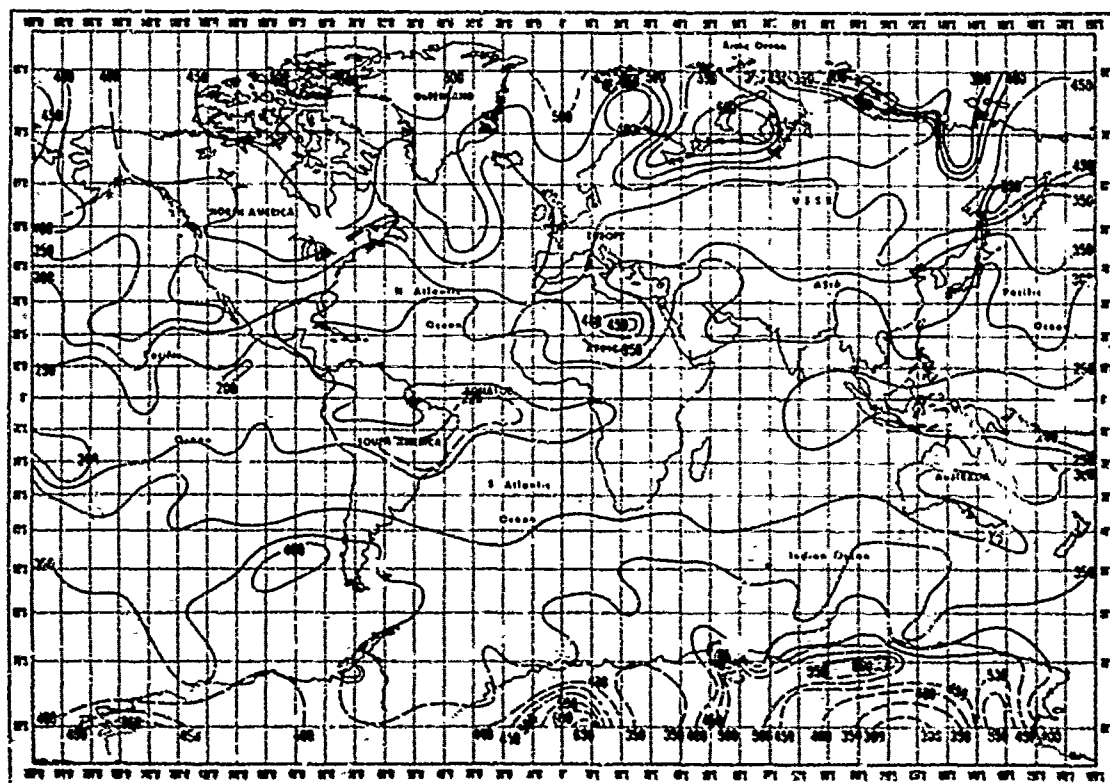
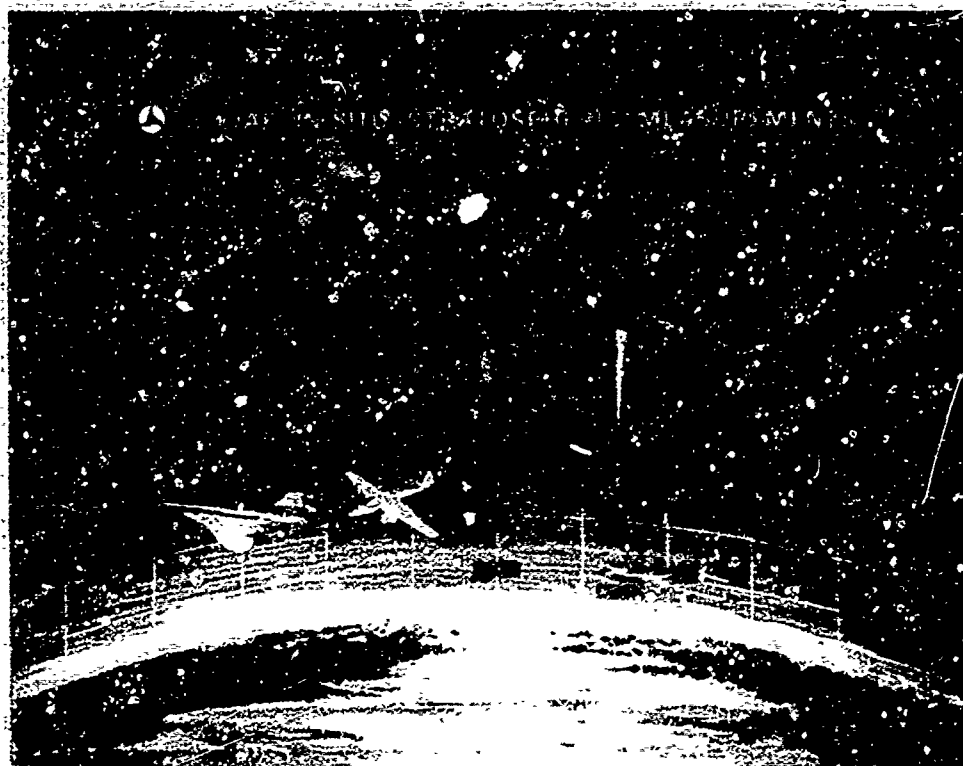


Figure 12. Total Ozone Content (10^{-3} cm STP) (C. Prabhakara, 1971 [Ref. 9])



I. 103 Measurements			
II. Experimental Results			
Values in Stratosphere (20 km)			
Component Measured	General Background	Over Thunderstorm Anvils Above Tropopause	ITCZ
1. Water *	3 ppm	5 to 7 ppm	15 ppm (?)
2. O ₃ *	N = Normal Value	30% > N	20% > N
3. NO	~0.1 ppb		
4. NO ₂	22 ppb		
5. N ₂ O	200 ppb		
6. HNO ₃	3 ppb		
7. Particulates			
Size	0.2 to 1 Micron		
Density	1 to 5 particles cm ⁻³		
Stratification - Layering - persistent			

* The simultaneous measurement of O₃ and H₂O indicates a positive correlation over thunderstorms and ITCZ.

Table 7. Achievements of AM&E to January 1973

Table 8 shows the U.S. Federal agencies which are coordinating with CIAP. Most of these are doing work important to CIAP, but funded by the individual agencies for their own purposes. The results, however, are essential to the accomplishment of CIAP objectives. Many of the U.S. Departments are administering DOT funds for the accomplishment of CIAP tasks which are deemed desirable by those agencies which could not independently fund the work. By and large the total "greater CIAP" effort, which includes in addition to that effort funded by the Department of Transportation the additional effort funded by other agencies of the U.S. Government, is likely to exceed fifty million dollars per year. In Table 9 are listed substantial participants in the CIAP program which are not DOT funded. These include not only other departments of the U.S. Government and their activities: NOAA, NASA, AEC, NSF, DoD, Agriculture, and HEW, but they also include activities abroad: the British Meteorological Office, in France CNES and Aerospatiale, in Belgium the Institut d'Aeronomie and Japanese activities under the Ministries of Education and of Transport.

The CIAP study must realize a "best effort" report in 1974. An important function of conferences such as this one is to solicit suggestions for the improvement of the study, which in its present form is by no means frozen. Augmentation of the study to provide the needed answers is a matter of urgency. DOT invites and welcomes suggestions and participation so that the report of the

AEC	NSF	DoD	DOI
LASL	NCAR	DNA	MINES
HASL		DDR&E	
LLL	USDA	ARPA	HEW
LBL		UCAF	
BNL	NBS	AEDC	NIH
SANDIA		APL	USPHS
ANL	NOAA	CRL	
		AWL	CEQ
NASA	ARL	AWS	
	ERL	APTAC	OST
AMES	BL	USN	
LEWIS	GFDL	ONR	NASC
GODDARD SFC		NRL	
GISS	EPA	USA	
HUNTSVILLE		WHITE SANDS	
	DURHAM		

Table 8. Federal Agencies Coordinating with CIAP

- NOAA GFDL—Modeling of Global Circulation (J. Mahiman) and Climatology (A. Oort)
- NASA Langley—Future Stratospheric Propulsion
- NASA—Definition and Conduct of Wake Sampling Experiment
- AEC—Project "Airstream" Atmospheric Sampling
- NSF NCAR—Modeling of Global Circulation
- DOD/USAF—RB-57F Aircraft Operations, Piggy Backed
- National Cancer Institute—Effects of u.v. on Skin
- USDA—Climatic Effects on Flora
- British Meteorological Office—Studies of the Stratosphere
- France CNES—Sampling of the Stratosphere
- Belgium Institut d'Aeronomie—Studies of the Stratosphere
- Japan Ministry of Education (Univ. of Tokyo, Nagoya, Sendai)—Studies of the Stratosphere
- Japan Meteorological Agency—Balloon-borne Measurements of the Stratosphere

Table 9. Other Substantial Participants (Not DOT Funded)

study in 1974 may have findings which are complete, comprehensive and acceptable to the scientific community. Already a committee under the auspices of the National Academy of Sciences and National Academy of Engineering (NAS/NAE) has assumed an advisory role for the conduct of this program.

In calendar year 1972 the effort was primarily to get people started. In calendar year 1973 the primary focus will be on the assimilation of results of experiments and the development of computational models for the projection of future changes in the stratosphere.

Most of the studies will have reports written during this calendar year in a way which may provide a partial basis for analysis, to be made available for worldwide dissemination in May 1974. At that time the monographs reviewing the studies in detail will be distributed for a variety of users:

1. They will be used by CIAP investigators as further bases for analyses leading to reports of findings.
2. They will be technically reviewed by groups other than the authors.
3. They will become a data base for the NAS/NAE summer study in July 1974.
4. They will be disseminated abroad for the benefit of similar analyses, possibly to be undertaken in Britain, France, Belgium, Japan, the USSR, Australia and elsewhere.

In conclusion let me say first that our mode of operation is to make the study details available as widely as may be possible in scientific communities both national and international. Second, the technical facts are expected to clear the way for world acceptance of the conclusions, whatever these may be. Third, the definition of specific problems which may be revealed by the CIAP program is expected to provide a basis for technical solutions to those problems.

And finally, the contributions to CIAP of the world's best-qualified scientists are invited.

The U.S. Department of Transportation desires that CIAP become regarded as "good science and engineering," a technically honest treatment of ecologic impacts. It desires to do this with a constructive attitude, pointing out directions to go and ways of going there, to do the things the world needs to have done in ways that clearly recognize ecologic values.

LIST OF REFERENCES

1. Y. Mintz, Appendix B- The General Circulation of Planetary Atmospheres, in *The Atmospheres of Mars and Venus*, Publ. 944, Washington, D.C., National Academy of Sciences and National Research Council, 1961, pp. 107-146.
2. H. Hoshizaki, High-Altitude Aircraft Wake Dynamics, Second Conference on the Climatic Impact Assessment Program, Washington, D.C., Dept. of Transportation, to be published March 1973.
3. R.E. Newell, Radioactive Contamination of the Upper Atmosphere, in *Progress in Nuclear Energy-Series XII: Health Physics*, vol. 2, Oxford, Pergamon, 1969, pp. 535-550.
4. Ernest Bauer, Dispersion of Tracers as a Function of Time, Second Conference on the Climatic Impact Assessment Program, Washington, D.C., Dept. of Transportation, to be published March 1973.
5. Frank Hudson, private communication.
6. A. K. Ferney, Engine Exhaust Emission Levels, AIAA 11th Aerospace Sciences Meeting, AIAA Paper 73-98, New York, American Institute of Aeronautics and Astronautics, 1973, p. 5.
7. R. W. Rummel, Supersonic Transport Routes, Climatic Impact Assessment Program Proceedings of the Survey Conference, DOT-TSC-OST-73-12, Washington, D.C., Dept. of Transportation, 1972, pp. 34-42.
8. M. H. Bortner and R. H. Kumbler, *The Chemical Kinetics and the Composition of the Earth's Atmosphere*, GE-500-FC-SR-1, Valley Forge, General Electric, 1968.
9. C. Prabhakara, D. J. Conard, L. J. Allison, and J. Strianka, Seasonal and Geographic Variation of Atmospheric Ozone Derived from Nimbus III, NASA-TN-D-6443, Greenbelt, Md., Goddard Space Flight Center, 1971.
10. H. Johnson, Chairman Chemistry Panel, CIAP Monograph 1. *The Natural Stratosphere of 1974*, Washington, D.C., Dept. of Transportation, to be published 1974.

Discussion on Paper 1
 "Research Programme for High Altitude Pollution"
 presented by A.J.Grobecker

P.Goldsmith: I note in Table 7 of your talk that you give a value of ~ 0.1 ppb for the NO concentration in the stratosphere. Could you tell us something of the details of the measurement and could you, or any photochemist present, comment on the implication of the value of NO concentration, taken together with the 22 ppb found by the British NPL measurements on the Concorde for NO₂, on the current theories of the role of nitrogen oxides in ozone photochemistry.

A.J.Grobecker: H.Schiff (Toronto, Canada) has measured NO at about 0.1 ppb on two occasions since January 1973 by a chemiluminescent detector, balloon borne between altitudes 15 and 23 kilometers.

C.B.Farmer has reported measurement by spectrometric technique, to find 1.0 ppb in NC 135 borne experiment observing extinction of solar infrared radiation.

The implications of these measurements are:

1. These two techniques give results differing from each other by an order of magnitude. On the basis of only one or two experiments, it is too early to prefer one technique over the other.
2. The Farmer data (1.0 ppb) compares with modelling estimates reported by Ackerman who used a standard-atmospheric model for computing the photochemistry.
3. Since there is great spatial and temporal variability of ozone or low stratospheric altitudes, similar variability of NO is also to be expected. Hence these data of different observations may be expected to differ widely by themselves.
4. The results suggest again the great importance of the role of the fluid dynamics in determining that the chemistry of the lower stratosphere may differ considerably from the motionless equilibrium condition.
5. It seems unlikely that these new measurements by themselves will introduce great change in previously derived theories of the role of nitrogen oxide in ozone photochemistry.

N.Chigier: In the studies which you have reported, has account been taken of the ingestion of engine exhaust into the trailing vortex system in the wake of the aircraft. For cases where engines are close to the wing tips, the high temperature and high concentration exhaust gases can be rapidly ingested in the core of the trailing vortex. Within the vortex, diffusion rates are very low and the net result could be the formation of long trails of high temperature and concentration.

A.J.Grobecker: The studies in behalf of CIAP by Lockheed Missile and Systems Corporation, have considered wakes generated by a variety of engine and wing configurations, in flights in the upper troposphere. In all of the cases, the engine exhaust seems to have been ingested into the wing-tip vortices, within a distance required for about 1½ rotations of these vortices. Thereafter, (after about two seconds) dispersion occurs chiefly dominated by diffusion, with minor contribution by forces due to aircraft induced motions. After about (10)³ seconds, only the eddy-like motions of the mesoscale atmosphere are expected to disperse the constituents of the aircraft wake.

Reaction of Ozone with Nitrogen Oxides at High Altitudes

Harold S. Johnston and Gary Whitten
 Department of Chemistry
 University of California
 and
 Inorganic Materials Research Division
 Lawrence Berkeley Laboratory
 Berkeley, California 94720

Abstract

Ozone is formed in the stratosphere by the dissociation of oxygen by ultraviolet radiation below 242 nm. Ozone is removed from the stratosphere by (a) the reaction of oxygen atoms and ozone, (b) by transport to the troposphere, (c) by catalytic reactions with free radicals based on water, and (d) by catalytic reactions with the oxides of nitrogen. The most important factor in the natural removal of stratospheric ozone appears to be catalytic cycles based on the oxides of nitrogen. The natural source of nitric oxide in the stratosphere has been tentatively identified, and the source strength has been calculated by three different investigators. There is about a factor of four uncertainty in the natural rate of injection of nitric oxide in the stratosphere. There is about a factor of four uncertainty in the calculated rate of introduction of nitric oxide in the stratosphere from full scale operation of supersonic transports of current and past designs. Within these two ranges of uncertainty, 500 supersonic transports would introduce nitric oxide in the stratosphere at a rate comparable to the known natural sources.

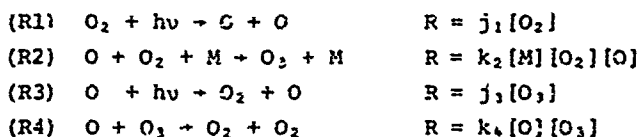
Introduction

During the period 1930-1960 it appeared that the global ozone balance could be explained in terms of the photochemistry of pure air and in terms of air motions. Doubts about the adequacy of this scheme became apparent in 1961 and became compelling by 1965. There appeared to be a large unbalanced production of ozone when only pure air photochemistry and air motions were considered. In efforts to explain this unbalanced ozone production, a set of "water reactions" was postulated in 1966, and a natural background of the oxides of nitrogen in the stratosphere was postulated in 1970. This article reviews the history of these considerations of the global ozone balance and gives a current estimate of the sufficiency of pure air reactions including air transport in giving a global ozone balance. The relative importance of the water reactions and reactions of the oxides of nitrogen is reviewed, and remaining unknown factors are discussed. Natural sources and sinks of the oxides of nitrogen in the stratosphere are discussed, and the natural sources are compared with the expected artificial source from the exhaust gases of supersonic transports.

I. Unbalanced Ozone Production

A. History¹

The basic photochemical theory of stratospheric ozone was developed by Chapman² in 1930. The mechanism involves two photochemical and two chemical reactions. These reactions and the corresponding rate relations are as follows:



Square brackets represent gas concentrations, in this report given as molecules cm^{-3} . The rate constants k are functions of temperature. The photochemical coefficients j are functions of incoming solar radiation, solar angle, all overhead species that absorb the chemically effective radiation, and on the molecular properties of oxygen and ozone.

Within a few seconds¹, oxygen atoms attain a steady-state with respect to local ozone

$$[\text{O}]_s = j_1 [\text{O}_2] / k_2 [\text{O}_2] [\text{M}] \quad (1)$$

If the stratosphere were static, ozone would attain a photochemical steady-state concentration

$$[\text{O}_3]_s = [\text{O}_2] \left(\frac{j_1 k_2 [\text{M}]}{j_3 k_4} \right)^{\frac{1}{2}} \quad (2)$$

The mean time for attaining this steady state is

$$\tau = \frac{1}{4} \left(\frac{k_2 [\text{M}]}{j_1 j_3} \right)^{\frac{1}{2}} \quad (3)$$

These relaxation times are a few hours at 45 km, a few days at 35 km, a few months at 25 km, and many years at 15 km. In the lower stratosphere, air motions are much faster than the photochemical equilibration rates. A comparison of observed ozone concentrations

with calculated vertical steady-state profiles indicates that much of the ozone at and below 20 km was brought there by vertical components of air motions rather than being produced there by photochemistry. A comparison of observed ozone at high latitudes with the quantities calculated from a static photochemical model shows that much of the ozone in polar regions was brought there by horizontal components of air motion.

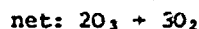
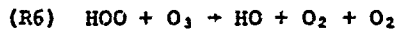
During the period 1930-60, it appeared that the Chapman photochemical mechanism plus considerations of air transport gave a satisfactory global balance between ozone production and destruction. The rate constants k_2 and k_3 had been measured in the laboratory in the 1930's. The cross sections σ for light absorption

$$-d \ln I = \sigma [A] dL \quad (4)$$

for O_2 (σ_2) and for O_3 (σ_3) had also been obtained from laboratory measurements. In early years of the Chapman model, the solar intensity above the atmosphere was calculated from the Planck radiation equation and a temperature for the surface of the sun. During the 1950's and early 1960's, new values of the rate constants k_2 and k_3 were obtained. The actual distribution of solar radiation above the atmosphere was obtained from rocket flights.

In 1961 Dütsch¹ pointed out that there appeared to be a discrepancy between global observed ozone and the amount calculated from the Chapman model with the new data for rate constants and solar intensity. Dütsch said that one should wait until the laboratory work was confirmed or not, and he advised ozone scientists to keep an eye on the developing field.

Between 1960 and 1965, there were major advances in the laboratory with respect to reactions of oxygen atoms, oxygen molecules, and ozone, including the effect of excited electronic states of oxygen atoms and molecules. By 1965 the discrepancy between the predictions of the Chapman mechanism and the observed patterns of ozone had become so great that Hunt² presented a strong case for "The Need for a Modified Photochemical Theory of the Ozonosphere". At first, Hunt assumed that excited electronic states of O and O_2 might account for the discrepancy, but he showed these reactions to be far too slow. Next, Hunt discussed the reactions of free radicals based on water (H, HO, HO₂), abbreviated HO_x. He examined two reactions that, although never observed directly, had been discussed in ozone photochemistry



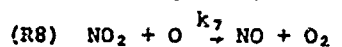
Hunt pointed out that if k_5 were as large as $5 \times 10^{-13} \text{ cm}^3 \text{ molecule}^{-1} \text{ sec}^{-1}$ and if k_6 were as large as $10^{-14} \text{ cm}^3 \text{ molecule}^{-1} \text{ sec}^{-1}$, then this catalytic chain reaction would be adequate to explain the apparently unbalanced production of ozone. Intensive laboratory studies of these reactions have been underway. The first direct measurements^{5,6} reactions 5 and 6 were reported late in 1972, and the observed rate constants are substantially less than the values required by Hunt. It appears that the water reactions are inadequate to account for the observed ozone in the stratosphere, although these reactions are important in the upper stratosphere (above 40 km). The role of HO_x free radicals has been the subject of several recent reviews.

A very careful analysis of the problem of unbalanced ozone production was given by Brewer and Wilson⁷ in 1968. They asked if the ozone balance could be reconciled within the combined uncertainties in solar intensity, in values of the rate constants for both the Chapman reactions and the water reactions, and in the magnitude of atmospheric motions. They concluded that a global ozone balance could be found within the framework of the accumulated uncertainties, but they were not satisfied with the pattern of air motions that was implied. Also the rate constants for the Chapman reactions that Brewer and Wilson used are not consistent with present-day values. With current values of the appropriate constants, one concludes that the Chapman reactions plus the water reactions are inadequate to account for the chemistry of ozone in the stratosphere.

The occurrence of oxides of nitrogen, NO and NO₂, (abbreviated as NO_x) in the stratosphere has been discussed by Nicolet⁸ since 1945. Although no direct measurements of these species in the stratosphere had been made until very recently, Nicolet has discussed the many reactions that they can undergo. He estimated (in 1965) that the order of magnitude of NO_x in the stratosphere is about one or so parts per billion by volume (parts in 10⁹, ppb). Ozone, on the other hand, is typically 1 to 10 parts per million in the stratosphere. Because of this great discrepancy in amount of NO_x and ozone, it did not appear to Hunt in 1966 that NO_x would be important in the stratospheric ozone balance. Two other lines of development, however, lead to a different conclusion.

During 1966-67, Johnston¹⁰ prepared a critical review of all available published laboratory studies of ozone chemical kinetics and photochemistry, going back to 1900. Much of the early data showed satisfactory precision, but very large discrepancies from one investigator to another. Such discrepancies were traced to catalytic destruction of ozone by certain surfaces, by catalytic cycles based on the water reactions, and by several catalytic cycles based on the oxides of nitrogen. This review was the immediate background of the proposal¹¹ made in 1971 that oxides of nitrogen in the stratosphere would be very active in the ozone balance, even if present at only 0.1 per cent of the ozone itself.

In 1968 and 1969 Murcray, Murcray, Kyle, and Williams¹² reported the direct observation of substantial amounts (about 3 ppb) of nitric acid vapor, HNO_3 , in the stratosphere. In the stratosphere nitric acid is, to some extent, broken down to the active oxides of nitrogen, NO_2 and NO , by sunlight and by active free radicals such as HO . Crutzen¹³ reasoned that if nitric acid vapor is present in the stratosphere, then the active oxides of nitrogen would be expected in comparable amounts, and he proposed the following catalytic cycle to rectify the unbalanced production of ozone

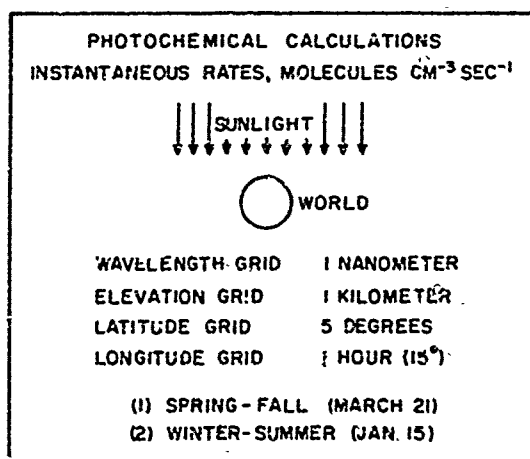


The combined effect of reactions 7 and 8 is the same as the direct effect of reaction 4 in the Chapman mechanism. At a typical stratospheric temperature, however, the rate constant for reaction 8 is 10,000 times greater than that for reaction 4.

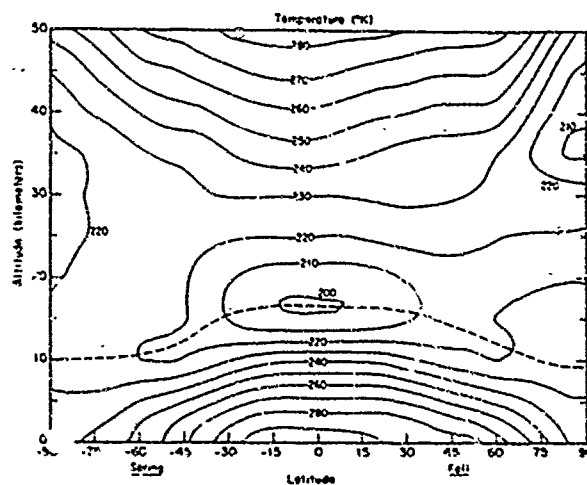
B. Current Status

A special computation was designed for the purpose of testing the sufficiency of the Chapman mechanism plus air transport in accounting for the global ozone balance.¹⁴ This computational procedure does not use the steady-state assumption for ozone. The computational procedure is indicated by Figure 1. We start with measured, average distributions of ozone (for example, Figure 3) and with standard distributions of temperature (for example, Figure 2). As indicated in Figure 1, a planar wave of sunlight (Figure 4, in part) impinges on the spherical earth. The grid of elevation, longitude, and latitude gives 43000 volume elements. The flux of sunlight for each nanometer wavelength above 190 nm is calculated in each volume element. The various orientations of the earth give rise to all hours of the day at one point in time. The steady-state concentration of oxygen atoms (Equation 1) is calculated in each volume element. The instantaneous rate of each elementary reaction, 1-4, is evaluated in each volume element. At a given elevation and latitude, the rates of the elementary reactions are averaged over longitude to give zonal averages of various rates, which are illustrated by figures analogous to Figure 2 or 3. Further integration over elevation from the tropopause to 45 km gives vertical column rates, and integration of column rates over latitude gives global stratospheric rates.

This computation has a narrow purpose, and in this way it avoids some of the complexities of atmospheric motions that are faced by more general analyses. The transport of ozone from one part of the stratosphere to another would cancel out in this computation, which sums over the entire stratosphere. The volume integral of the transport of ozone over the entire stratosphere is simply the flux of ozone across the boundaries. The flux of ozone across the tropopause has been evaluated by several different investigators^{15,6}, and the flux ozone across the stratopause in that region of photochemical steady state is not important. Sample results are given in Table 1.



XBL 728-6775



XBL 728-6776

Figure 1. Computational procedure for calculation of instantaneous photochemical rates.

Figure 2. Zonal average, standard temperature distribution for March 22. H.L. Crutcher, "Temperature and humidity in the troposphere" *World Survey of Climatology*, Volume 4, edited by D.F. Rex. Elsevier Publishing Company, Amsterdam-London-New York, pp. 45-83; *Handbook of Geophysics*, 1960.

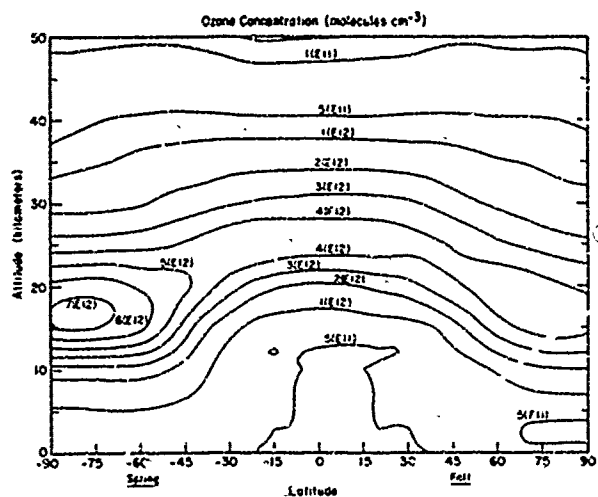


Figure 3. Zonal average standard ozone distribution for March 22. Dütsch, ref. 1; F.S. Johnson, J.D. Purcell, and R. Tousey, *Rocket Exploration of the Upper Atmosphere*, Pergamon Press, London, pp. 189-199, 1954.

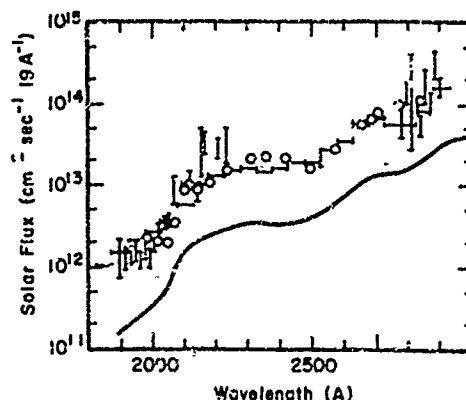


Figure 4. Intensity of solar radiation above the atmosphere. M. Ackerman, D. Frimout, and R. Pastiel, *Ciel et Terre*, 84, 408 (1968); O R.M. Bonnet, *Space Research* 8, 458 (1968); + C.R. Detwiller, D.L. Garrett, J.D. Purcell, and R. Tousey, *Ann. Geophys.* 17, 9 (1961) average value used: M. Ackerman, *Mesospheric Models and Related Experiments*, D. Reidel Publishing Co., Dordrecht, Holland, pp. 149-159 (1971).

Table 1. Instantaneous, global rates in the ozone balance (rates in units of 10^{23} molecules sec^{-1})

	Global reaction rates	
	Jan. 15	March 22
Gross rate of O_3 formation	500	486
Transport to troposphere (ref. 8)	-6	-6
Chemical loss (Chapman)	-86	-89
Unbalanced ozone production	408	391

Approximately 80 per cent of the ozone produced from sunlight fails to be balanced by the Chapman mechanism and by transport to the tropopause. This large unbalance between ozone production and destruction by Chapman reactions as given in Table 1 is based on the central values of a number of experimental quantities. The experimental quantities have a range of uncertainty, and one naturally asks whether the calculated unbalance of ozone can be due to experimental error in the rate constants or in other data. To examine this question, we deliberately varied the input data for one variable at a time by various arbitrary factors and repeated the entire calculation. It was found that the Chapman reactions plus transport could give a global ozone balance for each of the following highly perturbed conditions:

1. The intensity of radiation above the atmosphere at wavelengths below 300 nm is reduced by a factor of five (note the heavy line in Figure 4).
2. The ozone vertical profile retains its same shape but is displaced upward by $4\frac{1}{2}$ kilometers over the entire globe.
3. The absolute temperature is increased by 50°K everywhere.
4. The cross section σ_2 for radiation absorption by oxygen is decreased by a factor of five (note the heavy line in Figure 6).
5. The cross section σ_3 for radiation absorption by ozone is increased by a factor of five (note the heavy line in Figure 5).
6. The rate constant k_2 is decreased by a factor of five (note the heavy line in Figure 8).
7. The rate constant k_1 is increased by a factor of five (note the heavy line in Figure 7).

The primary data for the five quantities, I_0 , σ_2 , σ_3 , k_2 , and k_1 , are presented in Figures 4-8. The central curve drawn through the points corresponds to the values used to obtain Table 1. The heavy curve offset from the experimental data corresponds to how far one must go from the experimental data in order to force an agreement between ozone formation and destruction in terms of the Chapman mechanism alone. The results in Table 1 are derived from the data given by Figures 2-8. We have underway a "Monte Carlo" calculation that combines in a random way the errors from the various component quantities. Although these calculations are not yet complete, we are beginning to get an estimate of the standard deviation of the unbalanced ozone production from the combined effect of several sources of error. It appears improbable that the unbalanced ozone production shown in Table 1 is due to experimental error in the component quantities.

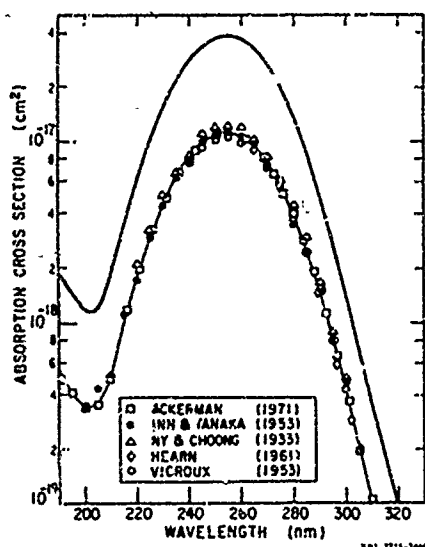


Figure 5. Ultraviolet radiation absorption cross section for ozone with experimental points, a curve through the experimental points, and a curve displaced from the points. E.C.Y. Inn and Y. Tanaka, *J. Opt. Soc. Amer.* 43, 870 (1953); A.G. Hearn, *Proc. Phys. Soc.* 78, 932 (1961); E. Vigroux, "Contribution à l'étude expérimentale de l'ozone, Masson et Cie, Paris (1953).

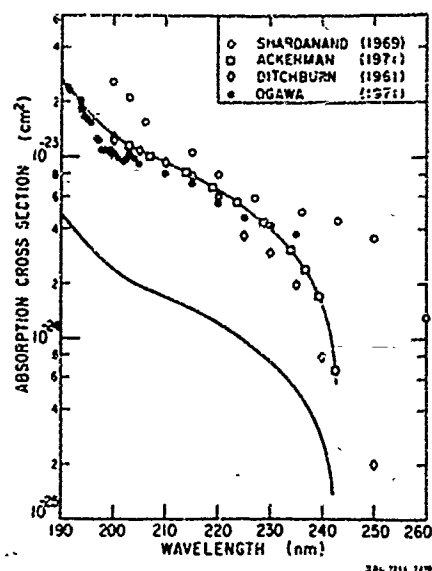


Figure 6. Ultraviolet radiation absorption cross section for molecular oxygen. Shardanand, *Phys. Rev.* 186, 5 (1969); R.W. Ditchburn and P.A. Young, *J. Atm. Terr. Phys.* 24, 127 (1961); M. Ogawa, *J. Chem. Phys.* 54, 2550 (1971).

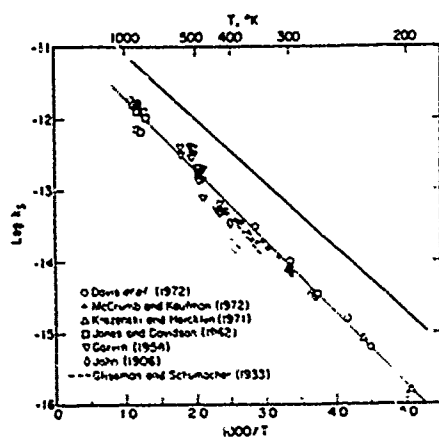


Figure 7. Rate constants for the reaction $O + O_2 \rightarrow O_3 + O_2$. D.D. Davis, W. Wong, J. Lephardt, in press (1973); J.L. McCrumb and F. Kaufman, *J. Chem. Phys.* 57, 1270 (1972); W.M. Jones and N. Davidson, *J. Am. Chem. Soc.* 84, 2868 (1962); D. Garvin, *J. Am. Chem. Soc.* 76, 1523 (1954); S. John, *Z. Anorg. Chem.* 48, 260 (1906).

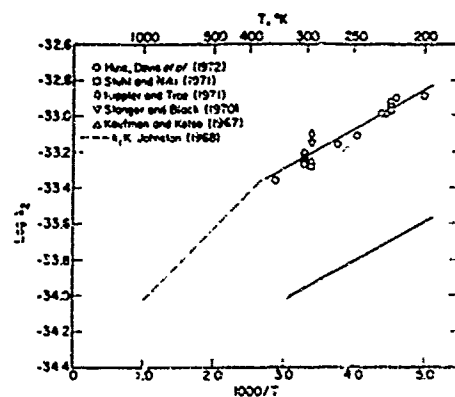


Figure 8. Rate constants for the reaction $O + O_2 \rightarrow O_3 + O_2$. R.E. Huie, J.T. Herron, and D.D. Davis, *J. Phys. Chem.* 76, 2653 (1972); F. Stuhl and H. Niki, *J. Chem. Phys.* 55, 3943 (1971); H. Hippler and J. Troc, *Ber. Bunsenges. Phys. Chem.* 75, 27 (1971); F. Kaufman and J.R. Kelso, *J. Chem. Phys.* 46, 4541 (1967); H.S. Johnston, "Gas Phase Reaction Kinetics of Neutral Oxygen Species" NSRDS-NBS-20 (1968).

It is instructive to examine in detail some of the data, which integrated to give the results of Table 1. Figure 9 gives contour lines for the concentration of oxygen atoms. This figure illustrates that the stratosphere is not a uniform region, but it is strongly stratified. Ozone is destroyed by oxygen atoms both by reaction 4 and reaction 8. The stratosphere at 60°N and 12 km, for example, has an average oxygen atom concentration of about 10^4 molecules cm^{-3} . It is, chemically speaking, a totally different region from the sunlit stratosphere at 20 km where the oxygen atom concentration is about 10^6 molecules cm^{-3} . Reaction 8 is vanishingly slow where the concentration of oxygen atoms is 10^4 cm^{-3} , but it occurs at a significant rate if $[\text{O}]$ is 10^6 and $[\text{NO}_2]$ is above 10^5 molecules cm^{-3} . This discussion pertains to the flight of regular jet planes in the polar stratosphere as compared to supersonic transports in the stratosphere at 20 km. With respect to rate of destruction of ozone, flights at 20 km are about 100 fold worse than the same flight at 12 km, even though both flights are "in the stratosphere".

Figure 10 gives the rate of photolysis of oxygen as zonal averages. If these rates are multiplied by two, they give the gross rate of production of ozone from sunlight. If ozone production persisted at each point at the rate given in Figure 10 for one year, the ozone concentration would build up to a value in molecules cm^{-3} that is 6×10^7 greater than the value given in Figure 10. For the contour 10^5 (written as E5) the concentration of ozone produced in a year would build up to the maximum concentration of ozone (compare Figure 3) in the entire stratosphere. This ozone production rate dips below 19 km in the tropical region and is about 24 km at the summer pole. Downward and horizontal air motions are dominant in setting the distribution of ozone in the lower stratosphere¹, but there is also a substantial amount of photochemical ozone production down to 20 km in the equatorial and summer temperate zones.

The rate of destruction of ozone by means of the Chapman reaction, $\text{O} + \text{O}_3 \rightarrow \text{O}_2 + \text{O}_2$, is given by Figure 11 for a standard January 15.

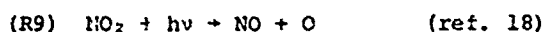
The difference between ozone production ($2j, [\text{O}_2]$) and destruction ($2k, [\text{O}][\text{O}_3]$) according to the Chapman mechanism is given by Figure 12. This unbalanced ozone production is 4×10^{11} molecules sec^{-1} on a global basis (Table 1). The global inventory of stratospheric ozone is about 4×10^{17} molecules. If the unbalanced production of ozone given by the Chapman mechanism persisted for 10^6 seconds (or about 12 days), it would double the world's inventory of ozone. Clearly, there must be some powerful mechanism for ozone destruction other than the Chapman reactions.

Table 1 and Figure 12 provide very strong evidence that the Chapman mechanism and air transport are insufficient to account for the present quantity and distribution of global ozone. "Something else" in the stratosphere must be very important in the natural ozone balance. At present, it appears that this "something else" is the oxides of nitrogen or the oxides of nitrogen plus the free radicals based on water.

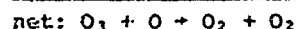
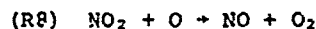
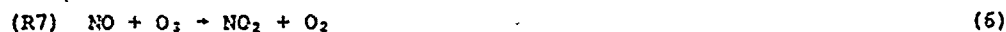
IV. Reactions of the Oxides of Nitrogen

A. The NO_2 Catalytic Cycle^{11,13,19}

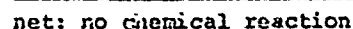
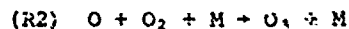
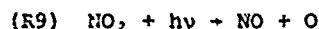
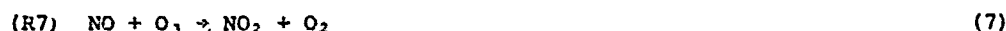
The most important reactions of the oxides of nitrogen with ozone are believed to involve the three reactions



The rate constants for these reactions have been obtained repeatedly in the laboratory, including studies at stratospheric temperatures and pressures. There is reasonably good agreement between different investigators of these reactions. The reactions combine in two different competing cyclic processes. The catalytic cycle for ozone destruction is



There is a parallel "do nothing" cycle



The rate of destruction of ozone with the oxides of nitrogen relative to the rate in "pure air" (that is, the Chapman model), is defined as the "catalytic ratio", ρ . The catalytic ratio^{11a} may be expressed either in terms of the variables NO_2 and O , or the variables NO and O . These expressions are

$$\begin{aligned} \rho &= \frac{\text{rate of ozone destruction with } \text{NO}_2}{\text{rate of ozone destruction in pure air}} \\ &= 1 + k_2[\text{NO}_2]/k_1[\text{O}] \end{aligned} \quad (8)$$

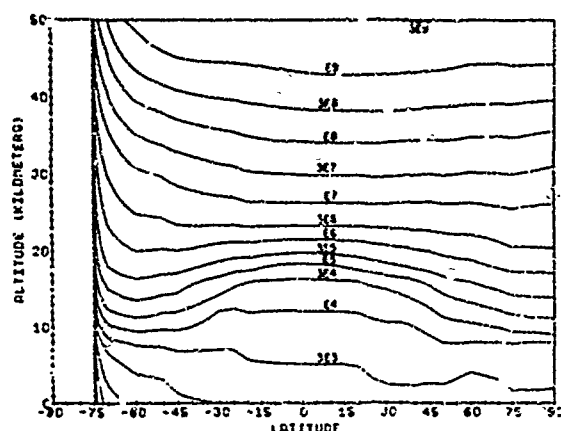


Figure 9. Oxygen atom, $O(^3P)$, concentration, Equation (1), for standard January 15.

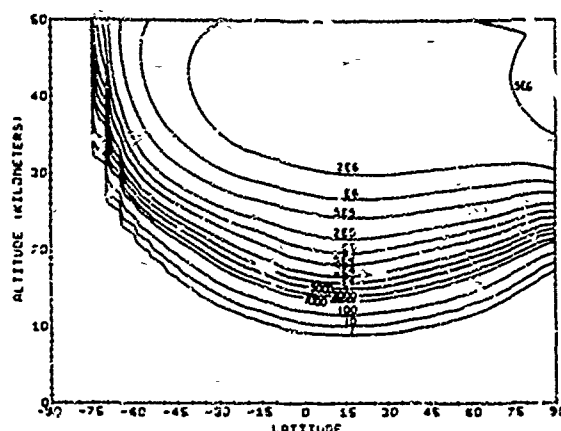


Figure 10. The rate of photolysis of molecular oxygen, $O_2 + h\nu \rightarrow O + O$, $j_1[O_2]$ for standard January 15. These data multiplied by two give the gross rate of formation of ozone.

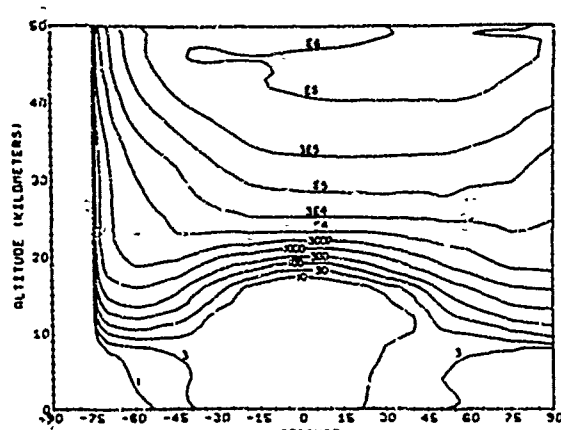


Figure 11. The rate of the reaction, $O + O_3 \rightarrow O_2 + O_2$. January 15.

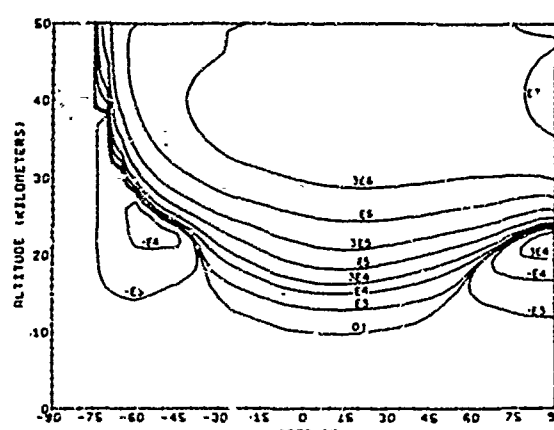


Figure 12. The net rate of ozone production according to the Chapman mechanism, $2j_1[O_2] - 2k_4[O][O_3]$. January 15.

$$= 1 + \frac{[NO](k_7k_8/k_4j_9)}{1 + k_4[C]/j_9} \quad (9)$$

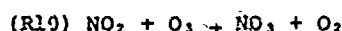
The instantaneous rate of destruction of ozone by NO_x catalysts may be expressed in the language of "ozone half life", τ (compare the use half life of radioactive decay to characterize instantaneous decay rates):

$$\tau = \ln 2 / 2k_4\rho[O] \quad (10)$$

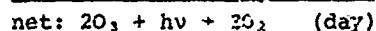
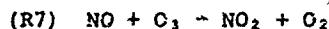
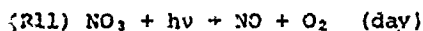
From Figure 9 it can be seen that the range of oxygen atom concentrations in the stratosphere is from about 10^5 at 15 km to almost 10^{10} at 50 km. Considerations of present and possible future sources of nitric oxide in the stratosphere give 10^8 to 5×10^{11} molecules cm^{-3} as the maximum probable range of NO concentration. From Figure 2 it can be seen that stratospheric temperatures vary from 200 to 260°K. For a typical temperature, 220°K, Figure 13 give values of the catalytic ratio, Eq. 9, for the full range of [NO] and [O] in a sunlit stratosphere. (Similar plots have been prepared for 200, 240, and 260°K.) The catalytic ratios vary from just under two to well over one thousand. For the same range of [NO] and [O] and for the same temperature, the half-time of ozone destruction, Eq. 10, is given by Figure 14. At low values of both [NO] and [O], the half-times are longer than a year. At 20 km, where [O] averages 10^6 , the rate of ozone destruction is significantly fast if [NO] exceeds 2×10^8 molecules cm^{-3} .

B. The NO_x Catalytic Cycle¹¹

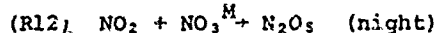
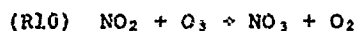
At low elevations, where [O] is low and the NO_2 cycle is slow, another catalytic cycle of the oxides of nitrogen may be important:



(11)



The radiation involved here is red light, which is abundant at all elevations. This reaction goes in another direction at night (including the polar night)

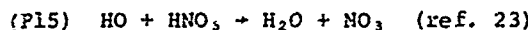
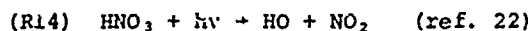
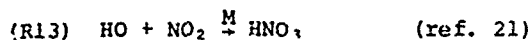


A few per cent of the NO_2 is converted to N_2O_5 in one night. The reactions of N_2O_5 during the next day are not well characterized, and the net effect of the reaction at night cannot be stated at this time.

The rate of reaction 10 has been studied only near room temperature, and the extrapolation to stratospheric temperatures is uncertain. However, the extrapolated values indicate the NO_3 catalytic cycle to destroy ozone faster than the NO_2 catalytic cycle below 22 km. and in the temperate region where the temperature is at least 220°K.

C. Nitric Acid Vapor

Nitric acid vapor is formed from the combination of hydroxyl radicals and nitrogen dioxide. It is destroyed by photolysis and by reaction with hydroxyl radicals.



The steady-state ratio of nitrogen dioxide to nitric acid is

$$\left(\frac{[\text{NO}_2]}{[\text{HNO}_3]} \right)_s = \frac{k_{13}}{k_{15}} + \frac{j_{14}}{k_{15}[\text{HO}]} \quad (12)$$

The half-time to approach the steady-state is

$$\tau = \ln 2 / (k_{13}[\text{HO}] + k_{15}[\text{HO}] + j_{14}) \quad (13)$$

Although these rate constants are not accurately known, they are well-enough known for order of magnitude calculations to be made. Near 20 km, k_{13} is about 10^{-12} , k_{15} is about 10^{-13} , and j_{14} is about 10^{-6} sec^{-1} . Thus the ratio of NO_2 to HNO_3 is approximately

$$\left(\frac{[\text{NO}_2]}{[\text{HNO}_3]} \right)_s \approx 0.1 + \frac{10^6}{[\text{HO}]} \quad (14)$$

If hydroxyl radicals are less than 10^6 molecules cm^{-3} , nitrogen dioxide will exceed nitric acid; and the half time, determined by the photolysis rate, is about one week. If the hydroxyl radicals are 10^7 molecules cm^{-3} , nitrogen dioxide is about one-fifth the nitric acid, and the half-time is less than a day. Although the constants k_{13} , j_{14} , and k_{15} are not firmly established, it appears that the ratio of NO_2 to HNO_3 is about 0.1 at 15 km, about 1 at 25 km, and substantially larger than 1 above 35 km. At all elevations, the half-time to establish the steady state between NO_2 and NO_3 appears to be two weeks or less. Thus it can be seen that nitric acid is a significant reservoir or temporary sink for the active oxides of nitrogen. In the lowest stratosphere nitric acid predominates over nitrogen dioxide, and the eddy diffusion of nitric acid into the troposphere where it is rained out is presumably a major loss process for stratospheric NO_x .

D. Effect of NO_x on the Unbalanced Ozone Production

The concentration and distribution of NO_x in the stratosphere is not known. To test the sensitivity of the global ozone balance to stratospheric NO_x , we arbitrarily assumed¹⁰ a range of possible amounts of NO_x in the stratosphere and repeated calculations leading to Table 1. For a constant concentration of 4.4×10^3 molecules cm^{-3} of NO_x throughout the stratosphere, the unbalanced ozone production given by Table 1 is turned into a global balance for standard conditions of January 15. It required 4.2×10^9 to produce a global ozone balance as of March 22.

Figure 15 presents the ratio of the rate of ozone production to the rate of ozone destruction, based on the Chapman model and the present actual distribution of ozone. Over most of the stratosphere ozone appears to be formed at least three times faster than it is being destroyed. In part of the tropical stratosphere ozone is being formed photochemically a thousand times faster than it is being destroyed by the pure-air reactions. It seems exceedingly improbable that stratospheric ozone would have assumed its present distribution if it is subject to such unbalanced production rates as is given by this figure.

With 4.2×10^9 molecules cm^{-3} of NO_x added throughout the atmosphere, the ratio of ozone formation to ozone destruction is changed from Figure 15 to Figure 16. In Figure 16, it can be seen that this addition of NO_x brings the entire atmosphere below 45 km within 20 per cent of photochemical equilibrium. The large local imbalances shown by Figure 15 are smoothed out almost entirely. In the ozone "source region" above 30 km,

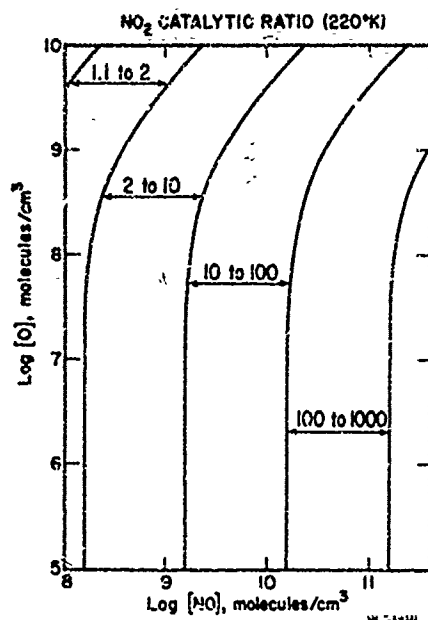


Figure 13. The catalytic ratio ρ . The ratio of the rate of destruction of ozone with the NO_2 cycle to the rate with "pure air", Equation 9. 220°K .

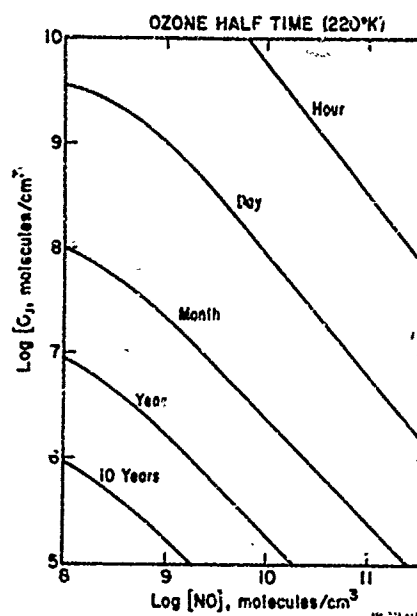


Figure 14. The half-time for ozone destruction by the NO_2 catalytic cycle, Equation 10. 220°K .

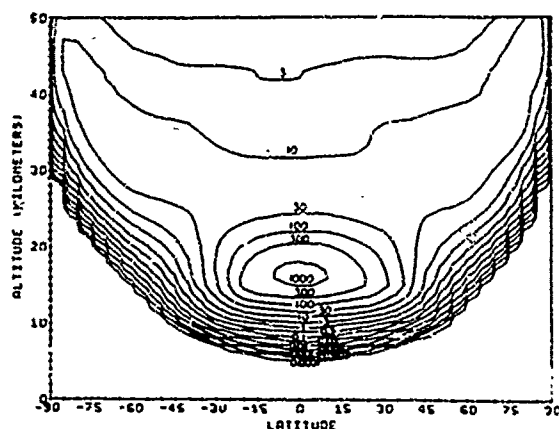


Figure 15. The ratio of the rate of photochemical ozone formation to its rate of destruction according to the Chapman mechanism, $j_1[\text{O}_2]/k_1[\text{O}][\text{O}_3]$. March 22.

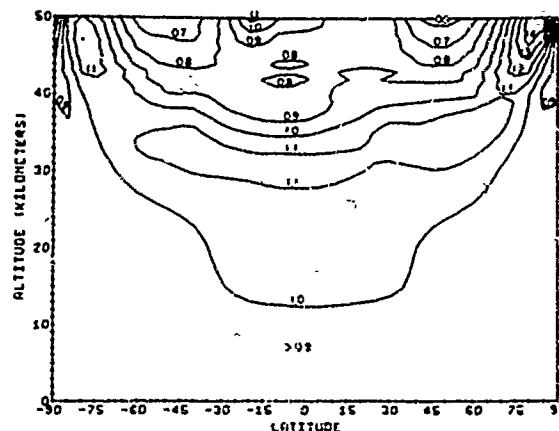


Figure 16. The same as Figure 15 but with 4.2×10^9 molecules cm^{-3} of NO_x added throughout the atmosphere.

the excess rate of ozone production to ozone destruction is a matter of 10 per cent, not the factor of 10 given by the Chapman mechanism.

At this time we have only a single report of the distribution of NO_x in the stratosphere, and it extends only to 28 km. Ackerman and Muller interpreted their own balloon data and those of Goldman et al.²⁵ Their reported concentrations of NO_x were about 8×10^9 at 15 km, 2×10^9 at 20 km, 3×10^9 at 25 km, and 5×10^9 molecules cm^{-3} at 28 km. Our assumed uniform concentration of 4.2×10^9 molecules cm^{-3} is consistent with Ackerman's values. On the other hand, it is demonstrated here that NO_x concentrations comparable to those observed (15 to 30 km) are very potent catalysts for ozone destruction.

The conclusion to this section is that the oxides of nitrogen are now a very active component of the stratosphere and are of major importance in the present ozone balance.

E. Comparison of Rates of Photochemical Destruction of Ozone from Various Mechanisms

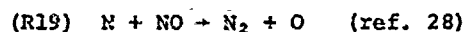
To carry through calculations of the relative rate of ozone destruction by the various mechanisms (O_x , HO_x , and NO_x), one must have data that is not yet available: the distribution of NO_x in the stratosphere and rate constants for HO_x reactions, including k_5 and k_6 . The Climatic Impact Assessment Program of the U.S. Department of Transportation is currently engaged in obtaining these numbers. By use of Park and London's²⁶ estimate of the NO_x background in the natural stratosphere and by use new, not yet published^{5,6} values for k_5 and k_6 , we can estimate which mechanisms predominate at various elevations for 45° latitude and the spring equinox. With these current data (which may change during the next few months) it appears that the predominant photochemical mechanisms for ozone destruction are:

- 15 to 20 km, the NO catalytic cycle
- 20 to 40 km, the NO_2 catalytic cycle
- 40 to 45 km, NO_2 , HO_x , and O_x mechanisms
about equal
- above 45 km, the HO_x reactions.

It appears that between 15 and 35 km, the oxides of nitrogen are by far the most important agent for maintaining the natural ozone balance.

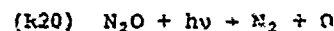
F. Natural Sources and Sinks of NO_x in the Stratosphere

Nitric oxide is produced high above the stratosphere from the photolysis of diatomic nitrogen. As this nitric oxide is transported down below where nitrogen is photolyzed, it is subject to the reactions

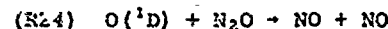
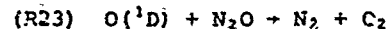
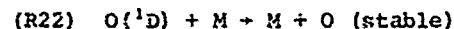
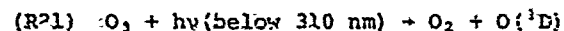


The destruction of nitric oxide by reaction 16 is reversed by reactions 17 and 18, but the destruction is reinforced by reaction 19. The net effect is a destruction of nitric oxide wherever reaction 16 can occur, but at a rate less than reaction 16 itself. Brasseur and Cieslik²⁷ have identified this mechanism as an important sink for nitric oxide at the top of the stratosphere.

The natural production of nitric oxide (NO) from nitrous oxide (N_2O) in the stratosphere has tentatively been identified as the most important source of stratospheric NO_x . Crutzen¹⁹ appears to be the first one to identify this natural source of stratospheric NO_x . Bacter in the soil and perhaps in surface ocean waters produce a small amount of nitrous oxide as a byproduct of the nitrogen cycle. Unlike NO and NO_2 , nitrous oxide is inert in the troposphere. It has a natural background of about 0.25 parts per million in the troposphere, and this value decreases rapidly in the lower stratosphere. In the eddy diffusion processes between the troposphere and stratosphere, nitrous oxide diffuses upward in elevation and down its mole fraction gradient into the stratosphere. In the stratosphere most of the nitrous oxide is photolyzed



but about 10 per cent of it reacts with singlet oxygen atoms, which are produced by short wavelength photolysis of ozone



Crutzen¹⁹ estimated that the flux of NO into the stratosphere from this source was between 0.3×10^8 and 1.5×10^8 molecules $cm^{-2} \text{ sec}^{-1}$. This mechanism for nitric oxide production in the stratosphere has also been analyzed by Nicolet and Peetermans²⁹ and by McElroy and McConnell.³⁰ The results of the three investigations are summarized in Table 2. They agree fairly well with each other and give as an average range (0.35 to 1.2×10^8 molecules $cm^{-2} \text{ sec}^{-1}$ for the natural source of NO_x .

Table 2. Natural NO_x Flux in the Stratosphere from the N_2O Mechanism

Range of Calculated Flux (molecules $cm^{-2} \text{ sec}^{-1} \times 10^8$)	Authors	Ref.
0.3 to 1.5	Crutzen	19
0.5 to 1.5	Nicolet and Peetermans	29
0.25 to 0.65	McElroy and McConnell	30
0.35 to 1.2	(average)	

Nitrogen dioxide and nitric acid are readily washed out by rain in the troposphere. There appears to be a higher mole fraction of NO_x in the stratosphere than in the troposphere. Thus in any diffusion or eddy diffusion process, NO_x would be transported

downward from the stratosphere to the troposphere. To the extent that tropospheric air is injected into the stratosphere in tropical regions, the amount of NO_x in the stratosphere is reduced by the influx of relatively clean air. Thus combustion processes that generate NO_x in the troposphere do not appear to be a source of stratospheric NO_x .

G. Artificial Increases in Stratospheric Nitrogen Oxides from SST Exhaust

There has been considerable discussion and some controversy on the amount of NO_x expected to be emitted from the SST exhaust. The quantity is conveniently expressed in units of grams of NO emitted in the exhaust per kilogram of fuel burned for conditions of cruise operation. The General Electric Company quoted the figure 42 g NO/kg fuel to the Study of Critical Environmental Problems³, SCEP, but they added a footnote that it might be a factor of 2 or 3 less. In part on this basis, Johnston¹¹ used the figure 15 g NO/kg fuel. The Concorde is said to emit 12.5 g NO/kg fuel.¹² On the basis of tests simulating the actual stratosphere, Forney¹³ has given a tentative estimate of 7 g NO/kg fuel. Experiments on engines similar to but not identical with SST engines, McAdams¹⁴ found a range of 20 to 30 g NO/kg fuel. Ferri¹⁵ estimated that current or previous models of SST engines would emit between 15 and 70 g NO/kg fuel, but he further stated that if SST engines were redesigned for the purpose of minimizing NO emission, these emissions could be reduced several hundred fold lower than existing engines. In view of this wide range of estimates, one might take 7 to 20 g NO/kg fuel as a reasonable estimate of what should be expected from the 1971 version of the American SST.

According to the Australian Academy of Sciences¹², the fleets of Concorde in 1985 would constitute a world wide average flux of NO in the stratosphere of 102×10^8 kg/day. This source strength corresponds to a world-wide average of 0.5×10^8 molecules $\text{cm}^{-2} \text{sec}^{-1}$. The average range of natural source strength of NO_x as given in Table 2 is 0.35 to 1.2×10^8 molecules $\text{cm}^{-2} \text{sec}^{-1}$. Thus it can be seen that the artificial source of NO_x from the Concorde is about the same size as the current estimates of the natural source of NO_x . The American SST would burn fuel at about three times the rate of the Concorde. If its emission index is the same as the Concorde, the American SST would increase stratospheric NO_x by about 1.2×10^8 molecules $\text{cm}^{-2} \text{sec}^{-1}$ as a world-wide average. This figure is equal to the upper range of the average estimates of the natural source in Table 2. If the large figures mentioned by McAdams or Ferri are appropriate, 500 American SST would constitute a world-wide source of stratospheric NO substantially greater than the maximum natural rate as given in Table 2. At latitudes of high traffic density, the regional emission rates would exceed the world-wide average emission rates discussed above. In many design problems, some safety factor is invoked between the expected central figure and an acceptable target figure. At present the central estimate of the effect of full fleets of SST (conventionally taken to be 500 for purpose of calculation) is that they would more or less double the natural source of NO_x in the stratosphere.

Table 3. Estimates of worldwide averages flux of NO_x from 500 SST

Estimated flux (molecules $\text{cm}^{-2} \text{sec}^{-1} \times 10^8$)		Ref.
0.5	Concorde (1972)	32
0.7	Forney (1972)	33
1.3	Johnston (1971)	11
2 to 3	McAdams (1971)	34
4.2	SCEP (1970)	31

0.5 to 2.0 (Probable range)

The quantity of NO_x in the stratosphere is not the whole story. The distribution of NO_x , both naturally and as it would be after full scale SST flights, is equally as important as the quantity of NO_x . In one simple model calculation¹¹, it was shown that a fixed quantity of NO_x (added globally to an assumed natural background of NO_x containing three times as much NO_x as the artificial increment) could reduce a local steady-state vertical column of ozone anywhere between 3 per cent and 50 per cent depending on the distribution of the added NO_x . Although steady-state calculations are not realistic enough to warrant detailed conclusions, this study was surely correct in identifying the importance of NO_x distributions in this problem. A world-wide, highly constrained vertical distribution gives an "overkill" of ozone in a narrow range of elevation, no contact with ozone elsewhere, and thus a small effect on the ozone vertical column. A highly constrained (10 fold local maximum) horizontal distribution with a moderate (10 km wide) vertical spread gave maximum ozone destruction and a factor of two reduction of the local ozone column. Both a highly constrained vertical distribution and a ten-fold "local maximum" over latitudes of high traffic density seem to be physically unreasonable, but the great difference between these extreme cases points up the importance of determining NO_x distributions in the stratosphere.

The conclusion of this section is that 500 SST (including the Concorde) promise more or less to double the rate of input of the oxides of nitrogen into the stratosphere, but the expected magnitude of ozone reduction is a very complicated problem requiring much more study before a satisfactory answer will be found.

References

1. H.U. Dütsch, Atmospheric ozone and ultraviolet radiation, World Survey of Climatology, Vol. 4, D.F. Rex, Ed., Elsevier Publishing Company, Amsterdam-London-New York, 1969, pp. 383-432.
2. S. Chapman, Memoirs of the Royal Meteorological Society, 3 (1930), 103; Philosophical Magazine, 10 (1930), 369.
3. H.U. Dütsch, "Chemical Reactions in the Lower and Upper Atmosphere", International Symposium, Stanford Research Institute (1961).
4. a. B.G. Hunt, J. Atmospheric Sci., 23 (1965) 98; b. B.G. Hunt, Jour. Geophys. Res., 71 (1966) 1385.
5. J. Anderson and F. Kaufman, in press (1973).
6. W.B. De More, submitted to Science (1973).
7. a. M. Nicolet, Annal. Geophys., 27 (1970) 531; Aeronomica Acta, 89 (1971); b. G. Paraskevopoulos and R.J. Cvetanovic, Chem. Phys. Letters, 9 (1971) 603; c. P.M. Scott and R.J. Cvetanovic, J. Chem. Phys., 54 (1971) 1440; d. D. Biedenkapp, L.G. Hartshorn, and E.J. Bair, Chem. Phys. Letters, 5 (1970) 488; e. R.J. Donovan and D. Husain, Chem. Rev., 70 (1970) 489; f. F. Kaufman, Canad. J. Chem., 47 (1969) 1924.
8. A.W. Brewer and A.W. Wilson, Roy. Meteorol. Soc. Quart. Jour., 94 (1968) 249.
9. M. Nicolet, J. Geophys. Res., 76 (1971) 8143; J. Atmos. Terrest. Phys., 7 (1955) 297; Inst. Prog. Meteorol. Belg. Mem., 19 (1945) 162.
10. H.S. Johnston, Gas Phase Kinetics of Neutral Oxygen Species, National Standard Reference Data Series - National Bureau of Standards Number 20, 1968.
11. a. H.S. Johnston, "Catalytic Reduction of Stratospheric Ozone by Nitrogen Oxides", Lawrence Radiation Laboratory Report, UCRL-20568, Berkeley, California (June 1971); b. H.S. Johnston, Science, 173 (1971) 517.
12. D.R. Murcray, T.G. Kyle, F.H. Murcray, and W.J. Williams, J. Opt. Soc. Am., 59 (1969) 1131; Nature, 218 (1968) 78.
13. P.J. Crutzen, Roy. Meteorol. Soc. Quart. Jour., 96 (1970) 320.
14. H.S. Johnston and G. Whitten, Symposium on Atmospheric Ozone, Arosa, Switzerland (1972).
15. a. H.A. Paetzold, "Vertical Atmospheric Ozone Distribution" Ozone, Chemistry and Technology, Advances in Chemistry No. 21 (American Chemical Society, 1959) 209-220; b. P. Fabian, Symposium on Atmospheric Ozone, Arosa, Switzerland (1972).
16. a. H.S. Johnston and H. Crosby, J. Chem. Phys., 22 (1954) 589; 19 (1951) 799; b. M.A.A. Clyne, B.A. Thrush, and R.P. Wayne, Trans. Faraday Soc., 60 (1964) 359; c. J.E. Marte, E. Tschuikow-Roux, and H.W. Ford, J. Chem. Phys., 39 (1963) 3277; d. L.F. Phillips and H.I. Schiff, J. Chem. Phys., 36 (1962) 1509.
17. R.E. Huie, J.T. Herron, and D.D. Davis, J. Phys. Chem., 76 (1972) 2653.
18. F.A. Leighton, Photochemistry of Air Pollution, Academic Press, New York and London, 1961.
19. P.J. Crutzen, Jour. Geophys. Res., 6 (1971) 7311.
20. a. H.S. Johnston, Environmental Affairs, 1 (1972) 735; b. H.S. Johnston, "Laboratory Chemical Kinetics as an Atmospheric Science", Survey Conference on Climatic Impact Assessment Program, Cambridge, Mass., Lawrence Berkeley Laboratory Report, LBL-497 (1972).
21. a. W. Tsang, private communication; b. C. Morley and I.W.M. Smith, Trans. Faraday Soc., 68 (1972) 1016.
22. H.S. Johnston and R. Graham, J. Phys. Chem., in press, 1972.
23. a. M. Adams, "Decomposition of Nitric Acid in the Presence of Carbon Monoxide", Stanford University, M.S. Thesis, 1956; b. D. Hussain and R.G.W. Norrish, Proc. Roy. Soc. (London), A273 (1953) 165.
24. M. Ackerman and C. Muller, Aeronomica Acta, No. 106 (1972).
25. A. Goldman, D.G. Murcray, F.H. Murcray, W. Williams, and F.S. Ronomo, Nature, 225 (1970) 441.
26. J. Park and J. London, "The Photochemical Relation Between Water Vapor and Ozone in the Stratosphere", Extended Abstract. Presentation by Department of Commerce Advisory Board for SST Environmental Effects, Boulder, Colorado (Mar. 18, 1971).
27. G. Srasseur and S. Cieslik, Symposium on Atmospheric Ozone, Arosa, Switzerland (1972).
28. D.L. Baulch, D.D. Drysdale, and D.G. Horne, "Critical Evaluation of Rate Data for Homogeneous Gas Phase Reactions of Interest in High Temperature Systems", Vol. 4. School of Chemistry, The University, Leeds, England, 1970.
29. M. Nicolet and W. Peetermans, Symposium on Atmospheric Ozone, Arosa, Switzerland (1972).
30. M.B. McElroy and J.C. McConnell, J. Atmos. Sci., 28 (1971) 1095.
31. Study of Critical Environmental Problems (SCEP), Man's Impact on the Global Environment (The MIT Press, Cambridge, Mass.) 1970.
32. Atmospheric Effects of Supersonic Aircraft, Australian Academy of Sciences, Report Number 15, 1972.
33. E. Forney, Climatic Impact Assessment Program, preliminary result (1972).
34. H.T. McAdams, Analysis of Aircraft Exhaust Emission Measurements: Statistics, Cornell Aeronautical Laboratory, Inc., Technical Report NA-5007-K-2, November 1971, p. III-4.
35. A. Ferri, Astronautics and Aeronautics, 37 (1972).

Acknowledgement

This work was supported by the Climatic Impact Assessment Program of the U.S. Department of Transportation.

Discussion on Paper 2
 "Reaction of Ozone with Nitrogen Oxides at High Altitudes"
 presented by H.S. Johnston

A. Goldberg:

1. The ozone profile you report is off by a factor of three, but rate calculations are only good as to order of magnitude. I think that represents agreement.
2. In your calculation of photochemical rates, transport phenomena were not given sufficient consideration.

H.S. Johnston:

1. Some rate data are valid only as to order of magnitude, but the data behind this calculation (Figures 7 and 8) are much better than that. The ozone column varies as the square root of the ozone destruction rate, and thus the discrepancy in profile is a factor of two, not three.
2. To the contrary, this calculation of integrated, instantaneous rates based on the observed ozone distribution gives full consideration to ozone transport (note particularly pages 3 through 6 and Table 1).

R.S. Scorer: The equilibrium level of components of the stratosphere is probably determined by a collection of reactions which have feedback on each other in such a way that a small increase in one component is absorbed without significantly altering any major component (including, of course, O_3). Most of the major injections of NO_x into the stratosphere are accompanied by a higher concentration of H_2O than the stratosphere average, so that it could be that a lower effective level of NO_x results from these injections than if the NO_x were mixed into a larger volume of air before its concentration could be reduced by the excess H_2O present. These considerations are important in addition to studying the details of the mixing mechanisms. It should be remarked that a greater mixing rate decreases the residence time and that in any case much of the NO_x will be removed into the troposphere before it achieves the mean dilution used to calculate the consequences of its presence. Prediction of direct consequences must consider the very complex interactions.

H.S. Johnston: In the natural stratosphere the ratio of water to NO_x ($NO + NO_2 + HNO_3$) is about 1000 to one, and in jet engine exhaust it is about 100 to one. Thus the point about increased ratio of water to NO_x is a valid one, which all careful studies of this problem must consider. We have made calculations of the injection of NO_x from supersonic transports, and there are very complex interactions, as Professor Scorer says. The formation of HNO_3 from NO_2 and NO does not remove NO_x from the stratosphere. The HNO_3 that is transported upward by vertical eddy diffusion is photolyzed by short wavelength ultraviolet radiation to form NO_2 in the important "ozone source region" above 25 kilometers.

NITROGEN OXIDES, NUCLEAR WEAPON TESTING, CONCORDE

AND STRATOSPHERIC OZONE

P GOLLSMITH, A F TUCK, J S FOOT, E L SIMMONS, R L NEWSON

Meteorological Office
London Road
Bracknell
Berkshire
RG12 2SZ
England

Summary

There has been much speculation in the literature recently that the oxides of nitrogen produced in the combustors of the jet engines of high flying supersonic aircraft could interact with, and so attenuate the Earth's ozone shield and increase the ultra-violet radiation reaching the planetary surface. It is fair to say that so far as the necessary full, quantitative, consideration of the interaction of radiation, photochemistry and the atmospheric circulation has not been made. However, it is incontrovertible that under laboratory conditions NO and NO₂ convert ozone and oxygen atoms to molecular oxygen.

In this paper calculations are presented suggesting that man may have already injected into the stratosphere, during the various nuclear testing programmes, amounts of nitrogen oxides greater than the annual emission expected from full operation of as many as 500 Concorde's. A study of some of the most reliable ozone records has failed to reveal any significant depletion in total ozone during the periods after nuclear weapon testing.

1. Introduction

At the present time man's understanding of the ozone layer, which is centred at a height of about 25 km in the stratosphere, is not complete. At one time it was thought that the oxygen reactions alone, the so called Chapman classical theory, could account quantitatively for the observed ozone profiles. But as knowledge of the relevant rate coefficients and the natural distribution of ozone became more exact, it became apparent that the classical theory gave theoretical ozone profiles with total ozone much greater than that observed. This discrepancy was for a while accounted for by turning to the so called 'wet chemistry' thesis in which it was postulated that reactions involving water and its dissociation products were responsible for a higher ozone destruction rate than that of the classical theory. Again better measurements of the relevant chemical rate coefficients led to this explanation falling out of favour. The current suggestion^{1,3,4} is that naturally occurring nitrogen oxides in the stratosphere, possibly originating from the troposphere and high atmosphere, may play a significant role as a means of converting stratospheric ozone and atomic oxygen to molecular oxygen. It would appear² that 1 to 10 ppb nitric oxide in the stratospheric air is required to produce agreement between measurement and the nitrogen oxide photochemical theory. The actual amounts of nitric oxide in the stratosphere have yet to be established.

It is in this context that there has been much speculation^{2,3,4} in the literature recently that the oxides of nitrogen produced in the combustors of the jet engines of high flying supersonic aircraft could interact with, and so attenuate, the Earth's ozone shield and increase the ultra violet radiation reaching the planetary surface. It is fair to say that none of these papers contain the necessary full, quantitative consideration⁵ of the interaction of radiation, photochemistry and the atmospheric circulation. However, it is incontrovertible that under laboratory conditions NO and NO₂ convert ozone and oxygen atoms to molecular oxygen. Such considerations have resulted in the initiation of a number of research programmes in the USA, UK and France to study the climatic consequences of the operation of fleets of supersonic aircraft.

Any process which heats air above ~2300K will produce significant quantities of NO, as an equilibrium constituent. Examples of such heating include the shock waves from nuclear explosions as well as the operation of the combustion chambers of aircraft jet engines. The actual amount of nitrogen oxides remaining at ambient temperatures will depend upon the rate at which the heated air cools through the 2300K temperature region. It may be that man has already injected massive amounts of nitrogen oxides into the stratosphere during the various nuclear testing programmes.

2. The Shock Wave

In order to calculate the amounts of nitrogen oxides produced in the shock waves of nuclear explosions, it is necessary to know the pressure - temperature history of each parcel of air through which the shock front passed. The mathematical description of the spherical shock wave as given by Taylor⁶ was used to calculate the pressure - temperature histories of seven spherical surfaces enclosing fixed masses of air around the explosion centre. Values of pressure and temperature of each spherical shell enclosed by these seven surfaces were then obtained by averaging the values at the two boundaries. The innermost

shell (1) which includes the explosion centre was taken to have the temperature and pressure history of the first spherical boundary. This was carried out for explosions of 1, 10 and 60 megaton TNT equivalent. The results of these calculations are given in Fig 1.

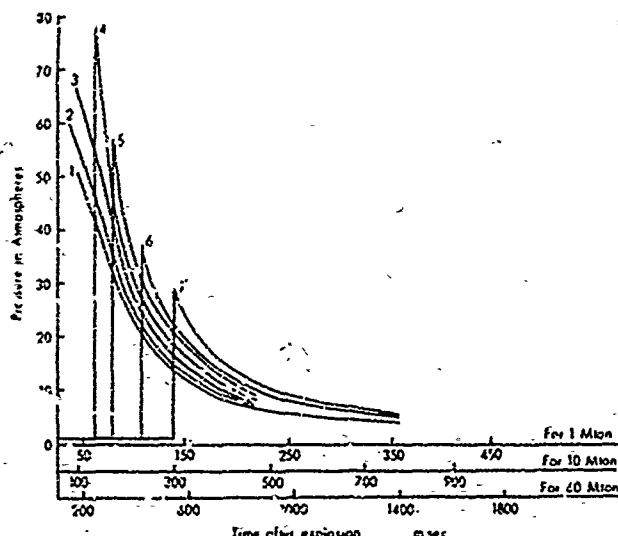


FIGURE 1a

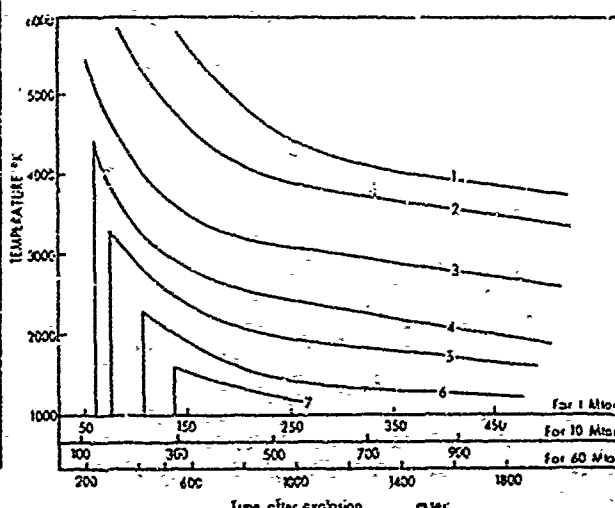


FIGURE 1b

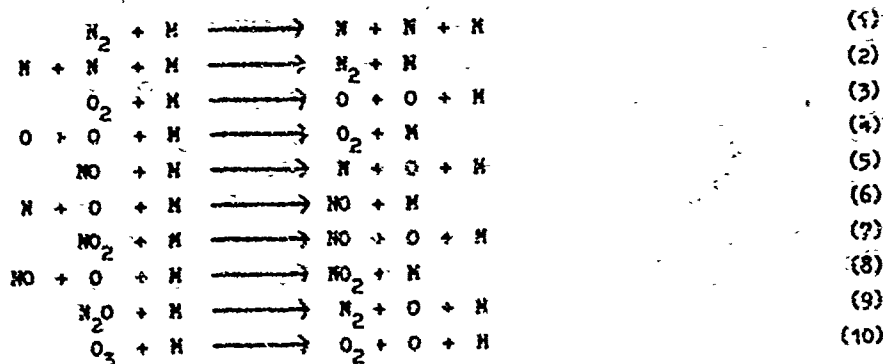
Zel'dovich and Raizer⁷ point out that the theory is not strictly applicable to the central regions of the explosion (shells 1 and 2) where radiative effects probably dominate. Also the theory becomes more approximate when the pressure in the shock front is less than about ten times that of ambient.

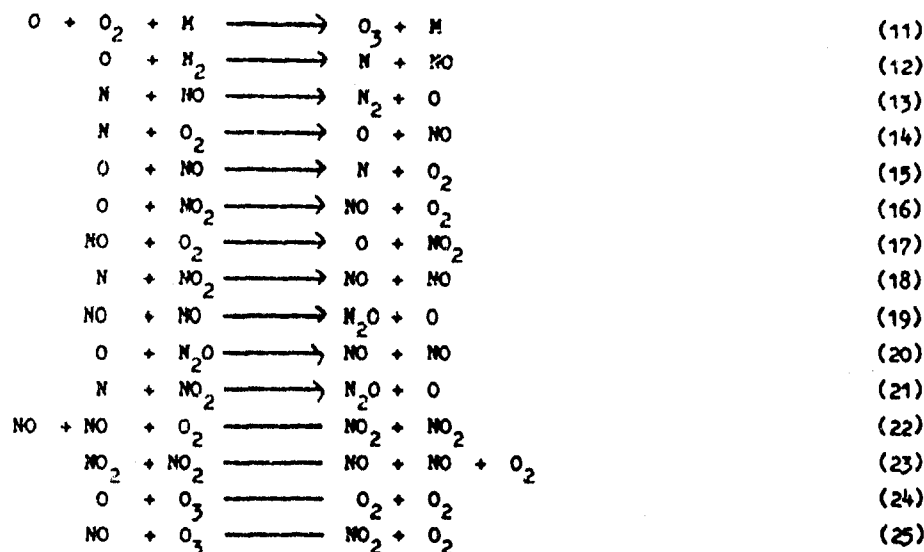
In arriving at the curves in Fig 1, a constant value of the ratio of specific heats γ , of 1.4, has been assumed. Although at higher temperature, γ is reduced from its ordinary tropospheric value of 1.4 by the absorption of energy in the form of molecular vibrational quanta, at very high temperatures increasing dissociation may be expected to compensate for this effect. Taylor noted that his calculations fitted the observed behaviour of the fireball in the first nuclear test in New Mexico better for $\gamma = 1.4$ than for $\gamma = 1.3$. The shock wave has been assumed to propagate spherically in a uniform atmosphere at 290K and 1000 mb. For the largest explosion considered (60 megatons), the radius of the 2000K surface is about 3 ks at which height this approximation is acceptable, as demonstrated by Korobeinikov's⁸ more accurate description of shock wave propagation in a real atmosphere.

3. Chemical Kinetics of Heated Air

The production of NO in shock-heated air has been directly measured in laboratory shock tube experiments at temperatures between 2300K and 6000K by Casaz and Feinberg⁹. Mole fractions of nitric oxide, $[NO]/[M]$, of up to 0.1 were observed; however, the experiments applied to short reaction times (several microseconds) and pressures from .01 to .07 atmospheres. This is in contrast to the conditions following a weapon burst, where, after a few hundred milliseconds, pressure relaxation rates are of the order of 50 atm s^{-1} and cooling rates are of the order of 2000K s^{-1} . The masses of the concentric shells of air heated above 2000K are typically of the order of 10^{12} grams. In these circumstances the best a priori way to calculate production of nitrogen oxides would be to start with a chemical kinetic mechanism composed of the elementary processes thought to be relevant and derive the set of simultaneous differential equations describing the variation in time of the number densities of the molecular species involved. These equations should then be solved, by numerical integration, for a particular air mass, through its pressure - temperature history as a function of time down to times and temperatures where the NO production and destruction rates are slow compared to the cooling rate.

The elementary chemical processes used in calculating the nitrogen oxide production in the hot air masses created by the nuclear shock wave are as follows:-





Excited species of both atoms and molecules have not been included, although some of these, for example $\text{O}(\text{ }^1\text{D})$, $\text{O}(\text{ }^1\text{S})$, $\text{O}_2(\text{ }^1\Delta)$, $\text{O}_2(\text{ }^1\Sigma^+)$,

$\text{N}(\text{ }^2\text{D})$, $\text{N}_2(\text{A}^3\Sigma^-)$, $\text{N}_2(\text{B}^3\Pi_u)$, $\text{NO}(\text{A}^4\Pi)$ and $\text{NO}(\text{A}^2\Sigma^-)$

may be expected to be populated or chemically produced at the higher temperatures. Justification for this omission is that the pressures which accompany the high temperature ensure that collisional deactivation of excited species is likely to be efficient.

Table I

Rate Coefficients

$$k = A T^N \exp(-E / 1.987T)$$

k in $(\text{cm}^3 \text{ mole}^{-1})^n \text{ sec}^{-1}$ units; E in calories per mole. ($n = 1$ for a 2 body process)
($n = 2$ for a 3 body process)

Reaction	A	N	E	Reference No.
(1)	3.73×10^{21}	-1.6	224, 900	10
(2)	2.25×10^{21}	-1.6	0	10
(3)	4.79×10^{18}	-1.0	118, 700	12
(4)	2.38×10^{17}	-1.0	340	12
(5)	2.27×10^{17}	-0.5	148, 830	13
(6)	6.45×10^{16}	-0.5	0	13, 11
(7)	1.54×10^{16}	0	65, 000	13
(8)	1.47×10^{15}	0	-1, 870	13
(9)	1.30×10^{15}	0	58, 000	14
(10)	3.89×10^{14}	0	22, 720	12
(11)	6.46×10^{12}	0	-2, 100	12
(12)	1.36×10^{14}	0	75, 400	13
(13)	3.10×10^{13}	0	334	13
(14)	6.43×10^9	+1.0	6, 230	13
(15)	1.55×10^9	+1.0	38, 640	13
(16)	1.00×10^{13}	0	600	13
(17)	1.00×10^{12}	0	45, 500	13
(18)	3.60×10^{12}	0	0	13, 15
(19)	9.40×10^{11}	0	66, 000	13
(20)	2.50×10^{13}	0	26, 900	13
(21)	1.20×10^{12}	0	0	13, 15
(22)	2.43×10^9	0	-1, 046	13
(23)	4.00×10^{12}	0	26, 900	13
(24)	1.20×10^{13}	0	4, 790	12
(25)	5.72×10^{11}	0	2, 460	33

The integrations were carried out using rate coefficients taken from recent authoritative reviews as summarized in Table I. With the exception of reactions 3 and 4, the rate coefficients have been adjusted for molecular nitrogen as the third body M. For reactions 3 and 4, the larger third body efficiencies of atomic and molecular oxygen were used. Where the reverse process of a reaction occurred, values were chosen to be compatible with the thermochemical equilibrium constant.

The integrations were carried out by a semi implicit scheme, programmed in ASSEMBLER, a low level IBM language. Initially, a simple Euler first order forward time step method was used to perform the integration. A prohibitively small time step of 10^{-10} seconds was required by this method. By setting nitrogen atoms and ozone to equilibrium, this was lowered to 5×10^{-7} seconds for shell 6, with its temperature of 2300K. The semi implicit method could run satisfactorily, without setting any species to equilibrium, using a time step of 10^{-6} seconds at 2300K, 5×10^{-7} seconds between 2300K and 3300K (shell 5), and 10^{-7} seconds between 3300K and 4400K (shell 4). The results obtained by the different methods at 2300K agreed closely; to have run the forward time step method at higher temperatures would have involved setting nitric oxide itself to equilibrium, defeating the purpose of the exercise. The semi implicit scheme used the relation:-

$$Y_{n+1}^{(i)} = \frac{Y_n^{(i)} + P_{(i)} \Delta t}{1 + Q_{(i)} \Delta t}$$

where $Y_{n+1}^{(i)}$ is the concentration of the i^{th} constituent at the $(n+1)^{\text{th}}$ time step, and $P_{(i)}$ and $Q_{(i)}$, functions of rate coefficients and concentrations of other species, are defined by the general chemical kinetic differential equation:

$$\frac{dY_{(i)}}{dt} = P_{(i)} - Q_{(i)} Y_{(i)}^m$$

where in this case $m = 1$ or 2 . At every time step each species was advanced in turn by this method, while the remainder were held constant. This method does not simultaneously solve all the continuity equations, and so cannot be guaranteed to conserve chemical identity (that is to say the total numbers of oxygen and nitrogen atoms). Chemical conservation was in fact obeyed quite well except in the few integrations which went to numbers of time steps greater than about 2×10^6 . However, in all cases, results are quoted from integrations where conservation of N atoms and of O atoms was ensured by scaling after each time step to the density implied by the pressure and temperature history derived from Taylor's equations. Results of typical integrations are shown in Fig 2. The rate coefficients were recalculated

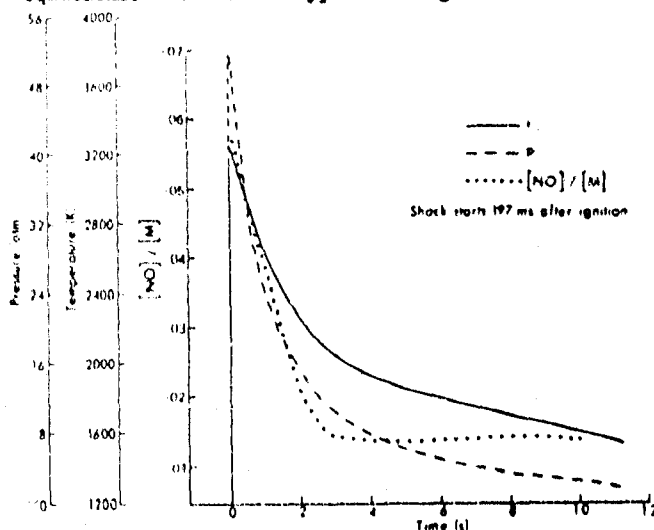


Figure 2b

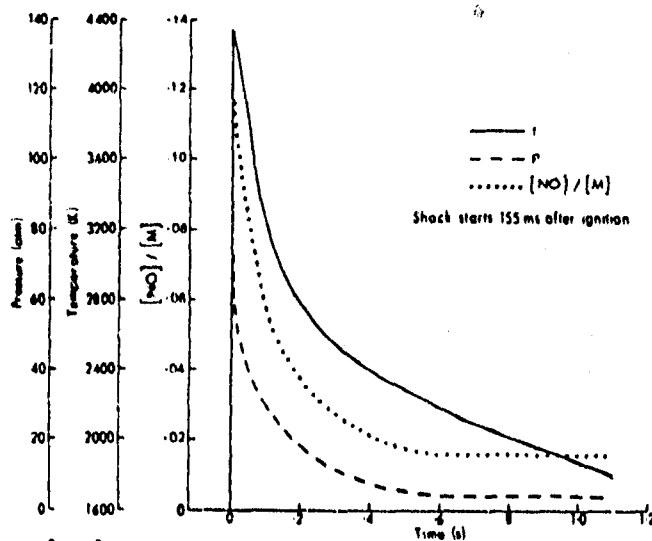


Figure 2a

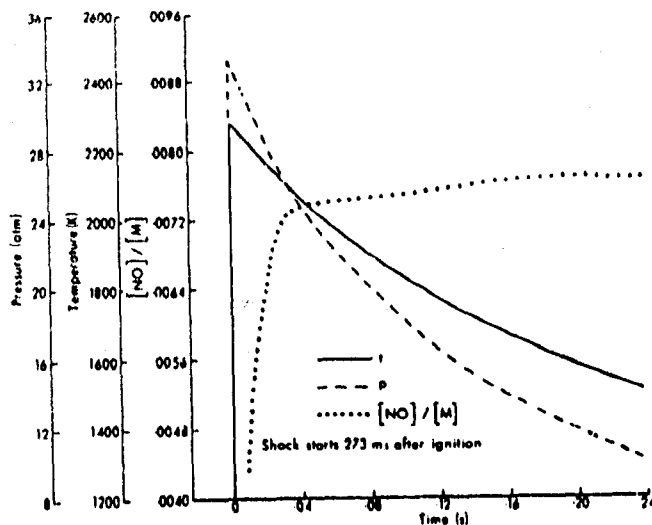


Figure 2c

at descending 50K intervals, after assuming a step perturbation of air from STP to the initial pressure and temperature values on each of the curves 4, 5 and 6 of Fig 1. The air in the outer shell 7 (Curve 7) never reaches a high enough temperature to produce significant amounts of NO.

The results of these calculations are given in Table II in which the nitric oxide yield for each concentric shell is listed, together with the total air mass in that shell for explosions of 1, 10 and 60 MT equivalent TNT.

It is seen that the NO yields for 1, 10 and 60 MT explosions were 0.49, 5.4 and 35.5 X 10¹⁰ gas respectively. The yield in the 1 to 10 MT range is about linear, with 5 X 10⁹ gas of NO being produced per MT of explosive energy. This linearity breaks down somewhat for the 60 MT explosion because in the outer-most of the shells producing significant amounts of NO (Shell 6), the NO production is slow enough to be dependent upon the time spent at high temperatures, rather than the cooling rate as is the case for the inner shells. 60 MT is about the size of the largest individual nuclear explosion ever made, in Russia in 1962.

The deduced production of 5 X 10⁹ gas per MT of explosive power can be compared with the findings of three previous studies:-

- (a) The first by D R Davies¹⁶ was primarily concerned with the chemical composition of the air in the shock wave and how the resulting changes in γ would affect the shock propagation. However,

Table II
Calculated NO production

Explosion Strength (megatons)	Shell No.	Air Mass in Shell (10 ¹² gas)	[NO] / [N]	[NO] 10 ¹⁰ gas	[NO] 10 ³² molecules
1	4	0.075	0.017	0.13	0.26
	5	0.145	0.016	0.23	0.46
	6	0.270	0.005	0.13	0.26
	TOTAL:-			0.49	0.98
10	4	0.75	0.015	1.2	2.4
	5	1.45	0.014	2.1	4.2
	6	2.70	0.008	2.1	4.2
	TOTAL:-			5.4	10.8
60	4	4.5	0.015	6.8	13.6
	5	8.7	0.013	11.1	22.2
	6	16.4	0.011	17.6	35.2
	TOTAL:-			35.5	71.0

he did conclude on the basis of a statistical mechanical treatment of equilibrium constants that at 4000K 4.6% of nitric oxide would be present. He also concluded that no NO would be produced at temperatures of 3000K or lower; that is because the statistical mechanical approach does not allow for the changes in the chemical reaction rates with temperature being slower than the rate of change of temperature. The amount of NO left after the passage of the shock wave was not of concern in this study.

- (b) In the second, Zel'dovich and Raizer¹⁷ assume that all the air that had been taken to temperatures greater than 2300K in the shock wave would ultimately have equilibrium NO concentrations frozen at values characteristic of 2300K when returned to ambient temperatures. On this basis they concluded that a 20 kiloton equivalent TNT explosion would yield a concentration of NO of about 1%, equivalent to about 50 tons. On a linear extrapolation this means that a 1 MT explosion would yield 2.5 X 10⁹ gas. This is about a half of the yield indicated by the more comprehensive calculations outlined in this paper.

- (c) In the third, Foley and Ruderman¹⁸ simply took one third of the liberated explosive energy yield as remaining as thermal energy in the buoyant hot air and assumed that this energy would be used in heating a mass of air to a temperature of 2000K. The physical basis of this assumption is not readily apparent from detailed studies of Taylor⁶ and Brde¹⁹. They further assumed that all this air instantaneously produced a concentration of 0.8% NO. The time scale for NO production for curve 6 of Fig 2 of the present paper demonstrates one limitation of this approach. However this simplified treatment of the physics and chemistry of nuclear explosions yielded a similar result (10¹⁰ gas of NO per MT explosive energy) higher than that of our method by a factor of two.

It is worthwhile at this stage to discuss some of the limitations of the treatment contained in this paper. In arriving at the nitric oxide production rate, the inner three shells, denoted in Fig 1, and containing 0.33 , 3.3 and 20×10^{12} gms respectively for 1, 10 and 60 MT events have not been included. This is not only because of the inapplicability of the Taylor formulations to these inner regions where radiative transfer may be relatively important but it might also be argued that these high temperature gases absorb the ionising radiations from the inner most region, so shielding the nitric oxide in the outer shells, 4, 5 and 6. The chemistry of a hot ionised air mass, subjected to radioactive emissions, is not easily modelled. Any nitric oxide production in these innermost shells will be additional to 5×10^9 gms per MT deduced from the outer shells. Also, all the calculations apply to a spherical shock wave. For explosions on or near the ground some of the energy would be absorbed in the earth rather than propagated in the atmosphere, leading to a somewhat smaller nitric oxide production.

As mentioned in section 2, a value of 1.4 for γ , the ratio of specific heats, was used in calculating the pressure-temperature histories of the shock wave. To test the effect of decreasing γ , the pressure-temperature histories were recalculated for a 10 MT event using $\gamma = 1.3$. The nitric oxide production was now attributed to shells 3, 4 and 5 rather than 4, 5 and 6. It was found that the total nitric oxide production was decreased to 4.5×10^9 gms per MT.

The overall calculated NO production for an explosion was found not to be very sensitive to variation to any one of the rate coefficients $k_3, k_4, k_{12}, k_{13}, k_{14}, k_{15}, k_{19}, k_{20}$ within their experimental limits. However, simultaneously setting the first six of these (k_3 to k_{15}) to their lower limits and the other two (k_{19} and k_{20}) to their upper limits, reduced total nitric oxide production to 2.7×10^9 gms per MT. Inspection of the course of the integrations showed that reactions 3, 12 and 14 were the main producers of nitric oxide and reaction 19 was the main destroyer. This is in agreement with the experimental observations of Camac and Feinberg. Thus the value of 2.7×10^9 gms per MT is a lower limit in the light of current knowledge of rate coefficients.

The amounts of NO_2 and O_3 generated by explosions also formed part of the solutions of the differential equations. It was found that NO_2 was always less than 1% of the nitric oxide production and that the O_3 production was negligible. The fact that the NO_2 amounts were so small provides some justification for omitting the higher oxides of nitrogen ($\text{NO}_3, \text{N}_2\text{O}_5$). In these calculations, the temperature history below 1500K was not considered. Needless to say there will be considerable conversion of NO to NO_2 as the air mass cools to ambient. This would account for the observations²¹ of an orange colour to the nuclear cloud at high altitudes.

The chemical model outlined in this paper is strictly speaking applicable only to dry air. In the real atmosphere, it is possible that a number of reactions involving water and its dissociation products should be incorporated. It is difficult to visualise a chemical mechanism at the relevant elevated temperatures by which water or its dissociation products at atmospheric mixing ratios could prevent the formation of NO. Species such as HNO , HNO_2 , HNO_3 have dissociation energies less than NO_2 , thus in the absence of some catalytic destruction of NO or NO_2 by H, OH, HO_2 and H_2O processes such as



cannot prevent the formation of NO in the shocked air masses. Further calculations on this point are in progress, but it is a fact that in the emissions of jet engines the gases contain high amounts of water and dissociation products and this does not apparently inhibit NO production.

3. Comparison with Nitrogen Oxide Production by Concorde

The recommended value²⁰ for the emission of nitrogen oxides from the Concorde's Olympus Mk 602 engines is 13.8 gms of NO per Kg of fuel consumed, which is rather larger than estimates based on measurements made at NGTE Pyestock. At a cruise altitude of about 55,000 feet the engine's fuel consumption is about 4550 Kg hr⁻¹ engine⁻¹. Thus assuming a trans-Atlantic crossing requires 2 $\frac{1}{2}$ hours flying time in the stratosphere, the total nitrogen oxide production per flight expressed in terms of NO is 670 Kg. Thus one Concorde crossing the Atlantic 4 times per day, each day of the year produces 9.8×10^5 Kg/yr of NO.

In Table III is given a year by year summation of all nuclear explosions^{18, 21, 22, 23} greater than 20 Kt TNT together with the associated NO production deduced from the calculated yield of 5×10^9 gms per MT. In the fourth column is the number of Concordes that would have to fly across the Atlantic four times per day, each day of the year to produce the same amount of NO as that year's nuclear weapon testing.

It is seen that the nuclear testing is equivalent during the period 1952 to 1958 to over 100 fully operational Concordes. During the two years 1961 and 1962, as many as 300 Concordes would have had to have been fully operational throughout the two years for the same gross NO injection. The assumption is made that all nitrogen oxides produced in explosions are ultimately transported into the stratosphere. Since the greater proportion of radioactive debris in an air burst of 1 Mt or greater is injected into the stratosphere²⁴, it is not unreasonable to assume that all nitrogen oxides will reach the stratosphere in a similar manner. Although Table III gives a summation of nuclear explosions greater than 20 Kt TNT, the total yield of explosions between 20 Kt, which probably do not inject material into the stratosphere, and 1 Mt, which probably do, is only a small proportion of the total. The inclusion of these low yield explosions will make no significant difference to the estimates of the stratospheric injection of nitrogen oxides.

Table III

The calculated annual NO production from all nuclear tests greater than 20 KT and the equivalent number of fully operational Concorde

Year	Megatons TNT	NO Production 10 ⁷ Kgm	Equivalent Number of fully operational Concorde
1952	11.1	5.5	54
1953	0	0	0
1954	48.5	24.2	237
1955	2.0	1.0	10
1956	26.0	13.0	127
1957	13.5	6.7	66
1958	61.9	30.9	303
1959	0	0	0
1960	0	0	0
1961	120.6	60.3	591
1962	213.5	106.7	1047
1963	0	0	0
1964	0	0	0
1965	0	0	0
1966	1.4	0.7	7
1967	3.5	1.7	17
1968	7.6	3.8	37
1969	3.0	1.5	15
1970	6.1	3.0	30
1971	1.6	0.8	8
1972	0	0	0

However, there will be obvious differences between the stratospheric cloud production due to aircraft emissions and that due to more rapid injections by explosives. In the latter case, the aircraft injections are confined to the limited region of air routes, and operate at flight altitudes in the lower stratosphere. The nuclear injections cover a much wider altitude range, depending upon the strength of the explosion; the cloud of debris from a 1 MT event typically stabilises at a height of about 22 km whilst that of a 10 MT event would reach about 32 km. Thus the Concorde emissions at the operational height of 17 km are always below the maximum in the vertical ozone profile, whilst the nitrogen oxides from nuclear explosions could well stabilise in the same height as the ozone maximum.

It must therefore be accepted that man has already directly injected into the stratosphere amounts of NO at least comparable with that expected from large fleets of Concorde aircraft. If the atmospheric ozone budget is sensitive to injections of anthropogenic nitrogen oxides then one would expect the effects of the nuclear testing programme to be reflected in the past records of total ozone amounts. This especially applies to the years 1961 to 1962.

4. Ozone Records

The total ozone amount in the atmosphere above any point on the earth's surface is highly variable, with large fluctuations from day to day and with a well established annual cycle which has a maximum in the early Spring and a minimum in the late Autumn. If the nitrogen oxides from the testing of nuclear weapons have affected total ozone amounts, then one would expect this to be reflected in the ozone records since 1952, with special emphasis on the years 1961 and 1962 when weapons yielding 334 MT were exploded, which is well over half the total explosive energy of all tests. Those tests prior to 1952 were all of less than 1 MT yield and contributed little to the total stratospheric injections.

Table IV

Ozone records of the stations used in figure 3

	Number of months	Mean total ozone	Slope % per decade	Error of slope (σ)
Arosa (47°N 10°E)	158	334	1.2	0.9
Cagliari Elmas (39°N 9°E)	161	329	8.6	0.9
Cambridge (50°N 5°W)	115	338	6.3	1.7
Edmonton (54°N 114°W)	162	357	2.9	1.0
Kagoshima (32°N 131°E)	151	289	1.9	1.2
Kodaikanal (10°N 77°E)	161	255	10.6	0.5
Lerwick (60°N 1°W)	151	348	7.2	1.2
Masaira (38°N 16°E)	141	346	3.5	0.9
Napoli (41°N 14°E)	137	301	-1.3	1.1
New Delhi (29°N 77°E)	159	270	7.8	1.1
Oxford (52°N 1°W)	162	353	4.3	1.0
Resolute (75°N 95°W)	143	351	3.6	1.8
Reykjavik (64°N 22°W)	134	339	-1.7	1.9
Sapporo (43°N 141°E)	155	371	1.0	0.8
Tateno (36°N 140°E)	160	325	0.0	0.9
Tromsø (70°N 19°E)	121	331	0.6	2.0
Vigna Di Valle (42°N 12°E)	162	341	1.1	0.9
Mean of stations	152	330	6.3	1.7

In Fig. 3, are plotted ozone data from the 17 stations in the N hemisphere with the longest continuous record. These are listed in Table IV. The deviation from the monthly mean, expressed as percentage of that mean, is plotted monthly as a function of time. In this way the annual and short term fluctuations are removed. Also the mean of the 17 stations was subjected to conventional five term binomial smoothing.

The stations were selected on the following criteria, the records (a) exist from 1957 or 1958, the beginning of the IGY period, when many more stations commenced operation (b) do not have gaps of more than 18 consecutive months in their data and (c) have over 110 monthly mean values for the total period 1957 to 1970. Stations making measurements with the Russian filter ozonometer were excluded because it has been demonstrated²⁵ that results from these instruments differ significantly from those of the Dobson ozone spectrophotometer for solar zenith angles greater than 60° or in the presence of haze. This may be important due to secular changes in haze (R. N. Kulkarni, private communication). Furthermore only ozone measurements in the N hemisphere are considered because the vast bulk of nuclear weapon debris has been injected there. In any case very few stations in the S hemisphere would have met the criteria of long term continuity. The periods of weapon testing together with total Megaton yield for each of nine periods are also indicated on Fig. 3. The 1961-62, American equatorial and Russian high latitude tests are separated on the diagram, with the American tests coming between the two periods of Russian tests.

It might be expected that if nitrogen oxides from the nuclear explosions are to modify the total ozone amount, then this would be reflected in the records, covering the N hemisphere, delayed by a period dependent upon stratospheric mixing times and relevant chemical reaction rates. It appears to us that these records do not provide evidence for such a modification.

However, it has been suggested by Johnston²⁶ et al on the basis of an analysis of the records of ozone measuring stations from 1960, including those in the USSR and some in the Southern hemisphere,

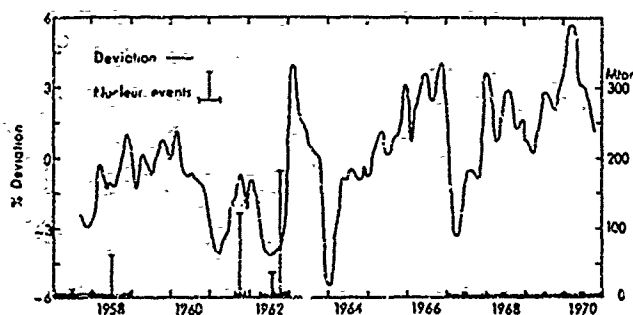


Figure 3

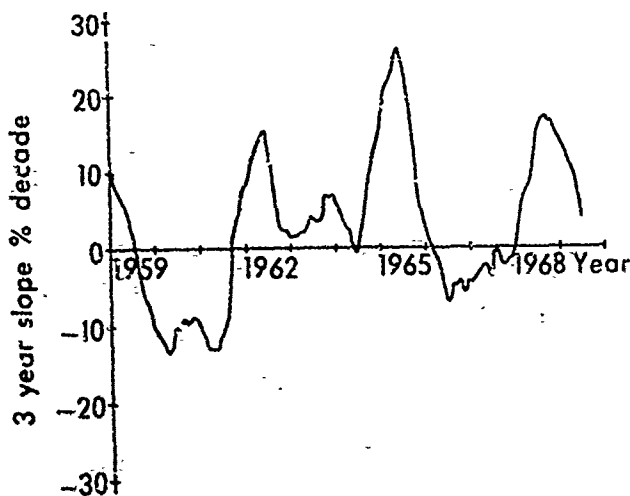


Figure 4

that in the Northern hemisphere there was a significant decrease (-7.6% per decade) in ozone during the period 1960-62, followed by an increase (+5.6% per decade) 1963-70. Johnston et al argue on the basis of these figures, that "oxides of nitrogen from nuclear bomb tests of 1952-62 constituted a measurable injection and the consequent reductions of ozone may be ascribable (perhaps only in part) to this injection experiment". They also speculate that the ozone increase 1963-70 may represent a recovery from the effects of the test period.

The ozone data going back to late 1957 given in Fig. 3, do not support the contention that the period 1960-62 is of any particular significance with respect to the periods of nuclear testing. Moreover there is considerable danger in comparing ozone trends over an interval of 3 years. This is demonstrated in Fig. 4, in which the three year slopes of the 17 station ozone records are plotted monthly. It is seen that the slopes vary between about +26% and -13% per decade and so there is no significance to the -7.6% per decade obtained by Johnston for the period 1960-62. Indeed during 1963-70, there was a period when the 3 years slope was also negative.

The upwards tendency of the trace of Fig. 3 since 1961 agrees with the findings of Koshyr et al²⁷ that there has been an increase of total ozone of up to 1% at a number of stations during the past decade (1961-1970).

There have been a number of other studies of trends of ozone based on much longer records of data. Notably Willett²⁸ and Christie²⁹, both on the basis of records going back to 1933, detected a negative and largely unexplained correlation of total ozone with sunspot number. The ozone minimum precedes the sunspot maximum by about 20 months. However, London and Olthaus³⁰ were unable to find such a correlation in the Arosa and Tromsø records, which formed the bulk of the Willett, Christie data before 1945. Paszold et al³¹,

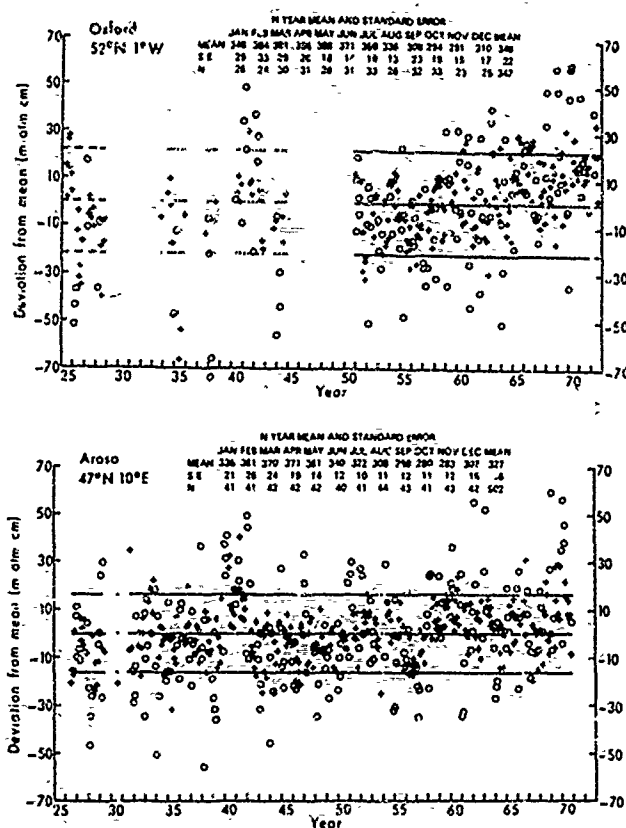


Figure 5

on the evidence of direct balloon-borne optical ozone soundings over central Europe between the years 1951 to 1972, report a positive correlation between sunspot number and the ozone amount between 20 and 30 km. The evidence for this correlation however is not conclusive due to the lack of data in the first half of the period.

There are only two ozone observing stations with reasonably complete long term records. These are Arosa and to a lesser degree Oxford, both from 1926. In Fig 5 the deviation from the monthly mean is shown for both these stations. The Oxford data between 1933 and 1944 have not previously been published, whilst those for Arosa are given by Perl and Dutsch³².

These long term records demonstrate the high variability in total ozone over a wide variety of time scales and indicate the difficulty in detecting any short term trends. In common with other data presented here, there is nothing to suggest that nitrogen oxides from the testing of nuclear weapons in the atmosphere have had any effect on the total ozone.

Final Remarks

In this paper the production of nitrogen oxides in the shock wave of explosions associated with the testing of nuclear weapons in the atmosphere has been calculated. This has allowed the total injection of nitrogen oxides into the stratosphere to be deduced for each year in which nuclear tests have taken place. These amounts have been compared with those expected from the engine exhaust products of fleets of Concorde each flying in the stratosphere for over 10 hours every day of the year. It is concluded that past nuclear explosions have been equivalent, as far as nitrogen oxide stratospheric injections are concerned, to large numbers of these fully operational Concorde. For instance, during the years of maximum nuclear activity, 1961 and 1962, the number of Concorde giving equivalent nitrogen oxide emissions would have been about 600 and 1000 respectively. Analysis of the ozone records reveal no detectable changes in the total atmospheric ozone during and after the periods of nuclear weapon testing. Although the two modes of nitrogen oxide injection may not be identical from the meteorological view point, the conclusion that massive injections of nitrogen oxides into the stratosphere do not upset the ozone layer seems inescapable. Such a conclusion has profound implications on our understanding of the photo-chemical processes in the stratosphere, since it is only by postulating an ozone sink due to natural nitrogen oxide at the 1 to 10 pph level that current theories are able to account for the natural concentrations of ozone in the stratosphere. It may be that other factors such as solar radiation, stratospheric circulation, refinement of chemical rate coefficients and hitherto unconsidered chemical sinks may all play a role in bringing theory closer to measurement.

Acknowledgements

The authors are grateful to Professor G M B Dobson for making available the hitherto unpublished Oxford ozone records and to R Smart who helped with the analysis of the ozone records. This paper is published by permission of the Director-General of the Meteorological Office.

REFERENCES

1. P J CRUTZEN J. of Geophys Research 76 p 7311 (1971).
2. H S JOHNSTON Catalytic Reductions of Stratospheric Ozone by Nitrogen Oxides. UCRL-20568 (1971).
3. H S JOHNSTON Science 173 p 517 (1971).
4. P J CRUTZEN Ambio 1 p 41 (1972).
5. Australian Academy of Science Report No 15. Atmospheric Effects of Supersonic Aircraft.
6. G I TAYLOR Proc. Roy. Soc. A201 p 159, p 175 (1950).
7. Ya. B. ZEL'DOVICH and Yu. P. RAIZER Annual Review of Fluid Mechanics 1, p 385 (1969).
8. V P KOROBENNIKOV Annual Review of Fluid Mechanics 3, p 317 (1971).
9. M CAMAC and R M FEINBERG 11th Combustion Symposium p 137 (1967).
10. J P APPLETON, M STEINBERG, D J LIQUORNIK J. Chem Phys 48 399 (1968).
11. I M CAMPBELL and B A THRUSH Proc. Roy. Soc. A296, p 201 (1967).
12. H S JOHNSTON "Gas Phase Reaction Kinetics of Neutral Oxygen Species" NBS-RS-NBS 20 Washington (1967).
13. D L BAULCH, D D DRYSDALE, D G JOHNS and A C LLOYD "High Temperature Reaction Rate Data" Vol 4 and 5
School of Chemistry, Univ. of Leeds (1969)(1970).
14. J TROE and H-Gg. WAGNER Ber. Bunsenges. Phys. Chem 71 p 937 (1967).
15. M A A CLYNE and B A THRUSH Trans Farad Soc 57 p 69 (1961).
16. D R DAVIES Proc. Phys. Soc. 111, p 105 (1948).
17. Ya. B. ZEL'DOVICH and Yu P RAIZER Physics of Shock Waves and High Temperature Phenomena. New
York Academic Press (1967).
18. H M Foley and M A RUDERMAN Institute for Defense Analyses Paper P 894 (1972).
19. H L Brode Ann Rev Nucl Sci 18 p 153 (1960).
20. M Z WILLIAMS Proceeding of Second Conference of the Climatic Impact Assessment Programme, Nov 1972.
21. S GLASSTONE E., Effects of Nuclear Weapons, revised edition, US Atomic Energy Commission (1962).
22. Federal Radiation Council, Estimates and Evaluation of Fallout in the UFA. (1968).
23. Health and Safety Lab (HASL) New York Report 142 (1964).
24. Report of the United Nations Scientific Committee on the Effects of Atomic Radiation (UNSCEAR)
General Assembly Official Records, 17th Session Supplement No 15 A/5216 (1962).
25. R J BOJKOV J. Applied Met. 8 p 362 (1969).
26. H S JOHNSTON, G WHITTEN and J HIRKS "The Effects of Nuclear Explosions in Stratospheric NO and
Ozone". Lawrence Berkeley Lab Report LBL 1421 (1972).
27. W D KOMBLY, E W BARRATT, G SLOCUM and R K WEICKMAN Nature 232 p 390 (1971).
28. H C WILLETT J. of Geophys Res. 67 p 661 (1962).
29. A D CHRISTIE Proceedings IAHAP Ozone Symposium, Arona 1972. Pure and Applied Geophysics (in
press).
30. J LONDON and S OLTMANS Abstracts of IAHAP Ozone Symposium, Arona 1972.
31. H K PAETZOLD, F FISCALAR and R H ZSCHORNIGER Nature, Phys Sci 240 p 106 (1971).
32. G PERL and H U DOTSCH Annalen der Schweiz Meteor Zentralanstalt 10.8. (1958).
33. M A A CLYNE, B A THRUSH and R P WAYNE Trans Farad Soc 60, p 359 (1964).
34. V M KOMASHENOK Fiz Atm i Okeana (Moscow) 4 p 797 (1968).

LEGENDS TO FIGURES

1. Pressure (a) and Temperature (b) histories for seven shells due to the shock wave around 1, 10 and 50 MT explosions;

Shell No	Mass in units of 10^{12} gm per shell		
	1 MT	10 MT	50 MT
1	0.115	1.15	6.9
2	0.115	1.15	6.9
3	0.103	1.03	6.2
4	0.075	0.75	4.5
5	0.145	1.45	8.7
6	0.273	2.73	16.4
7	0.283	2.83	17.0

- Fig 2. Nitric Oxide concentrations as a function of time for a 10 MT explosion for (a) shell 4 (b) shell 5 and (c) shell 6. The pressure and temperature histories are also plotted.
- Fig 3. Smoothed deviations from monthly means of total ozone from 17 stations in the period 1957 to 1970 and the intensity and timetable of nuclear explosions in this period.
- Fig 4. Percentage increase expressed in % per decade for the total ozone calculated from the deviations of the monthly means for 17 stations over 5 yearly intervals from 1959 to 1969.
- Fig 5. Deviation of monthly total ozone from the mean of that month for Oxford and Arosa from 1925 to 1971. Points for January to March inclusive, when the total ozone is at its most variable, are denoted by o, whilst + is used for all other months.

Discussion on Paper 3
 "Nitrogen Oxides, Nuclear Weapon Testing, Concorde and Stratospheric Ozone"
 presented by P. Go'smith

R S Johnston

As I pointed out in my talk, the effect of nitrogen oxides on stratospheric ozone depends both on the quantity and the distribution. Let me comment on each of these separately with respect to this paper:-

A. The shock-wave theory used in this paper involves simplifying approximations that profoundly change the very quantities they wish to calculate. It appears that Goldsmith et al did not apply corrections for the cooling of the shock wave by the endothermic dissociation of oxygen. At 6000°K, for example, O₂ is almost totally dissociated to atoms; and each such dissociation removes 118 kilocalories per mole from the kinetic energy of the shocked gases. This strongly endothermic reaction would reduce the temperature and slow down the shock wave in their zones 1, 2 and 3; and this attenuation of the strength of the shock wave would be propagated into regions 4, 5 and 6. The maximum temperature attained is thereby strongly reduced in all zones. It is not a matter of whether it should be 1.4 or 1.3; the failure to include the chemistry of dissociation in the fluid dynamics of the shock wave is to neglect one of the most important energy terms in the problem.

On this matter, it may not be necessary to speculate or to carry out calculations with highly approximate models of spherical shock waves. It appears that spectroscopic observations of NO_x in nuclear explosions were carried out in 1953. Let me quote excerpts from an unpublished document from the Lawrence Livermore Laboratory:

Memorandum, June 23, 1971 to Harry Reynolds from Norman Bonner. "...the only real data that emerged were the NRL spectral measurements on fireballs in the 1953 series at NTS. These were summarized in JAMS - 1955 by De Witt."

"(1). In JAMS - 1955, De Witt summarizes the data on NO_x. The presence of NO is not observed, but NO₂ and HNO₂ are observed. (The absence of NO is perhaps not surprising since there is about 20 times more ozone produced than NO₂. Ozone reacts rapidly with NO, so the presence of ozone almost automatically rules out NO)."

"For several shots of about 10 kt the light absorption by NO₂ bands reached a maximum at about the time of the temperature minimum. The amount of NO₂ was equivalent to roughly a 0.4 mm column of NO₂ at standard conditions (1 atm, 0°C)."

"The radius of a fireball at the minimum is $W^{0.4}$ ft if W is in kt (Glasstone). Thus a 10 kt fireball would have a radius of about 250 ft, or 75 metres."

"If the NO₂ is uniformly distributed in the fireball, the mole fraction of NO₂ will be $0.4 \text{ mm}/75 \text{ m} = 5 \times 10^{-6}$."

The volume of a sphere with 75 meters radius is $1.76 \times 10^{12} \text{ cm}^3$. If NO₂ is 5×10^{-6} of this volume, its partial volume is $8.8 \times 10^6 \text{ cm}^3$. At 2.68×10^{19} molecules cm^{-3} (STP), the number of molecules of NO₂ is 2.4×10^{26} for the 10 kiloton shot, which scales to 2.4×10^{28} for a megaton bomb. The figure derived by Goldsmith et al is 2×10^{32} molecules of NO per AT, which differs from experimental observations by a factor of 8000. Note that ozone was observed spectroscopically, whereas Goldsmith et al say ozone was negligible.

There appears to be a major conflict between this shock-wave theory and the observations made on the fireballs in 1953. It is possible that there were errors in the experimental data or in the interpretation of that data. In any case, the approximations used by Goldsmith et al are such as to cause them greatly to overestimate the amount of nitric oxide that would be produced by the shock mechanism.

A detailed treatment of the nuclear explosion, the radiation effects, the shock wave including molecular dissociation, and the state of the primary fireball after the shock wave has left and as it reaches 6000°K have been worked out by Bethe, Brode, Gilmore, and others. These results are summarized by Brode, and his article should be the starting point for studies of this problem. A mass of air equal to the 6000°K fireball is the minimum mass of air that will have a "frozen-out" solution of nitric oxide with a mole fraction of $(5 \text{ or } 8) \times 10^{-3}$ (the equilibrium value at 2000°K). The maximum mass of air that can attain the characteristic freeze-out mixture of nitric oxide is that which can be heated to 2000°K by mixing together the 6000° fireball and ambient air. If the cold air is blended with the hot air so that the coolant air always reaches a temperature of 2000° or more, the maximum yield of nitric oxide is attained. If the hot air is rapidly injected jet by jet, so to speak, into the surrounding cool air such that the coolant air never reaches 2000°, then the minimum yield of nitric oxide is realized. The ratio of the maximum yield to the minimum yield is the ratio of the enthalpy function ($H_T^\circ - H_{298}^\circ$) at 6000° to that at 2000°, including the energy of molecular dissociation in the enthalpy functions. This ratio is approximately 6.

Let me give another quotation from the memorandum by Norman Bonner:

"I have made an estimate of the maximum credible production of NO_x ... I have made the assumption that the 2000° equilibrium concentration exists throughout the volume of air that has been heated (by shock or otherwise) to at least 2000° ... (A. Brode, Annual Reviews of Nuclear Science, 1968)."

The maximum yield of nitric oxide found by Bonner is 0.8×10^{32} molecules of NO per megaton bomb yield. The revised estimate of the maximum nitric oxide production as given by Foley and Ruderman is 1.0×10^{32} molecules NO per MT. The minimum yield of nitric oxide predicted by this model is 5.13×10^{26} /MT by Bonner and 5.17×10^{26} /MT by Foley and Ruderman. The low NO_x yield observed (Lind - 1955) so short time is perhaps to be interpreted as showing the relative unimportance of the shock mechanism in forming NO_x. Perhaps these observations do not include the period of entrainment-

cooling of the fireball to 2000° . (The report LAMS - 1935 is still classified, and the experimental data are not given in the memorandum by Banner).

These estimates of NO production do not include the effect of wash-out by the precipitation that occurs in the bomb cloud as it approaches ambient temperatures in the upper troposphere or lower stratosphere.

The high solubility of HNO_3 and $(\text{NO} + \text{NO}_2)$ in water indicates a much higher primary wash-out of NO_x in the bomb-induced precipitation than the wash-out for products such as strontium-90.

B. The distribution of nuclear debris in the stratosphere is known, in terms of measured ^{90}Sr , excess ^{14}C , etc. Over 90 per cent of the explosion yield in the 1961-62 series occurred at 75°N , above the arctic circle at Novaya Zemlya. Over 75 per cent of this 90 per cent occurred in September through December, during or just before the arctic night. The nitric oxide catalyzed decomposition of ozone is a photochemical reaction, which does not occur during the arctic night. The ozone forming region of the globe is indicated by Figure 10 in my report. There is relatively little overlap between the spatial distribution of ^{90}Sr during 1962-70 and the ozone forming region. Much of the nuclear debris remained at low elevations and at far northern latitudes. If a realistic estimate is made of how much nitric oxide was produced by the nuclear bombs, it is found that the distribution in space and time was such that the ozone column should have been reduced by only a few per cent at most, and it should have taken at least five years, 1963-68 to build back up to pre-1961 levels.

P Goldsmith

The reply to Prof. Johnston's points is better made if the whole subject of nuclear weapon shock waves and the subsequent chemical kinetics is seen in context.

It is of course true that the propagation of a shock wave through a fluid medium requires knowledge of the internal energy on each side of the strong shock front (which for gases appears to be typically of the order of a mean free path thick). This presents no difficulties for the air in advance of the front; however, the composition and hence internal energy of the air immediately behind the shock front is determined by the recent history of the shock itself. Thus to solve the problem accurately, one should in principle, numerically integrate the equations of motion coupled with the appropriate kinetic equations describing the temporal evolution of the composition. At temperatures greater than about 7000K, air becomes ionized to a significant degree; there is insufficient knowledge of the individual chemical and physical processes in such conditions to successfully model the composition. This difficulty may be circumvented by using empirically measured values of γ , the ratio of specific heats, as a function of temperature. However, even this may not be satisfactory, for the reason that local thermodynamic equilibrium may not exist behind the shock front. It seems likely that the diatomic gas immediately behind the shock front will be in translational, and probably rotational equilibrium; however, it will not be in vibrational or chemical equilibrium. There may well not be time during the shock's traversal of a mean free path for large amounts of dissociation to take place; hence deposition of energy by the shock front in dissociation of N_2 and O_2 molecules may not slow the propagation to the degree that Johnston suggests. This may offer an explanation of why the Taylor theory predicts for a 1 Mt event, 130 msec to reach the 2000K surface when $\gamma = 1.4$ and 90 msec when $\gamma = 1.3$. This is in reasonable agreement with Brode's statement: "At a time of about 80 msec for this example of 1 Mt at sea level, the shock wave has expanded and weakened to such an extent that the shock temperature is relatively low, of the order of 2000°....". This suggests that our treatment, particularly with $\gamma = 1.3$ is not invalidated by Johnston's argument as far as speed of shock propagation is concerned. However, as the chemical kinetic processes use up energy, the resultant, shocked gas will cool more rapidly than in a non reacting gas. Our chemical kinetic modelling shows, however, that equilibrium calculations of composition are of little value in the 2000-7000K region. Thus, although pure oxygen is largely dissociated at 6000K, under the conditions in the cooling shocked air masses a "local equilibrium" is set up between our reactions 12, 13, 14 and 15, resulting in a much lower oxygen atom number density and a higher nitric oxide number density than predicted by an equilibrium calculation including reactions 3 and 4. This effect was predicted by Duff and Davidson, and observed by Camac and Feinberg; it is also apparent in our chemical kinetic results. This means that even if dissociation and hence chemical kinetics were important immediately behind the shock front, the energy loss in the 2000-7000K region would not be as large as if molecular oxygen were being dissociated; it costs ~ 118 kcal to dissociate a mole of oxygen molecules, but only ~ 42 kcal to produce two moles of nitric oxide from a mole of nitrogen and a mole of oxygen. The fact that one would be dissociating NO instead of O_2 also moves the effect to higher temperatures and smaller radii, so decreasing the impact upon our results. Because the ionization potential of nitric oxide is rather less than the dissociation energy of molecular nitrogen, modelling the composition above about 7000K is difficult. Above 10000K the strongly shocked air first cools and is then reheated by the diffusional advance of the radiation front; this further complicates consideration of the inner regions. We have therefore deliberately excluded any nitric oxide production from air gas - which have reached temperatures higher than about 5000K; it seems unlikely, however, that no nitric oxide will result from dissociated and ionized air upon cooling, so that we have probably underestimated in this respect.

However as far as coupling between chemistry of dissociation and the fluid dynamics of the shock wave is concerned, it must be remembered that since the time taken for the shock to traverse a mean free path, and the shock front is only a few mean free paths thick, is somewhat shorter than the time scale of the chemistry, the absorption of energy from the shock by chemical processes is not of major importance. In view of this the chemistry should be coupled with the cooling curve rather than the shock propagation. Because of the relatively small conversions to nitric oxide and the low concentrations of free nitrogen and oxygen atoms this should not greatly affect our calculations away from the hotter inner core.

Finally, an important point to be made on this issue concerns the definition of the shock strength of nuclear explosions. It is my understanding that the weapon energy yield, expressed in megatons of TNT equivalent, is defined by the observed shock. Taylor has analysed photographs of the first atomic explosion in New Mexico. He applies his blast wave theory to the position of the front as a function of time for radii between 10 and 185 metres. He deduces that the energy, in the absence of radiation, dissociation or ionisation, required to drive the observed blast wave is equivalent to about 17 KT taking $\gamma = 1.4$. One can also show that Taylor's analysis also predicts about the right temperature of the gas immediately behind the shock front when it ceases to be luminous; for air this is about 2000K. The photographs suggest that the shock wave and fireball separate at a radius of 130 metres. At this point Taylor's model gives a front temperature of about 2400°K for $\gamma = 1.4$.

If all other assessments of the energy of explosions describe the shock wave so accurately then our description of the temperature and pressure profiles for the regions around 2000°K must be fairly realistic.

Referring to the measurements quoted by Professor Johnston, it is difficult to comment upon quotations from unpublished documents. But, the following comments may be pertinent.

Dr Johnston himself has pointed out (LEL 1421) that the ultra-violet radiation from the fireball itself will produce ozone in the air outside the shocked air masses, and so the detection of this ozone in no way invalidates our finding that ozone production by the shock wave is negligible. Moreover the observations of nitrogen compounds must have been made through the ozone which would prevent reliable observation, whether by absorption or emission, of the spectra of gases in the shocked air mass at wavelengths less than 290 nm. It is perhaps no coincidence that the gases observed, NO_2 and HNO_2 , emit in the UV or visible beyond this wavelength. If infrared observation was used, it is again not likely that NO would be observed. I hope the observations will be published so that their full relevance to the nitrogen oxide production can be properly assessed.

With regard to the NO_2 measurement, a study of the temperature dependence of the $[\text{NO}]/[\text{NO}_2]$ ratio in our (non-equilibrium) calculations shows that it is extremely unlikely that NO_2 will be uniformly distributed in the fireball. In fact, it is likely to be in the cooler outer shell, where at 1500K we calculate a mole fraction of $\sim 10^{-4}$, in good agreement with Zel'dovich and Raizer, but a factor of 20 lower than De Witt's figure for a uniform distribution in the whole fireball. Again, without further detailed information about the nature and time resolution of the spectral observations, considered conclusions are impossible.

With regard to the last point, concerning the "freezing out" of $(7 \text{ or } 8) \times 10^{-3}$ mole fraction of NO, the equilibrium concentration at 2000K, it will be seen that we have covered this point in our paper, where we demonstrate the inadequacy of equilibrium treatments (consider the NO production in shell 6 for the different sizes of weapon). Further, the physical mechanism by which the 6000K air mass is produced is not satisfactorily explained; our point is that the shock wave has produced the nitric oxide in an air mass which has cooled well below 2000K before significant mixing or ascent has commenced.

The agreement between Bonner's figure of 0.8×10^{32} molecules of NO per megaton as the maximum credible production, Foley and Ruderman's figure of 10^{32} molecules of NO per megaton (apparently after reduction by a factor of two to allow for the specific heat of air at 2000K) and our figure of $\sim 10^{32}$ molecules of NO is fortuitous in view of differences in the treatments of the chemical kinetics used. We have used what is in principle the correct method, namely integration of the chemical kinetic equations through the pressure-temperature histories of the heated air as it cools to temperatures below 2000K. It is quite clear from this that equilibrium treatments are invalid, and that the relative rates of the chemical kinetics and the cooling processes need to be calculated properly for each individual pressure-temperature history.

The point about HNO_2 , NO and NO_2 being soluble in water is not relevant since we know that virtually all the radioactive debris from an air burst of greater than about 1 MT is transported into the stratosphere, despite the fact that many of these radioactive products are soluble or act as condensation centres for the cloud droplets. There is no reason why the soluble nitrogen compounds should not be similarly transported to and stay in the stratosphere.

Finally, Professor Johnston's point about the importance of the distribution of injected nitrogen oxides applies equally to its vertical, as well as its latitudinal distribution. Nor can the question of distribution be properly considered without taking into account the consequences of the atmospheric motions in the stratosphere. This especially applies to the ozone in the lower stratosphere which is not produced there by photochemistry but is itself a consequence of the transport processes. It is my view that an acceptable theoretical assessment of the impact of anthropogenic nitrogen oxides must await the outcome of complex numerical global models of the stratosphere which incorporate a realistic description of these motions and their driving forces interlinked with the photochemistry.

Meanwhile, there is no doubt that ozone records subsequent to the periods of nuclear tests, many of which were in equatorial regions and injected material at the levels of ozone maximum, show that these injections have not effected the ozone to any detectable degree. This fact gives some degree of confidence that the models will ultimately show that the ozone levels in the atmosphere are not in a delicate state of balance as far as nitrogen oxides from Concordia are concerned.

A K Oppenheim

The computations of the effect of atom bomb explosions on which the authors based most of their conclusions left out some important phenomena - principally those associated with transport processes - that may affect their results by perhaps orders of magnitude.

P Goldsmith

I think my reply to Dr Johnston covers this point.

R J Gelinas

Studies of O_3 response to NO injections by nuclear tests seem to consider only mean densities, which are subject to large fluctuations from natural causes alone. Consideration of mean square densities via autocorrelation functions, or their power spectra, on existing O_3 concentration data should provide a systematic means of assessing characteristic periods, or frequencies, associated with causal mechanisms, eg diurnal variations, seasonal forcing functions, solar variations, and "external" forcing functions eg nuclear tests. Better yet would be cross-correlation analysis of O_3 concentrations with radioactivity level data, in that such analysis often filters out unwanted noise. Indeed, correlation analysis on existing data can provide a guide as to the extent to which cause and effect has any significance at all in the available data.

Question: Have you, or others, attempted such an analysis on the existing data base?

P Goldsmith

The authors we have cited, Willett (1962), London & Oltman, and Christie (1972), have clearly made use of both autocorrelation and cross-correlation techniques, and we have ourselves considered the investigation of the contribution of various time scales to the total variance of the ozone amount by means of the F-test. But the fact that most of the testing of high yield nuclear weapons in the atmosphere was confined to two closely spaced campaigns in 1961-62 severely limits the usefulness of any cross-correlation techniques. It is computationally possible to find the cross-correlation of the ozone amount with a Heaviside step function, but it will not tell you anything that is not implied by the naive calculation of means before and after.

E Hestvedt

This paper certainly represents an important contribution to the discussion on the effect of NO_x emissions upon the ozone layer. I see no reason to doubt the computations and am fully willing to accept the figures given for bomb-injected NO_x . However, I have a feeling many will draw the conclusion that the bomb-tests had no effect on ozone. This is not what the author said. The conclusion to be drawn is that the bomb tests did not result in a decrease in ozone which can be seen in the ozone records. We know that large variations in ozone, from day to day and from year to year, are caused by variations in the circulation. Variations in ozone of the order of a few per cent, for instance caused by bombs or SST, are unlikely to show up in the records.

DETAILED EXHAUST EMISSION MEASUREMENTS OF THREE DIFFERENT TURBOFAN ENGINE DESIGNS

A. W. Nelson, Pratt & Whitney Aircraft, 400 Main Street, East Hartford, Connecticut 06108, USA

A series of test programs was conducted to better define the exhaust emission characteristics of three different P&WTM engine models: the JT3D, a low bypass ratio turbofan engine; the JT8D, a mixed flow turbofan engine; and the JT9D, a high bypass ratio turbofan engine. Special investigations were conducted on the JT3D and JT9D engines to investigate inlet temperature and humidity effects. Analysis of these data was supplemented with previously obtained data in order to increase the range of variables investigated. For the mixed flow JT8D engine, special tests were conducted using an engine especially modified to physically separate the fan and core engine streams so that true undiluted emission measurements could be obtained. Three different methods were used to evaluate the emission levels of each engine model: multipoint rake, exhaust case pressure probes and super-detailed traversing. Analysis of the latter method produced highly refined contour plots of CO, THC and NO_x emission footprints as well as exhaust temperature and pressure variations at the plane of the tailpipe. The average emission levels obtained by each of the three measurement methods are compared.

During the summer of 1971, the Environmental Protection Agency (EPA) contracted with several different test organizations to conduct a series of aircraft engine exhaust emission measurement programs. The results of these test programs were compiled and analyzed by the Cornell Aeronautical Laboratory, Inc., and were reported by References 1 and 2. The results showed a significant scatterband for practically all of the engine models tested. The scatter of the data for one standard deviation in the Environmental Protection Agency Parameter (EPAP) units (pounds of pollutant per 1000 pound thrust-hour per cycle) for the various turbojet and turbofan engines is shown in Figure 1. Included in the EPA documentation programs were the three Pratt & Whitney Aircraft (P&WTM) engines which are most widely used in today's commercial aircraft fleets, both U.S. domestic and world wide: the JT8D turbofan engine which powers the shorter range Boeing 737, 727, the McDonnell-Douglas DC-9 and Dassault Mercure aircraft; the JT3D turbofan engine which powers the longer range Boeing 707 and McDonnell-Douglas DC-8 aircraft; and the JT9D high bypass ratio turbofan engine which powers the Boeing 747 and the McDonnell-Douglas DC-10-40 jumbo jet aircraft.

ONE STANDARD DEVIATION AS A PERCENT AGE OF MEAN EMISSION LEVEL

ENGINE	JT3D	JT3C	JT3D	JT4A	JT8D*	JT9D	2PEY MK/5.1
NO. OF ENGINES MEASURED	8	7	26	3	26	9	4
CO	±11.8	±38.8	±47.5	±26.7	±43	±19	±22.2
THC	±21.8	±59.4	±60.8	±23.4	±40.0	±38.0	±28.2
NO _x	±13.5	±19.1	±11.8	±17.5	±15.5	±18.7	±6.7

* BASED ON SO-CALLED "DILUTED, SMOKELESS" JT8D EPA PROGRAM DATA

Figure 1 Data Scatter in EPAP Units for Various Turbojet and Turbofan Engines

Because of the importance of these engines in the world's commercial aircraft fleets, and in order to attempt to establish the causes for the significant data scatter in the EPA-sponsored programs, Pratt & Whitney Aircraft has conducted a series of independent programs involving these three engine models. The data scatter noted in the EPA-sponsored programs could be attributed, in varying degrees, to the following factors:

- Ambient temperature and humidity
- Run-to-run differences
- Engine-to-engine differences
- Instrumentation variations
- Facility-to-facility differences.

and in the case of mixed flow turbofan engines:

- Sampling problems due to fan air dilution.

JT3D Engine Test Series

Ambient temperature and humidity variations between test runs were considered to be two of the more important factors affecting the levels of exhaust emission constituents. A program was established to investigate the effect of these two factors on emission level, as well as to determine the emission variations in the plane of the tailpipe. The engine selected as the test vehicle for this investigation was the JT3D turbofan engine, which has a low (1.4:1) bypass ratio and is in the 18000 pound (EPA T2) thrust class. The results of this program are fully described in Reference 3. In summary it was found that the levels of carbon monoxide (CO) and the oxides of nitrogen (NO_x) are significantly affected by changes in both inlet temperature and humidity, while the level of hydrocarbons (HC) was found to be affected by humidity alone. These trends (and because of data set uncertainties, they should only be considered as trends) were obtained by the use of emission math models developed by statistical methods (regression analyses) using both the data obtained in the P&W independent program plus all of the JT3D data obtained in the EPA-sponsored programs. By

selecting specific engine power conditions, it is possible to examine, by the use of the models, the trends of emission level with changes of these ambient variations. The result at idle power for CO is shown in Figure 2. The variation of NO_x at takeoff power is shown in Figure 4.

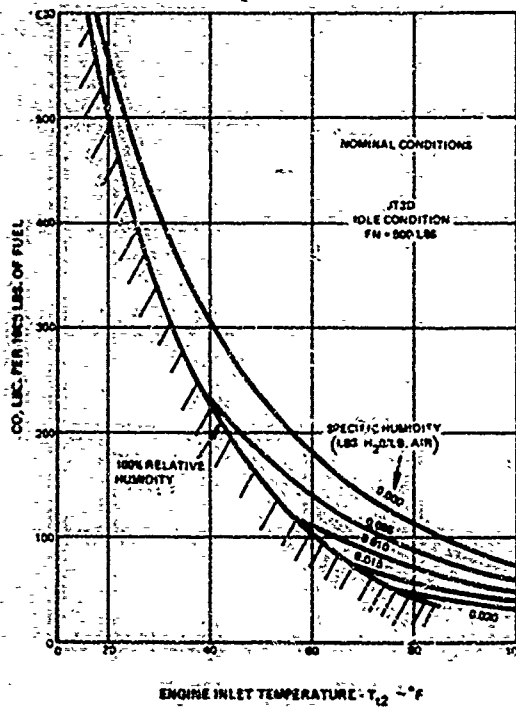


Figure 2 CO Trends with Ambient Changes at Idle Power

(FIGURE 3)
(NOT USED)

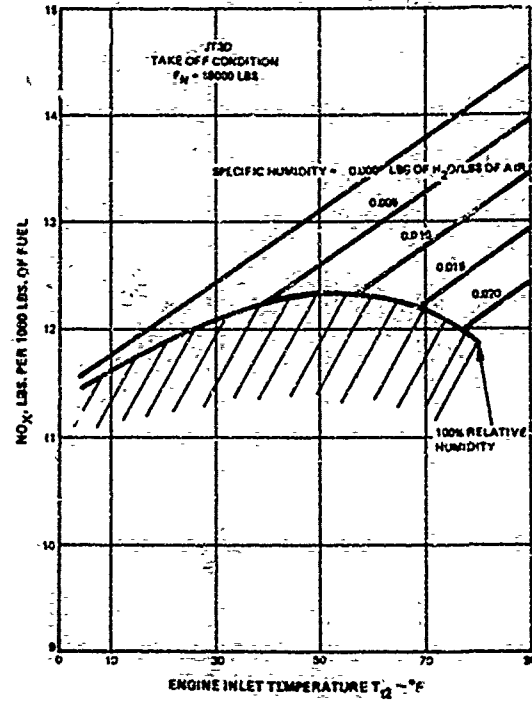
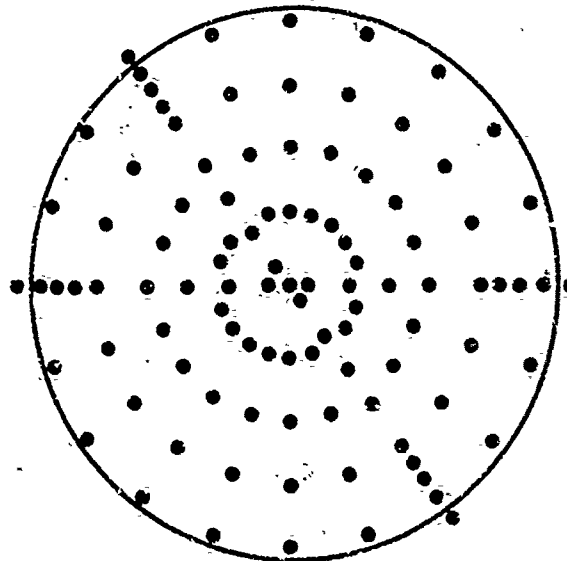


Figure 4 NO_x Trends with Ambient Changes at Takeoff power

Traverses taken at the plane of the tailpipe using the very detailed grid pattern shown in Figure 5 were analyzed to determine both the area-weighted average emission level and the variations in emission levels at the tailpipe plane. These isopleths for CO, HC and NO_x are shown in Figures 6, 7 and 8.



TAILPIPE VIEWED FROM REAR

Figure 5 Traverse Emission Sampling Points

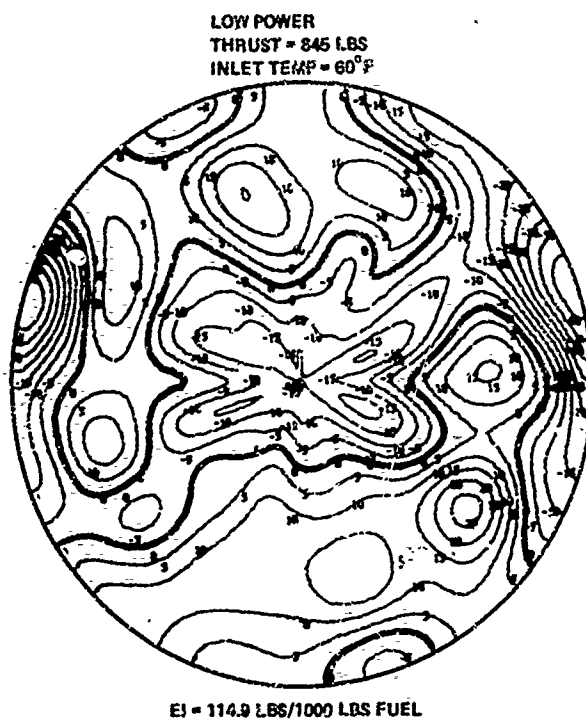


Figure 6 Isopleth for Carbon Monoxide at Low Power

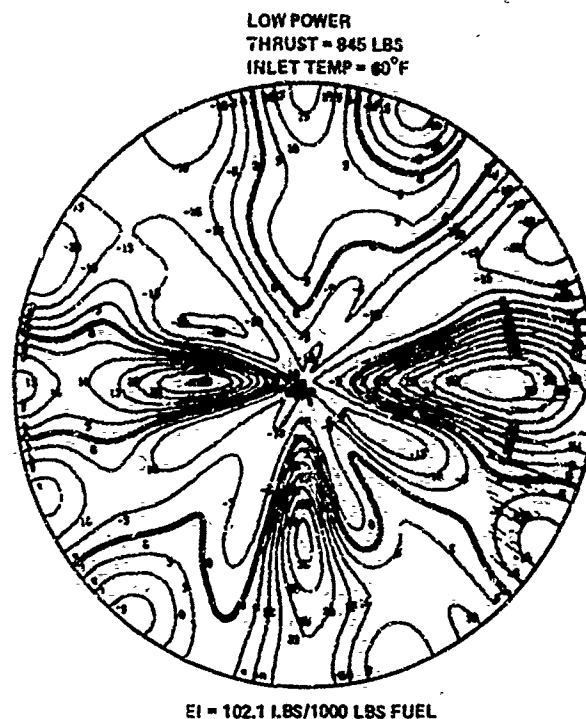


Figure 7 Isopleth for Total Hydrocarbons at Low Power

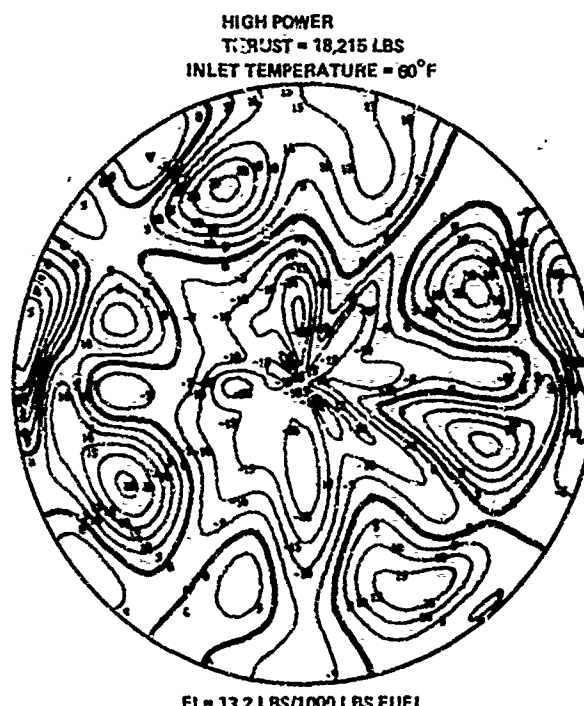


Figure 8 Isopleth for Oxides of Nitrogen at High Power

The heavy line on each of the plots represents the average emission level. It is interesting to note that the pattern of high hydrocarbon levels seems to reflect the pattern of the four struts in the exhaust case of the engine. The emission pattern for CO and NO_x appears to reflect the eight burner cans of the engine.

Because of the relatively large variations in the tailpipe plane, the emission figures obtained from the area-weighted traverse averages are believed to provide the most accurate value of actual emission levels. In this test series, a constant 60°F inlet temperature was maintained during such traverses, and also during certain of the engine emission calibration using the multipoint rake. Also, only a small specific humidity variation was recorded. Analysis of the traverse data together with the emission characteristics indicated by the multipoint rake data, permits fairly accurate estimates of emission levels for this engine model to be determined. By

the use of the emission trend math models developed during this test series, it can be computed that the EPAP (Environmental Protection Agency Parameter) for this engine can significantly vary with changes in ambient conditions as shown in Table 1 below.

ESTIMATED JT3D-3 EPAP VARIATION

Pounds of Pollutant/1000 Pound Thrust-Hour/Cycle

EPAP

Ambient Temperature	Specific Humidity	CO	THC	NO _x
25°F	.001	111.8	**	3.4
60°F	.008	31.0	**	3.7
85°F	.019	11.6	**	3.5

** Data Set Inadequate to Define Hydrocarbon Emission Trends

It should be recognized that these emission levels were obtained from the testing of experimental engine models. Because of development program demands, the operating characteristics of experimental engines frequently vary from those of engines of the same model currently in production. Although the emission levels shown here have not been verified by test results from production engines, the trends are considered to be representative.

JT8D Engine Test Series

A series of emission tests were also carried out for the JT8D engine model. This engine is in the 14,500 pound thrust class EPA (T4) and has a low (1.1:1) bypass ratio. Additional test programs were considered necessary not only because this engine model showed a large amount of data scatter during the EPA-sponsored programs (See Figures 9, 10 and 11) and also because of the difficulty in sampling the exhaust of mixed-flow-type turbofan engines in that both the non-vitiated fan air stream and the vitiated core engine gas stream are discharged through a common nozzle (Figure 12). Thus, there can be considerable mixing of the "clean" fan air with the pollutant bearing exhaust of the core stream. Although the effect of this complicating factor on emissions sampling was recognized by P&WA at the beginning of the EPA program, the only information available to us at the time was a detail traverse of the exhaust plane to obtain smoke readings made a year earlier. Inspection of a plot of these data suggested that a 12-point sampling rake, designed with sampling points at centers of equal areas for the exhaust plane of the JT3D engine, would provide sufficient coverage to the core engine stream of the JT8D engine. One of the other measurement organizations was also concerned about the sampling problem of mixed flow engines and reportedly used a single point probe at the engine centerline to record low power emissions.

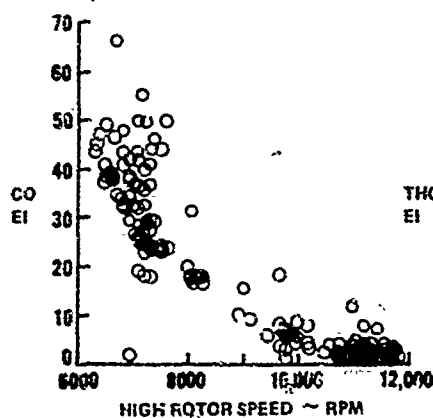


Figure 9 Data Scatter of Carbon Monoxide in JT8D Engine Emissions

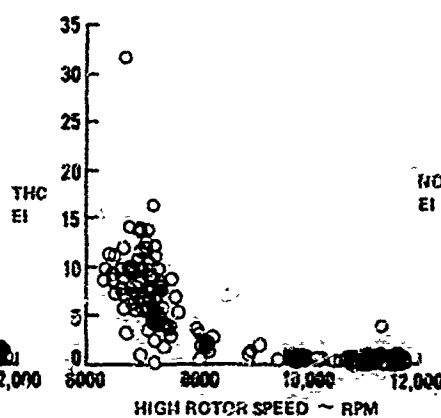


Figure 10 Data Scatter of Total Hydrocarbons in JT8D Engine Emissions

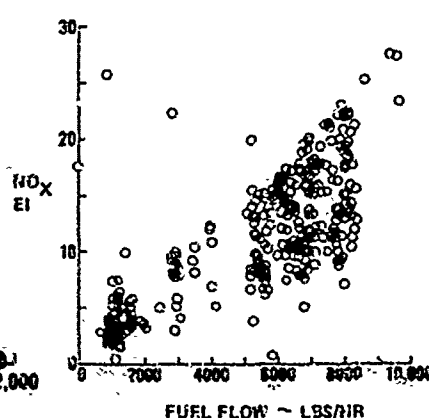


Figure 11 Data Scatter of Oxides of Nitrogen in JT8D Engine Emissions

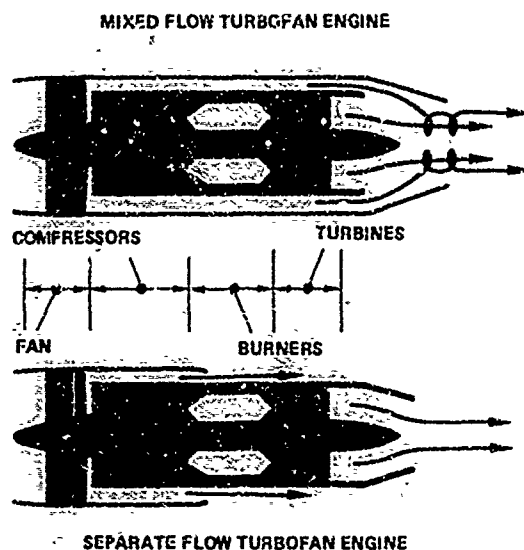


Figure 12 Comparative Diagrams - Mixed and Separate Flow Turbofan Engines

In recognition of the importance of the JT8D in the world's commercial aircraft fleet and because of the necessity to answer questions concerning the actual emission level and the best methods for measurement of this engine, Pratt & Whitney Aircraft undertook a series of test programs to try to better document and understand mixed flow engine emissions. It was then concluded that the best way to determine emission levels accurately for the mixed flow JT8D engine was to eliminate the effects of mixing by physically separating the fan and core engine gas streams and measuring, in great detail, the emission level of the core engine stream. A JT8D experimental engine was modified by removing the outer tailpipe plus the short core engine "mixer" duct (See Figure 13). A 96 inch long core engine tailpipe was fabricated and bolted to the core engine exhaust case. The long length of this tailpipe was provided in order to promote better uniformity of emission level at the plane of measurement and to preclude any interference of the fan stream with the core engine emission measurements. The exit nozzle was sized to closely match the normal core engine operating characteristics. The operating characteristics of this separated gas stream engine were found to approximate closely those of a standard JT8D engine, except for the expected thrust discrepancy, caused by the external support required for the extended exhaust nozzle.

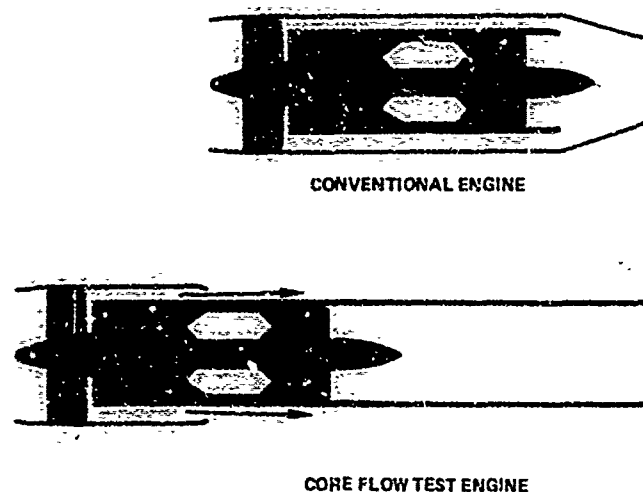


Figure 13 Modification of JT8D Engine for Core Stream Emission Test

Three sampling methods were used to measure the core engine exhaust emissions: (1) twelve point rake was modified to locate the respective sample pickup points at centers of equal area for the core engine tailpipe discharge area. The rake was used to collect exhaust samples to document emission characteristics during the complete power range engine calibrations; (2) emission measurements were taken during these calibration runs by extracting samples from the turbine case exhaust pressure probes; and (3) a traverse mechanism was also mounted behind the tailpipe for multipoint measurement of emissions. A grid spacing of 3 inches (Figure 14) was selected for the traverse testing providing 37-point coverage. An additional 8 traverse points were also taken to investigate boundary conditions at two different radial locations. Six such traverses were run at engine power settings spaced between idle to takeoff. Plots of these traverses disclosed relatively small gradients for all emissions measured, the largest gradients being observed for hydrocarbons at low power where again the hydrocarbon level appeared to be influenced by turbine case struts upstream.

Comparison of the emission data obtained from the various sampling methods used shows remarkably good agreement, as shown in Figures 15, 16 and 17.

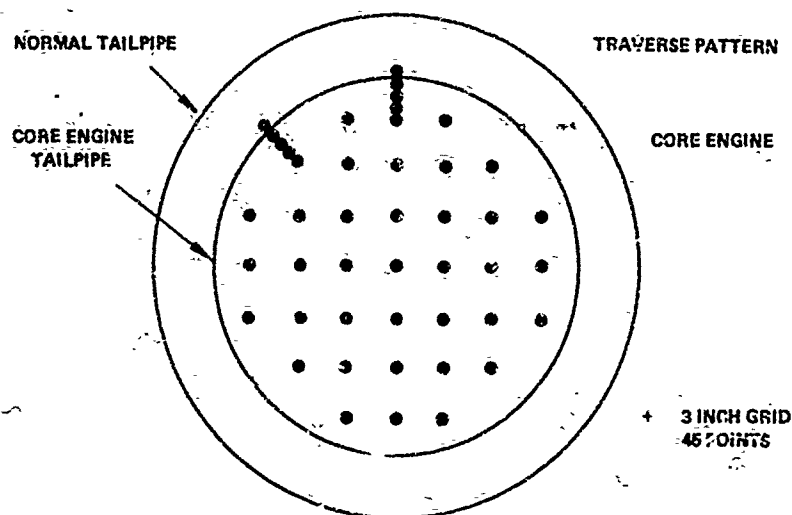


Figure 14 Core Engine Traverse Emission Sampling Points

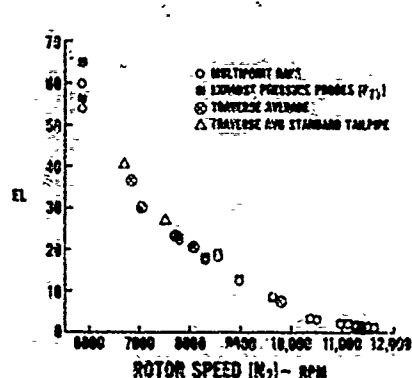


Figure 15 Core Engine Emission Test Results - Carbon Monoxide

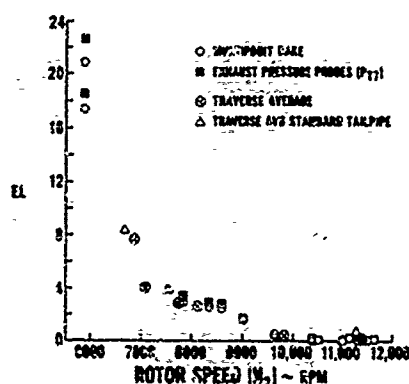


Figure 16 Core Engine Emission Test Results - Total Hydrocarbons

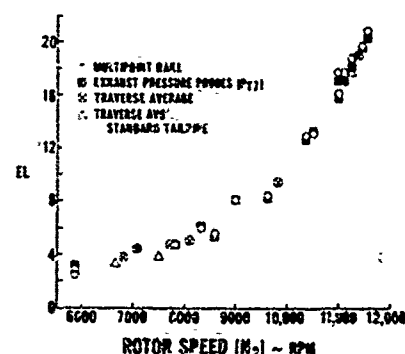
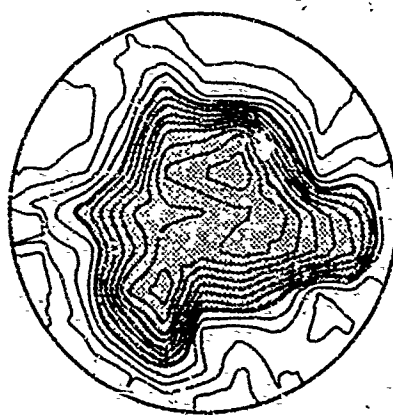


Figure 17 Core Engine Emission Test Results - Oxides of Nitrogen

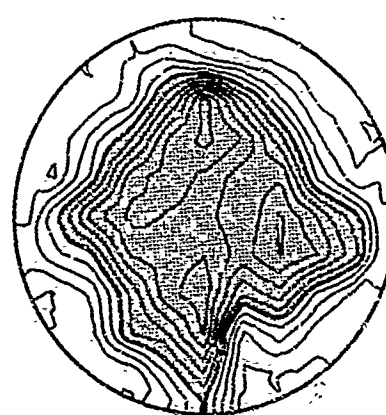
As a final check on emission level, the engine was reassembled with the standard mixed flow tailpipe, and three traverses were conducted: one at high power, and the other two near the idle power setting. The same 3-inch grid spacing that was used for the core engine emission level was also used for these traverses. This spacing together with additional points to investigate boundary effects produced a total of 90 separate points covering the tailpipe area. Isoleths of the traverse results confirmed the large variations in emission levels in the exhaust of a mixed flow engine, and are shown in Figures 18, 19, and 20. The heavy line in each isopleth represents the average emission level. The shaded area represents emissions higher than average and the unshaded areas lower. Each of the fine lines represent a 20 percent deviation from the average.



EI = 40.3 LBS/1000 LBS FUEL



EI = 8.31 LBS/1000 LBS FUEL



EI = 17.7 LBS/1000 LBS FUEL

Figure 18 Isoleth for Carbon Monoxide at Low Power

Figure 19 Isoleth for Total Hydrocarbons at Low Power

Figure 20 Isoleth for Oxides of Nitrogen at High Power

The data obtained in this program were analyzed several ways. They were first analyzed on the basis of high pressure rotor speed, this analysis producing emission levels generally higher than those previously measured in other test programs. Recently, the data were analyzed versus high compressor discharge (burner inlet) temperature (T_{T4}), and appeared to minimize the data variations due to inlet temperature. By entering this analysis using standard day values of production engine T_{T4} levels, significantly lower emission values are computed. These levels when transcribed into EPA units are listed in Table 2, below.

ESTIMATED JT8D-9 EPAP*
POUNDS OF POLLUTANT/1000 POUND THRUST-HOUR/CYCLE

CO	THC	NO _x
12.12	2.21	7.04

*EPAP Emission Level for 60°F and .008 Lbs.
H₂O/Lb of Air Specific Humidity

As noted for the JT3D engine, these data results have not been verified by comparable testing of production engines. In addition it has not been possible to obtain sufficient data, taken while using similar sampling methods, to develop trends of emission level with ambient changes for this engine, or variations in Emission index from engine to engine.

JT9D Engine Test Series

The test programs conducted for the JT9D engine were directed to investigate the following areas:

1. The ambient temperature effects on emission level for a large turbofan engine.
2. The emission level variation at the plane 2 inches behind the tailpipe for this engine.
3. The effect of water injection on exhaust emission levels.

The JT9D engine is a high (5:1) bypass ratio turbofan in the 45,000 pound (EPA T3) thrust class. In the normal sea level test stand configuration, the exhaust of the engine is readily accessible for emission measurement. A total of 631 separate emission test points were taken in the JT9D test series.

As an experiment, the exhaust emissions for the initial part of the program were sampled using two multi-point rakes mounted in tandem, one mounted in the normal vertical-horizontal orientation and the other rake rotated 45° from this position, as shown in Figure 21. The arrangement was selected to improve the emission measurement accuracy, but was found to be unnecessary, however, because of the relative uniformity of exhaust emissions from this engine. The initial test series was confined to baseline calibrations.



Figure 21 Tandem Multipoint Exhaust Emissions Sampling Rakes

This testing was followed by an investigation of the effects of water injection on the emission characteristics of the JT9D engine. Such testing was possible because certain models of the JT9D are equipped with water injection for takeoff augmentation. The normal water injection rate of 30,000 lbs/hr as well as water rate of 20,000 and 10,000 lbs/hr, were investigated at several engine power settings in the high power range. The results indicate that, although substantial decreases in the emission level of the oxides of nitrogen (NO_x) were obtained, there was a distinct trend toward substantial increases in the levels of both carbon monoxide (CO) and hydrocarbons (HC), as shown in Figures 22, 23 and 24. Although the base (dry) levels of these latter two emissions are very low at high power conditions, even slight increases in level cannot be tolerated with respect to the possibilities of achieving the proposed 1979 EPA goals, if the proposed 1979 goals are to be achieved.

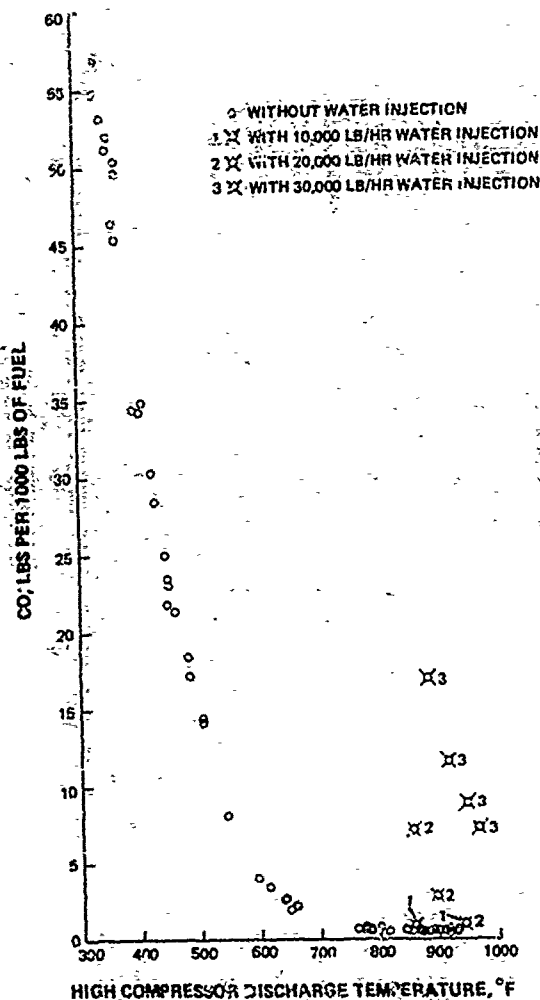


Figure 22 CO EI, With and Without Water Injection

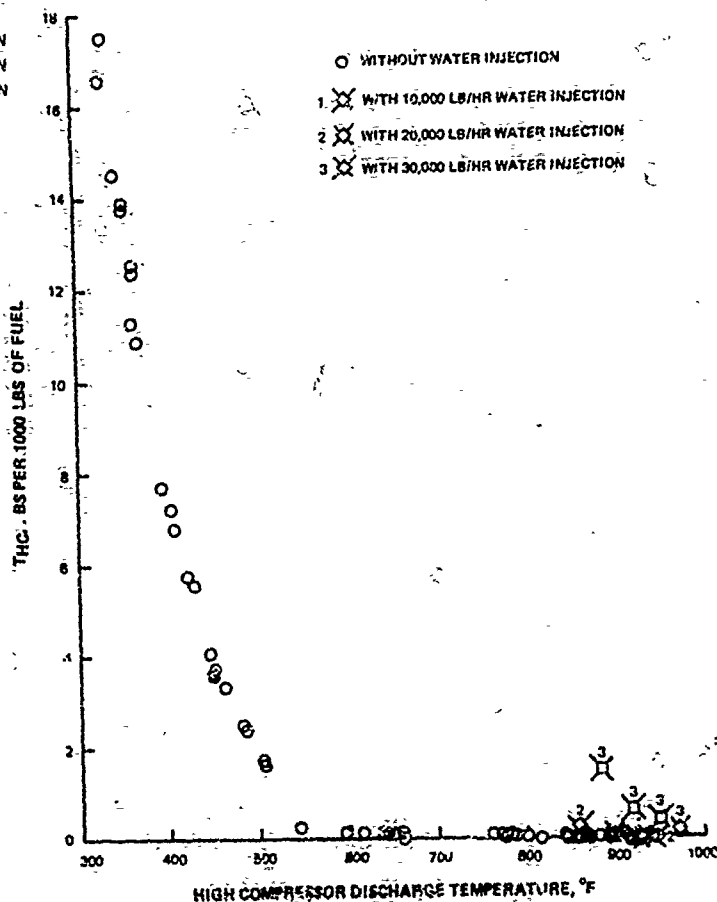


Figure 23 THC EI, With and Without Water Injection

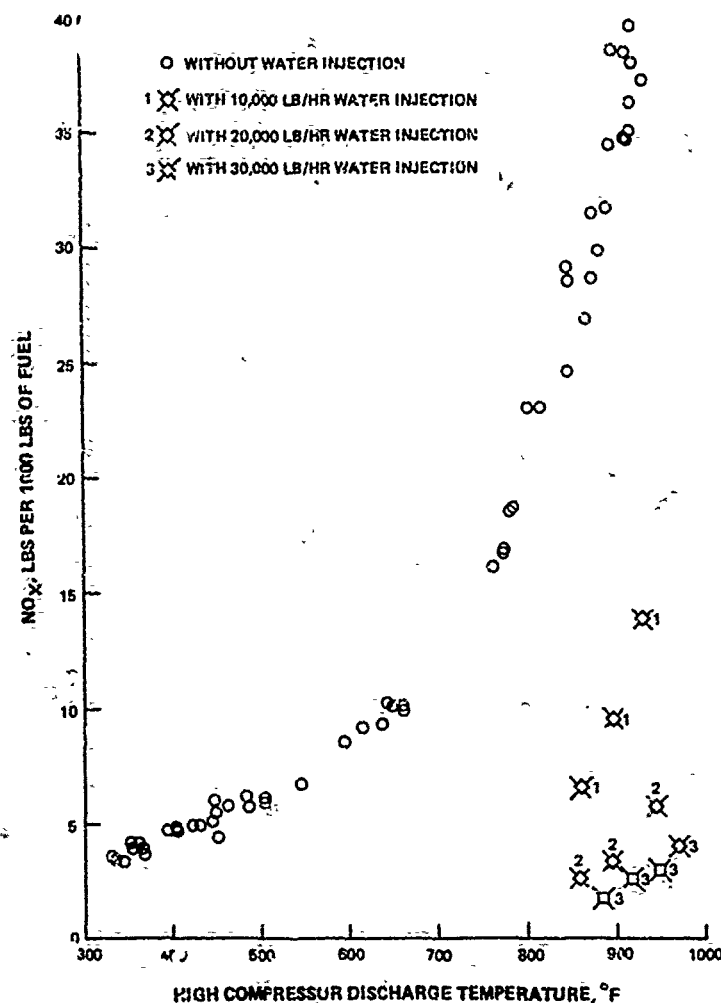


Figure 24 NO_x EI, With and Without Water Injection

The water injection testing was followed by a detailed investigation of the emission variation by traversing in a plane two inches behind the plane of the tailpipe. The traverses were made at five (5) engine power settings, with three of the traverses conducted at or near the idle power setting and two others in the high power range. Each traverse consisted of 81 individual emission test points arranged in a radial pattern, as shown in Figure 25. The isopleths of the emission data show relatively small emission gradients, as compared to similar isopleths obtained for the JT3D and JT8D engine models. Typical plots of CO and HC at idle power and NO_x at high power are shown in Figures 26, 27 and 28.

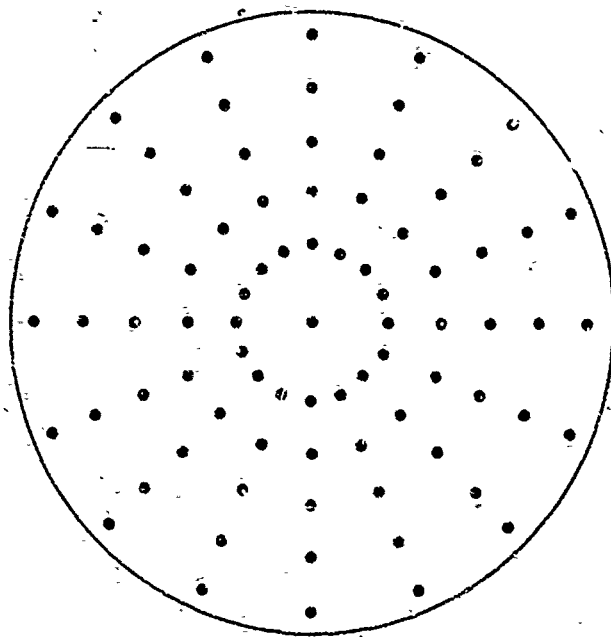


Figure 25 Traverse Emission Sampling Points

TAILPIPE VIEWED FROM REAR

EMISSION INDEX = 43.97 LB/K LB FUEL
HIGH ROTOR SPEED = 5000 RPM

NET THRUST = 3012 LBS
INLET TEMP = 71.1°F

EMISSION INDEX 12.21 LB/K LB FUEL
HIGH ROTOR SPEED 5000 RPM

NET THRUST 3012 LBS
INLET TEMP = 71.1°F



VIEW LOOKING FORWARD

Figure 26 Isopleth for Carbon Monoxide at Low Power



VIEW LOOKING FORWARD

Figure 27 Isopleth for Total Hydrocarbons at Low Power

EMISSION INDEX = 29.1 LB/K LB FUEL
HIGH ROTOR SPEED = 7402 RPM

NET THRUST = 36982 LB
INLET TEMP = 69.8°F



VIEW LOOKING FORWARD

Figure 28 Isopleth for Oxides of Nitrogen at High Power

Following the traverse test program, a limited program was conducted to investigate the effect of ambient temperature variations on emission level for this engine. The program was necessarily limited because the large airflow size of this engine prohibits the use of a non-recirculated type of inlet air heater. The normal inlet air heater used for this engine burns natural gas, and cannot be used for emission measurement testing because the combustion by-products of the heater would affect the level of exhaust emission measurements. It was therefore necessary to rely on natural ambient air temperature changes, a very time-consuming process. The test procedure followed was to record emission measurements each time the ambient temperature changed approximately 10°F. A total of 42 emission points were taken over a temperature range of 39°F to 59°F. The results of this testing were augmented by the results of the initial calibration testing, which was conducted at a temperature range of 60°F to 75°F. The humidity range for the data used for the ambient temperature effect analysis ranged from .0658 to .011 pounds of water/pound air specific humidity. Analysis of the data obtained during this limited testing suggested the following emission level trends with inlet temperature change.

$$CO_{Standard Day} = CO_{Measured} \times 1.06$$

$$\text{THC}_{\text{Standard Day}} = \text{THC}_{\text{Measured}} \times \theta^{1.3}$$

$$\text{NO}_x \text{ Standard Day} = \frac{\text{NO}_x}{\theta^4} \times \frac{T_{T2 \text{ Measured}}}{T_{T2 \text{ Standard Day}}}$$

where

$$T_{T2 \text{ Measured}} = \text{Ambient Inlet Temperature}$$

$$T_{T2 \text{ Std. Day}} = 519^\circ\text{F} (59^\circ\text{F})$$

The data, when plotted against compressor discharge temperature (T_{T4}), shows excellent consistency, as shown in Figures 22, 23, and 24.

By using the emission data obtained during this test series, together with the estimated inlet temperature trends evidenced by the data set, the variation in EPAP for the JT9D-7 engine can be estimated. These values are shown in Table 3, below:

Estimated JT9D-7 EPAP

Ambient Temperature	CO	EPAP THC	NO _x
25°F	9.73	2.65	1.83
59°F	7.84	1.76	5.46
85°F	6.50	1.28	7.04

Conclusions

Even though Pratt & Whitney Aircraft has conducted an extensive series of investigative programs for its major commercial engine models, accumulating more than 2200 separate emission test measurements, there remains a large number of questions to be answered. First, the testing conducted to date has verified significant effects of ambient temperature and humidity change on the levels of the three exhaust emissions (termed pollutants). It is considered however, that the testing conducted to date is only adequate for indicating trends, and not for indicating analytically acceptable correction factors. Much has been learned concerning test procedures and methods of analysis which can be applied to future, more definitive programs. Such programs are necessary to equilibrate emission data particularly when certifying engines to meet restrictive standards.

Much has also been learned in these programs concerning the procedures required to document adequately emission levels and characteristics of turbojets and separate flow turbofan engines. It appears that multipoint rakes can be calibrated to provide emission measurements reliable to the true emission level of the engine as established by detailed traversing. The accurate measurement of mixed flow turbofan engines presents a more difficult sampling problem because of large emission gradients, which are caused by fan air dilution. At present, accurate measurements can only be accomplished by very detailed traversing. Additional programs should be conducted to develop simpler methods of exhaust emission sampling for this type of engine.

There are other factors which require programs for more precise identification or reduction of their effect on exhaust emission levels. Instrumentation variation can effect exhaust emission far more than the electronic error stated by the manufacturers. Most of the instruments used are "laboratory type" instruments adapted for field use. Not only is the error of the instrument to be considered, but also the error of instrument operator or technician. Another source of instrument error can come from calibration procedures as well as from the reference gases used for calibration since most are not traceable to any nationally recognized standard (Reference 4). All of these factors can contribute to inaccurate emission measurement, and should be defined. These factors, as well as sampling differences, together make up what may be called "facility-to-facility" differences.

Programs should also be established to define possible "engine to engine" and "run to run" differences on a large number of production engines. Although these two differences may be small, they should be recognized and defined.

It is considered extremely important that these many factors affecting exhaust emission levels be accurately defined. This must be done before restrictive emission standards which require combustor technology levels close to the current state-of-the-art can realistically be applied or enforced for aircraft gas turbine engines.

REFERENCES AND BIBLIOGRAPHY

- | REF. NO. | TITLE |
|----------|---|
| 1 | Bogdan, Leonard and McAdams, H. T., "Analysis of Aircraft Exhaust Emission Measurements," Cornell Aeronautical Laboratories Report No. NA-5007-L-1, October 15, 1971. |
| 2 | McAdams, H. T., "Analysis of Aircraft Exhaust Emission Measurement: Statistics", Cornell Aeronautical Laboratories Report No. NA-5007-K-2, November 15, 1971. |
| 3 | A. W. Nelson, J. C. Davis and C. H. Medlin, "Progress in Techniques for Measurement of Gas Turbine Engine Exhaust Emissions", AIAA Paper No. 72-1159, New Orleans, Louisiana, December 1, 1972. |
| 4 | Report of the NBS-EPA Joint Conference on Problems in the Development of Standard Reference Gases for Mobil Source Emissions Measurement, July 27-28, 1972. |
- Nelson, A. W., "Collection and Assessment of Aircraft Emissions Baseline Data", Pratt & Whitney Aircraft Report No. PWA-4339, February 1972.
- Nelson, A. W., "Exhaust Emission Characteristics of Aircraft Gas Turbine Engines", ASME Publication 72-6T-75.

Discussion on Paper 4
 "Detailed Exhaust Emission Measurements of Three Different
 Turbofan Engine Designs"
 presented by A.W.Nelson

W.Blazowski: You said you had a very bad correlation between the calculated fuel air ration from the mission data and actual performance when you had a multi-point rake and then later said you had a good agreement between the CO hydrocarbon data that you obtained with the multi-point rake and that which you obtained with a very detailed traverse. Are you really saying that with a very detailed traverse you still got poor agreement between the fuel air ratio measured and fuel air ratio calculated?

A.W.Nelson: No. The multi-point rake data - all that data I have shown in the carbon monoxide curve were taken during the core engine test that we ran and on this test we used a multi-point rake which was designed for the core air flow only. This produced good results. That was the JT8D core multi-point rake data; and this agrees well with the detailed traverse that we made of the normal tail pipe. However, if we take the normal tail pipe and we put a multi-point rake that has centers of equal area with regard to that larger tail pipe, then we do not get representative results.

W.Blazowski: So the multi-point rake in the normal tail pipe and the detailed traverse in a normal tail pipe do not agree?

A.W.Nelson: That's right.

A.M.Mellor: How steady in time are the isopleths which you present?

A.W.Nelson: Many of the traverses, upon which the isopleths were derived, required over 100 test points to adequately define the emission characteristics at the engine exit. This required testing times on the order of 3 to 5 hours to complete. Inlet temperature conditions were maintained as steady as possible. On some of the tests, inlet heat exchangers were used. Analysis shows little change in actual engine conditions throughout each test.

R.W.Wheeler: Did you when you made your analyses use the EPA proposals, the ones published December 12, 1972? There are some curious analytical suggestions in there. One in which the carbon monoxide analyzer is heated, and the water of combustion is held up right through the whole system and passed right through the CO₂, presumably to keep the total volume of sample the same and to avoid correction for water. Many analyzers used in this regime will give an enormous water response and quite inaccurate results. Is it really necessary to have this EPA system in which the water is fully dropped out. Could we not correct for it instead and allow the analyzers to work in a nice condition.

A.W.Nelson: We did use the EPA recommended system all except for the oxides of nitrogen where we used the NDIR NDOV units rather than the chemi-luminescent measurements. I cannot answer your question with regard to the CO meter running dry rather than wet.

F.J.Verkamp: In your experiments, you measured large increases in CO with water injection. Reaction kinetic calculations predict simultaneous reductions in both NO_x and CO with water injection. Therefore the experimental increase in CO does not agree with the predicted decrease in CO and leads to two questions:

- (1) What type of water injection system did you use in the experiments?
- (2) Have you tested other water injection systems? Based upon experience with water injection in the 747 engines (some of which use water injection and some do not), does water injection adversely affect the durability and life of the engines which use water injection?

A.W.Nelson:

(1) The water injection system used in the JT9D engine injects water directly into the primary zone of the combustor.

(2) We have not measured effects on emission change with other types of water injection. The use of water injection can have an adverse effect on engine durability when the water used is not up to the stringent water purity standards which are recommended.

M.Whittaker: Could the speaker say to what extent the order of magnitude change in CO EPAP measurements on the JT3D-3 were accounted for by: (i) change in emission index; (ii) change in engine condition.

A.W.Nelson: The results shown were obtained from a math model developed using our own JT3D emission data plus the data collected for this engine during the 1971 EPA program. The constant input into the model was engine thrust or power condition. The variables are humidity and temperature. Therefore the EPAP change shown is in the emission index.

PHOTO-OXIDATION OF AIRCRAFT ENGINE EMISSIONS AT LOW AND HIGH ALTITUDES

by

K. H. BECKER and U. SCHURATH
Institut für Physikalische Chemie
der Universität Bonn, W. Germany

SUMMARY

Aircraft engines emit hydrocarbons, carbon monoxide, and oxides of nitrogen in addition to the main combustion products, which are carbon dioxide and water. The hydrocarbons undergo atmospheric oxidation by reactions with ozone, atomic oxygen, and various radicals. At low altitudes atomic oxygen and ozone production is initiated by the photo-dissociation of man-made nitrogen dioxide which is involved in complex chain reactions including radical intermediates of the hydrocarbon oxidation. At high altitudes, ozone formation by nitrogen dioxide photolysis is negligible compared with the photolysis of molecular oxygen leading to the natural ozone production. In medium altitudes, both natural ozone and ozone from the photolysis of anthropogenic nitrogen dioxide may be of importance, depending on geographic and meteorological parameters. At ground level the photo-oxidation of hydrocarbons in the presence of nitric oxides can lead to smog formation, whereas at higher altitudes it may affect the natural ozone content of the atmosphere. The sulfur dioxides emitted from aircraft burning sulfur-containing fuel is converted to aerosols which affect the physical conditions of the atmosphere.

1. INTRODUCTION

Jet engines emit essentially the same gaseous compounds as do internal combustion automobile engines. Relative pollutant concentrations, however, are different and depend also on the type and power setting of the jet engine.

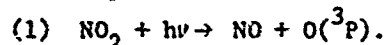
It is well known that photochemical reactions in diluted automobile exhaust can lead to photochemical smog formation. This process has been studied by many scientists and is thought to be basically understood, though many reactions are still speculative or based on indirect evidence only.

It will be the purpose of this lecture to outline the mechanism of photochemical smog formation and then to discuss its applicability to aircraft emissions, with certain modifications which take care of the differing environmental conditions.

2. THE MECHANISM OF PHOTOCHEMICAL SMOG

Photochemical reactions in the atmosphere transform solar energy as well as chemical potential of atmospheric pollutants into oxidizing power. The final products of the oxidation processes are carbon dioxide, water, nitric acid, and sulfuric acid, as well as their salts, and other gaseous or particulate products which are eventually removed from the atmosphere by rain or other physical processes.

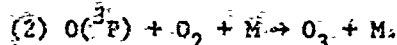
Very few atmospheric gases absorb light from the sun and undergo dissociation, which is essential for the initiation of chemical change under atmospheric conditions. We shall at first restrict our discussion to nitrogen dioxide, which is by far the most important photochemically active pollutant of the lower atmosphere. Figure 1 shows photoaction spectra of NO_2 at ground level for solar zenith angles of 40° and 60° with respect to reaction (1), which is the dissociation of NO_2 into NO and an $\text{O}(^3\text{P})$ ground state atom:



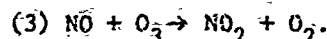
The photoaction spectra were obtained by multiplying the known solar spectrum,¹⁾ corrected for attenuation by the atmosphere, with the absorption cross section σ ²⁾ and the quantum yield ϕ for photodissociation of NO_2 .³⁾ The short wavelength cutoff at 290 nm results from light absorption from stratospheric ozone in the Hartley and Huggins bands. Above 398 nm, the dissociation limit of NO_2 , the quantum yield drops rapidly, thus restricting the photochemically active part of the solar spectrum to a narrow band between 290 nm and 420 nm. Integration of the photoaction spectra in figure 1 results in lifetimes of 2 and 3 minutes of NO_2 molecules with respect to photodissociation in sunlight, in good agreement with laboratory experiments.

At atmospheric pressure the lifetime of oxygen atoms from reaction (1) is only $14 \mu\text{s}$ with respect to the fast three body recombination with oxygen molecules

which produces ozone:



However, oxidation of NO by ozone is also fast at ambient temperatures and tends to reestablish the initial situation:

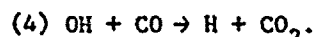


In an otherwise unpolluted atmosphere, ozone formation would therefore proceed to a photostationary state, depending on the concentration ratio of NO₂ and NO and the light intensity. This is not the situation observed in photochemical smog. It differs in four respects:

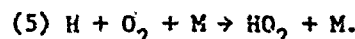
1. Hydrocarbons, especially olefins, are essential for photochemical smog formation and are used up in the process.
2. Nitric oxide, which is a primary pollutant in car exhaust, is quickly oxidized to nitrogen dioxide, much faster than can be explained by reaction with natural ozone or by reaction with molecular oxygen, which is extremely slow at low NO concentrations.
3. Excess ozone is formed in the course of smog formation.
4. Addition of carbon monoxide, usually considered chemically inert at ambient temperatures, changes reaction rates in photochemical smog.

These characteristics lead to the conclusion that intermediates are formed by the photolysis of NO₂ in the presence of hydrocarbons which eventually oxidize excess NO to NO₂ without using up ozone, and others which are capable of reaction with CO.

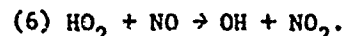
It has long been recognized that hydrocarbons are oxidized in polluted atmospheres by O-atoms from the photolysis of NO₂, and more efficiently by the ozone which accumulates. However, in the early stages of a smog situation, when much more NO is present than NO₂, and very little ozone, the oxidation of NO and the consumption of hydrocarbons would proceed at much slower rates than is actually observed were it not speeded up by radical chains. These chains are currently believed to be propagated by OH radicals. This assumption is corroborated by the observed CO effect on photochemical rates, which has been mentioned above and which can only be explained by the rapid reaction of OH radicals with CO:



H-atoms from (4) recombine with molecular oxygen to form HO₂ radicals:



The oxidizing species which convert NO to NO₂ are mainly HO₂ radicals and organic radicals containing a peroxy group, e. g. through reaction (6):



The rate constant of reaction (6) has recently been published by Stief and Payne⁴⁾ to be 3×10^{-13} cm³ molec.⁻¹ s⁻¹ with an uncertainty factor of 3. According to the same authors, oxidation of CO by HO₂ radicals is far too slow to play a part in photochemical smog. Organic peroxyacyl radicals are doubtless formed in the course of photochemical smog formation, because their recombination products with NO₂, e. g. PAN, have been identified among the noxious products. Alkyl peroxy radicals are also often considered as potential candidates for the oxidation of NO. However, Heicklen concluded from a recent study of the photo-oxidation of azomethane in the presence of NO that methylperoxy radicals and probably other alkyl peroxy radicals do not oxidize NO, they combine instead with NO to form alkyl peroxy nitrite, which is scarcely observed among the products of photochemical smog.

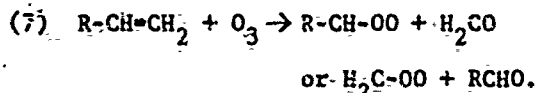
OH radicals formed in reaction (6) and other processes rapidly react with hydrocarbons or aldehydes, eventually reproducing NO₂ and other peroxy species which represent oxidizing power. Chain termination is by radical recombination and by H atom transfer from HO₂ to other radicals, which produces stable species and O₂.

Equations (1) through (6) comprise some of the most important reactions which are believed to occur in photochemical smog. Reliable rate constants are available except from reaction (6), which has been measured only to within a factor of 3.

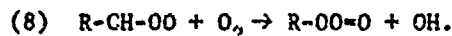
Thoroughly assessing the problem of photo-oxidation of pollutants, however, means considering all reaction sequences which are triggered by oxygen atom and ozone reactions with olefins and other hydrocarbons, and probably other initiation reactions such as the photolysis of HNO_2 . Elaborate sets of photochemical smog reactions have been worked out by several authors and computer tested on smog chamber data from such simple systems as clean air containing only oxides of nitrogen and propylene. E. g., 60 reactions were selected by Niki and co-workers,⁶⁾ and 81 by Hecht and Seinfeld.⁷⁾ Some results of Niki's computations are shown in figure 2, together with the experimental measurements provided by Altshuler. There is reasonable agreement between experiment and computation. It can be shown from these computations that OH chain reactions are very important during the induction period, that is, when most of the oxides of nitrogen are still in the form of NO. Later on ozonolysis accounts for up to 50% of hydrocarbon consumption.

One might argue that experimental data are easily fitted if a sufficient number of parameters is used. The situation is, however, less discouraging because most of the rate constants which are important in the scheme are known from reliable measurements. The computer calculations are therefore useful for predicting the effects of change in relative composition of pollutants, total concentration, and light intensity.

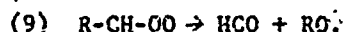
Comparing Niki's and Seinfeld's schemes reveals that considerable disagreement exists mainly with regard to ozone-olefin reactions, which are thought to contribute most to the consumption of olefins in photochemical smog. The primary reaction after addition of an ozone molecule is generally accepted to be the Criegee-split of the olefin into a carbonyl compound and a so-called zwitter ion:



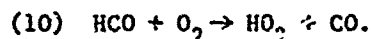
Reactions of the zwitter ion in the gas phase are, however, very little understood, most of the conclusions being drawn from product analyses of ozone-olefin-reactions at relatively high reactant concentrations. Niki⁶⁾ assumed a rate constant of $10^{-18} \text{ cm}^3 \text{ molec.}^{-1} \text{ s}^{-1}$ for reaction of the zwitter ion with molecular oxygen:



Reaction (8) provides both oxidizing power and chain propagating OH at one time. Seinfeld,⁷⁾ on the other hand, favors decomposition of the zwitter ion within about three minutes:



HCO is also formed by reactions of oxygen molecules with terminal olefins and is thought to react with molecular oxygen to produce HO_2 , which is then converted to OH by reaction with NO:



Ozone-olefin reactions at pressures ranging from 6 mtorr to 200 torr also have been investigated in our laboratory, using a 220 m^3 stainless steel spherical vessel⁸⁾ or a flow tube as a reactor. We find that the apparent rate constant of ozone consumption, by reaction with a 60fold excess of 6 mtorr propylene, strongly depends on oxygen pressure in the range 6 to 150 mtorr, being constant at the higher pressures.⁹⁾ This is shown in figure 3. No such dependence on He or N_2 pressure up to several 100 mtorr was observed, which excludes adiabatic heating or wall reactions as reasons for the observed effect. We conclude that oxygen selectively quenches or reacts with some product, probably the zwitter ion in an excited state, which otherwise decomposes into fragments, consuming further ozone.

Such a process is certainly quenched at atmospheric pressure. We have therefore also analysed the chemiluminescence spectra of olefin-ozone reactions up to 200 torr total pressure.¹⁰⁾ A representative spectrum at 3 torr pressure is shown in figure 4. Emission from electronically excited formaldehyde is common to all olefins reacting with ozone. When olefins with one or two substituents at one carbon atom react with ozone, glyoxal and biacetyl phosphorescence, respectively, are observed. These compounds result from the recombination of HCO radicals and CH_3CO radicals, respectively, and are therefore indicative of the decomposition of zwitter ions, according to reaction (9). In the red and infrared wavelength region, OH Meinel bands from vibrationally excited OH radicals, excitation up to $v = 9$, are observed from the reactions of various olefins with ozone. Vibrationally excited OH radicals are

formed by the reaction of free H atoms with ozone. Since the Mainel bands are also observed at 200 torr total pressure, and with little loss of intensity, H atom formation is not restricted to low pressures and may well provide a major atmospheric source of H atoms.

3. APPLICATION TO AIRCRAFT EMISSIONS

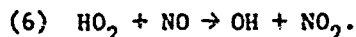
The photo-oxidations mechanisms of atmospheric pollutants which have been outlined so far were developed to apply to photochemical smog formation in diluted automobile exhaust, which governs pollutant composition in urban atmospheres. The question arises as to whether these mechanisms may be applied to aircraft emissions as well.

Jet engine emissions differ from automobile exhaust by a much higher ratio of nitrogen oxides to hydrocarbons during take-off, cruise, and approach. In the idling mode on the ground, hydrocarbon emissions of jet engines increase by an order of magnitude, olefins and aromatics accounting for up to 50% of the total, whereas NO is substantially reduced at the same time. The CO content is several times higher than under normal cruising conditions, but is still not comparable to automobile exhaust. Interestingly enough, the oxides of nitrogen from jet engines contain high percentages of NO₂ under certain conditions. Values of around 50% have been reported in the literature.¹¹⁾ This is clearly in contrast to automobile exhaust.

What are the consequences of these statements with respect to pollution and photo-oxidation reactions at airports? - It is highly improbable even at very busy airports that pollutant levels as high as in big cities will accumulate. Low concentrations, especially low hydrocarbon concentrations, tend to decelerate the process of NO to NO₂ conversion under the action of sunlight and, as a consequence, excess ozone formation. This is experimentally observed and is also predicted by computer calculations. The calculations predict that the higher percentage of NO₂ in NO_x from aircraft partly compensates for the dilution effect by increasing the initial rate of energy uptake from sunlight, thereby reducing the induction period of photochemical smog formation. Low or high CO concentrations at airports do not seriously affect the rate of photochemical change of pollutants. CO is oxidized by OH radicals from the photochemically induced reaction chain, if the CO concentration is high enough to compete with OH-olefin reactions, which are two orders of magnitude faster^{12, 13)}:



Reaction (4) is chain propagating because H atoms are quantitatively fixed as HO₂ radicals which re-enter the cycle, e. g. through oxidation of NO:



We conclude that photochemical smog formation at airports is possible and is enhanced if the NO₂ content is high for jet exhaust, since NO₂ is the light absorbing species of atmospheric photochemistry at ground level.

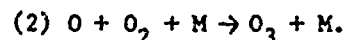
We shall now consider pollutants from aircraft which are not accumulated in the restricted area of an airport. These pollutants are emitted into the atmosphere at several km altitude. With the exception of SST, emission is in the troposphere. This part of the atmosphere is characterized by rapid vertical and horizontal mixing, which precludes any danger of accumulating high pollutant concentrations in limited air masses. At low concentrations of pollutants in vast air masses, photochemical smog formation in the usual sense of the word cannot occur. This does not mean that aircraft emissions at higher altitudes are not subject to photochemical change. NO₂ certainly absorbs sunlight which at higher altitudes is more persistent, if not more intense, in the important wavelength range 290 to 420 nm, NO is oxidized by ozone, and hydrocarbons undergo O-atom and ozone reactions to produce free radicals which trigger further reactions. But two very important deviations from the situation at ground level have to be taken into account: This is the effect of extreme dilution and the temperature effect.

Extreme dilution very much reduces reaction rates. Photostationary states are therefore no longer established within short periods of time. The starting point is no longer a highly unnatural ensemble of man-made pollutants which develop their own dynamics under the action of sunlight. The question is now, how long do pollutants persist in a more or less undisturbed natural surrounding.

This question can be assessed if the pronounced changes in temperature and pressure which characterize the vertical profile of the troposphere are taken into account. The temperature profile of the atmosphere is shown in figure 5. Pressure is on a logarithmic scale to the right of the figure, corresponding to an approximately

linear altitude scale which is plotted on the left.

The altitude dependence of the rate of the important three body reaction (2) is plotted in figure 6.



The plot shows lifetimes of oxygen atoms in the atmosphere with respect to reaction (2) as a function of altitude. Except for a very weak temperature dependence resulting from a negative activation energy of 1 kcal,¹⁴⁾ the change of lifetimes closely reflects the dependence of reaction rate (2) on the square of the air density. There is also a pronounced altitude effect on the rate constant of two body reactions which have activation energies. The rate constant for oxidation of NO by ozone¹⁵⁾ as a function of altitude is plotted in figure 7. The mean lifetime of NO molecules with respect to oxidation by natural ozone as a function of altitude is obtained by multiplication with the natural ozone profile of the atmosphere. This is plotted in figure 8, showing that NO has a maximum lifetime of 10 minutes at 6 km altitude.

Also, ozone-olefin reactions, which are of major importance in photochemical smog, are greatly retarded at higher altitudes by the temperature effect. They have activation energies of typically 2.5 to more than 5 kcal. Rate constants which have been measured in our laboratory at very low pressures are listed in figure 9.⁹⁾ In contrast to ozone reactions, reactions of oxygen atoms with olefins have very low activation energies.¹⁶⁾ Therefore, atom reactions with olefins become relatively more important at higher altitudes, also because of the prolonged lifetime of oxygen atoms with respect to ozone formation at low gas densities.

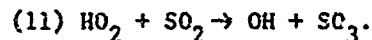
Important radical reactions, e. g. of OH radicals with CO, are known or assumed to have very little or no activation energies. Their rate constants undergo little change with altitude. Unfortunately, no information is available on the temperature dependence of NO oxidation by HO₂ radicals.

Metastable oxygen molecules in the $\text{O}_2(^1\Delta_g)$ state are produced in the higher troposphere and in the stratosphere by photolysis of ozone below 611 nm. A great number of quenching rate constants for $\text{O}_2(^1\Delta_g)$ have been measured in our laboratory under simulated high altitude conditions.^{17,18)} These long-lived metastables are extremely slowly quenched by atmospheric gases. It has been proposed that $\text{O}_2(^1\Delta_g)$ might react with olefins in polluted atmospheres to produce peroxides, opening up a new channel of pollutant photo-oxidation. Our measurements showed definitely that metastable oxygen does not react with simple olefins when oxygen atoms are excluded. This seemed to settle the question of chemical reactions of metastable oxygen with simple olefins in the atmosphere. The situation changed, however, when it was observed in our laboratory that intense infrared chemiluminescence is produced above 1.2μ , figure 10, when HCO radicals are reacted with metastable $\text{O}_2(^1\Delta_g)$.¹⁹⁾ The reaction is probably the fastest of metastable oxygen molecules in the gas phase with an organic compound. Work is in progress to further investigate this new type of chemical reaction and its products, which might contribute to the photo-oxidation processes in the higher troposphere and the stratosphere.

4. CONCLUSIONS

We conclude that the photo-oxidation mechanism of pollutants from aircraft and other sources in the troposphere undergoes fundamental changes with altitude, radical and atom reactions, and probably reactions of metastable oxygen molecules, becoming more important in the colder regions of the troposphere. The chain oxidation of CO by OH radicals is still effective at high altitudes and is enhanced by NO, which reacts with HO₂ to reproduce OH. Serious contamination of the troposphere by aircraft is not expected, because the residence time of pollutants is short compared with emissions rates. This is in contrast to SST emissions in the stratosphere. SST problems are, however, beyond the scope of this lecture, being treated in detail by other lecturers at this meeting.

So far I have not mentioned aircraft sulfur dioxide pollution, since jet fuel does not contain much sulfur. If, however, sulfur dioxide were to be released into the troposphere by aircraft to any great extent, the pollutant would be oxidized to SO₃ to form an aerosol through reaction with water vapour. Oxidation of sulfur dioxide is possible by HO₂:

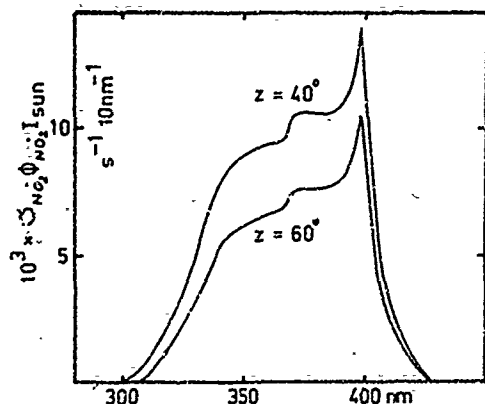


Stief and Payne⁶⁾ report a rate constant of 3×10^{-16} for this reaction. SO₂ is also oxidized by an unidentified intermediate of the ozone-olefin reaction, but not by metastable oxygen molecules $\text{O}_2(^1\Delta_g)$. Aerosol formation in the troposphere from aircraft sulfur dioxide does not seem to present a serious problem, because washout is

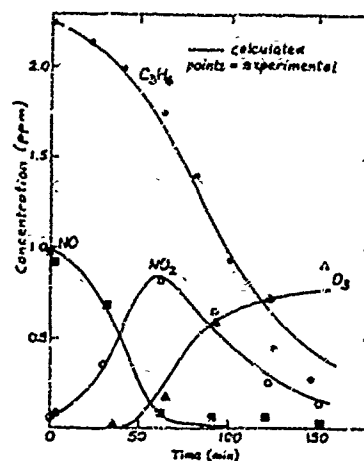
rapid. Here again, the situation is more serious with respect to aerosol formation in the stratosphere.

5. REFERENCES

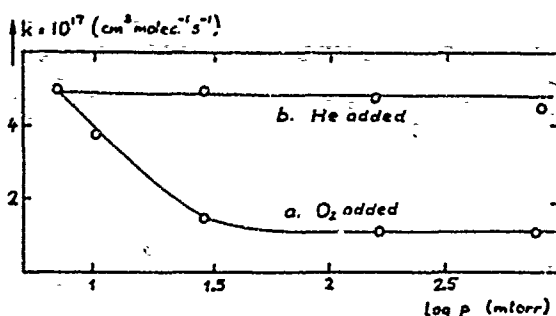
- 1) M. P. Thekarakara; Optical Spectra, March 72, 32.
- 2) P. A. Leighton, "Photochemistry of Air Pollution", Academic Press, New York and London 1961.
- 3) I. T. N. Jones, K. D. Bayes; to be published.
- 4) W. A. Payne, L. J. Stief; Science 179 (1973), 280.
- 5) C. W. Spicer, A. Villa, H. A. Wiebe, J. Heicklen; J. Am. Chem. Soc. 95 (1973), 13.
- 6) H. Niki, E. E. Daby, B. Weinstock; to be published.
- 7) Th. A. Hecht, J. H. Seinfeld; Environ. Sci. Technol. 6 (1972), 47.
- 8) W. Groth, K. H. Becker, G. H. Comsa, A. Elzer, E. Fink, W. Jud, D. Kley, U. Schurath, D. Thran; Naturwissenschaften 59 (1972), 379.
- 9) H. Seitz, Diplomarbeit, Bonn, Institut für Physikalische Chemie, Juli 1972.
- 10) K. H. Steinhoff, Diplomarbeit, Bonn, Institut für Physikalische Chemie, März 1973.
- 11) R. D. Siegel; J. Air Poll. Contr. Assoc. 22 (1972), 845.
- 12) K. Schofield; Planet. Space Sci. 15 (1967), 643.
- 13) E. D. Morris, H. Niki; J. Phys. Chem. 23 (1971), 3640.
- 14) R. E. Huie, J. T. Herron, D. D. Davis; J. Phys. Chem. 76 (1972), 2653.
- 15) M. A. A. Clyne, B. A. Thrush, R. P. Wayne; Trans. Faraday Soc. 60 (1964), 359.
- 16) a) D. D. Davis, R. E. Huie, J. T. Herron, M. J. Kurylo, W. Braun; J. Chem. Phys. 56 (1972), 4868.
 b) M. J. Kurylo; Chem. Phys. Lett. 14 (1972), 117.
 c) R. Atkinson, R. J. Cvetanović; J. Chem. Phys. 56 (1972), 432.
- 17) K. F. Becker, W. Groth, U. Schurath; Chem. Phys. Lett. 8 (1971), 259.
- 18) K. H. Becker, W. Groth, U. Schurath; Chem. Phys. Lett. 14 (1972), 489.
- 19) K. H. Becker, E. Fink, U. Schurath; to be published.



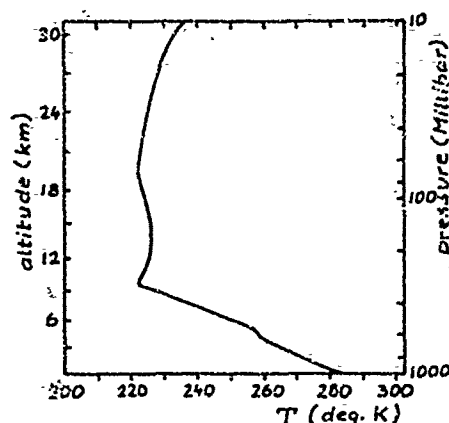
1. Photoaction spectra of nitrogen dioxide in natural sunlight; solar zenith angles 40° and 60° .



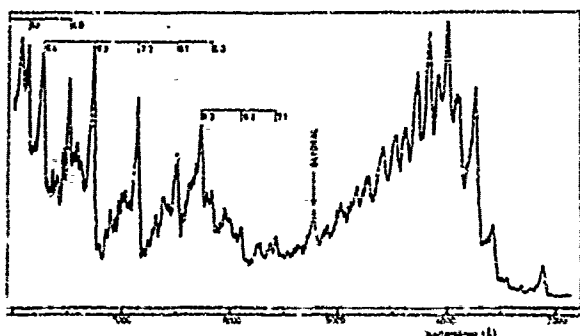
2. Comparison of experimental smog chamber data with calculated concentration-time behavior.



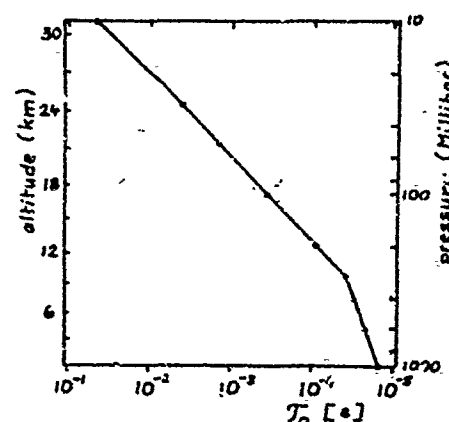
3. Rate constants of ozone reaction with propylene at low total pressures; dependence on oxygen and helium pressure:
a. Propylene-pressure 10 mtorr; ozone pressure = 0.15 mtorr; oxygen pressure variable.
b. Same propylene- and ozone pressure; helium pressure variable.



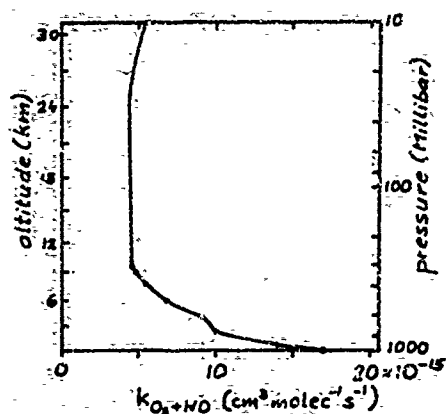
5. Typical temperature profile of the atmosphere.



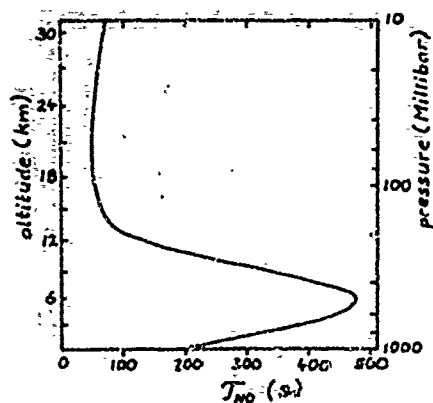
4. Chemiluminescence of the ozone-propylene reaction at 3 torr total pressure.



6. Altitude dependence of the lifetime of ground state oxygen atoms with respect to ozone formation in a normal atmosphere.



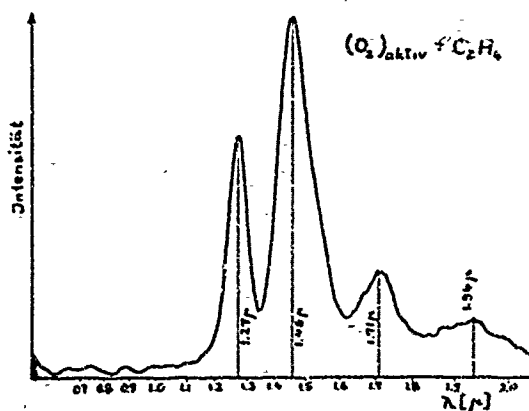
7. Altitude dependence of the rate constant of NO oxidation by ozone for a typical temperature profile of the atmosphere.



8. Lifetime of NO with respect to oxidation by natural ozone as a function of altitude in a typical atmosphere.

Compound	E ($\text{kcal} \cdot \text{mole}^{-1}$)	$A \cdot 10^{14}$ ($\text{cm}^3 \text{molec}^{-1} \text{s}^{-1}$)	k (298°K) ($\text{cm}^3 \text{molec}^{-1} \text{s}^{-1}$)
<chem>CH2=CH2</chem>	n.d.	n.d.	8×10^{-20}
<chem>CH2=CH-CH3</chem>	5.3 ± 0.15	5.1	6.7×10^{-18}
<chem>CH3-CH=CH-CH3</chem>	5.1 ± 0.1	1.5	2.8×10^{-18}
<chem>CH3-CH=CH-CH2-CH3</chem>	3.9 ± 0.15	1.1	1.5×10^{-17}
<chem>CH3-CH=CH-CH2-CH2-CH3</chem>	3.3 ± 0.1	0.97	2.0×10^{-16}
<chem>CH3-CH=CH-CH2-CH2-CH2-CH3</chem>	n.d.	n.d.	$(3 \pm 1) \times 10^{-17}$

9. Rate constants and activation energies of some ozone-olefin reactions measured at low reagent concentrations at 200 torr total pressure.



10. Infrared chemiluminescence of the reaction of HCO radicals with $O_2(a^1\Delta_g)$ at low resolution.

Discussion on the Paper
 PHOTO-OXIDATION OF AIRCRAFT ENGINE EMISSIONS
 AT LOW AND HIGH ALTITUDES
 (Paper 5)
 presented by
 K.H. Becker and U. Schurath

S.A. Mosier

With reference to your comment regarding the fact that large concentrations of NO_2 have been observed in the NO_x content of exhaust from gas turbine engines, will you please cite the references used and expand upon this information.

U. Schurath

My comment about the NO_2 content of NO_x from jet engines was based on publications by E.R. Lozano, W.W. Melvin, Jr., and S. Hochheiser, J.A.P.C.A. 18 (1968), 392, and by R. D. Siegel, J.A.P.C.A. 22 (1972), 845. Both papers present data and state explicitly that NO_2 concentrations from aircraft engine exhaust are not negligible under some conditions, and in fact may be rather high.

G.D. Kittredge

NO_2 in gas turbine exhaust, based on EPA studies, occurs to the extent of 70 to 48% of the total NO_x at low power settings, with increasing NO levels at higher power settings. This is strictly valid for relatively long residence time turboshaft engines, not turbojets.

U. Schurath

I would like to thank Mr. Kittredge for this comment which, as I understand it, confirms my assumption that the relative NO_2 output is markedly higher at the airport itself, where the risk of photochemical smog formation is greatest.

Prof. I. Glassman

Since it is now known that the concentration of OH radicals is not negligible in the lower atmosphere, should we be concerned with atmospheric reactions involving methane and OH radicals?

U. Schurath

Methane has a high natural background concentration of more than 1 ppm at ground level. Since the rate constant for the reaction of OH radicals with methane is $10^{-14} \text{ cm}^3 \text{ molecule}^{-1} \text{ s}^{-1}$ at room temperature, this reaction is certainly an important sink of methane and OH in the atmosphere. Reactions of olefins and aldehydes with OH are, however, about three orders of magnitude faster, so that the contribution of anthropogenic methane to chemical reactions in polluted atmospheres is negligible.

R.W. Wheeler

In your experiments with hydrocarbons, have you observed any reactions with methane, e.g. reactions of oxygen atoms with methane, and if not, is it not unnecessary to measure methane as an air pollutant?

U. Schurath

Reactions of ground-state oxygen atoms with methane are too slow to be of importance in the lower atmosphere. $\text{O}(^1\text{D})$ excited atoms react rapidly with methane, but this atom is only present at higher altitudes. OH radical reactions have already been discussed. Methane is neither toxic nor very reactive in the lower troposphere. Measuring methane as an air pollutant is therefore not very useful unless its concentration is considered indicative of the general degree of pollution of an air mass.

EFFECT OF SUPERSONIC TRANSPORT UPON THE OZONE LAYER, STUDIED IN A TWO-DIMENSIONAL PHOTOCHEMICAL MODEL WITH TRANSPORT

By

Egil Hesstvedt
Institute of Geophysics
University of Oslo
Blindern, Osl. 3, Norway

SUMMARY

A steady state two-dimensional model of the stratospheric ozone layer is presented. Photochemical reactions involving oxygen, hydrogen, and nitrogen are considered along with the effect of a parameterized, two-dimensional transport, by mean motion and by eddies. A parameterized meridional distribution of NO_x is applied, computed from one-dimensional models. The model is in fair agreement with observed ozone data. The reduction of ozone from emission of NO_x from supersonic aircraft is studied, assuming a fleet of 200 aircraft, flying at given altitudes and uniformly distributed over the globe. The effect is found to depend critically upon the flight level. For mid-latitude, summer, the ozone column density is reduced by 0.4% for a flight level of 18 km. For flight levels 23 km and 28 km the reduction is 1.6% and 2.3%, respectively. Accordingly, the increase in UV-radiation amounts to approximately 0.8%, 3.2%, and 4.6% for the same flight levels.

1. INTRODUCTION

The magnitude of the effect of future supersonic flights upon the ozone layer has been vividly debated over the last couple of years. The opinions cover a wide spectrum from "a negligible effect" to "catastrophe". It is the aim of this study to throw some more light upon the problem. Judging from our results, the effect lies between the two extremes: it is too small to represent an immediate danger, but large enough to cause a long term effect which should be seriously considered.

One way to approach the problem is to use photochemical models, including transport processes. One-dimensional models may give some indication of the magnitude of the effect, but since it is clear that horizontal transport plays an important role in the distribution of ozone, most of the work in this field is now concentrated on two- and three-dimensional models. Here is presented a steady state two-dimensional model, which is an extension of a more simplified model presented last year (1). In that model a constant mixing ratio of NO_x was applied and computations were made for different values of this mixing ratio. This model was later improved (2) by assuming a vertical profile of NO_x in accordance with available observational data (3). The same profile was applied for all latitudes, winter and summer. This gave a much better agreement between theoretical results and observed ozone data. The present model goes one step further: vertical profiles of NO_x have been computed from one-dimensional models, for different latitudes, winter and summer. The next step will be to include the effect of horizontal transport upon the NO_x distribution. Such an extension is now in progress.

2. TWO-DIMENSIONAL TRANSPORT MODEL

The model presented is a two-dimensional steady state model. Two versions of the model are computed, one for summer and one for winter conditions, both ranging from the Equator to the Pole and from the tropopause up to 35 km. The differentials in the analytical expressions for the transport are replaced by finite differences. The distance between the gridpoints in the model is 1 km vertically and 5° latitude horizontally. A relaxation method is applied to compute steady state solutions.

The boundary conditions for ozone are as follows: At 35 km photochemical equilibrium is assumed. Data for the column density of ozone above 35 km are taken from time dependent photochemical models for the region 35-70 km, computed by the author (unpublished). The values are given in Table 1. At the tropopause a constant value of 1012cm^{-2} is taken for the ozone number density. Both models (summer and winter) are extended 5° into the opposite hemisphere, and values computed for 5° latitude, winter, are used at the boundary in the summer model and vice versa for the winter model. Over the Pole the horizontal flux of ozone is taken to be zero.

Standard profiles have been used for temperature and density (4). The parameterized transport in the model is based upon data given by Gudiksen et al. (5). Their data for the vertical eddy diffusion coefficient K_{zz} have been modified, mainly in the upper part (6,7). The K_{zz} -profiles used in the present model are given in Figure 1. Also the data for K_{yy} , K_{yz} , v , and w are modified, since the original data fail to produce a realistic ozone distribution. In particular a stronger transport seems to be necessary to produce an ozone maximum at 18 km in high latitudes. In the present model Gudiksen's data for K_{yy} and K_{yz} are multiplied by 8, while data for v and w are multiplied by 2. This brings the transport data more in agreement with earlier data for atmospheric transport (8). With these modified data the theoretical ozone distribution appears more realistic.

	Summer					Winter			
	90°	60°	45°	30°	0°	30°	45°	60°	
$[O_3] (\times 10^{-12})$	1.24	1.65	1.96	2.17	1.99	1.51	1.36	0.68	
Column density ($\times 10^{-18}$)	1.00	1.11	1.28	1.36	1.25	0.94	0.85	0.55	

Table 1. Number densities of ozone ($\times 10^{-12} \text{ cm}^{-3}$) at 35 km and column density of ozone above 35 km ($\times 10^{-18} \text{ cm}^{-2}$)

3. OZONE PHOTOCHEMISTRY

The photochemical reactions considered in this model are specified in Table 2. The O-H reaction scheme, (reactions 1-36) is a standard one and quite similar to that used in most O-H atmospheric models. The nitrogen chemistry is much simplified and consists of only four reactions. However, the complexity of the nitrogen chemistry is implied in the computation of the NO_x profiles used as a parameter in our model. These profiles, given in Figure 2, are computed from one-dimensional models (6,7), which are based upon a complex scheme of O-H-N reactions.

Since the balance between NO and NO_2 is quickly established, the computation of these two components follows from a sharing of the available NO_x , given by the condition

$$\frac{d[NO]}{dt} = (k_{39}[O] + J_{NO_2})[NO_2] - k_{37}[O_3][NO] = 0$$

which gives

$$[NO_2] = k_{37}[O_3][NO_x] / (k_{37}[O_3] + k_{39}[O] + J_{NO_2})$$

The components $O(^1D)$, $O(^3P)$, H, and OH have very short lifetimes: for $O(^1D)$, it is less than 2×10^{-7} s, for $O(^3P)$ less than 0.2 s, for H less than 5×10^{-7} s, and for OH less than 5 min. Photochemical equilibrium is therefore a good approximation for these components, which, as well as NO, all vanish at night.

The lifetimes of O_2 , H_2 , and H_2O are many years in the lower atmosphere. We may therefore assume that these components are mixed and take 0.2095 , 5×10^{-1} , and 5.5×10^{-6} , respectively, for their mixing ratios.

HO_2 is in rapid exchange with H and OH. In the computations it is convenient to consider the sum (odd hydrogen) of these three components, which has a lifetime of one hour or less. The assumption of photochemical equilibrium for daytime conditions is therefore a fair approximation. The lifetime of H_2O_2 is less than 4 days in the region 10-35 km. The photochemistry is therefore faster than the transport, and photochemical equilibrium gives sufficient accuracy for our problem.

Since atomic oxygen is in photochemical equilibrium and is much less abundant than O_3 , the ozone budget is conveniently studied from the expression for odd oxygen

$$\frac{d[O_3]}{dt} = 2J_2[O_2] - 2k_{39}[NO_2][O] - 2k_3[O][O_3] - A$$

where A represents the loss rate of odd oxygen through oxygen-hydrogen reactions:

$$A = (k_{10}[OH] + k_7[HO_2])[O] + (k_{24}[OH] + 2k_{35}[O(^1D)] + k_{29}[O(^1)] + k_{29}[O(^1)] + k_{29}[H_2O])$$

It turns out that A is small compared to the loss rate through reactions 3 and 39. At levels where the photochemistry of ozone is not dominated by the transport, less than 10% of the total loss of ozone is due to O-H reactions. However, this figure depends on the value taken for k_{24} , which is, unfortunately, not known with a satisfactory accuracy.

Computations of dissociation rate coefficients are based upon Ackerman's data for the solar flux and absorption cross-sections for O_2 and O_3 (9).

4. THEORETICAL OZONE DISTRIBUTION

The computed steady state distributions of ozone, for summer and winter, are shown in Figure 3. A comparison of theoretical and observed ozone distribution seems to support the conclusion that our model is a plausible simulation of the processes which determine the mean ozone distribution in the real stratosphere.

The agreement between theory and observation is particularly good for summer conditions. At the Equator the maximum level is correctly reproduced at 26 km with an ozone number density of $4.9 \times 10^{-12} \text{ cm}^{-3}$. Polewards the maximum level falls down to 19 km with a peak value of $4.9 \times 10^{-12} \text{ cm}^{-3}$ at 60°, also in excellent agreement with observations. For winter conditions the agreement is quite good. One reason for this may be that a declination of -20° , as used in the winter model, excludes ozone production beyond 60° latitude. In the real atmosphere, such a situation only lasts for two months. However, even for the winter, the agreement is such that the model may be said to represent a reasonable simulation of the behaviour of stratospheric ozone.

Table 2. Reactions and reaction rate coefficients.

(1) $O(^3P) + O(^3P) + M \rightarrow O_2 + M$	$k_1 = 1.50 \times 10^{-34} \exp(1.4/RT)$
(2) $O(^3P) + O_2 + M \rightarrow O_3 + M$	$k_2 = 1.05 \times 10^{-34} \exp(1.014/RT)$
(3) $O(^3P) + O_3 \rightarrow 2 O_2$	$k_3 = 2.1 \times 10^{-11} \exp(-4.91/RT)$
(4a) $O_2 + h\nu \rightarrow O(^3P) + O(^3P)$	$175 \text{ nm} < \lambda < 242.4 \text{ nm}, J_{2a}$
(4b) $O_2 + h\nu \rightarrow O(^3P) + O(^1D)$	$\lambda < 175 \text{ nm}, J_{2b}$
(5a) $O_3 + h\nu \rightarrow O(^3P) + O_2$	$\lambda > 310 \text{ nm}, J_{3a}$
(5b) $O_3 + h\nu \rightarrow O(^1D) + O_2$	$\lambda < 310 \text{ nm}, J_{3b}$
(6) $OH + O(^3P) \rightarrow H + O_2$	$k_6 = 2.5 \times 10^{-11}$
(7) $HC_2 + O(^3P) \rightarrow OH + O_2$	$k_7 = 7 \times 10^{-11}$
(8) $H + O_2 + M \rightarrow HO_2 + M$	$k_8 = 1.89 \times 10^{-32} \exp(0.685/RT)$
(9) $H + O_3 \rightarrow OH + O_2$	$k_9 = 2.6 \times 10^{-11}$
(10) $OH + HO_2 \rightarrow H_2O + O_2$	$k_{10} = 2 \times 10^{-10}$
(11) $H_2O_2 + h\nu \rightarrow 2 OH$	$187.5 \text{ nm} < \lambda < 382.5 \text{ nm}, J_{H_2O_2}$
(12) $O(^3P) + H_2O_2 \rightarrow OH + HO_2$	$k_{12} = 1.87 \times 10^{-15}$
(13) $HO_2 + HO_2 \rightarrow H_2O_2 + O_2$	$k_{13} = 3 \times 10^{-11} \exp(-500/T)$
(14) $OH + H_2O_2 \rightarrow H_2O + HO_2$	$k_{14} = 10^{-11} \exp(-910/T)$
(15) $OH + OH \rightarrow H_2O + O(^3P)$	$k_{15} = 8 \times 10^{-11} (T/273)^{1/2} \exp(-2/RT)$
(16) $H_2O + h\nu \rightarrow OH + H$	$135 \text{ nm} < \lambda < 237.5 \text{ nm}, J_{H_2O}$
(17) $H + HC_2 \rightarrow H_2O + O(^3P)$	$k_{17} = 2 \times 10^{-10} \exp(-4/RT)$
(18) $H + HO_2 \rightarrow H_2 + O_2$	$k_{18} = 3 \times 10^{-12}$
(19) $H + H + M \rightarrow H_2 + M$	$k_{19} = 1.2 \times 10^{-32} (273/T)^{0.7}$
(20) $O(^1D) + M \rightarrow O(^3P) + M$	$k_{20} = 3.8 \times 10^{-11}$
(21) $O(^1D) + H_2 \rightarrow OH + H$	$k_{21} = 3 \times 10^{-10}$
(22) $O(^3P) + H_2 \rightarrow OH + H$	$k_{22} = 7 \times 10^{-11} \exp(-10.2/RT)$
(23) $HO_2 + O_3 \rightarrow OH + 2 O_2$	$k_{23} = 10^{-20}$
(24) $OH + O_3 \rightarrow HO_2 + O_2$	$k_{24} = 10^{-14}$
(25) $H + H_2O_2 \rightarrow H_2 + HO_2$	$k_{25} = 2.8 \times 10^{-12} \exp(-1900/T)$
(26) $H + O(^3P) + M \rightarrow OH + M$	$k_{26} = 8 \times 10^{-33}$
(27) $H + O_3 \rightarrow HO_2 + O(^3P)$	$k_{27} = 2 \times 10^{-10} \exp(-4/RT)$
(28) $H + O_2 \rightarrow OH + O(^3P)$	$k_{28} = 1 \times 10^{-9} \exp(-16.8/RT)$
(29) $O(^1D) + H_2O \rightarrow 2 OH$	$k_{29} = 3 \times 10^{-10}$
(30) $H + HC_2 \rightarrow 2 OH$	$k_{30} = 2 \times 10^{-11}$
(31) $H + OH + M \rightarrow H_2O + M$	$k_{31} = 2.5 \times 10^{-31}$
(32) $O(^3P) + CH_4 + M \rightarrow HO_2 + M$	$k_{32} = 1.4 \times 10^{-31}$
(33) $H + HO \rightarrow H_2 + O(^3P)$	$k_{33} = 3 \times 10^{-12} \exp(-8.3/RT)$
(34) $H_2 + OH \rightarrow H_2O + H$	$k_{34} = 10^{-10} \exp(-5.9/RT)$
(35) $O(^1D) + O_3 \rightarrow 2 O_2$	$k_{35} = 3 \times 10^{-10}$
(36) $HO_2 + h\nu \rightarrow OH + O(^3P)$	$J_{J_2} : J_{H_2O_2}$
(40) $CO + OH \rightarrow CO_2$	$k_{40} = 2.1 \times 10^{-13} \exp(-115/T)$
(41) $NO + HO_2 \rightarrow OH + NO_2$	$k_{41} = 3 \times 10^{-13}$
(79) $NO + O_3 \rightarrow NO_2 + O_2$	$k_{79} = 9.3 \times 10^{-13} \exp(-1235/T)$
(71) $NO_2 + h\nu \rightarrow NO + O$	$J_{NO_2} = 7 \times 10^{-3}$
(72) $NO_2 + O \rightarrow NO + O_2$	$k_{72} = 3 \times 10^{-11} \exp(-300/T)$

The photochemical lifetime of ozone increases rapidly with decreasing height. For 45° , summer, it is 4 days at 35 km, 2 weeks at 30 km, 3 months at 25 km, 1 1/2 years at 20 km, 5 1/2 years at 15 km, and 12 years at 10 km. Atmospheric transport therefore becomes increasingly important as we descend through the stratosphere. In the upper part of the model (30-35 km) ozone is nearly in photochemical equilibrium, while, below about 22 km, the chemistry is dominated by the transport. Argumentation about the influence of SST upon the ozone layer has very often been based upon purely photochemical models without the consideration of transport. From what is said above, such models are quite unrealistic. Conclusions drawn from such models should be appraised with scepticism.

5. EFFECT OF SUPERSONIC TRANSPORT UPON THE OZONE LAYER

The model described above may be used to estimate the effect of emission of NO_x from supersonic aircraft upon the ozone layer. If the rate of NO_x emission pr. engine is known, a realistic prognosis for future traffic density and routing makes it in principle possible to compute the perturbations in the NO_x distribution, as given in Figure 2, and consequently the decrease in total ozone, as a function of latitude and season. A computation along this line is presented here. Some simplifying assumptions have been made; these are, however, not likely to present a serious limitation. It is believed that the results obtained give a useful indication of the magnitude of the ozone depletion due to supersonic transport.

The basis for the computations is: A reference fleet of 200 four-engine aircraft is considered, each performing 1000 flights of 2 1/2 hours pr. year. The fuel flow is assumed to be 5,000 kg pr. hour pr. engine. The emission of NO_x (converted to NO_2) is assumed to be 21 g pr. kg. fuel. These 200 aircraft are assumed to fly at the same flight level, uniformly routed around the globe.

The perturbation of the NO_x distribution is now computed in the same way as we computed the NO_x profiles given in Figure 2, the only difference being that a point source, given by the above data, is introduced at the flight level. The results of such computations are given in Figure 2. Here the increase (in %) in NO_x is given as a function of flight level and height. As might have been expected, the increase in NO_x is very sensitive to the flight level. For 60° , summer, and a flight level of 18 km, the increase in NO_x in the "sensitive zone" (above 22 km) is seen to be around 2%. For flight level 23 km the NO_x increase in the same zone is between 5% and 10%, while flying at 25 km results in an NO_x increase by 10-20%.

The validity of these results is somewhat limited by the fact that the computations are based upon one-dimensional models. It is clear that horizontal transport will influence the NO_x distribution. However, the similarity in the curves in Figure 2 makes it unlikely that the consideration of horizontal transport would cause a drastic change in the theoretical NO_x distribution. The same may be said about the perturbation of NO_x from SST. On the other hand some change may be expected if we abandon the assumption of a uniform routing and instead introduce preferred routings, for instance along 50° latitude.

On the basis of the perturbed NO_x profiles, new steady state ozone distributions have been computed for flight levels of 18 km, 23 km, and 28 km, respectively. The changes in ozone are moderate, and the overall picture given in Figure 3 remains nearly the same.

Of special interest is the decrease in ozone column density above 10 km, shown in Table 3. It is seen that the ozone depletion is very sensitive to flight level. For latitudes around 50° , in the summer, the decrease in ozone is about 0.4% for flight level 18 km, while the decrease amounts to 1.6% (2.3%) for flight level 23 km (28 km). These figures may be converted to a corresponding increase in the erythemogenic UV-radiation (1), which will amount to 0.8% (3.2%, 4.6%) for flight level 18 km (23 km, 28 km).

The decrease in total ozone and increase in UV-radiation, as computed in this model, are not such that an immediate danger is to be expected. On the other hand, the cumulative effect of increased UV-radiation may, for all we know, be considerable. This is particularly true when flying at altitudes above 18 km.

Flight level	Summer					Winter				
	60°	45°	30°	15°	0°	15°	30°	45°	60°	
18 km	0.5	0.3	0.1	0	0	0	0.1	0.1	0.1	
23 km	1.8	1.4	0.6	0.5	0.4	0.7	0.8	0.9	0.9	
28 km	3.4	2.7	2.0	2.0	2.0	2.5	2.5	2.5	2.5	

Table 3. Decrease (in %) in total ozone caused by a "reference fleet" (see text) of 200 aircraft uniformly routed over the globe and flying at 18, 23, and 28 km.

REFERENCES

1. Hesstvedt, E. Water, Air & Soil Pollut. (in print).
2. Hesstvedt, E. CIAP Survey Conference Proceedings, November 1972 (in print).
3. Ackerman, M., and Muller, C. Aeronomica Acta, A., No.106, 1972.
4. Cole, A.E., Court, A., and Kantor, A.J. Handbook of Geophysics and Space Environments, (ed. by S.L. Valley), Bedford, Mass., Air Force Cambridge Research Laboratories, 1965.
5. Gudiksen, P.H., Fairhall, A.W., and Reed, R.J. J. Geophys. Res., 73, 1968.
6. Isaksen, I.S.A. Geofys. Publ., 30, 2, 1973 (in press).
7. Isaksen, I.S.A., and Hesstvedt, E. (to be published, 1973).
8. Reed, R.J., and German, K.E. Mon. Weath. Rev., 93, 1965, 313-321.
9. Ackerman, M. Mesospheric Models and Related Experiments (ed. by G. Fiocco), Doordrecht-Holland, D. Reidel Publishing Company, 1970, 149-159.

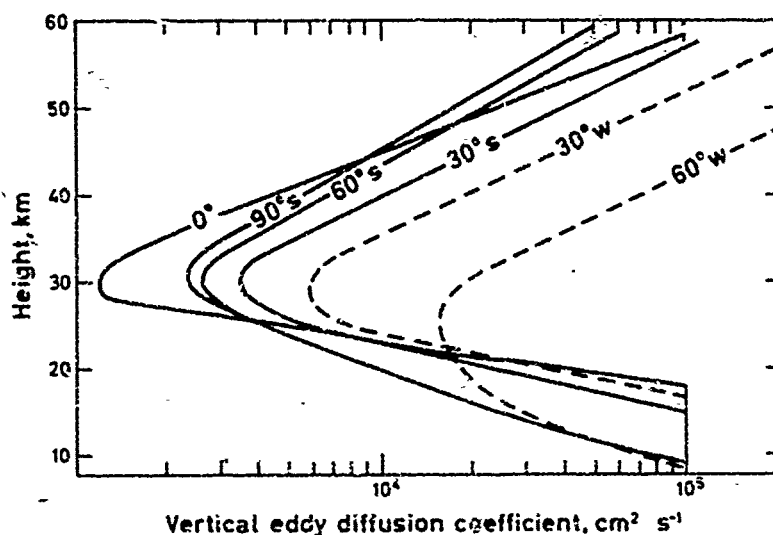


Figure 1

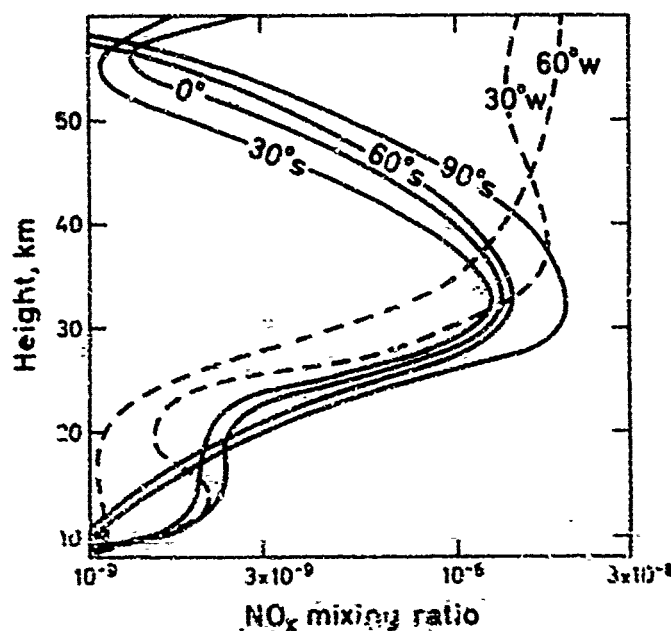


Figure 2

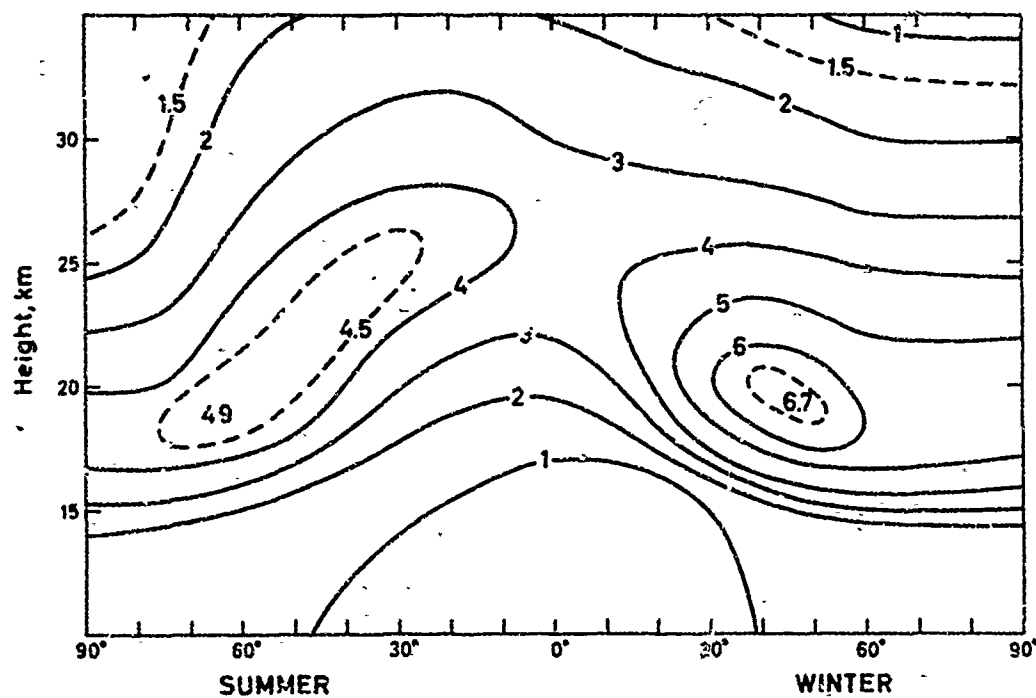


Figure 3

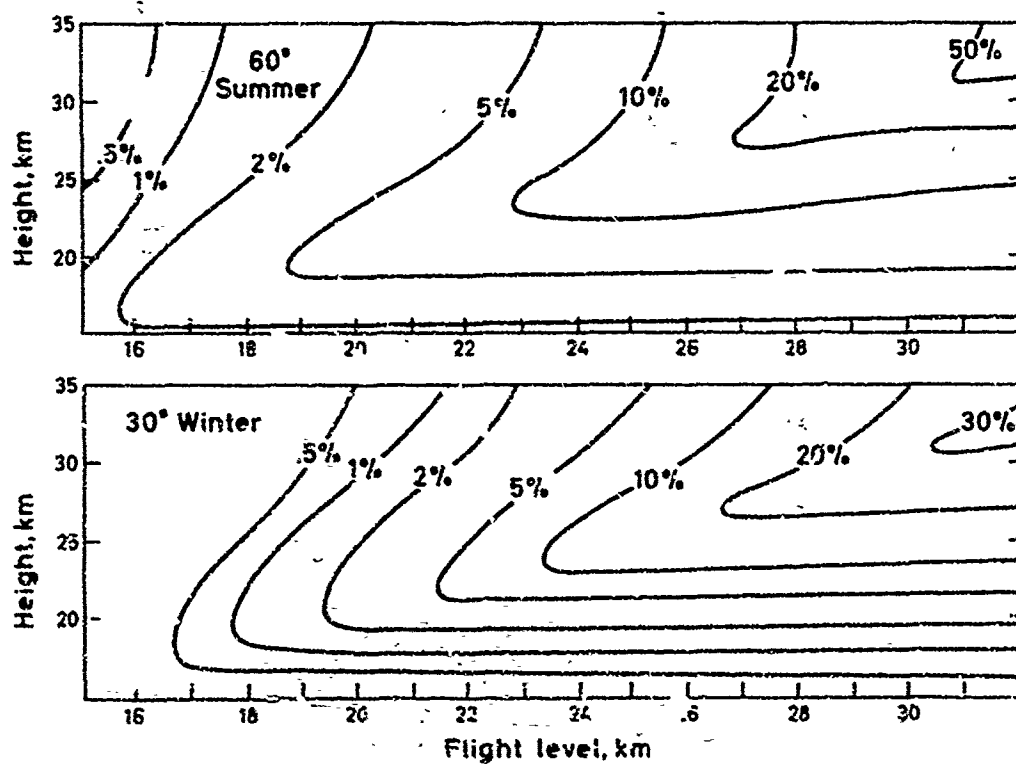


Figure 4

Discussion on Paper 6
 "Effect of Supersonic Transport upon the Ozone Layer, Studied in a Two-Dimensional
 Photochemical Model with Transport"
 presented by E.Hesstvedt

A.Goldburg: Figure 2 shows for NO_x 2×10^{-9} at 20 km and 10^{-8} at 30 km. In the first case this is much higher than 10^{-10} , reported in Paper 1, Table 7, and in the second case it is almost higher than possible according to Professor Johnston this morning. Would you comment?

E.Hesstvedt: My theoretical value of NO_x at 20 km corresponds to 10^{-9} for NO for the summer, probably a little less for the winter, but in both cases higher than the observed value. I cannot explain why. I would like to see more measurements of NO, at different heights. As for my theoretical value at 30 km I can only say that it agrees completely with Ackerman and Müller's measurements of NO_2 .

N.A.Chigier: Can you tell us how sensitive the computations you have made, are to the initial conditions. We could have initial conditions where the engine exhaust behaves like a turbulent jet with rapid dilution or alternatively the ingestion of the exhaust into the trailing vortices where high concentrations and temperatures would persist for periods of several minutes in small diameter trails of many kilometers in length.

E.Hesstvedt: Since my model has distances of 1 km (vertically) and 5° latitude (horizontally) between the grid-points, it is indirectly assumed that a point source is substituted by a large area source. It cannot be readily used to treat your second alternative. My guess is, however, that what happens the first few minutes after injection will be smoothed out over the relatively long time available, so that the difference between the two alternatives is, perhaps, not so great after all.

A.E.J.Eggleston: Have loss mechanisms for NO_x such as N_2O_5 and HNO_3 formation been included?

E.Hesstvedt: The formation of N_2O_5 and HNO_3 have been considered in the computations of NO_x on which this paper is based.

R.J.Gelinas: Two sets of measurements have recently been reported: NO concentrations of ≤ 0.1 ppb in the lower stratosphere (which seem on the low side) and O_3 column density measurements from the Concorde (which are on the high side of "normal"). What would your model indicate by consideration of such a negative deviation of NO and the resultant perturbation of the O_3 column density?

E.Hesstvedt: My model would simply say that, the less NO, the more ozone we get. But a point value, of say 0.1 ppb at 20 km, cannot be introduced in the model. I would need a profile.

P.Goldsmith: I have a comment and two questions:

It is interesting to note that Professor Hesstvedt's meteorologically more sophisticated treatment gives a much lower effect on the total ozone for a given amount of nitrogen oxides than the simpler approach outlined by Professor Johnston earlier. Perhaps, we will find that as our models of stratospheric ozone become more and more meteorologically realistic that this trend will continue.

In Professor Hesstvedt's model, he has used a rather high value for the stratospheric water vapour content; could he tell us whether the outcome of his model is very sensitive to this value?

Also, I note that he has used a constant ozone density at the tropopause as his lower boundary condition. If it were possible to use a lower boundary condition incorporating some factor to allow for the preferred regions of stratospheric/tropospheric exchange, in what direction would this affect the conclusions from the model?

E.Hesstvedt: Water is by volume; I admit it is slightly on the high side but this was done because we could not with the computer we had take methane and H_2 considerations into the model. We had to fix a number representative at the layer (say 25 kms) where chemistry is so fast that it competes with the transport. We are not too concerned with what goes on below that.

The model has not been changed to adjust to the freedom of the new computer, but we don't believe it will change significantly, in evaluating the SST. Past experience has not shown a major effect with increasing sophistication of our model.

R.C.Oliver: I note that you have changed Gudiksen's data for K_{yy} and K_{yz} by a factor of 8 and w by a factor of 2. Are such changes permissible in terms of fitting the W^{158} data on which Gudiksen based his calculations? And how would such changes impact upon stratospheric residence times?

E. Hestvedt: The changes we have made will clearly not fit the V^{155} data for that particular period of time. Our point is that with Gudiksen's data we do not get an ozone distribution which fits observations. Reed and German's data probably would.

These two sets of data differ approximately by the factors mentioned. The reason why we applied the adjusted Gudiksen data, rather than Reed and German's, is that Gudiksen's data have a format which is convenient for modelling. Since we have made only slight changes in K_{22} , the stratospheric residence time is not likely to be seriously altered by the adjustment.

CHEMICAL KINETIC IN THE STRATOSPHERE

G. BRASSEUR

Institut d'Aéronomie Spatiale
3, avenue Circulaire
B - 1180 Bruxelles (Belgique)

Summary

Ozone is produced by the photodissociation of molecular oxygen and can be destroyed by several reactions involving the nitrogen - hydrogen - oxygen atmosphere. In the lower part of the stratosphere, and for photochemical conditions, an important loss of ozone is due to the NO_x reactions. Nitric oxide is formed in the stratosphere after dissociation of nitrous oxide by the excited oxygen atom $\text{O}(^1\text{D})$. The formation of nitric acid is possible by the presence of hydroxyl radicals. Therefore a careful study of the hydrogen atmosphere is necessary. Water vapor, methane and molecular hydrogen have an indirect influence on the ozone distribution in the stratosphere.

1. INTRODUCTION

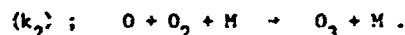
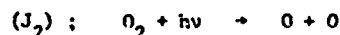
The aeronomy of the stratosphere has been studied with much attention for many years by different authors (see for example Nicolet [1], [2], [3]) but an increased attention has been given to these problems since it has been pointed out that high altitude aircrafts could have an impact on the earth's climate and on the U.V. radiation intensity at ground level.

Before trying to estimate the magnitude of such impacts, it is necessary to clearly understand the physical processes of the natural stratosphere. Many important questions still remain unsolved, e.g. transport mechanisms, specially through the tropopause; important reaction rates and absorption cross sections are not known with enough accuracy.

The purpose of this paper is to show that the problem of the stratosphere can not be solved without a good understanding of its photochemistry and the introduction of most minor constituents. A special attention will be devoted to the nitrogen oxides chemistry.

2. PRODUCTION AND DESTRUCTION OF OZONE

The minor constituent which plays the major role in the stratosphere certainly is ozone which is produced from the photodissociation of molecular oxygen for radiation of wavelength shorter than 242 nm:



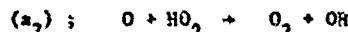
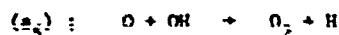
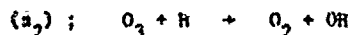
It is destroyed by reaction



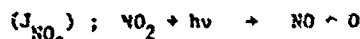
or by photodissociation



These reactions have been proposed in 1930 by Chapman [4] and explain the presence of a maximum of the ozone concentration in the middle of the stratosphere. But the obtained concentrations are too high compared with most experimental data since other loss processes have been omitted. In the upper stratosphere and above the stratopause, odd oxygen is destroyed by hydrogen compounds (Bates and Nicolet [5])



and in the lower stratosphere by the NO_x catalytic cycle (Crutzen [6], Johnston [7])



The production rate of ozone is thus given by

$$P(\text{O}_3) = J_2 n(\text{O}_2)$$

and is represented on fig. 1 for an overhead sun. Its integrated value between 10 and 50 km is of the order of $4 \times 10^{13} \text{ cm}^{-2} \text{ s}^{-1}$ but slightly varies with latitude and season since the penetration of solar radiation depends on the ozone content which is larger in the polar regions than near the equator.

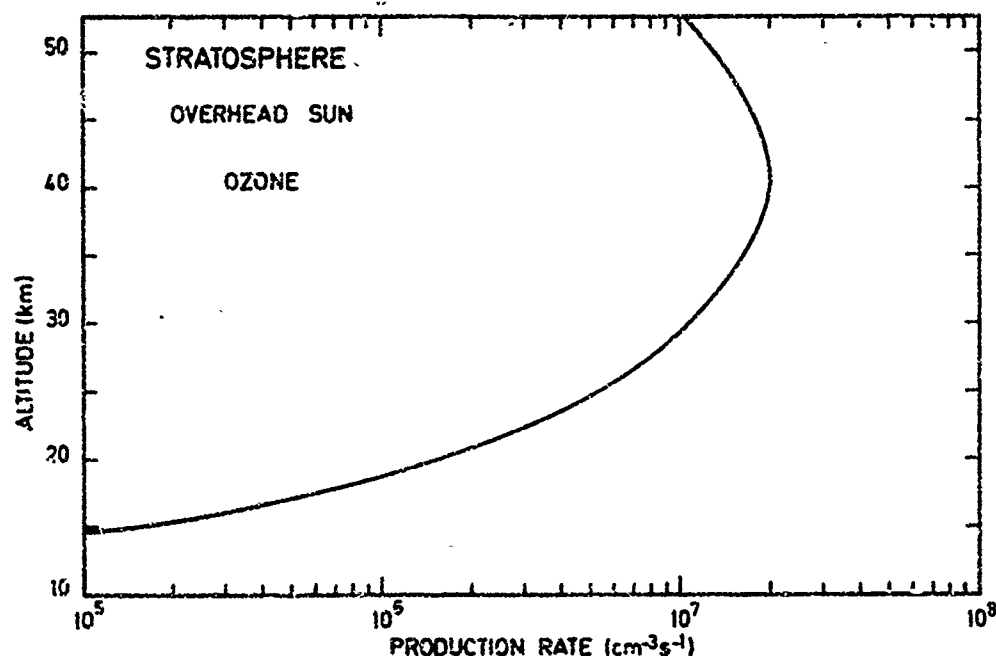


Fig. 1.- Production rate of odd oxygen for an overhead sun.

The loss rates of ozone are respectively given for the Chapman reactions by

$$L_1(O_3) = \frac{2 J_3 k_3 n^2(O_3)}{k_2 n(M) n(O_2)}$$

for the hydrogen compounds reactions by

$$L_2(O_3) = \frac{J_3 n(O_3)}{k_2 n(M) n(O_2)} [a_5 n(OH) + a_7 n(HO_2)] + a_2 n(H) n(O_3)$$

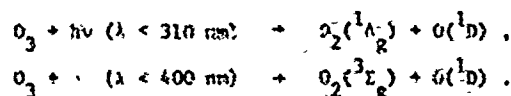
and for NO_x reactions by

$$L_3(O_3) = \frac{2 J_3 b_3 n(NO_2) n(O_3)}{k_2 n(M) n(O_2)}$$

The loss rates L_1 and L_3 are represented on fig. 2 for mid-latitude conditions and using respectively 10^{-9} and 3×10^{-9} as NO_x mixing ratio. Rate L_2 has not been represented since the rate constants a_5 and a_7 and the HO_x distributions are not well known. Nevertheless, order of magnitude calculations show that L_2 can be neglected in the major part of the stratosphere compared with L_1 and L_3 . The integrated loss between 10 and 50 km gives for L_1 $1.7 \times 10^{13} \text{ cm}^{-2} \text{ s}^{-1}$ and for L_3 $6 \times 10^{12} \text{ cm}^{-2} \text{ s}^{-1}$ and $1.8 \times 10^{13} \text{ cm}^{-2} \text{ s}^{-1}$ for 10^{-9} and 3×10^{-9} NO_x used again for the NO_2 mixing ratio.

3. THE NO_x CHEMISTRY IN THE STRATOSPHERE

The production of oxygen atoms in their electronically excited 1D state plays an important role in the stratospheric aeronomy.



A precise determination of the $O(^1D)$ distribution depends on the quantum yield of these processes. According to DeMore and Raper [8] the quantum efficiency at $\lambda < 310 \text{ nm}$ is equal to unity and it sharply decreases over this limit. At 334 nm (Jones and Wayne [9]), the photodissociation of ozone leads to $O(^3P)$ atoms only. In our models, two extreme values have been used in order to make a sensitivity evaluation. We prefer the maximum value since new measurements by Simonsick et al [10] indicate a quantum efficiency of about 0.5 at 312 nm.

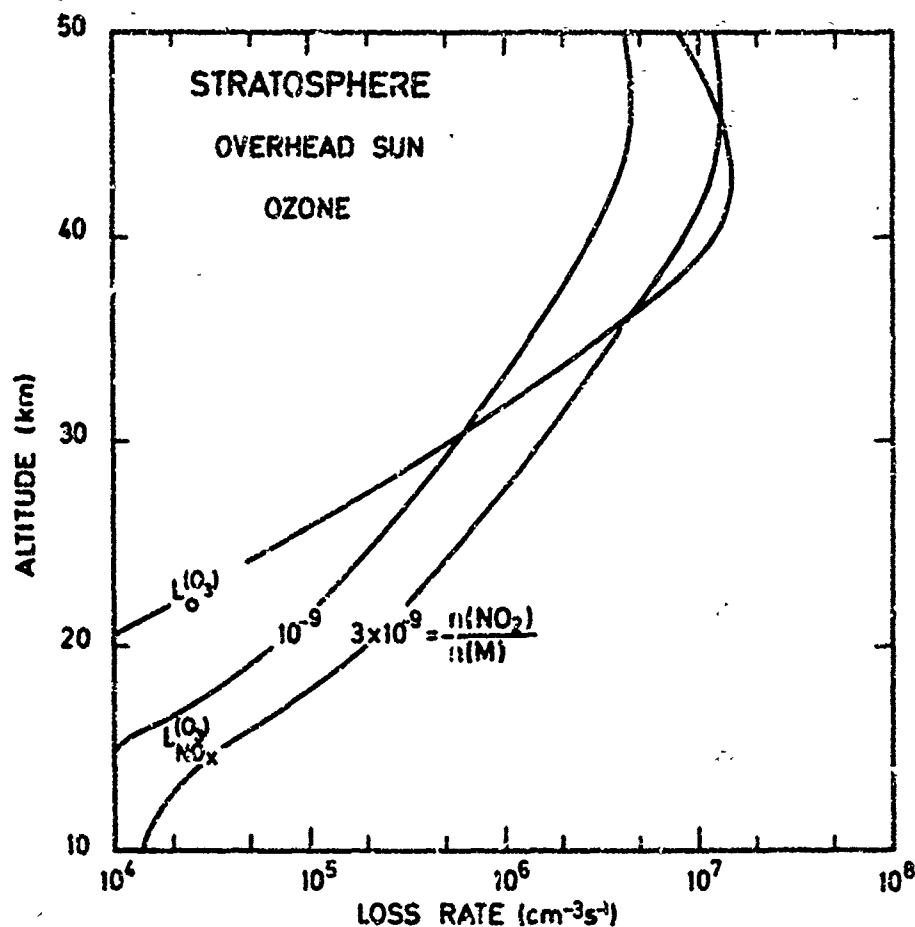
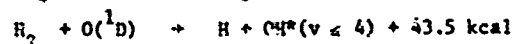
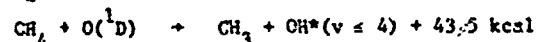
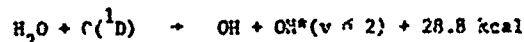


Fig. 2.- Loss rate of ozone by the Chapman reactions (L_O) and by the NO_x reactions (L_{NO_x}) for mid-latitude conditions and an overhead sun. L_{NO_x} has been computed using the constant values of 1 and 3 ppbv as NO_2 mixing ratio.

The $O(^1D)$ atoms are quickly destroyed by quenching with O_2 and N_2 but a fraction of them dissociate water vapor, methane and molecular hydrogen to produce OH and H radicals



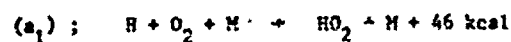
In the stratosphere, the water vapor mixing ratio remains constant and is of the order of 3 ppmv. Methane is produced at ground level, diffuses upward and is dissociated by OH or $O(^1D)$. Its mixing ratio at the tropopause is of the order of 1.5 ppmv. The corresponding value for molecular hydrogen is 0.5 ppmv.

Other reactions involving OH, H and HO_2 must be introduced in order to determine the equilibrium conditions between these radicals (fig. 3) :

- H formation and OH destruction :



- HO_2 formation and H destruction



- HO_2 formation and OH destruction



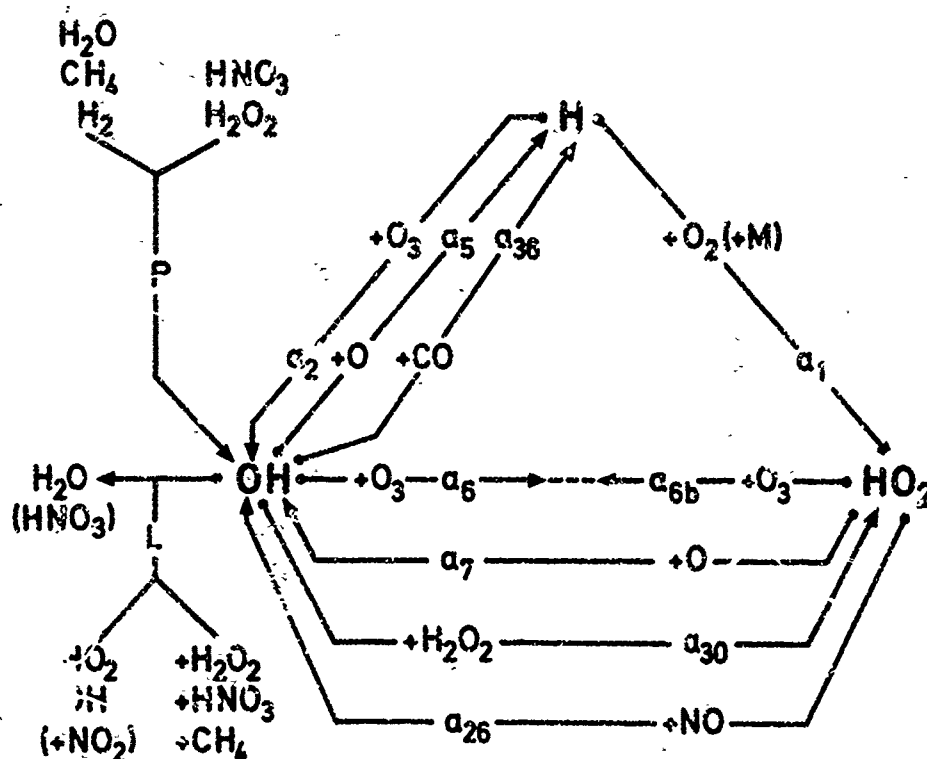
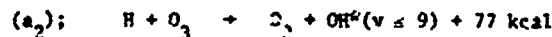
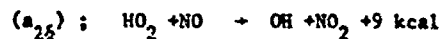
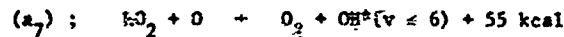


Fig. 3.- Reaction scheme showing the OH - H - HO₂ cycle in the stratosphere.

- OH formation and H destruction



- OH formation and HO₂ destruction



These different mechanisms have been studied with great attention by several authors (see e.g. Nicolat [2]) and won't be discussed in detail here. However, it can easily be seen that the ratio $n(HO_2)/n(OH)$ is

$$\frac{n(HO_2)}{n(OH)} = \frac{a_5 n(O) + a_{36} n(CO)}{a_7 n(O) + a_{26} n(NO)} \left[\frac{a_1 n(H) n(O_2)}{a_1 n(H) n(O_2) + a_2 n(O_3)} + \frac{a_{30} n(H_2O_2)}{a_5 n(O) + a_{36} n(CO)} \right]$$

In the upper stratosphere, it simply becomes

$$\frac{n(HO_2)}{n(OH)} = \frac{a_5}{a_7} \times \frac{a_1 n(H) n(O_2)}{a_1 n(H) n(O_2) + a_2 n(O_3)} = \frac{a_5}{a_7}$$

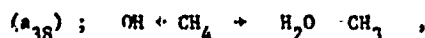
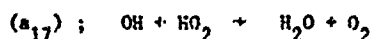
and near the tropopause

$$\frac{n(HO_2)}{n(OH)} = \frac{a_{36} n(CO) + a_{30} n(H_2O_2)}{a_{26} n(NO)}$$

This ratio, which plays a major role in the stratospheric photochemistry and specially (see below) on nitrogen oxides and acids cannot be correctly evaluated since the rate constants a_5 and a_7 and the concentrations of carbon monoxide, nitric oxide and hydrogen peroxide are not known with enough precision. However working values have been used, namely 1 and 9 for the $n(HO_2)/n(H)$ ratio.

If we finally introduce the net loss mechanisms of HO_x reforming water vapor





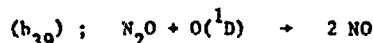
the global balance equation for HO_x can be written

$$a^* [n(\text{H}_2\text{O}) + n(\text{CH}_4) + n(\text{H}_2)] = a_{16} n^2(\text{OH}) + a_{17} n(\text{OH}) n(\text{HO}_2) + a_{38} n(\text{CH}_4) n(\text{OH})$$

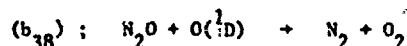
In a more detailed study, nitric acid should also be introduced in the HO_x problem since, as it will be seen below, it contributes to the OH formation and destruction. Nevertheless, it can be seen that the OH concentration closely depends on the nitrogen and the carbon oxides chemistry which must be studied with much attention. (see for example Brasseur and Nicolet [11] and Nicolet and Penner [12]).

4. THE NO_x PHOTOCHEMISTRY IN THE STRATOSPHERE

It was believed until a few years ago that the presence of nitrogen oxides in the stratosphere was due to its production above 90 km and its downward transport by eddy diffusion. However, in 1970, Nicolet [2] has identified an in situ source of NO due to the dissociation of nitrous oxide by ^1D oxygen atom



associated with



The stratospheric production of NO is thus given by

$$P(\text{NO}) = 2 b_{39} n(\text{N}_2\text{O}) n(\text{O}(^1\text{D}))$$

Nitrous oxide is formed by bacteria at ground level and diffuses into the stratosphere. But, during daytime, it is photodissociated by solar radiation and about ten per cent of it is destroyed by reactions (b_{38}) and (b_{39}) . The N_2O distribution is thus very sensitive to the transport conditions; the eddy flux ϕ is related to the concentration n by

$$\phi = -K \left[\frac{\partial n}{\partial z} + \frac{n}{H} + \frac{n}{T} \frac{\partial T}{\partial z} \right]$$

where H is the atmospheric scale height and T the temperature. In the troposphere, where the mean residence time is 1 month, the adopted value for the eddy diffusion coefficient K is $2 \times 10^5 \text{ cm}^2 \text{ s}^{-1}$. But in the stratosphere, where the mean residence time varies between 1 to 2 years, a value between 10^3 and $10^4 \text{ cm}^2 \text{ s}^{-1}$ must be adopted. Since there are variations with season and latitude, two analytical profiles (K_{\min} and K_{\max}) which seem to represent acceptable values have been chosen (fig. 4) in order to estimate the sensitivity of the profiles to the transport intensity.

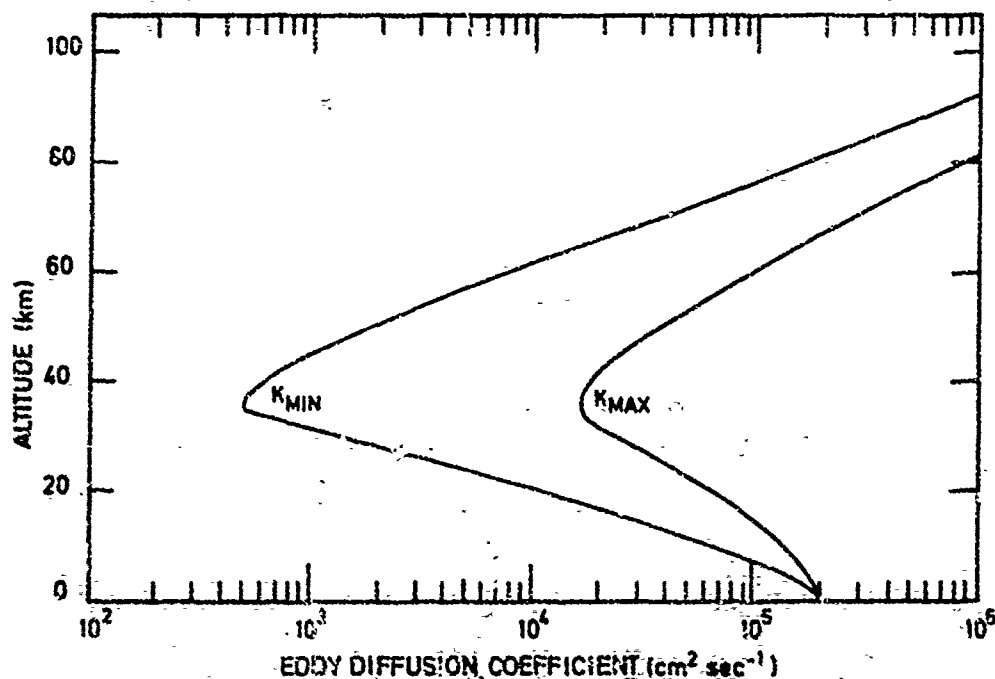


Fig. 4.-- Variable values of the eddy diffusion coefficient with altitude used in the computations.

The vertical distribution of the NO production (fig. 5) depends not only on the eddy diffusivity profile but also on the ozone distribution and the efficiency of its photodissociation to form $O(^1D)$ atoms. The NO production rate reaches a maximum value of the order of $100 \text{ cm}^3 \text{ s}^{-1}$ in the middle of the stratosphere. The values represented on fig. 5 have been divided by 2 in order to take into account the day and night effect.

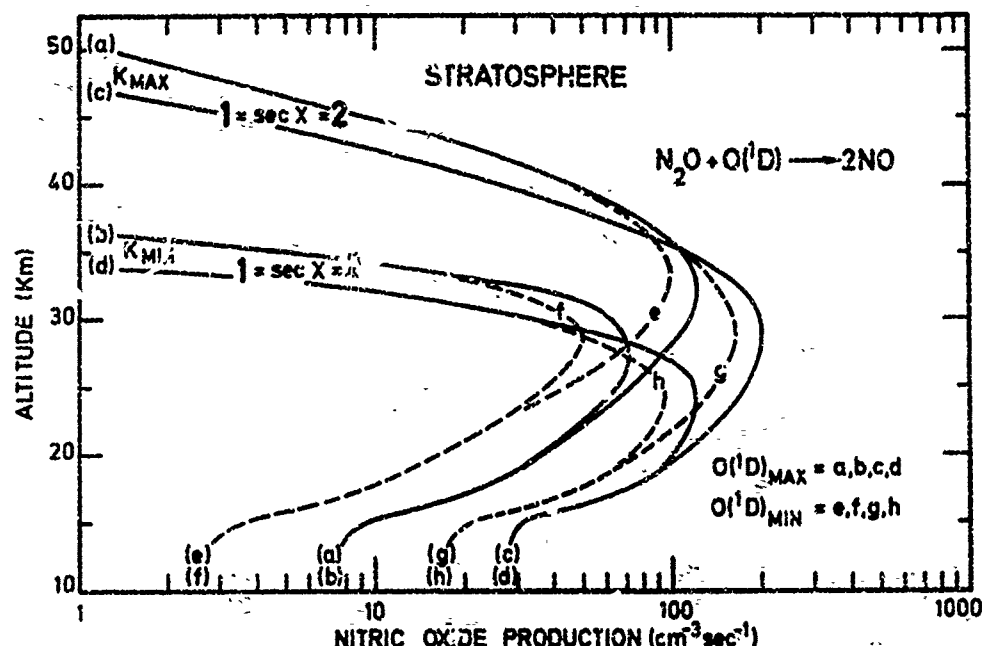


Fig. 5.- Vertical distribution of NO production for various stratospheric conditions.

The total NO production by reaction $O(^1D)$ with N_2O is about $(1.5 \pm 1) \times 10^8 \text{ cm}^2 \text{ s}^{-1}$ (Nicolet and Zeetermans [13]), which is the same order of magnitude as the artificial production by a conventional fleet of 500 SST aircrafts (334 equipped with 4 engines and 166 with 2 engines), flying 7 hours a day and emitting 10 ± 2.5 grams of NO per kilogram of fuel consumed.

As soon as it is produced a fraction of the NO molecules are converted into NO_2 molecules by reaction (b_4) which is associated with (b_3) and (JNO_2) (fig. 6). Since the lifetime of NO_2 is very short during daytime, photochemical conditions can be accepted and the NO_2/NO ratio is given by (fig. 7)

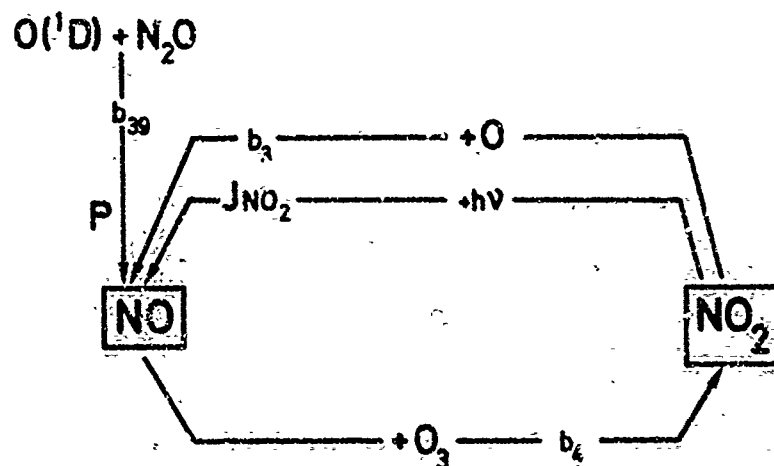


Fig. 6.- NO - NO_2 cycle.

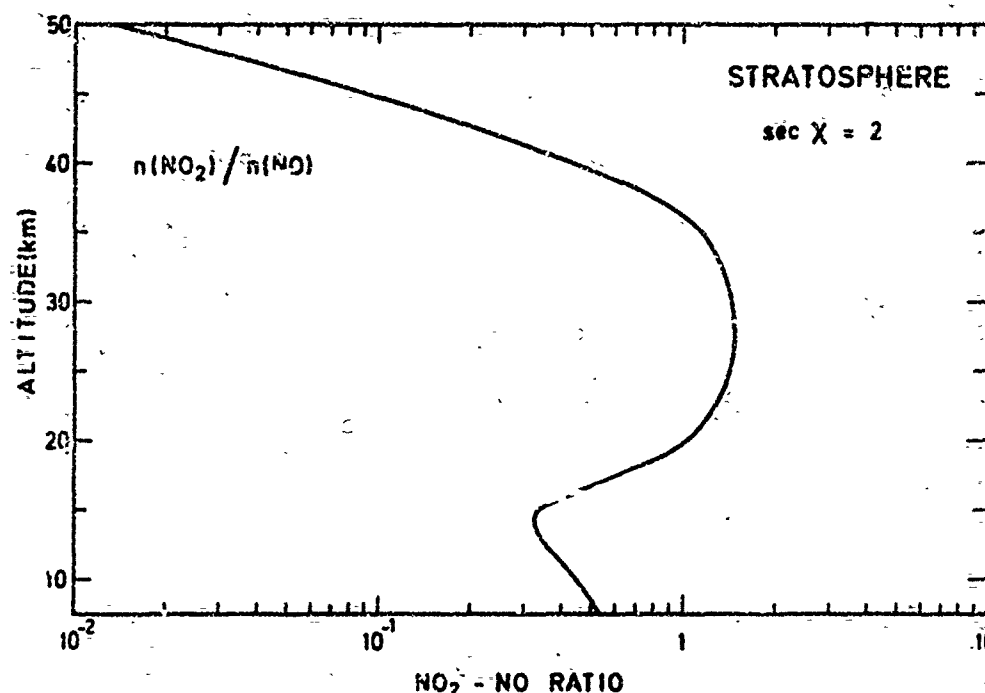


Fig. 7.- Vertical distribution in the stratosphere of the ratio $n(\text{NO}_2)/n(\text{NO})$ for a solar zenith angle of 60° .

$$\frac{n(\text{NO}_2)}{n(\text{NO})} = \frac{b_4 n(\text{O}_3)}{J_{\text{NO}_2} + b_3 n(\text{O})}$$

In the lower part of the stratosphere where the oxygen atom concentration is small, the ratio is proportional to the ozone concentration and its order of magnitude is one. Above 35 km, where $J_{\text{NO}_2} \ll b_3 n(\text{O})$, the ratio decreases rapidly to reach less than 0.05 at 50 km. During nighttime, NO is completely converted into NO_2 .

In the upper part of the stratosphere and above the stratopause, the photodissociation of NO must be considered as an important loss process for NO_x (Brasseur and Cieslik [14]) since we have (fig. 8)

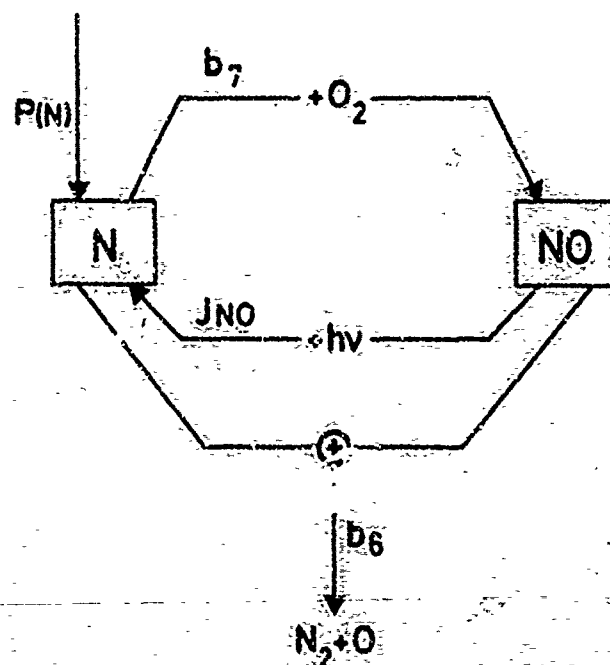
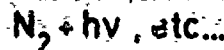
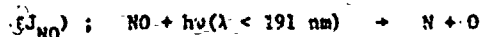


Fig. 8.- Important reactions involving N and NO in the mesosphere and stratosphere.



The most important contribution to the photodissociation coefficient J_{NO} is due to the predissociation in the δ bands, mainly the $\delta(O-O)$ and $\delta(I-O)$ bands since the ϵ band have been shown by Callear and Pilling [15] not to be predissociated and since the β and γ bands have very small absorption coefficients. In the spectral range that must be considered, the absorption of the solar radiation is due in part to the Schumann-Runge bands of molecular oxygen. So, a line by line integration is necessary in order to compute the J_{NO} coefficient (fig. 9). A detailed analysis of this question has been performed by Cieslik and Nicolet [16] who have shown that it is not possible to deduce equivalent average cross sections which are not altitude dependent.

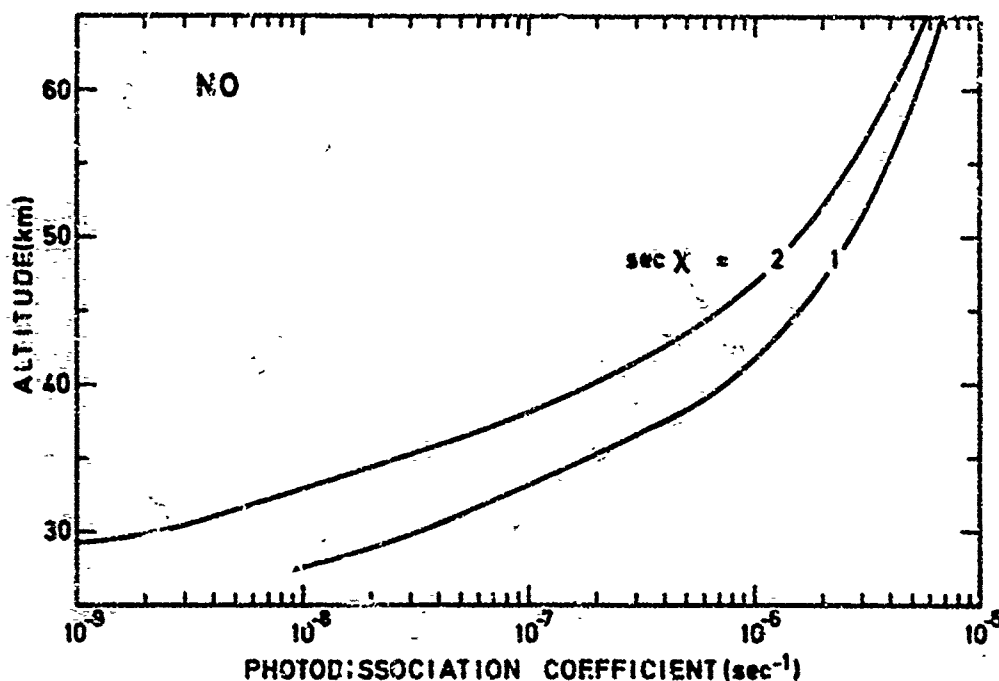


Fig. 9.- Photodissociation coefficient of NO versus altitude for an overhead sun and a zenith angle of 60°

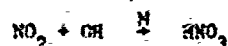
The net loss rate of nitrogen oxides $L(NO)$ is given by

$$L(NO) = \frac{2 b_6 J_{NO} n^2(NO)}{[b_7 n(O_2) + b_6 n(NO)]}$$

and is represented on fig. 10 where it is compared with the production and transport rate.

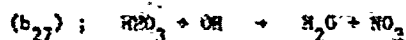
In the middle and lower stratosphere, other chemical reactions involving odd nitrogen atoms in polyatomic molecules must be introduced. The most important constituent certainly is nitric acid on which we shall confine our attention (fig. 11).

This constituent is mainly produced by the reaction

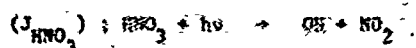


which can be considered as a three body reaction above 20 km and a two body reaction at sufficient high pressure.

Nitric acid is destroyed by hydroxyl radicals



and is photodissociated by ultraviolet light



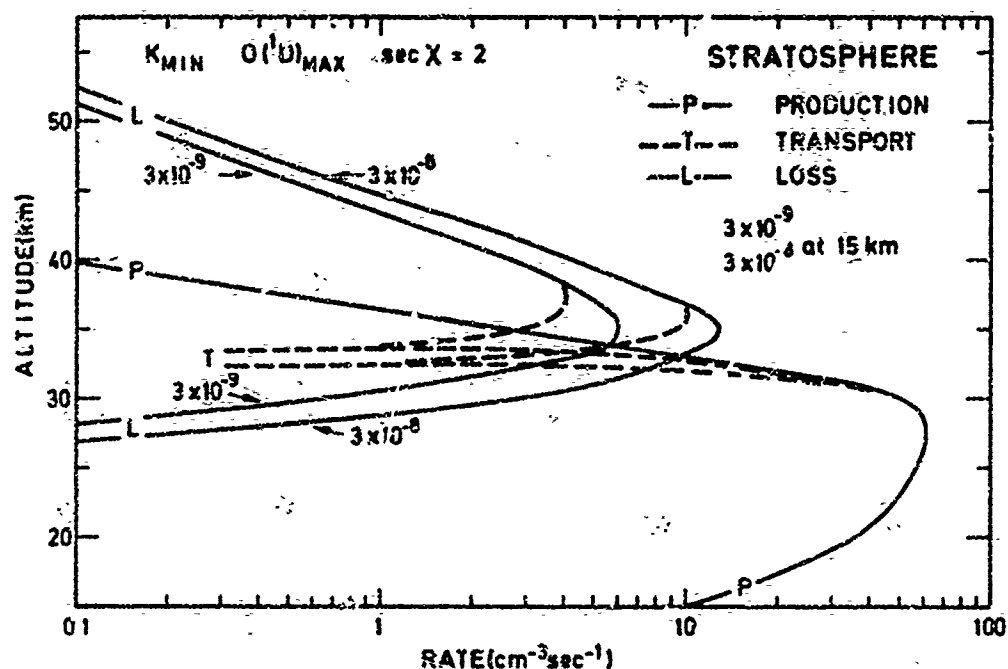


Fig. 10.- Production, transport and loss rates which can be considered as the most probable in the stratosphere. The production term may increase in the lower part of the stratosphere by the cosmic ray effect.

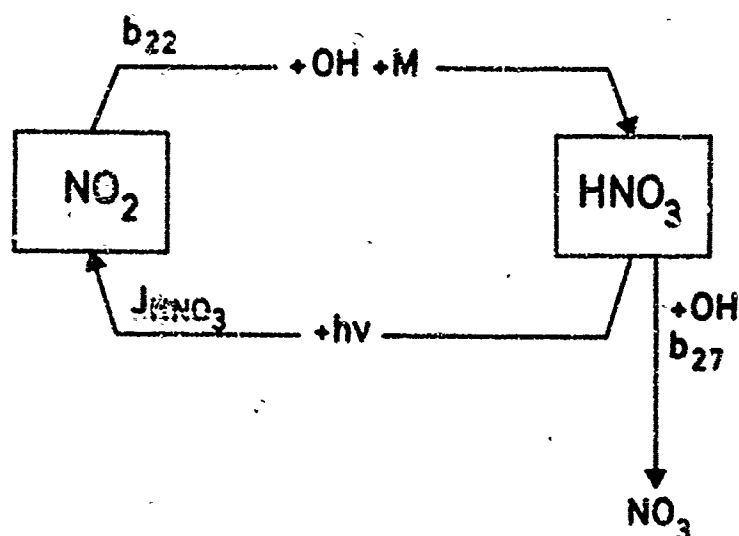


Fig. 11.- Reaction scheme showing the formation and destruction of nitric acid.

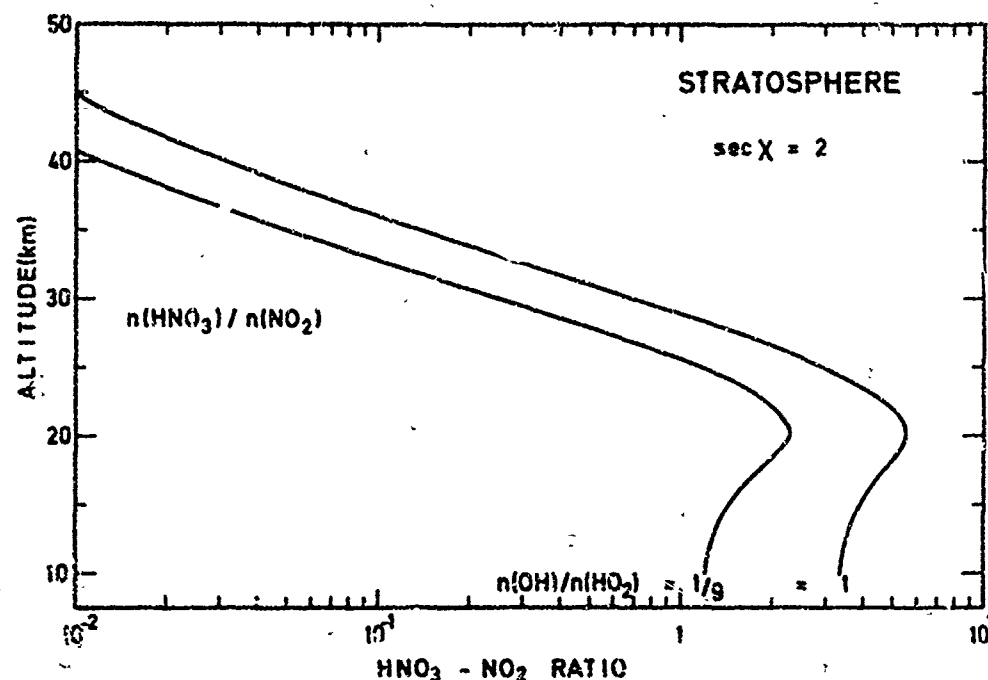


Fig. 13.- Vertical distribution in the stratosphere of the ratio $n(\text{HNO}_3)/n(\text{NO}_2)$ for a solar zenith angle of 60° and assuming two different ratios $n(\text{OH})/n(\text{HO}_2)$.

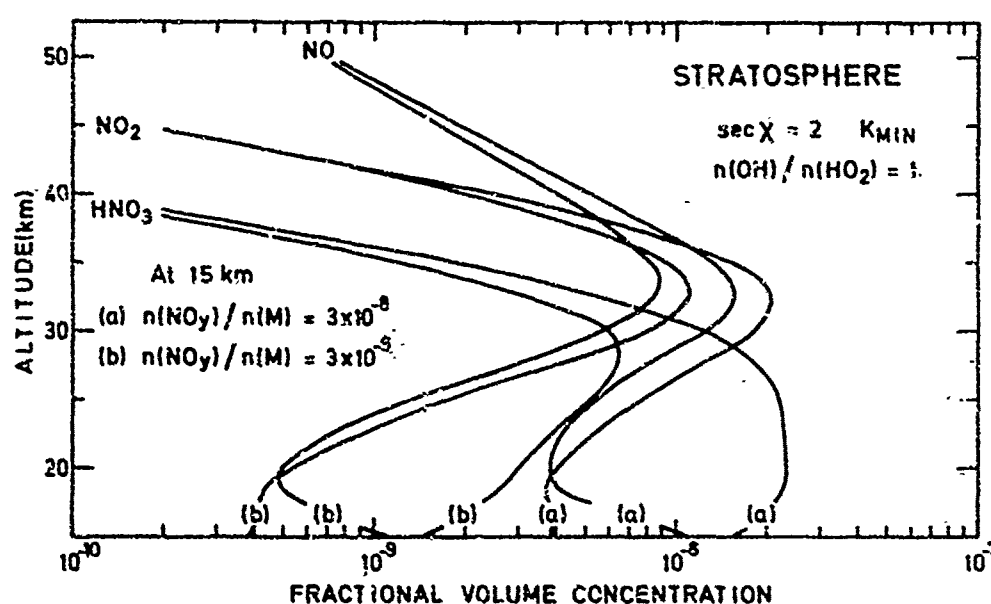


Fig. 14.- Vertical distribution of NO, NO₂ and HNO₃ calculated for two different values of the lower boundary condition of $\text{NO}_y = \text{NO} + \text{NO}_2 + \text{HNO}_3$ and assuming a solar zenith angle of 60° , $n(\text{OH}) = n(\text{HO}_2)$ and $K = K_{\text{min}}$.

Photochemical assumptions give

$$n(\text{NO}_3) = \frac{b_9 n(\text{O}_3) n(\text{NO}_2) + b_{32} n(\text{N}_2\text{O}_5) + b_{27} n(\text{OH}) n(\text{HNO}_3)}{b_{10} + b_{11} n(\text{NO}) + b_{12} n(\text{NO}_2)}$$

and

$$n(\text{H}_2\text{O}_5) = \frac{b_{12} n(\text{H}) n(\text{NO}_2) n(\text{NO}_3)}{b_{32} + b_{31} n(\text{H}_2\text{O})}$$

5. CONCLUSION

The effect of nitrogen oxides on ozone cannot be neglected in the lower stratosphere. In general, the NO chemistry can be explained considering only the oxygen atmosphere. However, hydrogen compounds play an important role in the formation of nitric acid by OH and therefore there is a need to introduce all aeronomic reactions dealing with the formation and destruction of hydroxyl and hydroperoxyl radicals. Since the ratio between the OH and HO₂ distribution is sensitive to the nitrogen and carbon oxides chemistry, a general aeronomic model of the stratosphere must be built.

New values of the important rate constants and cross sections with quantum yields are needed as well as new observational data such as the recent measurements of NO₂ by Ackerman and Muller [20] of HNO₃ by Murcray et al [21] of NO₂ and HNO₃ by Harries [22] of CO by Seiler and Warneck [23] and of CH₄ by Fehalt and Heidt [24].

REFERENCES

- [1] NICOLET, M., Nitrogen oxides in the Chemosphere, *J. Geophys. Res.*, **70**, 679, 1965.
- [2] NICOLET, M., Aeronomic reactions of hydrogen and ozone, *Aeronomica Acta* A n° 79 (1970) and in *Meso-spheric Models and Related Experiments* pp 1-51, Reidel Publ. Co., Dordrecht (1971).
- [3] NICOLET, M., Aeronomic Chemistry of the Stratosphere, in *Proceedings of the CIAP Survey Conference*, pp 44-70, U.S. Department of Transportation (1972).
- [4] CHAPMAN, S., A theory of upper atmospheric ozone, *Memoirs Roy. Met. Soc.* **3**, 103, 1930.
- [5] BATES, D.R., and NICOLET, M., Photochemistry of water vapor, *J. Geophys. Res.*, **55**, 301, 1950.
- [6] CRUTZEN, P.J., The influence of nitrogen oxides on the atmospheric ozone content, *Quart. J. Roy. Met. Soc.* **96**, 320, 1970.
- [7] JOHNSTON, H., Reduction of stratospheric ozone by nitrogen oxide catalysts from SST exhaust, *Science*, **173**, 517, 1972.
- [8] DEMORE, W.D. and RAPER, O.F., Primary processes in ozone photolysis, *J. Chem. Phys.*, **44**, 1780, 1966.
- [9] JONES, I.T.N., and WAYNE, R.P., Photolysis of ozone by 254-, 313- and 334 nm radiation, *J. Chem. Phys.*, **51**, 3617, 1969.
- [10] STMONAITIS, R., BRASLAVSKY, S., HEICKLEN, J., and NICOLET, M., Photolysis of O₃ at 3130 Å, *Chem. Phys. Letters*, **12**, 601, 1973.
- [11] BRASSEUR, G., and NICOLET, M., Chemospheric processes of nitric oxide in the mesosphere and stratosphere, *Aeronomica Acta* A **113**, 1973.
- [12] NICOLET, M., and PEETERMANS, W., On the vertical distribution of carbon monoxide and methane in the stratosphere, *Aeronomica Acta* A, **103**, 1972 and *PAGEOPH*, in press (1973).
- [13] NICOLET, M. and PEETERMANS, W., The production of nitric oxide in the stratosphere by oxidations of nitrous oxide, *Aeronomica Acta* A, **101**, 1972 and *Annales de Géophysique*, in press (1973).
- [14] BRASSEUR, G., and CIESLIK, S., On the behavior of nitrogen oxides in the stratosphere, *PAGEOPH*, in press (1973).
- [15] CALLEAR, A.B. and PILLING, M.J., Fluorescence of nitric oxide, Part 6. Predissociation and cascade quenching in NO D₂E⁺(v = 0) and NO C₂(v = 0) and the oscillator strengths of the c(O,O) and d(O,O) bands, *Trans. Faraday Soc.* **66**, 1886, 1970.
- [16] CIESLIK, S. and NICOLET, M., The aeronomic dissociation of nitric oxide, *Plan. Space Sci.*, **21**, 1973.
- [17] DALMON, R., Recherches sur l'acide nitrique et ses solutions par les spectres d'absorption dans l'ultraviolet, *Mém. Serv. Chim. Etat*, **30**, 141, 1943.
- [18] JOHNSTON, H.S. and GRAHAM, R., Gas phase ultraviolet absorption spectrum of nitric acid vapor, *J. Phys. Chem.*, **77**, 62, 1973.
- [19] BIAUME, Y., Nitric acid vapor absorption cross section spectrum and its photodissociation in the stratosphere, *J. of Photochem.*, to be published (1973).
- [20] ACKERMAN, M., and MULLER, C., Stratospheric Nitrogen Dioxide from Infrared Absorption Spectra, *Nature*, **240**, 3000, 1972.
- [21] MURCRAY, F.G., GOLDMAN, A., CSOKE-POECHK, A., MURCRAY, F.H. and WILLIAMS, W.J., Nitric acid distribution in the stratosphere, *J. Geophys. Res.*, to be published.
- [22] HARRIES, J.E., Measurements of some hydrogen - Nitrogen - Oxygen compounds in the stratosphere from Concord, NO₂, *Nature*, **241**, 515, 1973.
- [23] SEILER, W. and WARNECK, P., Decrease of the CO-mixing ratio at the tropopause, *J. Geophys. Res.*, **77**, 3204, 1972.
- [24] FEHALT, D.H. and HEIDT, V., Profiles of CH₄ in the troposphere and stratosphere, Paper presented at the "Sources, Sinks and concentrations of carbon monoxide and methane in the Earth's environment" meeting, St. Petersburg, Fla. 1972.

ACKNOWLEDGMENTS

I would like to express my gratitude to Professor M. NICOLET for his valuable advice during the preparation of this work.

Discussion on the Paper CHEMICAL KINETICS IN THE STRATOSPHERE

(Paper 7)

presented by

G. Brasseur

A. Goldburg

This question applies to all of the NO_x chemistry papers. What is the implication for next step if Schiff's data, table 7, paper 1, NO concentration in the stratosphere equal to 0.1 ppb, turns out to be correct?

G. Brasseur

There is still an uncertainty in the NO_2 - HNO_3 ratio since it is very sensitive to the hydroxyl radicals concentration which is not well known at the tropopause level. Thus the calculated values of NO, NO_2 and HNO_3 could slightly change if the OH concentration used in our model had to be modified.

But before trying to explain Schiff's data by the theory, we have to wait for other measurements, for example the data obtained with Girard and Farmer's instruments. Preliminary data seem to show values of NO which are higher than the results communicated by Schiff.

A NEW ANALYTICAL TECHNIQUE FOR CONTINUOUS NO DETECTION IN THE RANGE FROM 0.1 TO 5000 PPM

by

H. Meinel and Th. Just
FWLR - Institut für Reaktionskinetik
P.O. Box 800 320
D - 7 Stuttgart 80
West Germany

ABSTRACT

Similar to the technique of atomic resonance absorption spectrometry, the source radiation of NO is passed through an absorption cell supplied by the engine exhaust gas and the amount of radiation absorbed by the NO molecules in the gas is measured. As source lamp for NO, a hollow-cathode discharge tube has been developed producing very strong and sharp rotational lines ($\nu(0,0)=2269 \text{ Å}$). The spectral band-pass of the monochromator is about 20 Å. Background absorption due to soot, oil-droplets and molecular species is checked and compensated for by means of a nearby Bi-line ($\lambda = 2276 \text{ Å}$) from a Bi hollow-cathode source. For this reason, the light from the NO- and the Bi-source is alternately passed through the absorption cell and the ratio of the two resulting signals is measured.

I. INTRODUCTION

Nitric oxide (NO) is known to be one of the principal precursors of photochemical smog (1). Major sources of NO are internal combustion, automobile engines and gas turbines. The quantitative analysis of NO is therefore of importance both in smog and combustion research. While the literature concerning exhaust of other major atmospheric contaminants like hydrocarbons and carbon monoxide is quite extensive, the development of control methods for NO has been stimulated very recently (2). This is mainly due to the fact that the measurement of NO in the exhaust gas of engines and combustors is a more laborious and lengthy matter.

Lower emission standards becoming effective in the future, establish the need for instrumentation that is capable of measuring continuously at lower concentrations. Present methods commonly used for continuous NO analysis are the chemiluminescent NO optical detection (NOOD) (3) and the nondispersive infrared absorption technique (NDIR) (4). The other end of the optical spectrum, the ultraviolet, has received only little attention in terms of NO detection so far (5). This paper describes the initial development effort and application of an ultraviolet resonance absorption method for direct determination of NO as it exists in exhaust or ambient air.

II. NITROGEN OXIDE LEVELS

Approximately 99% of the oxides of nitrogen (NO_x) present in the immediate exhaust emissions have been shown to be in the form of NO (2). The NO concentration in the exhaust of automobiles ranges from about 30 - 3000 ppm dependent on the mode of operation. Concentration levels of NO from aircraft engines are much lower than from automobile engines, typically 10 - 50 ppm depending on fuel/air ratio. The 1980 emission goal for NO emission is - on the average - equivalent to approximately 10 ppm NO in a turbine-powered passenger vehicle.

Since actual mechanisms of oxidation to NO_2 (in the presence of olefins etc.) have been controversial, further laboratory studies directed towards air pollution should be performed at NO levels actually encountered in polluted atmosphere. The NO detector sensitivity is therefore expected to cover the range from 0.1 to 5000 ppm.

III. ABSORPTION METHOD

Nitric oxide is a strong absorber in the UV region. Absorption of light takes place at the 2270 Å region corresponding to the 0,0 transition of the γ system ($A^2\Sigma - X^2\Pi$) (6). The γ bands, which are sharply structured, appear to show four heads arising from two sub-bands to the $^2\Pi_{3/2}$ and $^2\Pi_{1/2}$ ground state multiplet, respectively (separation 121 cm^{-1}). Fig.1 presents a portion of the 0,0 band.

Transmission T is usually defined in terms of optical depth τ by the Lambert-Beer law (5)

$$(1) \quad T = \frac{I}{I_0} = e^{-\tau}$$

$$(2) \quad \tau = f \cdot kx$$

I, I_0 = light intensity after and before absorption

k = absorption coefficient (cm^{-1}) at STP

f = fractional concentration

x = length of absorbing path (cm)

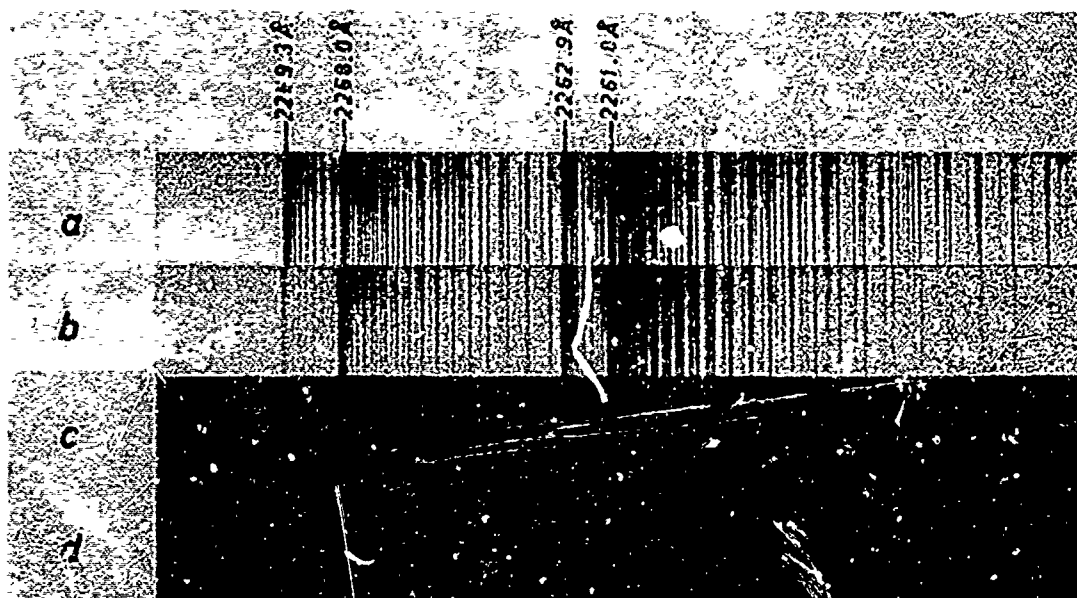


Figure 1 NO- γ (0,0) band, photographed in the second order of a 5 m Ebert spectrograph (reciprocal dispersion $\sim 0.8 \text{ Å/mm}$, 30μ slit). Absorbing path length 63.8 cm

- a) Absorption spectrum of NO at $p_{\text{NO}} = 0.4 \text{ mm Hg}$
- b) Automobile exhaust sample, 110 ppm NO
- c) Emission spectrum of NO from a hollow cathode discharge at $J = 2 \text{ mA}$
- d) Emission spectrum of c, absorbed by a 1200 ppm NO exhaust sample

Under careful laboratory conditions, an absorption exceeding about 2 per cent is detectable. According to Eq (1,2), this $T = 0.98$ criterion for estimating the limits of detectability corresponds to

$$(3) \quad \Delta\alpha \geq 0.02$$

which will be evaluated in chapter VI.

Using a continuum source for measuring the absorption of a sharply structured band, only an integrated absorption coefficient is obtained since any spectrograph has a finite spectral bandwidth (7). In order to measure the peak absorption at the line centers, a slit-width smaller than the line width of NO ($\sim 0.01 \text{ Å}$) would be necessary. This would require a high resolution spectrograph with an inherent low signal to noise ratio.

Similar to atomic absorption spectrophotometry (8), it appears therefore more attractive to measure the absorption at the center (λ_0) of the rotational lines by using a sharp-line source (source line width small compared to the absorption line width), which has emission lines at the same wavelength as the absorption peak (λ_0). In this case the effective bandwidth is defined by the half-width of the source emission line. The only requirement now is to isolate the selected resonance band from other neighbouring (nonabsorbed) emission features for which a small monochromator is adequate.

IV. NO SOURCE LAMP

As spectroscopic light source that meets the requirement to have a stable NO output and to emit sharp rotational lines, a hollow cathode discharge lamp has been developed. Regarding maximum NO emission, the hollow cathode lamp has proved to be most favourable since a discharge current of about 1 mA will suffice to obtain a high signal to noise ratio. Due to the small current (power consumption $\sim 0.1 \text{ W}$) the (gas-)temperature of the emitting source remains at room temperature (Doppler-width of NO lines at 300 K: $\sim 0.005 \text{ Å}$).

The discharge runs in flowing air at a pressure of about 1 mm Hg, maintained by a small rotary pump and controlled by a needle valve set to maximum NO emission. Providing a sufficient air flow through the tube, the amount of NO between cathode and viewing window is kept low so that self-absorption in the tube itself is negligible. The lamp is fed from a stabilized power supply similar to that used for powering photomultipliers.

Fig.1c shows the 0,0 band in emission. Fig.1d was recorded when placing an exhaust sample between source and spectrograph. From a comparison of Fig.1c and 1d it is evident that there is practically no interference due to other emission lines or bands within the 20 Å bandwidth of the monochromator ($2268 \pm 10 \text{ Å}$).

V. MEASURING METHOD

In order to eliminate errors due to an interfering absorption continuum e.g. by coexisting molecular compounds or scattering of droplets and soot particles, a double-beam design is used. The reference signal is obtained from a second, Bi hollow cathode source lamp which emits a strong nearby line

at 2276 Å (within the bandwidth of the monochromator) where the exhaust gas remains transparent to NO. As long as the background absorption at the NO- and Bi-wavelength is the same, the intensity of the NO- and Bi-emission is affected to the same extent. Therefore, by measuring the ratio of the intensity of the NO band to the intensity of the Bi line, background absorption can be compensated for.

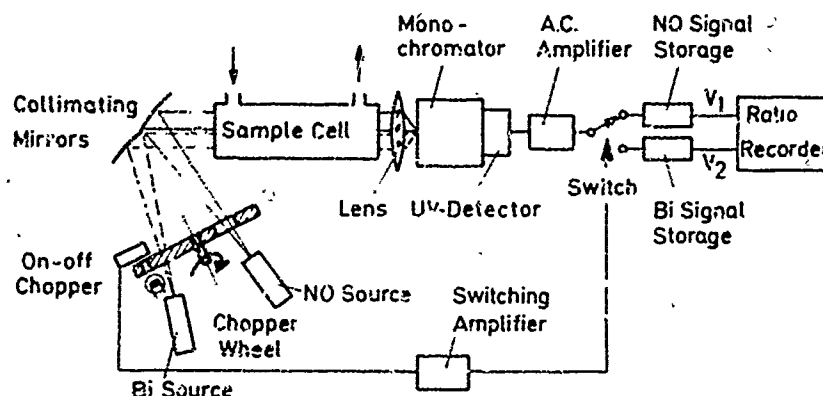


Figure 2 Schematic diagram of the UV resonance absorption NO detector

Fig. 2 shows a block diagram of the actual apparatus. Light from the two hollow cathode discharges passes alternatively through the chopper wheel, turning at 3000 rpm. The source radiation is collimated by a spherical mirror, consisting of two halves, before it is passed through the sample cell. The transmitted radiation is focused onto the monochromator entrance slit and detected by a solar blind spectral type photomultiplier (cut-off above ~ 3000 Å). The resulting a-c detector output is further amplified. An a-c signal obtained from an on-off chopper mounted in front of the chopping wheel drives a CMOS switch to positions corresponding at any instant to the NO or Bi source light. Potentials V_1 and V_2 , proportional to sample transmission at the NO- and Bi-wavelength, are stored in the storage elements, and their ratio is displayed on a recorder.

Since in the double-beam method only one optical path is used, effects of dust and condensation in the exhaust and drifts in the measuring system cancel out. The absorption method described is characterized by a fast response to concentration changes e.g. when installed in the vehicle exhaust sampling train. The response is dependent only on the rate of flow of the gas through the sample cell and the time constant of the electronic detection system.

VI. MEASUREMENTS

Prior to actual exhaust testing, an investigation using standard NO mixtures in different gas matrices was made to determine the sensitivity and the interference from other exhaust compounds, such as H_2O , CO , CO_2 , hydrocarbons etc. Results show that there is no indication of an interference of a sharp-line absorber at concentration levels present in combustion, exhaust or in polluted air. In exhaust samples from piston engines at different modes of operation, continuous absorption has been observed. Continuous absorption, however, is eliminated by the dual-beam method.

The absorption coefficient of NO was determined from optical density curves plotting $\log I_0/I$ versus concentration of NO (Fig. 3). For a sharply structured spectrum, the Beer-Lambert law (Eq 1) is a limiting relationship and only valid for sufficiently low optical depth (7). From the slope of the asymptote to the transmission density curves, the value of k can be calculated. At low total pressure ($p < 1$ mm Hg) a value of $k = 150$ is obtained. If the NO samples are diluted by 1 atm N_2 , the absorption is decreased due to pressure broadening and a k value of 56 is observed. For comparison, a plot of the absorbance is included in Fig. 3, using a deuterium continuum source and a 1 m monochromator with a bandwidth of 0.1 Å (reciprocal dispersor 16 Å/mm 1st order, 12μ entrance/exit slit) yielding $k = 57$ for the band head at 2269 Å. This indicates that even at the above mentioned resolution the resonance absorption method is more sensitive. With a medium resolution monochromator (slitwidth 0.85 Å) the effective absorption coefficient is further decreased to about 5 cm^{-1} (9). For comparison, the k value for the NO fundamental in the IR at 5.25μ is 2.35 cm^{-1} (4).

Evaluating Eq (3), the limits of detection can be determined. In order to detect 0.1 ppm NO ($\epsilon = 10^{-6}$, $k = 56$) an absorption path length of 36m is necessary. This has been realized by means of a multiple reflection cell of 2m length using 18 traversals. With the 63.8mm cell, the detection limit is about 5 ppm. Fig. 4 shows the calibration curve for this case.

In order to establish the usefulness of the UV resonance absorption technique, the method has been applied to exhaust NO measurement at the vehicle tailpipe and from exhaust samples. The most critical test was conducted during actual exhaust analysis by comparing its performance with a commercial chemiluminescent NO optical detector. Comparison of results shows that the agreement between the two methods is about 5 per cent at different NO levels ranging from 40 - 2000 ppm.

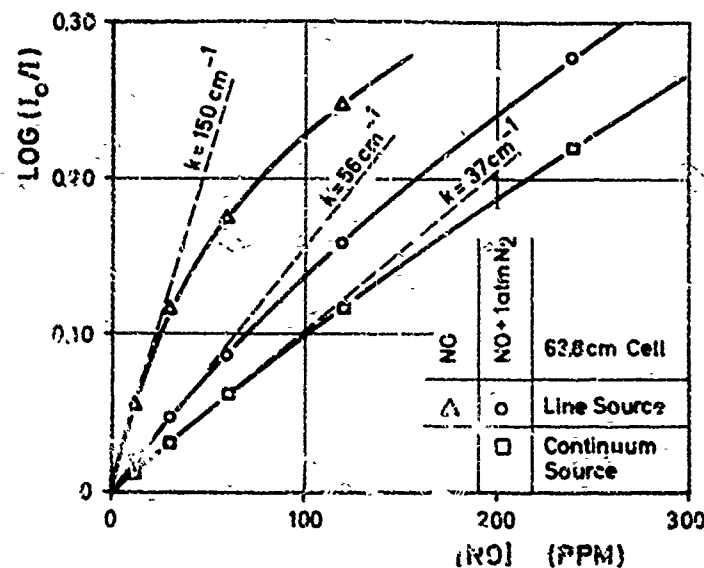


Figure 3

Optical density curves (cell length 63.8 cm)

- △ Low (total-) pressure sample, using resonance absorption technique, bandwidth 20 Å
- NO diluted by 1 atm N₂, resonance absorption technique
- NO diluted by 1 atm N₂, using continuum absorption technique, bandwidth of monochromator 0.1 Å

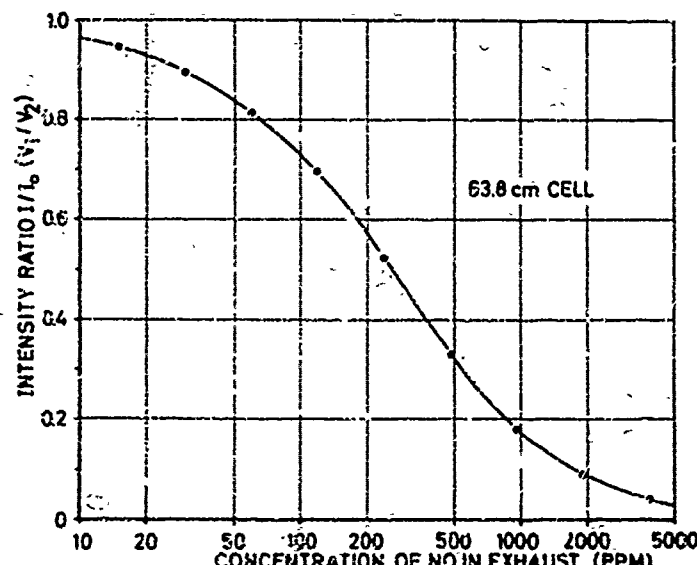


Figure 4

Calibration curve for a 63.8 cm exhaust sample cell

The good reproducibility and accuracy of the results is mainly due to the stability of the radiation sources. Observed drift is less than 0.5 per cent over several hours; the noise level at a time constant of ~ 1 sec is less than 0.5 per cent f.s.d. The extent to which these fluctuations can affect the final error depends on the values of the ratio I_0/I used in the experiment; the precision obtained is $\pm 2\%$.

VII. CONCLUSION

It has been shown that the UV resonance absorption technique is a very suitable, direct detection method for continuous NO measurement. In terms of sensitivity the new method is superior to conventional continuum absorption techniques in the UV and IR by a factor of about 10-30. Since the method requires for spectral filtering only a very small monochromator, it eliminates the need for delicate, expensive monochromators and its attendant service and adjustment problems. The method is characterized by fast response, unattended operation, low maintenance and low power consumption.

ACKNOWLEDGEMENTS

We wish to thank the Deutsche Forschungsgemeinschaft, Bonn, for financial support.

REFERENCES

- (1) A.C. Chamberlain and S.A. Penkett, *Contemp. Phys.*, **13** (1972), pp.179-198
- (2) W. Strauss, *Air Pollution Control*, Part I, **11**, Wiley-Interscience, New York, 1971/72
- (3) H. Niki, A. Warnick and R.R. Lord, An Ozone-NO Chemiluminescence Method for NO Analysis in Piston and Turbine Engines, Society of Automotive Engineers, Report 710072, Automotive Engineering Congress, Detroit, 1971
- (4) P. Campani, C.S. Fang and H.W. Frengle, Jr., *Appl. Spectrosc.*, **26** (1972), pp. 372-378
- (5) A.E.S. Green, *The Middle Ultraviolet: Its Science and Technology*, John Wiley & Sons, New York, 1966, pp. 158-164
- (6) A.J.D. Farmer, V. Jansson and R.W. Nicholls, *J. Quant. Spectrosc. Radiat. Transfer* **12** (1972), pp. 627-633
- (7) R.D. Hudson, Critical Review of Ultraviolet Photoabsorption Cross Sections for Molecules of Astrophysical and Aeronomic Interest, NSRDS-NBS 38 report, Washington, 1971
- (8) L. de Galan, W.W. McGee and J.D. Winefordner, *Anal. Chim. Acta* **37** (1967), pp. 436-444
- (9) B.A. Thompson, P. Hartek and R.R. Reeves, Jr., *J. Geophys. Res.*, **68** (1963), pp. 6431-6435

Discussion on Paper 8

"A New Analytical Technique for Continuous NO Detection
in the Range from 0.1 to 5000 ppm"
presented by H.Meinel

P.Goldsmith: Could you tell us whether this technique is capable of being developed for operation in the stratosphere? It would have to go down to values of 1 ppb or less and operate at low pressures of less than 1/10th of atmospheric.

H.Meinel: Of course, there are two possibilities, first use 50 traversals in a five meter cell, then you can obtain an increase in sensitivity by an order of magnitude, also electronics could be improved for a gain of 1 to 2 orders of magnitude.

J.P.Appleton: Could you tell me what advantage this technique has over conventional chemi-luminescent techniques, since a linear technique goes down to the parts per billion range and up to the many thousand parts per million range?

H.Meinel: First it's very easy to handle, plus you have relative measurement techniques where you only have to measure the ratio of intensities. In the chemi-luminescence technique you must measure absolute intensity with attendant calibration difficulties). Also you have a negative interference due to constituents in the exhaust.

PROBLEMS OF CHEMICAL POLLUTION BY AIRCRAFT
THE AIRPORT AND ITS IMMEDIATE ENVIRONMENT

T.V. Lawson

Reader in Industrial Aerodynamics,
 University of Bristol,
 Dept. of Aeronautical Engineering,
 Queen's Building, University Walk,
 Bristol BS8 1TR, England.

This paper is intended as an introduction to a series of papers concerned with the chemical pollution of the airport and its environment. It calls for a careful study of all surveys so that the inbuilt implications of the model are obvious, and it concludes that the problems of chemical pollution by the aircraft themselves are small. It suggests that much more progress will be made in attempts to reduce pollution around airports by concentrating upon organizations other than the engine manufacturers. It closes by suggesting that authors of technical papers be encouraged to supply an 'epilogue' in which they summarize the findings of their work for the benefit of the lay public.

INTRODUCTION

All forms of transportation pollute their environment, from the horse to the supersonic aircraft; in fact, all combustion processes pollute. But a problem only exists when local concentrations of pollution are excessive. The purpose of this meeting is to discuss the problems posed by the use of a transportation system based on aircraft. This does not mean to say that the parts of the system other than aircraft - the cars, buses, trains, etc. which have been used to move the passengers or goods from their starting point to their final destination - can be ignored. But as problems are caused by local concentrations, only the interface between the aircraft and the other parts of the whole system need be considered here. Consequently, a study of airports and their environments must take into consideration all other vehicles, as well as the aircraft, which constitute the local part of the overall transportation system, and in addition all stationary combustion processes and associated machinery required to satisfy the needs of all at the airport.

In his survey of atmospheric pollution by aircraft engines and fuels and related research work, Professor Sawyer listed 27 problem areas. These can be gathered into groups depending upon the height of the aircraft; the first consisting of problems for aircraft on the ground and in flight up to a height of, say, 1 km. The problems of this phase of the flight can be described in terms of the 'airport and its immediate environment'. A second group is made up of problems which arise when the aircraft is above about 18 km (to put a number to a strict dividing line which does not occur in practice): they arise from the nature of the stratosphere and can be described as 'stratospheric'. For flights at intermediate heights, normal operation of aircraft produces no pollution problem which has not been studied in one or other of the two groups; but a few special problems, such as cloud cover in the high troposphere, do exist and must be separately considered.

The second group of problems was discussed in Papers 1 to 8: these remarks essay to act as an introduction to papers 9 to 15 covering the first group of problems. The pollution of the environment by noise is expressly excluded from the discussion.

AIRPORT AND ITS NEIGHBOURHOOD PROBLEMS

At the start of a study, it is always beneficial to try to assess the magnitude of the problem, so that conclusions can be viewed in perspective. From a distillation of many surveys at different airports, the situation could be summarized as: 'By and large, taking all the commonly measured pollutants into consideration, the airport probably produces less pollution per unit of area than the surrounding urban community.' A closer look at the surveys suggests that about half of this pollution is produced by motor vehicles within the airport perimeter (fractions differ from one pollutant to another) and a considerable fraction of the remainder by aircraft while taxiing or idling prior to take-off. The contribution due to aircraft taking-off and climbing out or descending and landing is a small fraction of the pollution in a fairly clean area.

The attempt to make this summary highlights one of the major difficulties in this subject: it is a consequence of the different descriptions of the phenomena from which the details of each study have been isolated and inter-related. The in-phrase is 'the model'. The results of each survey are strongly affected by the thoughts and ideas of those who define the model - in the first instance by the choice of pollutants included and the method of their measurement. But this is an obvious bias which is at once clear to the reader. A slightly less obvious bias is introduced by the choice of assumptions made. These should not just be read through quickly as the preamble to the report, but pondered carefully and the implications of each individually and collectively weighed. There are subtler ways still of making a point, sometimes through the choice of a word, or the order in which items are presented. It is essential to read these surveys carefully from beginning to end, taking particular notice of assumptions made and all the remarks in small print. The reader should have a large coloured crayon in his hand with which to underline words and phrases which might be important to a full understanding of the results. As an illustration, consider Sawyer's statement in his survey 'The aircraft has been identified as a small but significant source of air pollution'. At first glance it is a better précis of the state of affairs than the one which started this section. But the interesting word is 'identified'. The usual procedure for an airport survey is to study aircraft movements, listing them by types; determine quantities of emission of the selected pollutants (either from the manufacturers or elsewhere) in all their operating conditions; evaluate average times

spent in all phases of operation, and, by combining all these, together with the chemical composition of the fuels, arrive at a value for the pollution emitted by the aircraft whilst within the confines of the airport.

The instantaneous output of the sensors placed on the airfield rarely shows spikes representing the movement of individual aircraft. Individual aircraft are not identified. The total pollution calculated as emitted by aircraft within the airport area is debited to the airport area. Surely a good assumption? On this same assumption the pollution produced by a 4,000 Megawatt power station must be debited to the area of the power station. If this were done, the resulting estimated level of pollution would be prohibitive. But the pollution from the power station is emitted from a tall chimney at a reasonably high temperature, so that it rises and disperses over a large area. Granted, the height of emission from aircraft is low in this phase of their operation, but the temperature of the efflux is high, much higher than from power stations. Perhaps this dispersion is the reason why the passage of individual aircraft has not been identified and why meteorological conditions at individual airports ought to receive more attention. Further mention of meteorological conditions will appear later in this paper.

Criticism of a survey or a particular model does not deny that aircraft emit pollutants: the purpose of the remarks was to draw attention to the fact that the numerical evaluation of the survey depends strongly upon the model of pollution used. It is to be hoped that very careful scrutiny of the assumptions in any model will be made before important and far-reaching decisions are taken as a result of the numerical results presented.

Turning to the pollutants themselves, they fall into three groups, depending upon how they are identified: those that can be seen, can be smelt, and require instruments for their detection. An understanding of the mechanisms of production of the first and third groups is developing and their control within prescribed limits appears probable; but at present understanding of the production of smells is minimal. Although the smell of airports is objectionable, I have a friend who enjoys it because he associates it with travelling and going to exciting places. Perhaps the answer to the smell problem is a P.R. campaign! To be serious, the smell problem is different because it is a difficult one to quantify in absolute or even comparative terms. More effort is required in this field; and difficulty, which has never stopped the aeronautical industry before, should not be given as a reason for doing nothing.

Great strides have been made in recent years to reduce the quantity of particulates in emissions so that, now, in one modern engine at least, while operating with reheat, the opacity from NO₂ emission is equal to that from particulates. Once this situation has been reached, and it will ultimately be reached in other engines with reheat, the problem of further reduction of visible emissions requires a two-pronged attack on particulates and NO₂ generation; and the cure for the NO₂ generation might conflict with the generation of NO_x in other modes of operation. This could result in a slowing down in the improvement of visible emissions, an improvement which has been particularly marked in recent years. It is unfortunate that the visible emission from aircraft is viewed against a clear blue or white background: the actual opacity is at least an order better than that proposed for motor vehicles, whose exhausts are usually viewed against the background of dirty, uneven road surfaces.

With a typical survey of airport pollution as a starting point, a quick study of the polluting machinery involved shows that action other than a meticulous attention to the jet engine exhaust could have a greater and more immediate effect. Cars create about half the present pollution at an airport such as Heathrow. Cars are used by the travelling public, by friends of the travelling public, by visitors and sightseers to the airport, and by the airport services. (Maximum pollution levels at Heathrow were measured in the approach tunnel through which visitors' cars reach the central passenger handling area). Control on the emission from cars will help this part of the problem, although control on the use of cars and their partial replacement by a non-polluting form of transport locally, both for passengers and services, could have a greater impact.

Taxying and idling are the phases of aircraft movement which contribute most strongly to pollution problems. Recent moves in engine design are producing engines with combustion efficiencies at idle of above 95%; but surely an improvement in the ground handling of aircraft could have a more immediate (even with existing engines with poor combustion efficiencies at idle) and more spectacular effect upon pollution levels at airports. Taxying times cannot be eliminated completely by using non-polluting traction methods, because engine checks have to be made prior to take-off and the 'jobbing' problem requires the engines to be run at low power for about 5 minutes before developing full power. The thrust developed might just as well be used for taxying, but any extension of the 5-minute period produces nothing but pollution and frustration. The layout of airports should consider the relative location of terminal buildings and the ends of runways, so that areas where excess pollution is emitted are not up-prevailing-wind of highly populated buildings, loading bays, or housing adjoining the airport.

This leaves the take-off and landing phases in which there is emission of pollution in spite of the extremely high combustion efficiencies, because of the large quantities of fuel burnt. Improvements in this phase of operation can only be achieved by reducing the quantities of pollutants emitted. Whereas it is always advantageous to reduce the pollution emitted, some attempt must be made to assess the effect of its high temperature on its ultimate diffusion, if accurate quantitative studies of pollution in airport vicinities are to be made.

In the last three paragraphs many people have been introduced into the arena wherein the engine manufacturer often stood alone. Only two have an incentive to cut pollution: the engine manufacturer whose cleaner engine would have a tremendous sales advantage providing its economics are comparable to those of his competitors, and the airline operator who pays for the excess fuel burned (it would be an interesting study to see a comparison between the cost of this fuel and the profit made on each flight). At present, most of the external pressure to reduce pollution is exerted on the engine manufacturer, who already has a strong incentive to improve. The fruits of his efforts will, however, be slow to manifest themselves because of the time delay before existing engine designs no longer form a majority of engines

in service, whereas reduction of pollution by the public, the airlines and the airport authorities can have an immediate impact. This would leave the improvements in engine design to compensate for increase in traffic in the years ahead.

The outside pressure for these changes must be applied upon the airport authorities, because they alone can react to it. In turn, they can apply pressure on other bodies in a number of ways, a few of which are listed below.

On the Planners to ensure that new airports are not built in areas which have adverse meteorological conditions. Sawyer discusses this under Problem Area 22, the 'atmospheric air pollution dynamics'. In layman's language, this means that the volume of traffic at certain airports could be limited by the local meteorological conditions due to which the local atmosphere reaches the maximum acceptable standard of impurity. Two conclusions from this statement ought to be emphasized; the first, as mentioned above, is that new airports (destined for high traffic density) ought not to be situated in regions sheltered from natural ventilation, and the second, that airports in current use ought not to be condemned or controlled by legislation arrived at as a result of studies at a few airports where the meteorological conditions are known to be particularly bad from the ventilation point of view.

On their Architects to ensure that the relative location of all buildings and the runway is such as to prevent the prevailing wind from blowing into an inhabited area the effluent from aircraft waiting at the end of the runway prior to take-off.

To design the loading bays for people and goods, so that they do not form traps for the pollution emitted when the engines are started.

To ensure that any area in which aircraft can stand with their engines running does not point to or adjoin residential areas outside the airport.

To arrange that all car parks for the public are so sited that their effluents during approach and parking (cars are bad at idle as well) are diffused before merging with another source of pollution.

On their Ground Controllers to ensure that no aircraft should start its engines until its lift-off time has been agreed; and even then only sufficient time should be allowed between start-up and lift-off for taxiing to the beginning of the runway and the concurrent engine checks and debowing routine. Obviously, slip arrangements for the aircraft in trouble with engine checks will have to be made, but surely in the age when we are talking of doing away with the stack at landing and giving an aircraft a touch-down time to within 10 seconds when it takes off thousands of miles away, we could solve this simple delay problem.

On the Public, whether the travelling public, their friends or sightseers, to accept some reorganization in the parking of their cars. This should include the supply of mechanised walkways from the car park to the terminal buildings, preferably under cover from the elements. It is essential that the public should feel wanted and encouraged to travel by air.

The bias of this paper is obvious: it agrees with Professor Sawyer that aircraft are a small but significant source of pollution, but it considers that the problems so caused by low level emissions are small. It suggests that pressure for improvements exerted on organizations other than the engine manufacturers will produce greater and more immediate benefits. The engine manufacturers, meanwhile, ought to be encouraged to do more research on the small problem, about which all too little is known.

EPilogue

Pollution is a highly emotive subject - and often those who know the least are the most vociferous. The scientist, announcing his results, does so in the way he has been taught, expressing uncertainties and assumptions clearly. In the hands of unscrupulous or misinformed commentators, these can be amplified or suppressed so as to change the overall meaning of the results. I see no solution to this predicament - except perhaps to suggest the addition of an epilogue to each report wherein the author can express his interpretation of the work in layman's terms, being, at the same time, exempt from the rigours of exactitude which usually bind him.

RELATIVE AIR POLLUTION EMISSIONS FROM AN AIRPORT
IN THE UK AND NEIGHBOURING URBAN AREAS

A.W.C. Keddie, BSc., PhD., J. Parker & G.H. Roberts, BSc.,
Air Pollution Division, Warren Spring Laboratory,
Department of Trade and Industry, P.O. Box 20, Gunners
Wood Road, Stevenage, Hertfordshire, SG1 2BX.

SUMMARY

This paper discusses air pollution levels at Stansted Airport in relation to emissions from four nearby towns. Calculations have been made of pollution emissions from these four sources and also from the airport and the expected contributions from these sources at three local sites have been examined. These values are compared with actual measurements at the three sites.

INTRODUCTION

One of the problems in air pollution is comparing major pollution emissions from different sources and the pollution levels arising from them. This has been previously attempted in a paper on pollution at Heathrow Airport¹. This paper gave details of measurements of pollution levels from both airport and urban sources, but at the time it was not possible to include data on urban emissions in the area, partly because no complete urban emission data existed at that time and partly because of the complexity of the urban pattern near Heathrow. Because of this complexity further studies were concentrated on Stansted Airport. While the total air traffic there is much less than at Heathrow, it represents an ideal site for basic work. It is situated in open country and has four towns in close proximity: Bishop's Stortford - 22,000 inhabitants, at about 5 km; Stansted Mountfitchet - 4,500 inhabitants, at about 7 km; Elsenham - 2,500 inhabitants, at about 3 km and Takeley - 1,500 inhabitants, at about 2 km.

Calculations based on actual fuel sales in Bishop's Stortford have been made of the likely pollution emissions from the four towns. Consumption in the three smaller towns has been estimated from the Bishop's Stortford figures on a population basis. Estimations have also been made for the aircraft, road traffic operations and heating plant at the airport.

The parts of the paper are as follows:

1. Annual fuel consumption in Bishop's Stortford
2. Estimated annual fuel consumption in Stansted Mountfitchet, Elsenham and Takeley
3. Pollution emissions from road traffic
4. Overall pollution emissions
5. Estimated pollution emissions from Stansted Airport
6. Environmental measurements at Stansted Airport
7. Predicted ground level concentrations from all sources
8. Conclusions.

The geographical area covered in this paper is illustrated in Figure 1.

ANNUAL FUEL CONSUMPTION IN BISHOP'S STORTFORD

With the assistance of the Chief Public Health Inspector at Bishop's Stortford, arrangements were made to check annual fuel consumptions in the town and these are shown in Table 1.

TABLE 1 - Annual Fuel Consumption in Bishop's Stortford - 1970/71

(Tonne Year⁻¹)

Fuel	Market	Annual Consumption
Coal	Domestic	4,000
"	Industrial	-
Smokeless Fuel	Domestic	9,000
"	Industrial	-
Oil	Domestic	1,000
"	Industrial	4,046
Gas	Domestic	2.295 x 10 ³ Therms
"	Industrial	0.405 x 10 ⁶ "

ESTIMATED ANNUAL FUEL CONSUMPTIONS IN STANSTED MOUNTFITCHET, EISENHAM AND TAKELEY

The annual consumption in these villages has been estimated on a population basis, as being directly proportional to the fuel consumption in Bishop's Stortford. In only one aspect will these estimations differ and that is in the actual fuel consumption for industry in Stansted Mountfitchet, where it has been possible to obtain figures of the fuel consumption in a factory in the town. The consumptions are shown in Table 2.

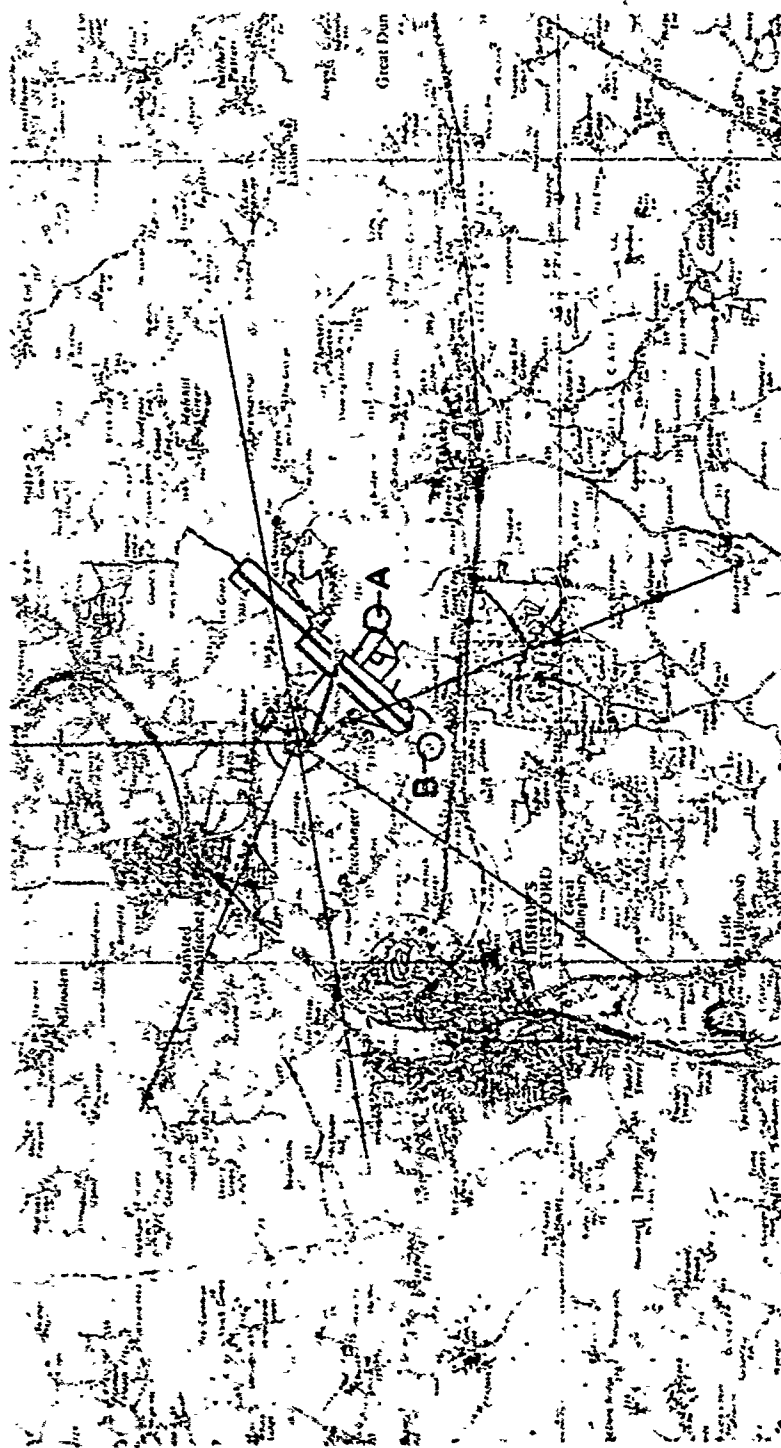


FIG.1 MAP OF STANSTED AREA SHOWING LOCATION OF SITES AND SAMPLING ANGLES

Based upon the Ordnance Survey map with the sanction of the Controller of H.M. Stationery Office,
Crown Copyright reserved.

TABLE 2 - Estimated Annual Fuel Consumption in Three Small Towns

(Tonne Year⁻¹)

Fuel	Market	Stansted Mountfitchet	Elsenham	Takeley
Coal	Domestic	818	454	273
Smokeless Fuel	Domestic	1841	1022	614
Oil	Domestic	205	114	68
Oil	Industry	19	-	-

POLLUTION EMISSIONS FROM ROAD TRAFFIC

When dealing with estimations of pollution from road traffic the position is more complex. It is not possible to obtain details of actual sales of motor fuel in a town, which would enable estimations to be made similar to those made for static sources. However, the Department of Trade and Industry publishes a Digest of Energy Statistics² in which total regional fuel sales are listed. The 1971 figures for the East Anglia Region in which the four towns are located, were: Petrol - 0.549×10^6 tonne; Diesel fuel - 0.201×10^6 tonne. The population of this region was 1.681×10^6 inhabitants. The pollution emissions in Bishop's Stortford are estimated in the ratios of the respective populations and also on the assumption that, on average, petrol vehicles travel 8.8 km l^{-1} and diesel 7.0 km l^{-1} . The factors for the vehicles are also the same as quoted in the Heathrow paper. In turn these estimations have been extrapolated down for Stansted Mountfitchet and Elsenham. One complication however, is that the town of Takeley is situated on the main A.120 road and therefore the traffic through the town will be much higher than would normally be expected in a similar small town not on a main highway. It was therefore decided to estimate road traffic pollution emissions in this town from the traffic census figures taken on this road in 1971. These showed that the traffic flow was 3569 diesel and 8326 petrol vehicles per day.

During the work at Stansted there was some evidence that the through road past Stansted Mountfitchet was being used by traffic going to the A.11 as a short cut to avoid passing through Bishop's Stortford. In the time available it was not possible to carry out a traffic count on this road to determine whether the estimates of emissions from traffic in Stansted Mountfitchet were too low. Because of the volume of traffic on the A.11 trunk road it is possible that the pollution emissions from road traffic used for Bishop's Stortford and Stansted Mountfitchet, may be about 5 per cent low.

OVERALL POLLUTION EMISSIONS IN THE FOUR TOWNS

For convenience it is proposed to summarize the estimated emissions from all sources in the four towns. The figures are shown in Table 3. It must be remembered, however, that it is not possible to predict the contributions to the ground level concentrations from these overall figures alone because the dispersion characteristics of each class of emission are different. For example, domestic emissions generally occur at a height of about 10 metres, industrial emissions from 20-30 metres (some larger industries emit at heights of over 200 metres) and road traffic at less than 1 metre.

TABLE 3 - Overall Pollution Emissions in the Four Towns

(Tonne d⁻¹)

Town	CO	NO _x	Hydrocarbons	SO ₂	Particulates
<u>Bishop's Stortford</u>					
Domestic	5.56	0.21	-	0.63	0.50
Industrial	0.01	0.07	-	0.58	0.04
Road Traffic	8.77	1.27	1.06	-	0.09
Total	14.34	1.55	1.06	1.21	0.63
<u>Stansted Mountfitchet</u>					
Domestic	1.14	0.04	-	0.13	0.11
Industrial	-	0.01	-	-	-
Road Traffic	1.80	0.26	0.18	-	0.02
Total	2.94	0.31	0.18	0.13	0.13
<u>Elsenham</u>					
Domestic	0.63	0.03	-	0.07	0.05
Road Traffic	0.99	0.19	0.11	-	0.01
Total	1.62	0.22	0.11	0.07	0.06
<u>Takeley</u>					
Domestic	0.38	0.02	-	0.05	0.04
Road Traffic	0.74	0.12	0.09	-	0.01
Total	1.12	0.14	0.09	0.05	0.05

ESTIMATED POLLUTION EMISSIONS AT STANSTED AIRPORT

It is not proposed to show in detail the complex calculations for estimating the emissions from aircraft operations. They have been estimated on the same basis as that used in the work at Heathrow.

Data supplied by the British Airport Authority for aircraft movements at Stansted Airport are shown in Table 4.

The general aviation category consists mainly of small petrol-driven aircraft used for private flying.

TABLE 4 - Total Aircraft Movements at Stansted Airport 1970-71

Types	Yearly Total
Turboprop	5,359
Short Haul Jets	9,581
Long Haul Jets	10,797
General Aviation	18,722

For estimating pollution emissions during taxi-ing operations a total ground movement time of 6.7 minutes per scheduled aircraft was chosen from the British Airport Authority records. Total ground movement time for the general aviation category was 2.25 minutes because this category seldom use the full length of the runway. For calculating the emission density at the airport a surface area of 3.54 square kilometres was used.

Road Traffic

During the work traffic counts were made of vehicles entering the airport terminal area. A detailed analysis of this traffic flow will be given in a later paper, but the mean flow during the period of the tests was 1419 vehicles per day, of which approximately 30 per cent were diesel.

Static Sources

There are a number of small package units providing the central heating plant at the terminal area. The pollution emissions from these plants during the periods November 1971, and February to April 1972 have been estimated from actual fuel consumption data. During these periods the total fuel consumption was 42,270 and 130,631 litres of 34 second oil respectively.

The total emissions of pollution from operations at the airport, i.e. aircraft operations, road traffic and heating plant, are given in Table 5.

TABLE 5 - Estimated Pollution Emissions at Stansted Airport

(Tonne d⁻¹)

Operation	CO	NO _x	Hydrocarbons	SO ₂	Particulates
<u>Aircraft Operations</u>					
Taxi-ing	1.58	0.03	0.63	-	0.005
Groundborne take-off	0.01	0.03	0.01	-	0.007
Airborne take-off	0.01	0.01	-	-	0.003
Aircraft Total	1.57	0.07	0.64	-	0.015
Road Traffic	0.06	0.01	0.01	-	0.001
Central Heating Plant	-	0.01	-	0.018	-
Gross Total	1.63	0.09	0.65	0.018	0.016

Taking Bishop's Stortford (area 15.30 km²) and Stansted Airport (area 3.54 km²), the emission densities have been estimated from the emission data in Tables 3 and 5 and are compared in Table 6.

TABLE 6 - Pollution Emission Densities - Stansted Airport and Bishop's Stortford

(Tonne km⁻² d⁻¹)

Location	CO	NO _x	Hydrocarbons	SO ₂	Particulates
Bishop's Stortford	0.87	0.10	0.07	0.08	0.05
Stansted Airport	0.46	0.02	0.18	0.01	0.01

From Table 5 it can be seen that, of the major pollutants emitted from both sources, it is only in the case of total hydrocarbons that the airport emission densities exceed those of Bishop's Stortford.

ENVIRONMENTAL MEASUREMENTS

Because of the low values of carbon monoxide and total hydrocarbons obtained near the runway at Heathrow

no measurements of these pollutants were undertaken at Stansted. Measurements were confined to smoke and sulphur dioxide and these determinations were carried out as described in the National Survey of Air Pollution, 1961-71, Volume 1, page 4.

Measurements were carried out in two stages:

1. Two standard volumetric instruments were installed to sample smoke and sulphur dioxide in the positions shown in Fig. 1, i.e. one in a hut to the east of the main runway (Site A) and the other in the Instrument Landing System enclosure at the end of Runway 05 (Site B).
2. At the end of the preliminary work a directional sampler⁵ was installed at the north west perimeter of the airport (Site C) to compare pollution levels arriving at the site from three different directions:
 - (i) a 50° sector from the direction of Bishop's Stortford,
 - (ii) a 60° sector from Stansted Mountfitchet, and
 - (iii) an 80° sector from the airport.

Preliminary Work

Measurements were carried out from September to November, 1971. The samples were changed daily by the Airport Fire Brigade and a summary of the results is given in Table 7.

TABLE 7 - Average Monthly Concentrations of Smoke and Sulphur Dioxide at Stansted Airport

($\mu\text{g m}^{-3}$)

Month	Site A		Site B	
	Smoke	SO ₂	Smoke	SO ₂
September	20	61	25	55
October	18	53	21	50
November	33	73	34	67
Average	24	62	27	57

It is interesting to note that in November with the arrival of the heating season the smoke concentrations rose by some 37 per cent, consistent with increased use of domestic fuel. Air traffic at the airport, however, decreased from 3,800 movements a month during September and October to 2,600 movements a month by November; a decrease of some 32 per cent.

This shows that any decrease in smoke emissions from reduced aircraft operations was swamped by increased emissions from domestic sources.

This is probably best explained by examining the mass emissions of smoke from aircraft operations and comparing the values with similar emissions from domestic sources. As can be seen in Table 5, the average daily emission of smoke from aircraft operations amounts to some 0.015 tonne d⁻¹. Because of the 32 per cent difference between summer and winter air traffic this would result in a smoke emission of approximately 0.018 tonne d⁻¹ in the summer and 0.012 tonne d⁻¹ in the winter, a difference of 0.006 tonne d⁻¹. On the other hand the average yearly emission of smoke from Bishop's Stortford amounts to some 0.50 tonne d⁻¹ (Table 6). Between winter and summer this value probably varies between 0.7 and 0.3 tonne d⁻¹ respectively, a difference of 0.4 tonne d⁻¹, or approximately 65 times the seasonal difference in emissions from aircraft operations.

Directional Sampler

The instruments used with this equipment were controlled by a wind vane and anemometer to switch on only when the wind was within the specified sectors. Using the M.B.T.H. technique⁴, determinations were also made of gaseous aldehyde concentrations in two of the sectors to compare aldehyde levels from the airport with levels from Stansted Mountfitchet. A summary of the average monthly concentrations is shown in Table 8.

TABLE 8 - Monthly Summary of Results at Site C

($\mu\text{g m}^{-3}$)

Month	Bishop's Stortford		Stansted Mountfitchet			Airport		
	Smoke	SO ₂	Smoke	SO ₂	Aldehydes	Smoke	SO ₂	Aldehydes
February	-	-	19	50	7	25	65	3
March	12	98	14	44	28	18	44	12
April	8	63	12	30	32	11	34	24
May	14	101	6	66	26	10	33	19
June	8	64	7	88	33	2	43	24
Average	11	82	12	80	25	13	45	17

From Table 8 it can be seen that the concentrations of smoke from the three sectors enclosing Bishop's Stortford, Stansted Mountfitchet and the airport plus Takeley were all low, as would be expected in a rural area such as this, although they do seem rather low in relation to the SO_2 values and some doubt must surround their validity. The amount of SO_2 emitted from the airport will be small and some of the SO_2 in this sector will come from Takeley. The highest concentrations came from the direction of Stansted Mountfitchet.

One surprising result of this investigation was noticed during comparison measurements of aldehyde concentrations in the sectors enclosing Stansted Mountfitchet and the airport. As may be seen from Table 8 the concentrations from the direction of the village were consistently higher than those from the airport. From the fuel consumption figures shown earlier in this paper this would not be expected. The major cause of this was probably traffic on the road from Stansted Mountfitchet as it passed close to the site. However, the series of measurements did coincide with the miners' strike in February and March and some contribution might have come from the burning of wood rather than coal and coke.

PREDICTED GROUND LEVEL CONCENTRATIONS

The results presented in the previous section give some idea of the concentrations of smoke and SO_2 prevailing in the neighbourhood of Stansted Airport. An indication is also given of the directional dependence of the observed concentrations. However, because there is a significant and variable transport of pollution into the Bishop's Stortford/Stansted Mountfitchet/Takeley area, it is not possible, from the directional measurements alone, to quantify the contributions made by the local sources. As a first attempt at quantifying these contributions some diffusion calculations were carried out based on the approximate emission and meteorological data available. The prediction method and the results are discussed.

The diffusion formula used to calculate the urban (domestic, industry and road traffic) and airport terminal (space heating and road traffic) contributions to ground level concentrations is of the Gaussian type and takes the form

$$x = \frac{Q}{\pi u \sigma_y \sigma_z} \exp \left[-\frac{1}{2} \left(\frac{y^2}{\sigma_y^2} + \frac{H^2}{\sigma_z^2} \right) \right] \quad (1)$$

where x is the concentration, (units m^{-3})
 Q is the emission rate, (units s^{-1})
 u is the mean wind speed, ($m s^{-1}$)
 σ_y, σ_z are the cross wind and vertical plume standard deviations, (m)
 H is the effective source height, (m)
 x, y and z are the down wind, cross wind and vertical distances, (m)

Following Turner⁵ and Singer and Smith⁶, σ_y and σ_z can be expressed in the form

$$\begin{aligned} \sigma_y &= \sigma_0 + 0.36 x^{0.86}, & \sigma_z &= 0.33 x^{0.86}; \text{unstable} \\ \sigma_y &= \sigma_0 + 0.32 x^{0.78}, & \sigma_z &= 0.22 x^{0.78}; \text{neutral} \\ \sigma_y &= \sigma_0 + 0.31 x^{0.71}, & \sigma_z &= 0.06 x^{0.71}; \text{stable} \end{aligned} \quad (2)$$

where σ_0 is the initial cross wind standard deviation of the plume.

Bishop's Stortford, Stansted Mountfitchet, Eisenham, Takeley and the airport terminal were treated as individual area disc sources for each pollutant and each type of source (e.g. domestic or road traffic). It was further assumed that each disc could be approximated by a normally distributed line source orientated cross-wind and passing through the centre of the disc with $4\sigma_0$ equal to the disc diameter (Turner). The effective height of road traffic sources was taken as 1m, domestic and terminal area space heating sources as 10m, and industrial sources as 30m. The effects of topography were neglected.

Domestic emissions of pollution were assumed to be dependent on the ambient air temperature (T °F) according to the formula

$$Q = \bar{Q} [a(60 - T) + 0.3] \quad (3)$$

where \bar{Q} is the mean emission rate and where $a = 0$ for $T > 60^\circ F$ and $a = 0.052$ for $T \leq 60^\circ F$ (Shieh⁷ et al). Typical monthly average values of $(60 - T)$ appropriate to the area were extracted from Column 11, Table IV of the Gas Council's Handbook on Degree Days⁸. Actual emission figures were used for the terminal space heating plant. All calculations were based on a mean wind speed of $4m s^{-1}$ and on the assumption that the frequency of occurrence of the stability categories in the area was 15% unstable, 35% neutral and 50% stable (Bannon⁹ et al).

For the present purposes it was assumed that the emissions from aircraft operations were entirely due to taxi-ing, occur at ground level and were distributed along the length of the airport. Although this approximation is reasonable for CO and hydrocarbons, it is pessimistic, in terms of air quality, for NO_x and particulates (see Table 5). It was also assumed that the aircraft emissions were constant throughout the year. The contribution made by these emissions to pollution concentrations at C was calculated by considering the airport as a line source of infinite length with an emission rate per unit length equal to the total emission rate divided by the airport length. In this case the appropriate diffusion equation is:

$$x = \sqrt{\frac{2 Q_a}{\pi \sigma_z u}} \quad (4)$$

where Q_a is the rate of emission per unit length.

In order to assess how good the predictions are, a comparison was made with the observed values of smoke and SO_2 at sites A and B for the month of November, 1971. The results from these two sites were chosen for comparison purposes in preference to the results from the site C because the smoke figures in particular are considered to be more reliable.

The observed smoke and SO_2 figures in Table 9 are the mean values for those days on which the wind blew predominantly from the relevant directions.

TABLE 9 - Comparison between Observed and Calculated Smoke and SO_2 Concentrations at Sites A and B during November, 1971

($\mu g m^{-3}$)

Source	Smoke			SO_2		
	Calculated	Observed	Calculated+ Background	Calculated	Observed	Calculated+ Background
Site A						
Bishop's Stortford	14	39	38	22	76	55
Stansted Mountfitchet	7	36	31	0	24	43
Site B						
Bishop's Stortford	17	41	41	25	62	58
Stansted Mountfitchet	7	29	31	10	70	43

From Table 9 it is apparent that the calculated concentrations, based on the assumption that the sites were directly downwind of Bishop's Stortford and Stansted Mountfitchet, were much less than the observed values for both pollutants. The difference could be due entirely to a poor prediction scheme but it seems probable that a large part of the difference is the result of neglecting the local background concentrations, or, more correctly, the pollution transported into the area from more distant sources. Insufficient observations have been made locally to quantify the transported contribution so, as an estimate, it was decided to take the average November concentrations for the two nearest sites forming part of the UK network of background sites. The average figures are $24 \mu g m^{-3}$ for smoke and $33 \mu g m^{-3}$ for sulphur dioxide, and these have been added to the calculated values in Table 9 to give the figures in the third and sixth columns of this table. The agreement between the calculated + background and the observed figures is much better and is remarkably good for smoke, although the almost perfect agreement for Bishop's Stortford is more fortuitous than the result of a highly accurate prediction scheme. In the case of SO_2 , the calculated + background values are still much less than the observed values, particularly for the Site A and the Stansted Mountfitchet direction. The remaining discrepancies may arise from a variety of factors, e.g. deficiencies in the model, neglect of unidentified emitters in the directions concerned, or an underestimation of the emission factors.

Accepting that the relatively crude prediction scheme gives a reasonable idea of the identified sources' contributions to pollution concentrations, it was used to calculate the various known sources' average contributions to the pollution levels at Site C for a typical February to April period. This period was chosen because it coincides with part of the period during which directional measurements of smoke and SO_2 were made at Site C. The contribution from each source was calculated on the basis that the source was directly up-wind of Site C. The results are shown in Table 10.

Putting the airport contributions into perspective relative to the urban contributions but bearing in mind the very approximate nature of the prediction scheme and emission data, it can be seen that the airport contributions to smoke concentrations at Site C are less than those for the town of Takeley, the smallest town, while the contributions to SO_2 and NO_x are comparable with those of Takeley. Carbon monoxide from the airport is more than that from Takeley but less than the contribution from the next largest town, Elsenham. It is only in hydrocarbons that the airport contribution exceeds the contributions from any of the urban sources. (90 per cent of the airport hydrocarbons come from aircraft operations). However, it should be pointed out that the airport contribution of under 10^{-2} ppm (based on hexane equivalent) to the hydrocarbon concentrations is at least an order of magnitude less than the typical hydrocarbon levels (excluding methane) in a polluted atmosphere (Barrett¹⁰). In the case of CO, the airport contribution is less than the typical concentration in an unpolluted atmosphere. Having made these comparisons for the central site, it must be pointed out that the concentrations of hydrocarbons and CO contributed by the aircraft operations will be higher closer to the airport and within the airport itself.

The relative contributions made by the airport will probably be higher during the summer months than the figures in Table 10 indicate because domestic emissions will be much smaller and there will be a 15 to 20 per cent increase in aircraft operations. On the other hand, the absolute concentrations due to the airport could be smaller due to the better dispersion during the summer months. Also, as noted earlier, taking the airborne take-off emissions as occurring at ground level will have meant some overestimation of the contribution made by the aircraft operations, particularly to smoke concentrations; these airborne emissions occur at heights ranging from 0 to 500 metres.

TABLE 10 - Average Calculated Contributions made by the Various Sources to Pollution Concentrations at the Site C for a typical February to April period

($\mu\text{g m}^{-3}$)

Source	Smoke	SO ₂	CO	NO _x	Hydrocarbons
<u>Towns (Domestic and Industry)</u>					
Bishop's Stortford	14	24	148	6	-
Stansted Mountfitchet	8	10	85	3	-
Elsenham	3.4	4.7	43	2	-
Takeley	2.5	3.1	24	1.3	-
<u>Towns (Road Traffic)</u>					
Bishop's Stortford	2.2	-	211	31	26
Stansted Mountfitchet	1.5	-	137	20	14
Elsenham	0.7	-	65	13	7
Takeley	0.6	-	42	7	5
<u>Airport</u>					
Terminal Area (Central Heating)	-	2.5	-	0.7	-
Road Traffic	0.3	-	21	3.5	3.4
Aircraft Operations	0.7	-	76	3.4	31
<u>Totals</u>					
Bishop's Stortford	16.2	24	359	37	26
Stansted Mountfitchet	9.5	10	220	23	14
Elsenham	4.1	4.7	108	15	7
Takeley	3.1	3.1	66	8.3	5
Airport	1.0	2.5	97	7.6	34.4

Note The above contributions are in addition to the background levels prevailing in the area e.g. during the February/April period background levels of smoke and sulphur dioxide were almost certainly in excess of $20 \mu\text{g m}^{-3}$.

CONCLUSIONS

This paper compares the approximated emissions of air pollutants from Stansted Airport and four neighbouring urban areas and also compares the calculated contributions these emissions will make at a central point. With the exception of hydrocarbons, total emissions from the airport are about the same as or less than the total emissions from Elsenham, the second smallest of the four urban areas. The airport total hydrocarbon emissions (98 per cent of which come from aircraft operations) amount to about 60 per cent of the approximated road traffic emissions of this pollutant in Bishop's Stortford, the largest of the four urban areas. However, on the basis of an emission rate per square km of urban or airport area, the airport hydrocarbon emissions are some 2.5 times the Bishop's Stortford emissions.

Using a fairly simple prediction scheme and the approximate emission data available, the contributions to the pollution concentrations at a central site, Site C, were computed for a typical February to April period. It was found that, with the exception of hydrocarbons and to a lesser extent CO, the airport contributions were relatively small in comparison with the other sources. Even in the case of hydrocarbons, the calculated typical contribution to concentrations at the central site (about 1100 metres from the airport) were at least an order of magnitude less than the typical hydrocarbon concentrations (excluding methane) in a polluted atmosphere.

As a broad generalization it could be said that replacing the airport by the smallest town, Takeley (population of 1,500), would have the effect at the central site of increasing the concentrations of all the pollutants except hydrocarbons. No attempt has been made to assess the effect on odours. No attempt was made to monitor odours because, to date, there is no satisfactory analytical technique which can be readily used to monitor the rapid changes in odour emissions from moving aircraft.

This paper has been able to give only some idea of the likely contributions to pollution levels from identified sources. Difficulties have arisen in trying to arrive at agreement between the predicted and observed concentrations of smoke and SO₂ presumably because the prediction scheme as used, is not valid; the simplifying assumptions are too crude and the background levels are highly variable and generally swamp the contributions from local sources. Also, the source inventory was rather limited. The same problems would also have arisen in any attempt to compare calculated and observed concentrations of the three other pollutants. In particular, the background levels are again as significant, or more so, than the local sources. It is therefore important that, for an exercise of this type to be completely successful, a detailed emission inventory be available and that there is adequate information on local background levels. The latter point raises the question of the sensitivity of the monitoring techniques available. In particular, the smoke concentrations observed at the central site were low and inconclusive, highlighting the defects of the filter paper technique for measuring smoke concentrations in such circumstances. Nevertheless the work carried out here for comparing the emissions from an airport and nearby urban areas and for comparing the contributions these emissions make to pollution concentrations, can serve as a guideline for similar work elsewhere on emissions from major industrial complexes and their overall contribution to the pollution of the local environment.

REFERENCES

1. Parker, J. "Air Pollution at Heathrow Airport, London: April-September, 1970". In Proceedings of SAE DOT Conference on Aircraft and the Environment, P.37, Part 1. New York: Society of Automotive Engineers, Inc, 1971 pp 121-146.
2. "Digest of Energy Statistics, 1971". H.M. Stationery Office, London.
3. Parker, J. "Transport of Air Pollution from the Scunthorpe Area". Stevenage: Warren Spring Laboratory, 1970, Report No. LR 126 (AP).
4. "Oxygenates in Automotive Exhaust Gas; Part 1. Techniques for determining Aldehydes by the MBTH Method". May, 1967, Project No. CM-59-65. Co-ordinating Research Council, New York, 20, N.Y.
5. Turner, D.B. "A Diffusion Model for an Urban Area". J. App. Met. 3, 1964, 85-91.
6. Smith, R.E. and Singer, I.A. "An Improved Method of Estimating Concentrations and Related Phenomena from a Point Source Emission". J. App. Met. 5, 1968, 631-639.
7. Shieh, L.J., Davidson, B. and Friend, J.P. "A Model of Diffusion in Urban Atmospheres: SO₂ in Greater New York". In Proceedings of Symposium on Multiple-Source Urban Diffusion Models. Chapel Hill, N.C.: U.S. Environmental Protection Agency, 1970 p 10-4.
8. Anon. "Degree Days". Technical Handbook No. 191. London, 1965, The Gas Council.
9. Fannon, J.K., Dods, L. and Mead, P.J. "Frequencies of Various Stabilities in the Surface Layer". Investigation Division Memorandum No. 85. Meteorological Office, 1952.
10. Barrett, C.F. "Air Pollution" U.K.C. Reviews, 3, 1970, 119-134.

Discussion on Paper 9

"Relative Air Pollution Emissions from an Airport in the UK
and Neighbouring Urban Areas"
presented by J.Parker

C.J.Scott: I wonder whether you have omitted one source of hydrocarbons which could be important - Hatfield Forest. Also, have you examined whether there is any photochemical conversion of such hydrocarbons to account for the aldehyde gradients across the airport that you have measured?

J.Parker: No attempts were made to relate aldehyde concentrations to sources from vegetation largely because the primary aim of the trials was to compare emissions and ground level concentrations from the airport with those from a number of nearby towns. However, from an examination of an ordnance survey map there would appear to be no extensive forests within six miles of Stansted Airport and under these conditions I think it would be unlikely that aldehydes from such a source would compare with levels from an airport only half a mile away.

No determinations of possible photochemical reactions were made during the work. Your suggestions however will be borne in mind during future work.

K.E.Grønsvik: Did you observe the characteristic smell/odour around the Stansted Airport?

J.Parker: Typical odours from paraffin fuel were observed close to the terminal area as would be expected. However, at the measuring site, which was about half a mile from the centre of the airport no odours were observed.

D.K.J.Tommel: Did you investigate the contamination by lead at Stansted Airport?

J.Parker: No estimations of lead were carried out during this work. The reasons for this are twofold: first some attempts were made to measure lead concentrations near the take off path at Heathrow without success, and second, as far as is known no lead additives are used with aircraft fuels.

GROUND CONTAMINATION BY FUEL JETTISONED FROM AIRCRAFT

by N.L. Oram and R.G. Picknett, PhD.

(Chemical Defence Establishment, Porton Down, Wiltshire, U.K.)

SUMMARY

This paper presents a study of the problem of ground pollution produced by fuel jettisoned from aircraft under emergency conditions, typically at 450 kg/min through a pipe 1 cm in diameter while flying at 120 m/s. Part I is concerned with the assessment of the likely size distribution of drops produced when fuel is jettisoned by aircraft. Trials are reported in which a Buccaneer aircraft jettisoned fuel at low altitude, the size distribution being measured at ground level. This spray represents a lower bound to the initial sizes of drops produced by civil aircraft. An alternative distribution is presented which is based on data from other sources and which represents an upper bound to the initial sizes of such drops. Part II is concerned with the proportions of jettisoned fuel which survive evaporation to reach the ground. The results are presented as functions of the initial drop size distribution, the fuel type, the height of jettisoning and the ground temperature. Under adverse combinations of these factors large quantities of fuel may reach the ground, e.g. roughly 50% of Avtur fuel jettisoned at 300 m will reach the ground if the temperature is -10°C. Consideration is also given to the heights of jettisoning required to ensure minimal ground contamination. The contamination density on the ground depends on atmospheric stability, wind speed and orientation of flight to wind direction, as well as on the amount of fuel reaching the ground. Only order-of-magnitude calculations have been made, but for fairly typical conditions with cross-wind flight at 300 m altitude, Avtur fuel can contaminate a strip of land about 4 km wide to a density of a few milligrams per square metre. Under the worst conditions of upwind flight at low wind speed, the strip of contamination can be only about 200 m wide and the density roughly 100 times higher.

INTRODUCTION

The study was undertaken in the context of suggestions made from time to time that fuel jettisoned by aircraft could be one cause of contamination on the ground. Scientific evidence was required to obtain more information about the discharge of fuel from aircraft. To put the results of the study in perspective in the circumstances applying in any particular country is a matter for separate consideration, but it is right to emphasise that civil aircraft do not jettison fuel except in an emergency so that jettisoning is a comparatively rare event. Moreover, long-range transport aircraft are the only ones fitted with jettisoning facilities and are also under instruction to jettison at the maximum possible height, preferably over the sea. It should also be emphasised that although in this paper a comparison has necessarily been made between the differing effects of using the two fuels, Avtag and Avtur, it is the latter (and less volatile fuel) which is almost exclusively used by aircraft operating in and out of the UK.

In a typical long-haul public transport aircraft jettisoning would take place at about 120 m/s through pipes of about 5 cm diameter at a rate of about 450 kg/min per pipe, and large quantities of fuel could be involved. Fuel leaving the aircraft is shattered by the airstream, forming drops of a range of sizes which start to evaporate as they fall under gravity. Small drops fall only a short distance before complete evaporation, whereas large drops fall a long distance. In order to predict the amount of fuel reaching the ground from an aircraft jettisoning at a given height the size distribution of the fuel drops must be determined at the point of release from the aircraft, and the fall speeds and rates of evaporation of the different sizes of drop must be evaluated.

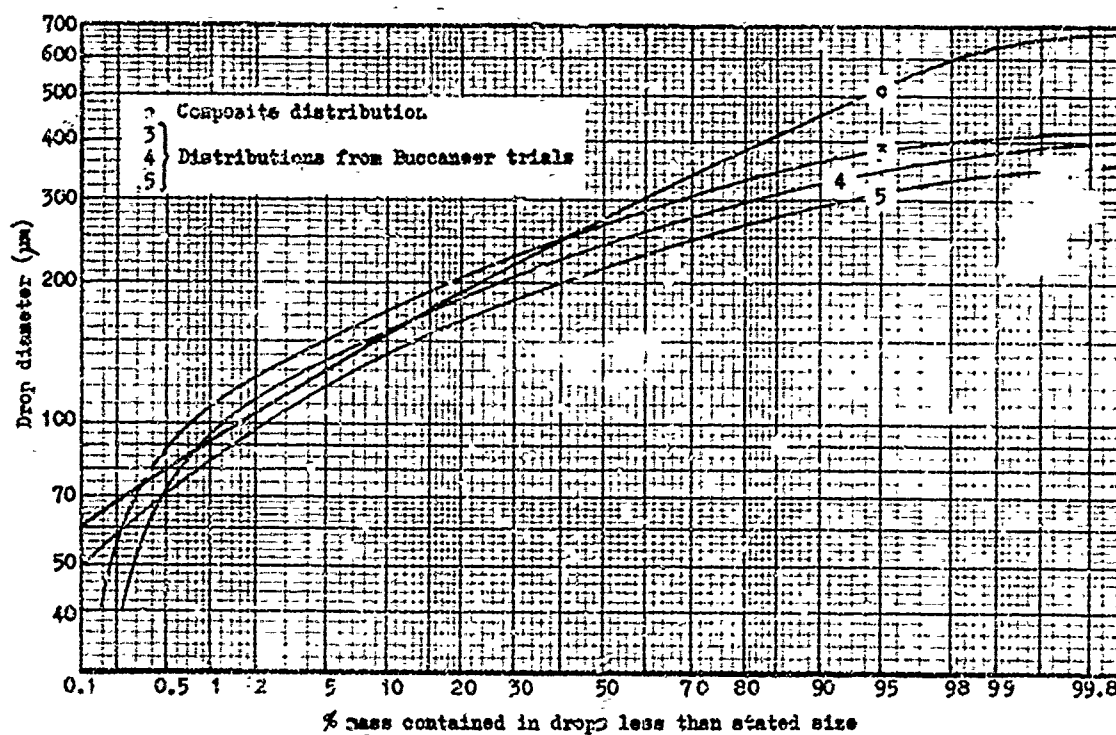
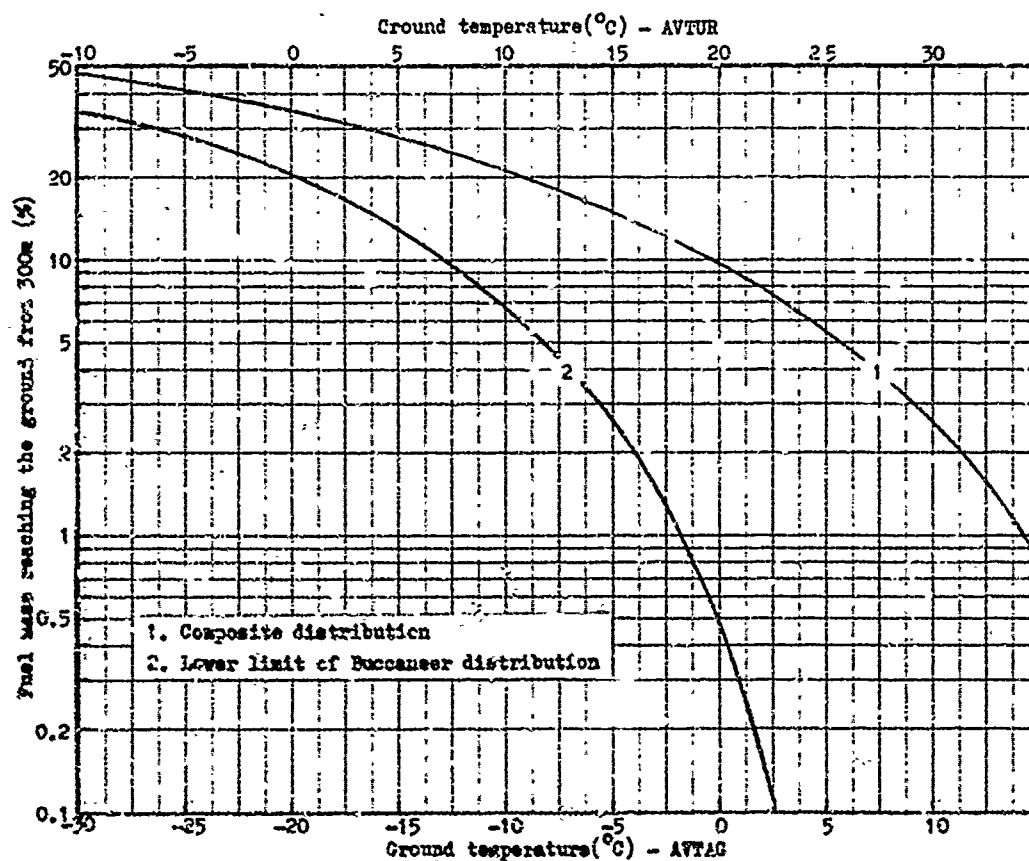
PART I: INITIAL DROP SIZE DISTRIBUTION OF JETTISONED FUEL

The size distribution of fuel drops at the point of release from the aircraft depends on a number of factors, including the air speed, the liquid flow rate, the physical properties of the fuel and the geometry of the ejection system. Although information is available for some liquids sprayed from aircraft through pipes similar to those used in jettisoning, it was thought necessary to determine the size distribution obtained when aviation fuel itself was sprayed. Typical conditions of spraying were modelled on the VC-10 aircraft and are given in the Introduction. Some aircraft have multiple jettisoning pipes, but, unless these are close together, each pipe may be considered separately.

An aircraft was chosen for these experiments because ground trials in a wind tunnel were considered to be hazardous. The only suitable aircraft available was a Buccaneer fitted with overload wing tanks from which it was possible to jettison fuel. Fortunately the jettisoning rate and jettisoning pipe size were almost identical to the figures quoted above. Furthermore, the fuel in the tanks could be isolated from the main fuel supply, thus enabling a chemical tracer to be added to the fuel without contaminating the aircraft's main fuel supply (a necessary feature on safety grounds). To minimise sizing errors due to evaporation between emission and sampling, the jettisoning height was made as low as possible and a relatively involatile fuel, Avtur, was used.

EXPERIMENTAL DETAILS

Five low-level trials were carried out during August 1972. The trial concept was that the aircraft should jettison fuel along a predetermined line across the wind direction, the spray produced being sampled by papers laid on the ground downwind. Detection and measurement of the fuel drops posed a problem due to the chemically inert nature of kerosenes. Preliminary investigations to find a means of assessing drops of unadulterated fuel having failed, it was decided to add 0.5% of Uvitex SH to the Avtur fuel. This material is a solid fluor, soluble in aviation spirit to about 0.8%, and has been used in many similar experiments because of its brilliant fluorescence under ultra-violet illumination. The drops produced by the jettisoning process were sampled on Whatman No. 50 filter paper sheets positioned on the

Figure 1. Drop size distributions for jettisoned fuelFigure 2. Fuel reaching the ground from 300 metres

ground in a predetermined pattern. The sampling points were on 3 lines parallel to the expected wind direction, 600 m long and 100 m apart. The flight path was across wind and passed over the sampling lines at a distance of 150 m from the upwind ends. Immediately under the flight path each sampling paper was covered with a rotating mask to prevent excessive deposition, but elsewhere this precaution was not necessary. After each trial, assessment of the sample papers was performed using photography under ultra-violet illumination, followed by counting and sizing of the images of the spots using an automatic particle size analyser (Quantimet).

RESULTS

The first two trials were not typical since the jettisoning rate achieved was much too low. This was a result of failure to pressurize the fuel tanks, a consequence of the aircraft being operated under non-standard conditions. Procedural alterations were made following the second trial which ensured that pressurization was obtained. The drop size distributions determined from the final three trials are shown in Figure 1. The mass median diameter of the drops was $240 \pm 30 \mu\text{m}$ and the maximum drop size was $400 \pm 15 \mu\text{m}$. (The method of assessment did not permit the detection of drops smaller than $40 \mu\text{m}$ diameter).

The trials were performed at an altitude of less than 15 m (not of course representative of conditions under which fuel would normally be jettisoned) to minimize drop evaporation which, if it had occurred to any significant degree, would have caused an erroneous estimate of the size distribution of drops at the point of release from the aircraft. To investigate the extent of evaporation, the Uvitex concentration in the drops at the moment of sampling was estimated and compared with the concentration in the fuel prior to spraying. The greater the drop evaporation, the larger would be the Uvitex concentration found in the drops. The estimation was made by cutting a number of small, equal-sized spots from the sampling papers and analysing them for Uvitex content. Since the size of the drops causing these spots was known by prior calibration, the Uvitex concentration in them at the time of sampling was calculable. In Trials 4 and 5 there was no evidence of evaporation, but in Trial 3 it appeared that drops initially of $117 \mu\text{m}$ diameter had evaporated to $100 \mu\text{m}$ before being caught by the sampling papers. This is only a small change in size and the relative change would be even less for bigger drops.

INITIAL SIZE DISTRIBUTION FROM FIELD TRIALS

The results from Trials 3 - 5 are reasonably consistent (see Figure 1), but there are two points worthy of consideration, i.e., did significant evaporation occur before sampling, and was the sample representative?

Evaporation. Evaporation begins as soon as the fuel is jettisoned and the effect would be most marked for small drops. Despite the fact that some evidence of slight evaporation was found in Trial 3, attempts to confirm it in subsequent trials were unsuccessful. It is therefore concluded that, by performing the trials at 15 m, it has been possible to prevent any significant evaporation occurring between the time of jettisoning and the time of sampling. The estimated size distribution of drops at the point of release from the aircraft is not in error from evaporation effects.

Representative sampling. The recovery of fuel on the ground as established by chemical analysis of Uvitex on the papers was never greater than 55%. Low recoveries are characteristic of aircraft spray trials and have been attributed to such factors as shielding of the sampling papers by tall grass and variations in drop concentration. From the point of view of the size distribution it is only necessary to consider whether there were initially present large numbers of small drops which evaporated before reaching the ground. This would mean that the measured distribution of Figure 1 represented the drop sizes 15 m below the flight path. If substantiated in future work then contamination levels on the ground must be reduced in proportion to the actual recovery of fuel as found in these low level trials.

FACTORS AFFECTING THE INITIAL SIZE DISTRIBUTION

Type of aircraft and discharge tube geometry. Investigations (1) have shown that the orientation of the discharge tube with respect to airflow has a marked effect on drop size. The efficiency of liquid shatter is governed by the way in which - discharge tube geometry enables the air stream to strip drops from the emerging column of liquid. A simple cylindrical tube projecting backwards along the flight path is an inefficient system and large drops should result. The jettisoning pipes of some aircraft (e.g., the VJ 10) are in fact of this type. On the other hand, a pipe emerging at right angles to the air flow would give rise to large shearing forces and small drops should result. The Buccaneer overload tank is of this type. The size distributions 3, 4 and 5 of Figure 1 probably represent a lower bound to the drop sizes produced during jettisoning. Trials with aircraft fitted with a simple pipe pointing rearwards should give size distributions representing an upper bound, and, indeed, such size distributions are available for a variety of liquids (1 - 4). The curve labelled "Composite Size Distribution" in Figure 1 gives a typical distribution for a light oil similar to kerosene sprayed at 120 m/s and about 440 kg/min. It has a mass median diameter of $275 \mu\text{m}$ with a maximum size of $680 \mu\text{m}$, which is significantly larger than the Buccaneer spray.

Fuel flow rate. Broadly speaking, the higher the fuel flow rate, the larger are the drops produced. There appear to be no significant differences between the results for the last 3 trials, but when the results of the first 2 trials are also considered some correlation can be claimed between flow rate and median drop diameter. The correlation is not good but the following empirical equation may be used for a Buccaneer flying at 120 m/s:

$$\text{mass median diameter } (\mu\text{m}) = 155 + (0.17 - 0.05)f,$$

where f is the fuel flow rate in kg/min.

Aircraft velocity. The air speed is as important as the fuel flow rate because it is the ratio of the flow rates of air and liquid which is the principal factor controlling drop size. The faster the aircraft, the smaller is the drop size, all other factors being equal. No direct evidence of this relationship can be offered from this series of trials since all spraying was at 120 m/s, but results from other trials (1 - 4) using a variety of aircraft and liquids can be employed to derive an empirical equation for the Buccaneer:

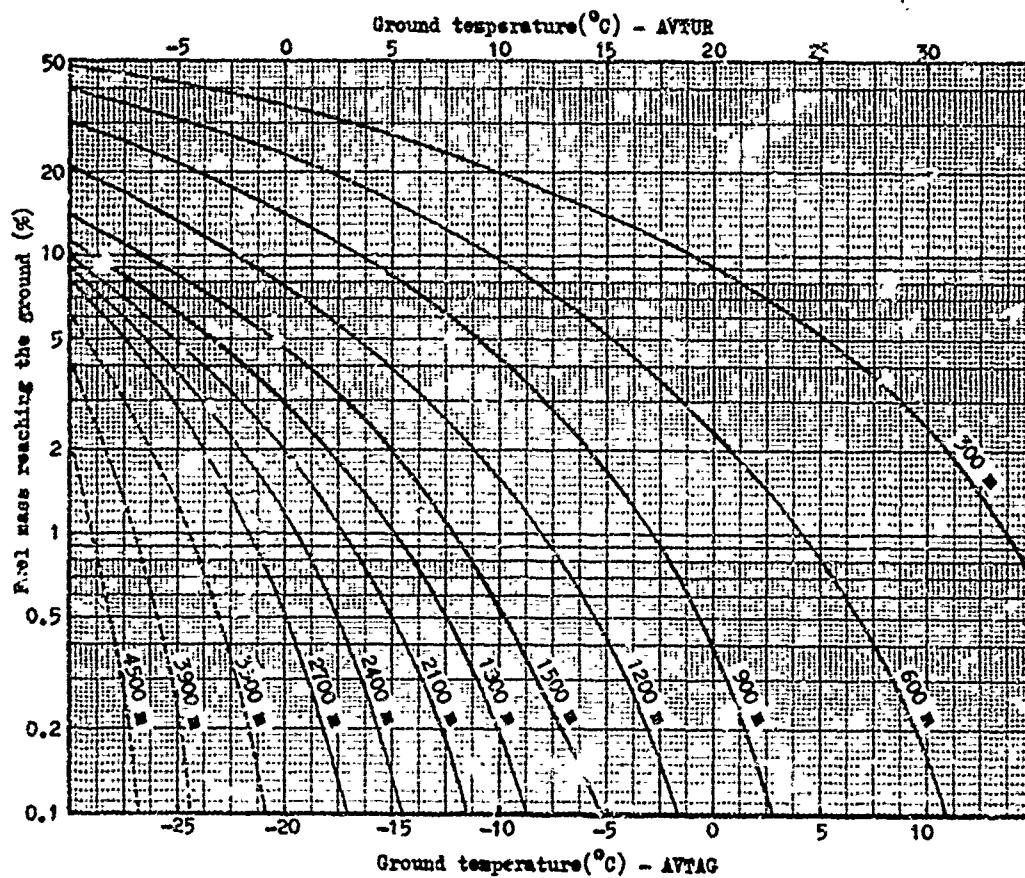


Figure 3. Maximum fuel reaching the ground for different heights of release

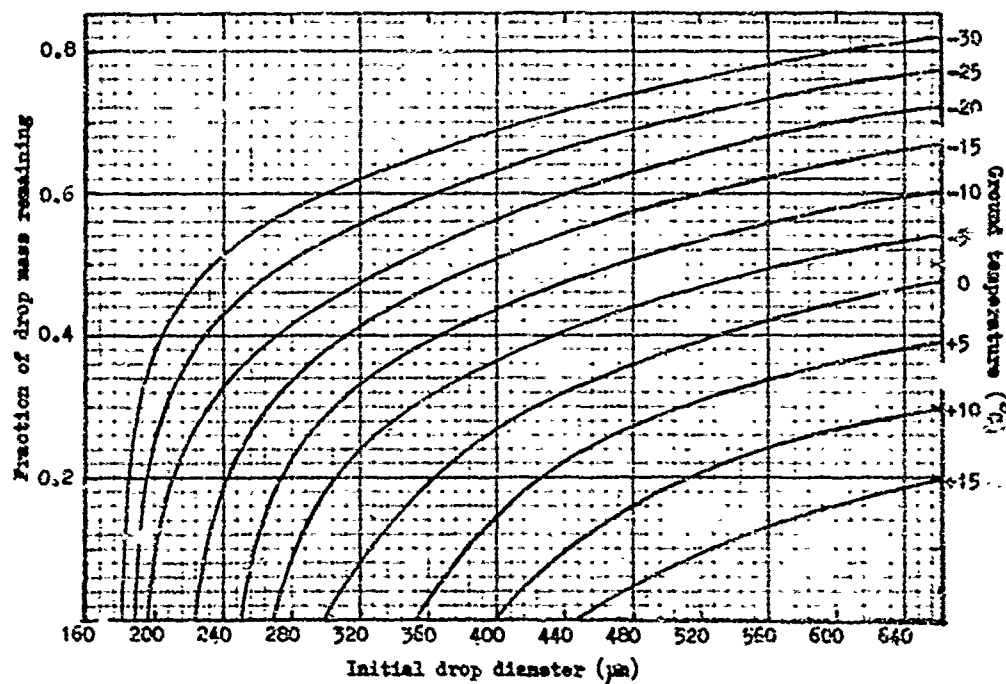


Figure 4. Residual mass ratio of AVTAG after falling 300 metres

mass median diameter (μ) = $540 - 1.5V$,

where V is the aircraft velocity in m/s. The error is $\pm 20 \mu$.

Type of liquid. In the aircraft sprays normally encountered the dominant factor in the relative flow rate of air and liquid, other factors such as surface tension, viscosity and density of the liquid being of secondary importance. Aviation fuels are sufficiently similar in their physical parameters for the same spray size distribution to apply to all fuels.

PART II: EVAPORATION AND DEPOSITION

To determine the amount of liquid carried to the ground by drops released from a given height, the fall speed and the rate of evaporation of the drops must be considered. Both are dependent on drop size, and so the initial drop size distribution is of paramount importance. In Part I it was established that no single distribution was applicable to fuel jettisoned by aircraft. Two representative distributions have therefore been taken which cover the likely extremes:

- Buccaneer drop size distribution (lower limit). This is described in Part I (Figure 1, curve 5) and is thought to give a lower bound for jettisoning systems where the pipe projects at right angles to the air flow, producing small drops.
- Composite drop size distribution (upper limit). This is also discussed in Part I (Figure 1) and is based on other work (1-4). It is thought to be typical of systems where the pipe projects backwards along the air flow, giving large drops.

Both apply to aircraft flying at 120 m/s while jettisoning at 450 kg/min through a pipe 6 cm in diameter, and are thus broadly applicable to aircraft jettisoning fuel in an emergency.

These size distributions represent the spray approximately 15 metres below the aircraft, at which level drop separations are so large as to give little probability of drop collision. Coalescence during the subsequent fall of the drops is therefore negligible. Any coalescence in the vicinity of the aircraft is considered to be an integral part of the spray production process and is included in the initial size distribution.

For each size of drop in these distributions, evaporation rates and fall speeds must be evaluated. The type of fuel affects the rate of evaporation, and two fuels are considered:

Avtur This is used almost exclusively, on safety grounds, by airlines operating within the UK. It has a relatively low evaporation rate.

Avtag This is used by some operators outside the UK and has a relatively high evaporation rate.

Other factors being equal, drops of Avtur reach the ground more readily than Avtag.

Temperature also has a major effect on the rate of evaporation. The lower the temperature, the less volatile are the aviation fuels, and the smaller is the rate of evaporation of drops from jettisoned fuel. This applies both to Avtur and Avtag. Ground temperatures from -30 to 15°C are considered here.

EVAPORATION AND DEPOSITION OF FUEL DROPS

Extensive calculations have been made by Lowell (5-6) on the evaporation of drops of aircraft fuel in free fall through the atmosphere. One report (6), dealing with JP-4 (Avtag), has considered the mass of liquid remaining after a drop had fallen a given distance, and plots were given of the results for a range of drop sizes, temperatures and distances of fall. These data have been taken as the starting point for the present work. Details of the procedures used are fully reported in the Appendix. The values required for final drop sizes, temperatures and distances of fall were obtained from Lowell's data by interpolation and were applied to two drop size distributions. One was the lower limit of the distributions found for the Buccaneer aircraft (Curve 5, Figure 1), representing the case of least deposition on the ground, and the other was the Composite distribution (also in Figure 1), representing the case of greatest deposition. Results for Avtag jettisoned from 300 m are illustrated in Figure 2 (lower scale). The percentage of fuel reaching the ground ranges from zero at 15°C to 47% at -30°C . The effect of the initial drop size distribution is clearly shown, being most marked at the higher temperatures.

With regard to Avtur fuel, Lowell (8) has stated that the evaporation rate of this liquid is identical with that of Avtag when the latter is colder by 20°C . Results for Avtur have been compiled using this information and are also shown in Figure 2 (upper scale). The far greater amount of Avtur reaching the ground under given conditions is apparent, demonstrating the significance of fuel volatility.

This work has also been extended to consider the effect of jettisoning from heights greater than 300 m. Again the method of calculation is described in the Appendix and only the results are given here. The accuracy is somewhat reduced as the height of fall is increased. Figure 3 shows the proportion of fuel reaching the ground from heights of up to 4,500 m for temperatures ranging from -30 to 15°C . The lower temperature scale refers to Avtag, while the upper scale refers to Avtur. Only the Composite size distribution has been considered in this respect.

A simplified table of the percentage of fuel reaching the ground from 300 m is given in Table 1, the ranges of the figures quoted being a result of the two size distributions used. Table 2 shows the minimum heights for jettisoning which will allow less than 0.1% of the fuel to reach the ground.

Minimum ground temperature (°C)	Percentage of fuel on ground	
	Avtur	Avtag
-10	35 - 47%	6 - 22%
5	13 - 28%	0 - 5%
15	3 - 15%	0 - 1%

TABLE 1. Jettisoning from 300 metres

Minimum ground temperature (°C)	Height in metres for:	
	Avtur	Avtag
-10	> 4,500	o 1,800
5	o 2,400	o 800
15	o 1,500	o 450

TABLE 2. Minimum jettisoning heights for 0.1% fuel on ground.

DENSITY OF GROUND CONTAMINATION

The problem of estimating the amount of fuel per unit area of ground is a difficult one which can only be solved by imposing rigid criteria with regard to meteorological factors such as wind shear and atmospheric stability. Even so, the result can only be approximate, and the data which are now presented must be regarded as indicating no more than the order of magnitude expected.

The maximum contamination density is obtained with the aircraft flying directly upwind under conditions where the wind is slight and does not veer with altitude. This eliminates any winnowing effect and leaves only diffusion by air turbulence, which can be analysed by Pasquill's theory (9) to obtain the density of ground contamination. The density is highest directly under the flight path and decreases on either side so that a clearly defined strip of ground contains most of the fuel. Using the standard conditions of jettisoning employed in this paper, together with the assumption that the spray plume diameter is negligible, it is possible to obtain density estimates. For Avtur fuel jettisoned at 300 m altitude in an atmosphere of neutral stability with a ground temperature 5°C, the strip of contaminated ground is about 200 m wide and the average density of contamination is about 0.1 g/m². This corresponds to a drop separation on the ground of about 0.5 cm, and such a deposit would presumably be readily detected.

A much lower, and perhaps more typical, density of contamination is obtained when the aircraft is flying across the wind so that winnowing of the spray drops occurs. The smaller drops, falling more slowly, get carried further downwind so that the strip of contaminated ground is wider than before and the density of contamination is less. For all but the lowest wind speeds this winnowing has a much greater dispersive effect than the diffusion just described, thus simplifying calculations. Taking the same meteorological and jettisoning conditions as before, but with a more typical wind speed of 10 m/s, the strip of contaminated ground is roughly 4000 m wide and the average density of contamination is about 0.004 g/m². (The average separation for the large drops is about 20 cm, while that for the small drops further downwind is about 2 cm.) Crosswind jettisoning under these conditions gives contamination densities which are only a few per cent of the maximum value estimated for upwind jettisoning. For both types of jettisoning the contamination density decreases with increasing altitude of release, wind speed and temperature.

CONCLUSIONS

The conditions of jettisoning which have been taken in this study are as follows:

aircraft speed:	120 m/s
diameter of discharge pipe:	6 cm
jettisoning rate per pipe:	450 kg/min

They are considered to be typical of aircraft jettisoning fuel under emergency conditions. Two aviation fuels are considered: Avtur and Avtag.

Different aircraft may give different initial drop size distributions when jettisoning fuel depending on whether the ejection pipe points rearwards or in a direction normal to the airstream. In the first case larger drops are expected, and a typical initial drop size distribution has a mean median diameter of 270 μ m with a maximum diameter of 680 μ m. In the second case smaller drops are expected, and the measured initial size distribution has a median diameter of 240 \pm 30 μ m with a maximum diameter of 400 \pm 15 μ m. Increasing the aircraft speed should give smaller drops and increasing the jettisoning rate should give larger drops. The type of fuel jettisoned should not significantly affect the initial drop size distribution.

The amount of fuel reaching the ground is governed by evaporation during the fall of the drops. Large drops fall quickly and suffer relatively little evaporation compared to small drops, and so the ground contamination from aircraft with ejection pipes pointing rearwards should be greater than for aircraft ejecting fuel normal to the airstream. There can be a 25-fold difference in contamination levels from this cause. Drop evaporation is also markedly dependent on fuel type. Avtur, being less volatile than Avtag, presents the greater risk of ground contamination: between 2 and 200 times as much Avtur as Avtag will reach the ground from 300 m under similar jettisoning conditions. Temperature is another important consideration. It affects the rate of evaporation, drops at high temperature evaporating much more quickly than at low temperature, making the risk of ground contamination more severe in winter.

The density of ground contamination depends on wind speed and atmospheric stability as well as on the parameters already discussed, and the problem is so complex that only order-of-magnitude values have been derived. The greatest contamination density occurs under conditions of slight wind when the aircraft flies upwind while jettisoning. With such jettisoning at 300 m in a 2.5 m/s wind at 5°C, a strip of ground about 200 m wide can be contaminated to a density of about 0.1 g/m² (drop separation about 0.5 cm).

This refers to jettisoning from a single pipe under the standard conditions given at the start of this Section. The contamination becomes more dispersed when the aircraft flies across the wind. Taking the same conditions as before except that the wind has a more typical speed of 10 m/s, the strip of contaminated ground becomes roughly 4000 m wide and the contamination density about 0.004 g/m². For both types of jettisoning the density of ground contamination decreases with increasing wind speed and altitude of release.

REFERENCES

1. H O HUSS. EDP dispersion from modified K10, K33A1 and 165-gallon jettisonable fuel tanks. Chemical Warfare Service TDR 1215 (1946).
2. G F COLLINS. Unpublished work.
3. R G DORMAN. The empirical spray equations of Nukiyama and Tanasawa and their practical applications. Chemical Defence Establishment PEP 213 (1950).
4. C L WHEELER. Unpublished work.
5. H H LOWELL. Free fall and evaporation of n-octane drops in the atmosphere as applied to jettisoning of aviation gasoline at altitude. National Advisory Committee for Aeronautics NR 552L21a (1953).
6. H H LOWELL. Free fall and evaporation of JP-4 jet fuel droplets in a quiet atmosphere. National Aeronautics and Space Administration TN D-33 (1959).
7. H H LOWELL. Dispersion of jettisoned JP-4 fuel by atmospheric turbulence, evaporation and varying rates of fall of fuel droplets. National Aeronautics and Space Administration TN D-88 (1959).
8. H H LOWELL. Free fall and evaporation of JP-4 jet fuel in a quiet atmosphere. National Aeronautics and Space Administration TN D-199 (1960).
9. P PASQUILL. The estimation of the dispersion of windborne material. Meteorological Magazine, London, 90, (1961).

ACKNOWLEDGEMENTS

The major part of this work was done under contract to the Chief Scientist's Division of the UK Civil Aviation Authority, formerly the Scientific Adviser's Division of the Department of Trade and Industry.

Grateful thanks are due to the many staff of the Chemical Defence Establishment who assisted in the field trials, including G P Collins, B Parmer, Mrs P White, B Whalley and the Range Staff. Thanks are also due to N Thompson for advice on atmospheric diffusion.

The Buccaneer aircraft was provided by the Royal Air Force and was flown from A & AEE, Boscombe Down. The skill and cooperation of the pilot, Wg/Cdr E D Frith, AFC, and his navigator, FI/Lt P J Wilde is gratefully acknowledged.

APPENDIX

CALCULATION OF GROUND CONTAMINATION

The fate of fuel drops jettisoned at altitude has been examined in some detail by Lowell (5 - 8). The results presented in this paper are based entirely on Lowell's calculations together with a knowledge of the initial size distribution of the drops. The form of presentation of data by Lowell was not directly applicable to present requirements, and extensive interpolation was necessary, but highly significant errors are not expected.

Lowell (6) has produced on pages 26-27 of his report on the evaporation of JP-4 (Avtag), curves relating residual mass and distance of fall for a range of drop sizes (250 μ m to 2000 μ m) over a range of ground temperatures (-30°C to +30°C) for jettisoning heights of 7000 feet, 5000 feet and 3000 feet. In the present analysis attention was confined to the case of 5000 feet (Figure 4b of Reference 6) since these curves were the most convenient for interpolation. Throughout his calculations Lowell assumed a standard lapse rate of 2°C/1000 feet. In order to produce a similar set of curves for a jettisoning height of 300 metres it was necessary to adjust the ground level temperature on the abscissa of his curves to maintain the correct temperature at the point of release. Figure 4 shows the relationship obtained between residual drop mass after a fall of 300 metres and initial drop size, using Avtag fuel and a range of ground temperatures. By presenting the curves in this form the fate of different sized drops can be determined very simply, e.g., if a drop of Avtag of 360 μ m diameter is jettisoned at 300 metres when the ground temperature is -25°C, then it will be seen from Figure 4 that the residual drop mass at ground level is 0.6, i.e. only 60% of the initial mass remains as liquid by the time the ground is reached.

Two drop size distributions were investigated, one representing the lower limit of the distributions found with a Buccaneer aircraft, and the other representing a composite size distribution from various experiments (see Figures 1 and 2). In each case the distribution was divided into size ranges such that a known proportion of the total mass was present in each range. A representative drop size for each range was calculated. The corresponding residual drop mass was determined from Figure 4 which, when multiplied by the initial mass percentage in the range, gave the mass of liquid reaching the ground, expressed as a percentage of the total fuel jettisoned. The procedure was repeated for all size ranges, and summation

Mass in Range		15	20	20	20	10	10	4	1	Percentage mass fuel reaching ground from 300 m
Size range (μm)		<100	100-200	200-250	250-300	300-350	350-400	400-450	450-500	
Representative size (μm)		100	150	215	245	270	290	315	350	
Ground temperature (°C)		15	-	-	-	-	-	-	-	
		10	-	-	-	-	-	-	-	
		5	-	-	-	-	-	-	-	
		0	-	-	-	-	-	0.055	0.160	
		-5	-	-	-	-	0.14	0.225	0.295	
		-10	-	-	-	0.19	0.27	0.33	0.38	
		-15	-	-	0.21	0.31	0.36	0.41	0.455	
		-20	-	0.215	0.34	0.40	0.44	0.472	0.515	Percentage mass fuel reaching ground from 300 m
		-25	-	0.35	0.44	0.49	0.525	0.55	0.59	
		-30	-	0.45	0.53	0.57	0.595	0.62	0.652	
		15	-	-	-	-	-	-	-	
		10	-	-	-	-	-	-	-	
		5	-	-	-	-	-	-	-	
		0	-	-	-	-	-	0.22	0.16	
		-5	-	-	-	-	1.4	0.9	0.295	
		-10	-	-	-	1.9	2.7	1.32	0.38	
		-15	-	-	4.2	3.1	3.5	1.54	0.455	
		-20	-	4.3	6.8	4.0	4.4	1.89	0.515	
		-25	-	7.0	8.8	4.9	5.25	2.20	0.590	
		-30	-	9.2	10.5	5.7	5.95	2.60	0.652	
		15	-	-	-	-	-	-	-	Percentage mass fuel reaching ground from 300 m
		10	-	-	-	-	-	-	-	
		5	-	-	-	-	-	-	-	
		0	-	-	-	-	-	120	190	
		-5	-	-	-	-	151	192	233	
		-10	-	-	-	155	187	218	254	
		-15	-	-	146	183	205	234	269	
		-20	-	129	171	199	221	245	281	
		-25	-	152	186	213	234	258	293	
		-30	-	165	198	224	244	269	303	

TABLE 3: Ground contamination data: 'Avtag' jettisoned from 300 m at 450 kg/min at 120 m/s.
(Data based on the 'lower limit' of the drop size distribution found from Buccaneer trials).

Mass in Range		15	20	20	20	10	10	4	1	Percentage mass fuel reaching ground from 300 m
Size range (μm)		<100	100-200	200-250	250-300	300-350	350-400	400-450	450-500	
Representative size (μm)		100	150	215	245	270	290	315	350	
Ground temperature (°C)		15	-	-	-	-	0.007	0.137	0.200	
		10	-	-	-	-	0.132	0.245	0.303	
		5	-	-	-	0.102	0.248	0.344	0.393	
		0	-	-	0.090	0.243	0.338	0.427	0.480	
		-5	-	-	0.250	0.322	0.420	0.505	0.545	
		-10	-	0.125	0.347	0.425	0.495	0.567	0.610	
		-15	-	0.275	0.425	0.495	0.562	0.633	0.675	
		-20	0.020	0.377	0.485	0.553	0.618	0.690	0.720	Percentage mass fuel reaching ground from 300 m
		-25	0.160	0.475	0.563	0.625	0.680	0.743	0.780	
		-30	0.250	0.552	0.628	0.680	0.733	0.793	0.835	
		15	-	-	-	-	0.07	0.55	0.20	
		10	-	-	-	-	1.32	0.98	0.30	
		5	-	-	-	1.02	2.48	1.38	0.39	
		0	-	-	1.80	2.43	3.38	1.71	0.48	
		-5	-	-	5.00	3.22	4.20	2.02	0.54	
		-10	-	2.50	6.94	4.25	4.95	2.31	0.61	
		-15	-	5.50	8.50	4.95	5.62	2.53	0.68	
		-20	0.40	7.54	9.90	5.53	6.18	2.75	0.72	
		-25	3.20	9.50	11.25	6.25	6.8	2.97	0.78	
		-30	5.0	11.04	12.56	6.80	7.33	3.17	0.84	
		15	-	-	-	-	87	291	385	Percentage mass fuel reaching ground from 300 m
		10	-	-	-	-	232	353	440	
		5	-	-	-	180	286	396	480	
		0	-	-	146	240	317	425	513	
		-5	-	-	205	264	341	450	535	
		-10	-	130	220	289	350	458	555	
		-15	-	169	244	305	375	485	575	
		-20	53	188	255	315	388	499	587	
		-25	105	203	268	329	400	512	603	
		-30	123	213	278	339	410	523	617	

TABLE 4: Ground contamination data: 'Avtag' jettisoned from 300 m at 450 kg/min at 120 m/s.
(Data based on the Composite size distribution).

gave the total mass percentage reaching the ground. Results were obtained for a range of ground temperatures. To complete the calculation the drop sizes reaching the ground were also determined from:

$$\text{Ground level diameter} = \text{Initial diameter} \times \sqrt[3]{\text{Residual mass ratio}}$$

Lowell's work was concerned with the evaporation of Avtag. It should be noted that Avtur is a less volatile fuel, and according to Lowell (page 8 of Reference 8) "in general the evaporative behaviour of JP-1 (Avtur) is comparable at a given temperature with that of JP-4 (Avtag) at a temperature about 20°C lower". It is on the basis of this statement that calculations of ground contamination by Avtur have been based. Results for Avtag with both distributions are given in Tables 3 and 4.

For calculations involving jettisoning from heights other than 300 metres the procedure outlined above was repeated using the drop size distribution after falling through 300 metres as the starting point for calculations for the next 300 metres, etc. Results for these calculations, based on the Composite drop size distribution, are shown in Figure 3 for both Avtag and Avtur.

Discussion on Paper 12
"Ground Contamination by Fuel Jettisoned from Aircraft"
presented by N.L.Cross

R.E.Huie: Do you have any information on the chemical composition of the fuel that reaches ground level. In particular, do the more reactive hydrocarbons tend to evaporate or survive to near ground level, potentially contributing to photochemical smog?

N.L.Cross: We have not considered it. The data probably has sufficient information in it to derive this.

A.E.Fuhs: What is the largest drop that can fall at terminal velocity without further break up?

N.L.Cross: Considerable work has been done on water drops. Laboratory experiments have established that the largest drop which can fall at terminal velocity depends on the degree of turbulence in the air and on the band number. The largest drops found in rain are about 6 mm diameter, and the corresponding size for aviation fuel would be about 4 mm. However, the high degree of turbulence and the large relative velocity between drop and air in the wake of an aircraft jettisoning fuel ensures that such large drops quickly shatter. The largest drops found from aircraft sprays are about 0.7 mm diameter.

N.A.Chigier: For calculating rates of evaporation you have a different evaporation rate constant for isolated droplets compared to surrounded droplets.

N.L.Cross: The interaction and turbulence behind the aircraft closely simulates the condition for isolated droplets and gives close correlation with actual results.

A.Goldburg: How frequently do commercial and military aircraft jettison fuel over land? The usual procedure, if possible, is to fly out over water which, of course, is possible in the USA on the coasts and in the UK.

N.L.Cross: Although information on the frequency of fuel jettisoning could be collected without undue trouble, no data have been published, as far as I am aware. It would certainly be of interest to have figures which would highlight the magnitude of the problem: perhaps someone here at this conference could help? It is usually only done in emergency.

J.Dunham: You showed two fuels with different dispersion rates. Is the fuel which disperses more rapidly disadvantageous for other reasons?

N.L.Cross: Yes, it is a more hazardous fuel with which to operate: it is more volatile.

POLLUTION LEVELS AT LONDON (HEATHROW) AIRPORT AND METHODS FOR REDUCING THEM

DR. D.M. BRUTON, Principal Medical Officer (Ground)
Air Corporations Joint Medical Service, Speedbird House,
London (Heathrow) Airport, Hounslow, Middlesex, U.K.

Information on exhaust fume pollution levels at London (Heathrow) Airport is available from a study carried out by the Warren Spring Laboratory (Department of Trade & Industry) in 1970-71. Additional studies have been made by the Air Corporations Joint Medical Service particularly in buildings. While pollution levels are below those of many urban areas and do not appear to represent either a short or long term hazard to health, local pollution problems constitute a source of annoyance to ground personnel employed at the airport. In an effort to alleviate some of the problems, the Air Corporations Joint Medical Service promoted a B.E.A. Working Group to study the factors involved and propose possible solutions. Reduction of exhaust fume emission by vehicle selection, engine tuning and maintenance and other techniques are described in the paper.

In my experience, scientists addressing medical meetings frequently start by apologising for their lack of medical knowledge. I feel even more anxious talking to engineers and scientists about exhaust fume pollution problems since, in the long run, alleviating these problems will depend on engineering and scientific technology at a level which is completely beyond me. Nevertheless, as a doctor, responsible for the health of large numbers of ground staff working at an international airport, it has been my experience that one cannot influence the working environment beneficially without being prepared to make practical suggestions as to how improvements might be achieved. This, in turn, has required some understanding of the disciplines and problems that occur in scientific, technological, and management areas.

It was this sort of involvement which led to my participation in a B.E.A. Working Group study of exhaust fume pollution problems at Heathrow and gives me, perhaps, some right to say a few words to you today.

Towards the end of 1970 I made an assessment of the medical hazards to B.E.A. and B.O.A.C. staff which might occur from exposure to exhaust fume pollution at Heathrow. On the limited information available at that time I came to the conclusion that there were no serious long or short term effects on the health of staff in respect of the three principal areas relevant to the toxicity of exhaust gases i.e. poisoning, respiratory irritation and carcinogenesis. An exception to this observation is the possibility of acute poisoning occurring if vehicles are permitted to exhaust into confined spaces. Additionally, short term effects such as irritation to the eyes, nose and throat are commonplace but cannot be regarded as seriously hazardous. Nevertheless, the problems of discomfort and physical irritation arising from fume pollution, in my opinion, justified further evaluation of the problem and exploration of possible remedial action.

In the months before the B.E.A. Working Group was set up for this purpose the Air Corporations Joint Medical Service were fortunate in being able to participate in the Warren Spring Laboratory Survey of Air Pollution at Heathrow (1) which produced a great deal of up-to-date information regarding pollutant levels and we were able to supplement this information with material gained from our own studies. Some representative examples of pollution levels found by the Warren Spring Laboratory and the Air Corporations Joint Medical Service are given in Tables 1 and 2 respectively.

CARBON MONOXIDE AND TOTAL HYDROCARBON LEVELS TERMINAL AREAS, HEATHROW AIRPORT - APRIL-SEPTEMBER 1970			
LOCATION	POLLUTANT	AVERAGE LEVEL (PPM)	PEAK LEVEL (PPM)
AIRSIDE	CARBON MONOXIDE	8.0	24.0
	TOTAL HYDROCARBONS	1.6	2.6
LANDSIDE	CARBON MONOXIDE	21.0	50.0
	TOTAL HYDROCARBONS	3.1	4.4

TABLE 1

CARBON MONOXIDE LEVELS - TERMINAL BAGGAGE AREAS				
DATE	AVERAGE LEVEL	PEAK LEVEL	LOCATION	REMARKS
11-13 Feb. 70	4 ppm	26 ppm	Open baggage area Terminal 1	Strong westerly wind Peaks in excess of 100 ppm due to vehicle exhaust immediately adjacent to CO monitor Both sets of the above figures apply to day operations only (6 am-midnight). Odd night traffic does not exceed 3 ppm.
18-19 Feb. 70	10 ppm	40 ppm	Open baggage area Terminal 1	
19-22 Feb. 70	15 ppm	100 ppm	Closed baggage area Terminal 1	
7 Oct. 70	18 ppm		Open Baggage area Terminal 1	
7 Oct. 70	8 ppm		Open Baggage area Terminal 2	
7 Oct. 70	30 ppm		Open Baggage area Terminal 3	

TABLE 2

While figures like these support the opinion that there is no serious hazard to health, Table 2 for example indicates that there is a need to keep a careful watch on the use of internal combustion engines within build

The Warren Spring Laboratory report was particularly valuable in indicating the contribution made by various exhaust fume sources to pollution levels at the airport. In the Terminal Area where pollution is heaviest and, as shown in Table 1, carbon monoxide levels reach 24 ppm, approximately fifty percent of the airside pollution is due to aircraft engines and the remaining fifty percent to ground vehicles. The ground vehicles involved are mainly those required for aircraft support functions such as refuelling bowlers, ground power units, catering vehicles, baggage tugs etc. On the other hand, the majority of landside pollution is caused by passenger vehicles bringing the travelling and visiting public to the airport. Another factor to remember is that many of the problems encountered in relation to staff complaint are often very localised, for example, the lachrymatory and irritant effects produced by prolonged running of stationary vehicles in a cul-de-sac area on a warm, still, summer day.

On consideration of the basic information it appeared that the solutions to some of the problems might be within our control and the Working Group concentrated most of its attention on vehicular rather than aircraft engine emissions.

The simplest anti-pollution manoeuvre is, of course, not to run an engine when it is not needed. Therefore an obvious first step, particularly in reducing local pollution, is to ensure that switch off disciplines are promoted and enforced. Secondly, it is often possible to use something other than an internal combustion engine. Electrically driven trucks, tugs and forklift vehicles can replace many of the internal combustion vehicles which currently operate at airports particularly those which operate predominantly within buildings and B.S.A. are in the process of replacing liquid petroleum gas forklift trucks in their Cargo Unit at Heathrow with electrically powered vehicles.

As far as the ground support vehicles that are to be found clustered around aircraft are concerned, it is possible to replace some of these with fixed power and fuel supply sources with the possibility of alleviating local pollution and even noise problems. An installation of this kind is currently under study by B.S.A. at Heathrow and there appear to be both economic and environmental benefits but I am not in a position, at present, to confirm objectively the environmental advantages and I cannot say whether such installations are likely to prove a practical proposition either at Heathrow or elsewhere.

Substitution of safe materials equipment or processes in place of hazardous materials equipment and processes is a basic principle of occupational health practice. All the anti-pollution measures described above follow this principle.

Several factors however, dictate the use of internal combustion vehicles for many of the activities concerned in airline operations. Limited power and range are two problems of battery operated vehicles and battery charging creates problems of toxic, explosive or corrosive fumes which must be properly dispersed.

Internal combustion vehicles are often, therefore, an inevitable choice, but it still remains possible to opt for diesel, petrol or gas powered engines. Of this trio diesels have the advantage of emitting low levels of carbon monoxide but smoke and odour may present difficulties. Choice of engine on the basis of emission characteristics is subject to many variables but these characteristics are factors worth considering.

Engine size should also be carefully considered since the total volume of exhaust emitted will be proportional to engine size.

Faced with the widespread use of internal combustion engines practical ways of reducing the emission of pollutants were considered.

Studies by the A.C.J.M.S. of the effect of catalytic exhaust purifiers on exhaust emissions produced by diesel and L.P.G. engines initially gave variable results due to failure on our part to control various parameters. One purifier manufacturer advised that the engine must be tuned to give low carbon monoxide and hydrocarbon emissions before fitting the purifier. When this was done we found that it was possible to obtain lower carbon monoxide and hydrocarbon emissions by tuning alone than by the use of tuning and catalyst. Figures for one of the tests are given in Table 3.

1½ LITRE MERCURY TUG - LPG FUEL		
TIME	CO Levels/ppm	
	WITHOUT CATALYST	WITH CATALYST
Start up	750	2,250
Start + 30 seconds	600	750
Start + 40 seconds	500	700-800
Start + 60 seconds	500	1,100
Start + 60 seconds with 2200 lb. loading	0	0
Other tests on a similar vehicle indicated that carbon monoxide levels of 5300 ppm could be reduced to 0 in all driving mode conditions by engine tuning and without the use of exhaust purifiers.		

TABLE 3

There are additional problems with the use of exhaust purifiers such as the need for regular maintenance, back pressure in the exhaust manifold causing adverse combustion conditions, durability limitations and the extra cost.

In view of these problems and the findings that it was possible to achieve low pollutant emissions by engine tuning alone, we decided to concentrate on maintenance as the key to lowering vehicle exhaust emissions as far as was practically possible. In addition, therefore, to promoting regular routine maintenance of all internal combustion vehicles, maintenance guide lines have been produced, which, it is believed, will achieve a significant reduction of pollution, fuel economy and extension of engine life. These recommendations are as follows:

ENGINE MAINTENANCE AND TUNING

In general, engines should be governed to give 90% of the manufacturers' rated performance. It follows that when engines are purchased, an engine should be selected with a maximum rating of approximately 10% higher than the maximum performance required.

Diesel Engines

- a. Fuel pumps and injectors should only be overhauled and installed by skilled staff with the necessary training and equipment.

- b. The maximum fuel delivery of each pump should be maintained within 1% of the manufacturers' recommendations.
- c. In establishing the fuel pump setting for a particular pump and engine duty, exhaust gas analysis should be taken into account.
- d. Where injectors are individually timed, they should be set to within half degree of the manufacturers' recommendations, and systematic checks should be made during scheduled maintenance that this tolerance is being maintained.
- e. Injectors after overhaul should be tested to the correct release pressure and spray pattern. Tests should be carried out to ensure that there is no pressure drop or fuel leakage at sustained high pressure.
- f. Engines should not be allowed to idle for long periods and should be switched off when not required.
- g. Vehicle drivers and engine operators should be instructed to report excessive emission of smoke or loss of performance.

Liquid Petroleum Gas and Petrol Engines

- a. Precise fuel/air ratios should be maintained with a tendency to lean stoichiometric mixture.
- b. The component parts of LPG fuel systems should be checked at frequent intervals to ensure correct line pressure and flow.
- c. Vaporisers of LPG fuel systems should be supplied with water from the engine cylinder block coolant system taken from a point on the engine side of the thermostat to ensure that warmed water is supplied as soon as possible after initial cold start. This will ensure that liquid gas is vaporised properly before reaching the engine.
- d. Timing should tend to be retarded, but not in excess to cause overheating, loss of performance or misfiring. Where appropriate, the distributor advance and retard mechanism should be locked and the ignition set to an optimum fixed position.
- e. Hard acceleration should be avoided as this not only wastes fuel but leads to unburnt fuel in the exhaust.
- f. Rapid deceleration and "over-running" of the engine leads to unburnt fuel in the exhaust.
- g. In general, the principles adopted to achieve maximum miles per gallon of fuel, are equally appropriate to the minimisation of exhaust fume pollution.

Finally, on the subject of controlling vehicle exhaust emissions, it should be mentioned that because many of the problems encountered are due to the annoying effects of fuel odours, some trials have been carried out using deodorizing fuel additives. Subjective impressions are that at least one of the additives tried produced a significant reduction in odour and smoke and the latter point was confirmed by the use of a "Hartridge" smoke meter, the results being shown in Table 4. Further studies will be made on the effects of masking agents in reducing discomfort problems.

SMOKE LEVELS - HARTRIDGE SMOKE UNITS (HSU'S) USING FUEL ADDITIVES		
Vehicle (2.5 litre tractors)	Without Additive	With Additive
A	50 HSU's	34 HSU's
B	55 HSU's	30 HSU's

TABLE 4

As half of the general pollution in apron areas is caused by aircraft engines, means of abating their effects should be considered. It appears neither practical nor necessary to attempt to alter aircraft engine emission characteristics to reduce their polluting effects while running on the ground. Measures designed to reduce the ground running time of aircraft engines will, however, be beneficial and tow-in push-out procedures, recently introduced, at Heathrow, have in some areas, reduced aircraft running on stands although their primary purpose is to promote quicker turn round for other reasons. It should be noted that the use of the fixed power installations previously mentioned also avoids the use of aircraft mounted gas turbine auxiliary power units and further emphasises the need to explore the use of such installations.

Aircraft orientation may play a part in reducing local pollution problems as the venting of exhaust down wind away from cul-de-sac areas or staff working around the aircraft is clearly going to be beneficial. However, this is rarely a practical proposition and, in any case, depends on airport designers and not airline operators although the opinion by the latter could bring influential pressure to bear.

Finally, as we have been led to the subject of airport design, I would like to conclude by noting that staff and passengers working in, or transiting through airport buildings require that these buildings are suitably supplied with air which is reasonably free from odour and definitely free from toxic levels of exhaust constituents. This frequently implies mechanical ventilation, filtration and continuously operating gas monitoring devices. A number of continuously operating carbon monoxide infra-red automatic gas analysers are installed in passenger and airline facilities at Heathrow. In some areas where internal combustion vehicles operate, the gas analysers control the ventilation system or actuate automatic warning devices. In addition, they provide valuable information which enables us to assess the safety of the working environment which, as a doctor, is of course my primary interest.

References: (1) Air Pollution at Heathrow Airport,
London: April - September, 1970. Parker J.
Warren Spring Laboratory. Department of Trade
and Industry, Stevenage, Herts, England.

Discussion on Paper 13
"Pollution Levels at London (Heathrow) Airport and Methods for
Reducing Them"
presented by D.M.Bruton

R.F.Sawyer: What is the nature of fuel additives used to reduce odor and smoke?

D.M.Bruton: I'm afraid I cannot recall the active constituents.

H.J.Judd: Barium sulphate.

R.F.Sawyer: Do you consider the use of barium sulphate a good idea from the medical standpoint?

D.M.Bruton: For our limited trials of masking agents I have been happy to accept the manufacturers' assurance that they are safe. However, when advising management on the possible use of masking agents I have repeatedly stressed that before their introduction we must be certain that the additives themselves do not introduce a new toxic element. I have also warned them that in certain situations removing odour and smoke could, at the same time, remove the only available warning of hazard.

D.J.K.Tommel: Are the carbon monoxide peak values real values or have they been integrated over a certain period of time?

D.M.Bruton: They are the peak values recorded during the sampling periods.

W.S.Blazowzki: You have compared your ambient carbon monoxide finding to the threshold limit value of 50 ppm. The US Environmental Protection Agency would use the ambient air quality standard of 9 ppm CO for the same comparison and this would have significantly changed the interpretation of results. Could you justify your use of 50 ppm and/or comment on the 9 ppm value?

D.M.Bruton: The threshold limit value of 50 ppm carbon monoxide is that recommended by ACGIH who thereby regard the level as a safe exposure for an eight hour shift, five days a week, etc. We are concerned with evaluating the risk to industrial staff with this type of working exposure and the threshold limit value is, in my opinion, the appropriate index. I do not know on what considerations the United States Environmental Protection Agency base their ambient air quality standards of 9 ppm for carbon monoxide. On physiological considerations alone 9 ppm seems too low but the EPA may have had other factors in mind.

C.J.Scott: Have you done, or are you planning, any studies of the effects upon piloting ability of prolonged exposure to the average carbon monoxide levels which you measured in terminal areas.

D.M.Bruton: We have already measured carbon monoxide levels on flight decks in taxiing aircraft and the levels give no cause for concern. The study carried out by Mr Judd for the Air Corporations Joint Medical Service has been published in the Journal of Aero Space Medicine.

C.J.Scott: I think you have misunderstood my question; I was talking about the exposure of pilots in the hour or two before take off. Do they spend that time in the terminal area where CO levels were higher than in cabins?

D.M.Bruton: This is not my area of responsibility but I think it is unlikely that carboxyhaemoglobin levels in operating air crew will be significantly affected by the very low levels of carbon monoxide found in terminal buildings. One could, of course, measure the carboxyhaemoglobin. I think it would be found that the most significant factor is cigarette smoking.

C.J.Scott: But do you forbid pilots to smoke?

D.M.Bruton: No. As far as I am aware no airline does.

POLLUTION CONTROL OF AIRPORT ENGINE TEST FACILITIES

by

T. L. Bailey, LT P. W. Tower, and Professor A. E. Fuhs
Department of Aeronautics
Naval Postgraduate School
Monterey, California 93940
United States of America

SUMMARY

Engine test facilities are required to meet the same environmental standards as any other industrial facility. To meet the standards for smoke, noise, gaseous pollutants, etc., control equipment must be installed. Due to large mass flow rates the control equipment is expensive; careful attention to design is necessary to control costs.

Pollution control forces new constraints on exhaust stack temperature, flow uniformity and pressure. Conversely, installation of pollution abatement apparatus may cause adverse operating conditions such as distorted flow into the engine and wrong augmentation ratio. The internal aerodynamics of engine test cells must be mastered to a level not possible previously.

Scale models (1:24) of test cells were fabricated in modules so that some 750 different combinations could be tested. Distortion at the engine face was measured and correlated in terms of component factors. Augmentation ratio and cell depression were measured. An analytical model correctly predicted the measured quantities except for distance from engine nozzle to augmentor inlet. With the data accumulated it should be possible to match pollution control requirements to test cell parameters.

I. INTRODUCTION

Through the 1960's satisfactory engine test facilities consisted of large rainproof buildings located and constructed in such a manner that the nearest neighbors were not permanently deafened. Today, the evolution of aircraft propulsion systems has rendered some of these installations unusable long before their physical deterioration would have done so. Turbojet test cells constructed during the next decade will be required to meet a greatly expanded and refined definition of satisfactory performance. Factors such as increased thrust, use of high bypass turbofans, proliferation of special-purpose turbine engines, inflation of real estate and utility costs coupled with reduced availability, and the recognition of the need for environmental protection will increase the cost and the challenge of designing test facilities operable through the 1990's.

By Executive Order No. 11282, May 26, 1966, Federal Government installations must meet local laws concerning the environment. In fact, the management of such installations is encouraged to assume leadership in pollution control. Engine test facilities must be designed with considerable care. Previously the penalties for design errors were not significant. After the test cell was built, adequate fixes could be incorporated. However, the addition of new environmental criteria to the facility performance specification makes design more critical.

Various techniques for control of pollutants are currently being screened for merit and feasibility as applied to engine test facilities. Unfortunately, there is not a suitable technology base from which to draw the design information. The technology base is weak for both pollution control and accurate internal aerodynamics of the test cell.

It is the purpose of this paper to identify the essential characteristics of the jet engine test facilities to be constructed during the 1970's and to provide a summary of the techniques available to meet these requirements. In the following sections the necessity of providing replacements for or modifications to current facilities is documented, and the factors which will ensure future production capability and economic feasibility are detailed.

From the background study for this paper there were two areas identified for further in-depth study. The first of these two topics is relationship between distortion at engine compressor face as determined by inlet design including pollution control features. The second study considers the influence of various design parameters on control of augmentation ratio, cell depression, and exhaust back pressure. Subsequent sections discuss these two studies.

II. ENGINES TO BE TESTED 1-23

A. Present

In its annual inventory issue, Aviation Week and Space Technology magazine presents a comprehensive summary of the types and sizes of aircraft propulsion systems in use with operational aircraft. The largest in each class is of primary interest to the test cell designer, but account must be taken of the wide variation within classes. Within the class of turbojet engines, thrust ranges from 30,000 pounds (J58 in the SR 71) to 170 (WR24-7 in drones), and the corresponding lengths vary from 22 to 2 feet.

The facility designed to service turboshaft engines would have to handle variations in shaft horsepower from 5000 SHP (J56-A-15) to 300 SHP (TSE 36) as well as length and weight changes. Similarly, turbofan engines in military use range from one-foot to nine-foot diameters (Harpoon and C5) and have weights of 100 to 7500 pounds. Review of current engine useage makes it obvious that the facility mission must be carefully established prior to initiation of design.

B. Future

In the past, varied aircraft types were powered by similar engines. New technology developments have changed matters dramatically, as evidenced by the present differences between characteristics of high bypass turbofans and afterburning turbojets. Future changes and developments will require more precise matching of engines and airframes for specific missions.^{1,2}

The Navy of the future will move strongly towards utilization of gas turbine powered surface vessels. These may be surface effect vehicles (SEV) or standard design vessels, but their propulsion systems will need overhaul and repair facilities similar to those of a Naval Air Rework Facility (NARF).

Because of the vast differences of engine types, it may not prove feasible to build a single test cell capable of testing all engines. Present Navy policy is to assign the overhaul and repair responsibility of a particular type engine to each NARF. The purpose of this section is to correlate engine characteristics and projected aircraft performance.

The first advanced technology engines for Navy fighter aircraft will be used in the F-14 Tomcat. Early versions will utilize the Pratt and Whitney TF-30 412 engine, and F-14B models will be equipped with the more powerful F401 PW 400 engines. The latter engine is in the 20-30,000 pound thrust class and will have an air flow rate at full power of about 300 pounds per second. If an augmentation ratio of 2.1 is chosen, a test cell flow rate on the order of 900 pounds per second will result. Other engine manufacturers are also developing afterburner equipped engines in the 25,000 pound thrust category.³

Further fighter aircraft developments will bring to the Navy the ADLI, or Advanced Deck Launched Interceptor. The ADLI will utilize an advanced technology engine with turbine inlet temperatures in excess of 3,000°F. Also, advanced hybrid multicycle engines are being developed and will be introduced to operational use during the life of test cells built in the present decade.⁴ Turbo-ramjets or supercharged ejector ramjets (SERJ) are also being developed. Advanced engines may not use familiar JP-4 or JP-5 as fuel. Fuels may include cryogenic methane, liquid hydrogen, or other exotic fuels. Test facility plans should consider this fact.

Future attack aircraft must combine the capability of high subsonic cruise speeds with the ability to loiter for long periods over target areas. Non-afterburning turbofan engines are presently in use, and their continued development and refinement is predicted. The U. S. Marine Corps presently has the Harrier (AV-8A) in operational use. The Navy may move toward procurement of Harrier-type aircraft in the near future and advanced vectored thrust V/STOL aircraft within the next ten or fifteen years. The Harrier utilizes the Pegasus turbofan engine with variable nozzles which is built by Rolls Royce. The advanced Pegasus 15 will have 25,000 pounds thrust and an airflow requirement of 450 pounds per second. A requirement for testing these engines is that shrouds and ducts be installed for directing the exhaust streams of the individual nozzles into a common exhaust.⁵ Total cell requirements for this engine will also be 900 pounds per second with a 1:1 augmentation ratio.

The Navy is currently developing the S-3 carrier based ASW aircraft, which is powered by the General Electric TF-34 turbofan engine. This is a 9,000 pound thrust engine with an airflow capacity of about 300 pounds per second and will be the first engine that the Navy operates that will be tested in the same configuration as it is mounted on the aircraft. That is, it will be pylon mounted, thereby requiring an overhead thrust bed. Because of the large mass flow through the turbofan engine, any pressure variations in the cell acting across the fan exhaust will cause errors in thrust measurement. The TF-34 has a bypass ratio greater than 6:1. Because of the exhaust characteristics of turbofan engines, care must be taken in matching the engine and augmentor to avoid excess air entrainment over that which is required for cooling purposes, thereby increasing the cell depression.⁶

Future patrol aircraft developed to be introduced in the 1980's may utilize large fan engines. Other aircraft using the same type engines may be those developed to replace the Navy's present transport fleet. Military transports with STOL capability will require turbofans in the 25-30,000 pound thrust category.⁷ The airflow through an engine of this size will be on the order of 1,000 pounds per second, and total cell airflow could run as high as 2,000 pounds per second, depending on the augmentor design.

Smaller logistic aircraft, successors to the C-2 COD aircraft, may use turbofans in the 5-10,000 pound thrust class. These will be similar to the above-mentioned TF-34 in flow requirements, and test facility requirements will be similar as well.

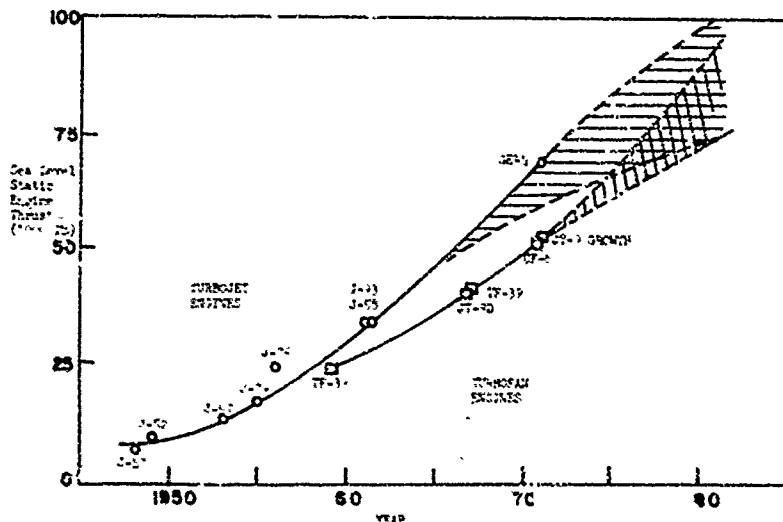
Future weapons system acquisition will have a bearing on aircraft design and therefore on engine design. For some missions, the effectiveness of a weapon may be proportional to the payload which can be carried in the transporting aircraft, and such systems may require a platform as large as the Lockheed C 5A.⁸ If the Navy were to acquire such a system, it would find itself in possession of turbofan engines in the 50,000 pound thrust category, having airflow requirements of 1,500 pounds per second and requiring a test facility capable of handling 3,000 pounds per second airflows.

Figure 1 shows the growth of military jet aircraft engines since WW II. The projection through 1980 is also given. Figure 2 gives the mass flow rate and sea level thrust for the next two decades. Curves labeled A are for facilities that can test the largest engines. Curves labeled B are for facilities limited to fighter and attack aircraft.

Consideration also must be given to the testing of turboshaft engines used in large rotary-wing aircraft. Facilities must be available for the measurement and absorption of the shaft energy generated by such engines. Similarly, turbine engines used for surface ship propulsion systems will require complex gearing and energy absorbing systems.^{9,10}

Other trends in engine/airframe mating techniques will require some modification of test cell design and operation. The F 14 aircraft will utilize non-interchangeable left-hand and right-hand engines. This may mean that reversible mountings, slave accessories, etc., will be required in cells.

In order to minimize drag associated with nozzle and airframe interaction, non-axisymmetric nozzles may be employed in the future. This possibility implies a requirement for an augmentor tube designed to permit replacement of the receptor bellmouth.



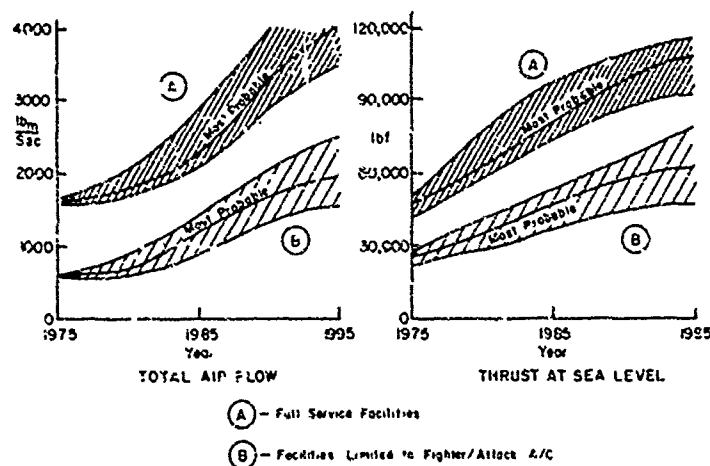


Figure 2 Future Test Cell Requirements.

test cells, both in the military and civilian communities, were designed and built to test the early generations of turbojet engines. These may be defined as the state of the art engines of the 1950's. In other instances, some even older test cells are in existence. The Naval Air Rework Facility at NAS North Island, California, has several operational cells which were initially built to test reciprocating aircraft engines. These are still in use testing J-57 and J-79 engines, but their performance is marginal now and will be aerodynamically and environmentally unsatisfactory for the engines which will reach operational status in the next twenty years.¹⁴

A. Test Facility Inlets

Many of the oldest test cells were engineered so as to take maximum advantage of existing construction and to minimize costs. The next generation of test cells built in the late 1950's was designed with some added sophistication. It was realized that the test section itself should be long enough to provide for some flow straightening forward of the engine bellmouth.

The cell aerodynamics were obviously cleaner than those previously built, and in operational use with present afterburner equipped engines these cells have been satisfactory. In all such installations certain compromises are made between the desired operational characteristics and economic constraints.

Modern turbine engines, particularly turbofan engines, have proven highly sensitive to aerodynamic distortion in poorly designed test cells. General Electric¹⁵ considers total pressure distortion greater than two inches of water above or below the mean measured at the fan or compressor face unacceptable and endeavors to reduce this difference to less than one inch H_2O .

Modern test facilities built in late 1960's to test these large fan engines, as well as any future engines, have been designed to reduce inlet distortion as much as possible. United Air Lines overhaul facility in San Francisco exhibits one of the simplest inlet designs. Air enters through the horizontal inlet, passes the acoustic treatment, and enters the test section without encountering any turns. This design is obviously easier to construct than one having a 90° vertical inlet.

A second example of modern design philosophy is exhibited in the test cell operated by Pacific Airmotive Corporation in Burbank, California. The vertical inlet is flush with the roof structure, turning vanes are installed to minimize the losses caused by the 90° turn. Turning vanes or flow straighteners will become increasingly necessary as test cell airflow design limits are approached. Some modern cells are designed so that turning vanes may be added in the future. The installation operated by AirResearch Manufacturing Co.¹⁶ in Torrance, California, has a vertical inlet. The only present requirement for flow treatment is a corner fairing to reduce separation at the inlet bend, but designs have been drawn for the addition of turning vanes when future requirements so dictate.

A prime consideration in the use of flow treatment is the method of installing the engine in the test cell. The simplest and cheapest method of construction is to build a front-loading cell. However, if flow treatments are installed this design requires that they be movable or that a portion of the treatment be hinged.

B. Exhausts for Test Facilities

The basic philosophy of present exhaust treatments is to remove the majority of the kinetic energy from the jet exhaust, to cool the exhaust by mixing with secondary air or water, and to lower the noise level of the exhaust. Removing the kinetic energy is also a method of acoustic treatment. The most common method of accomplishing the first two objectives is to utilize the kinetic energy of the exhaust to pump secondary air through the cell and into the exhaustor or augmentor tube where mixing of the two streams occurs. Augmentation ratio, defined as the ratio of secondary air mass flow to engine air mass flow, is an important consideration in determining overall cell design. With an excessive augmentation ratio, the depression limits of the cell may be exceeded; with too small a ratio, desired cooling may not be accomplished, and temperature limits of test cell exhaust components, such as installed acoustic treatment, may be exceeded. Figure 3 illustrates the dependence of exhaust temperature on augmentation ratio. Present design goals for augmentation ratios are 2:1 for turbojet engines and 0.25:1 to 0.5:1 for high bypass turbofan engines.^{3,12,15} Some facilities, however, still have augmentation ratios as large or greater than 1:1 for large turbofan engines.¹⁷ Turbulent mixing phenomena are not well understood, and much work remains to be done in analyzing the ejector system.

Water cooling is usually required for an engine operating in afterburner; the augmentation ratio required to cool the exhaust without water usually is greater than 6:1. The minimum amount of water usage is desirable in order that water supplies be preserved. Many cells utilize spray rings mounted inside the augmentor. These operate very inefficiently because of the difficulty of penetrating the hot, high speed core of the exhaust.¹⁸ Several attempts have been made to inject the water from within the core itself. The water sparger¹⁹ is an example. Care must be taken in the design of such items since they can produce undesirable acoustic phenomena if their natural frequencies correspond to the driving frequencies of the exhaust. Further development of water injection is a necessity for economical future operation.

forecast, it includes some uncertainty; but the information included is as authoritative as possible, having been collected from engine manufacturers, Department of Defense planning agencies, published reports of service sponsored research, and interviews with facilities planners for several test cell operators. These data make it clear that the decision as to facility capacity will restrict usage plans for extended periods and that the operator will require guidance by policy level managers to determine final construction requirements.

Gerend¹¹ provides a simple method of predicting turbine engine weights and dimensions. This method has been used to check the credibility of this summary information. These projections are specifically confined to facilities for sea-level testing only. Forecasts of requirements for altitude test facilities are available in Refs. 12 and 13.

III. PRESENT TEST CELL DESIGNS

Many currently operational jet engine

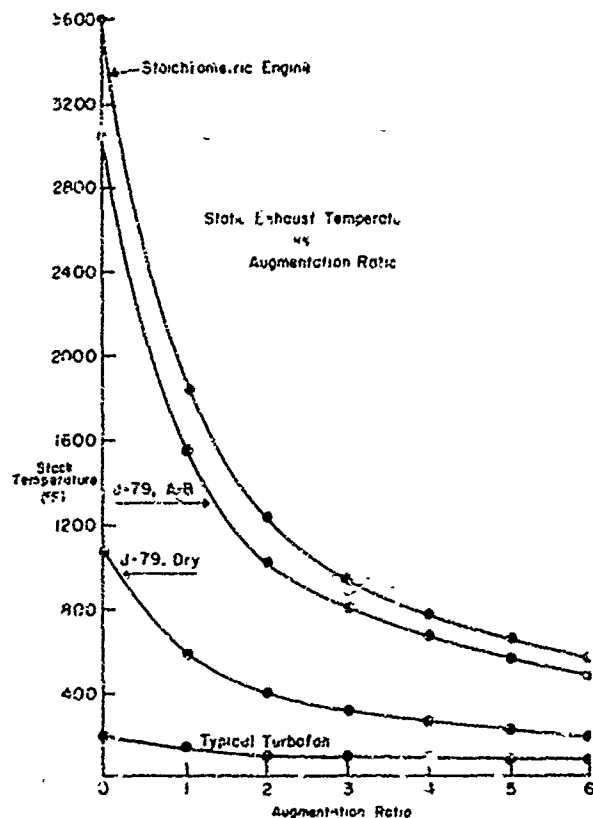


Figure 3 Static Exhaust Temperature vs Augmentation Ratio

sive heat transfer, they either must be monitored for temperature changes or kept at a constant temperature. United Air Lines facility in San Francisco has both such systems installed.¹⁷ Current thrust measurement accuracy²³ is typically ± 6 lbs. for an engine thrust of 41,100 lbs.

Overhead mounting systems have introduced a new problem to test operations in that the height of the engine when mounted in the cell makes accessibility difficult. United Air Lines¹⁷ has installed a hydraulically lifted platform beneath the mounting system. During actual testing the platform is lowered to a position flush with the floor, providing smooth passage for the secondary air past the engine. Another solution to this problem was developed for the previously mentioned AirResearch facility.¹⁶ The work platforms are suspended from the overhead at a convenient height and are swung up and locked next to the ceiling during engine operation.

In many older cells considerable time is used in preparing and mounting the engine for test. If this time is kept to a minimum, total cell running time can be maximized. Modern design philosophy reduces the man-in-cell time by allowing much of the preparatory work to be done in the handling area rather than in the cell itself. In the handling area the engine is fitted to a specially designed adapter. Necessary engine connections for starting air, fuel, instrumentation leads, and external power are made to the adapter. The entire assembly then is moved to the cell area and is hoisted to the thrust bed by a winch assembly in the thrust bed itself.^{16,17,20}

Means of handling and transporting the engine are also varied. Many facilities use wheeled dollies for transporting the engine and related assemblies.^{16,21} Some newer facilities utilize overhead monorail systems both in the handling and preparation areas and in the cell itself.^{19,24} Some problems have developed with monorail systems, however, and complete flow analysis must be accomplished before utilizing such a handling system. In one situation,²⁵ it has been found that vortices are formed by flow interaction with the monorail, causing serious flow distortion in a cell designed to test large turbofan engines.

Recently, attempts have been made to improve operator visual contact with the interior of the cell. The usual method of providing this contact is to provide a window between the control room and the cell. Whenever the cell structure is penetrated, additional acoustic problems are created; in order to provide minimum noise levels within the control room, there should be no direct connection between the cell and the control room. One alternative to windows has been to install closed circuit television. NARF North Island has installed three black and white cameras in their large cells. These cameras have no zoom or pan capability and have not met with complete operator approval. Also, they do not obviate the need for entrance into the cell by technicians to check for fuel or oil leaks when the engine is operating.

Because of the varied engines which must be tested in one cell, consideration must be given to the ease with which cell hardware can be adjusted for various engine sizes. NARF North Island utilizes the movable augmentor concept. The facility at United Air Lines uses a jackscrew arrangement to adjust the thrust bed position. The range of adjustment will depend on the size of engines projected to be tested, and the means of providing adjustment is an option of the designer.

Modern test facilities are being equipped with automatic data acquisition and processing capability. AirResearch Manufacturing Co.¹⁶ has an excellent example of a system designed for developmental engine testing, and United Air Lines¹⁷ provides a system designed for production testing of overhauled and repaired engines.

One method available for removing the kinetic energy of the jet exhaust is the "brute force" method. At NARF North Island in cells 13 and 14, the exhaust impinges on a solid concrete block lined with steel plate. This is effective in destroying the continuity of the stream but has failed to prevent serious damage to the walls of the plenum chamber.¹⁴ In the newer cells at North Island the exhaust impinges on a perforated steel plate.

A newer method of treating the flow, one coming into more general use,^{16,17,20,21} involves a colander in the form of a cylinder or a cone. The colander is the last section of the ejector tube and is perforated with holes, usually on the order of 1-1/4 in. in diameter.¹⁵ This serves to break up the flow and changes the low frequency noise of the exhaust into more easily attenuated higher frequencies. Research remaining to be accomplished in this area involves the study of placement and sizing of the holes so that uniform flow in the exhaust stack is attained.

Other methods of exhaust treatment will become necessary in the future. Environmental protection standards will require pollution abatement systems for engine test facilities. These systems will require close matching between the engine nozzle and the exhauster because any excess mass flow will unnecessarily load the abatement equipment. Also, in some cases, the flow needs to be properly conditioned before it reaches the abatement system.²²

C. General

Because of the relatively small flow rates, older turbojet engines could be tested in close proximity to cell boundaries. The larger engines now coming into use must be tested with adequate clearance from floors, walls, and ceilings to reduce velocity distortions. This clearance can only adequately be provided by overhead thrust bed systems. Because thrust measuring devices above the engine are subject to convective and conduc-

Most of the above information is applicable to depot level test cells for large overhaul facilities. Other proposals have been made for developing smaller test cells for use in intermediate level maintenance facilities. The Ground Support Equipment division of the Naval Air Engineering Center, Philadelphia, Pa., has designed a cell for intermediate level maintenance. This design differs greatly from those discussed in this section. A primary difference is the construction technique utilized. The cell is constructed from pre-fabricated sections and is designed to be demountable if the need should arise. The flow design is different in that separate intakes are provided for the primary (engine) and secondary (augmentation) airflows. Complete aerodynamic analysis is required for this and other major design alternatives.

IV. DESIGN OPTIONS

A. Test Facility Air Inlet

Acoustic Control. The current development of commercial STOL aircraft and increasingly stringent airport noise level restrictions²² have resulted in extensive on-going research directed at reduction of engine generated acoustic power. It is reasonable to expect that the engines now in service will be the noisiest, per point thrust, with which new test cells must cope.^{26,28} See Fig. 4 for sound power levels for several engines. It is equally certain that new test cells will require some form of inlet acoustic treatment for the following reasons:

- Current noisy engines will still be in service after the anticipated introduction of the replacement cells.²⁸
- Turbofan engines increase the acoustic power directed up-stream into the inlet.^{27,29,30}
- Military aircraft will continue at the least restricted in required acoustic abatement by virtue of their mission and environment.³¹⁻³³
- The test cell structure alone will not be able to absorb the acoustic power produced by even the quietest of projected future engines.^{12,25-28,31-33}

Accepting the necessity of including specific acoustic treatment, several options are available as shown in Fig. 5. Many of the designs for which performance data are available are proprietary ones, and the cost of acquisition must be weighed against that of locally produced designs which must be oversized to compensate for the less complete information on effectiveness.

Flat baffles are the simplest of the duct obstruction types. Of sheet metal and fiberglass composition they can, with careful streamlining, provide acceptably low levels of flow distortion. Adjustment of length, thickness, and spacing can match acoustic absorption characteristics to specified frequency ranges. The overall flow length required to meet both acoustic and aerodynamic limits may be the greatest for this option, and the increased cell length or stack height must be off-set by simplicity of installation and replacement. Both proprietary and non-proprietary designs are available.^{12,28} Staggered baffles require less total flow length for the same absorption and produce less aerodynamic distortion than the flat types. They are also more difficult to construct and replace though reduced total size may ease handling difficulties.^{28,34}

The sinuous passage treatment requires a length and produces a distortion level intermediate to those of the two baffle types. Construction and installation are more difficult and expensive than either of the baffles, but proprietary designs are available which permit single panel replacement.^{28,33}

The acoustic performance of the tubular treatment reduces the total flow length required below that of the other options, but the distortion level in some operating conditions may demand an increase in mixing length which offsets this gain. Additionally they may prove incompatible with good turning vane performance when used in a vertical inlet. The available designs with adequately documented performance levels are proprietary in nature.^{25,28}

Another option which is not in current use and which deserves to be fully evaluated as to effectiveness is the lined wall concept. By lining the considerable wall/overhead area forward of the engine inlet with suitable foam and lead septum material, it may be possible to eliminate entirely the need for duct obstructing devices with consequent simplification of distortion control. Since considerable absorbing thickness could be provided at low cost in a test cell, this option ought to be considered. Preliminary analysis by the treatment manufacturer indicates that this method would be restricted to a vertical inlet arrangement. The lining material is available from commercial sources, and it would be necessary to obtain their assistance in determining the type and quantity required.²⁹

Any of these alternatives can provide the required acoustic control and except as noted do not restrict the selection of inlet position. Detailed investigation is required to evaluate the possible trade-offs in cost, size, service life, and distortion. The construction contractor will require the services of a qualified acoustic engineer, but satisfactory inlet acoustic treatment can be provided at reasonable cost. Doelling and Rolz³⁵ provide an excellent summary of calculation procedures for design use. Before final selection can be made, the designer must, of necessity, consider compatibility with the aerodynamic requirements detailed in the next section.

Aerodynamics. Comprehensive design criteria are not available for this aspect of the inlet design. No general method is available for the prediction of streamline, pressure, or velocity patterns although these may limit the total test cell in its compatibility with future engines. Reference 12 is an example of a completed construction specification which treats

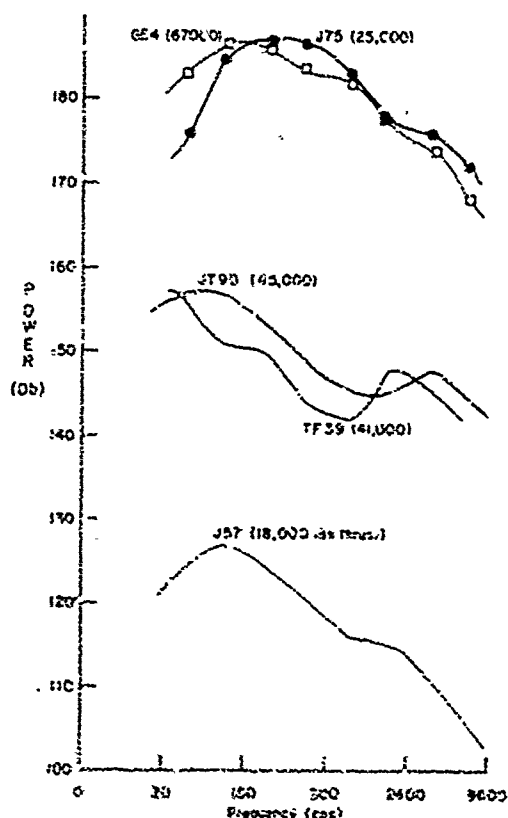


Figure 4 The Effect of Engine Type and Thrust on Sound Power Levels.

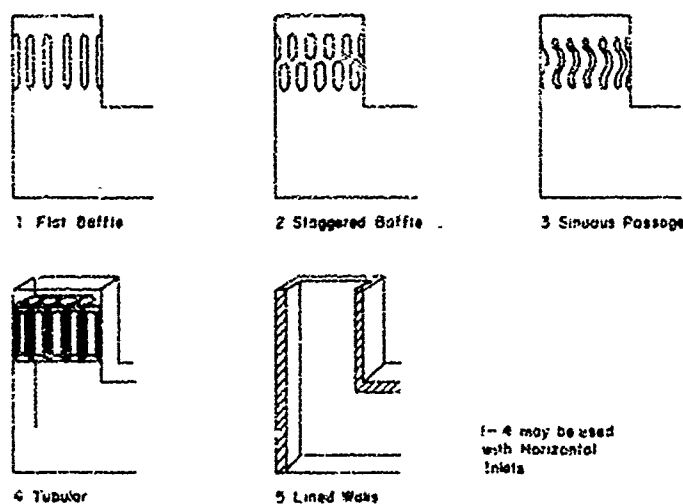


Figure 5 Inlet Acoustic Treatment Options.

requires that the exhaust treatment type and pollution control system be identified. In general, with exhaust directed vertically, increasing the inlet height and reducing inlet-to-exhaust separation distance reduce the probability of avoiding recirculation problems. A horizontal inflow naturally reduces the likelihood of exhaust gas capture.^{38,39} The references provide reasonably accurate prediction methods for proposed design susceptibility to recirculation.

Determination of the total inlet flow capacity requires identification of maximum projected engine requirements and facility type. With this available, using information from Figures 1 and 2 and similar data, it is necessary to select the augmentation ratio for the cell. Again, this cannot be freely chosen but is fixed by choice of exhaust treatment system since the various types have widely different requirements for excess air. Since a continuing trend toward higher exhaust temperature is evident, excess air to cool this exhaust will go the same way. Since this capacity may limit the facility growth potential and excess capacity is low in maintenance cost, it should be maximized consistent with construction costs. References 12, 28, 32, 37, and 40 illustrate typical current and anticipated augmentation requirements. From these a total airflow capacity three times the maximum engine requirement can be justified.

Since test cell operation ideally simulates free atmosphere engine performance, the approach velocity is limited in modern facilities to a maximum of 50 feet per second.^{28,37} This is an arbitrary limit but is reasonable since increasing velocity above this point rapidly increases the cost of distortion control, increases cell depression, and decreases the accuracy of thrust measurement. Accepting this limit, cross-sectional area required is calculated easily, and depression per foot of flow length may be accurately estimated using the standard duct flow loss techniques of Refs. 41, 42, and 43. Various depression limits have been used in the design of current facilities, but general agreement is found in considering the depression to be a free variable and altering the design to change it only in the most extreme cases, i.e., those in which pressure loads approach the structural load limit.^{37,40} The effect of greatly increased mass flows on depression and required cross-sectional areas is demonstrated in Fig. 6.

In the past, with these estimates, the designer could produce construction blueprints for the inlet. Prior to the introduction of the turbofan engine, the production test cell was required to produce a specified quantity of air at a reasonable velocity at the engine inlet. Only the grossest mismatch of engine, cell sizes or the ingestion of objects other than air molecules could produce compressor stall, flow reversal, overtemperature, or unstable engine oscillation. Today, test cells can be and are built which have more than sufficient inlet flow capacity but which cannot be used to test the engines for which they were designed.^{10,37} The condition responsible is nonuniformity of pressure or velocity distribution at the engine inlet. Turbofan engines, both high and low bypass, and special-use, lift type engines are the most sensitive to this distortion,⁴⁴ but when it exists, it affects every engine tested to an unpredictable extent. Its sources are numerous and effectively include everything in the cell between the open atmosphere and the engine face which is in other than a straight smooth-walled duct.^{37,45-46}

The design of distortion free inlets is an empirical matter with even the most experienced contractors in the field.³⁴ Until

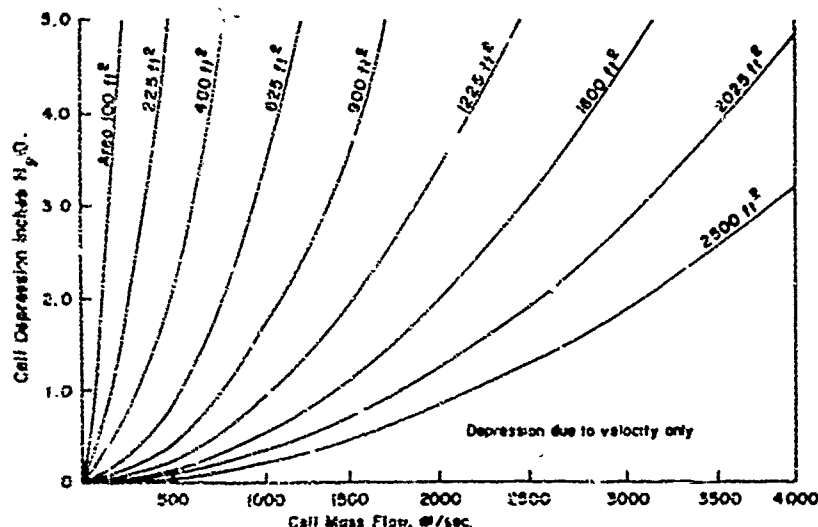


Figure 6 Effect of Increased Mass Flow on Cell Depression and Required Area.

this requirement lightly. The designer has available the choice of: a.) inlet shape: horizontal, vertical, inclined, open ended or capped; b.) number of turns, radii, and flow lengths; c.) shape of the flow dividers used in acoustic control; d.) duct shape: expanding, contracting, constant area; open or vane guided turns; and e.) duct wall finish: protrusion streamlining, the shrouding of fittings, and the installation of boundary layer trips or vortex generators.³⁶ The following diverse factors must be considered in selecting from these options: a.) Cost and availability of real estate at the proposed site; b.) effect of inlet stack height and position on the reingestion of exhaust gas; c.) required cell air flow capacity; d.) allowable pressure and velocity distortion of the flow at the engine inlet;³⁷ e.) allowable cell depression; f.) requirements for emergency air flow shut off to permit CO_2 flooding; g.) local weather conditions, especially winds and wind profiles; and h.) construction cost per square foot of cross sectional area and foot of length. Of these factors, a, g, and h may be accurately determined following the selection of the construction site.

Analysis of the effect of stack height and position

a method becomes available to predict the flow distortion for a projected engine in a proposed cell with variable augmentation ratio, the designer must accept the necessity of the following restrictions: a.) Minimize the number of turns in the inlet; b.) place no flow dividing surfaces in the inlet which are not absolutely necessary; c.) streamline all surfaces confining the flow or immersed in it; d.) provide flow length forward of the engine for vortex and wake damping;³⁸ e.) construct and test models of proposed designs;⁴⁹ f.) provide turning vanes⁴⁴ and flow straighteners for cell operations near design flow capacity; g.) test the finished cell with reasonable completeness at all flow levels and augmentation ratios, and h.) employ aerodynamic analysis methods in the design of duct curves.^{50,51} Reference 33 indicates an empirically determined pressure distortion maximum of ± 0.25 in H_2O . The persistence of wakes generated by flow obstructions may be estimated with the methods of Refs. 52,

1.2, and 54. However, total distortion cannot be predicted accurately, and no fixed limits have been established yet by test cell operators or designers. Distortion indices have been published by many manufacturers for production engines. Definitions vary, but each index may be measured by pressure survey rakes located forward of the compressor face. The variation with engine speed of this index may be measured for a given engine type in a particular cell, and the limit which will cause engine surge or stall is then available. Unfortunately, there is no method for predicting the value of the distortion index for a proposed cell design or a given engine. Extensive investigation also has failed to establish useful correlations between test cell stall margin and that of the same engine installed in an aircraft.⁵⁵ Therefore the best the designer can do now is to conform to the above guidelines and include provisions for repeated aerodynamic monitoring of cell performance throughout the service life of the facility. Current research may simplify vastly this aspect of design and increase confidence in the final performance of future high capacity cells.⁵⁶ For current installations, distortions caused by inlet vortices may be reduced by the employment of wall or deck fences or aspirated plates; this recent discovery is discussed in Ref. 3b.

Maintenance and Safety. Aside from basic structural integrity of all components, the contribution of inlet design to safe cell operation has been in the provision for airflow shut off and filtering for fire fighting and protection of the engine from foreign object damage. This latter requirement is accepted universally and is met by various combinations of wire mesh duct screens and bellmouth covers. The designer may locate these screens as convenient, but placement aft of distortion-producing acoustic treatment will provide a bonus of a reduced requirement for flow mixing length. References 42 and 50 may be used to calculate pressure loss due to screening.

Although CO₂ flooding systems are available in many present test cells, there is less than complete agreement about the necessity of their incorporation in future facilities. Increased size and the greater CO₂ capacity required to effectively flood large cells have escalated the associated installation costs. Larger cross sections also imply longer operating times for hatch shut-offs and further reduce system effectiveness. Operator experience indicates that the Cardox flood system may itself be more of a hazard than the fires it is intended to prevent due to casualties possible in an accidental actuation. Many aircraft powered by turbojet engines now incorporate quick shutdown systems and local application of extinguishing agents. Similar provisions in test facilities may eliminate the requirement for a quick-acting inlet shutoff. This is worth detailed investigation since it would remove the only inlet component requiring regular maintenance and would represent a considerable savings in construction cost.^{16,34}

The cell access doors and their actuation systems are the other inlet components with maintenance requirements in a side loaded configuration. If the front loaded layout is selected, it may be necessary to include articulated acoustic treatment and flow straighteners which will increase loading time somewhat and be sources of additional maintenance requirements. In either case, sliding or outward opening doors provide designed-in safety. Any door should be designed so that the forces from cell depression act so as to close the door, not open it.

Inlet design can make a substantial contribution to overall cell performance and to reduction of operating costs by the inclusion of a mounting frame for air filtration panels. Passing the flow through a ten micron filter will increase the life of all cell components from acoustic sheet metal to temperature probes.¹⁶ These panels are low in cost and are reusable; the increase in cell depression is minimal. The air quality at nearly all facility sites is now poor enough to make this a profitable addition to new designs; this quality is not likely to improve much in the future.

B. Test Sections³⁴⁻⁵⁴

Engine Handling and Access. Efficient operation of production type test cells requires that the non-running time of the engine in the cell be minimized. The engine-test bed adapter system is the best means of reducing this time and has demonstrated satisfactory performance at many modern facilities. Since the adapter is attached to the engine in the preparation area, the handling system must transport the completed unit. Selection of the optimum handling method requires consideration of the following factors:

- Tracked dollies prevent damage to concrete decking and eliminate traffic accidents that can occur with free dollies, but they are relatively inflexible in accepting widely varying engine sizes. They are also reasonably complex when used with engine-cell adapters and may require more maintenance than overhead handling systems of equal capacity.
- Free dollies may require special high cost decking for use with large, heavy engines; and when designed to handle the engine/adapter combination, they may not be suitable for general use elsewhere in the repair facility.
- Bridge cranes lack the ability to serve both the test cell and a large preparation area. They also require larger and more expensive cell access doors.
- The overhead monorail, either powered or free, minimizes access door size, can be tracked to multiple prep area stations, is suitable for the engine/adapter combination, can incorporate the hoisting unit required for cell loading, is flexible in size and shape capacity, and allows required maintenance to be performed outside the cell. This system is in operation¹¹ in present facilities; the only difficulty has been the effect of the rail on inlet aerodynamics. A streamlined track shroud or submergence in the overhead surface may reasonably be expected to eliminate unacceptable flow distortion.

Access to the installed engine must be convenient and safe. The access structure must not produce flow distortion or recirculation during test operation and must be adjustable in height and lateral position. Current systems utilize access structures which retract into the interior cell surfaces.^{16,35} Deck mounted service stands will be subject continually to corrosion damage from spilled engine fluids and cleaning solvents, and they must support transport dollies if an overhead system is not employed. A valuable addition to operational efficiency can be made by the designed inclusion of storage space for servicing and troubleshooting equipment which is convenient to the work area. Adequate lighting of the side and bottom engine surfaces is essential, and at some sites the installation of radiant heating units can greatly increase efficiency and safety.

Acoustic. In current test cells it is the acoustic portion of the engine environment which is least similar to that of the aircraft-installed engine. Reflection from the smooth concrete surfaces surrounding the engine subjects the engine casing and external accessories to acoustic power levels several times those present in an aircraft. No reliable data on damage caused by this are available, but it is certain that it is not beneficial. Some operators subjectively estimate that a 10-15% reduction in component life is attributable to this source. New cells should be designed to minimize the acoustic energy reflected onto the test engine either by absorbing it at the wall surface or directing it away from the test section. Reference 57 illustrates the substantial reduction possible with commercial absorbent materials. The effectiveness of directionally reflective surfaces is illustrated in Ref. 39; this option has the advantage of nominal cost in new construction.

Aerodynamics. The primary requirement for the test section is that the flow remain unidirectional and without recirculation of engine exhaust. Aft of the engine bellmouth there is no further necessity for streamlining or shrouding equipment except that even small variations of pressure along the engine casing may produce variation in the measured thrust. This will be minimized by keeping the exposed surface area between the engine and the thrust bed to a minimum, and, if constant, it can be included in cell correlation factors.^{16,37}

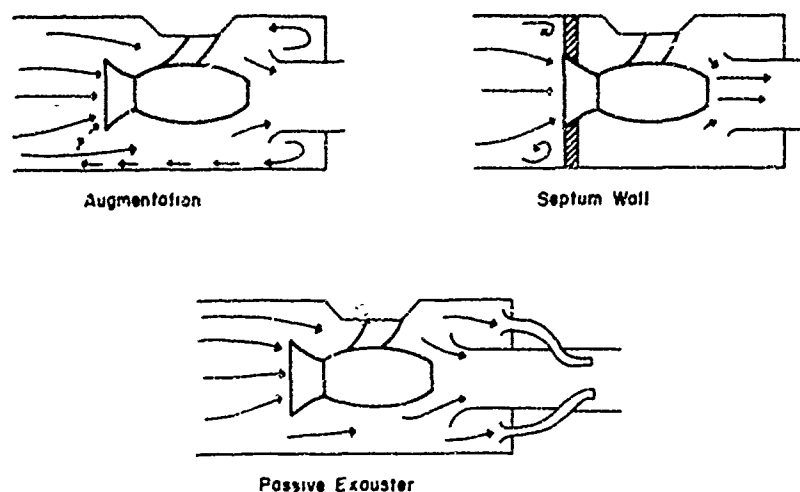


Figure 7 Recirculation Control Options.

separate electric motor is possible, but the flow capacity required and the additional cost and maintenance make it less than attractive. The drawback to inclusion of the passive venturi powered system is that the initial motivation for operation with a low augmentation ratio may be reduction of the flow volume to be handled by a pollution control system. If the afterburner method of pollution control⁶² is to be used, the exhaust air could be added to the exhaust aft of the secondary combustion zone. In any system, if the volume flow required for control of recirculation is low enough, inclusion of the passive exhauster must be considered since it has the advantages of low initial cost and minimum maintenance requirements.³³

Installation of cell instrumentation with the capacity to detect recirculation is a design feature which will return an enhanced profit on small initial investment by ensuring test reliability and preventing the accumulation of explosive mixtures when future engine augmentor positions are varied. It should be emphasized that explosions are a very real possibility, and care must be taken in design to avoid cavities where fuel-air mixtures can accumulate.

Instrumentation and Mounting. A key feature of the instrumentation design is flexibility. Effective use of the engine adapter system requires that the permanent test cell portion of the equipment require little or no modification when new engines are introduced. Each adapter will be customized to a particular engine, but all must appear identical to the test bed. This demands that the original design have sufficient capacity to accept the number and type of data transmission channels required by future engines and refined test techniques. References 12, 16, and 28 illustrate current estimates of this requirement, recent experience indicates that the savings possible by limiting this capacity almost certainly will be temporary ones since excess capacity is free of maintenance cost and can, in fact, greatly reduce cell down-time by permitting rapid shift to alternate channels when malfunctions occur. Maintenance can then be performed at scheduled times. The importance of this capability cannot be overemphasized since most operators report that the majority of cell down-time results from instrumentation malfunctions.

Instrumentation undoubtedly will be required for monitoring test facility performance relative to pollution. Many different instruments may be required,⁶⁶ although the production test facility requires less extensive instrumentation than a research test facility. Some of the instrumentation that may be needed includes infrared and ultraviolet spectrometers, gas chromatographs, smoke meters, acoustic measuring systems, and Raman spectrographs.

Knowledge of test facility pollutant emission is the essential first step to pollution control. Furthermore, community complaints, inadvertent shutdown ordered by control agencies, and possible fines are avoided by constant monitoring of pollution levels.

Although cell accessibility may be complicated by the use of the overhead thrust bed, its advantages more than compensate for this; and it is now recognized as the best design for future test cells. Among these advantages are: natural similarity to aircraft engine mounting methods, ready compatibility with monorail handling, freedom from corrosion by collected fluids, flexibility in engine positioning, and the availability of advanced design experience. It is possible to utilize a single step plug-in of the adapter to the test bed, but experience indicates that separating the connection of the physical support from the plug-in of the instrumentation leads enhances system reliability.¹⁶

For facilities required to anticipate a wide spectrum of thrust levels, it is possible to improve thrust measurement accuracy by using a three component system: test frame, thrust bed, and engine adaptor. With this arrangement the thrust bed may be changed to one having flexures with maximum sensitivity in the desired range.¹⁶ Investigation of the possibility of eliminating the direct thrust measurement system has shown that while it is technically feasible, the savings in engineering complexity are small and are offset by increased requirements for other types of instrumentation. In the view of most users, deletion of the direct thrust measurement system is not justified.^{12,16,39}

Auxiliary Subsystems. One of the most persistent failures in test cell design has been lack of subsystem growth potential. Rapidly increasing fuel consumption rates have made extensive rework of some facilities necessary and restricted the operation of others.^{12,16} At several installations the supply of starting air has proven inadequate almost before the cell was placed in operation.¹² For facilities requiring water for exhaust gas cooling or scrubbing, it is imperative that future capacities be determined since they may well be double or triple those required to test current engines. In all these subsystems, doubling the design capacity increases initial cost only about 20% while a similar change in an existing system may easily double the original cost and require extended facility closures.

In addition to sufficient capacity, the fuel system should be designed to permit future expansion to at least a two fuel operation.^{2,58} Again, providing this flexibility during design will cost far less than adding it later. Design of all subsystem controls should include maximum utilization of advanced control and monitor technology. The number and criticality of the subsystems which must be included in a turbojet test cell demand that careful attention be given to design of interlock controls providing fail-safe operation. There is no reason for operator error or an undetected malfunction to cause major damage to the engine or test facility. The electrical power dissipation, dynamometer, and fire extinguishing systems should also be routed through a master interlock control.

When the augmentation ratio is high, there is little likelihood of recirculation. When little or no augmentation air is used, the control of recirculation is more difficult; and, to be flexible, new facilities must be designed for possible operation in the zero augmentation mode.⁶⁷ Figure 7 illustrates the primary alternatives for recirculation control. The septum wall provides positive control but must be considered as a last resort due to the mechanical complexity involved in making it removable, useable with different engine inlets, and strong enough to resist the considerable pressure loading which is possible. The second alternative requires that excess air be drawn past the engine even when it is not required for exhaust cooling or mixing. Since this is needed only while the engine is in operation, it is logical to make the engine exhaust the power source and design the system to be entirely passive. An active exhauster powered by a

C. Control Center

The choice of data acquisition method will establish the requirements for the design of this area. In a facility requiring manual data recording, 25-30% of the total engine running time is occupied solely by data acquisition. Additionally, two to three minutes may elapse between the first and last data reading at each operating condition. Thus the justification for the higher cost of automatic data acquisition systems includes reduced cell time per engine (with accompanying reduction for fuel, utility, and pollution abatement loads) and increased test credibility due to the simultaneity and accuracy of data.

Sufficient incentive exists for the inclusion of automatic data scanning equipment in all future production test cells. It is possible to automatically acquire data and simply supply it as a printed record. But the nature of the data processing normally required is such that its inclusion within the automatic equipment in simple and effective. It can then be presented in a written format acceptable to the user as shown in Fig. 8 or as real-time operator assistance. Further extension of data system sophistication is possible and may be justified in the following areas: a.) Individual engine history records containing either rework/repair testing results or expanded to include in-service information;⁵⁸ b.) safety monitoring capability to provide warning of impending failure or to initiate shutdown or other corrective action; and c.) operator assistance in the form of step-by-step procedural instructions and malfunction analysis. The computer centered data system also can be operated in a closed loop mode with engines tested under fully automatic control.^{16,58} It is unlikely that this could be economically justified in future production type facilities since manpower savings would be small (installation and repair still required) and the cost of a reliable system high.

Long range economy is best served by including in the initial system design excess capacity to permit processing of additional data without major remodeling. Removable flooring in the control area is an excellent means of providing both maintenance access and ease of modification. Electronic data systems are more sensitive to interference and damage from acoustic, vibrational, and electromagnetic energy than the human operators, a fact which reinforces the necessity for the inclusion of appropriate types of shielding in the control area.^{12,14,28}

Replacement of the viewing window by a closed circuit TV monitor simplifies the insulation problem and increases safety. To justify its cost, the video monitoring system must be capable of providing resolution and discrimination comparable to that of an operator present in the cell. With carefully considered lighting and placement, accurate color reproduction, magnification to a one-foot focal distance, and full articulation, it will be possible to eliminate the necessity for in-cell operator inspection. This could reduce run times and allow leakage checks at other than idle power settings. For some facilities the addition of a video recording capability to the monitor system may be advisable. Having low initial cost, adaptable to fully automatic control, and requiring little maintenance, a video tape recorder could provide accurate records of malfunctions and permit continuing studies of cell efficiency. A recorder could also supply effective training material for operators when new engine models are introduced or new test procedures are initiated.

Modular design of the control station and provision of ready access to the installed equipment should be of prime concern to the designer.^{16,28} Some operators presently feel that audio monitor capability should be provided, and an earpiece adaptation of the required intercom system could be employed for this purpose.

D. Augmenter and Exhaust Treatment

General. An efficient, flexible, and reliable exhaust system is perhaps the most critical segment in test cell design, yet the present level of engineering sophistication in this area is still elementary. Justification for the above statement is recent changes in the design criteria for exhaust treatments. Early designs were built primarily to lower exhaust temperatures to levels that would not unacceptably shorten the life of installed noise abatement systems. This was accomplished by mixing the jet exhaust with secondary air. Past acoustic practices have been re-examined,^{60,61} and in many cases stricter requirements have been formulated.^{12,15,25,53}

Additionally, attention is now being focused on reducing the air pollution levels of jet engine test cells. Generally, test cells

are placed in a different regulatory category than are jet aircraft themselves. They are classed with other stationary sources.^{52,63}

Aerodynamics and Thermodynamics of Exhausts. A poorly designed augmenter system may be one that acts as an unnecessarily powerful jet pump. In this situation too much secondary or cooling air is entrained with the engine exhaust causing higher than designed cell airflows and cell depressions. Also, larger than design airflows will increase distortion levels and possibly disrupt smooth engine operation.^{6,15,37} Large air flow also can cause errors in thrust measurement. From the pollution point of view, excess exhaust mass flow rates increase abatement costs.

At the other end of the design spectrum is the system that fails to induce enough secondary airflow and thereby fails to prevent the problem of recirculation of exhaust gases. Excessive exhaust temperature may also result.

The problem of excess secondary airflow has been encountered at several facilities. At North Island a flange has been added to

***** ICE - 731 ENGINE *****			
GUARD SYSTEM DATA	SERIAL NO. 7307	DATE 27 7/72	
		TIME 39-22	
		DATA 14.76	
CYCLE 1			
TOLE FOR 1 MIN			
** CALCULATIONS **			
MIC2	5790.0	WT	14.76
MPC2	16233.5	TT	140.4
M2/M1	2.804	ENG	702.17
G-M POWER	0.400	HYD PUMP NO.1 PH	347.32W
TOTAL EXH POWER	513.647	HYD PUMP NO.2 PH	116.31W
** MEASURED DATA **			
SPR-DS-		THRUST (LBS)	203.05
N1 (RPM)	5790.0	POWER ANGLE	34.80
N2 (RPM)	16233.5	FUEL FLOW MAIN	198.00
		FUEL FLOW VERIF	199.13
PRESSURES - (PSI)			
COMP DISCH	27.74	OIL TANK VENT	0.00
FUEL PUMP INLET	47.51	NO.4 RRG SCV	0.00
F/O (OIL IN)	0.00	TOT ENG SCV	0.00
FAN G/A (OIL IN)	47.07	OIL PUMP DISCH	0.00
TEMPERATURES - (DEG F)			
FUEL	55.2	T17 LPT DISCH 180	0.0
F/O (OIL IN)	0.0	T17 LPT DISCH 181	0.0
FAN G/A (OIL IN)	134.4	T17 LPT DISCH 184	0.0
HYD PUMP IN	130.4	T17 LPT DISCH 185	0.0
FAN G/A SCV	124.1	NO.4 HEARING	0.0
NO.4-5 RRG SCV	151.0	NO.5 HEARING	168.7
VIBRATION - (MILS)			
THRU VERT	0.440	CORR VERT	0.590
THRU HORIZ	0.072	CORR HORIZ	0.770
		R-FAN OPA VERT	0.000
		A-FAN OPA VERT	0.000

Figure 8 Typical Data System Output.

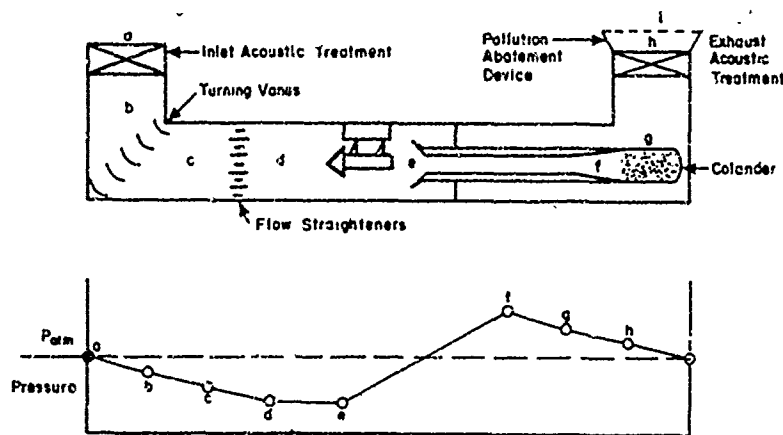


Figure 9 Test Cell Pressure Profile.

but the cell performance with advanced technology engines, which may reach the 100,000 pound thrust category, may require modifications. This not uncommon situation indicates the need for close attention to augmenter design and more thorough analysis of the ejector process.

Secondary air provides the necessary cooling of the engine exhaust and prevents recirculation. For a turbojet engine operating out of afterburner mode, an augmentation ratio of 2:1 has been set as a reasonable design goal.^{12,15} Augmenter performance is a function of the area ratio of the augmenter and exhaust nozzle, the length of the augmenter, the position of the exhaust nozzle relative to the entrance of the ejector tube, velocity ratio, and other variables. Most recommended test cell augmentation ratios for fan engines vary from 0.25:1 to 0.5:1 for high bypass engines and up to 1:1 for low bypass types.^{5,12,15,64} Appendix A contains the standard definitions of augmentation ratio for turbojets and turbopropeller jets.

Besides its function of providing the means of mixing and cooling the engine exhaust, the ejector system must overcome the various pressure drops in the inlet and the exhaust systems. Figure 9 shows the general pressure pattern within the test cell. Basically, momentum is transferred to the secondary air, thereby increasing its pressure.

Studies have been made to determine the mixing characteristics of jet pumps.⁶⁷⁻⁷⁶ These indicate that for each characteristic exhaust and secondary airflow combination there is an optimum length and diameter mixing tube. However, because of the cost of construction of the exhaust facilities many trade-offs must be made, and a flexible design must be selected that will work reasonably well over the range of engines to be tested.

A second method of cooling the exhaust is to use water spray cooling. This method is mandatory for engines operating in the afterburner mode but may be used in other modes as well. Studies have been carried out^{15,27} which indicate the amounts of air, water, or both which are required to cool exhaust gas temperatures to acceptable levels. When suitable amounts of water cooling are used, secondary airflow can become negligible. However, compromises must be made to determine the amount of water used. At the present time, most of the water used in spray cooling is lost through the stack. At several locations, including NAF North Island, fresh water supplies are at a premium; availability may dictate the design option chosen.

Water cooling has an impact on pollution control and may in itself be a source of pollution. Sulfur dioxide can be absorbed by the water. Droplets of water falling or condensing on surfaces, e.g. an automobile, can cause discoloration. Smoke particles can be entrained in the water. Humidity of exhaust stream can influence pollution abatement devices, e.g. electrostatic precipitators.

Where water cooling is necessary and available, difficulties remain in devising means whereby the high temperature jet core may be thoroughly penetrated by water streams. It is known¹⁸ that even high pressure water jets have little success penetrating into the core of a high speed flow. Various designs have been developed, including concentric rings, water spargers, and bounce sprays.^{19,20,77} These designs, however, have not been optimized for facilities required to test widely varying engine types.

Matching augmenter characteristics to individual engines will be difficult, particularly where low augmentation ratios are desired. Variable area nozzles are common for afterburning engines. The exhaust from the fans of high bypass engines is at a relatively low energy level; and since it contains no products of combustion, separate ducting may be desirable. The Pegasus engine used in the Harrier aircraft requires complex ducting during test cell operation.⁵

Prevention of thermal damage to the augmenter must be considered. In the entrainment zone, the walls are subject to radiant heating, while in the fully developed mixing zone they are heated by convection. Water jackets may be necessary during testing of afterburning or high turbine inlet temperature engines, particularly if the selected exhaust treatment system requires a low augmentation ratio.

Acoustic Treatment. Noise sources that must be treated by exhaust systems are: turbomachinery generated noise, combustion noise, turbulent noise generated by the interaction of the jet exhaust and the secondary air, and the turbulence in the exhaust itself.⁷⁸⁻⁸³ In the entrainment zone the shear stresses are high and the turbulence level is relatively low, creating most of the high frequency noise emanating from the jet.⁸⁴ Most of the low frequency sounds, those which contribute strongly to the overall sound level, come from the portion of the exhaust beyond the potential core; the peak of this sound is at a wavelength about three times the diameter of the jet.⁸⁴ It is this low frequency sound that is most difficult to attenuate. The higher frequency noise of machinery is easily abated with standard techniques which include baffles of all types, lined passages and bends, and tubular exhaust passages.^{15,33,37}

The properly designed augmenter can contribute to the overall reduction of noise; experimental results⁸⁵ have shown that jet noise can be reduced by a factor of 5 (7db) in an ejector noise suppressor. It was also shown that the initial mixing conditions and the length of the injector are more important factors in obtaining this attenuation than the area ratio of the tube and jet or the position of the primary jet relative to the ejector inlet.

Methods of breaking up the continuity of the jet and increasing the frequency of the exhaust noise were discussed previously. The utilization of a colander in the form of a cone or a cylinder is presently preferred over other options in modern cell designs. It has

the augmenter bellmouth restricting the flow of secondary air. This is not a smooth design aerodynamically, and the capability of this facility to handle large bypass fan engines or other high flow rate engine types is severely limited with the present flow restriction. A second solution is to install orifice plates within the augmenter itself to reduce the available flow area.²⁰ This type addition is slightly more flexible than the former since various size plates may be installed depending on the flow characteristics of the particular engine under test.

At the United Air Lines facility in San Francisco, secondary airflow in their new large jet engine test facility has been estimated as being almost twice as high as was originally anticipated.¹⁴ This condition has not exceeded cell structural limits with the present engines being tested (JT9D, CF6),

been found by experience that a hole size 1-1/4 in. in diameter is the smallest practical size.¹⁶ Holes smaller than this tend to be blocked easily due to impurities in cooling water as well as particulate matter present in the engine exhaust. Standard practice has been to space the holes uniformly over the surface of the colander, with total hole area 40 to 60% in excess of the cross-sectional area of the augmentor tube itself.^{16,21}

An exception to this practice has been introduced in some smaller Navy "C" cells.²¹ In these cells, holes were placed only in the lower half of the colander. This design has exhibited a serious shortcoming in that flow through the exhaust stack is very non-uniform; in fact, some points in the stack exhibit zero velocity. This causes portions of the acoustic treatment to be exposed to higher than design flow rates, thereby shortening useful life and decreasing overall performance.

Analysis must be done during design to ensure adequate flow conditioning over the operational range of the proposed test cell. The designer must ensure that enough pressure rise will be obtained to overcome any flow blockage that may be present under all operating conditions. See pressure from e to i in Fig. 9.

Unwanted acoustic energy may be generated by obstructions present in the ejector assembly. These include spray rings or nozzles, diffuser rings, and any other hardware installations. These obstructions increase the turbulence level of the flow, thereby increasing the noise sources within the flow. The merits of each proposed installation must be weighed according to the use intended for the individual test cell. Care must be taken that natural frequencies of installed components are not activated by the driving frequencies of the flow.

Possible exhaust stack treatments are as varied as those intended for use in the inlet. Options include lined bends and passages, tubular mufflers, sinuous passages, or straight passages.^{15,28,29} Steel Helmholtz resonators have been investigated by General Electric¹⁵ and have been found to be unsatisfactory for their own use; however, this approach has been successfully taken by Aero Systems Engineering.³⁹ Differences are in the cell utilization of the two operators and in the acoustic characteristics of the engines tested.

A primary concern is to develop a system which will withstand a moderate range of temperatures and wide range of velocities. Most installations¹⁵ have been designed to withstand exhaust stack temperatures in the 450-550°F range, with a maximum of 600°. At one time NARF North Island attempted to maintain temperatures below 200° in the non-afterburning mode by water cooling; however, it was impossible, with the existing water spray design, to operate the afterburner and maintain stack temperatures below 450°. The installed acoustic treatments were subjected to such severe thermal shock that their useful life was drastically shortened. Within practical limits a constant stack temperature should be maintained in all test modes.

Because of the varied sizes and characteristics of engines that will be tested in new construction test cells, consideration should be given to the possibility of providing variable area exhaust stacks. Methods of accomplishing this vary from simply blanking unnecessary portions of the stack with pre-fitted metal shutters according to the flow requirements of the engine under test to a movable cover over the stack opening which is programmed to provide optimum flow area (and available acoustic treatment) for a given engine power level. By designing the basic exhaust system to handle the largest forecast airflow with the additional capability of efficiently handling much lower flows, the problem of test cell obsolescence caused by advances in engine technology can be avoided.

Emission Control Devices. In the future, major design effort must be devoted to pollution abatement systems. It has been established by Executive Order that Federal installations comply with local environmental protection requirements. At the present time most emission requirements which are applicable to test facilities deal with the particulate emissions which cause visible pollution. Future legislation will limit emission levels of invisible noxious gases, unburned or cracked hydrocarbons, carbon monoxide, oxides of nitrogen, and sulfur dioxide. Studies have been conducted to determine exhaust emissions of gas turbine engines,^{43,46-51} and although the exact emission levels are not agreed upon, most figures mutually agree on an order of magnitude basis.

The abatement system chosen for test cell operation must first remove visible particulate emissions. California legislation limits the deviation from a maximum of 20% obscuration (Number 1 on the Ringleman scale) to three minutes out of every hour.

Except at idle, gas turbine engines emit very low levels of unburned hydrocarbons and CO, so that attempts to reduce these should concentrate on low flow rate conditions.⁸⁶

By 1975 Los Angeles County will limit emission of oxides of nitrogen to 225 ppm.⁶² New developments in engine technology resulting in high pressure ratios and high combustion temperatures have raised the levels of these oxides in engine exhausts.⁸⁶ The choice of abatement system must at the very least not add to these levels and ideally should reduce them.

The installed system must be able to remove unburned fuel from the exhaust flow. Estimates are that in the afterburner mode turbojets exhaust a few per cent unburned fuel; the combustion efficiency decreases with increasing altitude. Also, the ability must be retained to purge unwanted fuel from the exhaust drainage system. Prior to light-off it is Navy practice to "dry run" the engine; that is, the engine is windmilled, and the throttle fully opened to check for leaks. This results in relatively large amounts of fuel being dumped directly into the exhaust system.

Emissions of sulfur dioxide will not be a problem as long as the current restrictions on sulfur content of fuel are maintained.⁶⁵ Present restrictions limit the sulfur content to 0.3%, and most fuels contain even less. The economics of sulfur content in fuel is discussed briefly in Ref. 65.

Although advances have been made in combustor technology, completely clean jet engines are not yet a reality. NARF Alameda was recently cited in violation of local standards while testing a high time engine configured with "clean" combustor cans. One source⁶³ theorizes that reactions within the cell exhaust system change the character of particulate emissions, either in size or number, so that visibility obscuration is greater at the test cell exhaust stack than at the engine tailpipe.

Interim solutions for reducing smoke involve the use of fuel additives. United Air Lines in San Francisco utilizes CI-2 in their testing. Additives coat engine hot section parts, and the effect of adding heavy metallic vapors to the exhaust is under continuing investigation by the EPA.

Early studies of pollution abatement systems have resulted in the selection and development of a nucleation scrubber.⁷⁷ Other devices analyzed include filtering devices, venturi scrubbers, and electrostatic precipitators. These have been evaluated as unsatisfactory from considerations of safety, flexibility and economy in Ref. 77.

Filtering devices alone present problems because of their tendency to become clogged by particles entrained in the exhaust. Additionally, they require extremely low flow velocities and are not effective in removing noxious gases.

The primary drawback to the venturi system is its inability to operate efficiently over greater than a 10% interval away from its design point, which is an unacceptable restriction in light of the fact that air flows vary as much as 60 to 70% from idle to full power setting. A possible solution to this would be the installation of a bank of venturis, entailing high initial costs and complicated flow controls.

The present shortcoming of electrostatic precipitators is the inability to completely prevent fuel buildup on and around the electrodes; this condition creates the danger of an explosive discharge. Also, these systems cannot remove noxious gases or oxides of nitrogen. Afterburning engines require water cooling which is detrimental to electrostatic precipitators.

Nucleation scrubbers work by process of creating large particles by condensation of vapor from a saturated vapor. The nucleates are the particulate matter already present in the exhaust. The enlarged particles are then removed by impaction in the scrubbing system. A prototype scrubber system developed by Dr. A. Teller (Pat. #3,324,630) has been installed by the Navy at NARF Jacksonville. This particular scrubber has the capacity to handle large changes in flow volume, can reduce noxious gases and unburned fuel, and with modification can remove much of the oxides of nitrogen and sulfur if such action is required. Installation of this scrubber is also anticipated at NARF Norfolk. The primary drawback at present with the scrubber system is its high initial costs. At its present level of development, this system is not considered the ideal solution, and investigation is being carried out in other areas as well.

The nucleation scrubber as well as the other alternatives discussed are all similar in that they function by physically removing particulates and unwanted gases; a second class of installations acts by converting unwanted pollutants to harmless chemical species. These include afterburners and catalytic converters.

Northern Research and Engineering Corporation⁶² has proposed a thermal converter installation for test cells. This reference is a comprehensive discussion of the feasibility of such an installation and the justification for Navy procurement in light of future requirements for pollution control. At the present time much work remains to be done in conducting recommended studies and testing. The installation of a converter system will require close matching of the test section, engine, and exhaust itself since the proposed system requires a low augmentation ratio.

The final selection of an abatement system will be based on its flexibility and economy. It must be able to operate over a wide range of exhaust velocities and temperatures. The initial cost of procurement and installation must be low, as must be the cost of operation and upkeep. The system must be reliable enough to allow firm scheduling of cell down time with the minimum amount of unscheduled maintenance. An additional factor will be the ease with which the abatement system may be retrofitted to existing test cell structures.

The creation of secondary pollution must be avoided. Thermal pollution of natural water supplies is a real possibility in systems requiring heavy cooling. Also to be avoided is the creation of additional, unwanted noxious gases or other undesirable products of combustion if an additional combustion process is used.

Maximum allowable temperatures, pressures, and velocities will dictate the level of required protection of hardware exposed to the jet exhaust. Because of the temperatures encountered during afterburner runs, it may become necessary to water cool certain exposed parts. Refractory linings have been considered but were rejected for economic reasons.⁶²

Complete acoustic analysis must be completed to ensure that the natural frequencies of equipment exposed to the flow not be excited by the frequencies of turbulence generated noise.

Finally, the design of adjustable components should be kept as simple as possible. Operators are wary of too much gadgetry in test cell design,^{17,20} and cell down time increases with the addition of mechanical sophistication. All facilities must be designed to operate with the minimum amount of required upkeep.

V. DEPENDENCE OF COMPRESSOR FACE DISTORTION ON TEST CELL INLET CONFIGURATION⁵⁶

A. Model of Test Facility

Based on the background study discussed in the previous sections, an in-depth, parametric, experimental investigation was conducted. It was apparent that little information was available on the distortion level at the engine in a test facility as a function of inlet design parameters. The aim of the experiments was to identify the inlet designs giving the least distortion.

As shown in Fig. 5, various acoustic baffles may be placed in the inlet flow. To what degree do these disrupt the flow causing distortion? This is a typical question answered by the experiments.

Figure 10 shows the method of simulating an engine in a test facility. The flow in the bellmouth, which was pumped by the engine exhaust, was adjusted to be equal to the flow from the engine nozzle, which is labeled "metered compressed air supply" in

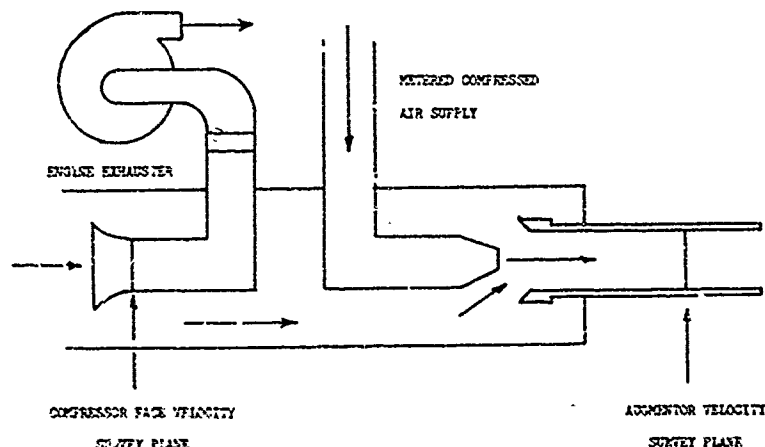


Figure 10 Augmented Flow Power System Layout.

Fig. 10. Section VI will discuss the augmentor investigation. In addition to the usual measurements of air temperatures, pressures, mass flow rates, etc., the primary data were compressor face velocity surveys and augmentor velocity surveys. The compressor face data were converted to distortion indices.

Table I provides the inlet configuration identification code. There were 5 different inlet arrangements, i.e. vertical, horizontal, etc. There were 5 different inlet covers, i.e. none faired, etc. From the various model components several thousand different test facilities could be assembled. More than a hundred configurations were tested.

The model components were constructed of plexiglass for reasons discussed by Tower.⁶³ Figures 11, 12, 13, and 14 show the vertical inlet stack, convertible duct bend,

flow straightener component, and triple turn inlet box component. Using the triple turn inlet box component, one can configure the A=5 inlet. The vertical inlet box component is used for the A=1 inlet.

Table 1. Inlet Configuration Identification Code

Configuration Number: ABCD.EFGHIJ

A. INLET	B. INLET COVER	C. ACOUSTICS	D. ACOUSTIC POSIT.	E. TURNING VANE
1 vertical	1 none	1 none	1 before turn and	1 none
2 horizontal	2 faired	2 flat baffle	transverse	2 one (#3)
3 none	3 bi-directional	3 staggered baffle	2 after turn, vert.	3 four
4 vert. w/o stack	4 flat plate	4 tubular	3 none	4 seven
5 S-turn	5 bi-dir, sideways	5 stag. baffle, crossways	4 before turn, and axial	5 one (#5)
			5 at inlet entrance	6 one (#1)
				7 one (#3) in turn 2
F. FLOW STRAIGHTENER	G. ENGINE BELL-MOUTH	H. AUGMENTATION	I. POWER MODE	J. ENGINE POWER LEVEL
1 none	1 neither	1 none	1 t/s-blower	1 maximum
2 rect. Xsection	2 engine w/o bell	2 zero	2 eng-blower	2 medium
3 screen before ac.	3 engine + bell	3 low	3 end+aug-blower	3 lowest
4 screen after ac.		4 medium	4 dual inode	
5 both screens		5 high		
6 distort screen				
7 honeycomb				

Figures 15, 16, and 17 show the bi-directional inlet cap, faired inlet cap, and flat plate inlet cap. From these components one can configure respectively the B=3 or 5, B=2, or B=4 inlet covers.

Figures 18 through 20 show the flat baffle acoustic treatment, staggered baffle acoustic treatment, and tubular acoustic treatment. The component of Figure 18 provides the C=2 configuration, etc.

Figure 21 shows the turning vane assembly for the E=4 configuration. Figure 22 shows the component used for the F=7 configuration. Figure 23 shows the component for the H=2 configuration, while Figure 24 shows the component for H=3, 4, or 5.

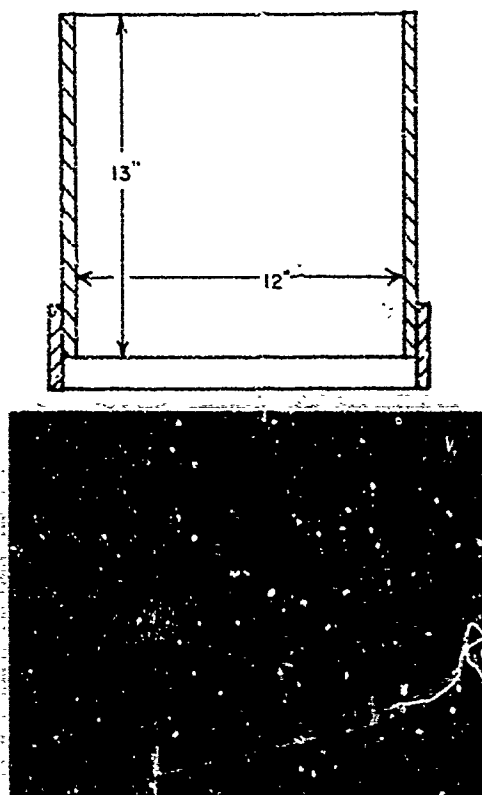


Figure 11 Vertical Inlet Stack.

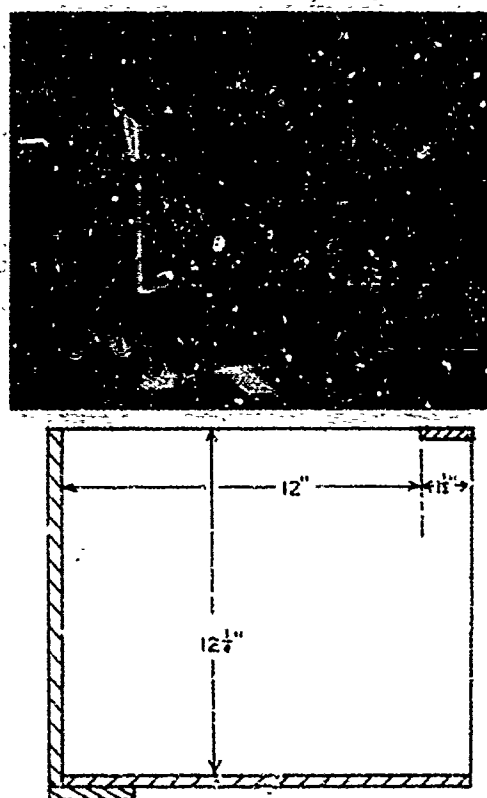


Figure 12 Convertible Duct Bend.

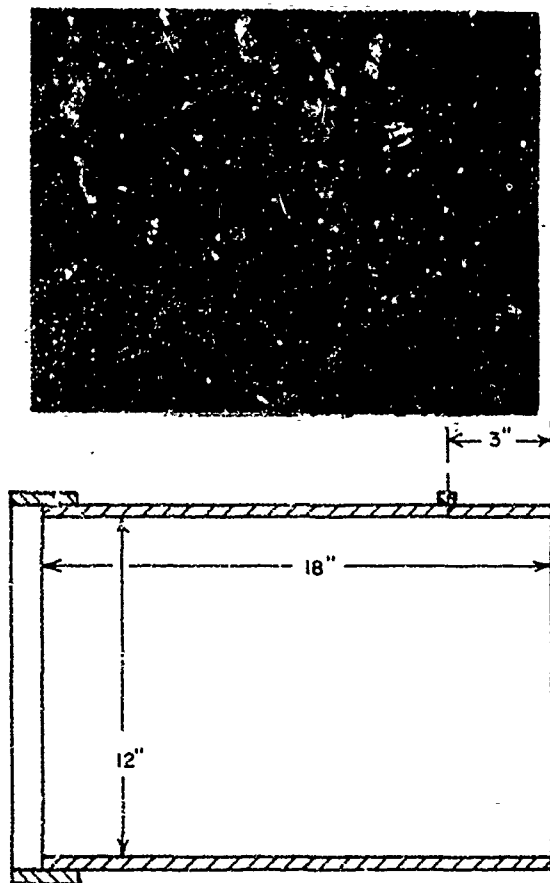


Figure 13 Flow Straightener Component.

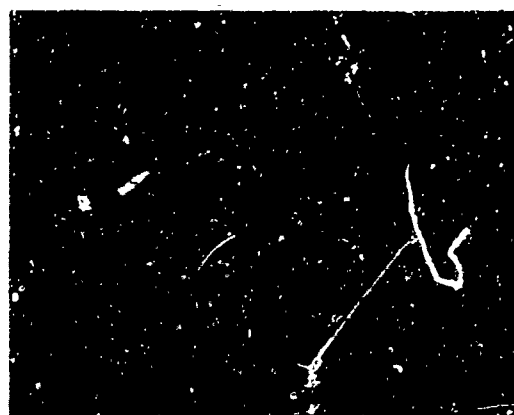


Figure 15 Bi-Directional Inlet Cap.

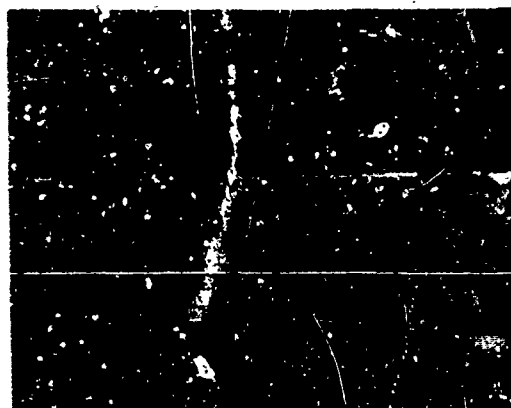


Figure 14 Triple Turn Inlet Box Component.

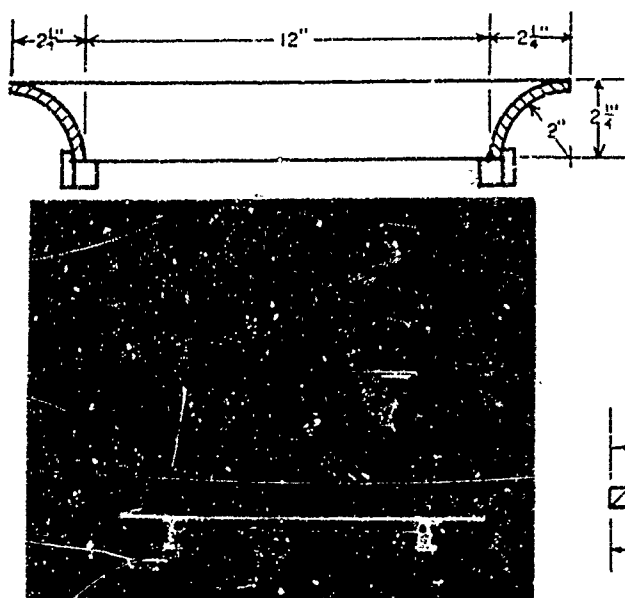


Figure 16 Paired Inlet Cap.

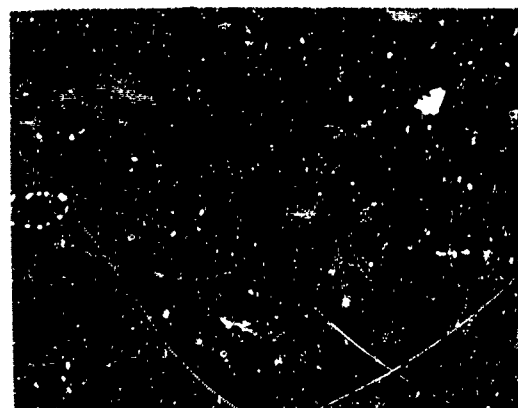


Figure 17 Flat Plate Inlet Cap.

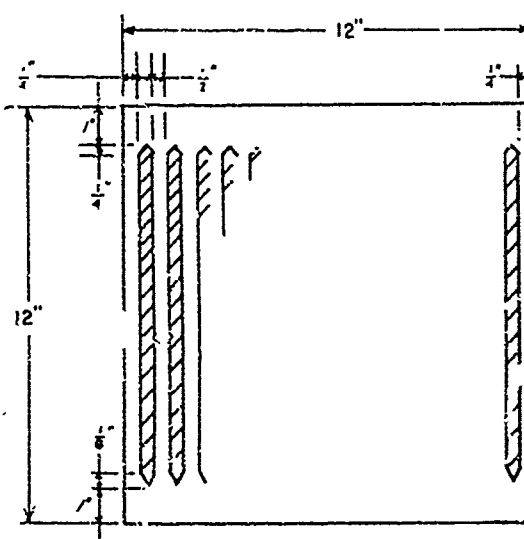
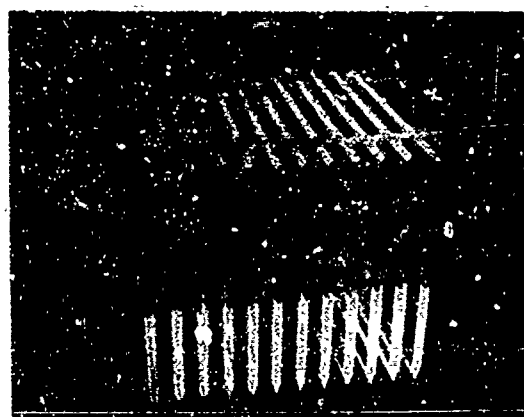


Figure 18 Flat Baffle Acoustic Treatment.

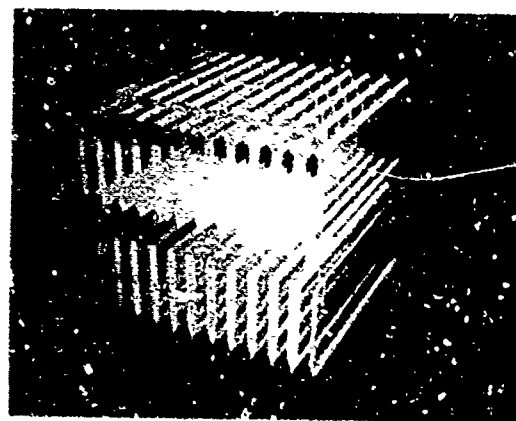
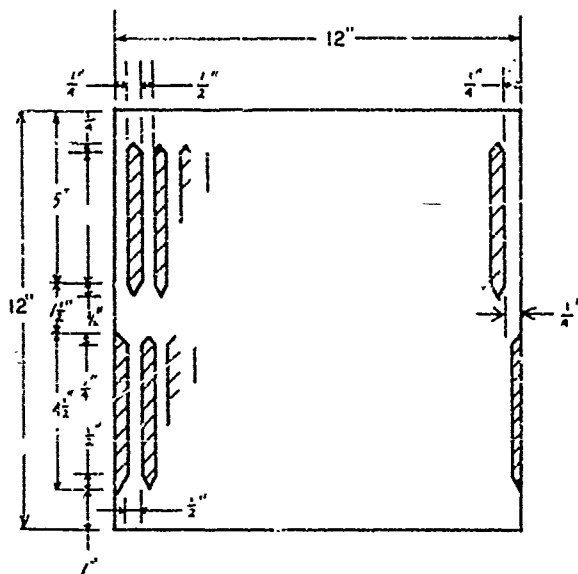


Figure 19 Staggered Baffle Acoustic Treatment.

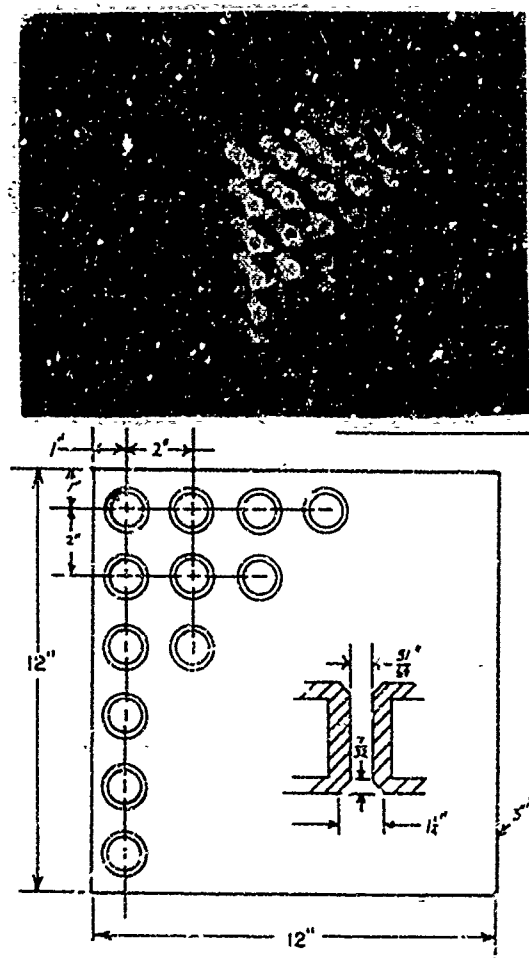


Figure 20 Tubular Acoustic Treatment.

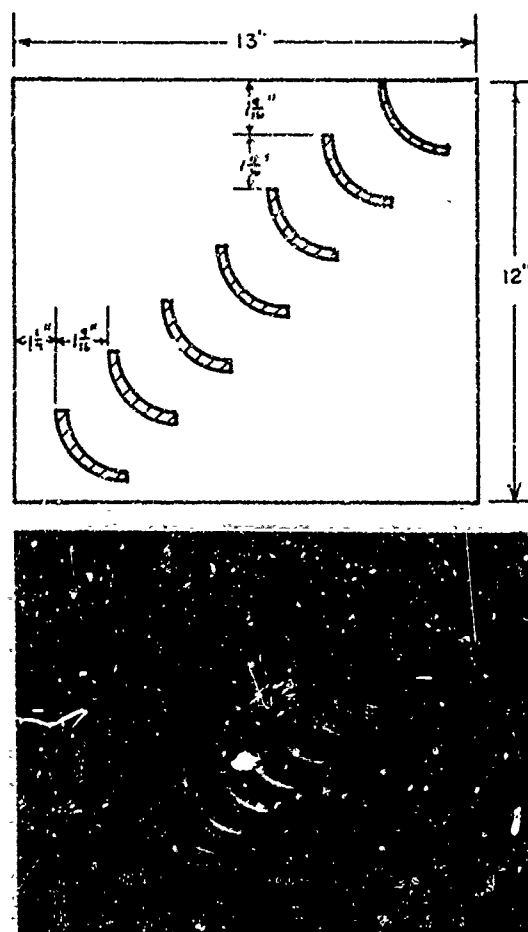


Figure 21 Turning Vane Assembly.

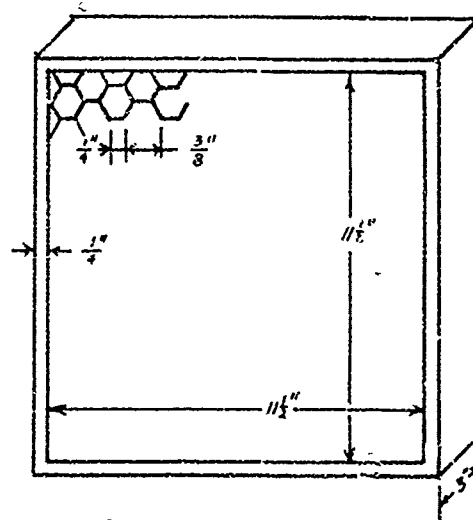


Figure 22 Hex Section Flow Straightener.

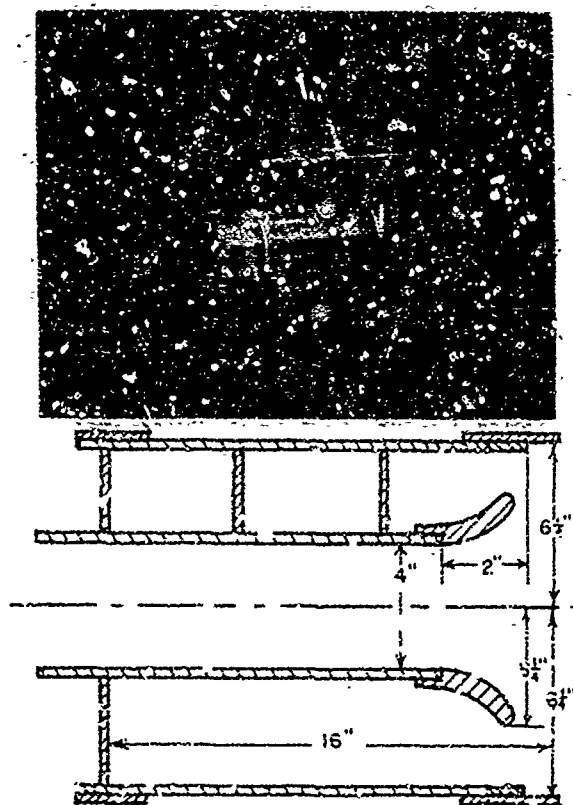


Figure 23 Zero Augmentation Test Section.

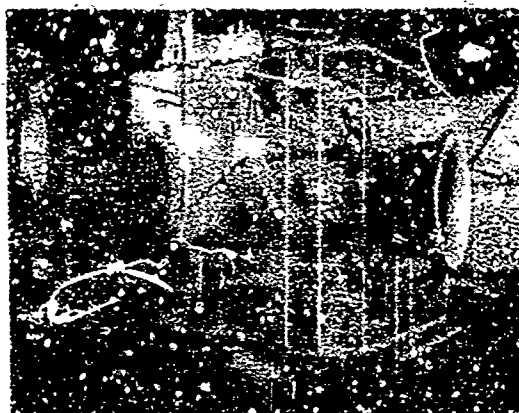
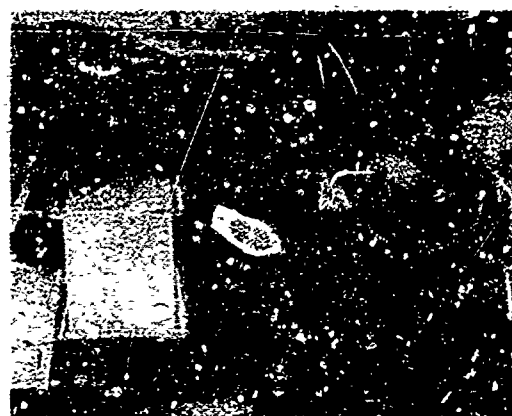


Figure 24 Dual Power Test Section.

Figure 25 shows assembled models for non-augmented flow for two different configurations. Figure 26 also shows assembled models but in this case for augmented flow. Once again two configurations are shown.

Figure 10 identifies a compressor face velocity survey plane. The pressure probes located at the survey plane are shown in more detail in Figure 27. There were a total of 24 total pressure probes with two static pressure ports identified as numbers 26 and 27.

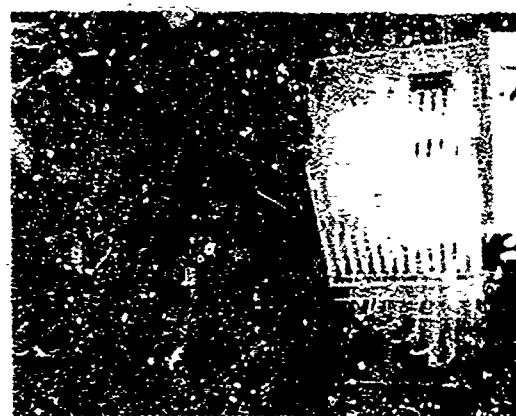


(a) Configuration 2125.123211



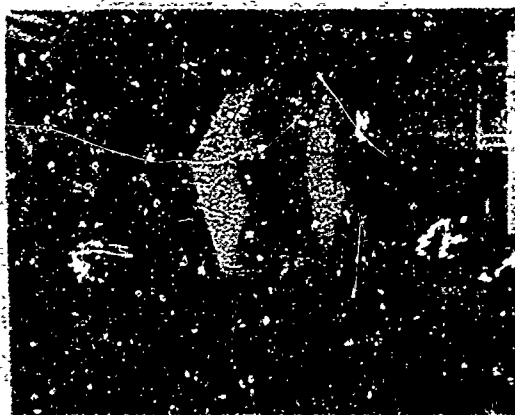
(b) Configuration 1213.422213

Figure 25 Assembled Model, Non-Augmented Flow.



(a) Configuration 5121.423512

Figure 26 Assembled Models, Augmented Flow.



cont'd (b) Configuration 5121.428542

Figure 26 Assembled Models, Augmented Flow.

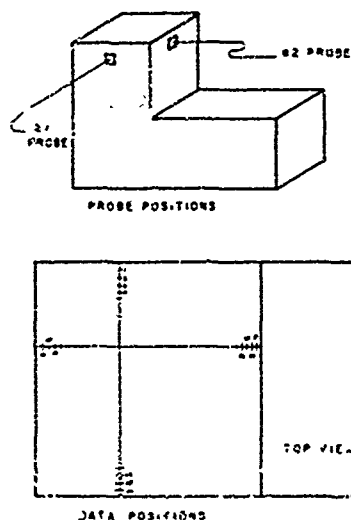


Figure 25 Inlet Velocity Survey Plan.



Figure 27 The Arrangement of Compressor Face Instrumentation.

As an example of supplemental information that was obtained, consider the inlet velocity survey plan illustrated by Figure 28. Velocity measurements were made at a total of 52 stations. Figure 29 shows results for the bi-directional cap. It is obvious that the cap causes a wake or a pair of vortex sheets from the line of symmetry. This is a source of flow distortion at the engine.

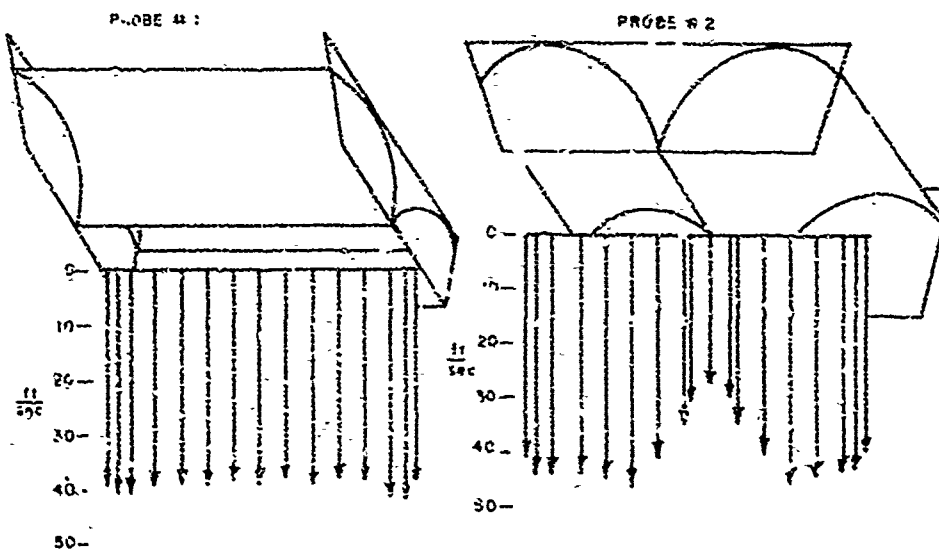


Figure 28 Typical Inlet Velocity Surveys.

B. Results

Distortion of the compressor face was characterized by a distortion index. Table II lists a few of the common indices which may be used by Rayleigh¹⁰⁴. The indices selected for this paper were K_D and the two indices developed by Brunda and Boytos.^{101,102}

Table II is a partial listing of results. The configurations are listed starting with least distortion and progressing to worst configurations. This is only a partial listing; the interested reader should obtain Truitt's thesis⁶⁶ from USA Defense Document Center for a complete listing of results.

As one may expect, the unconfined bellmouth (configuration 3113.113122) has the least distortion. The horizontal inlet with final baffle acoustic treatment (configuration 2122.113222) is next being very low in distortion level. The S-turn configurations, e.g. 5132.713342, gave unsatisfactory performance.

Based on the Brunda-Boytos radial and circumferential distortion indices, the test cell configurations were rated satisfactory (SAT) or unsatisfactory (UNSAT).

Table III provides a guide to test cell designers in regard to influence on distortion of various test facility geometries and the acoustic treatments.

Table II Measures of Distortion

NAME	DEFINITION
K	$\frac{(\theta/2\pi)(q/P)^{1/2}}{(q/P)^{1/2}/(q/P)^{1/2}}$ <p>Where $\theta \equiv$ radial extent of spoiled sector.</p>
\bar{Z}	$\left\{ \frac{(z/r_2)(z_2 - r_2) \left[z_2 Z_2(r) - z_1 Z_1(r) \right]}{\left\{ \left[1 - (\Delta F/r) \right] \sqrt{(q/P_1)/(q/P_2)} \right\} - 1} \right\} \times$ $\left[1 + (q/P) \right]$ <p>where Z is a complex function of position formed from eigenvalues of appropriate momentum equations and a linear combination of Bessel functions of the first and second kinds.</p>
K_D	$100 \frac{\sum \left[\frac{P_{ring}(avg) - P_{ring}(min)}{P_{ring}(avg)} \right] \bar{\theta}_{ring} C_{ring}}{\sum C_{ring}}$
D_1	$(P_{Tmax} - P_{Tmin})/P_{Tavg}$
D_{12}	$(P_{Tavg} - P_{Tmin})/P_{Tavg}$
D_{13}	$(P_{Tmax} - P_{Tmin})/P_{Tavg}$

VI. FACTORS AFFECTING EXHAUST SYSTEM PERFORMANCE¹⁰⁵A. Analysis^{57-76, 105-116}

Based on the background study reported in Sections II to IV, it is apparent that there are two serious deficiencies in available design information. First, it was not possible to adequately predict augmentation ratio given engine and test cell geometry and the operating conditions of the engine nozzle. Second, the amount of pressure rise in the augmenter could not be predicted. As pollution abatement devices are added to the test facility exhaust, the back pressure increases. At some point the engine ejector action will not be sufficient to overcome the pressure losses due to scrubbers, precipitators, or other pollution control devices. The work reported in this section partially fulfills the need for this design information.

A one-dimensional model was formulated for the geometry shown in Figure 30. The conservation equations are simultaneously solved to provide a solution for the static pressure at stations 1 and 2. It was assumed that $P_1 = P_2$. The static pressure at station 3 was given as an input quantity. Stagnation pressure at stations 1 and 2 was known. Knowing static and stagnation at station 2 permits evaluation of mass flow rate.

The location of the nozzle exit plane relative to the entrance to the augmenter tube has an effect on augmentation ratio. The model of Figure 30 cannot predict this dependence. A refined model was developed and is illustrated in Fig. 31. Within the entrainment zone defined in Fig. 31, there are three flow regions. The potential core has a flat velocity profile and is inside the mixing layer or shear layer. The velocity profile within the shear layer was described by an error function.⁵⁷⁻⁷⁶ In the annular space between the shear layer and the augmenter tube, a uniform velocity profile was assumed. The argument of the error function is $\eta = x/y$ where x and y are defined in Fig. 31. The jet spread parameter, σ , was evaluated using Abramovich's model^{70,118} which is $\sigma = 24 u_{jet}/u_0$. A dependence on x is introduced with the model of Fig. 31. For the model of Fig. 31, the flat-error-function-flat profile replaces the flat u_1 and u_2 profiles of Fig. 30. The conservation equations are solved once again. The analysis has been briefly sketched here, for complete details see Bailey's thesis.¹⁰⁵

Table III.
DATA SUMMARY
ORDERED BY DISTORTION LEVEL

CONFIG NUMBER	M	ENG VEL	RADIAL DISTORT.	CIRCUM. DISTORT.	K D	AUG. RATIO
3113.113122	3.671	133.692	0.0003 SAT	0.0396 SAT	0.2617	0.3
2122.113222	0.658	101.755	0.0009 SAT	0.0396 SAT	0.2661	0.0
1222.112222	0.669	103.435	0.0014 SAT	0.0396 SAT	0.4508	0.0
1131.413223	0.519	80.297	0.0009 SAT	0.0397 SAT	0.2334	0.0
1421.413223	0.519	80.191	0.0011 SAT	0.0397 SAT	0.1933	0.0
1221.413222	0.679	104.966	0.0009 SAT	0.0397 SAT	0.4455	0.0
1421.413142	0.511	79.058	0.0021 SAT	0.0397 SAT	0.2415	0.0
1331.413222	0.674	104.124	0.0007 SAT	0.0397 SAT	0.7611	0.0
1432.113223	0.521	80.516	0.0014 SAT	0.0397 SAT	0.2839	0.0
1122.112222	0.665	102.840	0.0006 SAT	0.0397 SAT	0.6558	0.0
1231.413222	0.677	104.620	0.0009 SAT	0.0397 SAT	0.6090	0.0
1113.413222	0.691	106.846	0.0012 SAT	0.0397 SAT	0.4010	0.0
1121.413222	0.680	105.098	0.0016 SAT	0.0397 SAT	0.5731	0.0
1432.413223	0.519	83.237	0.0011 SAT	0.0397 SAT	0.2605	0.0
1513.113222	0.660	102.011	0.0014 SAT	0.0397 SAT	0.8318	0.0
1252.113222	0.660	102.085	0.0010 SAT	0.0398 SAT	0.5323	0.0
1132.413222	0.662	102.366	0.0022 SAT	0.0427 SAT	0.7981	0.0
1232.113223	0.526	81.275	0.0013 SAT	0.0428 SAT	0.5152	0.0
1213.113223	0.523	80.814	0.0017 SAT	0.0428 SAT	0.2303	0.0
1131.313222	0.666	103.011	0.0020 SAT	0.0428 SAT	0.3638	0.0
1213.313222	0.676	104.564	0.0021 SAT	0.0428 SAT	0.7643	0.0
1413.313222	0.670	73.497	0.0025 SAT	0.0428 SAT	0.7493	0.0
1131.413222	0.575	104.380	0.0012 SAT	0.0428UNSAT	0.5851	0.0
1131.213222	0.665	102.824	0.0013 SAT	0.0428UNSAT	0.6107	0.0
1421.313222	0.662	102.262	0.0023 SAT	0.0428UNSAT	0.7317	0.0
1332.113222	0.670	103.538	0.0027 SAT	0.0428UNSAT	1.1801	0.0
1432.313222	0.663	102.476	0.0034 SAT	0.0428UNSAT	0.5861	0.0
1121.313222	0.672	103.800	0.0006 SAT	0.0428UNSAT	0.7879	0.0
1152.113222	0.660	102.017	0.0012 SAT	0.0428UNSAT	0.7284	0.0
1431.413222	0.672	103.867	0.0015 SAT	0.0428UNSAT	0.5602	0.0
1321.413222	0.676	104.553	0.0020 SAT	0.0428UNSAT	0.7551	0.0
1432.113222	0.666	102.801	0.0024 SAT	0.0428UNSAT	0.6691	0.0
5132.713342	0.477	73.793	0.0040UNSAT	0.0428UNSAT	0.6498	3.493
1213.113222	0.664	102.559	0.0005 SAT	0.0428UNSAT	0.7936	0.0
1113.213111	0.669	103.373	0.0017 SAT	0.0428UNSAT	0.4761	0.0
1213.213222	0.672	103.857	0.0017 SAT	0.0428UNSAT	0.8828	0.0
1213.413142	0.511	79.051	0.0019 SAT	0.0428UNSAT	0.7996	0.0
1352.112333	0.656	101.413	0.0022 SAT	0.0428UNSAT	0.8628	0.0
1113.113222	0.659	101.860	0.0007 SAT	0.0428UNSAT	0.9248	0.0

Table III. Continued

CONFIG NUMBER	M	ENG VEL	RADIAL DISTORT.	CIRCUM. DISTORT.	K D	AUG. RATIO
1441.513222	0.598	92.468	0.0014 SAT	0.0436UNSAT	1.9607	0.0
1431.213543	0.439	67.919	0.0036 SAT	0.0436UNSAT	1.5928	4.593
1513.413543	0.478	73.945	0.0042UNSAT	0.0436UNSAT	1.7761	3.761
1332.113542	0.465	71.940	0.0044UNSAT	0.0436UNSAT	1.4225	3.001
1222.313542	0.461	71.367	0.0055UNSAT	0.0437UNSAT	1.4443	3.120
1441.113142	0.486	75.162	0.0034 SAT	0.0437UNSAT	2.2344	0.0
1121.113342	0.493	76.219	0.0048UNSAT	0.0437UNSAT	1.8473	1.197
1221.313342	0.452	76.086	0.0032 SAT	0.0438UNSAT	1.6497	1.417
5134.213442	0.367	56.812	0.0054UNSAT	0.0439UNSAT	1.5316	3.1
1221.113342	0.491	76.016	0.0040UNSAT	0.0441UNSAT	1.9822	1.201
1321.413543	0.483	74.749	0.0040UNSAT	0.0441UNSAT	2.6631	4.125
1313.313342	0.458	70.041	0.0055UNSAT	0.0442UNSAT	1.3388	5.887
1421.413543	0.469	72.583	0.0027 SAT	0.0443UNSAT	1.8047	4.251
5132.413542	0.371	57.484	0.0046UNSAT	0.0444UNSAT	1.0127	6.376
1132.113542	0.477	73.851	0.0043UNSAT	0.0448UNSAT	2.0010	2.994
1222.113542	0.480	74.599	0.0075UNSAT	0.0450UNSAT	3.4913	2.871
5124.413442	0.395	61.407	0.0047UNSAT	0.0453UNSAT	2.8919	3.770
1213.113543	0.511	79.355	0.0067UNSAT	0.0456UNSAT	6.3772	3.542
1122.113542	0.473	73.467	0.0049UNSAT	0.0473UNSAT	5.9342	2.871
1131.213543	0.463	72.185	0.0056UNSAT	0.0479UNSAT	7.1440	4.374
5124.513442	0.373	58.359	0.0069UNSAT	0.0483UNSAT	5.1863	3.647
1331.213543	0.461	71.769	0.0032 SAT	0.0484UNSAT	7.8237	3.761
1131.213442	0.478	74.592	0.0058UNSAT	0.0488UNSAT	7.2430	3.419

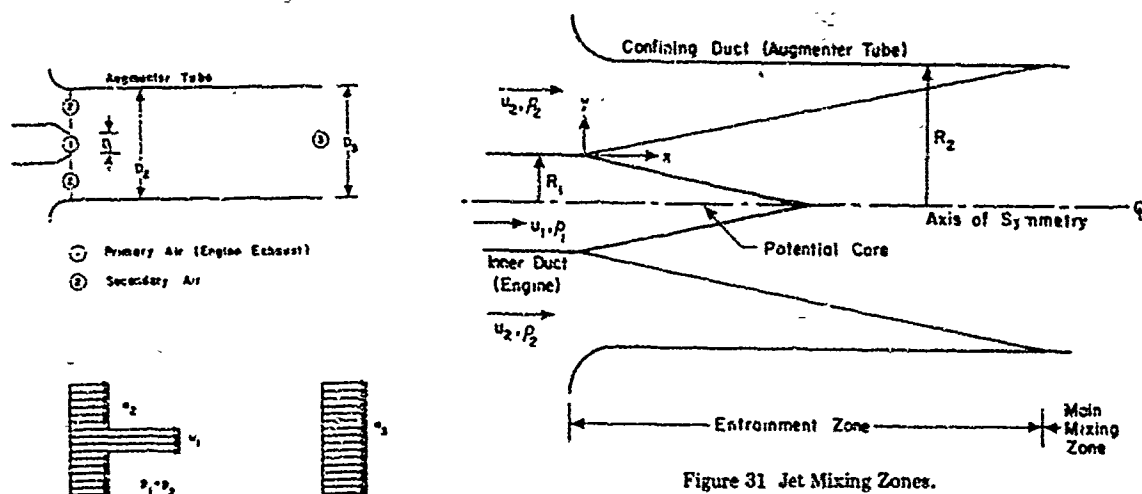


Figure 31 Jet Mixing Zones.

B. Experimental Apparatus

Figure 30 Station Designation and Ideal Velocity Profiles for Jet Pump Analysis.

different configurations could be tested. Table IV provides the configuration code for the exhaust system. The augmentor inside diameter was 3 in. Hence configuration A=1 provides a length/diameter ratio of 5. Figure 32 shows the augmentor entrance geometry. Configuration B=2 corresponds to the geometry of Fig. 32(b). The area of the holes in the colander was varied, and this provides the parameter identified as C in Table IV. The spacing positioned the nozzle exit plane relative to the augmentor tube entrance plane. For configuration E=3, the nozzle exit and augmentor entrance are coplanar. For configuration E=4, the nozzle exit is 1/2 in. upstream of (i.e. outside) the augmentor entrance. For configuration E=5, the nozzle exit plane is 1/2 in. inside the augmentor tube.

Figure 33(a) shows the two colanders employed in the experiments. Figure 33(b) is a photograph of a colander mounted in the apparatus. Figures 10 and 34 are comparable in that one is a sketch and the other a photograph of the dual mode installation. Figure 35 shows the nozzle and augmentor. Figures 36 and 37 show the nozzle and its air supply.

Table IV Exhaust System Test Configuration Code

ABC, DE	
A: Augmenter Length	B: Inlet Configuration
1.....15"	0.....None
2.....25"	1.....Conical
3.....40"	2.....Restricted
C: Colander	D: Nozzle Diameter
0.....None	1.....1"
1..1.3% x Aug Area	2.....1.25"
2..1.69 x Aug Area	3.....1.5"
E: Displacement (Spacers)	
1.....0"	
2.....1/2"	
3.....1"	
4.....1-1/2"	
5.....2"	
6.....2-1/2"	
7.....3"	
8.....3-1/2"	
9.....4"	

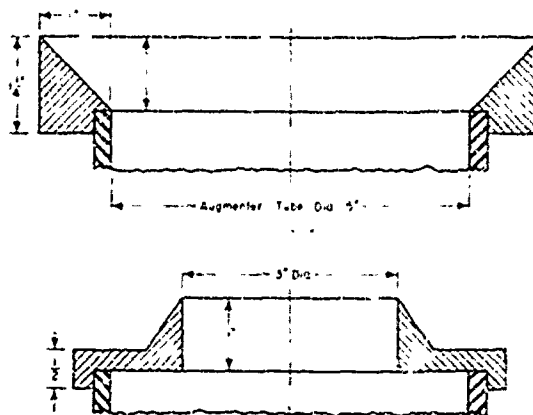
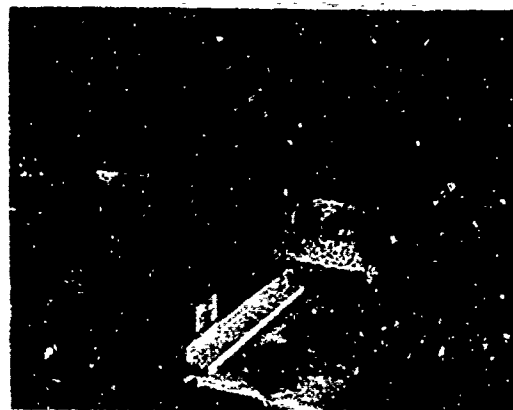


Figure 32 Inlet Schematic.



(a) Colanders Designed for Experiment.



(b) Colander Mounted on Apparatus.

Figure 33 Photographs of Colanders.

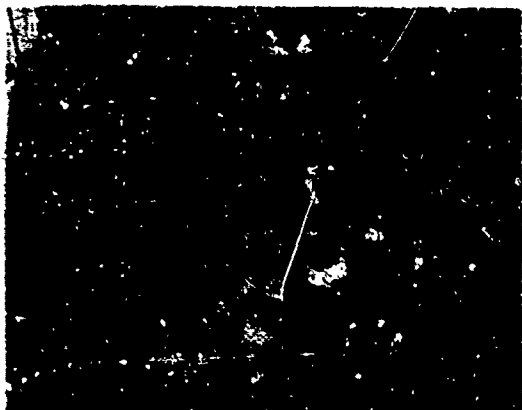


Figure 34 Dual Mode Installation.

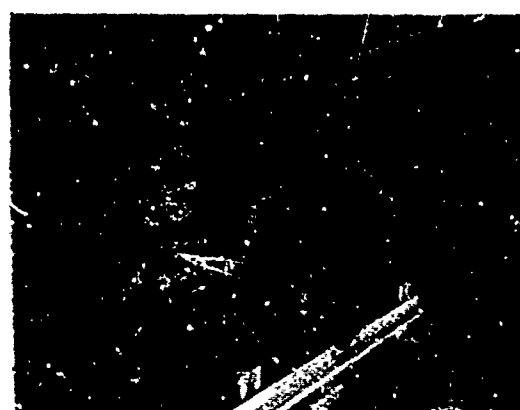


Figure 35 Nozzle and Augmenter.

Table V. Experimental Results

Configuration	Run	Station	\dot{m}_1 (pps)	\dot{m}_3 (pps)	\dot{m}_2/\dot{m}_1	$\frac{P_{noz}}{P_{atm}}$	U_{c1} (fps)
200.11	1.929	4	0.51	2.50	3.92	2.1	909
200.11	2.929	4	0.52	1.61	2.10	2.1	859
200.11	3.929	4	0.54	2.34	3.33	2.1	935
200.11	4.929	4	0.53	2.55	3.78	2.1	839
200.11	1.930	4	0.56	2.02	2.64	2.1	869
200.12	2.930	4	0.54	2.63	3.87	2.1	970
200.13	3.930	4	0.54	2.70	4.01	2.1	936
200.15	4.930	4	0.54	2.58	3.82	2.1	873
200.17	5.930	4	0.53	3.26	5.12	2.1	746
200.19	6.930	4	0.53	2.98	4.60	2.1	588
210.13	1.004	4	0.57	2.01	2.52	2.1	690
210.13	2.004	4	0.54	1.90	2.50	2.1	592
210.13	3.004	4	0.54	2.90	4.40	2.1	824
220.15	1.006	4	0.55	2.22	2.98	2.1	814
220.15	2.006	4	0.52	1.11	1.16	2.0	785
220.15	3.006	4	0.51	7.88	14.53	2.0	774
220.15	4.006	4	0.50	1.09	1.18	2.0	781
210.15	5.006	4	0.52	3.22	5.17	2.0	811
210.15	1.009	1	0.56	2.67	3.75	2.1	1375
		2		2.70	3.80		1334
		3		2.90	4.17		1107
		4		2.73	3.86		812
		5		3.04	4.40		658
		6		2.87	4.11		556
		7		2.98	4.29		490
200.15	2.009	4	0.53	3.23	5.21	2.05	857
		7		3.27	5.17		495
220.15	3.009	7	0.52	1.45	1.76	2.05	244
222.15	4.009	4	0.53	2.25	3.24	2.1	776
		7		1.60	2.01		243
210.10	1.011	7	0.54	2.17	3.03	2.05	432
210.10	2.011	7	0.50	1.91	2.84	1.9	445
210.10	3.011	7	0.41	1.77	3.29	1.6	344
210.10	4.011	7	0.41	1.77	3.29	1.6	349
210.10	5.011	7	0.41	1.90	3.63	1.6	331
210.10	1.013	7	0.42	1.87	3.41	1.6	346
200.10	2.013	7	0.42	1.79	3.30	1.6	334
220.13	3.013	7	0.42	0.81	0.94	1.6	158
220.15	4.013	7	0.54	1.26	1.32	2.1	215
210.15	5.013	7	0.53	3.38	5.32	2.1	392
200.15	6.013	7	0.54	2.39	3.47	2.1	393
200.15	7.013	7	0.37	1.54	3.19	1.45	248
200.17	8.013	7	0.37	1.62	3.42	1.45	248
200.19	9.013	7	0.36	1.77	3.84	1.45	258
200.12	10.013	7	0.36	2.27	5.23	1.45	280
202.13	1.015	7	0.49	2.03	4.40	1.45	290
201.13	2.015	7	0.37	2.02	4.45	1.45	290
200.13	3.015	7	0.22	1.20	4.60	1.15	169
200.13	4.015	7	0.29	1.67	4.83	1.28	232
200.13	5.015	7	0.42	2.44	4.83	1.62	352
200.13	6.015	7	0.46	2.67	4.86	1.38	394
200.13	7.015	7	0.50	3.03	5.12	1.94	432

pps is pounds per second.

C. Results

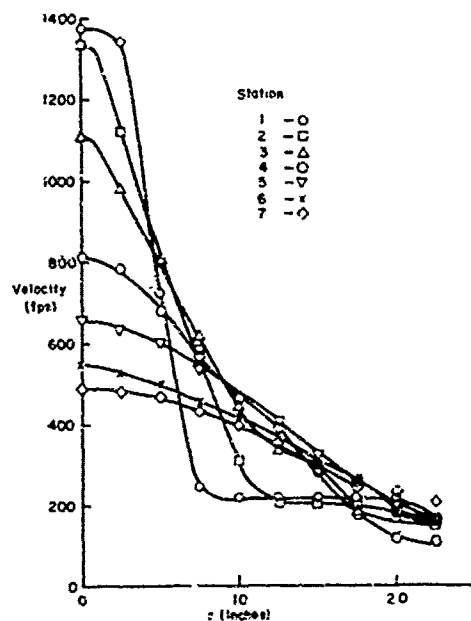
Table V summarizes the data obtained from the experimental apparatus discussed in the previous section. Runs 1.929 through 4.929, 1.004 through 3.004, 1.006 through 5.006, and 1.011 through 5.011 were conducted with Tower⁵⁶ to study the effects of changing the inlet configuration. Table VI correlates run numbers with configurations. Analysis of the data indicates two factors which affected the performance. Inlet acoustic treatments in the form of either flat or staggered baffles cut the augmentation ratio by a factor of 1/3. Compare run 1.004 with 5.006. It is seen that the installation of acoustic treatments, which is necessary if cells are to conform with local anti-noise ordinances, also helps to maintain the augmentation ratio at a reasonable level.



Figure 36 Inlet of Apparatus and Primary Air Piping.



Figure 37 Primary Nozzle.

Figure 38 Velocity Profiles for Configuration 210.15,
 $P_{T1} = 2.1$ atm.

Experimental results indicated that the conical inlet of Fig. 32 lowered the augmentation ratio when installed rather than improved it. The reason for this phenomenon may be that when the conical inlet was installed, it had the effect of moving the augmeter inlet away from the back wall of the test cell. Some turbulence or recirculation exists in the area between the inlet and the wall. It is thought that the change produced by moving the inlet caused some interference to occur in the streamlines into the augmeter decreasing the secondary flow rate. The particular model design tended to block the flow into the augmeter from the area behind the inlet.

Table VI. Dual Mode Inlet Configurations

Run	Augmeter Configuration	Inlet Configuration
1.929	200.11	1321.413543
2.929	200.11	1213.113543
3.929	200.11	1131.413543
4.929	200.11	1131.213543
1.004	210.13	1322.313542
2.004	210.13	1122.113542
3.004	210.13	5132.413542
1.006	220.15	5132.713342
2.006	220.15	1121.313342
3.006	220.15	1121.213342
4.006	220.15	1121.113342
5.006	210.15	1313.313342
1.011	210.10	7131.213442
2.011	210.10	5134.213442
3.011	210.10	5134.513442
4.011	210.10	5124.513442
5.011	210.10	5124.113442

The second major factor that was found to affect test cell performance was the presence of turning vanes. Turning vanes are necessary in some installations to reduce compressor face inlet distortion. Tower⁵⁶ discussed distortion limits for various engines. Results indicate that the decreased turbulence level obtained when turning vanes are installed leads to a decrease in total cell mass flow. This occurs because the mixing process in the augmeter becomes less effective. Increased turbulence in either the secondary or primary stream causes mixing to occur more rapidly as evidenced by the centerline velocity decay. Compare run 1.929 with run 1.004.

If it becomes necessary to install turning vanes in a given test cell, the designer may have to provide means of increasing the turbulence level of the secondary air prior to its entry into the augmeter or build a longer augmeter to provide distance needed to achieve complete mixing.

The compressor used for the experiments was capable of producing a total pressure in the nozzle of up to 2.1 atmospheres.

Figure 38 shows the velocity profiles measured at various augmeter stations for configuration 210.15 with a nozzle pressure ratio of 2.1 atmospheres. Station 1 was located 3 in. from the nozzle exit plane; station 7 was located 25 in. from the nozzle and 1 in. from the augmeter exit plane. Stations 2, 3, 4, 5, and 6 were 7, 11, 15, 19, and 23 in. respectively from nozzle exit plane. The profiles were calculated using data obtained in run 1.009. The mass flow rates calculated at the various stations indicate an accuracy of about 10%.

Figure 39 shows the rate of decay of centerline velocities as flow progresses in the augmeter. The velocities shown also were obtained from data of run 1.009 and are normalized to the centerline velocity at station 1.

Some configurations yielded unusual velocity profiles. Figure 40 shows a profile where the maximum velocity occurs at a point other than on the centerline. Monroe⁷⁵ encountered the same phenomenon and attributed it to the presence of oblique shocks at the nozzle. A second factor is the probable presence of a swirl component in the primary flow as it leaves the nozzle. The swirl component, if present, was probably caused by the three 90° turns in the inlet pipe between the orifice and the nozzle. It is recommended that if further work is carried out with the experimental apparatus, tubular flow straighteners should be installed in the nozzle section.

Experimental results were in close agreement with theoretical predictions. Figure 41 shows secondary mass flow as a function of primary mass flow for configuration 200.13. The experimental results closely match the theoretical predictions when no entry loss (ENTLOS) was included. The predictions which used an entry loss factor of 0.85 were less than the experimental results, which indicates that the loss factor was too severe.

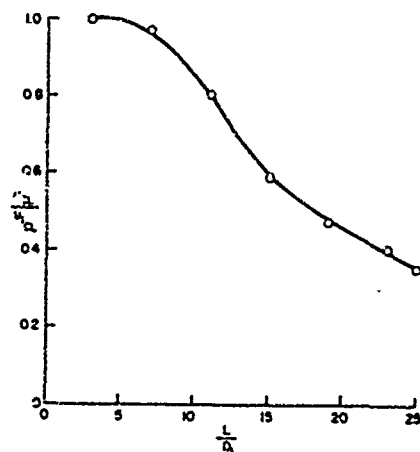
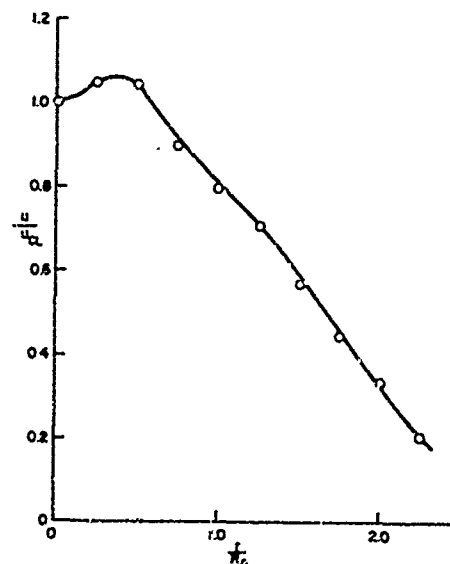
Figure 39 Centerline Velocity Decay, $P_{T1} = 2.1$ atm.

Figure 40 Nondimensional Velocity Profile, Station 4, Configuration 200.19, Run 6.930.

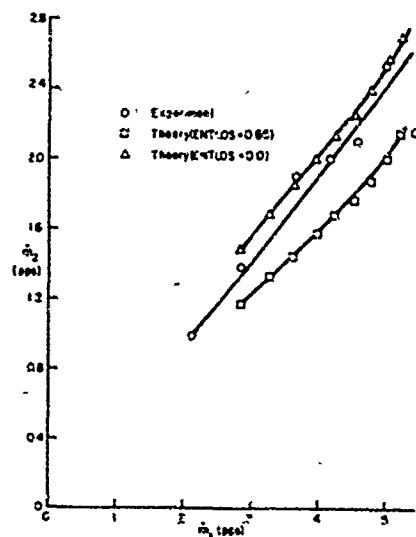


Figure 41 Secondary Mass Flow vs Primary Mass Flow for Configuration 200.13.

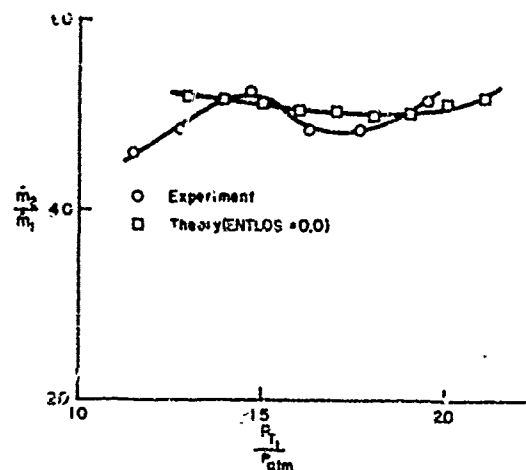
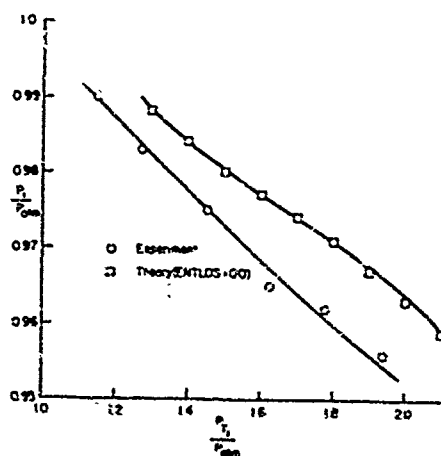
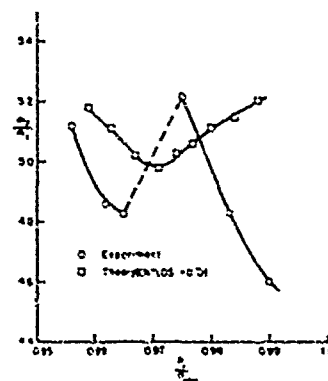
Figure 42 Variation of Augmentation Ratio with P_{T1} , Configuration 200.13.Figure 43 P_1 vs P_{T1} for Configuration 200.13.

Figure 44 Variation of Augmentation Ratio with Nozzle Exit Pressure, Configuration 200.13.

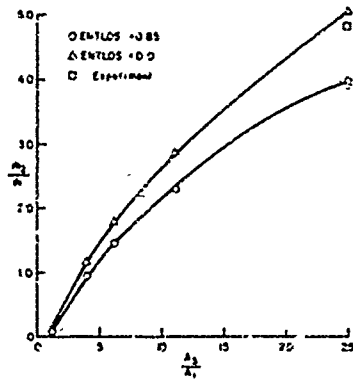


Figure 45 Augmentation Ratio as a Function of Area Ratio, $P_{T1} = 1.6 \text{ atm}$.

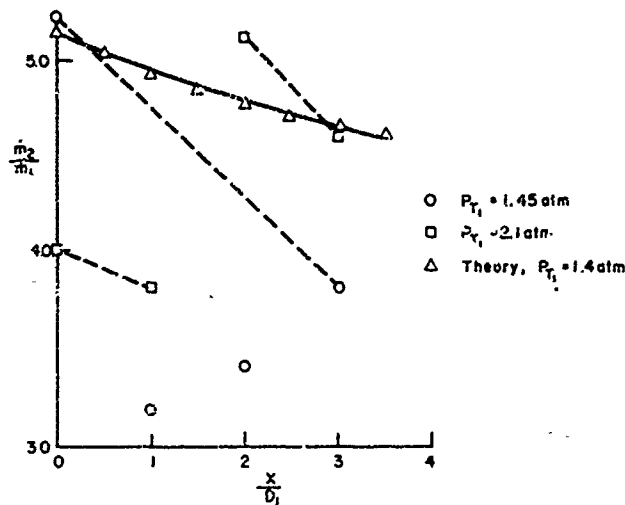


Figure 46 Augmentation Ratio as a Function of Nozzle Displacement Relative to Augmenter Entrance Plane.

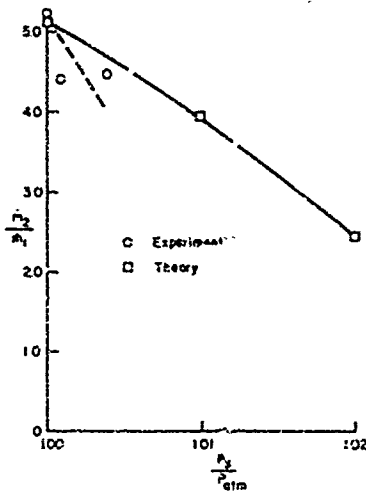


Figure 47 Augmentation Ratio as a Function of Augmenter Back Pressure, $P_{T1} = 1.45 \text{ atm}$.

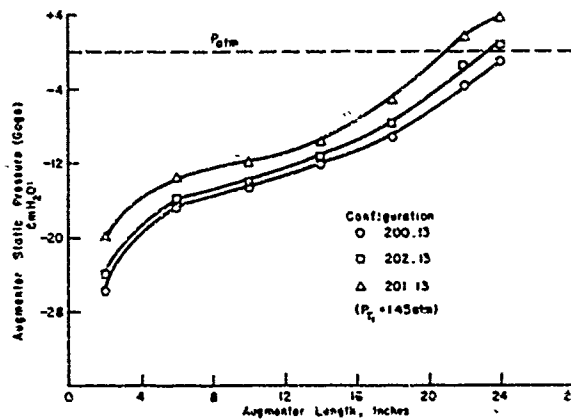


Figure 48 Augmenter Pressure Rise with Colanders Installed.

Figure 42 compares experimental and theoretical results of the dependence of augmentation ratio on nozzle pressure P_{T1} . Figure 43 shows the variation of P_1 , nozzle exit static pressure, with P_{T1} . In both figures good agreement between experimental and theoretical results is evident. Figure 44 compares the results showing variation of augmentation ratio with P_1 . The experimental results agreed with the trend predicted for supersonic flow (P_1 less than 0.97 in Fig. 44) but did not follow the predicted trend for subsonic flow. The probable cause for the disagreement is that the computer program assumed that complete mixing occurs at station 3 of the jet pump model, while in the experimental apparatus the amount of mixing that had been accomplished in the augmentor varied with the nozzle pressure ratio. An improvement might be made in the program by incorporating the jet spread parameter into the analysis. The present analysis only used the jet spread parameter to indicate the effect of nozzle position. The parameter is effectively a measure of the turbulence level, and, as previously discussed, increased turbulence causes higher augmentation ratios.

Figure 45 shows theoretical predictions of the dependence of augmentation ratio on area ratio A_2/A_1 . Present experiments have covered only one area ratio, so that further work is needed to validate the computed results.

Figure 46 illustrates the variation of augmentation ratio with nozzle displacement. The scatter of the data precludes any decision as to the validity of the predicted results. More data need to be collected for various nozzle displacements in subsonic flow situations. A form of the main computer program containing an improved turbulence factor should improve agreement between theory and experiment. A major addition needs to be made to the program in order to predict augmentation ratio as a function of nozzle displacement in the supersonic flow regime. At the present time the program is limited to zero-displacement in cases involving supersonic flow. It is thought that by applying the method of characteristics to the primary nozzle flow, it will be possible to predict exhaust system performance for all levels of supersonic flow as nozzle displacement is varied.

The back pressure against which the exhaust system operates greatly affects the augmentation ratio as seen in Figure 47. In its present form the computer program is able to predict the maximum back pressure allowable without encountering exhaust gas recirculation. This is particularly useful in situations where P_{T1} is low, such as an engine at idle power. Figure 48 shows the pressure rise in the augmentor system with various configurations.

Experimental results showed that the presence of a colander did little to influence the amount of mixing that occurred in the augmentor. Figures 49 and 50 show nondimensional velocity profiles at station 7 for various configurations and nozzle pressure ratios.

The maximum length augmentor required in a given system may be calculated with the jet spread parameter. The criterion for minimum length should be that all the secondary jet is contained into the main mixing region or, in other words, that the mixing zone

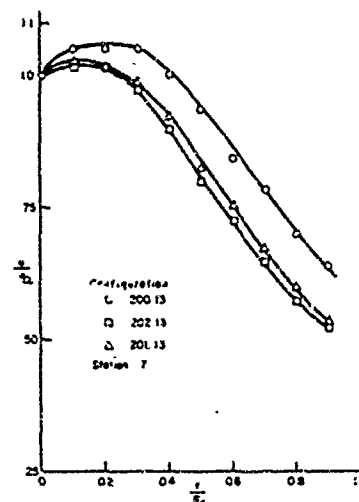


Figure 49 Effect of Colanders on Non-Dimensional Velocity Profile, $P_{T1} = 1.45$ atm.

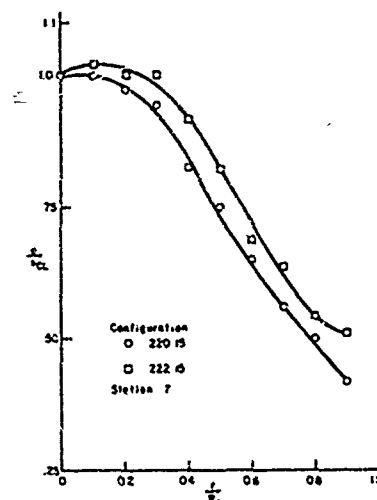


Figure 50 Effect of Colander on Non-Dimensional Velocity Profile, $P_{T1} = 2.1$ atm.

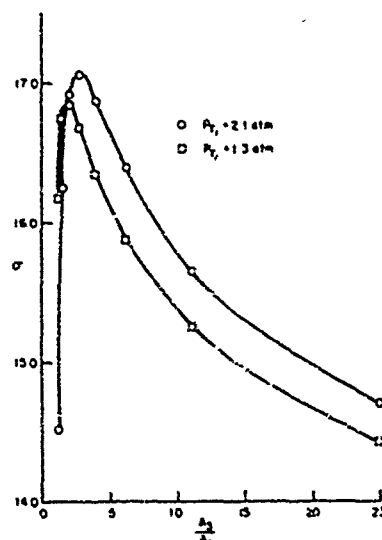


Figure 51 Jet Spread Parameter as a Function of A_2/A_1 .

has touched the augmenter wall. Figure 51 shows the jet spread parameter as a function of area ratio A_2/A_1 . The outer boundary of the mixing zone was defined to be $\eta = 1.84$, where η is the nondimensional coordinate in the y direction

$$\eta = \frac{oy}{x} \quad (1)$$

To find the minimum augmenter length define y_{\max}

$$y_{\max} = \frac{D_3 - D_1}{2} \quad (2)$$

D_3 is the augmenter diameter, and D_1 is the diameter of the nozzle. Pick σ from Fig. 51 using $A_2/A_1 = D_3^2/D_1^2$. Define x_{\min} as the required augmenter length

$$x_{\min} = \frac{\sigma(D_3 - D_1)}{3.68} \quad (3)$$

For example, consider an exhaust system with an augmenter 10 ft. in diameter in conjunction with a turbojet engine that is 3 ft. in diameter, operating with a nozzle pressure ratio large enough for supersonic flow. Figure 51 indicates a value of σ of about 15.5. Equation (2) then indicates a maximum augmenter length of 30 ft. for effective mixing.

Section VI summarizes Bailey's thesis;¹⁰⁵ the interested reader should obtain a copy of the thesis which provides considerably more detail. The computer programs and all equations for the analysis are given in the thesis.

VII. CONCLUDING REMARKS

Engine test facilities will be regulated by more restrictive environmental laws in the near future. In spite of the fact that the engine is the source of pollution, different regulations apply to test facilities. Additions of pollution abatement equipment makes it necessary to design the test facility to much closer tolerances in regard to flow distortion, augmentation ratio, cell depression, exhaust temperatures, and mass flow rates. The ability to design to the degree of precision required is rather primitive.

Methods of control of emissions are currently being explored. No single method, at present, appears to be the optimum. A variety of methods may evolve due to the variety of engine types, mass flows, exhaust properties and emission levels.

Flow distortion due to pollution abatement device was investigated experimentally; emphasis was on various acoustic treatments. Configurations yielding minimum distortion to the engine were identified.

Augmentation ratio was investigated both analytically and experimentally. A model was developed which predicts augmentation ratio; experiments indicate a precision of about 10%. The influence on augmentation ratio of location of exhaust nozzle exit plane relative to augmenter entrance plane was investigated.

APPENDIX A

Equivalent Augmentation Ratio for Turbofans⁸

Test Cell Augmentation ratio is defined as

$$A = \text{Augmentation ratio} = \frac{m_1 - m_0}{m_0}$$

where m_1 = total mass flow in the inlet stack

m_0 = mass flow passing through engine

Bypass ratio for a turbofan is defined as

$$B = \frac{m_c - m_e}{m_c}$$

where m_c = mass flow through engine core

Cooling air for a turbojet is $m_1 - m_0$. For a turbofan cooling air is $(m_1 - m_0) + (m_c - m_e)$. If energy added by fan is neglected. Manipulation leads to

$$A_{\text{eff}} = A + B + AB = \frac{m_1 - m_0}{m_0}$$

REFERENCES

- ¹Yaffee, Michael L., "Continued Engine Market Shrinkage Seen," Aviation Week & Space Technology, Vol. 96, No. 1, pp. 40-41, 3 January 1972.
- ²Yaffee, Michael L., "USAF Propulsion Interests Detailed," Aviation Week & Space Technology, Vol. 94, No. 9, pp. 54-57, 1 March 1971.
- ³Yaffee, Michael L., "New Versions of TP41 Designed," Aviation Week & Space Technology, Vol. 93, No. 16, pp. 42-47, 19 October 1970.
- ⁴Yaffee, Michael L., "Hybrid Fighter Engine Designed," Aviation Week & Space Technology, Vol. 95, No. 10, pp. 40-42, 6 September 1971.
- ⁵Rolls-Royce Limited Technical Report No. TP 148/E. E. D., Pegasus Facilities Planning Manual, 1970.
- ⁶Fluodyne Engineering Corporation Proposal No. P-1084, Proposal for Development and Design Criteria and Model Tests of a Universal Test Cell, October 1967.
- ⁷Hieronymus, William S., "Augmentor Wing Flight Tests Set," Aviation Week & Space Technology, Vol. 94, No. 1, pp. 48-50, 4 January 1971.
- ⁸Fuhr, A. E., "Aircraft Gas Turbine Test Cell Design Options," Naval Air Rework Facility, NAS North Island, Technical Memorandum No. E-41894, August 1971.
- ⁹"Aerojet Unveils Assault Vehicle," Aviation Week & Space Technology, Vol. 94, No. 3, p. 17, 18 January 1971.
- ¹⁰Courtney, William J., "Analysis, Test and Design of a Water Dynamometer," IIT Research Institute Report IITRI-J6143-FR, October 1969.
- ¹¹Gerend, R. P., and Roundhill, J. P., "Correlation of Gas Turbine Weights and Dimensions," AIAA Paper 70-669.
- ¹²Air Force Systems Command, Advanced Engine Research Facility, FY 71 MCP.
- ¹³Beavers, T. E., "An Engineering Analysis of Facilities for Altitude Testing of Large Turbojet and Turbofan Engines During the 1973-1990 Era, Arnold Engineering Development Center Report No. AEDC-TR-69-103.
- ¹⁴Naval Air Rework Facility, NAS North Island, MCON P-135, "Jet Engine Test Facility and Pollution Abatement; Facility Study and Present Value Analysis," 30 June 1971.
- ¹⁵Flight Propulsion Division of General Electric, Airline Planning Guide: Test Facilities for Large Advanced Turbojet and Turbofan Engines, 1 April 1967.
- ¹⁶Olve, R. L., "Modern Jet Engine Development Facility," ASME Paper 71-WA/GT-6, August 1971.
- ¹⁷Totmar, R. E., Staff Engineer, Personal Communication, United Airlines Overhaul Facility, 1 December 1971.
- ¹⁸Geery, E. L., and Margetts, M. J., "Penetration of a High Velocity Gas Stream by a Water Jet," AIAA Paper No. 68-604.
- ¹⁹Boe, R., Personal Communication, R. I. Corporation, Ogden, Utah.
- ²⁰O'Dell, D., Personal Communication, Naval Air Systems Command (Air 53431-D), Washington, D. C.
- ²¹Pulcher, G., Personal Communication, Naval Air Propulsion Center, GSE Division, Philadelphia, Pa.
- ²²Getter, G., Personal Communication, Getter and Associates, New Rochelle, New York.
- ²³Gall, E. S., "Thrust Stand Certification for the TF 39," Arnold Engineering Development Center Report AEDC TR-68-152.
- ²⁴Roscoe, C. F., Personal Communication, Naval Air Systems Command, 04 Group, Washington, D. C.
- ²⁵Surowiew, M. W., "Silencing Considerations for Large Gas Turbines," ASME Paper 71-GT-26, April 1971.
- ²⁶"Quiet Test Promises Cut in Noise Levels," Aviation Week & Space Technology, Vol. 94, No. 14, p. 21, 5 April 1971.
- ²⁷"Lockheed Research Aims at 50% Attenuation in Turbofan Noise," Aviation Week & Space Technology, Vol. 95, No. 3, pp. 54-55, 19 July 1971.
- ²⁸Naval Air Systems Command, Naval Facilities Engineering Command Committee, "Report on Standard Navy Depot Turbofan/Jet Engine Test Cell."
- ²⁹The Aeroacoustic Corporation, Bulletin B-31, R1, 1968.
- ³⁰Fink, M. R., "Shock Wave Behavior in Transonic Compression Noise Generation," ASME Paper 71-GT-7, April 1971.
- ³¹NASA SP-189, Progress of NASA Research Relating to Noise Alleviation of Large Subsonic Jet Aircraft.
- ³²Yaffee, Michael L., "U.S. Efforts Pace Engine Advance," Aviation Week & Space Technology, Vol. 92, 22 June 1970.
- ³³Burns & Roe, Inc., Standard Test Cell Design Study for Joint Airline Committee.
- ³⁴"New Jet Engine Test Cells," Architectural Products Review, June 1971.

- 35Doelling, N., and Bolt, R. H., Noise Control for Aircraft Engine Test Cells and Ground Run-up Suppressors, Volume 2: Design and Planning for Noise Control, Bolt, Beranek and Newman, Inc., November 1961.
- 36Colehour, J. L., and Farquhar, B. W., "Inlet Vortex," Journal of Aircraft, Vol. 8, No. 1, pp. 39-43, January 1971.
- 37The Aeroacoustic Corporation Bulletin B-37, R1, 1968.
- 38Leef, C. R., and Hendry, R. G., "Development of Nonrecirculating Wind-Tunnel Configuration Insensitive to External Winds," Journal of Aircraft, Vol. 6, No. 3, pp. 221-227, May-June 1969.
- 39Broberg, L. R., President, Letter of 10 February 1972, Aero Systems Engineering, Inc.
- 40Naval Air Rework Facility, NAS North Island, Memorandum, "Test Cell Conversion for TF34 Engine," 18 May 1971.
- 41Livesey, J. L., "Duct Performance Parameter Considering Spatially non-Uniform Flow," AIAA Paper No. 72-85, presented at AIAA Tenth Aerospace Sciences Meeting, San Diego, California, 17-19 January 1972.
- 42Carrier, W. H., and others, Modern Air Conditioning, Heating and Ventilating, Pitman Publishing Corporation, New York, 1959.
- 43Hoerner, S. F., Fluid Dynamic Drag, published by the author, 1965.
- 44Wenzel, L. M., "Experimental Investigation of the Effects of Pressure Distortion Imposed on the Inlet of a Turbofan Engine, NASA TM-X-1928, November 1961.
- 45Yaffee, Michael L., "AEDC Facilities Busy, Despite Cuts," Aviation Week & Space Technology, Vol. 94, No. 17, pp. 36-44, 26 April 1971.
- 46Pope, A., Wind Tunnel Testing, Section 3:11, John Wiley & Sons, New York, 1964.
- 47Vavra, M. H., Aero-Thermodynamics and Flow in Turbo Machines, Chapter 9, John Wiley & Sons, New York, 1960.
- 48Schlichting, H., Boundary Layer Theory, Chapter XI, McGraw Hill, New York, 1968.
- 49Idzeref, J. J., "Aerodynamic Model Study of Test Cells 2, 5, 6, 7, Building 300," Fluidyne Engineering Corporation Project No. 0482, August 1965.
- 50Valentine, E. F., "An Approximate Method for Design or Analysis of Two-Dimensional Subsonic-Flow Passages," NACA TN-4241.
- 51Deissler, R. G., Analysis of Turbulent Flow in non-Circular Passages, NACA TN-4384.
- 52Ljebiein, S., "Analytical Relation for Wake Momentum Thickness and Diffusion Ratio for Low Speed Tuning Vanes," NACA TN 4318.
- 53Burggaaf, O. R., "Analytic and Numerical Studies of the Structure of Steady Separated Flows," Journal of Fluid Mechanics, Vol. 24, Part 1, pp. 113-151, 1968.
- 54Dwyer, H. A., Doss, E. D., and Goldman, A., "Rapid Calculation of Inviscid and Viscous Flow Over Arbitrary Shaped Bodies," Journal of Aircraft Vol. 8, No. 2, pp. 125-127, February 1971.
- 55Matechak, J., and Thomas, L. A., "J52-P8A Engine Stall Margin Investigation, Naval Air Test Center Report No. ST-64R-69, 20 August 1969.
- 56Tower, P. W., "The Dependence of Compressor Face Distortion on Test Cell Inlet Configuration," Aeronautical Engineer Thesis Naval Postgraduate School, Monterey, Calif., December 1972. Available from DDC.
- 57The Soundcoat Company, Bulletins 701-704.
- 58Detroit Diesel Allison Division of General Motors, Research and Development Facilities, DDA Handbook.
- 59Pacific Airmotive Corporation Engineering Report, Reliability Program Support Services for Turbine Engines, 1 June 1971.
- 60Parsons-Vonseb Report, Sound Study for Aeronautical Propulsion Laboratory, Naval Postgraduate School, May 1961.
- 61Bureau of Aeronautics Specification XMA-51, Sound Measurement Tests for 30,000 Pound Thrust Capacity Turbojet Test Facility, January 1959.
- 62Northern Research and Engineering Corporation Report 950-313, Preliminary Design, Model Testing and Installation of a Prototype of a Thermal Converter for the Control of Exhaust Emissions from Navy Jet Engine Test Cells, Technical Proposal.
- 63Lindenhofen, H., Personal Communications, Naval Air Propulsion Center, Aero Engines Department, Philadelphia, Pa.
- 64General Electric Report No. 4DG 0006B01, Supplemental Airline Planning Guide: Test Facilities for Large Turbojet and Turbofan Engines, 1 June 1968.
- 65Fuhs, A. E., "Combustion Research Problems Associated with Advanced Air Breathing Engines," AIAA Paper 71-1, Ninth Aerospace Sciences Meeting, New York, N. Y., January 1971.
- 66Shaffernocker, W., "Current State of the Art for Air Breathing Combustor Testing," AIAA Progress Series in Aeronautics and Astronautics, Instrumentation for Air Breathing Propulsion, A. E. Fuhs and M. Kingery, Editors, MIT Press, 1973.
- 67Pai, S. I. Fluid Dynamics of Jets, D. Van Nostrand Co., Inc., 1954.

- 68 Birkhoff, G., and Zarantonello, L., Jets, Wakes and Cavities, Academic Press, New York, 1957.
- 69 Gurevich, M. I., The Theory of Jets in an Ideal Fluid, Translated by R. E. Hunt, Pergamon Press, 1966.
- 70 Abramovich, G. N., The Theory of Turbulent Jets, M. I. T. Press, 1963.
- 71 Christ, D. E., and Paulk, R. A., "Summary Report: An Experimental Investigation of Subsonic Coaxial Free Turbulent Mixing," Arnold Engineering Development Center Report AEDC-TR-71-236, February 1972.
- 72 Pindzola, M., Jet Simulation in Ground Test Facilities, AGARDograph 19, November 1963.
- 73 Pai, S. I., "Axially Symmetrical Jet Mixing of a Compressible Fluid," Quarterly of Applied Mathematics, July 1952.
- 74 Chia, K. N., Torda, T. P., Lavan, Z., "Laminar Mixing of Heterogeneous Axisymmetric Coaxial Confined Jets," AIAA Journal, Vol. 7, No. 11, p. 2072, November 1969.
- 75 Monroe, P. A., An Investigation of the Performance and Mixing Phenomena Associated with a Supersonic Exhauster Interacting with Subsonic Secondary Flow, Ae. E. Thesis, Naval Postgraduate School, Monterey, September 1967.
- 76 Wade, B. S., Parametric and Experimental Analysis of Ejector Performance, M. S. Thesis, Naval Postgraduate School, Monterey, July 1967.
- 77 Getter and Associates Report for the Naval Facilities Engineering Command, Pollution Abatement Study and Site Analysis for Jet Engine Test Cells.
- 78 Ribner, H. S., and others, Proceedings of a Short Course on Noise Generation and Suppression in Aircraft, 29 January-2 February 1968, UTSL.
- 79 NASA SP-5093, Acoustics Technology, A Survey, 1970.
- 80 Aerodynamic Noise, Proceedings of AFOSR-UCLA Symposium Held at Toronto, 20-21 May 1968, University of Toronto Press, 1969.
- 81 Richards, E. J., and Mead, D. J., Noise and Acoustic Fatigue in Aeronautics, John Wiley and Sons, Ltd., 1968.
- 82 Ferriss, D. H., and Johnson, R. F., "Turbulence in the Noise Producing Region of a Circular Jet," Journal of Fluid Mechanics, V. 19, Part 4, p. 591, August 1964.
- 83 Lighthill, M. J., "Jet Noise," AIAA Journal, Vol. 1, No. 7, p. 1507, July 1963.
- 84 Westervelt, P. J., and others, Proceedings of a Short Course on Noise Generation and Suppression in Aircraft, 29 January-2 February 1968, UTSL.
- 85 Middleton, D., Aeronautical Research Council, Reports and Memoranda No. 3389, The Noise of Ejectors, October 1963.
- 86 Sawyer, R. A., "Atmospheric Pollution by Aircraft Engines and Fuels-A Survey," Department of Mechanical Engineering, University of California, Berkeley, 1 September 1971.
- 87 Cornell Aeronautical Laboratory, Report No. NA-5077-K-1, Analysis of Aircraft Exhaust Emission Measurements, 15 October 1971.
- 88 Northern Research and Engineering Corporation, Report No. 11684, Assessment of Aircraft Emission Control Technology, September 1971.
- 89 Heywood, J. B., Fay, J. A., and Linden, L. H., "Jet Aircraft Air Pollutant Production and Dispersion," AIAA Journal, Vol. 9, No. 5, p. 841.
- 90 Henderson, R. E., AFAPL Technical Memorandum APTC-TM-69-11, "Turbo Propulsion Exhaust Smoke and Smoke Abatement," April 1969.
- 91 Study Group on Aviation Exhaust of the CRC Aviation Fuel, Lubricant and Equipment Research Committee, Report on Analysis of Exhaust Gases from Current Commercial Jet Engines, 23 July 1968.
- 92 North American Rockwell Corp., NA-69 57, An Investigation of Subsonic Duct Distortion, MacMillan, C. J., March 1969.
- 93 Arnold Engineering Development Facility, TR-71-50, Effect of Steady Inlet Distortion on the Stability and Performance Characteristics of an Augmented Turbofan Engine, Palmer, J. D., Parker, J. R., and Schwall, J. R., April 1971.
- 94 Reid, C., The Response of Axial Flow Compressor to Intake Flow Distortion, ASME Paper 69-GT-29 presented at the ASME Symposium, 9-13 March 1969.
- 95 Northern Research and Engineering Corp., Compressor Sensitivity to Transient and Distorted Transient Flows, Jansen, W., Swarden, M. C., and Carlson, A. W., December 1969.
- 96 Matechak, J., and Thomas, L. A., "J52-P8A Engine Stall Margin Investigation," Naval Air Test Center Report No. ST-64K-69, 26 August 1969.
- 97 Plourde, G. A., and Brimelow, B., "Pressure Fluctuations Cause Compressor Instability," AFAPL-AFFDL Airframe/Propulsion Compatibility Symposium, WPAFB, Ohio, June 1969.
- 98 Ball, W. H., and Ross, P. A., "Experimental Correlation of Installation Effects for Inlet/Airplane Integration," The Boeing Company, August 1969.

- 98 Roberts, R., Plourde, G., and Smakul, F., "Insights into Axial Compressor Response to Distortion," AIAA/SAE 4th Propulsion Joint Specialist Conference, June 1968.
- 100 Sherman, D. A., Metyska, D. L. and Ours, G. C., "Experimental Evaluation of a Hypothesis for Scaling Inlet Turbulence Data," Pratt & Whitney Aircraft Co., Contract Report F33516-67-C 1848, July 1971.
- 101 Brunda, D. F. and Boytos, J. F., "A Steady State Radial Inlet Pressure Distortion Index for Axial Flow Compressors," paper presented at the Gas Turbine and Fluids Engineering Conference, San Francisco, March 26-30, 1972.
- 102 Naval Air Propulsion Test Center Report NAPIC-ATD-193, Evaluation of a Circumferential Inlet Pressure Distortion Index on a TF30-P-12 Turbofan Engine, Brunda, D. F. and Boytos, J. F., July 1970.
- 103 Felchofer, W. J. and Smith, R. A., "Testing of Gas Turbine High Velocity Duct Systems," Naval Ships Engineering Command, Contract N00s22178, August 1966.
- 104 Farmer, C., Iverson, M., and Fuhs, A., "A New Approach to Distortion Induced Compressor Stall-Vorticity Maps," AIAA/SAE 5th Joint Propulsion Specialist Conference, AIAA Paper 72-1116, 1972.
- 105 Bailey, D. L., "An Analytical and Experimental Analysis of Exhaust System Performance in Sea Level Static Jet Engine Test Facilities," Aeronautical Engineer Thesis, Naval Postgraduate School, Monterey, Calif., December 1972. Available from DDC.
- 106 Weaver, T. E., "An Engineering Analysis of Facilities for Altitude Testing of Large Turbojet and Turbofan Engines During the 1973-1990 Era," Arnold Engineering Development Center Report No. AEDC-TR-69-103, July 1969.
- 107 Schetz, J. A., "Unified Analysis of Turbulent Jet Mixing," NASA CR-1332, July 1969.
- 108 Nagamatsu, H. T., Sheet, R. E., and Gill, M. S., "Flow and Acoustic Characteristics of Subsonic and Supersonic Jets from Convergent Nozzle," NASA CR-1633, December 1970.
- 109 Kerst, H. H., and Chow, W. L., "Non-Isoenergetic Turbulent ($P_{t1}=1$) Jet Mixing Between Two Compressible Streams at Constant Pressure," NASA CR-419, April 1966.
- 110 Morgenthau, J. H., Zelazny, S. W., and Herendorn, D. L., "Combustor Correlation Technique," Bell Aerospace Company Report No. 9560-920233, Buffalo, N. Y., February 1972.
- 111 Zelazny, S. W., Morgenthau, J. H., and Herendorn, D. L., "Shear Stress and Turbulent Intensity Models for Co-flowing Axisymmetric Streams," paper presented at AIAA 10th Aerospace Sciences Meeting, San Diego, California, 17-19 January 1972, AIAA Paper 72-47, 1972.
- 112 Engel, M. O., "Some Problems in the Design and Operation of Jet Ejectors," Proceedings of the Institution of Mechanical Engineers, Vol. 177, No. 13, p. 347, 1953.
- 113 Fabri, J., and Paulon, J., "Theory and Experiments on Supersonic Air-to-Air Ejectors," NACA TM-1410, September 1958.
- 114 Fejer, A. A., Hermann, W. G., and Tordo, T. P., "Factors that Enhance Jet Mixing," Aerospace Research Labs., WPAFB, ARL-63-0175, October 1969.
- 115 Keenan, J. H., Neumann, E. P., and Lortwerk, F., "An Investigation of Ejector Design by Analysis and Experiment," Journal of Applied Mechanics, Vol. 17, No. 3, p. 299, September 1959.
- 116 Krenkel, A. R., and Lipowsky, H. H., "Design Analysis of Central and Annular Jet Ejectors," ARL-66-0210, Polytechnic Institute of Brooklyn, October 1966.
- 117 Hanbury, W. T., "The Performance of an Air-Air Ejector According to a Quasi-One-Dimensional Theory," Aeronautical Research Council of Great Britain, A. R. C. 59-341, April 1967.
- 118 Bauer, R. C., "Characteristics of Axisymmetric and Two-Dimensional Isoenergetic Jet Mixing Zones," Arnold Engineering Development Center, AEDC-TDR-63-263, December 1963.

Discussion on Paper 14
 "Pollution Control of Airport Engine Test Facilities"
 presented by A.E.Fuhs

J.Poll: Could the authors confirm their testing of acoustic resonant liners for noise attenuation in test facility ducts? Such liners, suitably designed, would be expected to provide minimum flow distortion and pressure drop (compared to baffles, coolers, etc.), and would be most effective in the "medium" frequency range (say ~ 100 to 1000 Hz).

A.E.Fuhs: The case for acoustic resonant liners was studied. The configurations in Table III with the digit "1" in the third position are appropriate for an inlet with acoustic resonant liners.

P.A.Libby: Could you comment on the effect of disregard of the scaling laws in the qualitative and quantitative predictions of a test cell behaviour based on small scale models? Is it not risky to depend on such tests for an expensive facility?

A.E.Fuhs: One factor carefully studied prior to the experiments was scaling laws. Reynolds number was not duplicated. This influences viscous effects including vorticity generation, convection, and decay. However, the results of experiment will be conservative, i.e. a satisfactory design in subscale will remain satisfactory in full scale. An unsatisfactory design may or may not be unsatisfactory in full scale. The results of our experiments provide a guide for selection and identify cases where caution is appropriate.

The philosophy of the tests are consistent with wind tunnel tests where possible configurations are screened. In many wind tunnel tests full scaling is not accomplished: in fact, scaling is rarely observed.

Our paper provides the architect and engineer with guidance. Additional work is necessary for a specific facility design.

EXHAUST EMISSION MEASUREMENTS ON THE GE T64-7 TURBOPROP-ENGINE

W. Bergt, G. Koppler, G. Meikis

MOTOREN- UND TURBINEN-UNION MÜNCHEN GMBH

Engine Development and Testing Department

At MTU-Munich exhaust emission measurements have been carried out on the engine GE T64-7 with the objective to determine qualitatively the mass emission of the pollutants carbonmonoxide, unburnt hydrocarbons and oxides of nitrogen at different power ratings. Although for aircraft engine application the operating modes were just recently issued in the EPA proposed standards for control of air pollution, the engine was run through a 13-point California Test Cycle as applicable to Diesel engines for vehicles up to 6 000 lb gross weight. The numerical evaluation of the measured exhaust emissions was carried out using the method of analysis established for the above mentioned test cycle (Ref. 1). The measurements were taken for three different types of fuel: JP4, Diesel at 20°C and Diesel at 55°C.

The exhaust gas sampling using heated sampling lines and the analytical system set up for the measurements were in agreement with SAE Specifications. The instruments used in the analytical system are shown in the following table:

Component to be measured	Analyser	Measuring Range	Error of Analysis	Remarks
Carbon-Monoxide (CO)	N.D.I.R. (Maihak Co.)	Vol. %		Gauge is shifted
		0 - 0.1	$\pm 1\%$	electrically.
		0 - 0.5	$\pm 1\%$	Error at full scale.
Unburnt Hydrocarbon ΣC_6H_{14}	F.I.D. (IPM Co.)	Vol. ppm		
		0 - 10	$\pm 1\%$	4 ranges
		0 - 10 000		
Oxides of Nitrogen (NO ₂)	Chemo-luminescence (Scott Co.)	Vol. ppm		
		0 - 2.5	$\pm 1\%$	9 ranges
		0 - 10 000		

The results obtained from the exhaust emission measurements are represented in Figures 1 to 3. In these figures the emission levels of the pollutants (Vol. ppm) considered are superimposed on the load-time-spectrum of the California Test Cycle. Also pictured are the rated emission levels in gr/BHP-h relative to the presumed standards of 1975.

It can be seen from these figures that the emission levels of carbon monoxide, hydrocarbons and oxides of nitrogen are well below the most severe emission limits to be imposed on Diesel engines so far. The lowest values of emission levels being obtained for JP4 fuel. Figure 4 shows NO_x-emissions reported by Pratt and Whitney for the PT6 engine (Ref. 2) and for comparison the results obtained by MTU-Munich for the GE T64-7 using Diesel fuel. Although the rated power levels of the engines are different the measurements show good agreement and it can be seen that with increasing engine load the nitrogen oxide emission increases substantially. Figure 4 also includes on separate scale the Emission Index of nitrogen oxides as determined for the T64-7.

It is understood that the Proposed Emission Standards for operating modes simulating aircraft engine operation will be much lower in their numerical values than the ones reported simulating Diesel vehicles. The results shown are encouraging in view of the fact that the gas turbine, besides air transportation, becomes an increasingly important energy source for earth bound transportation as well.

Table of T64-7 Characteristic Data for Emission Evaluation

Engine Power Rating %	Mass Flow lbs/min	Break Power BPS	Weighting Factor
Idle	1347	0	0.2
2	1437	2400	0.08
25	1509	2800	0.08
50	1582	3200	0.08
75	1645	3600	0.08
100	1707	4000	0.08

References

- Ref. 1 State of California / Air Resources Board
California Exhaust Emission Standards, Test and Approval Procedures for Diesel Engines
in 1973 and Subsequent Model Year Vehicles Over 6 001 Pounds Gross Vehicle Weight
November 18 (1970)
- Ref. 2 E.S. Wright
The Potential of the Gas Turbine Vehicle in Alleviating Air Pollution
ASME Paper No. 70-WA/GT-8 (1970)

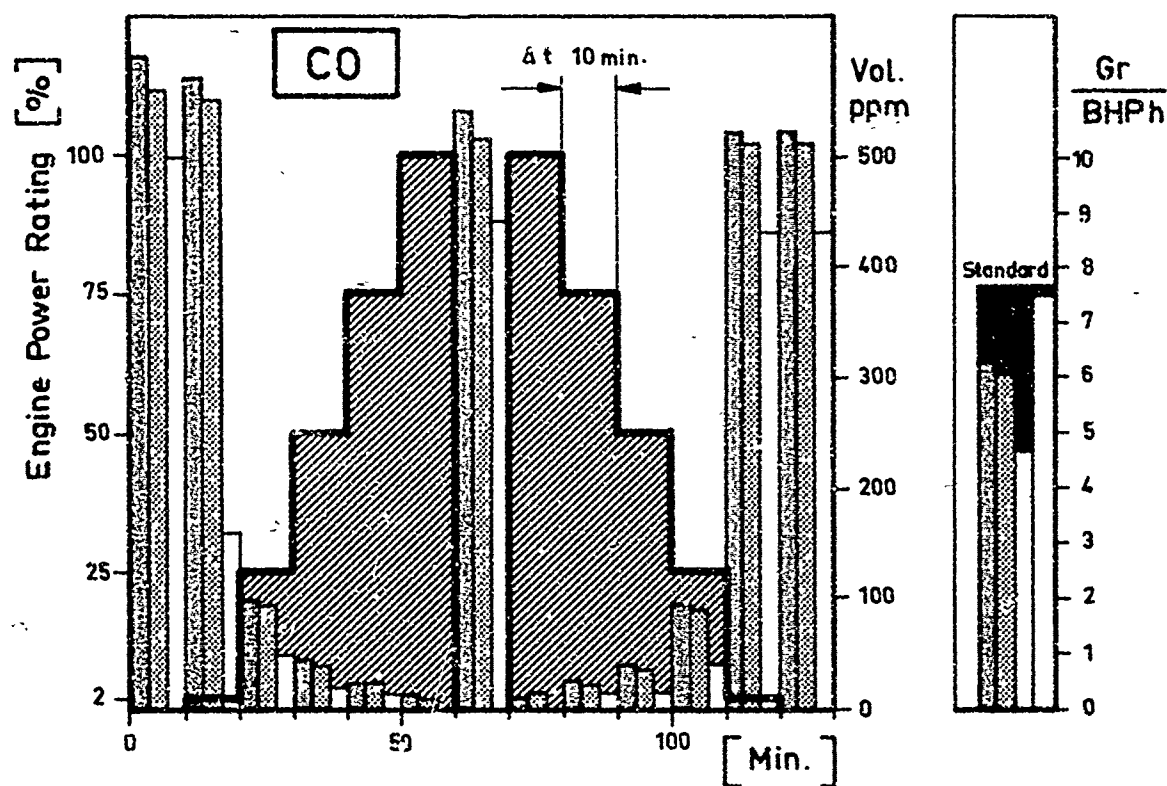


Fig. 1

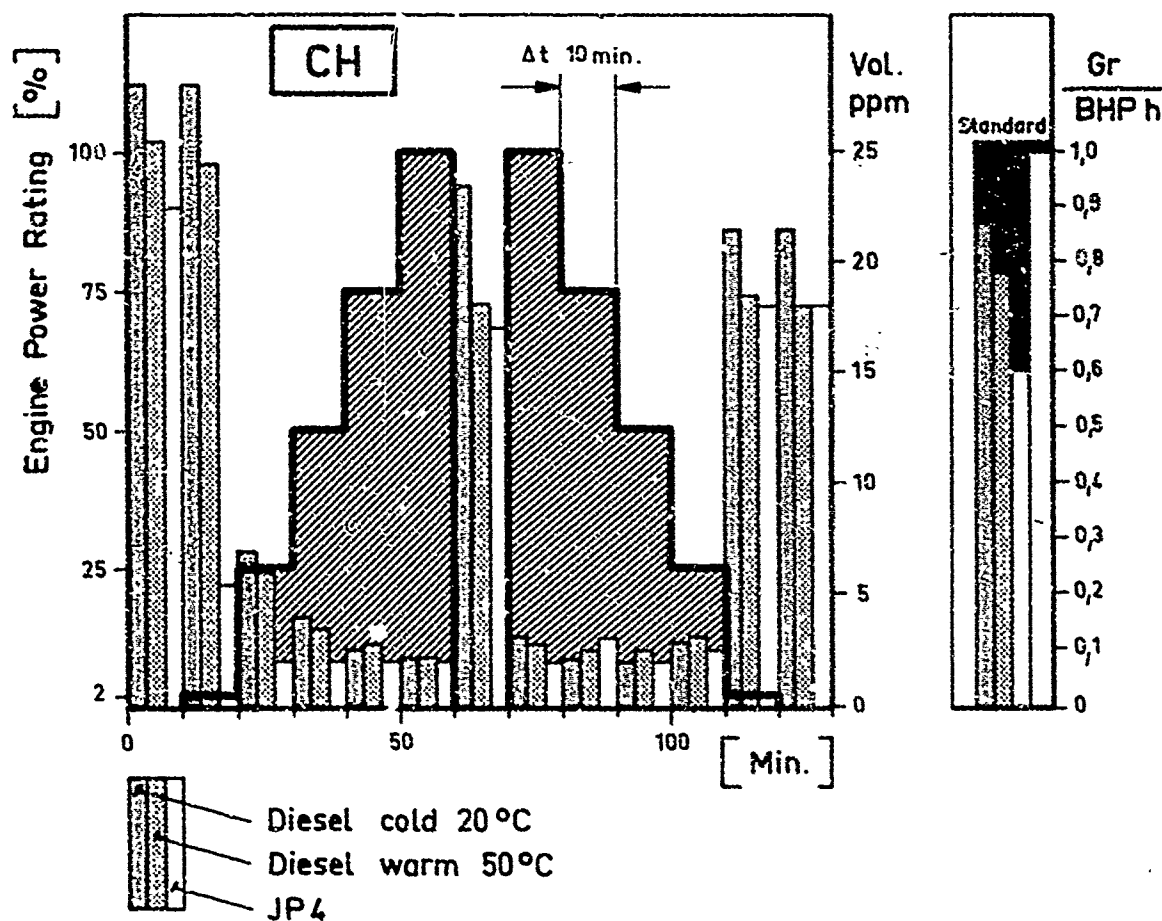


Fig. 2

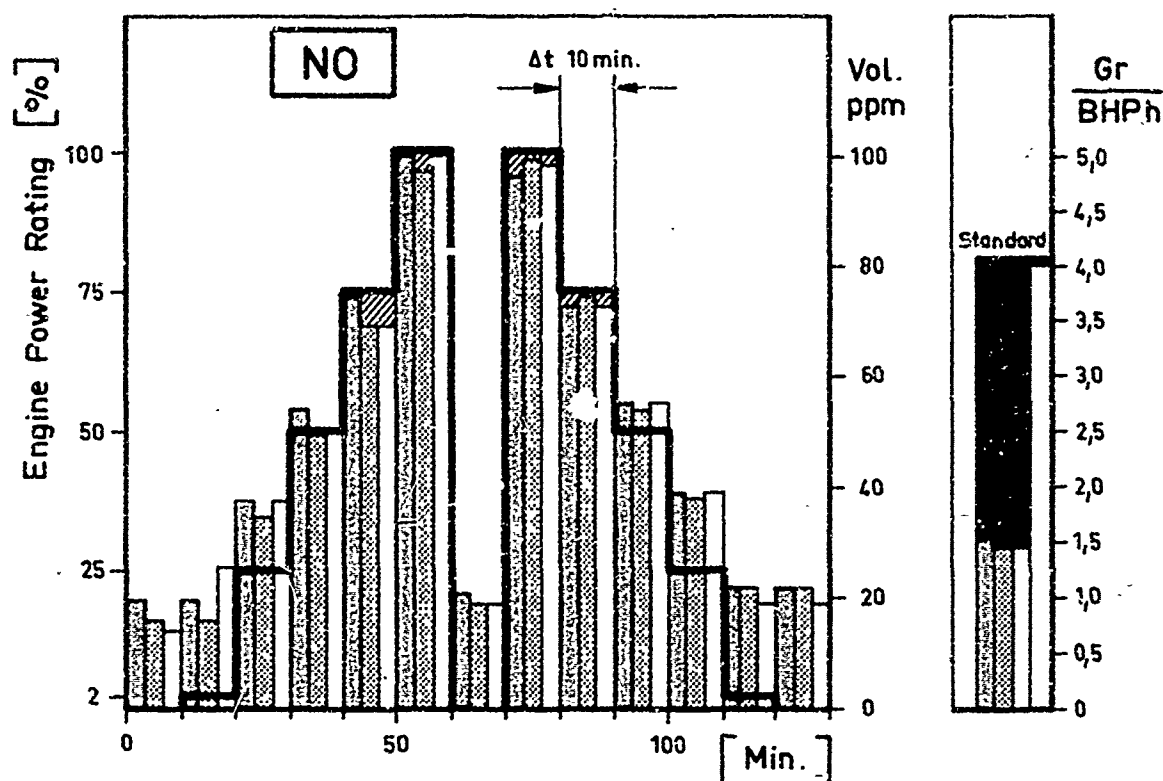


Fig. 3

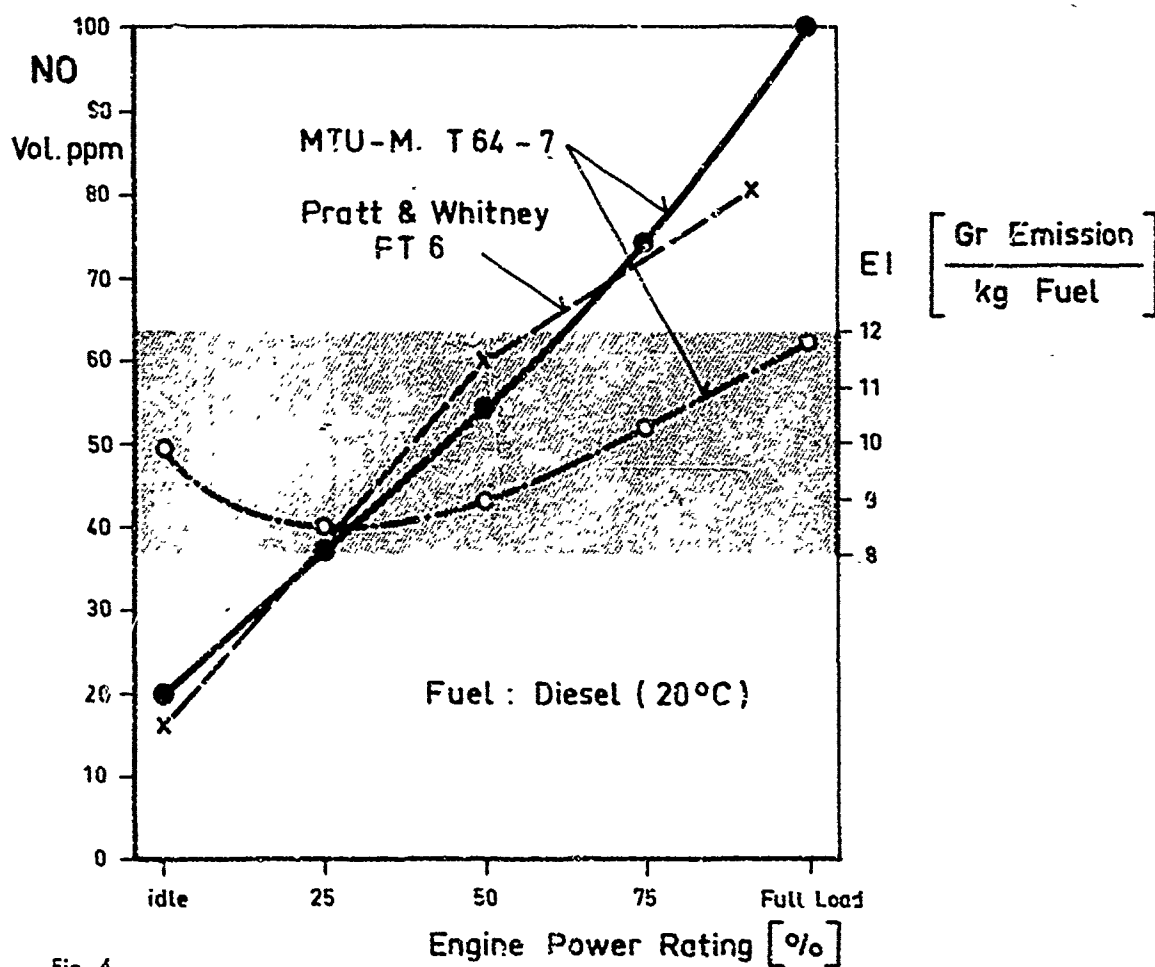


Fig. 4

NO FORMATION IN FUEL RICH FLAMES: A STUDY OF THE INFLUENCE OF THE HYDROCARBON STRUCTURE

K.H. Eberius and Th. Just

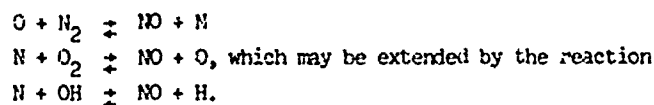
DFVIR - Institut für Reaktionskinetik, Stuttgart, Germany

SUMMARY

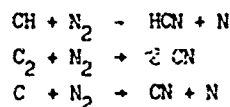
The formation of nitric oxide in premixed propane, ethylene and acetylene flames at 1 atm has been measured. Large overconcentrations of NO are found in very fuel rich flames. The NO formation in flames could be reasonably separated into three classes (a) Zeldovich mechanism with equilibrium O atom concentration, (b) Zeldovich mechanism with the remaining excess O atom concentration, (c) other reactions involving radicals as CH, C, C₂. The distinction of these classes can be made by studying the temperature dependence of the NO formation, by analysing the curvature of the NO profiles, by relating the rate of NO formation to O atom concentrations and by measuring HCN in some flames. The analysis of the temperature dependence of the NO formation in propane flames gave evidence, that in these flames with stoichiometric ratios between 1.2 and 1.4 and temperatures between 1850 °K and 2400 °K, reaction class (c) is the main reaction channel with the analytical formulation for the NO produced in these flames $[NO] = 0.0745 T^{-106}$ (dimensions in °K and ppm). A comparison of flames which have the same temperature at the same mixture strength, but differ in the chemical structure of the fuel, shows higher NO concentrations for acetylene flames and somewhat smaller NO concentrations for methane flames relative to the concentrations in propane flames.

1. INTRODUCTION

Detailed investigations of combustion processes showed, that various reaction channels contribute to the NO formation in flames. The relative importance of the channels depends of course on the nature of the actual flame. At high temperatures in the stoichiometric and fuel lean regime, the main NO formation can be attributed to the mechanism suggested by Zeldovich (1)



At high temperatures it is convenient and reasonable to calculate the NO production using equilibrium concentrations of the O atoms, which results for certain conditions in a linear relationship between NO concentration and time. At lower temperatures, however, the relatively more important O atom excess concentrations near to the main reaction zone should not be neglected in the calculations. In fuel rich flames additional reactions as proposed by Fenimore (2):



or by Bauer (3)

become important.

As the available data and their interpretations of NO formation in fuel rich hydrocarbon flames were contradictory, in a previous work (4) the NO formation in hydrocarbon-air flames has been investigated. The results were in agreement with Fenimore's measurements. The determination of HCN in propane flames supported his suggestions. Measurements of the nonlinear NO profiles in numerous adiabatic hydrocarbon-air flames made it possible to compute the NO formation in these flames by using these data together with the Zeldovich mechanism and O atom equilibrium concentrations. As the next step, the present paper deals with the influence of the temperature and the influence of the hydrocarbon structure on the formation of nitric oxide in or near the main reaction zone, the so-called "prompt NO", which together with the calculated NO, assuming Zeldovich mechanism and O atoms at equilibrium, gives the total NO formed in the adiabatic flames.

2. EXPERIMENTAL

The experimental set-up is nearly the same as described elsewhere (4). The flames were stabilized on a Meker-type burner of 7 cm diameter. The flow rates of the gases were metered by rotameters which were calibrated one against the other. The synthetic air was produced by feeding the burner with the appropriate amounts of normal air, oxygen and nitrogen. All gases were of technical purity. The mixture strength was changed by altering the fuel flow while the air flow remained constant. The cold gas velocities varied between 43 cm/sec and 70 cm/sec with respect to the burner area. Gas samples were withdrawn at different heights of the flames by a watercooled quartz probe and analysed for nitric oxide by an "W-light absorption technique. This technique avoids the condensation of water and shows no interferences with other components of the flame gases. The sensitivity is better than 1 ppm and the reproducibility is better than 5 per cent. The NO concentrations were measured between 2 and 5 cm above the burner. These NO profiles were linearly extrapolated, and the intercept at the height of the main reaction zone, which is for most flames between 1 and 10 mm above the burner, has been determined as the so-called "prompt NO". The extrapolation is accurate for mixture strengths greater than 1.1, but somewhat arbitrary for stoichiometric and lean flames as the slopes of these profiles are relatively large and not constant along the investigated distance.

3. RESULTS

Figures 1-3 show the "prompt NO" as a function of mixture strength for propane-, ethylene- and acetylene-synthetic air flames. The percentage r of oxygen in the synthetic air is constant along each profile. The equivalence ratio λ increases with increasing fuel concentration and is defined as the ratio of the actual fuel flow and the fuel flow, which would be needed for a stoichiometric conversion of the hydrocarbon to H₂O and CO₂ with the actual air flow. The temperature increases with increasing oxygen content r . The

temperatures of the propane flames $r = 25.9$ are about 550°K greater than the temperatures of the flames $r = 16.4$ for example. As a remarkable result the propane profiles show a strong increase of the "prompt NO" with increasing r resp. temperature at $\lambda = 1$. The $r = 24.6$ profile shows a maximum at $\lambda = 1$ and a less pronounced maximum at $\lambda = 1.35$. In contrast, the acetylene flames show maxima only in the fuel rich regime, while the character of the ethylene flames is between that of propane and acetylene flames.

4. DISCUSSION

a) INFLUENCE OF THE TEMPERATURE

To evaluate the influence of the temperature on the formation of "prompt NO", the "prompt NO" of the propane flames has been plotted as a function of temperature for various mixture strengths (Figure 4). These profiles correspond to profiles parallel to the ordinate in Figure 1, where some profiles had to be omitted for clarity of the diagram. The temperatures of the flames were assumed to be adiabatic flame temperatures calculated with the restriction that no hydrocarbons are present in the exhaust gases of the flames.

As a striking feature, the plot shows that the data points for $\lambda = 1.2$ up to $\lambda = 1.4$ and temperatures between 1850°K and 2400°K fit straight lines. For higher temperatures and near stoichiometric flames the profiles become much steeper. This behaviour could indicate that two mechanisms are responsible for the formation of the "prompt NO". In the fuel rich flames, NO may be formed by mechanisms as suggested by Fenimore (2), while in the stoichiometric regime and at high temperatures the influence of O atom super-equilibrium concentrations becomes dominant (3,4). With some reservation, the relative importance of such mechanisms could be obtained from the plot. If one would interpret the slope of the profiles as an activation energy and neglect dilution effects and the influence of the temperature on the flame structure and radical concentrations, which is certainly not correct, the straight line of Figure 4 for $\lambda = 1.3$ with the analytical representation $\text{NO} = 0.0745 T - 106$ (dimensions in $^\circ\text{K}$ and ppm) would correspond to an activation energy between 12 and 16 kcal/mol, whereas the steep profiles would correspond to an activation energy of 65 kcal/mol. This activation energy is of the same magnitude as the 75.4 kcal/mol activation energy of the reaction of oxygen atoms with nitrogen. For example it could be that for $\lambda = 1.1$ (Figure 4) and small temperatures the "prompt NO" is formed by the above mentioned mechanism, and above 2350°K the other mechanism becomes active, such that the profile represents the linear addition of both reaction paths. This interpretation of two reaction mechanisms is supported by our previous observations of HCN in fuel rich propane flames, and that the assumption of NO formation in rather fuel rich flames according to channel (b) would require unreasonable high concentrations of O atoms (4, 7). It should be noted that the low temperature values for $\lambda = 1.4$ in Figure 4 are much smaller than the other values, which will be discussed later.

b) INFLUENCE OF THE CHEMICAL STRUCTURE OF THE FUEL

To evaluate the influence of the hydrocarbon structure on the formation of "prompt NO", flames have to be compared, which have the same mixture strength and the same temperature, but differ in the structure of hydrocarbon. This comparison is made in the Figures 5-7. Figure 5 shows the "prompt NO" of adiabatic methane-air flames as a function of mixture strength. The appropriate propane and acetylene flames have the same temperature as the methane flame at the same equivalence ratio. A similar plot is made for adiabatic propane-air and ethylene-air flames, which give, according to the higher adiabatic flame temperatures of these flames, a comparison at higher temperature levels. Figure 5 shows that the "prompt NO" formation in methane flames is smaller than in propane flames, but the differences are not very significant. In the fuel rich regime, the NO concentration in methane flames and propane flames is about the same. The propane and acetylene flames of Figure 5 show similar concentrations in the fuel lean regime. At $\lambda = 1.3$ the acetylene flame, however, has produced 50 per cent more nitric oxide than the propane flame. The same difference of 50 per cent between acetylene and propane is shown in Figure 6 for the temperature level of the adiabatic propane-air flames from $\lambda = 0.85$ up to $\lambda = 1.4$. At $\lambda = 1.5$ the propane flame shows a NO concentration 6.5 times smaller than the acetylene flame. Ethylene shows a behaviour similar to propane, but the NO concentrations in the fuel lean regime are smaller. The same behaviour at higher concentrations is shown in Figure 7, where the temperature level is about 120°K higher than in Figure 6.

The behaviour of methane and ethylene is somewhat unexpected, while the high NO concentrations in the acetylene flames on the fuel rich side could be a consequence of high concentrations of C_2 and CH radicals and others supposed to be present in these flames.

It would be very difficult to interpret these results in terms of elementary chemical reactions. Direct measurements of the concentration of the species as O, CH, C, C_2 , C_3 should be made in the main reaction zone of flames to obtain more quantitative information.

c) INFLUENCE OF THE MIXTURE STRENGTH ON THE REACTION MECHANISM

It should be mentioned that the formation of the "prompt NO" in slightly fuel rich flames takes place up to several centimeters above the main reaction zone (curved NO profiles) whereas in richer flames this zone reduces to some mm and less (4, 8, 9). This behaviour becomes understandable if the hypothesis of the two reaction channels is accepted:

Previous measurements in a lean acetylene-oxygen flame at 0.1 atm show very sharp concentration maxima of H_2 and of radicals as excited OH and CH (10). The measured OH concentration, however, shows a broad maximum. The O atom concentration is about proportional because of partial equilibrium. In this particular case even a second maximum well downstream of the main reaction zone was found. It is not implausible to assume a similar behaviour in lean to stoichiometric flames at 1 atm. Therefore, if super-equilibrium O atoms are responsible for the "prompt NO" formation, the formation should be observable also at some distance of the main reaction zone. In fact, this statement agrees with the measurements for lean to slightly fuel rich flames. If radicals as excited CH are responsible, the formation should occur very close to and in the main reaction zone itself as in agreement with measurements in fuel rich flames. These considerations lead also to the conclusion that the "prompt NO" is formed predominantly by radicals as e.g. CH in fuel rich flames and by the amount of oxygen atoms which is above the equilibrium in fuel lean flames.

d) NO OVERCONCENTRATIONS

As the oxidation of N_2 to NO is a relatively slow process, the actual NO concentrations obtained in adiabatic flames are usually well below the equilibrium values of NO. However, in fuel rich propane flames at $\lambda = 1.4$ and temperatures below 2100 °K ($r = 21.85$ to $r = 17.25$, Figure 1), the measured NO concentrations are larger by a factor of 2 to 6 than predicted by calculations based on the assumption of thermodynamic equilibrium. Fenimore also quoted overconcentrations for his fuel rich acetylene flames (2). The measured values could eventually be explained partially by an error in the calibration of the gasflows. A small shift of the equivalence ratios calculated from the rotameter readings to smaller values would result in considerable smaller NO concentrations at the specified equivalence ratio.

Independent of the degree of the NO overconcentration, the measured NO concentrations decrease in a similar manner as the calculated equilibrium concentrations when the mixture strength increases. It is somewhat surprising that the "prompt NO" concentration in fuel rich flames observes equilibrium conditions as the "prompt NO" should be formed by radicals in large excess concentrations, and it is not quite understandable, that these concentrations, which are related to the total fuel conversion in the flame, should change by very large amounts, when the mixture ratio increases from 1.4 to 1.5 (Figure 1).

As it is unlikely, that the NO is formed by one step, other nitrogen containing hydrocarbons have to be postulated as intermediate species. The conversion of such intermediates to NO might be controlled by rates of reaction, which are related to species concentrations determined by thermal equilibrium. This could give an explanation of the strong decrease of the NO concentration in increasingly richer flames. Such an intermediate species could be HCN as observed in previous experiments (4). If for the propane flame $\lambda = 1.5$, $r = 21.0$, the measured HCN concentration was added to the measured NO concentration, the same value was obtained which is predicted by the straight lines of Figure 4 (the profile for $\lambda = 1.5$, which is similar to the profile for $\lambda = 1.4$ but shifted, has not been included in this figure because of clarity of the drawing). If the result could be observed also for other mixture ratios and temperatures, it would be possible to predict the sum of NO and HCN concentration in fuel rich flames. The measured overconcentrations of nitrogen compounds in flames of the fuel rich regime are then even higher if not only the NO is considered and measured.

5. ACKNOWLEDGEMENT

The financial support of the Deutsche Forschungsgemeinschaft is gratefully acknowledged by the authors.

6. LITERATURE

- (1) Zeldovich, J. (1946). The Oxidation of Nitrogen in Combustion and Explosions, *Acta Physicochimica URSS* 21, 577.
- (2) Fenimore, C.P. (1971). Formation of Nitric Oxide in Premixed Hydrocarbon Flames, Thirteenth Symposium (International) on Combustion, Combustion Institute, Pittsburgh, p. 373.
- (3) Bauer, S.H. (1971). Comment, Thirteenth Symposium (International) on Combustion, Combustion Institute, Pittsburgh, p. 379.
- (4) Bachmaier, F., Eberius, K.H. and Just, Th. (1973). Combustion Science and Technology (in press).
- (5) Sarofim, A.P. and Pohl, J.H. (1972). Kinetics of Nitric Oxide Formation in Premixed Laminar Flames. Fourteenth Symposium (International) on Combustion, Combustion Institute, Pittsburgh (in press).
- (6) Bowman, C.T. (1971). Investigation of Nitric Oxide Formation Kinetics in Combustion Processes: The Hydrogen-Oxygen-Nitrogen Reaction. *Combustion Science and Technology* 3, 37.
- (7) Iverach, D., Basden, K.S. and Kirov, N.Y. (1972). Formation of Nitric Oxide in Fuel-Lean and Fuel-Rich Flames. Fourteenth Symposium (International) on Combustion. Combustion Institute, Pittsburgh (in press).
- (8) Bowman, C.T. (1971). Comment, Thirteenth Symposium (International) on Combustion, Combustion Institute, Pittsburgh, p. 379.
- (9) Fenimore, C.P. (1971). Comment, Thirteenth Symposium (International) on Combustion, Combustion Institute, Pittsburgh, p. 379.
- (10) Eberius, K.H., Hoyermann, K. and Wagner, H.Gg. (1972). Structure of Lean Acetylene-Oxygen Flames. Fourteenth Symposium (International) on Combustion. Combustion Institute, Pittsburgh (in press).

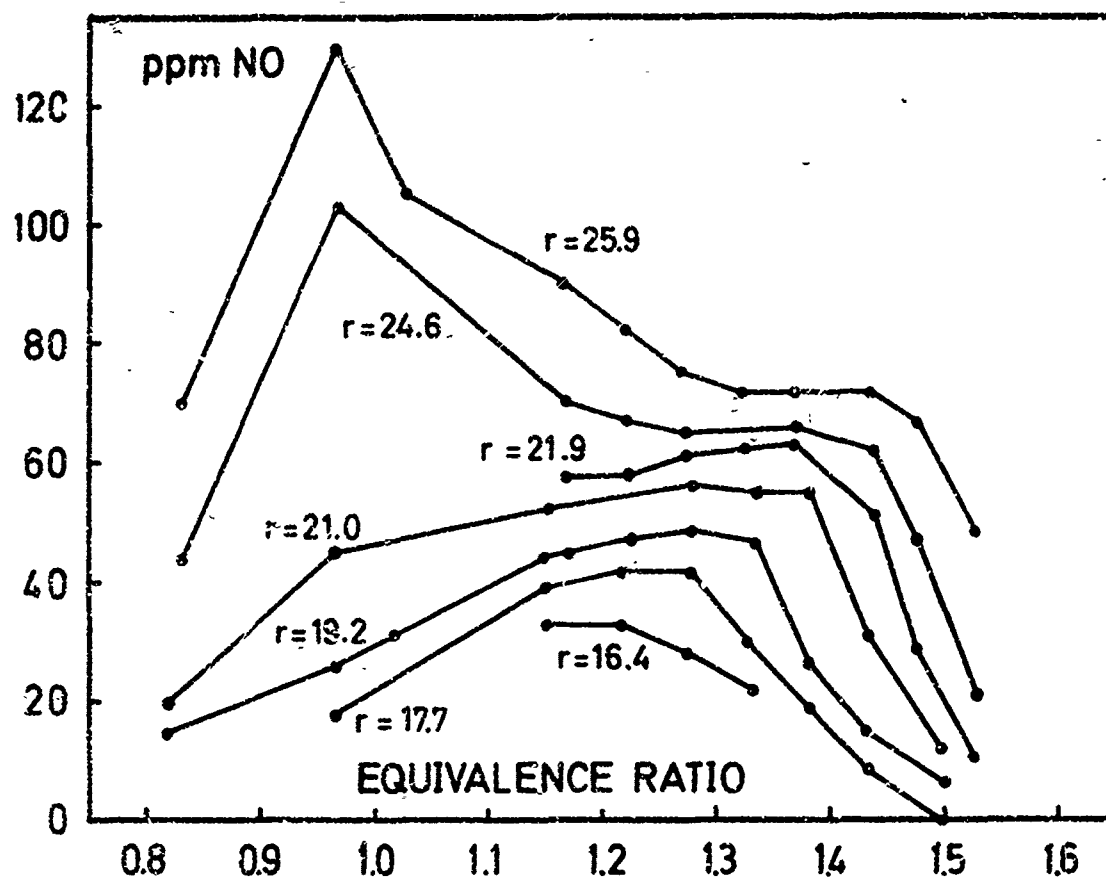


FIGURE 1: "PROMPT NO" IN ADIABATIC PROPANE-SYNTHETIC AIR FLAMES AS A FUNCTION OF THE MIXTURE STRENGTH (r = PERCENTAGE OF OXYGEN IN THE SYNTHETIC AIR)

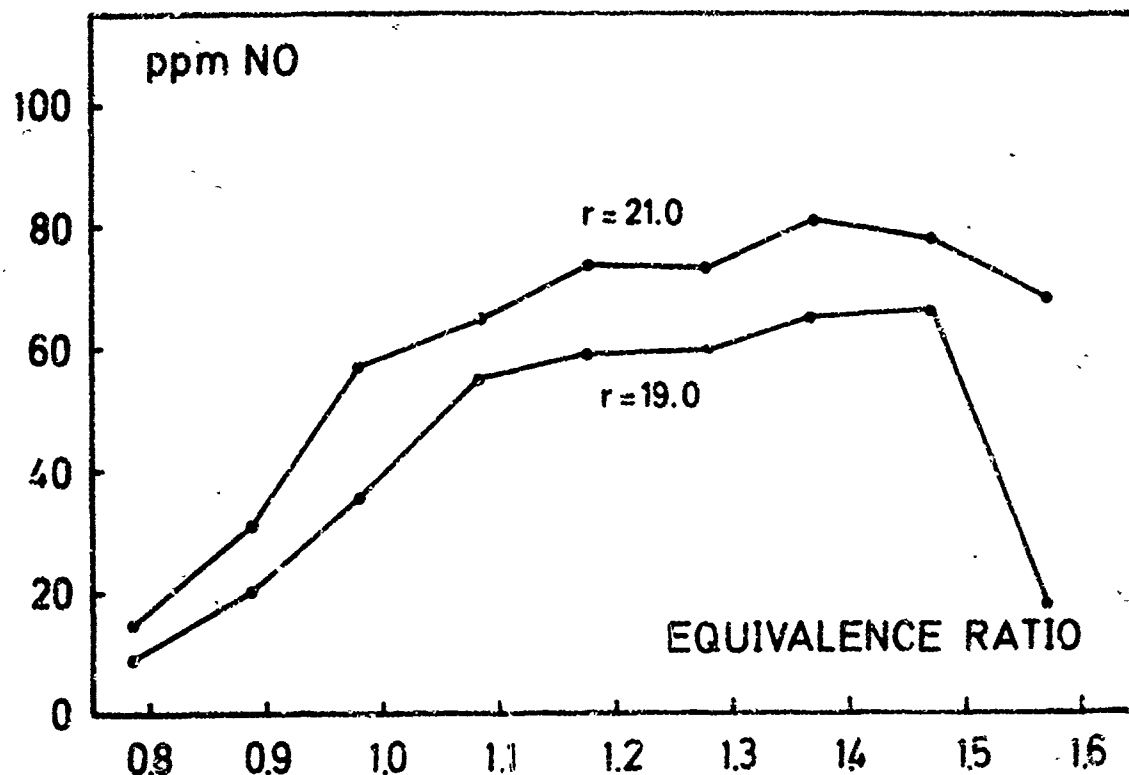


FIGURE 2: "PROMPT NO" IN ADIABATIC ETHYLENE-SYNTHETIC AIR FLAMES AS A FUNCTION OF THE MIXTURE STRENGTH (r = PERCENTAGE OF OXYGEN IN THE SYNTHETIC AIR)

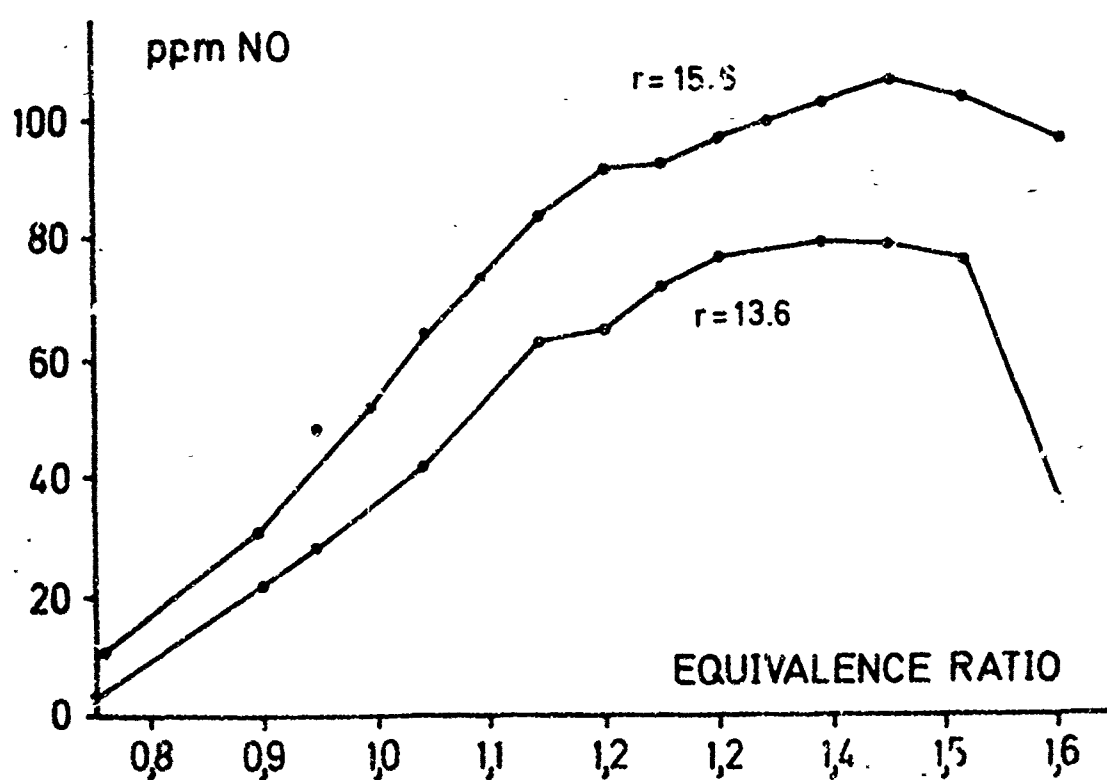


FIGURE 3: "PROMPT NO" IN ADIABATIC ACETYLENE-SYNTHETIC AIR FLAMES AS A FUNCTION OF THE MIXTURE STRENGTH (r = PERCENTAGE OF OXYGEN IN THE SYNTHETIC AIR)

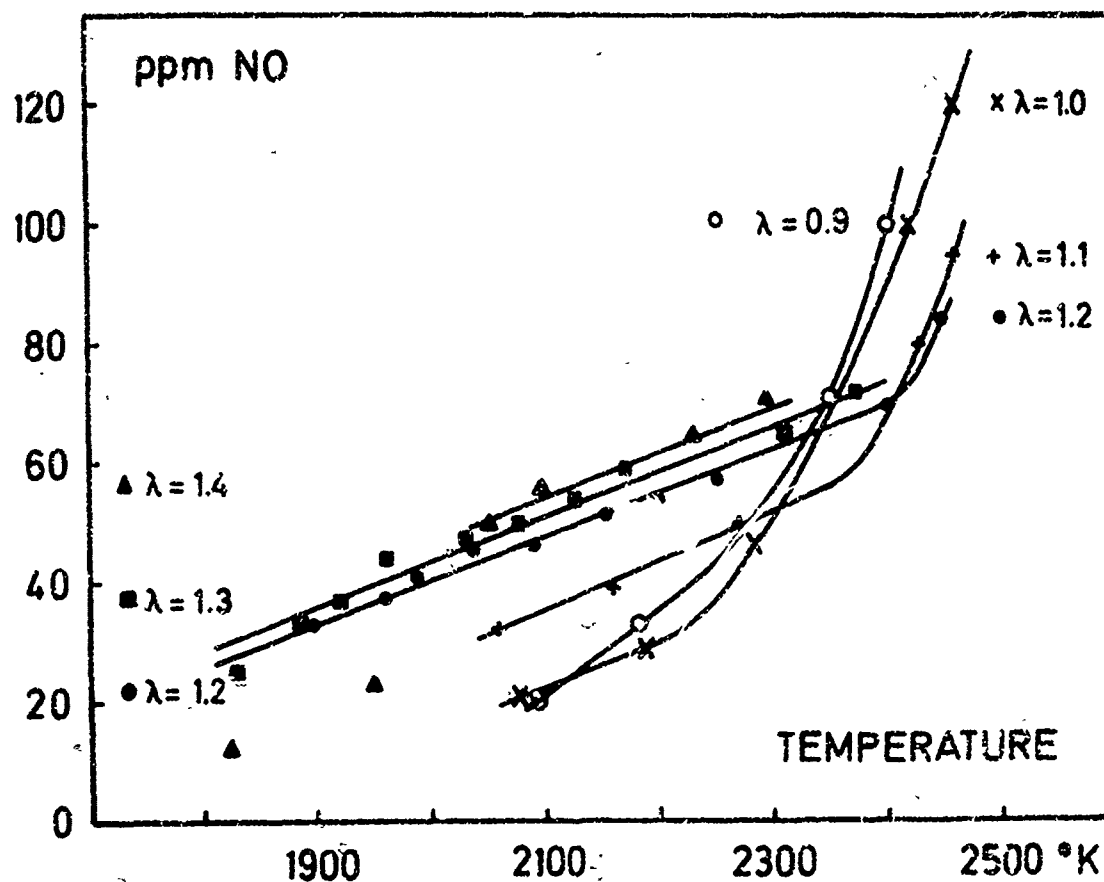


FIGURE 4: "PROMPT NO" AS A FUNCTION OF THE TEMPERATURE AT VARIOUS MIXTURE STRENGTHS λ IN ADIABATIC PROPANE-SYNTHETIC AIR FLAMES

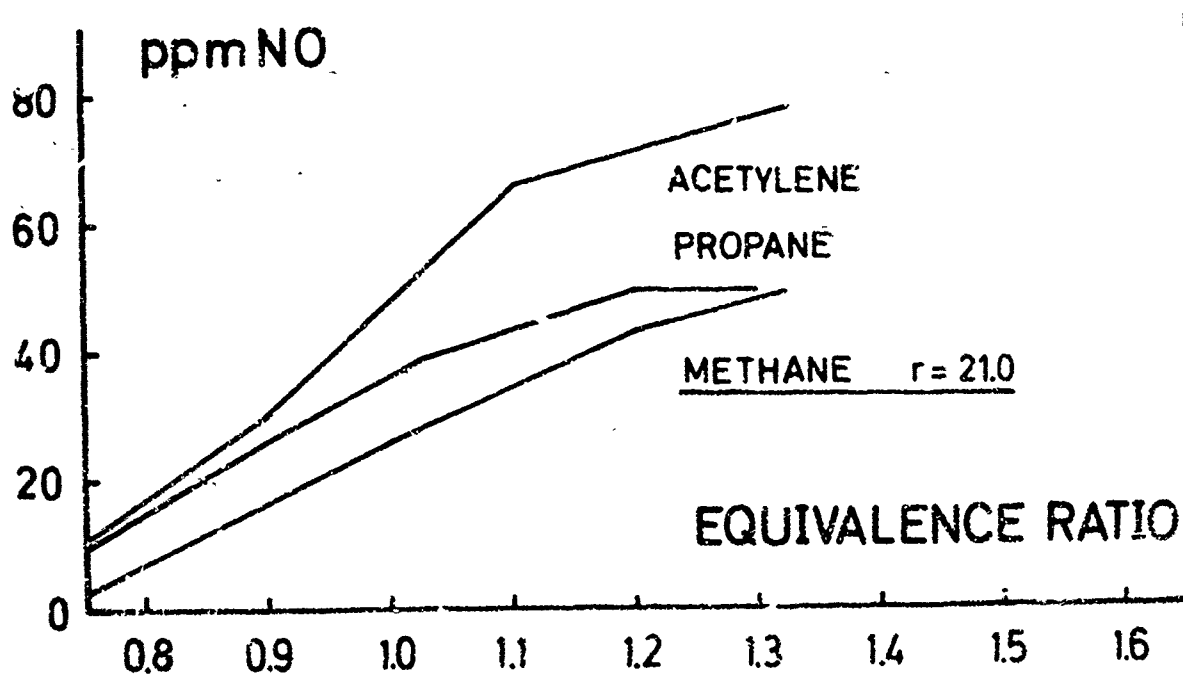


FIGURE 5: "PROMPT NO" IN ADIABATIC METHANE AIR FLAMES AND IN PROPANE-SYNTHETIC AIR RESP. ACETYLENE-SYNTHETIC AIR FLAMES FOR WHICH THE TEMPERATURES ARE THE SAME AT THE SAME MIXTURE STRENGTH

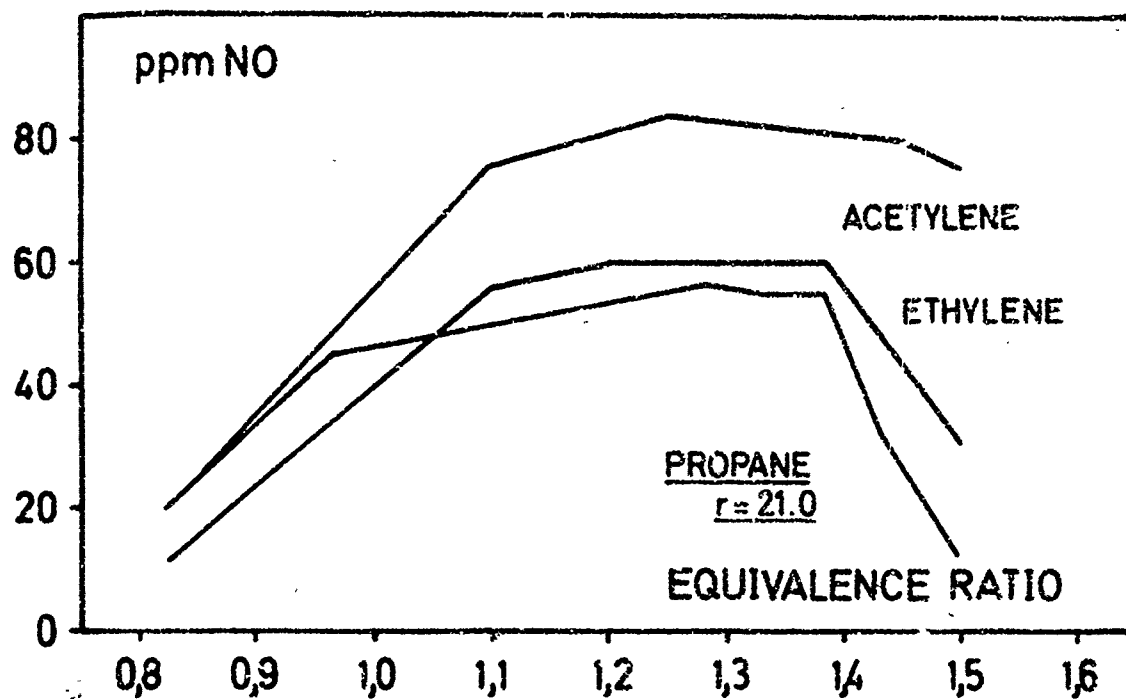


FIGURE 6: "PROMPT NO" IN ADIABATIC PROPANE AIR FLAMES AND IN ETHYLENE-SYNTHETIC AIR RESP. ACETYLENE-SYNTHETIC AIR FLAMES FOR WHICH THE TEMPERATURES ARE THE SAME AT THE SAME MIXTURE STRENGTH

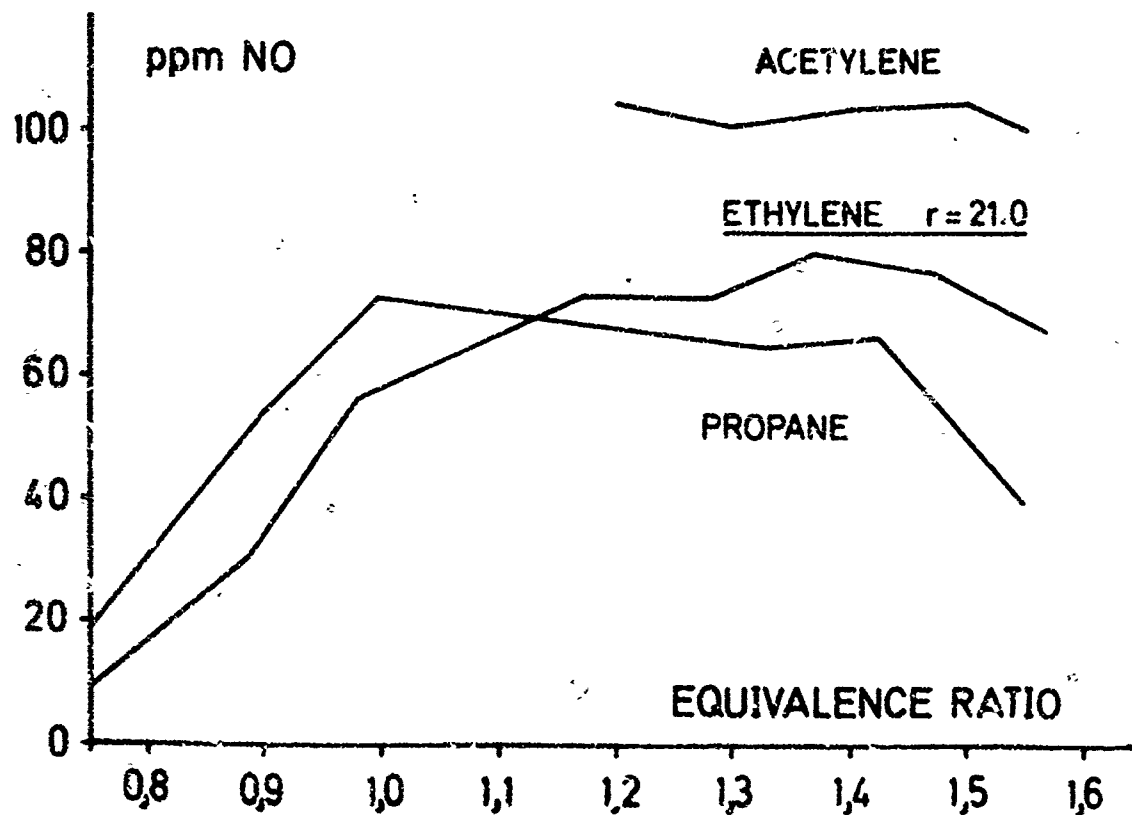


FIGURE 7: "PROMPT NO" IN ADIABATIC ETHYLENE AIR FLAMES AND IN PROPANE-SYNTHETIC AIR RESP. ACETYLENE-SYNTHETIC AIR FLAMES FOR WHICH THE TEMPERATURES ARE THE SAME AT THE SAME MIXTURE STRENGTH

Discussion on the Paper

NO FORMATION IN FUEL RICH FLAMES: A STUDY OF THE INFLUENCE OF THE HYDROCARBON STRUCTURE

(Paper 16)

presented by

K. H. Eberius and Th. Just

C. T. Bowman

The dependence of "prompt NO" on temperature, stoichiometry and fuel-type reported in this paper is additional information on the NO formation process in combustion of rich hydrocarbon fuels. Interpretation of the results, however, is hampered by the fact that the extrapolation technique used to determine "prompt NO" results in the "prompt NO" being dependent not only on the NO formation rate near the flame zone, but also on the rate late in the flame. This shortcoming aside, it is clear that the present experimental results are telling us that there are differences in the NO formation process in lean and rich hydrocarbon flames. The authors' interpretation of what their data mean in terms of the NO formation mechanism is plausible, but by no means unique. The possibility of non-equilibrium radical concentrations contributing significantly to NO formation in rich flames cannot be ruled out at this time. Until measurements of radical concentrations and NO formation rates have been made, preferably in low pressure flames where the structure of the flame zone can be adequately resolved, it will be difficult to draw definitive conclusions concerning the mechanism for NO formation in rich hydrocarbon flames.

Authors

In fact the extrapolation procedure for determining the "prompt NO" has to be handled with caution. Particularly in lean and near stoichiometric flames the errors may be considerable. However, in fuel rich flames, e.g. propane flames $\lambda > 1.2$, the NO concentration remains nearly constant in the burnt gas above 1 cm height above the burner (Fig. 3 of Ref. 4), thus the determination of the "prompt NO" is very accurate for these flames. The "prompt NO" determined for the investigated flames is the NO formed additionally to the NO which is formed assuming equilibrium conditions. In any case superequilibrium concentrations of radicals are responsible for the formation of the "prompt NO". Whereas in the fuel lean flames mainly O atoms appear to be responsible for the "NO prompt" formation, other radicals have to be postulated for fuel rich flames, as appropriate O atom concentrations are unreasonably high. The existence of radicals other than O atoms is supported by the HCN concentrations and by the temperature dependence of the "prompt NO" found in fuel rich flames. Which particle and which mechanisms contribute to the "prompt NO" formation is unknown at present. The HCN for example might be a precursor of the NO or it might only accompany the NO formation. It would be worthwhile to search for other nitrogen containing hydrocarbons in fuel rich flames. We agree that measurements of radical concentrations in low pressure flames should be made to elucidate the NO formation process in fuel rich flames.

MESURES DES CONSTITUANTS MINEURS DANS LA STRATOSPHERE PAR CONCORDE 001

par

R. JOATTON

Aérospatiale

Direction Technique Avions

Paris, France

1. L'AEROSPATIALE ET L'ENVIRONNEMENT STRATOSPHERIQUE

Les préoccupations liées au rapport de l'avion stratosphérique - c'est le cas de Concorde sur plus de 90% d'un trajet tel que PARIS-NEW YORK - avec l'environnement sont depuis près de 10 ans à l'ordre du jour en Grande-Bretagne et en France; c'est ainsi que le sous-groupe médical Concorde a animé depuis 1963 des expérimentations sur l'influence des conditions biologiques du vol sur l'équipage et les passagers, en ce qui concerne particulièrement le niveau de radiations cosmiques galactiques.

Dans le domaine du retentissement du véhicule stratosphérique sur son environnement, dès que les Conférences de Williamsburg (S.C.E.P.) et de Stockholm (S.M.I.C.) organisées en 1970 et 1971 par le M.I.T. eurent développé un certain nombre de recommandations concernant la stratosphère, l'Aérospatiale a décidé de mettre en œuvre leur application. Elle pouvait, ainsi que la B.A.C., apporter à cette tâche la disponibilité d'un prototype Concorde comme laboratoire volant pour l'exploration de la stratosphère.

L'Aérospatiale a donc défini en 1970 et 1971 un programme d'études théoriques et d'essais en vol avec la collaboration scientifique d'organismes européens (Centre National des Etudes Spatiales, Commissariat à l'Energie Atomique, Office National d'Etudes et de Recherches Aérospatiales (ONERA), Université de Paris, de Rennes et de Toulouse, etc...), et s'appuyait sur l'Institut d'Aéronomie Spatiale de Belgique en ce qui concerne les constituants mineurs.

La création en Octobre 1972 d'un organisme gouvernemental interministériel, le Groupe d'Etudes sur les conséquences des vols stratosphériques (COVOS), a permis d'élargir ce programme indépendant en harmonie avec les programmes internationaux de l'étude de la stratosphère (Climatic Impact Assessment Program des U.S.A., Committee of Consequences on Meteorology of Stratospheric Aircraft de Grande-Bretagne). Le groupe d'Etudes COVOS est présidé par le Professeur E.A. BRUN, et sa tâche est de gérer et d'élargir le programme précédent.

En ce qui concerne les constituants mineurs de la stratosphère, et les sources nouvelles de ces constituants apportées par les émissions des flottes stratosphériques, le programme français a abouti à la même logique que le C.I.A.P. en déterminant 3 phases principales d'études :

- a) Détermination de profils verticaux, à la période initiale actuelle du vol stratosphérique pour les principaux constituants mineurs, à l'aide de mesures au sol, ou portées par ballons ou avions. Pour ces dernières, le Concorde 001 doit mettre à leur service ses possibilités en altitude. Pour les ballons, le programme est défini en liaison avec le C.N.E.S. en prêtant une attention particulière aux projets que ce dernier développe avec la Météorologie Nationale, tels que ESSOR et SPEIRE.
- b) Détermination des ébits unitaires en constituants mineurs provenant des réacteurs Olympus, par essais ou simulation au sol. L'estimation du développement de la flotte et des principales routes aériennes correspondantes donne la source locale en constituants mineurs. Des mesures in situ sur panache d'émission d'un Concorde en vol stratosphérique, soit par avion quiveur qui pourrait du reste être un autre Concorde, soit par passage à proximité d'un ou plusieurs ballons formant simple ou double hôte ont été envisagées, mais non retenues pour l'instant.
- c) Préviation des perturbations éventuelle apportées par ces sources stratosphériques (a, b) aux profils verticaux initiaux mesurés (§ a). Cette forme de prévisions exige le développement de modèles mathématiques suffisamment approchés, notamment dans le domaine de la physicochimie des constituants mineurs, et la nécessité de tenir compte des mouvements atmosphériques.

2. PROGRAMME D'ETUDES DES CONSTITUANTS MINEURS

Les développements précédents expliquent que l'Aérospatiale se soit engagée à l'origine dans les voies suivantes :

2.1 - Dans le domaine des modèles mathématiques, définition d'un modèle bidimensionnel associant la cinétique au transport. Recherches des valeurs numériques adéquates par liaison avec l'ensemble des expérimentateurs.

2.2 - Dans le domaine des mesures stratosphériques, définition d'une instrumentation qui permette 3 phases de travail :

2.2.1 - Contribution à des profils verticaux actuels de la stratosphère concernant notamment NO , NO_2 , N_2O , NO^3H , CH_4 , CO , O_3 , H_2O . Dans la définition d'un appareillage de mesures correspondantes, les techniques par voie chimique, par prélèvement in situ, ont été rapidement écartées pour manque de sensibilité au profit des techniques optiques employées :

- soit in situ en définissant des chemins optiques suffisants à l'intérieur de l'avion pour les composants qui resteraient intacts à l'introduction à travers les étages du réacteur, qui porte l'air d'admission à 400°C , ou bien à l'extérieur de l'avion si les problèmes d'onde de choc et de vibration liés au régime supersonique le rendait possible. Ces solutions n'ont pas été retenues au premier stade;

- soit par des mesures de détection à distance à l'extérieur de l'avion, lesquelles sont susceptibles de donner des mesures locales par des méthodes différentielles.

2.2.2 - Les appareillages ainsi définis pourraient dans une 2ème phase conduire à une précision de quelques pour cents dans une série de mesures systématiques, dont le lissage permettrait d'effacer le caractère saisonnier. En relation avec le modèle mathématique cinétique-transport dont il a été question, l'occasion de perturbations naturelles ou artificielles permettrait de mesurer des évolutions qui, servant en quelque sorte de schéma inverse au modèle cinétique-transport, autoriseraient la détermination globale d'un certain nombre de paramètres.

2.2.3 - Une évolution distincte de l'appareillage de départ doit rapidement conduire à une miniaturisation permettant son embarquement sur certains avions de ligne. Ainsi sera réalisé le contrôle systématique des constituants mineurs : commandé au départ par les documents du MIT.

3. CHOIX DES METHODES DE MESURES OPTIQUES PORTEES DES CONSTITUANTS MINEURS

Le choix de la méthode de mesures déterminée fin 1971 en commun avec l'Institut d'Aéronomie de Belgique s'est basé sur les critères suivants :

- sensibilité aux principaux constituants mineurs
- rapidité et simultanéité de résultats concernant le plus grand nombre de constituants mineurs
- compatibilité avec la volée aérienne et les accélérations induites sur Concorde
- Facilité d'industrialisation dans un laps de 2 ans pour aboutir à un matériel simple de contrôle de routine.

La détection dans l'infrarouge, sans être sans doute la seule méthode possible, apporte une réponse favorable à ces différents points; en effet la plupart des constituants mineurs ont des signatures d'absorption individualisées dans la bande de $1\ \mu$ à $1\ \text{cm}$; la méthode paraît pouvoir faire face à la précision nécessaire, qui atteint l'ordre de la p.p.b. pour les oxydes de l'azote. Ce type d'appareillage est adapté aux vols et notamment aux accélérations induites. Il permet l'élaboration de générations ultérieures de très haute résolution, et répondant ainsi au 2° point du programme (détermination globale de paramètres numériques du modèle), aussi bien que celles d'appareils spécifiques d'industrialisation simple et travaillant dans une bande de longueur d'onde réduite correspondant à la réponse d'un constituant ; on aurait ainsi une réponse au 3° point du programme, qui est la définition d'appareillage de contrôle spécifique à un constituant.

Sans méconnaître les avantages des autres méthodes possibles, la décision fut prise fin 1971 d'axer la détection des constituants mineurs sur un "remote sensing" multiple dans la bande de l'infrarouge.

En fonction des ressources instrumentales "détection infrarouge" en France, de l'expérience acquise en vol, notamment sur Caravelle, et en complémentarité avec le programme britannique il a paru opportun dans la première phase des expérimentations Concorde (campagne 1973 du prototype 001) de combiner les différentes possibilités techniques en réunissant des résultats spectrométriques dans le domaine proche et dans le domaine lointain. Le domaine proche (vibration rotation) est le champ des expérimentations de l'ONERA (Dr GIRARD) et aussi du JPL (Jet Propulsion Laboratory) (Dr FARMER) avec qui la France fût mise en relation par l'intermédiaire du CIAP. Ces appareillages fonctionnent donc par absorption sur visée solaire.

Le domaine de l'infrarouge lointain (rotation pure) est le champ des expérimentations de l'Observatoire de Meudon (Dr LENA et Dr MARTEN) et du National Physical Laboratory (Docteurs STONE, HARRIES et BLACKMAN). La technique utilisée est l'émission du fond de ciel puisque le soleil n'est pas un émetteur dans cette bande (émission limitée à $0,6 \mu$).

La décision d'implanter sur Concorde 001, aussi simultanément qu'il était compatible afin d'avoir des résultats comparables, les appareillages précédents, fût prise en y ajoutant un fluxmètre de l'ultraviolet réalisé à Verrières par l'équipe du Pr BLAMONT et du Dr CHANIN; ce fluxmètre permet dans chaque bande de longueur d'onde de connaître l'énergie lumineuse disponible, et de remonter aux sources photochimiques des constituants mineurs.

Nous décrirons donc très sommairement les différents appareils implantés avant de passer aux problèmes liés à l'implantation à bord et au programme des mesures.

4. DEFINITION SOMMAIRE DES APPAREILLAGES EMBARQUES

4.1 - Rappelons brièvement les grandes catégories techniques auxquelles correspondent les appareillages retenus :

- spectromètre à fente où le pouvoir de collection et d'énergie lumineuse est proportionnelle à la largeur de la fente à laquelle la résolution est donc inversement proportionnelle
- spectromètre à grille, de principe semblable au précédent, mais où le découpage d'une mince plage de longueur d'onde se fait par réflexion sur une grille adaptée
- interféromètre qui, à la différence des précédents, travaille sur toutes les longueurs d'onde (effet multipler). En fonction d'un déplacement géométrique continu (chariot-miroir) on enrichit progressivement le spectre sur toute la plage de longueur d'onde et on dispose pour cela d'un grand pouvoir de collection et d'une grande résolution sous un encombrement réduit.

4.2 - Interféromètre du J P L

C'est un interféromètre de FOURRIER à grande rapidité, construit sur l'idée initiale de P. CONNES travaillant dans la bande de $1,2 \mu$ à $5,5 \mu$ (1.800 à 8.000 cm^{-1}). Le spectre entier est ainsi balayé dans un temps de 2 à 3". La résolution est de $0,25 \text{ cm}^{-1}$.

L'appareil, embarquable sur satellite et navette spatiale, a fait ses preuves dans l'étude de la pollution; il a, aux altitudes Concorde, une sensibilité de quelques p.p.b. (10^{-9}) aux espèces suivantes : CO , CO_2 , N_2O , NO , NO_2 , SO_2 , O_3 , H_2O et les hydrocarbures inférieurs. Il est adaptable à un certain nombre d'autres constituants mineurs.

L'interféromètre, contrôlé par une source monochromatique (Laser Helium-Néon 6328.Å) permet un balayage par sauts à vitesse non constante pour tenir compte des perturbations inévitables au cours des vols stratosphériques.

Une certaine réduction du poids et d'encombrement de l'appareillage associé, qui comprend 4 racks, a été réalisée facilement pour l'embarquement sur Concorde.

4.3 - Spectromètre infrarouge à grille de l'ONERA

L'ONERA a étudié et réalisé sur contrat D.R.M.E. depuis plusieurs années un spectromètre d'absorption à grande luminosité qui, associé à un pointeur solaire utilisé sur fusée sonde, répond au problème précédent et l'a prouvé sur des vols "Caravelle" réalisés dans le 2ème semestre de 1972. Il s'agit d'un spectromètre infrarouge à grille dont les spécifications techniques découlent du tableau suivant :

- domaine spectral d'utilisation
 - 1/ du spectromètre seul 4000 cm^{-1} à 700 cm^{-1}
 - 2/ du spectromètre associé à une optique d'entrée en fluorine = 4500 cm^{-1} à 1250 cm^{-1}
- limite de résolution spectrale $0,15/0,08\text{ cm}^{-1}$
- enregistrement des spectres sur enregistreur magnétique analogique
- poids : 150 kg
- dimensions : $150 \times 40 \times 60\text{ cm}$ (hors tout, héliostat inclus)
- consommation électrique : voisine de 500 watts
- précision de pointage exigée (par rapport au soleil par le travers : $\pm 5^\circ$)

La vitesse de balayage de $0,2\text{ cm}^{-1}$ par seconde implique que l'analyse d'un intervalle spécifique tel que $1350\text{ cm}^{-1}/1250\text{ cm}^{-1}$ (c'est-à-dire $7,4\mu$, 8μ) se passe en un peu plus de 4"; l'intérêt d'une telle bande est de contenir des zones d'absorption très intenses de CH_4 , NO , NO_2 , SO_2 , et N_2O , ainsi qu'une bande assez forte de HC HO . Par ailleurs la bande du méthane de 1306 cm^{-1} est bien connue de l'ONERA et l'étalonnage des spectres atmosphériques dans cette région en est grandement facilitée.

La stratégie des visées solaires implique que le trajet optique dans l'atmosphère devant être le plus grand possible, on prendra le soleil bas sur l'horizon (entre $+10^\circ$ et -2°). Une visée à élévation plus grande se fera pour la connaissance du spectre solaire lui-même.

4.4 - Interféromètre de l'Université de Maudon.

Il s'agit d'un spectromètre qui travaille dans l'infrarouge lointain dans la bande 40 à 200 cm^{-1} ; il utilise les techniques de la spectroscopie de FOURIER sur un interféromètre de MICHELSON, dont la modulation de phase est créée par un miroir secondaire vibrant. L'instrument a volé sur Caravelle expérimentale du Centre d'Essais en Vol de Brétigny (Juillet 1972), en travaillant en émission plutôt qu'en absorption. Le procédé permet des mesures de nuit, ce qui est fort intéressant pour la photochimie atmosphérique.

La course maximum du miroir de MICHELSON est de 40 cm donc la résolution théorique est de $0,067\text{ cm}^{-1}$ variant en fait entre $0,2$ et $0,07$. Chaque pas du mouvement de miroir a une longueur de 20μ . La lame de mylar qui crée les interférences a une épaisseur variant de 20 à 50μ . L'élément de détection est un bolomètre à germanium dopé (Infrared lab, Tucson, Arizona) travaillant à 2° K par refroidissement à l'hélium liquide. Les interférogrammes, qui représentent la transformée de FOURIER des échanges d'énergie entre la stratosphère et l'appareil expérimental, sont enregistrés magnétiquement, puis dépouillés à terre.

Le système ne présente pas d'interférence avec le système électrique à bord. L'appareil entier est monté sur un dispositif antivibratoire de coupure 7 Hz .

Les spectres obtenus sur Caravelle à 39.000 pieds montrent le plus nettement les lignes de rotation de H_2O , les triplets de O_2 et les branches principales de l'ozone. La mise en évidence de CO , NO , etc... paraît possible dans les conditions d'altitude.

Une simulation faite dans une chambre au sol sur source corps noir a montré qu'aucune des lignes faibles n'était des "Artifacts" expérimentaux.

4.5 - L'appareil du N P L.

Cet appareil est un interféromètre à transformée de FOURIER travaillant dans la limite de la zone d'infrarouge lointain (400 cm^{-1} à 10 cm^{-1}), dans une zone 33 cm^{-1} à 5 cm^{-1} limitrophe des ondes micrométriques; les mesures se placent donc en bonne position de compromis entre la haute précision requise en infrarouge et la complexité des installations micrométriques. Cet appareillage est celui qui a été monté sur COMET du N P L et sur le Concorde 002 durant son périple en Extrême-Orient de Juin 1972 par HARRIES et ses collaborateurs.

Le principe du fonctionnement de cet appareil est proche du précédent; le rayonnement pénétrant à travers le hublot est renvoyé en partie par un miroir à 45° , l'autre partie étant non déviée. Après réflexions sur 2 miroirs à 90° dont l'un mobile, le faisceau est reconstitué sur un détecteur à l'antimoniure d'indium refroidi à 2° K à l'hélium liquide;

* Le bolomètre a pour atout une grande détectivité presque constante dans toute la gamme des longueurs d'onde.

c'est la détection qui est différente de celle de l'appareil de Meudon. La résolution ainsi maximale est voisine de $0,05 \text{ cm}^{-1}$.

Durant sa tournée en Extrême-Orient, cet appareil semble avoir fourni des indications au moins qualitatives sur des raies liées à NO_x , HNO_3 , SO_2 . Des essais de profils tracés en fonction de la latitude ont été tentés.

4.6 - Fluxmètre du CNRS (Service d'Aéronomie).

Il sert à une mesure de flux solaire ultraviolet proche et visible durant les vols Concorde. Il mesure les variations de quantités totales d'ozone (bande d'absorption de HARTLEY) et d'oxygène (bande de SCHUMANN RUNGE).

Le photomètre est placé derrière un hublot en fluorine transmettant à 100°C entre 3.200 et 7.000 Å. L'angle de visée est de $+4^\circ$ par rapport à la normale horizontale. L'angle d'élévation solaire est de $+10^\circ$ à -2° . Le champ du photomètre est de 20° . Le photomètre se décompose en :

- un ensemble de détection photodiodes
- un ensemble de mesure électromètre et alimentation
- un enregistrement magnétique.

5. PROBLEMES LIES A L'IMPLANTATION SUR L'AVION CONCORDE 001

Ces problèmes liés à l'implantation sur l'avion des instrumentations définies au § 4 se situent au niveau :

- des vibrations et des accélérations
- de la disponibilité géométrique dans un avion chargé de dispositifs de contrôle opérationnel de performances
- du poids sachant que sur une trajectoire normale supersonique de 1 h. une surcharge de 300 Kgs représente 1 minute de vol
- de l'alimentation électrique et des servitudes du personnel en fonction des 2 lignes précédentes
- des ouvertures externes dans des matériaux parfois peu usuels, choisis en fonction de leur transparence infrarouge et qui auront à travailler au voisinage de 100°C
- des visées : y a lieu et des trajectoires associées.

5.1 - En ce qui concerne les vibrations et accélérations, les conditions suivantes correspondant à l'avion étant à retenir, les conditions verticales sont de 0,3 g au roulage, et en vol normalement inférieures à 0,1 g.

5.2 - Les nécessités des mesures opérationnelles normales suffisent à remplir l'appareil, qui par ailleurs se présente comme légèrement dissymétrique : le câblage électrique des mesures empruntant préférentiellement le côté droit. L'ampleur des moyens environnement à mettre en oeuvre aussi bien que les nécessités de visées ont donc conduit à consacrer une période de plusieurs semaines aux vols environnement prévus en Mai et Juin 1973. Un chantier occupant le mois d'Avril 1973 permettra de placer les appareillages dont les maquettes ont fait l'objet d'une présentation fin 1972.

5.3 - Poids

Le seul appareillage de poids vraiment important est le banc du J P L, de poids 900 kg. dont l'amarrage sur rail pose des problèmes. L'ensemble de l'équipement "études de l'environnement" correspond à un devis poids de 2 à 3 tonnes à comparer avec le devis de poids de 12 tonnes correspondant aux essais opérationnels de routine de l'avion.

5.4 - Compte tenu des contraintes correspondant à la géométrie et au poids 2 appareils se révèlent incompatibles et se substituent l'un à l'autre.

- appareillage ONERA (configuration 1)
- appareillage J P L (configuration 2)

Chaque des configurations se complètent des 2 appareils : Meudon et du photomètre, la configuration 1 seule se complète du spectromètre N P L.

Les vols "environnement" sont actuellement prévus, compte tenu des nécessités du planning d'essais opérationnels de l'avion, répartis en 2 phases couvrant chacune une configuration précédente durant les mois de Mai et Juin. Ils nécessiteront une optimisation de certains paramètres de visée solaire, à savoir :

- se maintenir dans le champ de visée du pointeur solaire à $\pm 14^\circ$ de la perpendiculaire à la trajectoire de l'avion (condition d'azimut)
- avoir une stratégie d'élévation qui donne une grande exploration au profil vertical en constituants mineurs et donc plage d'élévation maximale
- se maintenir à la plus haute altitude constante compatible avec les conditions opérationnelles de l'avion, qui est obligé de conserver une certaine marge vis-à-vis des accidents de température, donc de portance
- bien entendu, tenir compte de toutes les sujétions opérationnelles nécessaires au vol à cette altitude, et notamment en ce qui concerne l'autonomie, la durée du vol et les exigences du vol supersonique. Des trajectoires possibles correspondant à la période de vol sont de partir par des triangles dont l'un des côtés de près de 1.000 km va du cap Finistère (Espagne) au large du Finistère (France).

CONCLUSIONS

La campagne d'études sur la stratosphère par expériences embarquées sur le Concorde 001 est un témoignage de l'intérêt extrême porté par l'Aérospatiale, sous le contrôle du COVOS, aux problèmes de l'environnement; en particulier le problème de la source nouvelle en oxyde de l'azote et du carbone liée aux émissions de la flotte stratosphérique, mérite toute l'attention en tant que perturbation apportée à des équilibres naturels délicats dont il s'agit d'abord de mieux cerner la connaissance. Si elles devaient exister, les conséquences éventuelles de ces perturbations seraient progressives et non brutales, réversibles et non permanentes. On conçoit facilement comment un processus de contrôle continu, étendu à des avions de ligne, permet de conforter la théorie qui ne prévoit aucun effet avant des flottes où les véhicules stratosphériques se compteraient par dizaines de milliers.

Par ailleurs les prototypes Concorde pourront apporter une importante contribution à la science de la stratosphère, et ce n'est que juste retour des choses puisque cette région de l'atmosphère deviendra le support du transport aérien à longue distance : il ne s'agit pas là seulement du transport supersonique, mais du transport subsonique, puisque les gros porteurs à Mach élevé sillonneront de plus en plus la stratosphère, à l'exemple des avions classiques actuellement sur les lignes polaires où la tropopause descend au-dessous de 9 km. Actuellement le trafic militaire et civil en zone stratosphérique correspond à celui de la flotte Concorde vers 1980. Qui peut parler d'un effet décelable ?

Réf. : R.A. SCHINDLER (JPL) "APPLIED OPTICS" (1970) vol 9 p.301
 J.P. BALUTEAU & BUSSOLETTI (OBSERVATOIRE DE MEUDON) "NATURE" (à paraître)
 J.E. HARRIES, N.R. SWANN, J.E. BECKMAN, P.A. ADE (NPL & Queen Mary College) "NATURE" (1972) vol 236 p.159
 NASA SP 285 - REMOTE MEASUREMENT OF POLLUTION

Discussion on Paper 17
"Mesures des constituants mineurs dans la stratosphère par Concorde 001"
presented by R.Joatton

N.A.Chigier: For measurements made in the wake of the Concorde it is preferable to make traverses with a following aircraft across the path of the vortex, rather than parallel to the vortex. By rapidly crossing the vortex, samples can be taken without causing serious disturbance to the probe aircraft. When using balloons, if the balloons are at a lower density than the atmospheric environment, the balloons will centrifuge towards the central core of the vortex and allow measurements to be made in the high concentration region of the vortex. Helium balloons have been used to measure axial velocities in the core of trailing vortices.

R.Joatton: Nous avons effectivement songé à utiliser des haies de ballons. En ce qui concerne l'échantillonnage par avion d'accompagnement, on peut penser que si celui-ci croise le sillage de l'avion étudié, ou suit ce sillage, l'opération est délicate parce qu'elle présente deux risques: trop près de l'émission dans le sillage, des risques aéronautiques, trop loin de l'émission, des risques que la diffusion, qui est rapide, ait dispersé le sillage, et que les résultats ne soient plus représentatifs.

N.A.Chigier: I am surprised at your statement of rapid diffusion over 1 km. Vortex wakes can persist for distances from 30 km to possibly 100 km in the highly stable conditions of the stratosphere. After break up, vortex rings are formed which again persist for long periods of time with low rates of diffusion.

R.Joatton: J'ai dit seulement que la diffusion, lorsqu'elle joue seule, indépendamment de la dynamique du sillage, peut donner une dispersion de près de 1 km en 1 minute (Séminaire COVOS, Paris - Mars 1973).

Soot Formation in Rich Kerosine Flames at High Pressure

by

F H Holderness

J J Macfarlane

Procurement Executive, Ministry of Defence

National Gas Turbine Establishment

Pyestock

Farnborough

Hampshire

UK

SUMMARY

Soot appearing in gas turbine exhaust products originates within the primary flame. This paper summarizes model combustor experiments in which soot formation was measured in a reacting kerosine/air flame of uniform composition. Operating conditions are 6 to 21 bar and equivalence ratio 0.8 to 1.8.

Chemical equilibrium was not attained for equivalence ratios much above unity. The available oxygen reacted initially with a portion of the fuel, the remainder appearing as pyrolysis product. The total amount of this material, including soot, was roughly dependent on equivalence ratio, independent of other variables. The fraction fully degraded to soot increased sharply on raising pressure from 6 to 14 bar. There was a well defined threshold of soot formation at equivalence ratio 1.3 to 1.4 in premixed flames. Soot was observed at weaker conditions than this in spray flames and the formation rate rose to approximately 10 per cent of the input carbon at equivalence ratio 1.8.

1. INTRODUCTION

Soot is an unwanted constituent of gas turbine combustion products. Legislation against pollution by aircraft engine exhaust may require the adoption of SAE smoke number 20* as a maximum tolerable value⁽¹⁾. The source of soot is within the primary flame and the problem of eliminating its emission from the engine has two main aspects: the mechanism of formation at primary operating equivalence ratio levels of 1.0 and higher, and the processes of consumption or burnout when the flame gases are diluted to reduce equivalence ratio to 0.2 to 0.3.

The present paper is concerned only with the first of these steps.

Apart from the pollution aspect, the presence of soot in the flame is disadvantageous in the gas turbine because it raises flame emissivity; this increases heat transfer from the gas to the chamber walls and accentuates the mechanical problems of protecting them from overheating. The heat transfer behaviour has been shown to be amenable to mathematical prediction at the chamber design stage but development and use of the techniques for this are hampered by lack of basic data on the radiation properties of flame gases. Experimental work undertaken at NGTE to supply this data has included measurements of flame gas composition and soot burden. It is from this data that the nucleus of the present paper is derived.

2. EXPERIMENTAL WORK

Early work with very small high pressure flames

Soot formation at high pressure was first investigated in experiments with very small premixed flames⁽²⁾. In this work the combustion chamber was a 1.5 cm dia quartz tube, 5 cm long, open at the upper end, with reactant mixture supplied through a tube matrix in the base. Fuels were vaporized pure compounds (hexane and other 6 carbon atom hydrocarbons).

At pressures above 11 bar, high concentrations of soot were produced at equivalence ratios richer than a threshold of approx 1.5. The chemical and physical properties of the soot were dependent on equivalence ratio: at values near the threshold the material was dry and powdery; electron microscopy showed that the ultimate particles were mainly in the size range 150 to 250 Angstrom units, but were present on the collecting grids in large aggregations. Ultimate analysis of these dry powdery soots indicated a significant hydrogen content (empirical formula approximately $\text{CH}_{0.4}$). The tarry soots formed in richer, cooler, premixed flames had higher hydrogen contents (up to $\text{CH}_{0.65}$) and examination by dispersive UV absorption analysis⁽³⁾ showed that polycyclic carbon compounds, ranging from naphthalene to coronene, were present in significant amounts. Additional organic material, including methane and other light hydrocarbons, was found to be present in product gases from which the soot was filtered.

The encouraging broad conclusion drawn from the work was that soot-free flames could be achieved at high pressure (20 bar) in a range of equivalence ratios above 1.0 - ie richer than the average value in a typical primary flame zone.

The flames in the tiny burner could however scarcely be claimed to approach the simulation of engine operating conditions. Subsequently, radiation studies with a larger scale model primary zone gave an opportunity to follow up the soot investigation.

* Tentative correlation:- Smoke number 20 equivalent to 1.7 g/litre

Model primary zone chamber

The chamber design (Figure 1) is described in detail elsewhere⁽³⁾. It is intended to provide, for experimental study, a stream of reacting gas which is substantially uniform in all respects. Individual control of all operating parameters is available so that conditions occurring locally in stratified engine operational flame zones can be simulated at will.

Physically the chamber is a 7.6 cm internal diameter refractory lined tube fitted with a water cooled pressure shell and a pressure maintaining valve at the outlet end. The flame is stabilized in a short toroidal recirculation zone and may be fed with atomized liquid fuel (spinning disc atomizer) or with vaporized kerosene added upstream of the annular air injection jet to give fully premixed operation.

Gas analysis traverses showed that equivalence ratio was substantially uniform in a plane 7 cm downstream of the air inlet plane. Windows for radiation measurements were fitted at this point, and a fixed single point sampling probe immediately downstream was used for soot sample collection and routine sampling for chromatography.

The aim of the chamber design was to simulate conditions occurring locally in operational flames. In practice, limits were imposed by the air and fuel preparation facilities. The maximum chamber operating pressure was 21 bar. Maximum fuel flow was approximately 2.5 g/s (above the spinning disc atomizer performed unsatisfactorily). These values imposed a limit of approximately 21 g/s of combustion air at a maximum equivalence ratio of 1.8. To give comparable flow conditions throughout the test series (both spray and premixed) a standard air flow rate of 1 g/s/bar was therefore adopted. Tests were performed at four pressure levels (6, 11, 16 and 21 bar) and equivalence ratio was varied between 0.8 and 1.8 at each level. The maximum available air inlet temperature of 250°C was used throughout.

Mean residence time of the reactant mixture in the flame zone was in the range 30 to 40 ms.

The standard air flow rate of 1 g/s/bar was of necessity rather small. There was in consequence a disproportionately high percentage heat loss from the flame (12 to 17 per cent). This represents a defect in simulating operational flames - possibly a serious one. With this in mind, a series of tests with higher air flows (7 g/s/bar) was planned using a larger high pressure air supply. The spinning disc is replaced in the new system by an acoustic atomizer⁽⁴⁾ which gives fine atomization (estimated - less than 10 micrometres mass median diameter for the conditions used). At the time of writing, only one set of measurements - for soot formation at 6 bar - is available. This data is entered in Figure 2b.

3. TEST RESULTS

Details of gas composition in terms of its carbon content are summarized in Figures 2 to 5. The 'formation ratio' parameters plotted represent carbon in the measured constituent expressed as a fraction of the total carbon in the sample - ie as a fraction of the original fuel carbon.

Figures 2a and 2b give soot formation ratio for premixed and spray flames respectively. For comparison, results from the early premixed n hexane/air tests above are indicated on 2a, while the results of the later acoustic atomizer test series are entered on 2b.

The notable differences between premixed and spray flames are that the latter are more heavily soot forming and significant soot is observed at 11 to 21 bar in the range of equivalence ratio 1.0 to 1.4.

As in the very small scale tests, the nature of the soot varied from intensely black dry powders at the weaker equivalence ratios to tarry materials at richer conditions. Volatile organic material in the gas passing the soot filter pad was measured, without separation of individual compounds, as part of the routine chromatography⁽⁵⁾. (The method used here is a direct measurement by means of a flame ionization detector.)

The sum of soot and organic compounds in a sample, classified as "total unoxidized carbon", is plotted against equivalence ratio, for all tests, in Figure 3, while Figures 4 and 5 show the remaining carbon, present as CO and CO₂.

4. DISCUSSION

Oxygen availability

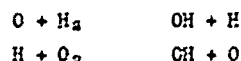
If the products of combustion of a mixture of kerosene and air remain in contact for a sufficiently long time the various reactions reach a balanced chemical equilibrium. If thereafter the operating conditions (temperature and pressure) remain steady, the composition of the products undergoes no further change. Figure 6 shows some relevant details of equilibrium composition for a wide range of equivalence ratio. It is immediately apparent that concentrations of free carbon and unoxidized hydrocarbon are so low as to be of no significance for equivalence ratio less than 3.0 - All carbon atoms are combined with oxygen in either CO or CO₂ molecules. The model primary zone equivalence ratio range is well below this (0.8 to 1.8) and one critical problem is therefore simply to explain the presence of the unoxidized constituents (soot and hydrocarbons) in product gas.

Free carbon, tarry hydrocarbons and indeed low molecular weight hydrocarbons can all be formed when a hydrocarbon mixture like kerosene is pyrolysed (ie destructively in the absence of oxygen). The observed facts may thus be explained as follows:

"The initial steps in combustion of rich mixture, involve consumption of all available oxygen by only a fraction of the fuel molecules. The process is accompanied by high rates of heat release and the remaining unoxidized hydrocarbons may be pyrolysed in the hot environment. The products of pyrolysis are determined by local temperature, pressure and residence time - the end product being free carbon, the basis

of soot. Reactions which redistribute the oxygen are slow so that in practice residence times typically available in a flame are too short to achieve complete conversion to equilibrium products."

The mechanism of the initial oxygen depletion can be attributed to the formation, at an early point in the combustion process, of excess oxygen atoms⁽⁶⁾. Fast reactions such as:-



give a similar available excess of OH radicals which in turn favours the removal of 'intermediate' combustion products:



The result can be the formation of CO_2 and H_2O in excess of the appropriate equilibrium concentrations (Figure 4) with an inevitable complementary depletion of available oxygen.

Total unoxidized material

Measurements of the total unoxidized material are plotted in Figure 3. There is an uncomfortably wide scatter (as might perhaps be expected of chemical measurements made on reacting flame gases). Some useful comments may however be made:-

The general impression given is that there is a dependence on equivalence ratio alone - not on pressure or on method of fuel/air mixture preparation.

The data from the 6 bar tests, both spray and premixed, fit the common curve quite well although there is virtually no soot at this pressure.

These observations suggest that the graph gives a rough guide to the availability of total unoxidized material and hence to a "soot formation potential".

The curve rises very sharply at high equivalence ratio and this feature emphasizes the importance of mixing in operational flames. A volume element of flame gas will retain a high soot formation potential until it becomes diluted with air to an equivalence ratio near stoichiometric.

Soot

Soot formation at 6 bar is comparatively slight for both premixed and spray flames (Figure 2). Unoxidized material is present in the flames but only a small fraction of it is degraded to free carbon. Moreover in spray flames there is little difference in soot forming tendency between the 1g/sec/bar spinning disc system and the 7g/sec/bar acoustic atomizer arrangement. It would appear therefore, that there is a marked and fundamental step increase in soot forming tendency when operating pressure is increased from 6 to 11 bar.

At 11 bar and higher pressures, much stronger soot forming tendencies are observed and there are notable differences between premixed and spray flames.

In premixed flames, there is a quite clearly marked threshold of soot formation at equivalence ratio 1.4 to 1.5. This was observed first in the early n-hexane tests and subsequently in the model primary zone tests with premixed kerosene vapour (Figure 2a). It seems probable therefore that this threshold value is also fixed by fundamental properties of the system: temperature, pressure and concentrations of chemical species. It follows that in operational chambers the possibility of completely eliminating soot may always exist. Mean operational primary zone equivalence ratio is near to 1.0; if therefore mixing processes can be made so efficient and rapid as to produce a substantially uniform mixture of fuel vapour and air before reactions begin, the threshold will never be exceeded.

This desirable end however is very difficult to achieve, as is shown by a consideration of the kerosene spray flame data (Figure 2). Spray flame conditions are optimized in the model primary zone; the spray itself, formed by the spinning disc atomizer technique, was 'mono-sized' (50 micronetre droplets⁽⁴⁾). The high initial velocity of the droplets together with the very strong recirculation, were expected to give very rapid evaporation and mixing. In spite of this however at pressures of 10 bar and higher soot is formed heavily in a range of equivalence ratios extending to weaker values than the premixed soot formation threshold. In the equivalence ratio range below 1.6, virtually all of the unoxidized material is carbonized - the full soot formation potential is used.

From these facts it would appear therefore that the droplet evaporation and mixing processes are not rapid and efficient enough, and there is a residual small scale non-uniformity of mixture strength present in the gases.

To appreciate the mechanics of this enhanced soot formation process, the reacting gas can be considered as a matrix of small elemental zones. Some are fuel-rich, representing the remnants of evaporated droplets, but intimately interleaved with these are leaner and hotter zones. Heat transfer from hot to rich zones will accelerate carbonization of the unoxidized material in the latter giving the observed high rates of soot formation.

5. CONCLUSIONS

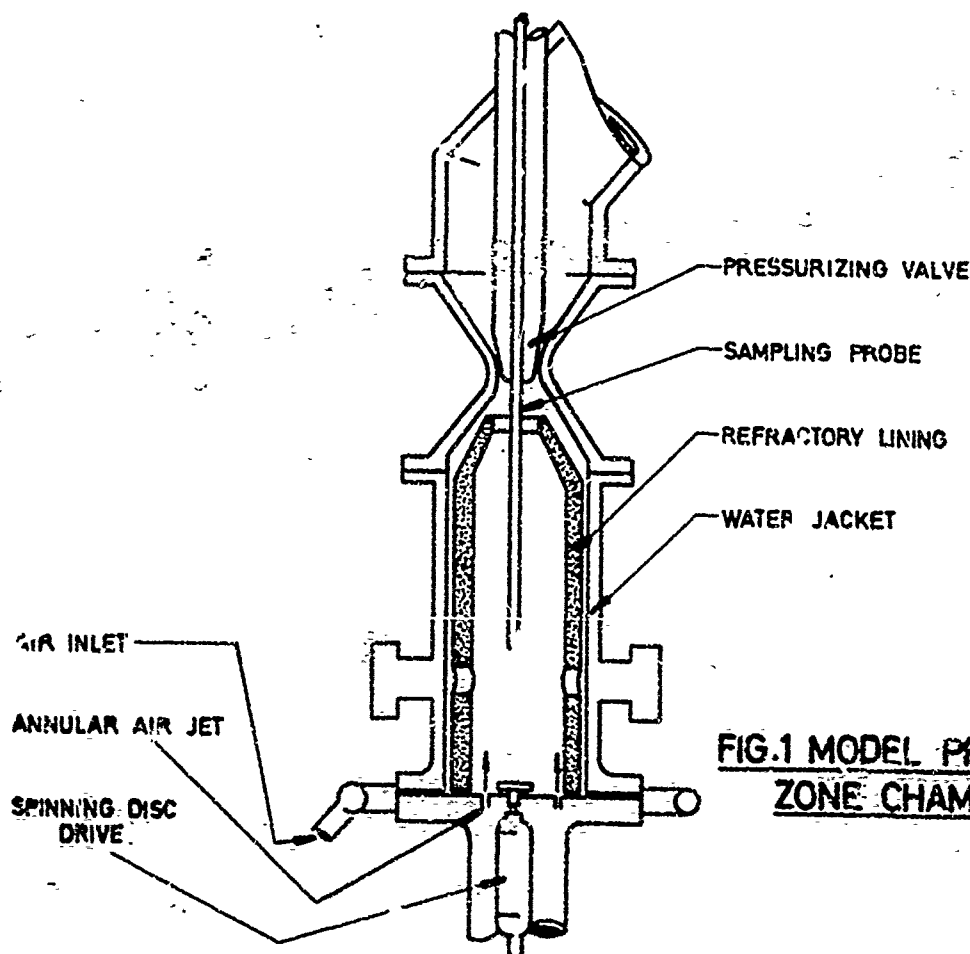
Measurements of soot formation have been made on product gases from a model combustion chamber operating as a primary zone at high pressure (up to 21 bar) and burning kerosine spray or premixed kerosine vapour/air mixtures. The observations are summarized and interpreted as follows:-

In richer than stoichiometric flames, all oxygen is initially consumed by a portion of the fuel. The remaining fuel becomes pyrolysed to soot and/or other organic products before the oxygen is redistributed in the final (soot-free) chemical equilibrium composition.

In premixed flames this mechanism only gives soot in mixtures richer than a threshold value of equivalence ratio 1.4 to 1.5. In spray flames the amount of total unoxidized material is similar to premixed but there is generally a more efficient conversion to soot. In particular there is significant soot formation at equivalence ratios less than the (premixed) threshold value. This behaviour is attributed hypothetically to a small scale non-uniformity of equivalence ratio, remnant of the original spray cloud. (Intimate contact between leaner, hot zones and richer ones with high soot formation potential would be expected to favour heavy soot formation.)

REFERENCES

- 1 Proposed standards for control of air pollution. Aircraft and aircraft engines. Federal Register. Vol 37. December 1972
- 2 J J Macfarlane
F H Holderness Soot formation in hydrocarbon/air flames. NGTE Report R253, December 1962
- 3 J J Macfarlane Flame radiation studies using a model gas turbine primary zone. Twelfth Symposium on Combustion 1969
- 4 J J Macfarlane 10 Liquid fuel atomizers for use in gas turbine combustion model experiments. Cranfield Symposium on heat transfer in gas turbine systems (No. 11) Pergamon Press 1971
- 5 F H Holderness
F S K Whitcher A gas chromatographic technique for the determination of all major components in combustion products. NGTE Report R299, 1967
- 6 G J Minkoff
G F H Tipper Chemistry of Combustion Reactions. Butterworths London 1962



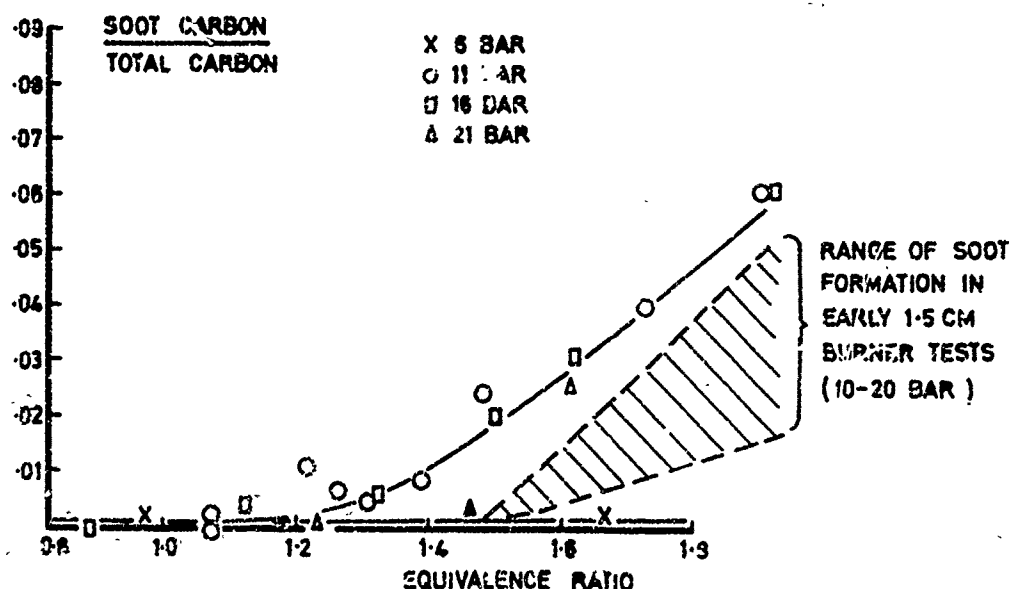


**FIG.2A SOOT FORMATION PREMIXED KEROSENE
VAPOUR / AIR**

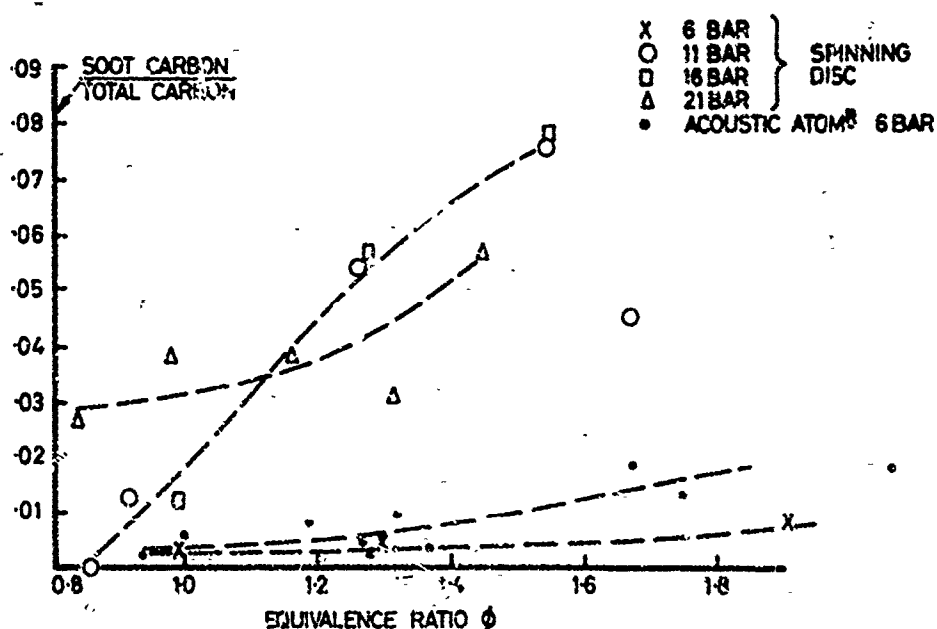


FIG.2B SOOT FORMATION, KEROSENE SPRAY

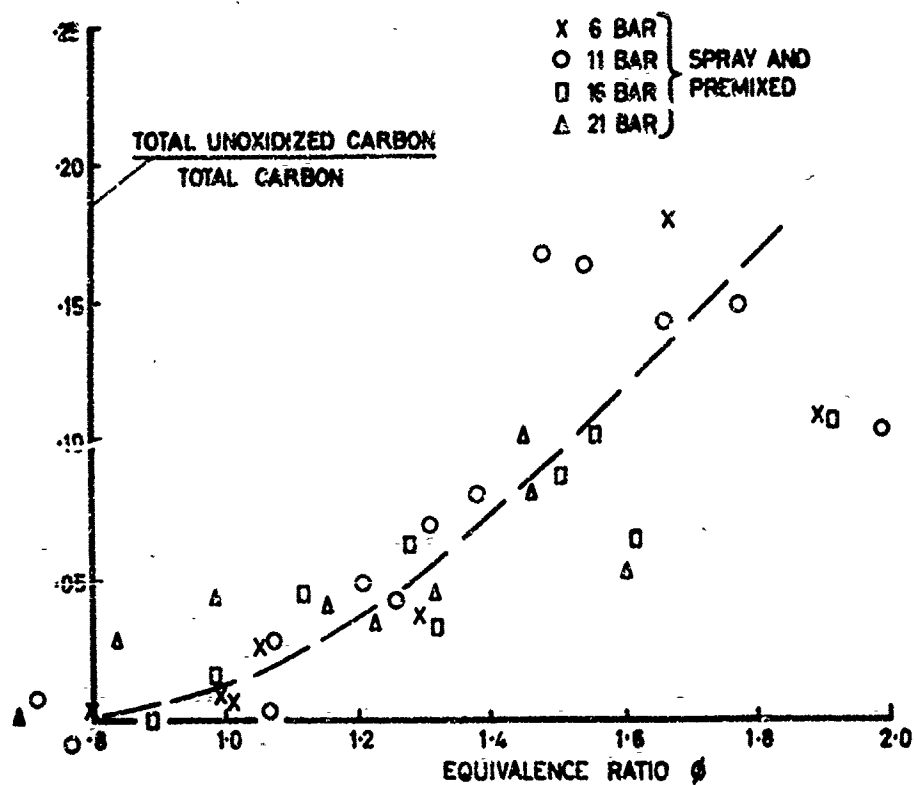


FIG. 3 TOTAL UNOXIDIZED CARBON

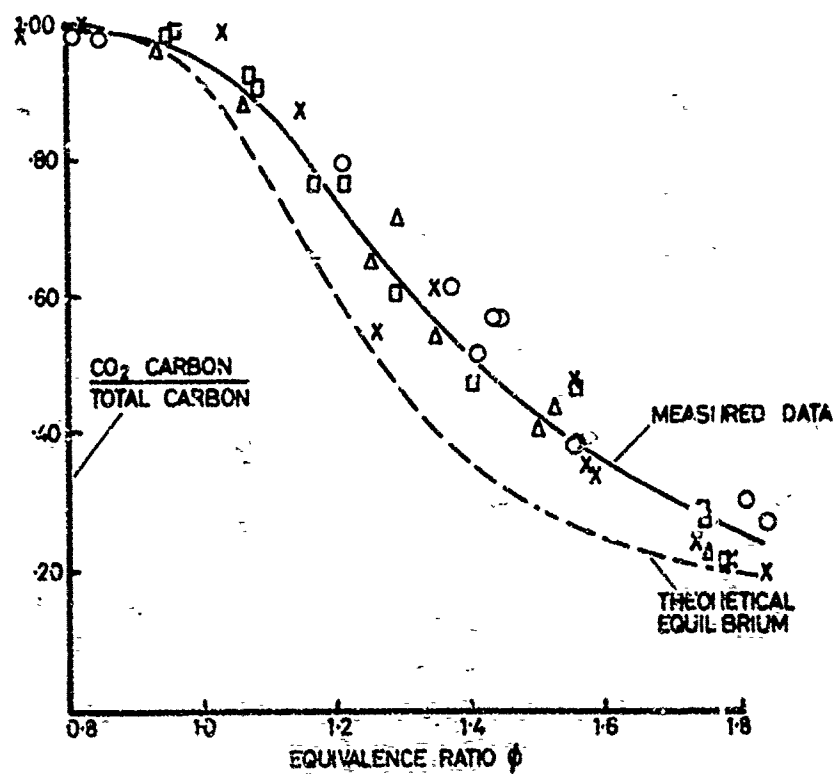


FIG. 4 CARBON DIOXIDE

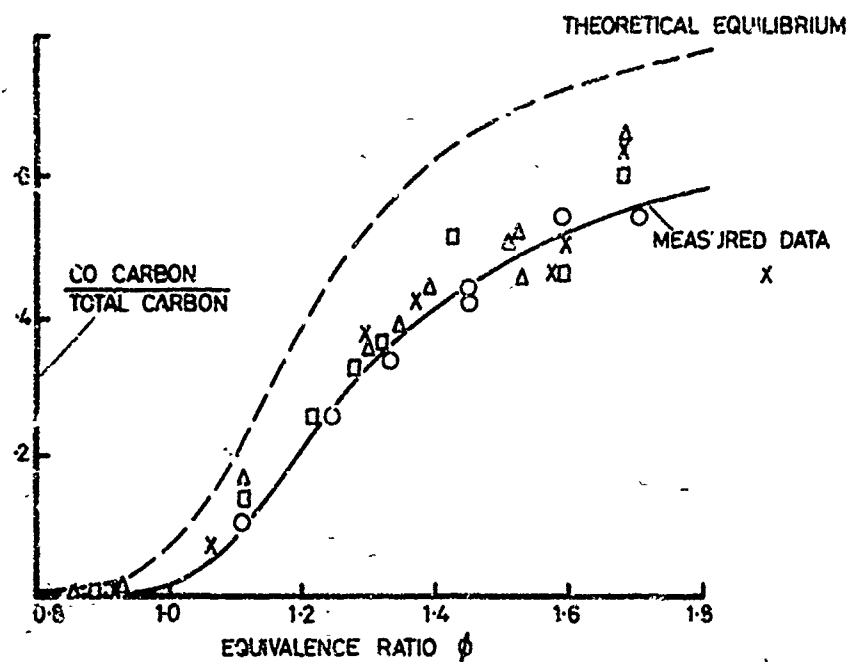


FIG.5 CARBON MONOXIDE

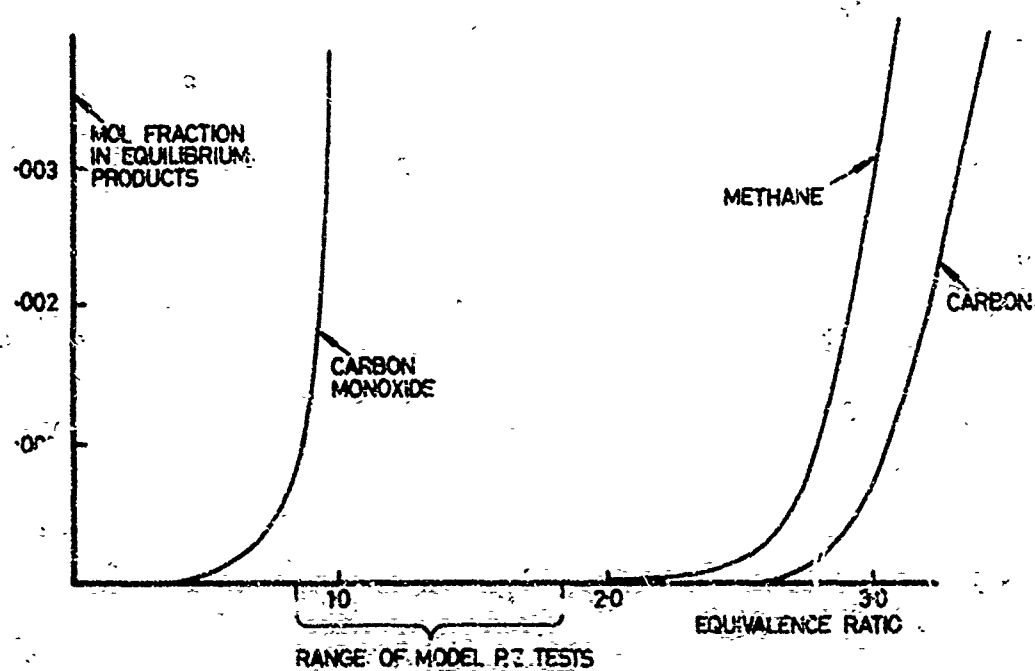


FIG.6 EQUILIBRIUM PRODUCT COMPOSITION

FROM "PROPERTIES OF COMBUSTION GASES" / SYSTEM $C_n H_{2n}$ - AIR VOL.2

Discussion on Paper 18
 "Soot Formation in Rich Kerosene Flames at High Pressure"
 presented by F.H.Holderness

G.Kappler: Since you have used a model combustion chamber with a cooled jacket, I wonder if your results are representative for actual combustors with hot walls. Our experiments clearly show that soot forms often on cold walls and is carried out by the gas streams. With hotter walls soot formation strongly decreases and no carbon or soot deposit can be observed on the walls. Can you, please, comment on this.

F.H.Holderness: In the experiments described in the paper, the cooled metal shell of the combustor was fitted for safety reasons. The shell was however lined with a 0.5 in thickness of ceramic to minimize heat loss from the flame. The inner surface of this liner, which formed the boundary of the combustion space, attained a steady high temperature (e.g. 660°C measured with gas temperature at axis = 1280°C).

Gas was sampled for soot measurements at the axis of the chamber, only one diameter downstream of the fuel injection plane. There was thus little doubt that the soot was generated within the reaction zone, away from the walls.

A.Quillevéré. Nous sommes, à la SNFCMA, très intéressés par les recherches faites par les auteurs qui donnent des résultats très concluants, en flamme de prémélange, sur l'influence de la richesse et de la pression.

Les auteurs ont-ils l'intention d'étudier, plus à fond, d'une part, l'influence de la température d'entrée et, d'autre part, de la recirculation des gaz brûlés?

F.H.Holderness: Inlet temperature variations were not possible except in a short range up to 250°C at the time of the experiments. The range now available (with new air supply plant) is increased to 750°C. A study of the effects of variations within the range is part of our future programme.

Assessment of the properties of the recirculation zone - in terms of reversal mass flow - is now possible using an omnidirectional velocity vector probe (described in NGTE Report R317 by J.J.Macfarlane).

The systematic study of the effect of this parameter on combustion product composition is therefore now a possibility.

We agree with the views expressed by Mikus and Heywood on the way in which spatial and/or temporal variations in FAR could influence product composition. It was in fact with this concept in mind that we conducted the two parallel series of tests with. (a) Spray flames, where FAR variations clearly must exist and (b) premixed flames where we did everything possible to eliminate such variations in the flame. One major point of interest in the results is therefore that in spite of the difference, the two series showed similar concentrations of total unoxidized material, CO₂ and CO (Figures 3, 4 and 5).

The dashed lines in Figures 4 and 5 show theoretical equilibrium composition derived from overall FAR and a temperature (T_F) calculated from the experimental data to be as near the true values as possible. If the value of FAR is calculated instead from the carbon in measured CO and CO₂ only, then the equilibrium curve (for T_F) lies much nearer to the experimental curve. It would thus appear that if the oxidized carbon only is considered, the reactions have virtually reached the equilibrium condition. In both premixed and spray tests, however, a portion of the original fuel has been left "stranded" (the unoxidized material). The total amount of this is approximately the same for the two series (Figure 3), but in the spray tests a larger fraction of it is pyrolysed to soot, particularly in the equivalence ratio range 1.0 to 1.5 at 11 bar and higher. It is this difference in pyrolytic effect which is, we propose, to be explained by the contact between very rich elements and very hot elements which can occur in spray flames only.

J.M.Beer: The authors have clearly illustrated the significance of pressure upon the soot formed in their flames. In flames with sprays I think that there are two principal reasons for the strong effect of pressure. Firstly that the kinetics of soot formation are favoured by pressure and secondly that the droplet spray when penetrating into a medium of higher density is compressed which in turn results in an increased local equivalence ratio. In a well controlled experimental series we observed the combustion of monosize sprays produced by a vibrating needle technique and found that the amount of soot formed was strongly dependent upon the interdroplet distance. When the experiments were carried out under conditions of elevated pressure (100 psi) the interdrop distance was greatly reduced with the effect of increased local fuel-air ratios and enhanced formation of soot.

While it is convenient for practical purposes to correlate data on soot formation with overall equivalence ratio, it seems to me that it would be of great help if they were given also as a function of local air-fuel ratio in the immediate vicinity of the root of the spray.

F.H.Holderness: The series of measurements with premixed kerosene vapour/air flames (Figure 3B) gives a valid correlation of soot with equivalence ratio (ϕ) since there were nominally no point-to-point variations in ϕ throughout the combustor.

In spray tests, radial traverses at the working plane (7 cms downstream of the fuel/air mixing plane, showed ± 5 per cent variation in FAR within the combustor walls. This sampling was not time-resolved and small scale non-uniformity (such as might exist as a relic of the droplet cloud) would not be revealed. We have no detailed knowledge of the macro-structure of the spray cloud near to the baseplate and the effect of pressure changes on this. Investigation of this point should be possible using the universal traversing gear which we have recently built.

A.M.Mellor: You used a probe fixed on the centerline to deduce that CO_2 is in excess of its equilibrium value. Did you check that CO_2 concentration was not lower near the wall?

F.H.Holderness: Diametral sampling was only possible in one plane of the combustor. The only measurements made were to check the distribution of equivalence ratio (found to be $\approx \pm 5$ per cent of a mean value). Analytically the measurements were made by completing combustion in the sample after addition of excess oxygen, and then measuring the ratio CO_2/N_2 in the products.

New traversing gear has now been built which enables all points within the combustor to be reached by a sampling probe. With this, more detailed investigation of variations in gas composition will be possible.

M.L.Barrère: When you computed the equilibrium condition, did you use the theoretical or experimental temperature?

F.H.Holderness: The equilibrium data shown in Figures 4 and 5 was calculated using values of temperature derived from the gas analyses by an enthalpy balance. Heat loss from the flame (12 to 17 per cent) was measured calorimetrically and a correction for this was applied. The single lines given in the graphs are for 10 bars operating pressure.

Equilibrium composition corresponding to a maximum temperature (no heat loss) shows a somewhat lower CO_2 content than that shown in Figures 4 and 5. The largest effect is at the stoichiometric condition - 1.1 per cent CO_2 lower.

SOOT OXIDATION KINETICS AT COMBUSTION TEMPERATURES

by

John P. Appleton
 Mechanical Engineering Department
 Massachusetts Institute of Technology
 Cambridge, Mass. 02139 U.S.A.

SUMMARY

Comparisons between soot oxidation rate measurements obtained in laboratory flames and in a recent shock-tube investigation are made with previously reported measurements of the surface oxidation rate of bulk samples of pyrolytic graphite. On the basis of these comparisons it is concluded that the surface oxidation rate mechanisms for soot and pyrolytic graphite are the same and that the rates are predicted by a semi-empirical expression, originally proposed by Nagle and Strickland-Constable for graphite oxidation, which expresses the specific surface oxidation rate in terms of the surface temperature and the gas-phase partial pressure of oxygen. This expression provides a method of estimating soot oxidation rates which is suitable for use in engineering design and performance studies of most practical combustion systems, such as gas-turbine combustors.

1. INTRODUCTION

Soot, normally observed as black smoke in the trails of jet aircraft, in the exhausts of many internal combustion engines (particularly diesels), and in the plumes from industrial chimneys and open free-burning fires, has given rise to considerable public concern because, together with carbon monoxide, oxides of nitrogen, and unburned hydrocarbons, it is generally thought of as being one of the primary contributors to the air pollution problem created by combustion. Although, in the context of air pollution, soot is clearly undesirable there are situations, such as in power plant furnaces, where the presence of soot in the high temperature combustion zone is advantageous; this is because the black-body radiation characteristics of the incandescent soot particles make radiative heat transfer much more effective than convection at high temperatures.

In order that combustion systems can be properly designed to eliminate soot from exhaust gases, it is obviously necessary that we at least have a reliable quantitative description of the oxidation kinetics of soot. The chemistry of soot formation, notwithstanding the vast literature which has been published on the subject, is still far from being understood for most practical combustion systems, and thus, still ranks as one of the major unsolved problems of combustion chemistry.

Palmer and Cullis [1], in their review of the formation of soot in the gas-phase, draw our attention to a number of general items of information concerning soot. For example, the properties of soots formed in flames are remarkably similar and little affected by the type of flame, i.e., premixed or diffusion, the nature of the fuel being burnt, and the other conditions under which they are formed. Soot is primarily composed of carbon, normally greater than ninety percent by weight, but may additionally contain other elements, usually hydrogen and oxygen, to some variable extent. Early electron microscope studies of soot showed that the constituent particles were roughly spherical with diameters typically ranging between 100 Å and 500 Å, and that they were grouped together in a necklace-like fashion. Other electron microscope and X-ray diffraction studies [2-7] showed that much of the carbon in the particles was present in the form of small graphite-like crystallites embedded in a polymeric material. More significantly, it appeared that each crystallite was composed of several graphite lamellae, each containing on the order of a hundred or so carbon atoms, which were stacked randomly on top of one another with a spacing of about 3.45 Å, i.e., a turbostratic structure [2, 3]. Furthermore, it was observed that the outermost crystallites were arranged so that their basal planes were approximately tangent to the particle surface and that heat treatment caused the crystallites to grow, presumably, at the expense of the polymeric material.

On the basis of this descriptive information it appears that, at the microscopic level, much of the surface structure of the small soot particles is similar to that of pyrolytic graphite which has found commercial application because of its high temperature resistance to oxidation and erosion, e.g., it has been suggested as a heat shield material for re-entry vehicles [8-11]. Pyrolytic graphite can be prepared by thermally cracking hydrocarbon vapors, such as methane or ethane, on high temperature solid substrates. Formed in this way, the graphite lamellae are oriented approximately parallel to the surface but with no layer to layer order, i.e., the structure is also turbostratic. Presumably, it is this highly anisotropic structure which provides the much higher resistance to surface oxidation by molecular oxygen at elevated temperatures than is observed for other more isotropic forms of commercially available graphite (see, for example, Nagle and Strickland-Constable [12] and Rosner and Allendorf [13]). Indeed, it has been suggested [13] that the reason for this difference in the oxidation resistance of pyrolytic graphite and isotropic graphite is that in the latter case a large proportion of the surface carbon atoms are likely to be in the more reactive prismatic plane or "edge" positions, whereas, with pyrolytic graphite, the surface atoms are those which are embedded within the basal planes.

The similarities in the surface structure of soot produced in flames and pyrolytic graphite prompted Radcliffe and Appleton [14] to make comparisons between the few major experimental investigations of soot oxidation [15-17] and the somewhat more extensive measurements of pyrolytic graphite oxidation [12, 13, 18-20]. The purpose of the comparison was that if good correspondence between the data were obtained where the experimental conditions of temperature and pressure overlapped, then, because the pyrolytic graphite rate measurements extended over a wider range of experimental conditions, they would

provide a sounder basis for extrapolation of the soot oxidation rate data to the higher temperature and pressure conditions of many practical combustion systems.* Figure 1, taken from Heywood, Fay and Linden [22] compares the ranges of oxygen partial pressure and temperature in which the major soot oxidation rate investigations have been made with the operating conditions of a typical gas-turbine combustor. The extensive extrapolation which is required to use the data is apparent.

In this paper we shall briefly review the previous soot and pyrolytic graphite oxidation rate measurements and also outline a theoretical model for surface oxidation [23] which yields the form of the expression proposed by Nagle and Strickland-Constable [12] to correlate their pyrolytic graphite oxidation rate measurements. Additionally, some new rate measurements for soot oxidation will be presented that cover the ranges of temperature between 1700 and 4000 °K and pressure between 0.05 and 13 atm. of oxygen; these results have recently been obtained in a shock-tube investigation by Park and Appleton [24]. It will be made apparent that the combined experimental measurements undoubtedly confirm the essential correctness of Nagle and Strickland-Constable's rate expression, thus providing a method of correlating and extrapolating soot oxidation rates which is suitable for use in engineering design and performance studies of practical combustion systems. Finally, an assessment of soot burn-up in a typical gas-turbine combustor using this rate expression will be presented in the final Section of this paper.

II. FLAME MEASUREMENTS OF SOOT OXIDATION

Lee, Thring and Beér [15] made measurements of soot oxidation rates in the hot laminar plume of a calor gas diffusion flame where the primary combustion products were oxygen, nitrogen, water vapor, carbon dioxide, and soot. At successive stations along the plume the local temperature was measured and samples of the product gases and the soot were extracted with suction probes for subsequent analysis. The gas analyses were made using chromatographic methods and the change in size of the soot particles was measured by means of electron micrographs. Within the limitations of their ability to vary the operating conditions, these investigators measured soot oxidation rates over the approximate temperature range: 1300 to 1700 °K, and oxygen partial pressure range: 0.04 to 0.12 atm. They correlated their results on the basis of the following empirical expression for the specific surface oxidation rate:

$$\omega = 1.085 \times 10^4 (P_{O_2}/T^{1/2}) \exp(-39.3/RT) \quad \text{gm.cm.}^{-2}\text{sec.}^{-1}$$

thus claiming a first order dependence on the oxygen concentration and an apparent activation energy of 39.3 k.cal.mole.⁻¹

In a similar type of investigation, Tesner and Tsibulevsky [16] measured the oxidation rate of soot in laminar diffusion flames burning acetylene-hydrogen and acetylene-water vapor mixtures. The kinetic data were obtained in the upper part of the flame where the oxygen concentration was relatively uniform over the cross section of the soot-gas column. These authors did not publish values of the oxygen partial pressure in the region of measurement (we estimated [14], $P_{O_2} \approx 0.01$ atm.), instead, they presented their reduced measurements of the specific surface rate referred to a unit atmosphere of oxygen on an Arrhenius plot, i.e., $\log(\omega/P_{O_2})$ versus T^{-1} . Because the data points all lay close to a straight line over the temperature range: 1400 to 2000 °K, they imply a first order dependence of the rate on the oxygen concentration, and the slope of the line yields an activation energy of about 40 k.cal.mole.⁻¹. Therefore, these results appear to be in substantial agreement with those reported by Lee, Thring and Beér.[†]

Fenimore and Jones' measurements [17] were made using an apparatus in which soot was first prepared by burning a premixed rich mixture of ethylene, oxygen and argon. The products were then cooled, mixed with additional fuel composed of hydrogen, oxygen and carbon dioxide, and then burned in a second fuel-lean sooty flame. The soot was thus oxidized in a known environment of constant oxygen composition and temperature. The rate of soot oxidation was again determined by sample analysis and the size of the soot particles measured using electron micrographs. The range of temperature covered by these measurements was 1530 to 1890 °K, and, for these fuel-lean flames, the oxygen partial pressure was varied between 0.04 and 0.3 atm. Three measurements were made in slightly fuel rich flames in which the oxygen partial pressure was estimated on the basis of equilibrium calculations to be about 10^{-4} atm. or less.

In a second series of experiments, Fenimore and Jones measured the rate of oxidation of dried soot in an atmosphere composed of dry nitrogen and oxygen using an electrically heated furnace through which the soot-gas suspension flowed at a known rate. Measurements of the oxidation rate were obtained for: $P_{O_2} = 0.12$ and 0.21 atm. at 1200 °K.

The distinguishing feature of the Fenimore and Jones results is the relatively weak dependence

*Magnussen [21] recently stressed the differences between the oxidation rates of soot and carbon by showing graphically that the Lee, Thring and Beér rate data for soot [15] was typically about a factor of one hundred times smaller than some carbon data obtained at comparable temperatures. The reason for Magnussen's observation appears to be that he chose to compare the soot data with data obtained using the much more reactive isotropic forms of graphite, such as Reactor graphite, which was also discussed by Nagle and Strickland-Constable [12].

[†]It is to be noted that in another publication [25], Tesner and Tsibulevsky presented measurements of soot oxidation by carbon dioxide. These results were also obtained in laminar diffusion flames burning acetylene diluted in nitrogen and carbon dioxide, but in a lower flame region where oxygen from the surroundings had not diffused to the soot column. For temperatures between 1800 and 1940 °K, they correlated their data by the expression:

$$\omega = 1.15 \times 10^5 P_{O_2} \exp(-75/RT) \quad \text{gm.cm.}^{-2}\text{sec.}^{-1}$$

which, in view of the large activation energy, shows that the oxidation of soot by carbon dioxide is extremely slow at normal combustion temperatures.

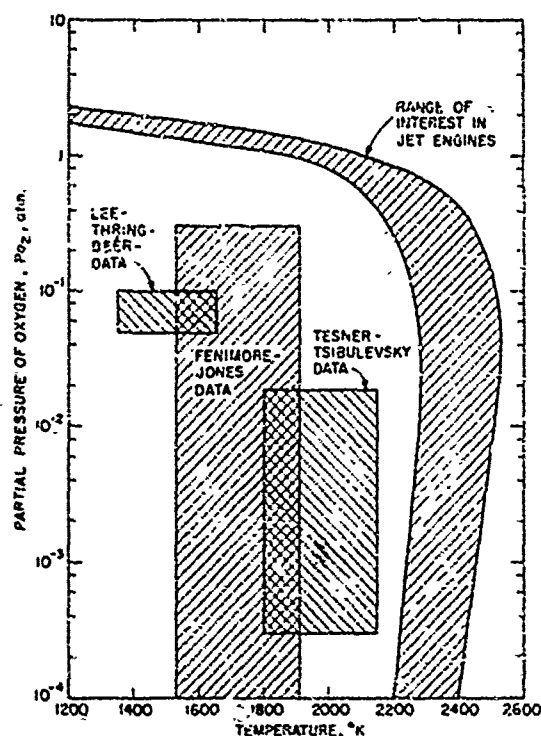


Figure 1. Comparison of regimes in which soot oxidation rate measurements have been made [15-17] with the range of operating conditions for a typical gas-turbine combustor.

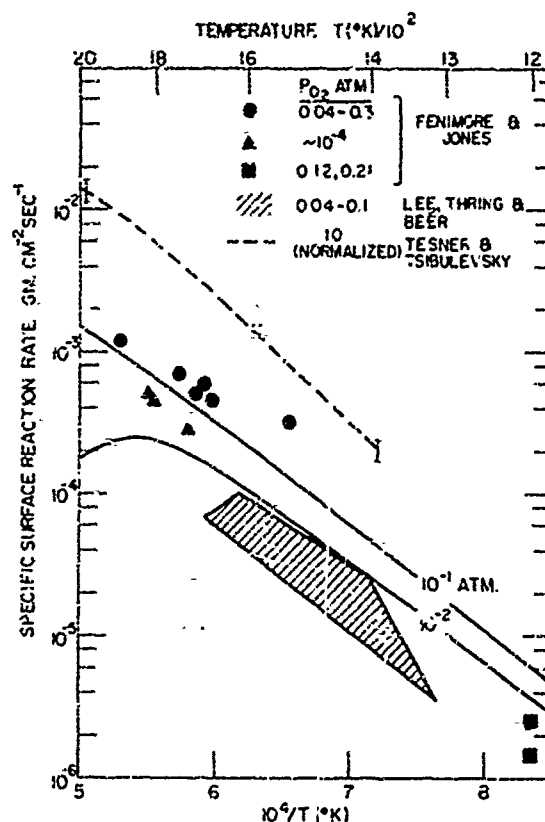


Figure 2. Summary of specific soot oxidation rate measurements obtained in laboratory diffusion flames as a function of temperature [15-17].

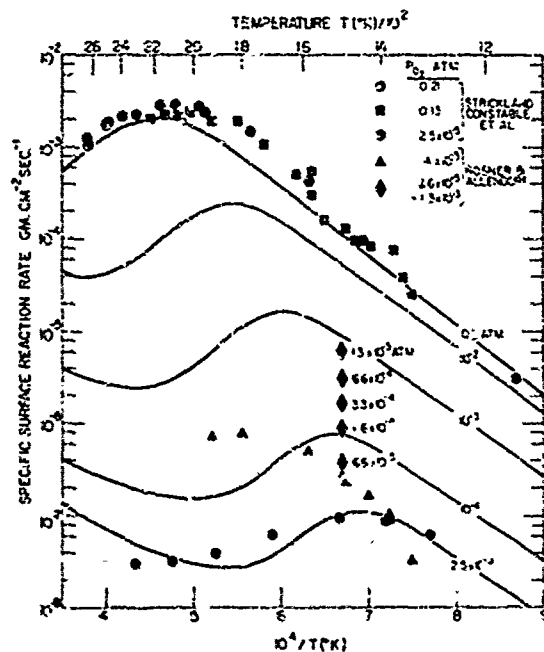


Figure 3. Measurements of the specific surface oxidation rates for pyrolytic graphite as a function of temperature and oxygen partial pressure [12,13,18-20].

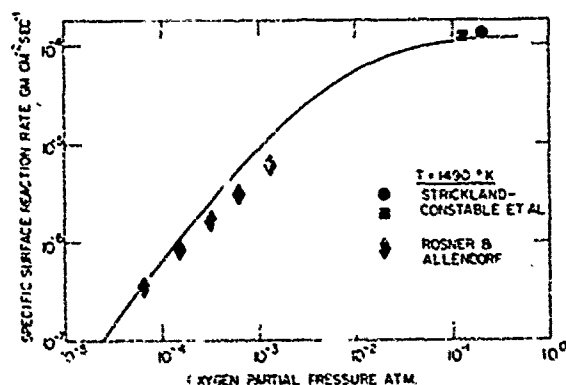


Figure 4. Specific surface oxidation rate for pyrolytic graphite as a function of the oxygen partial pressure at the fixed temperature, $T = 1490^\circ \text{K}$ [12,18,13].

which they observed for the oxidation rates on the oxygen concentration. Contrary to Lee, Thring and Beér and Tesner and Tsibulevsky, Fenimore and Jones claimed that the primary agent responsible for soot oxidation was not oxygen but the hydroxyl radical, OH. On the basis of other measurements from which they deduced to OH concentration in the reaction zones of the lean flames, they estimated that the OH radical was effective in removing a carbon atom from the soot in about ten percent of the collisions with the surface.

A summary of these flame measurements of soot oxidation rates is shown in Figure 2 where we have plotted $\log w$ against T^{-1} ; the individual results are identified in the legend of the figure. The full lines shown in Figure 2 are theoretical predictions of pyrolytic graphite oxidation rates calculated for different values of P_{O_2} using the formula proposed by Nagle and Strickland-Constable [12]; we shall return to discuss this comparison later.

171. PYROLYTIC GRAPHITE OXIDATION

Surface oxidation rate measurements of bulk samples of graphite have been reported by numerous investigators; a review of the work has been given by Lewis [26]. The investigations of primary interest to us are those by Strickland-Constable and his co-workers [12, 18, 19] and, more recently, by Rosner and Allendorf [13, 20].

Walls and Strickland-Constable [18] used small rods of pyrolytic graphite (2 cm. long and 0.4×0.5 cm. cross section) which were heated electrically between carbon supports. An inclined jet of oxygen was allowed to impinge on one of the surfaces of the specimen which was parallel to the basal planes. The surface temperature was measured with an optical pyrometer and the reaction rate determined by measuring the rate of recession of the surface. By maintaining the jet velocity at a relatively high value, nominally 70 m.sec.⁻¹, they were able to eliminate the effects of boundary layer diffusion and thus obtain measurements of the surface limited reaction rate. Walls and Strickland-Constable's results, which extend over the approximate temperature range: 1200 to 2700 °K, at an oxygen partial pressure of 0.21 atm. are illustrated in Figure 3. Other measurements reported by Nagle and Strickland-Constable [12] at $P_{O_2} = 0.13$ atm. were found to be in close agreement with those obtained at 0.21 atm. (not all of the $P_{O_2} = 0.13$ atm. data have been included in Figure 3 to avoid confusion), and thus it was concluded that the surface rate was independent of the oxygen concentration for these values of P_{O_2} . Earlier measurements of the oxidation rate of small carbon filaments (diameter: 0.05-0.1 mm) obtained at an extremely low pressure, $P_{O_2} \sim 2.5 \times 10^{-5}$ atm., were reported by Strickland-Constable [19] and these have also been included in Figure 3.

More recent pyrolytic graphite oxidation rate measurements have been made by Rosner and Allendorf [13, 20]. Their apparatus consisted of a glass vacuum flow system in which metered gas mixtures (e.g., oxygen and argon) were passed over an electrically heated pyrolytic graphite filament. The filament was prepared in situ by cracking ethane on an electrically heated tungsten filament substrate. The rate measurements were made by measuring the changes of the outer filament diameter after periods of known exposure to the oxidizing gas stream, and the surface temperatures were measured with an optical pyrometer. Rosner and Allendorf's results are also illustrated in Figure 3. At 1490 °K they cover the oxygen partial pressure range between 4×10^{-5} and 10^{-3} atm., and for the fixed value, $P_{O_2} = 4 \times 10^{-5}$ atm., they extend over the temperature range: 1140 to 2000 °K.

The important characteristic feature of the data shown in Figure 3 is that for fixed oxygen partial pressures, the rates pass through local maxima as the temperature increases. A second feature is illustrated in Figure 4 where we have cross-plotted from Figure 3 the oxidation rates at the fixed temperature of 1490 °K as a function of the oxygen partial pressure. Here it is apparent that the rate is first order in P_{O_2} at low pressures but tends to zero order as the pressure is increased.

The full lines shown in Figures 3 and 4 were calculated using Nagle and Strickland-Constable's semi-empirical formula which they claimed to correlate their pyrolytic graphite rate measurements. Indeed, apart from the temperature dependence of the results at $P_{O_2} = 4 \times 10^{-5}$ atm., the formula also appears to correlate Rosner and Allendorf's data as well. We shall outline the theoretical model of the surface oxidation mechanism on which this formula was based in the next Section. However, before doing that we shall briefly summarize Radcliffe and Appleton's arguments [14] for proposing that the oxidation rates of soot and pyrolytic graphite should be the same.

First, as pointed out in the Introduction, the surface structure of the crystallites contained in small soot particles and the structure of pyrolytic graphite is probably the same. Secondly, most of the soot oxidation rate measurements shown in Figure 2, exhibit a dependence on temperature which is about the same as the pyrolytic graphite rate measurements over the same temperature range. Thirdly, the magnitude of most of the soot rate measurements are predicted, to within a factor of two or three, by the Nagle and Strickland-Constable formula, the notable exceptions being Fenimore and Jones' results obtained in slightly fuel-rich flames.

Fenimore and Jones' contention that the OH radical is the primary agent responsible for the oxidation of soot in hot combustion gases does not appear to be supported by other experimental results obtained by Rosner and Allendorf [20] which indicate that, even for the more reactive isotropic graphite,

³ Rosner and Allendorf have also made measurements of the reactivity of both oxygen atoms and hydroxyl radicals on graphite surfaces. It is interesting to note that, whereas, they found large differences in the reactivity of oxygen molecules on isotropic graphite and pyrolytic graphite surfaces, the extremely high reactivity of both types of graphite surface with oxygen atoms was, to within a factor of two, about the same. We shall comment on their results for the reactivity of OH radicals at the end of this Section.

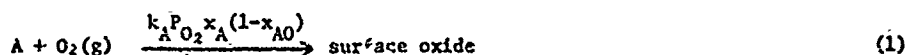
the OH radical only removes a carbon atom from the surface in less than one out of every hundred collisions with the surface, whereas, Fenimore and Jones' explanation of their results requires a ten percent efficiency for the OH collisions. We are inclined to suggest that the results obtained in the slightly fuel-rich flames could be explained by oxygen concentrations greater than Fenimore and Jones' estimates based on equilibrium calculations, i.e., 10^{-4} atm., but which were probably too small to measure. Certainly, the weak oxygen pressure dependence which Fenimore and Jones observed for their fuel-lean flame results is accounted for by the Nagle and Strickland-Constable correlation formula.

Finally, Lee, Thring and Beér's first order pressure dependence of the rate was deduced on the basis of quite a limited pressure range, i.e., 0.04 to 0.1 atm. of oxygen. When one bears in mind the probable experimental uncertainties associated with flame measurements and that Fenimore and Jones observed a much weaker dependence of the rate on P_{O_2} at comparable experimental conditions over a seven-fold change in the oxygen concentration, it seems probable that the Lee, Thring, and Beér's first order dependence on P_{O_2} is not justified.

In order to completely justify Radcliffe and Appleton's proposition that the oxidation rates of soot and pyrolytic graphite should be the same, it was apparent that measurements of soot oxidation rates should be made over more extensive ranges of temperature and pressure than had hitherto been obtained. It was for this reason that Park and Appleton [24] carried out their recent shock-tube investigation of soot oxidation rates. We shall present these results in Section V; however, before doing that we shall briefly outline the theoretical model of the surface oxidation mechanism which yields the form of the expression for the specific surface oxidation rate proposed by Nagle and Strickland-Constable.

IV. THEORETICAL MODEL OF SURFACE OXIDATION MECHANISM

The theoretical model of the surface rate mechanism was originally proposed by Blyholder, Binford and Eyring [23]. The theory assumes that there are two types of reaction sites on the exposed carbon surface, namely, an A-site which is more reactive, and a less reactive B-site. The fraction of the surface covered by A-sites is assumed to be x , and the remaining fraction, $(1-x)$, is assumed to be covered by B-sites. It is proposed that a steady-state fraction of the A-sites are covered by a surface oxide and that this fraction, x_{AO} , is given by a balance between the rate of activated adsorption of oxygen from the gas-phase on the A-sites to produce the surface oxide, viz.



and the rate of activated desorption of CO from the surface, viz.



Thus, the fraction of A-sites covered by the surface oxide is given by the steady-state expression:

$$x_{AO} = k_A P_{O_2} / (k'_A + k_A P_{O_2}) \quad (3)$$

and, therefore, the rate at which carbon leaves the surface due to A-site oxidation is:

$$k'_A x_A [k_A P_{O_2} / (k'_A + k_A P_{O_2})] = x_A [k_A P_{O_2} / (1 + k_Z P_{O_2})] \quad (4)$$

where we have written $k_Z = k'_A / k_A$, in accordance with Nagle and Strickland-Constable's notation.

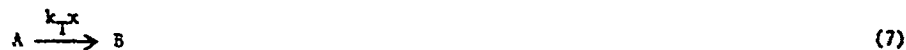
The theoretical model further assumes that oxygen reacts with B-sites in a slow endothermic first order reaction to yield an A-site and CO which is then desorbed from the surface:



The rate at which carbon leaves the surface via this mechanism is thus:

$$k_B P_{O_2} (1-x) \quad (6)$$

Finally, it is assumed that A-sites undergo a slow process of activated thermal rearrangement to yield B-sites:



For a steady-state value of x , the rates of reactions (5) and (7) must balance, thus

$$x = [1 + k_T / P_{O_2} k_B]^{-1} \quad (8)$$

and the overall specific surface reaction rate is then given by:

$$w_c / W_c = x [k_A P_{O_2} / (1 + k_Z P_{O_2})] + k_B P_{O_2} (1-x) \quad (9)$$

where $W_c = 12$, is the gram molecular weight of a carbon atom.

Nagle and Strickland-Constable chose the following values of k_A , k_B , k_T and k_Z , in order to fit their rate measurements:

$$k_A = 20 \exp(-30/RT) \quad \text{gm.cm.}^{-2} \text{sec.}^{-1} \text{atm.}^{-1}$$

$$k_B = 4.46 \times 10^{-3} \exp(-15.2/RT) \quad \text{gm.cm.}^{-2} \text{sec.}^{-1} \text{atm.}^{-1}$$

$$k_T = 1.51 \times 10^5 \exp(-97/RT) \quad \text{gm.cm.}^{-2} \text{sec.}^{-1}$$

and

$$k_Z = 21.3 \exp(4.1/RT) \quad \text{atm.}^{-1}$$

where all activation energies are expressed in the units of k.cal. mole⁻¹

It can be seen from Eq (6) that at low temperatures, the surface is entirely covered by A-sites, i.e., $x = 1$, and that at low oxygen partial pressures,

$$\omega = 2.4 \times 10^2 P_{O_2} \exp(-30/RT) \quad \text{gm.cm.}^{-2} \text{sec.}^{-1} \quad (10)$$

At higher partial pressures where the rate becomes zero order with respect to P_{O_2} ,

$$\omega = 11.3 \exp(-34/RT) \quad \text{gm.cm.}^{-2} \text{sec.}^{-1} \quad (11)$$

and at higher temperatures where thermal rearrangement produces an increasing proportion of B-site,

$$x = 3 \times 10^{-3} P_{O_2} \exp(21.6/RT) \quad (12)$$

i.e., the apparent activation energy of the A-site oxidation term in Eq (9) changes its value and sign with the net result that, for a fixed oxygen partial pressure, ω decreases with increasing temperature. At still higher temperatures the A-site oxidation term in Eq (9) becomes negligibly small by comparison with the B-site term, and ω again begins to increase with increasing temperature, i.e.

$$\omega = 5.35 \times 10^{-2} P_{O_2} \exp(-15.2/RT) \quad \text{gm.cm.}^{-2} \text{sec.}^{-1} \quad (13)$$

Although, as may be seen from Figures 3 and 4, this theoretical model clearly gives a good quantitative fit to both the Strickland-Constable and Rosner and Allendorf rate measurements over quite extensive ranges of temperature and oxygen partial pressure, the physical nature of the two surface sites and the type of surface oxide formed is obscure. For these reasons and the fact that the rate coefficients k_A , k_B , k_T and k_Z were chosen to fit a set of experimental data, we regard the theory as being semi-empirical.

V. SHOCK-TUBE MEASUREMENTS OF SOOT OXIDATION RATES

Park and Appleton's measurements [24] were made using a conventional pressure-driven stainless steel shock-tube having an internal bore of 3.8 cm. The soot was premixed as a dispersion in a prepared test gas, which contained between 2.5 and 30 percent by volume of oxygen in argon, using a specially designed aspirator. The measurements were made in the reflected shock-wave region where, close to the end wall, the rate of disappearance of the soot was determined by a simple laser-light transmission method. Figure 5 illustrates the schematic layout of the apparatus; a detailed description of the apparatus, including the aspirator, and the experimental procedure is described elsewhere [24].

The two types of soot used in these experiments were obtained in the form of commercially available carbon black [27]; i.e., channel black and furnace black. The primary difference between the two types was that the channel black had a mean particle radius, R_m , of 45 Å, whereas, the furnace black had a mean particle radius of 180 Å, both determined on the basis of electronmicroscope measurements. The particle size distributions were closely represented by a skewed Gaussian:

$$f(R) = (3N/2K_m^2) R \exp(-3K^2/4R^2) \quad (14)$$

such that the number density of particles in the size range: $R_a \leq R_m \leq R_b$, was given by the expression:

$$N(R_a:R_b) = \int_{R_a}^{R_b} f(R) dR$$

The amount of soot in the soot-test gas dispersion was maintained at a sufficiently low level that the heat release, even after complete combustion in the reflected shock-wave region, was sufficiently small that it was negligible in determining the thermodynamic properties of the test gas, i.e., the temperature and pressure in the reflected shock-wave region was calculated on the basis of the Rankine-Hugoniot relation for an ideal gas mixture and the measured primary shock-wave velocity.

A line tracing of an actual oscilloscope record of the transmitted laser light intensity as a function of time after shock reflection is shown in Figure 6. The ordinate, y , is the fraction of the light absorbed by the dispersed soot relative to the absorption obtained immediately following the passage of the reflected shock-wave past the observation station close to the end-wall, viz.

$$y = (I_f - I)/(I_f - I_0)$$

where I_f is the intensity of full light transmission with no absorption, and I_0 is the intensity measured immediately behind the reflected shock-wave at the time $t = 0$.

According to the small particle limit of the Lorentz-Mie theory for scattering and absorption of radiation by spherical particles, it can be shown that for a fixed wavelength, λ , such that $\lambda \gg R$, and a given constant value of the complex refractive index of the particle material, the extinction coefficient is proportional to the volume fraction occupied by the particles [28]. Thus, when the extinction coefficient is small, as was the case in these shock-tube experiments, y may be expressed in the form:

$$y = \int_0^\infty f(R) R^3 dR / \int_0^\infty f(R) R^3 dR \quad (15)$$

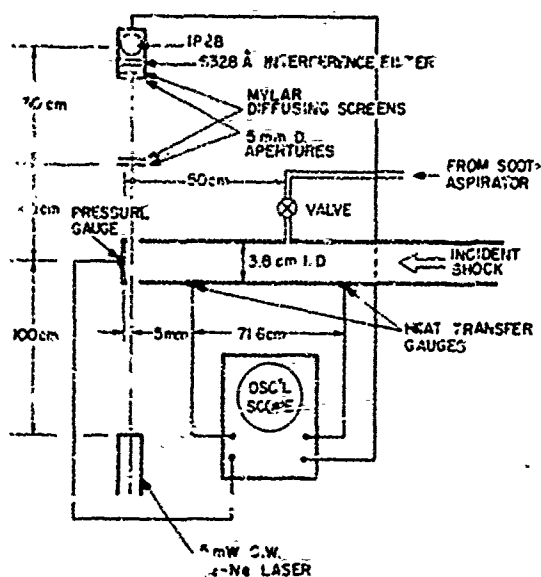


Figure 5. Schematic layout of shock-tube apparatus for soot oxidation rate measurements.

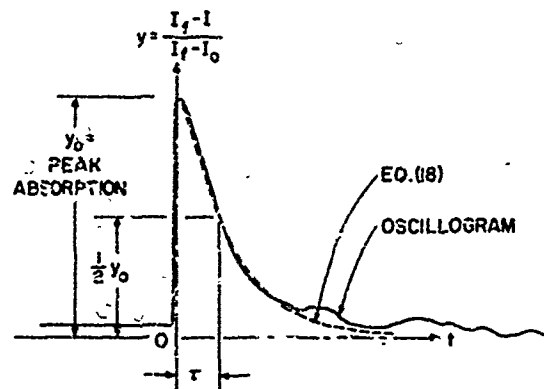


Figure 6. Y-profile of oscilloscope record of absorption profile obtained behind reflected shock wave. Initial channel pressure: 93 torr (8% O_2 , 92% Ar). Primary shock Mach number: 3.41. Characteristic time, $\tau = 150 \mu\text{sec}$.

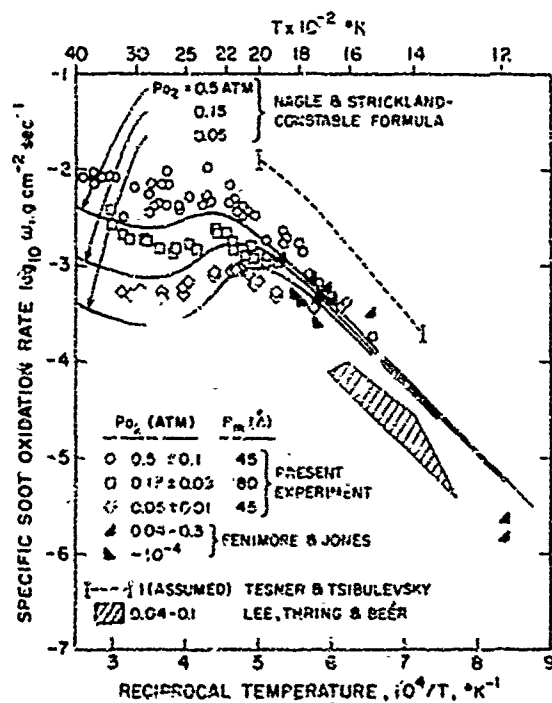


Figure 7. Specific soot oxidation rate measurements versus temperature as a function of the oxygen partial pressure.

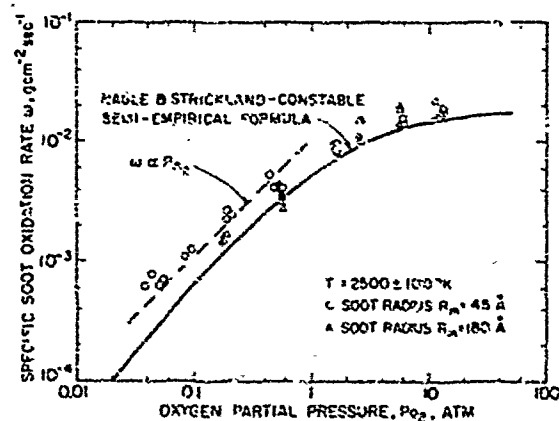


Figure 8. Specific soot oxidation rate as a function of the oxygen partial pressure at temperature $T = 2500 \pm 100 \text{ }^\circ\text{K}$.

where, $r = r(R, t)$, is the radius of individual particles at time t whose radius was originally R at $t \leq 0$.

Now the time rate of change of the mass of a single soot particle due to surface oxidation is given by the equation:

$$\rho \frac{d}{dt} \left(\frac{4\pi r^3}{3} \right) = -4\pi r^2 \omega \quad (16)$$

where ρ is the particle density ($\rho = 1.8 \text{ gm.cm.}^{-3}$ for the types of carbon black used), and ω is the specific surface reaction rate. Integration of this rate equation yields:

$$\begin{aligned} r &= R - S, & R > S \\ r &= 0, & R < S \end{aligned} \quad (17)$$

where, $S = \omega t / \rho$. With the particle size distribution function given by Eq (14) and r given by Eq (17), the integrals in Eq (13) can be evaluated to yield:

$$\begin{aligned} y &= \{1 + (3/2)(S/R_m)^2\} \text{erfc}[\sqrt{3}S/2R_m] \\ &+ \sqrt{3/\pi}(S/R_m) \exp[-3(S/2R_m)^2] \end{aligned} \quad (18)$$

In Figure 6 the y -profile shape given by Eq (18) is compared with the experimentally measured profile: it is apparent that the agreement is quite good. The value of y falls to half its initial value at $(S/R) = 0.33$ if the time corresponding to this point is designated by the characteristic time, τ , the specific surface reaction rate is given in terms of τ by the relationship:

$$\omega = 0.33R_m \rho / \tau \quad (19)$$

The method of determining ω is now obvious. The characteristic time, τ , is measured directly from the oscilloscope record, i.e., the time required for y to fall to half its initial value, and then substituted directly into Eq (19) to yield ω .

In the first series of experiments, the shock-tube operating conditions, i.e., the initial test gas pressure in the channel, the percentage of oxygen in the test gas mixture, the shock-tube driver pressure, etc., were arranged such that behind the reflected shock-wave a temperature range between 1700 and 4000 °K could be achieved at the three nominal oxygen partial pressures: $P_{O_2} = 0.05 \pm 0.01, 0.15 \pm 0.03, 0.5 \pm 0.1$ atm. The uncertainty of ± 20 percent in the oxygen partial pressure arose as a consequence of random variations in the shock velocity for the same initial test conditions. In a second series of experiments, the shock-tube operating conditions were so arranged as to keep the temperature in the reflected shock-wave region at about 2500 ± 100 °K whilst varying the oxygen partial pressure between 0.04 and 13 atm. The total pressure in the reflected shock region ranged between 35 atm. (33 percent O_2) for the highest oxygen pressure operation, to 1.4 atm. (2.5 percent O_2) for the lowest oxygen pressure operation.

The results of this shock-tube investigation are displayed in Figures 7 and 8 together with the previous rate measurements for soot oxidation [15-17], see legend for identification. The full lines were calculated on the basis of Nagle and Strickland-Constable's rate expression, Eq (9). First, it is apparent that the same characteristic features of the pyrolytic graphite oxidation rate measurements are reproduced by the soot oxidation rate measurements shown in Figure 7 and that the data are quite well correlated by Eq (9). The data shown in Figure 8 clearly illustrate that for a fixed temperature and low enough oxygen partial pressures, $P_{O_2} \leq 0.5$ atm., the surface oxidation rate is first order in the oxygen pressure, and that at high pressures, $P_{O_2} \geq 4.0$ atm., the rate asymptotes to a zero order limit. Again, the data contained in Figure 8 are in good accord with the prediction given by Eq (9). The separate results obtained for the channel black and the furnace black indicate that the specific surface reaction rate is independent of the particle size.

VI. DISCUSSION AND CONCLUSIONS

In the light of the foregoing discussions and the extensive shock-tube measurements of soot oxidation rates presented in the previous Section, we may conclude that Radcliffe and Appleton's proposition that the surface mechanisms for oxidation of pyrolytic graphite and those for soot are the same is correct, and that the rates may be adequately predicted, given the temperature and oxygen partial pressure, using the semi-empirical formula proposed by Nagle and Strickland-Constable. It thus appears that we have a reliable method of estimating soot oxidation rates which is suitable for use in engineering design and performance studies of practical combustion systems.

In their article on jet aircraft pollutant production, Heywood, Fay and Linden [22] investigated the problem of soot burn-up and nitric oxide formation using a simple plug-flow model of the combustion and mixing processes to represent the flow in a gas-turbine combustor. With the aid of this model they were able to calculate the mean temperature and composition of the flow as a function of the mean fuel:air equivalence ratio along the combustor length, on the assumption that all the major species were present in their local equilibrium proportions and that there was no heat loss to the combustion chamber walls. Figure 9 shows the results of this simple calculation for a combustor which is supplied with compressor air at 700 °K, and kerosene fuel, such that the mean primary zone equivalence ratio was 1.2 and the combustion chamber pressure was 15 atm.

Now the surface recession rate of a spherical soot particle may be written, using Eq (16), in the form:

$$\frac{dr}{dt} = -\omega / \rho \quad (20)$$

Thus, with the aid of a suitable expression for the specific surface reaction rate, such as Eq (9), the surface recession rate can easily be calculated from Eq (20) and the temperature and composition history given in Figure 9. Figure 10 illustrates the variations in the surface recession rate as a function of mean equivalence ratio for three different methods of correlating and extrapolating the soot oxidation rate data. It is apparent that the simple extrapolations of the Lee, Thring and Beér and the Penimore and Jones data* to the combustor operating conditions lead to gross overestimates of the soot burn-up rate. Indeed, Heywood, et al. concluded that on the basis of the Lee, Thring and Beér correlation formula, soot particles with initial diameters less than about $0.4 \mu\text{m}$ would be completely consumed in the combustion chamber before they entered the jet exhaust. Since a diameter of $0.4 \mu\text{m}$ is, typically, about a factor of ten times larger than the diameters of nonaggregated soot particles produced in flames, Heywood suggested that for soot particles to be observed in gas-turbine exhausts (see, for example, [29-31]), they would need to spend most of their time travelling in the relatively cooler regions of the combustion chamber near the inner liner.

Similar considerations [14] based on the Nagle and Strickland-Constable oxidation rate formula indicate that only particles with diameters less than about $0.04 \mu\text{m}$ would be totally consumed in the combustion chamber. Since this is typical of the expected initial size of the soot particles, it would appear that if the simple plug-flow model for mixing and combustion in the chamber is realistic, complete burn-up of the soot is only a marginal process. In fact, the simple plug-flow model does not provide an accurate representation of the combustor flow since it takes no account of the inhomogeneities in the composition and the temperature which are caused by turbulence. It is known that the mean nonequilibrium levels of nitric oxide and carbon monoxide produced in combustors [32, 33] are dependent on the turbulent mixing intensities; consequently, we anticipate that soot burn-up is similarly affected by turbulence [21]. However, it is to be noted from Figure 10, that the maximum in the surface recession rate of the soot particles, i.e., $17 \mu\text{m sec}^{-1}$, occurs at a local mean equivalence ratio of about 0.75; therefore, we might expect that the visibility of jet exhausts could be reduced by controlling the addition of secondary air so as to prolong the residence time of the soot particles at this mean condition. We note that the maximum rate of nitric oxide formation occurs when the equivalence ratio is close to unity [22], thus, prolonging the residence time at lower equivalence ratios (~ 0.75) should not cause significant increases in the emission of nitric oxide.

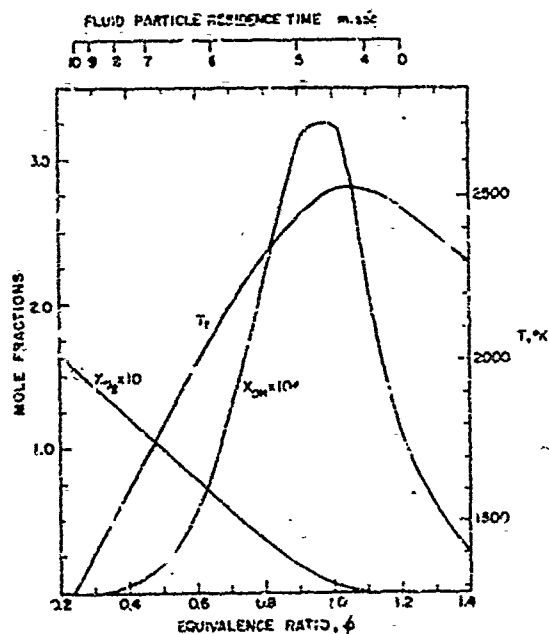


Figure 9. Calculated mean temperature and composition of combustor flow as a function of mean equivalence ratio and residence time [22].

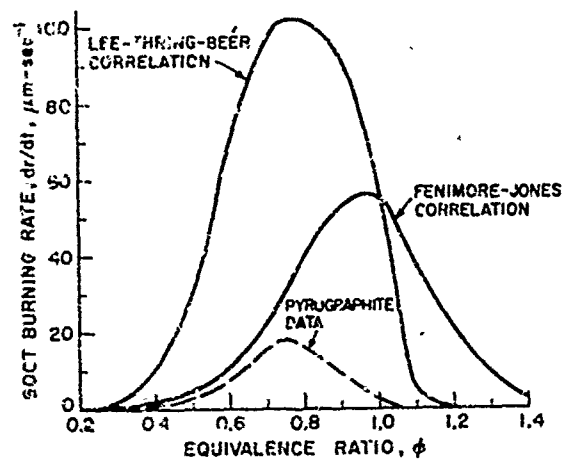


Figure 10. Surface recession rate of soot particles as a function of mean equivalence ratio for three different methods of extrapolating the soot oxidation rate data.

*Penimore and Jones' data were extrapolated by Heywood, et al. using the formula:

$$\omega = 12.7 P_{\text{OH}}^{1/2} \quad \mu\text{m.cm}^{-2}\text{sec}^{-1}$$

VII. REFERENCES

1. H. B. Palmer and C. F. Cullis, Chemistry and Physics of Carbon (P. L. Walker, Jr., Ed.) 1, 265 (1965).
2. B. E. Warren, Phys. Rev., 9, 693 (1941).
3. J. Biscoe and B. E. Warren, J. Appl. Phys., 13, 364 (1942).
4. J. H. L. Watson, J. Appl. Phys., 17, 121 (1946).
5. E. C. Hall, J. Appl. Phys., 19, 271 (1948).
6. R. O. Grisdale, J. Appl. Phys., 24, 1082 (1953).
7. H. Kuroda and H. Akamatu, Bull. Chem. Soc. Japan, 32, 142 (1959).
8. A. M. Garbar, Aerospace Engineering, 22, 126 (1963).
9. D. Schiff, Metals Engineering Quarterly, 2, 32 (1962).
10. E. J. Nolan and S. M. Scala, A.R.S. Journal, 32, 32 (1962).
11. A. M. Garbar and E. J. Nolan, Proceedings of the OSR/GE Symposium on Dynamics of Manned Lifting Planetary Entry (S. M. Scala, A. C. Harrison, and M. Rogers, Eds.), Wiley, New York, 1963, pp. 536-567.
12. J. Nagle and R. F. Strickland-Constable, Proceedings of Fifth Carbon Conference, 1, 154 (1962).
13. D. E. Rosner and H. D. Allendorf, AIAA Journal, 6, 650 (1968).
14. S. W. Radcliffe and J. P. Appleton, Combustion Science and Technology, 4, 171 (1971).
15. K. B. Lee, M. W. Thring, and J. M. Beer, Combustion and Flame, 6, 137 (1962).
16. P. A. Tesner and A. M. Tsibulevsky, Combustion, Explosion and Shock Waves, 3, 163 (1969).
17. C. P. Fenimore and G. W. Jones, J. Phys. Chem., 71, 593 (1967).
18. J. R. Walls and R. F. Strickland-Constable, Carbon, 1, 33 (1964).
19. R. F. Strickland-Constable, Trans. Faraday Soc., 40, 333 (1944).
20. D. E. Rosner and H. D. Allendorf, Heterogeneous Kinetics at Elevated Temperatures. Proceedings of International Conference in Metallurgy and Materials Science (G. R. Belton and W. L. Worrel, Eds.), Plenum Press, New York, 1970, pp. 231-251.
21. B. F. Magnusson, Thirteenth Symposium (International) on Combustion, The Combustion Institute, Pittsburgh, 1971, pp. 869-877.
22. J. B. Heywood, J. A. Fay, and L. H. Linden, AIAA Journal, 9, 841 (1971).
23. G. Blyholder, J. S. Binford, and H. Eyring, J. Phys. Chem., 62, 263 (1958).
24. C. Park and J. P. Appleton, Combustion and Flame, (in Press), 1973.
25. P. A. Tesner and A. M. Tsibulevsky, Combustion and Flame, 11, 227 (1967).
26. J. B. Lewis, Modern Aspects of Graphite Technology (L. C. F. Blackman, Ed.), Academic Press, New York, 1970, pp. 129-199.
27. Supplied by Cabot Corporation, Boston, Mass.
28. M. Kerker, The Scattering of Light and Other Electromagnetic Radiation, Academic Press, New York, 1969.
29. J. J. Faltani, "Smoke Reduction in Jet Engines through Burner Design," Paper 680348, Society of Automotive Engineers, 1968.
30. T. Durrant, "The Reduction of Smoke from Gas Turbine Engines," presented at 9th International Aeronautical Congress, A.F.I.T.A.E., Paris, June 1969.
31. S. M. DeCorso, C. E. Hussey, and M. J. Ambrose, "Smokeless Combustion in Oil Burning Gas Turbines," Paper 57-PWR-5, ASME, 1957.
32. F. Pompei and J. B. Heywood, Combustion and Flame, (in Press), 1973.
33. J. P. Appleton and J. B. Heywood, Fourteenth Symposium (International) on Combustion, The Combustion Institute, Pittsburgh, 1973 (in Press).

VIII. ACKNOWLEDGMENT

The preparation of this manuscript was supported under a grant (CK-33933) from the Division of Engineering Chemistry of the National Science Foundation, Washington, D.C.

Discussion on Paper 20
 "Soot Oxidation Kinetics at Combustion Temperatures"
 presented by J.P.Appleton

M.Beér: This is a paper with a valuable critical survey and it argues convincingly the case that the rate equation for soot oxidation be based on that developed for pyrographite oxidation. Professor Appleton refers to data by Lee Thring and Beér stating that the first order dependence found is "probably not justified". I disagree. Lee's data were obtained under closely controlled experimental conditions. The data showed clearly, within the range tested (0.04 - 0.1 atm), a linear dependence of the specific rate of combustion of soot upon oxygen partial pressure. The implied rate determining step was activated adsorption and it was emphasised in the paper that the rate equation was not considered to be valid outside the ranges of variables tested. If an activated adsorption step controls the overall rate it can be expected that the reaction order should decrease to fractional and, possibly, to zero order as the pressure increases and thus, the number of active sites for adsorption become gradually occupied.

The good agreement of experimental data with a rate equation of fractional order at high temperatures and pressures does not, therefore, provide evidence to suggest that the first order dependence of Lee et al's rate equation is not correct.

J.P.Appleton: Our primary purpose in carrying out the shock-tube study was to establish the rate law for the oxidation of soot at the higher combustion temperatures typical of gas turbine combustion chambers, see Figure 1. Unfortunately, with the limited hot gas residence times available to us in our shock-tube it was not possible to make measurements of the much slower soot oxidation rates obtained at temperatures below about 1700°K, i.e., in the temperature range which overlaps that of the Lee, Thring and Beér data.

In the light of Professor Beér's reassertion that the Lee, Thring and Beér measurements clearly showed a first order dependence of the rate on the oxygen partial pressure over their range of conditions, we must conclude that the Nagle and Strickland-Constable formula does not provide an adequate correlation of soot oxidation rates at lower temperatures. Although it might be possible to choose values of the empirical parameters appearing in Equation (9), which would bring the high temperature shock-tube measurements and the Lee, Thring and Beér measurements into better accord, it would then be difficult to explain Fenimore and Jones' lean flame results unless one were to invoke the possible importance of the OH radical as did Fenimore and Jones.

M.Barrère: You say that it's necessary to increase the length of the emission zone to burn out the soot but, if you do this, you increase nitric oxide formation. This may be a problem in future combustors with higher temperatures.

J.P.Appleton: For adiabatic combustion conditions, the maximum in the rate of formation of nitric oxide occurs at a fuel air equivalence ratio of about unity (see Figure 3, Paper 21 by Heywood and Mikus), whereas, according to the simple plug flow model of the combustion and mixing processes in a typical gas turbine combustion chamber, the maximum in the soot burning rate occurs in the secondary combustion zone where the mean fuel air equivalence ratio has fallen to about 0.75 (see Figure 10). At this condition the rate of formation of nitric oxide has fallen by at least one order of magnitude below its maximum value, i.e., the nitric oxide formation chemistry is effectively frozen, therefore, prolonging the fluid particle residence time at this condition should facilitate soot burn up without significantly increasing the total amount of nitric oxide formed.

PARAMETERS CONTROLLING NITRIC OXIDE EMISSIONS FROM GAS TURBINE COMBUSTORS

by

John B. Heywood and Thomas Mikus
 Department of Mechanical Engineering,
 Massachusetts Institute of Technology
 Cambridge, Massachusetts 02139 U.S.A.

SUMMARY

Nitric oxide forms in the primary zone of gas turbine combustors where the burnt gas composition is close to stoichiometric and gas temperatures are highest. It has been found that combustor air inlet conditions, mean primary zone fuel-air ratio, residence time, and the uniformity of the primary zone are the most important variables affecting nitric oxide emissions. Relatively simple models of the flow in a gas turbine combustor, coupled with a rate equation for nitric oxide formation via the Zeldovich mechanism are shown to correlate the variation in measured NO_x emissions. Data from a number of different combustor concepts are analyzed and shown to be in reasonable agreement with predictions. The NO_x formation model is used to assess the extent to which an advanced combustor concept, the NASA swirl can, has produced a lean well-mixed primary zone generally believed to be the best low NO_x emissions burner type.

1. INTRODUCTION

With the growth in air traffic, and the trend to bigger and higher pressure ratio gas turbine engines, aircraft emissions of oxides of nitrogen (NO_x) are expected to increase greatly over the next decade. Recent estimates suggest that by 1980, in the absence of emission controls, NO_x emissions will increase above their 1970 values by a factor of 2.2 at O'Hare Airport, 2.9 at John F. Kennedy Airport and 4.5 at Los Angeles International Airport(1). As a consequence, the U.S. Environmental Protection Agency has proposed NO_x emission standards for aircraft turbine engines for January 1, 1979(2). In addition, the effect of NO_x emissions from a fleet of SST's in the stratosphere on the ozone layer is a topic of intensive study and debate(3). There is an urgent need to understand the factors governing NO_x emissions from aircraft gas turbine engines, and use that understanding to develop combustor designs with much reduced emissions.

It is well known that jet aircraft NO_x emissions are most important at high engine power settings. Thus take-off and landing are the primary operating modes of concern for subsonic aircraft. For the SST, NO_x emissions during cruise in the stratosphere are of greatest concern. Experimentally it has been found that increases in combustor inlet temperature and pressure, and thus engine compressor pressure ratio, increase NO_x emissions. For a given engine operating condition, it is known that the fuel injection technique, the geometry of the combustor liner, and the pressure drop across the liner all affect NO_x emissions(4)(5).

The oxides of nitrogen which leave the engine are nearly all nitric oxide, NO , with only a few percent nitrogen dioxide, NO_2 . Several models for predicting the formation of NO inside actual gas turbine combustors have already been developed(6)-(10). These models have established that the exhaust NO concentration depends on rate-limited reactions occurring in the burning gases in the high temperature zones of the combustor. As additional air is mixed with the combustion products to cool the gases before entry to the turbine, the NO formation chemistry freezes. After this point, the NO concentration only changes due to dilution. In this paper, we will review how NO is formed in aircraft gas turbine combustors, and relate the combustor design parameters listed above to the thermodynamic variables which control the NO formation process.

We will then show that relatively simple models which include only the major parameters affecting NO formation can be used to predict NO_x emissions. The agreement obtained to date with predictions from such models and experimental data from conventional combustors will be reviewed. This type of model is then applied to the NASA swirl can combustor(11) and it is shown why this concept offers a significant reduction in NO_x emissions. To illustrate the usefulness of such models, predictions are then made for a swirl can combustor at take-off conditions for a JT9D or CF-6 engine.

Our intent in this review is to demonstrate that simple models of the type we describe can predict NO_x emissions with sufficient accuracy to be useful in the design process. The model can be used to extrapolate test data from a combustor on a test stand to actual engine operating conditions. By identifying the key design parameters which affect NO formation, and quantifying the effect on emissions of changing these parameters, such models can provide a structure for a combustor development program. With these goals our emphasis will be on relatively simple models which can easily be adapted to different types of combustors.

The results presented here come from our own group at M.I.T.(7)(12)(13) and from work at Northern Research and Engineering Corporation(6)(8). As a result of close collaboration, the models developed by these groups are conceptually similar and differ only in detail. The two groups have also analyzed different types of combustors, and an extensive model evaluation can therefore be carried out.

2. MODEL DESCRIPTION

2.1 Combustor Flow Characteristics

Most of the models proposed for predicting NO_x emissions from combustors contain two parts. The first is a kinetic scheme for nitric oxide formation, developed from a plausible physical description of

the turbulent flame structure within the primary combustion region. The second part is a fluid mechanic model which couples the NO kinetics to those aspects of the flow field which affect the NO formation process. Before each of these parts of the model is discussed in detail, the general nature of the flow in a conventional combustor will be reviewed.

The main features of the flow in a conventional annular jet engine combustor are shown in Figure 1. Both can and annular combustors can be divided roughly into two parts, a primary and a secondary zone. In the primary zone, at high power conditions, about 90 percent of the fuel is burnt and the mean fuel-air ratio is slightly rich of stoichiometric (equivalence ratio between about 1 and 1.5). To reduce gas temperatures to an acceptable level at turbine inlet, the overall equivalence ratio must be reduced to about 0.25. Thus only 20 to 25 percent of the total combustor airflow enters the primary zone.

Figure 1 indicates schematically the mean flow pattern in the combustor. Though a mean flow pattern in any given combustor is discernible from water analog studies, substantial fluctuations and unsteadiness occur. In the primary zone, the swirler air and the air jets through the first row of holes set up the recirculating flow pattern which stabilizes the flame. These air jets also vigorously mix the primary zone gases to obtain adequate distribution of the fuel.

In the secondary zone, the remaining air is mixed with the primary zone combustion products to complete combustion of the fuel, and cool the gas stream to the temperature distribution required at turbine inlet. About two-thirds of the secondary zone air enters the combustor transverse to the internal flow through large holes in the liner and mixes in the bulk of the flow. About one-third of the secondary zone air enters parallel to the liner through slots to film cool the combustor walls. The flow is primarily unidirectional.

2.2 Kinetics of Nitric Oxide Formation

At the temperatures and equivalence ratios found in all types of burners, NO forms via the extended Zeldovich mechanism:



Reaction (1) is endothermic left to right and relatively slow. Reactions (2) and (3) are exothermic and fast. In the absence of dilution the rate of change of NO concentration in a fluid element of volume V is

$$\frac{1}{V} \frac{d[\text{NO}]}{dt} = k_1 [\text{O}][\text{N}_2] - k_{-1} [\text{NO}][\text{N}] + k_2 [\text{N}][\text{O}_2] - k_{-2} [\text{NO}][\text{O}] + k_3 [\text{N}][\text{OH}] - k_{-3} [\text{NO}][\text{H}] \quad (4)$$

where [] denote concentrations in gram moles/cm³, and $k_{\pm i}$ are the forward and reverse rate constants of the i th reaction.

Before equation (4) can be used to calculate NO formation rates, two questions must be resolved: (i) the method for calculating [N], and (ii) the method for calculating [O], [O₂], [OH] and [H]. The N₂ concentration is essentially constant. The appropriate assumptions depend on the pressure, temperature and atomic composition of the system being analyzed. We are concerned here with typical gas turbine combustor conditions, i.e. pressures ~ 15 atm, peak temperatures ~ 2500 °K, residence times at these peak conditions ~ 3 msec, equivalence ratio for hydrocarbon - air combustion between about 0.7 and 1.3.

Since the N atom mole fraction is of order 10⁻⁸, the steady state approximation is usually made for [N]. This is a standard procedure in treating reacting mixtures wherever a species is present in very small amounts compared with species of interest.

The second question of the radical and O₂ concentrations is more complex, and a model for the flame front in the combustor must be formalized before appropriate assumptions can be made. Heywood⁽¹³⁾ and Westenberg⁽¹⁴⁾ have justified the assumption that under appropriate conditions, the O, O₂, OH and H concentrations are the equilibrium values. The argument can be summarized as follows.

In a premixed one-dimensional flame, there is a thin initial reaction zone where radicals are generated and react with the hydrocarbon fuel. Most of the temperature rise occurs in this zone. This region is followed by a thicker zone where CO is oxidized to CO₂, and radicals present in greater than equilibrium concentrations recombine through termolecular reactions. If the NO formed in this nonequilibrium region is much less than the amount formed downstream of the flame, then the O, OH, H and O₂ equilibrium assumption is a reasonable approximation. We have recently completed studies of CO equilibration in the flame zone at pressures, temperatures and equivalence ratios typical of a combustor primary zone⁽¹⁵⁾. These studies show that equilibration times are less than 10⁻⁴ sec. (for equivalence ratios between 0.7 and 1.3) which is much less than typical primary zone residence times, and that the effect of radical concentrations above equilibrium values will not be significant on NO formation. The amount of NO formed in the reaction zone of the flame is small compared with the amount formed downstream of the flame at gas turbine combustor conditions.

With these assumptions for [N], and [O], [OH], [O₂] and [H] equation (4) can be rearranged to give⁽¹²⁾

$$\frac{d[\text{NO}]}{dz} = \frac{2M_{\text{NO}}}{\rho} \frac{(1 - \alpha^2)R_1}{(1 + \alpha K)} \quad (5)$$

where $\{NO\}$ is the nitric oxide mass fraction; M_{NO} is the molecular weight of NO, ρ is the gas density, α is $\{NO\}/\{NO\}_e$ and subscript e denotes the equilibrium value, R_1 is the one-way equilibrium reaction rate for reaction (1) (e.g. $R_1 = k_1 [O]_e [N_2]_e = k_{-1} [N]_e [NO]_e$) and $K = R_1/(R_2 + R_3)$. Expressions for the rate constants for reactions (1) - (3), and typical values for R_1 , R_2 , R_3 and K are given in Table 1.

TABLE 1

Values of One-way Equilibrium Reaction Rates for Extended Zeldovich Mechanism

(T = 2500 °K, p = 10 atm, $\phi = 1.0$)			
	rate const., k_i^*	ref.	R_i^{**}
R_1	$1.4 \times 10^{14} \exp(-75,400/RT)$	(16)	2.1×10^{-5}
R_2	$6.4 \times 10^9 T \exp(-6250/RT)$	(16)	5.5×10^{-6}
R_3	4.2×10^{13}	(17)	2.9×10^{-5}
$K = R_1/(R_2 + R_3)$			0.61

* units: $\text{cm}^3 \text{mole}^{-1} \text{sec}^{-1}$

** units: $\text{mole cm}^{-3} \text{sec}^{-1}$, except K.

Since K is of order 1, for $\{NO\} \ll \{NO\}_e$ (i.e. $\alpha \ll 1$) the rates of reactions (2) and (3) have little effect on the NO formation rate. Either reaction provides a fast path to convert the N atom produced in reaction (1) to NO. As $\{NO\}$ approaches $\{NO\}_e$, the value of K starts to affect the NO formation rate. For lean mixtures $R_2 \sim R_3$, and the inclusion of reaction (3) makes little difference. For rich mixtures $R_3 \gg R_2$. Heywood(13) has shown that the omission of reaction (3) from the scheme results in an underestimate of the NO formation rate by a factor of 2 for a stoichiometric mixture with $\alpha \approx 0.5$.

Equation (5) shows that the NO formation rate depends only on the pressure, temperature, atomic composition and NO concentration downstream of the thin flame zone. NO profiles calculated with equation (5) as a function of time downstream of a one-dimensional flame for a stoichiometric mixture are shown in Figure 2. Since primary zone residence times are of order 3 msec and peak temperatures ~ 2500 °K, we would not expect NO concentrations to reach equilibrium levels within the high temperature zone of a gas turbine combustor.

Changes in equivalence ratio at a given temperature do not change the time required to equilibrate NO(12), but do substantially change the formation rate as shown in Figure 3. The gas turbine combustor is essentially adiabatic; the local flame temperature therefore depends only on the inlet air conditions and the local equivalence ratio. The dashed line in Figure 3 indicates the path a burnt gas eddy or pocket would follow as it is diluted in its passage through the combustor. NO formation rates peak sharply at $\phi = 1.0$, and rapid freezing of the NO forming reactions occurs as the mixture is then leaned out. Obviously those regions of the combustor where the burnt gas composition is close to stoichiometric are the regions where most of the NO is formed.

2.3 Fluid Mechanic Models

To develop a fluid mechanic model for the primary zone, we must now relate this description of a premixed one-dimensional flame to the flame structure in a conventional gas turbine combustor. Fuel as a liquid spray and air enter the primary zone separately in approximately stoichiometric proportions. The fuel droplets vaporize as they move relative to the primary zone gases in a time of order 2 msec(18) leaving fuel vapor rich wakes which then mix with air and already burnt gas and burn. Mixing of fuel and air to a uniform equivalence ratio would not be expected. As the fuel droplets vaporize, fuel vapor and air mix and form turbulent eddies or pockets of combustible mixture with a wide range of fuel-air ratios.

High speed movies of liquid fueled combustors and burners suggest that the thin flame front model described above is still applicable. In such combustors both nonluminous flame fronts propagating through eddies of fuel vapor and air which are essentially premixed, and soot forming luminous flames surrounding rich fuel vapor air eddies can be observed(19). Such an unsteady turbulent flame structure would be expected in the vigorously stirred primary zone where fuel and air enter separately. As each eddy containing fuel vapor and air ignites, either a thin flame front will propagate through the eddy, or envelope and consume the eddy, depending on the local fuel-air ratio and eddy size. Both "premixed" and "diffusion controlled" burning would be expected. As a consequence, burnt gas eddies are produced with a distribution in fuel-air ratio about the mean primary zone value. This distribution will change with time as these eddies mix with each other, and with diffusion air, through the action of turbulence and molecular diffusion. One expects the details of the fuel injection process (which determine droplet sizes and the distribution of droplets within the primary zone) and the air flow pattern (which determines the mixing intensity) to affect both the initial spread of the eddy fuel-air ratio distribution and its change with time. This physical description of the combustion process is the basis for the model we will now describe.

Several flow models for gas turbine combustors have been presented in the open literature(6)(9)(10)(20) and (21). These have recently been reviewed by Meller(18). We will concentrate on the simplest model which has been compared extensively with experimental data. In this model, developed by Fletcher

and Heywood(6) and the authors(7), no attempt is made to describe the details of the turbulent flow field. The primary zone of the combustor is treated as a partially stirred reactor. It is assumed that the fuel and air which enter the primary zone are rapidly dispersed throughout the zone to form discrete fluid elements or eddies of a scale small compared with combustor dimensions. We will assume these eddies are uniformly dispersed throughout the zone volume, and after combustion the gas within each eddy remains essentially together throughout its residence time in the primary zone. For such a partially stirred reactor model it can be shown that the fraction of the flow with residence time between t and $t + dt$ is given by $\psi(t)dt$ where

$$\psi(t) = (1/\tau) \exp(-t/\tau) \quad (6)$$

and τ , the mean residence time, is the primary zone volume divided by the volume flow rate of burnt gas out of the zone.

But since the fuel and air are not uniformly mixed, different burnt gas elements will have different average equivalence ratios during their residence time in the primary zone. A Gaussian distribution about the mean equivalence ratio ϕ (or mean fuel mass fraction which is almost equivalent(6)) is assumed; i.e., the fraction of the flow with equivalence ratio (or fuel fraction) between ϕ and $\phi + d\phi$ is given by $f(\phi)d\phi$ where

$$f(\phi) = (1/\sigma\sqrt{2\pi}) \exp[-(\phi - \bar{\phi})^2/2\sigma^2] \quad (7)$$

and σ is the standard deviation. A mixing parameter s , where

$$s = \sigma/\bar{\phi} \quad (8)$$

is used as a measure of the nonuniformity of the primary zone; $s = 0$ corresponds to perfect mixing. The mean primary zone equivalence ratio, $\bar{\phi}$, is determined from the fuel and air flows into the primary zone. Approximate correlations are available for estimating the fraction z of the fuel entering the primary zone which burns there(22). Techniques have been developed for estimating the air flow distribution within the combustor liner(23).

The importance of characterizing the uniformity of mixing is shown in Figure 4. Mean NO formation rates (for $\{NO\} \ll \{NO\}_e$) are shown as a function of mean primary zone equivalence ratio for combustor air inlet conditions of 843°K and 24.1 atm for $s = 0, 0.25$ and 0.5 . For stoichiometric mixtures, the mean NO formation rate is substantially reduced as the primary zone becomes less uniform; for rich ($\phi \geq 1.1$) and lean ($\phi \leq 0.8$) the mean NO formation rate is substantially increased. Note that the peak NO formation rate shifts to the lean side as s increases.

The remainder of the combustor, the secondary zone, is usually treated as a one dimensional flow with air addition. The importance of this zone in predicting exhaust NO_x emissions depends on the mean primary zone fuel-air ratio. Where most of the primary zone flow is stoichiometric or lean, addition of dilution air cools the burnt gases close to the primary zone exit and rapidly quenches the NO forming reactions as indicated in Figure 3. Mikus and Heywood(7) in their treatment of this type of burner made the reasonable assumption that the effect of the dilution air at the start of the secondary zone is to quench immediately the NO forming reactions. The NO mass fraction at burner exit is just the mean NO mass fraction at primary zone exit times the ratio of primary zone mass flow rate to total mass flow rate.

If a substantial part of the primary zone flow is fuel rich, this simplifying assumption is no longer valid. As rich burnt gas eddies mix with dilution air or leaner eddies and pass through the stoichiometric fuel air ratio, NO formation rates peak as shown in Figure 3. The rate of dilution is therefore an important parameter.

The approach taken by Fletcher, et al.(6)(8) was to specify the change in mean fuel mass fraction F (F = mass fuel/total mass) and mixing parameter s along the length of the secondary zone as eddies of diluting air and burnt gases mix and react, and any fuel not burnt in the primary zone is consumed. A simple eddy mixing model was used to take account of changes in NO concentration due to mixing. Since in typical aircraft turbine combustors, the NO concentrations in the stoichiometric regions of the combustor are about one third or less of the equilibrium level, changes in local NO concentration due to mixing have little effect on the NO formation rate (see equation (5)). The mean equivalence ratio profile along the length of the secondary zone is determined from the air flow through the liner. The flow through film cooling slots and dilution air holes in the liner can be calculated using standard techniques(23) and a plot of total mass flow in the liner as a function of length obtained. The average equivalence ratio across the cross section of the can is estimated by smoothing this plot. The variation of s along the combustor is discussed more fully in the next section. Only the first part of the secondary zone ($\phi \geq 0.6$ for a conventional combustor) is important. In the downstream section only dilution of previously formed NO occurs.

These models have been programmed for solution on a digital computer. Equation (5) is linked with a program for calculating equilibrium thermodynamic properties and species concentrations of kerosene-air burnt gas mixtures for given pressure, temperature and atomic composition. Equation (5) can be integrated to give $\{NO\}$ as a function of time for any burnt gas element. Suitable averaging over the residence time distribution, equation (6), and equivalence ratio (or fuel mass fraction) distribution, equation (7), yield the average nitric oxide concentration at primary zone exit. The two distributions are assumed statistically independent. In the dilution zone, the calculation procedure follows burnt gas eddies of given equivalence ratio along the burner in incremental steps. The mean NO mass fraction is found by weighting the NO mass fraction in eddies of different equivalence ratio according to equation (7). In each subsequent step along the burner, allowance is made for the change in NO mass fraction in each eddy due to mixing. Additional NO formed is then computed for a number of eddies of different equivalence ratio, and average NO mass fraction calculated. Because the eddy temperature and radical concentrations used are low values, they depend only on equivalence ratio and initial air conditions. And since $\{NO\}$ is significantly less than $\{NO\}_e$, the effects of mixing (which changes s and ϕ) can be accounted for in this approximate calculation procedure.

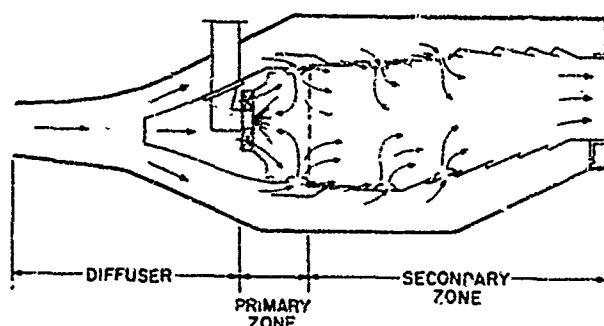


Fig. 1. Cross-section of typical annular gas turbine combustor showing mean flow pattern.

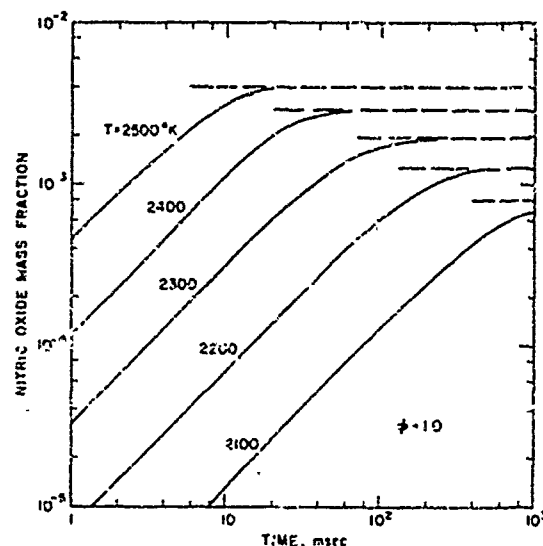


Fig. 2. Calculated NO mass fractions as function of time after combustion for different temperatures for a one-dimensional premixed flame. C_2H_5 -air mixture, pressure 10 atm, equivalence ratio 1.0. Dashed lines are equilibrium NO mass fractions.

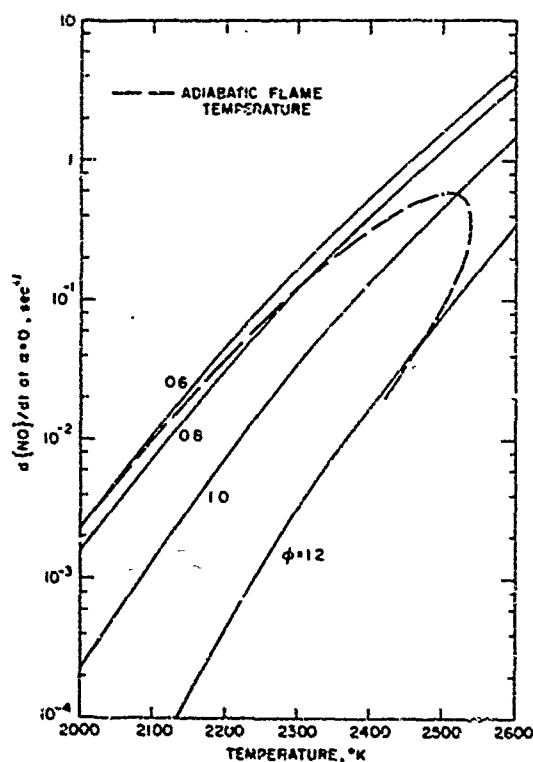


Fig. 3. NO formation rate, mass fraction per sec., for $\alpha=0$ as a function of temperature for different equivalence ratios and 15 atm pressure. Dashed curve shows adiabatic flame temperature for kerosene combustion with 700 °K, 15 atm, air.

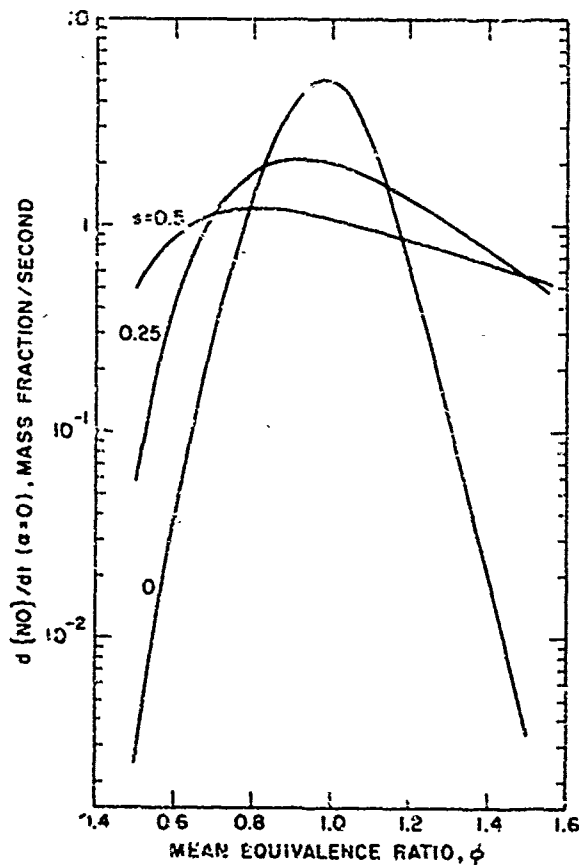


Fig. 4. Average NO formation rate for nonuniform kerosene-air burnt gas mixtures with different mean equivalence ratios and mixing parameters, 2. Air conditions: 843 °K, 24 atm.

3. MODEL EVALUATION

3.1 Sources of Uncertainty in Model Calculations

The previous sections indicate that the important model parameters are: air inlet temperature and pressure, T_a and p_a ; the mean equivalence ratio of the burnt gases in the primary zone, ϕ_p ; the mixing parameter in the primary zone, s_p ; and the rate of air addition in the early part of the secondary zone. With the exception of s_p , values of these parameters can be estimated for conventional combustors. However, before we examine the relationship of these parameters to predictions of combustor NO_x emissions, the major uncertainties in the model will be discussed.

The expressions used for rate constants are one possible source of error. Baulch, et al.⁽¹⁶⁾ give an uncertainty for k_1 as listed in Table 1 of \pm a factor of two up to 1600 °K increasing to a factor of four at 3000 °K. Examination of equation (5) shows that uncertainties in k_1 and k_2 are much less important. The uncertainty in $[\text{NO}]$ is thus approximately proportional to the uncertainty in k_1 , when, as is usually the case, the NO concentration in the highest temperature zones in the combustor do not approach equilibrium levels. The omission of radiation heat transfer is also a possible source of error in calculating the NO formation rate. While a gas turbine combustor is regeneratively cooled because the liner cooling air is eventually mixed with bulk flow, radiative heat losses from the gas in the primary and early part of the secondary zone will reduce peak burnt gas temperatures. In the primary zone, most of the radiation comes from soot particles formed in fuel-rich regions of the flame. Thus one expects error introduced by the omission of radiation from the primary and secondary zone models to be most significant in combustors with fuel-rich poorly mixed primary zones. The radiation heat flux to the liner wall will depend on the flame temperature and the amount of soot formed within the flame zone.

ϕ_p depends on measured fuel flow rate, estimated air flow into the primary zone and an estimate of the fraction of the fuel fed to the primary zone which burns there. The latter estimate is the most suspect, and existing correlations are probably inadequate. The correlation⁽²²⁾ used by Fletcher, et al.⁽⁹⁾ relates the primary zone combustion efficiency β to the primary zone fuel load factor, $\dot{m}_f/\sqrt{V_p p}$, where \dot{m}_f is the fuel flow rate, V_p is the primary zone volume and p the pressure level. The flame structure discussion in Section 2.3 suggests that the mixing characteristics would also be important. For the same fuel load factor, a better mixed primary zone will have a higher combustion efficiency.

The mixing parameter s must, as yet, be determined empirically by matching experimental NO_x emissions data. The dependence of s on fuel injection and air flow characteristics is examined in Section 3.4. More quantitative relationships for evaluating s are now being developed.

The quenching rate of the primary zone gases with dilution air, and the rate of burn up of fuel which leaves the primary zone unburnt must also be estimated. Fletcher, et al.⁽⁸⁾ carried out a sensitivity analysis to examine the effect of variations in these factors about their assumed average values and concluded that possible errors are quite small (≤ 25 percent). The fact that mixing with dilution air does not occur uniformly is not important in predicting overall NO emissions. The additional NO formed in burnt gas elements which are quenched more slowly than the mean compensates for elements quenched more rapidly than the mean since the combustor is almost adiabatic and the local NO formation rate is only weakly dependent on local NO concentration.

A comparison of model calculations with measured NO_x emissions from several combustors will now be made. Provided the absolute magnitude of the data can be predicted within about a factor of ± 2 , accurate prediction of the trends in the data is the more important test of model usefulness. The uncertainties in some model input parameters, and some of the approximations made preclude any expectation of more precise agreement.

3.2 Effects of Air Fuel Ratio, Air Inlet Temperature and Pressure

An extensive evaluation of the type of model described in Section 2 has been carried out by Fletcher, et al.⁽⁸⁾ Two combustors with different characteristics were tested over a range of operating conditions, and measured and predicted NO emissions compared. Tests were carried out with one operating variable changed at a time which does not correspond to normal combustor operation in a jet engine, but does facilitate model evaluation.

Figure 5 shows measured NO concentrations at combustor exit and the results of model calculations for two combustors A and B⁽⁸⁾. Each combustor was operated with inlet air at 85 psia and 700 °K and essentially constant air flow rate over a range of fuel flow rates. The measured emission characteristics of the two combustors are quite different, combustor A showing a more rapid decrease in emissions as air fuel ratio (AFR) increases. The solid lines show model predictions with constant values of s_p and with the primary zone burnt fuel fraction β given by the correlation in ref. (22). For combustor B, the $s_p = 0.7$ line is a good match to the data over the AFR range 55 to 130. For combustor A, the $s_p = 0.3$ curve matches the slope of the data but falls below the measurements. However, as explained in Section 3.1 the correlation used for β does not take account of differences in primary zone mixing characteristics. Jackson and Odgers, in their discussion of factors influencing heat release, recognized the importance of pressure loss factor on combustor efficiency,⁽²²⁾ but since pressure loss factor is relatively constant for gas turbine combustors they developed a single correlation. For the same fuel loading factor in the primary zone, better mixing should increase the value of β . Thus a correlation for β appropriate for $s_p = 0.3$ should give higher values than a correlation for $s_p = 0.7$. The scatter in the data used to develop the β correlation underline its approximate nature. s_p was treated as an adjustable parameter,⁽⁸⁾ and increasing β by 15 percent gives the dashed line in Figure 5 which matches the data over the AFR range 50 to 35. The idle NO emissions at an AFR of about 140 probably originate in the pilot flame.

The different NO emission characteristics of these two combustors can be explained as follows⁽⁸⁾. Combustor B burns with a rich primary zone for AFR less than about 70. Combustor A burns with a lean primary zone throughout its operating range. Though combustor A has a small primary zone with a higher loading factor than B, the primary zone combustion efficiencies (between 0.75 and 0.85) are similar since

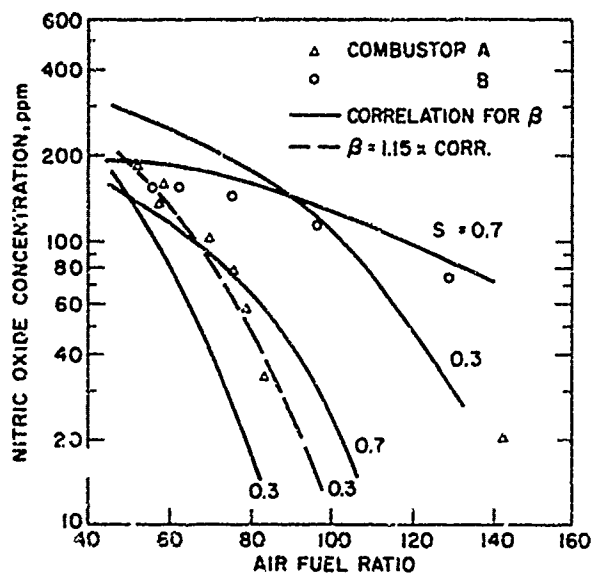


Fig. 5. Comparison of measured and predicted NO concentrations at combustor exit for two can combustors A and B for a range of overall air: fuel ratios. Kerosene fuel, 700 °K, 85 psia air. s is primary zone mixing parameter. β is fraction of fuel fed to primary zone which burns there. From Fletcher et al. (8)

Fig. 6. Calculated average burnt gas temperatures \bar{T} and equivalence ratios $\bar{\phi}$, and NO emission index along the length of two can combustors A and B. A has a fuel-lean and B a fuel-rich primary zone. From Fletcher et al. (8)

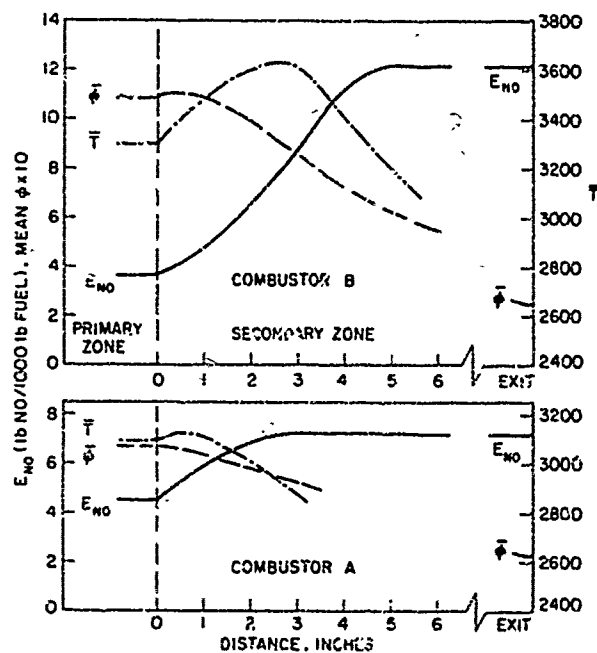
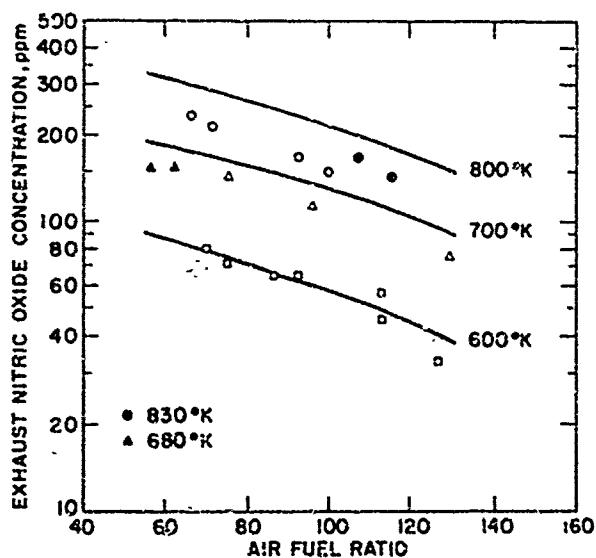


Fig. 7. Comparison of measured and predicted NO concentrations at burner exit for combustor B for a range of overall air fuel ratios and air inlet temperatures. Pressure is 85 psia. Predictions are for $s_p = 0.7$ and average air dilution rate. From Fletcher et al. (8)

A is better mixed.

This difference in emission characteristics is further illustrated in Figure 6 which shows calculated average burnt gas temperatures, \bar{T} , average burnt gas equivalence ratio ϕ , and NO emission index E_{NO} along the length of the two combustors(8). The NO emission index is lb NO/1000 lb fuel. It represents the amount of NO formed upstream of any axial position, and indicates that the NO chemistry is frozen at an equivalence ratio of about 0.6. However, the NO concentration continues to decrease along the length of the combustor due to dilution. The conditions for each calculation are given in the figure caption. As a consequence of the partially stirred reactor primary zone model, \bar{T} , ϕ and E_{NO} are constant within the primary zone.

In combustor B at the operating condition shown only one third of the exhausted NO is formed in the primary zone. Thus the rate of dilution of the gases just downstream of the primary zone has an important effect on total emissions. In combustor A with a lean primary zone, about two thirds of the exhausted NO is calculated as originating in the primary zone. When β is increased as described above to obtain a better match with the measured data, a higher fraction of the total NO originates in the primary zone. Thus the rapid quench assumption for a combustor with a lean well mixed primary zone which has been used by the authors(7) is a reasonable simplification.

The results of gas sampling and analysis inside the secondary zone of combustor B(8) lend support to these calculated profiles. Although a radial NO concentration gradient was measured at two axial locations ($x = 3$ and 7 inches) in the secondary zone, cross section average measured values were in close agreement with calculated mean values. The measured NO concentrations increase by about a factor of 2.5 from the edge of the film cooling layer to the can axis. These nonuniformities in time averaged NO concentrations presumably result from nonuniform dilution rates within the secondary zone.

The observed difference in NO emission characteristics with decreasing load (increasing AFR) for combustors with fuel-rich or fuel-lean primary zones is consistent with the variation in average NO formation rate shown in Figure 4. As the primary zone is leaned out (approximately in proportion to overall AFR), the average NO formation rate for the s_o value used above decreases substantially only after the primary zone becomes quite lean.

The effect of variations in combustor inlet air temperature at constant pressure on NO emissions for combustor B is shown in Figure 7(8). The solid lines are calculations based on an average secondary zone dilution rate obtained by smoothing a plot of air flow through the liner wall versus distance to allow for the delay in bulk mixing. The same value of s_o matches the measured data trends as overall AFR is increased. However, the effect of increasing air inlet temperature is overpredicted; a possible cause is omission of radiation heat losses in determining the burnt gas temperatures.

Data from Norster and Lefebvre(24) can be used to estimate the temperature drop below adiabatic flame temperatures resulting from radiation heat losses. Peak burnt gas temperatures would be about 20 °K below the adiabatic flame temperature with 600 °K inlet air, and 30 °K below with 800 °K inlet air for combustor B at an AFR of 65 and other conditions appropriate to Figure 7. An estimate of the change in NO formation rate resulting from these temperature decreases indicates the 800 °K air line would then lie about 24 percent lower and the 600 °K line about 10 percent lower at an AFR of 65. These approximate calculations support the conclusion that radiation heat losses account for the difference between measured and predicted effects of air inlet temperature.

The model also predicts the effect of changes in inlet air pressure. Experimental data show that, for a given combustor with fixed inlet air temperature, overall air fuel ratio and reference velocity, the NO emissions increase as the square root of air pressure(5). Equation (5) can be rearranged to show this dependence. Since the reaction



is in equilibrium,

$$[O] = \frac{x_{O_2}}{M} = \left(\frac{x_{O_2}}{K_p} \right)^{1/2} \quad (10)$$

where x_i is the mole fraction of species i , M is the molecular weight of the burnt gas mixture and K_p is the equilibrium constant for reaction (9). Using the perfect gas law, equation (5) can then be rearranged to give

$$\frac{d(NO)}{dt} = \frac{2H_{NO} k_1 x_{N_2}}{MRT} \left(\frac{x_{O_2}}{K_p} \right)^{1/2} \frac{(1 - \alpha^2)}{(1 + \alpha K)} \quad (11)$$

where R is the universal gas constant. For typical values of s_o for conventional combustors, Figure 3 shows the maximum NO formation rate occurs on the lean side of stoichiometric where x_{O_2} is essentially independent of pressure. For a fixed inlet air temperature, the burnt gas temperature T , k_1 and K_p only vary weakly with pressure. For $\alpha \leq 0.5$ which is usually the case, equation (11) shows that $d(NO)/dt$ increases as $(p)^{1/2}$. Thus for the same reference velocity, NO emissions will also vary approximately as $(p)^{1/2}$.

3.3 Predicting Emissions from the GM GT-309 Engine

The model can be fitted into an engine cycle and used to calculate NO emissions over the load range of an engine. Here air flow rate, air fuel ratio and combustor air inlet conditions all vary

simultaneously. The authors (7) have applied this model to the General Motors GT-309 regenerative gas turbine (25) (26) and compared predicted and measured NO emissions.

The GT-309 prototype engine has a can-type combustor with air-atomizing fuel injection. It has a well-defined primary zone because most of the dilution air is added at one axial station. Since the primary zone is operated at fuel-lean conditions, the assumption of rapid quenching of nitric oxide formation at the primary zone exit is a reasonable approximation, greatly simplifying the nitric oxide analysis.

The fraction of the total air flow through the combustor which enters the primary zone and takes part in primary zone combustion can be estimated from the sizes of the various orifices in the combustor liner and the approximate percentage of liner cooling air entrained into the primary flow. The mean primary zone equivalence ratio, obtained from the fuel flow and calculated primary air flow, is less than unity for all engine operating conditions. At each operating point a mean primary zone residence time, based on the volume flow rate at primary zone conditions, is calculated. Table 2 lists the values of combustor parameters over the engine's operating range.

TABLE 2
Data Used in GT-309 NO Emissions Study

Gasifier turbine speed %	Combustor inlet		Mean primary zone	
	Temperature °F	Pressure atm	Equivalence ratio	Residence time, msec
100	1091	3.68	0.81	6.8-7.3
90	1154	3.08	0.72	6.9-7.3
80	1233	2.53	0.62	7.2-7.5
70	1314	2.08	0.52	7.7-7.8
60	903	1.70	0.28	9.8
50	964	1.44	0.22	11.2

Treating the primary zone as a partially-stirred reactor, as described in Section 2.3, with 100% combustion efficiency and no heat losses, allows a computer analysis of nitric oxide formation with only one free parameter, the mixing parameter s . Figure 3 compares calculated NO concentrations at combustor exit with engine measurements. With $s \approx 0.5$ the calculations match the measured trends reasonably well from part load to full load (70-100 percent gasifier speed). The poor match of the uniformly mixed primary zone calculations (the $s = 0$ line) with the measured data underlines the importance of including nonuniformities in the NO formation model.

At lower gasifier speeds (50-55 percent) corresponding to idle, the model described here predicts NO concentrations orders of magnitude below the measured values. At the low gasifier speeds corresponding to idle and low power output modes, fuel and air flow rates are far away from the design point. The flow pattern and level of turbulence within the primary zone become radically different; considering the entire primary zone as a stirred reactor is no longer valid. Equivalence ratio and residence time distributions based on air flow rate for the whole primary zone are no longer good approximations to actual combustion conditions.

Results on tests on two modifications of the standard GT-309 burner with earlier quenching of the primary zone combustion products have been reported by Cornelius and Wade (26). The full power exhaust NO concentrations, relative to the standard burner are shown in Figure 9 as a function of relative residence time. The model predictions for $0 < s < 0.5$ are in close agreement; the value of s only weakly influences the relative effect of changes in residence time. This comparison does, however, support the conclusion that NO concentrations in the primary zone are below equilibrium levels.

3.4 The Mixing Parameter s

So far s has been treated as a floating parameter whose value is determined by matching predictions to measured emissions data. It has been found that a constant value of s_0 in the primary zone can be used for a given combustor over a wide range of operating conditions and gives acceptable NO predictions. But different types of combustors require different values of s_0 , and it is obvious that a better understanding of the relation of s to design and operating variables is required. Pompei and Heywood (27) have developed a more quantitative model for s in a kerosene fueled atmospheric pressure cylindrical burner which has several features in common with a gas turbine combustor. A high pressure air-assist atomizer was used to inject the fuel. For the same total air and fuel flow rates, variation in atomizer air pressure (over the range 10 to 30 psig) significantly changed combustion and emission characteristics.

The value of s along the burner length was determined from measured O_2 concentrations when the mean equivalence ratio was stoichiometric. Under these conditions, once combustion of the hydrocarbon fuels has occurred, any significant average O_2 concentration in the burnt gases is the result of imperfect mixing. Increasing the atomizer air pressure reduced s , flame luminosity and CO emissions at a given ϕ . The effect on NO emissions depended on the value of ϕ . These s profiles were used to calculate NO and CO concentrations along the burner length; these agreed well with measured values. Turbulent mixing theory was used to relate the decay of s with time (or distance along the burner) to a mixing rate intensity I as

$$s^2(t) = s_0^2 \exp(-It) \quad (12)$$

It was found that I varied approximately as the square of the atomizing air pressure (28). A simple model which assumed that the mixing rate intensity I was proportional to the one third power of the kinetic energy of the air entering the burner reaction zone predicted a one third power dependence of I on atomizing air pressure. This disagreement suggests that effects of atomizer air pressure on fuel droplet size, droplet velocity, and spray cone angle are likely to be important. This is obviously an area for

further work; the success of the mixing model in a simpler flow geometry is, however, encouraging.

A number of experimental studies in gas turbine combustors have shown that changing fuel injection techniques in a manner expected to reduce nonuniformities in the primary zone has reduced soot, CO, hydrocarbon and NO emissions. Norster and Lefebvre⁽²⁹⁾ have compared a dual-orifice atomizer and an "air spray" atomizer. Grohman⁽⁴⁾ has presented results showing how increasing the pressure drop across an air-assist fuel nozzle can significantly reduce CO and HC emissions and improve combustion efficiency. Dix and Bastress⁽³⁰⁾ have shown that increasing the air pressure drop across the air-assist fuel nozzle in an automotive gas turbine with a fuel-lean primary zone significantly decreases NO emissions. This corresponds to reducing s_0 in the NO prediction model, and Figure 4 indicates that for a lean system a substantial decrease in the NO formation rate would be expected.

Several combustor performance parameters in addition to emissions--combustion efficiency, blow-out, relight characteristics, primary zone soot formation and wall radiative heat flux--are also influenced by the extent of the fuel-air nonuniformities in the primary and secondary zones. Dix and Bastress⁽³⁰⁾ have already suggested how some of these performance parameters might be related to the mixing parameter s . It is therefore desirable that the role of nonuniformities in gas turbine combustors receive the utmost attention, both theoretically and experimentally.

4. NO EMISSIONS FROM THE NASA SWIRL CAN COMBUSTOR

To illustrate the versatility of the NO prediction model, we have applied it to a new combustor concept which shows promise of lower emissions. This concept, the NASA modular swirl can combustor Model 4-C, is an unconventional annular design.^(*) Fuel is introduced into 120 swirl cans mounted in three concentric rings at the same axial station. Most of the air flows through these modules and in between them at the plane of the "blockage plates" which are the maximum axial cross-sections of the swirl cans. Only about 6% of the total air flow (used as liner cooling air) does not pass through or between the swirl cans. Figure 10 shows the construction of a swirl can. Air flows from the left, entering the can and mixing with fuel, which is sprayed onto the swirler plate from a fuel tube inside the can. This fuel-air mixture passes through the swirler and burns in the wake of the module. Some of the air which has passed around the module is entrained into the recirculating wake flow. Cold-flow tests confirm that this recirculating wake extends approximately one blockage-plate diameter downstream. The air which flows around the module but is not entrained into this "primary zone" will mix with the combustion products from the primary zone further downstream. Figure 11 is a tangential view of the combustor showing the swirl can modules mounted at the entrance plane of the annular liner. At low fuel-air ratios the combustion occurs within small primary zones in the wake of each swirl can. As the fuel-air ratio approaches stoichiometric, the primary zones coalesce into a single "ring of fire."

The difficulty with analyzing the NASA combustor is that contrary to more conventional designs, the volume of the primary zone and the mass flow of air entering this zone are not well defined by the liner geometry. The fluid mechanics of entrainment into a reacting, swirling, recirculating flow are not tractable enough to be used in the relatively simple nitric oxide formation model being proposed here. The following simplifying assumptions are made to obtain a simple model applicable to combustion operation at low fuel-air ratios, i.e. not too close to the stoichiometric value of 0.067. (i) The volume of the primary zone in the wake of each swirl can module is taken to be 8.7 in.³, which is equal to the area of an averaged blockage plate multiplied by the plate's diameter. This aspect ratio of approximately one is verified by cold-flow tests. If the flow patterns in the combustor do not change much as the volume flow rate and combustion intensity are varied, the volume of the primary zones will remain nearly constant. Of course, as the fuel-air ratio approaches stoichiometric and the primary zones coalesce, this assumption becomes invalid. (ii) The average fuel-air ratio in the primary zones is proportional to the combustor's overall fuel-air ratio. Once again, if the combustor's flow patterns remain relatively fixed, this assumption will be approximately true. (iii) The nitric oxide formation reactions are rapidly quenched as the combustion products leave the primary zones. Consider a burnt-gas eddy whose local fuel-air ratio is less than the fuel-air ratio with the peak nitric oxide formation rate. A relatively small amount of dilution (from the air flowing between the swirl cans which was not entrained into a primary zone) will cause the temperature-sensitive nitric oxide reactions to freeze. Therefore, this quenching assumption appears reasonable when most of the primary-zone burnt-gas eddies are leaner than approximately stoichiometric.

A few comments on the above modelling assumptions are in order. (i) Primary zone residence times vary inversely with primary zone volume. Nitric oxide production is found to be almost linear with residence time for the region of interest, so that changing the primary zone volume will approximate sliding the nitric oxide prediction curves vertically on a log scale. (ii) Changing the proportionality factor between the primary and overall fuel-air ratios is equivalent to changing the fraction of the overall air flow which enters the primary zone. This changes both the primary zone residence time and the dilution factor on exit from the primary zone. The approximate linearity of nitric oxide with residence time mentioned above results in a cancellation of the residence time and dilution factor effects. Thus, changing the proportionality factor between the primary and overall fuel-air ratios merely slides the nitric oxide predictions horizontally on a log scale of overall fuel-air ratio.

At overall fuel-air ratios comparable to stoichiometric, the flow model described above clearly must be changed. (Even if the concept of 120 module-wake primary zones remained valid, these primary zones would be operating at fuel-air ratios well above stoichiometric and produce negligible nitric oxide compared to what would be formed during dilution to the overall fuel-air ratio.) A better model is to treat the entire combustor annulus inside the liner as a partially stirred reactor, driven by the swirlers and blockage plates at the entrance plane and the high combustion intensity. The model corresponds to the "ring of fire" flow pattern observed at high fuel-air ratio operating conditions. The swirl-cans then serve as crude versions of an air-assisted fuel injector, partially premixing the fuel before combustion with the main air flow. The combustion zone volume of interest for the high fuel-air operating conditions is approximately 4.1 ft.³, the entire annulus within the combustor liner. The average fuel-air ratio is about 1.03 times the overall value, to allow for adding half of the 6% of total air flow used to cool the

liner. The sampled exhaust gases were quenched at the combustor exit by the sampling probe, so downstream quenching is not considered in the calculations.

Figures 12, 13 and 14 are comparisons of measurements on the swirl can combustor reported by Niedzwiecki and Jones (11) with computations made using the two models described in this section. The data points shown as circles are measurements made at a combustor inlet pressure of 5 to 6 atma, with a combustor air flow of 85 to 110 lbm/sec. The data points shown as diamonds are known to be measured at 6 atma and 110 lbm/sec., which were the values used in the analytical computation.

The curves drawn for fuel-air ratios between 0.01 and 0.03 are calculated with the low fuel-air ratio model (120 separate primary zones), using a primary zone fuel-air ratio of 0.5 times the overall value. As mentioned earlier, a change in this parameter will simply proportion out the prediction curves horizontally. Also note that a change in primary zone volume simply shifts the curves vertically. The mixing parameter values 0.33 and 0.42 which are illustrated produce approximately the proper slope to match the data, especially for the higher combustor inlet temperature cases, Figures 13 and 14.

The curves drawn for fuel-air ratios greater than 0.03 are calculated using the model appropriate to fuel-air ratios comparable with stoichiometric. Here the primary zone volume and fuel-air ratios are well defined, so that the prediction curves are not shiftable without making basic changes in the model.

Table 3 gives some of the parameters relevant to the nitric oxide calculations for a few sample points from the $s = 0.33$ curves presented in Figures 12, 13 and 14.

TABLE 3

Combustor Inlet Temperature, °F	Overall Fuel-Air Ratio	Primary Zone Fuel-Air Ratio	Primary Zone Residence Time, msec	Nitric Oxide from Primary Zone, mass-fraction
602	0.0160	0.0400	0.93	4.55×10^{-5}
907	0.0187	0.0467	0.83	2.10×10^{-4}
1058	0.0214	0.0534	0.76	3.97×10^{-4}
602	0.0650	0.0669	1.89	2.20×10^{-4}
907	0.0500	0.0513	2.02	5.61×10^{-4}
1058	0.0400	0.0412	2.16	4.72×10^{-4}

The two models described in this section match the lean and rich ends of the NASA emissions data reasonably well. To cover the middle range of fuel-air ratios would require modelling the air entrainment and mixing processes. This goes beyond our present understanding of the processes occurring within the combustor. However, curves which are simply faired in between the model prediction curves of Figures 12, 13 and 14 produce good matches with the experimental data.

To show the use of the nitric oxide formation model in extrapolating experimental data, calculations were made for operation of the NASA combustor at sea level static dry takeoff conditions typical of combustors used in state-of-the-art engines in the 40,000-pound thrust class. Table 4 gives results based upon the following data: combustion inlet temperature = 1400 °R, combustor pressure = 23 atma, overall fuel-air ratio = 0.023, primary zone fuel-air ratio = 0.0575, mixing parameter $s = 0.33$. A correction factor of 1.25 is used to approximately compensate for the divergence of the $s = 0.33$ curve from the data at a fuel-air ratio of 0.023 as the rapid quench assumption becomes inadequate.

TABLE 4

Reference Velocity, ft./sec.	Nitric Oxide, mass fraction at exhaust	Emissions Index, lbm NO _x /1000 lbm fuel	"Corrected" Emissions Index
75	3.15×10^{-4}	21.5	26.9
100	2.56×10^{-4}	17.4	21.8
125	2.16×10^{-4}	14.7	18.4

5. CONCLUSIONS

(i) The nitric oxide formation process in conventional gas turbine combustors is now reasonably understood. The parameters important in determining exhaust NO concentrations are inlet air pressure and temperature, mean primary zone residence time and fuel air ratio, the uniformity of the fuel-air ratio distribution in the high temperature zones in the combustor and the air dilution rate at the upstream end of the secondary zone.

(ii) The model for predicting NO emissions we have described can match measured emissions data from several different types of combustor over a wide range of operating conditions. The major problem in applying the model is that the parameter characterizing the fuel-air ratio nonuniformities must be determined empirically. The potential for relating this parameter to injection and combustor design and operating parameters has already been demonstrated in simpler flow geometries. This is an area for intensive analytical and experimental research.

(iii) The NASA swirl can combustor concept, through a reduction of high temperature zone residence time, and leaner and better mixed primary zone compared with current conventional combustors, has achieved a significant reduction in NO emissions when compared with current "jumbo jet" engines.

6. REFERENCES

1. Anon. Aircraft Emissions: Impact on Air Quality and Feasibility of Control, U.S. Environmental Protection Agency, Dec. 1972.

2. Federal Register, vol. 37, No. 239, Part II, Dec. 12, 1972, p. 26491.
3. Barrington, A. E., ed., Climatic Impact Assessment Program: Proceedings of the Survey Conference, Feb. 15-16, 1972, Cambridge, Mass., U.S. Dept. of Transportation, 1972.
4. Grobman, J. S., "Effect of Operating Variables on Pollutant Emissions from Aircraft Turbine Engine Combustors," Emissions from Continuous Combustion Systems, ed. by Cornelius, W., and Agnew, W. G., Symposium held at General Motors Research Laboratory, Warren, Michigan, Sept. 27-28, 1971, Plenum Press, 1972, pp. 279-303.
5. Bahr, D. W., "Technology for the Reduction of Aircraft Turbine Engine Exhaust Emissions," AIAA Paper No. 72-1202, AIAA/SAE 8th Propulsion Joint Specialists Conference, New Orleans, Nov. 29-Dec. 1, 1972.
6. Fletcher, R. S., and Heywood, J. B., "A Model for Nitric Oxide Emissions from Air Gas Turbine Engines," AIAA Paper No. 71-123, presented at AIAA 9th Aerospace Sciences Meeting, New Orleans, Jan. 25-27, 1971.
7. Mikus, T., and Heywood, J. B., Comb. Sci. Tech., vol. 4, 1971, pp. 149-158.
8. Fletcher, R. S., Siegel, R. D., and Bastrom, E. A., The Control of Oxides of Nitrogen Emissions from Aircraft Gas Turbine Engines, vol. 1, Report No. 1162-1, Northern Research and Engineering Corporation, Cambridge, Mass., Dec. 1971.
9. Hammond, D. C., and Mellor, A. M., Comb. Sci. Tech., vol. 4, 1971, pp. 101-112.
10. Roberts, R., Arato, L. D., Kollrack, R., Bonnell, J. M., and Teixeira, D. P., "An Analytical Model for Nitric Oxide Formation in a Gas Turbine Combustion Chamber," AIAA Paper No. 71-715, AIAA/SAE 7th Propulsion Joint Specialist Conference, Salt Lake City, June 14-18, 1971.
11. Niedzwiecki, R. W., and Jones, R. E., "Pollution Measurements of a Swirl Can Combustor," AIAA Paper No. 72-1201, AIAA/SAE 8th Joint Propulsion Specialist Conference, New Orleans, Nov. 29-Dec. 1, 1972.
12. Heywood, J. B., Fay, J. A., and Linden, L. H., AIAA J., vol. 9, No. 5, 1971, pp. 841-850.
13. Heywood, J. B., "Gas Turbine Combustor Modelling for Calculating Nitric Oxide Emissions," AIAA Paper No. 71-712, AIAA/SAE 7th Propulsion Joint Specialist Conference, Salt Lake City, June 14-18, 1971.
14. Westerberg, A. A., Comb. Sci. Tech., vol. 4, Issue 2, 1971, pp. 59-64.
15. Morr, A., "A Model for Carbon Monoxide Emissions from Industrial Gas Turbine Engines," Ph.D. Thesis, M.I.T., Feb. 1973.
16. Saulsh, D. L., Drysdale, D. D., Home, D. G., and Lloyd, A. C., Critical Evaluation of Rate Data for Homogeneous Gas Phase Reactions of Interest in High Temperature Systems, Part 4, Dept. of Chem., The University, Leeds, Dec. 1969.
17. Campbell, I. M., and Thrush, S. A., Trans. Faraday Soc., vol. 64, 1968, pp. 1265-1274.
18. Mellor, A. M., "Current Kinetic Modeling Techniques for Continuous Flow Combustors," Emissions from Continuous Combustion Systems, ed. Cornelius, W., and Agnew, W. A., Symposium held at General Motors Research Laboratory, Warren, Michigan, Sept. 27-28, 1971, Plenum Press, 1972, pp. 23-49.
19. Appleton, J. P., and Heywood, J. B., "The Effect of Imperfect Fuel-Air Mixing in a Burner on NO Formation from Nitrogen in the Air and the Fuel," 14th Symposium (International) on Combustion, Penn State, August 1972, to be published by the Combustion Institute.
20. Edelman, R., and Economos, C., "A Mathematical Model for Jet Engine Combustor Pollutant Emissions," AIAA Paper No. 71-714, AIAA/SAE 7th Propulsion Joint Specialist Conference, Salt Lake City, June 14-18, 1971.
21. Pratt, D. T., Bowman, B. R., Crowe, C. T., and Sannichsen, T. C., "Prediction of Nitric Oxide Formation in Turbojet Engines by PSR Analysis," AIAA Paper No. 71-713, AIAA/SAE 7th Propulsion Joint Specialist Conference, Salt Lake City, June 14-18, 1971.
22. Jackson, S. R., and Odgers, J., "Factors Influencing Heat Release in Combustion Chambers and Consideration of the Related Materials and Structures," Combustion in Advanced Gas Turbine Systems, ed. Smith, I. E., London, Pergamon Press, 1966, pp. 137-208.
23. Grobman, J. S., Comparison of Calculated and Experimental Total-Pressure Loss and Airflow Distribution in Tubular Turbojet Combustors with Tapered Liners, NACA Memo 11-26-58E, National Advisory Committee for Aeronautics, 1958.
24. Norster, E. R., and Lefebvre, A. H., "Influence of Fuel Preparation and Operating Conditions on Flame Radiation in a Gas Turbine Combustor," ASME Paper No. 72-WA/HT-26, ASME Winter Annual Meeting, New York, Nov. 26-30, 1972.
25. Cornelius, W., Stivender, D. L., and Sullivan, R. E., "A Combustion System for a Vehicular Regenerative Gas Turbine Featuring Low Air Pollutant Emissions," SAE Paper 670936, SAE Combined Fuels and Lubricants, Power Plant and Transportation Meeting, Pittsburgh, 1967.
26. Cornelius, W., and Wade, W. R., "The Formation and Control of Nitric Oxide in a Regenerative Gas Turbine Burner," SAE Paper 700708, SAE Combined Farm, Construction and Industrial Machinery and Power Plant Meetings, Milwaukee, Wisconsin, 1970.
27. Pompei, F., and Heywood, J. B., Comb. Flame, vol. 19, to be published 1972.
28. Flagan, R., M.I.T. Ph.D. Thesis, to be submitted June 1973.
29. Norster, E. R., and Lefebvre, A. H., "Effects of Fuel Injection Method on Gas Turbine Combustor Emissions," Emissions from Continuous Combustion Systems, ed. Cornelius, W., and Agnew, W. A., Symposium held at General Motors Research Laboratory, Warren, Michigan, Sept. 27-28, 1971, Plenum Press, 1972, pp. 255-278.

30. Dax, D. M., and Bastress, E. K., "Approaches to Design of Low-Emission Gas-Turbine Combustion Chambers," SAE Paper 720728, SAE National Combined Farm, Construction and Industrial Machinery and Power Plant Meetings, Milwaukee, Wisconsin, Sept. 11-14, 1972.

ACKNOWLEDGMENT

This work was supported in part by the National Aeronautics and Space Administration under Grant NGR 22-009-378.

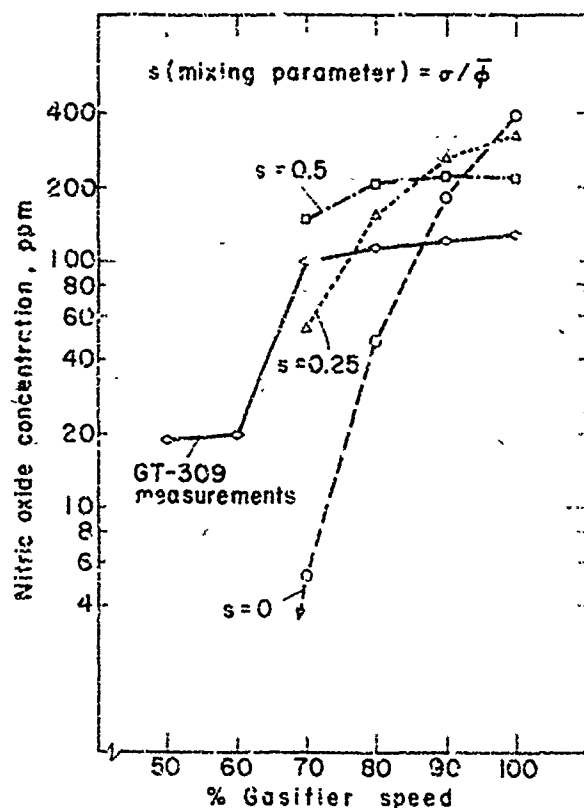


Fig. 8. Theoretical calculations of General Motors GT-309 engine combustor NO emissions versus gasifier speed, compared with engine exhaust measurements(7).

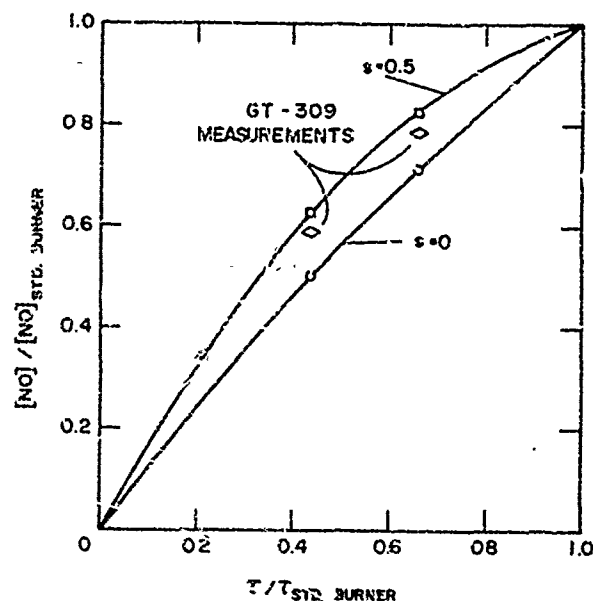


Fig. 9. Theoretical calculations of GT-309 combustor design-point NO emissions versus mean primary zone residence time, compared with measured values for the standard (std.) burner and two early quench design modifications(7).

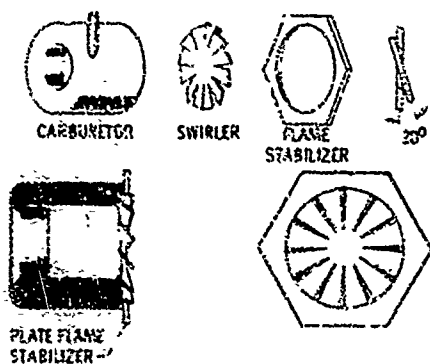


Fig. 10. NASA swirl can combustor module details(4).

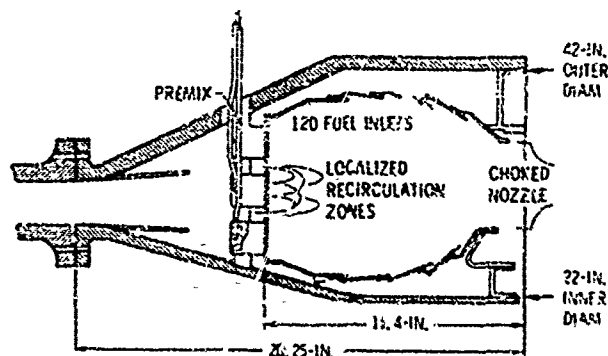


Fig. 11. NASA modular swirl can combustor schematic layout(4).

Fig. 12. Comparison of measured and predicted NO mass fractions at exit of NASA swirl can combustor as a function of overall fuel-air ratio. Curves at lower left are from single module model appropriate for low fuel-air ratios. Curves at upper right are from high fuel-air ratio model treating entire combustor as the primary zone. Data points shown as circles are measurements made at pressures of 5 to 6 atm with a combustor airflow of 85 to 110 lbm/sec. Data points shown as diamonds are at 6 atm and 110 lbm/sec, the values used in the computations. Nominal combustor inlet temperature is 600 °F. Data from Kucukerenci and Jones (11)

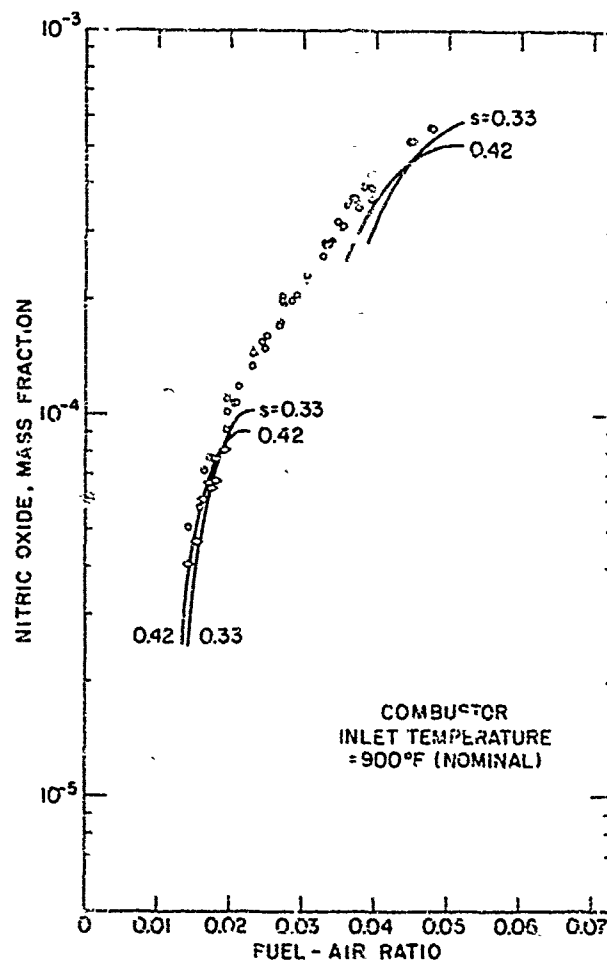


Fig. 13. Same as Figure 12 with nominal combustor inlet temperature of 900 °F.

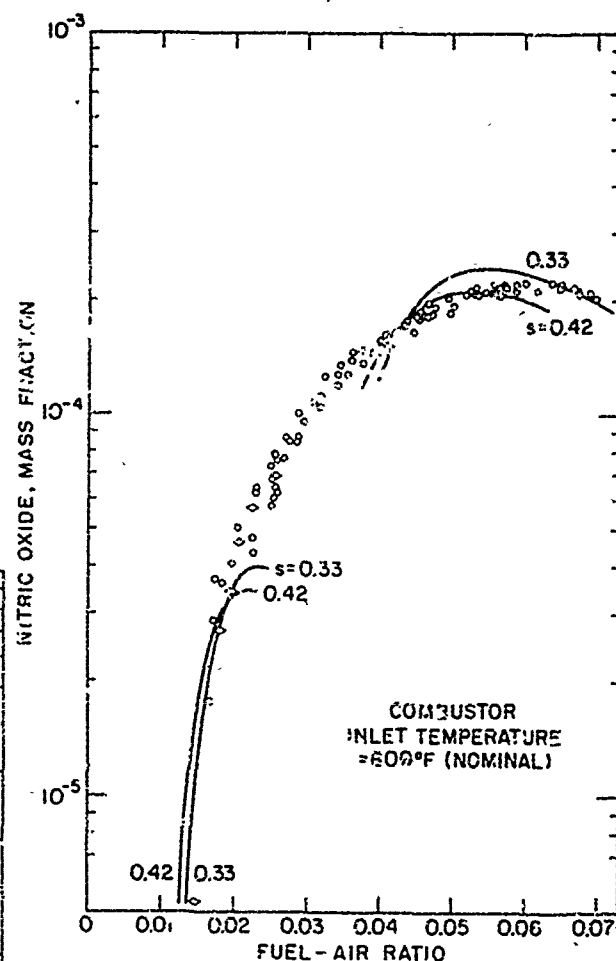


Fig. 14. Same as Figure 12 with nominal combustor inlet temperature of 1050 °F.

Discussion on Paper 21
 "Parameters Controlling Nitric Oxide Emissions from Gas Turbine Combustors"
 presented by J.B. Heywood

M. Whittaker:

- (a) Could the speaker indicate to what extent the reductions in NO emissions were due to reductions in residence time and to changes in degree of mixing?
- (b) Is the reduction a trade-off of NO_x pollution for CO pollution in the NASA Lewis combustor? What is the speaker's opinion regarding the merits of the two alternative methods of running rich or weak of stoichiometric?

J.B. Heywood:

- (a) In our calculations of emissions from the NASA swirl can combustor for take-off conditions with a pressure ratio of 24:1, the module wake region (the primary zone) was leaner, better mixed and had a shorter residence time (about 1 msec) than an equivalent conventional combustor. We did not estimate each of these effects separately. However, NO_x emissions would be reduced approximately in proportion to the reduction in residence time, and the effect of a leaner and better mixed primary zone on the NO formation rate can be estimated from Figure 4.
- (b) The CO emissions in the swirl can combustor depend both on the emissions of a single module and how many modules are operating. At light load when CO is a problem, the number of modules is reduced. There is no simple answer to this question.

N. Chigier: From the high speed movies which you have taken in the primary zone, could you observe envelope flames and individual droplets? The location of the flame front with respect to location of droplet surface can make large differences to vaporization rates of droplets.

J.B. Heywood: We have taken high speed movies of the combustion zone in an atmospheric pressure burner with an air blast atomizer and liquid kerosene as fuel. These movies show that luminous burning eddies are of order 0.2 inch in diameter, that is much larger than envelope flames around individual droplets.

R. Roberts: One must use caution when applying previously demonstrated results, i.e., the NASA swirl can combustor, to existing engines. It is likely that inlet reference velocity for the engine will be different.

J.B. Heywood: In our calculations of NO emissions from the NASA swirl can at simulated JT9D or CF6 take-off operating conditions, we have approximately matched the combustor inlet air temperature and pressure, turbine inlet temperature, and covered an appropriate range of reference velocities (75 - 125 ft/sec). So we believe the calculations are a reasonable simulation.

W.S. Blazowski: Our calculations with a simple model show that for future advanced engines and, for that matter, current designs on a hot day (25/1 pressure ratios at ambient temperatures exceeding 150°F) levels of NO produced are approaching primary zone equilibrium. Have you examined cases where combustor inlet temperatures are 1200-1300°F? How important might fuel distribution be in this case?

J.B. Heywood: Yes, we would expect that, as combustor pressures and flame temperatures increase somewhat above the values we have used, primary zone NO concentrations will approach equilibrium values. Since equilibrium NO concentrations depend on equivalence ratio in an adiabatic combustor, we would predict that the fuel distribution will be just as important.

A.H. Lefevre: I feel that your mixing parameter α_0 should be replaced by two mixing parameters, one to take account of the degree of fuel/air mixing prior to combustion and another which describes the intensity of mixing within the combustion zone. The value of the first parameter would be governed largely by the method of fuel injection employed, while the magnitude of the second parameter would be dictated mainly by the geometry of the liner and the pressure drop across it.

J.B. Heywood: Our choice of mixing parameter is in no way unique. Both the factors you mention would be expected to affect the parameters we have used. However, I doubt that these two factors can be separated in the way you describe.

A.M. Meller: It is a pleasure to see that your model can be extended to such a wide range of combustor types and still predict exhaust emissions of NO to within a factor of two. However, I think that the model should be subjected to two more demanding tests. First, comparison with detailed internal measurements which are now becoming available, and second, CO should also be included in some way for comparison as well. Other investigators have found it is impossible to get good agreement for both pollutants with a single set of curve fit parameters.

F.J.Verkamp: You presented data in your paper on the "Early Quench" GMR 309 combustor which showed that the NO_x was 25% less than the "Conventional" 309 combustor. However, you did not present any CO data for the "Early Quench" 309 combustor. Available CO data shows that the CC would increase. In fact, modifications to a conventional combustor simply cause a trade-off in CO and NO_x . Simultaneous reductions in both CO and NO_x emissions are required to provide advanced low emission combustors. In your analytical model, you predict only NO_x emissions. Do you plan to expand your model to predict CO emissions?

J.B.Heywood: We did compare NO measurements made by Fletcher, Siegel and Hastress (Ref. 8) with model calculations. The cross-section average NO concentrations along the combustor axis predicted by the model (Figure 7 in our paper is taken from reference 8 and shows the calculated profiles) are in reasonable agreement with the measured values when these are averaged over the liner cross-section. However, probing within the primary zone was not successful. Comparison between predictions and measurements must be done carefully. The model predicts NO concentrations in the burnt gases. In certain probe locations (e.g. the primary zone) the probe may sample a mixture of burnt and unburnt mixture and the data would not be directly comparable with predictions.

The model we have described obviously does not attempt to calculate CO emissions. We have developed a similar model which includes the kinetics of CO oxidation and the effects of imperfect fuel-air mixing and non-uniform dilution rates. This model predicts measured CO emissions trends quite well, with the same mixing parameter values.

P.A.Libby. It may be worthwhile to comment that the assumption of a gaussian distribution, e.g., of the fuel, in a turbulent flow can under some flow conditions be widely in error. We are comfortable with gaussian distributions so we can readily overlook the fact, which is obvious if we just think about it, that concentration in terms of mass fraction or some percentage is bounded, i.e., has values between zero and unity, and is not unbounded as many other fluid dynamical variables. A little reflection leads to the conclusion that for any mean concentration it is always possible to find an intensity of fluctuations of concentration which can only correspond to a non-gaussian probability density distribution.

Another consideration which raises further doubts about the assumption of a gaussian distribution in some cases relates to the possibility that turbulent eddies with either only fuel or only air within them may be significantly present. In this case the probability density distribution must be considered to consist of a continuous function plus two delta functions representing the fraction of time that only fuel and only air are present.

It should be understood that the behavior suggested by these comments does not always occur and in fact may not occur in the flow being treated by Professor Heywood and his co-worker. The converse of the statement made above is also true. for a given mean concentration one can always find a turbulent intensity sufficiently low so that a gaussian distribution might be expected to be a reasonable assumption.

In view of these comments we would certainly agree with the authors that the problem of turbulent flows with chemical reactions taking place in them requires and deserves much work.

J.B.Heywood: The gaussian distribution is, as is stated, an assumption. Some work being carried out by Professor John P.Appleton and Mr Richard Flagan at M.I.T. in a kerosene fueled atmospheric pressure burner suggests, however, that a gaussian distribution is attained quite rapidly. Note that the version of this NO model developed by Fletcher et al (References 6 and 8) does allow for unmixed and unburnt fuel through the parameter β , fraction of the fuel fed to the primary zone which burns there. Also, only that part of the distribution close to stoichiometric is really important in predicting NO emissions. Nonetheless, Professor Libby's comments are still appropriate.

FACTORS CONTROLLING POLLUTANT EMISSIONS FROM GAS TURBINE ENGINES

R.F. Sawyer
N.P. Cernansky
A.K. Oppenheim

University of California
Department of Mechanical Engineering
Berkeley, California 94720
U.S.A.

SUMMARY

Primary pollutants emitted by aircraft gas turbine engines are carbon monoxide, hydrocarbons, aldehydes, smoke, particulates, and nitric oxide. Factors controlling emissions of these pollutants are analyzed on the basis of aircraft engine exhaust composition and laboratory studies of gas turbine combustion processes. Moreover, an analytical prediction of the effect of aircraft operating parameters on the emission of nitric oxide is also given.

Measurements of aircraft engine exhaust compositions from several different turbojet, turbofan, and turboprop engines reveal striking similarities in their pollutant emission characteristics. Carbon monoxide, hydrocarbons, and aldehydes are at their peak values during idle operation and drop to very low levels as engine power is increased. Particulates, smoke density, and nitric oxide increase with power level, the latter depending exponentially upon the maximum local combustor temperature.

The formation and destruction of these pollutants were investigated in a laboratory gas turbine combustor. The oxidation of carbon monoxide, hydrocarbons, and aldehydes was measured in the dilution zone where thermal quench phenomena were observed. The apparent oxidation of particulates in the dilution zone was also observed; details of the particulate studies are reported in a companion paper, No. 28. The formation of nitric oxide was observed in the primary zone and in the first part of the dilution section of the combustor.

Operational conditions and engine parameters such as ambient temperature, pressure, and humidity, flight altitude, flight Mach number, water injection, fuel properties, and combustor characteristics have been studied analytically, yielding rational criteria for the prediction of their effect on the emission of nitric oxide.

SYMBOLS

EI	emission index, gm species/kg fuel
P	pressure, atm.
R	universal gas constant, 0.001986 kcal/gm-mole °K
t	time, sec
T	temperature, °K
X	mole fraction

INTRODUCTION

The present and potential significance of aircraft as contributors to air pollution remains still only partially established. Three regions of possible impact have been identified, 1) at or in the immediate vicinity of airports, 2) in an urban air basin, and 3) in the stratosphere. Studies at the Los Angeles International Airport (1,2) have shown aircraft to be the primary source of pollutants at the airport and in its immediate vicinity. Projections for future years (3) show in fact that, in the absence of aircraft emission controls, aircraft sources alone would prevent the attainment of U.S. Environmental Protection Agency air quality standards in the vicinity of this airport. The contribution of aircraft to the pollutant burden of an urban air basin is small, being currently less than about one percent of any pollutant species (3). The control of other pollutant sources and growth of air traffic, however, are predicted to increase the relative importance of aircraft as sources of air pollution, Table 1. The possible importance of aircraft emissions in the stratosphere focuses upon the effect of nitric oxide upon the ozone layer (4,5) and is the subject of Climatic Impact Assessment Program (CIAP) (6,7).

Aircraft contributions to low altitude air pollution have been judged to be of sufficient importance to cause the U.S. Environmental Protection Agency to propose emission standards for aircraft (8). These standards call for reductions or limitations of engine emissions over a period of years. The proposed 1979 emission standards for new gas turbine engines are summarized in Table 2. The proposed standards, expressed as pounds mass per 1600 pound-thrust-hours per cycle, offer a reward for low specific fuel consumption. The cycle is defined in terms of a simulated landing and take-off operation with the times in different engine power settings specified to correspond to taxi/idle, takeoff, climbout, and approach.

Although aircraft cannot now be considered as a major source of air pollution, future increases in both their absolute and relative contributions to air pollution is expected. The major force behind this increase is a rapidly expanding consumption of fuel by aircraft, again in both absolute terms and especially relative to fuel consumption in ground transportation (9). Figure 1. (The distribution of fuel consumption between ground and aircraft transportation can be somewhat misleading since the major portion of emissions from ground transportation impacts upon urban areas while only a fraction of the aircraft emissions, namely those emitted below roughly one kilometer altitude, are of any significance in this respect. It is estimated that 20 to 25% of all fuel consumed by U.S. civil aircraft is consumed during operations at air terminals, including take-off and landing (10).) Changing engine characteristics,

Table 1. Aircraft contributions (percent) to total air pollutant emissions. Los Angeles Air Quality Region with currently proposed controls on other sources and no controls on aircraft (3).

	1970	1975	1980
CO	1.0	5.8	13.6
HC	1.0	2.7	2.5
NO _x	0.7	2.8	5.7

Table 2. Proposed exhaust emissions standards for new aircraft gas turbine engines, 1979 (8).

thrust, lbf	< 6000	6000-29000	> 29000
CO	2.2*	2.1	1.7
HC	1.0	0.4	0.4
smoke number	35	25	20
NO _x	3.7	3.2	3.0

*Emissions of CO, HC, and NO_x in lb_m/10³ lbf-hr/cycle.
Smoke number refers to a filter smoke spot reflectance test.

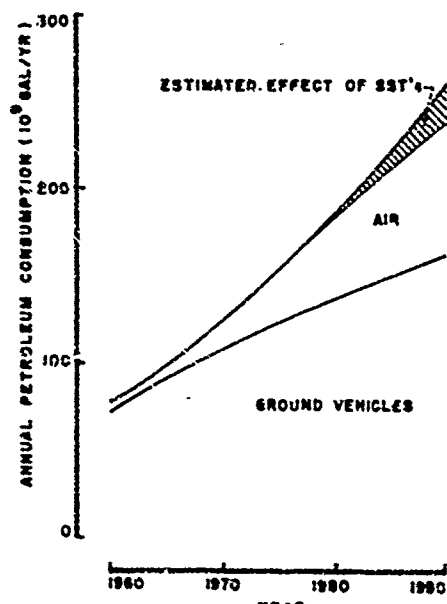


Figure 1. Annual United States petroleum consumption for transportation. Adapted from (9).

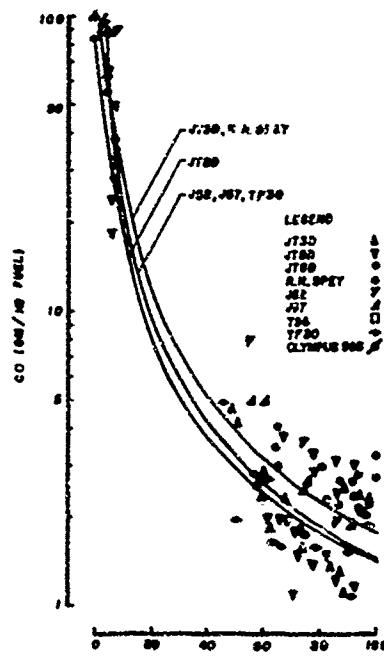


Figure 2. Aircraft gas turbine engine emissions: carbon monoxide.

especially those factors enhancing the formation of nitric oxide, will also affect total aircraft emissions. An understanding of the factors affecting the composition of gas turbine exhaust should prove useful in obtaining required emission reductions.

ENGINE EMISSIONS CHARACTERISTICS

Available data on engine emissions have increased greatly during the past two years (11-17). Much of this information was collected as part of an Environmental Protection Agency aircraft baseline emissions data program and it has been summarized and analyzed by the Cornell Aeronautical Laboratory (18, 19). Lipfert (20) has provided a particularly thoughtful analysis and correlation of these data. Most of the

engine data presented here comes from these sources and our interpretation draws freely upon the work of Lipfert.

The most important pollutants emitted by aircraft gas turbines are carbon monoxide, hydrocarbons, aldehydes, particulates, smoke, and the oxides of nitrogen. The term hydrocarbons generally refer to species detected by flame ionization. Smoke density, which is often erroneously equated with particulates (see Paper No. 28), is generally measured by a filter stain technique (21). The oxides of nitrogen (NO_x) in gas turbine exhaust are generally believed to be primarily nitric oxide (NO). High concentrations of nitrogen dioxide (NO_2) have been reported (12), however, and questions remain about whether nitrogen dioxide is indeed an important exhaust component or whether its measurement is the result of difficult sampling conditions. Nonetheless, the convention of treating the mass of NO_x as though it were all NO_2 is followed in this paper. Emissions are normalized with respect to the fuel consumption and are reported as grams of species per kilogram of fuel — a parameter referred to as the "emission index". The advantage of using this parameter is the fact that it eliminates the need to specify the local mixture ratio (degree of dilution) at the point of sampling. Mass emission rates are obtained from the product of the emission index and the fuel mass flow rate. The dimensions used by the Environmental Protection Agency in their proposed emissions standards are obtained by multiplying the emission index by the effective thrust specific fuel consumption, with proper attention paid, of course, to the use of consistent units.

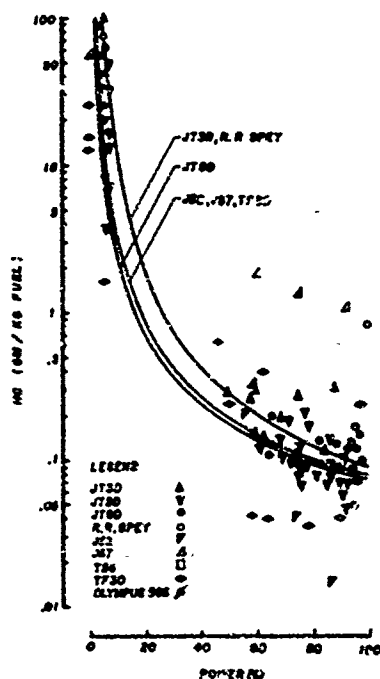


Figure 3. Aircraft gas turbine engine emissions: hydrocarbons.

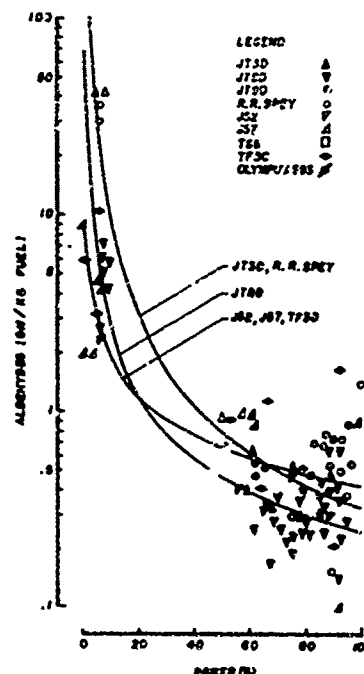


Figure 4. Aircraft gas turbine engine emissions: aldehydes.

Measured gas turbine exhaust emissions of carbon monoxide, hydrocarbons, and aldehydes are presented as a function of the engine power output in Figures 2-4. Similar trends are noted for all three of these gaseous reducing species. High emission levels occur at low power settings (idle) as the combined result of poor mixing and rapid cooling by an excess of air. At high power levels the emissions indices of all of these species drop to very low values. It is interesting to note that the concentrations of aldehydes are roughly comparable to those of hydrocarbons. The curves are least square fits of the data and the coefficients for their algebraic expressions are given in Table 3. Engine groupings are arbitrary. The correlation between hydrocarbons and carbon monoxide deduced by Lipfert (20) is shown in Figure 5. A direct relation of carbon monoxide and hydrocarbon emissions with combustor inefficiency, Figure 6, was pointed out by Lipfert (20) and others (22).

Smoke density tends to increase with power level, Figure 7. This property probably results from a combination of increased combustor pressure and increased sizes of fuel rich mixture regions in the combustor. Unlike the three gaseous reducing species, higher power levels apparently do not provide sufficiently increased oxidation rates to cause smoke levels to drop.

The oxides of nitrogen exhibit quite a different behavior from that of the previously described gaseous species, increasing rather than decreasing with power, as shown in Figure 8. Lipfert observed that the oxides of nitrogen are related directly to the combustor inlet air temperature, Figure 9. The striking degree of correlation among the emissions from a number of different engines is surprising and suggests a fundamental similarity between the processes controlling the formation of nitric oxide in these engines.

Table 3. Coefficients for the algebraic expression
 $\ln(\text{emissions index}) = \exp[A + B \ln(\% \text{ power})]$
 representing the least square fits to the gas
 turbine emissions data.

Pollutant	Group	Engines	A	B
CO	I	JT3D, R.R.Spey	2.79013	-.110670
	II	JT8D	2.73877	-.104240
	III	J52, J57, TF30	2.77706	-.112043
HC	I	JT3D, R.R.Spey	2.97357	-.227019
	II	JT8D	2.72515	-.180856
	III	J52, J57, TF30	2.76556	-.188982
Aldehydes	I	JT3D, R.R.Spey	2.78543	-.151952
	II	JT8D	2.59304	-.118274
	III	J52, J57, TF30	2.45164	-.0718543
NO _x	I	JT3D, R.R.Spey	2.30707	-.0983149
	II	JT8D	2.21816	-.0755872
	III	J52, J57, TF30	2.17307	-.0534085
Smoke Density	I	JT3D	1.96388	-.0595246
	II	JT8D	2.41608	-.147993
	IV	T56	1.66657	-.00494483

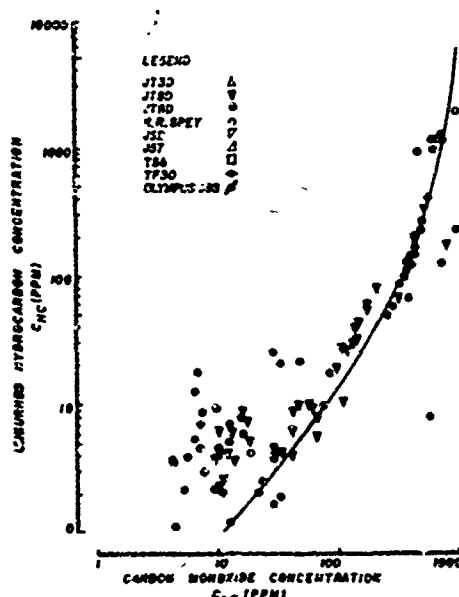


Figure 5. Correlation between hydrocarbons and carbon monoxide emissions from aircraft gas turbine engines. Adapted from (20).

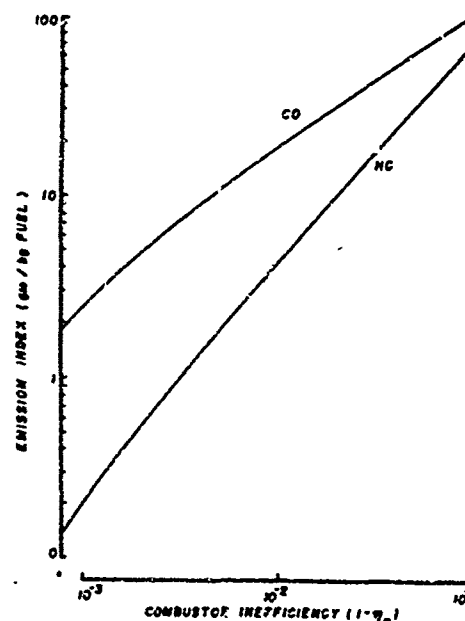


Figure 6. Relation of hydrocarbon and carbon monoxide emission indices to combustor inefficiency. Taken from (20).

Although the quantity of information on engine emissions has increased greatly in the past two years, the need for additional data still remains. Careful attention to sampling and analytical procedures and consideration of the effects of such parameters as ambient humidity and temperature should help reduce the scatter in the results of emission measurements. The trends shown in the available data are sufficient, however, to establish qualitatively the important factors controlling pollutant emissions.

LABORATORY COMBUSTOR STUDIES

All gas turbine engine and most gas turbine combustor emission studies have been concerned primarily with the measurement of exhaust composition. Exhaust composition, however, is controlled almost entirely

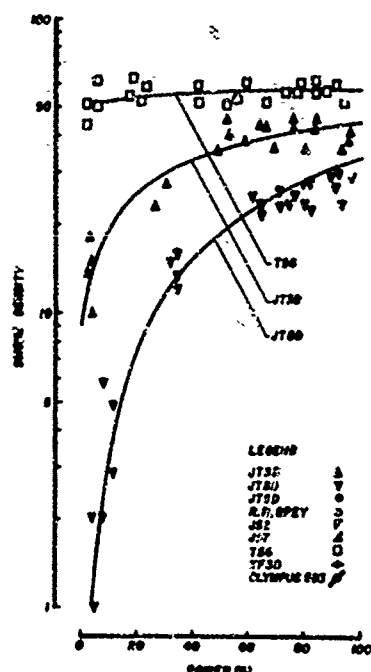


Figure 7. Aircraft gas turbine smoke density.

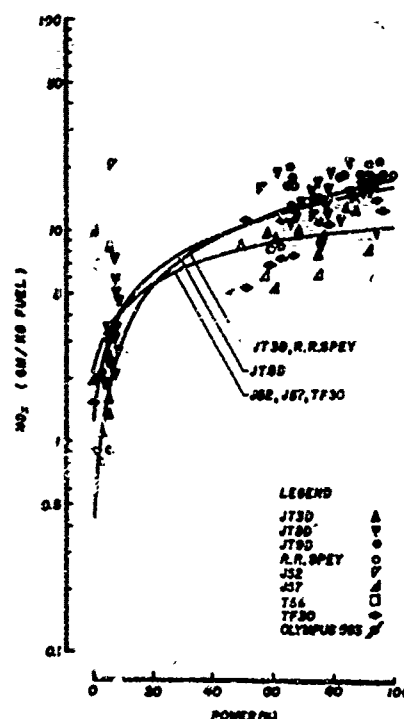


Figure 8. Aircraft gas turbine engine emissions: oxides of nitrogen, reported as NO_2 .

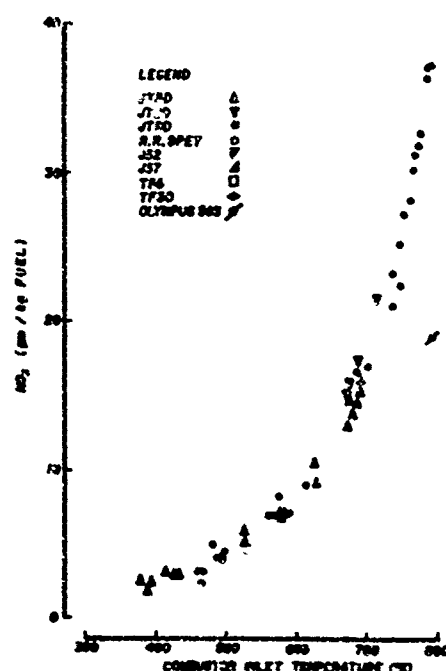


Figure 9. Aircraft gas turbine oxides of nitrogen correlation with combustor inlet temperature. Adapted from (20).

by processes taking place within the combustor. Consequently a series of laboratory combustor studies have been undertaken at Berkeley based on the sampling of combustion products from within the combustor. The major results of this continuing experimental research program, initiated approximately five years ago, have been reported in the literature (23-28). Given here in Figures 10-14 are selected centerline composition profiles for carbon monoxide, hydrocarbons, aldehydes, particulates, and oxides of nitrogen. In all cases the fuel was JP-4. Combustor pressure, combustor loading, and mixture ratio were the same only for the measurements of carbon monoxide, hydrocarbons, and oxides of nitrogen. This prevents making direct comparison of these data with those obtained for aldehydes and particulates.

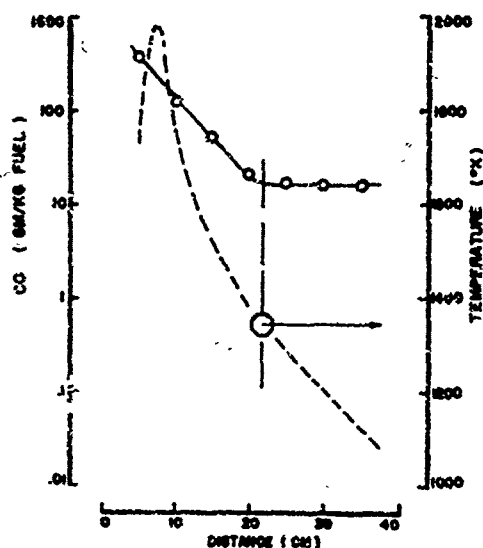


Figure 10. Laboratory gas turbine combustor centerline carbon monoxide and temperature.

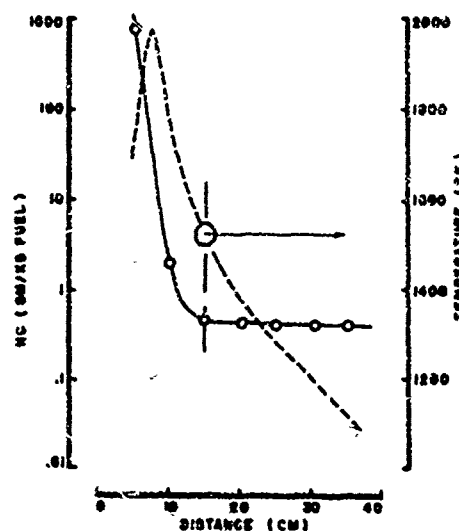


Figure 11. Laboratory gas turbine combustor centerline hydrocarbons and temperature.

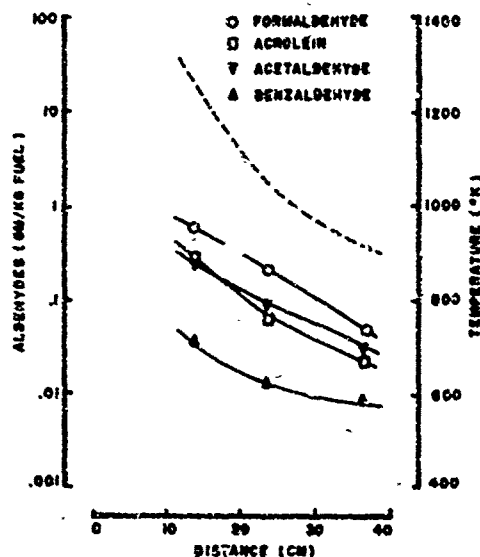


Figure 12. Laboratory gas turbine combustor centerline aldehydes and temperature.

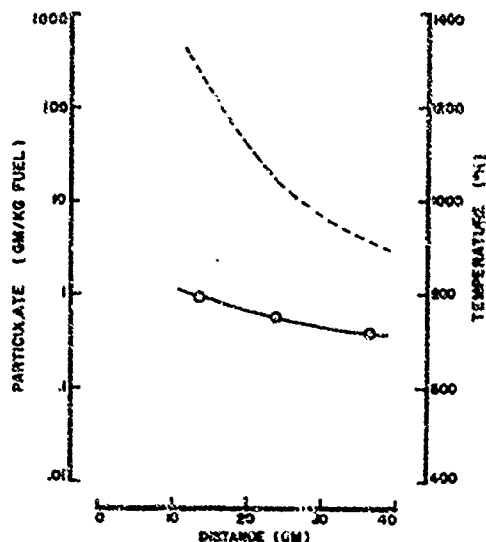


Figure 13. Laboratory gas turbine combustor centerline particulates and temperature.

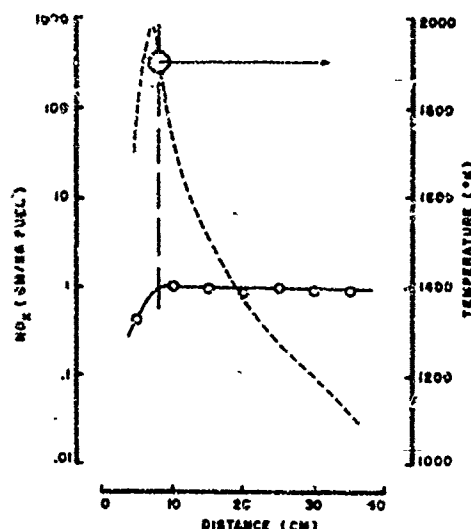


Figure 14. Laboratory gas turbine combustor centerline oxides of nitrogen (reported as NO_2) and temperature.

Carbon monoxide is oxidized in the dilution zone of the combustor. At a distance of about 20 centimeters from the fuel nozzle, however, the reaction of carbon monoxide is quenched as a result of cooling by the dilution air. The disappearance of carbon monoxide is controlled by the reaction, $\text{CO} + \text{OH} \rightleftharpoons \text{CO}_2 + \text{H}$. Since this reaction has low activation energy, the abrupt reduction in reaction rate is probably due to the disappearance of OH radicals. A simple, chemical kinetic model for the disappearance of CO, based on an equilibrium concentration of OH radicals, yields the following expression for its rate (29):

$$-\frac{d \ln X_{\text{CO}}}{dt} = 10^{11.763} T^{-1} \exp\left(-\frac{39,285}{RT}\right) X_{\text{O}_2}^{1/2} X_{\text{H}_2\text{O}}^{1/2} P^3 (\text{sec}^{-1})$$

The oxidation of hydrocarbons occurs much more rapidly than carbon monoxide. This leads to much lower concentrations of hydrocarbons, even though the quenching of the hydrocarbon reaction in this experiment occurred before that of carbon monoxide. The end result is consistent with the engine emission characteristics. The kinetic mechanism of hydrocarbon oxidation cannot be expressed in terms of a simple relation. The hydroxyl radical plays, no doubt, an important role in the process, so that quenching at a temperature close to that observed for carbon monoxide is expected.

Aldehydes are found in the combustor at low concentrations (less than hydrocarbons in the dilution zone whereas carbon monoxide is at a higher concentration than the hydrocarbons). The apparent slow disappearance, as illustrated in Figure 12, is somewhat misleading since these species are probably being formed as well as being destroyed in the dilution zone. The aldehydes are particularly reactive. Using a simple model similar to that employed for carbon monoxide, the disappearance of formaldehyde is predicted to take place at a rate given by the expression (29):

$$-\frac{d \ln X_{\text{H}_2\text{CO}}}{dt} = 10^{14.033} T^{-1} \exp\left(-\frac{38,685}{RT}\right) X_{\text{O}_2}^{1/2} X_{\text{H}_2\text{O}}^{1/2} P^3 (\text{sec}^{-1})$$

This reaction continues at temperature below the quench temperature for carbon monoxide.

The apparent oxidation of particulates in the dilution region is shown in Figure 13. As mentioned before, a detailed discussion of the behavior of this pollutant in the combustor is given in Paper No. 28.

The nitric oxide profile in the combustor is quite different from the species discussed so far. Nitric oxide is formed in the primary zone and in the first part of the dilution zone. Once formed, it shows no tendency to disappear. The observed dependence of nitric oxide formation on temperature is consistent with a highly simplified chemical kinetic model (30) based on the Zeldovich mechanism and equilibrium oxygen atom concentration. This model yields the rate (29):

$$\frac{dx_{\text{NO}}}{dt} = 10^{15.563} T^{-1} \exp\left(-\frac{135.5}{RT}\right) x_{\text{N}_2} x_{\text{O}_2}^{1/2} P^{1/2} \text{ (sec}^{-1}\text{)}$$

The quenching of the formation reaction takes place early in the dilution region and occurs well before the nitric oxide approaches an equilibrium concentration.

Extrapolation of these laboratory studies directly to engine characteristics is not intended or proposed. The pressures, temperatures, and loadings of the model combustor used for our studies are below those characteristic of modern gas turbines. It should be noted that important radial variations in the laboratory combustor have been observed (25), so that the one dimensional plug flow model suggested by our presentation here, based only on the centerline measurements, should be regarded as an oversimplification of the actual processes. Indeed the importance of a distribution of local mixture ratios has been pointed out by Heywood (31).

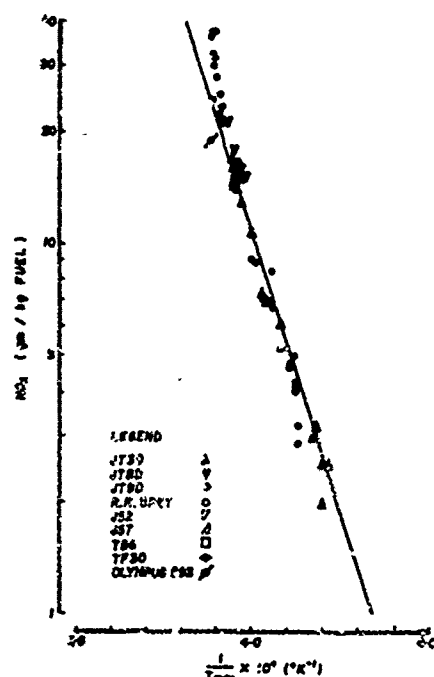


Figure 15. Arrhenius plot of oxides of nitrogen emissions index (reported as NO_2). Temperature refers to maximum local combustor temperature based on adiabatic, stoichiometric combustion.

EFFECT OF OPERATIONAL CONDITIONS AND ENGINE PARAMETERS ON NITRIC OXIDE EMISSIONS

The remarkable correlation of nitric oxide emissions from a number of different gas turbine engines operating over a range of power settings with the combustor inlet air temperature, Figure 9, may be interpreted in terms of the simple kinetic model given in the previous section. The rate of formation of nitric oxide is postulated to depend upon the mole fraction of nitrogen and oxygen, upon the square root of the combustor pressure, and, most importantly, upon the maximum local temperature within the combustor. The maximum local temperature was predicted from the inlet air temperature under the assumption of stoichiometric combustion. Such data, based in part on Figure 9, are plotted in standard Arrhenius form, $\text{Log}(\text{NO}_x)$ vs $1/T$ in Fig. 15. The straight line is drawn through the data with a slope corresponding to the effective activation energy of $-135 \text{ kcal/gm-mole } ^\circ\text{K}$ corresponding to the Zeldovich mechanism. Again, the agreement is most remarkable.

The engine data show a greater slope than predicted from the effective rate constant for the formation of nitric oxide. The difference is consistent with the predicted square root dependence of the rate of nitric oxide formation upon the combustor pressure. The engines having the greatest maximum combustor temperature also have the highest combustor pressures. The pressure effect also explains the difference between the high altitude nitric oxide emission from the Olympus-593 engine (solid circle) and the other data which were obtained from sea level tests.

These observations lead to the strikingly significant conclusion that the characteristic time for nitric oxide formation has been about the same for all of these engines.

A theoretical analysis was undertaken to determine the effect of aircraft operational conditions and engine parameters on the formation of nitric oxide. "Influence coefficients" indicating the sensitivity of nitric oxide formation to changes in these parameters were calculated. Two separate cases were examined: 1) typical take off conditions for a high performance, high bypass turbofan engine, and 2) supersonic cruise conditions, representative of an advanced turbojet.

Reference values for the operational and engine parameters were selected for the take off and

supersonic cruise cases described above. From these reference conditions, nitric oxide formation was calculated and then recalculated perturbing one parameter at a time. The changes in the nitric oxide levels due to parameter perturbations were noted and then used to calculate the "influence coefficients" which are reported in terms of the percent change in nitric oxide formation per unit change in the parameter.

It was assumed that nitric oxide production occurs largely in stoichiometric regions. Further, it was assumed that in the regions important to nitric oxide formation all important chemical species are at their equilibrium concentrations and nitric oxide levels remain sufficiently below their equilibrium values, so that nitric oxide decomposition reactions could be ignored. The following steps were then used for the calculation of nitric oxide formation: 1) combustor inlet conditions (temperature and pressure) were calculated from the operational conditions and engine parameters, 2) equilibrium concentrations of important chemical species, excluding nitric oxide, and the adiabatic flame temperature were evaluated for a stoichiometric mixture, 3) nitric oxide formation was computed using the simple model described previously.

The reference values of the operational and engine parameters assumed for the two cases are summarized in Table 4. Perturbed values of the parameters were chosen as 10 percent above and below the reference values, except where reason dictated that other values be used. The results of these nitric oxide influence coefficient calculations are presented in Table 5. Nitric oxide formation is shown to be extremely sensitive to altitude for the take off conditions and to altitude, pressure ratio and flight Mach number for the supersonic cruise conditions.

Table 4. Summary of reference point data for typical take-off and supersonic-cruise operating conditions

	High performance, high bypass, turbofan engine at take off	Advanced turbojet engine at supersonic-cruise
Ambient temperature ($^{\circ}\text{K}$)	298.	217.
Ambient pressure (atm)	1.0	0.0546
Relative humidity (%)	50.0	0.0
Altitude (km)	0.0	20.0
Mach number	0.0	2.7
Compressor pressure ratio	40.0	12.5
Polytropic compressor efficiency	0.9	0.9
Diffuser efficiency	1.0	1.0
Fuel hydrogen/carbon ratio	1.94	1.94
Fuel enthalpy of formation (cal/mole)	-5430.	-5430.
Equivalence ratio in pollutant formation zone	1.0	1.0
Residence time in pollutant formation zone (msec)	0.5	0.5
Water injection (wt. H_2O /wt. (H_2O +fuel))	0.0	0.0

It is important to note that the results of a linear perturbation analysis of this sort should be interpreted with some reservations and proper understanding of their significance. The operational parameters are not all independent. For example, a change in flight Mach number would usually also be accompanied by a change in flight altitude, pressure ratio, etc. No attempt was made to account for such multiple interactions in this study and therefore the influence coefficients presented represent only a first approximation of the effects of changes in operational parameters.

The effect of the operational conditions and engine parameters upon nitric oxide formation appears only through their effect on the combustor inlet temperature and combustor pressure. As discussed previously, there is some justification for the use of such a simplified model. The model is consistent with the dominant chemical kinetics and the experimentally measured values of nitric oxide emissions.

An important conclusion is that, in the absence of controls, nitric oxide emissions should increase with increasing engine performance. The most promising control technique appears to be the limitation of the maximum combustor temperature through lean combustion and uniform distribution of the reactants throughout the combustor.

CONCLUSIONS

Our review may be summarized by the following conclusions:

- 1.) Although aircraft pollutant emissions today are in most cases relatively minor, the potential exists in the future for aircraft to become major contributors.
- 2.) The dependence of aircraft gas turbine pollutant emission indices on the engine power level can be classified into two distinct groups: a) the hydrocarbons, aldehydes, and carbon monoxide which decrease with load and b) oxides of nitrogen and particulates which exhibit the opposite trend. With reference to the first group, unburned hydrocarbons and carbon monoxide correlate with combustor inefficiency

Table 5. Summary of influence coefficients for typical take off and supersonic-cruise operating conditions

Parameter	% Change in nitric oxide concentration*	
	Change in parameter	
	High performance, high bypass, turbofan engine at take off	Advanced turbojet engine at supersonic-cruise
Ambient temperature	-0.36%/°K increase)** 0.58%/°K decrease	2.7%/°K
Ambient pressure	0.10%/(0.001 atm)	3.4%/(0.001 atm)
Relative humidity	-0.5%/(% R.H.)	-
Altitude	-23%/(km)	-29%/(km)
Mach number	-	7%/(0.01 m)
Compressor pressure ratio	8.1%/(unit P.R.)	27%/(unit P.R.)
Polytropic compressor efficiency	-6.8%/(0.01 unit)	-4.4%/(0.01 unit)
Diffusor efficiency	-	3.2%/(0.01 unit)
Fuel hydrogen/carbon ratio	3.4%/(0.1 unit)	2.2%/(0.1 unit)
Fuel enthalpy of formation	-0.90%/(100 cal/mole)	-0.66%/(100 cal/mole)
Equivalence ratio in pollutant formation zone	-5.5%/(0.01 unit increase) 2.0%/(0.01 unit decrease)	-2.7%/(0.01 unit increase) 1.2%/(0.01 unit decrease)
Residence time in pollutant formation zone	20% (0.1 msec)	20% (0.1 msec)
Water injection	-2.5%/(0.01 unit)	-1.3%/(0.01 unit)

* A minus sign indicates that the nitric oxide changes inversely with the parameter, i.e., the nitric oxide concentration decreases as the absolute numerical value of the parameter increases.

** This surprising decrease in nitric oxide with increasing ambient temperature results because relative humidity was held constant. There is a disproportionate increase in water content with temperature; this water acts as a diluent to suppress combustor temperatures and hence nitric oxide formation.

and their emissions therefore can be minimized by maintaining high combustor efficiency. The absolute level of their emissions is relatively low because high emission indices occur at low fuel flow rates. With reference to the second group, their emissions become more significant because the high levels of their emission indices occur at the highest fuel flow rates.

3.) The oxides of nitrogen emissions correlate remarkably well to an Arrhenius law with respect to the maximum combustor temperature. The resulting effective activation energy is close to that for a simple chemical kinetic formation mechanism based on the classical Zeldovich mechanism. The formation of the oxides of nitrogen is sensitive to operational parameters which increase combustor inlet air temperature, especially compressor pressure ratio and flight Mach number.

4.) The minimization of oxides of nitrogen emissions requires control of the combustion process to avoid local regions of high temperature. The promotion of lean combustion with uniform mixture ratio distribution is a promising means of limiting oxides of nitrogen formation.

REFERENCES

1. Los Angeles County Air Pollution Control District, "Jet aircraft emissions and air quality in the vicinity of the Los Angeles International Airport," April 1971.
2. Lozano, E.R. and R.E. George, "Jet aircraft emissions and air quality in the vicinity of the Los Angeles International Airport," SAE #710429, 1971.
3. Environmental Protection Agency, "Aircraft emissions: impact on air quality and feasibility of control," 1972.
4. Johnston, H.A., "Catalytic reduction of stratospheric ozone by nitrogen oxides," University of California, Lawrence Radiation Laboratory Report No. UCRL-20563, June 1971.
5. Johnston, H.A., "Reduction of stratospheric ozone by nitrogen oxide catalysts from supersonic transport exhaust," *Science*, 173, 6 August 1971, 517-522.
6. Barrington, A.E. (Editor), "Proceedings of the survey conference," February 15-16, 1972, Climatic Impact Assessment Program, U.S. Department of Transportation, DOT-TSC-CST-72-13, September 1972.
7. Goldberg, A., "Climatic impact assessment for high-flying aircraft fleets," *Aeronautics and Astronautics*, December 1972, 56-64.

8. Environmental Protection Agency, "Aircraft and aircraft engines, proposed standards for control of air pollution," Federal Register 37, No. 239, Part II, 26488-26503, 12 December 1972.
9. Austin, A.L., B. Rubin, and G.C. Werth, "Energy, uses, sources, issues," Lawrence Livermore Laboratory, Report No. UCRL-51221, Livermore, California, 30 May 1972.
10. Northern Research and Engineering Corporation, "Nature and control of aircraft engine exhaust emissions," Cambridge, Massachusetts, November 1962, p.89.
11. Hare, C.T., H.E. Dietzmann, K.J. Springer, "Gaseous emissions from a limited sample of military and commercial aircraft turbine engines," Southwest Research Institute, Report No. AR-816, 1971.
12. AiResearch Manufacturing Company of Arizona, "Exhaust emissions test AiResearch aircraft propulsion and auxiliary power gas turbine engines," Test Report GT-8747-R, 1971.
13. Vaught, J.H., W.M. Parks, S.E.J. Johnson, R.L. Johnson, "Collection and assessment of aircraft emissions base-line data turboprop engines (Allison T56-A-15)," Final Technical Report EDR 7200, EPA, Ann Arbor, 1971.
14. Nelson, A.W., "Collective and assessment of aircraft emissions baseline data - turbine engines," PWA-4339, Final Report, Pratt & Whitney Aircraft, East Hartford, Connecticut, 1972.
15. Nelson, A.W., "Exhaust emission characteristics of aircraft gas turbine engines," ASME 72-GT-75, 1972.
16. Cox, F.W., et al., "A field survey of emissions from aircraft turbine engines," U.S. Department of the Interior, Bureau of Mines Report of Investigations RI-7634, 1972.
17. Forney, A.K., "Engine exhaust emission levels," AIAA Paper No. 73-98, 1973.
18. Begdan, L. and H.T. McAdams, "Analysis of aircraft exhaust emission measurements Technical Report CAL No. NA-5007-K-1, Cornell Aeronautical Laboratory, Inc., 1971.
19. McAdams, H.T., "Analysis of aircraft exhaust emission measurements: statistics," Technical Report CAL No. NA-5007-K-2, Cornell Aeronautical Laboratory, Inc., 1971.
20. Lipfert, F.W., "Correlation of gas turbine emissions data," ASME 72-GT-60, 1972.
21. Society of Automotive Engineers, "Aircraft gas turbine engine exhaust smoke measurements," Aerospace Recommended Practice, ARP 1179, 1970.
22. Grobman, J., "Effect of operating variables on pollutant emissions from aircraft turbine engine combustors," NASA Tech. Memo. NASA TM X-6788, presented at 1971 CM Lab. Symp., Warren, Michigan.
23. Sawyer, R.F. and E.S. Starkman, "Gas turbine exhaust emissions," SAE Paper No. 680462, 1968.
24. Sawyer, R.F., et al., "Air pollution characteristics of gas turbine engines," Transactions of the ASME, J. of Engineering for Power 91, A, 290-296, 1969.
25. Starkman, E.S., et al., "The role of chemistry in gas turbine emissions," Transactions of the ASME, J. of Engineering for Power 91, A, 290-296, 1969.
26. Sawyer, R.F., "Reducing jet pollution before it becomes serious," Astronautics and Aeronautics 8 62-67, April 1970.
27. Parikh, P.G., et al., "Pollutants from methane fueled gas turbine combustion," University of California, College of Engineering Report No. TS-70-15, 1970.
28. Sawyer, R.F., "Experimental studies of chemical processes in a model gas turbine combustor," Emissions from Continuous Combustion Systems (W. Cornelius and W.G. Agnew, editors), 243-254, Plenum, New York, 1972.
29. Kondratiev, V.N., "Rate constants of gas phase reactions," National Standard Reference Data System, N.B.S., Washington, D.C., January 1972.
30. Laurendeau, N.M. and R.F. Sawyer, "General solution of reaction rate problems via combined integration and steady state analysis: application to nitric oxide formation and decomposition," College of Engineering, University of California, Berkeley, Report No. TS-71-3; also Western States Section, The Combustion Institute Paper No. WSCI 71-72, October 19.
31. Heywood, J.B., "Gas turbine combustor modeling for calculating nitric oxide emissions," AIAA Paper No. 71-712, 1971.

ACKNOWLEDGMENTS

This work was supported in part by the Air Force Office of Scientific Research under Grants AFOSR-72-2299 and AFOSR-72-2200. The authors wish to thank Lynn Cohen, Carlo Vivo, and Robert Cheng for their help in data reduction and figure preparation.

Discussion on Paper 22
 "Factors Controlling Pollution Emissions from Gas Turbines"
 presented by R.F.Sawyer

K.Heuer: Comparative figures would be appreciated on the increase of oxides of nitrogen when using the so-called reduced smoke "JT8D" burner cans. If exact data are not available, what is the approximate percentage?

R.F.Sawyer: Limited test data indicate that NO increases with the JT8D "smokeless" cans are about 10-20%.

A.K.Forney:

(1) Figure 9 should be marked "Sea Level Static" except for the Olympus data point.

(2) Please comment on the problems associated with sampling engine exhaust, particularly the probe material, sampling line material, pumps, etc., associated with emission measurements in altitude test cells.

R.F.Sawyer: The first point is well taken. All of the data on Figure 9 are for sea level static tests with the exception of the Olympus data point which is for simulated, high altitude flight conditions and is not comparable to the other data.

Serious difficulties exist in the measurement of NO oxide as the result of reactions in stainless steel sampling probes. The problem is most serious with reducing atmospheres and uncooled probes but significant destruction of NO can occur with oxidizing atmospheres and cooled probes. Sampling from high velocity exhausts, especially with reheat, appears to present particular difficulties in obtaining *unaltered* samples for analysis.

F.J.Verkamp: General Motors has calculated combustion efficiency based upon CO and H/C exhaust gas analysis for approximately 15 years. If combustion efficiency is used as an index of emission performance or control, should nitric oxide be included in the calculation of combustion efficiency?

It was interesting to observe that CO and NO_x trade-off in all the emission data reported in your paper included the emission measurements inside the combustor.

The data presented in Figure 9 of your paper is often mis-used and mis-applied. Various people have concluded that low combustor inlet temperatures are required to achieve low NO_x. In fact, it is easier to achieve simultaneous low CO and NO_x emissions at high inlet combustor temperatures because new "non-conventional" combustor designs such as premix/prevaporization can be applied in gas turbine engines. It is interesting to note that data was presented at the annual ASME gas turbine meeting on April 9, 1973, which shows that NO_x decreases with increasing inlet temperature. Perhaps we are working on the wrong type of subsonic aircraft engine. Should we not be developing a regenerative low cycle pressure ratio engine which would have low fuel consumption and low emissions?

R.F.Sawyer: The presence of NO in the exhaust does represent a combustion inefficiency. If the NO were converted to N₂ and O₂, energy would be released. The amount of the energy so trapped is generally very small. Although there may be some justification to the suggestion that combustion efficiency be redefined to include NO, I would prefer to see the definition left in terms of hydrocarbons and carbon-monoxide.

Although the current practice tends to create trade-offs between CO and NO, there is no fundamental reason why both cannot be reduced simultaneously in gas turbine engines. This does not mean that both reach their absolute minimum levels at the same operating conditions.

If all other conditions are held unchanged, increasing combustor air inlet temperature will increase NO. I interpret the results to which you refer to be the consequence of other counteracting processes which act to reduce the local maximum combustor temperatures (which, in fact, control NO formation).

R.F.Jones: In Table 2 you showed some values of CO, hydrocarbon, NO_x which are the EPA goals for 1979 and you suggested these to arrive at the proper initial index values which we can use. That is not correct. You should multiply by approximately 4. If you insist on doing this, I would suggest rather that you use the proper *number* and make some conversion to get CO hydrocarbon NO_x numbers into the proper emission index.

Next, Figure 6. You showed combustion inefficiency. I don't believe I have ever seen the values of emission index for hydrocarbons as low as you showed for 1% inefficiency and I don't know what they assume the fuel to be. We standardly have taken the fuel to be CH₄ and the initial index for 1% inefficiency to be 10 for hydrocarbon and 42% for CO, and as far as I know, everyone is using these numbers.

And finally, the question on the effect of the relative humidity. In the paper I am going to give tomorrow, I find that the effect of humidity is exponential. It is approximately e - 19 times the humidity. This agrees with the work that has been done previously, in which they say, it is approximately 20 to 25%. These are not exactly correct either. Would you care to comment on all these comments?

R.F.Sawyer: Most of these are rather specific numerical questions. First, you are right on what factors you multiply by. It depends upon the engine, and the aircraft and the nature of the landing and take-off cycle.

I simply suggest that they are of the same order of magnitude; in some cases you multiply by 2 and sometimes by 4. Please accept that this is a very rough number. One thing I wanted to indicate is that automotive gas turbines for example are a factor of 10 or 20 below these.

As far as the CO to hydrocarbon ratio on the combustion inefficiency I defer to you on this. If you say it should be a 4 to 1 ratio instead of a 10 to 1 ratio, I accept that.

As far as the relative humidity numbers I suppose you are saying that these numbers don't agree with what your experimental numbers say it should be.

R.E. Jones: It is difficult to work with relative humidity.

R.F. Sawyer: I agree with the numbers 20/25%.

G. Kappler: First, exhaust emission measurements from a combustor situated behind a rotating heat regenerator have shown decrease in NO emission levels with increasing air inlet temperatures. However, since there was also evidence that exhaust gases were recycling because of leakages, the experimental data is as yet insufficient to attribute NO reduction results until after completion of detailed testing.

A. Ferri: In gas turbines with premixed fuel ratio and low fuel air ratio the reason why the NO_x index decreases with increase of air temperature is that at high air temperature the fuel evaporates, then the combustion occurs with low maximum temperature, due to the diffusion of the gases. The fuel does not evaporate, then the local combustion occurs at local ϕ of 1. This point has been discussed in my paper in the AIAA.

A SYSTEMATIC APPROACH TO THE STUDY OF THE CONNECTION BETWEEN EMISSION AND AMBIENT AIR CONCENTRATIONS

Simulation of the Short term variation of the SO₂
concentration in Oslo is used as an example

by

Knut Erik Grønskei
Research Meteorologist
NORWEGIAN INSTITUTE FOR AIR RESEARCH
P.O. Box 15
N-2807 Kjeller
Norway

SUMMARY

A systematic approach to study the effect of a complex source distribution on the ambient air quality is described. Measurements of emission, meteorological parameters and ambient air concentrations are used to develop a quantitative model describing the important physical and chemical processes. The model is mathematically formulated in a modified form of the continuity equation for the pollution component. To improve the model, regression analysis can be used. An example of this approach is given in the study of air pollution in Oslo where it has been shown that a systematic vertical motion is the most important process to clean the air in Oslo during inversion situations. Some comments are made on the "model approach" to the air pollution problem around an airfield.

1. INTRODUCTION

Much work has been carried out to determine the emission of pollutants from different kind of aircrafts during different phases of operation. Some work has also been performed to clarify the concentrations around the airfield.

These two studies may be looked upon separately, and their results will indicate whether an action against the air pollution near an airfield is necessary or not.

Often, the authorities are interested in using the measurements of ambient air concentration and of traffic density to extrapolate the data to other traffic conditions. In order to do this, it is necessary to have some model of the processes that describe the connection between the emission and the ambient air concentration. A linear dependence is often used for the extrapolation. In many cases, this is not allowable specially when reactions between the pollutants are important for the problem under consideration.

In this paper, the principles of development and use of an air pollution model will be presented in connection with the conditions around an airfield. Results from a numerical model study of the SO₂-pollution in the area of Oslo will be used as an example.

2. SYSTEMATIC APPROACH

Schematically, the development and use of a model in an air pollution study may be viewed as shown in Fig. 1. The three boxes on the top indicate natural processes. The emission of pollutants is transformed to ambient air concentration through transport, diffusion, chemical reactions and physical cleaning processes. Many transformation processes are known from general chemical and physical knowledge.

The emission rates, the ambient air concentration and parameters describing the pollutant transformation are required, and they are equally important in a systematic approach. Registrations and measurements are indicated in the next three boxes. The information from these separate studies may of course be used separately. Information about the emissions f.e. may show how to reduce the emission of pollutants in the most effective way. Information about the meteorological conditions may be used to select the best place for an airfield from this point of view. Information about the ambient air concentration may be compared with standards for the air content, and tell us whether a problem exists or not.

These types of information are combined in a model that uses emission information as input and generates ambient air concentration as output. Calculated concentrations may be compared with observed concentrations to test the model. A study of the resulting discrepancies may be used to improve the model.

To perform this comparison in a systematic way, a statistical method proposed by L. Nordø (1) is used.

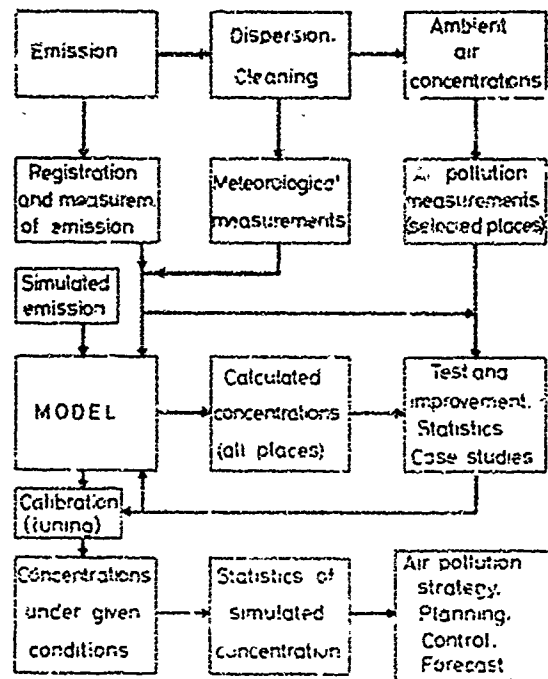


Fig. 1: Development and use of an air pollution model

This method consists of a multiple regression analysis that selects the best parameters describing a series of measurements. When several independent variables are used, the best set of parameters is selected without taking the best single parameter into consideration. New dependences with physical meaning may then evolve when a combination of parameters is used.

3. THE AIR POLLUTION MODEL

Many models for use in air pollution studies have been evaluated. All physical models concerning the connection between emission and ambient air concentrations of pollutants can be mathematically formulated by a modified form of the continuity equation for the pollutant compounds.

The general form of the continuity equation is given in equation (1)

$$(1) \quad \frac{\partial q}{\partial t} = - \nabla_h \cdot (\vec{v}_h q) - \frac{\partial}{\partial z} (wq) + \nabla_h \cdot (K_h \nabla_h q) + \frac{\partial}{\partial z} (K_z \frac{\partial q}{\partial z}) + \text{sources} + \text{sinks}$$

t	: time
x, y, z	: orthogonal coordinates with unit vectors. $\vec{i}, \vec{j}, \vec{k}$
q	: pollution concentration
K_h, K_z	: horizontal and vertical diffusion coefficients
$\vec{v}_h = u\vec{i} + v\vec{j}$: horizontal velocity
$\nabla_h = \vec{i} \frac{\partial}{\partial x} + \vec{j} \frac{\partial}{\partial y}$: horizontal gradient operator
w	: vertical velocity

The statement of the formula is simply that the local air pollution concentration changes with time because of systematic large scale transport, smaller scale transport by turbulence, and sources and sinks of the pollutant component.

If the parameters on the right hand side of the equation (three-dimensional velocity, diffusion coefficients, sources and sinks) and the initial value of the pollution concentration are known, the equation (1) may be solved for the pollution concentration as an initial value problem. A specific problem has to be analysed before relevant simplification can be made.

Air pollution is often caused by an emitting chimney that may be considered, in many cases, as a continuous point source. The pollutants are diluted by the atmospheric

turbulence in addition to a systematic air transport due to winds. Often the scale of the pollution cloud is small compared with systematic change in the horizontal wind field. Relevant approximations are:

1. stationary emission of an inert gas
2. stationary and homogeneous wind conditions.

These simplifications in relation to a point source lead to an analytical solution of the continuity equation. This solution may also be inferred from statistical consideration of the interaction between the pollution cloud and the atmospheric turbulence. The analytical formula describes the cone of pollution that extends from a chimney (A Gaussian plume model). The formula is empirically improved so that observations match calculations.

The success of the Gaussian plume model is dependent on the scales of the pollution cloud and the inhomogeneities in the systematic wind field. In addition to the notion of a point source, a line source is often considered as a simplification of the emission conditions (for instance when considering emissions of pollution from a highway).

In many cases, no simplifications of the field of emission and the other parameters that leads to an analytical solution of the continuity equation are possible.

A finite difference approximation of equation (1) then offers a more flexible solution. On the other hand, new difficulties are introduced, such as artificial diffusion, because of the finite difference system. A quasi Lagrangian system of integration like "the particle in cell" method applied by Sclarew (2) reduces this artificial diffusion.

A time dependent model offers an additional testing procedure in comparing the response of the model to changes in the parameters with observed time fluctuation in the ambient air concentration. The quantities that are assumed to be known have to be measured or estimated by sub-models.

4. THE OSLO MODEL

To give an example of model calculations that are carried out, some results from Oslo will be presented. A more complete description of these calculations may be found in the proceeding of the third meeting of the NATO/CCMS Panel on Modeling in Paris, on the 2nd-3rd October, 1972.

The Oslo region is shown in Fig. 2. The urbanized area is concentrated in about 30 km² and about 400 000 people are living there. The city of Oslo is surrounded by hills (height 3-500 m) on one side, and the Oslo-fjord on the other.

During winter time, this system of topography and local heat sources induce a local wind system that may create air pollution problems. This happens during inversion situations, and, statistically, a close connection is found between the vertical temperature gradient and the SO₂-concentration.

Six thermographs were placed along the hillside of Holmenkollåsen and were used together with the temperature recordings at the permanent meteorological stations to estimate the vertical stratification.

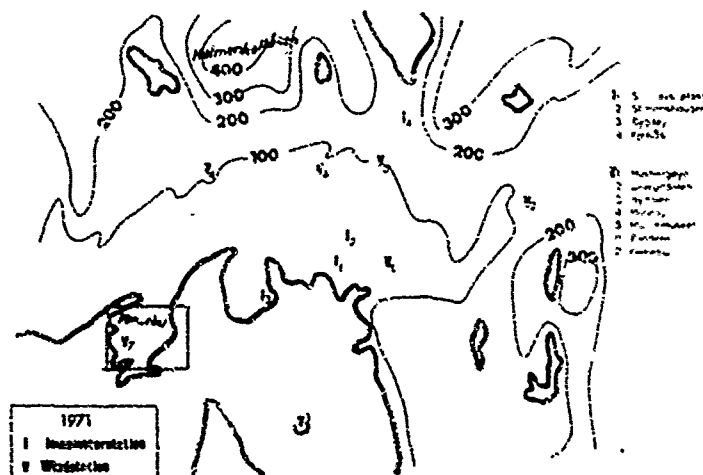


Fig. 2: The area of Oslo with measuring stations

The site of the continuous wind measuring stations (V_1, V_2, V_3 and V_4 on Fig.2) were chosen in order to measure the wind through the main valleys. Besides, two wind stations were placed in the centre of the city in addition to the permanent meteorological stations at Blindern (V_5) and Forneby (V_7). The airfield Fornebu is situated on the peninsula in the South-Western part of the area. This part of the map is shown in more detail in Fig. 8.

The air quality survey consisted of 25 stations measuring the daily mean SO_2 values together with the Just on filter (by light reflection). At four stations, the mean SO_2 concentration was measured each half hour (Bran and L  bbe imcometer). The imcometer and wind stations are marked in Fig. 2. Two of them are placed in the centre of the city, while the other two are placed North and South of this centre respectively.

These measurements were adapted to the model studies and the observation region is divided into a grid system shown in Fig.3. The regions with high elevation are excluded from our system. In the urban area, there exist a lot of small sources at different levels up to a certain height H . Within this area, the buildings and the heat sources at different levels lead to enhanced turbulence and a mixing of the air. In the computations, the mean concentration in this lowest part of the atmosphere is considered. In that way, the vertical mean value of equation (1) is used

$$(2) \quad \frac{\delta \bar{q}}{\delta t} = \bar{v}_h \cdot (\bar{v}_h q) - \frac{(\bar{w}q)H}{H} + \bar{v}_h \cdot (K_h \bar{v}_h q) + \left(\frac{K_z}{H} \frac{\delta q}{\delta z} \right) H + \text{sources} + \text{sinks}$$

($\bar{\quad}$) : the mean value in the lowest part of the atmosphere with height H .

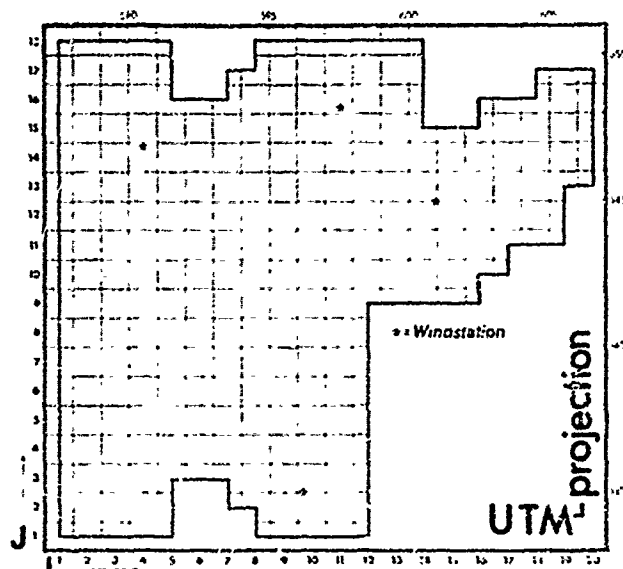


Fig. 3: The grid system

The grid distance is 1 km, and, in the finite difference approximation of eq. 2, a forward time step and an upwind finite difference system were used.

The finite difference approximation introduces an artificial diffusion. Reasonable estimates of the actual diffusion coefficient indicates that the horizontal diffusion term in eq. (2) is small compared with the artificial diffusion on a km scale and that the vertical diffusion above the mixing layer along the ground was small during inversion situations.

To estimate the three-dimensional windfield in the Oslo-area from the wind measurements, the horizontal windfield is separated in two parts, one divergent (\bar{v}_x) and one non-divergent part (\bar{v}_y)

$$(3) \quad \bar{v}_h = \bar{v}_x + \bar{v}_y; \quad \bar{v}_x = \bar{v}_h \chi; \quad \bar{v}_y = \bar{k} \times \bar{v}_h \psi$$

The divergent part is described by a velocity potential χ and the non-divergent part is described by a stream function ψ . Observed winds in the valleys (marked by a star in Fig. 3) are used to estimate the stream function along the boundary after correction with respect to the divergent part of the velocity.

A town represents a permanent heat source relative to its surroundings, and will cause vertical motions. As a first approximation it is proposed to put the horizontal divergence ($\bar{v}_h \cdot \bar{v}_h$) proportional to heat sources or some parameter describing the heat sources.

In Oslo this is done by estimating the heat sources from the emission of SO_2 over the centre of the city and from the temperature difference between the air and the

water over the Oslofjord, (equation 4).

$$(4) \quad \vec{v}_h \cdot \vec{v}_h = \nabla^2 \chi = \begin{cases} a_1 Q_{SO_2} & \text{over the centre of the city} \\ a_2 (T_A - T_W) & \text{over the open Oslo Fjord, when} \\ & (T_A - T_W) < 0 \end{cases}$$

Q_{SO_2} : areal sources of SO_2 in the region

$T_A - T_W$: temperature difference between air and water

a_1 : $-1.5 \cdot 10^{-5} \text{ s}^{-1} (\text{ton S}/(\text{km}^2 \cdot 3 \text{ months}))^{-1}$

a_2 : $+3.0 \cdot 10^{-4} \text{ s}^{-1} \text{ deg}^{-1}$

The values are regarded as empirical estimates of the combined effect of gravitational forces and heat sources in the area. It is believed that these factors are functions of other meteorological parameters within the region (f. ex. inversely proportional to the stability in the air), but no definite relationship of this kind was found in the present investigation.

The vertical velocity w is determined by assuming that three dimensional air-streams are non-divergent.

$$(5) \quad w_h = -H \cdot \nabla_h \cdot \vec{v}_h$$

To estimate the stream function describing the horizontal non-divergent part of the wind field in Oslo, the wind measurement from each of the valleys was used. The wind observations were corrected with respect to the convergent wind field, and the corrected measurements on Husbergøya V_1 , Groruddalen V_2 , Nydalen V_3 and Husby V_4 , were used to estimate the streamfunction along the boundary, in their neighbourhood. No air stream was allowed to cross very steep hillsides (for example Holmenkollåsen). To estimate the streamfunction within the region, the following equation is used:

$$(6) \quad \nabla^2 \psi = 0$$

A way to estimate the vorticity within the region has not been found without taking a more complete set of the hydrodynamical equations into consideration. The intention of the presented wind approximation is to calculate the air pollution concentration within an urban area, and it is believed that this concentration is strongly dependent on the vertical motion, but not very sensitive to small changes in the horizontal wind-direction. The mentioned approximations represent a better approximation than the assumption of an homogeneous wind-field in the urban area, when the wind-field is weak. This wind-field model was generated from the measurements in two meteorological case-studies in Oslo and tested against the results of nine other case-studies.

The existence and the location of a stagnation point over the urban area of Oslo is reflected in our model calculations. The main features of the air stream round the Oslo Fjord are also reflected in the different case-studies.

This indicates that our approximation of the convergent wind-field works fairly well and that the resulting vertical velocity may be regarded as a first approximation on the scale that is resolved in our grid system.

The observed and calculated winds in one of the case-studies used for testing are presented in Fig. 4. The arrows (+) show the calculated wind directions in each grid point. The hatched arrows (H) show observed wind directions at the given time. The observations are mainly built on the drifting of smoke from chimneys (10-20 m above ground level), but also on the drift of soap bubbles about 2 m above the ground. In the lower right part of the Fig. 4, the measurements from the thermographs show the dependence of temperature on height. Date and time of the case study are given on Fig. 4.

Case study 3: 11 a.m., 4th January 1969 (Fig. 4)

The vertical temperature stratification in the area is stable with a neutral part over the centre of the city. The general wind field shows a weak wind from the West. Because of this, the stagnation point is moved North-Eastwards, relative to the maximum convergence zone. In this case, the observed and calculated winds correspond well. One exception is a wind observation in the Western part of the town.

Summary of the case-studies

In some case-studies, the presented wind model does not work well in some regions of Oslo. This may be due to local canalization of the air flow which is not resolved in the model, or to wind fluctuations which the semi-stationary wind model does not take into consideration. Besides, the wind model is sensitive to the meas-

ments from the key observing stations in the valleys. Some discrepancies are evidently due to measurements from these stations that are not representative for their region.

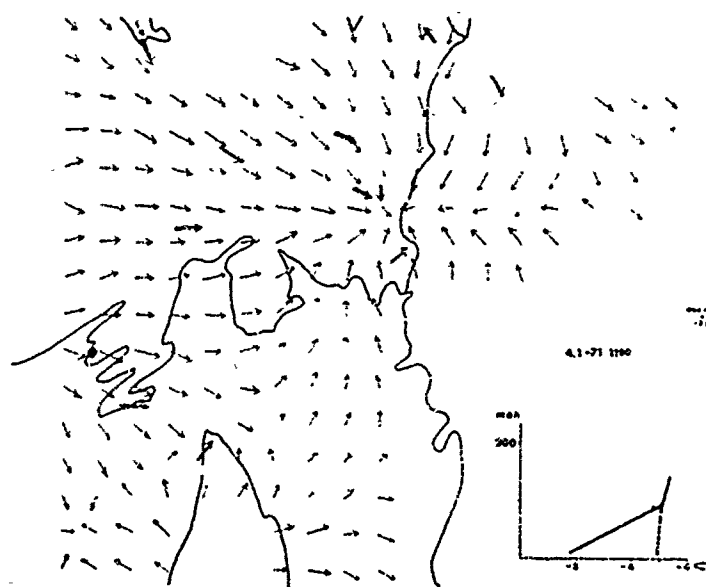


Fig. 4: Observed (H) and calculated (+) wind directions

The existence and the location of a stagnation point over the urban area of Oslo is reflected in our model calculations. The main features of the air streams round the Oslo Fjord are also reflected in the different case studies.

This indicates that our approximation of the convergent wind field works fairly well and that the resulting vertical velocity may be regarded as a first approximation on the scale that is resolved in our grid system.

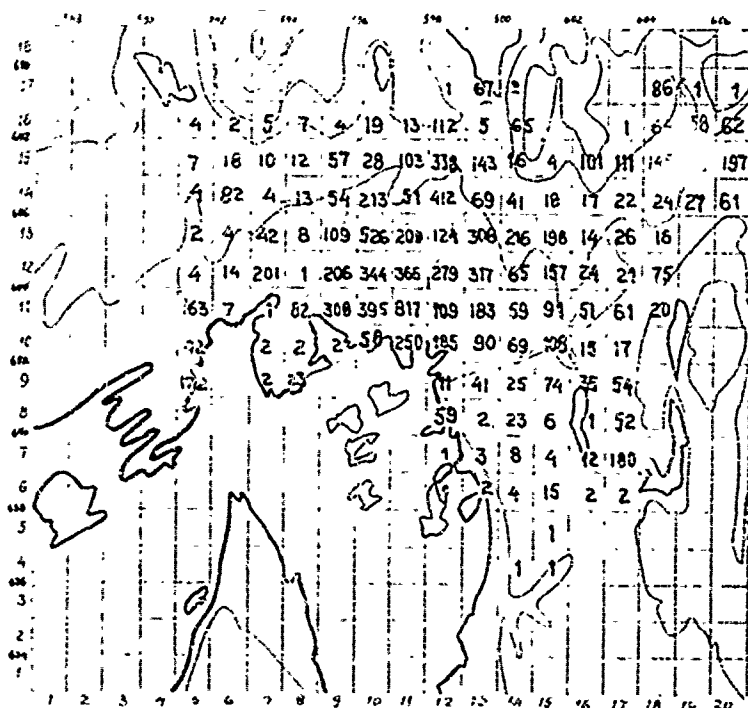


Fig. 5: Delivery of sulphur in oil, January-March 1971 (100 kg/S/km²)

An emission inventory was mostly carried out by the oil companies in Norway. A result of this inventory has been an estimation of the delivery of sulphur in oil to each square km within the region during the first three months of 1971. This estimate is shown in the above Fig. 5.

The emission survey has also shown that the emission of SO_2 in Oslo is mainly due to domestic heating. There exists a large number of small sources and few isolated stacks. The emission height is connected to the height of the houses in the region. In this way, the sources of SO_2 in the Oslo region may be considered as volume sources and the height of the volume is connected to the maximum emission height (H) in each square (1 side: 1 km). This height is used as the height of vertical integration of equation (2).

The daily emission of SO_2 was estimated from the mean seasonal delivery of sulphur in oil by using the daily degree-day number and the seasonal sum of these numbers. The degree-day number denotes how many degrees centigrades the daily mean temperature is below 17°C . The hourly emission was estimated from the empirically determined daily emission fluctuations.

The sink-term of SO_2 (A) was assumed to be a function of the SO_2 concentration in the following way:

$$(7) \quad A = cq + dq^2$$

$$c = 1.0 \cdot 10^{-6} \text{ s}^{-1} \quad d = 0.25 \text{ s}^{-1}(\text{g/m}^3)^{-1}$$

The functional form of A and the values c and d are estimated by J. Nordø in connection with modelling long range transport of air pollutants.

The wind model was used together with the presented estimates of the sources and sinks for SO_2 in the region, and the SO_2 concentration was calculated in all the grid points during the 4 days: 17-18th Dec./1970, 3-4th Jan./1971, 4-5th Jan/1971 and 5-6th Jan./1971.

The timing of the daily measurements was the reason for choosing the calculation interval from 2 p.m. to 2 p.m. the next day. The initial values of SO_2 -concentration was chosen to be zero. This approximation will influence the calculations during the first few hours. There was not found any reason to improve this approximation although it could easily be done, as for example by using the steady state solution for the given wind field as an initial value.

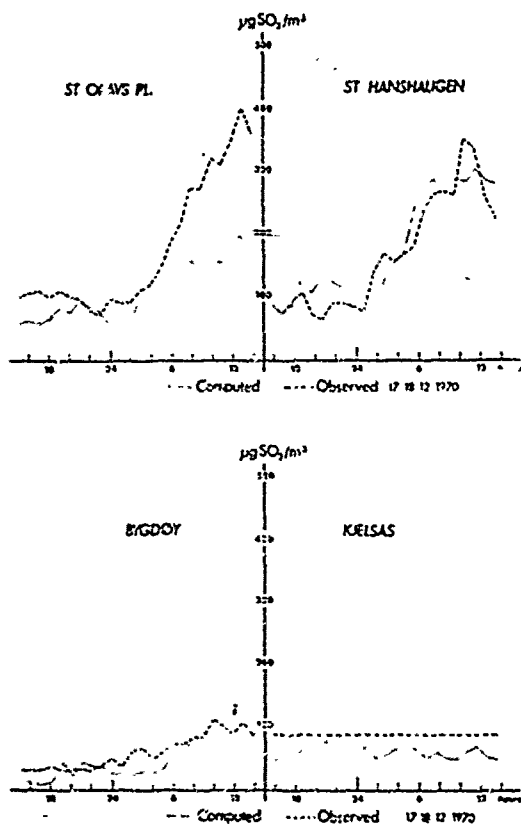


Fig. 6: The observed and calculated SO_2 concentrations in Oslo

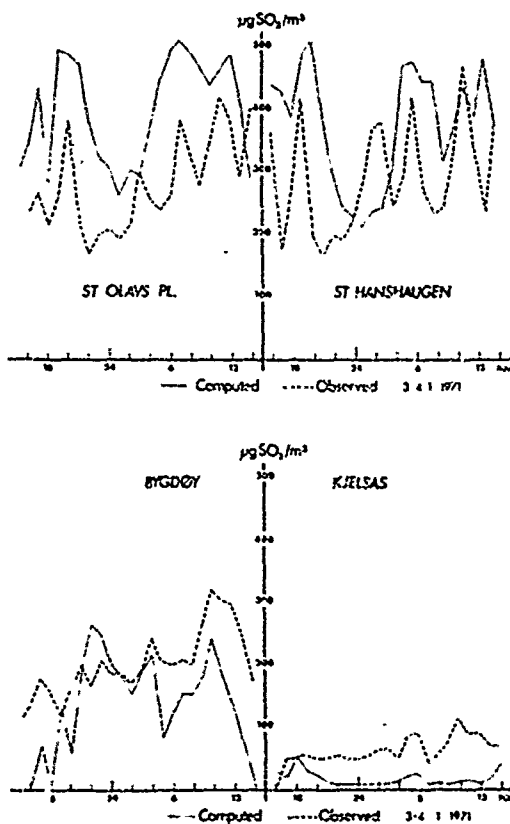


Fig. 7: The observed and calculated SO_2 concentrations.

Fig. 6 shows the calculated and observed values at the four stations from 3 p.m. the 17th December to 2 p.m. the 18th December. During the night, the windspeed slowed down from about 5 meters per second to an irregular wind of about 1 m per second. This is the reason for the increase of the SO_2 concentration that is observed and calculated. The calculated increase at St.-Olavs-Plass is too low compared to the observed values. An increase from about $100 \mu\text{g SO}_2/\text{m}^3$ to about $300 \mu\text{g SO}_2/\text{m}^3$ at St. Hanshaugen and an increase from about $30 \mu\text{g SO}_2/\text{m}^3$ to $100 \mu\text{g SO}_2/\text{m}^3$ at Bygdøy compared well. The calculations at Kjelsås do not show any large change, and the measurements do not show any fluctuation at all. The reason for this may be the limited sensitivity of the instrument used.

From the presented calculations, it may be concluded that the response of the SO_2 concentration to larger changes in wind velocity is correct with respect to time and

space. This indicates that the emission of SO_2 and the wind field are taken into consideration as a fair approximation.

In Fig. 7, the calculated and observed concentrations between the third and fourth of January are shown. In the centre of the city, the calculated SO_2 concentrations are somewhat too high and somewhat too low in the suburbs. On the other hand, the calculated fluctuations of some hours duration are largely observed in the same manner at the stations St. Olavs-Plass, St. Hanshaugen and Bygdøy. One exception is a three hour increase between 1 and 3 a.m. at St. Hanshaugen. This increase is observed somewhat later and with smaller amplitude at St. Olavs-Plass. The reason for this might be a local increase of the emission which is not considered in the calculation.

The short term fluctuations in the calculated SO_2 concentrations are mainly due to changes in the wind field. These fluctuations are not easily recognized when the wind at one of the wind stations is studied. The total ventilating effect resulting from the air flow in several valleys has to be considered. It may therefore be concluded that one wind station is not enough to describe actual short term fluctuations of the air pollution concentration in Oslo. Further, it indicates that small fluctuations in the wind field over the centre of Oslo are fairly well reflected by the net of wind measuring stations placed in the valleys (V_1 , V_2 , V_3 , V_4).

Two of the stations, St. Olavs-Plass and St. Hanshaugen were in the centre of the city (Fig. 2). The difference in height between these stations was about 70 m. It did not seem that this difference made any deviation in concentration. This supports our assumption of mixing in the lowest layer. The two other stations were placed South (Bygdøy) and North (Kjelsås) of the city centre.

The dust on the daily exposed filters in Oslo has been analysed with respect to sulphur. The sulphur content on the filters appeared to be closely connected to the measured SO_2 concentration, the temperature and the humidity in the air.

If the applied sink-term for SO_2 is regarded as a source for particulate sulphur, the computed concentrations were of the same order of magnitude as the referred measurements. To show the relative importance of the different removal processes of SO_2 from the ground level in Oslo, the different terms of equation (2) were integrated over the Oslo region, and the results are given in percent of the SO_2 emission:

- removal by vertical transport: 40 - 80 %
- " by horizontal transport 0 - 50 %
- " by the applied sinkterm: 5 - 20 %

Due to the organised vertical lifting of the air over Oslo, the SO_2 pollution within the city remains tolerable despite the high frequency of stagnating periods during winter.

In order to improve the model, statistical calculations of the calculated SO_2 -concentrations in relation to the observed concentrations have been carried out.

The correlation coefficient between the hourly calculated and observed SO_2 concentrations from four stations during the four days turned out to be 0.75. This means that much of the variations remain to be explained. On the other hand, many of the calculated short term fluctuations may be recognized in the observations at several stations. The difference between the calculated and observed values has been correlated with other meteorological parameters and it turns out that the correlation between this difference on one hand and temperature and humidity on the other hand, is about 0.80 on all stations. This indicates that more sophisticated chemical processes should be considered when trying to improve the model.

On the other hand, when results from different periods are investigated, different parameters become important to explain the deviations between observed and calculated values. At the present stage, it is difficult to identify one single process that ought to be considered in order to improve the model.

5 GENERAL COMMENTS ON MODEL STUDIES OF AIRFIELDS

When an airfield is considered, the emission configuration is very complex. Different kinds of activities may be regarded as pollutant sources. Among them are the running of aircraft engines, the heating of hangars and other buildings, and the auto-traffic in connection with the airfield. It is important to evaluate the contribution of individual sources to the observed air concentrations.

A map of Fornebu near Oslo is shown in Fig. 8 as an example of an airfield. Besides, the site of Fornebu is shown in relation to the Oslo region in Fig. 2. The definition of the study area will be possible after formulation of the problem. Since most of the sources are ground sources, it is the airfield itself and the immediate neighbourhood that has to be considered from a local point of view. Runup of aircraft engines, taxiing, take off and landing zones represent relatively high pollution sources on a local scale.

If the local air pollution problem in the surroundings of an airfield is studied, a horizontal resolution of 160 m would be chosen. If the contribution from the airfield Fornebu to the air pollution in Oslo is to be clarified, this may be done by the model presented in section three. Regarding the SO_2 pollution in winter, the airfield was

assumed to be a small source and in that way not considered. On the other hand, if the pollution of carbon monoxide (CO), nitrogen oxides (NO_x) or hydrocarbons (HC) is to be studied on a regional scale in Oslo, the airfield has to be considered as a significant source. In this kind of problem, the airfield may be looked upon as a volume source in a similar way as described in section three.

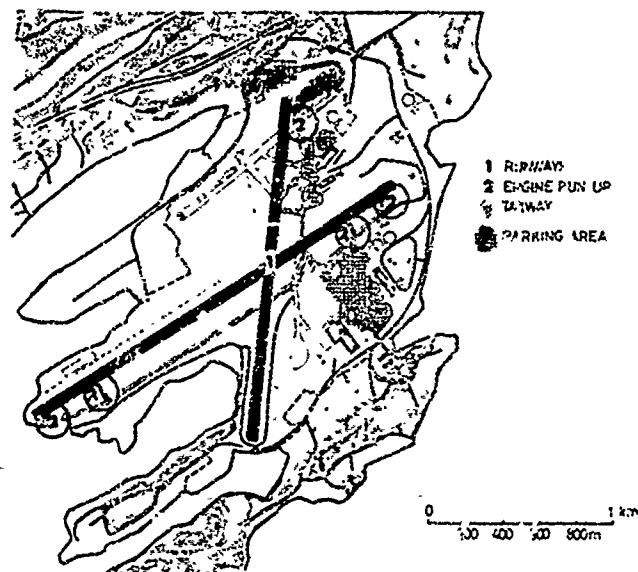
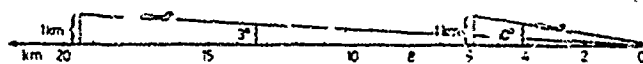


Fig. 1. Fornebu airfield in Oslo



The operation of the airplane engines is accompanied by an increased turbulence which leads to an initial mixing of the pollutants. In this way, the pollutant sources may be regarded as volume sources of 10-30 m height. Subsequently, the pollutants will be dispersed further by atmospheric mean wind transport and turbulent diffusion.

Turbulence generated in the air will remain for some time before dissipation. Therefore, different wind directions may give different mixing conditions over an airfield as a result of different roughness of the ground in the neighbourhood.

Regarding the systematic transport of pollutants, the area around an airfield is generally flat and the wind field may be assumed constant close to the airfield. This assumption depends on the extent of the study area. Very little is known about the application of the theory of systematic vertical motion on a regional scale, although some comments may be made. Horizontal differences of the atmospheric heat sources and topography may be regarded as the causes of local differences in the wind field. The heat sources and sinks are normally connected to the ground. In this way, topography also leads to horizontal differences in the heat sources, and take part in the generation of local air streams that interact with the larger scale winds. Differences in the thermal properties of the ground may also create important horizontal differences in the heat sources. This should be kept in mind when the meteorological measurements are planned in a region.

The connection between emission and immission ought to be studied with an inert gas such as carbon monoxide (CO). A study like this may serve as a starting point for a study of a set of gases that interact with each other. A model of this interaction has to be combined with the emission and dispersion processes. The chemical processes may be very complex and different processes are important under different meteorological conditions. From a chemical point of view, it is difficult to transfer results from experiments in a laboratory to the actual atmosphere. A model study as described may be useful in this connection.

Changes in parameters describing the processes influence the ambient air concentrations of the different components. Therefore, the model should be tested in a time scale that is appropriate considering the changes in the ambient air concentration. This is probably the best way of testing the model properly.

When a pollution plume from a point source is considered, the meandering of the plume is a wellknown fact, and it is accepted that instantaneous observations of the pollution concentration may deviate considerably from the values predicted by a Gaussian plume model. On the other hand, the observed and calculated mean values match fairly well. If this test method is used, great care must be taken not to misinterpret observational facts that point in the direction of other important processes that are not included in the model. These processes should be pointed out from an analysis of the scales of the

terms in the relevant mathematical formulation of the model.

Development and use of a model for an airfield will give information about local air pollution distribution as a result of different activities in connection with the airfield. This information may be used to reduce the local ambient air concentrations effectively. Further, the model will estimate trends in the ambient air concentration as a result of emission tendencies. The contribution of the air pollution from an airfield as a whole on a regional scale compared to other sources may be clarified by a relevant model on this scale.

REFERENCES

- (1) J. Nordø: On Empirical Deduction of Laws from Geophysical Records. Det Norske Meteorologiske Institutt, Scientific Report No 5 (1966).
- (2) R.C. Sclarew et. al.: The Particle in Cell Method for Numerical Solution of the Atmospheric Diffusion Equation and Application to Air Pollution Problems. Vol. 1 Systems, Science and Software. La Jolla. California Nov. 1971 NTIS-PB-209 290.

Discussion on Paper 23 "A Systematic Approach to the Study of the Connection between Emission and Ambient Air Concentration" presented by K.E.Grønskei

M.Wittaker: The author seems to be over modest and this study seems a very fine piece of work. I would like to ask whether the occurrence of mountains in his model makes it easier or more difficult to apply. I am thinking that application of the model to the Stansted Airport study of Farker would be very interesting.

K.E.Grønskei: In principle, mountains make no difference. We did not consider return of pollutants to ground which might be important on flat terrain.

ÉTUDE THÉORIQUE DE L'ÉVOLUTION RÉSIDUELLE DES PRODUITS POLLUANTS DANS LES JETS DE TURBORÉACTEURS

par

Roland BORGHI

Ingénieur de Recherches

OFFICE NATIONAL D'ÉTUDES ET DE RECHERCHES AÉROSPATIALES

29, avenue de la Division Leclerc - 92320 CHÂTILLON

France

RÉSUMÉ

De nombreuses études sont actuellement en cours pour prévoir et maîtriser la quantité de produits polluants CO et NO délivrés à la sortie de la tuyère d'un turboréacteur. Dans de nombreux cas, ces quantités ne doivent pas être prises directement en considération pour définir le taux de pollution du moteur car des évolutions sensibles se poursuivent dans le jet à l'extérieur du réacteur, soit que l'équilibre chimique n'ait pu être atteint dans la tuyère, soit que le mélange de gaz brûlés avec l'air ambiant modifie, déclenche ou fige des réactions.

Nous avons abordé ce problème sur le plan théorique, en établissant une méthode de calcul numérique prenant en compte à la fois les phénomènes de mélange turbulent et les réactions chimiques hors d'équilibre. Ainsi nous avons pu, d'une part comparer plusieurs modèles réactionnels dont l'un tient compte de la présence des radicaux H, O, OH, N, d'autre part constater qu'effectivement CO peut se transformer rapidement après la sortie en CO₂ alors que c'est beaucoup plus difficile à NO de disparaître.

THEORETICAL STUDY OF THE RESIDUAL EVOLUTION OF POLLUTING PRODUCTS IN TURBOJET EXHAUSTS

SUMMARY

Many studies are currently under way to predict and control the quantity of CO and NO polluting products delivered at the outlet of a turbojet nozzle. In many cases, these quantities should not be directly taken into consideration to define the engine pollution rate, as noticeable evolutions take place in the jet outside the engine, either because chemical equilibrium has not been reached in the nozzle, or because mixing of the burnt gases with external air modifies, triggers or freezes reactions.

We tackled this problem on the theoretical view point, establishing a numerical computing method taking into account turbulent mixing phenomena as well as non-equilibrium chemical reactions, in this manner we obtained, on the one hand, a comparison between several reaction models, one of which taking account of the presence of H, O, OH and N radicals, and on the other hand, the proof that CO can effectively get transformed into CO₂ quite quickly after exhaust, while it is much more difficult for NO to disappear.

1. INTRODUCTION

Les gaz brûlés produits par un turboréacteur contiennent une grande variété de produits, dont certains, comme NO, CO, C sont considérés comme polluants. Le problème général de prévoir les proportions de ces produits est actuellement à l'ordre du jour : il nécessite d'une part l'étude de la cinétique des réactions chimiques, et d'autre part la représentation réaliste de l'évolution aérodynamique des gaz dans les voyers des turboréacteurs. Nous avons abordé ici le problème plus simple de l'évolution de ces produits polluants après la sortie du turboréacteur, au cours du mélange du jet avec l'air ambiant ; c'est surtout dans le cas d'un turboréacteur avec réchauffe, qui délivre des gaz relativement chauds ($T > 1500^\circ\text{K}$), relativement rapides ($M \approx 1$, $u > 700 \text{ m/s}$), et hors d'équilibre chimique, que ce problème se pose actuellement.

Cette étude est abordée d'un point de vue analytique. Les réactions chimiques hors d'équilibre qui se produisent dans le jet ont été représentées soit par des schémas globaux simples, soit par tout un processus réactionnel faisant intervenir les espèces, O, O₂, H, H₂, OH, H₂O, CO₂, NO₂, N, N₂ et les espèces polluantes auxquelles nous nous sommes limités pour l'instant : CO et NO ; les phénomènes de mélange turbulent des gaz chauds avec l'air (avec ou sans vitesse) sont pris en compte en utilisant le schéma de longueur de mélange de Prandtl. Une méthode de calcul numérique a alors été établie, permettant de suivre le déroulement des réactions chimiques et l'évolution des divers corps dans les différentes zones du jet ; les réactions importantes sont alors mises en évidence, il est possible de voir si certaines espèces sont proches de l'équilibre ou au contraire presque figées. L'influence de l'état des gaz dans la section de sortie de la tuyère sur leur évolution ultérieure peut être aussi analysée ; en particulier les proportions des espèces dissociées O, OH, H et la forme des profils transversaux de températures se sont avérés être des paramètres très importants.

2. REPRÉSENTATION DES RÉACTIONS CHIMIQUES

2.1. Evolution du CO

Les taux de combustion d'hydrocarbures ont été étudiés expérimentalement il y a un certain temps par Longwell, Malcolm, Weiss [1], dans un foyer homogène ; comme la dernière étape de cette combustion est l'oxydation de CO, on peut en déduire une forme de disparition de CO :

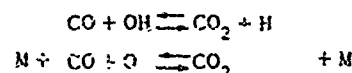
$$(1) \quad \left(\frac{dC_{\text{CO}}}{dt} \right)_{\text{chim}} = -k C_{\text{CO}} C_{\text{O}} T^{1/2} \exp \left[-\frac{E_0/R_0}{T} \right]$$

Récemment, des études expérimentales sur l'oxydation du CO dans une post-flamme, de Howard, Williams, Fine [2] ont conduit à faire intervenir l'eau comme un catalyseur ; ils ont proposé :

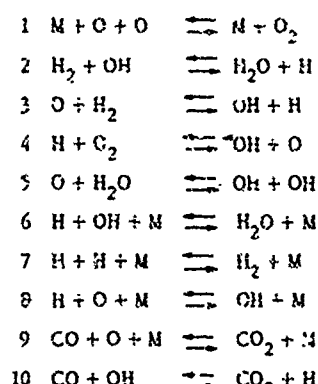
$$(2) \quad \left(\frac{dC_{CO}}{dt} \right)_{\text{chim}} = -k C_{CO} C_{O_2}^{1/2} C_{H_2O}^{1/2} \exp \left[-\frac{E_0/R_0}{T} \right]$$

avec d'autres valeurs de k et de E_0/R_0 que précédemment.

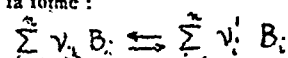
Ces relations globales traduisent en fait, plus ou moins exactement, tout un ensemble de réactions élémentaires qui ont été étudiées séparément par différents auteurs ; le mécanisme d'oxydation du CO se produit en effet grâce à deux réactions élémentaires :



la première semblant la plus importante dans les phénomènes de combustion ; pour connaître les proportions de O, OH, H qui interviennent, il faut alors tenir compte d'un grand nombre d'autres réactions avec les nouveaux corps OH_2 , H_2 , O_2 , et même HO_2 . On peut trouver ces réactions, avec leurs constantes cinétiques, chez divers auteurs [3, 4, 5, 6]. Nous avons retenu, pour notre part, l'ensemble des réactions ci-dessous ; la série est très complète, puisqu'il nous avons éliminé seulement celles faisant intervenir HO_2 (pour lesquelles les constantes cinétiques sont les moins sûres ([6])).



pour chacune de ces k réactions, de la forme :



le taux de production (par unité de masse et de temps) de l'espèce i , s'écrit :

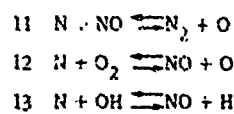
$$(3) \quad \rho(\dot{w}_i)_k = (\nu'_{ik} - \nu_{ik}) \frac{dL_i}{dt} \left(\dot{w}_k - \dot{w}'_k \right) \quad \left(\dot{w}_k = \sum_{i,k} \nu_{ik} m_i \right)$$

$$\text{ou} \quad \dot{w}_k = k_k \cdot T^{n_k} \cdot \exp \left[-\frac{E_{0k}}{R_0 T} \right] \cdot \prod C_i^{y_{ik}} ; \quad \dot{w}'_k \text{ a la même forme.}$$

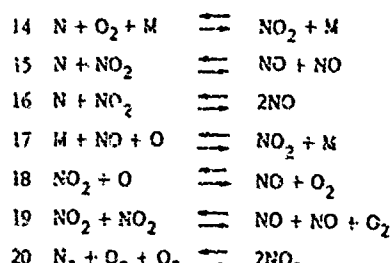
Les constantes $k_k, k'_k, p_{ik}, p'_{jk}, E_{0k}, E'_{0k}$ peuvent être trouvées dans les références citées plus haut, avec plus ou moins de précision ; le tableau 1 donne les valeurs adoptées ici, pour les résultats de calculs présentés.

2.2. Évolution de NO

Divers auteurs ont montré que la formation de NO était bien représentée par trois réactions élémentaires, les deux réactions du mécanisme de Zeldovitch, valables pour de l'air, et une réaction supplémentaire due à la présence de radicaux OH [7, 8, 9].



Nous n'avons pas tenu compte ici du corps N_2O , mais avons rajouté du NO_2 , dont la présence dans les jets de turboréacteur a été constatée expérimentalement [10] ; de sorte que d'autres réactions élémentaires doivent être prises en compte :



Les constantes cinétiques relatives à ces réactions, choisies d'après les références citées, ainsi que (11) et (12), figurent dans le tableau 2.

TABLEAU 1

		k	p	E_0	k'	p'	E'_0
1	$M + O + O \rightarrow M + O_2$	$8,9 \cdot 10^{14}$	-0,34	0	$2,5 \cdot 10^{16}$	-0,5	-117 945
2	$H + OH \rightarrow H_2O + H$	$1,5 \cdot 10^{12}$	0	-5300	$5,55 \cdot 10^{13}$	-0,01	-19 707
3	$O + H_2 \rightarrow OH + H$	6×10^{12}	0	-30 000	$1,94 \cdot 10^{13}$	-0,03	-8 052,5
4	$H + O_2 \rightarrow OH + O$	2×10^{14}	0	-16 652,5	$1,65 \cdot 10^{12}$	-0,27	0
5	$O + H_2C \rightarrow OH + OH$	$1,76 \cdot 10^{13}$	-0,02	-16 734,5	$1,55 \cdot 10^{12}$	0	0
6	$H + O + M \rightarrow H_2O + M$	$1,5 \cdot 10^{17}$	-0,5	0	$3,96 \cdot 10^{17}$	-0,31	-117 027
7	$H + H + M \rightarrow H_2 + M$	$1 \cdot 10^{18}$	-1	0	$7,15 \cdot 10^{18}$	-0,82	-102 240
8	$H + O + M \rightarrow OH + M$	$3 \cdot 10^{14}$	0	0	$6,96 \cdot 10^{13}$	0,21	-101 292,5
9	$CO + O + M \rightarrow CO_2 + M$	6×10^{12}	0	0	$1,31 \cdot 10^{13}$	-0,58	-125 735
10	$CO + OH \rightarrow CO_2 + H$	$4,2 \cdot 10^{12}$	0	-1080	$5,5 \cdot 10^{13}$	0	-23 500

TABLEAU 2

		k	p	E_0	k'	p'	E'_0
11	$N + NO \rightarrow N_2 + O$	$2,13 \cdot 10^{13}$	-0,04	0	$4,8 \cdot 10^{13}$	0	-75 011,5
12	$N + O_2 \rightarrow NO + O$	$2,67 \cdot 10^{10}$	+0,52	-7 042,5	$3,2 \cdot 10^{12}$	1	-39 100
13	$N + OH \rightarrow N_2 + OH$	$3 \cdot 10^{14}$	0	-16 000	-	-	-
14	$N + O_2 + M \rightarrow NO_2 + M$	10^{17}	-1	0	10^{13}	-1,5	-104 730
15	$N + NO_2 \rightarrow 2NO$	$3 \cdot 10^{10}$	0	0	10^{10}	0	-87 436
16	$N + NO_2 \rightarrow N_2 + O_2$	$1,2 \cdot 10^{10}$	0	0	$1,7 \cdot 10^{11}$	0	-135 130
17	$M + NO + O \rightarrow NO_2 + M$	$2 \cdot 10^{18}$	0	0	$5,3 \cdot 10^{11}$	-1	-73 350
18	$NO_2 + O \rightarrow NO + O_2$	$3,82 \cdot 10^{12}$	0	0	$2,4 \cdot 10^{12}$	0	-44 000
19	$NO_2 + NO \rightarrow NO + NO + O_2$	$2,5 \cdot 10^{12}$	0	-35 900	$7,2 \cdot 10^{10}$	0	0
20	$N_2 + 2O_2 \rightarrow 2NO_2$	$2 \cdot 10^{12}$	0	-75 510	10^{11}	0	-52 616

2,3.

Dans la méthode de calcul que nous allons exposer au paragraphe 3, c'est le système de réactions chimiques le plus compliqué que nous avons pris en compte, c'est-à-dire 20 réactions faisant intervenir les espèces : O, O₂, H, H₂, OH, H₂O, Cu, CO₂, NO, NO₂, N, N₂.

Il est aisé, bien entendu, d'utiliser à la place des schémas réactionnels plus simples, tels que celui de Lengweil ou Howard pour la transformation du CO₂; ceci a aussi été fait et nous comparerons les différents modèles.

Il est possible de rajouter des réactions élémentaires nouvelles. L'influence de NO sur les réactions d'oxydation de H₂ ou CO, qui, encore assez mal connue, peut par exemple, justifier l'addition de réactions supplémentaires, comme on le verra, le nombre de réactions n'est pas très gênant pour le calcul numérique, le nombre d'espèces à prendre en compte étant par contre le principal responsable de la longueur des calculs.

3. METHODE DE CALCUL

3.1. Equations

Le mélange d'un jet de turboréacteur (fig. 1), est décrit avec une bonne approximation par le système classique d'équation (en mouvement permanent) ci-dessous, qui traduisent les bilans de quantité de mouvement, de l'enthalpie totale, et des masses des différentes espèces :

$$(3) \quad \frac{\partial}{\partial x}(\rho u u) + \frac{\partial}{\partial x}(\rho u v) = \frac{\partial}{\partial x}(\rho E \frac{\partial u}{\partial x})$$

$$(5) \quad \frac{\partial}{\partial x}(\rho u n H) + \frac{\partial}{\partial z}(\rho v n H) = \frac{\partial}{\partial x} \left(n A \frac{\partial H}{\partial x} \right) + \frac{\partial}{\partial z} \left(\epsilon \left(1 - \frac{1}{P} \right) u \frac{\partial H}{\partial z} \right)$$

$$(6) \quad i = 1, \dots, n \quad \frac{\partial}{\partial x}(\rho u v Y_i) + \frac{\partial}{\partial z}(\rho v v Y_i) = \frac{\partial}{\partial x} \left(n D \frac{\partial Y_i}{\partial x} \right) + \rho \dot{w}_i$$

Les grandeurs μ, ν, ρ, Y_i, H , sont considérées ici comme des valeurs moyennes des valeurs turbulentes et ϵ, A, D sont donc des coefficients de transfert mixtes (moléculaire plus turbulent), indépendants de l'espèce considérée.

Dans cette approximation, la pression est constante dans tout le champ d'écoulement, ce qui implique que le jet soit assez proche de l'adaptation par rapport au milieu extérieur.

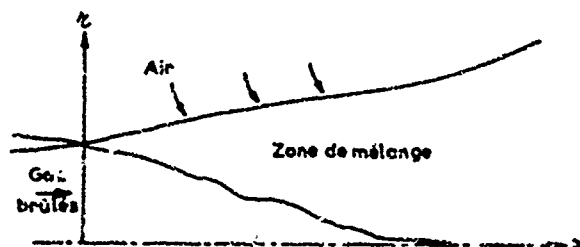


Fig. 1 - Schéma de l'écoulement.

Les grandeurs \dot{w}_i sont les taux de production moyens des espèces i ; on les écrira ici

$$(7) \quad \dot{w}_i = \sum_k (\dot{w}_i)_k$$

en exprimant les $(\dot{w}_i)_k$ par les formules (3) où les concentrations C_j et T seront assimilés à leurs valeurs moyennes; ce faisant on néglige donc l'influence de la turbulence sur ces taux de réaction chimique.

Entre les \dot{w}_i existe des relations traduisant la conservation des atomes, du type :

$$(8) \quad \sum_{i=1}^n \mu_{ij} \frac{\dot{w}_i}{M_i} = 0$$

où μ_{ij} est le nombre d'atomes de j dans l'espèce i . On peut donc définir des fonctions auxiliaires φ_j , formes linéaires des Y_i :

$$(9) \quad \varphi_j = \sum_{i=1}^n \mu_{ij} \frac{Y_i}{M_i}$$

qui satisfont à une équation sans terme de production :

$$(10) \quad \frac{\partial}{\partial x}(\rho u v \varphi_j) + \frac{\partial}{\partial z}(\rho v v \varphi_j) = \frac{\partial}{\partial x} \left(n D \frac{\partial \varphi_j}{\partial x} \right)$$

Dans notre cas, nous considérons 12 espèces, on peut en remplacer quatre par des fonctions φ exprimant la conservation des atomes C, O, N, H; de plus la conservation de la masse totale (qui prend la place alors de la conservation d'une espèce d'atome) permet de faire disparaître d'une équation les termes de diffusion et de réaction pour donner l'équation de continuité :

$$(11) \quad \frac{\partial}{\partial x}(\rho u n) + \frac{\partial}{\partial z}(\rho v n) = 0$$

Le système d'équations différentielles le plus simple est alors composé de (4), (5), (11), 3 équations (10), $n - 4 = 8$ équations (6).

A ces équations, il faut ajouter les équations d'état :

$$(12) \quad \frac{p}{P} = RT \quad \text{ou } R \text{ est fonction des } Y_i;$$

$$(13) \quad H = \frac{u^2}{2} + \int C_p dT + Q_0 \quad \text{où } Q_0 \text{ et } C_p \text{ sont fonctions des } Y_i \text{ et des équations donnant } \epsilon, A, D, \text{ les paramètres du mélange turbulent.}$$

La forme la plus simple, et cependant très réaliste, pour représenter les phénomènes de mélange turbulent est celle de Prandtl; ϵ est rattaché à une longueur de mélange ℓ par :

$$(14) \quad \epsilon = \ell^2 \left| \frac{\partial u}{\partial z} \right|$$

et D et A sont proportionnels à ϵ :

$$(15) \quad D = \frac{\epsilon}{Sc}, \quad A = \frac{\epsilon}{R}$$

longueur $2\pi r \delta$ étant proportionnelle à l'épaisseur δ de la couche de mélange :

$$(6) \quad C = \lambda \delta(\pi)$$

Les valeurs numériques : $\lambda = 0,09$

$$P_2 = S_2 = 0,63$$

semblent représenter convenablement un grand nombre d'expériences [13].

3.2. Résolution

Nous avons donc à résoudre un système de 14 équations aux dérivées partielles et 3 équations ordinaires, dans le domaine constitué par le quart de plan $x \geq 0, r \geq 0$, pour trouver en chaque point :

- les fractions massiques Y_i des 14 espèces (la douzième s'en déduisant car $\sum_{i=1}^{14} Y_i = 1$) ;
- les vitesses u et v ;
- les grandeurs thermodynamiques H, T, p .

Il existe différentes méthodes numériques pour résoudre les équations aux dérivées partielles paraboliques, nous avons choisi ici celle de Patankar-Spalding, que nous avons adaptée pour les termes de productions complexes dus à toutes les réactions, le lecteur se rapportera à la référence [13] pour détail de la méthode.

Remarquons simplement que l'emploi des fonctions Φ_i définies par (9) à la place des Y_i demande quelques précautions : il importe de les utiliser à la place des Y_i qui ont la plus grande valeur absolue, et non pas les plus faibles, en effet, lors du calcul de ces Y_i par des formules inverses de (9) :

$$P_{ij} \frac{Y_i}{m_i} = \Phi_i - \sum_{j=1}^N \mu_{ij} \frac{Y_j}{m_j}$$

toutes les erreurs numériques faites dans le calcul des Y_i sont reportées sur Y_i , si l'on choisit pour les Y_i des espèces en faible quantité, elles seront donc entachées d'une erreur relative grande, dans certains cas on peut même obtenir des valeurs négatives de Y_i ; ce qui est désastreux pour la suite du calcul.

3.3. Pas de calcul

La méthode numérique de calcul employée minimise les risques de divergence, cependant les pas de calcul (en x et r) doivent être choisis suffisamment petits pour conserver une certaine précision. En ce qui concerne le pas de calcul en r , l'habitude nous fait utiliser un découpage radial du jet, proportionnel aux débîts, en 30 à 40 sections.

Pour Δx nous avons utilisé un critère lié à la vitesse chimique d'évolution des Y_i : en un point donné, ce limite Δx par

$$\Delta Y_i = \frac{dY_i}{dx} \Delta x = \Delta x \frac{P_{wi}}{\rho u} = \Delta x \frac{S_{wi} + Y_i S_{oi}}{\rho u}$$

de façon que le ΔY_i ne soit qu'une fraction ϵ du ΔY_i maximum supposé possible en ce point, Y_i est atteint lorsque $\dot{w}_i = 0$ c'est-à-dire $Y_i = -S_{wi}/S_{oi}$, ce qui donne :

$$(17) \quad \Delta x = -\epsilon \frac{\rho u}{S_{oi}}$$

comme plusieurs espèces, en plusieurs points du jet sont à considérer, il faudrait choisir le plus petit des Δx , cependant, comme certaines espèces peuvent être en quantité très faible et très peu affectée par les phénomènes chimiques (un peu près « stationnaires » de ce point de vue), il y a intérêt à les maintenir en dehors du critère, c'est ce que nous avons fait en particulier pour N .

L'influence de ϵ sur les résultats a été étudiée, la valeur nominale de 0,5 a été retenue, assurant une précision excellente sur les espèces CO et NO qui nous intéressent au premier chef, cependant pour avoir une aussi bonne précision sur OH et O, on a constaté qu'il fallait une valeur 2 à 4 fois plus faible. Compte tenu de ces précautions, les temps de calcul sont assez importants sur une IBM 360-50 (en double précision, c'est-à-dire avec 14 chiffres significatifs). Par exemple le calcul d'un jet de 5 cm de rayon sur une distance de 50 cm a pris 10 minutes sans oxydes d'azote, 15 minutes avec les oxydes d'azote, comme le pas de calcul est assujéti aux réactions chimiques, il est d'autant plus faible que la température est élevée (ce qui augmente le temps de calcul) ; d'autre part le nombre d'espèces à considérer, relié au nombre d'équations à résoudre, est pratiquement proportionnel au temps de calcul, par contre le nombre de réactions chimiques prises en compte n'a que peu d'importance en ce qui concerne le nombre d'espèces.

4. QUELQUES RÉSULTATS DE CALCUL

4.1. Comparaison de schémas chimiques

Avec un jet d'air effectif la comparaison des différents schémas d'oxydation du CO, sur un cas de calcul type : un jet chaud ($T = 1500^\circ K$) à $u = 500$ m/s, de 5 cm de rayon se mélange avec de l'air au repos à température ordinaire ($300^\circ K$), à la pression atmosphérique ; il est composé de 3 % de CO, de 5 % de CO_2 , 3 % d' H_2O , 11,98 % de O_2 (en masse) comme constituants principaux, les calculs différents ont été effectués avec le schéma réactionnel complet et avec les formules globales (1) et (2), la comparaison est faite sur la figure 2 où sont tracés les Y_{CO} sur l'axe du jet.

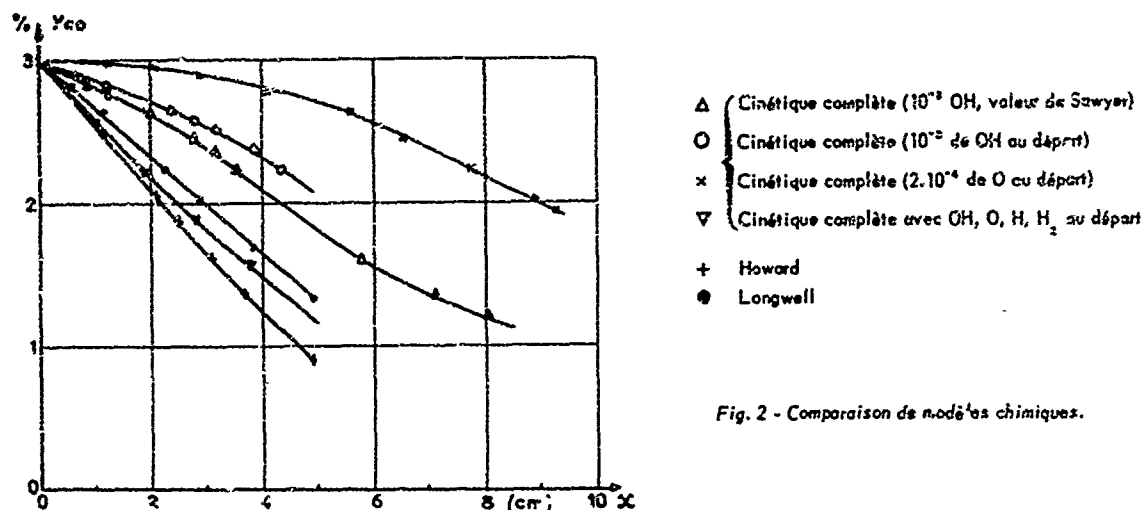


Fig. 2 - Comparaison de modèles chimiques.

La schématisation tirée de [1] donne une disparition de CO assez rapide ; on a pris pour ce calcul $E_0/R_0 = 20\,000^\circ\text{K}$ et $\bar{X} = 11,25, 10^7$ (SI), valeurs calculées d'après les résultats expérimentaux de [1]. La schématisation de Howard, avec 5 % de vapeur d'eau, donne une disparition un peu plus rapide. En ce qui concerne le schéma plus complet, nous avons effectués plusieurs calculs en mettant dans la section initiale différentes quantités des espèces dissociées, O, OH, H, on voit que la disparition de CO est extrêmement influencée par ces quantités, et que l'on peut retrouver une disparition sensiblement équivalente à celle des modèles simplifiés en mettant au départ : $Y_O = 10^{-3}$, $Y_H = 10^{-4}$, $Y_{H_2} = 10^{-4}$, $Y_{OH} = 10^{-3}$; ces proportions sont très supérieures aux valeurs de ces espèces à l'équilibre dans les conditions de pressions et de températures considérées, mais nous nous plaçons justement hors de l'équilibre, car il reste beaucoup de CO ; remarquons de plus que nous avons employé pour la constante k_{20} de la réaction principale



deux valeurs légèrement différentes, l'une conseillée par Baulch (qui figure dans le tableau 1), l'autre conseillée par Singh et Sawyer d'après des expériences récentes [14].

Il apparaît donc une assez bonne concordance entre les trois schémas cinétiques, dans notre cas de calcul qui entre effectivement dans le domaine pour lesquels les formules de Longwell et Howard ont été établies ; à l'extérieur de ce domaine, c'est-à-dire par exemple pour des valeurs de la température plus faibles ou plus élevées, et pour des concentrations plus diluées, ce qui peut se produire dans d'autres parties du jet considéré, il faut accorder plus de confiance à la cinétique plus élaborée ; cependant son utilisation, on le voit, nécessite la connaissance de données de départ plus complètes, car il faut connaître les proportions de O, OH, H en particulier, dont l'importance apparaît clairement.

4.2. Analyse de calcul

Le calcul prenant compte de la cinétique compliquée permet de décrire les différents phénomènes en tous les points du jet.

Considérons par exemple un jet chaud (1500°K) à Mach 1 (760 m/s) environ

$$\begin{array}{lll} Y_O = 10^{-3} & Y_{OH} = 10^{-3} & Y_{H_2O} = 10^{-3} \\ Y_{O_2} = 11,99 \cdot 10^{-2} & Y_{H_2O} = 5 \cdot 10^{-2} & Y_{H_2O_2} = 0 \\ Y_H = 10^{-4} & Y_O = 3 \cdot 10^{-2} & Y_H = 0 \\ Y_{H_2} = 10^{-4} & Y_{H_2} = 5 \cdot 10^{-2} & Y_{H_2} = 1 - \sum_{i=1}^4 Y_i \end{array}$$

et de l'air à 300°K (23 % d' O_2 et 77 % d' N_2).

La figure 3 représente la vitesse et la température dans l'axe du jet, la fin du cœur potentiel se situe à environ 8,5 cm, là où la vitesse commence à décroître, dans le cœur, la température n'est pas constante, mais s'élève légèrement, à cause de la disparition de CO ; par la suite les décroissances de M et de T sont très semblables, T décroissant un peu moins vite car nous avons pris un nombre de Prandtl égal à 0,85.

La figure 4 représente la variation de débit global des espèces CO, CO_2 , NO, NO_2 (en $\text{kg/s}/2\pi$) le long du jet. On constate une disparition assez nette de CO et une apparition de CO_2 , corrélativement. Le NO et le NO_2 au contraire apparaissent, mais varient beaucoup moins (noter la différence d'échelle), l'absence (artificielle) de NO_2 au début est rapidement compensée par une disparition de NO, puis les quantités de NO et NO_2 croissent de concert, d'une manière plus constante que CO_2 , qui atteint un plateau assez peu de temps après la fin du cœur potentiel, la bosse de la courbe de NO correspond à la fin du cœur potentiel.

La figure 5 donne les taux de réaction \dot{W}_i et \dot{W}_i^+ (taux global et taux de production : $\dot{W}_i^+ - \dot{W}_i^-$), en unités arbitraires, sur l'axe du jet, pour les espèces CO et NO. On voit, puisque \dot{W}_i^+ est presque partout 100 fois plus petit que \dot{W}_i^- , que NO est toujours proche de sa composition d'équilibre (sauf dans les tout premiers centimètres), d'ailleurs un calcul d'équilibre avec les

proportions initiales ci-dessus donne $(Y_{NO})_{eq} = 9,57106 \cdot 10^{-4}$ à $1500^\circ K$. Au contraire CO est très hors d'équilibre dans les 10 premiers centimètres ; il a tendance à se mettre en équilibre (\dot{W}_{CO}^+ croît et \dot{W}_{CO}^- décroît), mais l'arrivée d'air froid fige la réaction et à partir de 20 cm environ \dot{W}_{CO}^+ et \dot{W}_{CO}^- sont tous les deux très petits. L'examen des valeurs \dot{W}_{CO}^+ et \dot{W}_{CO}^- sur l'axe montre aussi que d'autres espèces peuvent être proches de l'équilibre, dans le cœur potentiel ($T \approx 1500^\circ K$), H_2 au bout de 2 cm, H au bout de 5 cm, NO_2 au bout de 4 cm, et O et OH tendent vers l'équilibre, mais leur production est plus forte et celui-ci ne sera pas atteint avant la fin du cœur ; lors du refroidissement par l'air extérieur, après le cœur potentiel, les espèces H et H_2 restent encore un peu en équilibre, puis s'écartent progressivement de celui-ci et se figent ; NO, comme on l'a vu, et aussi NO_2 restent en équilibre.

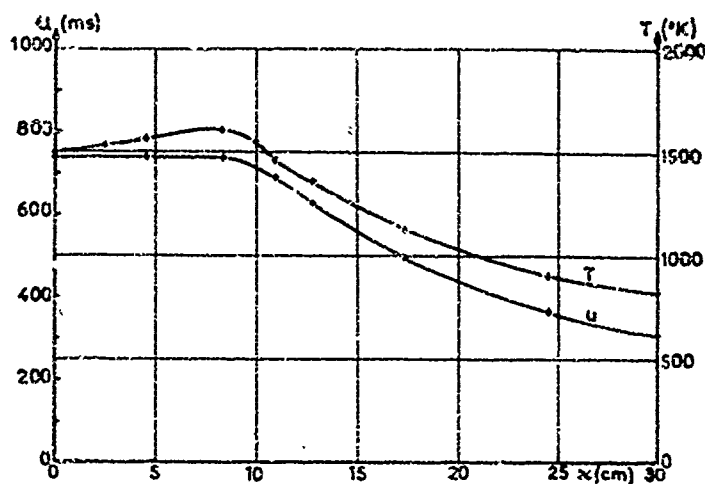


Fig. 3 - Vitesse et température sur l'axe du jet.

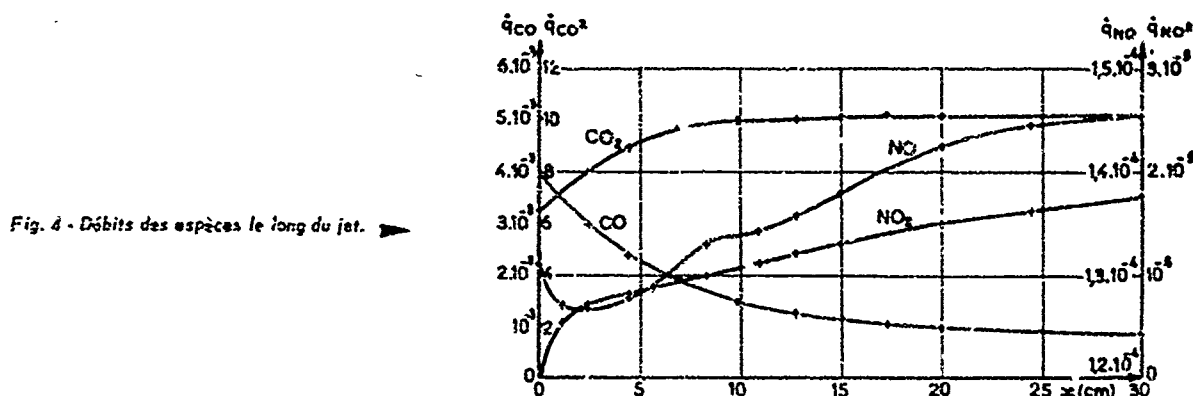


Fig. 4 - Débits des espèces le long du jet.

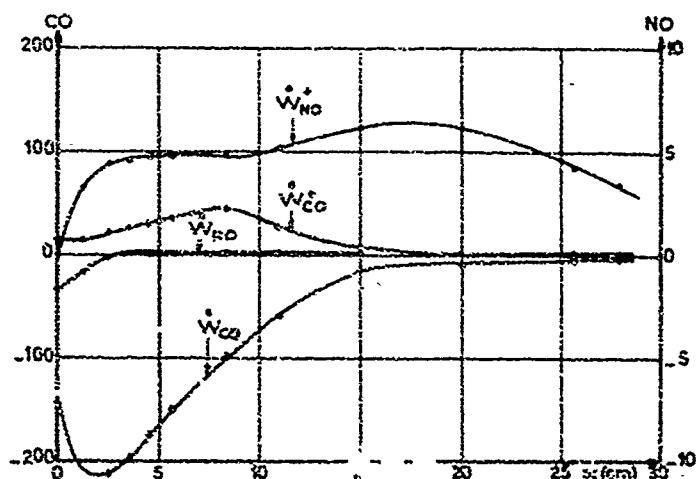


Fig. 5 - Taux de production sur l'axe du jet.

Les figures 6 donnent des répartitions transversales pour deux abscisses, l'une avant et l'autre après la fin du cœur potentiel. La figure 6a donne l'évolution de la température ; elle décroît bien sûr assez rapidement quand l'air froid pénètre dans les gaz.

On constate sur la figure 6a que la disparition de CO est pratiquement confinée au centre du jet, c'est parce que la température est la plus importante, d'ailleurs à 15,9 cm, lorsque le mélange a déjà refroidi le jet ($1050^\circ K$ au centre du jet, d'après la figure 2) \dot{W}_{CO} est nettement plus faible qu'à 5,5 cm, l'apport d'oxygène par l'air ambiant ne semble donc avoir aucune influence notable sur la disparition de CO.

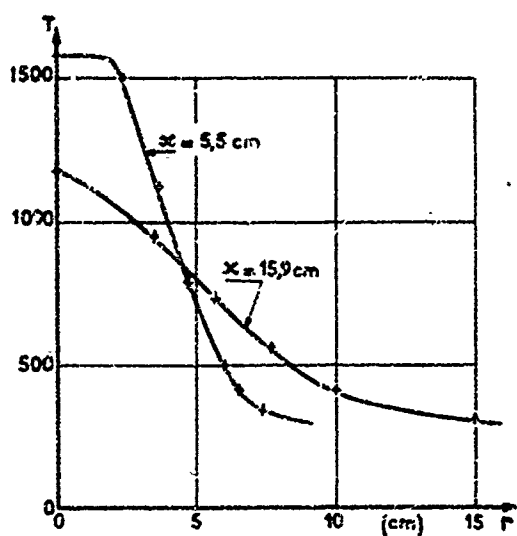


Fig. 6a - Profils transversaux de température.

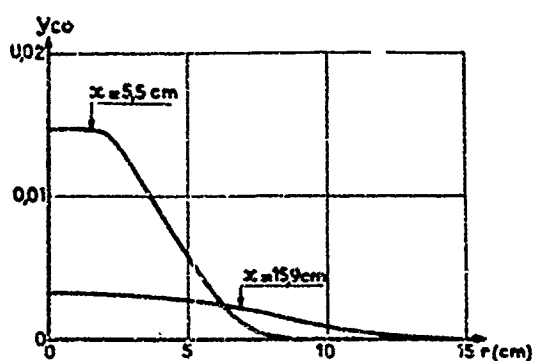


Fig. 6b - Profils transversaux de CO.

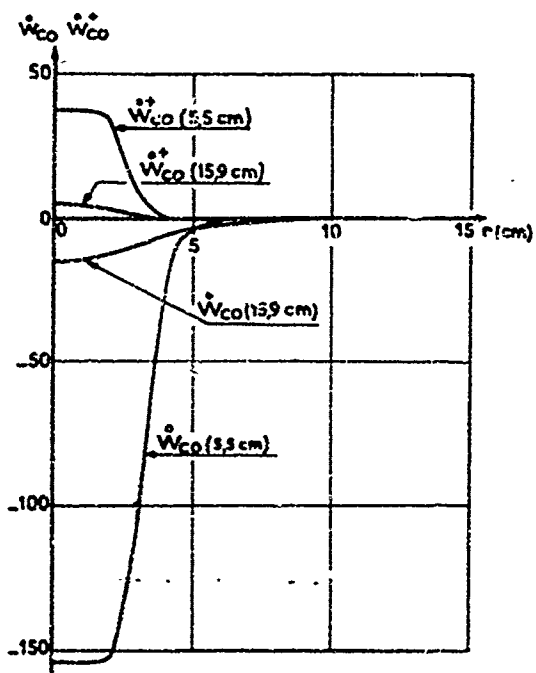


Fig. 6c - Profils transversaux des taux de production de CO.

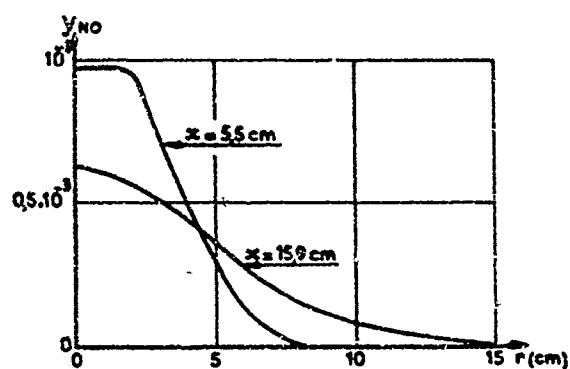


Fig. 6d - Profils transversaux de NO.

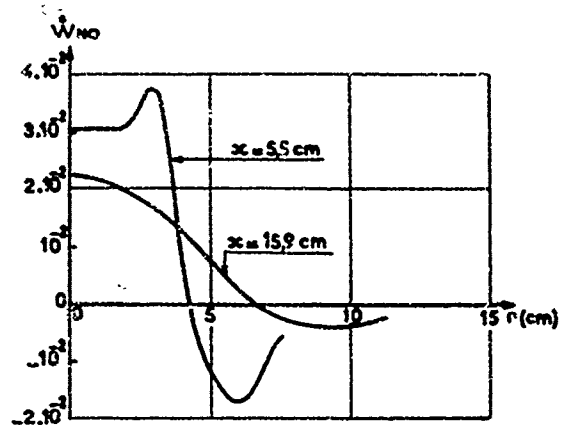


Fig. 6e - Profils transversaux du taux de production de NO.

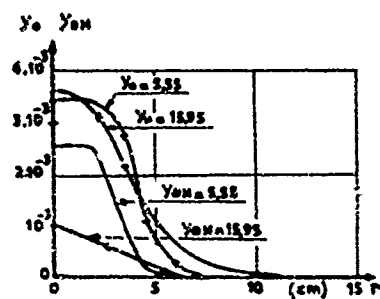


Fig. 6f - Profils transversaux de O et OH.

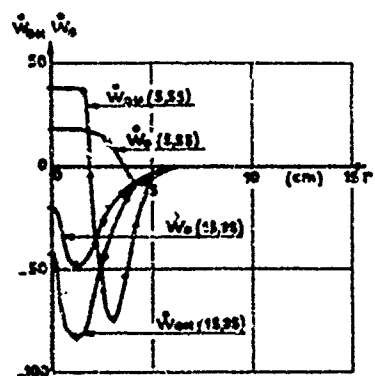


Fig. 6g - Profils transversaux des taux de production de O et OH.

Bien que d'un ordre de grandeur différent, les répartitions transversales de CO et NO (figures 6b et 6d) sont d'allure analogue ; on remarque cependant que la différence entre les courbes pour 5,5 cm et 15,9 cm est bien moins faible pour le NO que pour le CO ; ceci est dû à ce que NO ne disparaît pas comme CO. La figure 6e montre d'ailleurs que NO apparaît au centre du jet, mais disparaît à la périphérie ; cependant W_{H_2} est toujours très faible, de sorte que l'on peut considérer NO comme figé, bien que très proche de l'équilibre (figure 5).

Les figures 6f et 6g montrent les répartitions relatives à OH et O ; elles sont en quantité relativement faible par rapport à CO, mais leurs taux de production chimique sont cependant assez forts ; ces derniers s'évanouissent rapidement (les réactions se figent) en dehors de la zone centrale du jet, où T est la plus forte ; lorsque T est faible, que ce soit à la périphérie du jet pour $x = 5,5$ cm, ou dans tout le jet pour $x = 15,9$ cm, les réactions chimiques ont tendance à provoquer la disparition de O et OH.

4.3. Influence de profils non uniformes en sortie de tuyère

La disparition de CO par combustion résiduelle dans le jet est un fait à prendre en compte lors de la conception des foyers de rechauffe ; on peut, avec la méthode de calcul que nous avons exposé, étudier comment cette disparition est influencée par les caractéristiques du jet chaud dans la section de sortie de la tuyère. En particulier, on peut mettre en évidence que les profils transversaux de température et de concentration en CO (en pratiques liés) ont une importance notable. Nous avons effectué deux calculs pour lesquels la température moyenne, la poussée et les débits des différentes espèces sont identiques dans la section de sortie, mais où T , μ , Y_i présentent des répartitions différentes : dans un premier calcul, leur répartition est uniforme, dans le second, c'est une répartition à deux niveaux, l'écoulement étant plus chaud, plus rapide, plus chargé en CO et CO_2 sur une couronne périphérique qu'au centre.

Pour le premier cas nous avons pris les valeurs suivantes :

$$\begin{array}{lll} \mu = 760 \text{ m/s} & T = 1400^\circ \text{K} & r_{jet} = 4 \text{ cm} \\ Y_O = 2 \cdot 10^{-4} & Y_{CO} = 2 \cdot 10^{-2} & \\ Y_{O_2} = 10,98 \cdot 10^{-2} & Y_{CO_2} = 7 \cdot 10^{-2} & \\ & Y_{H_2O} = 5 \cdot 10^{-2} & \end{array}$$

toutes les autres concentrations étant nulles (sauf N_2 bien sûr).

Pour le second calcul, dans un cercle de 2 cm de rayon :

$$\begin{array}{ll} \mu = 642 \text{ m/s} & T = 1000^\circ \text{K} \\ Y_O = 2 \cdot 10^{-4} & Y_{CO} = 1,2 \cdot 10^{-2} \\ Y_{O_2} = 13,62 \cdot 10^{-2} & Y_{CO_2} = 4,2 \cdot 10^{-2} \\ & Y_{H_2O} = 3 \cdot 10^{-2} \end{array}$$

Dans la couronne extérieure :

$$\begin{array}{ll} T = 1490^\circ \text{K} & \mu = 784 \text{ m/s} \\ Y_O = 2 \cdot 10^{-4} & Y_{CO} = 2,26 \cdot 10^{-2} \\ Y_{O_2} = 10,08 \cdot 10^{-2} & Y_{CO_2} = 7,51 \cdot 10^{-2} \\ & Y_{H_2O} = 5,66 \cdot 10^{-2} \end{array}$$

Dans les deux cas le débit réduit de CO ($\dot{q}/2\pi$) est de $2,89 \times 10^{-3} \text{ kg/s}$.

La figure 7 montre la diminution de ce débit réduit en fonction de x , dans le jet ; elle est notablement plus forte dans le premier cas que dans le second : au bout de 40 cm, 21,8 % de CO ont disparus dans le premier cas, seulement 10 % dans le second.

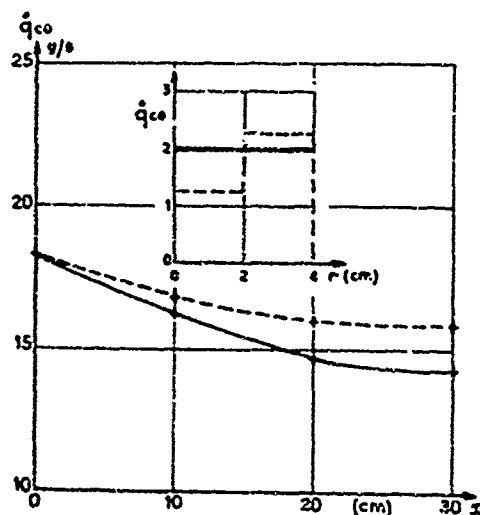


Fig. 7 - Influence du profil initial sur la disposition de CO.

Nous avons vu précédemment que les réactions qui entraînaient la disparition du CO étaient pratiquement dues à la température, on peut expliquer alors facilement le résultat précédent : dans le second cas de calcul, la couronne extérieure la plus chaude et la plus chargée de CO devrait être principalement le siège de ces réactions, mais c'est celle qui est le plus rapidement refroidie par l'air extérieur, et c'est cela qui limite la possibilité de disparition du CO.

5. CONCLUSIONS

A l'occasion de l'étude de l'évolution de CO et NO dans les jets de turboréacteur nous avons développé une méthode numérique de calcul où les phénomènes chimiques peuvent être représentés par un grand nombre de réactions.

Cette méthode de calcul permet l'étude de l'influence des caractéristiques de sortie du turboréacteur - en particulier nous avons présenté ici le cas d'une distribution de température non uniforme - sur les taux de disparitions dans le jet. Dans ce but, d'ailleurs, des schématisations des réactions chimiques, telles [1] et [2], peuvent être utilisées, car elles recourent assez bien les calculs plus complexes que nous avons effectués ici. Cependant, ces derniers permettent de comprendre les différents phénomènes qui se produisent dans les diverses parties de l'écoulement, et ont un domaine d'application plus étendu que le cas particulier du jet de turboréacteur.

RÉFÉRENCES

- [1] LONGWELL, MALCOLM, WEISS - *Heat release rate in hydrocarbons combustion*. I.E.C., vol. 47 n° 8 (1954).
- [2] HOWARD J.B., WILLIAMS G.C., FINE D.H. - *Kinetics of carbon monoxide oxidation in post flame gases*. 14th Symposium (international) on Combustion (1972).
- [3] BROWN W.G., WHITE D.R., SMOOKLER G.R. - *A study of the chemical kinetics of shock heated $H_2/CO/O_2$ mixtures*. 12th Symposium (International) on Combustion (1968).
- [4] BAULCH D.L., DRYSDALE D.D., LLOYD A.C. - *Critical evaluation of rate data for homogeneous, gas-phase reactions of interest in high-temperature systems - N° 1 - (1968)*. Dep^t of Physical Chemistry - The University - Leeds.
- [5] SEERY D., and BOWMAN C.T. - *An experimental and analytical study of methane oxidation behind shock waves*. Combustion and Flame, vol. 14 n° 1 (1970).
- [6] BAULCH D.L., DRYSDALE D.D., LLOYD A.C., HORNE D.G. - *Evaluated kinetic data for high temperature reactions. Vol. 1 - Homogeneous gas-phase reactions of the H_2-O_2 systems*. Butterworths - London - 1972.
- [7] HEYWOOD J.B. - *Gas turbine combustor modeling for calculating nitric oxide emissions*. AIAA paper n° 71/712.
- [8] WESTENBERG A.A. - *Kinetics of NO and CO in lean, premixed hydrocarbon-air flames*. Combustion Sciences and Technology, vol. 4 (1971), p. 59-64.
- [9] HEYWOOD J.B., FAY J.A. and LINDEN L.H. - *Jet aircraft air pollutant production and dispersion*. AIAA paper n° 70/115.
- [10] QUILLEVERE A. - Communication non publiée.
- [11] PRUD'HOMME R., LEQUOY C. - *Talieu des vitesses spécifiques de réactions chimiques utilisables en aérothermochimie*. Note Technique ONERA n° 147 (1969).
- [12] SULZMAN K.G.P., LEIBOWITZ L., PENNER S.S. - *Shock tube studies on mixtures of NO, CO and Ar*. 13th Symposium (International) on Combustion (1970).
- [13] PATANKAR S.V., SPALDING D.B. - *Heat and mass transfer in boundary layers*. 2^e édition, Intertext Books - London (1970).
- [14] SINGH T., SAWYER R.F. - *Co-reactions in the after-flame region of ethylene/oxygen and ethane/oxygen flames*. 13th Symposium (International) on Combustion (1970).



Discussion on Paper 24
 "Etude théorique de l'évolution résiduelle des produits-polluants
 dans les jets de turboréacteurs"
 presented by R.Borghi

R.E.Hule: Have you determined the sensitivity of your model to variation in the rate constants used? Some of those used seem to be significantly in error. In general, a sensitivity analysis should be applied to all of the models presented at this meeting. If the model shows significant sensitivity to a rate constant, how well this number is known should be investigated?

R.Borghi: Nous avons seulement testé la sensibilité des résultats aux variations de la constante relative à la réaction $\text{CO} + \text{OH}$; la sensibilité est notable.

Les valeurs des constantes sont tirées de différents articles; bien sûr, d'autres valeurs existent, qui peuvent être estimées meilleures. Il sera facile de les utiliser dans de nouveaux calculs.

A.Feni: The reactions selected exclude some important reactions. The details of the initial conditions are important. I believe that the complete list of reactions to be used, would give more accurate results, without much larger work required.

I.Glassman: The controlling factor is the mixing time not the reaction time.

R.Borghi: Les conditions initiales sont très importantes en effet, aussi bien avec ce groupe de réactions qu'avec un autre plus compliqué.

D'autre part, s'il est possible d'inclure d'autres réactions, il est d'abord nécessaire de connaître des valeurs plus précises des constantes cinétiques, ce qui n'est pas le cas actuellement, même pour les réactions utilisées ici.

I.Glassman: There is some evidence that at the higher temperatures the $\text{CO} + \text{OH}$ reaction has been very much under estimated, people did what seemed logical in the past when other information was not available, that is assume simple Arrhenius kinetics for that reaction with very low activation energy. Simple transition state theory which gives much greater weight to the pre-exponential factor is a much more appropriate way of analyzing and reporting kinetic results for certain free radical reactions, the reaction rate changes significantly at high temperatures. At temperatures above 1500-1700 K there is a difference of several orders of magnitude.

R.Borghi: La réaction $\text{CO} + \text{OH}$ est très importante; nous avons choisi les valeurs de constantes cinétiques pour cette équation dans un récent article de Singh et Sawyer (14), qui ont effectué des expériences dans un cas semblable de post-flamme.

DEVELOPMENT AND VERIFICATION OF AN ANALYTICAL MODEL FOR PREDICTING EMISSIONS FROM GAS TURBINE ENGINE COMBUSTORS DURING LOW-POWER OPERATION

Stanley A. Mosler, Senior Assistant Project Engineer, Pratt & Whitney Aircraft Division of United Aircraft Corporation, West Palm Beach, Florida, USA, 33402; Richard Roberts, Assistant Project Engineer, Pratt & Whitney Aircraft Division of United Aircraft Corporation, East Hartford, Connecticut, USA, 06108; and Robert E. Henderson, Technical Area Manager, Air Force Aero Propulsion Laboratory, Air Force Systems Command, Wright-Patterson Air Force Base, Ohio, USA, 45433

SUMMARY

A theoretical combustor model has been formulated for predicting concentrations and distributions of unburned hydrocarbons, and carbon monoxide from gas turbine engine combustors. Essential components of this model include an internal flowfield model, a treatment of the physical combustion process, and a treatment of hydrocarbon oxidation kinetics. Model components were incorporated into a computer program with a single model structure for simplicity. An experimental program was also conducted to evaluate combustor design techniques for lowering emission levels and to provide experimental data against which the theoretical model could be tested. Burner exit-plane measurements of unburned hydrocarbons, carbon monoxide, nitrogen oxides, temperature, and pressure were made. Predictions of exhaust species concentrations and distributions were made using the theoretical combustor model in support of the experimental program. Results are discussed with respect to internal aerodynamic and chemical kinetic arguments within the framework of the theoretical formulation.

LIST OF SYMBOLS

A	= area	w_r	= recirculation mass flowrate
$\overline{C_{8H_{16}}}$	= partial equilibrium products of combustion (CO_2 excluded) corresponding to temperature, pressure, and fuel-air ratio	w_t	= rate of turbulent mass exchange between adjacent streamtubes
C_D	= aerodynamic drag coefficient	x	= axial coordinate direction
C_p	= specific heat	Δx	= axial distance required for full jet penetration
D_c	= diameter of combustion air-jet entry hole	Y	= transverse air-jet penetration distance
D_d	= diameter of liquid fuel droplet	Y_{O_2}	= weight fraction of oxygen in ambient gas
I	= stoichiometric oxygen-fuel weight ratio	α_j	= fraction of recirculation mass flow entering or leaving the j th streamtube
L	= heat of vaporization of the fuel	β_0	= angle of jet entry
\dot{m}_f	= rate of mass vaporization from liquid fuel droplet	λ	= thermal conductivity
P	= static gas pressure	μ	= viscosity
Q	= heat of combustion of the fuel	ρ	= density
\dot{Q}	= rate of combustion heat release	ϕ	= equivalence ratio, local fuel-air ratio/stoichiometric fuel-air ratio
R	= streamtube radius	Subscripts	
r	= streamtube radius	B	= bulk gas parameters
T	= static gas temperature	c	= air addition jet parameters
T_0	= total gas temperature	d	= fuel droplet parameters
T_f	= fuel droplet surface temperature	eq	= equilibrium
U	= axial velocity component	g	= local gas parameters
V	= tangential velocity component	j	= identifying the j th streamtube
w_c	= external mass addition flowrate	l	= liquid fuel parameters

1. INTRODUCTION AND PROBLEM DEFINITION

During the past several years, significant technological advancements have been realized in turbine engine combustion system design and performance. Advanced and future primary combustors will have the operational flexibility to accept wide variations in compressor discharge pressure, temperature, and airflow with minimum pressure loss and good design point combustion efficiency while providing an acceptable exhaust-gas temperature profile into the turbine. More recently, however, an additional requirement has been imposed: to reduce objectionable exhaust emissions.

Increased citizen awareness of environmental issues coupled with the obvious visible smoke emissions from jet aircraft has brought substantial public attention to aircraft-contributed pollution. Although smoke by itself may not be harmful, it focused attention on the gas-turbine engine as a potential source of additional undesirable gaseous emissions: carbon monoxide, CO ; unburned hydrocarbons, UHC ; and oxides of nitrogen, NO_x . Additionally, even though turbine engine powered aircraft contribute but a small amount to the overall air pollution problem, these aircraft can become significant contributors in and around high-traffic airports and military air installations.

Of particular concern are the relatively high levels of invisible emissions produced during part-power or low-power (idle/taxi) engine operation. These invisible emissions are principally UHC and CO . Both are nonequilibrium by-products of the combustion process between engine fuel and air. Under ideal thermodynamic conditions, neither should be present as combustion products; however, under low-power operating conditions, the efficiency of current

gas turbine engine combustors tends to be low. Consequently, thermodynamic equilibrium is not attained during the combustion process and these toxic, objectionable exhaust emissions are produced. Minimizing turbine engine exhaust pollution requires that emission control and abatement techniques become a major consideration in the design and development of future combustion systems.

To provide effective emission control without compromising required aerothermodynamic performance of the combustor, two basic approaches may be considered. One approach is to conduct an extensive experimental combustor development program involving the evaluation of many design changes and variations addressed to reducing emissions without incurring system performance degradation. Unfortunately, this approach is often very costly and time consuming and generally requires, ultimately, some system performance compromises and penalties. Another approach is to develop a generalized, analytical combustor model that realistically describes the coupled physical and chemical processes occurring within the combustor and predicts the exhaust product concentration and distribution produced by the combustion system as a function of combustor design, aerothermodynamics, and general operating conditions. Such a model could then become a vital engineering tool permitting the designer to assess the impact of design changes for exhaust emission control on component performance prior to initiating costly development testing.

It is, therefore, the purpose of this paper to present the analytical development and verification of a theoretical combustor analytical design procedure, or model, formulated to serve as an effective tool for evaluating emissions control techniques. The theoretical formulation was developed, initially, to assess combustor emission performance during low-power engine operation, i.e., to predict the concentration and distribution of UHC and CO as a function of combustor operating conditions, geometry, and fuel injection characteristics. The essential components of the overall model are described first; this description is followed by a discussion of an experimental program conducted in conjunction with the modeling effort to evaluate combustor design techniques for lowering emission levels and to provide experimental data against which the theoretical model could be tested. The paper is concluded by comparing the analytical predictions and experimental data for two combustor configurations.

2. APPROACH TO COMBUSTOR MODELING

The approach taken in the development of the low-power emissions combustor model has been to formulate mathematical treatments for the principal physical and chemical mechanisms that influence the combustion process, and to integrate these mechanisms through a sequence of thermodynamic states obtained from the coupling of these mechanisms with the physical combustor flowfield. The simultaneous solution of the combustion rate mechanisms and the fluid dynamics provides the gas temperature, flow velocity, and chemical species concentrations as a function of position within the combustor, which in turn influence subsequent combustion. The principal elements of the analysis are a combustor internal flowfield model, a physical combustion model, and a treatment of hydrocarbon-air chemical kinetics.

The primary objective of the modeling effort is to develop an engineering tool to assist in the design and development of low-emissions combustor hardware. For this reason, the analysis must include sufficient detail to draw a correspondence between the combustion process and combustor geometry, fuel injection characteristics, and engine operating conditions. Development of individual submodels and combination in modular fashion allows the requisite detail to be incorporated in a tractable mathematical analysis. The combustor model to be described here represents an outgrowth of the work reported in Reference 1.

3. DESCRIPTION OF THE COMBUSTOR MODEL

The combustor flowfield model, with input quantities of chamber area as a function of axial distance, inlet air temperature, pressure, and axial location of air addition sites, defines the physical system upon which the gas dynamic and combustion rate calculations are based. The experimentally determined internal flowfield for a conventional swirl-stabilized, can-type combustor is shown in figure 1. The flowfield is seen to include a region of highly turbulent, reversed flow in the front of the chamber, surrounded by a region of relatively uniform downstream flow. The forward or recirculating flow region is designated the primary zone and the downstream region the secondary or dilution zone. The primary zone serves the purpose of stabilizing the combustion process. Liquid fuel is conditioned for burning and combustion is largely completed in this zone. The products of high-temperature combustion and reactants leaving the primary zone continue to burn in the secondary zone. The secondary zone is frequently mixed with dilution air in the secondary zone to provide a suitable temperature profile for entrance to the turbine.

The combustor flowfield model employed in the present analysis is shown schematically in figure 2 for the case of a can-type combustor. The two-dimensional internal flowfield has been approximated by a set of co-annular, one-dimensional reacting streamtubes. The recirculation zone boundary, enclosing region (1), defines the location and size of a zero net flow, one-dimensional streamtube representing the recirculating flow. The recirculation zone boundary has the physical significance of separating the net upstream and downstream portions of the primary-zone airflow. Air entering the front of the combustor is assigned to the main flow streamtubes on an equal basis. Downstream combustion and dilution jet air is apportioned to the streamtubes by means of a jet penetration and mixing model described below. All wall cooling air is assigned to the outer streamtube, which begins at the first cooling

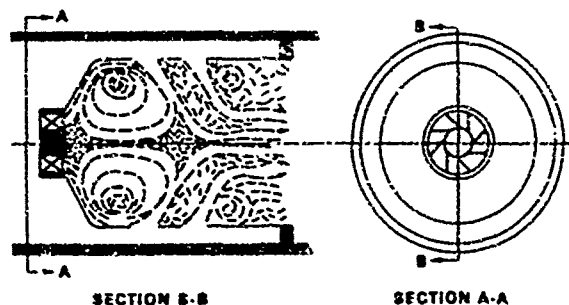


Figure 1. Primary Zone Flow Pattern

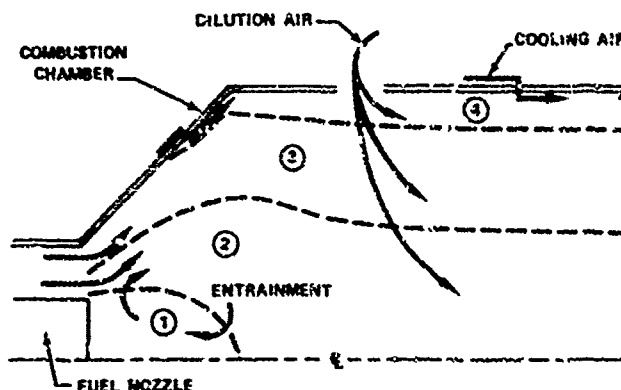


Figure 2. Internal Flowfield Streamtube Model

air addition site. The airflow distribution to combustion and cooling holes is specified as model input. The streamtube boundaries are defined by inner and outer radii, computed as dependent variables. The outermost streamtube is bounded by the location of the chamber wall, which is provided as input.

The applicability of the model to particular combustor types is determined by the flowfield analysis, and includes can and annular configurations that are adequately described by a radial array of one-dimensional, co-annular streamtubes, symmetric about the geometric combustor axis. The recirculation region(s) may either be symmetric about the combustor axis or be symmetric about individual, regularly spaced axes themselves symmetrically arranged about the combustor axis. In the latter case, transition to the annular streamtube arrangement is made at the end of the recirculation region. The can and annular versions of the model are presently limited to 4 and 7 streamtubes, respectively.

The steady-state, one-dimensional analysis of the flow in a streamtube for the downstream direction, x , is obtained by solving the equations for conservation of mass, momentum and energy. It is assumed that wall friction, drag of internal bodies, gravity forces and external heat exchange are negligible. With these assumptions, the differential equations for continuity, linear momentum, and energy, respectively, for the j th streamtube bounded by R_j and R_{j-1} may be written as shown in equations (1) through (3).

$$\frac{d}{dx} (\rho_j U_j A_j) = \frac{dw_c}{dx} \Big|_j \quad (1)$$

$$\frac{d}{dx} (\rho_j U_j^2 A_j) = -\frac{d}{dx} (P_j A_j) + 2\pi P_{j+1} R_j \frac{dR_j}{dx} - 2\pi P_{j-1} R_{j-1} \frac{dR_{j-1}}{dx} + \frac{dw_t}{dx} \Big|_{j-1,j} (U_{j-1} - U_j) + \frac{dw_t}{dx} \Big|_{j,j+1} (U_{j+1} - U_j) \quad (2)$$

$$\frac{d}{dx} (\rho_j U_j A_j C_{p_j} T_{o_j}) = \rho_j U_j A_j \dot{Q}_j + \frac{dw_t}{dx} \Big|_{j-1,j} (C_{p_{j-1}} T_{o_{j-1}} - C_{p_j} T_{o_j}) + \frac{dw_t}{dx} \Big|_{j,j+1} (C_{p_{j+1}} T_{o_{j+1}} - C_{p_j} T_{o_j}) \quad (3)$$

The equation of state, $\rho = P/RT$, is employed to express $d\rho/dx$ in terms of dP/dx and dT/dx in equation (1). In the structuring of a computational procedure, the energy equation is replaced by a number of species conservation equations for fuel and combustion products, which together specify the enthalpy of combustion. In the case of a non-swirling flowfield, static pressure is uniform in the radial direction. For nonzero inlet swirl, additional conservation equations for angular momentum and radial equilibrium are written for the j th streamtube. They are shown, respectively, as equations (4) and (5).

$$\begin{aligned} \frac{d}{dx} \left[\rho_j U_j A_j V_j \frac{(R_j + R_{j-1})}{2} \right] &= \frac{dw_t}{dx} \Big|_{j-1,j} \left(V_{j-1} \frac{(R_{j-1} + R_{j-2})}{2} - V_j \frac{(R_j + R_{j-1})}{2} \right) + \\ &+ \frac{dw_t}{dx} \Big|_{j,j+1} \left(V_{j+1} \frac{(R_{j+1} + R_j)}{2} - V_j \frac{(R_j + R_{j-1})}{2} \right) \end{aligned} \quad (4)$$

$$\frac{d}{dx} (P_j - P_{j-1}) = \frac{d}{dx} \left[\rho_j V_j^2 \left(\frac{R_j^2}{R_j^2 - R_{j-1}^2} \ln \left(\frac{R_j}{R_{j-1}} \right) - \frac{1}{2} \right) \right] \quad (5)$$

A calculation procedure has been devised to determine the rate of transfer of mass, momentum, and energy between the recirculation zone and the outer streamtubes. With the definition of a mass flowrate, w_r , representing entrainment flow entering or leaving the recirculation region, the conservation equations (continuity, linear momentum, and energy) for region (1) may be written as follows.

$$\frac{d}{dx} (\rho_1 U_1 A_1) = \frac{dw_r}{dx} \quad (6)$$

$$\frac{d}{dx} (\rho_1 U_1^2 A_1) = -\frac{d}{dx} (P_1 A_1) + 2\pi P_2 R_1 \frac{dR_1}{dx} + \begin{cases} U_1 \frac{dw_r}{dx} & w_r < 0 \\ \sum_{j=2} \alpha_j U_j \frac{dw_r}{dx} & w_r > 0 \end{cases} \quad (7)$$

$$\frac{d}{dx} (\rho_1 U_1 A_1 C_{p_1} T_{o_1}) = \rho_1 U_1 A_1 \dot{Q}_1 + \begin{cases} C_{p_1} T_{o_1} \frac{dw_r}{dx} & w_r < 0 \\ \sum_{j=2} \alpha_j C_{p_j} T_{o_j} \frac{dw_r}{dx} & w_r > 0 \end{cases} \quad (8)$$

where w_r has been defined to be positive for mass entering the recirculation zone and $\alpha_j dw_r/dx$ defines the fractional exchange rate with streamtube j . Entrainment exchange with the outer streamtubes requires that terms including dw_r/dx in equations (6) through (8) be applied to equations (1) through (3) in proportion α_j such that total entrainment mass flow is conserved. Experience has shown that satisfactory results are obtained when entrainment flow is uniformly exchanged with all outer streamtubes, with the exception of the wall cooling streamtube(s).

Specification of the recirculation boundary, $R_1(x)$, allows the computation of w_r as an additional dependent variable. However, for arbitrary recirculation-zone size, the computed entrainment flow may not be consistent with the required boundary conditions that the recirculation zone contain zero net mass flow and that the axial recirculation velocity, U_1 , approach zero at the upstream and downstream limits of the recirculation-zone envelope. By expressing the recirculation zone boundary in functional form, $R_1 = f(x)$, it is possible to iterate on zone length until the boundary conditions are satisfied. Satisfactory results have been obtained employing elliptical zone contours following the work of Reference 3. With this treatment of recirculation entrainment, both recirculation-zone size and magnitude of recirculation flow may be computed as dependent variables.

Turbulent mixing between adjacent streamtubes may be expressed in terms of a rate of mass exchange between the streamtubes, w_t . The change in momentum resulting from this mass exchange may be related to the Reynolds'

shear stress acting at the boundary between the streamtubes $\tau A = (U_j - U_{j-1}) w_j$, where $A = 2\pi R_{j-1} dx$. The Reynolds' stress may be expressed in terms of the turbulent eddy viscosity coefficient, μ_t , such that $\tau = \mu_t (\partial U / \partial r) \approx \mu_t (U_j - U_{j-1}) (r_j - r_{j-1})^{-1}$, where r_j , r_{j-1} are internal streamtube radii corresponding to the "half-jet" approximation. μ_t may be related to local flow quantities by an expression of the form $\mu_t = \rho k b |U_{\max} - U_{\min}|$ where k is an empirical constant fitted to experimental mixing data for two-dimensional turbulent jets, and b is proportional to the width of the mixing region (Reference 4). With appropriate selection of eddy viscosity model, the rate of mass exchange between adjacent streamtubes is written:

$$\frac{dw_t}{dx} \bigg|_{j-1, j} = \frac{2\pi R_{j-1}}{40} \left| \rho_j (U_j^2 + v_j^2)^{1/2} - \rho_{j-1} (U_{j-1}^2 + v_{j-1}^2)^{1/2} \right| \quad (9)$$

The rate of external air addition, w_e , to the streamtubes defining the internal flowfield is determined from a jet penetration and mixing model. With reference to Figure 3, a transverse jet is assumed to enter the combustor with negligible momentum in the streamwise direction. In the process of mixing with the streamtube flow, the jet is turned in the downstream direction and is accelerated up to the local stream velocity. The trajectory of the jet centerline at the point of uniform velocity defines the jet penetration. An empirical correlation is utilized to express the penetration of a single transverse jet in terms of local jet and mainstream flow properties (Reference 5):

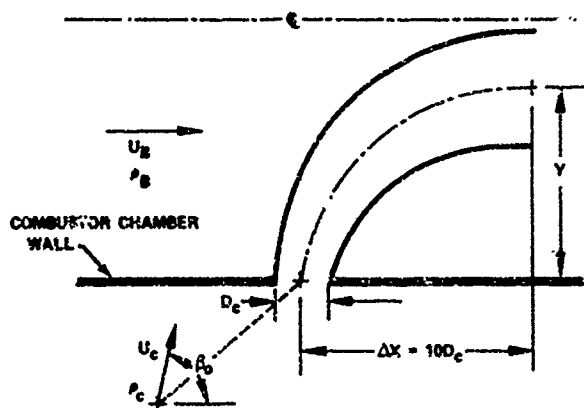


Figure 3. Transverse Jet Penetration Model

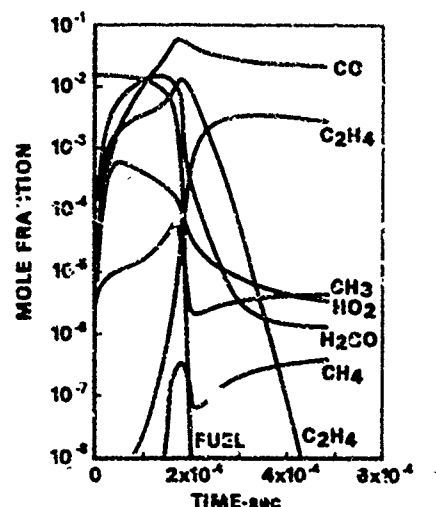


Figure 4. Variation in Species Concentration with Time

$$Y = 0.87 D_c \left(\frac{U_c}{U_B} \right)^{0.85} \left(\frac{\rho_c}{\rho_B} \right)^{0.47} \sin \beta_0 \left(\frac{\Delta x}{D_c} \right)^{0.32} \quad (10)$$

where the subscript B denotes bulk-averaged streamtube velocity and density. The quantity Δx , defined as the distance required for full penetration, has been assumed equal to $10 D_c$. The jet cross-sectional area is computed with the assumption that jet pressure is equal to the local stream pressure at the point of maximum penetration. If the shape of fully developed jet cross-section is assumed to be an ellipse with ratio of major to minor axes of 5:1 (Reference 6), the jet cross-section may be positioned with respect to the streamtube boundaries. Jet air addition to the j th streamtube is proportional to that fraction of the jet cross-sectional area intersected by the streamtube boundaries located at R_{j-1} and R_j . The jet is assumed to be fully mixed with the respective streamtube flows at a position $\Delta x = 10 D_c$ downstream of the air-addition site, consistent with the assumption of full penetration in that distance. Jet air addition rate is specified as linear over the mixing length.

The rate of combustion of liquid fuel is governed by the respective rates of fuel-droplet vaporization and mixing of vaporized fuel and air in the presence of diffusive burning. It is assumed that fuel droplets are uniformly distributed within a streamtube, that interaction between burning droplets is insignificant, and that the fuel droplets within a given streamtube are adequately described by a single value of Sauter mean diameter (SMD). The fuel droplet vaporization rate for a burning droplet is calculated from the following expression due to Wood, Lorell, Rosser and Wise (References 7 and 8):

$$\dot{m}_f = \frac{2\pi D_d \lambda_g}{C_{p_g}} \ln \left[\frac{1 + Q Y_{O_2}}{L I} - \frac{C_{p_g}}{L} (T_f - T_g) \right] \quad (11)$$

Equation (11) is based on assumptions of spherical symmetry, steady-state conditions, independence of transport properties on temperature and composition, and negligible radiation effects. The liquid surface temperature, T_f , is taken to be the ASTM 50% distillation point in accordance with the conclusions reached in Reference 8 for multicomponent fuel blends. Equation (11) is multiplied by $1.0 + 0.276 Re^{1/2} Pr^{1/3}$ where the Reynolds number is given by $Re = \frac{\rho_g U_g - U_d}{\mu_g} D_d$ and the Prandtl number by $Pr = \frac{C_{p_g} \mu_g}{\lambda_g}$ to account for convection (Reference 9).

Since the fuel-droplet velocity typically differs from that of the streamtube flow, acceleration or deceleration of the droplet due to aerodynamic drag must be included. This is accomplished by including a drag force term in the droplet momentum equation. The resulting differential equation for droplet velocity is:

$$\frac{dU_d}{dt} = \left(\frac{3C_D \rho_g}{4D \rho_f} \right) |U_g - U_d| \cdot (U_g - U_d) \quad (12)$$

The drag coefficient is calculated from one of the following equations, depending on Reynolds number (Reference 10):

$$C_D = 27 \text{ Re}^{-0.84}; 0 < \text{Re} \leq 80; C_D = 2.271 \text{ Re}^{0.217}; 80 < \text{Re} \leq 10^4; C_D = 2.0; 10^4 < \text{Re} \quad (13)$$

Initial values of mean droplet size and injection velocity are determined from fuel-injector characteristics. Initial fuel mass distribution among the streamtubes is specified as model input. Separate droplet vaporization equations are written for each streamtube containing liquid fuel. All fuel that enters the recirculation zone is assumed to be fully vaporized and mixed with the region (1) airflow.

In keeping with the physical droplet burning model represented by equation (11), fuel, once vaporized, is assumed to react in stoichiometric proportion with the surrounding air in the streamtube. Excess air or vaporized fuel is withheld from the reacting mixture for the purpose of computing combustion-product temperature and species concentrations. The combustion-product mixture reverts to bulk-streamtube conditions when the fuel vapor within a streamtube has been exhausted. The computation of streamtube aerodynamic parameters is based on bulk-mixture conditions at all times. In the case of premixed fuel and air, combustion occurs at the injected mixture proportions. Combustion of injected fuel vapor or partially evaporated fuel droplets is assumed to occur on a stoichiometric basis as above.

The quantity of fuel vapor produced by an increment of combustor length, when added to the preexisting fuel-air-combustion product vapor mixture at that axial station, is available for combustion. Chemical reaction of the hydrocarbon fuel and air determines the gas temperature and concentration of active combustion species. The degree of completion of the combustion reactions determines the exhaust concentration of carbon monoxide and unburned hydrocarbons. The number of possible reactions involved in the breakdown of hydrocarbon fuels is extremely large, and few have been investigated with respect to their rates. It is, therefore, convenient to assume that fuel breakdown into final species occurs in a small number of global steps. The hydrocarbon kinetics system employed in the present analysis is shown in the following table.

As represented by this mechanism, the complex oxidation of hydrocarbon fuel is viewed as occurring in 3 broad stages. The first stage, represented by global reactions (1) through (3), produces light, unburned and partially oxidized hydrocarbons. The rate constants for these reactions have been adjusted to fit experimental ignition delay data following the approach of Edelman and Fortune (Reference 11). The hypothetical aldehyde intermediate ($\text{C}_4\text{H}_8\text{O}$) is introduced for computational convenience. The subsequent sequence of reactions, comprising the second stage of combustion, includes the principal exothermic reactions and produces large amounts of H_2O and CO . The particular reactions included in the present system are considered to represent families of intermediate species of similar character. The final stage of combustion is characterized by the conversion of CO to CO_2 via reaction (19). The reaction rate constants shown in the table have been taken from References 11 through 19 with the exception of reaction (7), where the rate has been deduced from results presented in References 13 through 15 and 19. JP-5 fuel is represented chemically by the formulation C_8H_{16} , although it is not meant to be a true olefin. The thermodynamic properties (specific heat, heat of formation) for C_8H_{16} are consistent with those of JP-5.

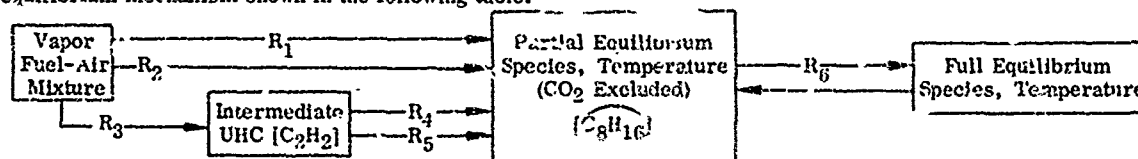
Reaction	Rate Constant, $\text{cm}^3 \cdot \text{mole}^{-1} \cdot \text{sec}^{-1}$	Reference Source
(1) $\text{C}_8\text{H}_{16} + \text{O}_2 = 2\text{C}_4\text{H}_8\text{O}$	$k_1 = 7.5 \times 10^6 \text{ T}^{1.5} e^{-7900/\text{T}}$	See Text
(2) $\text{C}_4\text{H}_8\text{O} + \text{O}_2 = \text{HO}_2 + \text{CO} + \text{CH}_3 + \text{C}_2\text{H}_4$	$k_2 = 10^{11} \text{ T}^{1.5} e^{-10000/\text{T}}$	See Text
(3) $\text{C}_8\text{H}_{16} + \text{OH} = \text{H}_2\text{CO} + \text{CH}_3 + 3\text{C}_2\text{H}_4$	$k_3 = 3 \times 10^{10} \text{ T} e^{-4500/\text{T}}$	See Text
(4) $\text{CH}_3 + \text{O} = \text{H}_2\text{CO} + \text{H}$	$k_4 = 2 \times 10^{13}$	12
(5) $\text{CH}_3 + \text{O}_2 = \text{H}_2\text{CO} + \text{OH}$	$k_5 = 10^{12}$	13
(6) $\text{H}_2\text{CO} + \text{OH} = \text{H}_2\text{O} + \text{CO} + \text{H}$	$k_6 = 10^{14} e^{-4000/\text{T}}$	12
(7) $\text{C}_2\text{H}_4 + \text{O}_2 = 2\text{H}_2\text{CO}$	$k_7 = 3 \times 10^2 \text{ T}^{2.5}$	See Text
(8) $\text{C}_2\text{H}_4 + \text{OH} = \text{CH}_3 + \text{H}_2\text{CO}$	$k_8 = 5 \times 10^{13} e^{-3000/\text{T}}$	14
(9) $\text{CH}_3 + \text{H}_2 = \text{CH}_4 + \text{H}$	$k_9 = 6 \times 10^{11} e^{-5500/\text{T}}$	15
(10) $\text{C}_2\text{H}_4 = \text{C}_2\text{H}_2 + \text{H}_2$	$k_{10} = 7 \times 10^8 e^{-23250/\text{T}}$	16
(11) $\text{C}_2\text{H}_2 + \text{OH} = \text{CH}_3 + \text{CO}$	$k_{11} = 10^{13} \times e^{-3500/\text{T}}$	13
(12) $2\text{H} + \text{M} = \text{H}_2 + \text{M}$	$k_{12} = 2 \times 10^{18} \text{ T}^{-1}$	11, 16
(13) $2\text{O} + \text{M} + \text{O}_2 = \text{M}$	$k_{13} = 10^{17} \text{ T}^{-1}$	13, 17
(14) $\text{OH} + \text{H} + \text{M} = \text{H}_2\text{O} + \text{M}$	$k_{14} = 7 \times 10^{19} \text{ T}^{-1}$	17, 18
(15) $\text{H} + \text{O}_2 = \text{OH} + \text{O}$	$k_{15} = 2.24 \times 10^{14} e^{-9400/\text{T}}$	18
(16) $\text{O} + \text{H}_2 = \text{OH} + \text{H}$	$k_{16} = 1.74 \times 10^{13} e^{-4730/\text{T}}$	18
(17) $\text{H} + \text{H}_2\text{O} = \text{H}_2 + \text{OH}$	$k_{17} = 8.41 \times 10^{13} e^{-16050/\text{T}}$	18
(18) $\text{O} + \text{H}_2\text{C} = 2\text{OH}$	$k_{18} = 5.75 \times 10^{13} e^{-9000/\text{T}}$	18
(19) $\text{CO} + \text{OH} = \text{CO}_2 + \text{H}$	$k_{19} = 5.6 \times 10^{11} e^{-540/\text{T}}$	18
(20) $\text{HO}_2 + \text{M} = \text{H} + \text{O}_2 + \text{M}$	$k_{20} = 2.4 \times 10^{15} e^{-22950/\text{T}}$	18
(21) $\text{HO}_2 + \text{H} = 2\text{OH}$	$k_{21} = 6 \times 10^{13}$	17, 19

While it is felt that the kinetic mechanism presented in the present table offers an adequate representation of the detailed hydrocarbon combustion process, the simultaneous solution of the system of equations does not lend itself

to coupling with the streamtube flow field model. In particular, computational step size must be very small as species equilibrium is approached, resulting in excessively long computation time. The approach taken in the development of the model was to replace the full kinetic mechanism with a reduced kinetic-partial equilibrium system capable of predicting those aspects of the full system behavior that are important to the determination of exhaust emissions.

The kinetic mechanism presented in the preceding table is readily solved for the plug-flow combustion of premixed fuel and air. The computed behavior of selected intermediate species is shown in figure 4 for the case of a stoichiometric mixture at a pressure of 2 atm (2.026×10^5 N/m²) and an initial temperature of 1000°K. The combustion is characterized by a period of abrupt change in species concentration corresponding to rapid temperature rise, followed by a period of relatively slow approach to equilibrium. From the point of view of emissions modeling, the relatively slow "post-flame" reactions are most significant, representing the reaction of intermediates on a time scale comparable to the combustor residence time. The time spent in the transitory, rapid temperature rise period is an order of magnitude less than typical values of combustor residence time. In addition, the ignition delay period for raw fuel can be significant at lower mixture temperatures. Thus, a reduced system which provides the ignition delay and post-flame behavior of the full hydrocarbon kinetics mechanism will adequately predict the influence of the chemical combustion rate on exhaust emissions.

The behavior of the full kinetics mechanism was documented by performing plug-flow computations for a range of initial temperatures, pressures, and fuel-air ratios. This behavior was then fitted with the reduced kinetic-partial equilibrium mechanism shown in the following table.



	Reaction	Rate Constant, (m ³ ·mole ⁻¹ ·sec ⁻¹)	Reference Source
(R ₁)	$C_8H_{16_{\text{vapor}}} + O_2 \rightarrow C_8H_{16}$	$k_{R_1} = 7.5 \times 10^6 T^{1.5} e^{-7900/T}$	Preceding Table
(R ₂)	$C_8H_{16_{\text{vapor}}} + OH \rightarrow C_8H_{16}$	$k_{R_2} = 3 \times 10^{10} T e^{-4500/T}$	Preceding Table
(R ₃)	$C_8H_{16_{\text{vapor}}} + H \rightarrow 4C_2H_2$	$k_{R_3} = 1.3 \times 10^{13} e^{-4000/T}$	See Text
(R ₄)	$C_2H_2 + O_2 \rightarrow 1/4 C_8H_{16}$	$k_{R_4} = 10^{10} e^{-6500/T}$	14
(R ₅)	$C_2H_2 + OH \rightarrow 1/4 C_8H_{16}$	$k_{R_5} = 2 \times 10^{12} e^{-3500/T}$	20
(R ₆)	$CO + OH \rightleftharpoons CO_2 + H$	$k_{R_6} = 5.6 \times 10^{11} e^{-540/T}$	Preceding Table

This system provides for the rate controlled conversion of raw fuel-air mixtures to partial equilibrium products, both directly (R₁ and R₂) and via an unburned hydrocarbon intermediate (R₃ through R₅). CO₂ has been removed as an allowable species in the partial equilibrium state. Subsequent conversion to full equilibrium products is controlled by reaction (R₆). The combustion product temperature and species concentrations are determined by interpolation between the partial and full equilibrium states based on [CO₂]/[CO₂]_{eq}. It should be noted that this treatment of hydrocarbon combustion kinetics requires only that carbon atoms be conserved. Therefore, with the exception of reaction (R₆), only the characteristic reaction products are stated and no reverse reaction is provided. The reaction rate constants for reactions (R₁), (R₂) and (R₆) correspond to those given in the first table for the same reactions.

Reaction (R₃) represents direct formation of light, intermediate, unburned hydrocarbons typified by C₂H₂. Examination of results obtained from the full-kinetic system indicated that intermediate unburned hydrocarbons appear in significant quantities after about half the original fuel is consumed. Furthermore, the dependence of unburned hydrocarbon concentration on fuel-air ratio and inlet temperature was not simply related to either the OH or O₂ equilibrium concentration. The qualitative behavior of the intermediate unburned hydrocarbons was fitted best by relating the formation to [H]_{eq}. This "reaction" has no chemical significance, representing only a fit to the observed behavior. The rate indicated in the preceding table has, likewise, been fitted to the observed behavior of the full system. Reactions (R₄) and (R₅) represent reaction of the intermediate unburned hydrocarbons with HO₂ and OH to partial-equilibrium products. The rates indicated in the preceding table are representative values for reactions involving light, intermediate hydrocarbons, obtained from References 14 and 20, respectively. Since the species [HO₂]_{eq} is not provided by the equilibrium chemistry computation, reaction (R₄) has been written in terms of [O₂]_{eq}, with the assumption that [O₂]_{eq} is 2 orders of magnitude greater than [HO₂]_{eq} for the conditions of interest. The calculation subroutine employed for the equilibrium hydrocarbon thermochemistry is based on procedures of Brinkley (References 21 and 22).

The number and initial location of the streamtubes is specified based on combustor geometry. Initial values of the independent and dependent variables are determined from combustor geometry and input conditions. The aerodynamic equations of motion are written in differential form for each streamtube. These equations, when coupled with an equation describing the recirculation-zone boundary and arranged in matrix form, constitute a set of linear differential equations which may be solved simultaneously for parametric derivatives with respect to x . These differentials are numerically integrated over the interval Δx utilizing a Runge-Kutta procedure to obtain values of parameters at $x + \Delta x$. Integrated values of parameters at $x + \Delta x$ are then used to obtain new derivatives which are integrated to yield values of parameters at $x + 2 \Delta x$, and so on, until the exit plane is reached.

Production of vaporized fuel, chemical reaction of fuel and air, external air addition and turbulent exchange between streamtubes are evaluated in subroutines external to the streamtube equation matrix. Updated values of derivatives with respect to x are provided at the end of each computational step for integration in the next step. For this approach to succeed, it is necessary that variation in parameters not included as dependent variables in the differential equation matrix be small across the computational step. This arrangement of the computational procedure permits concentrations and flow properties of combustion product species to be calculated as a function of position along the individual streamtubes for fairly arbitrary specification of the physical and chemical combustion models. The model is presently limited to equilibrium combustion of a fixed fuel-air mixture outside the recirculation zone. Satisfactory results have been obtained with the assumption of stoichiometric burning within this zone. Typical computed values of pressure, velocity and stream temperature are shown in figures 5a and 5b for a can-type combustor with zero inlet swirl.

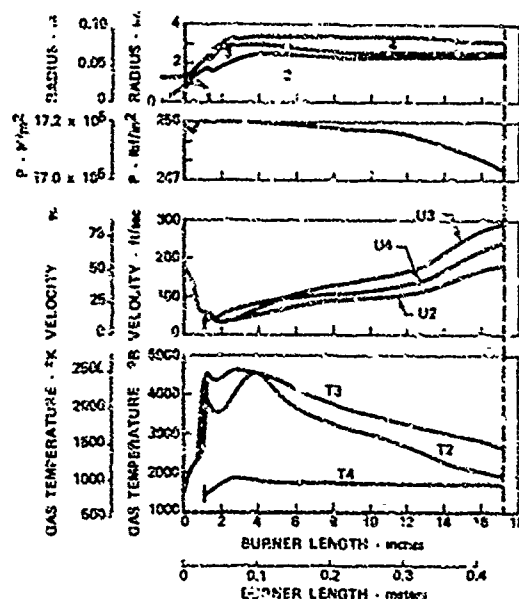


Figure 5a. Analysis of Can Type Combustor with Zero Inlet Swirl

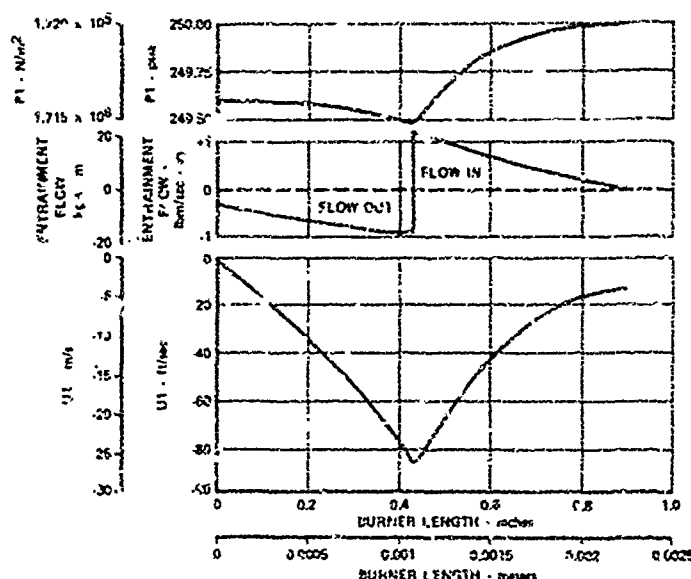


Figure Recirculation-Zone Parameters from Analysis

4. EXPERIMENTAL ASSESSMENT

An experimental research program was conducted concurrently with the development of the analytical model. The objective of this program was to evaluate component design techniques for lowering pollutant emission levels at part-power engine operation and to provide experimental data to assist in refining the theoretical combustor model. Continuous interchange of information between the analytical and experimental programs served to enhance the successful accomplishment of both.

Two promising means of reducing pollutant emission levels during low-power operation were evaluated during the experimental program: air staging and axial fuel staging. The principal objective of each was to closely control the environment within the combustor to effect a more complete reaction between fuel and air; thereby minimizing the formation of the products of incomplete combustion UHC and CO.

It is virtually impossible to closely control or regulate the environment within current fixed-geometry burners at both high and low-power operating conditions because of the nature in which they operate. Even at full power, the overall fuel-air ratio lies well below the lower flammability limit for mixtures of aircraft fuel and air. Consequently, it is necessary to burn the fuel with but a fraction of the available air at a local fuel-air ratio well within the flammability limits for the fuel-air mixture, and then add the remaining combustor-designated air to the combustion products.

Conventional combustors are typically operated at near-stoichiometric fuel-air ratios in the primary zone at a selected design point such as full power. They are then operated below this design-point fuel-air ratio at all other conditions. At full-power and near-full-power conditions, the reaction temperature in the combustor is high and reaction rates are fast. Consequently, combustion efficiencies are typically very high and both UHC and CO concentrations in the exhaust gas are very low. On the other hand, at low- or part-power conditions, these combustors operate at overall and local fuel-air ratios well below those achieved at high power. As a result, combustion temperatures are low and reaction rates are slow; consequently, combustion efficiencies are low and concentrations of both UHC and CO in the exhaust gas are high.

With the air-staging concept, combustion chamber environmental control is achieved by changing the distribution of air entering the combustor as the rate of fuel flow is changed so that the local fuel-air ratio in the primary zone is kept at a constant value. Hence, although the overall fuel-air ratio increases as the rate of fuel flow is increased and decreases as the rate of fuel flow is decreased, the primary-zone fuel-air ratio does not change.

With the axial fuel staging concept, on the other hand, control of the environment within the combustor is achieved by changing the distribution of fuel entering the combustor as the rate of fuel flow is changed. As a result, a pre-established local fuel-air ratio is achieved but not exceeded in the vicinity of each injection station. Although the overall fuel-air ratio increases as the rate of fuel flow is increased, local fuel-air ratios in the vicinity of the axial fuel injection stations do not exceed a predetermined value.

With both methods, near-stoichiometric, primary-zone fuel-air ratios at low-power operating conditions can be theoretically achieved by properly distributing fuel and air to the combustor. Consequently, both UHC and CO concentrations in the exhaust from gas-turbine engine combustors at low- and part-power operations can be theoretically reduced or eliminated.

With reference to figure 6, the air staging and fuel staging concepts evaluated in the experimental program can be described by 4 primary parameters. The first, PSAR, is the ratio of the air flowrate in the primary zone to the air flowrate in the secondary zone. The second, PSFR, is the ratio of the fuel flowrate in the primary zone to the fuel flowrate in the secondary zone. The next, PHIP, is the fuel-air equivalence ratio in the primary zone. The fuel-air equivalence ratio is defined as the ratio of the local and stoichiometric fuel-air ratios for the fuel-air mixture of interest. The last, FA, is the overall fuel-air ratio for the combustor.

Three of the preceding 4 variables are independent. If any 3 are specified, the fourth can be readily derived from the combustor geometry shown in figure 6.

$$PSAR = \frac{(PHIP)(0.068)}{FA} \left(\frac{PSFR + 1}{PSFR} \right) - 1 \quad (14)$$

$$PSFR = \frac{1}{1 - \frac{(PHIP)(0.068)}{FA} \left(\frac{PSAR}{PSAR + 1} \right)} \quad (15)$$

$$PHIP = \left(\frac{FA}{0.068} \right) \left(\frac{PSFR}{PSFR + 1} \right) \left(\frac{PSAR + 1}{PSAR} \right) \quad (16)$$

$$FA = \frac{(PHIP)(0.068)}{\left(\frac{PSFR}{PSFR + 1} \right) \left(\frac{PSAR + 1}{PSAR} \right)} \quad (17)$$

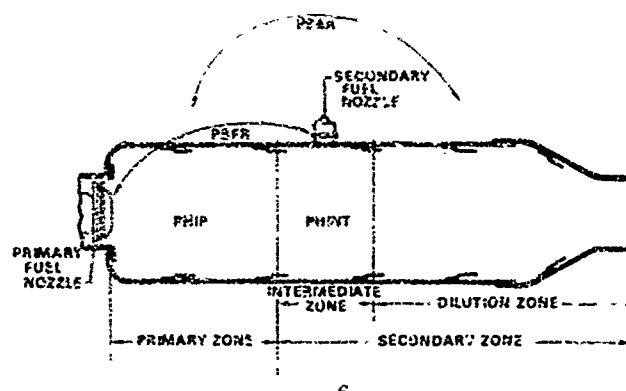


Figure 6. Research Combustor Arrangement and Nomenclature

Evaluation of the air-staging concept involved determining the variation in distribution and concentration of exhaust pollutants with the air distribution parameters PSAR and PHIP, and the overall fuel-air ratio, FA, at specific values of combustor inlet air temperature, pressure, and flowrate. A description of the experimental hardware and of the testing conditions is presented later in this paper. A practical combustor design based upon the air-staging concept would require means to continuously vary the air distribution as FA is varied. No attempt was made to synthesize such a configuration in this program, however. Instead, a research combustor was designed and built with flexibility to facilitate the predetermined variation of airflow distribution into the burner. For discrete values of PSAR, the variation in emission concentration and distribution at the exit plane of the research burner was determined over a range of overall fuel-air ratios. Results from tests involving the systematic variation of PSAR were then combined to describe results that should be obtainable from a combustor having a continuously modulating air distribution system.

Evaluation of the axial fuel-staging concept involved determining the variation in distribution and concentration of exhaust pollutants with the air distribution parameters PSAR and PHIP, the fuel distribution parameters PSFR and PHINT and the overall fuel-air ratio, FA, at specific values of combustor inlet temperature, pressure, and flowrate. PHINT is the intermediate-zone equivalence ratio. Each test series consisted of selecting a discrete value of the air distribution parameter PSAR, which established the primary-zone equivalence ratio PHIP, and increasing the overall fuel-air ratio by introducing additional fuel into the combustor through a second set of fuel nozzles located downstream of the primary zone. (See figure 6.) As FA was increased, then PSFR decreased and PHINT increased.

Tests conducted to evaluate the air and axial fuel staging concepts were accomplished using an annular research combustor of the basic configuration shown schematically in figure 6. This hardware was designed to be generally representative of conventional static-iced combustors. Diameters of the outer and inner liners of the flametube were 10 and 10 inches, respectively (0.381 and 0.254 meter, respectively). The length of the burner from the primary fuel nozzle injection station at the dome to the exit plane of the discharge transition duct was 16 inches (0.106 meter). The combustor was fabricated from heavy-gauge (0.0625 inch; 0.0016 meter) Hastelloy-X sheet stock. This unusually thick material was selected for the research burner to provide physical resistance to overcome both geometrical distortions associated with thermal stresses developed during testing and mechanical forces generated during programmed modifications. The walls and dome were film-cooled by air entering the combustor through judiciously placed louvers along the inner and outer liners.

In accomplishing the air-staging evaluation tests, changes in airflow distribution were achieved simply by changing the size of the air-entry holes in the burner, as required. This was done by affixing sheet-metal patches, predrilled to the sizes required to achieve the PSAR of interest, atop air-entry holes in the liners of the basic burner. To change from one air distribution to another, then, all that was involved was to remove the existing patches and replace them with a new set. In all air-distribution arrangements, the entry holes in the outer and inner liners were diametrically opposed to effect impingement of the incoming airstreams. Once the burner had been modified to provide a specific air distribution, fuel-staging tests could also be conducted. Operationally, as noted earlier, this simply involved distributing and regulating the fuel flowrate to the primary and secondary zones of the burner, as required.

The research combustor was provided with 2 fuel-injection stations, as shown schematically in figure 6. One, located in the dome, served the primary zone in both air and fuel-staging tests; the other, located halfway between the dome and the exhaust plane, served the secondary zone in the fuel-staging tests. The primary-zone fuel system consisted of 14 fuel nozzle-swirler combinations that were evenly spaced along the circumference of the mean height of the flametube. The fuel nozzles used were pressure-atomizing, simplex-type, oil-burner nozzles that had a design-point flowrate of 4 gallons (U. S. liquid) of JP-5 fuel/hr ($4.21 \times 10^{-4} \text{ m}^3/\text{sec}$) at a differential pressure of 12.1 lbf/in² ($8.62 \times 10^5 \text{ N/m}^2$). At this condition, each nozzle produced a hollow-cone fuel spray having a dispersion angle of 90 deg (1.57 rad). The axial-flow air swirler around each fuel nozzle had an outer diameter of 1.58 in. (0.0427 m), an inner diameter of 1.20 in. (0.0305 m), and incorporated 16 vanes. In alternating locations, swirlers contained vanes arranged at an angle of 45 deg (0.785 rad) to the horizontal axis; in the remaining 7 locations, swirlers contained vanes arranged at an angle of 135 deg (2.36 rad) to the horizontal axis.

The secondary fuel system incorporated 14 fuel nozzles of the type used in the primary system. Each nozzle was affixed to the outer liner of the combustor such that its spray axis was normal to the horizontal axis of the combustor (figure 6), and that its face was at the same diameter as the inner wall of the outer liner. The nozzles were centered within holes drilled in the outer liner through which secondary combustion air entered. No swirlers were used for the injection of this secondary air.

The test rig used in the experimental program, shown schematically in figure 7, consisted of a large upstream plenum chamber, a test section in which the combustor was mounted, and a traverse case containing temperature, pressure, and gas-sampling probes. The traverse case was also used to collect exhaust gas from the test section and direct it into the exhaust system of the test facility. The upstream plenum chamber was designed to diffuse the combustor inlet airflow to very low velocities to minimize the possibility of obtaining nonuniform flow distributions around the combustor.

Airflow, unutilized, to the combustor was supplied from the bleed ports of a T75 turbojet slave engine. An indirect heat exchanger was provided in the airflow system to maintain combustor inlet air temperature at the desired level. In the tests conducted in this program, the rate of airflow to the combustor was approximately 6 lb_m/sec.

(2.72 kg/s); the air temperature was maintained at approximately 100°F (477°K). All tests were conducted at combustion chamber pressures slightly above atmospheric.

Temperature, pressure, and exhaust gas composition distributions for the entire exhaust gas flowfield at the exit plane of the annular research burner were determined in each experimental test. A 4-arm, rotating traverse probe assembly, shown in figure 8, was used in the accomplishment of these measurements. Each of 2 of the probe arms, located 180 deg (3.14 rad) apart, had 5 equally spaced, radially positioned platinum-platinum-10% rhodium, aspirated thermocouples alternating with 4 comparably spaced total-pressure probes. Each of the remaining 2 probe arms, also located 180 deg (3.14 rad) apart, but positioned circumferentially halfway between the first pair of arms, contained inlet ports at 5 equally spaced, radial position, through which a small quantity of exhaust gas from the combustor was continuously abstracted. Gas entering these ports discharged into a common line in each arm. The gas samples from each line then discharged into a single manifold. This consolidated sample was directed through a heated transfer line to a set of on-line gas analysis instruments from which the average composition of the exhaust gas at a fixed circumferential location was obtained.

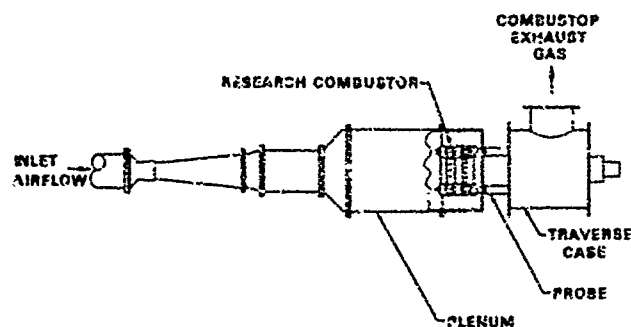


Figure 7. Experimental Test Rig

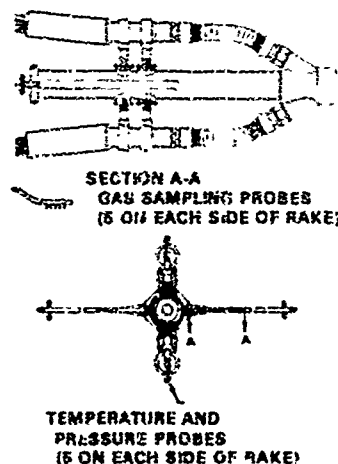


Figure 8. Sampling Probe

As the traversing probe was rotated through an angle of 180 deg (3.14 rad) around the centerline of the burner, each pair of arms surveyed half of the combustor discharge annulus. An entire 360 deg (6.28 rad) survey was thereby accomplished by rotating the traversing probe system through only 180 deg (3.14 rad). For the tests conducted in this program, exit plane measurements for a full traverse were taken at 12 deg (0.209 rad) intervals during the 180 deg (3.14 rad) survey. A total of 150 discrete temperature measurements, 120 discrete pressure measurements, and 15-10 point average exhaust gas composition measurements were obtained in each survey.

The composition of exhaust gas abstracted at the exit plane of the research combustor was determined using an on-line instrumentation system shown in figure 9. The system consisted of the appropriate circuits, controls, and quantitative analytical instrumentation to determine the concentrations of total unburned hydrocarbons, carbon dioxide, carbon monoxide, nitric oxide, nitrogen dioxide, and water vapor. Unburned hydrocarbon concentrations were determined using a flame ionization detector; carbon dioxide, carbon monoxide, nitric oxide, and water vapor concentrations were determined using nondispersive infrared analyzers, and the concentration of nitrogen dioxide was determined using a nondispersive ultraviolet analyzer.

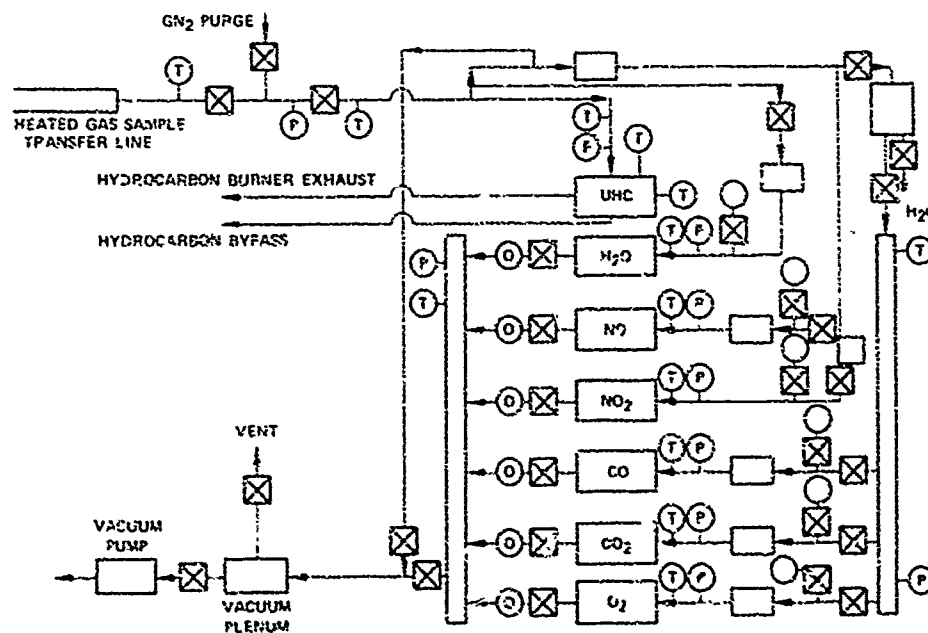


Figure 9. Schematic Diagram of Instrumentation System

The instrumentation system incorporated 2 independent gas-sample circuits. These circuits emanated from the single, heated, exhaust-gas supply line that delivered gas from the traverse probe to the instrumentation system. One circuit, which delivered exhaust gas to the flame ionization detector, was heated to prevent condensation of hydrocarbons. The other circuit, which delivered exhaust gas to a manifold supplying the remaining instruments was unheated. Gas from the second circuit was directed through the proper drier and/or absorber upstream of each analyzer to eliminate those species that might interfere with the analysis of a desired species.

5. COMPARISON OF ANALYTICAL AND EXPERIMENTAL DATA

Of the tests conducted to evaluate the air and fuel staging concepts, those from 2 typical series were selected for use in this paper to compare analytical and experimental emissions data. The hardware used in both series was identical. However, in the air staging tests, although the intermediate-zone (axial-staging) fuel nozzles were in place, no fuel was supplied to the combustor through these nozzles. For the test series in question, the research combustor was designed to operate with a liner pressure loss of 1.8% and a primary zone equivalence ratio of unity when the overall fuel-air ratio was 0.016. At values of FA less than 0.016, PHIP was less than unity. To achieve the design-point fuel-air ratio, the total airflow to the combustor (which was built to have a PSAR of 0.31) was distributed, approximately, as follows: 23% for the primary zone; 13% for the intermediate zone; and 64% for the dilution zone. Primary-zone air was defined as that air entering the primary zone of the combustor through the swirlers (6.7%); through the penetration holes in the inner and outer liners (6.7%); and through the cooling louvers (10.2%). Intermediate-zone air was defined as that air entering the intermediate zone of the combustor through the penetration holes in the outer liner around the intermediate-zone fuel nozzles (7.6%); and through the cooling louvers (5.0%). Dilution-zone air was defined as that air entering the dilution zone of the combustor through the penetration holes in the inner and outer liners (49.5%), and through the cooling louvers (14.8%). With this airflow schedule, when the axial fuel staging option was used, an intermediate zone equivalence ratio of approximately 0.7 was theoretically achieved when the overall, full-power fuel-air ratio was 0.022.

Fourteen tests comprise the test series described in this paper. The air staging tests were conducted by increasing the rate of fuel flow through the primary fuel nozzles until the desired fuel-air ratio was achieved. With the combustor operating at this condition, measurements of temperature and pressure, and samples of exhaust gas were taken at the exit plane. In this series, data were obtained at fuel-air ratios of 0.0039, 0.0059, 0.0091, 0.0132, 0.0162 and 0.0196. The fuel staging tests were conducted by establishing a predetermined primary zone equivalence ratio, using the primary fuel nozzles, and then increasing the overall fuel-air ratio by adding additional fuel through the intermediate zone fuel nozzles. Data were obtained in this series as they were in the air-staging series. Three values of PHIP were investigated: 0.38, 0.50, and 0.75; at each of these values FA was varied. For a PHIP of 0.38, the discrete values of FA examined were 0.0076, 0.0153, and 0.0196; for a PHIP of 0.50, the values of FA were 0.0119, 0.0160, and 0.020; and for a PHIP of 0.75, the values of FA were 0.015 and 0.020. The measured values of carbon monoxide, unburned hydrocarbon and oxides of nitrogen concentration are presented in figures 10 through 12.

The combustor emissions prediction model and calculation procedures described in Section II have been programed for solution on a digital computer. In addition to the aerodynamic parameters shown in figure 5, the computer program provides a detailed history of fuel droplet size, droplet velocity, vaporized fuel-air ratio, and hydrocarbon combustion product species concentrations for each streamtube. The model was utilized to predict carbon monoxide and unburned hydrocarbon emission levels for selected configurations and operating conditions represented in figures 10 through 12. The particular configurations chosen were the air staging test series (Scheme 2-1A) and the fuel staging test series (Scheme 2-1B) operated at PHIP = 0.50. The predicted exit plane carbon monoxide and unburned hydrocarbon concentrations are indicated as dashed lines in figures 10 and 11. The model is not presently configured to predict formation of nitrogen oxides. As indicated in figures 10 and 11, reasonable agreement in absolute concentration and trend with change in operating condition (fuel-air ratio) and configuration (fuel staging) has been obtained.

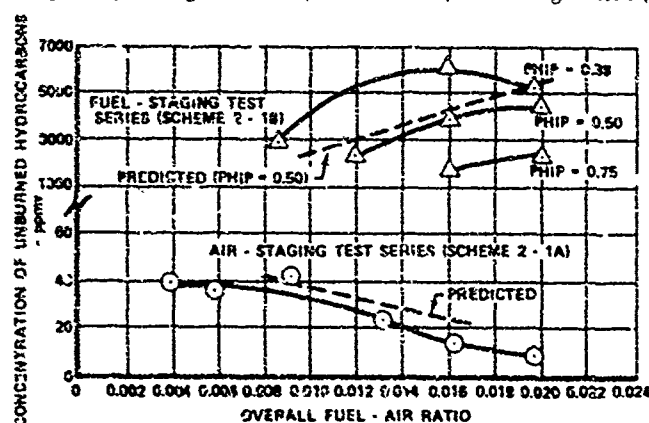


Figure 10. Variation in CO Concentration with Fuel-Air Ratio

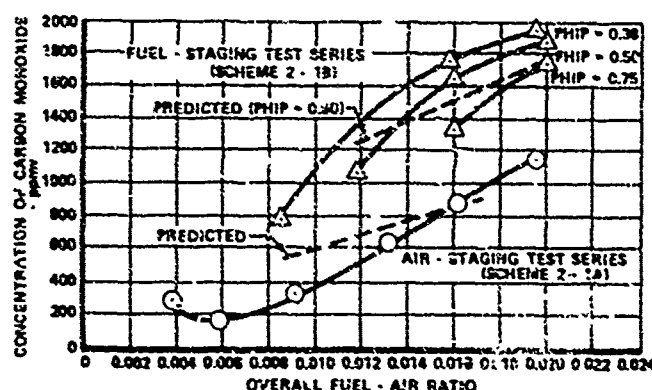


Figure 11. Variation in UHC Concentration with Fuel-Air Ratio

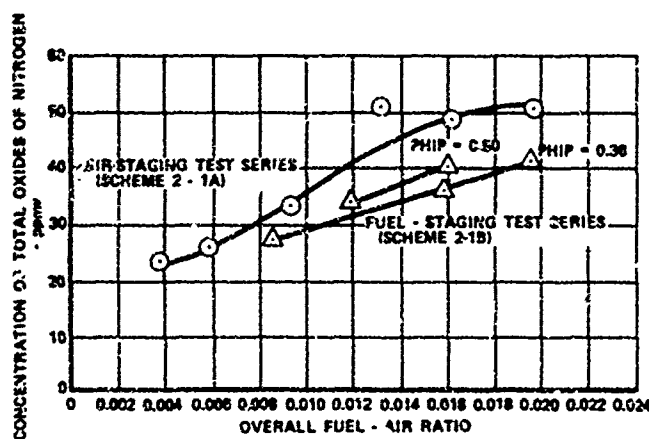


Figure 12. Variation in NO_x Concentration with Fuel-Air Ratio

Examination of the predicted carbon monoxide and unburned hydrocarbon concentrations within the combustor indicates that these emissions result from premature quenching of the respective chemical reaction mechanisms as streamtube temperature is reduced by air addition. Carbon monoxide level is controlled by the kinetic conversion to carbon dioxide, while the total unburned hydrocarbon level reflects both raw fuel which has failed to ignite and intermediate hydrocarbons for which oxidation has been halted. Examination of the detailed predictions indicates that carbon monoxide conversion is quenched at a higher temperature than the hydrocarbon oxidation reactions. Thus continued hydrocarbon reaction produces carbon monoxide below the temperature at which conversion to carbon dioxide can occur. With respect to the combustor internal flowfield, carbon monoxide is quenched in the downstream portions of the central streamtubes, following dilution air addition, and everywhere in the wall cooling streamtube. Quenched unburned hydrocarbons are principally confined to the outer wall cooling air streamtube.

The increase in exit plane carbon monoxide and particularly unburned hydrocarbon concentration with combustor wall fuel injection (fuel staging) is the result of severe quenching by dilution air addition downstream of the fuel injection site. Examination of the detailed model predictions indicates that for the particular configuration investigated, insufficient time has been provided for the rate limiting processes of fuel droplet vaporization and chemical reaction of the secondary fuel.

6. CONCLUSIONS

The streamtube combustor model developed in the present study has been shown to predict absolute levels of carbon monoxide and unburned hydrocarbon emissions and to predict trends with change in operating condition and configuration which are in reasonable agreement with the cited experimental data. In addition, the predicted concentrations of carbon monoxide and unburned hydrocarbons are sensitive to variations in combustor geometry, fuel injection characteristics and engine operating conditions, in direct relation to the corresponding variations in aerodynamic parameter and fuel-air mixture distributions within the combustor. For these reasons, it is concluded that the present modeling approach provides a useful means of identifying significant features which influence the levels of these emissions from gas turbine combustors and for assessing the emissions characteristics of proposed combustor configurations.

7. REFERENCES

1. Roberts, R., L. D. Aceto, R. Kollback, D. P. Teixeira, and J. M. Bonnell, "An Analytical Model for Nitric Oxide Formation in a Gas Turbine Combustor," *AIAA Journal*, Vol. 10, No. 6, 1972, pp. 820-826.
2. Clarke, J. S., "The Relation of Specific Heat Release to Pressure Drop in Aero-Gas-Turbine Combustion Chambers," *Proceedings of the 1955 IME-ASME Conference on Combustion*, 1955, pp. 354-361.
3. Winterfeld, G., "On Processes of Turbulent Exchange Behind Flameholders," *10th Symposium (International) on Combustion*, The Combustion Inst., 1965, pp. 1265-1275.
4. Alpineri, L. J., "Turbulent Mixing of Coaxial Jets," *AIAA Journal*, Vol. 2, No. 9, 1964, pp. 1560-1567.
5. "Computer Program for the Analysis of Annular Combustors, Volume I: Computational Procedures," Rept. 1111-1, 1968, Northern Research and Engineering Corp., Cambridge, Mass.
6. Abramovich, G. N., "The Theory of Turbulent Jets," MIT Press, Cambridge, Mass., 1963, Chapter 12, Section 4.
7. Wise, H., J. Lorell, and B. J. Wood, "The Effects of Chemical and Physical Parameters on the Burning Rate of a Liquid Droplet," *Fifth Symposium (International) on Combustion*, The Combustion Inst., 1955, pp. 132-141.
8. Wood, B. J., W. A. Rosser, and H. Wise, "Combustion of Fuel Droplets," *AIAA Journal*, Vol. 1, No. 5, 1963, pp. 1076-1081.
9. Williams, F. A., *Combustion Theory*, Addison-Wesley, Reading, Mass., 1965, pp. 56-57.
10. Dickerson, R. A., and M. D. Schuman, "Rate of Aerodynamic Atomization of Droplets," *Journal of Spacecraft*, Vol. 2, 1965, pp. 99-100.
11. Edelman, R. B., and O. F. Fortune, "A Quasi-Global Chemical Kinetic Model for the Finite Rate Combustion of Hydrocarbon Fuels with Application to Turbulent Burning and Mixing in Hypersonic Engines and Nozzles," *AIAA Paper 69-86*, New York, 1969.

12. Browne, W. G., R. P. Porter, J. D. Verlin, and A. H. Clark, "A Study of Acetylene-Oxygen Flames," Twelfth Symposium (International) on Combustion, The Combustion Inst., 1969, pp. 1035-1047.
13. Cooke, D. F., and A. Williams, "Shock-Tube Studies of the Ignition and Combustion of Ethane and Slightly Rich Methane Mixtures with Oxygen," Thirteenth Symposium (International) on Combustion, The Combustion Inst., 1971, pp. 757-766.
14. Sorensen, S. C., P. S. Myers, and O. A. Uyehara, "Ethane Kinetics in Spark-Ignition Engine Exhaust Gases," Thirteenth Symposium (International) on Combustion, The Combustion Inst., 1971, pp. 451-459.
15. Baker, R. R., R. R. Bahr, and R. W. Walker, "The Use of the $H_2 + O_2$ Reaction in Determining the Velocity Constants of Elementary Reactions in Hydrocarbon Oxidation," Thirteenth Symposium (International) on Combustion, The Combustion Inst., 1971, pp. 291-299.
16. Benson, S. W., and G. R. Haugen, "Mechanism for Some High-Temperature Gas-Phase Reactions of Ethylene, Acetylene, and Butadiene," J. Phys. Chem., Vol. 71, 1967, pp. 1735-1746.
17. Camac, M., and R. M. Feinberg, "Formation of NO in Shock-Heated Air," Eleventh Symposium (International) on Combustion, The Combustion Inst., 1966, pp. 137-145.
18. Baulch, D. L., D. D. Drysdale, D. G. Horne, and A. C. Lloyd, "Critical Evaluation of Rate Data for Homogeneous, Gas Phase Reactions of Interest in High-Temperature Systems," No. 1-4, 1968-1969, Dept. of Physical Chemistry, Leeds Univ., England.
19. Franklin, J. L., "Mechanisms and Kinetics of Hydrocarbon Combustion," Annual Review of Physical Chemistry, edited by H. Eyring, C. J. Christensen and H. S. Johnston, Annual Reviews, Inc., Palo Alto, Calif., 1967, pp. 261-282.
20. Drysdale, D. D., and A. C. Lloyd, "Gas Phase Reactions of the OH Radical," Oxidation and Combustion Revs., Vol. 4, 1970, pp. 157-250.
21. Brinkley, S. R., "Computational Methods in Combustion Calculations," Combustion Processes, Sec. C; High Speed Aerodynamics and Jet Propulsion, Vol. 2, edited by B. Lewis, R. N. Pease, and H. S. Taylor, Princeton University Press, Princeton, N. J., 1956.
22. Brinkley, S. R., "Calculation of the Thermodynamic Properties of Multicomponent Systems and Evaluation of Propellant Performance Parameters," Proceedings of the First Conference on Kinetics, Equilibrium and Performance of High Temperature Systems, edited by G. S. Bahn and E. E. Zukoski, The Combustion Inst., 1960, pp. 74-81.

Discussion on Paper 25

"Development and Verification of an Analytical Model for Predicting Emissions
from Gas Turbine Engine Combustors during Low Power Operation"
presented by S.A. Mosier

A.M. Mellor:

- (1) Are the HC results presented as ppmC?
- (2) As in your earlier model (your Ref. 1) do you assume that as the fuel evaporates it mixes infinitely fast across its stream tube?
- (3) Have you studied the sensitivity of your results to the number of streamlines of type 2 or 3 which you include in the analysis?

S.A. Mosier:

- (1) The UHC results are presented as ppmv of equivalent CH_4 , which is equivalent to ppmv of C atoms.
- (2) Yes, the fuel is assumed to mix infinitely fast with surrounding streamtube air following evaporation. However the fuel and air mixture thus formed is limited to stoichiometric preparations. Excess vaporized fuel or excess streamtube air is withheld from the reaction mixture. The effect of fuel-air mixture preparation rate on the chemical combustion rate is approximated in this manner.
- (3) No.

R.E. Sampson: You have shown the model agrees with experimental data. Would you comment as to how accurately you feel the results represent the effectiveness of these control techniques and how the experimental combustors compare to the same combustor configuration with no emission controls?

S.A. Mosier: The emissions results presented for the non-fuel staging experiment are considered representative of conventional liquid fuel injection annular combustors when run at the indicated inlet values of pressure, temperature and fuel-air ratio. The fuel-staging results presented here should not be considered representative of the potential of fuel staging as an emission control technique. The test reported here is simply one of a number of such tests run, and does not represent an attempt to optimize the configuration for minimum emissions. The present test sequence was run for the primary purpose of verifying the analytical model.

AN EXPERIMENTAL RESEARCH ON THE BEHAVIOR OF A CONTINUOUS FLOW COMBUSTION CHAMBER

by

C. CASCI, A. COGHE, U. GHEZZI, S. PASINI
Istituto di Macchine, Politecnico di Milano
P. za Leonardo da Vinci, 32
20133 Milano, Italy

SUMMARY

Related to combustion phenomena area, a continuous flow test bench was developed, to study gas turbine combustion. The feeding system could provide a wide range of air-fuel ratio and working pressure to investigate different test conditions. The combustion chamber was arranged to sample the gas composition in different positions, and obviously to measure other magnitudes such as pressure, air and fuel mass flow rate, etc. The species analyzed were carbon monoxide, unburned hydrocarbons, and nitrogen oxides.

The primary concern was the evolution of the above species along the can-type liner and the determination of the most opportune working conditions. The typical design features (dimensions, flow rate, etc) of the combustion chamber described in this paper, allow to translate reasonably the results obtained to real systems, but the kinetic and fluidodynamic phenomena concerned with combustion process make quite arduous the extrapolation of the results to conditions very far from the ones experimented in this research.

1. INTRODUCTION

In the Laboratories of Istituto di Macchine of Politecnico di Milano, an analysis program has been planned in the research of some typical features of gas turbine combustion chambers. Basically, the primary concern of the research is a contribution to the knowledge of emission mechanisms of such combustion systems.

In this area, theoretical and experimental works have already been presented by numerous authors; it seems however necessary to insist on the experimental aspect of the problem, also to better support the theoretical study. Particularly, sophisticated techniques are needed to allow multipoint measurements of the parameters interested, being not enough the study of the exhaust conditions alone. In fact, only the information made available by such techniques will give the possibility to investigate the mechanism of the processes which take place inside the burner, thus deducing meaningful design criteria.

The whole research program foresees the employment of a series of combustion chambers of different architecture and parallelly includes also a series of different fuel injection systems (the research will naturally be completed by testing in several working conditions).

In this paper are presented the results obtained by employing only one kind of liner (the first and simplest of the above mentioned series). Therefore, no optimization process endeavored, at least from the point of view of the best liner architecture.

2. TEST FACILITIES AND PROCEDURES

The test facilities installed to serve the research purpose are here briefly described; for a more detailed description, information are available from Ref (1). In Fig (1) the air and fuel feeding systems are schematically represented; the eventual back pressure is generated by a butterfly valve placed at the exhaust pipe end and led by an electrical engine.

The plant has been designed to achieve a maximum air mass flow rate equal to 15.000 kg/h and a maximum air pressure, in the test chamber, equal to 10 kg/cm² absolute. The maximum values of air pressure and air mass flow rate were never reached during this test series.

The longitudinal section of the combustion chamber and the development of the can-type liner are shown in detail in Fig (2). The test section has been arranged to accomplish six contemporary samplings, four of which inside the liner (see Fig (3) and (4) and the other two immediately after the chamber exit section. Each probe could move in the radial direction, to sample at different distances from the liner center line, and bore coaxially and internally a thermocouple, placed in opportune way (see Ref (2)) to allow temperature measurements in the sampling zone (see Fig (5)).

The sampling procedures were discontinuous (except nitrogen oxides); therefore, finite volume samples (around few liters) were analyzed. Anyway, particular attention was given to sampling, controlled directly by the plant operator by means of a solenoid valve

system. The sampling operation as therefore conducted under the most opportune conditions, thus avoiding also possible contaminations, especially during the transitories (see Ref (1)).

3. ANALYSIS OF RESULTS

Tests were held by varying air-fuel ratio and chamber pressure. The maximum pressure was not particularly elevated (3 kg/cm^2 absolute) for this test series; however, a sensible difference was observed among the results when the pressure increased from the atmospheric to the higher values. The air-fuel ratio AFR was generally varied by keeping constant the fuel mass flow rate (22 kg/h ; injection pressure: 18 kg/cm^2) and changing therefore the air mass flow rate. However, to extend the investigation of the burner working mechanism, other tests were held with a higher fuel mass flow rate (29 kg/h ; injection pressure: 34 kg/cm^2). In all tests, the inlet air temperature was kept between 275 and 295°K .

For all the six stations ("A" through "F") chosen for the test section (see Fig (6)), each test condition was characterized by gas samples taken at the radial positions "1" and "3" and by temperature measurements obtained at all the radial positions "1", "2", "3", and "4". The behavior of CO , CO_2 , HC (referred to hexane), NO , and NO_x was then analyzed.

Only the most meaningful data among all the results obtained are reported in this paper, allowing a better idea of the behavior of the combustion chamber for different working conditions. Particularly, results referring to $\text{AFR} = 70$ and $\text{AFR} = 100$ are reported in this work.

4. TEMPERATURE DISTRIBUTION INSIDE THE LINER

The examination of temperature distribution inside the liner is particularly important because reaction kinetics are strictly related to local temperature level; the temperature knowledge can therefore explain some typical pollutant emissions. In Fig (7) through (12), temperature maps inside the liner are shown, corresponding to two values of AFR and three values of combustion chamber pressure.

As a typical behavior, in the primary zone, close to liner center line, a relatively cold region can be observed; this region gets larger for higher AFR and lower pressure values. Moving radially outward from the liner center line, the temperature becomes before higher, to fall down again when close to the liner wall. The highest temperature region extends along the liner axis and its area is larger as higher the pressure and lower the air-fuel ratio.

It can therefore be pointed out, as intuitive, that the temperature level decreases with the increasing AFR and increases with the increasing pressure. For this combustion chamber, the high temperature zone extends very much forwardly, mainly for the highest pressure values; the extension of the high temperature zone, along the liner center line, could easily be limited by increasing the secondary air jet penetration. As a consequence, also a better temperature profile would be achieved at the exit section "F".

5. CARBON MONOXIDE

CO concentration data were observed to vary from a maximum of few per cent (highest value, in the primary zone: 5%) to a minimum which was, for the most favourable cases, around 0.02% (percentage in volume, dry basis). Concentration data show therefore that CO reduction (from the point of maximum to the exit section "F") should be attributed only in a small part to dilution, being on the contrary originated mostly by oxidation reactions controlled by opportune reactants concentrations and temperature level.

In Fig (13) through (15), as an example, the behavior of carbon monoxide is shown versus the probe positions, for samples taken on the liner center line (corresponding to radial position "1") and close to its wall (corresponding to radial position "3") and for $\text{AFR} = 70$ and 100 , and pressure = 1 , 2 and 3 kg/cm^2 absolute.

For both central and peripheral samples, CO reaches maximum concentration around station "B"; then the concentration reduces quite sharply up to station "I" for the peripheral samples and (generally) up to exit station "F" for the central ones. This phenomenon should probably be related to the higher temperature level of the central zone. With other parameters at identical values, it may then be noted that in the primary zone too the lower values of CO correspond to the higher values of AFR.

It seems reasonable the hypothesis the above CO behavior should be due to a larger oxygen availability; however, it must be kept in mind (as it will be seen later on) that if only the emissions at exit section "F" are considered and then referred to the AFR stoichiometric value (taking into account in such a way the dilution effect), the CO behavior becomes less simple and, mainly at higher pressures, an increasing in CO concentration with the increasing AFR may be noted (see also Fig (22)).

Keeping constant the values of the other parameters, an increasing of thermal level (and therefore of combustion efficiency) created by an increasing of pressure, results in a better situation from the point of view of CO emissions. For identical AFR values and by increasing the fuel mass flow rate (29 kg/h), curves of CO concentration versus probe positions were noted to behave like the other ones above illustrated, yet being observed in most cases quite an increasing of CO emissions in the exhausts.

Carbon monoxide measurements were by gas chromatography.

6. UNBURNED HYDROCARBONS

Generally, the behavior of unburned hydrocarbons (whose measurements, referred to hexane, were by gas chromatography) shows analogy with that of carbon monoxide. The maximum concentration (about 10,000 ppm) was reached around station "B"; then a decay took place (naturally due also here only in a small part to dilution) and at the exit station "F" a concentration was found around few tens of ppm. Fig (16) through (18) show the behavior of unburned hydrocarbons for central (corresponding to radial position "1") and peripheral (corresponding to radial position "3") samples and for AFR = 70 and 100, and inlet air pressure = 1, 2 and 3 kg/cm² absolute.

The unburned hydrocarbons concentration at the exit station "F" points out that moving outward, from the liner central line to its wall, large changes are not found, if the particular case at atmospheric pressure is excluded. Anyway, like carbon monoxide, the behavior at atmospheric pressure should be considered anomalous by comparison to those at higher pressure values (see at this purpose Fig (22) and (23)). Again like carbon monoxide, unburned hydrocarbons too showed a reduction of the emissions when the pressure increased, causing a higher thermal level.

The HC behavior becomes more complicated because of the main role played by fuel injection and atomization system. Anyway, test runs with higher fuel mass flow rate (29 kg/h) did not show any relevant change of HC concentration.

7. NITROGEN OXIDES

The process of NO creation is regulated mainly by the temperature (which must be particularly high) and by oxygen availability. From this point of view and keeping in mind the temperature maps shown in Fig (7) through (12), the NO behavior, for the combustion chamber under test, becomes quite easy to understand. Fig (19) through (21), as already done, show NO concentration versus probe position, for AFR = 70 and 100, and for inlet air pressure = 1, 2 and 3 kg/cm² absolute.

For the cases considered, a reduction of AFR gives higher NO emissions, for both central (corresponding to radial position "1") and peripheral (corresponding to radial position "3") samples; similarly, an increase of pressure generates an increase of NO emissions. With no doubt, the above effects are due to higher thermal levels related to both AFR reduction and higher pressure values.

Along the combustion chamber, NO concentration and temperature were found to behave almost in the same way; at this point, as an example, NO behavior (for the radial positions "1" and "3" at each station "A" through "F" and for AFR = 70) and temperature map at the same conditions could be compared to demonstrate the above statements.

NO sampling data emphasize here again that the dilution alone cannot explain completely the decay of concentration. Therefore, the hypothesis may be advanced, under certain conditions in the combustion chamber, reactions exist which bring to NO destruction. While sampling, also NO_x were measured; usually, they were found to be just a little higher than the corresponding NO.

At this point, it must be noted that the sampling probe was directly connected to the data acquisition system, and therefore sampling and measuring were almost contemporaneous. NO and NO_x were by chemiluminescence.

8. CONCLUSIVE CONSIDERATIONS

The study of a can-type combustion chamber, like that employed in this work, involves phenomena of kinetic and fluidodynamic nature, playing a role of primary importance for the determination of temperature level and local composition. This two aspects of the problem, considered together, make quite arduous the extrapolation of the results for conditions very different from those experimented in this research, mainly if the changed working conditions are joined by different combustion chamber architectures. However, the whole results achieved by a systematic study can with no doubt clarify the working mechanism of the system under examination, thus suggesting modifications to improve its performance.

In the present work, the emissions of some polluting substances (CO, HC, NO) were taken into consideration and tried to be correlated with the combustor behavior in different working conditions. The mechanisms which can favor the formation of polluting substances are well understood; if these emissions are to be reduced, inside the combustion

chamber opportune conditions should be established. As long as NO is concerned, it is well known its formation being conditioned by particularly high temperature levels, together with a certain oxygen availability for nitrogen oxidation; the destruction of CO and HC is on the other hand favored by quite high thermal levels and by keeping in the primary zone an AFR very close to the stoichiometric value (mixture just a little lean). Also the typical injection system features should not be neglected, being clear that better fuel atomization and distribution improve combustion efficiency, reducing therefore some pollutant emissions.

What above stated can be compared with the graphs shown in Fig (22) through (24); here, measured at the exhaust section "F", respectively the behavior of CO, HC, and NO are plotted versus AFR, for different pressures. The emissions are then referred to stoichiometric conditions, to consider dilution effects. The results can be very well correlated to the temperature maps before mentioned.

As far as CO and HC are concerned, an increase in pressure brings (generally) to reduced emissions or increased thermal levels. On the other hand, for all the cases considered, NO emissions are monotone versus pressure and AFR. A pressure increasing results in higher NO emissions (see at this purpose the temperature maps), while an AFR increasing causes a reduction of NO emissions. It seems therefore quite evident NO formation being controlled mainly by temperature levels, which, with no doubt, are correlated to the mixture formed in the primary zone.

The considerations before developed bring to the conclusion that generally those parameters which are favorable to NO reduction are on the other hand in contrast with CO and HC reduction. It becomes therefore necessary to respect an opportune compromise if a design of a new kind of combustion chamber wants to be avoided.

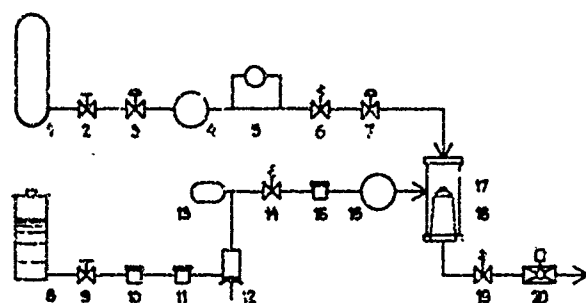
9. REFERENCES

1. S. Pasini, et alii Un impianto per lo studio sperimentale della combustione a flusso continuo - Internal Report of C.N.R. (National Research Council), 1972.
2. A. Coghe, et alii Taratura di un sistema di misura della temperatura in un combustore a flusso continuo - Internal Report of C.N.R. (National Research Council), 1972.
3. E.E. Starkman, et alii The Role of Chemistry in Gas Turbine Emissions - A.S.M.E. Paper 70-GT-81, 1970.
4. D.C. Hammond, A.M. Mellor Analytical Calculations for the Performance and Pollutant Emissions of Gas Turbine Combustors - Comb. Sci. Tech. 4, 101-112, 1971.
5. A.M. Mellor, et alii Emissions from and within an Allison J-33 Combustor - Comb. Sci. Tech. 6, 169-176, 1972.
6. F.F. Sawyer, et alii Air Pollution Characteristics of Gas Turbine Engines - Journal of Engineering for Power, Trans. A.S.M.E., Series A, Vol. 91, No 4, Oct 1969, pp 290-296.
7. A. Liberman Composition of Exhaust from a Regenerative Turbine System - Journal of the Air Pollution Control Association - Vol. 18, 1968, pp 149-153.
8. E.R. Lozano, et alii Air Pollution Emissions from Jet Engines - Journal of the Air Pollution Control Association, Vol. 18, 1968, pp 392-394.
9. D.S. Smith, et alii Oxides of Nitrogen from Gas Turbines - Journal of the Air Pollution Control Association, Vol. 18, 1968, pp 30-35.
10. W. Cornelius, W.R. Wade The formation and Control of Nitric Oxide in a Regenerative Gas Turbine Burner - S.A.E. Paper 700708, Sept 1970.
11. L.T. Pratt, et alii Prediction of Nitric Oxide Formation in Turbojet Engines by PSK Analysis - A.I.A.A. Paper No 71-713, June 1971.

12. J.B. Heywood Gas Turbine Combustor Modeling for Calculating Nitric Oxides Emissions - A.I.A.A. Paper No 71-712, June 1971.
13. D.C. Hammond, A Preliminary Investigation of Gas Turbine Combustor Modeling - Comb. Sci. Techn. 2, pp 67-80, 1970.
A.M. Wallor
14. R.P. Sawyer Atmospheric Pollution by Aircraft Engines and Fuels (A Survey) - AGARD-AR-40, 1972.
15. W. Cornelius, Emissions from Continuous Combustion Systems -
W.G. Agnew, Editors Plenum Press, 1972.

10. ACKNOWLEDGMENT

The authors wish to thank Mr. S. Benecchi, Mr. T. Ferrari, Mr. F. Gamma, Mr. A. Morelato, Mr. A. Mosca, and Mr. G. Zizak (C.N.P.M. Center) for helping in the experimental part of the work, and S.N.A.M. Progetti for the assistance in NO_x sampling.



- | | |
|---------------------------|---------------------------|
| 1 AIR PRESSURE TANK | 11 FINE STRAINER |
| 2 MANUAL VALVE | 12 PLUNGER-TYPE FUEL PUMP |
| 3 PRESSURE REDUCING VALVE | 13 HYDRAULIC COMPENSATOR |
| 4 AIR FLOW METER | 14 SAFETY VALVE |
| 5 AIR DENSITY METER | 15 COARSE STRAINER |
| 6 SAFETY VALVE | 16 FUEL FLOW METER |
| 7 AUXILIARY VALVE | 17 FUEL INJECTOR |
| 8 FUEL TANK | 18 COMBUSTION CHAMBER |
| 9 MANUAL VALVE | 19 SAFETY VALVE |
| 10 COARSE STRAINER | 20 BUTTERFLY VALVE |

FIG (1)

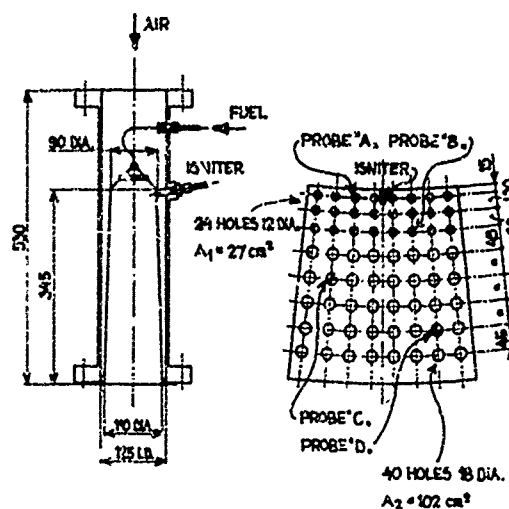


FIG (2)

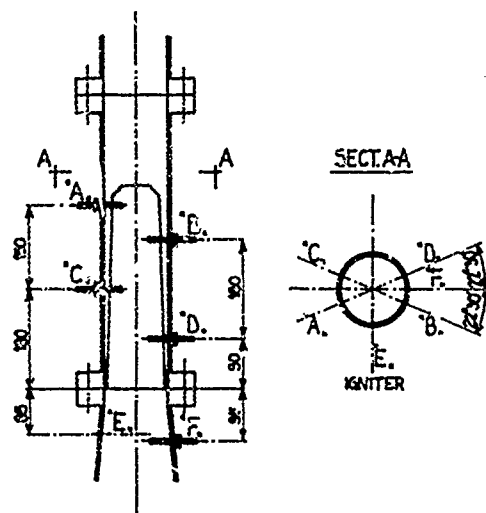


FIG (3)



FIG (4)

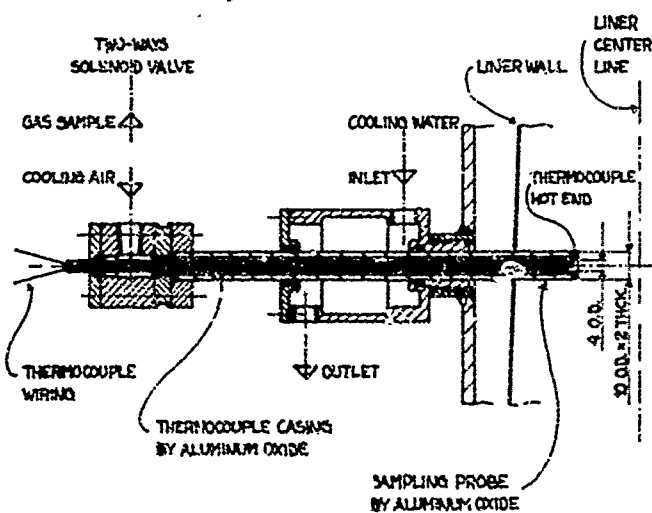


FIG (5)

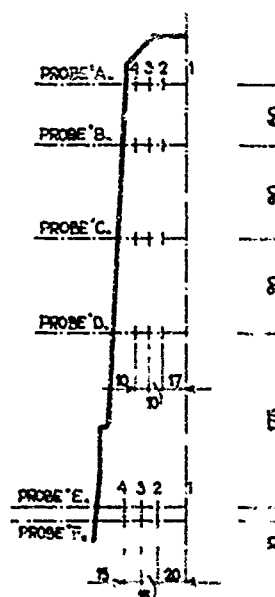
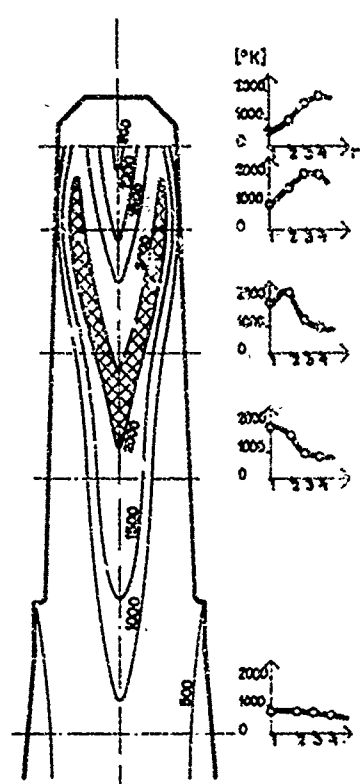
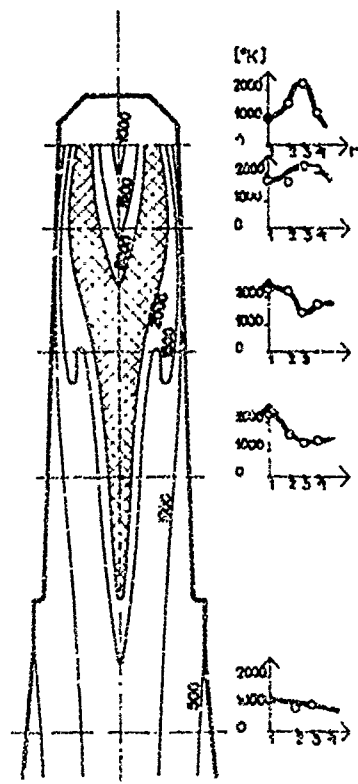


FIG (6)



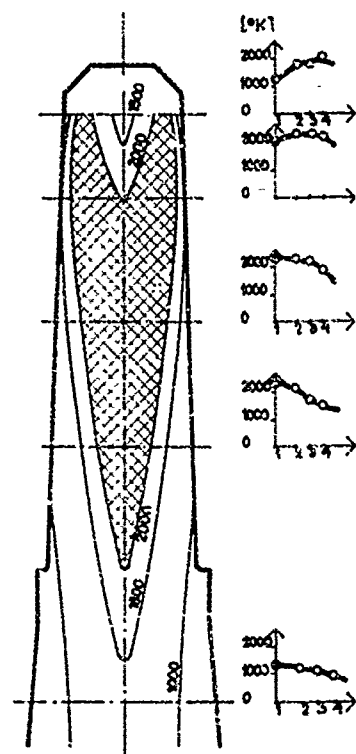
INLET AIR PRESSURE = 1 kg/cm^2
FUEL MASS FLOW RATE = 22 kg/h
AIR-FUEL RATIO = 70

FIG (7)



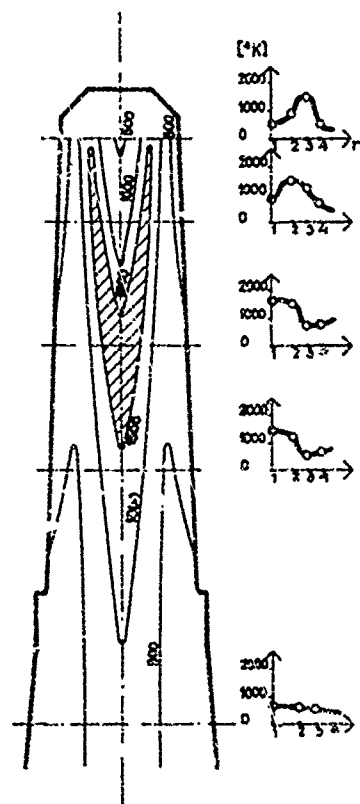
INLET AIR PRESSURE = 2 kg/cm^2
FUEL MASS FLOW RATE = 22 kg/h
AIR-FUEL RATIO = 70

FIG (8)



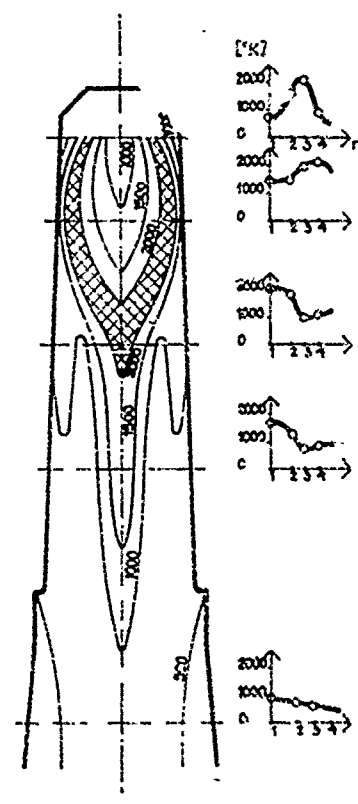
INLET AIR PRESSURE = 3 kg/cm^2
FUEL MASS FLOW RATE = 22 kg/h
AIR-FUEL RATIO = 70

FIG (9)



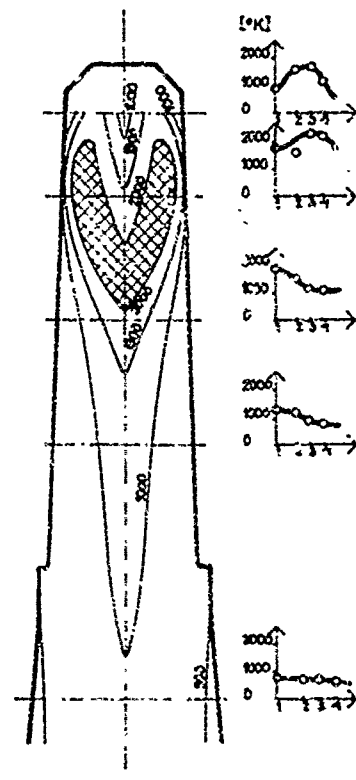
INLET AIR PRESSURE = 1 kg/cm^2
FUEL MASS FLOW RATE = 22 kg/h
AIR-FUEL RATIO = 100

FIG (10)



INLET AIR PRESSURE = 2 kg/cm^2
FUEL MASS FLOW RATE = 22 kg/h
AIR-FUEL RATIO = 100

FIG (11)



INLET AIR PRESSURE = 3 kg/cm^2
FUEL MASS FLOW RATE = 22 kg/h
AIR-FUEL RATIO = 100

FIG (12)

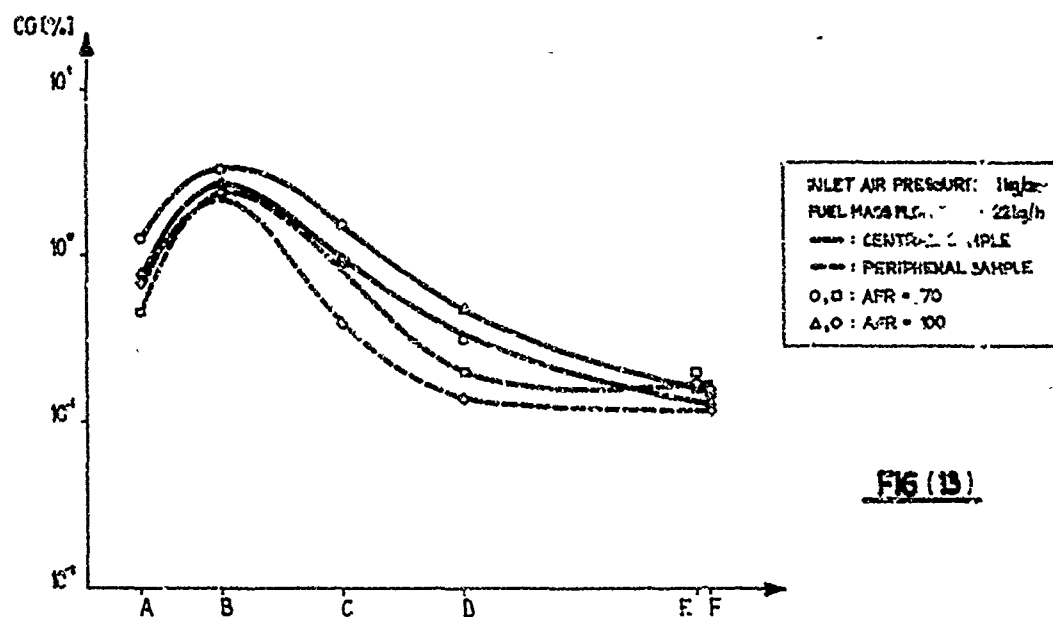


FIG (13)

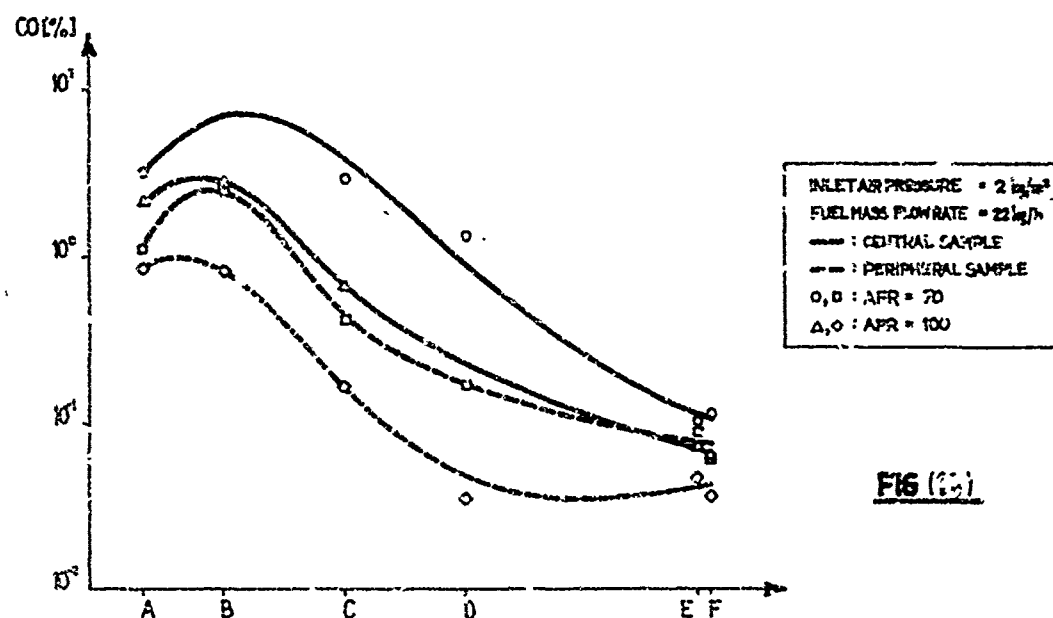


FIG (14)

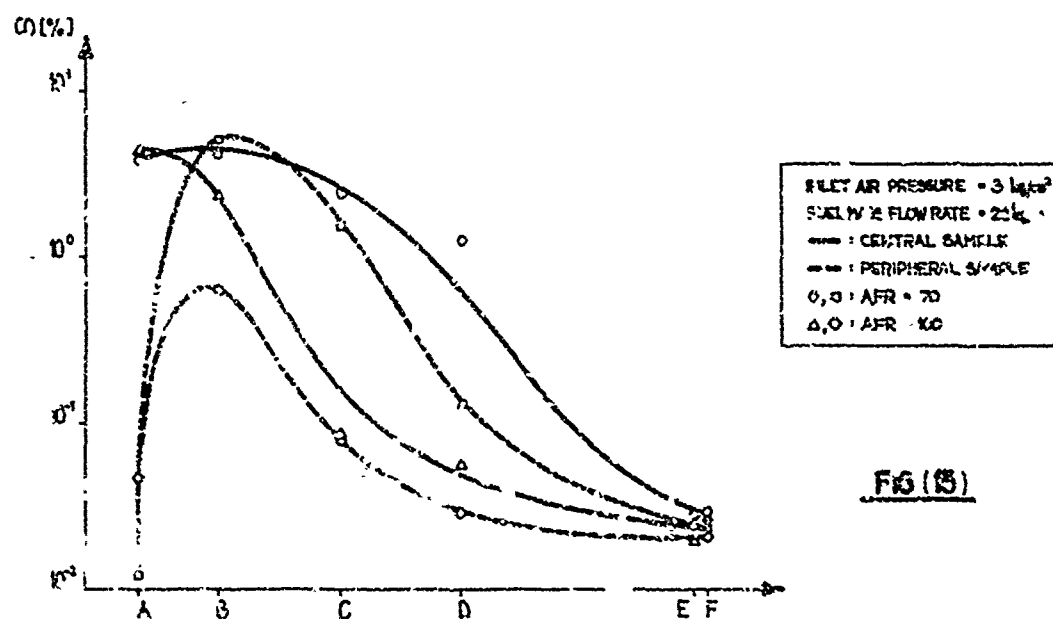


FIG (15)

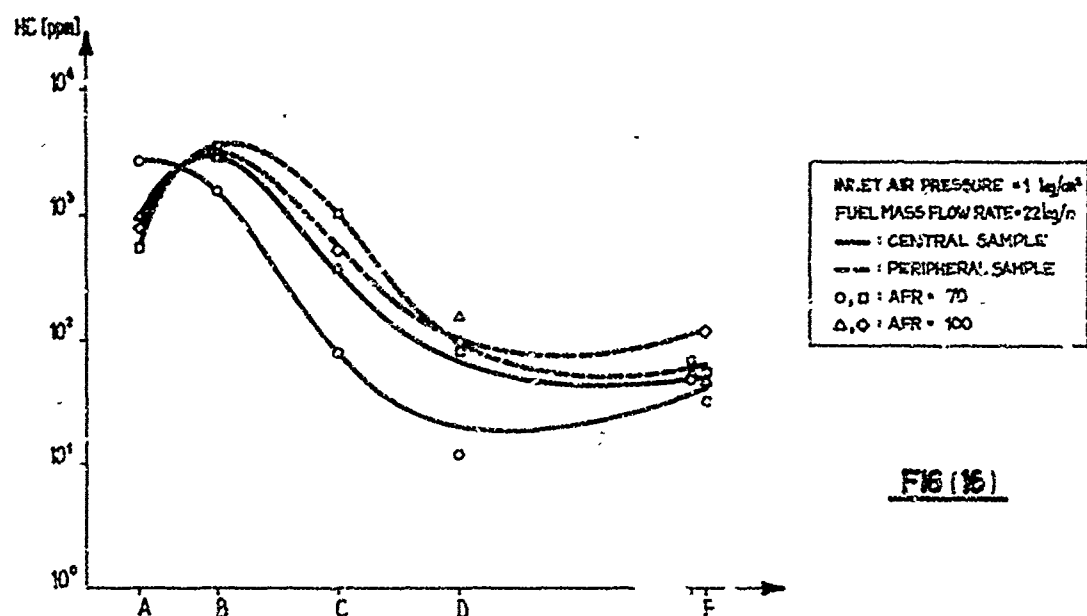


FIG (16)

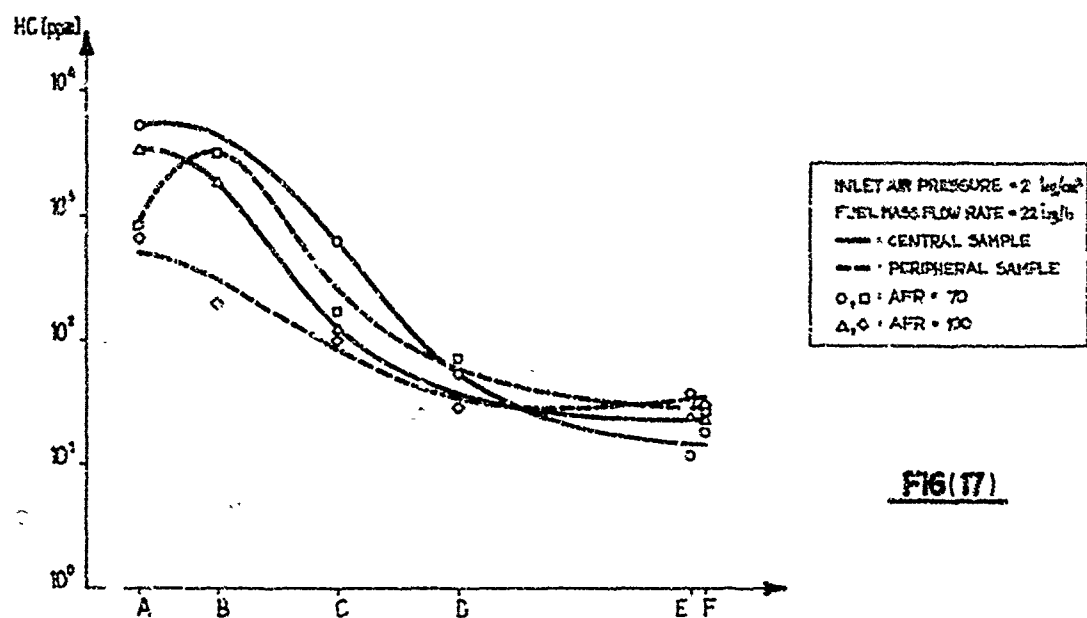


FIG (17)

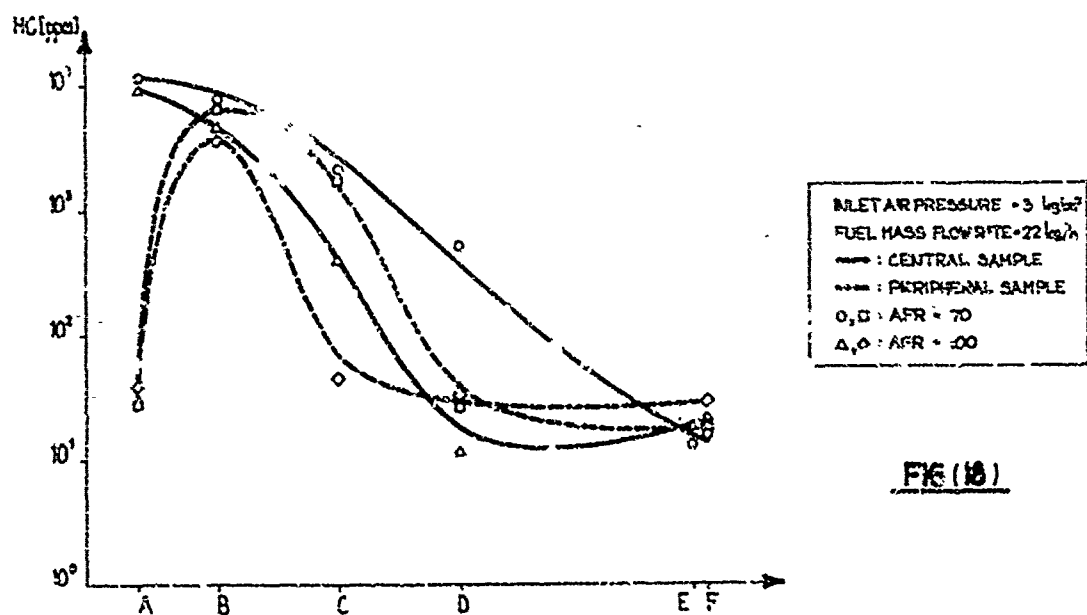
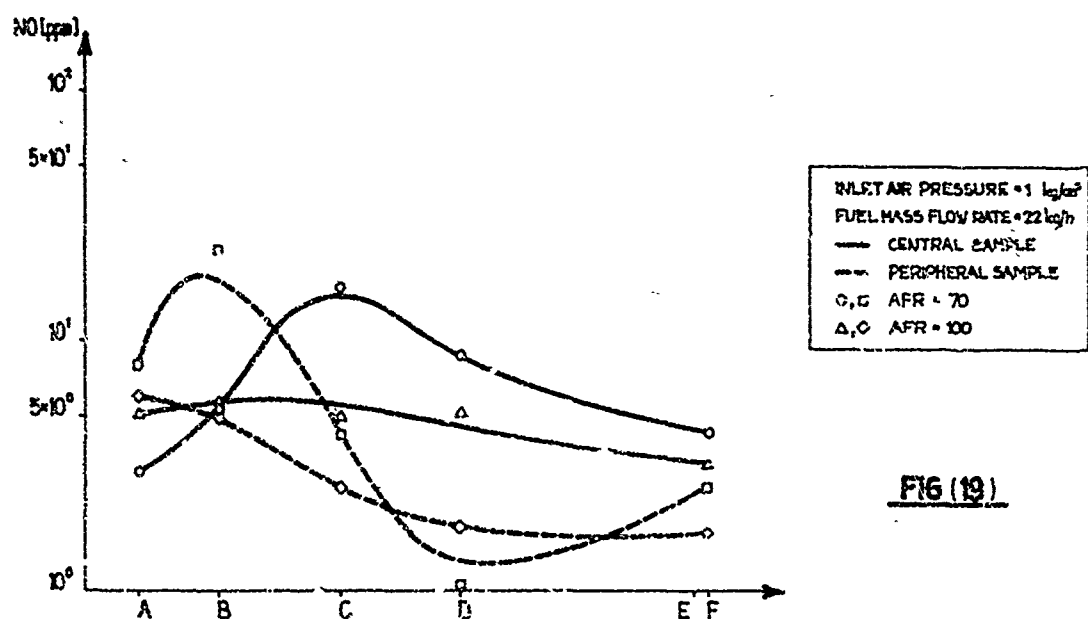
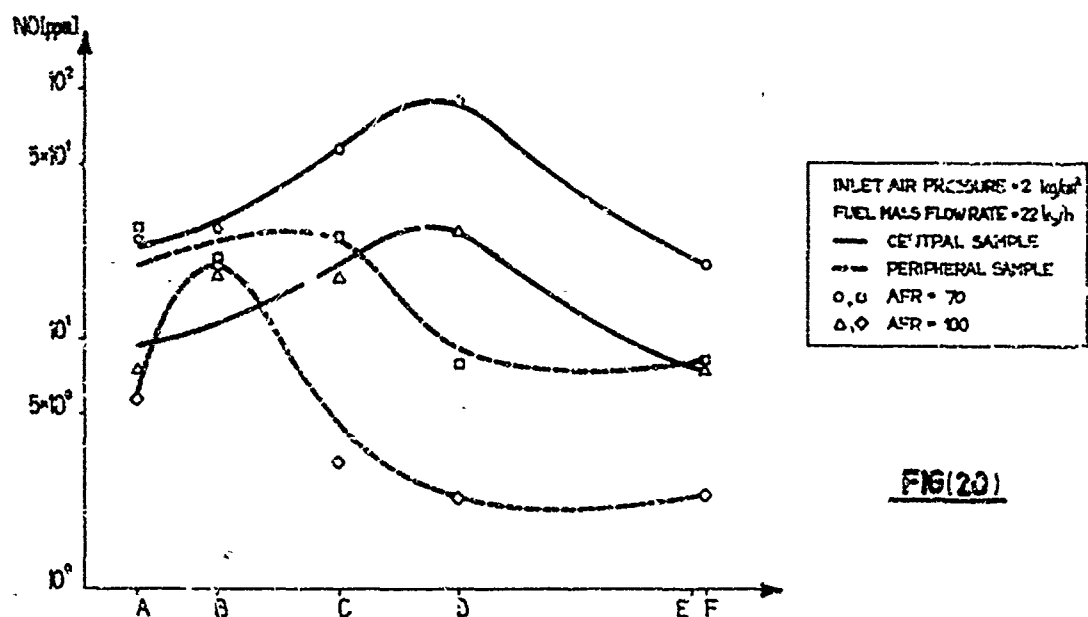


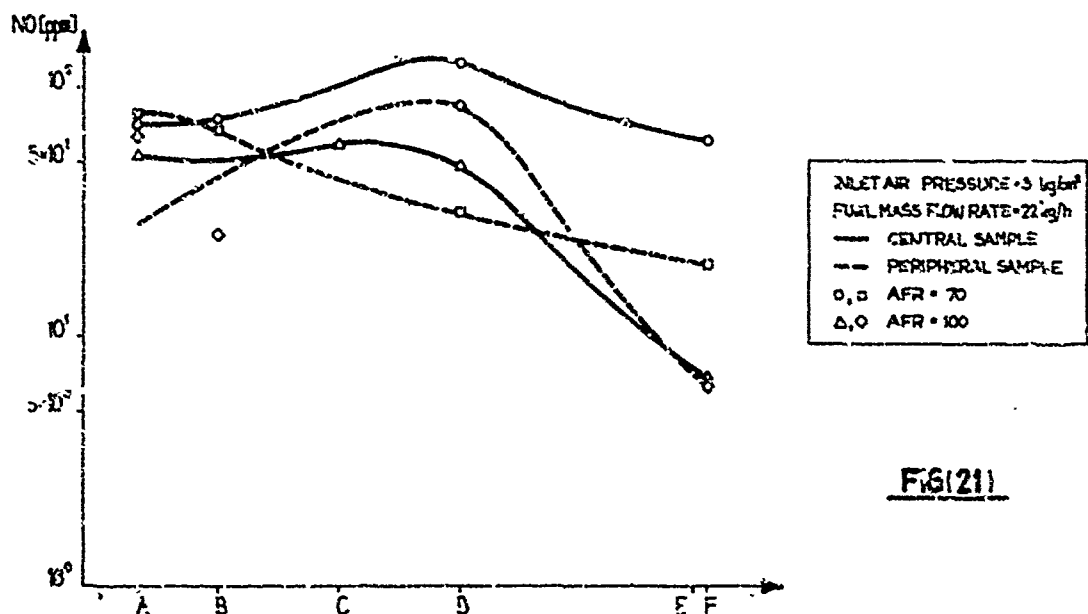
FIG (18)



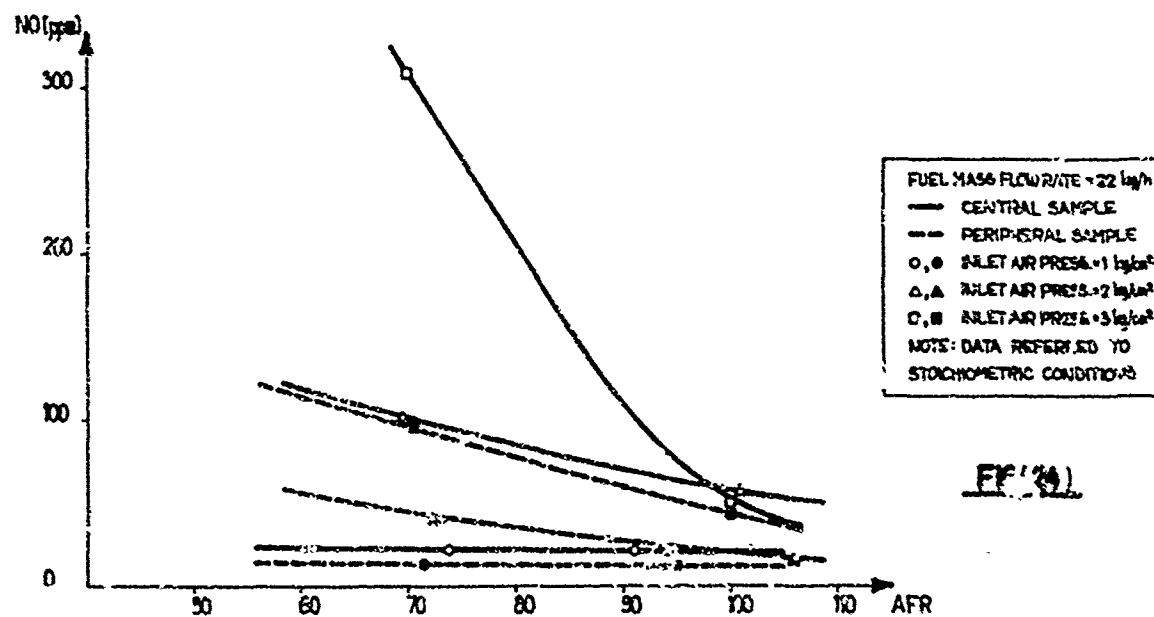
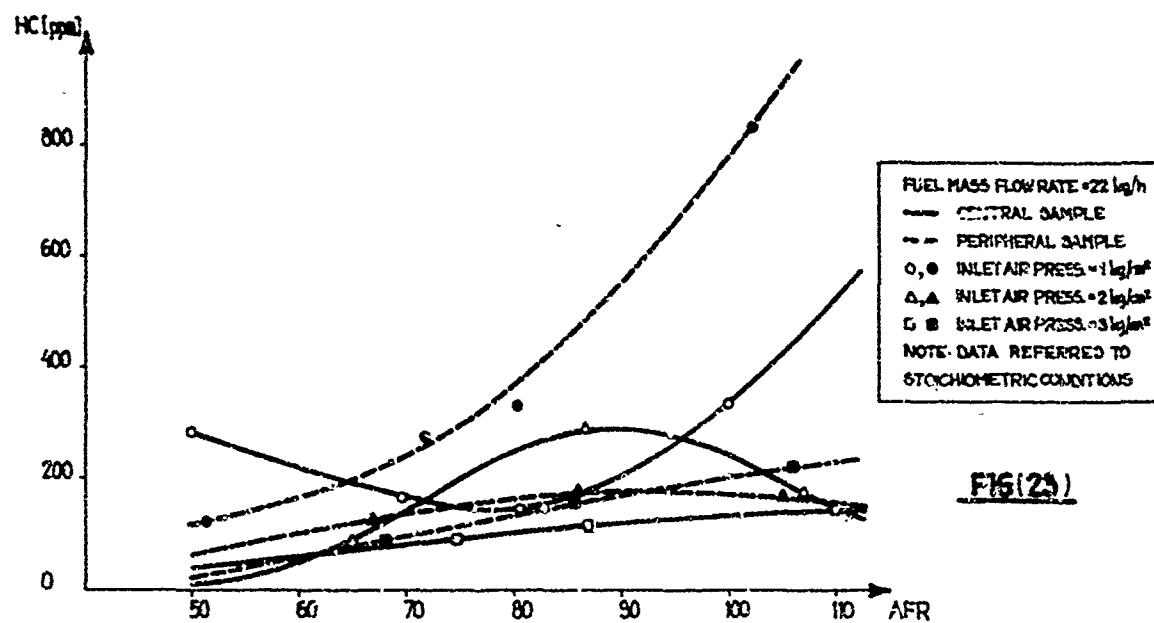
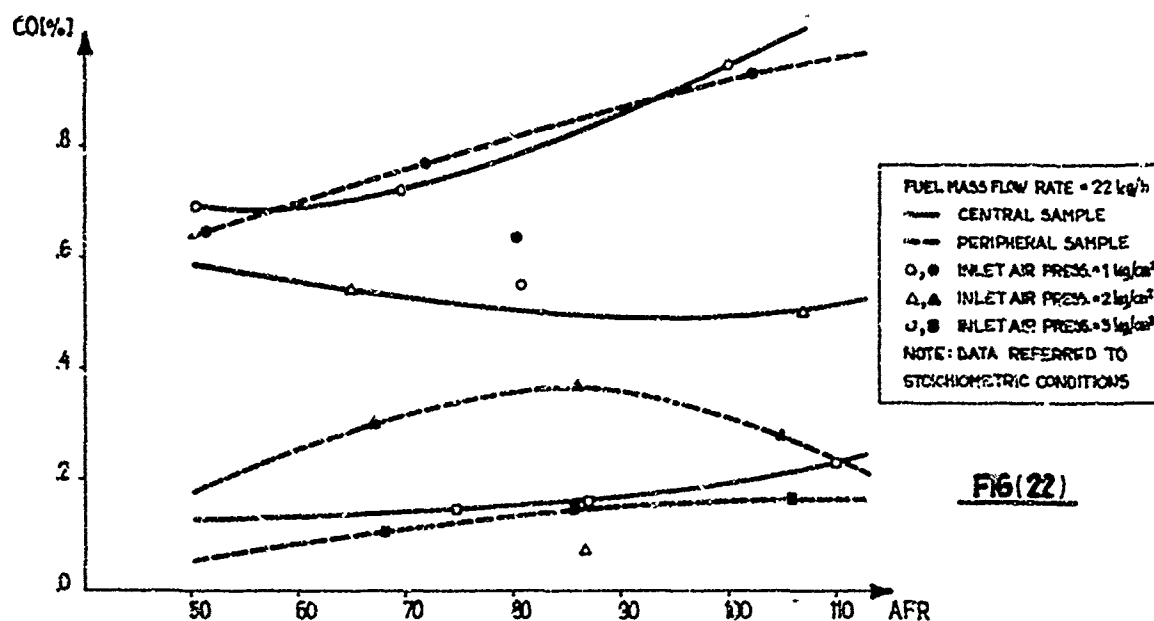
FIG(19)



FIG(20)



FIG(21)



SESSION IV - DESIGN

OPENING REMARKS

by Colonel W. Moe, USAF

So far this week we have largely concerned ourselves with two very important aspects of jet engine generated chemical pollution. They are:

1. the effects of such pollution, particularly at high altitudes and in the immediate vicinity of airports, and
2. the chemical reactions which are responsible for the unwanted products of combustion or, if you wish, a determination of the ultimate levels of these products.

Today we will turn our attention to the design of the combustor. Although the burner is the actual source of the aircraft chemical pollution problem, it also provides us with our principal means of control. Such control will not come easily, for the pollutants are formed in a complex process which involves aerodynamics, heat transfer, and reaction chemistry. Furthermore, any useful burner must conform to such practical constraints as performance, length, volume, weight, durability and cost. The result of all these considerations is that burner design is not a precise science, but an engineering art.

We are very fortunate today to have available for presentation papers written by experienced professionals who are willing to share their special knowledge with us. I am substituting today for Mr. Bill Heiser, Chief Scientist of the Air Force Aero Propulsion Laboratory, who was invited by NSARD to say a few words about the role of the United States Air Force in aircraft chemical pollution control. I was pleased to make some introductory comments because I have been impressed by the strong start that our Air Force has made in this area, and I would like you to know a bit about it. I wish to emphasize, however, that these are intended only as generalized comments in view of the fact that U.S. standards and Air Force policy with respect to those standards have not yet been established.

The Air Force is involved in the subject because:

1. All U.S. Federal Agencies have been charged by President Nixon to assume a cooperative role in all relevant aspects of environmental protection.
2. The U.S. Air Force has historically played an important role in the development of new military and commercial derivative engines, this being the most appropriate time in their life cycle to introduce major technological advances.
3. The applicability of the new laws to the military has yet to be determined. Since our military forces are the biggest single American consumer of aviation fuel, we are unlikely to be overlooked in the long term.
4. Finally, since U.S. Federal regulations will be applied in the near future, we are co-operating with the Environmental Protection Agency in discussions and actions relating to the setting of standards.

As a result of such reasoning, our programs and efforts have the objective of being an active and co-operative agency, pending the outcome of the present legislation and policy making. At this point I must re-emphasize that the process of policy making is only now going into action, and that there is as yet no official military position. To begin the definition of future Department of Defense posture, the Air Force Aero Propulsion Laboratory is recommending pollution control goals which are now under consideration at higher levels. These goals do not conflict with the intent of the proposed Environmental Protection Agency regulations. You will be hearing more about these suggested goals in the presentation to be given this afternoon by Mr. Henderson.

Let me briefly review some of the problems of pollution control that are peculiar to the military. To begin with, any control techniques that rob high performance military aircraft of their tactical margin will obviously be unacceptable and that must represent the military position for combat aircraft. For example, reduction of oxides of nitrogen via water injection will probably never be applied to fighter aircraft. Next, we find that there are some conflicts between the direction in which high performance engine technology is moving and that implied by the Environmental Protection Agency goals. The most notable here is the fact that burner temperatures will continue to increase through the foreseeable future. Since generation of oxides of nitrogen increases with temperature, the environmental targets will become increasingly difficult to reach. Another issue is that of exhaust trail visibility. The military criterion for a sufficiently invisible exhaust plume, which is not yet clearly defined, is likely to be more stringent than the environmentalists will require.

A further unique aspect of the military situation is that a standard landing and take-off cycle cannot reasonably be defined for military aircraft. This has caused us to seek goals that are based upon the technology required to meet the intent of the proposed environmental regulations.

Finally, there are features of the problem which are principally military. Here I can cite afterburner emissions as an outstanding example. Since early work indicates that the chemical reactions continue a considerable distance downstream of the nozzle exhaust plane, we are not even certain as to the magnitude of this problem. I doubt, however, that it is about to simply disappear. In response to all of this, the Air Force has spent the past year laying the foundations necessary for progress. We believe that our posture will allow us to respond to the challenges ahead. Among other actions:

1. We have worked closely with our Army and Navy to develop a coordinated program to reduce pollution.
2. We have participated extensively with our Environmental Protection Agency during its regulation development phase in order to provide technical assistance and to clearly understand their intentions and proposed standards.
3. We have initiated technology base programs, some in conjunction with our Department of Transportation and Federal Aviation Administration, for the measurement and control of pollution.
4. We have encouraged the engine industry to accelerate their own investments in this area.
5. We have encouraged coordination and information exchange through conferences and short educational courses intended to inform key personnel of the most recent developments.
6. We have determined that university support for related work should be greatly increased.
7. An office has been established which directly serves the Secretary of the Air Force and is concerned only with environmental quality.
8. The Air Force position is not completely firm, but it is fairly obvious that we will incorporate new technology to reduce pollution, which may not be acceptable in some cases involving combat aircraft. Non-superiority aircraft, such as military transports, will no doubt be considered quite differently.

This, however, is only the beginning. The stringent goals proposed for 1979 might well be surpassed by even more stringent goals for 1983, and so on. One can only conclude that better and better practical jet engine chemical pollution control techniques will have to be found. Obviously, without strong support from the entire technological community, none of our goals can be met. In the long term, then, our future really rests in your hands. In the near term, on the other hand, we are in the hands of that small band of brave men known as designers. And that brings us back to the purpose of today's meeting.

MODÉLISATION DES FOYERS DE TURBORÉACTEUR EN VUE DE L'ÉTUDE DE LA POLLUTION

par

Marcel BARRÈRE

Directeur Scientifique

OFFICE NATIONAL D'ÉTUDES ET DE RECHERCHES AÉROSPATIALES (O.N.E.R.A.)

29, avenue de la Division Lefevre - 92320 CHÂTILLON

France

RÉSUMÉ

Après un examen des différents modèles actuellement proposés pour calculer l'évolution des espèces polluantes dans un foyer de turboréacteur, une étude critique de ces modèles est faite en vue de leur amélioration afin de pouvoir :

- prédire le taux d'espèces polluantes des foyers pour diverses conditions de fonctionnement,
- dégager les principaux paramètres qui agissent sur ce taux de polluants,
- concevoir de nouveaux foyers optimisés pour avoir une production minimale de polluants tout en conservant les mêmes performances.

SUMMARY

MODELIZATION OF TURBOMACHINE COMBUSTORS FOR POLLUTION STUDIES

After a survey of the various models currently proposed to calculate the evolution of polluting species in a turbomachine combustor, a critical study of these models is presented with a view to improve them in order to :

- predict the polluting species generation rate of the combustor for various functioning conditions,
- bring out the main parameters acting on this polluting rate,
- design new optimized combustors generating a minimum of pollutants while retaining the same performance.

1. INTRODUCTION

Un foyer de turboréacteur moderne est caractérisé non seulement par l'efficacité de la combustion, les pertes de charge, les pressions limites de fonctionnement, l'uniformité de la température de fin de combustion mais encore par le pourcentage des produits polluants formés. Cette nouvelle contrainte a donné naissance à tout une activité scientifique qui comprend sur le plan théorique l'élaboration de modèles mathématiques permettant d'évaluer le taux de production des espèces polluantes comme les oxydes de l'azote et du soufre, l'oxyde de carbone, les hydrocarbures imbrûlés et les particules solides.

L'objectif de ces modèles est tout d'abord de prédire avec suffisamment de précision le taux de production des espèces polluantes du foyer principal et de la réchauffe. Les turboréacteurs actuellement utilisés ; il doit également permettre de dégager l'influence des principaux paramètres qui agissent sur ce taux de production ; ces modèles doivent enfin pouvoir guider l'ingénieur dans la conception de nouveaux foyers, dans la façon dont il faut organiser la combustion de manière à produire le minimum de polluants tout en respectant les critères d'efficacité et de pertes de charge. Cette optimisation de foyer ne pourra se faire qu'à partir de modèles valables. Le but de ce travail est de présenter les différents modèles qui sont actuellement proposés et d'indiquer de quelles manières ils pourraient être améliorés pour résoudre les trois problèmes précités :

- prédire le taux de polluants des foyers pour les diverses conditions de fonctionnement ;
- dégager les principaux paramètres qui agissent sur ce taux de polluants ;
- concevoir de nouveaux foyers optimaux à production minimale de polluants tout en conservant les performances du foyer.

2. ANALYSE DES DIFFÉRENTS MODÈLES PROPOSÉS

Nous distinguons deux classes de modèles, les modèles simplifiés ou modulaires où chaque fonction du foyer est représentée par un bloc ayant certaines propriétés et les modèles à combustion évolutive qui tiennent compte de la structure de la zone de combustion et des hétérogénéités apportées par les conditions d'injection du combustible et de l'air par la structure tourbillonnaire de l'écoulement. Avant d'aborder cette schématisation examinons brièvement le fonctionnement des foyers actuels (1).

Nous avons représenté sur la figure 1A la structure de la zone de combustion d'un foyer principal. Une injection latérale et axiale d'air crée une zone de recirculation ; le combustible finement pulvérisé est injecté dans cette zone, ce noyau de recirculation est le siège d'une combustion très intense due aux échanges de masse et d'énergie entre les produits brûlés formés, l'air et les gouttes de combustible, c'est la zone de combustion primaire. Le rapport de mélange dans cette zone est voisin du mélange stœchiométrique. De ce noyau s'échappent des gaz imparfaitement brûlés, la combustion se poursuit dans le foyer tubulaire grâce à un apport latéral d'air, c'est la zone de combustion secondaire. Pour limiter la température à l'entrée de la turbine les gaz brûlés sont mélangés à une nouvelle injection latérale d'air, c'est la zone de dilution.

La figure 1B représente l'organisation de la combustion dans un foyer de réchauffe, la stabilisation de la flamme dans cet écoulement pré-carburé à grande vitesse est obtenue par des obstacles. En aval des obstacles une zone de recirculation conditionne la stabilisation de la flamme ; à partir de cette zone une flamme turbulente se propage tout d'abord sans interaction avec la paroi ou les flammes voisines, c'est la zone de jet ; par la suite il y a rencontre des différentes flammes turbulentes, c'est la zone d'inter-pénétration ; à l'extrémité du foyer on rencontre, si le foyer est suffisamment long, une zone de combustion plus homogène. Ce foyer est donc caractérisé par une forte stratification de l'écoulement.

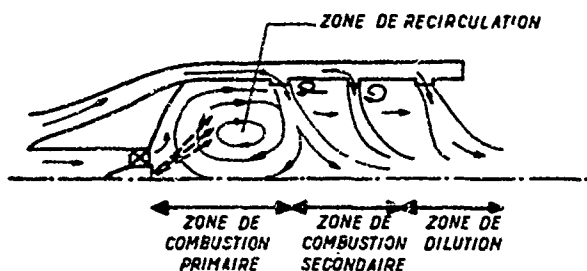
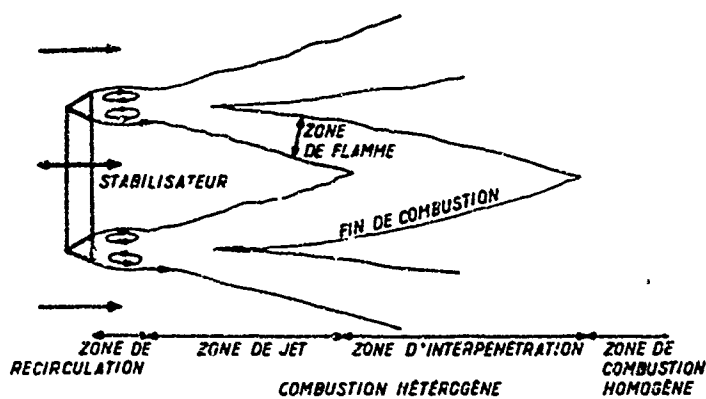


Fig. 1 A - Organisation de la combustion dans un foyer principal de turboréacteur.

Fig. 1 B - Organisation de la combustion dans un foyer de réchauffe.



2.1. Foyer principal de turboréacteur

Nous allons tout d'abord aborder les modèles simplifiés ou modulaires.

2.1.1. Modèles simplifiés

Un foyer principal de turboréacteur peut être représenté (fig. 2) par un ensemble de réacteurs plus ou moins parfaitement mélangés et de réacteurs tubulaires. Cette figure en donne trois exemples qui sont utilisés à l'heure actuelle. Pour mieux comprendre cette analyse il nous paraît utile de donner les principales caractéristiques de ces réacteur

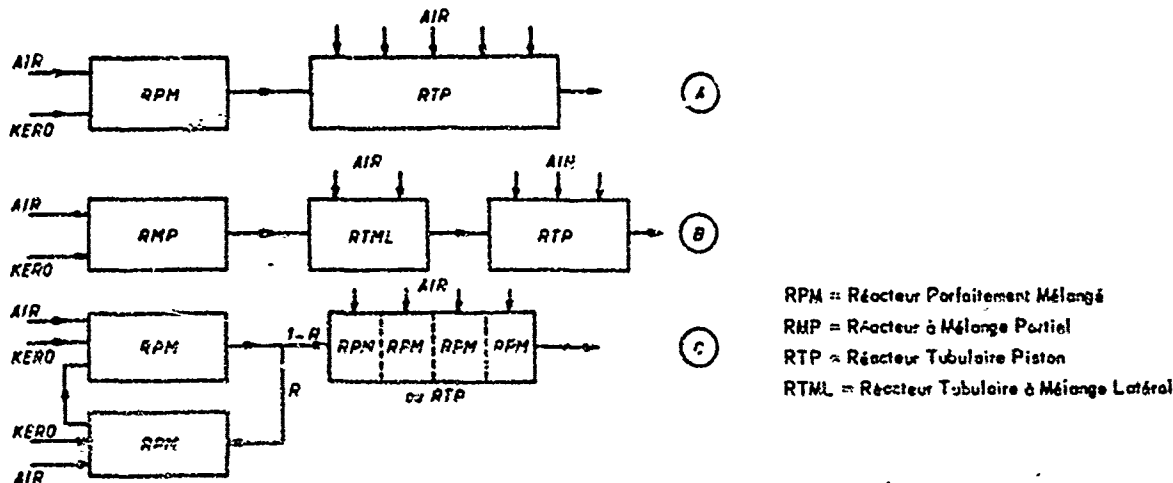


Fig. 2 - Représentation schématique d'un foyer principal de turboréacteur.

a) réacteurs parfaitement mélangés

Pour mieux saisir l'intérêt de ce modèle il nous semble utile de rappeler brièvement la théorie de ce réacteur. On admet tout d'abord que les temps nécessaires au mélange sont négligeables devant les temps nécessaires aux réactions chimiques. Les conditions dans le réacteur correspondent donc aux conditions de sortie. Les équations de conservation s'écrivent :

- équation de continuité globale :

$$V \frac{d\rho}{dt} = \dot{m}_{ae} + \dot{m}_{re} - \dot{m} = \dot{m}_e - \dot{m}$$

- équation de continuité des espèces :

$$V \frac{d\rho_i}{dt} = \dot{m}_{ie} - \dot{m}_i + V \dot{W}_i$$

- équation de conservation de l'énergie :

$$\frac{d}{dt} \left(\sum_i m_i e_i \right) = \sum_i \dot{m}_{ie} h_i(T_e) - \sum_i \dot{m}_i h_i(T) - \dot{Q}(T),$$

V est le volume du réacteur et \dot{W}_i le taux de production de l'espèce i ; en introduisant la fraction massique $Y_i = \frac{\dot{m}_i}{\dot{m}} = \frac{\rho_i}{\rho}$ l'équation de continuité des espèces devient :

$$(1) \quad t_s \frac{dY_i}{dt} = Y_{ie} - Y_i + t_s \frac{\dot{W}_i}{S}$$

où t_s est le temps de séjour $t_s = SV/\dot{m}_e$, \dot{m}_e étant le débit d'entrée dans le réacteur.

L'équation de conservation de l'énergie, en remplaçant l'énergie interne par l'enthalpie $\sum_i Y_i e_i = \sum_i Y_i h_i - P$, en supposant le produit VP constant et en mettant l'enthalpie sous la forme

$$\sum_i Y_i h_i = \sum_i Y_i \left[\int_{T_0}^T C_{pi} dT + q_i^0 \right] = \sum_i Y_i [h_{Ti} + q_i^0]$$

où h_{Ti} est la partie de l'enthalpie sensible à la température et q_i^0 la chaleur de formation à pression constante de l'espèce i , a pour expression :

$$(2) \quad t_s \frac{d}{dt} \left(\sum_i Y_i h_{Ti} \right) = \sum_i (Y_{ie} h_{Tie} - Y_i h_{Ti}) - \frac{t_s}{S} \sum_i \dot{W}_i q_i^0.$$

Le réacteur est supposé adiabatique $\dot{Q}(T) = 0$.

Les conditions d'entrée dans le réacteur (Y_{ie} et h_{Tie}) étant connues, le système constitué par les équations (1) et (2) donne les conditions de fonctionnement du réacteur (composition et température pour une pression donnée), il est donc possible d'avoir la composition des produits polluants comme NO_x , SO_x , CO ... à condition de bien connaître la cinétique chimique de formation de ces substances. Ces différentes façons de résoudre ce problème peuvent être résumées de la manière suivante :

1. On suppose le régime permanent, le système d'équations se réduit alors

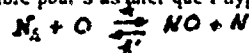
$$(3) \quad \begin{cases} Y_i = Y_{ie} + t_s \dot{W}_i / S \\ \sum_i Y_i h_{Ti} = \sum_i Y_{ie} h_{Tie} - \frac{t_s}{S} \sum_i \dot{W}_i q_i^0 \end{cases}$$

Les conditions d'entrée dans le réacteur sont connues (richesse, débit, pression) le paramètre que l'on fait varier est le temps de séjour qui limite le processus réactionnel ; on peut toutefois le déterminer si le volume du réacteur est connu, moyennant une hypothèse sur la masse volumique ρ , les débits étant également connus. La détermination de concentrations des espèces polluantes repose alors sur les hypothèses faites pour représenter la cinétique chimique. Examinons les plus utilisées :

a. L'écriture d'un système d'équations chimique complète constitue la solution idéale mais qui conduit à des méthodes de résolution compliquées, les équations étant non linéaires, mais souvent guère plus complexes que le calcul de la composition à l'équilibre et des méthodes similaires peuvent être utilisées pour la résolution.

b. Une deuxième façon de procéder consiste à admettre que le temps de réaction chimique est, pour certaines réactions, petit devant le temps de séjour de telle manière qu'il sera possible de supposer ces réactions à l'équilibre et de conserver dans le système régissant la cinétique chimique, les réactions lentes qui freinent le processus. Le mode opératoire est alors le suivant :

on calcule la température et la composition en supposant tout le système en équilibre ; on évalue ensuite le paramètre de BRAY qui est un critère d'écart à l'équilibre pour s'assurer que l'hypothèse est valable. Ce critère pour une réaction du type :



s'écrit : (4)

$$B = 1 - \frac{k}{k'} \cdot \frac{\rho_m \rho_N}{\rho_{N_2} \rho_O} \cdot \frac{Y_{NO} Y_N}{Y_{N_2} Y_O}$$

k et k' sont les vitesses spécifiques de réaction fonction de la température, ρ_m est la masse molaire. B est calculé avec les conditions de l'équilibre B^e , l'équation chimique précédente peut être supposée à l'équilibre si B^e est voisin de zéro. Ce calcul est valable si on admet que la température calculée avec l'hypothèse de l'équilibre n'est pas très éloignée de la température calculée avec la méthode a. [2].

On calcule ensuite la composition en supposant certaines réactions régies par l'équilibre et d'autres par la cinétique chimique. [3].

c • Une troisième manière d'opérer consiste à séparer les différentes formations des espèces polluantes, on suppose donc qu'il n'y a pas d'interférence entre les différentes espèces.

• On calcule tout d'abord les fonctionnements du réacteur à partir d'un système chimique simplifié vérifiant en particulier le bilan d'énergie, on peut par exemple utiliser une équation du deuxième ordre pour représenter les phénomènes de combustion de type :



ou même un système simplifié plus complexe qui donne les imbrûlés.

• Connaissant les conditions dans le réacteur, on écrit pour chaque espèce polluante le système de réactions chimiques correspondant : système donnant la concentration en CO - système donnant la concentration de NO - système donnant la concentration en SO_x ... et on résout ces systèmes séparément. On fait donc l'hypothèse (vérifiée pour le NO) que la concentration de l'espèce polluante est suffisamment faible pour ne pas perturber le bilan énergétique.

2 ■ Une deuxième manière de résoudre le système d'équations relatif au réacteur homogène consiste, comme le font EDELMAN et ECONOMOS [4], à considérer le système complet constitué par les équations (1) et (2) du régime transitoire et à résoudre ces équations sous une forme différentielle, la résolution étant poursuivie jusqu'au régime permanent.

b) réacteurs à mélange imparfait

L'imperfection du mélange joue un très grand rôle dans la production des espèces polluantes. On sait en effet que la production de CO, de NO, des hydrocarbures imbrûlés, du carbone est très sensible au rapport de mélange local et à la température ; cette production sera donc sensible aux hétérogénéités rencontrées dans le foyer, hétérogénéités qui peuvent être dues aux procédés d'injection du combustible (gouttes) et de l'air (jets), à la turbulence de l'écoulement, fonction de paquets plus ou moins riches et plus ou moins mélangés, à la stratification de l'écoulement. La caractérisation de cette hétérogénéité est un point important du modèle si l'on désire obtenir correctement la production des espèces polluantes à la sortie du foyer. Dans le cas de réacteur du type que nous venons d'étudier on peut tenir compte de l'imperfection du mélange de différentes manières.

1 ■ Le temps de séjour tout d'abord n'est pas le même pour toutes les molécules entrant dans le réacteur, il existe donc une fonction de distribution du temps de séjour. Pour la déterminer on utilise la technique du traceur consistant par exemple à ajouter celui-ci pendant un intervalle de temps bref (méthode de l'impulsion) ou encore on fait subir au débit un échelon (méthode de l'échelon) ou une variation sinusoïdale. Si nous désignons par $C(t)$ la concentration du traceur, l'évolution de la concentration est donnée par l'équation du bilan :

$$(5) \quad t_s \frac{dC(t)}{dt} + C(t) = C_0(t)$$

$C_0(t)$ étant la concentration à l'entrée.

Si nous supposons que le traceur est injecté pendant un temps très court la solution s'écrit :

$$(6) \quad C(t) = \frac{1}{t_s} \exp[-t/t_s]$$

L'évolution de C en fonction du temps définit la fonction densité de probabilité

$$(7) \quad p(t) = \frac{1}{t_s} \exp[-t/t_s]$$

représente la distribution du temps de séjour dans le réacteur, la fraction de l'écoulement dont le temps de séjour est compris entre t et $t+dt$ est $p(t)dt$; la fonction de distribution s'écrit :

$$(8) \quad F(t) = 1 - \exp[-t/t_s]$$

c'est la fraction d'espèces possédant un temps de séjour inférieur au temps t . Le temps de séjour moyen correspondant au moment d'ordre un est $m_1 = t_s$ et la variance $\sigma^2 = t_s^2$.

Les fonctions de distribution utilisées dans le réacteur sont en général plus complexes et de la forme :

$$(9) \quad F(t) = 1 - \exp[-\alpha(t-\theta)/t_s]$$

α et θ étant deux constantes déterminées par l'expérience ; ces deux constantes tiennent compte de la stratification de l'écoulement ou des volumes morts c'est-à-dire des zones du réacteur où le taux de production chimique est nul. Si nous prenons par exemple un écoulement stratifié dans le réacteur relatif à deux régions une fraction f est parfaitement mélangée et une fraction $1-f$ non mélangée

$$(10) \quad F(t) = 1 - \exp\left\{-\frac{t - (1-f)t_s}{t_s}\right\}$$

$$\alpha = 1/f, \quad \theta = (1-f)t_s$$

2 ■ Examinons le cas où l'imperfection du mélange se traduit par des variations de composition, la variable d'espace x est le cas la grandeur définissant la composition du mélange ; prenons par exemple la concentration molaire $C = n/V$ à l'instant t . La fonction densité de probabilité est alors $p(C, t)$ la proportion d'espèces ayant au temps t une concentration comprise entre C et $C+dC$ est égale à $\int p(C, t) dC$. Il en résulte la définition de la concentration moyenne $\bar{C}(t) = \int C p(C, t) dC$ et de la variance $\sigma^2 = \int (C - \bar{C})^2 p(C, t) dC$. La non uniformité en concentration peut être décrite par la variance σ^2 , un mélange turbulent isentropique conduit à une décroissance de σ^2 . En introduisant un temps caractéristique de mélange t_m ,

$$(11) \quad t_m \frac{d\sigma^2}{dt} = -\sigma^2$$

$$\sigma^2 = \sigma_0^2 \exp[-t/t_m]$$

Ce temps de mélange intervient par comparaison au temps de séjour t_s , dans le cas d'un réacteur avec injection latérale on obtient sensiblement :

$$(12) \quad t_s / t_m \approx (1/4) (D^2 / S)^{2/3}$$

où D est le diamètre du réacteur et S la surface des jets entrant dans le réacteur. En utilisant la technique du traceur on peut également avoir une idée de la valeur de t_m .

La densité de probabilité $p(c, t)$ peut être obtenue à partir d'une équation de bilan du type de BOLTZMANN [5]. L'évolution des espèces dans le réacteur va dépendre de deux paramètres de DANKHÖLLER : le rapport t_c / t_s du temps chimique au temps de séjour et le rapport t_c / t_m du temps de séjour au temps de mélange.

3. FLETCHER et HEYWOOD, dans la zone primaire de combustion, supposent que l'écoulement est rapidement divisé en éléments discrets de dimensions plus petites que celles du réacteur. Ces éléments sont rapidement dispersés et brûlent avec des richesses φ différentes. Ils supposent pour φ une distribution gaussienne avec une valeur moyenne $\bar{\varphi}$ et une déviation standard σ ; ils caractérisent la non uniformité du réacteur par le paramètre de mélange $s = \sigma / \bar{\varphi}$. La densité de probabilité du temps de séjour est représentée par l'équation (7). Les résultats obtenus sont représentés sur la figure 3.

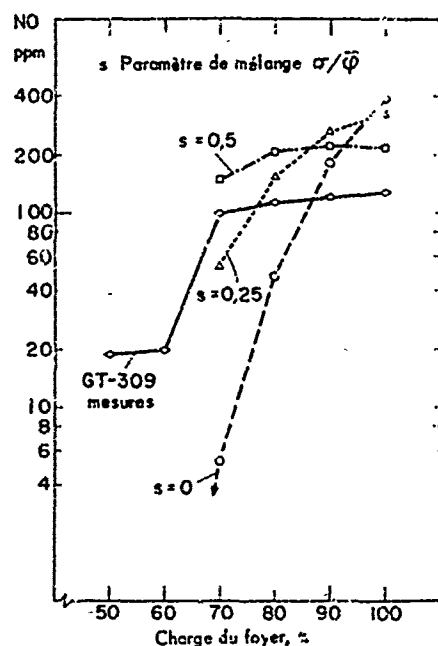


Fig. 3 - Formation théorique et expérimentale de NO dans un foyer principal de turboréacteur en fonction de la charge, calcul avec trois rapports de mélange $s = 0$, $s = 0,25$ et $s = 0,5$ [11].

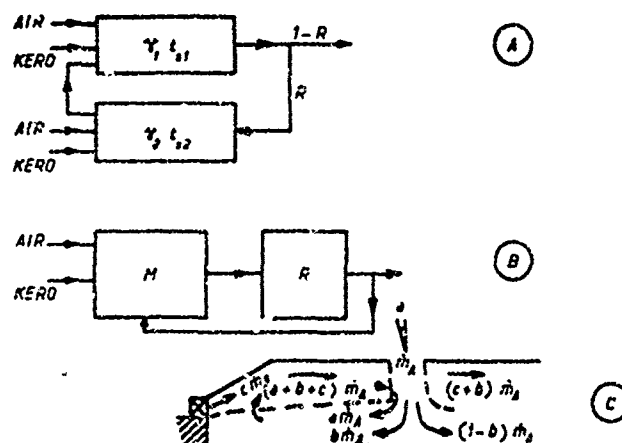


Fig. 4 - Schématisation de la zone primaire.

4. La représentation de l'hétérogénéité de la zone de combustion primaire peut être obtenue en considérant plusieurs réacteurs [6] homogènes (fig. 3). Une façon de faire est celle représentée sur la figure 4A où sont couplés deux réacteurs homogènes de volumes V_1 et V_2 correspondant à deux temps de séjour t_{s1} et t_{s2} . Le deuxième est à recirculation, une fraction R des gaz brûlés sortant de (1) pénètre dans le réacteur (2) la fraction $(1-R)$ allant dans le réacteur tubulaire. Les gaz brûlés sortant de (2) pénètrent dans (1). Cette schématisation a été adoptée par HAMMOND MELLOR [7]. Compte tenu des équations donnant le fonctionnement d'un réacteur, il est facile d'écrire le bilan des espèces et le bilan d'énergie pour chacun des réacteurs. On peut également utiliser le couplage, figure 4B, d'un mélangeur prenant en compte l'aspect physique désigné par (M) et d'un réacteur homogène (R), avec recirculation, le mélangeur est sans réaction chimique et dans le réacteur parfaitement mélangé n'interviennent que des réactions chimiques. Le partage des différents débits de la zone primaire peut se faire comme indiqué sur la figure 4C. Le débit \dot{m}_A qui pénètre dans les orifices latéraux sous forme de jet faisant un angle α avec la normale à la paroi latérale du foyer, ce débit se divise en trois parties, $a\dot{m}_A$ qui reste dans la zone de recirculation, $b\dot{m}_A$ qui pénètre dans la zone de recirculation mais qui en ressort et le débit $(1-b)\dot{m}_A$ injecté vers la zone de combustion secondaire. Dans la partie avant du foyer pénètre le débit $C\dot{m}_A$ par le dispositif de mise en rotation de l'air (swirl). La valeur de b est donnée par :

$$(13) \quad b = 0,5 (T_c / T_{s1})^{1/2} \cos \alpha$$

T_s est la température de l'air à l'entrée et T_c la température moyenne de la zone primaire.

c) réacteur tubulaire unidimensionnel du type piston

Ce réacteur suppose à l'entrée un mélange parfait de l'air, du combustible et des gaz brûlés s'il est placé après la zone primaire de combustion. On admet également que les phénomènes de diffusion sont négligeables de sorte que les équations de continuité s'écrivent :

• équation de continuité globale $G = \rho v = \text{constante}$

• équation de continuité de l'espèce j

$$(14) \quad G \frac{dY_j}{dx} = \dot{W}_j$$

où $\frac{dY_j}{dx}$ étant le gradient de concentration le long du réacteur.

L'équation de conservation de l'énergie devient :

$$G \frac{d \sum Y_j h_j}{dx} = \dot{Q}$$

ou encore d'après la définition de h_j

$$(15) \quad G \frac{d \sum Y_j h_{f,j}}{dx} = \sum q_{f,j} \dot{W}_j + \dot{Q}(T)$$

\dot{Q} est la chaleur échangée avec l'extérieur, on suppose qu'il n'y a pas d'échange par conduction, l'énergie cinétique est négligeable devant l'énergie thermique et chimique. L'évolution de la combustion est supposée sensiblement isobare ce qui élimine l'équation de conservation de la quantité de mouvement.

L'évolution des concentrations des espèces polluantes est obtenue à partir de l'intégration de l'équation :

$$(16) \quad \int_0^x dx = \int_{Y_{j,e}}^{Y_{j,f}} \frac{Y_j}{\dot{W}_j} dY_j,$$

tout le long du foyer, ou encore en remplaçant la distribution spatiale par une distribution temporelle :

$$(17) \quad \int_0^t dt = \int_{Y_{j,e}}^{Y_{j,f}} \frac{Y_j}{\dot{W}_j} dY_j$$

Ce modèle peut être amélioré en introduisant une injection progressive d'air tout le long du réacteur ou encore en tenant compte de la stratification de l'écoulement ou de la présence de phases condensées.

d) représentation du foyer principal à l'aide de réacteurs élémentaires

À l'aide de ces deux types de réacteurs : réacteurs parfaitement mélangés (RPM) ou tenant compte du degré de mélange et réacteurs tubulaires du type piston (RTP) il est possible de schématiser un foyer principal de turboréacteur. Sur la figure 2 nous donnons trois schémas qui ont été utilisés pour évaluer la production de NO et de CO.

Dans le modèle A dû à HEYWOOD [8] la zone primaire de combustion est représentée par un réacteur du type RPM et la zone secondaire de combustion et de dilution par un réacteur tubulaire avec injection d'air à différentes abscisses. Le modèle B dû à FLETCHER et HEYWOOD [9] comporte un réacteur à mélange imparfait en introduisant une fonction de distribution du temps de séjour et de la richesse (RPM) la zone de combustion secondaire est représentée par deux réacteurs tubulaires. Le modèle C dû à HAMMOND et MELLOR [10] représente la zone primaire par deux réacteurs parfaitement mélangés avec recirculation et la zone de combustion secondaire par une série de réacteurs à mélange parfait. Le réacteur tubulaire du type piston peut en effet être représenté par une succession de réacteurs du type (RPM) avec injection partielle d'air dans chacun des réacteurs. À l'aide de cette schématisation il est possible d'évaluer tout le long du foyer la variation de concentrations des polluants. La figure 5 en est un exemple dû à HEYWOOD [8], [11]. La zone de combustion primaire correspond à la partie à richesse ϕ constante (0-4 ms), la production de NO est limitée par le temps de séjour. La zone de combustion secondaire (4-10 ms) à richesse décroissante par suite de l'injection d'air est caractérisée par une augmentation de NO due à la zone de combustion secondaire puis par une décroissance dans la zone de dilution.

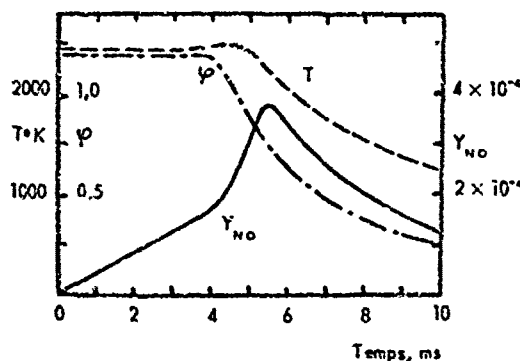


Fig. 5 - Variations en fonction du temps de la température, de la richesse et de la fraction massique de NO calculées par le schéma de la figure 2C [8].
 $p = 15 \text{ bars}$, température d'entrée = 700°K

2.1.2. Modèles à combustion évolutive

a) phase gazeuse

Les modèles précédents reposent sur une conception spatiale simple, réaction dans un volume donné ou réaction chimique suivant une direction, problème unidimensionnel. Dans un foyer par suite de l'organisation de la combustion des problèmes bi et tridimensionnels apparaissent [12]. Le schéma le plus simple que l'on rencontre et qui a été traité par D.B. SPALDING est celui représenté sur la figure 6 où deux écoulements A et B se rencontrent, se mélangent avec des réactions chimiques dans cette zone de mélange. Cette configuration correspond par exemple à un écoulement de gaz brûlés chauds (A) rencontrant des gaz frais précarburés (B). Une zone de combustion s'étale après le point de rencontre de ces deux jets. Cette configuration correspond également à une flamme de diffusion représentée par un jet de combustible (A) rencontrant un jet d'air (B). Ce problème est traité par R. BORGHI dans la communication : « Etude théorique de l'évolution résiduelle des produits polluants dans les jets de turboréacteur », les équations de conservation et les méthodes de résolution sont données [13]. On peut de cette manière avoir l'évolution des produits polluants le long d'une ligne de courant ; cette évolution étant régie par l'équation de continuité de l'espèce j :

$$(18) \quad \rho u \frac{\partial Y_j}{\partial x} + \rho v \frac{\partial Y_j}{\partial y} = \frac{\partial}{\partial y} \left[\rho D \frac{\partial Y_j}{\partial y} \right] + \sum_{i=1}^N \dot{w}_{j,i}$$

dans laquelle on admet que les gradients transversaux de composition sont les plus importants, où D est le coefficient global de diffusion et comprend donc les coefficients de diffusion moléculaire et de diffusion turbulente. On peut de cette manière connaître en chaque point (x, y) de l'espace l'évolution des espèces NO, CO et des hydrocarbures imbrûlés. La figure 7 est un exemple de résultats obtenus par cette schématisation.

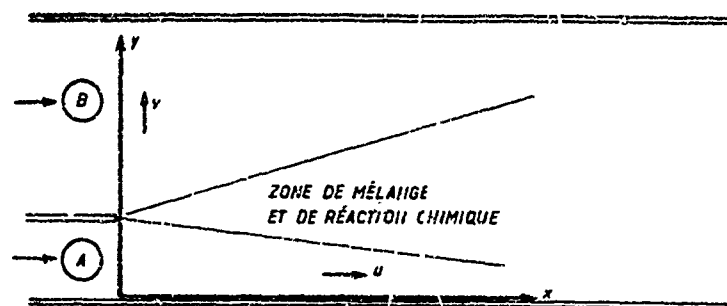


Fig. 6 - Modèle bidimensionnel.

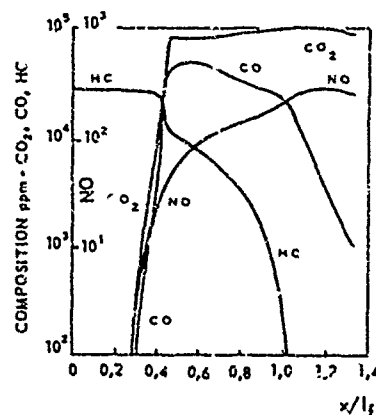


Fig. 7 - Variation de la formation des espèces CO_2 , CO, NO, hydrocarbures (HC) tout le long du foyer [4].

b) écoulement à deux phases

Dans la plupart des foyers le combustible est injecté sous forme de fines gouttelettes, il est donc important de connaître les répercussions qu'entraînent, sur le taux de production des polluants, la présence dans le foyer de gouttes en combustion.

• Formation du NO à l'échelle de la goutte :

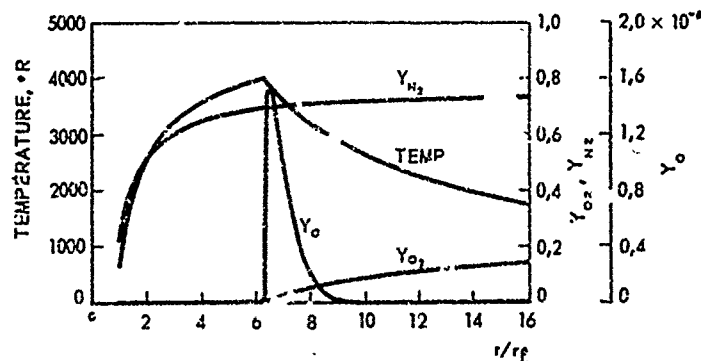
Cette goutte est donc considérée comme une source de NO dont le débit est fonction du diamètre de la goutte, de la nature de la goutte, de la pression, de la température et de la composition du gaz entourant la goutte. La détermination de la concentration du NO autour de la goutte et de la quantité de NO produite peut se faire de diverses manières.

• On utilise une théorie quasi stationnaire pour évaluer autour de la goutte le champ de températures et la distribution des espèces les plus importantes comme N_2 , O_2 etc. La concentration des espèces étant évaluée en tenant compte des phénomènes de diffusion. Cette analyse est justifiée par le fait que le rayon de la flamme est connu avec une certaine imprécision. Williams signale en particulier que la convection naturelle a pour effet de rapprocher la flamme de la goutte et la valeur donnée par la théorie qui ne tient pas compte des phénomènes de convection est en général trop élevée ; dans ce cas, le rapport entre le rayon de la flamme donné par la théorie et celui de l'expérience est de l'ordre de deux de sorte que le fait de considérer le rapport $r_f(t)/r_g(t)$ comme

constant (r_g est le rayon de la goutte) et une hypothèse valable, cette valeur étant d'ailleurs corrigée par l'expérience. On suppose également que le profil des températures et des concentrations exprimé en fonction de r/r_g est indépendant du temps. Il existe donc une courbe unique que l'on utilise pour donner l'évolution de la température et des concentrations. Ces profils sont donnés en figure 8. Dans ce calcul, l'épaisseur de la zone de flamme est supposée petite par rapport au rayon de la goutte (combustion concentrée) [14].

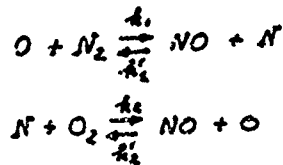
Fig. 8 - Variation de la température et de la fraction massique de N_2 , O_2 et O à partir de la surface de la goutte

[15]



A partir de ces courbes, on calcule pour chaque rayon r la température ; la concentration en oxygène atomique et azote atomique est calculée en considérant l'équilibre de O_2 avec O et N_2 avec N .

Devant toutes ces hypothèses, il est normal de négliger la diffusion de NO . Si on admet par exemple une cinétique de formation de NO du type :



à chaque rayon r la fraction de NO est donnée par l'équation

$$(19) \quad \frac{\dot{m}}{4\pi r^2} \frac{dY_{NO}}{dr} = \dot{W}_{NO} = K_1 N_2^{1/2} \left\{ \left(\frac{Y_{O_2}}{K_2 K_{O_2}} \right)^{1/2} \left(1 - \frac{Y_{NO}}{K_1 N_2} \right) + \left(\frac{Y_{N_2}}{K_4 K_{N_2}} \right)^{1/2} \left(1 - \frac{Y_{NO}}{K_3 O_2} \right) \right\}$$

\dot{m} étant le débit de combustible issu de la goutte et K_1 et K_2 les constantes d'équilibre de formation de O et N à partir de O_2 et N_2 .

Dans le cas d'un combustible ne contenant pas d'oxygène, la formation de NO commence à l'extérieur de la flamme, passe par un maximum puis décroît, il n'y a pas de formation de NO entre la goutte et la flamme qui est une zone très riche. Par contre si le combustible contient de l'oxygène, la formation de NO peut commencer plus près de la goutte.

On peut, comme le fait KESTEN [15], tenir compte de la diffusion et utiliser l'équation de continuité en instationnaire :

$$(20) \quad \frac{\partial Y_{NO}}{\partial t} + \frac{\dot{m}}{4\pi r^2} \frac{\partial Y_{NO}}{\partial r} - \frac{1}{r^2} \frac{\partial}{\partial r} \left(r^2 D \frac{\partial Y_{NO}}{\partial r} \right) = \dot{W}_{NO}$$

et intégrer cette équation dans le champ de température et de composition précédemment défini. On obtient en fonction de r/r_g l'évolution de Y_{NO} qui est représentée sur la figure 9, chaque courbe correspondant à des instants de combustion différents. Il s'agit de goutte d'éthanol brûlant à la pression atmosphérique. Une étude paramétrique montre que la masse de NO produite ramenée à la masse de combustible Ξ_{NO} est très sensible au diamètre de la goutte. On obtient des relations de la forme :

$$(21) \quad \Xi_{NO} = 5 \cdot 10^{-4} D^2$$

D étant le diamètre de la goutte exprimé en millimètres (goutte d'éthanol, $p = 1$ atm.). Ξ_{NO} est très sensible à la pression, peu sensible à T_{∞} jusqu'à des températures de 1500°K. Ξ_{NO} dépend étroitement du rapport r_g/r_c . Ξ_{NO} augmente lorsque r_g/r_c croît.

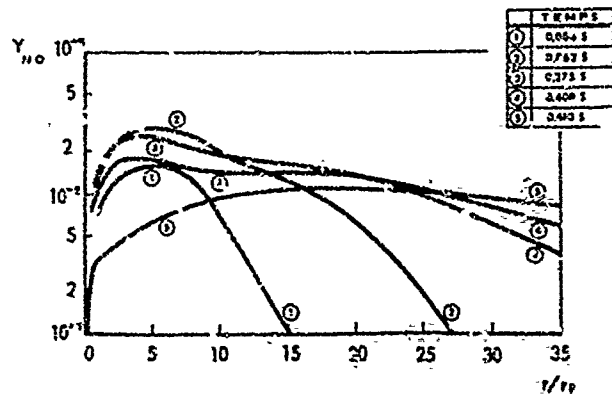


Fig. 9 - Variation de la fraction massique de NO le long de la goutte à différents instants de sa combustion (t_g en ms).

Un deuxième modèle repose sur l'analyse de la combustion en régime transitoire toujours avec l'hypothèse d'une combustion concentrée. En prenant le domaine situé à l'extérieur de la flamme ($t_f < t < \infty$) l'intégration en transitoire de l'équation de conservation de l'énergie et de la continuité des espèces (O_2 en particulier) conduit aux expressions :

$$(22) \quad T - T_\infty = \frac{\dot{q}_f}{2} (T_f - T_\infty) \operatorname{erfc} \left(\frac{t - t_f}{2\sqrt{\alpha t}} \right)$$

$$Y_{O_2} = Y_{O_2\infty} \left(\frac{t - t_f}{t} + \frac{t_f}{t} \operatorname{erf} \left(\frac{t - t_f}{2\sqrt{\alpha t}} \right) \right)$$

Le rayon de la flamme t_f est déterminé par l'équation de continuité globale et la condition de stoechiométrie. Ce calcul a été développé par SPALDING à la référence [16] donnant l'évolution de t_f en fonction du temps pendant la combustion de la goutte. Dans le cas d'un nombre de Lewis égal à l'unité, la diffusivité thermique, α , est égale au coefficient de diffusion D .

A partir des équations précédentes et en supposant que $Y_{N_2} = Y_{N_2\infty}$, SAWYERS [14] a calculé la formation de NO autour de la goutte en combustion en considérant uniquement la première équation chimique de production de NO prépondérante dans le sens direct de sorte que :

$$(23) \quad \frac{1}{\Omega} \frac{dY_{NO}}{dt} = \frac{2 \dot{q}_f^2}{\sqrt{K_0}} \frac{Y_{N_2}}{H_2 O_L} \sqrt{\frac{Y_{O_2}}{H_2 O_L}} \frac{1}{H_2 O_L}$$

Il est certain qu'une théorie complète de combustion de la goutte pourrait être entreprise en tenant compte de l'écoulement externe et en mettant en jeu une cinétique chimique plus complète qui tiendrait compte de la formation de tous les polluants gazeux (NO, CO et hydrocarbures imbrûlés).

• Production du NO par un ensemble de gouttes

Pour déterminer le taux de production de polluants par un ensemble de gouttes, il importe tout d'abord de connaître l'évolution de la fonction de distribution des gouttes dans le foyer. Cette fonction de distribution est donnée par une équation du type Boltzmann qui tient compte de l'évolution du diamètre des gouttes due à la combustion, de la position des gouttes et du champ de vitesses relatives des gouttes, des collisions et des phénomènes de coalescence ou de pulvérisation secondaire des gouttes. Il faut également tenir compte, dans l'équation de continuité de l'espèce considérée, de ceux termes de production. Le terme de production en phase gazeuse tel qu'il a été écrit plus haut et le terme de production en considérant chaque classe de goutte de même diamètre comme source de l'espèce considérée. On peut de cette manière calculer la fraction massique $Y_j(x, t)$ de l'espèce j considérée à chaque instant t et pour une position x choisie.

• Formation et évolution des particules de carbone

Dans ce paragraphe se rapportant à des écoulements à deux phases, il nous paraît important de donner quelques indications sur les modèles utilisés relatifs à la formation et à l'évolution des particules de carbone dans un foyer.

Il existe très peu de modèles qui permettent de prédire la formation du carbone dans les flammes [8] [17], le dernier stade chimique précédant sa formation étant l'acétylène. On connaît plutôt les conditions qui réduisent cette formation, à savoir la richesse qui doit être localement au-dessous d'un certain niveau, ce niveau étant fonction de la pression et de la température locale. Il est certain qu'à l'échelle de la goutte, où l'on rencontre toutes les richesses, la formation de carbone est possible, on peut cependant montrer que cette production nécessite un certain temps critique et si le temps de séjour dans la zone riche en combustion entourant la goutte est inférieur à ce temps critique, la formation de carbone n'est pas possible, d'où l'intérêt d'introduire vers le foyer des gouttes de petit diamètre ou même de combustible prévaporisé qu'il faut mélanger le plus rapidement possible avec l'air (mélangeurs situés en amont du foyer). Cette formation de carbone peut être due également au contact de gouttes combustibles avec des parois chaudes.

Il est ensuite très difficile de brûler ces particules de carbone formées dans la zone primaire, combustion qui pourrait avoir lieu dans la zone secondaire ou la zone de dilution. Bien que de faibles dimensions (quelques centièmes à quelques dixièmes de micron) ces particules de carbone s'avèrent très difficiles à brûler. Les modèles utilisés pour étudier cette combustion sont analogues à ceux mis au point pour l'étude de la combustion des gouttes dans les foyers [18]. Les lois d'évolution du rayon r sont de la forme :

$$(24) \quad r \frac{dr}{dt} = -a \frac{p_{O_2}}{\sqrt{T}} e^{-T_a/T}$$

où p_{O_2} est la pression partielle d'oxygène entourant la particule [18]. Les lois proposées doivent tenir compte des phénomènes de diffusion et des phénomènes chimiques, la loi précédente mettant l'accent sur les phénomènes chimiques, BRYANT [19] a proposé une loi de la forme :

$$(25) \quad \frac{dr}{dt} = \frac{p_{O_2}}{K_c + K_d r}$$

ajoutant au processus chimique par l'intermédiaire de K_c un processus de diffusion dépendant du rayon r de la particule.

Quoi qu'il en soit, par suite du temps de séjour dans le foyer du turboréacteur, il est très difficile de brûler ces particules, il est plus sûr pour diminuer la pollution due aux particules de carbone d'organiser la combustion de manière à empêcher leur formation.

2.2. Foyers de réchauffe

La figure 1B représente l'organisation de la combustion dans un tel foyer et l'étude de la pollution se fait avec les modèles présentés au paragraphe 2.1.

• La zone de recirculation peut être schématisée par un réacteur homogène et peut être considérée comme une source de gaz brûlés.

• La zone de jet et la zone d'interpénétration ont été étudiées au paragraphe 2.1.2-a, le modèle correspond à celui de la figure 6 où l'écoulement A est constitué par les gaz brûlés et l'écoulement B par un écoulement de gaz préchauffés. En suivant une ligne de courant il est possible de calculer les variations de concentration en NO, CO et hydrocarbures imbrûlés.

• La zone de combustion homogène peut être assimilée à un réacteur tubulaire ou à une succession de réacteurs homogènes.

A la sortie de la zone d'interpénétration des jets de flamme, les concentrations en NO, CO et en hydrocarbures imbrûlés varient suivant une période qui correspond à la géométrie de l'accroche flamme d'une manière analogue aux variations de température données sur la figure 10. La production globale à la sortie du réacteur est une intégration de toutes ces fluctuations, il faut tenir compte des réactions secondaires du jet du réacteur avec l'air extérieur ainsi que des variations de température et de concentration à la sortie de la tuyère [13].

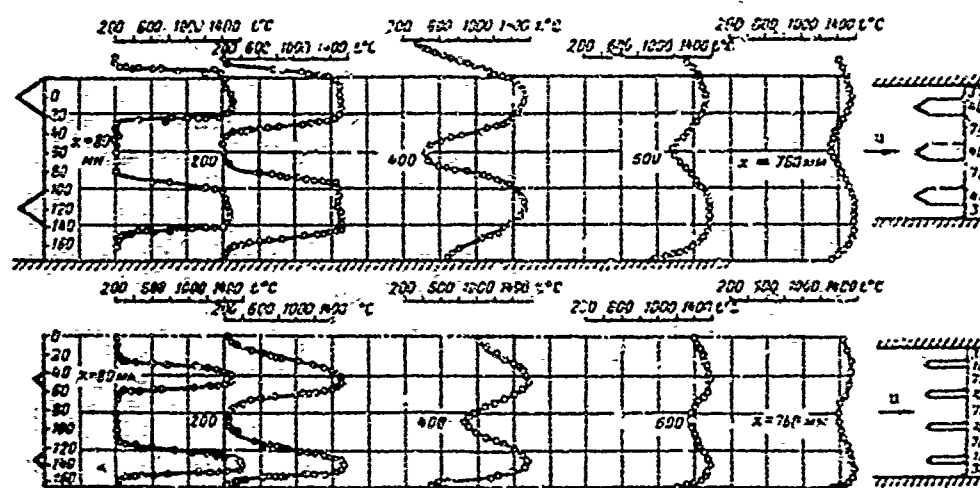


Fig. 10 - Profils des températures en différentes sections du foyer prises à partir des stabilisateurs pour deux configurations de foyer [27]. $T_{air} = 200^\circ C$, vitesse $u = 70 \text{ ms}^{-1}$.

3. ÉTUDE CRITIQUE DE CES MODÈLES

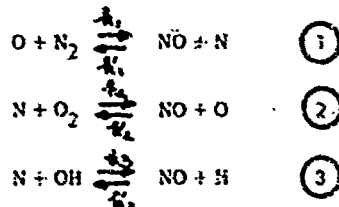
3.1. Evaluation du taux de production

3.1.1. Cinétique chimique de formation :

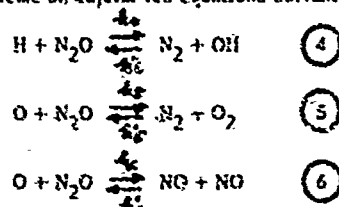
Les schémas retenus sont fonctions de la nature des espèces. Examinons chacun d'eux pour les espèces considérées.

a) Cinétique de formation de NO

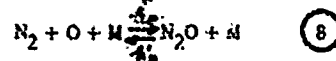
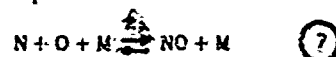
Les réactions élémentaires retenues sont :



mettant en évidence l'importance des trois radicaux O, N et OH et correspondant au mécanisme de formation de NO proposé par ZELDOVITCH. A ce système on adjoint les équations suivantes relatives à N_2O



on ajoute parfois les deux équations :



M jouant le rôle de diluant.

Ces réactions sont sensiblement classées par ordre d'importance, les réactions faisant intervenir l'espèce NO_2 sont en général négligées. Pour déterminer un système simplifié donnant la production de NO on utilise en général trois façons de procéder.

1 On suppose qu'à l'exception de NO, toutes les autres espèces entrant dans la production de NO sont à l'équilibre. Cette hypothèse est assez bien vérifiée dans certains cas comme l'indique la figure 11 ; exception faite pour N, la fraction molaire des autres espèces ne varie pas au cours du temps. Partant des équations chimiques (1), (2) et (7) le taux de production de NO s'écrit :

$$(26) \quad \dot{w}_{\text{NO}} = k_{\text{NO}} [-AC_{\text{NO}} + B]$$

$$\text{avec } A = k_1' C_{\text{N}}^e + k_2' C_{\text{N}}^e + k_3' C_{\text{N}}^e, \quad B = k_1 C_{\text{O}}^e C_{\text{N}_2}^e + k_2 C_{\text{O}}^e C_{\text{O}_2}^e + k_3 C_{\text{O}}^e C_{\text{N}}^e$$

Les concentrations C_{O_2} , C_{O} , C_{N_2} , C_{N} et $C_{\text{N}_2\text{O}}$ étant évaluées à l'équilibre et k_1 , k_1' , k_2 , k_2' , k_3 , k_3' à la température T choisie.

Dans le cas d'un réacteur homogène parfaitement mélangé en introduisant la variable de composition $\epsilon_i = \frac{C_i}{S} = \frac{Y_i}{w_i}$ la production de NO s'écrit :

$$(27) \quad \epsilon_{\text{NO}} = (B/S) / (A + 1/\tau_s)$$

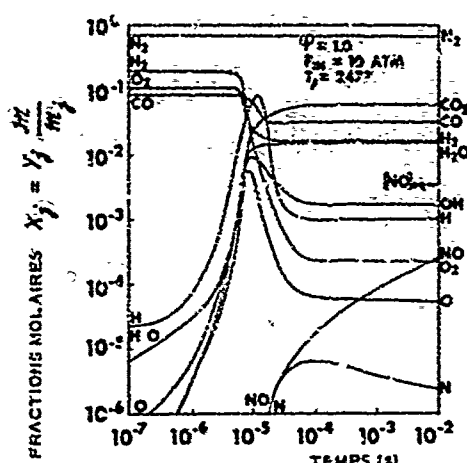


Fig. 11 - Variation de la composition en fonction du temps pour une température d'entrée dans le foyer de 1000°K [21].

A est la somme des inverses des trois temps chimiques $(k_1' C_{\text{N}}^e)^{-1}, (k_2' C_{\text{N}}^e)^{-1}, (k_3' C_{\text{N}}^e)^{-1}$ l'importance relative conditionne la production de NO, le temps de séjour dans le réacteur limite également cette production, on a donc intérêt à avoir des noyaux de recirculation de faible volume pour diminuer la production de NO, ce volume doit cependant être compatible avec une bonne stabilisation de la flamme et une efficacité de combustion élevée. Lorsque $A\tau_s$ est petit devant l'unité : $\epsilon_{\text{NO}} = \frac{B}{SA}$ et dans l'autre cas extrême $A\tau_s \gg 1$: ϵ_{NO} tend vers la valeur limite : B/S . $A\tau_s$ joue le rôle du paramètre de DAMKÖLLER comparant le temps mécanique τ_s au temps chimique A^{-1} . Dans le cas d'un réacteur tubulaire en l'absence de diffusion :

$$(28) \quad \frac{d\epsilon_{\text{NO}}}{dt} + R\epsilon_{\text{NO}} = B/S$$

ayant pour solution :

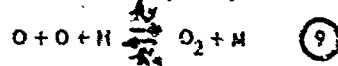
$$(29) \quad \epsilon_{\text{NO}} = \epsilon_{\text{NO}}^e (1 - e^{-At})$$

avec

$$\epsilon_{\text{NO}}^e = B/SA$$

2 Une deuxième manière de simplifier le calcul du taux de production consiste à choisir les réactions prépondérantes et à considérer :

réactions à l'équilibre : adretrons que l'équation fournissant l'oxygène atomique est à l'équilibre



(30)

$$C_{\text{O}}^e / (C_{\text{O}_2}^e)^2 = K_{\text{O}}(T) = k_2/k_3$$

On suppose également que la réaction prépondérante est la réaction (1) dans le sens direct de sorte que le taux de production est égal à [20] :

$$(21) \quad \dot{W}_{N_2} = K_{N_2} (k_1 / K_2^{1/2}) C_{N_2} C_{O_2}^{1/2}$$

faisant intervenir l'azote et l'oxygène moléculaire.

Cette expression a été améliorée par P.J. MARTENEY [21] en supposant que NO et N sont donnés par les équations chimiques (1) et (2) prises dans le sens direct de sorte que

$$(32) \quad \begin{cases} \dot{W}_{NO} = K_{NO} [\alpha C_N + \beta] \\ \dot{W}_N = K_N [-\alpha C_N + \beta] \end{cases}$$

avec

$$\alpha = k_1 C_{O_2}^c, \quad \beta = (k_1 / K_2^{1/2}) C_{N_2}^c (C_{O_2}^c)^{1/2}.$$

Dans le cas d'un réacteur tubulaire et en supposant des concentrations nulles au temps $t=0$

$$(33) \quad \begin{aligned} C_{NO} &= 2\beta t - \frac{1}{\alpha} (1 - \exp(-\alpha t)) \\ C_N &= \frac{1}{\alpha} (1 - \exp(-\alpha t)). \end{aligned}$$

Cette relation est assez bien vérifiée dans le cas des flammes propane-oxygène [22].

3. Une troisième façon de faire est de supposer que le taux de production de certaines espèces est nul, la concentration ne variant pas au cours du temps. Partons des équations chimiques (1), (2), (3), (4), (5), (6), (7) et (8). Supposons que les espèces O, O₂, H, OH et N₂ sont à l'équilibre, les taux de production de NO, N, N₂O supposés hors d'équilibre s'écrivent :

$$(34) \quad \begin{aligned} \dot{W}_{NO} &= K_{NO} [-x_{NO} (R_1 x_N + R_2 + R_3 + 2R_4 x_{N_2O} + R_5) + R_1 + x_N (R_2 + R_3 + R_4) + 2R_5 x_{N_2O}] \\ \dot{W}_N &= K_N [x_{NO} (R_2 + R_3 + R_4) + R_1 - x_N (R_1 x_{NO} + R_2 + R_3 + R_4)] \\ \dot{W}_{N_2O} &= K_{N_2O} [x_{NO}^2 R_4 - x_{N_2O} (R_4 + K_1 + R_5 + R_6) + R_4 + R_5 + R_6] \end{aligned}$$

R_1 correspond au premier membre ou au deuxième membre de l'équation relative à l'équilibre $R_1 = k_1 C_O^c C_{O_2}^c = k_1' C_{O_2}^c C_O^c$ et $x_i = C_i / C_i^c$. En admettant que $\dot{W}_N < \dot{W}_{N_2O} \neq 0$ on obtient deux relations donnant x_N et x_{N_2O} en fonction de x_{NO} de sorte que, en posant

$$K_1 = R_1 / (R_2 + R_3 + R_4) \quad \text{et} \quad K_2 = R_6 / (R_4 + R_5 + R_6),$$

$$x_N = (K_1 + x_{NO}) / (1 + K_1 x_{NO})$$

$$x_{N_2O} = (1 + K_1 x_{NO}) / (1 + K_2)$$

Il en résulte que :

$$(36) \quad \dot{W}_{NO} = K_{NO} 2(1 - x_{NO}^2) [R_1 / (1 + K_1 x_{NO}) + R_6 / (1 + K_2)].$$

Cette relation est la plus utilisée dans les modèles donnant la production de NO [23] [24] [11] [8]. K_1 et K_2 sont fonctions de la température et de la richesse, leur valeur est inférieure à l'unité en particulier dans le cas des mélanges riches, les valeurs de K_1 et K_2 sont très nettement inférieures à l'unité.

Dans la zone primaire d'un foyer de turboréacteur pour laquelle la concentration en N₂O est faible ($K_2 \ll 1$) et $x_{N_2O} \approx 1$, $R_1 = 2,1 \cdot 10^{-5}$, $R_2 = 5,5 \cdot 10^{-6}$, $R_3 = 2,3 \cdot 10^{-5}$, $R_4 = 4,2 \cdot 10^{-3}$ pour $T = 2500^\circ K$, $P = 10$ bars, richesse $\varphi = 1$; on constate que R_1 est petit devant R_2 et R_3 et $K_1 \approx 0,6$. Il en résulte que $R_1 / (1 + K_1 x_{NO})$ est le terme prédominant, le mécanisme de formation de NO dépend surtout des équations (1), (2) et (3). Le mécanisme de formation de N₂O est important à basse température et pour les mélanges pauvres.

Dans le cas d'un réacteur tubulaire, l'évolution de NO en fonction du temps est donnée par :

$$(37) \quad \frac{d x_{NO}}{dt} = \frac{A}{2} \frac{1 - x_{NO}^2}{1 + K_1 x_{NO}} + B \frac{1 - x_{NO}^2}{1 + K_2}.$$

En négligeant le terme relatif à N₂O la solution de cette équation différentielle s'écrit :

$$(38) \quad (1 - x_{NO})^{K_1+1} (1 + x_{NO})^{K_1-1} = e^{-At}$$

avec :

$$A = 4 k_1 C_{N_2}^c C_{O_2}^c / C_{NO}^c = 4 k_1' C_N^c,$$

qui est à rapprocher de la valeur définie au premier paragraphe.

La figure 12 donne les variations de x_{NO} en fonction de At et pour différentes valeurs de k_1 . Lorsque l'on change k_1 pour une valeur donnée de x_{NO} , les différentes valeurs de k_1 modifient At mais ces modifications sont indépendantes de k_2 , et ne dépendent que de x_{NO} : $\Delta(At) = -\log(1-x_{NO})/k_1$. L'influence de k_2 est faible. Pour la zone de combustion secondaire d'un mélange air-kérosène ($P = 3$ bars) la figure 13 donne les variations de A et de k_1 en fonction de la richesse φ pour deux températures d'entrée de l'air 600 et 900°K [25].

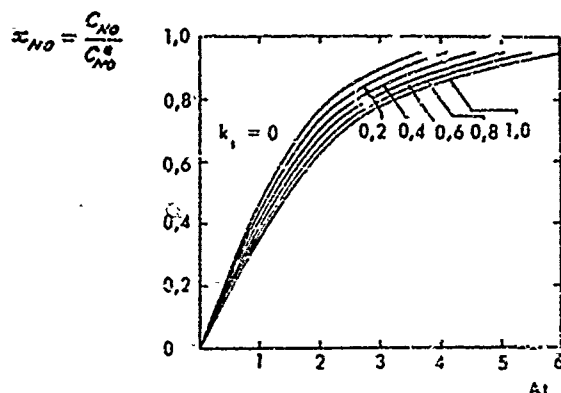


Fig. 12 - Variation de x_{NO} en fonction de At pour différentes valeurs de k_1 [25]

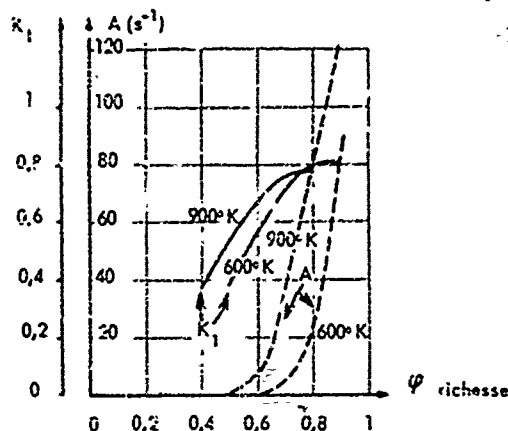


Fig. 13 - Variation de A et k_1 en fonction de la richesse.

Nous venons de voir trois méthodes pour simplifier le taux de production chimique. La première consiste à évaluer le taux de production de l'espèce choisie et à supposer, ce qui est sensiblement vérifié dans le cas du NO que toutes les autres espèces sont à l'équilibre. La deuxième consiste à simplifier au maximum le système des réactions chimiques pour ne garder que les réactions principales et à supposer les autres réactions à l'équilibre. La troisième, la plus rationnelle, consiste à écrire qu'une partie des espèces sont hors d'équilibre, qu'une autre partie a un taux de production nul et que les espèces restantes sont à l'équilibre. A propos de ces différentes méthodes, il est important de faire les remarques suivantes :

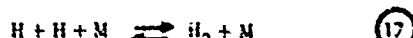
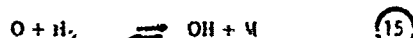
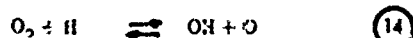
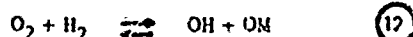
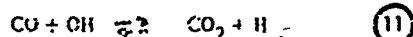
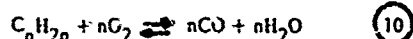
1■ Le calcul de la composition à l'équilibre repose sur un système parfaitement déterminé qui pour N substances de C éléments comporte C équations de conservation des espèces et $N-C$ équations d'équilibre qui sont formées à partir d'un système de base en dehors de toute considération chimique.

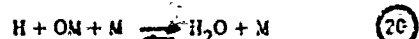
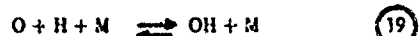
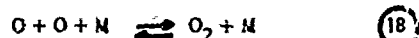
Le calcul de la composition hors d'équilibre repose sur les lois de la cinétique chimique qui n'imposent pas le nombre de réactions chimiques, la matrice des coefficients stoechiométriques entrant dans les réactions chimiques permet de s'en rendre compte, des réactions chimiques peuvent être obtenues par combinaison de plusieurs autres mais elles ne peuvent être éliminées par suite des valeurs différentes des vitesses spécifiques de réaction, après réduction cette matrice des coefficients stoechiométriques est de rang $N-C$. Lorsque l'on utilise les équations de l'équilibre les équations obtenues en annulant le taux de production et les équations de la cinétique chimique, il faut bien prendre soin de construire un système cohérent et de ne pas utiliser sous une forme différente deux fois la même équation.

2■ Les simplifications du système chimique en écoulement relaxé sont utiles mais il faut les faire avec le plus grand soin et, dans certains cas, un système d'une écriture plus complexe n'offre pas pour cela plus de difficultés à la résolution.

b) Cinétique de formation du CO

Dans la zone primaire de combustion, le CO est surtout formé par un processus d'oxydation du combustible et correspond donc à un processus de combustion que l'on peut représenter par le système d'équations :





faisant appel à trois types de réactions :

- une oxydation partielle de l'hydrocarbure (10)
- une réaction limitant la destruction du CO (11)
- une série de réactions produisant des radicaux libres ne contenant pas de carbone (12) - (20).

Dans la zone secondaire, la production de CO est due principalement à la réaction (11), la réaction :



est également possible mais par suite du niveau de température rencontré, la concentration de HO_2 est négligeable compare à OH.

Le taux de production de CO est donc donné par :

$$(39) \quad \dot{W}_{CO} = \kappa_{CO} \left(k_{11} C_{CO} C_{OH} + k'_{11} C_H C_{CO_2} \right).$$

Dans le cas d'un réacteur tubulaire en remarquant que : $C_{CO} + C_{CO_2} = C_{CO}^0 + C_{CO_2}^0$

$$(40) \quad C_{CO} = C_{CO}^0 + C_{CO_2}^0 e^{-Ae}$$

avec

$$A = k_{11} C_{CO}^0 (1 + C_{CO}^0 / C_{CO_2}^0).$$

Dans les conditions rencontrées dans la zone de combustion secondaire les temps d'oxydation du CO sont courts par rapport au temps de séjour ; pour des pressions comprises entre 1-5 bars et pour des températures d'entrée de l'air comprises entre 600 et 1000°K, CO est converti en CO_2 en un temps de l'ordre de la milliseconde. ($k_{11} = 5,6 \cdot 10^8 \exp(-540/T)$).

3.1.2. Taux de production en écoulement turbulent

Dans un milieu turbulent, le taux de production est évalué en tenant compte des concentrations moyennes et, en général, la contribution due aux fluctuations de concentrations est négligée.

Si nous caractérisons la concentration C_i par sa valeur moyenne \bar{C}_i et la fluctuation C_i' de sorte que $C_i = \bar{C}_i + C_i'$, pour une réaction du deuxième ordre du type :



le taux de production moyen est égal pour l'espèce C par exemple à :

$$(41) \quad \langle \dot{W}_C \rangle = \kappa_C [(k + k') (\bar{C}_A + C_A') (\bar{C}_B + C_B')]]$$

Examinons le cas où, par suite du mélange, les fluctuations de température sont négligeables, l'équation précédente devient :

$$(42) \quad \langle \dot{W}_C \rangle = \kappa_C \bar{k} \bar{C}_A \bar{C}_B (1 + \epsilon_{AB})$$

avec

$$\epsilon_{AB} = \langle C_A' C_B' \rangle / \bar{C}_A \bar{C}_B.$$

Le terme relatif à la moyenne des produits des fluctuations des concentrations est en général négligé. Cependant, dans l'évaluation du taux de production, le coefficient de corrélation des concentrations ϵ_{AB} peut être positif, négatif et même approcher la valeur -1, ce qui conduit à un taux de production moyen nul bien que les réactants soient en moyenne en concentration non nulle ; la turbulence peut en effet être telle qu'un point de l'espace voit alternativement l'espèce A puis l'espèce B, ce qui conduit à $\epsilon_{AB} \rightarrow -1$. C_A et C_B satisfont à l'équation du bilan, en multipliant l'équation de C_A par C_B , celle de C_B par C_A et en additionnant terme à terme on obtient l'équation du bilan du produit $C_A C_B$, en passant aux fluctuations

$$(43) \quad \frac{d}{dt} \langle C_A' C_B' \rangle = \partial_m \nabla^2 \langle C_A' C_B' \rangle - 2 \partial_m \langle \bar{C}_A' \cdot \nabla C_B' \rangle + \partial_c \bar{C}_A \cdot \nabla \bar{C}_B - \bar{C}_B \langle \nabla C_A' \rangle - \bar{C}_A \langle \nabla C_B' \rangle - \bar{k} [(\bar{C}_A + \bar{C}_B) \langle C_A' C_B' \rangle - \bar{C}_A \langle C_B'^2 \rangle - \bar{C}_B \langle C_A'^2 \rangle - \langle C_A' C_B' (C_A' + C_B') \rangle]$$

d/dt correspondant à la dérivée d'Euler, ∂_m est le coefficient de diffusion moléculaire, ∂_c est un coefficient de diffusion turbulente tel que :

$$(44) \quad \langle \nabla C_A' \rangle = -\partial_c \nabla \cdot \bar{C}_A, \quad \langle \nabla C_B' \rangle = -\partial_c \nabla \cdot \bar{C}_B.$$

La résolution de cette équation a été effectuée dans le cas où on néglige les triples corrélations et en tenant compte des équations du bilan pour $\langle C_A'^2 \rangle$ et $\langle C_B'^2 \rangle$ (il y a trois temps caractéristiques, τ_m relatif à la diffusion moléculaire, τ_c correspondant à la diffusion turbulente et τ_r un temps caractéristique de la réaction chimique. La comparaison de ces trois temps permet de définir certains types d'écoulement :

• Lorsque la diffusion turbulente est le phénomène prépondérant, le produit $\langle C'_A C'_B \rangle$ est positif si A et B sont introduits prémélangés dans la zone de réaction et négatif lorsqu'ils sont introduits séparément. L'effet de diffusion turbulente se traduit par un accroissement de la valeur absolue de $\langle C'_A C'_B \rangle$.

• Lorsque la réaction chimique est le phénomène prépondérant $\langle C'_A C'_B \rangle$ tend vers une valeur limite qui dépend des valeurs initiales des produits de fluctuations des concentrations $\langle C'_A C'_A \rangle$, $\langle C'_B C'_B \rangle$, $\langle C'_A C'_B \rangle$.

• Lorsque la diffusion moléculaire est le phénomène prépondérant, $\langle C'_A C'_B \rangle$ décroît et tend vers zéro, dans ce cas l'hypothèse d'un taux de production calculé à partir des valeurs moyennes est justifiée.

Il est donc important, dans le calcul du taux de production chimique, de tenir compte du produit $\langle C'_A C'_B \rangle$ qui, suivant la structure de l'écoulement peut être négatif ou positif, le signe dépendant des conditions d'injection ainsi que de l'importance relative des phénomènes de diffusion moléculaire et turbulente et de la cinétique chimique turbulente (fig. 14).

Le calcul du taux de production en écoulement turbulent est discuté aux références [2], [26].

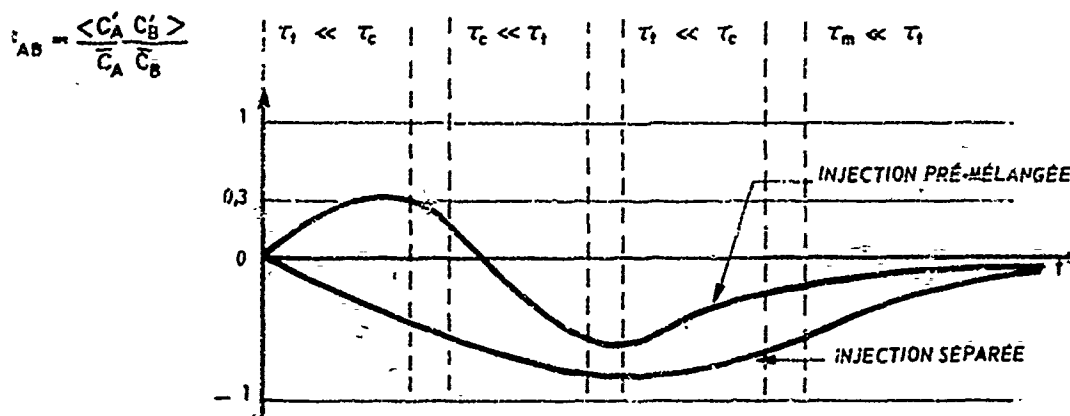


Fig. 14 - Evolution de $\langle C'_A C'_B \rangle$ le long d'une ligne de courant pour une injection prémélangée et séparée.

3.2. Aspect physique du mélange en milieu turbulent

Une description complète des écoulements turbulents n'est pas actuellement possible, il est donc nécessaire en l'absence de théorie satisfaisante de construire des modèles plus ou moins simplifiés. Une amélioration sensible de l'analyse présentée au paragraphe 2 peut être obtenue en utilisant les modèles représentant les écoulements turbulents avec mélange et réactions chimiques [27, 28].

Par suite de la variation de la masse molaire tout le long du foyer, il est utile comme le fait FAVRE [29] de remplacer les moyennes temporelles définies au paragraphe précédent par des moyennes massiques.

Avec les paramètres vitesse et fraction massique on obtient par exemple :

$$(45) \quad \bar{v} = \frac{\langle \rho v \rangle}{\bar{\rho}} + v'' = \tilde{v} + v'' \quad \text{au lieu de :} \quad v = \bar{v} + v''$$

et

$$(46) \quad \tilde{Y}_i = \frac{\langle \rho Y_i \rangle}{\bar{\rho}} + Y_i'' = \tilde{Y}_i + Y_i''$$

La comparaison des moyennes massiques et temporelles conduit à la relation :

$$(47) \quad \tilde{Y}_i = \bar{Y}_i + \frac{\langle \rho' Y_i \rangle}{\bar{\rho}}$$

L'hypothèse $\tilde{Y}_i \approx \bar{Y}_i$ suppose donc que $\langle \rho' Y_i \rangle / \bar{\rho} \bar{Y}_i \ll 1$.

Les flux relatifs aux transferts turbulents de masse, de quantité de mouvement et d'énergie sont représentés par les groupements : $\langle (\rho v)' Y_i' \rangle$ pour le transfert de masse, $\langle (\rho v)' u' \rangle$ pour le transfert de quantité de mouvement et $\langle (\rho v)' \epsilon' \rangle$ pour le transfert d'énergie. Pour faciliter la résolution du système d'équations traduisant le bilan de masse, la forme donnée plus haut est préférée à $\langle \rho' (Y_i)' \rangle$. Il est possible, par analogie avec l'écoulement laminaire, d'introduire des coefficients de transfert turbulent \mathcal{D}_t , \mathcal{M}_t , λ_t tels que

$$(48) \quad \mathcal{D}_t = - \langle (\rho v)' Y_i' \rangle / \bar{\rho} \frac{\partial \tilde{Y}_i}{\partial y}, \quad \mathcal{M}_t = - \langle (\rho v)' u' \rangle / \bar{\rho} \frac{\partial \tilde{u}}{\partial y}, \quad \lambda_t = \langle (\rho v)' \epsilon' \rangle / \bar{\rho} \frac{\partial \tilde{T}}{\partial y}$$

ainsi que les nombres adimensionnels de Prandtl Pr_t , Schmidt Sc_t et Lewis Le_t .

Suivant l'hypothèse de DONALDSON [30], la moyenne du produit des gradients des fluctuations de concentration est remplacée par :

$$(49) \quad \langle \nabla Y_A' \cdot \nabla Y_B' \rangle = \frac{\langle Y_A' Y_B' \rangle}{\lambda^2}$$

où λ est une longueur caractéristique telle que

$$\lambda^2 = C_1 \delta^2 / (C_2 + C_3 R_{ch})$$

où

$$R_{ch} = \frac{\bar{\rho} [\langle u'^2 \rangle + \langle v'^2 \rangle]^{1/2} \delta}{\mu}$$

où δ est l'épaisseur de mélange. Le coefficient de viscosité turbulent μ_t est déterminé par la loi de Prandtl ou des modèles plus complexes :

$$\mu_t = \rho l^2 \left| \frac{\partial \bar{u}}{\partial y} \right|, \quad \partial_t = \mu_t / \text{Sc}_0, \quad \lambda_t = \mu_t / \text{Pr}_t$$

avec

$$l = C_4 \delta$$

Les constantes $C_1, C_2, C_3, C_4, \text{Pr}_t, \text{Sc}_0$ sont d'après DONALDSON [30] et PATANKAR-SPALDING [31] égales à : 0,0041 ; 2,5 ; 0,008 ; 0,09 ; 0,83. L'intervention de l'énergie cinétique de la turbulence $\bar{k} = \frac{1}{2} [\langle u'^2 \rangle + \langle v'^2 \rangle]$ impose une équation du bilan supplémentaire relative à \bar{k} . D'après LEE et HARSHA [32] cette équation s'écrit dans un écoulement bidimensionnel :

$$(50) \quad \langle u \rangle \frac{\partial \bar{k}}{\partial x} + \langle v \rangle \frac{\partial \bar{k}}{\partial y} = \frac{\partial}{\partial y} \left(\frac{\mu_t}{\text{Pr}_k} \frac{\partial \bar{k}}{\partial y} \right) + \mu_t \left(\frac{\partial \bar{u}}{\partial y} \right)^2 - D_k$$

avec

$$D_k = \alpha \bar{k}^{3/2} l_k$$

l'ordre de grandeur des constantes est le suivant : $\alpha = 1,5$, $\text{Pr}_k = 0,7$, l_k est de l'ordre de δ .

De nombreux chercheurs [28] [32] [33] [34] ont appliqué ce modèle introduisant l'énergie cinétique turbulente pour décrire la combustion turbulente dans les foyers et de ce fait ces modèles peuvent être également utilisés pour prédire la production des espèces polluantes. Il est certainement trop tôt pour répondre de leur valeur et des confrontations avec l'expérience sont encore nécessaires. On dispose en particulier de peu de données sur l'intensité de la turbulence dans les foyers et de mesures de cette intensité sont nécessaires pour aller plus loin. Les modèles présentés sont utilisés en fait sous leur forme incomplète et les équations tenant compte d'une façon rigoureuse de la variation de \bar{k} sont très complexes.

Dans l'équation du bilan de l'énergie cinétique turbulente il serait également important de pouvoir assurer qu'il n'y a pas de couplage entre \bar{k} et l'énergie libérée par la réaction chimique.

Dans ce court paragraphe, nous avons voulu souligner les améliorations que l'on pouvait attendre d'une représentation plus réaliste du taux de production chimique en écoulement turbulent et du processus de mélange turbulent pour prédire la formation des espèces polluantes. Ces améliorations ne vont pas sans une grande complexité, c'est pourquoi les modèles simplifiés présentés au paragraphe 2 seront encore utilisés dans la plupart des cas.

4. OPTIMISATION DU FOYER EN VUE DE LA PRODUCTION MINIMALE DE POLLUANTS [35]

Dans une représentation de foyers à partir de réacteurs parfaitement mélangés et de réacteurs tubulaires, la recherche de la stratégie optimale pour produire le moins d'espèces polluantes est relativement simple : ce problème peut être résolu en utilisant des techniques classiques d'optimisation comme les méthodes de programmation dynamique, le principe du maximum ou diverses versions des méthodes du gradient.

Pour résoudre ce problème d'extremum nous allons utiliser ici l'algorithme de KATZ [36] [37] bien adapté à une série de réacteurs parfaitement mélangés. Dans sa généralité un foyer peut être représenté par une succession de réacteurs comme indiqué sur la figure 15. Prenons N réacteurs et caractérisons chaque variable de composition par x_j , le repère placé en exposant caractérisant le réacteur, pour le réacteur n la composition est x_j^n , il entre dans ce réacteur pour l'espèce j , x_j^{n-1} et il sort x_j^n , j variant de 1 à L . Chaque réacteur est caractérisé par le temps de séjour τ^n et la température T^n puisque nous considérons une série de réacteurs parfaitement mélangés. Dans chacun des réacteurs peuvent entrer également des espèces u et sortir les espèces v , u ne vient pas d'un réacteur placé en amont et v ne pénètre pas dans le réacteur placé en aval. Des circuits de recirculation peuvent être également prévus sur certains de ces réacteurs.

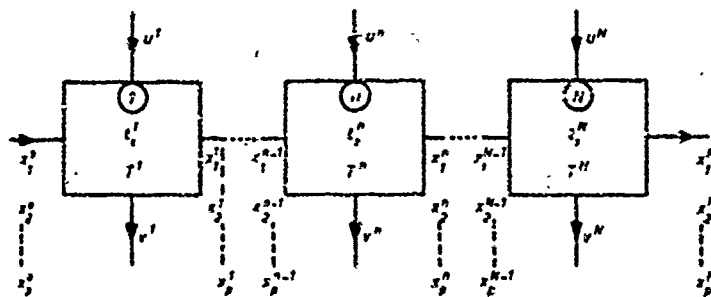


Fig. 15 - Représentation schématique en vue de l'optimisation d'un foyer à combustion étagée.

Dans ce cas précis, il s'agit de choisir le temps de séjour t_i^n de chacun des réacteurs de manière à obtenir à la fin des N réacteurs une espèce particulière (par exemple NO) ayant une concentration minimale (x_N^n minimal). Cet extremum peut être recherché en imposant des contraintes comme la température de fin de réaction T^n limitée à une certaine valeur, ou en imposant, pour certaines espèces, un niveau d'efficacité de transformation (efficacité de combustion). Pour limiter ce problème nous allons considérer deux types d'espèces, l'espèce repérée par l'indice 1 qui traduit l'évolution de la combustion, le taux de production, calculé à partir d'une seule réaction chimique du type $H + O \rightarrow P$.

Dans le cas du réacteur homogène d'ordre 2 nous obtenons en régime permanent :

$$(51) \quad x_2^{n+1} = x_2^n + t_2^n f(x_1^n, T^n)$$

caractérise donc le degré d'avancement de la réaction de combustion. Pour chaque réacteur, l'équation de continuité et l'équation de conservation de l'énergie, fait apparaître une relation linéaire entre T^n et le degré d'avancement de la réaction de combustion x_1^n , de sorte que l'équation précédente devient :

$$(52) \quad x_2^{n+1} = x_2^n + t_2^n f(x_1^n) = x_2^n + t_2^n f^n$$

avec $n = 1, 2, \dots, N$ et $x_1^n = \alpha$, valeur initiale à l'entrée du premier réacteur. L'espèce polluante a pour composition dans chacun des réacteurs x_1^n et le taux de production de cette espèce est une fonction d'une valeur locale du degré d'avancement de la réaction x_1^n et de la température T^n de sorte que, d'une manière générale, la concentration de l'espèce polluante est régie dans chaque réacteur par :

$$(53) \quad x_2^{n+1} = x_2^n + t_2^n g(x_1^n) = x_2^n + t_2^n g^n$$

où f^n et g^n sont des fonctions de x_1^n .

A partir du système représenté par les équations (52) et (53) il faut donc déterminer les temps de séjour respectifs de manière à ce que x_2^n soit minimum.

Exprimons tout d'abord x_1^n et x_2^n en fonction de x_1^{n-1} , x_2^{n-1} et t_2^n

$$(54) \quad \begin{cases} x_1^n = F_1(x_1^{n-1}, t_2^n) \\ x_2^n = F_2(x_1^{n-1}, x_2^{n-1}, t_2^n) = x_2^{n-1} + t_2^n g[F_1(x_1^{n-1}, t_2^n), t_2^n] \end{cases}$$

Nous introduisons à ce stade un nouvel ensemble de variables y_i^n tel que :

$$(55) \quad y_i^{n+1} = \sum_{j=1}^2 \frac{\partial F_j(x_1^n, t_2^n)}{\partial x_j^n} y_j^n$$

En partant du système (54) nous obtenons :

$$(56) \quad \begin{cases} y_1^{n+1} = y_1^n \frac{\partial F_1(x_1^n, t_2^n)}{\partial x_1^n} - y_2^n t_2^n \frac{dg^n}{dx_1^n} \frac{\partial F_1(x_1^n, t_2^n)}{\partial x_1^n} \\ y_2^{n+1} = y_2^n \end{cases}$$

Les x_2^n sont aux conditions initiales et les y_i^n $\begin{cases} y_1^n = 1, i=1 \\ y_2^n = 0, i=2 \end{cases}$, donc $y_1^n = 1$

En différentiant l'équation (52) par rapport à x_1^n nous obtenons :

$$(57) \quad 1 = \frac{\partial x_1^n}{\partial x_1^n} \left(1 + t_2^n \frac{df^n}{dx_1^n} \right)$$

de sorte que :

$$(58) \quad \frac{\partial x_1^n}{\partial x_1^n} = \frac{\partial F_1(x_1^n, t_2^n)}{\partial x_1^n} = \frac{1}{1 + t_2^n \frac{df^n}{dx_1^n}}$$

La première équation de (56) devient :

$$(59) \quad y_1^{n+1} = \frac{y_1^n - t_2^n (dg^n/dx_1^n)}{1 + t_2^n (df^n/dx_1^n)}$$

Les divers temps de séjour t_2^n sont déterminés par la condition rendant l'Hamiltonien H^n minimum :

$$(60) \quad H^n = \sum_{j=1}^2 y_j^n F_j(x_1^n, t_2^n) \quad \text{c'est-à-dire :} \quad \partial H^n / \partial t_2^n = 0$$

Dans le cas traité, l'Hamiltonien devient :

$$(61) \quad H^n = y_1^n F_1(x_1^n, t_2^n) + x_2^n - t_2^n g[F_1(x_1^n, t_2^n)]$$

et :

$$(62) \quad \frac{\partial H}{\partial t_2} + \gamma_1 \frac{\partial F_1}{\partial t_2} - g[F_1] - \gamma_2 \frac{d\gamma}{dx_2} \frac{\partial F_1}{\partial t_2} = 0$$

En différenciant l'équation (52) on obtient l'expression de $\partial F_1 / \partial t_2$ et en portant cette expression dans (62) le temps de séjour optimal, t_2^{opt} , s'écrit :

$$(63) \quad t_2^{opt} = \frac{\gamma_1 t_1^{opt} + g}{f \frac{d\gamma}{dx_2} - g \frac{d\gamma}{dx_2}}$$

L'élimination de t_2^{opt} entre (59) et (63) détermine γ_1^{opt} :

$$(64) \quad \gamma_1^{opt} = -g/f \quad \gamma_2^{opt} = g^{opt}/f^{opt}$$

d'où l'expression du temps de séjour en posant : $R = g/f$

$$(65) \quad t_2^{opt} = \frac{1}{f} \left(\frac{R - R^{opt}}{dR/dx_2} \right)$$

La relation donnant le degré d'avancement de la réaction principale obtenue à partir de (52) s'écrit :

$$(66) \quad x_1^{opt} = x_1 + (R - R^{opt}) / (dR/dx_1) \text{ au départ : } x_1^{opt} = x_1 + R / (dR/dx_1);$$

dans le plan $R(x_1)$ la détermination de x_1^{opt} peut se faire par une construction géométrique simple.

Et pour x_2^{opt} nous obtenons à partir de (63) :

$$(67) \quad x_2^{opt} = x_2 + R(R - R^{opt}) / (dR/dx_2).$$

Le processus itératif de résolution est le suivant, pour les N réacteurs donnés à partir de x_1^{opt} , on calcule à partir de l'équation (66) les x_1^{opt} successifs, le choix de x_1^{opt} est convenable si on retrouve la valeur d'entrée dans le système x_1^{opt} . On calcule ensuite les temps de séjour t_2^{opt} à partir de l'équation (65), ce qui détermine le volume de chacun des réacteurs ; à l'aide de l'équation (67), on calcule ensuite l'évolution de l'espèce polluante.

La résolution de ces problèmes d'optimisation est très utile pour le constructeur car, après avoir découpé le foyer en plusieurs sous-ensembles, il est possible de déterminer la disposition de ces sous-ensembles, leur géométrie et leur condition de fonctionnement, de manière à réaliser un compromis entre plusieurs contraintes : longueur du foyer, température de fin de combustion, refroidissement des parois, pertes de charges, limite de stabilité, pression limite de fonctionnement, pollution. Ces problèmes d'optimisation ont une portée plus générale que l'étude de la pollution minimale.

5. CONCLUSION

Nous allons pour conclure reprendre un certain nombre de points qui nous paraissent importants.

• Précisons tout d'abord que nous avons volontairement limité notre exposé à la seule question relative à l'élaboration des modèles. Nous n'avons pas cherché à exploiter cette schématisation afin d'en déduire des conclusions sur les performances des foyers les moins polluants, ou sur la conception de tels foyers. Cette partie est abordée dans d'autres mémoires présentés à ce meeting.

• Le fait de schématiser le foyer par un assemblage de réacteurs nous paraît une solution simple mais réaliste, de tels modèles sont utiles aux constructeurs pour déterminer les paramètres qui ont une action prépondérante dans la production des espèces polluantes. Leur étude peut également les guider dans la conception de nouveaux foyers moins polluants. Ces modèles peuvent être améliorés en tenant compte des temps nécessaires au mélange turbulent et aux réactions chimiques.

• Les modèles du type SPALDING basés sur la propagation de fluxes turbulents sont également très intéressants mais il est nécessaire de pouvoir évaluer plus correctement le taux de production chimique d'une part et de représenter avec plus de rigueur le mélange turbulent d'autre part. Il semble toutefois que les études de mélanges turbulents sans combustion peuvent être utilisées lorsque le milieu est le siège de réactions chimiques. Il faut cependant qu'un plus grand nombre d'expériences soient effectuées pour confirmer cette hypothèse.

• Nous n'avons pas parlé du peu de précision avec laquelle sont connues les vitesses spécifiques de réaction, il n'est pas sûr par exemple que les valeurs de k déterminées au tube à choc soient utilisables dans l'étude des foyers, il serait souhaitable que ces vitesses spécifiques soient déterminées dans des conditions aussi voisines que possible de celles rencontrées dans les foyers.

• La représentation du foyer par un ensemble de réacteurs est féconde lorsque l'on aborde les problèmes d'optimisation du foyer ; il est certain que la résolution de ces problèmes d'extremum conduit à une meilleure définition du foyer en fonction des critères choisis.

REFERENCES

- [1] BARRERE M. - *Optimisation des foyers de turbines à gaz*. Colloque ATMA, session 1972.
- [2] BARRERE M., PRUD'HOMME R. - *Equations fondamentales de l'aérothermochimie*. Masson et Cie (1972).
- [3] PRATT D.G., BOWMAN B.R., CROWE C.T., SONNICHSEN T.C. - *Prediction of nitric oxide formation in turbojet engines by P3R analysis*. AIAA paper n° 71-713.
- [4] EDELMAN R., ECONOMOS C. - *A mathematical model for jet engine combustor pollutant emissions*. AIAA paper n° 71-714.
- [5] EVANGELISTA J.J., SHINNAR R., KATZ S. - *The effect of imperfect mixing on stirred combustion reactors*. XIIth Symposium on Combustion. The Combustion Institute, p. 901-911.
- [6] ESSENHIGH R.M. - *A new application of perfectly stirred reactor. Theory to design of combustion chambers*. Technical report FS67-1 (U). The Pennsylvania State University (1967).
- [7] HAMMOND D.C., Jr., MELLOR A.M. - *Analytical calculations for the performance and pollutant emissions of gas turbine combustors*. AIAA paper n° 71-711.
- [8] HEYWOOD J.B., FAY J.A., LINDER L.H. - *Jet aircraft air pollutant production and dispersion*. AIAA paper n° 70-115.
- [9] FLETCHER R.S., HEYWOOD J.B. - *A model for nitric oxide emissions from aircraft gas turbine engines*. AIAA paper n° 71-123.
- [10] HAMMOND D.C. Jr., MELLOR A.M. - *A preliminary investigation of gas turbine combustor*. Combustion Science and Technology. Vol. 2 n° 2 et 3, nov. 1970. p. 67-81.
- [11] HEYWOOD J.B. - *Gas turbine combustor modeling for calculating nitric oxide emissions*. AIAA paper n° 71-712.
- [12] PATANKAR S.V., SPALLING D.B. - *A computer model for three-dimensional flow in furnaces*. Imperial College of Science and Technology. March 1972 - C/TN/A/8.
- [13] BORGHİ R. - *Etude théorique de l'évolution résiduelle des produits polluants dans les jets de turboréacteurs*. Meeting AGARD - Pollution, London, April 1972.
- [14] ALTENKIRCH R.A., SHADED S.M., SAWYER R.F. - *Nitric oxide formation around droplets burning at elevated pressures*. Combustion Science and Technology. Vol. 5 n° 4, June 1972, p. 147-155.
- [15] KESTEN A.S. - *Analysis of formation in single droplet combustion*. Combustion Science and Technology. Vol. 6, p. 115-123.
- [16] SPALDING D.B. - *Theory of particle combustion at high pressures*. ARSJ n° 29, p. 828.
- [17] WERSTORF B.L., HOWARD G.B., WILLIAMS J.C. - *Physical Mechanisms of carbon formation in flames*. T.R. MIT 66 PU June 1972. Project Squid.
- [18] LINDEN L., HEYWOOD J.B. - *Smoke emission from jet engines*. Combustion Science and Technology. Vol. 2 n° 5 et 6, January 1971, p. 401-413.
- [19] BRYANT J.T. - *The combustion of premixed leaner graphite dust flames at atmospheric pressure*. Combustion Science and Technology. Vol. 2, n° 5 et 6, January 1971, p. 389-401.
- [20] CRYNES S.L., MADDOX R.N. - *Status of NO_x control from combustion sources*. Chemical Technology, August 1971, p. 502-509.
- [21] MARTENEY P.J. - *Analytical study of the kinetics of formation of nitrogen oxide in hydrocarbon-air combustion*. Combustion Science and Technology. Vol. 1 (1973), p. 461-469.
- [22] LIVESY J.B., ROBERTS A.L., WILLIAMS A. - *The formation of oxides of nitrogen in some oxy-propane flames*. Combustion Science and Technology. Vol. 4, n° 1, September 1971, p. 9-17.
- [23] LAVOIE G.A., HEYWOOD J.B., KECK J.C. - *Experimental and theoretical study of nitric oxide formation in internal combustion engines*. M.I.T. Fluid Mechanics Laboratory, Publication n° 69-10 (1969).
- [24] ROBERTS R., ACEYO L.D., KOLLBACK R. - *An analytical model for nitric oxide formation in a gas turbine combustion chamber*. AIAA paper 71-715.
- [25] WESTENBERG A.A. - *Kinetics of NO and CO in lean, premixed hydrocarbon-air flames*. Combustion Science and Technology. Vol. 4 (1971), p. 59-64.
- [26] BARRERE M., BORGHİ R. - *Taux de production chimique en régime turbulent*. Combustion Institute, section française, réunion du 14-15 septembre 1972.
- [27] RECHENBACH B.V., BELII C.A., BESPALOV I.V. - *Physique de la dynamique des jets et de la stabilisation des flammes*. Machinostroenie, Moscou 1964.
- [28] BRAY K.N.C. - *Engineering applications of nonequilibrium flow theory*. International center for mechanical sciences Udine (Italy), septembre-octobre 1972.

- [29] FAVRE F. - *Equations des gaz turbulents compressibles*. J. de Mécanique n° 4 (1965), p. 361-391.
- [30] DUP C., DONALDSON, SULLIVAN R.D., ROSENBAUM M. - *A theoretical study of the generation of atmospheric clear air turbulence*. AIAA journal, vol. 10 n° 2 February 1972.
- [31] PATANKAR S.V., SPALDING D.B. - *Heat and mass transfer in boundary layers*. 2nd edition - Intertext Books, London 1970.
- [32] LEE S.C., HARSHA P.T. - *Use of turbulent kinetic energy in free mixing studies*. AIAA journal. Vol. 8 n° 6 June 1970, p. 1026-1032.
- [33] BRADSHAW P., FERRISS D.H., ATWELL N.P. - *Calculation of boundary layer development using the turbulent energy equations*. J. Fluid Mech. 28 1967, p. 593.
- [34] HARSHA P.T. and LEE S.C. - *Correlation between turbulent shear stress and turbulent kinetic energy*. AIAA journal. Vol. 8 (1970), p. 1508.
- [35] FERRI A. - *Better marks on pollution for the SST*. Astronautics & Aeronautics, July 1972.
- [36] KATZ S. - *Ind. Eng. Chem. Fundamentals* 1. 1962, p. 226.
- [37] WANG C.S., LIANG-TSENG-FAN - *Optimization of some multistage chemical processes*. Ind. Eng. Chem. Fundamentals. Vol. 3, n° 1, February 1964, p. 38-42.



Discussion on Paper 27

"Modélisation des foyers de turboréacteur en vue de l'étude de la pollution"
presented by M.L. Barrère

N.Chigier: The oxides of nitrogen concentrations that you have computed for liquid sprays are based upon the model of an envelope flame around individual droplets. Experimental studies at Sheffield have shown that in a cloud of droplets no combustion takes place within the spray. The flame front is located at the outer periphery of the spray sheath and the combustion of the spray is similar to that of a gaseous turbulent diffusion flame. Within the cloud of drops temperatures are too low and oxygen concentrations are too low to allow combustion to take place within the spray.

If we wish to achieve the controlled temperature change along the length of the combustor as recommended by Mr. Barrère, we can inject the liquid spray and by controlling the entrainment of the air into the spray we can obtain an effective control of temperature starting with low temperatures and increasing the temperature towards the exit of the combustor.

M.Barrère: Je suis d'accord avec la remarque du Dr N.Chigier; dans certain cas, il n'existe pas de flammes de diffusion autour des gouttes, mais alors, suivant le processus de combustion turbulente, il peut exister des paquets avec combustion à la périphérie en proportion stoechiométrique qui sont une source de production de NO. Nous pensons, et cela constitue notre deuxième commentaire, qu'il faut réaliser tout le long du foyer une augmentation progressive de température pour réduire au maximum la production de NO.

A.Ferri: The combustion around the droplet is complex. We can have combustion in a cloud of droplets, then the diffusion scheme does not work. Turbulence is an important parameter, and the scale of turbulence related to the size of the droplet is a parameter of combustion.

M.Barrère: La combustion autour des gouttes est complexe dans un milieu turbulent et la position du front de flamme par rapport à la surface de la goutte est un paramètre important dans la production de NO. Nous avons voulu dans notre présentation insister tout particulièrement sur l'importance de l'hétérogénéité de l'écoulement dans la production de NO, hétérogénéité dont il faut tenir compte dans le modèle; cette hétérogénéité peut être due soit au procédé d'injection (gouttes, injection séparée de l'air et du combustible), soit à la turbulence de l'écoulement (formation de paquets).

J.B.Heywood: High speed movies I have seen of spray combustor indicate some combustion is nonluminous, which suggests that there is some burning in turbulent eddies where the fuel is premixed, which changes conditions downstream.

M.Barrère: A partir de photographies de combustion de brouillard en milieu turbulent, il n'est pas possible d'affirmer, bien qu'on observe des flammes non lumineuses, qu'il n'y a pas de réactions chimiques exothermiques autour des gouttes qui produisent du NO. Ce qu'il faut éviter c'est d'avoir des zones locales en proportion stoechiométrique, ce qui peut arriver dans le cas de combustion de gouttes, de combustion de paquets gazeux riches en combustible, ou de combustion dans des zones tourbillonnantes de gaz prémélangés.

A. Quillevère: Des mesures sur l'émission des oxydes d'azote ont été faites à l'échappement d'une turbine à gaz Hispano-Suiza - Division du Groupe SNECMA - dont la chambre de combustion est de technologie classique et comporte des injecteurs mixtes gaz-fuel. Dans les cas de fonctionnement au gaz seul, l'indice d'émission est inférieur à celui obtenu au fuel seul, mais seulement de 20 à 30 %. Ces résultats confirment, selon nous, que les processus de combustion ne doivent pas être fondamentalement différents dans les deux cas.

Le modèle de formation proposé par l'auteur dans le cas de l'injection liquide, fondé sur l'existence autour de chaque goutte d'un front de flamme de diffusion, ne nous semble pas pouvoir représenter valablement la réalité.

M. Barrère: On constate déjà que le passage d'un combustible liquide à un combustible gazeux réduit la proportion des oxydes d'azote. La faible réduction observée peut être due à la manière d'injecter le combustible gazeux; en milieu turbulent, on peut avoir des poches de combustible qui brûlent avec une flamme de diffusion exactement comme des gouttes. Il faut, à notre avis, réaliser un prémélange air - combustible gazeux pour pouvoir réduire notablement la production de NO.

SMOKE SUPPRESSANT ADDITIVE EFFECTS ON PARTICULATE EMISSIONS FROM GAS TURBINE COMBUSTORS

P.J. Pagni, L. Hughes, and T. Novakov

Mechanical Engineering Department
University of California
Berkeley, California 94720
U.S.A.

ABSTRACT

The effects of manganese based additives on the mass, size distribution and chemical composition of particulate emissions from gas turbine combustors are described. Experiments show that the additive, 2-methylcyclopentadienyl manganese tricarbonyl, can increase mass emissions if used excessively. The additive shifts the emitted particle size distribution toward many more much smaller particles, thereby reducing visibility primarily by reducing the size of the emitted particles. X-ray photoelectron spectroscopy studies have determined that the chemical state of the emitted manganese is manganese monoxide. The health effects of this pollutant and the many small carbon particles emitted when the additive is used may be of concern. It is recommended that combustor redesign and collection techniques be employed whenever possible to suppress particulate emissions from aircraft and test facilities.

I. INTRODUCTION

Undesirable emissions from aircraft, automotive and stationary gas turbine engines are produced in the combustion chamber. Generally, neither pollutant compositions nor their concentrations undergo significant changes during subsequent flow through the turbine. One can, therefore, characterize gas turbine emissions by studying the combustion chamber exhaust. A model gas turbine combustor (1) was used in the investigations reported here.

Exhaust Smoke

Exhaust smoke from gas turbine combustors consists of small, graphite like carbon particles. The high visibility of exhaust smoke results from the fact that mean particle diameters are of the order of the wavelengths of visible radiation. The Mie theory (2) for radiation scattering from spherical particles predicts a maximum in the scattering cross-section near a particle size parameter, $\alpha = 2\pi r/\lambda = 3$. Electron micrographs of gas turbine smoke from distillate fuel (3) indicate that smoke particles are irregularly shaped agglomerates, with major dimensions of (1.0 μ) composed of approximately spherical particles of 0(0.01 μ).

There are two competing processes (4) which determine the amount of smoke in the exhaust: a) the formation of carbon particles in the fuel rich regions of the primary zone and b) the heterogeneous combustion of these particles in the fuel lean secondary zone. Thus, the presence of solid carbon in the exhaust may be attributed to either of two factors: the success of the formation mechanism, or the inadequacy of the subsequent oxidation. The kinetics of carbon particulate formation is not well understood (5); however, it is possible to say qualitatively that the carbon particles originate in fuel-rich regions of the primary combustion zone due to the local nonhomogeneity of the fuel-air mixture. Whether this formation process is dominated by agglomeration of small particles nucleated on hydrocarbon ions (6, 7) or by a polymerisation process (8) is not yet clear and is the subject of much current interest. In a gas turbine engine the variables most strongly affecting the formation of solid carbon are operating pressure, fuel composition, fuel-air ratio and the detailed fluid mechanics of the fuel-air mixing in the primary zone.

The oxidation of solid carbon particles is also complex; however, the available information has been applied to the particulate burning in a gas turbine combustor (9-11). These calculations, using the burning rate expression of Nagle and Strickland-Constable, indicate that significant oxidation of carbon particles occurs in the secondary zone of a typical aircraft combustor, eliminating the smaller particles and diminishing the size of the initially larger agglomerates.

With the information these studies provide it should be possible to optimize the combustor temperature and composition fields under the constraint of eliminating particulate emissions. From extensive testing two methods of controlling exhaust smoke have evolved: a) combustion chamber modification and b) the use of smoke suppressing fuel additives. The design approach (12, 13) has minimized particulate emissions by enhancing oxidation via a lower overall fuel-air ratio and by reducing formation through improved mixing to provide a more uniform fuel-air distribution in the primary zone. The alternate approach (14, 15), addition of a small amount of metallic-organic smoke suppressant to the fuel, offers a solution easily applicable to existing combustors.

Manganese-Based Additives

Various additives containing soluble metallic compounds have been developed for smoke inhibition and reduction of combustor system deposits (16, 17). Additives with a composition of ~ 25% manganese by weight, e.g. 2-methylcyclopentadienyl manganese tricarbonyl, have proved to be the most effective smoke suppressants with the least adverse effects on long range engine performance. The mechanism by which this additive reduces smoke is currently not well understood; two possibilities are: 1) surface catalysis of soot oxidation (18, 19) and 2) inhibition of the agglomeration mechanism present with pure carbon particles (7, 20).

Manganese additives have been extensively tested in laboratory combustion chambers, engines and furnaces to determine the effects of the additive on smoke, performance, and deposition. Engine tests using a concentrated blend of manganese additive, 0.08% (vol.) which effectively eliminated visible exhaust smoke were reported by Shayeson (14). Endurance tests using 0.04% (vol.) were performed to determine the degree of additive induced deposit buildup. Inspection after fifty hours of running exhibited no deposit buildup anywhere in the engine and clean combustors essentially free of carbon but coated with a thin, dusty, black or orange deposit of manganese oxide. Flight tests were performed with 0.1% (vol.) CI-2. It was recommended that additives be seriously considered as a practical means of alleviating engine exhaust smoke.

While manganese-based additives seem to be attractive smoke suppressants based on smoke reduction, solubility, availability, and fuel system performance, their long term effect on the environment is a cause for concern (17, 21, 22). It has not been clear whether metal based additives actually reduce total carbon particulate mass emission or simply redistribute particle sizes to reduce their visibility while forming metal oxides which are themselves pollutants. Future utilization may be limited by concern for their role in creating pollutants (23, 24).

Model Experiments

To determine the effects of manganese-based additives on combustor particulate emissions, a model combustor, shown schematically in Fig. 1, was used. Jet fuel type JP-4, with a hydrogen to carbon mole ratio of 2 to 1 served as a convenient fuel. A commercial manganese-based fuel additive, CI-2 (Ethyl Corporation Combustion Improver No. 2) was mixed with the JP-4. The average equivalence ratio, ϕ , in the primary combustion zone was slightly greater than unity (stoichiometric) whereas the overall equivalence ratio due to the dilution air ranged from 0.1 to 0.3. Soot formation occurs in locally rich, $\phi > 1$, carbules in the primary zone. Oxidation of these particles is apparent from the visible continuum radiation emitted through the pyrex housing. The temperature field within the combustor has been reported (1). The exhaust from the combustor is passed through a constricting orifice plate which serves as both a sampling probe holder and a combustor pressure control.

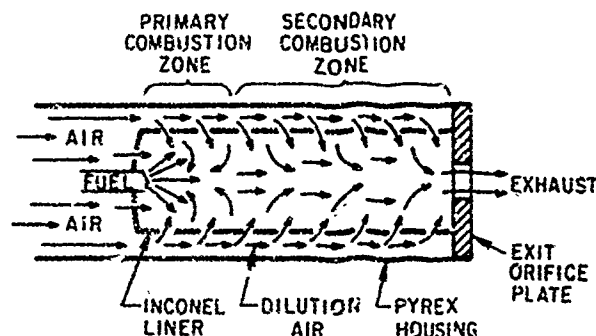


Fig. 1. Schematic of the model gas turbine combustion chamber in which particulate measurements were performed.

Figure 2 shows the particulate mass and gas concentration sampling system comprised of: 1) an isokinetic sampling probe, 2) gaseous analyzers, and 3) a particulate filtration assembly. Tortuous path sintered bronze filters with 7 μ nominal pores were initially used for emitted mass measurements. Nuclepore filters, ~ 50 μ thick, with a .8 μ pore diameter were used for electron microscopy and most mass measurements. Experimental details are reported elsewhere (25, 26).

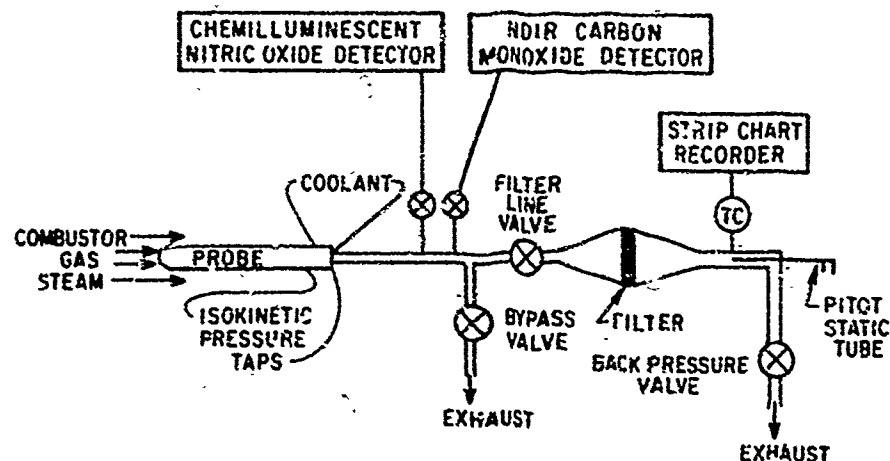


Fig. 2. Sampling system used to obtain particulate mass and gas concentration measurements along the axis of the combustor shown in Fig. 1.

II. PARTICULATE EMISSIONS

Mass Measurements

The emissions index, defined as the grams of species per kilogram of fuel, describes the emitted particulate mass. The values obtained are lower than those reported (27, 28) for typical turbojet and turbofan engines which range from 2-14 (gm/kgm of fuel). There are two reasons for this difference: 1) typical engine chamber pressures are from five to ten-fold those used here, and 2) the model combustor geometry produces a resident time that is longer than typical in an aircraft engine, hence carbon oxidation is enhanced.

Experimental emission indices as a function of the nondimensional position along the combustor axis are presented in Fig. 3. The orifice plate defining the combustor exit plane is located at 4.6 combustor diameters from the fuel inlet nozzle as indicated by the light dashed line. The additive data points are indicated by solid triangles and the JP-4 data points are given by the solid circles. The solid and dashed lines are the best fits to the additive and pure JP-4 results along the combustor axis. For these operating conditions, there is an increase in the emissions index for the runs with the additive blend.

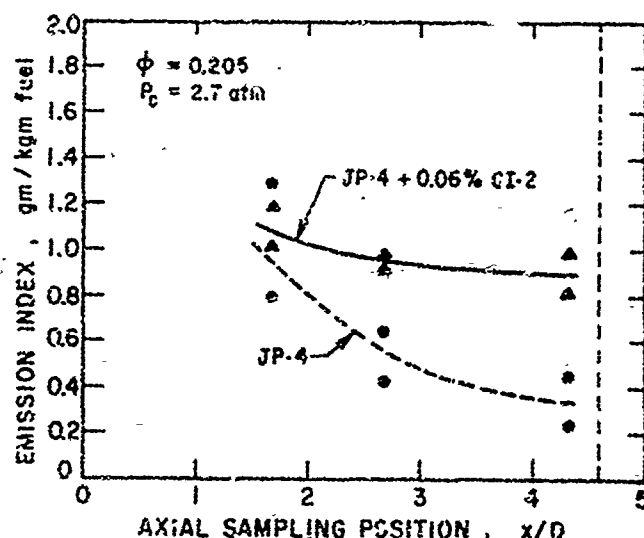


Fig. 3. Sample particulate emission index (gm/kgm of fuel) with and without CI-2 as a function of nondimensional axial probe position, x/D , where x is the distance from the fuel injector and $D = 7.6$ cm is the combustor diameter. The chamber pressure is 2.7 atm.

It was noted that the additive prevented buildup of carbon deposits in the combustor. Examination after ten test hours using JP-4 showed heavy carbon deposition, while after 20 test hours using the additive blend no deposition was apparent. It was suspected that the increase was therefore due to inhibition of carbon deposition within the combustor. Similar manganese additives are used in stationary power plants as deposition inhibitors (29). It is curious that 2-methylcyclopentadienyl manganese tricarbonyl increases mass emissions at concentrations which were reported to have eliminated smoke. These observations can be consistent only if the additive significantly alters the size distribution of the emitted particles.

Size Distributions

To study the mechanism by which additives reduce exhaust visibility, it is useful to measure the size of the emitted particles. Optical techniques are available (30) which permit accurate size distribution determination provided the function form of the distribution and the refractive index of the particles are known *a priori*. One aim of the experiments described here was to determine whether the particle size distribution emitted by a model combustor could be presented by a power law such as

$$n(r) = cr^{-b} \quad (1)$$

where $dN = n(r)dr$ is the number of particles per unit volume with radii in the range r to $r + dr$; b and c are constants.

This distribution was obtained experimentally by Junge (31), and theoretically by Friedlander (32), for a steady state atmospheric aerosol where $b = 4$. The emissions from a combustor cannot be considered well-aged; however, if the dominant physical process occurring in the aerosol is coagulation, the power law given by Eq. (1) is approximately applicable (33) with $b = 2$ over the range of particle sizes significant to radiation scattering. The two mechanisms which effect the particle size distribution in a combustor exhaust are surface oxidation and coagulation. Since the rate of oxidation is proportional to the surface area, oxidation preferentially eliminates the smaller particles. Thus, if oxidation and coagulation occur simultaneously, the expected value of the power law exponent would be $b < 2$.

In these experiments the manganese-based fuel additive was mixed with jet fuel type JP4 at the concentrations shown in Table I. Electron micrographs of the collected particles were taken at several

Table I

Summary of Particle Size Data and Combustor Operating Conditions

Manganese additive (% by vol)	0.0	.0015	.01	.015	.03
c ($\text{cm}^{-3} \mu^b$)	2.7×10^3	1.4×10^2	6.3×10^2	7.8×10^2	6.6×10^2
b	0.36	1.54	1.43	1.16	1.07
r_{\min} (μ)	.05	.07	.03	.04	.04
r_{\max} (μ)	5.0	0.4	1.5	2.5	2.5
correlation coefficient	.65	.99	.95	.93	.96
total number counted	217	431	462	521	523
total flow through filter (cm^3)	2.0×10^4	2.1×10^4	1.8×10^4	2.5×10^4	2.7×10^4
combustor equivalence ratio	.2	.3	.3	.3	.2
combustor pressure (atm.)	3.6	1.3	2.7	3.1	2.6

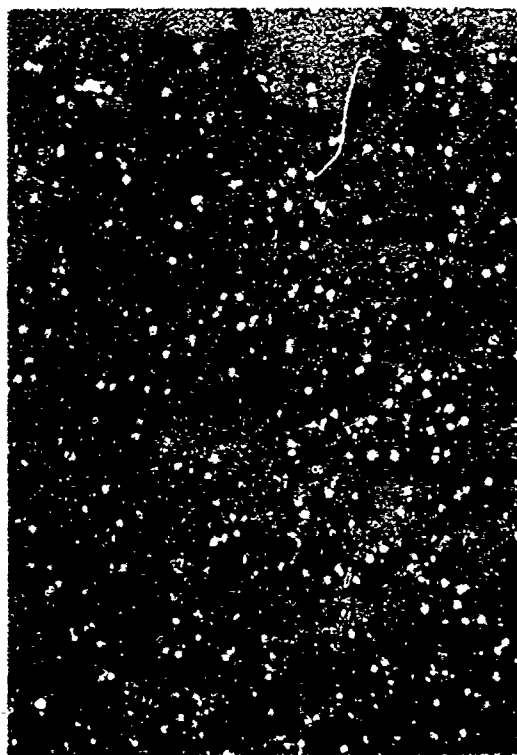


Fig. 4. Electron micrograph at a magnification of ~ 2000 of particles sampled at the combustor exit plane for JP-4 plus 0.06% (vol.) CI-2. The white dots are pores of diameter 0.8μ in the Nuclepore filter. The black areas are large particles, and the gray rings are artifacts of the replication technique.

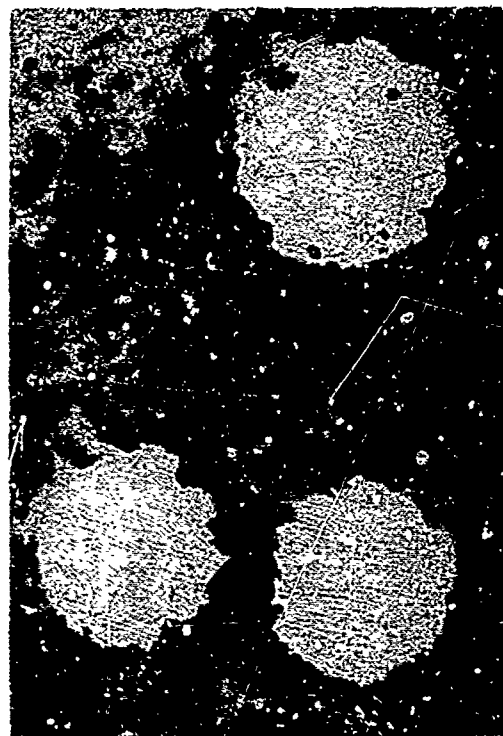


Fig. 5. Electron micrograph at a magnification of $\sim 40,000$ of particles sampled at the combustor exit plane for JP-4 plus 0.061% (vol.) CI-2. Pores have a diameter of 0.8μ . Average particle size is approximately 0.03μ . Apparent concentration in the pores is due to the optical effect of looking down a long pipe.

magnifications. Shadowed silicon monoxide replicas of .8 μ Nuclepore filters were used to minimize sample manipulation. Figures 4 and 5 show typical electron micrographs at ~ 2000 and $\sim 40,000\times$ apparent magnification. The particles in similar photographs were sized and counted using a projected area equivalent radius as a measure of particle size. The constants b and c in Table I are least square fits of Eq. (1) to data obtained at the conditions listed. The maximum in b at low additive concentration is consistent with a minimum observed in mass emissions at a similar concentration (17). The unusual units of c, $\text{cm}^3 \mu\text{b}^{-1}$, were chosen for convenient integration of Eq. (1) over size range to obtain total number or mass concentration. Since the correlation coefficients listed are acceptable, a power law is adequate to approximately describe the particle size distribution. Due to the small data base, the values listed are only indicative of the appropriate order of magnitude of the constants in Eq. (1). More data are required to quantify these results. Photographic counting is also clearly biased toward particles which impact on the surface rather than diffuse to the pore walls. Calculations based on Spurny's approximations (34) for the number of impacted and trapped particles at these sampling conditions show that particles below .03 μ in radius are underestimated by this technique. Accounting for this effect increases b for both JP4 and JP4 + CI2, but does not alter the comparison.

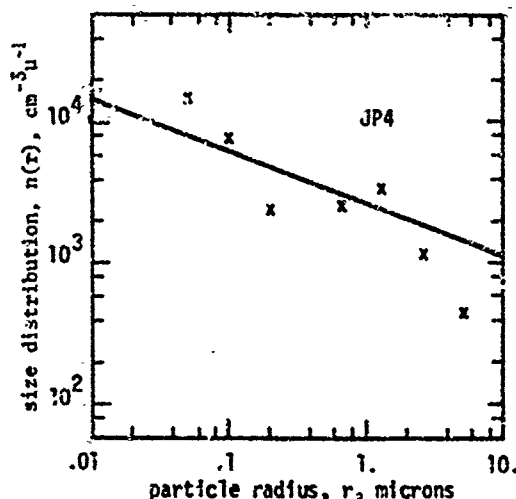


Fig. 6. The size distribution of particles emitted from a combustor burning pure JP4. Note the relatively large number of particles with $r \geq 1 \mu$. The distribution is $n(r) = 2.7 \times 10^3 r^{-1.36} \text{ cm}^{-3} \mu^{-1}$.

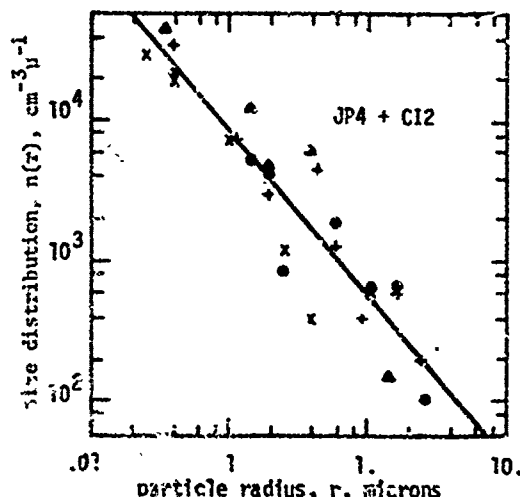


Fig. 7. Mean size distribution of emitted particles using JP4 with the manganese additive, CI2, at: x, 0.0015%; Δ , 0.01%; o, 0.015%; +, 0.03% by vol. Note the relatively large number of particles with $r < .1 \mu$. The distribution is $n(r) = 6.6 \times 10^2 r^{-1.15} \text{ cm}^{-3} \mu^{-1}$.

Figure 6 gives the emitted particle size distribution obtained using pure JP4 fuel. Figure 7 shows the size distribution data obtained using the manganese additive. The distributions at each operating condition show good agreement with a power law. The purpose of combining these data is to permit easy comparison with the size distribution obtained without the additive. The increase of the power law exponent when CI2 is added to JP4 indicates that the net effect of the manganese-based additive is to redistribute the mass emitted to small particle sizes where it is no longer visible. The mechanisms by which the additive alters the size distribution are still not clear. The increase in b upon manganese addition however implies that deposition or agglomeration inhibition occurs in addition to any oxidation catalysis since simply increasing the oxidation rate would decrease b. Detailed measurements of the evolution of the size distribution along the combustor axis are underway to determine the responsible mechanisms.

Chemical Composition

Other questions raised by the observed mass emissions increase include 1.) which of the many possible manganese oxides exist in the exhaust and 2.) what is the amount of manganese emitted. Two recently developed techniques were utilized to provide this information. X-ray photoelectron spectroscopy determined the manganese oxidation state and neutron activation techniques gave a quantitative measure of the total manganese in the exhaust samples.

The method of photoelectron spectroscopy consists in the measurement of the kinetic energies of photoelectrons expelled from a target irradiated with approximately monoenergetic X-rays (35). Since the incident photon energy is known, the determination of the kinetic energy of the photoelectrons provides a direct measure of the electron binding energy. A broad range photoelectron spectrum from an irradiated exhaust sample is shown in Fig. 8. It is evident that the major constituents are manganese, carbon and oxygen. Trace amounts of sulfur are also seen. The manganese photoelectron lines are identified as Mn(2p), Mn(3s) and Mn(3p). While electron binding energies are characteristic of an element, their precise values are modified by the valence electron distribution. The difference in binding energy between an electron on an atom in a molecule and the binding energy of the same electron on the elemental atom is known as the chemical shift. These shifts are highly correlated to the effective charge of the atom in the molecule. For oxidized species the electron binding energies will generally be greater than for the neutral configuration, while the binding energies for reduced chemical species will

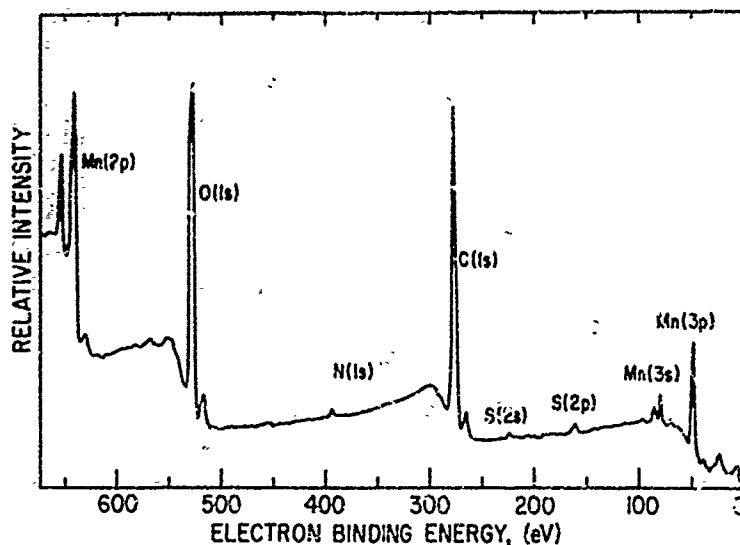


Fig. 8. X-ray photoelectron spectrum of particles collected on a Nuclepore filter from JP-4 with .25% (vol.) CI-2 exhaust. Since only the surface atoms respond, this spectrum is characteristic of the particles alone. Large amounts of manganese, carbon and oxygen are indicated with traces of nitrogen and sulfur.

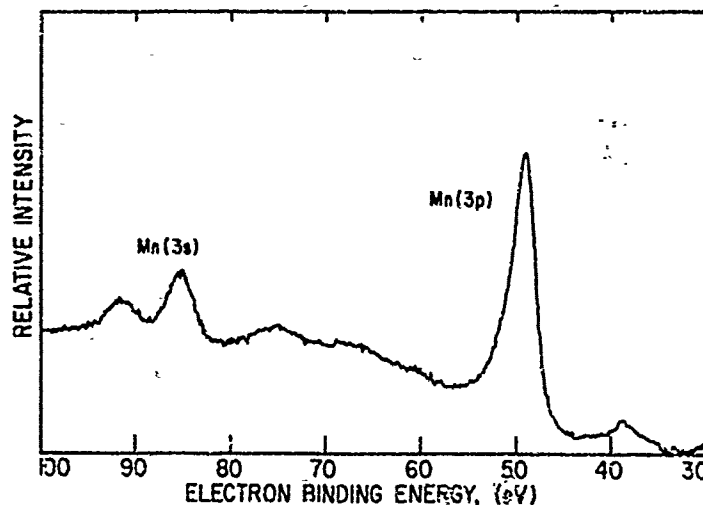


Fig. 9. X-ray photoelectron spectrum similar to Fig. 8 over the range of interest to the manganese oxide state determination. The sharpness of both the 3p and 3s peaks indicate the manganese is present in a single oxidation state.

show a negative shift.

Precise Mn(3p) binding energy values were determined for the exhaust particulate samples and for the compounds MnO, Mn₂O₃ and MnO₂ from short scans such as Fig. 9. These values, corrected for sample charging using the hydrocarbon contaminant C(1s) binding energy of 285.0 eV, are listed in Table II. An inspection of the measured binding energies shows that the particulate manganese binding energy is compatible with both MnO and Mn₂O₃, while eliminating MnO₂. The possibility of Mn₂O₃ can be eliminated by examining the shapes of the 3p photoelectron peak. Mn₂O₃ is broader than MnO or MnO₂, probably indicating a composite peak. This is expected since Mn₂O₃ is essentially a mixed oxide MnO·MnO₂, and therefore the manganese in Mn₂O₃ is in two oxidation states. The exhaust sample Mn(3p) peak is definitely single. This evidence suggests that the manganese is present as MnO.

Table II

Chemical Shift of the Mn(3p) Electron Binding Energy

Sample	Exhaust	MnO	Mn ₂ O ₃	MnO ₂
Binding energy, (eV)	48.9 ± 0.2	48.8 ± 0.2	49.0 ± 0.3	49.9 ± 0.2

It is however, difficult to unambiguously assign an effective charge to the exhaust manganese oxide from a measurement of the chemical shift alone since the binding energies are so similar. Therefore, multiplet splitting was employed to confirm the determination of the oxidation state. Multiplet splitting of core electron binding energies has been observed in the photoelectron spectra of transition metal compounds and other paramagnetic species. Consider the example of a Mn^{2+} ion. This ion has five unpaired 3d electrons in the valence shell which will interact with the two 3s electrons in the core of the same ion. These two 3s electrons are paired, i.e., their spins are oriented antiparallel. In any atomic or molecular system with unpaired valence electrons, the 3s-3d exchange interaction affects core electrons differently, depending on whether they are oriented spin up or spin down. This so called core polarization effect, well known in the NMR spectroscopy, causes the 3s core level to be split into two components.

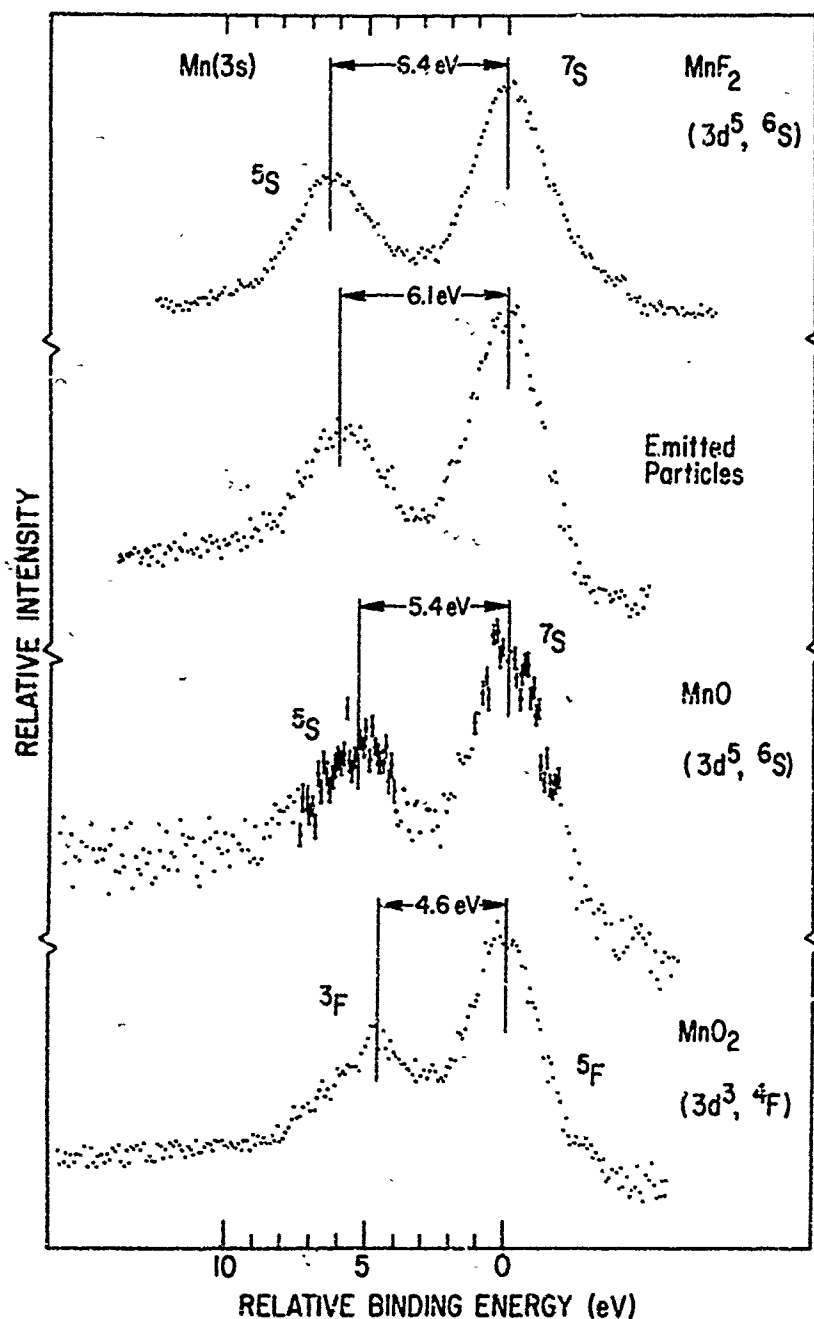


Fig. 10. Comparative X-ray photoelectron spectra for MnF_2 , exhaust particulates, MnO and MnO_2 , near 90 eV electron binding energy where multiplet splitting of the 3s level of manganese occurs. From this evidence it is concluded that MnO is the only manganese oxide in the exhaust.

Figure 10 shows the multiplet splitting of the 3s level for MnO_2 , MnO , the particulate sample, and MnF_2 . MnF_2 is included since it is the most ionic compound of divalent manganese and therefore its Mn^{2+} ion must exhibit the largest possible 3s multiplet splitting. The exhaust sample results lie between the 3s splitting of the MnO and that of the MnF_2 . On this basis alone it can be concluded that the manganese is in the 2^+ oxidation state as MnO . The small apparent difference between the 3s splittings of the reagent MnO and the combustion product could be caused by oxidation of the bottled MnO , or by different solid state interactions for the ions in the regular MnO matrix than for those in the extremely small exhaust particles. A photoelectron spectrum from a MnO single crystal would be useful. The narrowness of the combustion product 3s peaks again indicates that the manganese is present in only one oxidation state.

Similar details of the neutron activation analysis have been reported (36). Exhaust samples collected on Nuclepore filters were irradiated with thermal neutrons in the reactor at Berkeley. The cross-section of manganese is sufficiently large, $\sim 1.4 \times 10^{-23} \text{ cm}^2$, to permit easy excitation of ^{55}Mn to ^{56}Mn which subsequently decays with a half life of ~ 2.5 hrs. By measuring the intensity of the gamma radiation at 846 keV emitted when ^{56}Mn decays to ^{56}Fe , the amount of manganese is determined with a sensitivity of 10^{-12} gm . Average results for several operating conditions are given in Table III. Total emission indices were obtained by weighting the Nuclepore filters with a sensitive balance before and after sample collection.

Table III

Average Mass of Manganese Emitted as Measured by Neutron Activation Analysis

CI-2 % (vol.)	gm Mn/kgm fuel	total gm/kgm fuel	equivalence ratio, ϕ	chamber pressure (atm.)
0.0	2.8×10^{-3}	1.1	.30	2.0
0.005	3.5×10^{-2}	0.65	.20	2.5
0.01	4.0×10^{-2}	1.0	.30	2.5
0.015	5.1×10^{-2}	1.3	.20	3.0
0.03	1.6×10^{-1}	2.9	.20	2.5

The neutron activation analysis indicates that approximately all the manganese added to the fuel is emitted. This lends credence to the mass sampling procedure and indicates negligible deposition of manganese within the combustor.

Armed with the amount of manganese emitted and knowledge of the oxide state as MnO , one can calculate the mass of manganese monoxide emitted. Since the total mass of particulate emissions has been measured, the mass of carbon emitted is immediately obtained assuming the particles contain only MnO and carbon. The resulting emission indices are shown in Fig. 11 as a function of additive concentration. Small amounts of the additive, less than .01 % (vol.), decrease the emitted mass. This implies either agglomeration inhibition or surface oxidation catalysis by manganese. However, at additive concentrations greater than .01 % (vol.) both the total mass and the mass of carbon emitted increase. The carbon emission index reaches a plateau as additive concentration increases at $\sim 1.7 \text{ gm/kgm fuel}$ above the no additive level for this combustor at the operating conditions given in Table III.

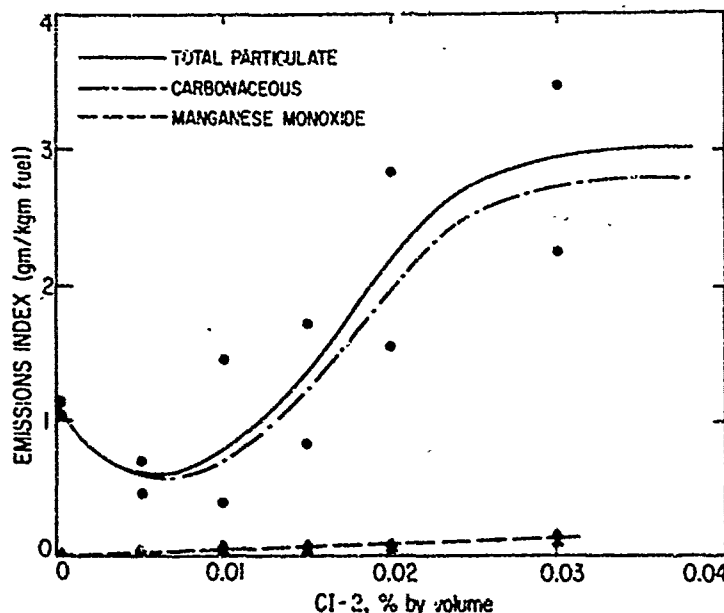


Fig. 11. The circles are typical experimental results for the total particulate emission index. The solid line is an average total particulate EI. The carbonaceous EI is the difference between the total EI and the MnO EI. The significant result is that additive concentrations $> 10^{-2}$ % (vol.) increase the mass of carbon emitted.

Using a similar model combustor, Starkman, Cattaneo and McAllister (37) measured a carbon deposition rate within the chamber of 1.56 gm/kgm of fuel for kerosene at $\phi = .25$ with a chamber pressure of 2.3 atm. This is incredibly close to the observed increase in the carbon emission index and leads to the conclusion that the prohibition of carbon deposition within the combustor by manganese is the cause of the increased mass emission. This effect of manganese has also been reported by Shaysen (15), who observed a significant transient increase in emitted carbon when the additive was injected into the fuel line of an engine operating without CI-2. The mechanism by which manganese effects carbon deposition is not yet clear.

III. CONCLUDING REMARKS

In summary, the following conclusions are drawn:

- 1.) A power law, $n(r) = cr^{-b}$ where c and b are constants, approximately describes the measured size distribution of particles emitted by a model gas turbine combustor.
- 2.) The additive, 2-methylcyclopentadienyl manganese tricarbonyl (CI-2), alters the emitted size distribution to produce fewer larger particles ($\geq 0.2 \mu$) and many more small particles ($\leq 0.2 \mu$).
- 3.) Approximately all the manganese added to the fuel is emitted with negligible manganese deposition within the combustor.
- 4.) The emitted manganese is in the $2+$ oxidation state as manganese monoxide.
- 5.) The manganese additive either inhibits carbon particle agglomeration or catalyzes carbon particle oxidation. Further size distribution and composition studies are underway to determine which mechanism dominates.
- 6.) It has been shown that the manganese additive inhibits carbon deposition within the combustion chamber.
- 7.) Under the conditions of these experiments, the manganese additive decreased the emitted particulate mass at concentrations less than .01 % (vol.). However at concentrations greater than .01 % (vol.), the additive increased the emitted carbonaceous particulate mass substantially. The low concentration decrease is consistent with both agglomeration inhibition and oxidation catalysis. The increase at high concentration is due to carbon deposition inhibition by the manganese.

The use of this additive has two consequences potentially important to health: a.) manganese monoxide can be a significant pollutant at sufficiently high concentrations, and b.) increasing the number of small carbon particles emitted is deleterious since these particles serve as adsorption and nucleation sites and thus promote smog producing heterogeneous reactions. On the basis of these conclusions it is recommended that 2-methylcyclopentadienyl manganese tricarbonyl be used at the lowest possible additive concentrations, $0(10^{-3} \text{ \% by vol.})$. Combustor and test facility redesign are preferable methods of particulate emission suppression.

ACKNOWLEDGEMENTS

This research was supported by the National Science Foundation through Grant GK-27895 and the Environmental Protection Agency through Grant AP-385. The authors are grateful for the valuable assistance of R.F. Sawyer, A. Harker, and J. Murchio.

REFERENCES

1. R.F. Sawyer, "Experimental Studies of Chemical Processes in a Model Gas Turbine Combustor," in *Emissions from Continuous Combustion Systems*, Plenum Pub. Corp., New York, 1972, pp.243-254.
2. M. Kerker, *The Scattering of Light*, Academic Press, New York, 1969, p.105.
3. S.M. DeCorso, C.E. Huxsey, and M.J. Ambrose, "Smokeless Combustion in Oil Burning Gas Turbines," ASME Publication No. 67-PWR-5, 1967.
4. L.H. Linden and J.B. Heywood, *Comb. Sci. and Tech.* 2: 5, 1971, pp.401-411.
5. H.B. Palmer and C.R. Cullis, "The Formation of Carbon from Gases," in *Chemistry and Physics of Carbon*, (ed. P.L. Walker) Marcel Dekker, New York, Vol. 1, 1965.
6. J.B. Howard, "On the Mechanism of Carbon Formation in Flames," Twelfth Int'l. Symp. on Combustion, The Combustion Institute, Pitts., Pa., 1969, pp.877-887.
7. K.S.B. Addecott and C.W. Nutt, "Mechanism of Smoke Reduction by Metal Compounds," Preprints. Am. Chem. Soc., Div. Pet. Chem. 14: 4, 1969, A69-A80.
8. A.G. Gaydon and H. Wolfhard, *Flames - Their Structure, Radiation and Temperature*, 3rd Ed., Chapman and Hall, London, 1970, Chap. 8.
9. J.B. Heywood, J.A. Fay, and L.J. Linden, *AIAA Journal* 9: 5, 1971, pp.841-850.
10. S.W. Radcliffe and J.P. Appleton, *Comb. Sci. and Tech.* 4, 1971, pp.171-175.

11. J.P. Appleton, "Soot Oxidation Kinetics at Combustion Temperatures," this volume.
12. T. Durrant, "The Control of Atmospheric Pollution from Gas Turbine Engines," SAE Paper No. 680347, 1968.
13. J.J. Faitani, "Smoke Production in Jet Engines Through Burner Design," SAE Paper No. 680348, 1968.
14. M.W. Shayeson, "Reduction of Jet Engine Exhaust Smoke with Fuel Additives," SAE Paper No. 670866, 1967.
15. W.G. Tayler, "Smoke Elimination in Gas Turbines Burning Distillate Oil," ASME Publication No. 67-PWR-3, 1967.
16. K.C. Salooja, Combustion, January 1973, pp.21-27.
17. G.L. Martin, D.W. Pershing, and E.E. Berkau, U.S. Environmental Protection Agency, Office of Air Programs Publication No. AP-87, 1971.
18. D.H. Cotton, N.J. Friswell, and D.R. Jenkins, Comb. and Flame, 17, 1971, pp. 87-98.
19. N.J. Friswell, "Emissions from Gas Turbine Type Combustors" in Emissions from Continuous Combustion Systems, Plenum Pub. Corp., New York, 1972.
20. R.M. Schirmer, "Effect of Fuel Composition on Particulate Emissions from Gas Turbine Engines" in Emissions from Continuous Combustion Systems, Plenum Pub. Corp., New York, 1972.
21. G.C. Cotzias, Physiological Reviews, 38, 1958, pp. 503-532.
22. R. Penahuer, Industrial Medicine and Surgery, January 1955, pp. 1-11.
23. W.K. Poole and D.R. Johnston, Research Triangle Institute Report No. RTI-AU-229-FR-InNIH-E5-2433, Durham, North Carolina, 1969.
24. R.J. Sullivan, Preliminary Air Pollution Survey of Manganese and Its Compounds, National Air Pollution Control Administration, Raleigh, North Carolina, 1969.
25. D.V. Gicvanni, P.J. Pagni, R.F. Sawyer, and L. Hughes, Comb. Sci. and Tech., 6, 1972, pp. 107-114.
26. P.J. Pagni and L. Hughes, Chemosphere, 1, 5, 1972, pp. 209-214.
27. R.F. Sawyer, Aero. and Astro 8, 1970, pp. 62-67.
28. R.F. Sawyer, A.K. Oppenheim, N.P. Cernansky, "Factors Controlling Pollutant Emissions from Gas Turbine Engines," this volume.
29. Y. Kukin, "Effects of Additives on Boiler Cleanliness and Particulate Emissions," presented at the 1972 Int'l. Meeting of the Society of Engineering Science, Tel Aviv, Israel.
30. T.O. Caulfield, J.A. Caton, P.J. Pagni, and D. Gilson, "Lead Additive Effects on Particulate Emissions from a CFR Engine," College of Engr. Report ME-72-12, Univ. of Calif., Berkeley, 1972.
31. C. Junge, J. Meteorol. 12, 1952, pp. 13-25.
32. S.K. Friedlander, J. Meteorol. 17, 1960, pp. 479-483.
33. S.K. Friedlander, J. Meteorol. 18, 1961, pp. 753-759.
34. K.R. Spurny, J.P. Lodge, E.R. Frank, and D.C. Sheesley, Environ. Sci. and Tech. 3, 5, 1969, pp. 453-468.
35. J.M. Hollander and D.A. Shirley, Annual Review of Nuclear Science, 20, 1970, pp. 435-466.
36. L. Hughes, "The Effect of a Manganese Fuel Additive on Air Quality," in publication.
37. E.S. Starkman, A.G. Cattaneo and S.H. McAllister, Indus. and Engr. Chem., 43, 1951, pp. 2822-2826.

Discussion on the Paper
 SMOKE SUPPRESSANT ADDITIVE EFFECTS ON PARTICULATE EMISSIONS FROM GAS TURBINE COMBUSTORS
 (Paper 28)
 presented by
 P.J. Pagni

G. Kittredge

With respect to the comment that total carbonaceous particulates increase under these operating conditions, did this include the manganese oxide? Was the MnO contained within the basic particle structure?

This paper is very timely and much needed.

P.J. Pagni

As shown in Fig. 11, the MnO mass contribution is included in, but does not account for the observed increase. The purely carbonaceous fraction of the total emissions also increased substantially.

We cannot now say with certainty whether the MnO is imbedded in the carbon particles or whether it exists as separate particles. From the change in size distribution, however, I suspect the combined form predominates.

J.P. Appleton

Do you think it's possible that manganese monoxide can actually inhibit oxidation just by covering the surface oxidation sights?

P.J. Pagni

No. Under average conditions for our experiments, there are approximately 10 MnO atoms per carbon particle. This is not sufficient to inhibit surface oxidation by coverage.

W.S. Blazowski

1.) I notice that the combustor pressures are much lower than in an actual engine and I further note absence of the specification of temperature. Lower P and T seriously compromise the usefulness of your results. Could you comment.

2.) Shayson indicated that carbon particles (in mg/m^3) were decreased with the use of CI-2 in a J79 combustor test operated at the correct temperature and pressure (SAE Paper 67-0866). Would you comment on this disagreement with your results?

P.J. Pagni

1.) There is no question that our results are strictly limited to the conditions of the experiment, i.e. chamber pressures < 3 atm. and room temperature inlet air. However, it is still surprising and significant that the emissions index increases when a smoke suppressant is used. The quantitative results will differ at engine operating conditions, where the emission indices are much higher, however the same qualitative picture will probably emerge. I suspect that some of the difficulties encountered in the operational use of the additive are due to the effects described here.

2.) No disagreement exists since Shayson never measured carbon particles in mg/m^3 (See Ref. 14). Two emission measurement methods were used: a) attenuation of visible light and b) Densichron Reflectometer readings of filter samples. Neither of these techniques could detect the mass increase since it is coupled with a shift to smaller particle sizes as shown in Figs. 6 and 7.

TECHNOLOGY FOR THE REDUCTION OF AIRCRAFT TURBINE ENGINE EXHAUST EMISSIONS

by

Donald V. Bahr
Manager - Advanced Combustion And Emissions Control Technology
General Electric
Aircraft Engine Group
Cincinnati, Ohio (45215)

SUMMARY

Within recent years, development efforts have been underway at General Electric to provide technology for the design of turbine engine combustors with reduced levels of objectionable gaseous emissions, in addition to low smoke particulates emissions. As an important part of these efforts, tests of both production and advanced engines have been conducted to determine the emissions characteristics of aircraft turbine engines. The results of these engine evaluations are presented. Also presented are the results of exploratory investigations to define and develop design approaches for reducing the carbon monoxide, unburned hydrocarbons and nitrogen oxides emissions levels of high performance, annular combustors - with already developed low smoke emission characteristics. In these latter investigations, the emissions level reductions obtainable through the use of advanced primary combustion zone stoichiometry control methods and advanced fuel injection techniques were evaluated. In addition, results are presented on the use of water injection techniques to suppress the formation of nitrogen oxides in combustors. Based on the results of these various investigations, it is concluded that future engines can be developed with significantly lower levels of these gaseous emissions than those of current engines.

INTRODUCTION

Within recent years, the number of turbine engine-powered aircraft in both commercial and military service has increased at an extremely rapid rate. This rapidly increasing usage of turbine engine-powered aircraft has logically resulted in increased interest in assessing the possible contributions of aircraft turbine engines to the air pollution problems confronting many metropolitan areas throughout the world. Several studies, to evaluate the extent of any air pollution resulting from the operation of aircraft turbine engines have been conducted, as is discussed in Reference 1. These studies have shown that the overall contributions of aircraft turbine engines to the air pollution problems of the world are quite small, as compared to those of other types of contributors. These studies have also shown that the exhausts of aircraft turbine engines generally contain low concentrations of gaseous and particulate emissions considered to be in the category of air pollutants. The typically low concentrations of objectionable emissions are due to the continuous, well controlled and highly efficient nature of the combustion processes in turbine engines and to the use of fuels which contain very small quantities of impurities.

Nonetheless, even though relatively low concentrations and total amounts are generated in most instances, the exhaust emissions in the category of air pollutants resulting from the operations of aircraft turbine engines are of possible concern. The specific aircraft turbine engine exhaust emissions which are of possible concern from an air pollution standpoint consist of carbon monoxide, unburned or partially oxidized hydrocarbons, carbon particulates as soot or smoke and oxides of nitrogen. To minimize possible adverse environmental effects, significant development efforts have been and are being conducted within the industry and government to provide technology for the control and reduction of the levels of these objectionable exhaust emissions. To date, extensive engine evaluations have been conducted to determine the exhaust emissions characteristics of both production and development aircraft turbine engines. Major efforts have also been conducted to develop technology for the design of engines with much reduced smoke emission levels. As a result of these latter efforts, engines with virtually invisible smoke emission levels have already been developed and been placed into service. More recently, efforts have been initiated to develop technology for the design of aircraft turbine engines with reduced carbon monoxide, hydrocarbons and nitrogen oxides emissions levels, as well as low smoke emission levels.

Development efforts to provide technology for the control and reduction of the levels of the objectionable exhaust emissions of aircraft turbine engines have been in progress at General Electric for the past several years. This paper presents a summary of the results obtained to date in these various General Electric investigations, with particular emphasis on the results obtained in investigations to develop methods of reducing the levels of the objectionable gaseous emissions of non-afterburning engines.

EXHAUST EMISSIONS CHARACTERISTICS OF AIRCRAFT TURBINE ENGINES

A typical illustration of the exhaust carbon monoxide, hydrocarbons, nitrogen oxides, smoke and sulfur oxides emissions characteristics of a non-afterburning aircraft turbine engine is presented in Figure 1. In this figure, the measured emissions characteristics of a large, operational General Electric turbofan engine are presented. This engine is equipped with a low smoke emission combustor. The emission levels shown in Figure 1 are the average values measured in tests of several different units of this particular turbofan engine. As is indicated in this figure, the carbon monoxide and hydrocarbons emissions levels of non-afterburning engines occur mainly at idle and other low engine power operating conditions and are typically very low at higher engine power settings. The peak levels of the nitrogen oxides emissions, on the other hand, typically occur at takeoff and other high engine power operating conditions. At low engine power operating conditions, the levels of the nitrogen oxides emissions are typically quite low.

In the case of this turbofan engine, the engine exhaust smoke concentrations are very low and are virtually invisible at all operating conditions, as is shown in Figure 1. In general, the peak smoke

emission levels of non-afterburning engines occur at high power operating conditions. In the case of some older technology engines, exhausts which contain visible concentrations of smoke are produced, particularly at takeoff operating conditions. Even in engines with visible smoke emissions, these emissions represent extremely small losses in engine combustion efficiency. While the peak smoke concentrations in the exhausts of engines with visible smoke emissions are low on an absolute basis, typically less than 0.003 percent (by weight) of the core engine exhaust gas, these concentrations are considerably greater than those of an engine of equal size with invisible smoke concentrations. Exhaust gas smoke concentrations of this order are typically equivalent to about 2 grams per kilogram of fuel, as compared to values of 0.1 or less gram per kilogram of fuel for engines with invisible smoke emissions. Thus, although not generally regarded as a significant health hazard, visible smoke emissions represent an objectionable condition because of the higher associated smoke quantities per kilogram of fuel consumed as well as the visibility itself. In commercial aircraft operations, visible smoke emissions are of concern primarily because of air pollution and related localized atmospheric visibility reduction considerations. In military aircraft operations, visible smoke emissions are, in addition, of concern because they can result in unsatisfactory conditions from a tactical standpoint.

As is illustrated in Figure 1, the sulfur oxides emissions levels of aircraft turbine engines are normally low at all operating conditions. These typically low emissions levels are a direct consequence of the low sulfur contents of aircraft turbine engine fuels. Also, metal compound emissions, such as metal oxides, are also normally very low at all engine operating conditions. The only significant sources of this latter category of emissions are the inorganic impurities in the fuel. Aircraft turbine engine fuels, however, are generally very clean and are free of such contaminants. Thus, the magnitude of any metal compound concentrations in engine exhaust gases would generally be expected to be less than 10 parts per billion parts (by weight) of core engine exhaust gas.

At cruise operating conditions, the levels of the various objectionable emissions of non-afterburning engines are normally quite low. Of these emissions, only the nitrogen oxides emissions are normally generated to any significant extent at cruise operating conditions. For all engine applications, with the possible exception of supersonic aircraft applications, even the nitrogen oxides emissions levels of a given engine at cruise are significantly lower than those at takeoff and climbout operating conditions. Thus, the highest levels of the various objectionable exhaust emissions of non-afterburning engines are primarily generated at engine operating conditions that occur in and around airports. Further, because large numbers of aircraft operations can occur in and around a given airport, the exhaust emissions resulting from these many localized aircraft operations tend to be concentrated to some extent. Accordingly, the primary concern associated with these exhaust emissions appears to be their possible impacts on the environments of major metropolitan airport localities.

At the present time, therefore, the primary exhaust emissions reduction technology needs of non-afterburning engines appear to involve the elimination of visible smoke emissions, the reduction of carbon monoxide and hydrocarbons emissions levels at idle operating conditions and the reduction of nitrogen oxides emissions levels during takeoff and climbout operations. Reductions in the levels of these emissions at these specific operating modes would also be generally expected to provide more favorable characteristics at other engine operating conditions, including cruise conditions. In any non-afterburning engine, the source of these emissions is, of course, its main combustor. The attainment of these more favorable exhaust emissions characteristics in future engines, thus, primarily involves providing improved and modified main combustors for use in these engines. For engines with afterburners, methods of reducing the carbon monoxide, hydrocarbons, oxides of nitrogen and particulates emissions generated in the reheat combustion system may also be required.

The engine exhaust products of aircraft which cruise in the stratosphere are another possible area of concern, because of the relatively slow mixing rates between the stratosphere and the troposphere and the resulting tendencies for materials introduced into the stratosphere to accumulate. The introduction of nitrogen oxides into the stratosphere has, for example, been identified as a possible area of concern by some investigators. The possible impacts of the introduction of engine exhausts into the stratosphere are the subject of a very extensive Climatic Impact Assessment Program, currently being conducted by the U.S. Department of Transportation. This major study, which is described in Reference 2, is scheduled to be completed by the end of 1974 and is expected to result in a determination of whether or not modifications may be needed in the exhaust emissions characteristics of engines for aircraft which are to operate in the stratosphere.

REDUCTION OF SMOKE EMISSIONS

In the initial General Electric development efforts to provide engines with more favorable exhaust emissions characteristics, major emphasis was directed at reducing smoke emission levels. Thus, an extensive number of investigations was conducted to develop technology for the design of low smoke emission combustors. During the past several years, these efforts have included the development of both annular and can-type combustor designs with low smoke emission characteristics. These efforts have also included the development of low smoke emission combustors for a wide variety of engine applications, including engines with high pressure ratios and engines designed to operate with low grade distillate fuels. A summary of some of these investigations is presented in Reference 3. These investigations have conclusively shown that the design of low smoke emission combustors involves providing both leaner fuel-air mixtures and more effective fuel-air mixing in the primary combustion zone, as compared to those of combustors with high smoke emission levels. These investigations have demonstrated that both of these provisions are needed to eliminate any fuel-rich mixtures within the primary combustion zone and, therefore, that both are of major importance. Providing the required leaner fuel-air mixtures and improved mixing in the primary zone has been found in these investigations to involve significant changes in the overall design approaches used in the combustors of present day engines. Also, combustor design features added to reduce smoke emission levels have been found, in some instances, to result in losses in other aspects of combustor performance, especially ignition performance. Thus, the design and definition of low smoke emission combustors has generally been found to entail careful, iterative development efforts to provide the required low smoke

emission characteristics, as well as to meet all the usual ignition, stability, efficiency, exit temperature distribution, life and other performance requirements.

One of the major results of these smoke reduction technology efforts has been the development of an advanced annular combustor design approach in which large amounts of the combustor air flow are introduced through swirl cups, containing axial flow swirlers, which surround each of the fuel nozzles. With this design approach, lean and relatively uniform primary zone fuel-air mixtures are obtained within short distances downstream of the fuel nozzles, as a result of the large swirl cup air flows and the rapid and effective fuel-air mixing provided by the air swirlers. With this design approach, much reduced smoke levels have been obtained without any significant losses in ground ignition or altitude flight performance capabilities and no losses in other combustor performance characteristics. A more detailed description of this combustor design approach is contained in Reference 3. An illustrative axial swirler array of this kind and the smoke emission levels obtained with this design approach in the J6-6 engine are presented in Figure 2. To date, this design approach has been successfully used in the combustor designs of the TF39, LM250 and CF6 engines and has resulted in low smoke emission combustor designs for these large engine applications. These advanced engines, equipped with these low smoke emission combustors, are already in service. The smoke emission levels of these high performance engines are virtually invisible at all operating conditions.

The smoke emission levels shown in Figure 2 are expressed in terms of the SAE ARP 1179 smoke number. On this scale, which runs from zero to 100, low smoke numbers indicate low smoke particulates emission levels. Engine tests conducted at General Electric have shown that the visibility threshold smoke numbers of various types of engines range from about 20 to 40. The visibility threshold of any given engine is strongly dependent on its size. Thus, larger size engines have lower smoke numbers as their visibility thresholds than smaller engines, because of the larger sizes of their exhaust plumes. Larger size plumes result in greater path lengths and, accordingly, greater amounts of light scattering and absorption for the same smoke concentration in the exhaust gas. The visibility of a given exhaust plume is also strongly influenced by the angle at which the plume is viewed. The smoke emissions of a given plume, of course, appear less visible when the plume is viewed at a right angle. For engines in the larger size class, visibility threshold smoke numbers are normally in the range of about 20 to 30. Engines in the smaller size class generally have visibility threshold smoke numbers in the range of about 30 to 40. The core engines of high bypass turbofan engines also generally have somewhat higher threshold smoke numbers than pure turbojet engines of a similar size, because of the dilution of the core engine exhaust by the bypass air. Generally, a SAE ARP 1179 smoke number of about 20 is at or below the smoke number visibility thresholds of most aircraft turbine engines - regardless of engine size or the angle at which the exhaust plume is viewed. Based on tests conducted at General Electric, a SAE smoke number of 20 has been found to be equivalent to a smoke concentration of less than 2 parts per million parts of core engine exhaust gas, by weight. Thus, a smoke number of this magnitude not only results in an invisible exhaust in most instances, but also results in smoke concentrations by weight which are extremely low.

Additional data on the smoke emissions characteristics of various General Electric engines are presented in Figure 3. All of the engines in this group are equipped with annular-type combustors. As is shown in this summary chart, the peak smoke emission levels of the older engines are generally well above the visibility threshold band and are strongly affected by cycle pressure ratio rating. The peak smoke emission levels of the more advanced engines are generally below a SAE smoke number of 20 and, therefore, are below the nominal threshold of visibility. These advanced engines encompass a wide range of sizes and cycle pressure ratios. Considerable experience in commercial and military service has already been obtained with these advanced, low smoke emission engines. Based on the extensive results obtained to date with these engines, it is concluded that technology for the design of low smoke emission combustors, which also fulfill all engine ignition and other performance requirements, is reasonably well defined.

REDUCTION OF CARBON MONOXIDE & UNBURNED HYDROCARBONS EMISSIONS

More recently, investigations have been initiated at General Electric to identify and develop methods of reducing the carbon monoxide and hydrocarbons emissions levels of these already developed low smoke emission combustors. A major objective of these emissions reduction development efforts is to retain the already developed low smoke emission characteristics of these advanced combustors. Major emphasis in these development efforts is being focused on providing technology applicable to annular-type combustors for advanced turbofan engines. Summaries of some of the results of these investigations are presented in References 4 and 5.

The carbon monoxide and hydrocarbons emissions are, of course, products of inefficient combustion. As is illustrated in Figure 1, these emissions are primarily produced at idle and other low power operating conditions. These emissions mainly occur at these operating conditions because the combustion efficiency levels of most engines at these low power operating conditions are not optimum and are typically in the 90 to 95 percent range. At higher engine power settings, the combustion efficiency levels of most engines are generally well in excess of 99 percent and, therefore, the quantities of incomplete combustion products produced at these operating conditions are very small. The somewhat reduced combustion efficiency performance of most existing aircraft turbine engines at idle and other low power operating conditions is due to the adverse combustor operating conditions that normally prevail at these engine operating conditions. At the low power operating condition, the combustor inlet air temperature and pressure levels are relatively low, the overall combustor fuel-air ratios are generally low and the quality of the fuel atomization and distribution within the combustor primary zone is usually poor because of the low fuel and air flows. For any given engine, all of these adverse combustor operating conditions are rapidly eliminated as the engine power setting is increased above idle power levels and, accordingly, its combustion efficiency performance is quickly increased to near-optimum levels.

As a first step in these carbon monoxide and hydrocarbons emissions reduction investigations, analytical and experimental studies were conducted to determine the relationships between the levels of these emissions and the combustion efficiency performance characteristics of engines. As a part of these efforts, these relationships were determined in tests of several General Electric engines. The ranges of

carbon monoxide and hydrocarbons emissions level combinations measured in these engine tests at various combustion efficiency values are presented in Figure 4. As is shown, wide ranges of emissions levels combinations were measured at the lower combustion efficiency values. The specific ratios of carbon monoxide to hydrocarbons emissions levels of engines at the low power operating conditions, where these low efficiency values occurred, were found to be dependent on engine size and the specific design features of the engine combustor. At the higher power operating conditions, where the combustion efficiencies are high the hydrocarbons levels were found to be relatively low. These low hydrocarbons emissions levels are consistent with combustion chemical kinetics considerations which show that hydrocarbon compounds are consumed much faster than carbon monoxide. Therefore, as near-ideal combustion performance is approached, any remaining non-equilibrium combustion products - or inefficiencies - tend to exist mainly as carbon monoxide.

These investigations also showed that the emissions levels, at idle operating conditions, of the high cycle pressure ratio engines are considerably less than those of the lower cycle pressure ratio engines. Some measured idle power combustion efficiency performance levels, along with carbon monoxide and hydrocarbons emissions level data, are presented in Figure 5 as a function of engine cycle pressure ratio rating. This correlation generally indicates that the increased combustor inlet temperatures and pressures, at idle, that are associated with the higher pressure ratio cycles result in improved combustion efficiency performance. At a given set of combustor inlet air temperature and pressure operating conditions, combustion efficiency performance at idle is also effected to a significant extent by the fuel-air ratio of the primary combustion zone and the quality of the fuel atomization. At idle and other low power operating conditions, the overall engine and combustor fuel-air ratios are generally low and, thus, the primary zone fuel-air ratios are also low - typically one-half of the stoichiometric value. Further, fuel atomization quality tends to be relatively poor at these low engine power levels because of the low fuel flows and air flows. In pressure atomizing combustors, these low fuel flows result in low fuel nozzle pressure drops and, thus, poor atomization. In combustors with low fuel injection pressures, in which the fuel is airblast atomized by compressor discharge air, these low air flows result in low air velocities and, thus, poor atomization. In both types of combustors, poor atomization results in slow fuel vaporization and poor mixing of the fuel with the air. Therefore, methods of providing either higher primary combustion zone fuel-air ratios at idle or improved fuel atomization at idle, or both, are needed. Approaches of this kind are being defined and developed in the investigations currently underway at General Electric. In addition to evaluations of methods of obtaining improved fuel atomization at idle, investigations of methods of minimizing or eliminating any combustion quenching tendencies within combustors are being investigated, as well as methods of obtaining higher average or local primary zone fuel-air ratios at idle. These latter investigations involve the use of fuel staging methods to localize the fuel concentrations at idle or decreased primary zone air flows at idle.

To date, some promising results have been obtained in these investigations. An advanced full annular combustor has been tested, at engine idle operating conditions, with modified fuel nozzles to evaluate the effects of improved fuel atomization in improving low power combustion efficiency performance. A significant improvement in combustion efficiency, from about 95 percent to about 98 percent at the nominal idle fuel-air ratio operating condition, and much reduced carbon monoxide and hydrocarbons emissions levels were obtained. These test results, which are presented in Figure 6, showed that the relatively poor atomization quality provided by the existing dual orifice fuel nozzle design at the idle power operating conditions caused a loss of combustion efficiency. As is also shown in Figure 6, increases in the fuel-air ratio above the nominal value resulted in even further decreases in the carbon monoxide and hydrocarbons emissions levels, particularly in the case of the hydrocarbons. These latter findings provide an indication of the significant reductions obtainable by operating the combustor at higher fuel-air ratios at idle. One attractive means of obtaining these beneficial higher fuel-air ratios at idle is to extract and dump overboard increased amounts of compressor discharge air. Some results obtained in tests of an advanced annular combustor, in which various amounts of compressor bleed air extraction were simulated, are presented in Figure 7. These results illustrate the effects of increasing primary combustion zone fuel-air ratio - at a constant fuel flow rate. As is shown, significant carbon monoxide and hydrocarbons emissions level reductions were obtained. Since many advanced engines have provisions for extracting large amounts of compressor discharge flow, this concept appears to be an attractive one.

Based on the results obtained to date in these investigations, it appears that significant reductions in carbon monoxide and hydrocarbons emissions levels are obtainable by combustor design modifications involving improved fuel atomization and/or improved primary zone stoichiometry at idle. Although progress has been made, methods of providing further reductions, especially in the case of the carbon monoxide emissions are needed. It is expected, however, that engines to be developed and placed in service in future years will have significantly lower carbon monoxide and hydrocarbons emissions levels.

REDUCTION OF OXIDES OF NITROGEN EMISSIONS

In parallel with the investigations to develop methods of reducing the carbon monoxide and hydrocarbons emissions levels, analytical studies and exploratory investigations to identify and develop techniques of reducing the nitrogen oxide emissions levels of advanced combustors have also been underway at General Electric. As in the carbon monoxide and hydrocarbons emissions level reduction investigations, a major objective of these efforts is to retain the already developed low smoke emission characteristics of these advanced combustors. Also, as in the carbon monoxide and hydrocarbons emissions level reduction investigations, major emphasis is being focused in providing technology applicable to annular-type combustors for advanced turbofan engines. Summaries of some of the results of these investigations are presented in References 4 and 5.

Small amounts of nitrogen oxides are generated, to some degree, in any combustion process and result from the oxidation of atmospheric nitrogen. In the combustion systems of turbine engines, these emissions are formed within the primary combustion, or flame zones, and within the dilution zones immediately downstream of the primary zones. These emissions consist primarily of nitric oxide together with small amounts of nitrogen dioxide. The small amounts of nitrogen dioxide emissions result from the

further oxidation of the nitric oxide that is formed in the combustion or flame zones. Once discharged into the atmosphere, however, the nitric oxide is gradually converted to nitrogen dioxide. The thermochemical equilibrium quantities of nitric oxide that can be generated are strongly dependent on the flame temperature levels of the hot combustion gases and on the availability of oxygen. Thus, these equilibrium quantities increase rapidly as the initial air temperature is increased and as the combustion zone fuel air equivalence ratio (ratio of actual fuel-air ratio divided by stoichiometric fuel-air ratio) approaches values in the order of 0.9.

As a first step in these investigations, analytical studies of the nitric oxide formation process in combustors were conducted. These studies showed that the formation rates increase very rapidly as flame temperature is increased. Thus, these rates increase very rapidly as the initial air temperature level is increased and as the combustion zone fuel-air equivalence ratio approaches unity. Increases in the inlet air pressure level were also found in these studies to increase the formation rates. For these reasons, the nitrogen oxides emissions levels of turbine engines generally reach levels of any significance only at the high power operating conditions, where the combustor inlet air temperature and pressure levels are high. These studies showed, however, that the formation rates are relatively slow at all operating conditions, as compared to the fuel combustion reactions. Therefore, the quantities of the nitrogen oxides emissions that are generated, even at the high engine power levels, are usually much less than the thermochemical equilibrium values, since they are limited by the short residence times of the hot combustion gases within engine combustors. As a result, very high fuel combustion efficiencies can be obtained without the generation of thermochemical equilibrium nitric oxide concentrations. Some typical nitric oxide formation rate data, that were generated in these studies, are presented in Figure 8.

Because of the very strong dependence of formation rate on the initial air temperature level and, since combustor inlet air temperature level is a direct function of cycle pressure ratio, the nitrogen oxides emissions characteristics of turbine engines are directly related to overall engine cycle pressure ratio. The nitrogen oxides emissions characteristics of several General Electric engines have been determined in engine tests. Some of the results of these engine tests are presented in Figure 9. As is shown in this figure, the flame power (takeoff) emissions levels of the high cycle pressure ratio engines are significantly greater than those of the low cycle pressure ratio engines.

At any specific set of combustor inlet air conditions, control and reduction of the nitrogen oxides emissions levels of a given combustor involve control of the flame temperatures within the primary combustion zone and the dilution zone immediately downstream and/or control of the residence times of the hot combustion gases in these zones. To minimize the quantities of nitrogen oxides emissions formed, the flame temperatures and/or residence times of the gases in these zones must be minimized. One general approach for reducing flame temperatures involves the addition of inert liquids or gases into the primary combustion zone. The introduction of water into the primary zone is an approach of this kind. Some results of experimental studies to evaluate the use of water injection as a means of reducing nitrogen oxides emissions levels are presented in Figure 10. As is shown, water injection in amounts of 1 to 2 percent, by weight of the combustor air flow, provides considerable reductions. These investigations showed that, to achieve these reductions, the water must be injected directly into the primary combustion zone and must be uniformly distributed with the primary zone fuel-air mixtures. If effective atomization of the water and rapid mixing with the fuel-air mixtures are not obtained, greater quantities of water are needed for the same degree of suppression.

Based on results of this kind, water injection appears to be a generally effective method of obtaining significant reductions in nitrogen oxides emissions levels during takeoff and climbout operations. The use of water injection at cruise operating conditions is, of course, unacceptable. However, the use of water injection in aircraft engines, even when limited to takeoff and climbout operations, does involve some weight penalties and does require the addition of water tankage, pumping, valving and plumbing provisions to the engine. As such, the use of water injection has some significant drawbacks. Accordingly, means of reducing the levels of these emissions by combustor design modifications, rather than by the use of water injection, represent an important development need. Further, if nitrogen oxides emissions level reductions at cruise operating conditions are identified as an important need, reductions by means of combustor design modifications will be essential.

Another general approach for reducing flame temperatures and, thereby, minimizing the quantities of nitrogen oxides emissions formed in a given combustor is to minimize the quantities of combustion gas mixtures with near-stoichiometric fuel-air proportions. This type of approach offers a potential means of reducing nitrogen oxides emissions levels by combustor design features rather than by the use of water injection. Analytical and experimental studies to define and develop methods of this kind, which involve the difficult problems of precisely controlling the average and local fuel-air ratios within the primary combustion and dilution zones, have been conducted as a part of the General Electric investigations. Some potentially promising results have been obtained in these investigations. The use of advanced fuel injection methods involving airblast fuel atomization has been found, for example, to result in somewhat lower emissions levels as compared to those of combustor designs with more conventional fuel injection provisions - at the same combustor operating conditions. As is shown in Figure 9, emissions levels reductions in the order of 30 percent have been obtained in tests with these advanced fuel injection techniques. These lower emissions levels appear to be the result of the very effective fuel-air mixing obtained in carbureting combustors of this kind. Tests have shown that this highly effective mixing process results in more uniform mixtures in the primary combustion and dilution zones than those obtainable with more conventional fuel injection methods, thereby permitting the use of shorter gas residence times in these zones. As a result, more rapid elimination of any localized fuel-air mixtures with near stoichiometric proportions and, thus, reduced nitrogen oxides emissions levels may be attained.

Other investigations have shown that significant reductions in nitrogen oxides emissions levels may be obtained by operating with either much richer or much leaner average primary combustion zone fuel-air ratios than those normally used in current combustor designs. Some experimental results of this kind are shown in Figure 11. As is shown, the use of lean primary zone mixtures, in particular, results in significantly decreased nitrogen oxides emissions levels. Operation with such lean primary mixtures may, of course, require the use of considerably more advanced and complex combustor design approaches to obtain

satisfactory ignition characteristics and operation over the required wide ranges of combustor fuel-air ratios. Combustors designed to operate with lean primary zones at full power operating conditions may, for example, require the use of variable geometry features to modulate and reduce the air flow into the primary combustion zone at the low power operating conditions. Or they may involve the use of modular combustor designs, comprised of many small combustor modules each equipped with fuel injection and fuel-air mixing provisions, with which staging of the combustion process may be obtained.

Also shown in Figure 11 are the effects of higher primary zone fuel-air ratios. Only small reductions in the nitrogen oxides emissions levels, as compared to those of the baseline combustor design, were obtained in these tests with higher primary zone fuel-air ratios. These findings suggest that the nitrogen oxides formation process is apparently merely shifted from the primary zone to the dilution zones downstream, with little net change in the emissions levels. These findings provide an indication as to why the nitrogen oxides emissions of low smoke emission combustors have generally been found to be about the same as those of similar combustor designs with high smoke emission levels, rather than being significantly higher as had been predicted by some investigators. Conversion of a given combustor design to a low smoke emission design generally involves providing leaner average primary zone fuel-air ratios. The results of Figure 11 suggest that a reduction from an average primary zone fuel-air ratio of 2 or more, which is typical of many high smoke emission combustor designs, to a value of about 1.3, which is typical of current low smoke emission combustor designs, would only be expected to result in small increases in the nitrogen oxides emissions levels of a given combustor. These findings are corroborated by the data shown in Figure 12, where the nitrogen oxides emissions characteristics of an advanced turbofan engine, equipped first with a combustor with visible smoke emissions and then with a low smoke emission version of this same combustor, are compared.

Thus, some preliminary progress has also been made in these exploratory investigations. These investigations indicate that the oxides of nitrogen emissions will probably be the most difficult of the emissions problems associated with aircraft turbine engines to solve by combustor design modifications. Based on the results obtained to date, however, it is anticipated that suitable reduction techniques involving combustor modifications, rather than the use of water injection, will be successfully developed. Thus, it is anticipated that the nitrogen oxides emissions levels of the advanced engines, especially the high pressure ratio and high performance engines, to be developed and placed into service in future years will be reduced to values significantly lower than those being measured in current engine models with equivalent pressure ratio ratings. However, it appears, at present, that such additional combustion research and development effort will be required to bring this nitrogen oxides emissions abatement technology to the point where it can be satisfactorily applied and significant emissions level reductions can be realized in future engines.

CONCLUSIONS

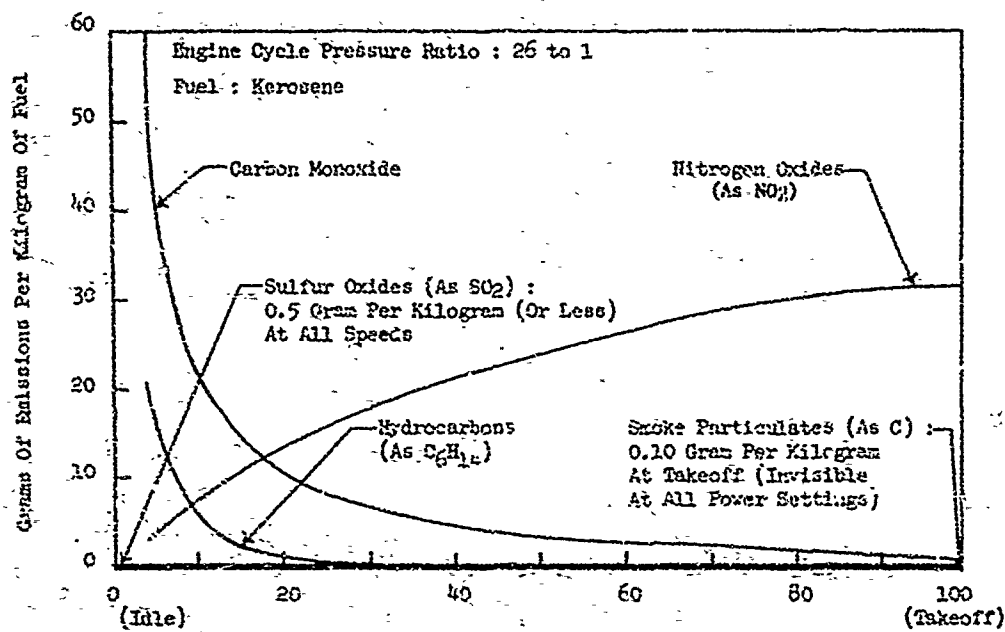
1. Significant progress has been made in the development of technology for the design of combustors with much reduced smoke emission levels. As a result of these efforts, combustors with virtually invisible smoke emission levels at all engine operating conditions have been developed and placed into service. The peak SAE ARP 1179 smoke numbers of these advanced combustors are typically in the order of 20 or less. Smoke numbers of this order correspond to very low concentrations of smoke particulates in engine exhausts, only about 2 parts per million parts (by weight) of the core engine exhaust gas.

2. Based on the results of investigations conducted to date, much reduced carbon monoxide and hydrocarbons emissions levels appear to be attainable through the use of combustor design modifications which provide improved fuel atomization at idle and/or higher primary combustion zone fuel-air ratios at idle.

3. Some potentially promising approaches for providing suppression of the nitrogen oxides emissions levels of combustors have been identified in the exploratory development efforts conducted to date. The introduction of water into combustors has been found in these studies to be an effective method of reducing the levels of these emissions. While this latter approach appears to be effective as a way of suppressing the peak nitrogen oxides emissions levels associated with takeoff and climbout operations, there are some significant disadvantages associated with its use. The use of advanced fuel injection and atomization methods has also been found to be an effective method of reducing nitrogen oxides emissions levels. Further, the use of precisely regulated primary zone fuel-air ratios appears to offer considerable promise.

REFERENCES

1. Exhaust Emissions From Gas Turbine Aircraft Turbine Engines, Sub-Council Report, National Industrial Pollution Control Council, February, 1971.
2. Grobecker, A. J. Presentation To The Second Conference On The Climatic Impact Assessment Program, U.S. Department Of Transportation, November, 1972.
3. Bahr, D. W., Smith, J. R., and Kenworthy, M. J. Development Of Low Smoke Division Combustors For Large Aircraft Turbine Engines, AIAA Report 69-493, June, 1969.
4. Bahr, D. W. Control And Reduction Of Aircraft Turbine Engine Exhaust Emissions, Proceedings Of The Symposium On Emissions From Continuous Combustion Systems, 1972.
5. Bahr, D. W. Technology For Reduction Of Aircraft Turbine Engine Exhaust Emissions, AIAA Report 72-1262, November, 1972.



Percent Of Full Power-At Sea Level Static Operating Conditions (Standard Day)

Figure 1. Exhaust Emissions Characteristics Of Advanced Turbofan Engine.

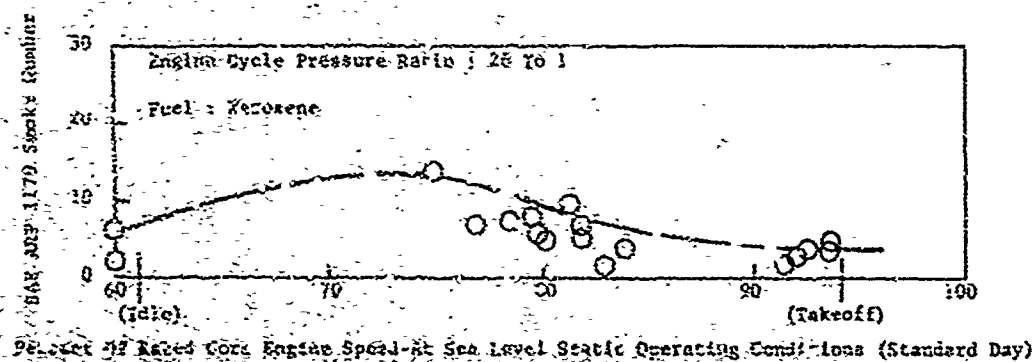


Figure 2. Typical Axial Swirl Cup Array and Measured Smoke Emission Characteristics.

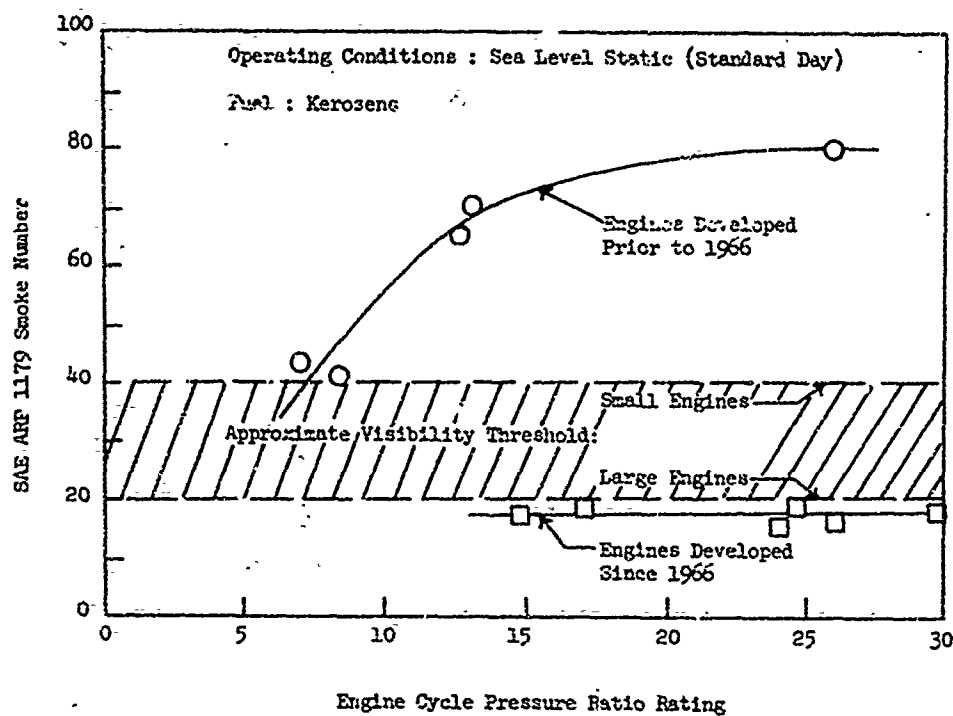


Figure 3. Comparison Of Peak Engine Smoke Emission Characteristics Of Various General Electric Engines.

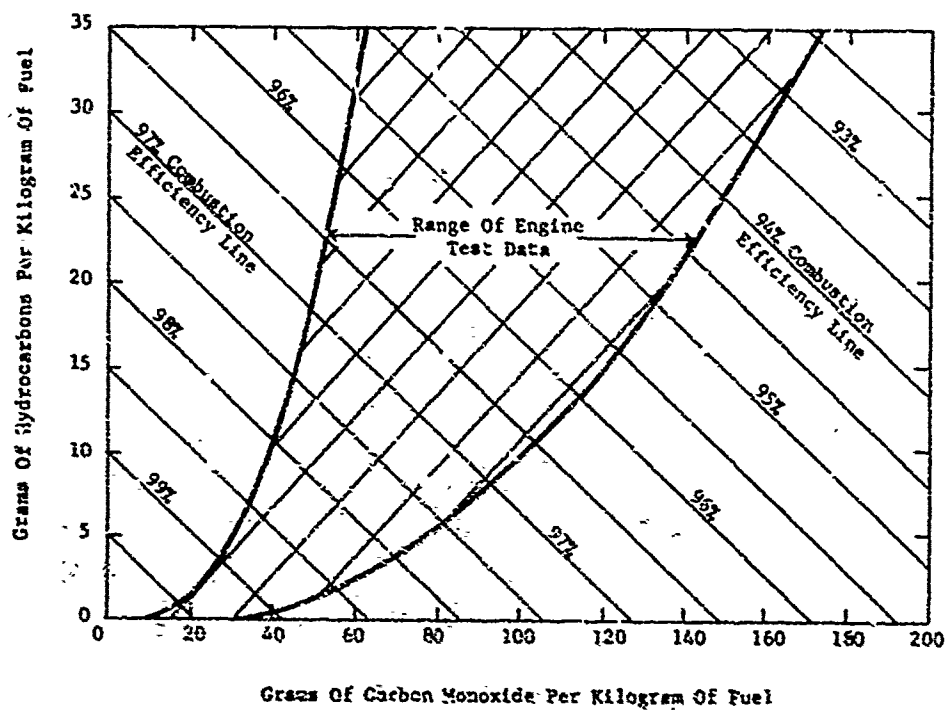


Figure 4. Relationships Between Combustion Efficiency and Levels Of Carbon Monoxide and Hydrocarbons Emissions.

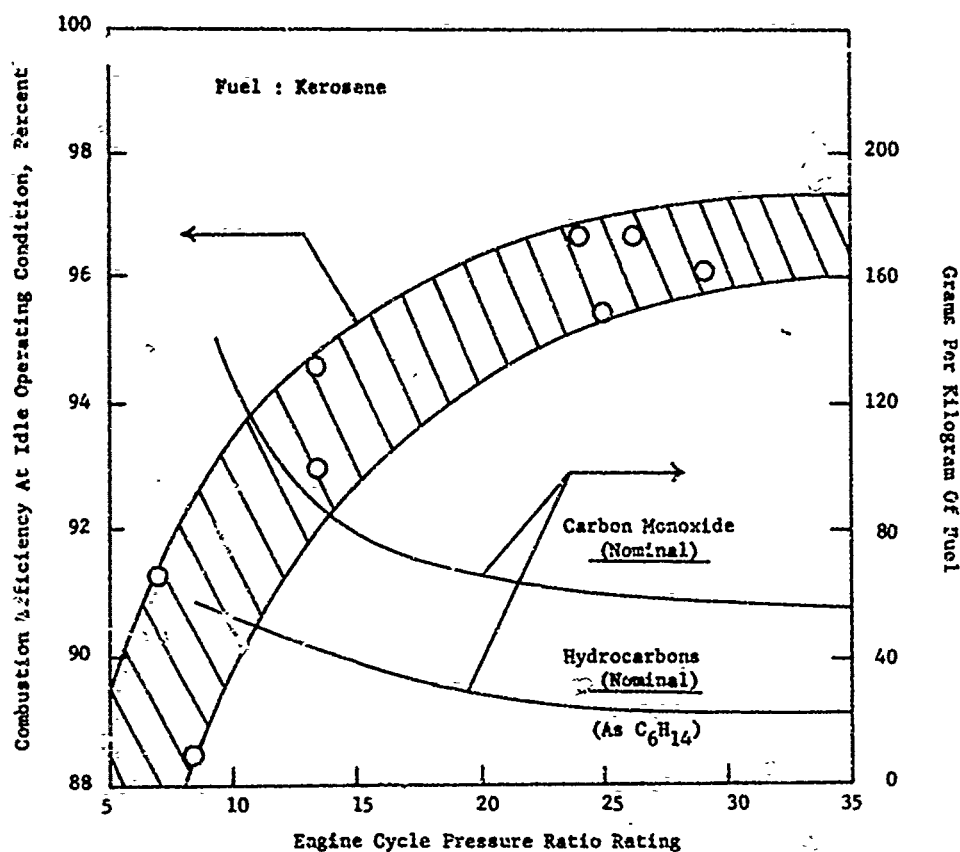


Figure-5. Idle Power Combustion Efficiency Performance And Emissions Trends-At Standard Day Operating Conditions.

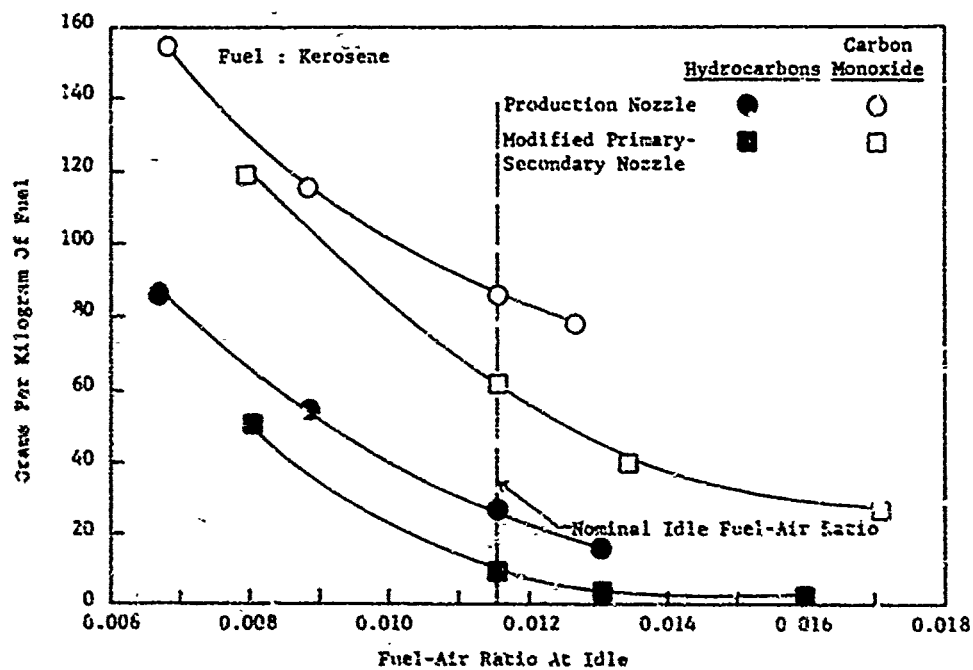


Figure 6. Carbon Monoxide And Hydrocarbons Emissions Characteristics At Idle Of An Advanced Combustor-At Standard Day Operating Conditions.

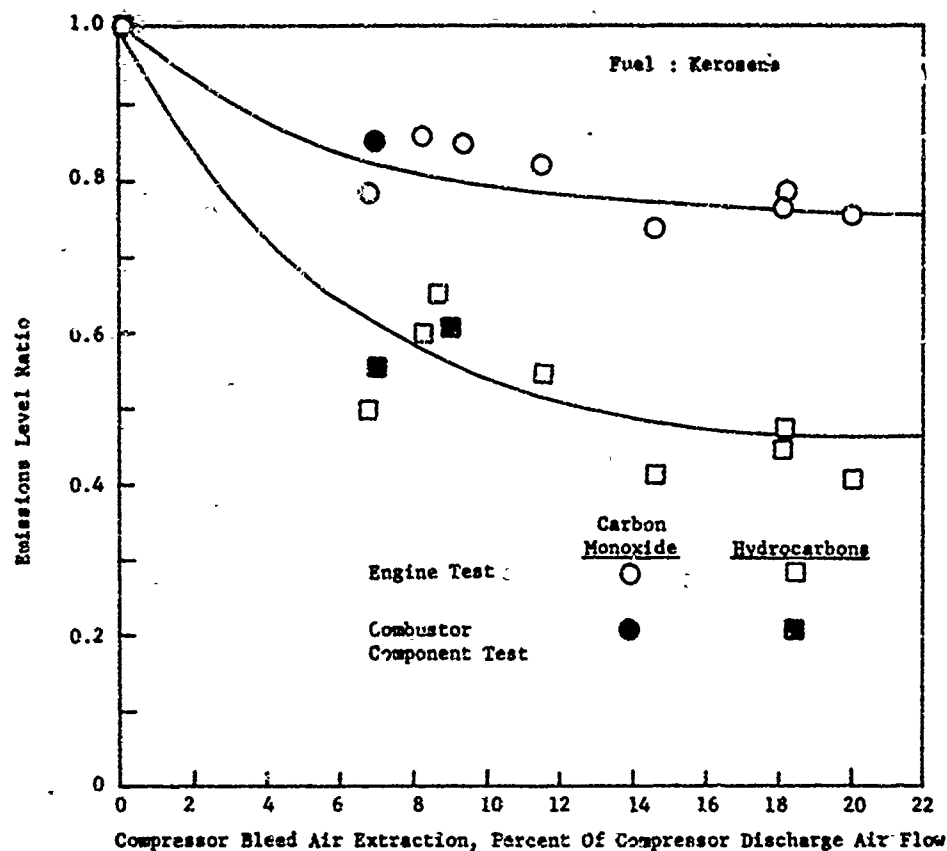


Figure 7. Effect Of CDP Bleed Extraction At Idle On Carbon Monoxide And Hydrocarbons Emissions Characteristics Of An Advanced Combustor-At Standard Day Operating Conditions.

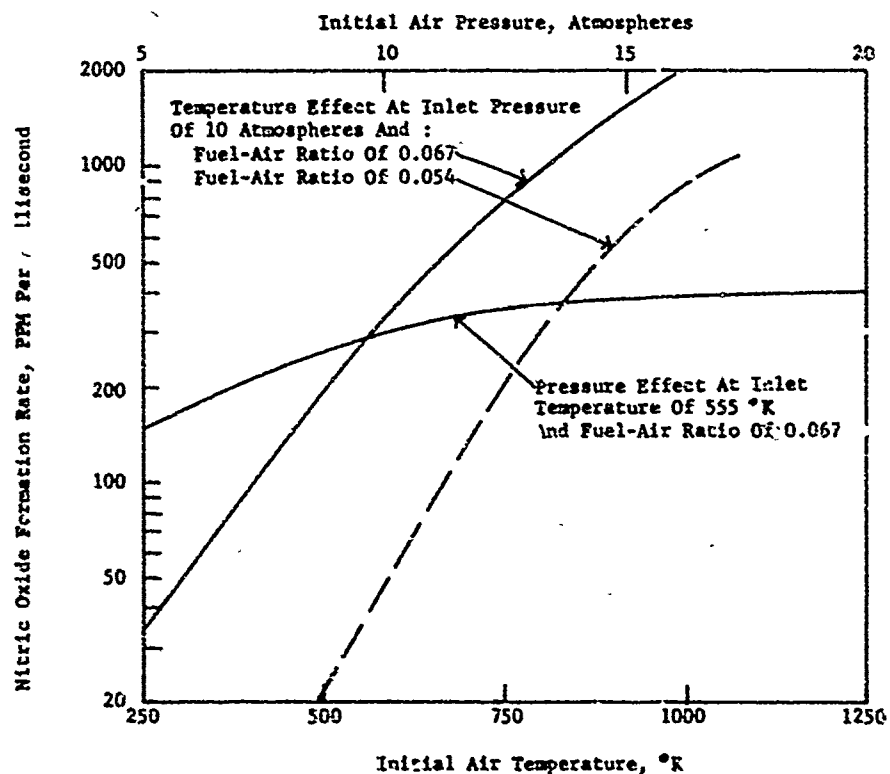


Figure 8. Effects Of Initial Temperature And Pressure On Nitric Oxide Formation Rates.

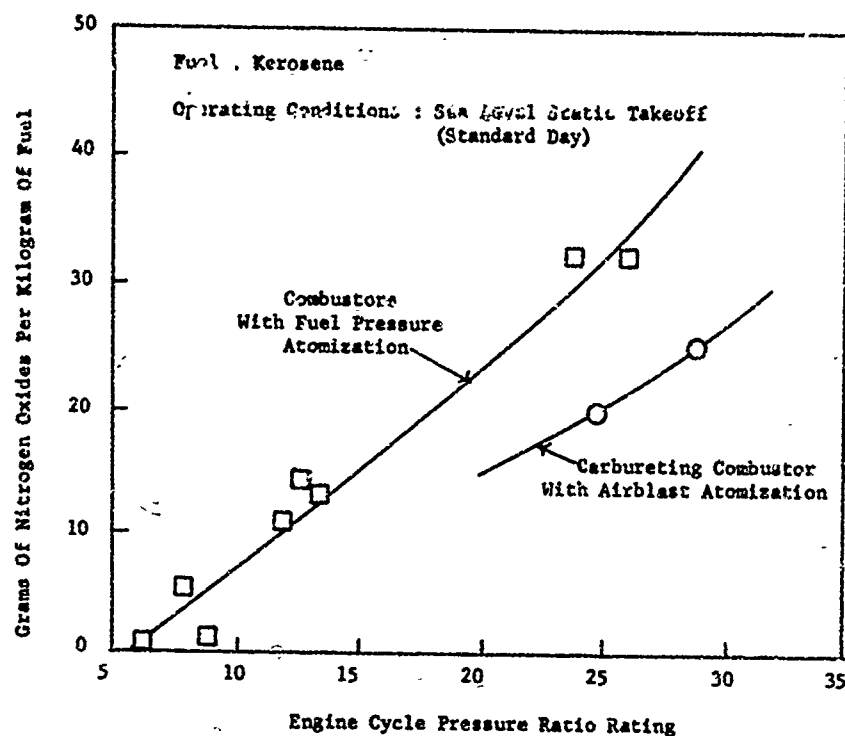


Figure 9. Comparison Of Nitrogen Oxides Emissions Characteristics Of Advanced Carbureting Combustor With Those Of Conventional Fuel Injection Combustors.

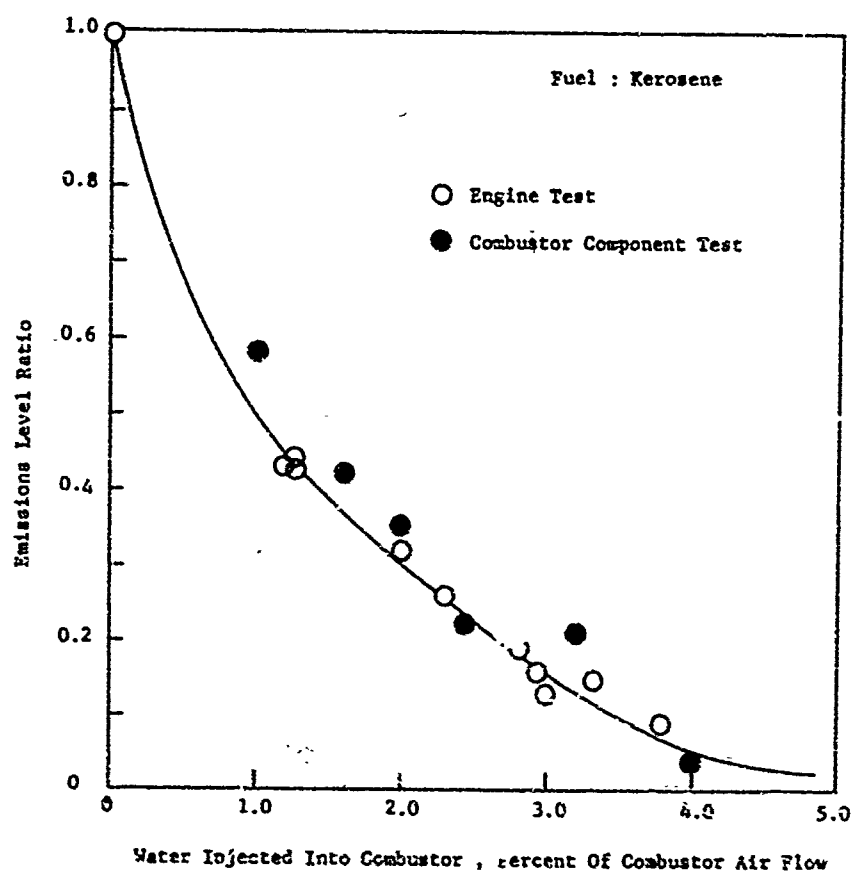


Figure 10. Effect Of Water Injection On Oxides Of Nitrogen Emissions Characteristics Of Advanced Combustors-At Standard Day Sea Level Static Takeoff Operating Conditions.

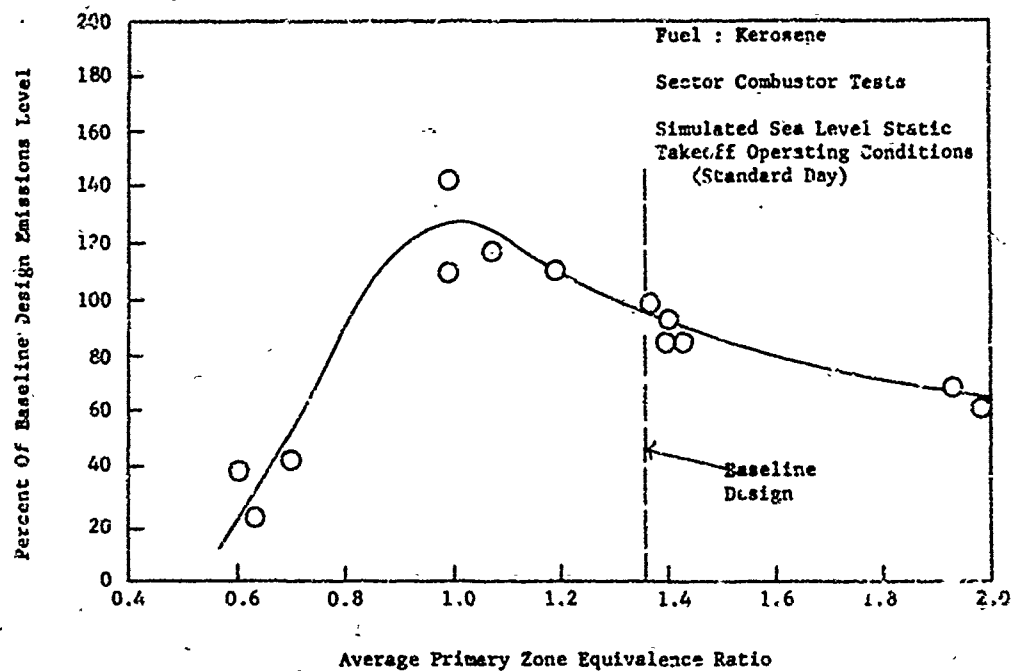


Figure 11. Effect Of Primary Combustion Zone Stoichiometry On Nitrogen Oxides Emissions Level.

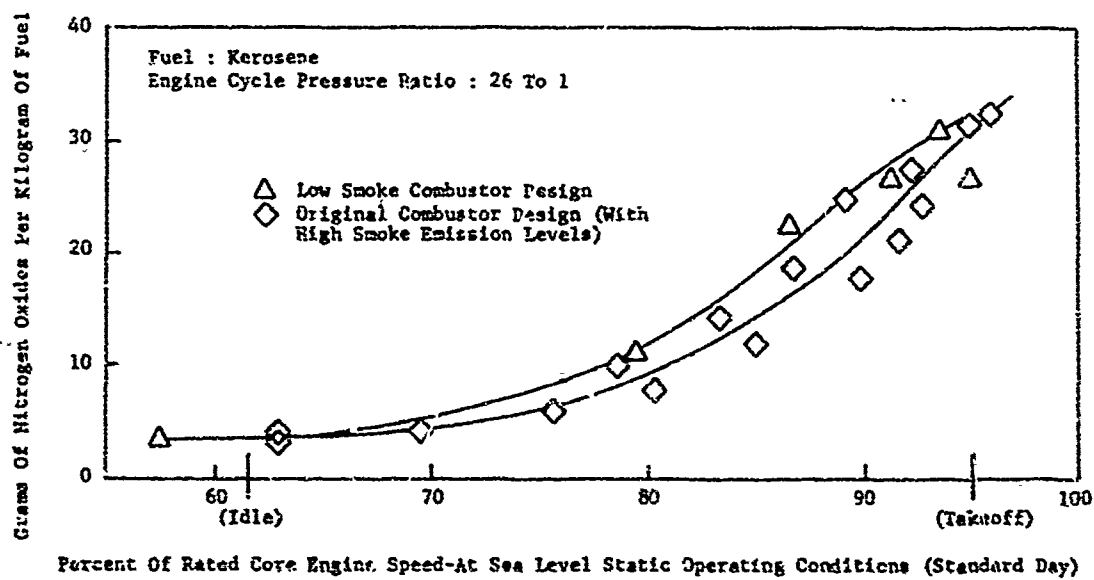


Figure 12. Comparison Of Nitrogen Oxides Emissions Characteristics Of Low Smoke Emission Combustor With High Smoke Emission Version Of The Same Combustor.

Discussion on Paper 29
 "Technology for the Reduction of Aircraft Turbine Engine
 Exhaust Emissions"
 presented by D.W.Bahr

H.C.Eatock: In Figure 9, NO_x emissions level data points in the range of 1 to 2 pounds per 1000 pounds of fuel are shown for the low pressure ratio engines. Any comments?

D.W.Bahr: In these low cycle pressure ratio engines, the peak NO_x concentrations contained in the engine exhaust gases are relatively low, generally less than 20 ppm. These specific data were obtained in some of our original engine emissions measurements tests. The sensitivity of the gas analysis methods used in these particular tests to low NO_x concentrations is slightly limited and, therefore, the measured NO_x emissions levels may be slightly low. Our NO_x emissions cell models, which were developed subsequently, predict levels in the range of 3 to 4 pounds per 1000 pounds of fuel for these engines. In more recently conducted tests of these low cycle pressure ratio engines in which further improved on-line exhaust emissions measurement capabilities were used, NO_x emissions levels in the range of 3 to 4 pounds per 1000 pounds of fuel were, in fact, obtained. All other NO_x emission data shown in Figure 9, and in the other figures containing such data, were obtained with this improved measurement system.

H.C.Eatock: Are the smoke emission characteristics of the baseline design combustor, referred to Figure 11, similar to those shown in Figure 2 for the low smoke combustor design?

D.W.Bahr: Yes. The baseline design, which is specified in Figure 11, is the same as the Figure 2 low smoke design.

F.J.Verkamp: With CDP bleed air extraction at idle, how much of an increase in NO_x emissions level at idle was observed?

D.W.Bahr: No measurable increases were observed in these tests, even with highly sensitive NO_x analysis equipment. While some small increases in the NO_x emissions levels at idle might be theoretically expected with increased bleed air extraction, any such increases are apparently very slight and not of significance. The NO_x emissions levels of turbojet and turbofan engines at idle are, of course, quite low — generally less than 3 pounds per 1000 pounds of fuel even in high cycle pressure ratio engines — and not of any significant concern.

F.J.Verkamp: What was the effect of water injection on the measured CO emissions levels?

D.W.Bahr: No changes in the measured CO emissions levels were observed up to a water mass flow rate of about 5 percent of the combustor air mass flow rate. Above this water flow rate, slight increases in the CO levels were detected.

A PRELIMINARY STUDY ON THE INFLUENCE OF FUEL STAGING ON NITRIC OXIDE EMISSIONS FROM GAS TURBINE COMBUSTORS

by

A. H. Lefebvre and R. S. Fletcher
School of Mechanical Engineering,
Cranfield Institute of Technology,
Cranfield, Bedford, England.

SUMMARY

The performance characteristics of present-day gas turbine combustors are significantly constrained by a design philosophy which attempts to achieve all the performance requirements in a single zone. Clearly these constraints can be lifted if the combustor employs two or more separate combustion zones, as it is then possible to design each zone to satisfy differing performance requirements. This paper presents the results obtained from a preliminary investigation carried out on a tubular aircraft combustor chamber which was perfectly standard apart from an additional fuel injector located just downstream of the primary zone. Measurements of nitric oxide exhaust emissions were carried out over a range of fuel flows to both primary and secondary zones and the results compared with predictions based on a previously derived mathematical model.

INTRODUCTION

Advances in gas turbine combustor design philosophy over the past three decades have been characterized more by gradual evolution than marked step change. Most of the early aircraft engines featured tubular combustion chambers. These were gradually superseded by tubo-annular systems which were widely used until the ascendance of the annular chamber, which now tends to dominate the scene, at least for aircraft applications. Over the same period some significant changes have occurred in fuel injection techniques. The early simplex swirl atomizer gave way in due course to more sophisticated designs, such as the duplex or dual-orifice atomizer, but growing concern over the problem of exhaust smoke eventually led to the advent of fuel-injection systems which involve a substantial element of fuel/air premixing prior to combustion. A notable example of this type of 'premix' device is the airblast atomizer.

It is, however, of interest to note that although the size and general appearance of combustor liners have altered appreciably, their basic design characteristics have remained substantially unchanged. Thus almost all combustors comprise three main zones - first a primary zone in which fuel is injected into a recirculating airstream and where most of the burning takes place, followed by an intermediate zone in which combustion proceeds to completion and where much of the soot produced in the primary zone is consumed. Downstream of this zone is the dilution zone where further air is injected to cool the gas down to the turbine inlet temperature. On some combustors these three zones are quite separate and distinct; on others the demarcation between zones is more blurred. Nevertheless, in all conventional combustors these three zones exist and their purpose is broadly to fulfill the functions outlined above.

The primary zone has by far the most arduous role to perform. It has to provide easy ignition and wide burning limits, coupled with high combustion efficiency and low soot formation over a wide range of operating conditions. Some of the requirements are difficult to reconcile. For example, most of the recognized methods of improving altitude relighting performance, such as reducing the cone angle of the fuel spray, or injecting less air into the primary flow reversal, tend to increase both flame radiation and exhaust smoke. Consideration of the other important pollutant species generated in kerosene/air combustion, namely carbon monoxide (CO), unburned hydrocarbons (HC) and oxides of nitrogen (NO_x) poses additional formidable problems. High flame temperatures and long residence times are advantageous from the viewpoint of minimizing CO and HC, but low flame temperatures and short residence times are essential to avoid excessive production of NO_x . Thus, in general, any modification to the primary zone that helps to reduce CO and HC will tend to enhance the formation of NO_x , and vice versa.

Disquiet over pollutant emissions from gas turbines has led in recent years to a searching re-examination of all the key processes taking place within the combustor. As a result two main lines of development towards "low emissions" combustors have emerged. One approach, which is attractive in the short term, is aimed at improving the emissions performance of existing combustor concepts by careful distribution of air to the various zones, by the adoption of more advanced methods of fuel injection, and by the practical exploitation of new wall-cooling techniques that discourage CO and HC accumulation in the lean cool regions near the liner wall. The merit of this approach is that the combustor retains its existing general size and configuration, and improvements can be made without trespassing far outside the bounds of established technology. Its main drawback is that the end product must inevitably be a compromise of some kind, both in regard to emissions and other aspects of combustion performance.

The other approach is essentially a rejection of the present design philosophy which is too rigid in its control of fuel and air distribution characteristics. An attempt is made to vary the distribution of fuel and/or air with engine operating speed and power output in such a manner that conditions within the combustion zone are always conducive to low pollutant emissions. One possible way of achieving this aim is by the use of variable geometry to regulate and control the amount of air entering the primary zone. This introduces the complexity of moving parts but has the potential to minimize pollutant emissions over the entire power range. Another alternative is to replace the conventional primary zone with two or more combustion zones each with its own separate supply of fuel. This offers the prospect of 'tuning' the flow and mixing characteristics of each zone to achieve conditions that best satisfy one or more aspects of combustion performance. This might suggest that the number of zones should ideally equal the number of

combustion performance parameters but, in practice, considerable simplification is possible because some performance requirements are sufficiently analogous to be accommodated into a single zone. For example, the conditions that promote good ligating performance, i.e. low air velocity, low turbulence and small spray angle, also tend to widen the burning range.

Clearly the simplest form of "staged" combustor would be one in which the normal primary zone is replaced by two separate combustion zones, each designed specifically to optimize certain aspects of performance. One proposed arrangement comprises a lightly-loaded primary zone, which is supplied with fuel either "premixed" or from a conventional pressure atomizer, depending on the stability range required. At low fuel flow conditions such as idling, combustion is confined to this zone, which being lightly loaded, ensures easy light-up, high combustion efficiency and low exhaust emissions. Downstream of the primary zone is located the main combustion zone. This is supplied with a large amount of air, premixed with fuel, to give soot-free combustion and low nitric oxide emissions.

The construction of a combustor designed along these lines is proceeding. In the meantime it was decided to carry out a preliminary investigation on a modified conventional combustor, with the following objectives;

- (1) to obtain some guidance on the potential of staged combustion for the reduction of nitric oxide
- (2) to examine whether the previously-derived model for predicting nitric oxide emissions could be satisfactorily applied to multi-staged combustion systems.

EXPERIMENTAL PROGRAMME

The test programme was carried out using a single, tubular, fully-developed and operational gas turbine combustor which featured air admission through an upstream axial swirler, secondary holes, tertiary holes and film cooling slots. The main dimensions and flow proportions of the combustor are given below:-

TABLE 1
Details of Combustor

Liner length	50cm.
Liner diameter	25cm.
Primary zone volume	3,850cm. ³
Total combustion volume	12,900cm. ³
Total liner volume	24,000cm. ³
Primary zone air	12 per cent
Total combustion air	48 per cent

The primary-zone fuel injector consisted of a piloted airblast atomizer and the secondary zone injector of a conventional swirl atomizer with a 60 degree angle. The secondary atomizer was installed within a water-cooled jacket and located with its point of injection about 3cm. downstream of the primary zone exit. A schematic diagram of the test combustor is given in Figure 1.

The results reported here represent only the preliminary ones in a continuing research programme in which measurements of combustion efficiency and certain pollutant emission levels namely oxides of nitrogen, unburned hydrocarbons, smoke and carbon monoxide, will be determined for a family of staged combustors. The discussion will consider the results obtained for nitric oxide over the following range of operating conditions.

TABLE 2
Test Conditions

Combustor Geometry	As designed	Modified to vary airflow into primary zone
Fuel Injection	Conventional	Staged
Air-Fuel Ratio	68 to 107	
Pressure	2.7 bars	
Temperature	450 deg.K	

Air heating was effected by means of in-line electrical heaters and the fuel employed was aviation kerosene. In order to investigate the influence of varying airflow proportions on NO emissions, with and without fuel staging, a number of tests were carried out with partial blanking of either the primary or dilution air admission holes. This gave, in effect, three separate combustor builds, as follows:-

- Build 1 - standard liner, having 12 percent primary air plus 36 percent secondary air. Total combustion air = 48 percent of chamber mass flow.
- Build 2 - dilution air holes partially blanked off giving 17 percent primary air and 50 percent secondary air. Total combustion air = 67 percent.
- Build 3 - primary air holes partially blanked off, giving 10 percent primary air and 32 percent secondary air. Total combustion air = 42 percent.

The air flow proportions quoted above are based on the manufacturer's estimates which have been modified for Builds (2) and (3) to allow for the effect of the blanking strips in redistributing the air to the various zones. In estimating flow proportions for Builds (2) and (3) no attempt was made to recalculate hole discharge coefficients and therefore no great accuracy is claimed for the values quoted above. In all

tests on Builds (2) and (3) the chamber reference velocity was modified by appropriate amounts in order to maintain a constant value for the mean residence time in the combustion zone.

MEASUREMENT OF EMISSIONS

Exhaust gases were extracted at the combustor exit through a diametral probe containing nine holes of 1mm. diameter, spaced to give equal area sampling. Although the probe itself was water cooled, the line between the test rig and the adjoining control room was electrically heated to between 180° and 200°C. A small positive pressure was maintained on all instruments to overcome possible problems of leakage. A freezing trap and spray trap were included to cool the sample and remove excess water. The nitric oxide concentration in parts per million by volume was measured on a chemiluminescent analyzer.

MATHEMATICAL MODEL OF NITRIC OXIDE EMISSIONS

The predominant oxide of nitrogen produced in aircraft gas turbines is nitric oxide, (NO), and mathematical methods are presently being developed to predict the formation characteristics of this species. One model^{2,3} has already demonstrated the ability to predict NO from conventional combustors and it can be simply modified to apply to staged combustion systems. A brief description of the model follows:

Method of Approach

The main assumptions made in the derivation of the model are, that,

1. The major chemical species in the combustion process can be considered to be in thermodynamic equilibrium.
2. The NO formation process can be isolated from the flow and combustion processes.

These assumptions follow from observations of practical combustor systems that show nitric oxide levels to be sufficiently low for changes in concentration to have negligible effect upon gas temperatures, and the NO formation process to be so slow relative to the combustion process that most NO is formed in the post-flame gases.

Nitric oxide kinetics are represented in a manner after that first proposed in Reference (4) which leads to the following overall NO reaction rate equation:

$$\frac{d(NO)}{dt} = \frac{2M_{NO}}{\rho} (1-\alpha^2) \frac{R_1}{1 + \alpha K} \quad (1)$$

where (NO) = nitric oxide mass fraction, M_{NO} = molecular weight of NO, ρ = gas density, $\alpha = (NO)/(NO)_e$, where e indicates equilibrium conditions, and R_1 and K relate to three controlling kinetic rate equations which involve the species O_2 , O, M_2 , N, NO and OH.

The model of the flow behaviour in the gas turbine combustor treats each of the three zones defined previously (see Figure 2) in a separate manner. The NO emission characteristics of the primary zone are related to three controlling processes, namely, the lack of complete combustion that occurs within the zone, the nonuniformities in concentration and temperature, and the residence time characteristics of the fluid elements. Incomplete combustion is accounted for by defining an effective mass mean equivalence ratio ϕ_E to be equal to ϕ/ϕ_p where ϕ_p is the actual mass mean value and ϕ is a primary zone combustion efficiency as correlated in Reference (5). The 'mixedness' of the primary zone is characterized by the single dimensionless parameter $S_0 = \sigma/\phi_E$ where σ in statistical terms is called the standard deviation and represents the degree of distribution about ϕ_E . Regions with equivalence ratios bounded between e and $e+\phi$ are then represented by the mass fraction $f(\phi)$ where

$$f(\phi) = (1/\sigma\sqrt{2\pi}) \exp [-(\phi-\phi_E)^2/2\sigma^2] \quad (2)$$

The residence time for each fluid element in the zone is assumed to obey the distribution characteristics that follow from the theory of well-stirred reactor, in which the characteristic mean residence time is defined as the primary zone volume divided by the volumetric flow rate.

Factors modelled in the intermediate zone are those that influence the axial mass-mean temperature profile and the distribution characteristic about this mean. These are the rate at which air enters the zone and is entrained into the bulk flow, the rate of mixing to the homogeneous state (T-c), and the rate at which the unburned fuel is ignited. It is assumed that these processes are proportional to the square root of distance travelled in the zone. The assumptions have been tested parametrically³ and found to influence predictions by less than fifteen percent. Conditions in the dilution zone are assumed to be homogeneous and, therefore, readily calculated.

Previous Comparisons with Experimental Data from Conventional Systems

The limitation in the model described above is that the mixedness parameter, S_0 , must be considered to be a matching parameter as its value can only be determined by comparison of predictions with measured values. Practically its value can vary from 0.5 to 2.0 for a premixed fuel-air system, to unity for the very poorly mixed case. It has been used with fair success to predict NO_x emissions over a wide range of operating conditions for two fully developed aircraft gas turbine combustors, once the value of S_0 was obtained, and some results are shown in Figure 3.

EXTENSION OF MODEL TO STAGED COMBUSTION

The simplest method of approach in applying the model to the staged combustor concept is to assume that it comprises two combustion zones in series. The dilution zone is of no significance as previous calculations have shown that NO ceases to be formed once the effective mass mean equivalence ratio reduces below about 0.5. Such values tend to occur a little further than one radius distance from the

primary zone exit in conventional gas turbine combustors.

If this approach is adopted an assumption has to be made concerning the details of the mixing process that occurs between the two stages and its influence upon the subsequent NO formation characteristics. It is assumed that these have no significance in the well designed system and the initial concentration of all elements in the second stage calculation is set equal to the average value that exists at the first stage. Examination of equation (1) shows this to be a valid assumption as the rate of formation of NO, though dependent upon the NO concentration, is essentially linear until it exceeds approximately 0.3. The value of α , which is the fractional concentration of NO produced in relation to the equilibrium value, rarely exceeds this figure in gas turbine systems. This assumption implies that the NO generated in the two stages can be considered separately and that the total emission is the sum of the individual contributions.

Calculations were made based upon the assumption that the first stage length terminated with the point of injection of the second stage fuel. The secondary burning zone was assumed to contain all the air added up to the downstream edge of this zone. The combustion efficiency of the second stage burning zone was measured at the standard rig test condition and found to be close to 60 percent. This value was used in all calculations.

DISCUSSION

The results obtained for all three builds are shown plotted in Figures 4, 5 and 6. When the standard liner was operating with two stages of fuel injection, approximately 75 percent of the fuel was injected into the primary combustion zone and the remainder into the secondary combustion zone. The effect of staging the fuel injection in this manner was to reduce appreciably the exhaust concentration of NO, as shown in Figure 4. It is apparent from Figures 5 and 6 that fuel staging was less effective in reducing NO emissions with Builds (2) and (3), in which approximately one-third of the fuel was employed in primary-zone combustion and the remainder injected downstream. Nevertheless, taking the results as a whole, and bearing in mind the rudimentary nature of the test programme, in which no attempt was made to optimize flow quantities or airflow pattern or fuel distribution in either stage, it is clear that fuel staging has considerable potential for lowering NO emissions from gas turbine combustors.

The full lines drawn in Figures 4 to 6 represent the values of NO as predicted from the mathematical model described above. The mixedness parameter, S_0 , was determined by trial and error to give good agreement between measured and calculated values of NO for the standard liner. This same value of S_0 was then employed to calculate all the NO emissions data corresponding to the lines shown in full in Figures 4, 5 and 6. In all figures the experimental and predicted values tally reasonably well and thereby strengthen the validity of the mathematical model used to simulate NO emissions.

CONCLUSION

The results of this preliminary investigation confirm that fuel staging has considerable potential for reducing nitric oxide emissions from gas turbine combustors.

REFERENCES

1. Lefebvre, A. H., "Emissions from Continuous Combustion Systems" Edited by W. Cornelius and W. G. Agnew - General Motors Symposium, p.321, Plenum Press, 1972.
2. Fletcher, R. S. and Heywood, J. B., "A Model for Nitric Oxide Emissions from Aircraft Gas Turbine Engines", AIAA Paper 71-123, presented at the AIAA 9th Aerospace Sciences Meeting, New York, January 1971.
3. Fletcher, R. S., Sierel, R. D. and Bastress, E. K., "The Control of Oxides of Nitrogen Emissions from Aircraft Gas Turbine Engines", (NREC Report 1162-1) Northern Research and Engineering Corporation, Cambridge, Massachusetts, December 1971. Also Federal Aviation Authority report FAA-RD-111-2.
4. LeBlond, G. A., Heywood, J. B. and Keck, J. C., "Experimental and Theoretical Study of Nitric Oxide Formation in Internal Combustion Engines". Combustion Science and Technology, Vol. 1, pp.316-326, 1970.
5. Jackson, S. H. and Odgers, J., "Factors Influencing Heat Release in Combustion Chambers and Consideration of the Related Materials and Structures". Combustion in Advanced Gas Turbine Systems, Proceedings of International Propulsion Symposium, Cranfield, England, April 1967.

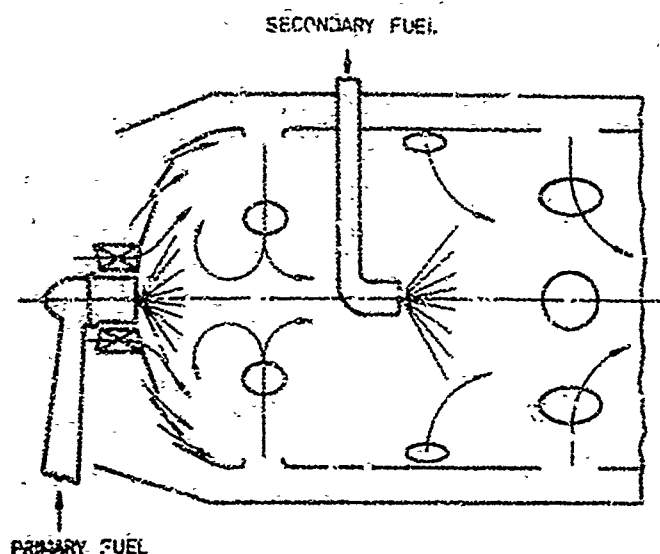


Figure 1 SCHEMATIC DIAGRAM OF TEST COMBUSTOR

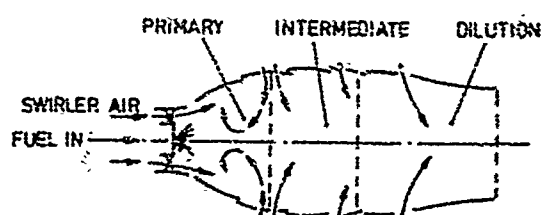
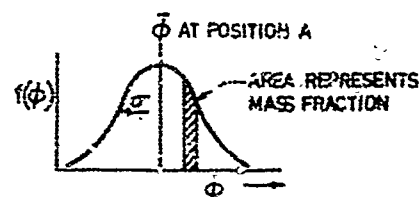


Figure 2 ASSUMED FLOW AND DISTRIBUTION PATTERNS THROUGHOUT CONVENTIONAL COMBUSTOR LINER

(a) CROSS SECTION OF COMBUSTOR LINER SHOWING MEAN FLOW PATTERN



(b) DISTRIBUTION OF MASS AS A FUNCTION OF EQUIVALENCE RATIO

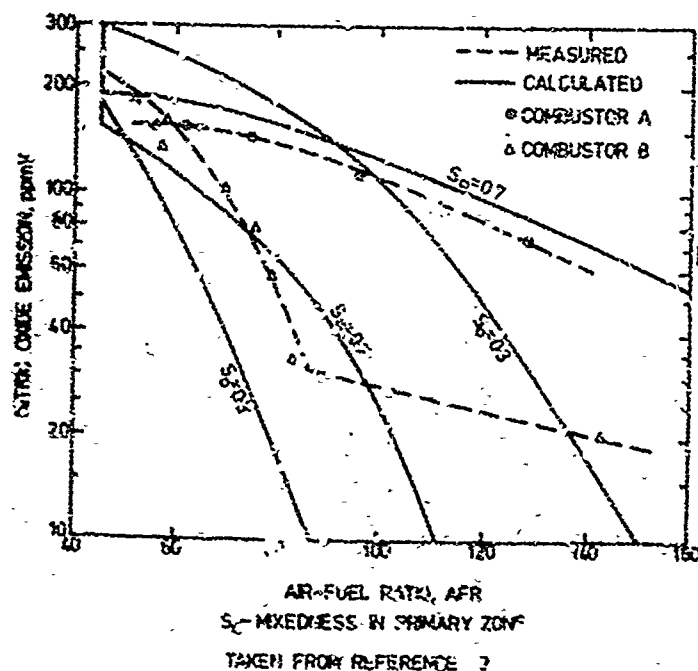


Figure 3 PREDICTED versus MEASURED NITRIC OXIDE EMISSIONS

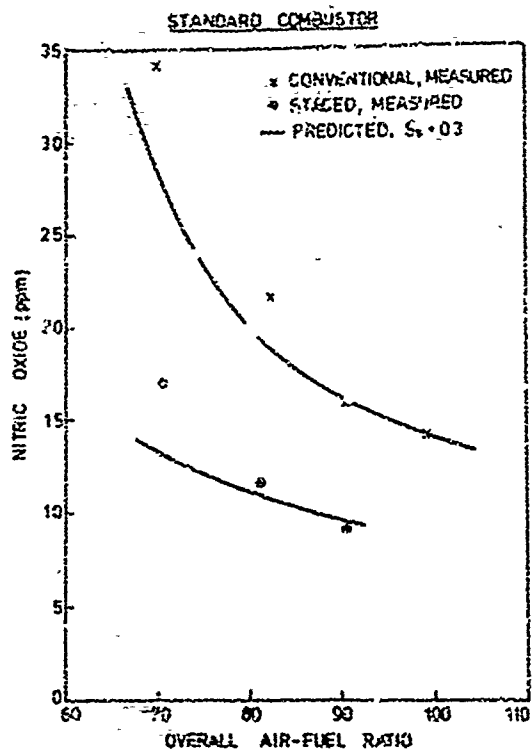


Figure 4 NITRIC OXIDE EMISSION
CHARACTERISTICS FOR BUILD 1

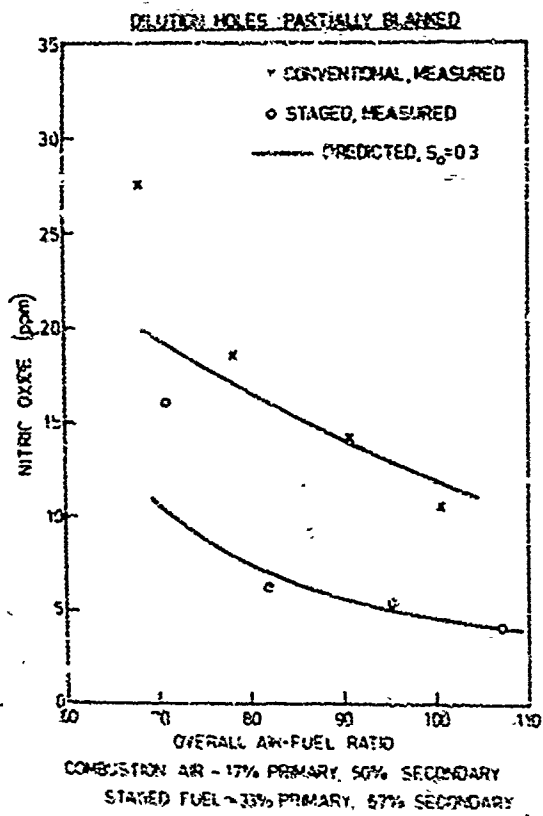


Figure 5 NITRIC OXIDE EMISSION
CHARACTERISTICS FOR BUILD 2

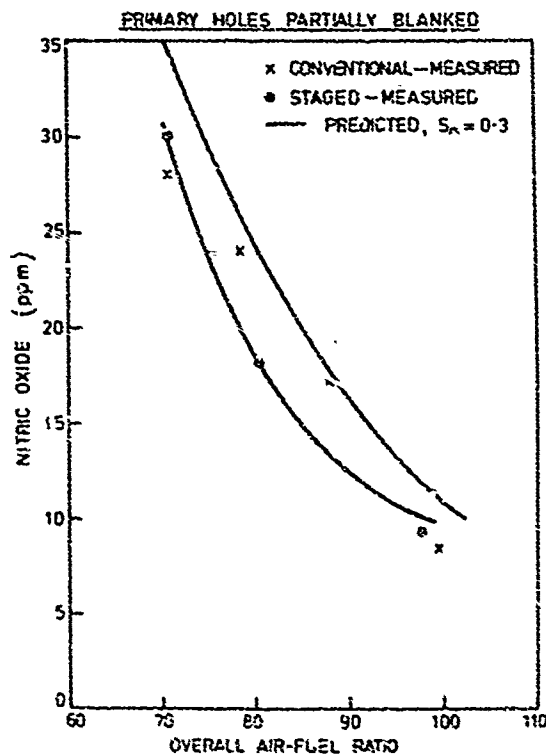


Figure 6 NITRIC OXIDE EMISSION
CHARACTERISTICS FOR BUILD 3

Discussion on Paper 30
 "A Preliminary Study on the Influence of Fuel Staging on Nitric Oxide
 Emissions from Gas Turbine Combustors"
 presented by A.H. Lefebvre

S.A. Mosier: With due respect to your comment that the results shown are preliminary in nature, I must reject the burner configuration shown in your Figure 1 as being non-pragmatic. The insertion of a fuel injection system into the flame zone of a combustor leads to a great many safety and maintenance problems. Also, reducing nitric oxides using the staged fuel concept is not necessarily a great feat. I would suggest that you pay close attention to unburned hydrocarbon and carbon monoxide concentrations. Your poor combustion efficiency (80 percent) reveals that the carbon monoxide and unburned hydrocarbons concentrations are very high under the conditions at which you were testing. Your work appears to be too preliminary to draw any promising extrapolations.

A.H. Lefebvre: The method employed to introduce the second-stage fuel was adopted for rig test convenience and is not being advocated as a practical design. The quoted value of 80 percent combustion efficiency for the pre-dilution zone is, in fact, fairly typical of aircraft combustors when operating at relatively low inlet air temperatures and pressures. Mr Mosier's reference to "high concentrations of carbon monoxide and unburned hydrocarbons" are, I believe, based on a misunderstanding of our objectives. We contend that low emissions of these species is best achieved by single-stage fuel injection into a primary zone that is specifically designed in terms of flow velocity and equivalence ratio to give optimum combustion performance at low power conditions. Such a system would, of course, tend to give high concentrations of nitric oxides at high power conditions, but it is hoped to avoid this situation by injecting a large proportion of the fuel downstream of the primary zone when operating at maximum power. The primary purpose of our work was to test the validity of this contention, and we feel that these initial results presented in our paper suffice to illustrate the high potential of the two-stage concept for low-emission combustors.

G. Kappeler: With fuel staging, energy is locally introduced into the gas stream and also fluctuations caused by the combustion process. It seems feasible that with an unfortunate tuning the fluctuations might be aggravated (as it is often observed in afterburners) and the noise level might increase and buzz be detected. Could you please comment on this possibility.

A.H. Lefebvre: Previous work at Cranfield has shown that the noise emanating from a gas turbine combustor is primarily a function of the velocity and flow rate of the exhaust gases and is virtually independent of variations in fuel injection method and liner geometry. I do not consider that a two-stage combustor is inherently more susceptible to combustion instability than a conventional combustor. We have not encountered buzz or any other form of flow instability in the admittedly limited amount of running carried out so far.

A. Quillevéré: L'étude expérimentale présentée par les auteurs est instructive. Toutefois, le niveau de température à l'entrée du foyer étant modeste, l'importance du mécanisme "thermique" de formation des oxydes d'azote est moins grande qu'elle ne l'est, à régime élevé, dans une chambre de combustion de moteur. Compte tenu de l'existence du mécanisme dit du "prompt NO", trouverait-on les mêmes gains avec une température d'entrée plus élevée?

A.H. Lefebvre: We would expect the results obtained at relatively low inlet air temperatures to be indicative of what might be expected with the engine operating at high power settings. (Since the presentation of this paper further tests have been conducted at much higher inlet air temperatures and significantly greater reductions in nitric oxides obtained.)

A.B. Wessel: I should appreciate your comment on whether a staged fuel concept, which of necessity introduces fuel further downstream the combustor, will require additional length to enable the dilution mixing process to be completed so as to maintain the outlet temperature traverse quality at the levels currently found acceptable.

A.H. Lefebvre: This is an interesting and important question. At first sight it would appear obvious and logical that an additional combustion zone must entail additional liner length. However, I am not convinced that this is necessarily true. Firstly, I would argue that we are now providing a more positive function for the intermediate zone which, on most conventional combustors plays an ill-defined and somewhat nebulous role. Secondly, it is not fundamental to the two-stage concept that the two combustion zones should be located in series. Although this configuration was found convenient for our tests, a "parallel" arrangement for the two combustor zones is equally practical and, in some cases, may be considered more desirable.

DESIGN AND EVALUATION OF COMBUSTORS FOR REDUCING AIRCRAFT ENGINE POLLUTION

by

Robert E. Jones and Jack Grotsman
Lewis Research Center
National Aeronautics and Space Administration
Cleveland, Ohio 44135

SUMMARY

This report summarizes some of the NASA Lewis Research Center's recent efforts in reducing exhaust emissions from turbine engines. Various techniques employed and the results of testing are briefly described and referenced for detail. The effort arises from the increasing concern for the measurement and control of emissions from gas turbine engines. The greater part of this research is focused on reducing the oxides of nitrogen formed during takeoff and cruise in both advanced CTOL, high pressure ratio engines and advanced supersonic aircraft engines. The experimental approaches taken to reduce oxides of nitrogen emissions include the use of: multizone combustors incorporating reduced dwell time, fuel-air premixing, air atomization, fuel preevaporation, water injection and gaseous fuels. In the experiments conducted to date, some of these techniques have been more successful than others in reducing oxides of nitrogen emissions. In all cases, considerably more research will be required to develop combustors employing one or more of these experimental techniques without sacrificing over-all combustor performance. Tests are being conducted on full-annular combustors at pressures up to 6 atmospheres and on combustor segments at pressures up to 30 atmospheres.

Emissions of unburned hydrocarbons and carbon monoxide are caused by poor combustion efficiency at conditions such as engine idle. The use of fuel staging in multizone combustors and air assist fuel nozzles have indicated that large reductions in hydrocarbon and carbon monoxide emissions can be achieved. Studies are also being conducted on the use of diffuser area and variable combustor geometry to try to optimize the combustor airflow distribution over the wide range of operating conditions.

The effect of inlet-air humidity on the generation of oxides of nitrogen was studied as well as the very effective technique of direct water injection. The emission characteristics of natural gas and propane fuels were measured and are compared to those of ASTM-A1 kerosene fuel.

INTRODUCTION

This report describes some of the present efforts of the NASA Lewis Research Center in reducing the pollutant levels of gas turbine engine combustors with the primary emphasis on reducing oxides of nitrogen at takeoff and cruise conditions. Concern over air pollution has drawn the attention of combustion engineers to the quantities of exhaust emissions produced by gas turbine engines. Two general areas of concern have been established; urban pollution in the vicinity of airports and pollution in the stratosphere (refs. 1 and 2). The principal urban pollutants are emissions of unburned hydrocarbons and carbon monoxide during engine idle and taxi, and oxides of nitrogen and smoke during take-off. Oxides of nitrogen are presently considered to be the most critical emission product during high altitude cruise (ref. 3).

Redesigning the gas turbine combustor to accomplish a significant reduction in oxides of nitrogen will be a difficult task, since oxides of nitrogen are formed during any combustion process involving air. The amount formed is controlled by the chemical reaction rate and is a function of the flame temperature, residence time of combustion gases at the highest temperatures, the concentrations of oxygen and nitrogen present, and to a lesser extent the combustor pressure. Trends in combustor operating conditions indicate a steady rise in combustor inlet air temperature due to increases in engine pressure ratios and increasingly higher flight speeds (ref. 4). These effects increase the flame temperature with subsequent increases in the production of oxides of nitrogen.

The combustion work reported in this paper is pursuing several varied techniques for reducing the formation of gaseous pollutants. To reduce concentrations of oxides of nitrogen, combustors are being tested that have reduced reaction zone dwell time. Also, studies are also being conducted on ways to reduce the reaction zone temperature. Idle emissions are being reduced by improving combustion efficiency at off design operating conditions. Combustor smoke is being minimized by careful control of the reaction zone equivalence ratios and by rapid mixing in the reaction zone.

These techniques for gaseous pollutant control are being evaluated on several full-annular combustors as well as in high pressure combustor segment tests. Techniques under study include the use of many small recirculation zones to reduce reaction zone dwell time, the use of premixing; air atomization and preevaporation of fuel; fuel staging and simulated variable combustor geometry; the use of direct water injection; and tests with a variety of fuels including natural gas and propane.

TEST PROCEDURES

Combustor testing is conducted in a variety of connected-duct test facilities at the Lewis Research Center. All inlet-air temperatures are obtained without vitiating the inlet air flow. Several test facilities have vitiating heaters to raise the inlet temperature still higher. However, they are never used during tests where the measurement of combustor pollutant levels is required. For full-annular combustors, tests can be conducted at exact conditions simulating high-altitude, high Mach number flight. Each test facility is equipped with on-line gas analysis instruments for pollutant measurements. The exhaust constituents, CO_2 and CO , are measured using nondispersive infrared (NDIR) instruments, oxides of nitrogen, NO and NO_2 are measured using chemiluminescence instruments equipped with a thermal converter to reduce NO_2 to NO prior to measurement. Unburned hydrocarbons are measured using a flame-ionization detector

maintained at a temperature of 450 K. Unburned hydrocarbons from kerosene fuels are assumed to have the composition $C_{12}H_{22}$.

Gas sampling techniques vary from test to test. Most samples are taken from one or more internally manifolded fixed rakes. Some gas samples are taken with traversing probes on both segment and annular combustor tests. The samples are transported to the gas analysis instruments through heated stainless-steel tubes. Sample transit time through the transfer tube is minimized by venting a large amount of the sample flow at the instruments and by maintaining the pressure in the transfer tube at approximately 2 atmospheres. The sampling procedures and techniques used, follow the guidelines specified in SAE ARP 1256 (ref. 5). Smoke measurements are also made by sampling at the combustor exhaust plane. The smoke number is determined by collecting the particulates on filter paper and obtaining a reflectance reading of the stain. This technique has been standardized in SAE ARP 1179 (ref. 6).

The representativeness of the gas sample is checked by comparing the computed gas-sample fuel-air ratio to the fuel-air ratio calculated from flow rate measurements. Only data obtained where these fuel air ratios agree to within ± 5 percent is accepted.

EMISSION REDUCTION RESULTS AND DISCUSSION

Multizone Combustors

Combustor descriptions. - Full annular combustor testing at NASA-Lewis has emphasized two combustor concepts for decreasing burning zone length. These are the swirl-can combustor and the double annular combustor. The swirl-can combustor is shown in Fig. 1 and 2. The combustor is of annular design, 0.514 m long and 1.057 m in diameter. The combustor consists of 120 individual swirl-can modules which distribute combustion uniformly across the annulus. The modules are arranged in three concentric rows with fuel flow independently controlled to each row. There are 48 modules in the outer row, 40 in the center and 32 in the inner row.

The combustor module design is shown in Fig. 3. Each module premixes fuel with air in the carburetor, swirls the mixture, stabilizes combustion in its wake, and provides interfacial mixing areas between bypass air through the array and the hot gases in the wake of the module. More detailed information on swirl-can combustors can be found in Refs. 7 to 9.

The other full-annulus combustor being investigated with a shortened burning zone is referred to as a double-annular, ram induction combustor. A cross-sectional sketch of this combustor is shown in Fig. 4. Constructing the combustion zone as a double-annulus permits the reduction of overall combustor length while maintaining an adequate ratio of length to annulus height in each combustion zone. This feature allows a considerable reduction in length to be made over a single annulus with the same overall height.

Individual control of the inner and outer annulus fuel systems of the double annular combustion zone provides a useful method for adjusting the outlet radial temperature profile.

The ram-induction combustor differs from the more conventional combustors in that the compressor discharge air is allowed to penetrate into the combustion and mixing zones without diffusing to as high a static pressure. The kinetic energy of the inlet air is thereby used to promote rapid mixing of air and fuel in the primary zone, and of diluent air and burned gases in the mixing zone. The airflow is efficiently turned into the combustor by two rows of vaned turning scoops that penetrate into the combustor. A more detailed discussion of the ram-induction concept is provided in Refs. 10 through 14.

Oxides of nitrogen emissions. - The emissions of oxides of nitrogen ($NO + NO_2 = NO_x$) for the multizone combustors are shown in Fig. 5. Also shown on this figure are data from a single-annular combustor, Refs. 15 and 16. The NO_x emission index, grams of NO_x produced per kilogram of fuel burned, is shown as a function of the combustor exit average temperature. The test conditions; pressure, inlet-air temperature and reference velocity were the same for all three combustors. The numbers in parentheses are the number of fuel injection sources of each combustor. Increasing the number of fuel injection sources and spreading the combustion zone uniformly throughout the combustor appears to be a very effective way of reducing the emission of NO_x . The techniques of premixing fuel and air and rapid quenching of the combustion reaction, both incorporated into the swirl-can approach, are also considered to be a principle factor for producing the lower NO_x emissions of these combustors. Figure 6 compares the NO_x emission level for the three combustor types with increasing inlet-air temperature and a constant exit temperature of 1500 K. The trend with increasing inlet-air temperature is an exponential increase in NO_x emission index. The use of multizone combustors or combustors that spread combustion as much as possible is a very effective way to reduce NO_x emissions. At an inlet-air temperature of 755 K the swirl can combustor produces only 8 percent as much NO_x as the more conventional single-annular combustor. Figure 7 shows the emissions of NO_x for the swirl-can combustor for inlet-air temperatures up to 840 K and fuel air ratios up to 0.0695. For the ASTM-A1 fuel used in these tests, the stoichiometric fuel-air ratio is 0.0876. This swirl-can combustor was designed for near stoichiometric operation and as such is larger than would be required for operation at more usual turbine inlet temperatures. The figure shows a strong dependence of NO_x emissions on both inlet-air temperature and on fuel-air ratio. However as the fuel-air ratio is increased the formation of NO_x eventually reaches a constant level and as stoichiometric fuel air ratios are approached the measured concentration of NO_x was noticed to decline. Though this effect is only clearly demonstrated at an inlet-air temperature of 550 K, there is no reason to believe that similar effects would not be observed at the higher inlet-air temperatures. A more complete discussion of all the emission characteristics of swirl-can combustors can be found in Refs. 7 and 8.

The effects of combustor residence time on NO_x emissions is shown in Fig. 8 for the two multizone combustors. Increasing the combustor reference velocity (decreasing the residence time) causes a corresponding decrease in the NO_x emission level. The effect is actually linear with residence time as is indicated by the dashed line with a slope of minus one.

Smoke number. - The smoke emissions of the swirl-can combustor are shown in Fig. 9. These data were

obtained during a test to stoichiometric operating conditions at a pressure level of 6 atmospheres, (ref. 9). No smoke was detected when the combustor exit temperature was below 1950 K. The smoke increases rapidly as the overall stoichiometric fuel-air ratio is approached. For comparison, the smoke number of the double-annulus combustor at an exit average temperature of 1500 K and the same operating conditions as on Fig. 9 is approximately 14. This illustrates the point that fuel-air premixing as occurs in swirl-cans is a very effective way of reducing combustor smoke.

Air Atomization

High pressure combustor tests were made to determine pollutant emissions and performance characteristics obtained with low fuel pressure drop air-atomizing fuel nozzles designed to utilize the air-stream momentum in atomizing ASTM A-1 fuel (ref. 17). Similar tests were made with pressure-atomizing fuel nozzles for comparison. With the present trend in development toward advanced turbojet engines with high compressor-pressure ratios, the problem of developing low pollutant combustors has become more difficult at the resulting high levels of inlet-air pressure and temperature.

One of the main advantages of air atomizing fuel nozzles is their flexibility in design in producing fuel sprays which spread out fairly uniformly across the airstream. With improved atomization and mixing obtained from air atomizing fuel nozzles, it would be expected that nitric oxide concentrations could be reduced (ref. 18). Besides being relatively simple in design and fabrication, air atomizing fuel nozzles are less susceptible to fuel fouling at high inlet-air temperatures as compared with the pressure atomizing type.

Air atomizing nozzles were tested under ambient flow conditions in a full scale Lucite model of an experimental combustor to determine spray patterns produced with water injection. Photographs taken at several water air ratios and reference velocities showed that a splash cone type of air atomizing nozzle gave a better distribution of liquid and a finer spray of water droplets than that obtained with a radial jet type of air atomizer. As expected from water spray tests, radial jet nozzles gave high smoke numbers in preliminary combustor tests. Thus, the splash cone air atomizing nozzle, shown in Fig. 10, was selected for the high pressure combustor tests.

The fuel nozzle assembly shown in the figure consists of a diffuser snout in which a portion of the air from the compressor is captured and flows through the air swirler and around the splash cone nozzle. The air swirler produces a rotating airflow which assists in evenly distributing the fuel droplets and stabilizing the subsequent flame. Low pressure fuel is injected from the combination fuel supply and splash cone support through four 0.16 cm diameter orifices onto the curved face of the nozzle. Fuel splashes over the nozzle lip and is atomized by the swirling airstream. At the point where the airstream first contacts the fuel, the diffuser passage converges to accelerate the flow of the resultant fuel-air mixture which is then suddenly expanded into the combustor by the diverging portion of the diffuser. The nozzle assembly can be used either singly or in combination to provide the required distribution for can combustors, can-annular combustors, or annular combustors.

A high pressure combustor segment 0.456 m (18 in.) long with a maximum cross section of 0.153 by 0.305 m (6 by 12 in.) was tested with the splash-cone air atomizing and conventional simplex pressure atomizing fuel nozzles (ref. 17) at inlet-air pressures of 4 to 20 atmospheres, inlet air temperatures as high as 590 K, reference velocities of 12.4 to 26.1 m/sec (41 to 86 ft/sec), and fuel air ratios of 0.008 to 0.020. Pollutant emissions obtained with the splash cone air atomizing nozzle configuration are compared with results obtained with pressure atomizing fuel nozzles. Most of the results to be described herein were obtained at an inlet total temperature of 590 K, a reference velocity of 21.4 m/sec, and a fuel-air ratio of 0.015.

The variation of the nitrogen oxide emission index with pressure is shown in Fig. 11. Emission index generally increased with increasing inlet air pressure. However, there was a considerable drop in emission index with the splash cone nozzle when inlet air pressure was increased from 10 to 20 atmospheres. This was attributed to improved atomization of the fuel when airstream momentum was increased. In this case, momentum was increased by increasing the airstream density. Thus, at an inlet air pressure of 20 atmospheres, it was found that the nitrogen oxide emission index was considerably lower with the splash cone air atomizing nozzle than with the pressure atomizing nozzle. These tests were conducted with a fixed air entry hole geometry. It is conceivable that further reductions in oxides of nitrogen might be attained by adjustments in liner airflow distribution.

Increasing inlet air pressure from 4 to 10 atmospheres increased exhaust smoke numbers for all of the fuel nozzles that were tested. However, smoke number decreased slightly with the splash cone nozzle when inlet air pressure was increased from 10 to 20 atmospheres. As previously mentioned, nitric oxide emission index decreased in a similar manner which was attributed to improved fuel atomization when airstream momentum was increased. Thus, with the air atomizing splash cone nozzle, an improvement in fuel atomization at high inlet air pressure tended to counteract the general tendency of smoke number to increase with increasing inlet air pressure. However, at 20 atmospheres inlet air pressures, the splash cone nozzle had a smoke number of about 35, somewhat higher than one of the pressure atomizing nozzles tested out lower than that of another. It should be noted that the inlet air temperature of 590 K was somewhat below the design "takeoff" condition of 20 atmospheres and 755 K (1360° R). Thus, smoke numbers are somewhat higher than might be expected at the design takeoff condition since increasing inlet temperatures tend to reduce smoke number.

Increasing either inlet-air pressure or temperature decreased carbon monoxide and unburned hydrocarbon emission indexes with both the splash cone and pressure atomizing nozzles. The comparison between the splash cone and the pressure atomizing nozzle indicated that both carbon monoxide and unburned hydrocarbons were lower with splash cone nozzles at an inlet air temperature of 590 K (1060° R) over a range of pressure of 4 to 20 atmospheres although the combustion efficiencies for both fuel nozzles were near 100 percent. Initial results for the air atomizing splash cone fuel nozzle are promising but a great deal more research

is required to attain further reductions in oxides of nitrogen and smoke, and to evaluate combustor durability and altitude relight capabilities.

Fuel Prevaporization

A study was conducted to determine the effect of prevaporization on the exhaust emissions from an experimental combustor (ref. 19). Two methods for reducing oxides of nitrogen are to reduce the reaction zone temperature (flame temperature) and to reduce the reaction zone dwell time. The reaction zone temperature may be reduced by operating with a more homogeneous fuel air mixture that is either fuel rich or fuel lean. The fuel air mixture could be made more homogeneous either by increasing mixing intensity, by premixing the fuel and air before they enter the reaction zone, or by prevaporizing the fuel before it enters the reaction zone. A more homogeneous fuel air mixture should also minimize emission products caused by incomplete combustion. Eliminating the process of fuel droplet evaporation within the reaction zone could enable a reduction in reaction zone dwell time.

Operating a combustor with prevaporized kerosene fuel would require a heat exchanger to convert the liquid fuel to vapor prior to injection into the reaction zone. Due to limitations that might be imposed by the heat exchanger, the combustor may operate with only partially vaporized fuel over a part of the flight conditions. One of the objectives of the tests described herein was to determine emission levels with varying degrees of vaporization. Vaporized propane was used to simulate vaporized kerosene. Propane was chosen to eliminate the complexities of operating a liquid fuel boiler and because its burning characteristics are similar to kerosene. Two different dual fuel nozzles were used to inject varying proportions of liquid ASTM A-1 fuel and gaseous propane into the test combustor as shown in Fig. 12. The experimental combustor that was used is similar to that described in the previous section. At a given fuel-air ratio, the summation of the mass flowrates for liquid ASTM A-1 and gaseous propane was held constant as the proportion of gaseous propane was varied from 0 to 100 percent. Fuel injector No. 1 consists of a simplex nozzle located in the center of the assembly for injecting liquid kerosene and a series of eight evenly spaced holes concentric with the simplex orifice for injecting gaseous propane. Fuel injector No. 2 is a commercial duplex nozzle in which the center orifice was used for injecting liquid kerosene and the annular orifice was used for injecting gaseous propane. The tests described herein were conducted over a range of inlet pressure and temperature of 4 to 20 atmospheres and 475 to 700 K, respectively, a fuel-air ratio of 0.014 and a reference velocity of 21.3 m/sec.

Figure 13 shows the variation in the emission index for oxides of nitrogen with inlet temperature for varying proportions of gaseous propane. The results obtained using fuel injector No. 1 indicate that as the inlet temperature is increased from 478 to 700 K, the emission index for oxides of nitrogen increases from 6 to 22 for 0 percent vapor. The effect of vapor fuel on the NO_x emission index is negligible up to an inlet temperature of about 590 K. The reduction in NO_x that occurred as the proportion of vapor fuel was increased became more significant as inlet temperature was increased further. At 700 K, a considerable improvement was obtained, amounting to a 24 percent decrease in NO_x , as the proportion of vapor was increased from 0 to 100 percent. The results obtained with fuel injector No. 2 were similar with the exception that the general level for the NO_x emissions was lower.

Figure 14 shows the variation in smoke number with inlet pressure for varying proportions of gaseous fuel. As inlet pressure was increased from 4 to 20 atmospheres, the smoke number for fuel injector No. 1 increased from 12 to 17 with 0 percent vapor. At a pressure of 20 atmospheres, increasing the proportion of vapor from 0 to 100 percent, decreased the smoke number by 60 percent. Fuel injector No. 2 produced a marked increase in smoke number as pressure was increased.

Fuel injector No. 1 displayed a higher level for the NO_x emission index but a lower level of smoke number than injector No. 2. The observed differences are attributed to differences in degree of fuel air mixing between the two configurations. It appears that fuel injector No. 2 had less mixing causing it to operate at locally fuel rich conditions thus producing more smoke but lesser amounts of NO_x . No attempt was made to alter reaction zone airflow distribution in these tests. The results indicate, however, that further reduction in NO_x might be obtained by improvements in fuel air mixing (premixing) or by adjusting the amount of primary zone airflow.

The combustor operated at combustion efficiencies near 100 percent for all test conditions described herein. Nevertheless, the emission index for carbon monoxide decreased significantly as the proportion of vapor increased from 0 to 100 percent as shown in Fig. 15. The corresponding emission indices for total hydrocarbons were negligible for all test conditions.

Idle Emissions

Emission of unburned hydrocarbons and carbon monoxide are often prevalent during engine idle and taxi. These emissions are of primary concern in the vicinity of airports. The cause of these emissions is poor combustion efficiency at the combustor operating conditions typical of ground idle. Typically these conditions are low combustor pressure, 2 to 4 atmospheres; low inlet-air temperature 365 to 460 K, and low fuel-air ratios of 0.0075 to 0.01. Measured engine combustion efficiencies vary from 89 to 96 percent. Two approaches are being tried in an attempt to improve idle combustion efficiency. These are the use of fuel staging in multizone combustors and use of an air-assisted fuel nozzle.

Fuel staging. - Fuel staging as applied to multizone combustors means that only one of the several possible zones receives fuel during idle. When the overall fuel-air ratio is maintained at that value required for idle the burning zone has a significantly higher than average fuel-air ratio. With pressure atomizing fuel nozzles this means a higher pressure drop during idle which in turn gives finer atomization and better combustion efficiency. With swirl-can modules the fuel flow to the active row is high enough so that a well developed spray is formed. At very low fuel flow rates per module the fuel has been observed to dribble rather than be sprayed from the swirl cans. The results of the fuel staging tests are shown in table I and reported in detail in Refs. 8 and 20. The double annulus combustor emissions are compared with combustion in both annuli and staged to inner annulus. Similar data are shown for the swirl-can combustor.

It is apparent that large reductions in emission levels can be obtained by this simple technique. The levels of pollutant reduction demonstrated still may not be sufficient and further improvements may be required.

Air assist fuel nozzles. - Improving fuel atomization by using an air assist fuel nozzle can significantly reduce unburned hydrocarbon and carbon monoxide emissions at idle operating conditions by improving combustion efficiency. This might be done as shown in Fig. 15. Here a conventional dual orifice fuel nozzle is modified so that during idle, high pressure air is injected through the secondary orifice. Only small amounts of air are needed. For higher power settings the air would be shut off and secondary fuel would be injected in the conventional manner.

Figure 17 illustrates the reductions in hydrocarbons and carbon monoxide that were obtained by using air assist fuel injection in a dual orifice nozzle, in a single J-57 engine combustor can at simulated engine idle conditions. Increases in atomizer air pressure (Δp) represent increases in the air through one orifice of the fuel nozzle. Fuel is supplied through the other orifice. The addition of air through the nozzle improved fuel atomization with the main effect being a dramatic improvement in combustion efficiency. Attendant reductions of approximately 80 percent in hydrocarbons and 50 percent in carbon monoxide emission index levels were realized. More details on this technique, including a description of the nozzle configuration, are given in Ref. 21.

Control of Combustor Airflow Distribution

Another technique which may have substantial potential for reducing emissions is the control of the combustor airflow distribution as a way of controlling the primary zone equivalence ratio. Two approaches are being taken: the use of short diffusers incorporating bleed for airflow profile control; and the use of variable combustor geometry.

Diffuser tests. - Short diffusers incorporating bleed on both walls are being tested in a full annulus test facility described in Ref. 22. This test facility has the capability to test many different diffuser geometries. Tests have been conducted on an asymmetric wall diffusers (ref. 23), dump diffusers and a wide variety of short length diffusers incorporating bleed on both diffuser walls. We find that large changes in the diffuser exit flow profile can be caused by the application of small quantities of bleed flow. Additionally, bleed can cause the diffuser to flow more efficiently and diffuser total pressure losses can be significantly reduced.

An application of diffuser bleed is illustrated in Fig. 18. As shown in Fig. 18(a) the combustor inlet velocity profile without bleed has the majority of the airflow bypassing the primary zone. This condition should be optimum for low pollutant emissions at idle and enhanced altitude relight capability. At takeoff and cruise conditions, Fig. 18(b), the combustor inlet velocity profile is straightened by applying outer wall bleed for optimum operation.

Variable geometry. - Variable combustor geometry could be a very effective way of controlling the combustor primary zone equivalence ratio. At conditions such as engine idle variable geometry could be used to optimize the primary zone equivalence ratio to minimize the emissions of hydrocarbons and carbon monoxide. Similarly at altitude relight conditions the primary zone fuel air ratio could be optimized for reignition. At take-off or cruise the combustor geometry would again be changed and now optimized to minimize smoke and oxides of nitrogen. At present the only variable geometry configurations being studied are for improved altitude relight and improved idle emission control. This work is being done on a modified version of the double-annulus combustor.

Water Injection Tests

Direct injection of water into the primary zone of a combustor is another very effective way to minimize the emissions of oxides of nitrogen. However, practical aircraft considerations limit the use of water injection only for takeoff. Water injection lowers the flame temperature and serves as a diluent in the air stream. Both effects reduce the maximum combustion temperature and thereby reduce the emissions of NO_x . Figure 19 compares data for three different combustors all using slightly different techniques for direct water injection. The ratio of NO_x emission indices with and without water injection is shown as a function of the water-air ratio. Water injection in the single annular combustor was by spraying water into the combustor snout upstream of each fuel nozzle. Water injection in the segment combustor was from the secondary ports of the nozzles used for comparison of propane fuel injection (nozzle No. 1, fig. 12). Water injected in this manner mixes much more intimately with the fuel and is significantly more effective in reducing NO_x emissions. These effects however do influence the levels of other pollutants as combustion efficiency may be lowered by water injection. Some increase in CO levels during water injection have been observed but are not considered to be significant in view of the low values without water injection.

Inlet air humidity. - Variations in inlet-air humidity have been shown to reduce the level of oxides of nitrogen emissions. Tests were conducted using the single annular combustor described previously. Water was sprayed into the inlet-air far enough upstream of the combustor so that it would be completely vaporized before reaching the combustor. The results of these tests are shown in Fig. 20. Data were obtained over a wide range of inlet-air temperatures and humidities. The trends with increasing humidity are the same; an exponential decrease in the NO_x emission index with increasing humidity.

Alternate Fuels

The single annular combustor of Ref. 15 has been tested with natural gas fuel. Reference 25 gives details of the work done to determine an optimum method of injecting natural gas fuel. Natural gas does not display stable combustion over as wide a range of operating conditions as conventional kerosene fuels used in aircraft turbine engines in spite of its higher heating value. The narrow combustible limits and high chemical stability account for the poor performance of natural gas fuel at off design engine operating conditions, Refs. 26 and 27.

Natural gas does have an advantage over kerosene fuels in its well documented tendency to produce lower emissions of NO_x (ref. 28). Figure 21 compares the emissions of NO_x for ASTM-A1 fuel and natural gas fuel over a range of inlet-air temperatures. Exit temperature was constant at approximately 1500 K, combustion efficiency was approximately 100 percent and test pressure was 6 atmospheres. In general, the use of natural gas resulted in approximately a fifty percent reduction in NO_x emissions. In an attempt to further reduce the emissions of NO_x , direct water injection was tried. As expected, the combustor performance was severely degraded. At an inlet-air temperature of 590 K, the combustor blew out at a water-air ratio of 0.025. Direct water injection was marked by noisy, unstable combustion and reduced combustion efficiency. Gas analysis data show that about 90 percent of the combustion inefficiency is due directly to unburned fuel. Where combustion could be maintained, the use of direct water injection did decrease the emissions of NO_x .

CONCLUDING REMARKS

Research on most of the combustor concepts mentioned will be continuing in an effort to better understand ways of minimizing the pollutants from combustors. The goals that have been established for future gas turbine engines will require that there be new technology in combustor design. Several trends and approaches are well understood but with the exception of exhaust smoke have yet to be demonstrated on flight engines. In addition to the aircraft engine emissions research being conducted "in-house" by NASA/Lewis, a contracted effort designated as the "Experimental Clean Combustor Program" has recently been initiated. The goal of the "Experimental Clean Combustor Program" is to make a substantial reduction in all pollutant levels of advanced CTOL engines. The primary emphasis of these contracts will be to demonstrate a 75 percent reduction in NO_x emissions. However there will also be attempts to significantly reduce the emissions at idle. Demonstration of the best combustor concepts will eventually include ground static tests in a large high pressure ratio engine.

REFERENCES

1. Flott, M.; Baker, R. C.; Bastress, E. K.; Change, K. M.; and Siegel, R. O.: The Potential Impact of Aircraft Emissions Upon Air Quality. Rep. 1167-1, Northern Research and Engineering Corp., 1971.
2. Sawyer, R. F.: Atmospheric Pollution by Aircraft Engines and Fuels. WARD-AR-40, 1972.
3. Anon.: Proceedings of the Survey Conference, Climatic Impact Assessment Program. Rep. DOT-TSC-OST-72-13, Department of Transportation, 1972.
4. Grobman, J.; Jones, R. E.; Marek, C. J.; and Niedzwiecki, W.: Combustion. Aircraft Propulsion. NASA SP-259, 1971, pp. 97-134.
5. Anon.: Procedure for the Continuous Sampling and Measurement of Gaseous Emissions from Aircraft Turbine Engines. Rep. ARP 1256, SAE, Oct. 1971.
6. Anon.: Aircraft Gas Turbine Exhaust Smoke Measurement. Rep. ARP 1179, SAE, May 1970.
7. Niedzwiecki, R. W.; and Jones, R. E.: Pollution Measurements of a Swirl-Can Combustor. NASA TM X-58163, 1972.
8. Niedzwiecki, R. W.; Trout, A. M.; Mularz, E.: Performance of a Swirl-Can Combustor at Idle Conditions. NASA TM X-5578, 1972.
9. Niedzwiecki, R. W.; Juhasz, A. J.; and Anderson, D. N.: Performance of a Swirl-Can Primary Combustor to Outlet Temperatures of 3600° F (2256 K). NASA TM X-52902, 1970.
10. Perkins, P. J.; Schultz, D. F.; and Wear, J. D.: Full-Scale Tests of a Short Length, Double-Annular Ram-Induction Turbojet Combustor for Supersonic Flight. NASA TN D-6254, 1971.
11. Clements, T. R.: 90-Degree Sector Development of a Short Length Combustor for a Supersonic Cruise Turbofan Engine. Rep. PWA-FR-3790, Pratt & Whitney Aircraft (NASA CR072734), 1970.
12. Schultz, D. F.; and Perkins, P. J.: Effects of Radial and Circumferential Inlet Velocity Profile Distortions on Performance of a Short-Length Double-Annular Ram-Induction Combustor. NASA TN D-5705, 1972.
13. Schultz, D. F.; and Mularz, E. J.: Factors Affecting Altitude Relight Performance of a Double-Annular Ram-Induction Combustor. NASA TM X-2630, 1972.
14. Clements, T. R.: Development of a Short Length Combustor for a Supersonic Cruise Turbofan Engine Using a 90 Degree Sector of a Full Annulus. Rep. PWA-FR-4854, Pratt & Whitney Aircraft (NASA CR-120503), Apr. 1972.
15. Wear, J. D.; Perkins, P. J.; and Schultz, D. F.: Tests of a Full-Scale Annular-Induction Combustor for a Mach 3 Cruise Turbojet Engine. NASA TN D-6041, 1970.
16. Rusnak, J. P.; and Shadowen, J. H.: Development of an Advanced Annular Combustor. Rep. PWA-FR-2832, Pratt & Whitney Aircraft (NASA CR-72453), May 30, 1969.
17. Ingebo, R. D.; and Morgren, C. T.: High Pressure Combustor Exhaust Emissions with Improved Air-Atomizing and Conventional Pressure Atomizing Fuel Nozzles. Proposed NASA Technical Note.
18. Pongei, F.; and Heywood, J. R.: The Role of Mixing in Burner Generated Carbon Monoxide and Nitric Oxide. Rep. 723; Dept. Mech. Eng., Massachusetts Inst. Tech., Feb. 1972.

19. Norgren, C. T.; and Ingebo, R. D.: Investigation of the Effect of Pre-vaporized Fuel on the Exhaust Emissions from an Experimental Gas Turbine Combustor. Proposed NASA Technical Memorandum
20. Clements, T. R.: Effect of Fuel Zoning and Fuel Nozzle Design on Pollution Emissions at Ground Idle Conditions for a Double-Annular Ram-Induction Combustor. Pray & Whitney, Aircraft (NASA CR-120194), 1972.
21. Briehl, D.; and Papathakos, V.: Use of an Air-Assist Fuel Nozzle to Reduce Exhaust Emissions from a Gas-Turbine Combustor at Simulated Idle Conditions. NASA TN D-6404, 1971.
22. Juhasz, A. J.; and Holdeman, J. D.: Preliminary Investigation of Diffuser Wall Bleed to Control Combustor Inlet Airflow Distribution. NASA TN D-6435, 1971.
23. Juhasz, A. J.: Control of Exit Velocity Profile of an Asymmetric Annular Diffuser Using Wall Suction. NASA TM X-2710, 1972.
24. Bahr, D. W.: Control and Reduction of Aircraft Turbine Engine Exhaust Emissions. Symposium on Emissions from Continuous Combustion Systems. General Motors Research Lab., Warren, Mich., Sept. 1971.
25. Wear, J. D.; and Schultz, D. F.: Effects of Fuel Nozzle Design on Performance of an Experimental Annular Combustor Using Natural Gas Fuel. NASA TN D-7072, 1972.
26. Hibbard, E. A.: Evaluation of Liquified Hydrocarbon Gases as Turbojet Fuels. NACA RM ES6121, 1956.
27. Wear, J. D.; and Jones, R. E.: Comparison of the Combustion Characteristics of ASTM A1, Propane and Natural Gas Fuels in an Advanced Annular Combustor. NASA TN D-7135, 1972.
28. Hilt, M. B.; and Johnson, R. H.: Nitric Oxide Abatement in Heavy Duty Gas Turbine Combustors by Means of Aerodynamics and Water Injection. Paper #72-GT-53, ASME, Mar. 1972.

TABLE 1. - EFFECT OF FUEL STAG

Idle Operation

 $P_3 = 4 \text{ atm}$ $T_3 = 480 \text{ K}$ $f = 0.008$

Type of combustor	Annulus	Efficiency	H/C	CO
Swirl Can	All	< 50	> 200	100
	Inner	~100	15	40
Double Annular	Both	92	33	132
	Inner	~100	15	78

Discussion on Paper 31

"Design and Evaluation of Combustors for Reducing Aircraft Engine Pollution"
presented by R.E.Jones

G.Kappler: To round out your excellent paper for me, could you please give me some figures concerning the pressure loss of the swirl can combustors.

R.E.Jones: Total pressure losses for swirl-can combustors generally vary between 3.5 to 6 percent. Reference 9 of my paper gives more specific data.

A.Glassman: On the swirl atomizers you have a small flame holder plate; do you have photographs of these plates during combustion?

R.E.Jones: We have taken movie photography of these combustors during operation but they are not in any referenced work.

A.M.Mellor: You have shown that air-assisted fuel injection can decrease CO and H/C emissions at idle. Do you have any data on its effect on NO over the entire engine operating range?

R.E.Jones: The air-assist nozzle scheme described in this paper has only been tested at idle conditions as the variation of the air-assist nozzle is considered to be a "quick-fix" to decrease idle pollutants. We do observe a slight increase of 10 to 15 percent in the amount of NO_x produced using this approach. We have not evaluated the effect of air-assist nozzles over the entire engine operating range.

M. Whittaker: Comparing Figure 13 with Professor Sawyer's correlation of 700 K gives a higher value of 22 compared to 15 for conventional chambers. I am comparing your combustor with production combustors; isn't this combustor to reduce NO?

R.E. Jones: No. These sector combustors were done only to illustrate the potential reduction in NO_x by using vaporized fuel. This combustor was not designed to be a low NO_x emission combustor.

C. Eatock: I wish to congratulate the authors for a fine job of surveying a large amount of work in one concise paper. Figure 20 shows humidity effects which from memory, appear close to theoretical. On our recently concluded program on low NO_x auto gas turbine combustors for EPA, we confirmed this for non-regenerative engines at about 500 K while at higher temperatures characteristic of regenerative engines, we found only half the effect for reasons not understood. What percentage of air was used at ΔP 80 psi in Figure 17? The efficiency indicates almost a 10 times reduction of pollutants - perhaps a little more than the CO and H/C graphs show.

R.E. Jones: You are correct. These humidity values are close to theoretical particularly at higher inlet-air temperatures. At lower inlet air temperatures the theory predicts a greater reduction in NO_x than was measured. I suspect that this partially accounts for the results you have obtained with regenerative engines.

The effects shown on Figure 17 at a ΔP = 80 psi require about 1/4 of 1 percent of the combustor air flow. The discrepancy in efficiency versus emissions measurement is due primarily to calculating the efficiency at low temperature rises from thermocouple data. The emissions data was obtained initially from batch samples but has been recently confirmed using the on-line gas analysis instruments.

POINT DE VUE DU MOTORISTE
SUR LA CONCEPTION DES FOYERS A FAIBLE TAUX DE POLLUTION

par

Alain Quiliévré - Raymond Briançon - Jean Decouflet
SNECMA
77550 Moissy-Cramayel
France

RESUME

Les moyens propres à réduire la pollution des turboréacteurs sont examinés du point de vue du constructeur. Les rendements au ralenti des moteurs modernes à chambres annulaires, ont atteint des niveaux assez élevés. Il est possible d'éliminer pratiquement les émissions de fumées visibles par l'emploi de techniques d'injection appropriées. Mais, l'augmentation des taux de compression et les vitesses de vol supersoniques sont responsables d'un accroissement des émissions d'oxydes d'azote. L'injection d'eau est un moyen efficace pour combattre la formation de ces oxydes, mais elle n'est pas applicable en croisière. D'autres méthodes sont concevables pour réduire, dans tous les cas, l'émission des oxydes d'azote, tout en diminuant celle des imbrûlés au ralenti (CO et HC), mais elles conduisent à des chambres de combustion plus complexes et posent des problèmes de poids, d'endurance, de fiabilité et de prix. Le foyer de rechauffe de l'Olympus ne produit ni oxydes d'azote, par suite du niveau modeste de la température de la flamme, ni particules de carbone. Mais, dans certains cas de fonctionnement, on constate la transformation d'une partie de l'oxyde nitrique NO émis par la chambre en peroxyde NO₂ visible à l'échappement. Les réactions de combustion de l'oxyde de carbone et des hydrocarbures produits par la rechauffe se poursuivent après la sortie de la tuyère dans le cône potentiel du jet et dans les premières phases du mélange avec l'air ambiant. Le rendement atteint est dans certains cas assez élevé (de l'ordre de 0,995). Pour un taux de rechauffe maximal, l'ingénieur ne peut guère améliorer la situation présente, mais pour des taux plus modestes une réduction de la masse finale d'imbrûlés émise est possible par une meilleure optimisation.

PLAN

1. Introduction.
2. La technologie actuelle des foyers.
3. La formation des polluants.
4. Les niveaux de pollution.
5. Modèle mathématique de la combustion "externe".
6. La réduction de la pollution.
7. Conclusions.

1. INTRODUCTION

L'importance du trafic aéronautique est à l'heure actuelle telle qu'il est apparu nécessaire de réduire l'importance de la pollution au sol, sinon en altitude. Ces nouvelles exigences peuvent-elles être satisfaites par des modifications de la technologie de combustion ? C'est une question qui se pose aux motoristes, et que nous examinons dans cette communication. Il nous a semblé souhaitable de faire, en premier lieu, une brève revue de la technologie actuelle, des mécanismes de production des polluants et des niveaux de pollution des moteurs, en mettant l'accent sur les résultats acquis à la SNECMA, particulièrement pour la rechauffe utilisée sur le moteur Olympus. Ensuite nous indiquons les voies qui, selon nous, peuvent être suivies pour diminuer les niveaux de pollution. Il convient de signaler que la nature et la quantité des polluants émis dépendent du combustible. Les carburéacteurs d'aviation sont des mélanges d'hydrocarbures dont les propriétés physiques et chimiques varient quelque peu en fonction de l'origine du brut. Ces propriétés sont réglementées par des normes qui fixent certaines limites. Le problème de la pollution se poserait de façon différente si l'on envisageait de modifier le carburant par des traitements chimiques (par exemple : désaromatisation) ou d'utiliser des combustibles nouveaux comme le méthane ou l'hydrogène. Les carburéacteurs classiques du "kérosène" seront seuls considérés ici.

2. LA TECHNOLOGIE ACTUELLE DES FOYERS

La technologie résulte des qualités exigées et des conditions de fonctionnement. Les qualités exigées, bien connues, sont les suivantes :

- faible masse et faible volume,
 - faible perte de charge (diminution de pression totale),
 - stabilité de combustion dans toutes les conditions de fonctionnement et facilités d'allumage et de réalumage en vol,
 - rendement de combustion le meilleur possible (diminution de la consommation de carburant),
 - longue durée de vie, entretien facile, prix acceptable.
- En outre la chambre principale doit être conçue en sorte que la répartition de température à l'entrée de la turbine soit assez uniforme.

Certaines de ces exigences sont contradictoires. Elles ne peuvent être satisfaites que de façon approchée en acceptant des compromis.

La réduction de la pollution est une exigence nouvelle qui accroît la complexité du problème, déjà très difficile à résoudre pour les moteurs modernes à hautes performances (réf. 1 et 2).

Il faut cependant noter qu'un effort a déjà été accompli, avec succès, pour la réduction des fumées visibles.

Les conditions thermodynamiques de fonctionnement de la chambre principale sont très variables suivant le régime du moteur, la vitesse de vol et l'altitude : la température et la pression d'entrée sont très basses pour les conditions de réallumage en altitude (températures de l'ordre de 240 à 290°K et pressions de 0,3 à 0,5 bar).

Ces conditions sont très sévères pour la combustion.

Aux régimes de décollage et de croisière les grandeurs correspondantes sont, au contraire, très élevées, ce qui pose des problèmes de tenue thermique et de tenue mécanique de la chambre.

Pour les moteurs modernes, la température à l'entrée de la chambre peut atteindre 700 à 870°K et la pression 30 bars.

Le rapport de mélange D_c/D_a (quotient du débit de combustible par le débit d'air) est très variable. La valeur maximale est atteinte au décollage (0,020 à 0,030 suivant les moteurs), mais la combustion doit pouvoir se maintenir à des richesses plus élevées pendant les accélérations.

La valeur minimale est atteinte en décélération : une limite pauvre de stabilité de l'ordre de 0,003 est nécessaire.

Le débit réduit ou fonction d'écoulement, $D_a/T/P$, est par contre assez peu variable.

Dans le cas de la rechauffe, les conditions thermodynamiques de fonctionnement sont fort différentes, mais elles sont moins variables.

Pour l'Olympus, la pression est de l'ordre de 3 bars pendant le décollage et de 1,8 bar pendant l'accélération transsonique (entre 8000 et 14000 m), la température des gaz à l'entrée étant de 1660°K et 960°K pour ces mêmes phases de vol. Le rapport de mélange global du moteur Olympus est assez loin du rapport stoechiométrique : de l'ordre de 0,036 au décollage et variable de 0,030 à 0,025 pendant le vol transsonique.

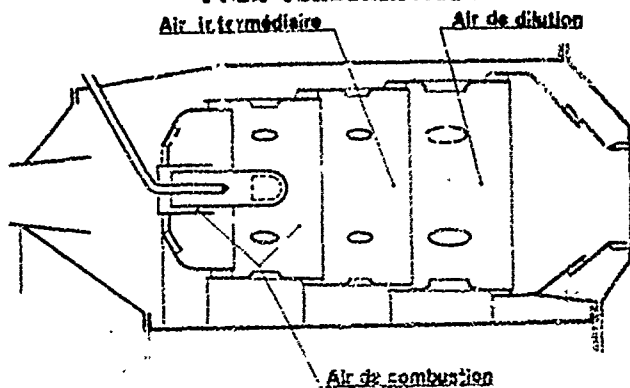
Cette rechauffe n'est que "partielle".

Les conditions de fonctionnement et les qualités réclamées pour la rechauffe étant très différentes de celles de la chambre principale, les techniques employées sont nécessairement, elles aussi, très différentes.

La figure 1 représente la coupe d'une chambre de combustion principale annulaire typique.



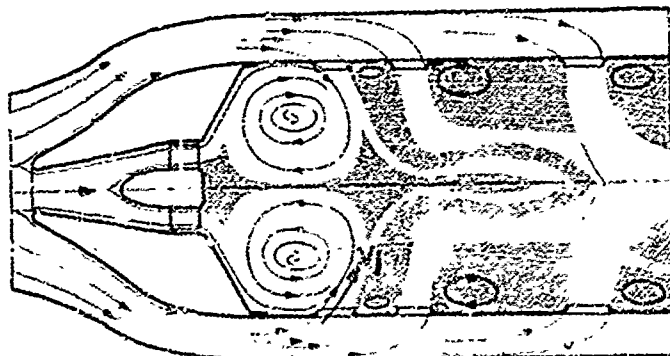
SCHEMA DE CHAMBRE DE COMBUSTION ANNULAIRE POUR TURBOREACTEUR



ZONES DE COMBUSTION ET DE DILUTION



ECOULEMENT DANS UNE CHAMBRE DE COMBUSTION

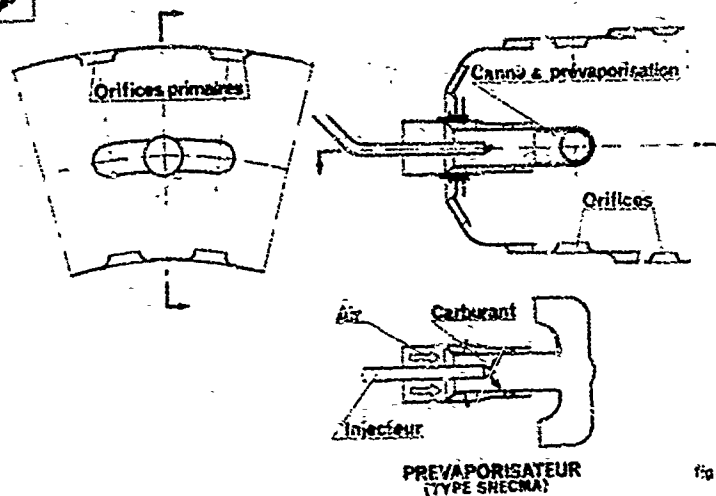


L'air sortant du réservoir traverse le "tube à flamme" par un ensemble d'orifices régulièrement répartis.

La première fonction du tube à flamme est le partage de l'air en au moins trois fractions : l'air de combustion, l'air de dilution et l'air de protection thermique (par effet de "film-cooling"). En second lieu, le tube à flamme doit créer une structure d'écoulement de jets turbulents propre à assurer, d'une part, les recirculations de gaz brûlés nécessaires à la stabilisation de la flamme et, d'autre part, le niveau de turbulence suffisant (figure 2).

La troisième fonction du tube à flamme est la protection thermique des carter. L'injection du combustible se fait par la tête dans la zone de combustion, soit directement dans la flamme par des injecteurs à pulvérisation mécanique, soit après prémélange plus ou moins complet avec une partie de l'air de combustion par "prévaporisation" (figure 3 et réf. 1 et 3) ou par "pulvérisation aérodynamique" ("air blast atomisation").

SYSTÈME D'INJECTION A PREVAPORISATEURS EN "T"



Pour que la stabilité et le rendement de combustion soient suffisants dans les conditions thermodynamiques défavorables au démarrage au sol et du réalumage en altitude, il est nécessaire que la richesse moyenne de la zone de combustion soit assez proche de l'unité (rapport de mélange de 0,068 environ, pour le kérosène). Cette condition justifie le fractionnement de l'air par le tube à flamme. Une zone de combustion assez homogène et courte est obtenue par une recirculation de l'écoulement sous la forme d'un double vortex occupant toute la section droite de la zone primaire du tube à flamme (figure 2, réf. 1 et 2). La structure d'écoulement adéquate dépend de la géométrie du tube à flamme, de l'espacement des orifices et de leurs dimensions.

Des critères déduits de l'expérience fixent le choix de ces paramètres. Il en résulte des nombres de Mach moyen d'écoulement de l'ordre de 0,04 à 0,07 environ, suivant le type de moteur (ce nombre de Mach moyen de référence est conventionnellement calculé dans la section droite maximale entre carters pour les conditions de sortie du compresseur).

Le nombre de Mach des jets d'air déterminés par les orifices du tube à flamme est de l'ordre de 0,17 à 0,25.

Le choix de la valeur du débit d'air de combustion est important.

Les facteurs à prendre en compte sont les rendements et les stabilités de combustion de différents régimes et aussi d'autres qualités telles que l'uniformité de température au décollage, l'absence de fumées visibles etc...

Généralement, la richesse moyenne dans la zone de combustion pour la croisière est choisie au voisinage de l'unité. La chambre de combustion est, dans ces conditions, "adaptée" en croisière.

La masse volumique des gaz à l'entrée du foyer de reheating est beaucoup plus faible qu'à l'entrée de la chambre principale. Il faut, par conséquent, admettre, à l'entrée de la chambre de reheating, un nombre de Mach pour l'écoulement moyen beaucoup plus élevé que dans la chambre principale (il atteint 0,30 à 0,40).

Il n'est plus possible d'envisager une structure d'écoulement analogue à celle d'un foyer homogène à taux de recirculation élevé.

Les zones de recirculation sont localisées en aval d'un ou de plusieurs obstacles ou "accroche-flamme" situés dans la veine préalablement carburée (figures 4 et 5).

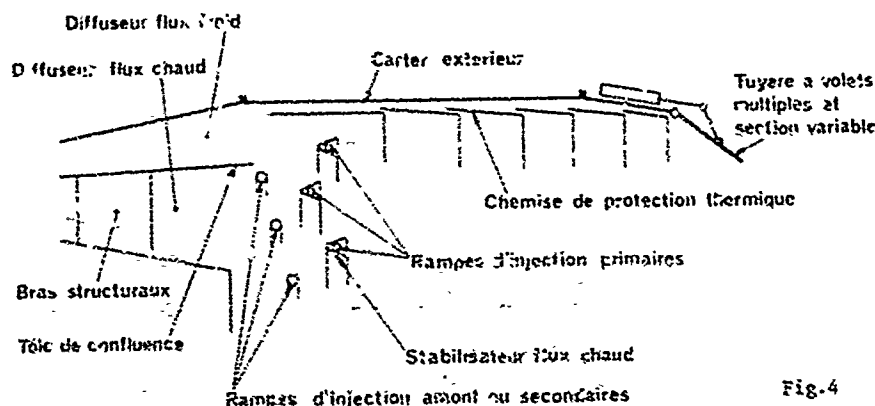


Fig. 4

Schéma d'une chambre de reheating

L'écoulement des gaz brûlés en aval d'une zone de recirculation joue le rôle d'une flamme pilote à partir de laquelle la combustion se propage au reste de l'écoulement carburé. La zone de propagation s'accroît par l'effet des transferts turbulents qui résultent de l'accélération des gaz brûlés. La combustion se poursuit ensuite dans une zone de post-flamme où les vitesses s'uniformisent et la turbulence s'amortit. La protection thermique du carter est assurée par une chemise simple ou à film cooling (Fig. 4). L'injection est faite

directement dans l'écoulement en amont des stabilisateurs de flamme

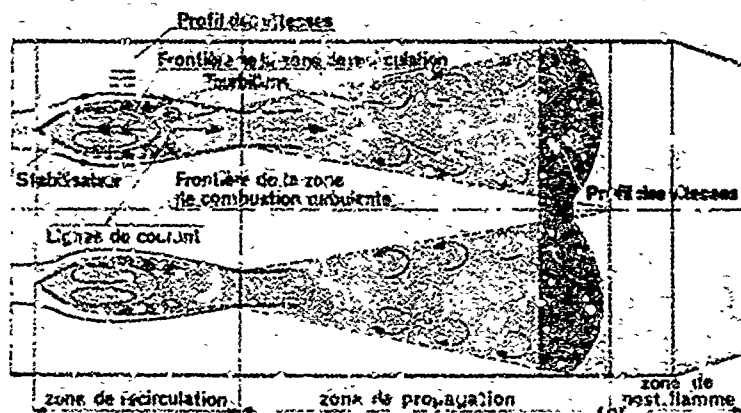


Fig. 5- Schéma de principe de la combustion dans un foyer de chauffe de turbo-réacteur.

3. LA FORMATION DES POLLUANTS

Il est bon de noter, tout d'abord, que le but à atteindre n'est pas d'éviter la formation des polluants, mais bien finalement leur rejet dans l'atmosphère, ce qui n'est pas la même chose. Le carburant injecté dans la chambre est un polluant préalablement "formé", le problème majeur est de le brûler. Une telle combustion s'accompagne nécessairement de la formation de polluants intermédiaires, tels que CO.

Il y a donc bien un double aspect de "formation" et de "destruction" des polluants.

3.1. Les processus fondamentaux de combustion

Ces processus de combustion sont déterminés, au premier lieu, par la rapidité des transformations chimiques résultant de l'état physique et chimique local. Il s'agit de transformations irréversibles qui obéissent à des lois de cinétique en milieu gazeux homogène ou en milieu hétérogène (combustion des particules de carbone).

En deuxième lieu, la combustion dans un foyer est conditionnée par la rapidité des transferts, essentiellement turbulents, qui sont nécessaires pour obtenir un état local favorable aux réactions chimiques.

Ces transferts turbulents sont déterminés par les gradients de la vitesse d'écoulement.

Dans certaines zones du foyer, le processus global est essentiellement gouverné par la cinétique chimique, c'est le cas des zones de post-flamme. Par contre, dans d'autres régions, comme la zone de propagation d'une flamme, les gradients de vitesse sont accompagnés de gradients de température. Les phénomènes chimiques et aérodynamiques sont couplés et la rapidité de l'évolution chimique dépend des deux phénomènes.

La cinétique de combustion des hydrocarbures est, on le sait, très complexe mais, cependant, on peut souvent obtenir une représentation valable en considérant la combustion comme une réaction chimique simple d'ordre voisin de 2, définie du point de vue cinétique par une énergie d'activation et un facteur de fréquence.

Pour connaître les lois des mécanismes complexes pour lesquels cinétique et turbulence sont couplés, on peut, dans certains cas, corréler les performances (stabilité et rendement) des foyers de moteurs en utilisant comme paramètre des expressions déduites de ce modèle simple de réaction.

Ce schéma cinétique s'appliquera d'autant mieux que la combustion s'accomplit dans un mélange gazeux de richesse uniforme, ce qui est assez bien réalisé dans la chauffe, au moins à régime de chauffe élevé. Dans la chambre principale, le carburant injecté n'est jamais complètement vaporisé avant de pénétrer dans les zones de combustion. Cependant, par suite du niveau élevé de la turbulence, les vitesses relatives entre les gouttes de combustible et le milieu gazeux sont, en moyenne, suffisantes pour que se stabilise pratiquement l'amorçage de la combustion de la goutte par un front de flamme de diffusion qui l'entoure.

Les mécanismes de combustion sont, par conséquent, assimilables à ceux d'une flamme de combustible gazeux, de rapport de mélange non uniforme. Il y a lieu d'examiner cependant si les gouttes peuvent se vaporiser assez vite et si la répartition du carburant dépend peu ou beaucoup de la technique d'injection.

Un calcul, présenté dans la référence 4, montre que, dans une zone primaire type, une goutte de 80 μ m s'évapore en 1 ms environ.

Par conséquent, la durée d'évaporation de la goutte n'est pas généralement un facteur limitatif, sauf pour les conditions de démarrage, de rallumage, en altitude et, dans une certaine mesure, du ralenti au sol. En contre, la vitesse d'injection du liquide détermine la répartition du combustible dans la zone de combustion. Certaines techniques d'injection ont l'avantage de répartir le carburant d'une façon très peu sensible aux variations des conditions thermodynamiques (en particulier le niveau de pression dans la chambre).

En conclusion, sauf pour les régimes extrêmes et, pourvu que l'on emploie une technique d'injection adaptée à l'écoulement des gaz, on doit, pour la chambre principale, pouvoir éliminer la plupart des difficultés propres à l'injection liquide.

3. Les mécanismes de formation des polluants

La formation et l'évolution des polluants dans le foyer dépendent essentiellement des processus de combustion que nous venons de passer en revue.

On doit distinguer parmi les polluants deux catégories : d'une part l'oxyde de carbone, les particules de carbone, les hydrocarbures divers, aldéhydes, alcools, et, d'autre part, les oxydes d'azote qui ne se forment qu'à température élevée, sans pratiquement participer aux mécanismes cinétiques de la combustion. Comme on le sait, ces mécanismes sont extrêmement complexes, même pour un combustible aussi simple chimiquement que le méthane.

Examinons, en premier lieu, la formation des divers hydrocarbures et de l'oxyde de carbone.

Au cours des premières étapes de la combustion, le carburant se transforme en donnant naissance à des hydrocarbures particuliers comme le méthane, qui eux mêmes donnent, par la suite, naissance à des intermédiaires tels que CO et H_2 . Ces transformations s'accomplissent suivant des chaînes de réactions faisant intervenir comme centres propagateurs divers atomes et radicaux.

L'oxyde de carbone CO est, parmi les corps formés, celui qui brûle le plus lentement (son oxydation n'est d'ailleurs possible que par un mécanisme cinétique faisant intervenir le radical OH).

Quand le moteur fonctionne à régime élevé (décollage, croisière, etc...) les conditions de pression, de température et de richesse moyenne (proche de 1) de la zone de combustion de la chambre principale sont très favorables à la combustion et les vitesses de réactions sont assez rapides pour que, à la sortie de la zone de combustion, l'équilibre chimique soit pratiquement atteint pour les constituants N_2 , O_2 , CO_2 , H_2O , CO, H_2 , O, OH, H. Cependant l'équilibre complet donnant naissance, par dissociation de N_2 , à des atomes de N et des oxydes d'azote NO, NO_2 n'est jamais atteint dans les foyers des moteurs, le temps de séjour étant insuffisant.

Dans la zone de dilution, le mélange progressif des gaz primaires avec l'air complémentaire devrait aboutir finalement à une combustion quasi complète (N_2 , O_2 , CO_2 , H_2O). Mais, au dessous d'une certaine température, les réactions de recombinaisons deviennent trop lentes et l'état chimique se fige en cours d'évolution.

On trouve donc toujours, même dans les conditions les plus favorables, un peu de CO dans les gaz d'échappement (et des oxydes d'azote).

Cette description est cependant schématisée. Le mélange du carburant avec l'air de combustion n'étant, dans la zone primaire, que partiellement réalisé avant la combustion, celle-ci n'a pas lieu à une richesse uniforme. Dans les régions les plus pauvres, les températures de combustion atteintes sont plus faibles et par conséquent les vitesses de réactions sont trop lentes pour que l'équilibre soit atteint. Après traversée de la zone de dilution, les gaz brûlés de ces régions peuvent être figés dans un état chimique de combustion partielle comportant, non seulement de l'oxyde de carbone mais encore des imbrûlés du type hydrocarbure.

Les films d'air de refroidissement du tube à flammes constituent toujours une zone d'évolution pauvre.

Pour les raisons analogues, les combustions trop riches sont pénétrées d'imbrûlés supplémentaires.

Quand le moteur fonctionne à des régimes faibles, les conditions de pression, de température (ralentissement, démarrage) et de richesse moyenne de la zone de combustion (ralenti) sont défavorables à la fois à la combustion et à la vaporisation du combustible et l'équilibre chimique n'est pratiquement atteint même dans les régions les plus favorables.

A l'échappement, les concentrations de l'oxyde de carbone et des hydrocarbures HC sont alors beaucoup plus importantes et la proportion des hydrocarbures devient importante dans l'ensemble des imbrûlés (CO et HC).

La formation des particules de carbone résulte de conditions particulières de combustion.

Comme l'ont montré des expériences de laboratoire aux flammes plane et sphaériques (réf. 5, 6 et 7), la combustion à pression élevée (supérieure à 10 bars) de mélanges gazeux de richesses supérieures à $\phi = 1,5$ ne conduit pas à l'équilibre mais à un état de faux équilibre caractérisé par la formation d'hydrocarbures particuliers et aussi de particules de carbone.

L'état final de faux équilibre dépend des conditions physiques de l'évolution.

La turbulence diminue la production de hydrocarbures et de suies.

Les aromatiques présents dans le carburant sont, parmi les composants du carburant, ceux qui produisent ces particules en proportions importantes, dans les conditions indiquées.

Par conséquent, et contrairement à une opinion assez répandue, si un combustible tel que le méthane ne produit pas de particules de carbone, ce n'est pas parce qu'il est injecté à l'état gazeux, c'est une conséquence de sa structure chimique.

Les réactions qui produisent les hydrocarbures et les particules de soie sont des réactions de cracking en phase gazeuse. A l'échappement, la plupart des particules ont des diamètres inférieurs à $0,1 \mu$.

Certains fuels lourds non utilisés en aviation peuvent donner naissance en fin de vaporisation de la goutte à un cracking en phase liquide, conduisant à des particules plus grosses et plus dures, appelées émulsions.

Les particules formées dans les zones riches de la flamme brûlent ensuite partiellement quand, au cours des phases d'extinction (zone de combustion, zone de diffusion et flamme de rechauffe), de l'oxygène complémentaire est apporté, avec formation d'un rayonnement thermique.

Les oxydes d'azote sont essentiellement formés, comme nous l'avons déjà noté, par dissociation thermique à température élevée. Le mécanisme cinétique qui conduit de l'équilibre partiel (N_2 , O_2 , CO_2 , H_2O , CO, O, OH, H) à l'équilibre total avec en plus NO, NO_2 , N, est assez bien connu (voir par exemple, réf. 4).

Dans les conditions du cycle-moteur, la rapidité du mécanisme n'est jamais suffisante pour que l'équilibre complet soit atteint.

Ce mécanisme "thermique" de formation n'est rapide que si, dans la zone de combustion, les températures de flamme sont élevées, ce qui suppose à la fois des températures élevées à l'entrée de la chambre et des richesses moyennes voisines de 1 dans la zone de combustion. Ces conditions sont obtenues, dans les chambres principales des moteurs modernes au décollage, en montée et en croisière. L'oxyde qui se forme est presque exclusivement l'oxyde nitrique NO. Sa vitesse de formation à l'état d'équilibre "partiel" est donnée approximativement (26f.4) par l'expression :

$$\frac{d[NO]}{dt} = \frac{2 K_{NO}}{R} \frac{2 R}{1}$$

où $[NO]$ est la fonction massique de NO, t le temps en s, R la constante molaire, K_{NO} la constante molaire de NO et R , une constante de réaction donnée par :

$$R = k [N]_e \times [O]_e$$

$[N]_e$ et $[O]_e$ sont les concentrations en nombre de moles par unité de volume à l'équilibre "partiel" et :

$$k = 2 \times 10^{-11} \text{ cm}^3 \text{ s}^{-1}$$

Les calculs d'équilibre qui donnent les valeurs de $[N]_e$ et $[O]_e$ montrent que la vitesse de formation de NO ne doit qu'un peu varier avec la pression, mais énormément avec la température, la température d'extinction apparente étant de l'ordre de 55 000 à 65 000 °K.

Une augmentation de 100°C de la température du mélange multiplie la vitesse de production de NO par environ 5. Au-dessus de 1800 à 1850°C, la production de NO devient vraiment lente à l'échelle des foyers de moteurs aéronautiques.

Dans la zone de diffusion de la chambre principale, une faible partie du NO formé se transforme en NO₂.

Le nombre global de moles de NO se stabilise rapidement dès que la température diminue.

On a constaté (voir plus loin) que, dans la flamme de rechauffe de l'Olympus, une part importante du NO formé dans la chambre se transforme en NO₂.

On peut interpréter cette transformation comme le résultat d'une évolution s'effectuant à température moyenne dans les zones de mélange des gaz brûlés de la rechauffe avec le flux plus froid et oxygéné qui les encadre, l'état stable à basse température étant le peroxyde NO₂.

L'expérience (26f.4) suggère l'existence, dans les zones de réactions vives de la flamme, d'un deuxième mécanisme de formation de NO à température plus basse que celle du mécanisme thermique de la "post-flamme", faisant intervenir un certain nombre des radicaux présents dans la flamme. Cette production de NO "précoce" ("prompt" NO) est plus forte à richesses élevées, mais son importance est finalement nettement moins grande, dans les turbomachines, que celle du NO thermique dans la post-flamme.

4. LES NIVEAUX DE POLLUTION

4.1. Les coefficients caractéristiques de la pollution

Les analyseurs continus de type industriel dosent les volumes respectifs d'atomes de carbone et d'azote contenus par unité de volume des gaz analysés, sans distinguer la nature chimique des divers hydrocarbures et oxydes d'azote.

Il est toutefois possible de doser séparément NO.

Des appareils permettant la mesure des aldéhydes sont seulement en cours de commercialisation.

Les polluants sont donc classés en quatre catégories :

- l'oxyde de carbone, CO,
- les hydrocarbures, HC,
- les oxydes d'azotes, NO_x,
- les particules de carbone solides.

L'émission de polluant i est caractérisée par un indice d'émission IE_i, exprimé en g du polluant i émis par kg de carburant injecté.

Le rendement de combustion η peut se définir comme le rapport de l'enthalpie chimique effectivement libérée à celle qui est théoriquement libérable.

La relation donnant η en fonction des indices IE est de la forme :

$$\eta = 1 - 10^{-3} \sum a_i (IE)_i \quad (1)$$

Les coefficients a_i varient légèrement avec les températures de l'air et du carburant à l'entrée du foyer.

On a :

$$a_{CO} = 0,24 \quad a_{HC} = 0,07$$

Pour les hydrocarbures totaux (HC) et les oxydes d'azotes totaux (NO_x) définis par des concentrations volumiques en atome de C et N, il est nécessaire de définir un état moléculaire conventionnel. Généralement, pour HC on prend CH₄ ou pour NO_x, NO.

Le coefficient a_{NO} de la formule (1) dépend des propriétés du mélange HC.

Si l'on considère le méthane comme étant le seul constituant, on a :

$$a_{CH_4} = 1,19$$

Si, par contre, on considère que les hydrocarbures imbrûlés ont, par atomes de C, le même pouvoir calorifique que le carburant de formule $C_n H_{1,9 n}$, on a :

$$a_{CH_4} = 0,87.$$

On pourrait convenir de prendre arbitrairement $a_{CH_4} = 1$.

Pour le carbone solide $a_C = 0,8$. Mais la masse des particules n'étant pas mesurée directement, on néglige, en général, le terme relatif au carbone solide, dans l'expression de n de même que les termes relatifs aux oxydes d'azote.

On définit ainsi un rendement de combustion simplifié n' par la relation, la forme :

$$n' = 1 - 10^{-3} (0,24 IE_{CO} + IE_{CH_4}) \quad (2)$$

Les analyseurs mesurent en fait des concentrations molaires (CO) , (CH_4) .

L'indice $(IE)_i$ du polluant i s'exprime en fonction de la fraction molaire $[i]$ en ppm par la relation :

$$(IE)_i = [i] = \frac{M_i}{28,97} \times \frac{D_A + D_C}{D_C} 10^{-3} \quad (3)$$

où M_i est la masse molaire de i , D_A et D_C les débits d'air et de carburant du foyer.

Les projets de réglementation de la pollution des avions au sol, considèrent les masses totales de chaque polluant qui sont émises au cours d'un cycle type défini par des durées de fonctionnement pour différents régimes (roulage au sol, décollage, montée, approche).

4.2. Moteurs sans rechauffe

Les moteurs en exploitation sur les avions de transports civils ont fait l'objet de mesures assez nombreuses qui ont été publiées. Citons, en particulier, l'étude du Cornell Aeronautical Laboratory (réf.9).

Une assez grande dispersion se révèle dans certains de ces résultats.

La cause en est, d'une part, l'influence non négligeable des conditions ambiantes, mais sans doute, plus encore, la difficulté de prélever un échantillon moyen représentatif par suite de l'hétérogénéité des concentrations de polluants, à la sortie de certains moteurs.

Nous n'entreprendrons pas ici une analyse des résultats qui se trouvent ailleurs. Le lecteur pourra se documenter en conséquence.

Nous donnerons simplement des ordres de grandeur et ferons quelques remarques générales.

La phase de roulage au sol (allier et atterrir) est responsable de 50% de l'émission de CO au sol.

Au décollage et en croisière, les indices $(IE)_{CO}$ sont de l'ordre de 0,5 à 1.

Pour le roulage, l'indice varie de 40 à 120 environ suivant les types de moteurs.

L'émission des hydrocarbures aux régimes élevés est assez faible ($IE_{HC} < 0,2$). Au ralenti, la dispersion est grande (indices variant de 10 à 120).

L'émission des oxydes NO, est prépondérante aux régimes ou la température à l'entrée de la chambre est la plus élevée (décollage pour les avions subsoniques, croisière pour les supersoniques).

Au décollage, l'indice est essentiellement fonction du taux de compression des moteurs et varie (en NO_x) de 10 à 40.

Au ralenti, il est beaucoup plus faible, mais non négligeable, de l'ordre de 10 à 15 % de la valeur au décollage. La proportion de la masse totale de NO_x émise au sol pendant le décollage et la montée est prépondérante (~ 30 %).

L'émission des particules de carbone dépend non seulement des conditions thermodynamiques, mais aussi de la technique d'injection et de préparation du mélange.

Les moteurs des premières générations d'avions à "réaction" étaient faiblement comprimés, et malgré l'emploi fréquent de techniques d'injection favorisant la formation des fumées, les émissions visibles n'étaient pas très importantes.

Quand les taux de compression se sont accrus au-delà de 15 environ, les émissions sont devenues très importantes.

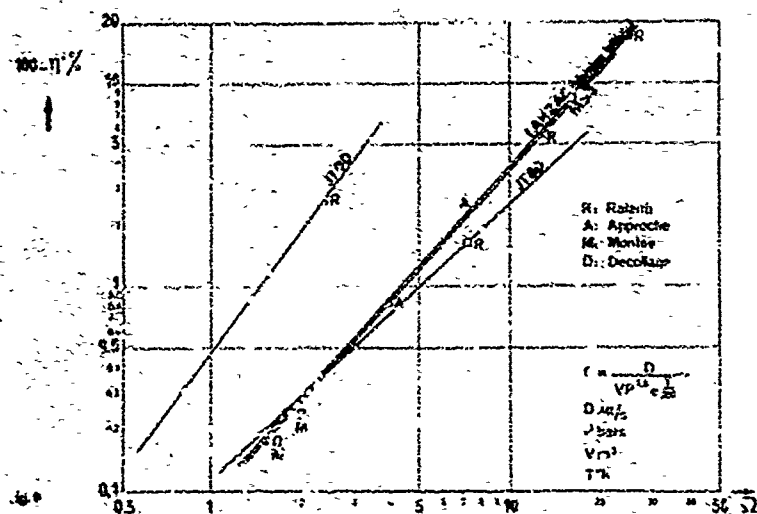
Les constructeurs de moteurs ont alors étudié des techniques nouvelles, anti-fumées, favorisant un prémélange partiel du combustible avec l'air de combustion. Pratiquement on sait maintenant, sans trop de difficulté, réduire les émissions au voisinage ou au-dessous du seuil de visibilité (de 35 à 20 SAE suivant la taille du moteur).

Nous allons maintenant l'influence du type de moteur (rapport de dilution, rapport de compression) et de la taille du moteur sur les émissions.

Sur la figure sont représentées, à titre d'exemple, des courbes donnant pour quatre moteurs (JT9D, JT8D, A3000, SNECMA LARZAC), le rendement n' de combustion (relation 2) en fonction de la charge $\frac{P}{P_0}$ et de la charge de combustion $\frac{D_C}{D_A}$ définie par :

$$\frac{D_C}{D_A} = \frac{1,3}{V_e} \sqrt{\frac{T}{T_0}} \quad (4)$$

où D_A est le débit d'air à l'entrée de la chambre en kg/sec, P la pression d'entrée en bar, V_e le volume intérieur au cône de flamme en m^3 et T la température à l'entrée en $^{\circ}K$.

Fig. 6. Rendements de combustion η' de quelques moteurs

Les données relatives aux moteurs JT9D et JT8D sont issues de la référence 9. Les moteurs SNECMA, en cours de développement, sont figurés dans leur état initial de développement (à titre d'exemple).

Le paramètre Ω est un paramètre de corrélation classique fondé sur une cinétique simplifiée globale. Les courbes représentatives de chaque moteur joignent les points correspondant aux divers fonctionnements types (décollage, ralenti, approche...).

Les deux moteurs M.53 et LARZAC ont des chambres de technologies voisines ; il est normal que leurs courbes $\eta' = f(\Omega)$ le soient aussi. De plus, leurs taux de compression sont voisins et faibles (9 et 10). Mais ces moteurs sont très différents du point de vue de la taille.

Le rapport de Mach moyen d'écoulement dans la chambre, la charge Ω varie approximativement comme l'inverse du temps de séjour, c'est-à-dire l'inverse de l'échelle du moteur. Il est donc logique que la charge du plus petit moteur soit la plus forte et par conséquent son émission de CO et HC la plus grande (voir tableau ci-dessous).

Les moteurs JT9D et JT8D sont plus comprimés (taux de compression 16 et 22) que les deux moteurs SNECMA, prévus pour des utilisations militaires. Plus le taux de compression est élevé, plus, au ralenti, les pressions et températures à l'entrée de la chambre sont élevées elles aussi ; pour un taux de compression de 10, la pression et la température sont de l'ordre de 2 bars et 90°C alors que, pour un taux de compression de 20, les valeurs correspondantes sont approximativement de 10 bars et 150°C.

Il en résulte que la charge aérodynamique Q de la chambre et les émissions de CO et HC d'un moteur fortement comprimé sont plus faibles que celles d'un moteur moins comprimé.

Régime de ralenti

Moteurs	JT9D	JT8D	M.53(*)	LARZAC(*)	LARZAC Etape II
Charge Ω	2,36	6,9	12,8	26	26
Rendement de combustion η'	0,972	0,983	0,945	0,83	0,88

(*) Etat initial de développement.

Il est clair que les caractéristiques générales du moteur jouent un rôle au moins aussi important, sinon plus, que le niveau de perfection technologique de la chambre, caractérisé par la courbe $\eta' = f(\Omega)$.

4.3. La rechauffe de l'Olympus - Niveau de pollution -

Les conditions de combustion de la rechauffe (pression et température d'entrée, vitesse moyenne d'écoulement) sont beaucoup plus défavorables que celles de la chambre principale et, par conséquent, le rendement atteint à la sortie de la tuyère du moteur est relativement faible, de l'ordre de 0,30 à 0,35 suivant les moteurs.

La rechauffe de l'Olympus n'est que partielle, une fraction du flux étant seule intéressée par la "post-combustion". La stabilisation de la flamme est réalisée par un anneau stabilisateur et la caractérisation par une rampe du type à "enclume" située en amont de l'anneau.

Le profil de température à la sortie n'est donc pas uniforme et, de plus, les températures maximales à la sortie du jet sont plus faibles que celles d'un moteur militaire fonctionnant à pleine rechauffe.

Ces températures sont cependant assez élevées pour que les réactions chimiques de "post-flamme" continuent dans le jet, après la sortie du moteur.

Le mélange progressif des gaz brûlés avec l'air ambiant abaisse la température du jet. A une certaine distance du moteur les réactions sont figées.

Ce n'est qu'au-delà de cette distance de figeage que doivent être faits les prélèvements de gaz définissant les niveaux de pollution.

4.3.1. Méthodes de prélèvements et d'analyse

Les mesures, dont il est question ici, ont été faites derrière un moteur fonctionnant à l'air libre (en banc "ouvert"). Une sonde de 6 mètres de longueur est placée horizontalement dans l'axe du jet, à une distance à l'aval du moteur qui varie de 7 à 12 m. Les quinze points de prélèvement sont placés tous les 30 cm le long de la sonde (figures 7 et 8).

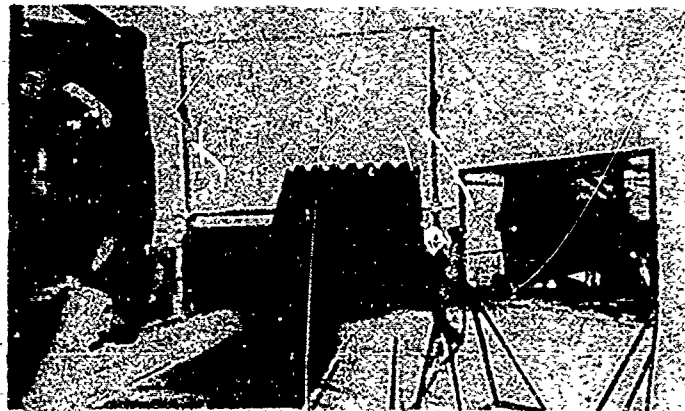


Fig. 7. Prélèvement de gaz à l'arrière de l'Olympus avec réchauffe

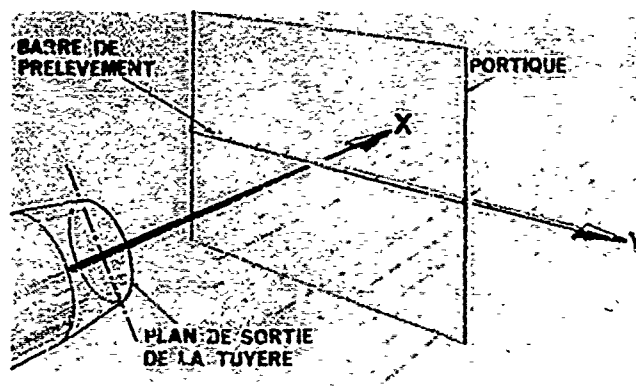


Fig. 8. Schéma pour la définition des axes de coordonnées

Les concentrations de CO_2 et CO sont mesurées, soit par chromatographie en phase gazeuse, soit par analyseur infrarouge non dispersif (NDIR), et les concentrations d'oxydes d'azote soit par la méthode à l'acide phénol-disulfonique (PDSA), soit par chimiluminescence.

4.3.2. Résultats d'essais

Nous donnons les résultats obtenus pour trois dispositifs prototypes, repérés par les lettres A, B et C.

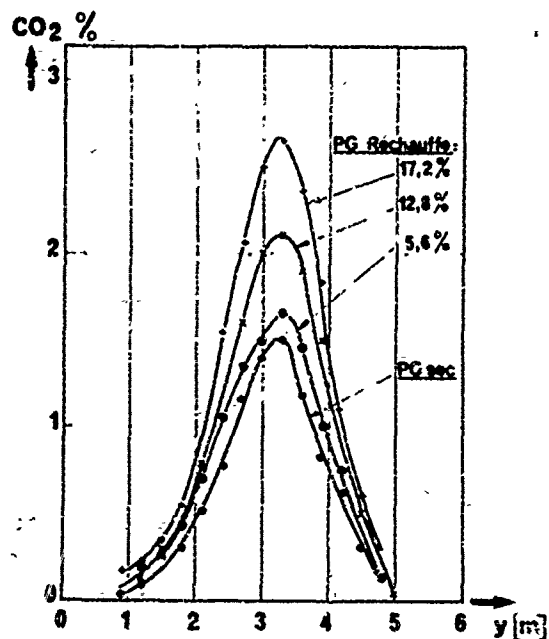
Le diamètre de l'anneau de stabilisation est le même pour les trois systèmes.

Pour les deux systèmes A et B, le diamètre de la rampe d'injection, située à 100 mm environ en amont de l'anneau est égal à celui de l'anneau. Ces deux systèmes ne diffèrent entre eux que par des caractéristiques particulières de la rampe d'injection.

Le système C est caractérisé essentiellement par le fait que la rampe est située plus en amont et que son diamètre est supérieur à celui des systèmes A et B.

Les planches des figures 9, 10, 11 donnent, pour la type C, les profils des concentrations des constituants CO_2 , CO et NO_x , à 10 mètres en arrière de la tuyère du moteur, pour différents taux de réchauffe (le taux de réchauffe est défini par le pourcentage d'accroissement de la poussée).

La figure 12 montre les profils des pressions totales dans les mêmes conditions.



Pollution à 10 m
en arrière
de l'Olympus

Système de réchauffe
type C

$T_{ET} = 1380^\circ\text{K}$

$Z = 0$

Fig. 9.

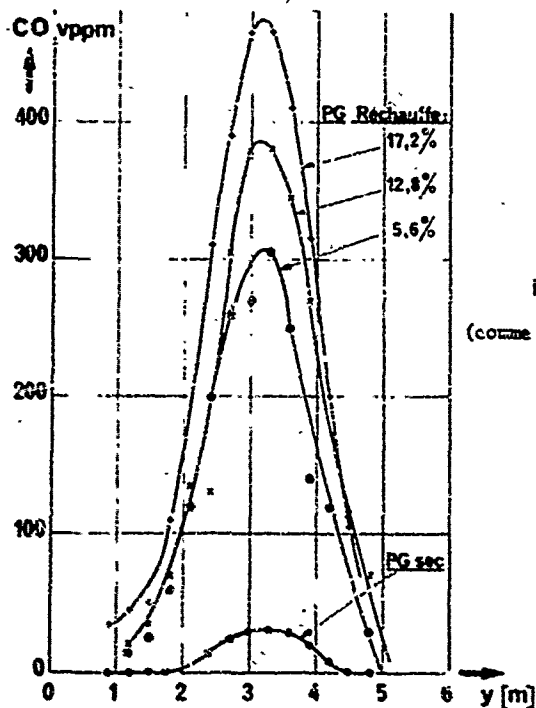


Fig. 10.

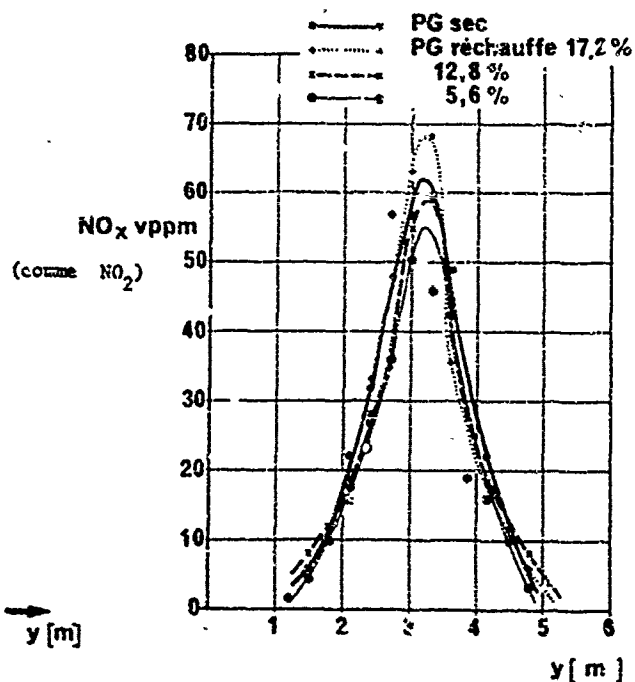
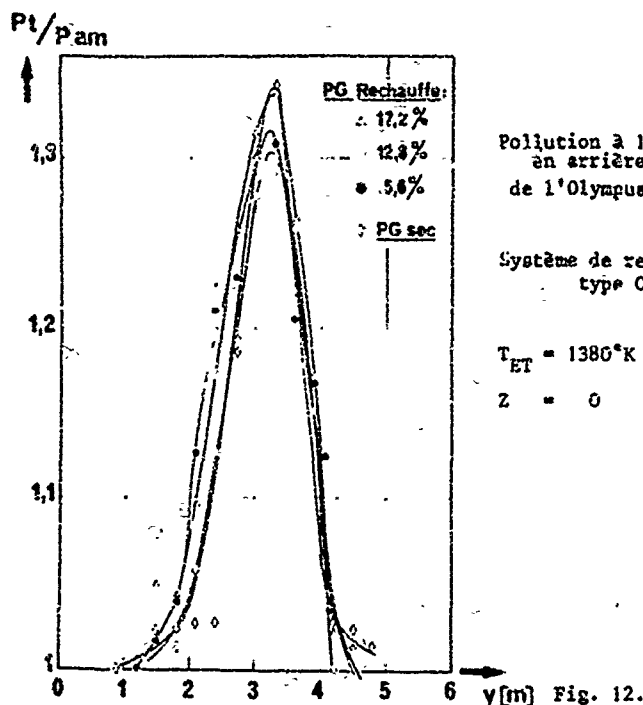


Fig. 11.



Ces différents résultats donnent, par intégration, les masses des divers constituants rejetés ; le débit de carburant pris en compte pour le calcul de l'indice d'émission est celui qui résulte du bilan des atomes de carbone fourni par l'intégration.

La masse totale du carburant ainsi calculée est inférieure de 7 à 16% à celui qui correspondrait au carburant injecté.

Le tableau suivant donne les indices d'émission de CO et d'hydrocarbures imbrûlés de chaque système de rechauffe, pour un taux d'accroissement de poussée de 17 % et une température T_{ET} d'entrée de la turbine de $1380^{\circ}K$.

Dispositif de rechauffe	A	B	C
IE_{CO}	9	15	37
$IE_{Hydrocarbures}$ exprimé en CH_4	0,12	0,19	3,2

- Pour le système C, quel que soit le taux de rechauffe, l'indice d'émission IE_{CO} est pratiquement constant et égal à 37.

Sur la figure 13, on voit que l'indice de pollution local de CO varie assez peu, sauf en bordure du jet.

Pollution à 10 m en arrière de l'Olympus

Système de rechauffe type C

$T_{ET} = 1380^{\circ}K$

$Z = 0$

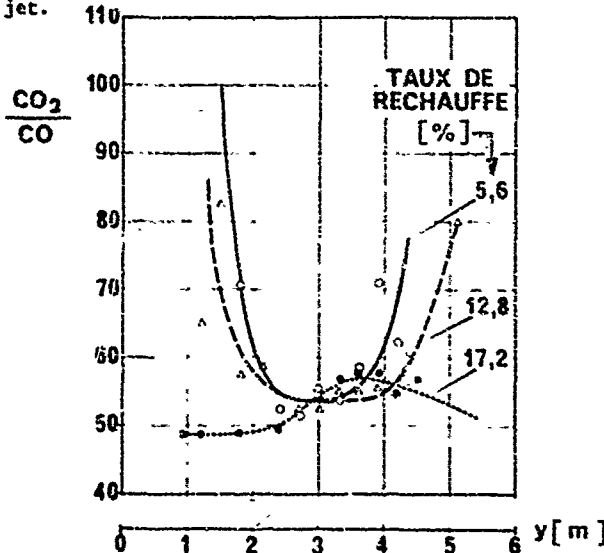


Fig. 13

Les prélèvements de NO_x montrent que, dans le cas de l'Olympus, la production des oxydes d'azote dans la flamme de la rechauffe, est indécidable.

Par contre, alors que, pour le moteur "sec", la proportion de NO est de 88 %, elle n'est plus que de 32 % pour un taux de rechauffe voisin de 17 %.

- Des mesures faites à des distances x de 7 et 12 mètres ont donné les mêmes indices qu'à 10 mètres, ce qui montre que les réactions chimiques sont figées avant 7 mètres.
- Pour les trois versions essayées, le rendement de combustion η est supérieur à 0,99. L'évolution chimique "externe" est très importante, le rendement à la sortie du moteur n'étant pas supérieur à 0,85 (pour un taux de rechauffe de 17 %).
- Les systèmes types A et B sont très intéressants au point de vue pollution, mais ils ne permettent pas d'obtenir l'accroissement de poussée demandé par le développement du moteur.
Il convient de noter l'influence très importante des modifications du système d'injection sur le niveau de pollution, par l'intermédiaire de la combustion "externe". En effet, le système C qui est le plus polluant est par contre celui qui, aux charges les plus élevées, a le meilleur rendement à la sortie du moteur.
- De nouvelles mesures ont été faites dans un banc d'essai traditionnel insonorisé à la sortie du conduit d'évacuation. Les indices d'émission sont plus faibles qu'en banc ouvert, mais le pourcentage d'abaissement de 30 % est le même pour tous les systèmes. Les résultats des essais en banc ouvert que nous avons donnés correspondent tous à une température T_{ET} à l'entrée de la turbine égale à 1380°K.
Les essais dans le banc "fermé" à température T_{ET} plus élevée montrent un abaissement sensible de la pollution pour CO (-30 % pour $\Delta T_{ET} = + 80^\circ K$).

5. MODELE MATHEMATIQUE DE LA COMBUSTION "EXTERNE"

(Moteur Olympus avec rechauffe)

Pour concevoir de nouvelles chambres de combustion moins polluantes ou simplement pour améliorer les chambres existantes, il serait très utile de pouvoir décrire, par des relations mathématiques, l'évolution des phénomènes à l'intérieur des chambres de combustion. C'est ce qui est actuellement entrepris par beaucoup de chercheurs. Des résultats intéressants ont été obtenus en schématisant les phénomènes. Mais si l'on essaye de les décrire plus fidèlement, on se heurte souvent à de grandes difficultés. C'est le cas pour la zone de combustion de la chambre principale. Une de ces difficultés tient au "couplage" qui existe entre la turbulence et la cinétique chimique dans les zones de propagation de la flamme, transversalement à l'écoulement.

On ne sait pas évaluer correctement le taux volumétrique de production et de destruction des espèces par réactions chimiques, dès lors que le gradient transversal de vitesse est associé à un gradient de composition chimique. Mais on sait que, si l'on néglige l'effet de la turbulence en exprimant la vitesse globale de la réaction chimique, sur des bases purement cinétiques, déduites, par exemple, de mesures faites dans un foyer sphérique "homogène", on obtient une valeur qui peut être dix fois plus élevée que la valeur réelle.

La raison principale du désaccord entre le calcul et la réalité tient au défaut d'homogénéité à petite échelle liée à la nature de la turbulence.

Un élément de volume dont le degré moyen d'avancement chimique est de l'ordre de 0,7 n'a pas, généralement, du fait de l'échelle de turbulence, une composition uniforme.

Cet élément comprend, en réalité, des fractions dont les degrés d'avancement sont très élevés (voisins de 1) et des fractions dont les degrés d'avancement sont très faibles (voisins de 0). Or la vitesse de la réaction de combustion globale (schéma cinétique simplifié) est nulle dans ces deux cas alors qu'elle est maximale au voisinage du degré d'avancement moyen de 0,7. Par conséquent, en négligeant l'effet de la turbulence on surestime gravement la rapidité du processus réel de combustion (voir la communication de Mr. BARREPE, réf.12).

Dans le cas de la rechauffe, les zones de propagation (voir figure 5) jouent un rôle très important.

Pour prévoir la valeur du rendement de combustion à la sortie du moteur en fonction des données thermodynamiques et géométriques, nous utilisons, à la SNECMA, des méthodes simplifiées semi empiriques dont l'exposé sortirait du cadre de cette communication.

Nous allons, par contre, donner les résultats des premières tentatives que nous avons faites, avec l'ONERA, pour modéliser les processus de la combustion "externe" (après la sortie du moteur).

L'intérêt de cette étude tient à l'importance prépondérante, dans le cas de la rechauffe, de l'évolution chimique externe et de l'aide que présente un modèle mathématique, non seulement pour mieux comprendre les résultats des mesures faites au sol, mais aussi pour prévoir l'évolution externe pendant l'utilisation de la rechauffe en vol, pour laquelle la mesure est difficile.

5.1. Hypothèses fondamentales

Les hypothèses que nous avons faites simplifient beaucoup le problème. Des améliorations devront être apportées par la suite.

a) Hypothèses aérodynamiques

La vitesse d'écoulement du milieu ambiant, dans le plan de sortie de la tuyère est prise nulle. On suppose le jet à pression constante et vitesse initiale sonique.

Comme la pression totale initiale P_0 du jet de l'Olympus, au point fixe au sol, est voisine de 3 bars (valeur choisie pour le calcul), nous avons été conduits à prendre une pression ambiante fautive, égale à la pression de l'écoulement sonique, soit 1,55 bars.

Le mélange du jet est décrit par un programme de calcul mis au point par l'ONERA (communication de Mr. BORGHI), que nous avons utilisé avec les hypothèses de cinétique exposées plus loin. Les transferts turbulents sont introduits au moyen de la notion classique de longueur de mélange à laquelle on associe des valeurs fixées des nombres de Prandtl et Schmidt.

Dans un plan transversal, la longueur de mélange est supposée constante dans la zone de mélange et proportionnelle à l'épaisseur de celle-ci (coefficient de proportionnalité voisin de 0,1). Les nombres de Prandtl et Schmidt ont été pris constants et égaux à 0,83 (nombre de Lewis égal à 1).

b) Influence de la turbulence sur les taux de réactions

Cette influence a été négligée pour deux raisons :

En premier lieu le niveau de turbulence dans le cœur potentiel du jet est vraisemblablement assez faible ; en second lieu, et surtout, il s'agit d'une évolution chimique en post-flamme qui ne fait intervenir que des degrés d'avancement chimique assez élevés ; par conséquent, même si dans les zones de turbulence élevée (par exemple, dans les zones de mélange avec l'air ambiant) un élément de volume est bien hétérogène en composition, l'influence sur le taux moyen de réaction par unité de volume devrait être plus faible, puisqu'à degré d'avancement élevé la vitesse globale de réaction est une fonction monotone décroissante du degré d'avancement.

c) Hypothèses de cinétique chimique

Théoriquement la méthode la plus rigoureuse consisterait à tenir compte d'un grand nombre de réactions chimiques élémentaires faisant intervenir les radicaux libres. Cette méthode présente, quant à son application à un jet de turboréacteur, plusieurs difficultés. Outre la complexité du système chimique envisagé, il existe des incertitudes non négligeables sur les constantes cinétiques (facteur de fréquence et énergie d'activation). De plus, l'évolution des espèces polluantes suivant l'abscisse x du jet dépend d'une manière considérable des concentrations initiales en radicaux libres (dans le plan de la tuyère $x = 0$). Ces concentrations ne sont pas aisément mesurables et l'on ne dispose pas d'hypothèses de calcul suffisamment sûres pour en estimer les valeurs.

Nous avons finalement représenté les réactions de combustion, comme cela se fait de façon classique, par une loi cinétique globale donnant le taux de consommation du combustible par unité de temps, en fonction de la température de l'élément de volume considéré et des concentrations en oxygène et en combustible de cet élément.

En fait, le combustible à considérer n'est pas le carburant injecté mais un mélange de CO et d'hydrocarbures divers.

Nous avons, de plus, admis que l'ensemble des imbrûlés pouvait être représenté valablement par l'oxyde de carbone CO seul.

C'est l'hypothèse qui a déjà été faite, par exemple, par LONGWELL (réf.10) pour interpréter sur des bases purement cinétiques les limites de stabilité d'un foyer sphérique "homogène" (1953).

Nous avons fait nos calculs avec la même expression de vitesse de réaction que celle de LONGWELL, à savoir :

$$\frac{dX_{CO}}{dt} = 2 \frac{dX_{O_2}}{dt} = 12.10^7 \sqrt{T} \times \frac{P}{R T} e^{\frac{-21000}{T}} \times X_{O_2} \times X_{CO} \quad (5)$$

où X_i est la fraction molaire du constituant i ,

P , la pression en Pascal,

T , la température en $^{\circ}K$,

R , la constante des gaz parfaits = 8,314 J/mole $^{\circ}K$

t , le temps en s.

En réalité la combustion de CO s'accorde avec les étapes intermédiaires dans lequel le radical OH joue un rôle fondamental.

C'est pourquoi certains auteurs ont proposé d'autres expressions globales faisant intervenir non seulement les concentrations de CO et O, mais encore celles de l'eau formée par combustion.

Une synthèse des différentes lois possibles figure dans l'article de G.B. HOWARD, G.C. WILLIAMS et D.H. FINE présenté au 14ème symposium de combustion (réf.11).

Ces auteurs proposent la loi moyenne suivante valable, en principe, sur une grande échelle de température.

$$\frac{dX_{CO}}{dt} = 1,3 \times 10^8 e^{\frac{-15000}{T}} \times \frac{P}{R T} \times X_{CO} \times X_{O_2}^{0,5} \times X_{H_2O}^{0,5} \quad (6)$$

(mêmes unités que pour (5)).

Nous avons, en plus de l'équation (5), utilisé l'expression (6) pour quelques calculs.

Ces lois ne peuvent prétendre représenter d'une manière très précise les résultats car elles dépendent d'une manière notable des conditions expérimentales dans lesquelles elles ont été établies (type d'écoulement, richesse, niveau de turbulence, domaine de température etc...) et ces conditions font apparaître une dispersion notable dans les résultats.

d) Hypothèses thermodynamiques

Elles concernent le profil de température dans le plan de la sortie de la tuyère, qui n'est pas uniforme pour une reheating partielle telle que celle de l'Olympus. Pour simuler les différentes possibilités, nous avons envisagé, outre le cas d'une répartition uniforme, à la température moyenne du jet $T_{tjm} = 1370^\circ\text{K}$, celui d'une répartition du débit total D en deux débits : l'un D_1 qui subit une reheating jusqu'à la température d'arrêt T_{tj1} , l'autre D_2 qui reste à la température d'arrêt T_{tj2} à l'entrée du canal, c'est-à-dire à la température d'arrêt en aval de la turbine. La répartition entre le flux chaud et le flux froid est supposée faite de manière à assurer une poussée globale constante et égale à celle donnée par la répartition uniforme de température T_{tjm} . On a donc approximativement :

$$D_1 \sqrt{T_{tj1}} + D_2 \sqrt{T_{tj2}} = D \sqrt{T_{tjm}}$$

Les calculs présentés ici ont été réalisés avec les valeurs suivantes :

$$T_{tjm} = 1370^\circ\text{K} \quad T_{tj1} = 1500^\circ\text{K} \quad T_{tj2} = 1020^\circ\text{K} \text{ soit un rapport } \frac{D_1}{D} \approx 0,75$$

Nous avons envisagé, pour ce même rapport D_1/D , les deux répartition (A) et (B) portées sur la figure 17. La répartition (A) correspond à une reheating localisée au voisinage de l'axe, alors que la répartition (B) schématise une reheating concentrée vers l'extérieur du canal.

5.2. Evolution dans le coeur potentiel du jet

L'évolution résulte directement de l'intégration des relations (5) ou (6) compte tenu des hypothèses faites. Elle est caractérisée par la valeur du rendement η de combustion.

La figure 14 présente la variation de η en fonction de temps, pour diverses températures totales initiales supposées uniformes dans tout le jet. Il s'agit donc d'un calcul paramétrique préalable, destiné à donner l'ordre de grandeur de l'influence de T_{tj} , en ignorant les hypothèses thermodynamiques du cas de l'Olympus (paragraphe 5.1.d) qui seront reprises plus loin pour l'étude complète du jet.

Nous avons traité le calcul avec un rendement de combustion initial au droit de la tuyère de 0,75 (valeur nettement plus faible que celle de l'Olympus au décollage).

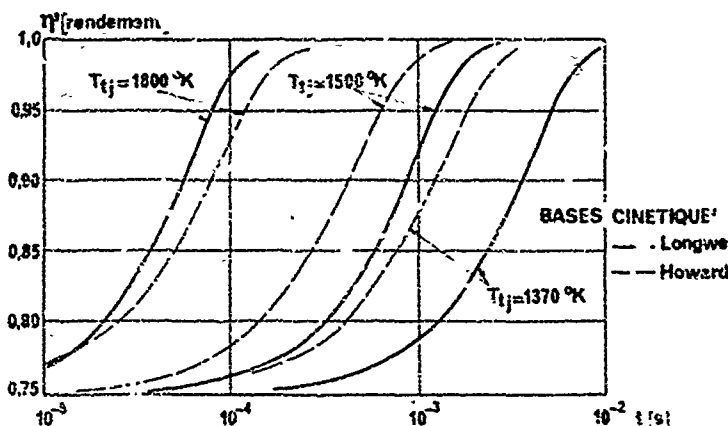


Fig. 14 Evolution théorique dans le coeur potentiel (rechauffe)

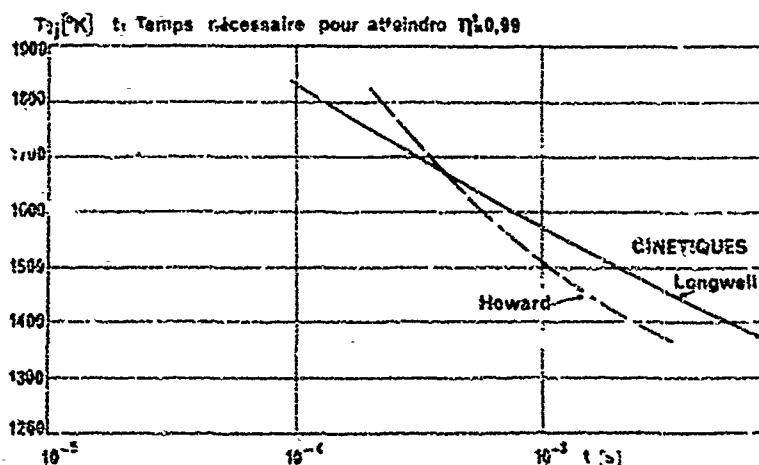


Fig. 15. Evolution théorique dans le coeur potentiel (rechauffe)

On peut remarquer qu'en augmentant T_{tj} de 200° on atteint le même rendement en un temps 10 fois plus petit (voir aussi figure 15) et que, d'autre part, aux basses températures 1400°K , la loi (5) aboutit à des évolutions plus lentes que la loi (6) alors que cet effet s'inverse aux hautes températures. Ces résultats sont la conséquence normale des valeurs différentes des énergies d'activation des expressions (5) et (6).

Les variations de η en fonction de t sont, pour les deux cinétiques, très semblables.

La longueur axiale L du coeur potentiel vaut approximativement 10 fois le rayon, soit dans le cas de la tuyère de l'Olympus une longueur de 4 m à 4,5 m environ.

Il en résulte, compte tenu de l'hypothèse simplificatrice d'un champ de pression uniforme, un temps de parcours sur l'axe d'environ 6 ms. Dans ces conditions les figures 14 et 15 montrent que, pour le filet de courant sur l'axe, le rendement dépasse 0,99 dès que T_{tj} atteint 1400°K .

Par contre, pour les filets externes, le temps de séjour est plus faible et, à la sortie du coeur potentiel, il reste une proportion de CO plus importante.

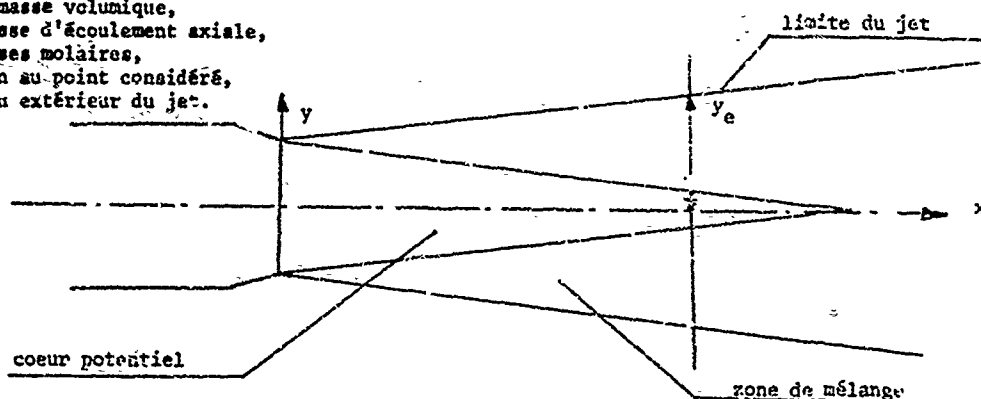
5.3. Evolution chimique dans l'ensemble du jet

Seule la loi de cinétique chimique bimoléculaire représentée par l'expression (5) a été utilisée pour ces calculs.

Le niveau de pollution dans un plan y perpendiculaire à l'axe du jet (voir croquis ci-contre), est caractérisé par le débit de CO dans cette section, soit :

$$D_{CO} = \int_0^{y_e} \rho V X_{CO} \frac{M_{CO}}{M} 2 \pi y dy \quad (7)$$

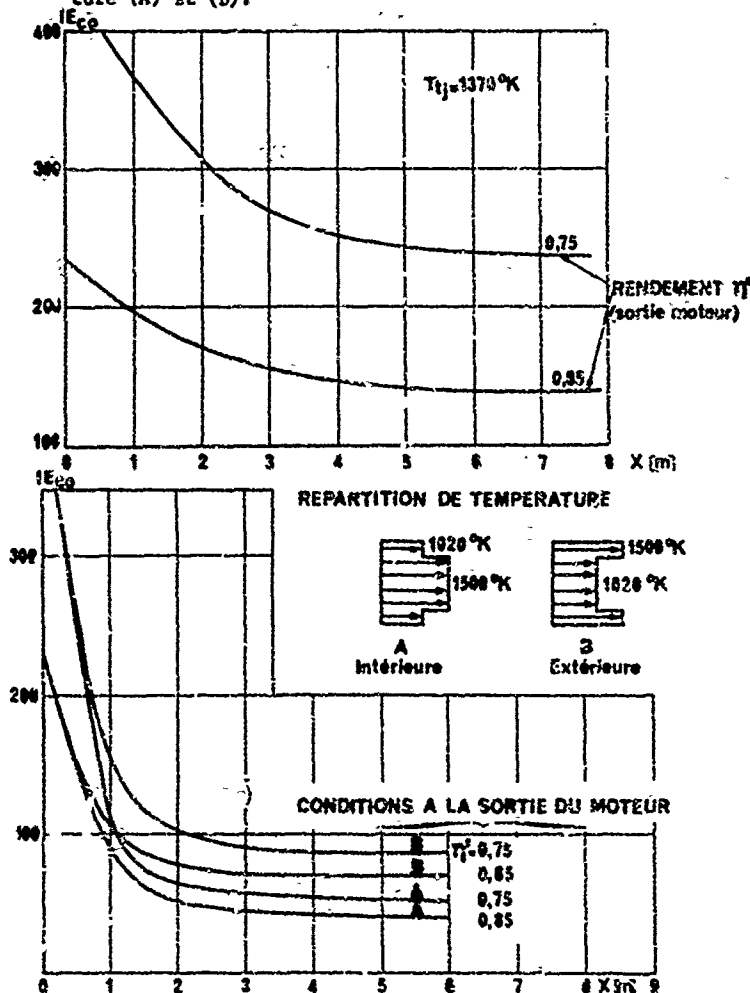
ρ est la masse volumique,
 V la vitesse d'écoulement axiale,
 M les masses molaires,
 y le rayon au point considéré,
 y_e le rayon extérieur du jet.



L'intégration dans le plan x, y est faite en utilisant le programme ONERA (voir 5.1.a). Les résultats sont représentés en employant l'indice d'émission IE_{CO} déduit de D_{CO} .

La figure 16 représente l'évolution de l'indice IE_{CO} en fonction de l'abscisse x comptée à partir du plan de sortie de la tuyère, pour une répartition uniforme de température $T_{tj} = 1370^\circ K$ et pour deux valeurs du rendement η' au droit de la tuyère (0,75 et 0,85).

La figure 17 montre l'évolution de IE_{CO} en fonction de x dans le cas des répartition de température (A) et (B).



On constate que la décroissance initiale de CO est rapide mais qu'au delà d'une distance d'environ 6 m, les réactions chimiques sont pratiquement figées, le niveau de pollution ne variant plus. Pour la répartition (A), en particulier, la valeur finale de l'indice (~ 40) est assez proche des valeurs qui ont été mesurées (paragraphe 4.2.). La répartition (B) est nettement plus défavorable car les filets de courant externes, à la température maximale, rencontrent plus rapidement la zone de mélange dans laquelle intervient un figage plus précoce. Du strict point de vue pollution, il serait donc nécessaire de concentrer la recharge au voisinage de l'axe. De plus, on constate que, dans le cas d'une répartition uniforme, les niveaux de pollution finaux restent approximativement dans le rapport des niveaux initiaux (rapports des quantités 1 - η').

Par contre, dans le cas des répartition (A) ou (B), l'amélioration du rendement initial n'entraîne qu'une diminution beaucoup plus faible de la pollution résiduelle. L'importance de l'évolution chimique externe sur la pollution est prépondérante.

Figures 16 et 17 - Evolution théorique de l'indice moyen de CO après la sortie du moteur.

5.4. Conclusions

Bien que fondé sur des hypothèses très simplifiées, le modèle présenté dans ce texte donne une représentation assez satisfaisante des phénomènes les plus importants de l'évolution chimique dans le jet d'un turboréacteur avec rechauffe.

On note, en particulier, que du point de vue pollution au sol, les transformations chimiques après la sortie du moteur ont une influence prépondérante.

L'ordre de grandeur des indices d'émission calculés à 6 m pour les répartitions de température (A) et (B) (assez voisines des répartitions réelles) est assez proche de la réalité.

On constate, par conséquent, que le fait de négliger l'influence de la turbulence sur la disparition de CO, ne semble pas affecter les résultats comme cela est le cas lorsque l'on cherche à modéliser, par exemple, la propagation turbulente de la combustion à l'intérieur du foyer de rechauffe. Néanmoins, il est clair que, pour obtenir une représentation plus fidèle des phénomènes, il est nécessaire d'améliorer par étapes le modèle décrit, le premier stade étant, à notre avis, une description aérodynamique correcte du jet supersonique.

Nous pourrions envisager alors d'utiliser la méthode à l'étude de la pollution en vol.

6. LA REDUCTION DE LA POLLUTION

6.1. Cas de la rechauffe

Le cas de la rechauffe est très différent de celui de la chambre principale. La rechauffe ne produit aucun particule de carbone (elle brûle en particules qui sont formées dans la chambre principale) et aucun oxyde d'azote, au moins dans le cas de l'Olympus.

La poussée maximale du moteur est obtenue pour la température maximale des gaz de sortie. Généralement cette température est atteinte pour une richesse globale d'injection (chambre principale plus rechauffe) voisine de 1. Cette richesse n'est pas favorable à une évolution complète des réactions chimiques après la sortie du moteur par suite du défaut d'oxygène

$$\left[\frac{d[CO]}{dt} \times \frac{1}{1-\eta} \rightarrow 0 \text{ quand } \eta \rightarrow 1 \right]$$

Par contre, pour une rechauffe moins poussée, correspondant à une richesse de l'ordre de $\phi = 0,80$, les vitesses de réaction de post-flamme deviennent optimales ce qui devrait être plus favorable du point de vue de la pollution.

Dans le cas d'une rechauffe partielle telle que celle de l'Olympus, la situation est, à cet égard, plus favorable et une certaine optimisation de l'injection peut diminuer au sol, l'émission de CO. On doit noter que, dans l'état actuel des techniques, la part de la rechauffe dans l'émission de CO est, de toute façon, modeste (de l'ordre de 10 à 20 % dans le cas de l'Olympus), par suite du temps d'utilisation restreint.

6.2. Chambre principale - Remarques préliminaires

Avec une technique classique (un étage d'injection et une géométrie fixe), les moyens propres à réduire l'émission de CO et des hydrocarbures au ralenti ont tendance à augmenter l'émission totale des oxydes d'azote et réciproquement.

Seules des techniques dites "avancées", du point de vue pollution, utilisant l'injection étagée ou une géométrie variable permettent, a priori, une optimisation simultanée pour l'ensemble des polluants. Il convient de noter que la généralisation récente des tubes à flamme annulaires à rapporté, du point de vue pollution, un progrès. En effet, la chambre annulaire réduit, en gros par deux, les surfaces des tôles mouillées par les gaz et protégées par les couches d'air des "films" de refroidissement, ce qui diminue (paragraphe 3.2., page 32.5) les émissions de CO et HC, en particulier au ralenti.

Nous avons déjà signalé, d'autre part, que des progrès importants, sinon décisifs, avaient été faits dans la maîtrise des techniques propres à supprimer les fumées visibles.

6.3. Chambre principale - Amélioration des techniques classiques

a) Considérons tout d'abord le problème de la réduction des "inabrupts" CO, hydrocarbures et fumées. Leur réduction revient à l'amélioration du rendement de combustion η .

Le moyen le plus évident consiste à diminuer la charge aérodynamique Ω (relation (4), page 32-7) par augmentation du volume V du tube à flamme.

On est cependant limité dans cette voie par des questions d'encombrement, spécialement en longueur de chambre et particulièrement pour les moteurs faiblement comprimés dont les chambres ont des volumes déjà importants, même pour des Ω élevés. D'autre part, une diminution trop grande des vitesses d'écoulement n'est pas favorable à la rapidité de la préparation du mélange carburé (vaporisation des gouttes).

Un allongement de la chambre n'est pas bon du point de vue refroidissement des parois du tube à flamme (réf. 2).

Un deuxième moyen, pour améliorer le rendement au ralenti consiste à augmenter, à ce régime, la richesse moyenne de la zone de combustion qui est trop pauvre, en diminuant le pourcentage de l'air de combustion. On change ainsi "l'adaptation" de la chambre. Toutefois, il y a des limites à ce procédé, en particulier pour les moteurs fortement comprimés pour lesquels l'augmentation de la richesse, au décollage, accroît l'émission des fumées au décollage.

Le rendement de combustion, au ralenti, devrait aussi être amélioré en évitant le fléage par présence des résistances, soit par l'air de dilution, soit par les "films" de refroidissement. Il y a donc théoriquement intérêt à introduire l'air de dilution, le plus tard possible. Une augmentation du niveau de turbulence est de nature à améliorer les rendements de combustion mais on est limité dans cette voie par la perte de charge et les problèmes de refroidissement du tube à flamme.

Pour éviter les fumées et, dans une certaine mesure les hydrocarbures, il faut, comme on l'a vu, diminuer l'importance des zones riches. Un prémélange total avec l'air de combustion n'est pas admissible car la limite d'extinction pauvre de la chambre serait alors trop élevée. Mais on doit favoriser le mélange rapide du carburant avec une fraction de l'air de combustion, avec mélange ultérieur avec les gaz brûlés recirculant dans la zone primaire. Avec l'injection classique à "pulvérisation mécanique", ce prémélange partiel est obtenu en faisant passer un débit d'air à l'intérieur de l'injecteur et en ménageant certains orifices d'entrée d'air de combustion dans la fond du tube à flamme (voir, par exemple, les études de Pratt and Whitney).

Il nous paraît préférable de modifier la technique d'injection.

La planche de la figure 3 schématisée, sous la forme mise au point à la SNECA (voir réf. 1 et 2), la technique dite de la prévaporisation développée initialement et toujours utilisée par les Britanniques sur certains de leurs moteurs.

Une fraction de l'air de combustion et le combustible sont introduits ensemble à l'entrée du prévaporisateur.

Ce système présente, en outre, d'autres avantages déterminants (réf. 1), mais pose des problèmes de tenue mécanique et thermique pour les moteurs à performances élevées.

Une autre technique est celle de la pulvérisation pneumatique : le combustible est injecté directement dans une fraction de l'air primaire, sans conduit pénétrant à l'intérieur de la zone de combustion. La vitesse de l'air résultant de la perte de charge du tube à flamme permet, en principe, d'obtenir une pulvérisation fine. Mais l'adaptation d'un tel système à une structure d'écoulement convenable dans la zone de combustion n'est pas facile. Nous avons développé un dispositif de ce genre dont les premiers résultats aux bancs partiels sont prometteurs.

- b) La réduction de l'émission des oxydes d'azote implique celle des temps de séjour à température élevée.

Malheureusement, la plupart des procédés énoncés plus haut pour améliorer les rendements de combustion et diminuer, au ralenti, l'émission de CO et des hydrocarbures, sont de nature à favoriser la production des oxydes de l'azote.

Il faudrait, en effet, éviter de maintenir, aux régimes élevés, les gaz brûlés à des richesses voisines de 1.

Un réglage pauvre, aux régimes élevés, de la zone de combustion ne permet pas les rallumages en altitude et les bons rendements au ralenti.

Un réglage riche est néfaste du point de vue des émissions de fumées et se traduit, dans la zone de dilution, par un passage à des richesses voisines de 1.

De toute façon, l'hétérogénéité des richesses de la zone de combustion atténue les effets attendus de ces réglages (réf. 13).

Le seul procédé vraiment efficace est l'injection d'eau déminéralisée, aux régimes élevés, dans la zone de combustion, injection qui baisse comme il convient les températures de flamme. Sur une turbine à gaz Hispano-Suiza, nous avons obtenu au point fixe une réduction de 40 % de l'émission de NO_x en injectant un débit d'eau de 39 % du débit de combustible.

Malheureusement l'injection d'eau, utilisée systématiquement au décollage et en montée, est une servitude lourde et pose des problèmes de durée de vie des parties chaudes du moteur. De plus, ce procédé est inapplicable pour réduire les émissions en croisière.

6.4. Chambre principale - Réduction de la pollution par des techniques "avancées"

"L'écoulement de l'injection" est soit radial, soit axial. La NASA a publié certains résultats concernant un écoulement radial à "modules" identiques.

L'injection axiale est souvent citée mais nous ne connaissons aucun résultat publié.

Dans son principe l'injection étagée est un moyen propre à réduire, à la fois les imbrûlés et les oxydes d'azote puisque les richesses moyennes des diverses zones de combustion peuvent être optimisées.

Toutefois, pour que le bénéfice à en retirer soit réel, il faut que les techniques d'injection et la structure de l'écoulement d'air dans les différentes zones soient correctement réalisées, ce qui n'est pas une tâche facile.

La géométrie variable est évidemment, a priori, un moyen d'adapter les richesses par variation des orifices de passage d'air, mais la complexité technologique est un lourd handicap.

La figure 18 montre le schéma de principe d'une chambre conçue, a priori, pour réduire l'émission de l'ensemble des imbrûlés sans géométrie variable.

Le flux sortant du compresseur est divisé en deux parties alimentant deux chambres annulaires concentriques.

La chambre extérieure A comporte une zone de combustion de type classique alimentée par des injecteurs constituant la zone d'injection. Le débit d'air de combustion est optimisé pour le ralenti (richesse moyenne voisine de 1). Un crépissage d'air est introduit dans une zone secondaire de la chambre A. Les gaz brûlés sortant de la chambre A sont introduits sous forme de jets, à travers une cloison P dans une zone où ils se mélangent au flux sortant de la chambre B.

La chambre B assure l'essentiel de la combustion à régime élevé, la chambre A fonctionnant alors à très faible charge.

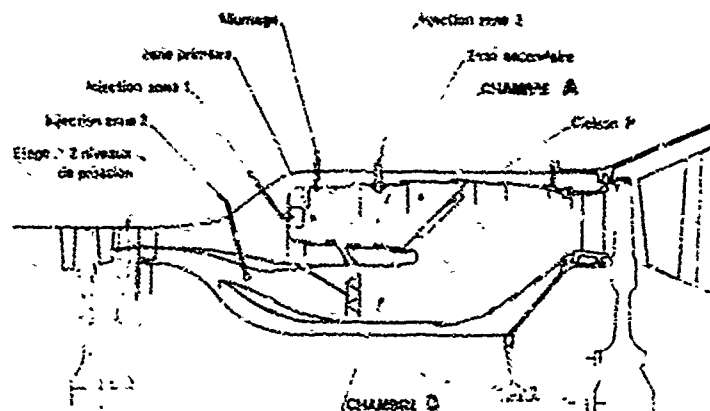


Fig. 13 - Schéma d'une chambre antipollution à deux écoulements -

L'injection dans la chambre B (zone d'injection 2) est du type à prémélange, comme pour une rechauffe, et la stabilisation est elle aussi semblable à celle d'une rechauffe. On peut ainsi adapter cette chambre à une richesse éloignée de 1 (de préférence pauvre) et choisir le temps de séjour de façon à réduire le plus possible les oxydes d'azote (réf.14). Le prémélange, s'il est bien uniforme au niveau des stabilisateurs, garantit un fonctionnement sans fumées visibles.

Une difficulté se pose dans le cas des moteurs pour avions supersoniques : si la richesse de décolage de la chambre B est nettement pauvre, en croisière la richesse de cette même chambre risque d'être insuffisante.

Plusieurs solutions peuvent alors être envisagées suivant l'importance respective des problèmes de la pollution par les oxydes d'azote au sol et en vol (multiplication des zones d'injection de la chambre B ou utilisation d'une zone d'injection complémentaire 3).

L'allumage de la chambre A est classique, celui de la chambre B pouvant se faire par l'intermédiaire d'une intercommunication entre A et B.

La division des flux peut être faite préalablement, au niveau du dernier étage de compression du compresseur. Ainsi la perte de charge de la chambre A est plus élevée par suite d'une compression supplémentaire, ce qui favorise les rendements de combustion au ralenti et le mélange des flux des chambres A et B, la perte de charge de B étant plus faible.

Les gains à attendre d'une telle technique, pour le même volume global que celui d'une chambre classique, sont difficiles à estimer avec précision.

Il y a, bien sûr, beaucoup de problèmes à résoudre tels que celui du refroidissement des parois (en particulier la cloison P), celui de la répartition de température à l'entrée de la turbine et celui des régimes intermédiaires.

De toute façon, le poids de la chambre serait augmenté, la régulation du carburant rendue plus complexe et le prix du moteur accru.

7. CONCLUSIONS

Les principaux problèmes de la pollution des moteurs d'avion à réaction sont l'émission d'oxyde de carbone et d'hydrocarbures imbrûlés divers pendant les phases de roulage au sol, l'émission de particules et des oxydes d'azote au décollage, en montée et en altitude pendant la croisière. Un progrès notable a déjà été fait pour les imbrûlés au ralenti (CO et HC) par l'emploi systématique de la chambre annulaire et pour les fumées visibles par l'utilisation de techniques d'injection améliorées favorisant un prémélange partiel.

Des améliorations peuvent être apportées aux techniques classiques, mais elles sont limitées.

Il faut remarquer, de toute façon, que les problèmes ne sont pas les mêmes suivant le type de moteur. Les turboréacteurs de faible puissance et ceux dont le taux de compression est modeste sont défavorisés pour l'émission des imbrûlés au ralenti, les moteurs à taux de compression élevés et de forte puissance, pour les oxydes d'azote.

Des techniques "avancées" (injection étagée, géométrie variable) devraient, en principe, réduire l'ensemble des émissions mais leur application pose des problèmes technologiques très importants qui nécessitent de longues recherches.

La rechauffe ne pose au sol qu'un problème relativement peu important d'émission de CO et HC, mais les moyens d'action sont limités.

Références bibliographiques

1. Le développement des chambres de combustion annulaires à hautes performances à la SNECMA -
J. CARUEL - 1st Symposium on Air Breathing Engines - 1972 MARSEILLE -
2. Développement des chambres de combustion à haute intensité -
A. QUILLÉVÉRE - AGARD Conference proceedings part.2 - 1968 TOULOUSE -
3. A Survey of Annular Vaporizing Combustion Chambers -
E.C. PARNELL and M.R. WILLIAMS - 1969 CRANFIELD -
4. Jet Aircraft Air Pollutant Production and Dispersion -
J.B. HEYWOOD - J.A. FAY - L.H. LINDEN -
A.I.A.A. Paper n° 70.115 - 1970 -
5. Soot Formation Rates in premixed C_2 and C_6 Hydrocarbon Air Flames at Pressures upto 20 Atm -
J.J. MCC FURLANE - F.H. BOLDRENESS and F.S.E. WHITCHER -
Combustion and Flame 3 - 1964 -
6. F.J. WRIGHT
Combustion and Flame 15 n° 3 - 1954 -
7. Le carbone-suie dans les flammes -
A. FEUCIER - Revue de l'Institut Français du Pétrole XXIV n° 11 - Novembre 1969 -
8. Formation of Nitric Oxide in Premixed Hydrocarbon Flames -
C.P. FEMINORE -
13th Symposium of Combustion - 1970 -
9. Analysis of Aircraft Exhaust Emission Measurements -
H.T. Mac ADAMS et L. BOGDAN -
Carnell Aeronautical Laboratory Inc. - 1971 -
10. High Temperature Reaction Rates in Hydrocarbon Combustion
J.P. LONGWELL and M.A. WEISS - Industrial and Engineering Chemistry - 1955-
11. Kinetics of Carbon Monoxide Oxidation in Post Flame Gases -
J.B. HOWARD - G.C. WILLIAMS - D.H. FINE -
14 th Symposium of Combustion (1972) -
12. Modélisation des foyers de turboréacteur en vue de l'étude de la pollution -
M. ZARRENE -
Propulsion and Energetics Panel 41 st Meeting - 1973 -
13. A model For nitric oxide Emissions from Aircraft gas Turbine Engine -
R.S. FLETCHER et J.B. HEYWOOD -
A.I.A.A. Paper n° 71.123 - 1971 -
14. Better Marks on Pollution for the S.S.T. -
A. FERRI - Astronautics and Aeronautics - 1972 -

Discussion on Paper 32

"Point de vue du motoriste sur la conception des foyers à
faible taux de pollution"
presented by A.Quillévére

A.K.Forney:

- (1) Reference Figure 11 shows NO_x formed in afterburner. Would there be more NO_x formed at higher rates?
- (2) We have run at higher levels up to Mach 2 (main fuel = afterburner fuel). This yields 20% increase in NO_x and at Mach 2.6 a 25% increase in NO_x .

A.Quillévére: Il nous est difficile de répondre à la question posée car nous n'avons mesuré les oxydes d'azote, avec rechauffe, que sur l'Olympus et nous n'avons pas entrepris, non plus, l'étude d'un modèle mathématique pour la formation de NO_x dans la rechauffe. Un accroissement de production de NO_x avec rechauffe de 20% n'est évidemment pas négligeable.

La différence entre vos résultats et les nôtres tient, peut-être, au fait que la rechauffe de l'Olympus est une rechauffe partielle, dont la température de flamme est en moyenne relativement basse. Il est possible que, pour des taux de rechauffe plus élevés, la production de NO_x ne soit plus négligeable.

AIRCRAFT GAS TURBINE POLLUTANT LIMITATIONS ORIENTED TOWARD MINIMUM EFFECT ON ENGINE PERFORMANCE

Robert E. Henderson
Tech Area Manager, Combustion
Air Force Aero Propulsion Laboratory (TEC)
Wright-Patterson Air Force Base, Ohio 45433

and

William S. Blazowski, 1/Lt
Laboratory Mechanical Engineer
Air Force Aero-Propulsion Laboratory (SFF)
Wright-Patterson Air Force Base, Ohio 45433

SUMMARY

The proposed Environmental Protection Agency (EPA) regulations for aircraft engine emissions are examined in terms of their impact on the application to military aircraft gas turbine engines. A quantitative assessment of current engine emission levels, design trends and potential emission control techniques is presented. It is concluded that special considerations must be afforded to military aircraft relative to direct application of EPA regulations; however, many future emission-reducing advances will be applicable to military gas turbines. U. S. Air Force goals have been established to insure that new engines take advantage of this technology, and are in accordance, to the greatest degree possible, with what EPA requires of commercial aircraft. These goals are in terms of minimum idle combustion inefficiency, maximum allowable oxides of nitrogen (lb/1000 lb-fuel) and maximum allowable smoke number. The rationale behind using these parameters and the means by which the numerical limitations were derived are described.

INTRODUCTION

In recent years, increased citizen awareness of environmental issues coupled with the obvious visible smoke emissions from jet aircraft has brought substantial public attention to aircraft-contributed pollution. Although smoke by itself may not be harmful, it did focus attention on jet engines as a source of invisible toxic gaseous emissions (carbon monoxide, hydrocarbons, and oxides of nitrogen). As airports became busier with more frequent operations, it became evident that at least the possibility existed that these individual mass emissions, when concentrated in the local airport environment, could result in ambient levels which exceed allowable levels.

Concern within the United States culminated in the inclusion of mass emissions from aircraft engines in the considerations of the Clean Air Act Amendments of 1970. This legislation requires that the Environmental Protection Agency (EPA) assess the extent to which aircraft emissions affect air quality, determine the technological feasibility of controlling such emissions, and establish aircraft emission standards, if necessary.

The resulting EPA assessment of the impact of aircraft exhaust emissions¹ has indicated the necessity to regulate aircraft emission of carbon monoxide (CO), total hydrocarbons (CxHy), oxides of nitrogen (NOx) and visible smoke. It should be noted that NOx as used herein represents the summation of emissions of NO and NO₂. Specifically, the emissions of non-methane hydrocarbons by aircraft are estimated to be "far in excess" of the hydrocarbon standard at many airports. Carbon monoxide emissions in some areas of public access, where contributions of CO by aircraft are major, exceed the standard, and aircraft generated NO₂ concentrations are significant but well below the standard. The EPA study also indicated that particulate emissions due to aircraft alone resulted in concentrations in excess of the secondary (welfare-related) air quality standard. The limitations presently being considered by EPA were derived from these conclusions.

Although carbon monoxide, hydrocarbons, oxides of nitrogen and smoke are the most often mentioned jet engine pollutants, a more detailed description of pollutants could be considered. (a) total hydrocarbons can be further organized into unreactive hydrocarbons and reactive hydrocarbons or even finer subgroups; (b) besides the considerations of visible smoke, the problem of total particulates may be addressed; (c) sulfur oxides, although not a significant problem because of the low levels present in aviation fuels, can be considered as one of the pollutants; and (d) emissions responsible for odor, although part of the total hydrocarbon class, could be addressed as a separate entity. The present scope of understanding, however, does not allow the more detailed problems associated with each of these categories to be discussed here. Consequently, the four principal pollutant categories mentioned above are employed as the main format for discussion of pollutants in this paper. Occasional reference is made to the various more detailed aspects of the problem.

Planned EPA regulations are based on reducing aircraft engine emissions during their operation below 3000 feet. However, an additional environmental problem has been associated with aircraft -- the potential problem of high altitude emissions. There are many mechanisms by which this might arise: (1) Emission of water vapor and carbon dioxide into the stratosphere may cause a "greenhouse effect", (2) hydrocarbons emitted might react with nitrogen oxides both emitted into and naturally present in the stratosphere to form a smog type condition at high altitude; and (3) increased concentrations of water (H₂O) and NO_x due to emissions into the stratosphere might deplete the ozone layer and allow increased penetration of solar ultraviolet radiation. Much more investigation is needed, however, before the problem can be suitably defined.

This paper will not address the ground level or the stratospheric environmental questions per se, but rather, it will assess the possibility of reducing aircraft engine pollutants at all operating levels and describe emission goals presently being considered for current and future U. S. Air Force aircraft propulsion systems.

In consideration of pollutant characteristics, piston, non-afterburning and afterburning turbine engines are in separate categories. Each group will be discussed below.

POLLUTANT FORMATION

1. Piston Engines

Presently, the U. S. Air Force employs relatively few piston-type aircraft engines; hence, current philosophy is to apply pollutant controls outside the basic existing engine rather than reduce emissions by major engine design changes. Pollutant formation in piston aircraft engines is virtually the same as that in automobile piston engines in that they both operate at fuel-rich conditions. Since, under these conditions, it is not possible to convert all of the fuel into carbon dioxide (CO_2) and H_2O , as is necessary for maximum extraction of the fuel chemical energy, emissions of CO and C_xH_y become of primary concern. Considering the extent of aircraft piston engine operation, NO_x is not considered to be a very serious problem. Oxides of sulfur (SO_x) emissions from aircraft piston engines are also regarded as a secondary problem. The sulfur content of the fuel is extremely low (below 0.05% by weight) and so, when compared with other sources of SO_x (i.e., stationary power generating plants burning coal and other high sulfur fuels), the sulfur oxides emitted by aircraft piston engines are not considered to be cause for concern.

Particulate emissions from aircraft piston engines consist mainly of the lead which was added to the fuel as an anti-knock. No applicable limitation currently exists but future regulation is conceivable. Hence, a need for an anti-knock additive which does not contain lead may exist in the future.

2. Non-Afterburning Turbine Engines

Of the three classes of aircraft engines being discussed here, the non-afterburning turbine engine has by far received the most attention in characterization of emissions. The non-afterburning turbine class includes turbojets, turboshafts, and turboprops. Pollutant formation characteristics of all of these engines are similar due to the fact that each type uses the same basic core -- a compressor, combustor, and turbine.

Recently, there have been many attempts to correlate and explain emission trends for these engines. Basically, it is well known that emissions of CO and C_xH_y are a significant problem at idle conditions while smoke and NO_x emissions tend to be a greater problem at the higher power settings. These trends are illustrated in Figure 1. As in the case of piston engines, sulfur content of the fuel is low (usually less than 0.05% by weight) and, therefore, SO_x emission is not a problem. Furthermore, total particulate emissions arising from lead-based additives are not a problem -- no such additive is required for the gas turbine engine. Emitted particulates are composed largely of carbon and the principal remaining problem is one of defining that point at which the carbonaceous particulates become visible.

Since the majority of the present and future U. S. Air Force (USAF) aircraft fleet will be powered by turbine engines, methods of pollutant control for these engines must be developed. As a basis for later consideration of control techniques, the following discussion addresses the means by which each of the general pollutants from gas turbine engines is generated.

a. Hydrocarbons and Carbon Monoxide

Aircraft turbine engine combustors are designed for peak efficiency operation at cruise and higher power settings. The idle and taxi power condition is appreciably different from the cruise setting and, consequently, the engine operates inefficiently at these points. The major effect of inefficient operation is the emission of species which represent unused chemical energy -- CO and C_xH_y . A relationship between combustion inefficiency and emission of these two pollutants is given by the following equation:

$$1 - \eta_b = \frac{(EI)_{\text{CO}} (QL)_{\text{CO}} + (EI)_{\text{C}_x\text{H}_y} (QL)_{\text{C}_x\text{H}_y}}{(QL)_{\text{fuel}} \times 10^3} \quad (1)$$

where: η_b = combustion efficiency of main burner.

$1 - \eta_b$ = inefficiency of main burner.

$(EI)_i$ = emission index in lb/1000 lb fuel for exhaust constituent i.

$(QL)_i$ = constant pressure lower heating value for exhaust constituent i (BTU/lbm). Although chemical energies should be used in the above equation, the error incurred in using QL values is slight.

The value of Q_L for carbon monoxide is known to be 4343 BTU/lb., and that for JP-4 is 18,700 BTU/lb. However, the actual composition of C_xH_y emitted from an aircraft gas turbine engine is not known and, consequently, its value of Q_L is unknown. Measurement of hydrocarbons is usually made with a flame ionization detector which actually senses total carbon atoms, and the reduced data are represented as pounds of hydrocarbons per pound of fuel. Most hydrocarbons have Q_L values between 16,000 and 21,000 BTU/lb, but those that would be emitted from the engine (as unburned fuel or as other organic species) would probably have a hydrogen-carbon ratio similar to that of the original fuel. Consequently, the value of Q_L for Eq. (1) has been taken as the same as for JP-4.

Inserting the Q_L values into Eq. (1), the following relationship is obtained:

$$1 - \eta_b = \frac{(E1) \cdot 4343 + (E2) \cdot 18,700}{18,700 \times 10^3} \quad (2)$$

This relation is graphically shown in Figure 2. A equation has been used to reduce some engine emission data to combustion inefficiency values for various engines. The results are given in Table 1 below:

TABLE 1

AVERAGE COMBUSTION INEFFICIENCY VALUES AT IDLE FOR
SOME CONTEMPORARY AIRCRAFT GAS TURBINE ENGINES

<u>ENGINE</u>	<u>IDLE COMBUSTION INEFFICIENCY</u>
T56-A7	1.8
T56-A15	1.9
J52-P6A	4.2
GJ805	4.2
JT3C	9.7
JT2D	14.4
JT8D (Regular)	2.2
JT8D (Smokeless)	2.0
JT9D	2.9
TF30	3.3
J57-P21A	5.5
T53-A-13A	3.2
JT9	3.3
TF39	2.7

Engine emission data has been extracted from many sources, the majority coming from the EPA survey of engine emission factors.³ These same data plotted against engine pressure ratio at idle are shown in Figure 3. A reasonable correlation is obtained indicating that higher inlet temperatures and pressures at idle result in improved combustion efficiency. Consequently, it is reasonable to say that larger high-pressure ratio engines are less of a low power emissions problem than those of low pressure ratio design.

b. Oxides of Nitrogen

Although highest at full power, the emissions of NO_x in the exhausts of aircraft turbine engines predominate during take-off, climbout and landing approach. The problem stems from the molecular oxygen and nitrogen in air being exposed to the extremely high temperatures of the combustor primary zone where for stability considerations, the fuel-air ratios have been designed to be approximately stoichiometric.

A reported correlation of data from many engines has shown that NO_x emission is strongly related to the combustor inlet temperature.⁴ This correlation is presented in Figure 4. None of these engines has had any design modifications specifically intended to reduce or control NO_x emissions. Therefore, Figure 4 is referred to here as the "uncontrolled engine correlation."

An extremely important aspect of this correlation is that the emission characteristics are expressed as pounds of pollutant per thousand pounds of fuel -- the Emission Index (EI). In non-afterburning engines, considerations such as specific fuel consumption and total thrust depend on the engine cycle parameters; but the emission of NO_x is solely dependent on how it was formed in the region of combustion. The successful correlation of Figure 3 confirms that EI versus combustor inlet temperature is the proper means to characterize NO_x emission. Further, this strongly suggests that NO_x control techniques should be judged on the basis of reductions from uncontrolled engine emissions expressed in pounds per thousand pounds of fuel.

c. Visible Particulates (Smoke)

Visible smoke emitted from aircraft turbine engines is principally composed of carbon. It is generated usually in systems which operate unusually fuel-rich in local zones of the combustor. It has been established that the presence of exhaust smoke seems to have little effect on the overall operation and performance of the engine system -- any combustion inefficiency associated with this emission is negligible. Nevertheless, the aesthetic nuisance and tactical vulnerability arising from smoke emissions require that the problem be eliminated.

Efforts to abate visible smoke from aircraft gas turbine engines date back nearly a decade. The engineering know-how to design smokeless combustors for new engines without sacrificing any desirable engine characteristics is now in hand. The purpose of this brief section is to describe the background upon which smoke emissions may be quantified.

An important factor in smoke visibility is the relative position of the observer to the exhaust plume -- the worst possible case is observation of the exhaust plume just slightly skewed from the centerline of the engine. Although attempts have been made to account for plume dispersion and turbulent mixing behind the aircraft⁵, the quantitative relationship between visibility from this position and a smoke measurement remains a very complicated, unsolved task.

Investigation of the perpendicular-view case has yielded useful quantitative information. Analytical correlation of exhaust plume visibility as viewed perpendicularly and smoke number as measured by the techniques described in Reference 6 has been performed by Champagne.⁷ This important relationship between smoke number and path length for noticeable visible light attenuation is graphically shown in Figure 5. Smoke number data for some engines has been taken and these results have also been plotted in Figure 5. A reasonable agreement between data and theory is apparent.

Very little has been done regarding total particulates and, as previously mentioned, this is considered to be a problem which eventually may be regulated. Hopefully, the modifications to reduce visible particulates will reduce the total particulates emitted as well.

3. Afterburning Turbine Engines

To gain additional thrust during critical points of an aircraft mission, afterburners are employed. Thrust augmentation by afterburning involves injection and combustion of fuel in the exhaust gases exiting the turbine section of the engine. The temperature rise in the afterburner results in expansion of these exhaust gases which in turn increases the exhaust velocity and resultant thrust. The fact that the afterburner is normally used during takeoff and climbout accents the potential seriousness of emissions in this mode -- currently only emissions below 3000 feet are considered in expected EPA aircraft emissions standards.

Very little information is presently available for pollutant emissions from afterburning engines; however, general trends in available data (Reference 8, 9, & 10) indicate possible significant emissions of CO and C_xH_y , especially at the lower afterburner power settings. NO_x emissions appear to be similar to emissions during non-afterburning high-power operation when emissions are expressed on an EI basis. These results, however, are presently described only as trends because truly quantitative data is extremely difficult to obtain. Combustion product gases at the exhaust plane are extremely reactive and at high temperature. Much of the CO and C_xH_y present at the exhaust plane is reacted to CO_2 and H_2O further downstream. Consequently, accurate measurement of afterburner emissions involves determination after these reactions have been completed; i.e., placement of sampling probes downstream of the exhaust plane is necessary. Presently, no well-defined method exists to do this.

The fact that reactions in the plume are important indicates that the conditions of the ambient air could also significantly influence the resulting emissions. Cooler ambient temperatures would tend to cool the plume more quickly and thus quench the plume reactions which are responsible for converting CO and C_xH_y to CO_2 and H_2O . Further, the ambient pressure could also be expected to influence emission via an effect on the rate of mixing -- data obtained at sea level may not be applicable to altitude operation where both pressure and temperature differences may effect the extent of plume reaction.

Considering the problems cited above, it is not possible at this time to assess the emissions characteristics of or to specify emissions limitations for afterburning engines. Consequently, this should be an area of concerted research over the next few years.

MILITARY RELEVANCY

Several considerations indicate that the military aircraft contribution to environmental degradation is not as significant as that of commercial operations. Nevertheless, in recognition of the leadership role required of U. S. Federal Agencies in protecting the environment, appropriate research and development efforts are underway and in planning. Moreover, some pollution problems are unique to the

military. For example, the U. S. Armed Services presently account for all afterburning engines within the U. S., operate most helicopters, and conduct most stratospheric aircraft operations.

Military aircraft operations are responsible for approximately half of all aviation fuel consumed by U. S. users. This, however, is not considered a representative indication of the military contribution to the environmental problem. In general, military air bases are much more widely dispersed than commercial airports where air quality violations have been observed. Furthermore, the traffic patterns at most military air bases are much less active than those at commercial airports such as Los Angeles International, Kennedy and Washington National. Only limited studies concerning aircraft-related ambient air quality violations have been made at military installations; hence, no conclusive results are available. Assessments of air base ambient air quality at several selected military installations are currently being conducted.

Some specific problems and factors are unique to the larger turbine engines employed in fixed-wing aircraft within the military.

1. Unknown severity and lack of control techniques, if required, for afterburning turbine engine emissions.
2. High performance aircraft of the future will require higher pressure ratio engines operating at overall combustor fuel-air ratios close to stoichiometric -- factors which will make emission control of NO_x more difficult.
3. Military aircraft operations at high altitude are a matter of concern.

Rotary wing aircraft engine emissions are uniquely relevant to the military as the primary user of helicopter systems. Helicopter engines are relatively small -- usually much less than 6000 hp (the upper limit for the smallest engine size class defined by EPA regulations) -- and therefore, consume a small percentage of total aviation fuel. In addition, helicopters spend very little time in the taxi-idle mode where emissions of CO and C_xH_y are highest. There are, however, unique emissions control problems associated with these small engines as outlined below.

1. Lower levels of CO and C_xH_y at low power are difficult to achieve due to flame quenching effects along the liner walls in these high surface-volume ratio combustors.
2. These engines generally operate at low pressure ratio and have low fuel atomization pressures -- both having the effect of increasing CO and C_xH_y emissions.
3. The small size of helicopter engine combustion chambers places unique restrictions on integration of emissions control techniques.
4. Relative to the EPA 3000 foot ground rule, NO_x emissions from helicopters are more serious as these aircraft spend a large fraction of their total operating time below 3000 feet.

EMISSION CONTROL TECHNOLOGY

Many techniques and procedure modifications are being considered to reduce exhaust gas emissions from piston and turbine engines. The degree of suppression effectiveness to be realized, however, is dependent upon the specific combustion system design being addressed. Specific application of these techniques to existing engines will normally entail a special component development program. Future or new engines, however, can be designed to employ many of these emission control procedures. The following subsections address the feasibility of emission control for aircraft engines.

1. Piston Engines

From the military standpoint, the U. S. Department of Defense will be procuring relatively few piston engines in the future; therefore, emission control for Air Force piston engines is not considered a major issue. Commercially developed emissions control technology shall be applied in those situations where it is cost effective and practical. A realistic approach at this time is to support control techniques development for turbine engines because engines of this type will predominate in the future.

2. Non-Afterburning Turbine Engines

Control techniques for turbine engine emissions can be categorized into current technology and future technology. Candidate approaches are presented relative to these basic categories.

a. Current Technology

There are many ways in which current technology may be utilized to reduce emissions. Some of these methods involve the basic combustor design while other techniques concern those components which supplement combustor operation.

(1) Minor Combustor Redesign - This consists of a minor modification of the combustor liner and/or fuel nozzle not involving a change in design concept. Design changes such as these will affect, but may not simultaneously decrease, the four principal exhaust pollutants (CO, C_xH_y , NO_x and smoke). For instance, a reduction in CO due to a small combustor design change often results in a corresponding increase in NO_x , and vice versa.

(2) Major Combustor Redesign - This consists of a major design change to the combustor liner and/or fuel system perhaps introducing an alternate fuel injection concept; i.e., airblast

atomizers/vaporizers. A combustor liner change could involve converting from a can-annular to an annular configuration. The new combustor, however, would still be required to fit within the same engine envelope. All exhaust pollutants can be addressed if a major design change is permitted.

(3) Controlled Fuel Injection - This consists of a modification to the fuel supply system to allow a fraction of the fuel nozzles to be shut off during low power operation. A localized fuel-flow increase to the operating nozzles permitting a higher local fuel-air ratio in the combustion region results in more efficient combustion with attendant reductions in CO and CxHy emissions during idle and taxi operation. This, however, necessitates minimal reaction quenching between nozzles. The effectiveness of this control technique has not yet been fully investigated.

(4) Water Injection - This entails introducing demineralized water to the combustor primary zone lowering the local flame temperature and thus reducing the formation rate of NO_x during high power (take-off and climb) operation. Although large cargo transport and other non-combat aircraft might consider this method, it will most likely be an impractical emissions control technique for combat/tactical aircraft operations from a weight consideration.

(5) Compressor Air Bleed - This consists of increasing the bleed air rate from the compressor during low power engine operation. The resulting decreased airflow to the combustor increases the primary zone fuel-air ratio allowing operation at higher combustion efficiency. It is expected that this method will provide the primary near-term means for low power emissions control.

(b) Future Technology

(1) Variable-Geometry Combustor - This combustor design concept achieves fuel-air ratio control by airflow modulation. During low power operation, CO and CxHy pollutants are controlled by increasing the fuel-air ratio in the primary zone with attendant high combustion efficiency. The higher fuel-air ratio is the result of mechanically blocking part of the primary zone airflow. During high power operation, NO_x and smoke are controlled by mechanically opening more primary zone airflow area, thus leaning the primary zone to a fuel-air ratio below stoichiometric and permitting a lower primary zone flame temperature and hence, a lower NO_x formation rate. Because of increased design complexity, the variable-geometry combustor cost is expected to be substantially higher, weight will increase and reliability, maintainability and durability will no doubt be somewhat compromised.

(2) Staged Fuel Injection - In this control concept, combustion occurs in discrete steps or stages. In general, the combustor will employ either an axial or radial staged fuel injection technique. In either case, the first stage will serve as a pilot zone for low and part power operation; whereas, the second stage will provide high power operation. The fuel-air mixture can be carefully controlled through staging to minimize CO, CxHy, and NO_x and smoke at all operating conditions. Radial fuel staging has been successfully demonstrated to a limited extent; axial staging has been less successful due to durability problems. Some potential disadvantages with such a system include increased complexity of the fuel distribution and control system, increased total combustor weight and volume, and the durability problem discussed above.

(3) Premix Combustion - Recent progress in premix/carburetion fuel injection technology has demonstrated the feasibility of premix combustion to reduce exhaust emissions while enhancing combustor performance. Premixing the fuel and air prior to introduction to the primary zone permits combustion of a more uniform fuel-air mixture. Combustion efficiency is increased at low power, and NO_x and smoke can be substantially reduced. The premix/carburetion approach currently offers the most promise as an effective control for all exhaust pollutants of consequence, without serious compromise to other engine performance requirements. Some integration problems may be encountered, however, with small annular burners due to combustion chamber volume restrictions.

3. Afterburner Exhaust Emissions

Little can be said relative to the control and abatement of afterburner exhaust emissions as only limited emissions data has been obtained to date. Consequently, a firm definition of the afterburner emissions problem has yet to be made. Therefore, until the basic problem is defined, no major undertaking in control techniques development can be considered. Presently, no control techniques for afterburner operations are known to exist.

4. Fuel Additives

Fuel additives, as an approach to emission control can offer many advantages. Most importantly, basic engine design is not altered and sacrifices in performance are not required. Unfortunately, the following disadvantages are associated with presently available emission control additives: (a) Use incurs depositions which are harmful to the engine; (b) cost and logistics of supplying and handling a separate additive are substantial; (c) in some cases, toxicity of the additive imposes a special hazard and environmental problem.

Previous application of fuel additives has been to reduce smoke emission in aircraft turbine engines. Metal-bearing organic compounds can be employed with the most effective metals being manganese, iron, and barium. However, no formulation has yet been produced which will effectively eliminate smoke, and not cause harm to the engine over long periods of use. Specifically, deposits in the engine hot section and plugging of afterburner spraybars have resulted.

Recent developments in additive formulation have shown promise of alleviating some of these drawbacks. Should this work be successful, it is expected that fuel additives for smoke abatement may yet be employed in many older systems for which redesign and retrofit are impractical.

The decision to employ an additive must weigh the above factors. Currently, the additive approach is being considered for use in engine test cells to prevent violations of stationary source

emissions limits. In the past year investigations have also been conducted to determine the feasibility of NO_x control by fuel modification¹¹.

PROPOSED EPA STANDARDS

The purpose of this section is to describe the commercial engine standards presently being considered by EPA and their implications with respect to various types of military aircraft. Standards for piston and non-afterburning turbine engines will be discussed in the following subsections. No standards applicable to afterburning turbines have been seriously considered. Furthermore, there are no standards being considered at this time to limit aircraft emissions in the stratosphere.

1. Piston Engines

The first set of applicable limitations for aircraft piston engines as presently planned by EPA will take effect in 1979. These standards have been defined for all piston engine designs with exception of the radial configuration -- a design common to many operational military piston aircraft, but a limited number in the general aviation class. To meet these limitations 50% reduction in CO and C_xH_y from typical present values is anticipated. An oxide of nitrogen limitation has been included only to prevent a substantial increase in NO_x via a control technique. The NO_x limitation is calculated to represent the NO_x emission from a piston engine operating at the increased air-fuel ratio necessary to attain the above 50% reduction in CO and C_xH_y assuming no other control techniques are applied.

2. Non-Afterburning Turbine Engines

a. General

The basic purpose of the EPA standards is to reduce emissions of aircraft to the point necessary to insure that air quality standards are not violated. This requires limitation of emissions at the passenger loading areas, during taxi-out to the main runways, during take-off and climbout, during approach and landing, during taxi-in to the passenger loading area and during final idle and shutdown. Emission during each of these modes contributes differently to the ambient pollutant levels at the various airport locations which have been found to have concentrations in excess of air quality standards. Analytical models which might be expected to assign a degree of importance to emissions at each mode are far too underdeveloped at this time. Consequently, EPA considers it reasonable to place limitations on the total pollutants which are emitted into the immediate environment of the airport below 3000 feet.

The parameter which is used to express total pollutants is critical. For example, it is possible to specify a commercial aircraft limitation in terms of pounds of pollutant per passenger seat per landing take-off cycle. This would be the most fundamental approach, requiring limitation of pollutant emissions by engine improvements, airframe considerations, considerations of choosing the proper type and number of engines for a particular airframe design and even by optimized seating arrangements. It is also possible to specify emission limitations based on pounds per thousand pounds of fuel or pounds per thousand pounds of thrust, EI or EIT respectively. These units are related in the following way:

$$\text{EI} \times \text{SFC} = \text{EIT} \quad (3)$$

Where: SFC = thrust specific fuel consumption,
lbm fuel/hr/lbf thrust

$$\text{EIT} = \frac{\text{lbm pollutant/hour}}{1000 \text{ lbf thrust}}$$

When on a per-pound-of-fuel basis, the emissions of CO and C_xH_y can be translated back to the considerations of idle combustion inefficiency discussed earlier. Also, as previously mentioned, the NO_x emissions based on a pound per thousand pounds of fuel basis are known to be closely tied to the combustor inlet temperature, or pressure ratio.

Since SFC is an indication of engine efficiency and EI indicates how all the combustor was designed from the exhaust pollution standpoint. The use of EIT would imply then that pollution has been designed from the exhaust pollution standpoint. The use of EIT would imply then that pollution emission criteria should be included in the selection of basic engine cycle parameters (pressure ratio and turbine inlet temperature). This, however, may adversely affect optimization of system performances.

The approach which EPA has adopted for their proposed regulations for gaseous emissions is intermediate between specification of emission per passenger seat and specification of EI and EIT. It involves the use of a parameter based on the emission per thrust-hour summed over a typical landing take-off (LTO) cycle. The EPA parameter has the dimension:

$$\frac{\text{lbm pollutant}}{\text{lbf thrust-hour cycle}}$$

Data-reduction details to obtain this parameter are presented in Reference 3. EPA considers this to be the most practical parameter from the commercial aircraft engine standpoint since it:

(1) Gives a number which is physically recognizable as the total emission of the engine into the airport environment per unit of power output.

(2) Ties pollutant emission to an engine, not an engine/airframe combination.

(3) Represents the effect of total engine cycle (LTO) pollutant reductions.

The EPA exhaust smoke limitation is a specified smoke number which is not to be exceeded at any engine power setting.

Since the EPA parameter, EPAP, makes use of a landing-take-off cycle, the cycle must be defined. Duty cycles have been specified for the following classes of turbine engines.

Class T1	Thrust below 6000 lbf
Class T2	Thrust between 6000 lbf and 29,000 lbf
Class T3	Thrust greater than 29,000 lbf
Class T4	JT9D Family Engines

For shaft-power engines, EPA has assumed a 1:1 equivalence between pound-thrust and shaft-horsepower.

b. Discussion

The EPA parameter (EPAP) is not simply related to EI or EIT because it represents a summation over a specified duty cycle. However, some significant simplifications are possible in the case of CO and C_xH_y. As previously mentioned, emissions of these species are only significant during the idle/taxi power setting. The following list shows the average emissions for each operating mode for a JT9D engine.³

Mode	CO Emissions (lbm)	C _x H _y Emissions (lbm)
Taxi/Idle (Out)	32.25	8.65
Take-Off	.10	0.03
Climbout	.43	0.10
Approach	2.17	0.20
Taxi/Idle (In)	11.88	3.19

Note that 94.3% of the CO emissions and 97.3% of the C_xH_y emissions are from the idle power setting. Therefore, the EPA for total CO and C_xH_y over the LTO cycle can be well approximated by the taxi/idle emissions contribution.

NO_x emission from today's uncontrolled engines cannot be attributed to one mode. The following list shows the contribution of various modes for a JT9D engine over the LTO cycle.³

Mode	NO _x Emissions (lbm)
Taxi/Idle (Out)	1.92
Take-Off	8.40
Climbout	16.81
Approach	3.61
Taxi/Idle (In)	0.71

Only the taxi/idle power settings are low in the case of NO_x emissions.

It might be thought that by virtue of the fact that the thrust dependency is included in the denominator, the EPAP favors engines with a low SFC. This is true for the emission of CO and C_xH_y because the idle emission characteristics are related to an engine's pressure ratio. Further, it is true that if two engines have the same NO_x, EI, the one with the lower SFC will have a lower EPAP value. Although an engine's SFC value is dependent on its pressure ratio, the dependence of NO_x emission on combustor primary zone temperature is dominant; hence, an increased NO_x EPAP results from increased pressure ratio. This fact is extremely important. Engine design motivation for commercial subsonic aircraft has always been toward minimum SFC. Although this motivation is in concert with combustor design techniques for reduction of CO and C_xH_y emission, it is opposed to reduction of NO_x emission. EPA proposes techniques such as water injection and advanced combustor design concepts to solve the NO_x problem for commercial aircraft without compromising SFC.

IMPACT ASSESSMENT AND GOALS

The recommended U. S. Air Force position regarding any emission limitation on military engines is summarized as follows:

1. In no case shall pollutant controls be allowed to infringe on military engine design or operation in a manner which compromises system effectiveness.
2. Pollution control technology for aircraft gas turbine engines developed in commercial as well

as military programs shall be used to the greatest extent possible.

3. Military engines shall approach the related EPA commercial regulations to the greatest extent possible.

4. For the present time, the U. S. Air Force shall issue pollution limitation goals -- not procurement regulations.

The needs, requirements and operational use of military aircraft are entirely different from those of the commercial fleet. One glaring example, in this respect, involves military rotary-wing aircraft. EPA has currently limited its studies to fixed wing aircraft; consequently, the relatively few non-military rotary-wing types are not included in proposed EPA regulations. However, pollutant emission goals for military aircraft do include rotary-wing engines as well as fixed-wing types. Goals have not been set for emission from piston engine or afterburning turbine engines for the reasons stated previously. Those for non-afterburning turbine engines are discussed below. These goals do not consider a landing/take-off cycle -- a more fundamental approach, which utilizes combustion efficiency for CO and CxHy control and the uncontrolled NOx data correlation of Figure 4, has been chosen. These parameters relate more directly to the combustor design and allow pollutant reduction considerations apart from performance considerations.

1. Low Power Emission

For large turbine engines used in fixed-wing applications, CO and CxHy (the low power pollutants) have limitation goals expressed as maximum allowable combustion inefficiency. Since CO and CxHy are the only exhaust emissions which contain chemical energy, combustion inefficiency is a direct quantitative measure of these emissions. At the present time, it is realistic to expect that a combustion inefficiency of 1% could be attained by the "target dates" discussed below -- further expectation would depend too strongly on techniques which cannot be presently identified. Therefore, a combustion inefficiency goal of 1% has been established. This goal would be applicable to classes T3, T2 and most of class T1. Some relaxation of the inefficiency goal will be necessary for small engines in class T1 having combustors of large liner area relative to combustion volume: i.e., large S/V ratios. For small gas turbines used primarily in rotary-wing aircraft, technology demonstration goals and dates are specified rather than production engine compliance dates, since control technology for small engines is not yet available. CxHy and CO levels corresponding to a combustion inefficiency of 1% shall not be exceeded for combustors having a liner surface area-to-volume (S/V) ratio less than 1.0 in.⁻¹. Slightly higher values will be allowed for combustors of higher S/V ratio. It is estimated that this goal can be achieved in advanced technology engine programs by 1977.

2. NOx Emissions

Establishment of goals for NOx emissions from U.S. Air Force aircraft must be considered with respect to whether or not the water injection, staged combustion, premix and variable geometry control methods are applicable. Weight penalties prohibit the application of water injection to combat aircraft, but the method could be considered for large non-combat applications; i.e. C-130, C-141. Consequently, two separate NOx goals are discussed below -- those for non-combat and those for combat aircraft.

a. Non-Combat Aircraft - Those Air Force aircraft which can employ water injection (principally large transport-type aircraft) will have goals as described below. Significant reductions (approximately 50%) in NOx emission during the take-off and climbout modes of operation are anticipated by the use of water injection. Further, the effects of staged combustion, variable geometry and premix when combined with water injection are expected to produce even lower levels of emission (approximately 75% reduced from the uncontrolled engine) at the high power operating points. Although the effective control of NOx by staged combustion and variable geometry has not yet been adequately demonstrated, based on the technology expected to be available by 1979, the non-combat aircraft engines employing water injection should exhibit an NOx emission profile during take-off and climbout not to exceed the 75% reduction curve shown in Figure 6. Non-combat aircraft not employing water injection should exhibit a 50% reduction. Furthermore, the NOx profile for the idle/taxi and approach modes should not exceed the uncontrolled data correlation curve of Figure 6.

b. Combat Aircraft - Since water injection, the only near term control method for NOx emission, is not a viable approach for combat aircraft, no limitation goal can be set which reflects its application. The goal for military aircraft engines would depend only on whether or not the variable geometry, staged combustion and premix approaches are judged to be applicable to combat aircraft. Should they not be applicable, no goal is appropriate other than insistence that the data correlation for uncontrolled emission not be exceeded. Emission reductions with the advanced technique alone could be expected to be approximately 50% of the uncontrolled value. Therefore, should the advanced techniques prove viable, the military goal is that engines used in combat aircraft have an NOx emission profile for idle/taxi and approach modes not to exceed the data correlation curve and that the emission during the take-off and climbout modes not exceed the 50% reduction curve shown in Figure 6. Again, some relaxation of this goal may be necessary for certain small engines for which volume limitations prohibit integration of NOx control concepts. Furthermore, for engines having low combustor inlet temperatures with inherently low NOx levels, it may be unnecessary and/or impractical to further reduce the levels. The very small turboshaft engines used in rotary-wing aircraft shall have as a goal the demonstration of technology to effect a 50% reduction of emission at the high power settings by 1979.

3. Smoke Emissions

The Air Force smoke goals for future engines are shown in Figure 7, and are based directly on the visibility criterion previously discussed with respect to Figure 5. Rather than use the absolute term "path length for light attenuation", the parameter δ has been employed where δ is the

exhaust diameter of the engine and n is the maximum number of engine exhaust streams through which an observer could possibly sight. For example, the value of n for the case where two engines are spaced far enough apart so that the smoke density has been significantly diluted before the exhaust plumes intersect, the value of n need not be taken as two. Use of this goal will assure, without being overly demanding, that the system will not emit visible smoke. Absence of an overly demanding goal is important in that it could create difficulty in attaining other emission limits and performance requirements. As more information is gained on visibility when the exhaust plume is sighted at a distance, a new smoke goal which more directly addresses the tactical vulnerability problem will be considered. Should this criterion be more stringent than that discussed above, it will be substituted for the present limitation.

4. Implementation

The "target dates" proposed for achievement of the USAF emission goals defined above depend upon the development stage of an engine. Engines falling into the following categories are expected to meet these goals:

- a. Engines for which development has begun after 1976.
- b. Engines produced in significant quantity after 1979.

The above stated goals for large engines are based on a careful assessment of the state-of-the-art. Technology demonstration goals specified for small engines are based on an assessment of the present small engine emissions control technology status and the results expected from current and planned control technology programs.

COMPENDIUM

The important factors to be considered in setting emission limitation goals for military aircraft engines have been presented. EPA regulations for commercial aircraft have been discussed with respect to their applicability to military aircraft. Most importantly, reductions in emissions which may result in performance compromises have been eliminated from the military goals set forth. Only those control techniques which involve emission reductions without system performance compromise are considered to be applicable for military aircraft.

Goals for carbon monoxide and total hydrocarbon emissions control are based on combustion inefficiency. Goals for oxides of nitrogen require a reduction during take-off and climbout modes by a specified fraction of the uncontrolled value. A smoke specification which will insure exhaust plume invisibility has also been set. It is believed that these goals will result in Air Force aircraft having the lowest pollutant emission levels possible without restricting the performance and mission for which the aircraft was intended.

REFERENCES

1. "Aircraft Emissions: Impact on Air Quality and Feasibility of Control", Environmental Protection Agency, February 1972.
2. Bahr, Donald W., "Control and Reduction of Aircraft Turbine Engine Exhaust Emissions" presented at: The Symposium on Emissions from Continuous Combustion Systems, G. M. Research Laboratories, Warren, Michigan, 27-28 September 1971.
3. Bogdan, L., and McAdams, H. T., "Analysis of Aircraft Exhaust Emissions Measurements", Cornell Aeronautical Laboratories Report Number MA-5007-K-1, 15 October 1971.
4. Lipfert, F. W., "Correlation of Gas Turbine Emissions Data", ASME Paper 72-GT-60.
5. Chesters, A. K., "Prediction of the Effect of Engine Geometry on Aircraft Smoke Visibility", ASME Paper No. 71-WA/GT-10.
6. JAE Aerospace Recommended Practice 1179, "Aircraft Gas Turbine Engine Exhaust Smoke Measurement", Society of Automotive Engineers, New York, N. Y., 4 May 1970.
7. Champagne, D. L., "Standard Measurement of Aircraft Gas Turbine Engine Exhaust Smoke", ASME Paper No. 71-GT-28.
8. Palcza, J. L., "Study of Altitude and Mach Number Effects on Exhaust Gas Emissions of an Afterburning Turbofan Engine", Federal Aviation Administration Report FAA-RD-72-31, December 1971.
9. Burnett, J. Z., "Noise and Air Pollution Emissions from Noise Suppressors for Engine Test Stand and Aircraft Power Check Pads", Professional Report 71M-19, January 1972.
10. Latalier, G. R., and Gearhart, J. W., "Measurement of Pollution Emissions from an Afterburning Turbojet Engine at Ground Level, Part II - Gaseous Emissions", AEDC-TR-72-70, August 1972.
11. Shaw, H., "Fuel Modification for Abatement of Aircraft Turbine Engine Oxides of Nitrogen Emissions", AFAPL-TR-72-80.
12. Blazowski, W. S., "Simplified Correlation of Aircraft Turbine Engine NO_x Emissions", AFAPL/SFF TM-72-16, October 1972.

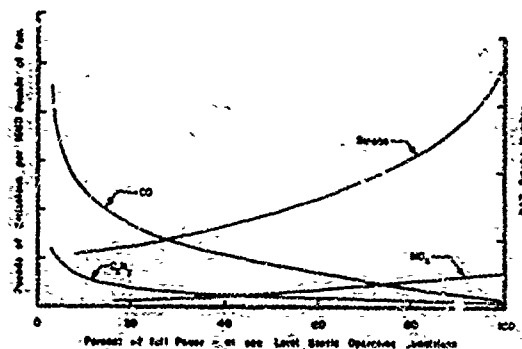


Figure 1. Typical Non-Afterburning Turbine Engine Exhaust Emissions Characteristics (From Reference 2)

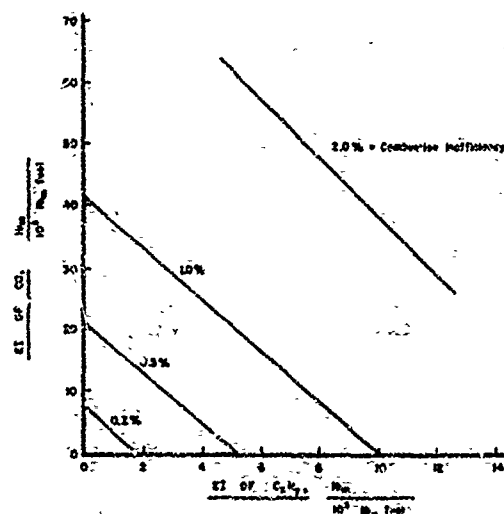


Figure 2. Relationship Between Combustion Inefficiency and Pollutant Emissions

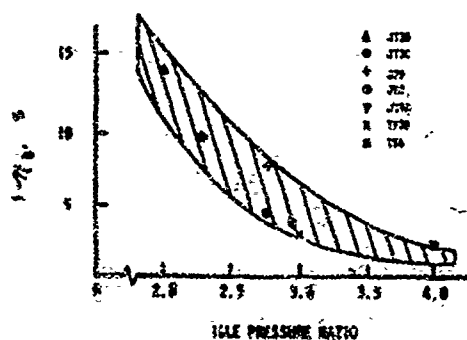


Figure 3. Idle Performance Correlation

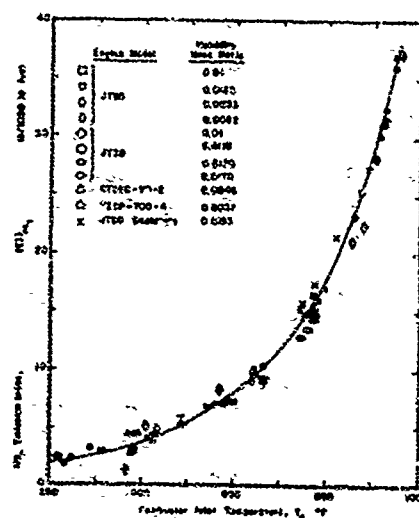


Figure 4. Correlation of NO_x Emissions Data with Combustor Inlet Temperature (From Reference 4)

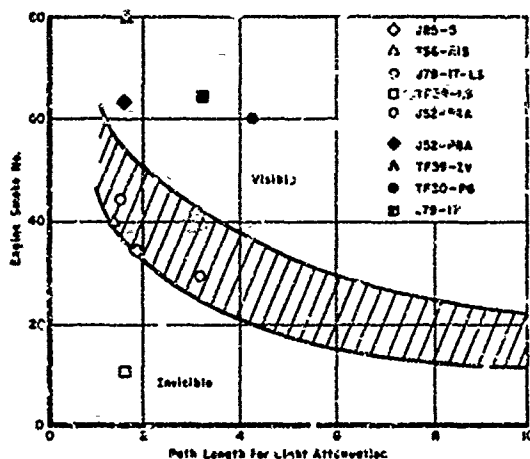


Figure 5. Measured Smoke Numbers in Comparison with Visibility Criterion (Band indicates uncertainty in analytical model of Ref. 7)

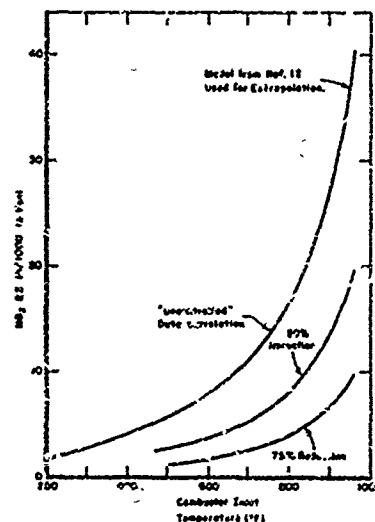


Figure 6. NO_x Emission Curves

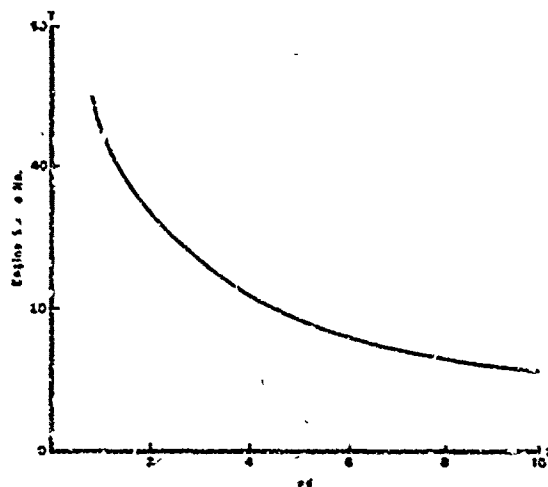


Figure 7. Smoke Emission Goal

Discussion on Paper 33
 "Aircraft Gas Turbine Pollutant Limitations Oriented Toward
 Minimum Effect on Engine Performance"
 presented by R.E.Henderson

M.Whittaker: We have seen one formula for inefficiency by A.Quillévére and one by yourselves, and at Rolls Royce we have yet another. It would help if we could develop a common formula. Ours would give a 16% larger inefficiency than yours (at a high efficiency level) due to the fact that we allow for typical ratio of unburned hydrogen to carbon monoxide.

R.E.Henderson: Our inefficiency equation is intended only for application at idle conditions. At this power setting emission of hydrogen is negligible - carbon monoxide and unburned hydrocarbons are the principal emissions resulting in inefficiency. Past experience has shown that the average hydrogen-carbon ratio is close to that of the original fuel and, accordingly, we have used the lower heating value of the initial fuel in our equation.

R.Sawyer: In setting your goals, did you consider limiting aldehydes?

R.E.Henderson: Following the lead of EPA we have not chosen to specify limits for individual hydrocarbon species. However, we feel that this is an extremely important point in that not all hydrocarbons contribute equally to environmental problems. We have initiated some work at AFAPL to resolve a typical hydrocarbon spectrum emitted from aircraft gas turbine engines and strongly encourage others to do the same.

A.Lefebvre: You are critical of variable-geometry and staged-fuel injection while you advocate premixing. It seems premixed systems call for excess air, have a narrow burning range, poor altitude relight and require a pilot burner.

R.E.Henderson: It is not our intent to be overly critical of variable-geometry and staged fuel injection techniques. However, we do consider these techniques to be much more complex and would require extensive development. This is not completely true of premixed systems which have been under development for several years and do not necessarily exhibit all the problems you allude to in your question. To further qualify this we refer you to Paper 31 by R.Jones, NASA, and Paper 29 by D.Bahr, General Electric.

T.Mikus: Would you please specify the units for the abscissas of Figure 5 and Figure 7?

R.E.Henderson: In both cases the units are in feet. In Figure 5, this length represents the linear distance of exhaust for a given Smoke Number through which one could sight. In Figure 7, this length, L_d , represents the number of engine exhaust plumes through which an observer could sight perpendicularly times the engine exhaust exit diameter.

Mr Jaarsma: What are your experiences with fuel additives for NO_x reduction?

R.E.Henderson: The AFAPL sponsored a program to develop fuel modifications for abatement of aircraft NO_x emissions. This work is fully described in Reference 11 of our paper. It was found that the same metal-bearing additives used for smoke abatement also reduced NO_x . However, only 30% reductions were achieved for large additive concentrations like 0.5% by weight.

PHOTOMETRIC MEASUREMENTS OF EXHAUST SMOKE
TRAILS BY JET ENGINES

M. Lucchesini and D. Dini
Istituto di Macchine
University of Pisa, Italy

SUMMARY

The purpose of the present work is twofold:

- developing a photographic photometry method to measure density and visibility of exhaust smoke trails;
- obtaining an objective index for the smoke emission degree by turbojets during take-off and landing.

Photographic photometry is based on light scattering theory. Assuming the light transmission percentage value, T , as an index of engine contaminating level, tests here conducted show the P.W. JT8D9 as being one of the most contaminating jet engines on airline service, giving T values of about 74%.

Transmission T values have been measured in many cases at different distances from the nozzle and for several angles between optical and trail axes. This has been done to show dependence of T from the aerodynamic airplane/engine configuration and from the optical path L through the trail.

A similar method has been adopted from the IIT Research Institute (Ref. 1). A comparison between the results is here made.

SMOKE TRAILS FROM AIRCRAFT TURBINE ENGINES are a symbol of air pollution. Smoke is currently determined by an indirect reflection measure according specifications and procedures described by Aerospace Recommended Practice, ARP 1179, Ref. 2. The results are expressed by a numerical value known as the AIA smoke number. This technique is normally applied to engines operating in test cells. But, from a practical point of view, it is required to evaluate an engine smoke degree during its actual operating conditions of aircraft in flight, especially at takeoff and approach power, i.e. an objective index taking into account the visibility of smoke trails.

At present, the only accepted method for describing the visual qualities of smoke trails is the Ringelmann method, a subjective measurement highly dependent upon the environmental test conditions.

Photographic photometry is a relatively simple and inexpensive technique in determining the transmission T of light through the smoke. This T index is expressed as the percentage of the intensity of transmitted light in respect to the intensity of incident light. Since both particle volume concentration and trail visibility are simple functions of T , the corresponding numerical value may be assumed as a valid one to objectively evaluate the optical density of smoke plumes and, more in general, to establish the polluting characteristics of the engine.

The light attenuation through a smoke trail is due to the exhaust particle absorption properties. It is known from optical physics that, where a smoke particle is small, say about 0.05 micron, in relation to the wavelength of incident light, say about 0.5 micron, the total attenuation of light, E , is substantially due to absorption phenomenon.

The following values are normally accepted, Ref. 1:

$$E = \text{light extinction} = 0.9$$

$$S = \text{light scattering} = 0.1$$

$$A = \text{light absorption} = 0.8$$

That is, the extinction of light by aircraft turbine engine smoke is due to 89% absorption of light and 11% scattering of light. This meaning that absorption is most responsible of smoke trail obscuration, smoke particle sizes being of the order of 0.05 micron at the nozzle.

Regarding small particles, absorption is only depending upon their concentration per unit mass or volume of gas.

The attenuation of light, expressed as an extinction coefficient E , modifies the intensity of transmitted light as given by the expression

$$I = I_1 e^{-\pi r^2 c L E} \quad (A)$$

where:

I_1 = intensity of incident light

I = intensity of transmitted light

c = number concentration of smoke particles

E = extinction coefficient

r = particle radius

L = optical depth through the smoke trail between I_1 and I

Considering the transmission index $T = I/I_1$, the expression (A), Ref. 1, may be written

$$2,303 \log T = -\pi r^2 c L E \quad (B)$$

or

$$\log \frac{1}{T} = D_T = c K \quad (C)$$

where:

D_T = optical transmission density of the smoke trail

$K = \pi r^2 E, 2,303$ = specific absorption coefficient

conclusion, the number of particles per unit volume, c , may be determined as function of: the distance, from the nozzle, at which the smoke trail density or visibility has to be measured; the particle radius, r ; the optical path, L ; the extinction

coefficient, B . It is to be noted that: r is varying as function of the distance from the nozzle (higher radius at more distance from the nozzle and for a more powerful engine, Ref. 1). The optical path L depends upon the angle between optical and smoke trail axes, the number and superposition degree of the trails left behind the airplane, and finally the aerodynamic aircraft/engine configuration. The single trail light transmission T may be determined by the experimental expression

$$T = \sqrt[n]{T_m}$$

where n is the number of engines and T_m is the light transmission of the superimposed smoke trails.

It is therefore evident that, once transmission T is determined by photometric method, the c value obtained through the expression (C) is accurate to an increasing degree as more reliable are the r and L values.

Consequently it is convenient to be restricted to the determination of the transmission, T , of light through the smoke, disregarding the evaluation of c , and to assume the T value as an absolute degree of the engine emission.

The visibility of jet smoke trail is substantially depending upon two factors: jet trail sizes and luminance contrast coefficient, C_p , between smoke plume and extended background.

No limitation is introduced in our case by the first factor, but a threshold contrast value has to be selected for jet exhaust trails.

If the contrast coefficient is given by the expression

$$C_p = \frac{B_p - B_b}{B_b}$$

where B_p and B_b are the luminances, respectively, of a smoke plume and of an extended background, a black smoke plume will have a contrast coefficient ranging from 0 to 1, depending on the amount of background light transmitted through the plume.

From Ref. 3 we have, in the case of luminance levels that approach conditions under which jet engine exhaust plumes are usually viewed, i.e. with a negligible amount of light scattering,

$$C_p = T - 1 \quad (D)$$

The threshold contrast coefficient of 2% is necessary for the visibility of jet carbon particle smoke.

Therefore, substituting 2% into Eq. D indicates that jet smoke with $T \geq 96\%$ will be invisible. According Ref. 1, a J-57 engine, must have, for $T = 98\%$, a particle concentration c less than $1.7 \cdot 10^7$ particles/cc to be invisible.

It is evident, from what above mentioned, that the T value is relative to that specific aircraft/engine combination.

It is necessary to specify the distance from the nozzle and the angle between optical and trail axes, in order to exactly interpret the T transmission value.

PHOTOGRAPHIC PHOTOMETRY METHOD

IN ACTUAL PRACTICE, photographic photometry technique is used to photograph the smoke trails against the sky as background, recovering the luminance values from the photograph, and to record a gray step scale on a photogram different from that one of the subject, but on the same film.

Once the negative is developed, the corresponding density of each step is measured by a microdensitometer, Fig. A.

If the density of the steps in the gray step negative is plotted against the logarithm of the exposures (product of the exposure time with the luminance), the characteristic curve γ of the photographic emulsion is obtained.

The absolute values of the exposures are not to be known, whereas the exposure ratios between various gray steps are sufficient. Exposure ratio is proportional to the density difference between steps of the original gray scale.

It is therefore convenient to have the γ curve plotting densities of the negative against the corresponding density steps measured on the original gray scale.

If the densities corresponding to the smoke trails and the background are measured by microdensitometer and plotted as ordinates of the γ curve relative to that negative, the exposure ratio and, consequently, the light transmission T may be determined.

The density is defined as

$$D = \log_{10} \frac{I_0}{I} = \log_{10} \frac{1}{T}$$

where $T = \text{antilog}_{10} \left[- (D_{\text{trail}} - D_{\text{background}}) \right]$

The density values measured by a densitometer depend upon the geometry of the exploration optics, and upon the scattering and the light absorption relative to the examined negative.

That is, for a scattering subject, the density measured through an instrument having a large solid angle, is differing from the density obtained through a small solid angle instrument. The first instrument is measuring a scattered density, the second one a specular density larger than the other.

The two densities are interdependent through the Calliers coefficient. In photographing the original gray scale to calibrate the film, the densities obtained by the camera are specular, because of the small angle subtended by the lens on the gray scale, whereas the densities measured by the densitometer on the original gray scale (plotted as abscissa) may be not specular.

A better approach could be obtained through an accurate determination of the Calliers coefficient. Otherwise, the following procedure may be suggested:

- determination by a microdensitometer of the increments of the gray scale reproduced on the negative, Fig. A;
- plotting as abscissas, in suitable scale, the nominal density values of the original gray scale, avoiding every measurement. The density increment, measured from any reference (line A-A in Fig. A) is plotted in correspondence of each original density;
- a γ curve is obtained, to draw in tracing paper, Fig. B. In fact, it is sufficient to superpose the tracing paper B on the graph C to obtain the desired density increments; that is possible if the scale, relative to the density values plotted as ordinates in Fig. A and B and to the graphs obtained by microdensitometer for the density increments in the transition sky-trail-sky (points A and B in Fig. C), is the same one;
- the real density values may be read as abscissas, in correspondence of the intersections between the curves of Fig. C and B. The antilogarithm of their difference gives the transmission T value of the smoke trail.

INSTRUMENTATION

TWO 35 mm SINGLE LENS REFLEX PHOTOCAMERAS TTL, with 135 and 50 mm lenses, have been used to photograph the smoke trails. They have been set up a tripod for horizontal and vertical angular displacements.

Camera and gray scale were inside a dark chamber having the wedge on a terminal slit, in order that the scale could be illuminated only from the sky light. In addition to photographing the subject, whose luminance was to be measured, a transparent gray-step wedge was also photographed.

It was used the same background of the smoke trail, even though this is not limitative, in as much as, for a panchromatic emulsion, the slope of the curve γ is not changing for cloudy or bright sky exposures.

The sensitive material was Ilford Pan-F, developed in Ilfosol 1 + 29, at $T = 20^\circ\text{C}$ for 10 min.

For measuring density, a MK 111 DS Double Beam microdensitometer by Joyce Loebel Ltd was used.

EXPERIMENTS AND RESULTS

DIFFERENT TYPES OF ENGINES and airplanes have been examined during this study. Static and in flight measurements were obtained at the Airport of Pisa-S. Giusto. In flight observations of aircraft exhaust were made on the DC-9-30, B-737-200, BAe-111, S.A. Caravelle. Engines examined were P.W. JT8D-7, R.A. Spay, P.W. JT8D-9, R.R. Avon 532 R.

- 1) In flight tests - Photographs and visual estimates of the obscuring power of the smoke were made, with several viewing angles, from two sites 600 feet right and left the runway strip. Records were made in more days. In general, airplanes moved away from the measuring sites during take-off. Table 1 summarizes the results of DC-9 I-DIZB. When viewed at 90° deg, visual transmission typical values were of the order of 77%. At more distance from the nozzle, transmission through smoke trail is increasing (86.5% and 79.5%). With the DC-9 I-ATIK, Table 2, the results correspond to transmission values of 74-76% with viewing angle of 90° at take-off. The measurements 14), 15 and 16) show clearly as transmission is decreasing with less viewing angle between optical and trail axes. More results have to be obtained from the DC-9 I-ATIX airplanes, Table 4. The Caravelle I-DABF, equipped R.R. Avon engines, show polluting characteristics quite inferior in respect to the other examined airplanes, Table 3.

Measurements obtained from the Boeing-737-200, J-AWSY, even though insufficient for general conclusions, show transmission values of the same order of the DC-9. The same result has been taken from observations of the BAC-1-11, R.R. Spay, Table 4. Fig. 1 and 2 show typical photograms of the DC-9 I-ATIK, under viewing angles of 90° and 45°.

Fig. 3 and 4 are referred to the Caravelle I-DABP; like the case of the DC-9, the smoke trail visibility is increasing as the viewing angle is decreasing.

- 2) Static tests - Measurements were taken during thrust reversal on landing, take-off starting, taxiing, engine idling.

Some results during thrust reversal of the DC-9 I-DI2B are summarized in Table 5. The relative smoke emission is shown on Fig. 5.

Measurements made for the DC-9 I-ATIK during runway show a quite invisible smoke trail, corresponding to $T = 96 - 97\%$.

CONCLUSIONS

PHOTOGRAPHIC PHOTOMETRY IS OFFERING an effective technique to determine the smoke trail visibility and the carbon particle volume concentration at some distances from the exhaust nozzle. Restricting observations to the smoke trail near the engine exhaust, it is possible to have an indication of the polluting degree of an engine simply through the transmission T value.

Developing such measuring method applied to several conditions and many kinds of airplanes, and using a more sophisticated instrumentation, it is possible to establish the influence on the optical transmission values of the aerodynamic engine/airplane configuration and of the atmospheric conditions.

Each airplane has been photographed from two different sites, using photocameras with different focal length. The two negatives have been developed and analyzed according the indicated procedure. The transmission values, obtained for the same viewing angle and nozzle distance, coincide, to confirm the validity of the system.

REFERENCES

1. J. Stockham, H. Betz, "Study of Visible Exhaust Smoke from Aircraft Jet Engines", SAE 710428, National Air Transportation Meeting, Atlanta, Ga., 1971.
2. Aerospace Recommended Practice Aircraft Gas Turbine Engine Exhaust Smoke Measurement, ARP 1179, Society of Automotive Engineers, Inc., 1970.
3. W. Connez and J. Hodgkinson, "Optical Properties and Visual Effect of Smoke Stack Plume". PHS Publ. 999-AP-30, 1967.

Table 1 - DC-9 I-DIBZ, P.W. JT8D-7 engine

Engine Thrust Setting	Viewing Angle, d.g.	Distance from Nozzle (feet)	Transmission T%
Take-off	80°	25	77,5
a) Take-off	45°	25	72,5
b) Take-off	25°	25	72,5
Take-off	25°	130	88
Take-off	15°	—	—
Take-off	90°	16,6	77,5 H
a) Take-off	45°	23,3	76 K
b) Take-off	45°	76,6	79,5
Take-off	30°	26,6	68,5 J
Take-off	20°	46,6	75

Note that, for H, K, J, the transmission is decreasing with less viewing angle, at about constant distance from the nozzle of the smoke trail in which transmission is measured.

Table 2 - DC-9 I-ATIK, P.W. JT 8D-7 engine

Operation	Viewing Angle, deg.	Distance from Nozzle (feet)	Transmission %
1) Take-off	90°	20	76
2) Take-off	45°	20	68,5
3) Take-off	45°	60	71
4) Take-off	20°	70	76
5) Take-off	20°	160	84
5) Take-off	15°	53	67,5
7) Take-off	15°	18	80
8) Take-off	15°	330	80
9) Take-off	15°	530	80
10) Take-off	10°	53	70
11) Take-off	10°	175	77
12) Take-off	10°	330	81
13) Take-off	5°	330	69
14) Take-off	90°	33	74
15) Take-off	45°	33	73
16) Take-off	30°	33	58

Table 3 - S.A. Caravella I-DABP, R.R. Avon 532 R engine

Operation	Viewing Angle, deg.	Distance from Nozzle (feet)	Transmission %
Take-off	90°	33	95
Take-off	45°	33	93
Take-off	45°	100	100
Take-off	15°	33	93
Take-off	3°	33	90
Take-off	90°	33	90
Take-off	30°	—	—
Take-off	15°	—	—

At the same distance from the nozzle, transmission is decreasing, with less angle between optical and trail axes.

Table 4 - Measurements on airplanes in flight.
Airport of Pisa, S. Giusto.

Operation	Viewing Angle, deg.	Distance from Nozzle (feet)	Transmission %
<u>DC-9 I-ATIX</u>			
Take-off	90°	—	85
Take-off	90°	—	—
<u>Boeing 737-20 G-AWSY, P.W. 3 engine</u>			
Take-off	90°	83	65
Take-off	45°	83	62,5
<u>BAC 1-11 G-AXCP, R.R. Spay engine</u>			
Take-off	90°	32	70
Take-off	45°	32	65

Table 5 - DC-9 I-DIZB, JT 8D-7 engine

Operation	Viewing Angle, deg.	Transmission %
Thrust reversal	80°	89
Thrust reversal	45°	86,5
Thrust reversal	45°	89
Thrust reversal	90°	93

Table 6 - DC-9 I-ATEK, JT 8D-7 engine

Idling	90°	100
Runway starting	90°	97
Runway starting	90°	96

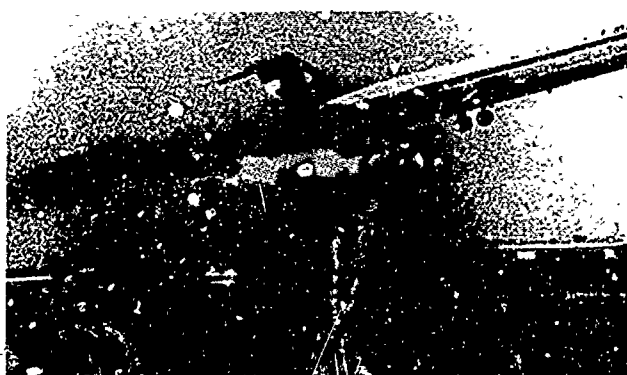


Fig. 1

I-ATIK, take-off,
angle = 90°
 $T = 74\%$



Fig. 2

DC-9 I-ATIK, take-off,
angle = 45° . Points of
densitometer measure-
ments: $T' = 68\%$, $T'' = 71\%$.

Fig. 3

Caravelle I-DABP,
take-off, angle = 90° ,
 $T = 95\%$



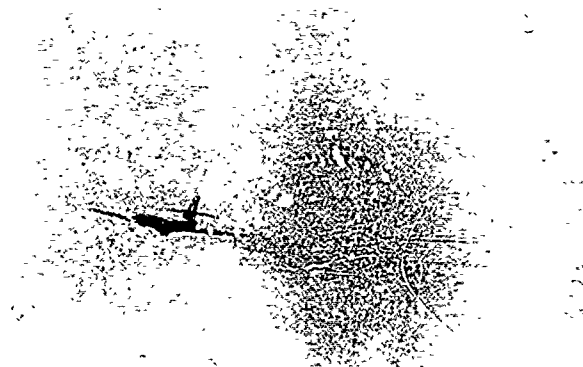


Fig. 4

Caravelle I-DABP
take-off, angle = 30° ,
T = 90%. Decreasing
the viewing angle, is
increasing smoke
trail visibility



Fig. 5

DC-9 I-DIBZ,
landing, thrust
reversal, angle = 45° ,
T = 89%

D SCALE A

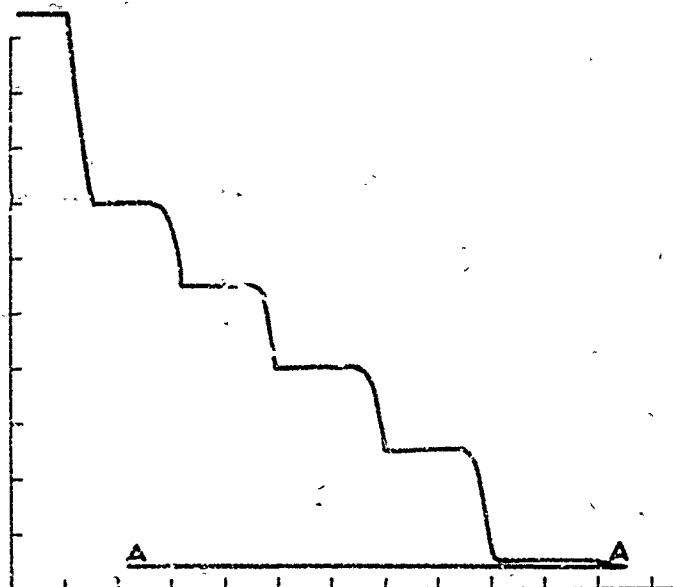


FIG. A

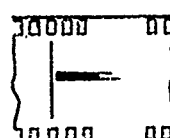
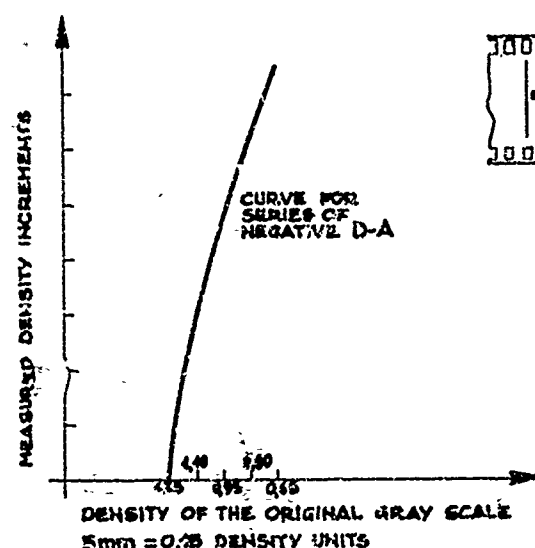


FIG. B

D 25 PP

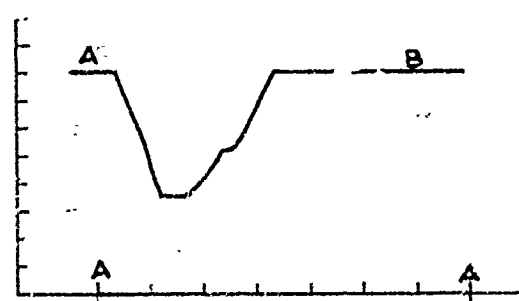
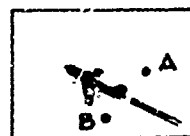
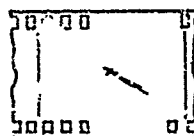


FIG. C

ENVIRONMENTAL TOXICOLOGICAL IMPACT OF AIRCRAFT OPERATIONS

by

Dr Kenneth C. Back
 CHIEF, Toxicology Branch, Toxic Hazards Division
 6570th Aerospace Medical Research Laboratory
 Wright-Patterson Air Force Base, Ohio, 45433, USA

SUMMARY

The environmental toxicologist must define the adverse effects of aircraft operations on all forms of life in the operational and peripheral environment. The scope includes soil and aquatic organisms, all forms of plant life, domestic and wild animals, and the entire spectrum of human population. Sources of pollution from aircraft operation include such chemical substances and decomposition products thereof as aviation gasoline, jet fuels, advanced fuels, oils, lubricants, hydraulic fluids, coolants, deicers, and various additives used in these formulations. These may enter the environment as the result of normal mission accomplishment and attendant ground operations, inadvertent malfunctions and spillage, and necessary periodic disposal processes. To enable the formulation of both comprehensive and sensible environmental assessments and environmental impact statements, definitive toxicological criteria and standards must be available. This paper will discuss some of the physiological effects of the more important compounds which are current problems with aircraft pollutants, indicate some of the problems associated with obtaining such biological data, discuss mechanisms necessary to comply with current pollution control directives, and point out the standards which are now functional.

INTRODUCTION

In the last decade, the introduction of jet aircraft employing low bypass turbofan engines at airports located in or near population centers has brought increasing public attention to aircraft-contributed pollution. As airport aircraft activity increased, the emission of visible exhaust smoke and the attendant noise generated by jet engines were viewed by many citizens with increasing concern. Although smoke, per se, is not too harmful, it focused attention on jet aircraft as a source of some invisible toxic gaseous emissions (carbon monoxide, hydrocarbons, and oxides of nitrogen). In the USA, the Environmental Protection Agency (EPA) has indicated the necessity to regulate aircraft emission of the three aforementioned groups of compounds. The EPA has provided consistent evidence that aircraft are important contributors to air pollutant concentrations in excess of primary (health related) and secondary (welfare related) Federal ambient air quality standards in localized areas of US airports. The planned EPA regulations are based on reducing emissions by aircraft during their operation below 3000 feet. However, the additional environmental problems of high altitude emissions will soon be dealt with.

The environmental toxicologist must define the adverse effects of aircraft operations on all forms of life in the operational and peripheral environment. The scope includes soil and aquatic organisms, all forms of plant life, domestic and wild animals, and the entire spectrum of human population.

Sources of potential pollution from aircraft operations include such chemical substances and decomposition products thereof as aviation gasoline, jet fuels, advanced fuels, oils, lubricants, hydraulic fluids, coolants, deicers, and various additives used in these formulations. These may enter the environment as the result of normal mission accomplishment and attendant ground operations, inadvertent malfunctions and spillage, and necessary periodic disposal processes. To enable the formulation of both comprehensive and sensible environmental assessments and environmental impact statements, definitive toxicological criteria and standards must be available.

This paper will discuss some of the physiological effects of the more important compounds which are current problems with aircraft pollutants, indicate some of the problems associated with obtaining such biological data, discuss mechanisms necessary to comply with current pollution control directives, and point out the standards which are now functional.

PERTINENT LAWS AND DEFINITIONS

The Clean Air Act as amended in 1970 has promulgated a group of companion laws and regulations which will be of consequence not only to the airlines and aircraft industry of the United States, but also to foreign carriers and manufacturers of aircraft operating in the United States as well. Section 231 of the Clean Air Act as amended by Public Law 91-604, directs the Administrator of the Environmental Protection Agency (EPA) to "establish standards applicable to emission of any air pollutant from any class or classes of aircraft or aircraft engines which in his judgement cause or contribute to, or are likely to contribute to, air pollution which endangers the public health or welfare." Regulations insuring compliance with these standards are required to be issued by the Secretary of Transportation in accordance with Section 232 of the Act. As a means of complying with the Clean Air Act, the US Air Force has implemented an active program for the "Protection and Enhancement of Environmental Quality" as outlined in AF Regulation 19-1. This regulation establishes policies, assigns responsibilities, and provides criteria and standards for an environmental pollution abatement program. The following is quoted (in part) directly from this regulation:

"1. Environmental Pollution Explained: As used in this regulation, environmental pollution is the presence of physical, chemical, and biological elements or agents that adversely affect human health or welfare, unfavorably alter ecological balances of importance to human life, adversely affect species of animal or plant life, cause damage to and deterioration of man-made materials or property, or degrade

the utility of the environment for aesthetic and recreation purposes. Control of environmental pollution requires consideration of air, water, and land, and must extend to noise, improper solid waste management, and electromagnetic energy, as well as things conventionally thought of as pollutants.

2. Air Force Policy:

a. Eliminate or control environmental pollutants generated by or resulting from Air Force operations or from contractor operations on real property owned, leased or controlled by the Air Force consistent with the overall mission of the Air Force.

b. Lead in preventing, controlling, and abating environmental pollution by accelerating corrective measures at Air Force installations, and by initiating and supporting local area programs of local communities in developing area-pollution abatement programs.

c. Provide for environmental pollution control measures in designs for new Air Force buildings, facilities, weapon systems, operations, tests, exercises, procedures, and projects for rehabilitation or modification of structures.

d. Provide preventive pollution control by:

- (1) Reducing or eliminating waste at the point of generation.
- (2) Considering potential environmental pollution control problems when selecting chemical compounds and materials to be used in Air Force operations.
- (3) Including pollution abatement as an element in specifications.

e. Comply not only with Air Force directives relating to pollution criteria and standards, but also with criteria and standards published by the Environmental Protection Agency (EPA) and by state and local pollution abatement agencies in the area. Either Air Force or EPA standards and criteria, depending on which is more restrictive, will be applied when state or local agency standards are less stringent or nonexistent.

Other laws which have direct impact on the aircraft industry are the "National Environmental Policy Act", the "Occupational Safety and Health Act", and the most recently proposed "Toxic Substances Act". The latter act will undoubtedly require that any chemical which will be utilized in large quantities will be given a thorough screening and evaluation process in terms of its total effect on the environment (air, water, soil, biological activity, etc), how it is to enter the environment, how it will move or be transported within the environment, and ultimately how it will be disposed of or removed from the environment. Routine studies will be required to determine the physical, chemical and biological properties of each compound as it pertains to the physical environment as well as its effects on living organisms. Special attention will be given to toxic, carcinogenic, mutagenic, teratogenic and reproductive processes. As one can readily see, compliance with all these rules and regulations can become exceedingly costly and, as shall be seen, may require long lead-times for acquisition of biological data. Since these laws will ultimately affect every new fuel, fuel additive, oil, lubricant, hydraulic fluid, coolant, etc., it is readily apparent that all aircraft design engineers and propulsion chemists must become intimately aware of the biological aspects involved.

AIRCRAFT AND AIRCRAFT ENGINES (PROPOSED STANDARDS)

The proposed standards of the EPA were published in the Federal Register V. 37, No. 239, 12 December 1972. It is pertinent to note that the proposed regulations would establish:

1. Fuel venting emission standards for new and in-use aircraft gas turbine engines.
2. Crankcase emission standards for new aircraft piston engines.
3. Exhaust emission standards for new and in-use aircraft gas turbine engines.
4. Exhaust emission standards for new aircraft piston engines.
5. Exhaust emission standards for new gas turbine aircraft.
6. Test procedures applicable to aircraft gas turbine engines and gas turbine aircraft.
7. A test procedure applicable to aircraft piston engines.

Goals of the EPA are to complete a formal analysis of technology development by 1 January 1975 in order to reflect a best estimate of gaseous emission standards for turbine and piston engines which may be technically feasible by 1979. Of particular interest is paragraph 87.71 which states that ASTM D 1655-67 Jet A fuel shall be used for testing purposes. This fuel may contain non-metallic additives but may not contain additives used for the purpose of smoke suppression (such as organometallic compounds). It is not clear whether organometallic compounds may be used for normal operation.

It is not necessary nor desirable to present standards here since they may be read in the document and they are subject to great changes before becoming law. For purposes of illustration, the following are noted as standards for a new gas turbine engine manufactured on or after 1 January 1976 (Class T4-JT8D model family):

1. Hydrocarbons - 2.5 lb/1000 lb thrust hrs/cycle.
2. Carbon Monoxide - 11.5 lb/1000 lb thrust hrs/cycle.

In contrast, for engines of the same class manufactured after 1 January 1979, the emission limits are:

1. Hydrocarbons - 0.4 lb/1000 lb thrust hrs/cycle.
2. Carbon Monoxide - 2.1 lb/1000 lb thrust hrs/cycle.
3. Oxides of Nitrogen - 3.2 lb/1000 lb thrust hrs/cycle.
4. Smoke - Smoke number of 35.

Notice that there are no limits for NO_x or smoke for the 1976 standards but they are proposed for 1979 engines.

It is obvious then, from the proposed standards and the general tenor of this meeting that the primary concerns of the EPA are toward control of carbon monoxide and the oxides of nitrogen. Smoke abatement has already received a good deal of work and has been greatly reduced with new advances.

TOXICOLOGY OF AIRCRAFT ENGINE EXHAUST PRODUCTS

In a recent paper by R.F. Sawyer (AGARD Report No. 40 on Atmospheric Pollution by Aircraft Engines and Fuels) there is an interesting summary of pollutant species and their primary effects in Table II. A primary effect of toxicity was noted for carbon monoxide, oxides of nitrogen, oxides of sulfur, lead, metals, sulfur compounds, halogenated acids and aldehydes. It is true that all of these compounds can be considered toxic if the concentration in the atmosphere is great enough to cause harmful effects. One must recognize that pollution from aircraft engines is not a problem of acute toxicity. That is, single exposures do not cause harmful effects to humans as does a single exposure to a high concentration of a chemical such as hydrogen fluoride gas. Rather, the toxicity is manifest only as it adds to the whole complex of chronic air pollution effects. Further, at present, aircraft are probably only responsible for significant pollution in highly populated cities where high pollutant levels are already prevalent from other vehicular sources.

NATIONAL PRIMARY AND SECONDARY AMBIENT AIR QUALITY STANDARDS

The following can be found in the Federal Register Vol 36, No. 84, dated 30 April 1971, and in Vol 36, No. 206, dated 23 October 1971. It is necessary to understand these standards in order to understand the really low levels of contaminants which the EPA is trying to achieve.

National primary ambient air quality standards define levels of air quality which the Administrator judges are necessary, with an adequate margin of safety, to protect the public health. National secondary ambient air quality standards define levels of air quality which the Administrator judges necessary to protect the public welfare from any known or anticipated adverse effects of a pollutant. For your convenience the data have been placed in Table 1.

In an emergency situation where any of the contaminants, alone or in combination, reach levels deemed significantly harmful to health, it is likely that all out contingency laws would prevail. It is likely that all abatement strategies including decrease in air traffic might be brought to bear on the situation. Keep in mind that these levels are designed to protect all people from harmful effects, including the healthy, very young, the aged and persons in poor health.

TOXICOLOGY OF CARBON MONOXIDE

In order to shed some light on the problems associated with obtaining biological data which can be used for establishing environmental quality standards, emergency exposure limits and threshold limit values, I should like to use as an example the work performed in our laboratories during the past few years on carbon monoxide. Keep in mind that long-term continuous exposure data are required to establish environmental quality standards. For emergency exposure limits, high level, short-term exposures are necessary, while 8 hour, five-day per week exposures are needed to establish threshold limit values for the working population. This presentation is not intended to be an extensive review dealing with all aspects of carbon monoxide toxicity. The interested reader is referred to several reviews¹⁻⁴ and to the recent New York Academy of Sciences symposium, "The Biological Effects of Carbon Monoxide",⁵ which explored the subject in great depth.

Although the toxicity of carbon monoxide was well established, the Air Force developed a keen interest as a result of the following considerations:

1. Once the reality of man in space was established, it soon became apparent that carbon monoxide might become a major problem on long-term space flights, i.e., missions of greater than 90 days duration. Studies on space cabin materials revealed that a major gas-off product was CO. Of the first 206 materials tested, 127 or 62 per cent evolved CO.⁶⁻⁸ Another potential source of CO contamination stemmed from considerations of O_2 regeneration systems, which would be needed for long missions. Such systems could utilize the Sabatier reaction or others which utilize CO in the reaction cycle to generate O_2 . Finally, man himself could contribute to the CO. Coburn studied endogenous CO production and the CO pool in man.⁹ He measured the rate of endogenous CO production at 0.42 ml/hr in a normal resting male, with production primarily from hemoglobin catabolism.

2. The detrimental effects of CO have been primarily derived from acute exposures to relatively high concentrations. Under such circumstances the central nervous system (CNS) is the most vulnerable, followed by cardiovascular collapse late in the intoxication cycle.¹⁰ Although these effects are part of an acute CO exposure, this same relationship does not necessarily apply to chronic (intermittent) or continuous exposures to low concentrations of CO. The major question at present is, "Does chronic continuous exposure to CO adversely affect the CNS or the cardiovascular system at low levels which are considered safe during transient exposures?"

TABLE 1
NATIONAL AMBIENT AIR QUALITY STANDARD

POLLUTANT	PRIMARY		SECONDARY		WARNING	EMERGENCY	SIGNIFICANT HARM TO HEALTH
	ANNUAL ARITHM. MEAN	MAX. FOR 24 HRS (*)	ANNUAL ARITHM. MEAN	MAX. FOR 24 HRS (*)			
NITROGEN DIOXIDE	0.05 ppm 100 µg/m ³		0.05 ppm 100 µg/m ³		1.2 ppm/1hr 0.3 ppm/24hr	1.6 ppm/1hr 0.4 ppm/24hr	2 ppm/1hr 0.5 ppm/24hr
PHOTOCHEMICAL OXIDANTS		0.08 ppm 160 µg/m ³		0.08 ppm 160 µg/m ³	0.4 ppm/1hr	0.6 ppm/1hr	0.4 ppm/4hr 0.6 ppm/2hr 0.2 ppm/3hr
SULFUR DIOXIDE	0.03 ppm 80 µg/m ³	0.14 ppm 365 µg/m ³	0.02 ppm 60 µg/m ³	0.1 ppm 260 µg/m ³ 0.5 ppm for 3 Hr	0.6 ppm/24hr	0.8 ppm/24hr	1 ppm/24hr
PARTICULATE MATTER	75 µg/m ³ (geometric mean)	260 µg/m ³	60 µg/m ³ (geometric mean)	150 µg/m ³	625 µg/m ³ 24hr	875 µg/m ³ 24hr	1000 µg/m ³ 24hr
HYDROCARBONS (6 to 9 a.m.)		Max. for 3Hr (*) 0.24 ppm 160 µg/m ³		Max. for 3Hr (*) 0.24 ppm 160 µg/m ³			
CARBON MONOXIDE		Max. for 8Hr (*) 9.0 ppm 10.0 mg/m ³ For 1Hr (*) 35.0 ppm 40.0 mg/m ³		Max. for 8Hr (*) 9.0 ppm 10.0 mg/m ³ For 1Hr (*) 35.0 ppm 40.0 mg/m ³	30 ppm/8hr	40 ppm/8hr	50 ppm/8hr 75 ppm/4hr 125 ppm/1hr

(*) MAXIMUM CONCENTRATION NOT TO BE EXCEEDED MORE THAN ONCE PER YEAR

3. Since the CNS is the most sensitive to hypoxia, could CO disrupt the more complex cognitive, mental, or the highly integrated functions of the brain? Several studies report decrements in human performance with COHb levels as low as 3 to 5%;^{11,12} however, others have not seen impairment at these levels.^{13,14} The importance of determining whether real effects from CO exist at such low levels of COHb becomes apparent when the COHb levels of cigarette smokers are taken into consideration. Goldsmith and Landaw found smokers to have COHb levels between 3.8 and 6.8%.¹⁵ If these COHb levels are compared to the 3 to 5% levels associated with performance decrements as reported by several investigators, then one must consider the possibility that large segments of the population may be performing certain functions at depressed levels.

Our studies can be divided into three major areas: (1) the effects of continuous long-term CO exposure on various animal species; (2) the effects of continuous long-term CO exposure on the performance of rhesus monkeys; and (3) the effects of short-term low level CO exposure on human performance. Previous workers have indicated marked changes in the central nervous system (brain), cardiac lesions, vascular lesions (increased susceptibility to lipid depositions in the aorta) and performance decrement at exposure levels as low as 50-100 ppm CO. In order to accelerate the development of such changes, monkeys, batons, dogs, rats, and mice were exposed to CO continuously for 168 days in the Thomas Domes (Exposure Chambers). The exposed animals received CO at concentrations of 460 mg/cuM for the first 71 days, followed by 575 mg/cuM for 97 days. Control animals were kept under identical conditions except for the presence of CO. This high level exposure initially resulted in obvious clinical signs of anorexia and depression which disappeared in three days to a week after onset of exposure. The ultimate result of the exposure was an increase in hemoglobin which closely correlated with the amount of circulating carboxyhemoglobin. There was a commensurate rise in hematocrit and the number of red blood cells with a slight decrease of plasma volume so that a marked increase in blood viscosity resulted. Despite the marked increase in blood carboxyhemoglobin (40%) this study has demonstrated the adaptive mechanisms available to provide oxygen transport in the blood during exposure to CO at levels more than eight times that of the current industrial Threshold Limit Value (TLV). In addition, detailed pathological examination revealed no discernible lesions of the central nervous system, heart or vascular system. In rats and mice there was a statistically significant rise in heart weight and in heart to body weight ratio. The increase seemed to be predominantly in the left ventricle and can be explained by the increase in blood volume and viscosity which, in turn, increases the workload for the heart. Apparently the most significant limiting factor in adapting to slowly increasing carbon monoxide concentrations is the blood forming system's ability to produce more and more red blood cells and the cardiovascular system's ability to move high viscosity blood. Blood viscosity was increased to such critical levels in this experiment that any further increase in the concentration of carbon monoxide would almost certainly have resulted in catastrophic heart failure. This study has gone a long way to dispel some of the entrenched theories as to the direct toxic effect of carbon monoxide on the cells, other than tissue anoxia, which can result from reducing the blood oxygen carrying capacity by tying up too much hemoglobin with carbon monoxide. Results are of practical significance to the protection of both ground and flying personnel in environments where carbon monoxide becomes a toxic hazard.

The US Air Force has a very high interest in the short- and long-term effects of carbon monoxide (CO) since studies of gas-off products of space cabin materials and processes (including man's contribution) reveal that the compound is likely to be found in space cabins if not properly removed. Recent investigations by others have indicated that very low concentrations of CO can cause subtle decrement in high level performance. In order to test performance changes in animals, a continuous 100-day CO (220 mg/M³ concentration) exposure study in a space cabin atmosphere of 5 psia total pressure (27,000 ft simulated altitude), mixed gas environment consisting of 68% oxygen and 32% nitrogen (pO₂ = 160 mmHg) was performed. The experiment was performed on 12 trained Macaca mulatta monkeys in which operant behavior was conditioned to both continuous and discrete avoidance tasks by both audio and visual cues. The animals performed 15 min/hour, 8 hours/day and 5 day/week during the continuous exposure period. Extensive clinical laboratory determinations were performed, including blood carboxyhemoglobin levels, at regular intervals before, during, and following the exposure period. Results of the 100-day exposure indicated a rapidly plateauing carboxyhemoglobin saturation of approximately 22% in all animals. There was also a concomitant increase in hematocrit and hemoglobin. Exposure caused no detectable performance changes in any of the monkeys tested.¹⁶

Other workers have reported performance decrement in humans and animals exposed to 50 to 100 ppm of CO which produce carboxyhemoglobin levels of 4 to 10% saturation at equilibrium. In a previous in-house experiment, 9 human volunteers were subjected to 50-200 ppm CO levels for three hours. These levels caused no significant deterioration in performance of time estimation, tracking, or ataxia tests. In a more recent study, 4 human volunteers were exposed overnight for approximately 9 hours in a Thomas Dome to 0, 75, or 150 ppm of carbon monoxide in a double-blind designed experiment. This exposure produced blood carboxyhemoglobin levels of 6% and 12% for 75 and 150 ppm CO, respectively. No effects were noted on sleep patterns obtained from continuous EEG recordings, indicating a restful sleep. Ataxia tests, psychopharmacological workload tests, tracking tests and flicker fusion tests were not different from control values during non-exposure nights. Time estimation was also unaffected by exposure. These results are clearly different from those of Beard and Wertheim who found decrement at these levels.¹² Our data indicate that CO at the levels used in our experiments would not impair those pilot performance skills required to execute instrument landings of aircraft, or landing heavy aircraft under adverse conditions such as a strong crosswind.¹⁷

In summary, please note that in all these experiments carboxyhemoglobin levels were from 4 to as high as 40% saturation. Remember from Table 1 that the primary standard for carbon monoxide is 9 ppm for 8 hours which can't be exceeded more than once a year. This level should not produce a carboxyhemoglobin level of more than 1-2% saturation. These are much below a level obtained by a man who smokes 1 pack of cigarettes per day.

I do not wish to leave the reader with the impression that we are opposed to more stringent control of environmental pollution or that carbon monoxide is completely harmless. The general public, and those responsible for its general health, must establish levels of carbon monoxide which contain wide safety margins to insure the well-being of the total population. However, these limits must be established by realistic criteria in order to be meaningful. In the case of the Air Force, which deals with a more select

population, it needs such criteria in order to operate within the economic and practical engineering constraints placed on operational systems and still be certain that the human element is unimpaired.

OTHER STANDARDS OF IMPORTANT COMPOUNDS

In contrast, then, to the standards outlined in Table 1, the following criteria are followed for Emergency Exposure Limits and Threshold Limit Values for US Air Force use:

	TLV (ppm)	EEL (ppm)		
		MIN		
		10	30	60
Carbon Monoxide	50	1500	800	400
Nitrogen Dioxide	5	30	20	10
Sulfur Dioxide	5	30	20	10
Ozone	0.1	--	--	--
Hydrogen Chloride	5	30	20	10
Hydrogen Fluoride	3	20	10	8
JP-5 Fuel				
Benzene (Aromatic Hydrocarbon)	5	5mg/l	5mg/l	5mg/l

If nothing else is gained from perusal of this paper, it must become apparent that the propulsion engineer must be aware of the rules and regulations regarding the introduction of a new chemical additive, or old chemical which may be used in a new and novel way, into the inventory. It may take a great deal of time and money to obtain the necessary biological data, and to have it accepted by governmental authorities charged with making sure it will have little effect or impact on the environment.

REFERENCES

1. Dinman BD: Pathophysiologic determinants of community air quality standards for carbon monoxide. *J. Occup Med* 10:14-31, 1968.
2. Root WS: Carbon monoxide. In *Handbook of Physiology, Section 3: Respiration II*, edited by W.O. Fenn and H. Rahn. Washington, D.C., the American Physiological Society, 1965, pp 1087-1098.
3. Lilienthal JL: Carbon monoxide. *Pharmacol Rev* 2:324-354, 1950.
4. Effects of chronic exposure to low levels of carbon monoxide on human health, behavior, and performance. Library of Congress Catalogue Card No. 73-602110, National Academy of Sciences and National Academy of Engineering, Washington, D.C., 1969.
5. Biological Effects of Carbon Monoxide, New York Academy of Sciences, *Annals of the New York Academy of Sciences* 174:1-430, 1970.
6. Pustinger JV Jr, Hodgson FN: Identification of volatile contaminants of space cabin materials. AMRL-TR-66-53, Wright-Patterson AFB, Ohio, 1966.
7. Pustinger JV Jr, Hodgson FN: Identification of volatile contaminants of space cabin materials. AMRL-TR-67-58, Wright-Patterson AFB, Ohio, 1967.
8. Pustinger JV Jr, Hodgson FN: Identification of volatile contaminants of space cabin materials. AMRL-TR-68-27, Wright-Patterson AFB, Ohio, 1968.
9. Coburn RF, Blakemore WS, Forster RE: Endogenous carbon monoxide production in man. *J. Clin Invest* 42: 1172-1178, 1963.
10. Gleason MM, Gosselin RE, Hodge HC, et al: *Clinical Toxicology of Commercial Products*, 3rd ed. Baltimore, The Williams and Wilkins Company, 1969, p: 60-65.
11. Schulte JH: Effects of mild carbon monoxide intoxication. *Arch Environ Health* 7:524-530, 1963.
12. Beard RR, Wertheim GA: Behavioral impairment associated with small doses of carbon monoxide. *Amer J Public Health* 57:2012-2022, 1967.
13. Vollmer EP, King BG, Birren JE, et al: The effects of carbon monoxide on three types of performance at simulated altitudes of 10,000 and 15,000 feet. *J Exp Psychol* 36:244-251, 1946.
14. Lawther MB, Commins BT: Cigarette Smoking and Exposure to Carbon Monoxide. Presented at New York Academy of Sciences Conference on the Biological Effects of Carbon Monoxide, *Annals of the New York Academy of Sciences* 174:1-430, 1970.
15. Goldsmith JR, Landaw SA: Carbon monoxide and human health. *Science* 162:1351-1359, 1968.
16. Theodore J, O'Donnell RD and Beck KC: Toxicological evaluation of carbon monoxide in humans and other mammalian species. *J Occup Med* 13:242, 1971.
17. O'Donnell RD, Chikos P, and Theodore J: Effect of carbon monoxide exposure on human sleep and psychomotor performance. *J Appl Physiol* 31:513-518, 1971.

ROUND TABLE DISCUSSION

On Friday, 13 April a round table discussion on the topic of aircraft pollution was conducted. This section includes only those comments for which a written record was provided by the person making the comment.

Round Table Discussion Members

Chairman:

Professor A.FERRI	Department of Aero and Astronautics, University of New York	USA
-------------------	--	-----

Members:

ICA G.P.A.CASANDJIAN	Direction Générale de la Protection de la Nature et de l'Environnement, Paris	FRANCE
Mr A.QUILLEVERE	SNECMA, Centre d'Essais de Villaroche, Moissy-Cramayel	FRANCE
Dr-Ing.G.KAPPLER	MTU München GmbH, Munich	GERMANY
Mr T.V.LAWSON	Department of Aeronautical Engineering, University of Bristol	UK
Mr J PARKER	Air Pollution Division, Warren Spring Laboratory, Stevenage, Herts.	UK
Mr A.B.WASSELL	Rolls-Royce (1971) Ltd, Derby	UK
Mr D.D.WILLIAMS	Rolls-Royce (1971) Ltd, Bristol Engine Division, Filton	UK
Mr A.W.NELSON	Pratt & Whitney Aircraft, East Hartford, Connecticut	USA
Professor R.F.SAWYER	Department of Mechanical Engineering, University of California, Berkeley	USA

A.FERRI

The problem of pollution due to aircraft engines presently is considered to be important for two conditions of flight: (1) take-off conditions; and (2) high-altitude supersonic speed.

The first part of the problem, in my opinion, is a simpler problem to be solved either from a technical or operational point of view. As stated clearly during the meeting, such a problem could immediately be reduced substantially by changing operational procedures, without the immediate necessity of engine redesign. Unfortunately, this approach has not yet been considered, and as often happens, in order to improve conditions legislature is introduced that requires rapid improvements in engine performances. Because of the time limits considered, this approach imposes the development of "fixes" on existing engine designs. Such "fixes" are difficult to find and often solve a problem and produce another. However, the problem can be solved in new engines where the time required for development is available without the necessity of new technology, and possibly without a substantial increase in cost.

The second part of the problem is more difficult to define accurately; even the magnitude of the problem has not yet been assessed. The problem has two aspects: (1) one is related to the physics of the phenomena taking place in the stratosphere; and (2) the other related to the consequences of possible depletion of ozone. Recently Dr. Johnston clearly summarized the present position with respect to the ozone depletion by stating that: "There is strong evidence that nitrogen oxide from SST exhaust could seriously reduce stratospheric ozone; but in any case, the evidence can be matched by a possibility that the SST could have little or no effect". I would like to qualify this statement by adding "when flying continuously and in large numbers". Even if the effects on the ozone are real, presently it is possible to estimate the actual consequences of a moderate reduction of ozone concentration within the framework of all the other changes taking place at the same time in the atmosphere. In order to emphasize this point, it could be useful to recall, for example, that it has been mentioned at this meeting (during the discussion by a meteorologist) that this effect could be beneficial to reduce the detrimental effects due to the gradual increase in turbidity of the air.

A quantitative definition of these two aspects is extremely complex and will require long investigations. The possibility exists that no clear conclusion will be reached for quite some time. Therefore, the alternate possibility of eliminating the problem with changes in engine design appears important for acceptance of flight in the stratosphere. Fortunately, the time available for the solution of this problem from an engine design point of view is sufficiently long to make possible a systematic effort directed to large reduction of NO for the engine exhaust. The knowledge of basic technology is in hand in order to achieve such goals. Such knowledge indicates that the problem can be solved, or at least substantially reduced, by development of a burner based on a combustion mechanism that does not produce regions of high temperature which are not required for good performance of the engine. Then a technically sound approach to this problem consists in continuing the effort to define the magnitude of the problem as accurately as possible, and at the same time, carrying out a parallel effort directed to developing engine burners designed for the main purpose of decreasing NO an order of magnitude without penalizing the performance. I am confident that this burner design can be developed in the 10 year time period available to industry.

Any discussion on the acceptance of the SST's on the basis of the possibility of the existence of the pollution problem alone, as carried out presently by some groups, is unsound and not justifiable, and is justified only if it is considered to be an effective means for forcing the engine designers to concentrate their efforts on solving the problem by developing in time the required technology, and introducing this new technology in the engine used.

A.B.WASELL

1.0 Introduction

Despite any impression that may have been given by some speakers from this side of the water, the European zero-engine industry recognizes that it has to assist in developing the solutions to the problem of pollution by aircraft engines. The extent of this problem, however, is somewhat conjectural since the pollution from aircraft has not been specifically related to the acceptable air quality standard. We even see that the standard defined as acceptable on either side of the Atlantic can differ by a factor of at least 5. In addition the models used to predict the interaction between the airport and the surrounding community need considerable refining.

Also the direct control of aircraft engine emissions by combustor design modifications, the introduction of ground operational procedures to reduce emissions and the control of emissions from ground vehicles servicing parked aircraft need to be coordinated, otherwise the finite resources available for the development of emission control techniques will not effect the desired emission reduction.

2.0 The Setting of Pollution Goals

It has been stated that the emission controls which are contemplated are based on present or achievable technology. This is a very laudable objective, but it leaves open to debate what is achievable and what time-scale is required to achieve it. Two sources of data are currently available on which to base this forward projection of technology. These are theoretical combustor models and laboratory experiments.

2.1 Combustion Models

This technique is beginning to produce some very interesting results which will obviously form the basis of future work, but some comments are in order here:

- (a) the reaction rate constants need regular review since new data are continually becoming available and at present it appears that most researchers have their own favourite values. Some agreed standardization would seem desirable.
- (b) the majority of models have concentrated on predicting reactions either at idle or at take-off, whereas it is essential that any model should be capable of predicting with reasonable accuracy at least one species predominating at idle and one predominating at take-off (e.g. CO plus NO).
- (c) to date models seem to have been designed to fit existing sets of data rather than to optimise preferred configurations before committing the manufacture of test hardware. This seems to demonstrate an apparent lack of faith in the models (with the possible exception of the Ford Motor Company in their recent ASME paper). Indeed it was even stated during the week that "data . . . are analysed and shown to be in reasonable agreement with the predictions" rather than vice versa.

2.2 Laboratory Experiments

It would be considerably more helpful if all data could be presented in a consistent form - say, always using the emission index. Apart from this adoption of this procedure two other points are considered important:

- (a) that investigations should never be restricted to only one of the gaseous pollutants, this will ensure that adequate data will be available for comparison with predictions from improved modelling techniques. It will also indicate either the extent of exchange rates between pollutant species or whether a significant advance in the state-of-the-art can be achieved.
- (b) that predictions based on small scale laboratory experiments carried out at unrealistic levels of inlet temperature and pressure are treated with caution as they deserve. Through-flow velocities should also be of representative values and not changed during comparative tests.

3.0 Full Scale Concept Evaluations

Once the initial laboratory experiments have been completed successfully at realistic conditions, the effect of combustor design changes on the other important combustion parameters must be considered. Experimental evaluation of liner temperatures over the whole operating range, the altitude relighting and cold starting characteristics and combustor outlet temperature pattern factors will be required, before the development of the finally acceptable compromise for engine operation can begin.

The above work which has to be completed before any in service evaluation can start indicates why Mr Nelson stated that his company had taken 8 years from programme go-ahead to complete the retrofits of the reduced smoke JT8D's in service with the US Airline fleets. This is an example of a relatively small redesign based largely on existing technology, when initiated, and demonstrates the reason for the caution adopted by the industry in relation to implementation times for the proposed legislation.

4.0 Total Atmospheric Pollution

It appears that two problem areas for aircraft engine pollution have been identified (viz. local to the airport and above the tropopause) and these are currently treated quite independently. Since the higher operational altitudes now being used by subsonic aircraft brings them within the scope of C.I.A.P., it is suggested that an overall pollution assessment be made to ensure that standards set for one type of environment do not ensure a consequent increase in pollution in the other. Viewed from an overall position, this type of solution would be highly suspect as an improvement concept. The use of water injection to cure take off NO_x leaving cruise NO_x emissions at an unacceptable level would be an example.

Additionally the thermodynamic cycle for a new engine should be chosen on the basis of minimising the pollution over the total flight mission rather than at any particular point in that mission.

J.J. MACFARLANE

There are two aspects of the aircraft emissions control problem which particularly concern the National Gas Turbine Establishment. The second of these is the artificial constraints placed on engine designers by the proposed EPA rules in limiting his freedom of choice - for a given level of combustion, technological expertise - in selecting the type of engine cycle to be used for a particular airframe duty. This I can safely leave to my friend and colleague Mr J.A. Lang to expand for you.

I would like myself to deal with an equally fundamental limitation of the EPA proposed rules - the methods laid down for emissions sampling and analysis.

1. Sampling probe design

There are well established techniques which have been in use on combustion test rigs for 25 years or more in the UK which permit truly representative weighted mean samples of highly stratified exhaust gas streams to be obtained easily. These are based on water cooled multi-hole sampling probes in which the main area restriction is at the inlet port (the diameter for which, in common usage, is in the region of 0.020 to 0.030 inch). In use, the static pressure in the probe manifold (i.e. downstream of the sampling ports) is made equal to the free stream static pressure. The sample flow rate for a given port is then a direction function of free stream local dynamic head. By arranging that there is a geometrically adequate coverage of the exhaust plane by ports located in equal areas of the traverse, a single stream of automatically mass weighted mean sample gas is obtained.

2. The use of this technique implies an adequate number of sample ports and for a typical present day large engine exhaust cross section (3 ft ϕ in diameter) the number to consider is in the range 50 to 150 ports rather than the 10 or 12 mentioned by EPA.

3. The technique also connotes a uniform static pressure field in air stream being sampled. This is not likely to obtain at the 0.5 diameter distance downstream of the propelling nozzle required by EPA.

4. From a test economy point of view, it is desirable to take gas samples for emissions measurement during normal engine check-out tests and for this purpose, interference with thrust measurement must be avoided. This also connotes a sample plane farther downstream than required by EPA.

5. One can find very little with which to quarrel in the methods proposed for on line measurement of gaseous exhaust constituents, they are, after all, normal commercially available experimental techniques.

6. The measurement of exhaust smoke however is a very different case. The proposed EPA technique can be criticised from a number of points of view.

- (a) It is seriously proposed by the EPA that engines should be operated for a period of 20 minutes steady running (including max take-off thrust) for each operating RPM being examined, just to obtain the smoke sample.
- (b) The sampling technique deliberately selects a filtration medium which is made specifically for filtering coarse gelatinous precipitates in wet chemical analysis, and uses this to filter solids, the ultimate particle size of which is known to be in the region of 20 nanometers.
- (c) The filter material is ordinary cellulose so that, having made a reflectance measurement, there is no direct means for calibrating this in terms of mass of carbon collected.
- (d) I went to some trouble to draw the attention of the SAE 41 committee, (whose brainchild this technique seems to be) to the benefits to be obtained from substituting glass fibre filters which, being of adequately fine porosity, and being stable to heating up to at least 500°C, are an ideal means for measuring mass concentration directly.
- (e) There is no doubt that for routine purposes, some form of optical density smoke measurement technique, either on an abstracted sample as in the smoke meter designed and used by my friend Brian Toone at Rolls-Royce (1971) Ltd, or by a development which involves measurement of optical density of the whole exhaust jet at a suitable point downstream of the exhaust nozzle. The latter technique has been described in a recent technical paper emanating from a US source - the exact reference escapes me.

In conclusion Mr Chairman, in my opinion, it is only by adopting rapid techniques of this kind taking only minutes for complete analyses of a given exhaust condition, and designed to avoid interference with routine engine performance measurements, that we shall be able to collect enough information covering the service life of gas turbine propulsion engines.

A.W.NELSON

There is no doubt that certain local areas of the world do have serious air pollution problems. However, much of the remaining areas do not have a problem because of natural air circulation which has a cleansing action. None of us would argue that it is desirable to decrease the pollution from any source. Granted, too, that the best incentive for getting this accomplished is through regulatory action. But such regulations must be both practical and economically viable and commensurate with the overall contribution of the source to the affected area as a whole. Assessment of the commercial aircraft pollution contribution has not yet been well established.

There are some emissions reductions that can be effected. In order to accomplish the greatest reductions of aircraft turbojet emissions, new combustor concepts are required. However it must be recognized that the combustors in today's commercial aircraft engines, although highly refined, are basically the same pressure atomized fuel injection concept used in the original jet engine designs and, as such, have a vast background of development experience which contributes to the excellent safety and reliability records of today's commercial airlines.

The new combustor concepts now being considered are still in the early stages of development, that of rig testing. Rig tests are, of course, required for basic research, but these results must be kept in proper perspective. Rig test, and limited engine test results, have indicated significant reductions in CO and HC. NO_x reductions are also indicated by such testing however, much of these NO_x achievements have been accomplished using different methods than those used for the low power emissions. Interactions or the conflicts of these different methods have not yet been thoroughly defined.

Those of us who are associated with engine development are well acquainted with the differences that often occur between rig test results and engine test results of similar concepts. We must also test and develop combustor operational characteristics over the entire planned flight altitude - Mach number envelope. Inevitably modifications are encountered which may effect emission levels.

Programs are underway, both in-house and under government sponsorship to minimize exhaust emissions using new combustor concepts. It appears at present that approximately 3 years are required to reach the point where these new concepts can be properly evaluated in engines. Assuming these full scale engine test results show that emission reductions, at or near the goals have been achieved, it characteristically takes a minimum of 4 to 5 years, or more, for a new engine model to be developed incorporating such a new combustor concept once the concept has been proven.

Retrofit of in-use engines or engines already in manufacture (certified) status with new (different) combustor concepts is expected to be difficult and perhaps require complete redesign of major parts of the engine and as well as the aircraft itself which can be very (if not prohibitively) expensive. The ultimate environmental value to be gained by such a requirement should be carefully considered. As pointed out in my paper, there is much to be done to improve instrumentation and analysis corrections for ambient and other effects.

On the aspect of water injection for "super" control of NO_x, such a requirement would impose both economic and potential safety penalties on the airline operators and the traveling public. Also, it would appear that little, if any, real work has been done to evaluate the effect of water injection on emission levels for the premix, prevaporizing and other new concepts now being considered for emission reduction. It has been proposed at this meeting that if one is able to prevaporize and premix at the overall fuel/air ratio, and burn to completion, very low values of NO_x will be achieved. In fact combustion must be forced to occur at lean mixtures if significant NO_x reductions are to be achieved. There are however strong reasons in the form of physical limitations why prevaporized, premixed combustion at the overall fuel/air ratio does not offer a realistic solution for low pollution combustors. This is not simply a development problem because:

- (1) there is an order of magnitude increase in burning time required to get high efficiency (i.e. low CO and HC);
- (2) the real probability of premix passage self-ignition;
- (3) the pilot burner will contribute strongly to NO_x levels;
- (4) air is needed for liner cooling and temperature pattern adjustment.

The operational requirements mentioned earlier also further complicate these limitations.

To conclude then, we can say that we are actively working both to research and develop low emission combustor techniques and concepts, but let us be realistic about what can be practically achieved together with consideration of the necessary long lead times required to translate resulting new technology, both safely and economically into engines which will most usefully benefit the public as a whole.

A.QUILLEVERE

Nous admettons qu'un effort important de réduction de la pollution peut être fait, mais nous sommes persuadés, comme l'ont souligné dans leurs déclarations A.W.Nelson (Pratt and Whitney Aircraft) et G.Kappler (M.T.U.), que cet effort demanderait beaucoup de temps et d'argent. Il ne faut pas perdre de vue, en effet, que la mise au point d'une chambre de combustion fiable, de longue durée de vie et convenant à un moteur de performances élevées est déjà un problème difficile dont la solution résulte d'une longue expérience.

Il convient, cependant, de noter que les recherches et les essais partiels préliminaires qui sont indispensables pour valider de nouvelles formules anti-pollution, ne devraient pas se solder par des dépenses inutiles. En effet, même si les objectifs de réduction de la pollution se révélaient, par la suite, excessifs, les résultats obtenus permettraient d'approfondir les connaissances des processus de combustion, ce qui est souhaitable pour réduire le coût des mises au point.

Une diminution importante de l'émission de tous les polluants, au sol et en altitude, exige l'emploi de nouvelles technologies dites avancées (injection étagée, géométrie variable etc. . .). La meilleure solution ne pouvant être qu'un compromis, il importe de ne pas mettre en application des réglementations arbitrairement sévères et de bien définir les priorités dans la réduction des divers polluants en envisageant l'ensemble du problème au sol et en altitude.

Pratiquement, nous pensons qu'il faut déterminer, par des essais de principe représentatifs, les possibilités extrêmes de réduction des polluants (ce qui n'est pas encore fait) et dégager des moyens financiers complémentaires pour que les constructeurs puissent vérifier par des essais sur moteur la faisabilité des solutions dégagées.

Nous terminerons cette déclaration par des remarques plus particulières.

Dans les communications présentées, diverses méthodes ont été proposées pour réduire l'émission soit de l'oxyde de carbone et des hydrocarbures, soit des oxydes d'azote, mais très souvent ces méthodes ne peuvent être appliquées simultanément et les répercussions sur le refroidissement des parois de la chambre ou sur la répartition des températures à l'entrée de la turbine ne sont pas toujours considérées.

Enfin, nous avons noté un sujet à controverses: est-il possible d'envisager, pour diminuer l'émission des oxydes de l'azote, d'envisager une combustion en prémélange uniforme à richesse pauvre? Certains le pensent, d'autres se posent des questions concernant les niveaux de rendement d'un tel procédé ou ces possibilités réelles d'application.

G.KAPPLER

We don't argue about the fact that the air is polluted from many sources and that the reduction of air pollution is a vital necessity. We are also aware that the gas turbine, by burning fossil fuel, is a contributor to pollution although a very small contributor. Since for commercial reasons the design of combustors is anyway going toward complete combustion the pollutants from engine exhausts will be reluctantly diminished. Although for CO and NO reduction different approaches must be taken a compromise is feasible and smoke is perhaps no longer a problem. We think therefore, that imposing standards is not the efficiency way to reduce air pollution especially not if the impact of the pollutants on the ecology is not well known.

We think, on the other hand, that standards are necessary and should be established keeping in mind the job the engine is supposed to do. It is strongly felt that if stringent standards are imposed, the combustor designer has to concede because there is no way of designing a combustor chamber for high power, very high combustion efficiency, good temperature distribution and no NO and CO emission at very low costs. We have therefore concentrated our activity on improving first the emission levels at idle, when the aircraft is on the ground and second on ground transportation using gas turbines, because gas turbines may become a challenger of diesel engines for heavy vehicles.

To sum up, we are in full agreement with the trend to reduce air pollution and have started work on our own and on the European scale. However, we have strong feelings against any severe imposed standards when their ultimate necessity is not proved and their ecological impact is small against other sources, when these requirements for the engine combustor design result in enormous costs with today's technology.

R.ROBERTS

With regard to aircraft safety and the impact of rapid change over to new or unique combustor designs, all current engines and those scheduled for introduction in the near future employ burners which are extrapolations of existing designs. The wide experience with this type of burner, and the certain knowledge of its behavior, contribute to the safety record which has been a hallmark of the aircraft gas turbine industry. If unconventional designs, such as premixed burners as have been widely discussed at this meeting, are to be employed, extreme care will have to be taken to ensure that considerations of operational safety are not compromised. This will be made difficult by the lack of a body of experience gained over a long history of operations.

A.K.FORNEY

Comment on a comment by Professor Ferri:

Information available to the US C.I.A.P. Program that is supported by published papers of John Leach and his associates of the British Aircraft Corporation indicates that there is today a significant amount of flying by the subsonic jets in the stratosphere. Therefore, if the nitrogen oxides produced by engines prove to be a problem, that problem will not wait until supersonic aircraft are flying in quantities.

J.DUNHAM

It has been pointed out that numerous subsonic jets operate currently at sufficient high altitude to have some potential influence on stratospheric ozone. Have the various models of ozone depletion been applied to predict their effect, and if they are what answer will they give?

How could the large fleet of subsonic aircraft be introduced as an NO_x source in models like Hesstvedt's?

E.HESSTVEDT

Subsonic aircraft sometimes fly in the troposphere, sometimes in the stratosphere. The tropopause fluctuates at a given latitude. The emissions of NO_x can therefore not readily be introduced in two-dimensional models. Three dimensional models would solve the problem. But approximations of the effect of subsonic transport in the stratosphere could be obtained even from two-dimensional models if flight levels were given relative to the tropopause rather than in absolute altitude.

My model indicates that a limited fleet of SST's, not flying too high, would have a small influence on the ozone layer. I must, however, warn against the conclusion which has obviously been drawn by this audience, that a small effect is no effect. Apart from the instantaneous effect on life we also have to consider the possibility of a long term, cumulative, effect. This we know very little about.

S.A.MOSIER

With respect to Prof. Ferri's comment regarding the increase in income tax or other public tax to accommodate modifications regarding means for reducing pollution by operational procedures at airports, I suggest that this can be handled in the same manner in which search procedures are handled at many American airports. By law, each passenger boarding an aircraft in the USA must be searched. However, only the passenger boarding is assessed a fee. The user pays for what service he receives. Whatever procedures are implemented to accommodate airport problems should be simply paid for by airport users. No increase in public taxation is necessary.

I.A. LANG

My comments concern the problems of applying legislation to a problem as complex as aero-engine emissions. For example, the present EPA proposals favour the high bypass ratio turbofan, since the emissions parameter is essentially the product of emissions index and specific fuel consumption. No account is taken, however, of the aircraft mission objectives. It seems to me that, by biasing the engine/airframe optimisation procedure to meet a given set of emission requirements, the resultant system could be far from optimum for the mission as a whole. It is not inconceivable that under these circumstances the overall mission pollution could be increased.

A. GOLDFURG

It has always seemed to me that the richness of the observational phenomena of ozone, specially with respect to its time dependent qualities, make it inappropriate to attempt to understand it in depth from basically steady state equilibrium theories. Attempts to explain perturbations to ozone must in the end give way to theories which have their origins in time dependent phenomena. Such an approach, as an example, is that of H.C. Willet of M.I.T. which he reported in "The Seasonal Changes of Temperature and O_3 in the Arctic and Antarctic Stratosphere", *Jr. Atmos. Sci.*, May 1968, 341-360. In this article Willet treats the annual regimes of temperature in the Arctic and Antarctic stratospheres with special reference to the sporadic winter warmings of the Arctic and the explosive spring warming of the Antarctic stratospheres. There follows a discussion of the inadequacy of the usual advective-dynamic explanation, at least in terms of any model presented to date, (1968) to account quantitatively for any of these phenomena in their more extreme manifestations. The seasonal regimes of total atmospheric ozone in the Arctic and Antarctic are likewise contrasted again with special reference to the differing thermal regimes and sudden stratospheric warmings. The strong annual period of auroral frequencies are discussed in relation to the Arctic and Antarctic thermal regimes, as is the relationship of sudden stratospheric warmings to auroral and solar activity.

Finally, variability of the solar wind, i.e., the solar corpuscular penetration of the higher atmosphere, is tentatively suggested as a possible alternative explanation to the advective-dynamic hypothesis to account for the variation, shared in common, of the Polar temperature, ozone and auroral activity.

M. WHITTAKER

Present estimates of growth in air traffic seem to ignore the rapidly changing world fuel supply situations and the effect this will have upon price. Would anyone making these type of predictions care to comment.

A.K. FORNEY

The traffic predictions to be made as part of the C.I.A.P. Program include all the factors, and many others also, brought up by Mr Whittaker. These factors include fuel costs, alternate fuels, as well as many others.

R.E. HUIE

I would like to point out that the stratospheric models presently used are not highly accurate. A change in the ozone concentration predicted by these models is more an indication of the direction of change, not the magnitude. Therefore, if a model predicts a few per cent reduction, this should be considered important, and it should be realized that the actual reduction could be much larger or much smaller.

Someone commented earlier that the technological solution to environmental problems would not improve the standard of living, at least as measured by the Gross National Product. They will, however, improve the quality of life, which is more important.

SUMMARY

A.FERZI

The main topics discussed were the following:

1. Pollution around and at the airports

Several objections have been directed toward the tendency of trying to solve the problem by imposing standards on the airplane engines. It was the consensus that a different approach, where changes in operational procedures are introduced, could go a long way in solving the problem without the requirement for engine retrofitting that would increase the cost of transportation.

2. Knowledge of atmospheric phenomena

Substantial discussions have taken place on the possible effects of an increase in NO_x concentration on the upper atmosphere. No basic conclusions can be reached from the discussions. The following important information was presented:

- (a) Recent preliminary measurements of NO_x concentration in the upper atmosphere do not agree with predictions.
- (b) Substantial disagreement exists among scientists interested in the problem on the interpretation of available data.
- (c) The present program of Climatic Impact Assessment Program (C.I.A.P.) is in the process of reducing, or eliminating many of the disagreements by making available results of crucial experiments.

3. Engine pollution in the upper atmosphere

It is accepted that the level of NO_x produced by the present generation of engines can be substantially reduced. The amount of decrease predicted varies substantially from group to group; however, the decrease will be substantial even if only the lower limit predicted is realized.

APPENDIX A

AGARD PROPULSION AND ENERGETICS PANEL

- AGARDograph 89 - "V/STOL Aircraft". Proceedings of a Meeting held at NATO Headquarters, Paris. September 1964. (Two volumes.)
- AGARDograph 98 - "Graphical Methods in Aerothermodynamics" by O.Lutz and G.Stöffers. November 1967.
- AGARDograph 117 - "Behaviour of Supercritical Nozzles under Three-Dimensional Oscillatory Conditions" by L.Crocco and W.A.Sirignano. 1967.
- AGARDograph 122 - "Selected Topics in Electrofluid Dynamic Energy Conversion". Editors M.Lawson and F.Wattendorf. December 1968.
- Publication Hors-Série (contact AGARD). - "Properties of Air and Combustion Products with Kerosine and Hydrogen Fuels". Editor R.W.McIntyre. (13 volumes.) 1967.
- Conference Proceedings 8 - "Fundamental Studies of Ions and Plasmas". Editor H.Dean Wilsted. Proceedings of the PEP 26th Meeting held in Pisa, September 1965. (Two volumes.)
- Conference Proceedings 9 - "Gas Turbines". Papers presented at the PEP 27th Meeting held in Paris, April 1966. (Two volumes.)
- Conference Proceedings 12 - "Recent Advances in Aerothermochemistry". Editor I.Glassman. Selected papers presented at the PEP 28th Meeting (7th Colloquium) held in Oslo, May 1966. (Two volumes.)
- Conference Proceedings 21 - "Performance Forecast of Static Energy Conversion Devices". Editors G.W.Sherman and L.Devol. Proceedings of the PEP 29th Meeting held in Liège, June 1967.
- Conference Proceedings 31 - "Helicopter Propulsion Systems". Editor R.P.Hagerty. Proceedings of the PEP 31st Meeting held in Ottawa, June 1968.
- Conference Proceedings 34 - "Advanced Components for Turbojet Engines". Editor R.P.Hagerty. Proceedings of the PEP 32nd Meeting held in Toulouse, September 1968. (Two volumes.)
- Conference Proceedings 42 - "Aircraft Engine Noise and Sonic Boom". Editors R.Barth and R.P.Hagerty. Proceedings of the Joint FDP/PEP (33rd Meeting) held in St.Louis, France, May 1969.
- Advisory Report 22 - "Technical Evaluation Report on AGARD Specialists' Meeting on Aircraft Engine Noise and Sonic Boom" by W.R.Sears. January 1970. (Primarily treats sonic boom.)
- Advisory Report 26 - "Technical Evaluation Report on AGARD Specialists' Meeting on Aircraft Engine Noise and Sonic Boom" by J.O.Powers and M.Pianke. June 1970. (Primarily treats engine noise.)
- AGARDograph 123 - "Space Power Systems". Editor G.C.Szego. Lecture Series held in October 1967. (Two volumes.)
- AGARDograph 135 - "Fluidic Controls Systems for Aerospace Propulsion". Editor R.J.Reilly. XXXV Lecture Series. September 1969.
- Conference Proceedings 52 - "Reactions between Gases and Solids". Editor R.P.Hagerty. February 1970. Proceedings of PEP 34th Meeting held in Dayton, Ohio, October 1969.
- Advisory Report 32 - "Technical Evaluation Report on AGARD Propulsion and Energetics Panel's 34th Meeting (3th Colloquium) on Reactions between Gases and Solids" by S.S.Penner and F.G.Abbott Jr. February 1971.

App.A-2

- AGARDograph 108 - "Combustibles, Lubrifiants et Fluides Auxiliaires pour l'Aviation Supersonique" by G.J.Souillard, J.Ducanne and T.H. de Menten. June 1970.
- AGARDograph 141 - "Propergels Hautement Energétiques" by P.Tavernier, J.Boisson and B.Crampel. August 1970.
- Lecture Series 39 - "Advanced Compressors". Editor J.Chauvin. August 1970.
- Conference Proceedings 64 - "Advanced Technology for Production of Aerospace Engines". Editor R.P.Hagerty. September 1970. Proceedings of PEP 35th Meeting held in London, England, April 1970.
- Conference Proceedings 73 - "High Temperature Turbines". Editor R.P.Hagerty. January 1971. Proceedings of PEP 36th Meeting held in Florence, Italy, September 1970.
- Advisory Report 29 - "Technical Evaluation Report on AGARD Technical Meeting on High Temperature Turbines" by J.B.Esgar and R.A.Reynolds. February 1971.
- Lecture Series 46 - "Small Gas Turbines for Helicopters and Surface Transport". Editor J.Fabri. May 1971.
- Conference Proceedings 84 - "Aircraft Fuels, Lubricants, and Fire Safety". Editor R.P.Hagerty. August 1971. Proceedings of PEP 37th Meeting held in The Hague, Netherlands, May 1971.
- Advisory Report 44 - "Technical Evaluation Report on Propulsion and Energetics Panel 37th Meeting on Aircraft Fuels, Lubricants, and Fire Safety" by R.B.Whyte and L.Gardner. May 1972.
- Advisory Report 36 - "Report of the AGARD Ad Hoc Committee on Engine-Airplane Interference and Wall Corrections in Transonic Wind Tunnel Tests". August 1971.
- AGARDograph 148 - "Heat Transfer in Rocket Engines" by H.Ziehl and R.C.Parkinson. September 1971.
- Conference Proceedings 91 - "Inlets and Nozzles for Aerospace Engines". Editor R.P.Hagerty. December 1971. Proceedings of PEP 38th Meeting held in Sandefjord, Norway, September 1971.
- Advisory Report 41 - "Technical Evaluation Report on Propulsion and Energetics Panel 38th Meeting on Inlets and Nozzles for Aerospace Engines" by D.N.Bowditch and R.Monti. February 1972.
- Advisory Report 40 - "Atmospheric Pollution by Aircraft Engines and Fuels - A Survey" by R.F.Sawyer. March 1972.
- Advisory Report 50 - "Technical Evaluation Report on Propulsion and Energetics Panel 39th Meeting on Energetics for Aircraft Auxiliary Power Systems" by R.H.Johnson, C.E.Oberly and R.E.Quigley, Jr. November 1972.
- AGARDograph 164 - "Boundary Layer Effects in Turbomachines". Edited by V.Surugue. December 1972.
- Conference Proceedings 104 - "Energetics for Aircraft Auxiliary Power Systems". Editor A.E.Fuhs. December 1972. Proceedings of PEP 39th Meeting held in Colorado Springs, Colorado, USA. June 1972.
- Conference Proceedings 112 - "Impact of Composite Materials on Aerospace Vehicles and Propulsion Systems" May 1973. Proceedings of Structures and Materials Panel and Propulsion and Energetics Panel Joint Symposium held in Toulouse, France, September 1972.
- AGARDograph 167 - "Modern Methods of Testing Rotating Components of Turbomachines". Edited by M.Pianko, May 1973.
- AGARDograph 168 - "Gas Sampling and Analysis in Combustion Phenomena" by G.Lengelle and C.Verdier, June 1973.
- AGARDograph 168 (FR) - "Élevement et Analyse de Gaz dans les Phénomènes de Combustion" par Lengelle et C.Verdier, June 1973.

APPENDIX B

LIST OF PARTICIPANTS

PANEL MEMBERS

ALPAUGH, Mr R.T.	US Army Materiel Command, Washington, DC, USA.
*BARRERE, Mr M.L.	ONERA, Châtillon-sous-Bagneux, France.
*CASCI, Prof.C.	Politecnico di Milano, Ist. di Macchine, Milano, Italy.
CHAUVIN, Prof.J.	VKI, Rhode-St-Cenèse, Belgium.
*DINI, Prof.D.	Università degli Studi, Istituto di Macchine, Pisa, Italy.
DUCARME, Prof.J.	Université de Liège, Institut de Mécanique, Liège, Belgium.
DUNHAM, Dr J.	NGTE, Pyestock, Farnborough, Hants, UK.
*FERRI, Prof.A.	Department of Aero and Astronautics, University of New York, Bronx, New York, USA.
*FUHS, Prof.Allen E.	Department of Aeronautics, Naval Postgraduate School, Monterey, California, USA.
GIORGIERI, Colonel L.	Ministero Difesa Aeronautica, Roma, Italy.
GLASSMAN, Prof.Irvin	Engineering Quadrangle, Princeton University, Princeton, New Jersey, USA.
HARGIS JR, Mr Calvin B.	Office of the Assistant Secretary of the Air Force for R&D, The Pentagon, Washington, DC, USA.
JAARSMA, Mr F.	National Aerospace Laboratory, NLR, Amsterdam, Netherlands.
JOHNSON, Mr Elmer G.	Aerospace Laboratory, Wright-Patterson AFB, Ohio, USA.
LANE, Mr R.J.	Rolls-Royce (1971) Ltd, Bristol Engine Division, Filton, Bristol, UK.
*LEFEBVRE, Prof.A.H.	School of Mechanical Engineering, Cranfield Institute of Technology, Cranfield, Bedford, UK.
MONTI, Prof.R.	Università di Napoli, Naples, Italy.
PAVLIDIS, Brig.Gen.A.	Chief of Staff, 30th Air Materiel Command, Pafos Phaleron, Athens, Greece.
PIANKO, M. l'Ing. en Chef M.	Service Technique Aéronautique, Paris, France
REKOS, Mr Nelson F.	Office of Aeronautics and Space Technology, NASA Headquarters, Washington, DC, USA.
RIPOLL, M. l'Ing. en Chef J.	Centre d'Essais des Propulseurs de Saclay, Orsay, France.
SCHOLZ, Prof.Dr-Ing.N.K.	MTU München GmbH, Munich, Germany.
SEZGEN, Prof.H.	Makina Müh Bölümü, Orta Doğu Teknik Üniversitesi, Ankara, Turkey.
SURUGUE, Mr J.	ONERA, Châtillon-sous-Bagneux, France.
WHYTE, Dr R.B.	Fuels and Lubricants Laboratory, Division of Mechanical Engineering, NRC, Ottawa, Ontario, Canada.
WINTERFELD, Dr-Ing.G.	DFVLR, Institut für Luftstrahlantriebe, Perz-Wahn, Germany.

HOST NATION

SEDDON, Dr J.	Ministry of Defence (London), UK.
SMITH, Mr D.B.	Ministry of Defence (London) Coordinator, UK.

AGARD HQ

YARYMOVYCH, Dr M.I.	Director, AGARD.
CATILLER, Major J.B.	PEP Executive.
SCOPES, Mrs P.C.	Secretary.

AUTHORS/SESSION CHAIRMEN

ALVERMANN, Dr Ing.W.	DFVLR, Institut für Luftsaugende Antriebe, Braunschweig, Germany.
APPLETON, Prof.J.P.	Mechanical Engineering Department, MIT, Cambridge, Mass., USA.
BACK, Dr K.C.	AMRL/THT, Wright-Patterson AFB, Ohio, USA.
BAHR, Mr D.W.	General Electric Company, Cincinnati, Ohio, USA.
BAILEY, Lt-D.L.	Department of Aeronautics, Naval Postgraduate School, Monterey, California, USA.
BECKER, Prof.Dr K.H.	Institut für Physikalische Chemie, Universität Bonn, Germany.
BERGT, Dipl.Ing.W.	MTU München GmbH, Munich, Germany.
BLAZOWSKI, Lt W.	AFAPL (AFSC), Wright-Patterson AFB, Ohio, USA.
BORGHI, Mr R.	ONERA, Châtillon-sous-Bagneux, France.
BRASSEUR, Mr G.	Institut d'Aéronomie Spatiale de Belgique, Bruxelles, Belgium.

BRIANCON, Mr R.	SNECMA, Service Combustion, Centre d'Essais de Villaroche, Moissy-Cramayel, France.
BRUION, Dr D M.	Air Corporations Joint Medical Service, London (Heathrow) Airport, Hounslow, Middlesex, UK.
CERNANSKY, Mr N.P.	Department of Mechanical Engineering, University of California, Berkeley, California, USA.
COGHE, Mr A.	Istituto di Macchine, Politecnico di Milano, Italy.
CROSS, Mr N.L.	Chemical Defence Establishment, Porton Down, Wiltshire, UK.
DECOUFLET, Mr J.	SNECMA, Service Combustion, Centre d'Essais de Villaroche, Moissy-Cramayel, France.
EBERIUS, Dr H.	Institut für Reaktionskinetik, DFVLR, Stuttgart, Germany.
EISFELD, Mr F.	DFVLR, Institut für Antriebssysteme, Braunschweig, Flughafen, Germany.
FLETCHER, Prof.R.S.	School of Mechanical Engineering, Cranfield Institute of Technology, Cranfield, Bedford, UK.
FOOT, Dr J.S.	Meteorological Office, Bracknell, Berkshire, UK.
GHEZZI, Mr U.	Istituto di Macchine, Politecnico di Milano, Milano, Italy.
GOLDSMITH, Mr P.	Meteorological Office, Bracknell, Berkshire, UK.
GRÖBECKER, Dr A.J.	Department of Transportation, Washington, DC, USA.
GROBMAN, Mr J.	NASA Lewis Research Center, Cleveland, Ohio, USA.
GRÖNSKEI, Mr K.E.	Norwegian Institute for Air Research, Kjeller, Norway.
HENDERSON, Mr R.E.	AFAPL - TBC - Wright-Patterson AFB, Ohio, USA.
HESSTVEDT, Prof. E.	Institute of Geophysics, University of Oslo, Blindern, Norway.
HEYWOOD, Prof.J.B.	Department of Mechanical Engineering, MIT, Cambridge, Massachusetts, USA.
HOLDERNESS, Mr F.H.	NGTE, Pyestock, Farnborough, Hants, UK.
HUGHES, Dr L.	Department of Mechanical Engineering, University of California, Berkeley, California, USA.
JOATTON, Mr R.	Aérospatiale, Direction Générale/DTA, Paris, France.
JOHNSTON, Prof.H.S.	Department of Chemistry, University of California, Berkeley California, USA.
JONES, Mr R.E.	NASA Lewis Research Center, Cleveland, Ohio, USA.
JUST, Dr T.	DFVLR, Institut für Reaktionskinetik, Stuttgart, Germany.
KAPPLER, Dr Ing.G.	MTU München GmbH, Munich, Germany.
KEDDIE, Dr A.W.C.	Air Pollution Division, Warren Spring Laboratory, Stevenage, Herts, UK.
LAWSON, Mr T.V.	Department of Aeronautical Engineering, University of Bristol, Bristol, UK.
LUCCHESINI, Mr M.	Istituto di Macchine, Università di Pisa, Italy.
MACFARLANE, Mr J.J.	NGTE, Pyestock, Farnborough, Hants, UK.
MEIKIS, Dr Ing.G.	MTU München GmbH, Munich, Germany.
MEINEL, Dr H.	DFVLR, Institut für Reaktionskinetik, Stuttgart, Germany.
MIKUS, Mr T.	Department of Mechanical Engineering, MIT, Cambridge, Massachusetts, USA.
MOE, Colonel W.S.	AFAPL, Wright-Patterson AFB, Ohio, USA.
MOSIER, Mr S.A.	Pratt & Whitney Aircraft, Florida R&D Center, West Palm-Beach, Florida, USA.
NELSON, Mr A.W.	Pratt & Whitney Aircraft, United Aircraft Corp., East Hartford, Connecticut, USA.
NEWSON, Dr R.L.	Meteorological Office, Bracknell, Berkshire, UK.
NOVAKOV, Mr T.	Department of Mechanical Engineering, University of California, Berkeley, California, USA.
OPPENHEIM, Prof.A.K.	Department of Mechanical Engineering, University of California, Berkeley, California, USA.
PAGNI, Prof.P.J.	University of California, Department of Mechanical Engineering, Berkeley, California, USA.
PARKER, Mr J.	Air Pollution Division, Warren Spring Laboratory, Stevenage, Herts, UK.
PASINI, Mr S.	Istituto di Macchine, Politecnico di Milano, Milan, Italy.
PICKNETT, Dr R.G.	Chemical Defence Establishment, Porton Down, Salisbury, Wiltshire, UK.
QUILLEVERE, Mr A.	SNECMA, Centre d'Essais de Villaroche, Moissy-Cramayel, France.
ROBERTS, Dr R.	Pratt & Whitney Aircraft, United Aircraft Corporation, East Hartford, Connecticut, USA.
ROBERTS, Mr G.H.	Air Pollution Division, Warren Spring Laboratory, Stevenage, Herts, UK.
SAWYER, Prof.R.F.	Department of Mechanical Engineering, University of California, Berkeley, California, USA.
SCHMIDT, Dipl.Ing.J.	MTU München GmbH, Munich, Germany.
SCHURATH, Mr U.	Institut für Physikalische Chemie, Universität Bonn, Bonn, Germany.
SIMMONS, Dr E.L.	Meteorological Office, Bracknell, Berks, UK.
TOWER, Lt P.W.	Department of Aeronautics, Naval Postgraduate School, Monterey, California, USA.
TUCK, Dr A.	Meteorological Office, Bracknell, Berks, UK.
WHITTEN, Mr G.	Lawrence Berkeley Laboratory, Berkeley, California, USA.

OBSERVERS

- ALEXOPOULOS, Prof.J.B.
 ALLEN, Mr F.D.
 *BEER, Prof. J.M.
- BERTIN, Madame
 BONING, Mr R.W.
 BOUMA, Ir.W.J.
 *BOWMAN, Dr C.T.
- BRAY, Prof.K.N.C.
 BRIFFA, Mr G.F.F.
 BRIX, Dipl.-Ing.W.
 BRODERICK, Mr A.
- BUJAC JR, Mr J.N.
 *CASANDJIAN, ICA G.P.C.
- CHAMBON, Ing.
 *CHIGIER, Dr N.A.
- COX, Dr R.A.
- COX, Mr R.A.
 DORAN, Mr D.
 *EATOCK, Mr H.C.
 *EGGLETON, Dr A.E.J.
- FACY, Dr E.E.R.M.
 FEJER, Prof.A.A.
 *FORNEY, Mr A.K.
 FRISWELL, Dr N.J.
 *GELINAS, Dr R.J.
- GERONIMI, Mr J.L.
 GERRARD, Mr A.J.
- *GOLDBURG, Mr A.
 GOLDSTONE, Dr L.
 GRAYSTONE, Mr P.
 GREENSTONE, Mr R.
 GRISSOM, Mr J.L.
 GUYOT, Mr P.
 HAYS, Mr G.E.
 *HEUER, Ing.Grad K.O.
 HOFMAN, Ir. A.M.
 HOLCOMBE, Mr V.R.
 HOUTMAN, Ir. C.J.
- HUDSON, Dr F.P.
 *HUIE, Dr R.E.
- JONES, Dr I.T.N.
 *JUDD, Mr H.J.
 *KITTREDGE, Mr G.D.
- LAGNEAU, Mr J.P.
 LAGUZZI, Mr F.
 *LANG, Mr J.A.
 LEACH, Mr J.F.
 LEWIS, Mr A.
 *LIBBY, Prof.P.A.
- LIVERMORE, Mr H.E.
- Hellenic Air Force Academy, Tatoi, Near Athens, Greece.
 Rolls-Royce (1971) Ltd, Small Engine Division, Leavesden, Watford, Herts, UK.
 Department of Chemical Engineering and Fuel Technology, The University, Sheffield, UK.
 Aérospatiale, Courbevoie, France.
 Hawker Siddeley Aviation Ltd, Hatfield, Herts, UK.
 Civil Aviation Department (RLD), Schiphol-East, Netherlands.
 United Aircraft Corporation Research Laboratory, East Hartford, Connecticut, USA.
 Department of Aeronautics, The University, Southampton, UK.
 Rolls-Royce (1971) Ltd, Small Engine Division, Leavesden, Watford, UK.
 VFW-Fokker, Bremen, Germany.
 US Department of Transportation, Transportation Systems Center, Cambridge, Massachusetts, USA.
 US Army Aviation Systems Command, Saint-Louis, Missouri, USA.
 Direction Générale de la Protection de la Nature et de l'Environnement, Paris, France.
 SNECMA-Villarcche, Moissy-Cramayel, France.
 Department of Chemical Engineering & Fuel Technology, The University, Sheffield, UK.
 Atomic Energy Research Establishment, Health Physics & Medical Division, Harwell, Berks, UK.
 Imperial College of Science and Technology, London, UK.
 BEA/BOAC, Heathrow Airport, Hounslow, Middlesex, UK.
 United Aircraft of Canada Ltd, Longueuil, Quebec, Canada.
 Atomic Energy Research Establishment, Health Physics & Medical Division, Harwell, Berks, UK.
 Meteorology Nationale, Paris, France.
 c/o Engineering Department, The University, Cambridge, UK. (USA)
 Department of Transportation, FAA, Washington, DC, USA
 Shell Research Ltd, Thornton Research Centre, Chester, UK.
 Lawrence Livermore Laboratory, University of California, Livermore, California, USA.
 Laboratoire Central de la Préfecture de Police, Paris, France.
 Engineering Laboratories, Lucas Equipment Division, Wood Top Works, Burnley, Lancs, UK.
 The Boeing Company, Seattle, Washington, USA.
 Civil Aviation Authority, Strand, London, UK.
 Meteorological Office, Bracknell, Berks, UK.
 Department of Transportation, Office of the Secretary, Washington, DC, USA.
 ARO Inc., Arnold AF Station, Tennessee, USA.
 Aérospatiale, Châtillon-sous-Bagneux, France.
 The Boeing Co., Seattle, Washington, USA.
 Deutsche Lufthansa German Airlines, Hamburg, Flughafen, Germany.
 Netherlands Agency for Aerospace Programs. (NIVR), Delft, Netherlands.
 Pratt & Whitney Aircraft, East Hartford, Connecticut, USA.
 Technische Hogeschool Lab. voor Verbrandingsmotoren en Gasturbines, Delft, Netherlands.
 Sandia Labs., Albuquerque, New Mexico, USA.
 National Bureau of Standards, Elementary Processes Section, Washington, DC, USA.
 Meteorological Office, Bracknell, Berks, UK.
 BEA/BOAC, Heathrow Airport, Hounslow, Middlesex, UK.
 Office of Air and Water Programs, Environmental Protection Agency, Washington, DC, USA.
 ACEC, Charleroi, Belgium.
 FIAT, Divisione Aviazione, Direzione Progettazione, Torino, Italy.
 NGTE, Pyestock, Hants, UK.
 British Aircraft Corporation, Commercial Aircraft Division, Filton, Bristol, UK.
 Shell Research Ltd, Thornton Research Centre, Chester, UK.
 c/o Imperial College of Science & Technology, Department of Aeronautics, London, UK. (USA)
 Hawker Siddeley Aviation Ltd, Hatfield, Herts, UK.

- LOITIERE, Mr B.
MÉTÉOROLOGIE NATIONALE, Observatoire de Magny-les-Hameaux, St-Rémy-les-Chevreuses, France.
- MACNAIR, Miss E.J.
MOD(N), Ship Department, Foxhill, Bath, UK.
- MASON, Dr D.M.
ONR, London, England. (USA)
- MATTINGLY, Dr S.R.
Meteorological Office, Bracknell, Berks, UK.
- *MELLOR, Prof.A.M.
School of Mechanical Engineering, Purdue University, West Lafayette, Indiana, USA.
- MILWARD, Mr R.A.
British Airport Authority, London, UK.
- MORBIOLI, Ing.R.
SNECMA, Corbeil, France.
- MORLEY ENGLISH, Prof.J.
c/o Technical University of Denmark, Electrical Power Engineering Department, Lyngby, Denmark. (USA)
- MOURANCHE, IA D.
Centre d'Essais des Propulseurs de Saclay, Orsay, France.
- CDGERS, Prof.J.
Laval University, Département du Génie-Mécanique, Québec, PQ, Canada.
- *OLIVER, Dr R.C.
Institute for Defense Analyses, Arlington, Virginia, USA.
- OVERTON, Mr D.L.
Rolls-Royce (1971) Ltd, Bristol Engine Division, Filton, Bristol, UK.
- PARKE, Dr D.A.
Shell Research Ltd, Thornton Research Centre, Chester, UK.
- PATERSON, Mr M.P.
Air Pollution Research Group, Department of Mathematics, Imperial College, London, UK. (AUSTRALIA)
- *POLL, Dr I.
Department of Mechanical Engineering, The University, Sheffield, UK.
- POOK, Mr N.W.
Engelhard Industries Ltd, Cinderford, Glos, UK.
- PRATT, Dr N.H.
Department of Aeronautics & Astronautics, The University, Southampton, UK.
- RFED, Dr L.E.
Central Unit on Environmental Pollution, Department of the Environment, London, UK.
- *ROBERTS, Dr R.
Power Program, Office of Naval Research, Arlington, Virginia, USA.
- ROSNER, Prof. D.E.
Yale University, Mason Laboratory, New Haven, Connecticut, USA.
- SABETTA, Prof.F.
Istituto di Aerodinamica, Scuola di Ingegneria Aerospaziale, Roma, Italy.
- *SAMPSON, Dr R.E.
Environmental Protection Agency, Ann Arbor, Michigan, USA.
- SCHONFELD, Mr C.W.
KLM, Schiphol-Oost, Netherlands.
- *SCORER, Prof.R.S.
Imperial College of Science & Technology, London, UK.
- *SCOTT, Mr C.J.
Rolls-Royce (1971) Ltd, Bristol Engine Division, Filton, Bristol, UK.
- SIMONI, Mr G.
Italian Embassy, London, England. (ITALY)
- SMITH, Dr I.W.M.
Department of Physical Chemistry, University Chemical Laboratories, Cambridge, UK.
- SPRENGEL, Dr-Ing.U.
DFVLR, Forschungsplanung, Porz-Wahn, Linder Höhe, Germany.
- STAECHELIN, TA, Dipl.phys.P.
Musterprüfstelle der Bundeswehr für Luftfahrtgerät, Munich, Germany.
- STAPLES, Mr G.E.
BEA, Technical Services Branch, Eng. Head Office, London, Heathrow Airport, UK.
- STRINGER, Mr F.W.
Engineering & Research Laboratory, Lucas Aerospace Ltd, Fabrication Group, Wood Top Works, Burnley, Lancs, UK.
- SWITHENBANK, Dr J.
Department of Chemical Engineering, The University, Sheffield, UK.
- TAILLET, Dr J.
ONERA, Châtillon-sous-Bagneux, France.
- THRANE, Dr E.
NDRE, Kjeller, Norway.
- *TOMMEL, Dr D.K.J.
Department of Public Health and Environmental Hygiene, Leidschendam, Netherlands.
- UNDERWOOD, Dr R.L.
US Department of Transportation, Office of the Secretary, Washington, DC, USA.
- *VERKAMP, Mr F.J.
Detroit Diesel Allison Division, General Motors Corporation, Indianapolis, Indiana, USA.
- VICKERY, Mr D.I.
British Aircraft Corporation, Commercial Aircraft Division, Bristol, UK.
- VOKAER, Mr D.P.R.
Institut de Mécanique Appliquée, Université Libre de Bruxelles, Bruxelles, Belgium.
- WAKELING, Mr D.J.N.
BOAC, Environmental Control, Heathrow Airport, Hounslow, Middlesex, UK.
- WARDLE, Mr D.I.
Atmospheric Environment Service, Downsview, Ontario, Canada.
- *WASELL, Mr A.B.
Rolls-Royce (1971) Ltd, Derby, UK.
- WEYER, Ir. W.F.P.M. van de
Cent. RNLAf, Scientific Research Branch, Vliegbasis Ypenburg, Gebouw A-16, Rijswijk, Netherlands.
- *WHEELER, Mr R.W.
Ricardo & Co., Bridge Works, Shoreham-by-Sea, Sussex, UK.
- WHITCHER, Mr F.S.E.
NGTE, Pyestock, Farnborough, Hants, UK.
- *WHITTAKER, Mr M.
Rolls-Royce (1971) Ltd, Bristol Engine Division, Filton, Bristol, UK.
- WILLIAMS, Mr R.E.
Shell International Petroleum Co. Ltd, Shell Centre, London, UK.
- ZELLNER, Dr rer nat. R.
The University, Leasfield Road, Cambridge, UK. (GERMANY)
- ZIMMER, Dipl. Ing.F.
Dornier GmbH, Friedrichshafen, Germany.
- WILLIAMS, Mr
Rolls-Royce (1971) Ltd, BED, Filton, Bristol, UK.